The Chiari Malformations

R. Shane Tubbs
Mehmet Turgut
W. Jerry Oakes
Editors

Second Edition

Springer

The Chiari Malformations

R. Shane Tubbs • Mehmet Turgut
W. Jerry Oakes
Editors

The Chiari Malformations

Second Edition

Springer

Editors
R. Shane Tubbs
Department of Neurosurgery
Tulane University School of Medicine
New Orleans, LA
USA

Department of Neurosurgery and
Ochsner
Neuroscience Institute, Ochsner Health
System
New Orleans, LA
USA

W. Jerry Oakes
Departments of Neurosurgery and
Pediatrics, University of Alabama
Birmingham, AL
USA

Mehmet Turgut
Department of Neurosurgery
Aydın Adnan Menderes University
School of Medicine
Efeler, Aydın
Turkey

ISBN 978-3-030-44861-5 ISBN 978-3-030-44862-2 (eBook)
https://doi.org/10.1007/978-3-030-44862-2

This Springer imprint is published by the registered company Springer Nature Switzerland AG
The registered company address is: Gewerbestrasse 11, 6330 Cham, Switzerland

Foreword

While the brain malformations that carry Hans Chiari's name continue to be listed on the National Institutes of Health (NIH) Website under *Genetic and Rare Diseases Information Center*, we now recognize that the low-lying cerebellar tonsil that has long been pathognomonic of Chiari I is a common, albeit age-dependent, anatomical variant. This and other observations came to light since publication of the first edition of this book, and have contributed to refueling the diagnostic and therapeutic controversies associated with these entities, with debates on what combination of anatomical and clinical features we should consider pathological, and when and how we treat them. Concurrently, investigations into the diagnosis and surgical management of hindbrain hernias have shifted from an exploratory twentieth century period to an analytical twenty-first.

Alongside other pediatric neurosurgical disciplines, the Chiari field was defined and developed by a group of inspired young neurosurgeons—now hailed as pioneers and senior authorities—who believed children deserved their own surgical specialists, and proceeded, among others, to categorize and define the various field disciplines and their surgical management.

As the reigns of the specialty were gradually passed down from mentor to mentee, the new generation began to shepherd the field into an era of science, quality improvement, and technology. Consequently, the observations and suppositions of the past are now being scrutinized and analyzed through the lens of evidence-based medicine; the diagnostic and surgical challenges are being steadfastly vanquished by previously unimaginable technology; and the pathophysiology is being unraveled using the scientific method.

A necessary complement has been the acquisition of additional expertise and the bridging of professions. Accordingly, the Chiari research network, much of which is represented here, now comprises an amalgam of experts in the basic sciences, biostatistics and epidemiology, genetics, engineering, and others, as well as pediatric neurosurgeons, some of whom have also procured supplemental training in these areas. The result is a comprehensive 52-chapter second edition, in which gray-haired and

emerging world authorities on the anatomical, physiological, radiological, clinical, and surgical features of the Chiari malformations and related disorders join hands to report on the history, present-day status, and future prospects of this ripening field.

Bermans J. Iskandar, MD
Department of Neurological Surgery
Pediatric Neurosurgery
University of Wisconsin
Madison, WI, USA

Preface

During the last 50 years the Chiari malformations in both children and adult populations have been the topic of much controversy in the literature. Nowadays, the increased use of magnetic resonance imaging has shown that Chiari malformations may be much more common than previously believed. Nevertheless, the optimal choice of the surgical intervention itself is even more controversial, ranging from craniovertebral decompression alone to posterior cranial fossa decompression with duraplasty and cerebellar tonsillar resection.

Since the publication of our first edition on the Chiari malformations, additional topics have been identified that necessitate conversation. These include chapters on additional embryological and anatomical topics, ventral compression, craniosynostosis, diagnostics, advanced imaging, what to do with the so-called "benign" Chiari malformation, experimental models, and predictive and treatment analyses. This has increased the number of germane topics by 20 chapters. As in the first edition, this book includes chapters from leaders in the field. We hope that neuroscientists and clinicians at all levels will find this book to be a useful resource.

New Orleans, LA, USA — R. Shane Tubbs
Efeler, Aydın, Turkey — Mehmet Turgut
Birmingham, AL, USA — W. Jerry Oakes

Contents

Contributors

Niyazi Acer, PhD Department of Anatomy, Erciyes University School of Medicine, Kayseri, Turkey

Olufemi Ajani, MD, FRCSC Department of Surgery, McMaster Children's Hospital, Hamilton, ON, Canada

Elizabeth N. Alford, MD Department of Neurosurgery, University of Alabama at Birmingham, Birmingham, AL, USA

Davis P. Argersinger, BS Surgical Neurology Branch, National Institute of Neurological Disorders and Stroke, National Institutes of Health, Bethesda, MD, USA

Saritha Aryan, MS, MCh Department of Neurological Sciences, Sri Sathya Sai Institute of Higher Medical Sciences, Bangalore, Karnataka, India

Anastasia Arynchyna, MPH Department of Neurosurgery, Division of Pediatric Neurosurgery, University of Alabama at Birmingham, Birmingham, AL, USA

Allison E. Ashley-Koch, PhD Departments of Medicine, and Biostatistics and Bioinformatics, Duke Molecular Physiology Institute, Durham, NC, USA

A. James Barkovich, MD Departments of Radiology, Neurology, Pediatrics and Neurosurgery, University of California, San Francisco, San Francisco, CA, USA

Katherine Barnes, BS Department of Neurosurgery, University of Alabama at Birmingham, Birmingham, AL, USA

Ulrich Batzdorf, MD Department of Neurosurgery, David Geffen School of Medicine at UCLA, Los Angeles, CA, USA

David F. Bauer, MD Department of Surgery, Division of Neurosurgery, Dartmouth-Hitchcock Medical Center, Lebanon, NH, USA

Pierre-Aurélien Beuriat, MD, PhD Department of Pediatric Neurosurgery, Hôpital Femme Mère Enfant, Lyon, France

Jeffrey P. Blount, MD Department of Neurosurgery, Children's of Alabama, University of Alabama at Birmingham, Birmingham, AL, USA

Christopher M. Bonfield, MD Department of Neurological Surgery, Vanderbilt University Medical Center, Nashville, TN, USA

Frederick A. Boop, MD Department of Neurosurgery, University of Tennessee Health Science Center, Le Bonheur Children's Hospital, Memphis, TN, USA

Stephen J. Bordes Jr, MD, BA Department of Anatomical Sciences, St. George's University School of Medicine, St. George's, Grenada, West Indies

Edson Bor-Seng-Shu, MD, PhD Laboratory for Neurosonology and Cerebral Hemodynamics, Division of Neurological Surgery, Hospital das Clínicas, São Paulo University Medical School, São Paulo, Brazil

Nadine Bradley, BSN Department of Pediatric Neurosurgery, Children's of Alabama, Birmingham, AL, USA

Roger Schmidt Brock, MD, PhD Department of Neurosurgery, Hospital das Clínicas, University of São Paulo, DFV Neurology and Neurosurgery Service S/C Ltda, Bela Vista, São Paulo, Brazil

Douglas L. Brockmeyer, MD Department of Neurosurgery, Primary Children's Hospital, University of Utah, Salt Lake City, UT, USA

Joshua J. Chern, MD, PhD Department of Neurosurgery, Children's Healthcare of Atlanta, Emory University School of Medicine, Atlanta, GA, USA

Michael J. Cools, MD Department of Neurosurgery, University of North Carolina, Chapel Hill, NC, USA

Abby E. Deans, MD, PhD Department of Radiology and Biomedical Imaging, University of California, San Francisco, San Francisco, CA, USA

Marcelo de Lima Oliveira, MD Department of Neurology, Hospital das Clínicas, University of São Paulo, São Paulo, Brazil

Matheus Fernandes de Oliveira, MD, PhD Department of Neurosurgery, Hospital das Clínicas, University of São Paulo, DFV Neurology and Neurosurgery Service S/C Ltda, Hospital do Servidor Público Estadual de São Paulo, São Paulo, Brazil

Curtis W. Dewey, MS, DVM, DACVS, DACVIM, CTCVMP Department of Neurology/Neurosurgery, College of Veterinary Medicine, Cornell University, Ithaca, NY, USA

Federico Di Rocco, MD, PhD Department of Pediatric Neurosurgery, Hôpital Femme Mère Enfant, Université de Lyon, Lyon, France

Esther Beeson Dupépé, MSPH, MD Department of Neurological Surgery, St. Louis Children's Hospital, Washington University School of Medicine, St. Louis, MO, USA

Leon S. Dure, MD Department of Pediatrics/Pediatric Neurology, University of Alabama at Birmingham, Birmingham, AL, USA

Rami W. Eldaya, MD, MBA Department of Neuroradiology, Mallinckrodt Institute of Radiology, Bames Jewish Hospital, Washington University School of Medicine, St. Louis, MO, USA

Richard G. Ellenbogen, MD Department of Neurological Surgery, University of Washington Medicine Neuroscience Institute, Seattle, WA, USA

Scott W. Elton, MD Department of Neurosurgery, University of North Carolina, University of North Carolina School of Medicine, Chapel Hill, NC, USA

Manu S. Goyal, MD, MSc Department of Neuroradiology, Mallinckrodt Institute of Radiology, Washington University School of Medicine, St. Louis, MO, USA

Jacob K. Greenberg, MD, MSCI Department of Neurological Surgery, Washington University School of Medicine, St. Louis, MO, USA

Simon G. Gregory, PhD Department of Neurology, Duke Molecular Physiology Institute, Durham, NC, USA

Hatice Susar Güler Department of Anatomy, Bozok University School of Medicine, Yozgat, Turkey

Todd C. Hankinson, MD, MBA Departments of Neurosurgery and Pediatrics, Children's Hospital Colorado/University of Colorado School of Medicine, Aurora, CO, USA

John D. Heiss, MD Surgical Neurology Branch, National Institute of Neurological Disorders and Stroke, National Institutes of Health, Bethesda, MD, USA

David S. Hersh, MD Department of Neurosurgery, Connecticut Children's/UConn School of Medicine, Hartford, CT, USA

Bermans J. Iskandar, MD Department of Neurological Surgery, Pediatric Neurosurgery, University of Wisconsin, Madison, WI, USA

Skyler Jenkins, MD Department of Anatomical Sciences, St. George's University School of Medicine, Grenada, West Indies

James M. Johnston, MD Division of Pediatric Neurosurgery, Department of Neurosurgery, University of Alabama at Birmingham, Children's of Alabama, Birmingham, AL, USA

Kyung Hyun Kim, MD Division of Pediatric Neurosurgery, Seoul National University Children's Hospital and Neural Development and Anomaly Laboratory (NDAL), Department of Anatomy and Cell Biology, Seoul National University College of Medicine, Seoul, South Korea

Seung-Ki Kim, MD, PhD Division of Pediatric Neurosurgery, Seoul National University Children's Hospital, Seoul, South Korea

Jörg Klekamp, MD Department of Neurosurgery, Christliches Krankenhaus Quakenbrück, Quakenbrück, Lower Saxony, Germany

Joyce Koueik, MD, MS Department of Neurological Surgery, University of Wisconsin Hospital and Clinics, Madison, WI, USA

Sandi Lam, MD, MBA Division of Neurosurgery, Ann & Robert H. Lurie Children's Hospital of Chicago, Chicago, IL, USA

Ji Yeoun Lee, MD, PhD Division of Pediatric Neurosurgery, Seoul National University Children's Hospital and Neural Development and Anomaly Laboratory (NDAL), Department of Anatomy and Cell Biology, Seoul National University College of Medicine, Seoul, South Korea

Marina Liebsch Department of Neurosurgery, University Hospital Tübingen, Tübingen, BW, Germany

David D. Limbrick, MD, PhD Departments of Neurological Surgery and Pediatrics, St. Louis Children's Hospital, Washington University School of Medicine, St. Louis, MO, USA

Cormac O. Maher, MD Department of Neurosurgery, University of Michigan, Ann Arbor, MI, USA

Subramaniyan Mani, MTech Hospital Management Information System and Telemedicine, Sri Sathya Sai Institute of Higher Medical Sciences, Bangalore, Karnataka, India

Dominic J. Marino, DVM, DACVS, DACCT, CCRP Department of Surgery, Long Island Veterinary Specialists, Plainview, NY, USA

Christina A. Markunas, PhD Behavioral Health Research Division, RTI International, Durham, NC, USA

Bryn A. Martin, PhD Department of Biological Engineering, University of Idaho, Neurophysiological Imaging and Modeling Laboratory, Moscow, ID, USA

Panagiotis Mastorakos, MD, PhD Surgical Neurology Branch, National Institute of Neurological Disorders and Stroke, National Institutes of Health, Bethesda, MD, USA

Arnold H. Menezes, MD Department of Neurosurgery, University of Iowa Hospitals and Clinics, Iowa City, IA, USA

Kenneth A. Moore, MD Department of Neurosurgery, University of Tennessee Health Science Center, Memphis, TN, USA

Carmine Mottolese, MD, PhD Department of Pediatric Neurosurgery, Hôpital Femme Mère Enfant, Lyon, France

Robert P. Naftel, MD Department of Neurological Surgery, Monroe Carell Jr Children's Hospital at Vanderbilt/Vanderbilt University, Nashville, TN, USA

Vincent N. Nguyen, MD Department of Neurosurgery, University of Tennessee Health Science Center, Memphis, TN, USA

W. Jerry Oakes, MD Departments of Neurosurgery and Pediatrics, University of Alabama, Birmingham, AL, USA

I-Wen E. Pan, PhD Department of Health Services Research, Division of OVP, Cancer Prevention and Population Sciences, The University of Texas MD Anderson Cancer Center, Houston, TX, USA

Tae Sung Park, MD Division of Pediatric Neurosurgery, Department of Neurosurgery, Washington University School of Medicine, St. Louis Children's Hospital, St. Louis, MO, USA

Carolyn S. Quinsey, MD Department of Neurosurgery, University of North Carolina School of Medicine, Chapel Hill, NC, USA

Nathan J. Ranalli, MD, FAANS, FAAP Department of Neurosurgery, Division of Pediatric Neurosurgery, University of Florida Health Science Center – Jacksonville, Lucy Gooding Pediatric Neurosurgery Center, Wolfson Children's Hospital, Jacksonville, FL, USA

Vijay M. Ravindra, MD, MSPH Department of Neurosurgery, University of Utah, Clinical Neurosciences Center, Salt Lake City, UT, USA

Thomas Ridder, MD Pediatric and Adult Neurosurgery, Children's Hospital of Colorado – Colorado Springs/UCHealth Brain and Spine, Colorado Springs, CO, USA

Luigi Rigante, MD Department of Neurosurgery, Cleveland Clinic Abu Dhabi, Abu Dhabi, United Arab Emirates

Cleveland Clinic Lerner College of Medicine of Case Western Reserve University, Cleveland, OH, USA

Rima S. Rindler, MD Department of Neurosurgery, Emory University School of Medicine, Atlanta, GA, USA

Brandon G. Rocque, MD, MS, FAANS Department of Neurosurgery, University of Alabama at Birmingham, Birmingham, AL, USA

Lucy B. Rorke-Adams, MD (retired) Department of Pathology, The Children's Hospital of Philadelphia, Philadelphia, PA, USA

Florian Roser, MD, PhD Department of Neurosurgery, Cleveland Clinic Abu Dhabi, Abu Dhabi, United Arab Emirates

Cleveland Clinic Lerner College of Medicine of Case Western Reserve University, Cleveland, OH, USA

Curtis J. Rozzelle, MD Department of Neurosurgery, University of Alabama at Birmingham, Birmingham, AL, USA

R. Raghunatha Sarma, PhD Department of Mathematics and Computer Science, Sri Sathya Sai Institute of Higher Learning, Puttaparthi, Andhra Pradesh, India

Akal Sethi, MD, MBA Department of Neurosurgery, University of Colorado, Aurora, CO, USA

Mohammadali M. Shoja, MD Division of General Surgery, Tabriz University of Medical Sciences, Tabriz, Iran

University of Illinois at Chicago, Metropolitan Group Hospitals, Chicago, IL, USA

Ki-Bum Sim, MD, PhD Department of Neurosurgery, Jeju National University College of Medicine, Jeju, South Korea

Matthew D. Smyth, MD Department of Neurological Surgery, Washington University School of Medicine, St. Louis, MO, USA

Susan J. Staulcup, MSPH Department of Neurosurgery, Children's Hospital Colorado/University of Colorado, Aurora, CO, USA

Jennifer M. Strahle, MD Department of Neurosurgery, Washington University School of Medicine, Orthopedic Surgery and Pediatrics, Washington University School of Medicine, St. Louis Children's Hospital, St. Louis, MO, USA

Alexandru Szathmari, MD, PhD Department of Pediatric Neurosurgery, Hôpital Femme Mère Enfant, Hospices Civils de Lyon, Claude Bernard Lyon 1 University, Lyon, France

Mario Augusto Taricco, MD, PhD Department of Neurosurgery, Hospital das Clínicas, University of São Paulo, DFV Neurology and Neurosurgery Service S/C Ltda, Bela Vista, São Paulo, Brazil

Manoel Jacobsen Teixeira, MD, PhD Department of Neurology, Division of Neurosurgery, Hospital das Clínicas, University of São Paulo, University of São Paulo School of Medicine, São Paulo, Brazil

Sumit Thakar, MCh Department of Neurological Sciences, Sri Sathya Sai Institute of Higher Medical Sciences, Bangalore, Karnataka, India

R. Shane Tubbs, MS, PA-C, PhD Department of Neurosurgery, Tulane University School of Medicine, New Orleans, LA, USA

Department of Neurosurgery and Ochsner Neuroscience Institute, Ochsner Health System, New Orleans, LA, USA

Mehmet Turgut, MD, PhD Department of Neurosurgery, Aydın Adnan Menderes University School of Medicine, Efeler, Aydın, Turkey

Elizabeth Tyler-Kabara, MD, PhD Department of Neurological Surgery, Department of Bioengineering, Department of Physical Medicine and Rehabilitation, Neural Enhancement Laboratory, University of Pittsburgh School of Medicine, McGowan Institute for Regenerative Medicine, UPMC Children's Hospital of Pittsburgh, Pittsburgh, PA, USA

E. Haley Vance, DNP, APN, CPNP-AC Department of Pediatric Neurosurgery, Vanderbilt University Medical Center, Vanderbilt Children's Neurosurgery, Nashville, TN, USA

Kyu-Chang Wang, MD, PhD Division of Pediatric Neurosurgery, Neural Development and Anomaly Laboratory (NDAL), Department of Anatomy

and Cell Biology, Seoul National University College of Medicine, Seoul National University Children's Hospital, Seoul, South Korea

John C. Wellons III, MD, MSPH Department of Neurological Surgery, Division of Pediatric Neurosurgery, Monroe Carell Jr Children's Hospital at Vanderbilt/Vanderbilt University, Nashville, TN, USA

Seher Yilmaz, PhD Department of Anatomy, Bozok University School of Medicine, Yozgat, Turkey

Kathrin Zimmerman, BA Department of Neurosurgery, Division of Pediatric Neurosurgery, University of Alabama at Birmingham, Birmingham, AL, USA

Part I

History and Classifications

1 A History of the Chiari Malformations

R. Shane Tubbs, Mehmet Turgut, and W. Jerry Oakes

Early Descriptions of Hindbrain Herniation

Although a thorough study of hindbrain herniations associated with spina bifida aperta would not take place until the late nineteenth century, rare reports are found in earlier literature. For example, in *Observationes Medicae*, published in 1641, the famous Dutch physician and anatomist Nicolaes Tulp (1593–1674) (Fig. 1.1) described a myelodysplastic individual and may have referred to hindbrain herniation [1, 2].

In 1829, the French pathologist and anatomist Jean Cruveilhier (1791–1874) (Fig. 1.2) of Paris also described a patient born with myelomeningocele in whom "…the considerably dilated cervical region contained both the medulla oblongata and the corresponding part of the cerebellum, which was elongated and covered the fourth ventricle, itself enlarged and elongated" [3]. What was described by Cruveilhier is now called the Chiari type II malformation. However, Cruveilhier's observation of the malformation occurred

Fig. 1.1 Nicolaes Tulp

R. S. Tubbs (✉)
Department of Neurosurgery, Tulane University School of Medicine, New Orleans, LA, USA

Department of Neurosurgery and Ochsner Neuroscience Institute, Ochsner Health System, New Orleans, LA, USA

M. Turgut
Department of Neurosurgery, Aydın Adnan Menderes University School of Medicine, Efeler, Aydın, Turkey

W. J. Oakes
Departments of Neurosurgery and Pediatrics, University of Alabama, Birmingham, AL, USA

R. S. Tubbs et al. (eds.), *The Chiari Malformations*, https://doi.org/10.1007/978-3-030-44862-2_1

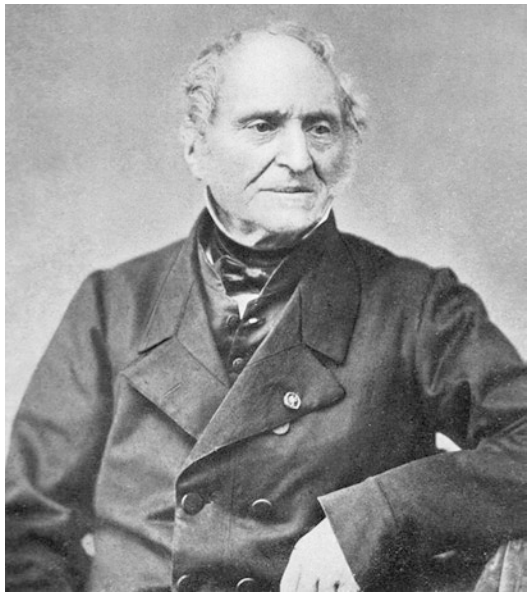

Fig. 1.2 Jean Cruveilhier

55 years before it was definitively described by Arnold and Chiari. In fact, some have used the term "Cruveilhier-Cleland-Chiari malformation" to describe this subset of patients with hindbrain herniation [3]. John Cleland published on spina bifida in 1883 [4]. The patient described by Cruveilhier was a child with a myelomeningocele who succumbed from sepsis secondary to meningitis [3]. His description on autopsy revealed bony anomalies of spina bifida with the associated split cord malformation as well as the variations in the posterior cranial fossa and cerebellum that are now known as a Chiari type II malformation. Two other cases with similar findings were noted by Cruveilhier, leading him to conclude that spina bifida occurred secondarily to a developmental abnormality. Further observations by Cruveilhier revealed clinical cases that involved a sac covering the myelomeningocele. There were no dangerous findings associated with the child until the sac was opened. When the sac was punctured, the child would end up with one or more of the following symptoms: fever, convulsions, infections, paraplegia, sepsis, and seizures, with death usually occurring in several hours to days.

Probably the first description of hindbrain herniation in the absence of myelodysplasia and what would become known as Chiari I malformation was described by Theodor Langhans (Fig. 1.3) as "pyramidal tumors." Langhans was born September 28, 1839, in Usingen (Nassau), Germany, and studied under Henle in Göttingen and von Recklinghausen in Berlin [5]. He was also a student under such names as Virchow (Fig. 1.4), Trauber, and Frerichs [6]. He served as assistant to von Recklinghausen until 1867 [6]. He was later made *professor ordinarius* in Giessen and then moved to Switzerland in 1872 where he was appointed Professor and Chair of Pathological Anatomy in Bern succeeding Klebs. Langhans with the physician Sahli and the surgeon Kocher formed a triumvirate, which made the medical school at Bern famous [7].

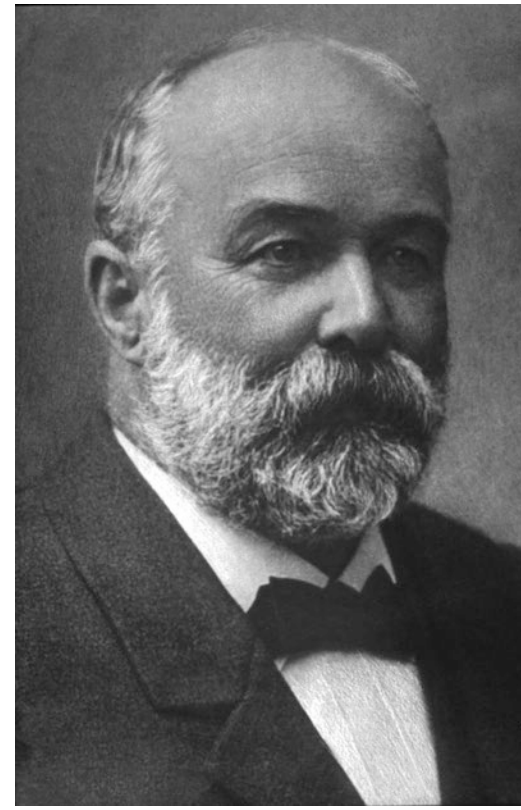

Fig. 1.3 Theodor Langhans

In his 1881 publication *Über Höhlenbildung im Rückenmark in Folge Blutstauung* (*Regarding Cavity Creation in the Spinal Cord as a Consequence of Obstruction to Blood Flow*), Langhans made many observations and hypotheses that were far ahead of his time [8]. For example, he speculated that pathology at the foramen magnum resulted in syrinx formation

Fig. 1.4 Rudolph Virchow

[9]. The following is a translation of excerpts of Langhan's publication *Über Höhlenbildung im Rückenmark in Folge Blutstauung* [8]:

> In the case, which first brought to my attention the necessity to look for cavity formation in the spinal cord following a change in the cerebellar cavity, I could not find a cause for the increase in pressure; but great pressure on the pons and medulla oblongata from above was indeed apparent. Upon dissection of the cerebellum, nothing was of note except for an obvious/significant development of both tonsils, which protruded down in the form of two symmetrical pyramidal tumors and pushed the medulla oblongata in a frontal direction at almost a right angle.
>
> The formation of the cavities, according to my observations, was connected to other changes in the central nervous system, more specifically to changes in the cerebellar cavity, which must have impeded the circulation to a great extent. The increase in pressure in the cerebellar cavity will hinder or greatly impede the outflow of blood and cerebral spinal fluid.
>
> In all cases, the ventral part of the spinal cord is affected and if at all, only a small portion of the dorsal part. The cavities do not start in the medulla oblongata at the calamus scriptorius or in the upper 1–2 cm of the spinal cord.
>
> The direction in which the central canal extends is constant – to the side and posteriorly. In my opinion, the decisive factor for this is the consistency of the white matter. The cavity creation starts there where the increased pressure, which exists in the cerebellar cavity stops and, therefore, a diverticulum can only occur toward the area of less pressure.
>
> According to my theory, a diverticulum is more likely to occur than a widening of the central canal, because the development of the diverticulum in the dorsal part meets less resistance than a central expansion. [8]

These descriptions are striking for several reasons including Langhans first describing pathologic tonsillar ectopia and hypothesizing that this obstruction at the foramen magnum results in development of syringomyelia. Additionally, the fact that syringomyelia normally does not include the first segment of the cervical cord was clearly recognized by Langhans [8]. Lastly, Langhans realized that fluid accumulation within the spinal cord could occur via dilation of the central canal or outside of this region.

Hans Chiari will most be remembered for his 1891 paper *Ueber Veränderungen des Kleinhirns infolge von Hydrocephalie des Grosshirns* (*Concerning Changes in the Cerebellum due to Hydrocephalus of the Cerebrum*) that described what is now regarded as the Chiari malformations [10–13]. Chiari (Fig. 1.5a) was born on November 4, 1851, in Vienna. Chiari came from a family of physicians, and his father, Johann Baptist Chiari (1817–1854), is credited with describing prolactinomas [10]. Chiari studied medicine in Vienna, assisting one of the most revered pathologists at the time, Karl Rokitansky (1804–1878), at the Vienna Institute of Pathology. Chiari was hired as a prosector at the Vienna Institute, which was renowned for its knowledge and research under the control of Rokitansky. In 1875, Chiari completed medical school and Rokitansky retired. Richard Ladislaus Heschl (1824–1881) succeeded Rokitansky as head of Pathological Anatomy in Vienna, and Chiari assisted him until Heschl's death in 1881. In 1878, Chiari habilitated in pathological anatomy in Vienna, and 4 years later, he became *extraordinarius* at the German University in Prague. One year later, he was appointed *ordinarius* and superintendent of the pathological-anatomical museum in Prague [10].

Most of Chiari's accomplishments occurred while he was in Prague. For example, in 1877,

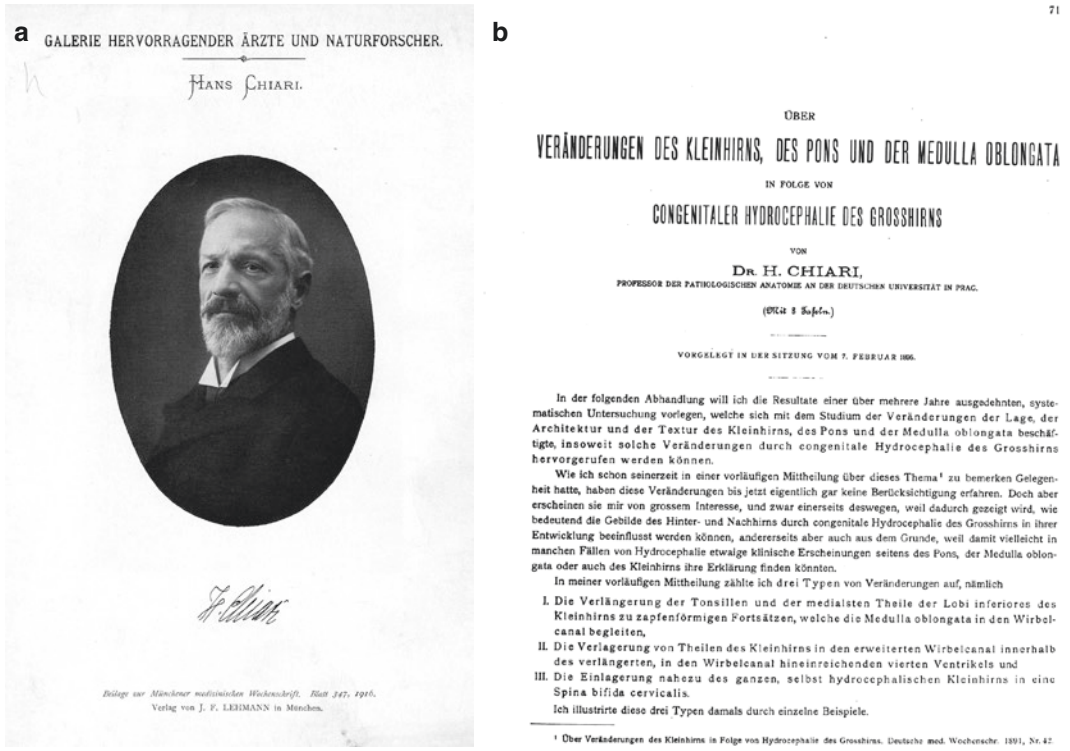

Fig. 1.5 (**a**) Hans Chiari. (**b**) First page of Chiari's seminal 1891 publication

Chiari was noted as the first to describe the features of a choriocarcinoma [10]. In 1899 and in conjunction with British internist George Budd (1808–1882), Chiari provided a clinical and pathological explanation of hepatic vein thrombosis—the so-called Budd-Chiari syndrome [10]. Prior to Chiari, such a syndrome had been described but never explained to any extent. Among his other accomplishments, Chiari studied the relationship between carotid artery plaques and thrombosis. Chiari's name is also attached to the symptoms associated with aortoesophageal fistula after foreign body ingestion or gunshot wound. In 1883, Chiari probably described the first and only authentic case of traumatic pneumocephaly prior to roentgenography. He demonstrated a fistulous connection between a pneumatocele in the frontal lobes and the ethmoid sinuses in a patient who died of meningitis following rhinorrhea and thus first indicated a mechanism to explain meningitis in this context. Interestingly, Chiari implicated sneezing as a precipitating factor for this pathogenesis. Chiari also made significant contributions with his observations of pituitary adenomas and, in 1912, developed a novel transnasal approach to lesions of the pituitary gland [14]. Of note, Schloffer, who first performed a transsphenoidal pituitary operation in Innsbruck, Austria, examined pituitary adenomas from specimens that he obtained from Chiari in Prague.

In 1888, Chiari observed that syrinxes usually communicate with the central canal of the spinal cord. It was in 1891 in the journal *Deutsche Medizinische Wochenscriff* [11] and later in 1896 (*Über Veränderungen des Kleinhirns, des Pons und der Medulla oblongata in Folge von congenitaler Hydrocephalie des Großhirns* (*Changes in the Cerebellum, Pons, and Medulla Oblongata due to Congenital Hydrocephalus of the Cerebrum*)) [12] (Fig. 1.5b) that Chiari first published his works regarding hindbrain malformations (Fig. 1.6a–h). Chiari's type I malformation was first described by him in a 17-year-old woman who died of typhoid fever

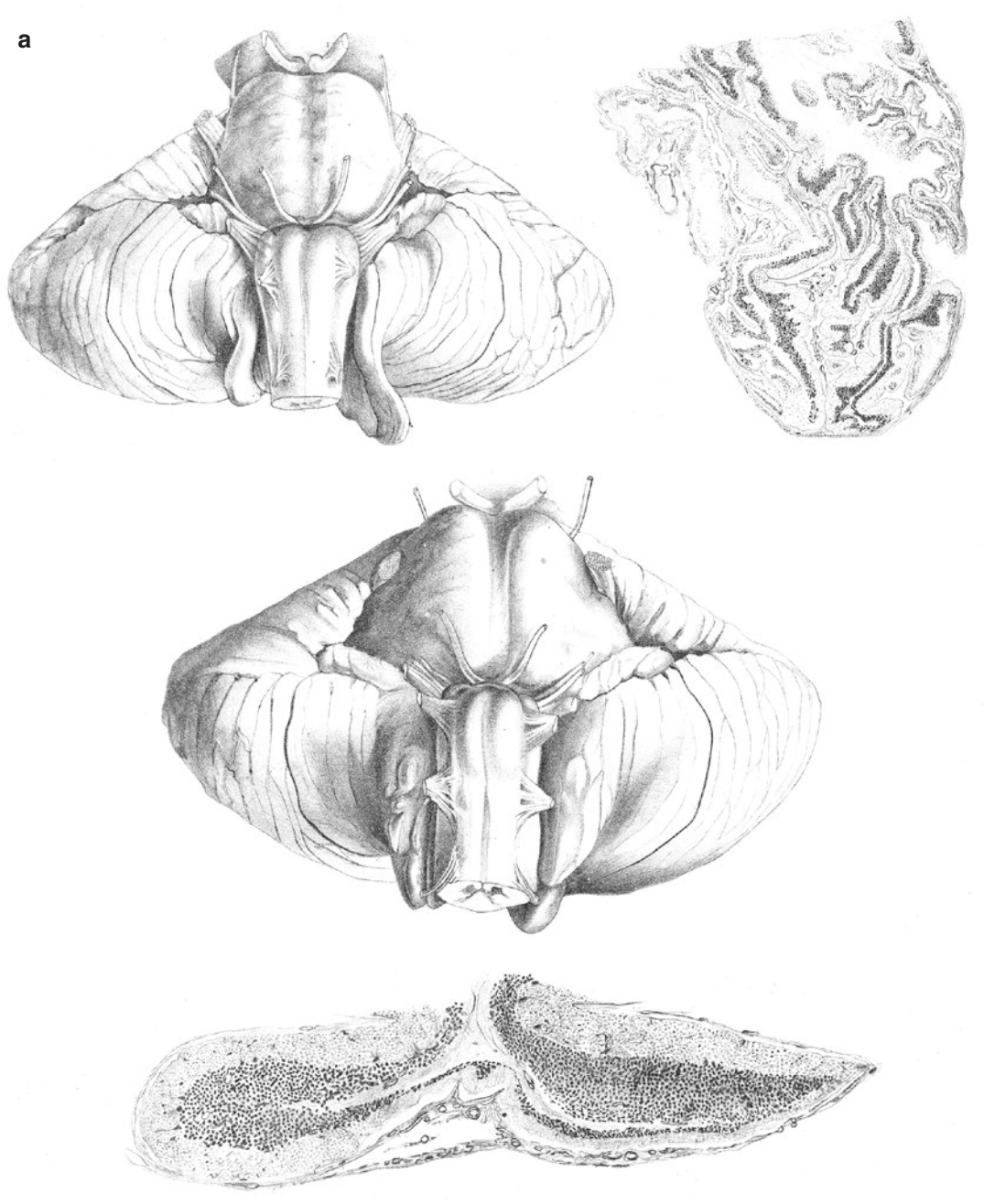

Fig. 1.6 (**a–h**) Drawings from Chiari's descriptions of the hindbrain hernias noting the findings at autopsy that would propagate in what are known today as the "Chiari malformations"

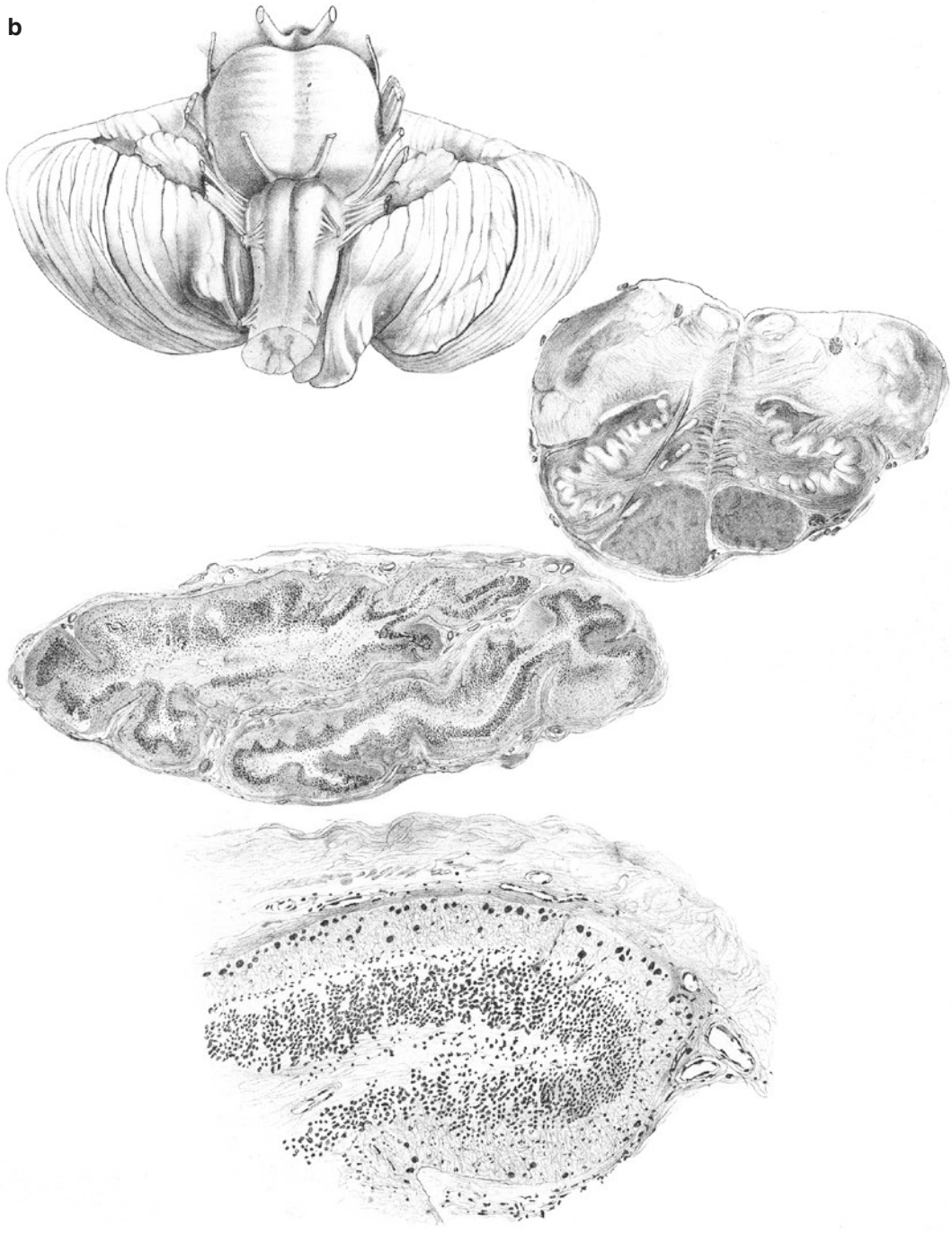

Fig. 1.6 (continued)

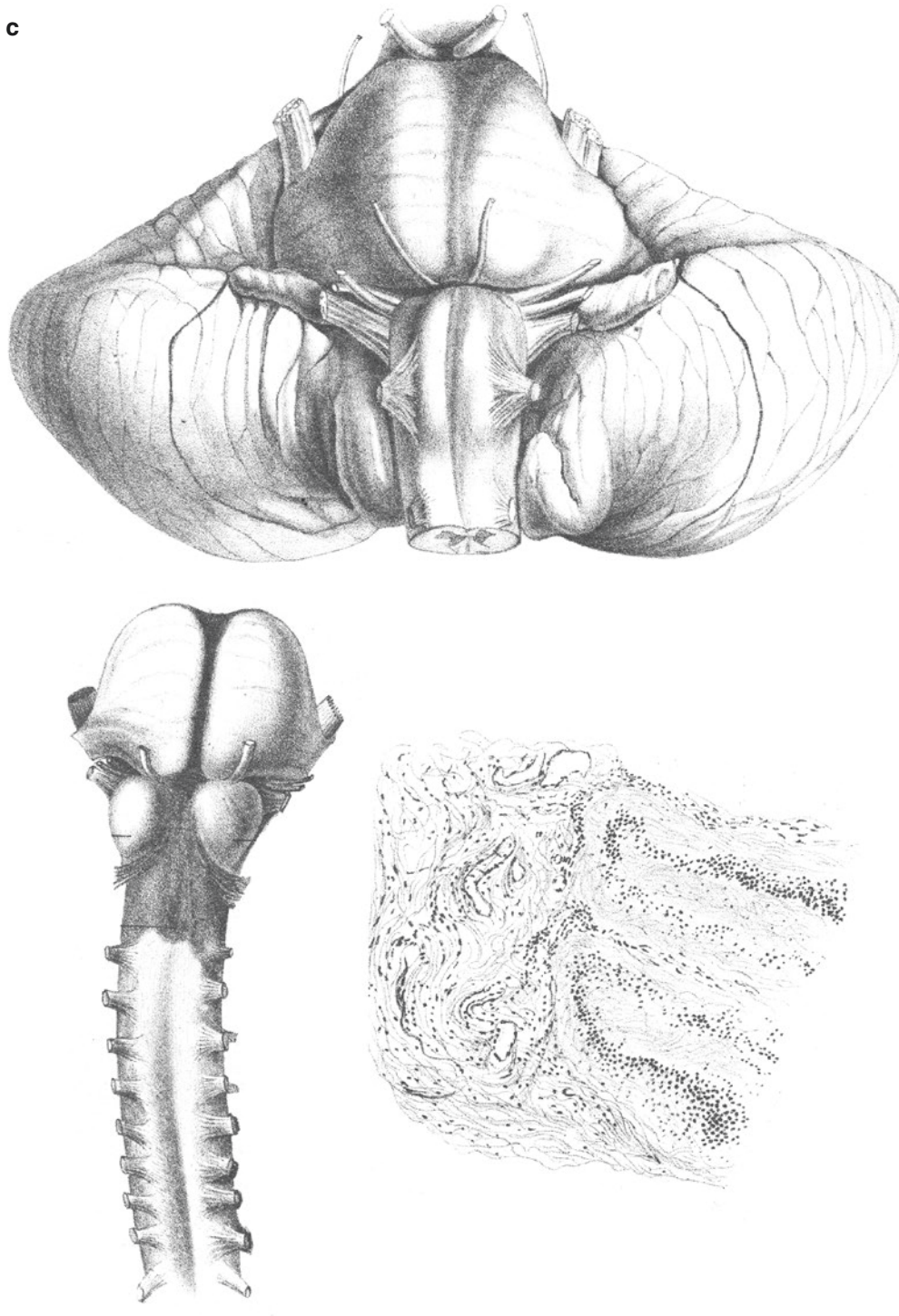

Fig. 1.6 (continued)

Fig. 1.6 (continued)

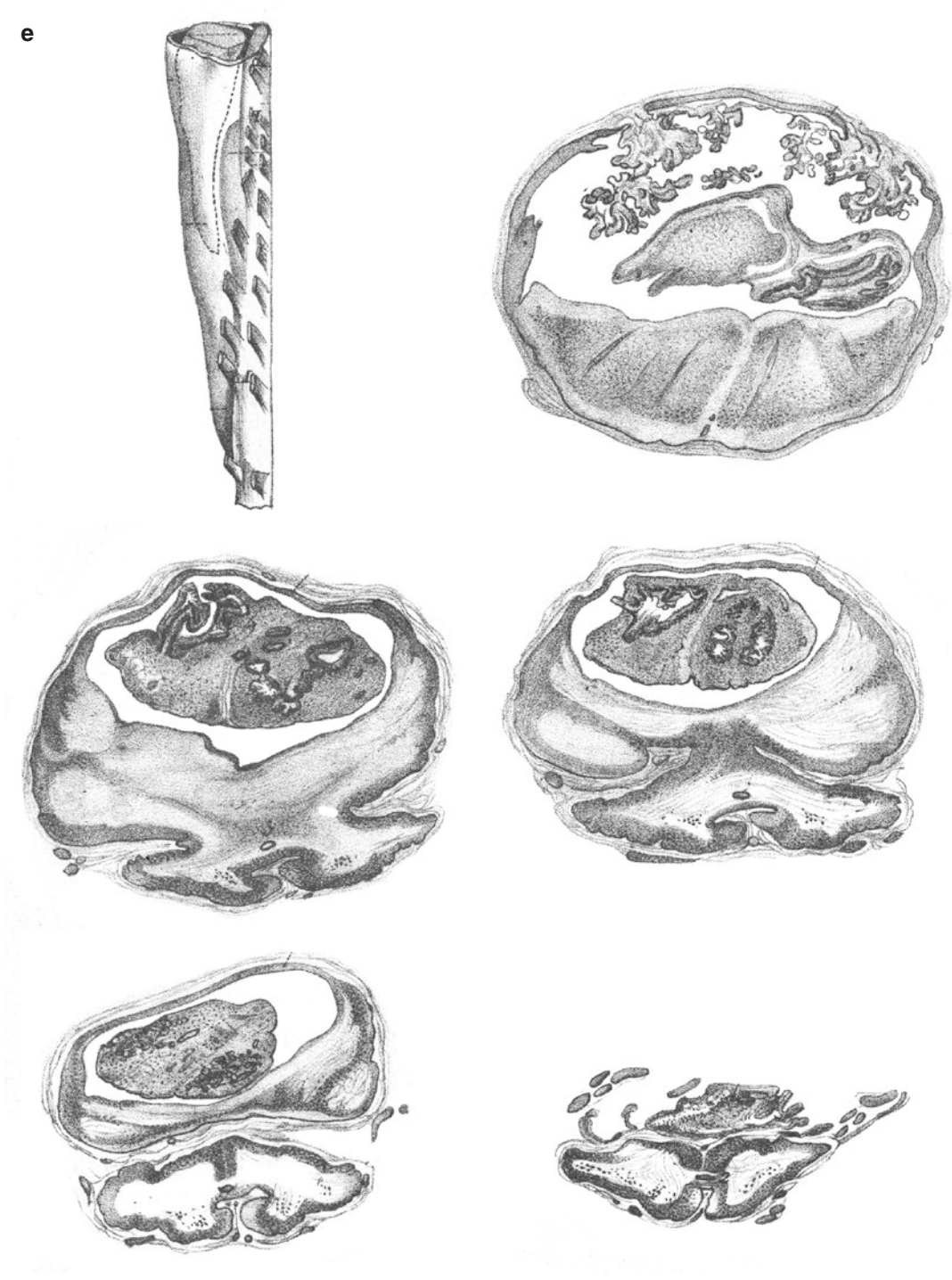

Fig. 1.6 (continued)

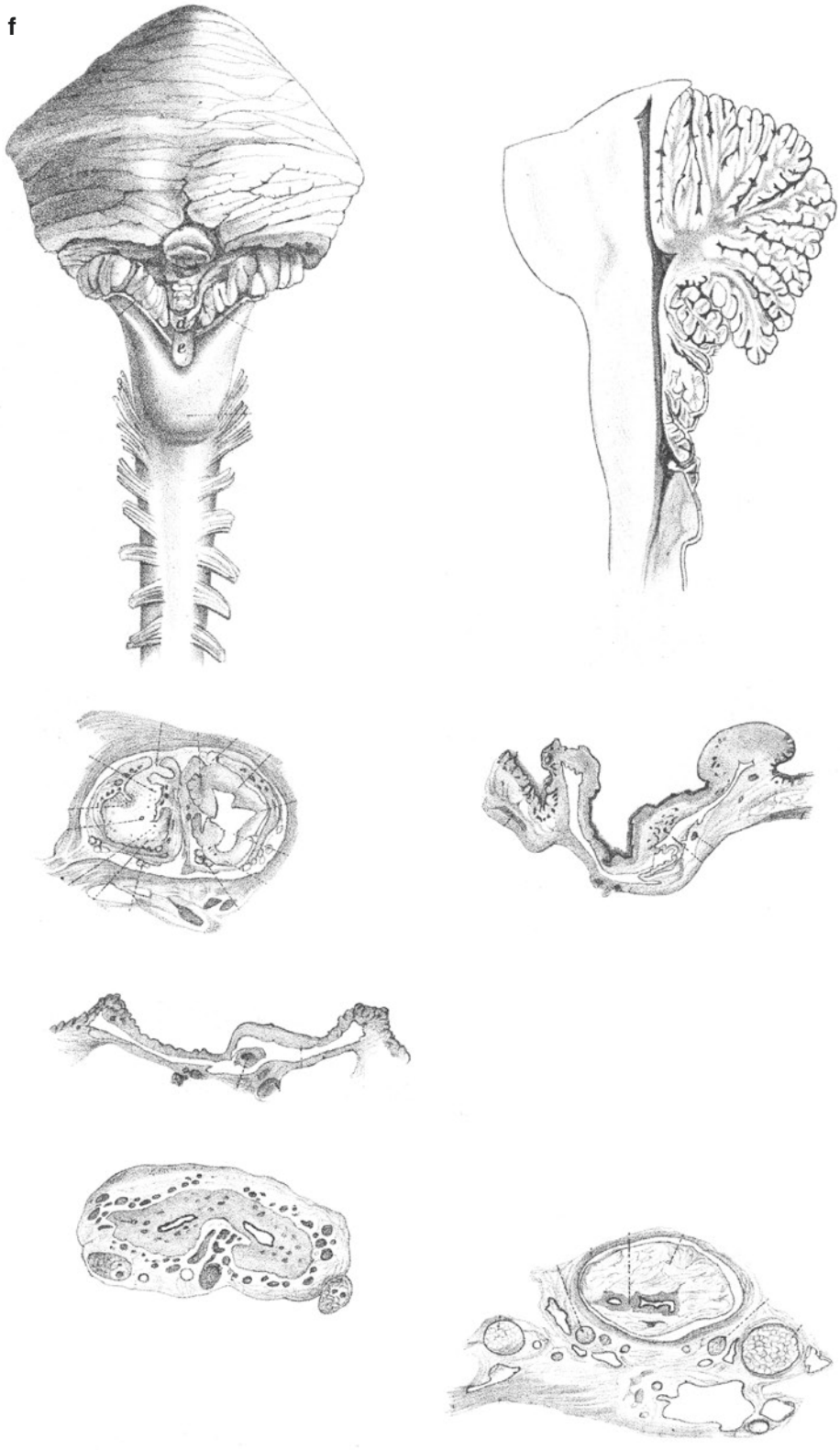

Fig. 1.6 (continued)

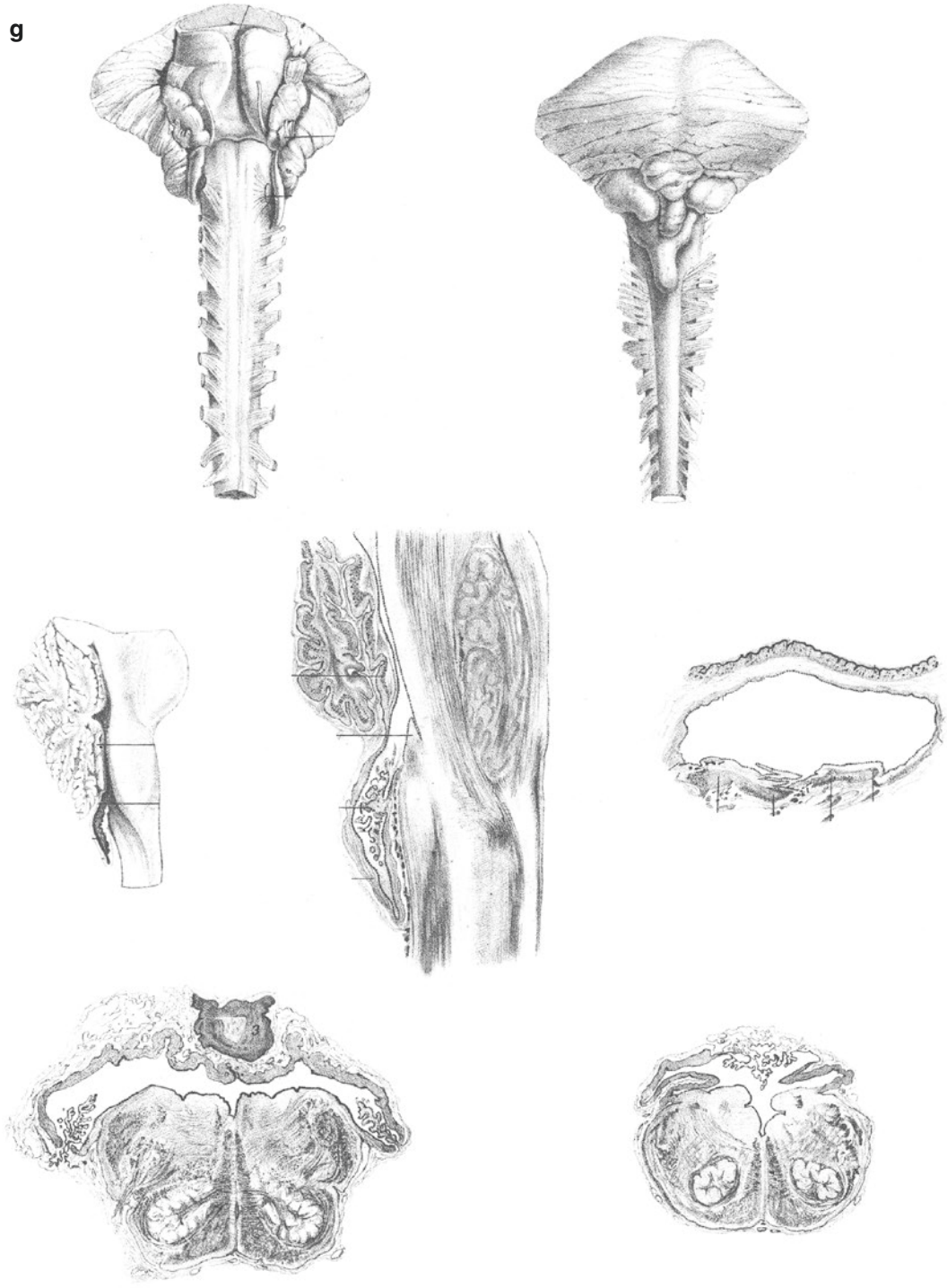

Fig. 1.6 (continued)

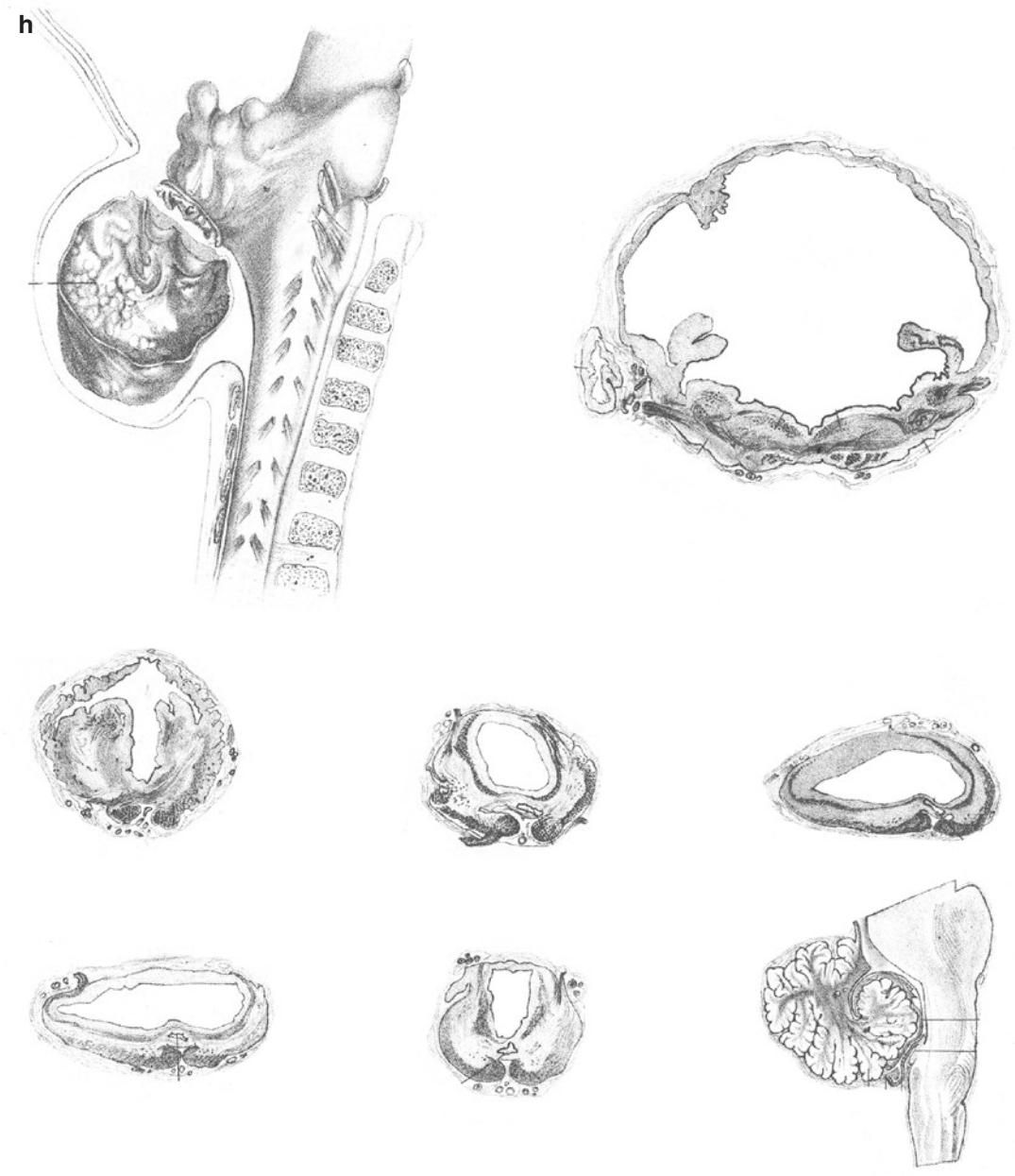

Fig. 1.6 (continued)

and suffered from hydrocephalus but had "no symptoms referable to the cerebellum or medulla." Her malformation was described as a "peg-like elongation of tonsils and medial divisions of the inferior lobes of the cerebellum into cone shaped projections which accompany the medulla oblongata into the spinal canal" while sparing the medulla [15]. For the "Chiari" malformations in general, Chiari made the following comments based on his work:

> In this paper, I will be discussing the results of my extensive and systematic research, which lasted several years on alterations to the architecture and texture of the cerebellum, the pons and the

> medulla oblongata to the extent that such changes may be secondary to congenital hydrocephalus of the cerebrum.
>
> As I have mentioned in my preliminary memorandum on this topic [11], such changes received little attention in the past. However, they are of great interest to me, because they show how significantly the developmental formation of the hind- and afterbrain is influenced by congenital hydrocephalus of the cerebrum, and because this may, in some cases of hydrocephalus, explain possible clinical expressions concerning the pons, medulla oblongata and/or cerebellum. I listed three types of changes in my preliminary memorandum, namely:
>
> I. Elongation of the tonsils and medial divisions of the inferior lobes of the cerebellum into cone-shaped processes which accompany the medulla oblongata into the upper spinal canal;
> II. Elongation of divisions of the cerebellum into the enlarged spinal canal within the elongated fourth ventricle which extends into the spinal canal; and
> III. Herniation of almost the entire hydrocephalic cerebellum into a cervical spina bifida.
>
> Previously, I illustrated these three types by giving specific examples of each. It is my intention to bring the entire research material concerning this topic, which I gathered over a four-year period from 1889 to 1892 (based on dissection of 4,276 bodies and a total of 63 cases of congenital hydrocephalus), to the reader's attention. I will be discussing the previously mentioned three types in detail as well as an additional type: Type IV, namely cerebellar hypoplasia without herniation of the cerebellum into the spinal column. [12]

In 1891, the German Otto Mennicke reported two autopsy specimens, both with syringomyelia, and one of whom was found to have an associated cerebellar tonsillar ectopia [16]. Mennicke reported on one case of severe syringomyelia of the cervical and upper thoracic spinal cord including secondary degeneration of the spinal cord and inferior beak-shaped elongation of the tonsils in a 29-year-old woman. The hemispheres of the cerebrum were noted to be normal. The following are translations of excerpts from Mennicke's dissertation *Ueber Höhlenbildung im Rückenmark* and specifically of portions of the document that discuss his observations of tonsillar ectopia from his second case:

> This case is about a severe destruction of the medulla oblongata, especially in the area of the decussation of the pyramids and the upper part of the cervical spinal cord and a strong squeezing of the cerebellar tonsils downwards apparently causing pressure on the medulla oblongata. The cause of these changes is not completely defined, but is probably due to a dislocation of the bony parts in the area of the foramen magnum. As a consequence, we find extensive degeneration of primarily the posterior funiculus as well as the gray matter at the bottom of the rhomboid fossa and the pyramid, which is extremely flattened from the front to the back parts of the medulla. [16]

In 1894, Julius Arnold (1835–1915) described a single myelodysplastic infant without hydrocephalus, whereby the fourth ventricle and cerebellum herniated through the foramen magnum while sparing the medulla [17]. Arnold studied under Rudolf Virchow (1821–1902) (Fig. 1.4) and Nikolaus Friedreich (1825–1882) in Heidelberg, later becoming Professor of Anatomy [10]. Chiari's type II malformation was similar to Arnold's case and was described as a "displacement of parts of the cerebellum and elongated fourth ventricle, which reach into the cervical canal" [3]. Chiari later refined his description of type II malformations to include greater hindbrain involvement, as a "displacement of part of the lower vermis, displacement of the pons and displacement of the medulla oblongata into the cervical canal and elongation of the fourth ventricle into the cervical canal" [3]. In 1907, the Chiari type II malformation was renamed the Arnold-Chiari malformation by Schwalbe and Gredig while working in Arnold's laboratory [18]. Although little attention was given to the posterior fossa abnormalities in this report, Arnold's students seized this opportunity to immortalize their professor by affixing the moniker "Arnold-Chiari malformation" to this condition [19, 20]. In the end, however, it was the significant contributions of Chiari that shed the most light on these forms of hindbrain herniation; thus, now referring to them as Chiari malformations is appropriate.

Chiari type II malformation was described earlier by the Scottish physician John Cleland in 1883 [4] who called it the "basilar impression syndrome." Cleland noticed the malformation from autopsies and described it as the "inferior vermiform process, which extends

up so far that what appears to be the pyramid touches the corpora quadrigemini, while the uvula looks backward and the laminated tubercle hang down from an exaggerated velum posticum, as an appendix three fourths of an inch in length, lying in the fourth ventricle" [4, 21]. Cleland argued that the malformation resulted from primary dysgenesis of the brain stem and that "hydrocephalus was obviously of much later origin, when the different parts of the brains were already formed" [4]. Though it preceded Chiari's, Cleland's work had little impact on the scientific community's attempt at better understanding these malformations of the hindbrain [2, 22]. Chiari believed these malformations were due to hydrocephalus [11]. Chiari described one example of the most severe malformation of the hindbrain observed by him, type III; cervical spina bifida, whereby there is a partially absent tentorium cerebelli with prolapse of the fourth ventricle and cerebellum into the cervical canal, associated with a hydromyelic cavity communicating with the fourth ventricle [12]. The salient findings of Chiari's type IV malformation include an occipital encephalocele containing occipital lobe, hydrocephalus, cerebellar hypoplasia, and a small posterior fossa [23]. In 1896, Chiari described an additional 63 cases of congenital hydrocephalus with an associated type I malformation in 14/63 and a type II malformation in 7/63 [12, 24].

In 1906 and as a result of tensions within the Habsburg Empire, Chiari left Prague (as head of the university and *professor extraordinarius* and superintendent of the Prague pathological-anatomical museum) to travel to the University in Strasbourg, France, where he was appointed *ordinarius* of pathological anatomy. On May 6, 1916, after an accomplished career, Hans Chiari passed away due to a throat infection. This prolific writer published approximately 180 papers between the years 1876 and 1916 and was always very careful to give credit to the discoveries of others [25].

Many years later, in 1935, Russell and Donald [26], at the London Hospital, described ten additional pathological specimens of hindbrain herniation.

Surgical History of the Chiari Malformations

Although many have attributed the first successful patient series to James Gardner (see below) in the 1950s, earlier attempts at surgical decompression were attempted [27, 28]. In the late 1930s, Wilder Penfield in Montreal commented "the anomaly [Chiari malformation] may present itself as an unexpected clinical problem to be dealt with by the neurosurgeon." In 1938, Penfield and Coburn [29] reported a 29-year-old woman with loss of hearing and weakness on the right side of the face. Her history included removal of a thoracic "spina bifida" in infancy. On physical examination, she was noted to have nystagmus, absence of the right corneal reflex, truncal ataxia, and decreased peripheral reflexes. The patient underwent posterior cranial fossa exploration with the authors not considering hindbrain herniation in their differential. Later, they stated:

> In retrospect it seems that we should have suspected the Arnold-Chiari malformation. Instead, a suboccipital craniotomy was carried out, with a tentative diagnosis of a tumor of the acoustic nerve bilaterally. [29]

Unfortunately, the patient of Penfield and Coburn never regained consciousness and died 2 months later. At autopsy, the authors identified a Chiari II malformation and hydrocephalus. These authors suggested that in the future, the cerebellar tonsils be left intact and that the posterior margin of the foramen magnum be removed with the posterior elements of C1 and C2 [29].

Not known to many is that 8 years prior to the publication of Penfield and Coburn, the Dutchman Cornelis Joachimus van Houweninge Graftdijk (1888–1956) (Fig. 1.7) operated a patient, in 1930, with myelomeningocele and ventriculogram-proven hindbrain herniation who had rapid head growth [30]. This contribution was published in his thesis for a Doctorate of Medicine entitled *Over Hydrocephalus* (About Hydrocephalus) (Fig. 1.7) [31]. With surgery, he attempted to relieve cerebrospinal fluid (CSF) obstruction at the craniocervical junction by redundant cerebellar tissue. Although his patient died, this report marks the first known attempt at

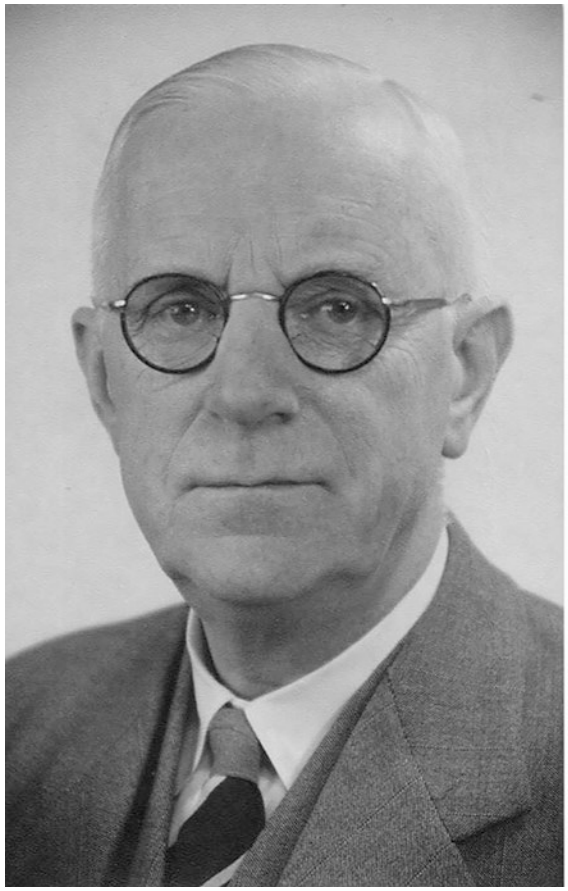

OVER HYDROCEPHALUS

PROEFSCHRIFT TER VERKRIJGING VAN DEN GRAAD VAN DOCTOR IN DE GENEESKUNDE AAN DE RIJKSUNIVERSITEIT TE LEIDEN, OP GEZAG VAN DEN RECTOR-MAGNIFICUS Dr. J. J. BLANKSMA, HOOGLEERAAR IN DE FACULTEIT DER WIS- EN NATUURKUNDE, VOOR DE FACULTEIT DER GENEESKUNDE TE VERDEDIGEN OP DINSDAG 21 JUNI 1932, DES NAMIDDAGS TE 4 UUR,

DOOR

Cornelis Joachimus van Houweninge Graftdijk

GEBOREN TE GIESSENDAM.

N. V. BOEK- EN STEENDRUKKERIJ EDUARD IJDO — LEIDEN.

Fig. 1.7 Cornelis Joachimus van Houweninge Graftdijk and cover page of his sentinel work

surgical correction of a hindbrain herniation. Van Houweninge Graftdijk said:

> I decided to try widening the space through which the brain had herniated in order to allow for better flow of CSF. [31]

The idea that displacement of the foramina of the fourth ventricle into the upper end of the spinal canal might precipitate hydrocephalus, and that the whole of the anomaly might act as a valve, was first expressed by van Houweninge Graftdijk in 1932 [31]. For this case, part of the occipital bone and posterior elements of the first two vertebrae were removed. Unfortunately, the patient developed fever on postoperative day 2, and 84 days after the operation, the bladder was perforated, so on day 98 postoperative, the patient died.

Van Houweninge Graftdijk also presented evidence that fluid could flow more readily from the spine to the head than vice versa [32]. It was in children with spina bifida that he concluded that the pressure within the meningocele was lower than the pressure within the cranium [33]. Conversely, Russell and Donald [26] commented on van Houweninge Graftdijk's theory but hypothesized that hindbrain hernias did not cause hydrocephalus in these patients. Interestingly, in 1935, these authors stated:

> If hydrocephalus, either congenital or post-operative, were due to such a malformation, then air injected by the lumbar route would collect in the ventricles and not in the sulci upon the cerebral convexities. Such a result would be not only of academic interest but of clinical importance. It would point to the desirability of decompressing the spinal cord at the foramen magnum to facilitate

> the circulation of fluid in the leptomeningeal spaces. Such an operation has not yet been carried out. [26]

However, these authors, in a footnote, stated that while their aforementioned paper was in press, their attention was drawn to the writings of van Houweninge Graftdijk. Van Houweninge Graftdijk also surmised that cerebrospinal fluid can readily escape in an upward direction from the vertebral canal into the ventricles or cerebral subarachnoid spaces but has difficulty in passing from the ventricles down into the vertebral canal. To address such issues surgically, he excised redundant cerebellar tissue and/or bone over the posterior surface of the malformation as previously mentioned [26, 31]. Van Houweninge Graftdijk also postulated that caudal traction theory by the myelomeningocele is responsible for "pulling" the hindbrain caudally, thus resulting in a Chiari II malformation [33].

Van Houweninge Graftdijk was born in Giessendam, Holland. His father was a family doctor in Giessendam, and his brother died young as the result of hydrocephalus. Although his brother and sisters were given the family surname "Graftdijk," Cornelis was given the name "van Houweninge Graftdijk" as his parents did not want this surname to die out. Cornelis graduated from the University of Leiden and became a physician in 1913 and, following the advice of his teacher Professor Korteweg, became a ship doctor so that he could gain some "practical knowledge." In 1914, he studied surgery with Professor Zaaijer for 5 years and then began his own practice in Leiden at the hospital Diaconessenhuis. He maintained his affiliation with Professor Zaaijer at the University Hospital in Leiden and, in addition to practicing general surgery, treated pediatric patients with hydrocephalus. This interest probably arose from his concern over his older brother who had hydrocephalus. Van Houweninge Graftdijk trained doctors in surgery and for many years was *Chef de Clinique* of the Department of Surgery at the University Hospital.

In the early 1930s, van Houweninge Graftdijk wrote his dissertation [31] on hydrocephalus, and on June 21, 1932, he obtained his doctor's degree cum *laude.* Soon after, Professor Zaaijer left the university and was replaced by Professor Suermondt who had no interest in hydrocephalus. It is not clear why van Houweninge Graftdijk did not succeed Prof. Zaaijer, but as a result of this, he left the University Hospital and was not able to continue working on hydrocephalus. He continued to practice at the hospital Diaconessenhuis. He became chairman of the Dutch Association of Surgery, and in 1940, he wrote the book *Heelkunde voor Den Medicus Practicus* [34], a textbook of surgery for family doctors.

In 1938, McConnell and Parker [35] published their results of posterior fossa decompression for Chiari I malformation in five patients. Two of these patients had successful outcomes. In 1945, Bucy and Lichtenstein [19] reported successful decompression for a Chiari I malformation of a 40-year-old woman without hydrocephalus, and in 1948, Chorobski and Stepien [36] operated a woman with life-altering Valsalva-induced headache and Chiari I malformation that had full resolution of her symptoms. Most remembered for his direct approach to the hindbrain was James Gardner (Fig. 1.8) from the Cleveland Clinic. In 1957, he and Goodall [27] reported their efforts at surgically addressing syringomyelia by decompressing the hindbrain and sealing off the hypothetical communication between the syrinx and fourth ventricle in 17 patients. They reported improvement in 13, decline in 3, and death in 1. In their series, some patients had improvement of preoperative symptoms. The publication of Gardner and Goodall appears to have resulted in the widespread adoption of posterior fossa decompression for hindbrain herniation with larger reports following over the next few decades [2, 15, 23, 24, 37, 38]. It was Gardner in the 1950s who showed in a large series of patients that decompression of the hindbrain herniation in patients with syringomyelia often improved symptoms in patients. This report led to widespread adoption of this method of treatment. In fact, a Pub Med search of the terms Chiari malformation and surgery yielded roughly 2000 publications between 1950 and 2019. More recently, W. Jerry Oakes (Fig. 1.9) has contributed to our understanding of the Chiari malformations and

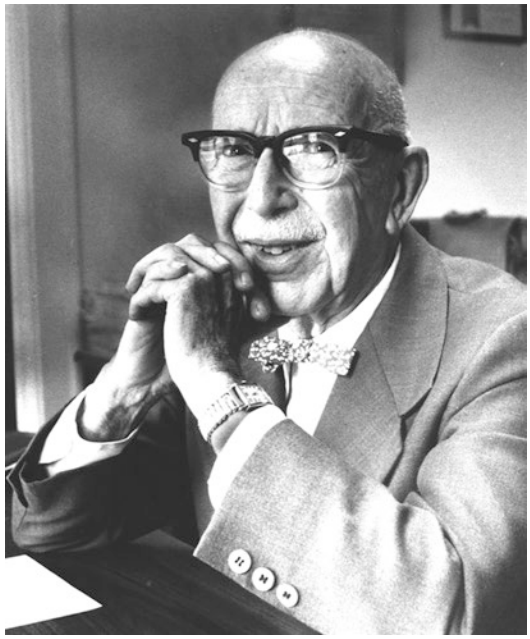

Fig. 1.8 James Gardner

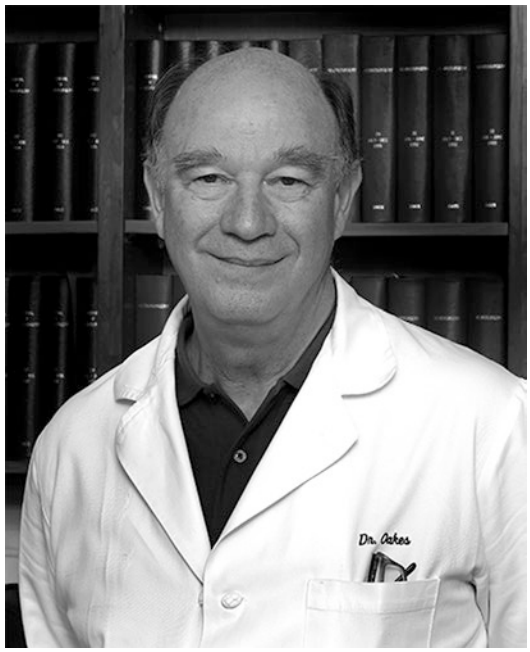

Fig. 1.9 W. Jerry Oakes

coined such terms as the Chiari 0 and 1.5 malformations. He has written more than 100 papers and chapters dedicated to this topic.

The evolution of surgery for hindbrain herniation is indebted to pioneers such as those described herein. Our current understanding and treatment of these embryological derailments are based on years of observation and surgical trial and error.

References

1. Tulp N. Observationes medicae. Amsterdam: Lodewijk Elzevir; 1641.
2. List CF. Neurologic syndromes accompanying developmental anomalies of occipital bone, atlas and axis. Arch Neurol Psychiatr. 1941;45:577–616.
3. Pearce JMS. Arnold Chiari, or "Cruveilhier Cleland Chiari" malformation. J Neurol Neurosurg Psychiatry. 2000;68:13.
4. Cleland J. Contribution to the study of spina bifida, encephalocele, and anencephalus. J Anat Physiol (London). 1883;17:257–91.
5. Holubar K. Dermatopathology in historical perspective. Am J Dermatopathol. 1990;12:534–5.
6. Pritchard J, Foley P, Wong H. Langerhans and Langhans: what's misleading in a name? Lancet. 2003;362:922.
7. Ashwal S. Founders of child neurology. San Francisco: Norman Publishing; 1990. p. 190.
8. Langhans T. Über Höhlenbildung im Rückenmark in Folge Blutstauung. Arch Pathol Anat Physiol. 1881;85:1–25.
9. Theodor Langhans (1839–1915). Nature. 1939;144:546.
10. Greenblatt SH. A history of neurosurgery in its scientific and professional contexts. Park Ridge: American Association of Neurological Surgeons; 1997.
11. Chiari H. Ueber Veränderungen des Kleinhirns infolge von Hydrocephalie des Grosshirns. Dtsch Med Wochenschr. 1891;17:1172–5.
12. Chiari H. Ueber Veranderungen des Kleinhirns, des Pons und der Medulla oblongata Infolge von congenitaler Hydrocephalie des Grosshirns. Denkschriften Kais Akad Wiss Math-Naturw. 1896;63:71–116.
13. Koehler PJ. Chiari's description of cerebellar ectopy (1891) with a summary of Cleland's and Arnold's contributions and some early observation on neural-tube defects. J Neurosurg. 1991;75:823–6.
14. de Lotbinière ACJ. Historical considerations. In: Anson JA, Benzel EC, Awad IA, editors. Syringomyelia and the Chiari malformations. Park Ridge: American Association of Neurological Surgeons; 1997. p. 1–26.
15. D'errico A. The surgical treatment of hydrocephalus associated with spina bifida. Yale J Biol Med. 1939;11:425–30.
16. Mennicke O. Ueber Syringomyelie mit anatomischer Untersuchung zweier Fälle. Inaugural-Dissertation zur Erlangung der medicinischen Doktorwürde

der hohen medicinischen Fakultät der Universität Marburg. 1891.
17. Steele GH. The Arnold-Chiari malformation. Br J Surg. 1947;34:280–2.
18. Koehler PJ. Chiari's description of cerebellar ectopy (1891). With a summary of Cleland and Arnold's contributions and some early observations on neural tube defects. J Neurosurg. 1991;75:823–6.
19. Bucy PC, Lichtenstein BW. Arnold-Chiari deformity in an adult without obvious cause. J Neurosurg. 1945;2:245–50.
20. Carmel PW, Markesbery WR. Early descriptions of the Arnold-Chiari malformation; the contribution of John Cleland. J Neurosurg. 1972;37:543–7.
21. Pearce JMS. Fragments of neurological history. London: Imperial College Press; 2003. p. 395–8.
22. Tubbs RS, Pugh J, Oakes WJ. The Chiari malformations. In: Winn R, editor. Youman's neurological surgery. 5th ed. Philadelphia: Elsevier; 2004.
23. Ogryzlo MA. The Arnold-Chiari malformation. Arch Neurol Psychiatr. 1942;48:30–46.
24. Paul KS, Lye RH, Strang FA, Dutton J. Arnold-Chiari malformation. J Neurosurg. 1983;58:183–7.
25. Tubbs RS, Cohen-Gadol AA. Hans Chiari (1851–1916). J Neurol. 2010;257:1218–20.
26. Russell DS, Donald C. The mechanism of internal hydrocephalus in spina bifida. Brain. 1935;58:203–15.
27. Gardner WJ, Goodall RJ. The surgical treatment of Arnold-Chiari malformation in adults: an explanation of its mechanism and importance of encephalography in diagnosis. J Neurosurg. 1950;7:199–206.
28. Tubbs RS, Oakes WJ. Chiari malformations. In: Winn HR, editor. Youmans neurological surgery. 5th ed. Philadelphia: Saunders; 2004. p. 3347–61.
29. Penfield W, Coburn DF. Arnold-Chiari malformation and its operative treatment. Arch Neurol Psychiatr. 1938;40:328–36.
30. Bejjani GK. Definition of the adult Chiari malformation: a brief historical overview. Neurosurg Focus. 2001;11:1–8.
31. van Houweninge Graftdijk CJ. Over hydrocephalus. Leiden: Eduard Ijdo; 1932.
32. Williams B. Further thoughts on the valvular action of the Arnold-Chiari malformation. Dev Med Child Neurol. 1971;13:105–12.
33. Williams B. Cerebrospinal fluid pressure-gradients in spina bifida cystic, with special reference to the Arnold-Chiari malformation and aqueductal stenosis. Dev Med Child Neurol. 1975;17:138–50.
34. van Houweninge Graftdijk CJ. Heelkunde voor Den Medicus Practicus. Leiden: HE Stenfert's Kroese; 1940.
35. McConnell AA, Parker HL. A deformity of the hindbrain associated with internal hydrocephalus. Its relation to the Arnold-Chiari malformation. Brain. 1938;61:415–29.
36. Chorobski J, Stepien L. On the syndrome of Arnold-Chiari. Report of a case. J Neurosurg. 1948;5:495–500.
37. Adams RD, Schatzki R, Scoville WB. The Arnold-Chiari malformation. Diagnosis, demonstration by intraspinal Lipiodol and successful surgical treatment. N Engl J Med. 1941;225:125–31.
38. Saez R, Onofrio BM, Yanagihara T. Experience with Arnold-Chiari malformation, 1960–1970. J Neurosurg. 1976;45:416–22.

2 Defining the Chiari Malformations: Past and Newer Classifications

R. Shane Tubbs and Mehmet Turgut

Introduction

Hans Chiari (1851–1916) gave the first detailed illustrations of what is now termed the Chiari malformations. In 1891, he described several congenital anomalies affecting the cerebellum due to hydrocephalus, and this paper listed three different types of abnormalities [1]. Four years later, in 1895, Chiari wrote a second paper that described the type IV malformation in two patients [2]. Traditionally, these embryological derailments have been classified as Chiari I, II, III, and IV malformations. However, some malformations do not fit neatly into any of these four categories as many of these differ anatomically or symptomatically. Chiari's original system recognized these malformations as specific, individual conditions. His nomenclature does not refer to tonsillar variations on a continuous spectrum [3]. As a result, additional subclassifications have been established [4, 5]. Currently, the following eight classifications have been used: Chiari 0, Chiari I, Chiari 1.5, Chiari II, Chiari III, Chiari 3.5, Chiari IV, and Chiari V malformations.

According to Chiari's classification, malformations are grouped as discrete categories. Type I (Fig. 2.1) consists of a herniation of the cerebellar tonsil that extends inferiorly to the foramen magnum. However, in light of more recent advancements in clinical medicine, Chiari 0 (Figs. 2.2 and 2.3) and 1.5 malformations (Fig. 2.4) have been recognized as variations of the Chiari I malformation. Chiari 0 malformations are considered borderline defects in which a syringohydromyelia responds to decompression of the posterior cranial fossa, although there is little to no cerebellar tonsillar herniation (<3 mm). Chiari 1.5 malformations are more severe forms of Chiari I malformation in that more brain tissue crowds the foramen magnum. While symptoms and anatomical considerations are quite similar, treatment outcomes differ between Chiari I and 1.5 malformations. As a result, a thorough understanding of a newer classification system is crucial for the proper recognition and treatment of individuals with Chiari malformations that do not fit into traditional subtypes. The following is a description of the original malformations described by Chiari and the newer subsets.

Chiari I Malformation

Chiari's description of the Chiari malformation type I (CM I) herniation was of cerebellar tonsils

R. S. Tubbs (✉)
Department of Neurosurgery, Tulane University School of Medicine, New Orleans, LA, USA

Department of Neurosurgery and Ochsner Neuroscience Institute, Ochsner Health System, New Orleans, LA, USA

M. Turgut
Department of Neurosurgery, Aydın Adnan Menderes University School of Medicine, Efeler, Aydın, Turkey

R. S. Tubbs et al. (eds.), *The Chiari Malformations*, https://doi.org/10.1007/978-3-030-44862-2_2

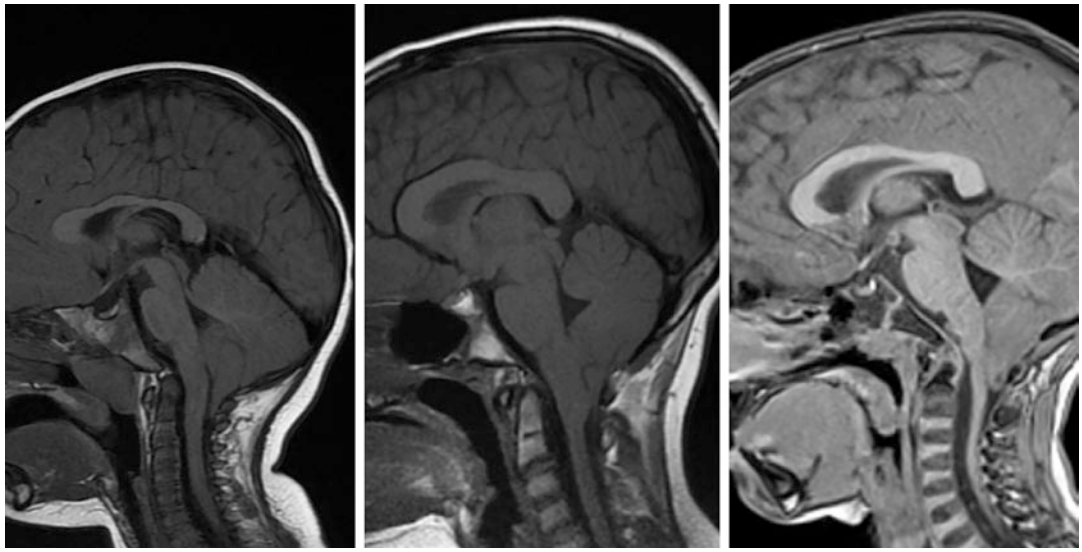

Fig. 2.1 Midsagittal MRI of three patients with CM I noting variable anatomy

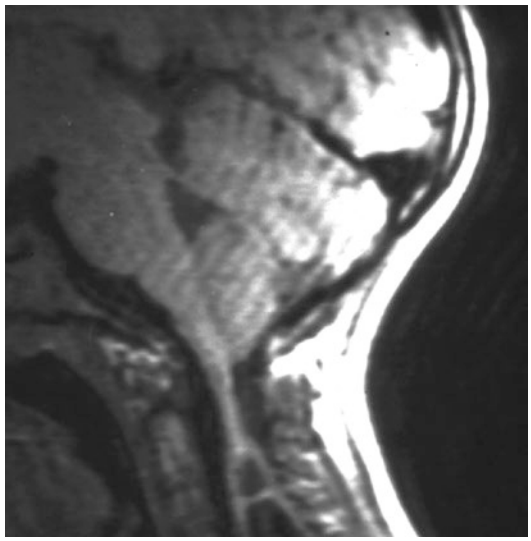

Fig. 2.2 Preoperative image of a patient with a large cervicothoracic syringomyelia and no hindbrain herniation. This cannot be classified as CM 0 until it is proven that the syrinx improves following posterior fossa decompression

cerebellar tonsils may herniate up to 3 mm through the foramen magnum [10]. Barkovich et al. concluded that a minimal cutoff for the CM I would be 3 mm of tonsillar herniation [11]. It has been widely accepted that the inferior cutoff for CM I herniations is 5 mm of tonsillar ectopia, although interobserver differences in measurements of tonsillar herniation are well known [12]. nique does have its limitations since the cerebellar tonsils are bilateral structures, the basion and opisthion are challenging to identify (especially in a younger population), evaluation of the degree of caudal descent is challenging postoperatively following removal of the opisthion, and flexion/extension of the head may change the location of the tonsils (Figs. 2.5 and 2.6) [14, 15]. Because the basion and opisthion on sagittal MRI are more challenging to locate in younger children due to underdeveloped intraosseous medullary spaces, there is an increased risk for overestimation of the amount of cerebellar tonsillar displacement.

Using coronal MRI, Tubbs et al. found asymmetry between the right and left cerebellar tonsils in 96% of patients, positing that CM I usually involves asymmetric tonsillar ectopia (Fig. 2.7) [16]. When studying a pediatric population showing symptoms related to CM I, 18% of the patients had clinical symptoms due to the unequal herniation. In addition, for those patients who also had a coexisting syringomyelia, 95% showed a greater amount of herniation of the right tonsil (Fig. 2.7). Furthermore, asymmetric tonsillar ectopia can lead to a misdiagnosis in the event midsagittal MRI captures the less descended tonsil while missing the contralateral tonsil.

In another study conducted by Tubbs et al., there was discrepancy between coronal and mid-

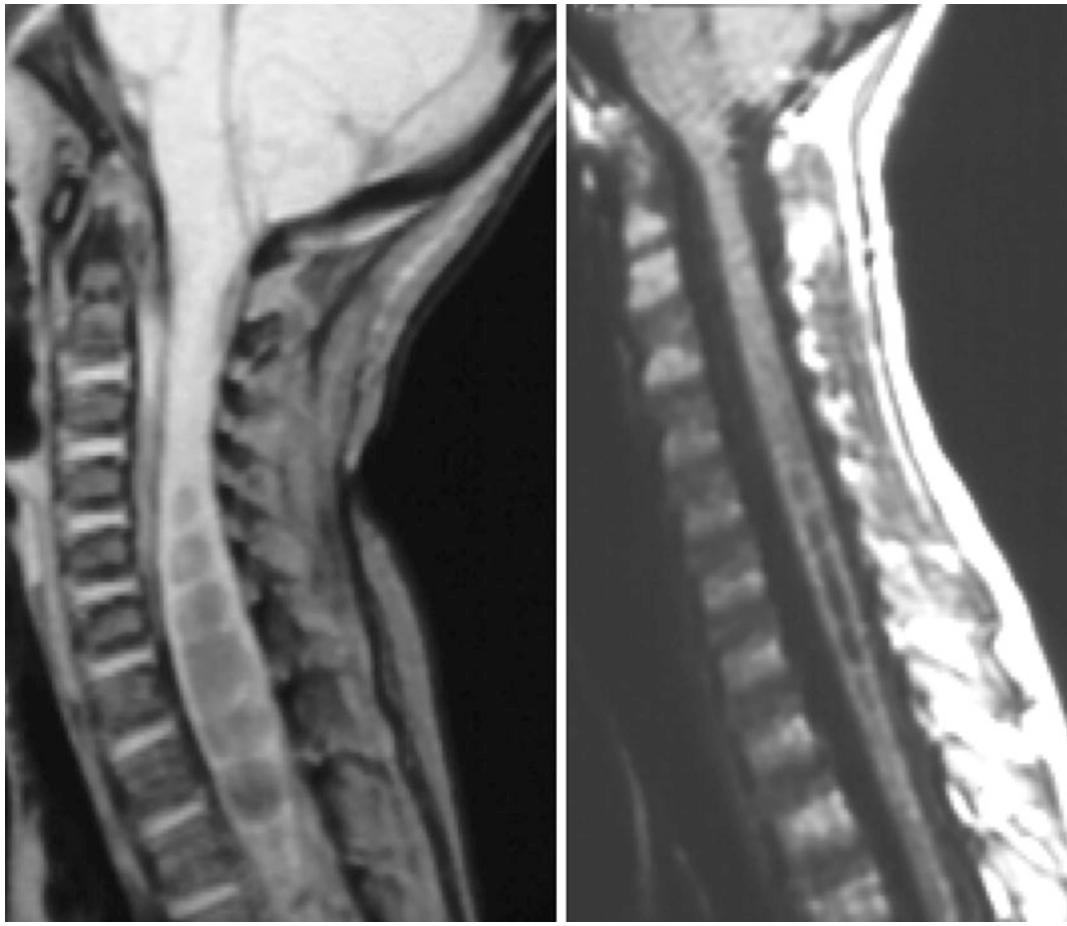

Fig. 2.3 Postoperative decompression of the craniocervical junction reveals a large preoperative syrinx (left) and no hindbrain herniation and a diminished postoperative syrinx (right), thus confirming the diagnosis of CM 0

sagittal planes when diagnosing CM I (Fig. 2.8) [16]. In most of the cases, coronal MRI did not meet the criteria for CM I, whereas midsagittal MRI qualified the patient for such a diagnosis. In addition, these studies found that one tonsil was often more caudally descended in coronal sections [16]. It was concluded that midsagittal MRI may overestimate CM I [16].

Treatment

According to Bindal, decompression surgery should be performed for all symptomatic CM I patients to alleviate symptoms and arrest progressive deterioration [13]. This surgical technique includes resection of the posterior foramen magnum and the posterior arch of C1 and +/− duraplasty. There may also be indications for possible anterior decompression, especially with a retroverted odontoid process.

Chiari 0 Malformation

Type 0 Chiari malformation (CM 0) is a subset of Chiari malformations in which patients have a syringomyelia with little to no associated hindbrain herniation (<3 mm) that responds to craniocervical decompression (Figs. 2.2 and 2.3) [4, 6].

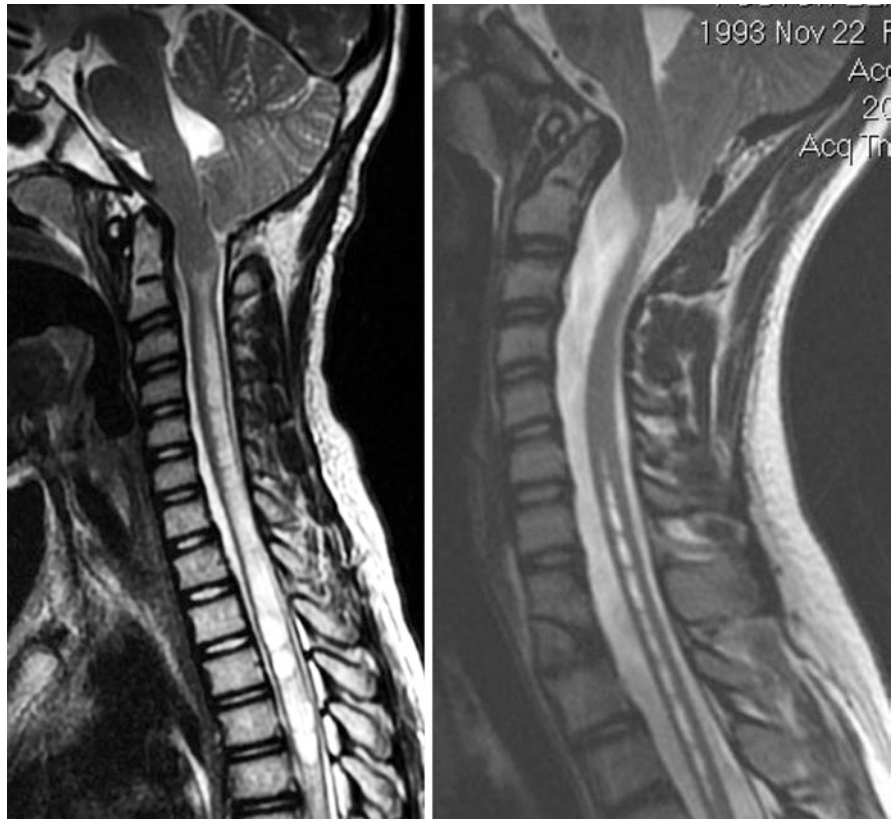

Fig. 2.4 Midsagittal, T2-weighted MRI of two patients with tonsillar ectopia consistent with CM I but with the addition of an elongated and caudally displaced brainstem, thereby forming the so-called Chiari 1.5 malformation. Note the posteriorly displaced odontoid process in the patient on the right

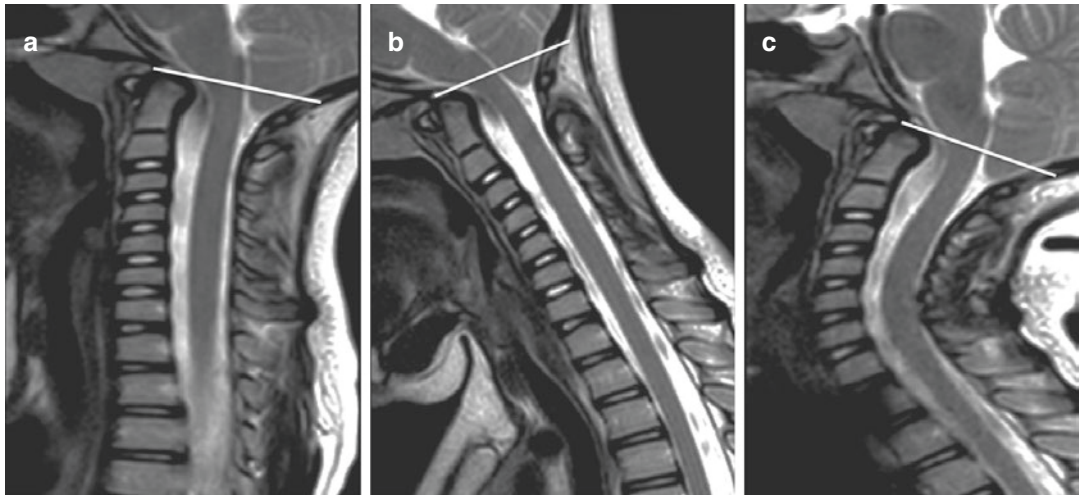

Fig. 2.5 Sequential images of a patient with CM I noting the position of the cerebellar tonsils in neutral (**a**), flexion (**b**), and extension (**c**). In this case, flexion results in the tonsils being located at a more inferior angle

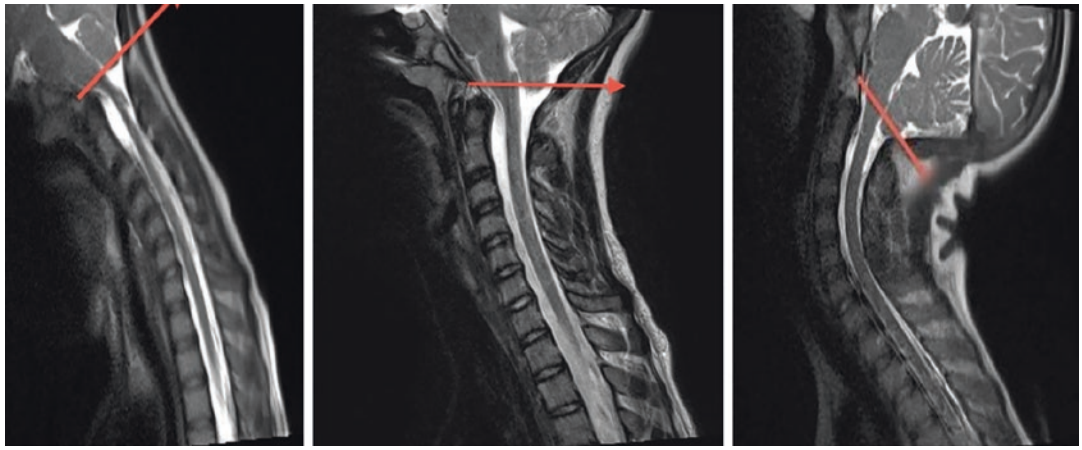

Fig. 2.6 Similar images as seen in Fig. 2.5, but in this patient with CM I, extension results in the tonsils being located at a more inferior level

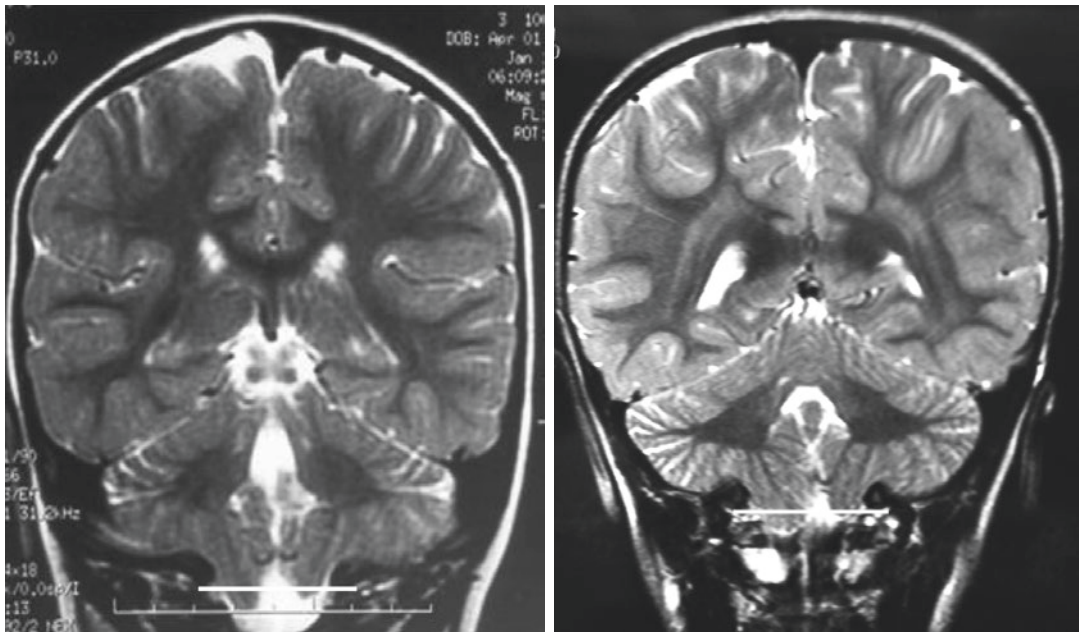

Fig. 2.7 Coronal images from two patients with CM I. Note on coronal imaging, the asymmetry between the left and right tonsils is seen and that in these two patients, the left tonsils alone would not qualify as CM I

Similar to CM I, symptoms are thought to be precipitated by a craniocervical junction disruption to the flow of cerebrospinal fluid (CSF). This similarity has given CM 0 synonyms such as "borderline Chiari" or "Chiari-like pathophysiology" with a "tight cisterna magna" [17].

Originally termed syringohydromyelia without hindbrain herniation in 1969 by Newton, Iskandar et al. termed this condition CM 0 after analyzing cases in which the symptoms and syrinx size improved after posterior cranial fossa decompression [4, 18]. Although there have been a number of reported CM 0 cases since then, the overall number of case presentations has been few. CM 0 might also represent intermittent hindbrain herniation not seen on static imaging.

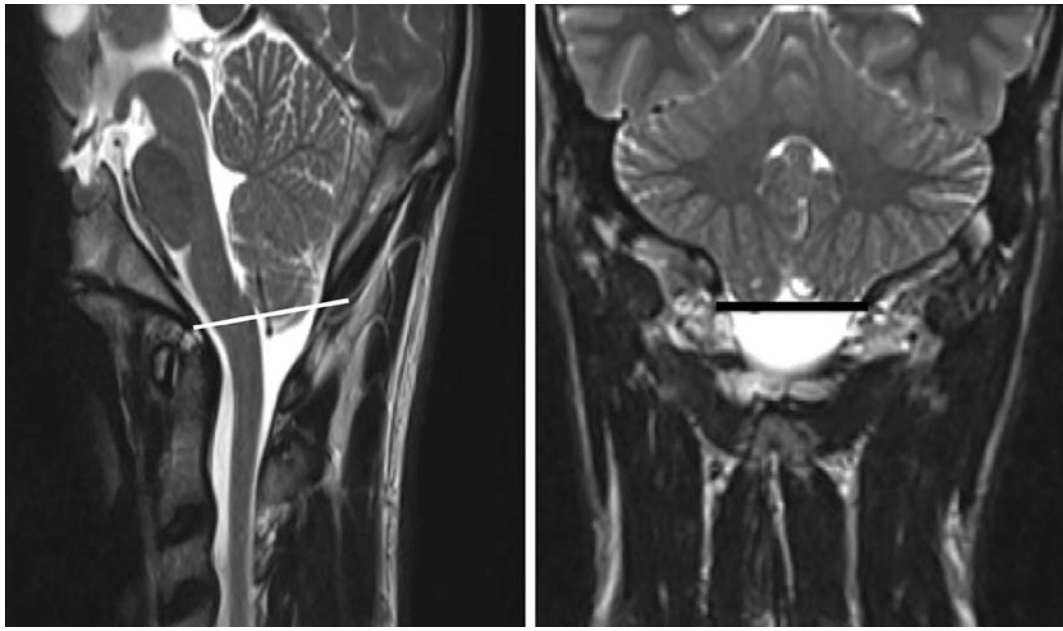

Fig. 2.8 A patient diagnosed with a minimal (3–4 mm) CM I via sagittal MR imaging (left), but with analysis of coronal MRI (right), no cerebellar tonsillar herniation is evident

Features

Tubbs et al. completed a study of the posterior cranial fossa in patients with CM 0 and found deviations from controls [19]. Radiological imaging showed that the tips of the obices could be found in excess of two standard deviations beneath the mean value [19]. The spinomedullary junction midsagittal anteroposterior distance was increased at the level of the foramen magnum [19]. The angle between the base of the fourth ventricle and the clivus was elevated; however, the clival angles and prepontine spaces were found to be within normal limits [19]. Similar findings were also reported in other studies [20, 21].

In this population, Sekula et al. found that the angle of the tentorium cerebelli was greater, whereas the clivus, basisphenoid, and basioccipital were significantly shorter when compared to controls [22]. In addition, it was found that certain cases of syringomyelia lacking hindbrain herniation had impacted cerebellar tonsils in the plane of the foramen magnum with an open arachnoid space anterior to the brainstem [17].

Pathogenesis

In cases of a near-virtual absence of cerebellar herniation as in CM 0, syrinx formation is most likely due to obstructed CSF circulation. This obstructed flow could be attributed to the veils or arachnoid adhesions in the fourth ventricle foramina that are often found during surgery. This usually involves the foramen of Magendie. CSF flow could also be obstructed as a result of a distorted posterior fossa [4, 17, 19].

Since there is more evidence of pathophysiological similarity between CM 0 and CM I, familial clustering suggests genetic as well as multifactorial factors, such as epigenetic and environmental causes, for the differentiation of the two [23]. Therefore, CM 0 and CM I may fall on a continuum rather than be distinct abnormalities.

Clinical Presentation

CM 0 and CM I have similar reported presentations such as limb weakness, scoliosis, and pares-

thesias [24]. In addition, posterior Chiari-like headaches of short duration are typically present and can be induced by Valsalva maneuver [24]. These headaches are suggested to be symptoms of intermittently herniating tonsils, not seen on MRI [20].

Diagnosis and Treatment

Though many techniques have been proposed to treat Chiari malformations, restoring normal CSF flow is required and performed via a posterior cranial fossa decompression [24, 25]. Badie et al. (1995) found that occipital craniectomy, with or without duraplasty, led to cessation of symptoms postoperatively due to decreased craniocervical pressure dissociation [26]. This operation consists of removing a portion of the skull at the posterior aspect of the foramen magnum, removal of the posterior arch of the atlas, and +/−incision of the dura, lysing the arachnoid adhesions/veils to reestablish normal CSF flow through the foramen of Magendie [4, 17]. This can be done with or without duraplasty.

Preoperatively, the diagnosis of CM 0 is one of exclusion and is only confirmed postoperatively with the improvement of clinical symptoms [24]. Finally, though this malformation has been used to describe tonsillar herniation of less than 3 mm in the absence of syringomyelia, this is not a proper use of the term [24].

Chiari 1.5 Malformation

Chiari 1.5 malformation (CM 1.5) (Fig. 2.4) is a more complicated form of CM I with the tonsillar herniation seen in CM I but with the addition of lengthening and inferior displacement of the brainstem and obex being located caudal to the basion-opisthion line [5, 27, 28]. Though the exact incidence of CM 1.5 is not known, it is proposed to be less common than CM I [29]. Since CM I and CM 1.5 share morphological and anatomical similarities, diagnostic distinction needs to be made because the operative outcomes can differ between them [27]. According to Tubbs et al., patients with CM 1.5 were more likely to fail the initial posterior fossa decompression compared to patients with CM I and usually manifested as continued presence of a syringomyelia [5, 30, 31].

Clinical Presentation

The presentation of CM 1.5 is similar to CM I, yet no signs or symptoms differentiate the two. However, patients have reported headaches in the presence and absence of the Valsalva maneuver, shortness of breath, jaw pain, difficulty speaking, opisthotonos, absent gag reflex, lethargy, and drop attacks [5, 6, 24, 28].

Treatment

Treating CM 1.5 first depends on determination of the root cause of the pathology, including hydrocephalus, craniosynostosis, and/or a brain tumor. For patients with craniosynostosis, posterior occipital decompression is recommended [5, 32–34]. In addition, determination as to whether a syrinx is present should be made. If present, decompression surgery is recommended to decrease the compression of the spinomedullary junction.

As with other Chiari malformations, posterior decompression surgery is the only effective treatment; however, syringosubarachnoid shunting has been reported in treatment of CM 1.5 [5, 35]. In many cases of symptomatic CM 1.5 with inferior displacement of the brainstem, patients have a poorer response to posterior cranial fossa decompression, more so if they have concomitant syringomyelia [5, 30, 31].

Other

Some hindbrain herniations are not clear. Most often, a compressed and tapered cerebellar tonsil greater than 3 mm inferior to the foramen magnum is considered a CM I. However, is a rounded, normal-appearing cerebellar tonsil with minimal

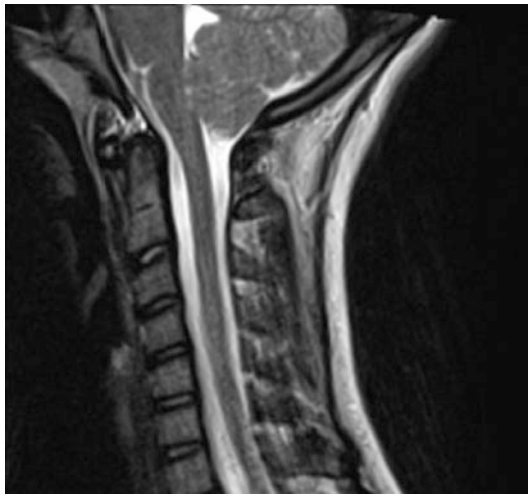

Fig. 2.9 Minimal descent of the cerebellar tonsils, but in this patient there are no signs of compression, and these structures have a normal rounded appearance

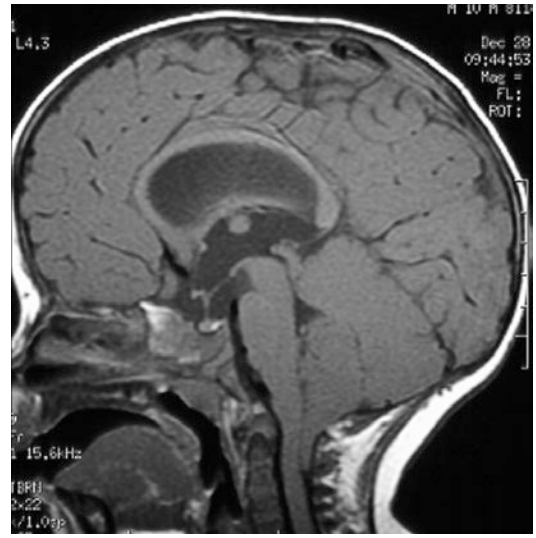

Fig. 2.10 Ventriculomegaly is an asymptomatic patient. Note the caudal displacement of the cerebellar tonsil that to some qualifies as a CM I but to others is simply a result of the enlarged ventricles

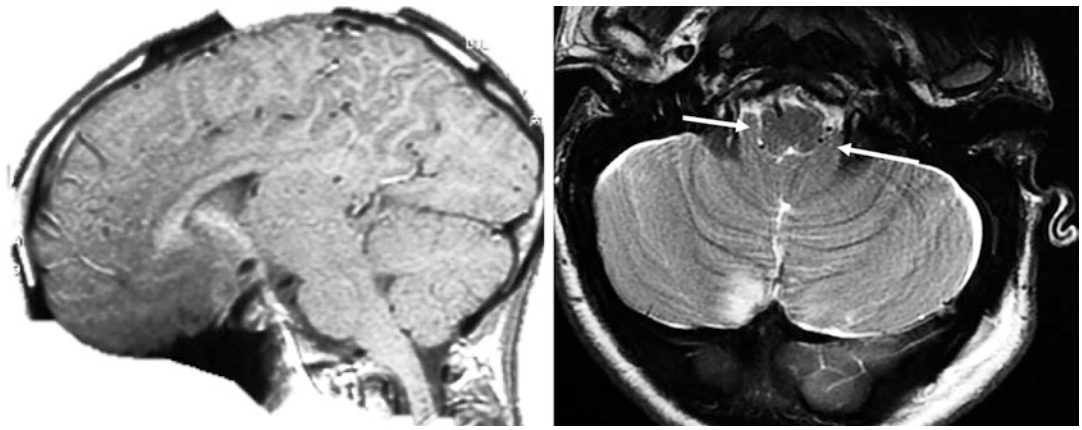

Fig. 2.11 A patient where no tonsillar ectopia is seen on midsagittal imaging (left), but with axial imaging (right), the cerebellar tonsils are seen lateral to the spinomedullary junction

caudal displacement (Fig. 2.9) in an asymptomatic patient also a CM I? Such patients with a rounded tonsil at or below the foramen magnum might be misinterpreted as a CM 0, which as previously stated must have syringomyelia that responds to posterior cranial fossa decompression. Additionally, are cerebellar tonsils that are found below the foramen magnum in the presence of ventriculomegaly or hydrocephalus to be considered CM I (Fig. 2.10)? Some have argued that the hydrocephalus precedes the hindbrain herniation; thus, the hindbrain hernia is secondary and should not be considered in the spectrum of CM I. Lastly, some forme fruste of CM I might not be adequately classified or diagnosed as they fall outside of the "normal" presentations. For example, a stenotic foramen magnum might result in cerebellar tonsils that are herniated inferior to the foramen magnum but not posterior to the brainstem/spinal cord as is usually seen. In these cases, the typical midsagittal imaging might miss this anatomical variant (Fig. 2.11), which should be considered in the spectrum of CM I.

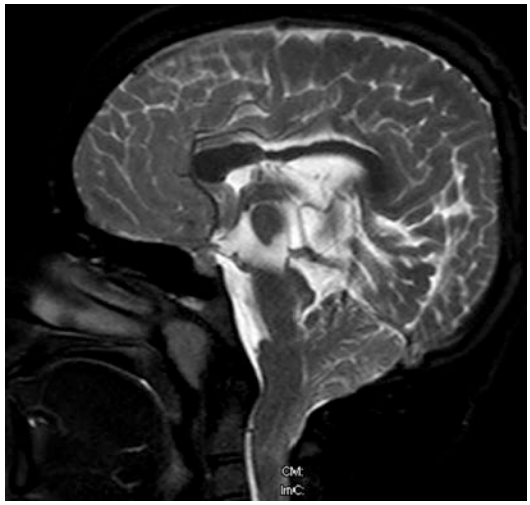

Fig. 2.12 Midsagittal, T2-weighted MRI of patient with Chiari II malformation. Note the enlarged massa intermedia, deformed tectum and corpus callosum, and herniation of the cerebellar vermis through the foramen magnum

Fig. 2.13 Midsagittal section of the cranium and upper spine in a fetal specimen with Chiari II malformation. Note the degree of rhombencephalic derivatives in the upper cervical canal

Fig. 2.14 Specimen in Fig. 2.13 with brain removed and noting the descent of the posterior fossa and its small size

Chiari II Malformation

The Chiari II malformation (CM II) is seen almost exclusively in the setting of myelodysplasia and hydrocephalus. In type II malformations, the structures herniating through the foramen magnum include the cerebellar vermis, brainstem, and fourth ventricle (Figs. 2.12, 2.13, and 2.14). In addition to these neural structures, the accompanying choroid plexus and the associated basilar artery and posterior inferior cerebellar arteries may also be caudally displaced. The posterior cranial fossa is often small and the foramen magnum larger than normal, and syringomyelia is seen in many of these patients.

The CM II occurs in most (>95%) patients with myelomeningocele and is the leading cause of death in treated myelodysplastic patients today. About one-third of these patients develop brainstem symptoms by 5 years of age, and in excess of one-third of those die, usually of respiratory failure. In fact, as many as 20% of patients with symptomatic CM IIs may present as a neurological emergency. When presenting acutely, there is dysfunction of the glossopharyngeal and vagus nerves, affecting respiration, swallowing, and vocal cord functions; this is often accompanied by stridor, opisthotonos, and nystagmus.

Symptomatic deterioration with progressive brainstem dysfunction may be irreversible and lead to death, irrespective of the type of therapy given or the speed with which treatment is instituted. Especially difficult to treat are neonates who fail to initiate adequate ventilation from birth. Although suspected of having inadequate respiratory drive centers, and therefore little or no potential of sustained independent ventilation, their management is associated with a poor outcome and difficult ethical decisions.

Unlike patients with CIM, there is a strong relationship between the type of symptoms and the age of onset. Newborns usually have no symptoms. Older children and young adults most commonly display symptoms and signs of spinal cord and cerebellar dysfunction. A multitude of other symptoms and signs may occur in older patients. Common among these are ophthalmologic findings, which include strabismus**,** horizontal nystagmus (especially when looking upward), abnormalities of pursuit movements and convergence, and defects of optokinetic movements.

CM IIs are characterized by the elongation and caudal displacement of the cerebellar vermis and brainstem, the presence of a myelomeningocele in virtually all cases and hydrocephalus in most, and the common (40–95%) existence of syringomyelia, especially in the lower cervical cord. However, the changes of the CM II constitute a set of cranial and spinal malformations ranging from the posterior cranial fossa, upper cervical canal, ventricular system, and neural tissues of the brain.

Associated neurological anomalies include tectal beaking, secondary to partial or complete fusion of the colliculi into a single backward pointed peak, and kinking at the level of the cervicomedullary junction. The latter anomaly is caused by caudal displacement of a portion of the medulla in conjunction with a spinal cord that is held in relative immobility by the denticulate ligaments. The cerebellum is usually smaller than usual, and upward herniation of the cerebellum may be evident. Finally, callosal agenesis or dysgenesis and abnormalities of the cerebral cortical pattern termed polygyria (not to be confused with the abnormal four-layered cortex seen in polymicrogyria) have frequently been described in Chiari II malformation patients.

In addition to hydrocephalus, the ventricular system displays multiple abnormalities. The third ventricle may be only mildly dilated and contain a large massa intermedia. The fourth ventricle is typically small, flattened, and elongated and extends into the cervical canal. The lateral ventricles may be asymmetrically dilated, with prominence of the atria and occipital horns (colpocephaly), and the septum pellucidum is frequently absent. This sharpness of the frontal horn (lemon sign) and the caudal displacement of the fourth ventricle (banana sign) are relatively easily seen on in utero ultrasound examinations.

The upper cervical canal also displays several bony and spinal cord anomalies in association with the CM II. The posterior arch of C1 is often missing or bifid. Klippel-Feil fusion anomalies of the cervical spine are present in a small group of patients. Basilar impression and C1 assimilation are uncommon in CM II. Significant shortening and scalloping of the clivus can be seen. Other radiographic signs of CM II include Lückenschädel, scalloping of the posterior surface of the petrous pyramid, falx cerebri hypoplasia, falx cerebri fenestration, tentorial hypoplasia with a wide incisura and tiny posterior cranial fossa, and enlargement of the foramen magnum.

Chiari III Malformation

Chiari malformations are complex hindbrain deformities first described and characterized by Hans Chiari in 1891 [1]. Chiari III, one of the rarest of the Chiari malformations, is characterized by high cervical or occipital encephalocele and osseous defects and some but not all of the anatomical characteristics of Chiari II malformation including herniation of posterior cranial fossa contents, medullary abnormalities, hydrocephalus, and a small posterior fossa (Figs. 2.15, 2.16, 2.17, and 2.18) [1]. Only 57 cases have been reported in the literature since 1891 [36]. Patients with Chiari III malformation have poorer outcomes than patients with Chiari I and II malformations, with high mortality rates and/or severe neurological and developmental deficits in those who survive.

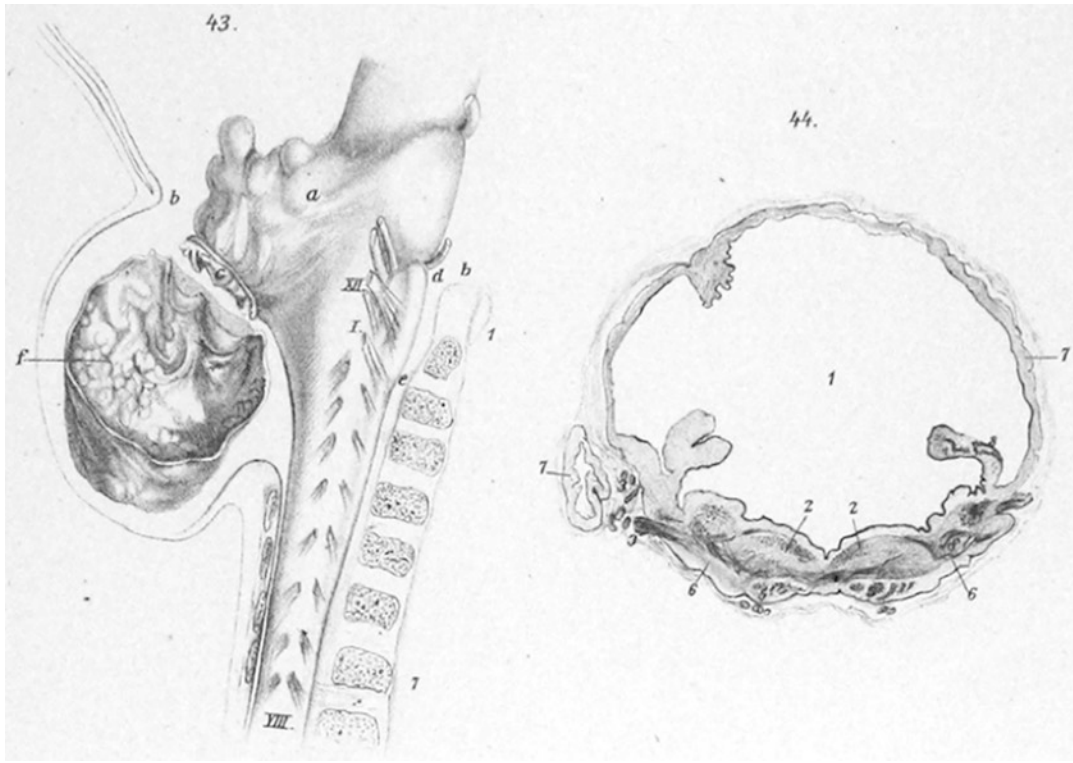

Fig. 2.15 Chiari's drawings of the Chiari III malformation. (Reprinted from Chiari [40])

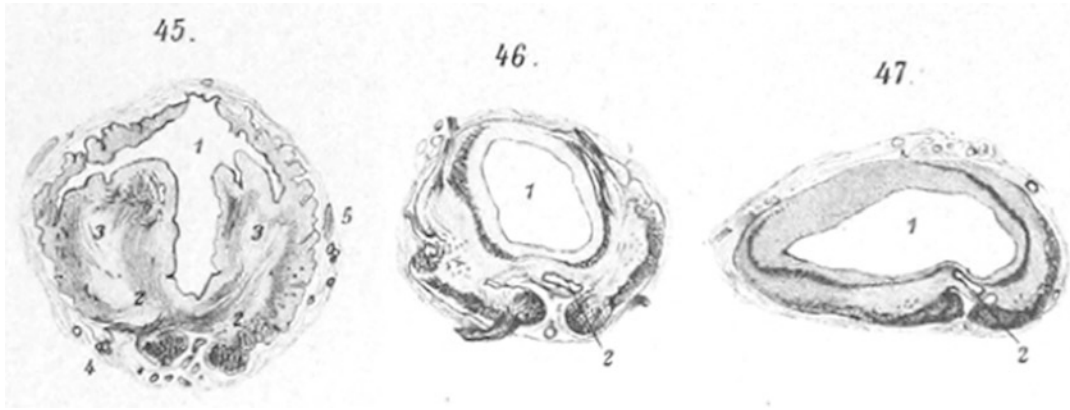

Fig. 2.16 Transections including through the spinal cord for the patient depicted in Fig. 2.15

Chiari's Original Description of the Type III Malformation (1891)

The following is a translation of Chiari's observations and descriptions of the type III malformation [1]:

Of the third type of serial changes of the cerebellum caused by chronic congenital hydrocephalus there was only one case available to me. It demonstrated the greatest degree of displacement of the cerebellum, out of the cranial cavity through the foramen magnum into the vertebral canal, involving the displacement of nearly the entire cerebellum (Figure 2.15),

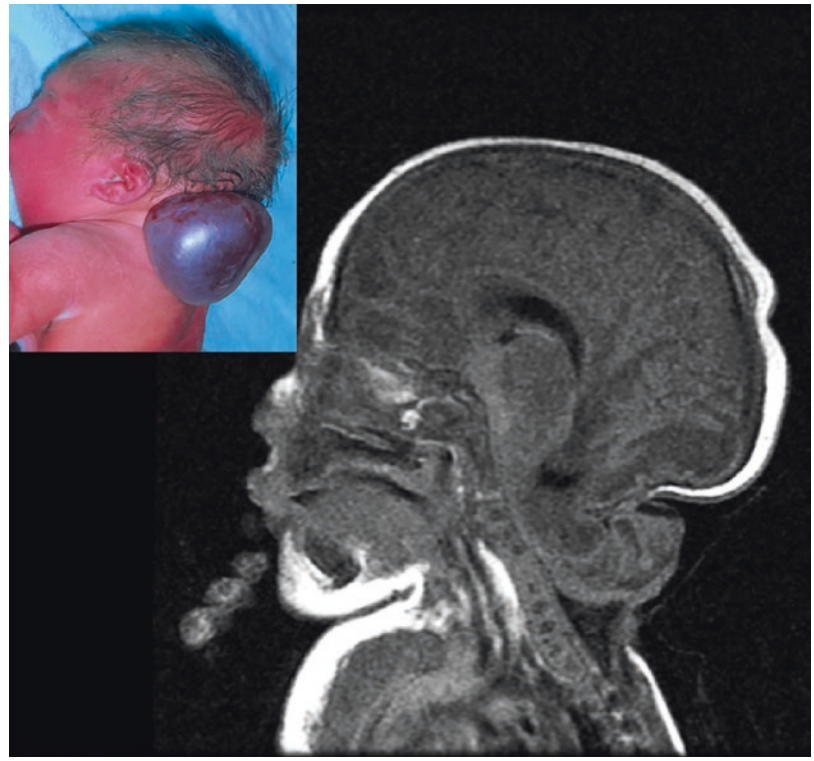

Fig. 2.17 Photograph and sagittal MRI of patient with Chiari III malformation

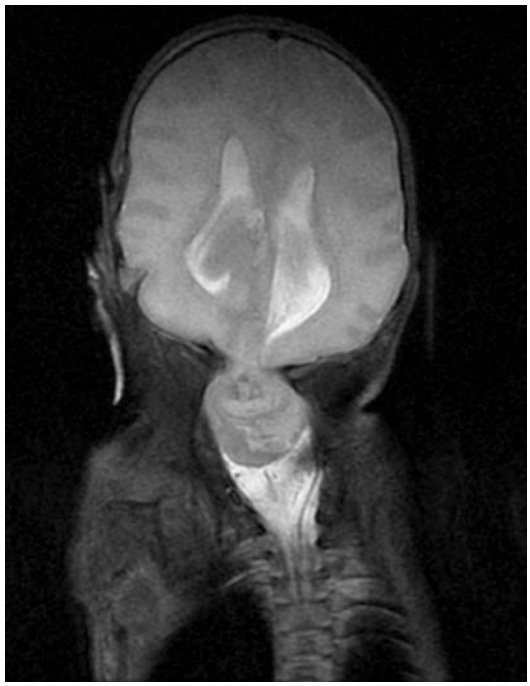

Fig. 2.18 Coronal MRI of patient seen in Fig. 2.17

which was itself hydrocephalic, into a cervical spina bifida.

This case, also from the surgical division of Dr. Bayer in the Kaiser Franz Joseph Children's Hospital was that of a 5-month-old girl who was admitted in November 1890 for operation. The child had a large head and a convergent strabismus. On her neck was a fluctuant, tender, and easily compressible tumor about the size of a hen's egg, extending from the occiput to the seventh cervical vertebra. It was covered with thin skin and was considered to be a cervical hydromyelocele at the base of which a wide cleft in the upper vertebrae could be palpated. There was no paralysis.

On November 15, Dr. Bayer removed the mass by cutting around its base and pulling it away, during which a finger-sized central stalk was ligated and detached. On postoperative day 1, the wound remained free of reaction. However, a CSF leak occurred on November 18 and the wound was oversewn. Meningitis developed on November 21 and the child died on November 23.

The tumor, given to me immediately after the operation, was prepared in Müller's solution. It was a

hemispheral sac with a wall of several layers. The most external layer was the cutis with numerous sweat glands and sparse hair follicles and sebaceous glands. Next was a rather thick stratum subcutaneum, almost free of adipose tissue, to which the dura mater was attached near the base of the mass. The next layer was formed by a rather easily detached thin membrane with a smooth inner surface, which I believe to be arachnoid. The innermost portion of the sac consisted of a cavity with a thumb-sized opening, externally covered with a loose and heavily vascularized tissue. Its wall on the average was only 1 mm thick and consisted of a whitish gray firm tissue covered with numerous nodules, which microscopically was reminiscent of sclerotic central nervous tissue.

At autopsy on November 24, I found that the tissue removed at operation was that of the cerebellum. The lateral ventricles and the third ventricle appeared vastly expanded. The tentorium cerebelli was absent and in place of the cerebellum there was only a nut-sized protuberance, resting on the dorsal surface of the pons and medulla. This remnant of the cerebellum lay inside the enlarged foramen magnum. The posterior arches of the upper three vertebrae were split and widely separated. The inferior margin of the ventral surface of the pons was located at the level of the tip of the odontoid process and the medulla oblongata was completely within the vertebral canal.

Cross-sections through the pons and medulla showed them to be flattened. The Sylvian aqueduct and fourth ventricle were dilated. The remnants of the cerebellum consisted of a cavity opened at the amputation site, with walls about 1 mm thick and knobby widenings up to 5 mm thick. The spinal cord had a large hydromyelia. (Figure 2.16)

Based on the anatomical findings, this represents a cervical cerebellar hydroencephalocele. Occipital encephaloceles often include the cerebellum but what is noteworthy in the present case is the exit of the cerebellum from the cranial cavity through the foramen magnum and into a cervical spina bifida. This displacement of the cerebellum was probably due to hydrocephalus and from this I believe that it is justified to offer this case as representative of a third type of the alternations of the cerebellum due to hydrocephalus [1].

Clinical Presentation

The incidence of Chiari III among all of the Chiari malformations varies between different clinical centers, with a reported incidence of 0.65–4.4%. The incidence of encephaloceles is higher, at 1–2 of every 5000 births with 75–90% of these being occipital [36]. Malformations commonly present as an occipital mass at birth, expanding as the child grows older. Clinical findings include disordered eye movement such as titubation and downbeat nystagmus, sensory loss, weakness, ataxia, respiratory insufficiency, respiratory failure, amyotonia, hyperreflexia, dysphagia with secondary aspiration, spastic or decreased muscle tone, and inspiratory stridor.

Anatomy

Encephalocele tissue in the Chiari III malformation (Figs. 2.17 and 2.18) is usually abnormal and nonfunctional and contains gliosis, necrosis of neural tissue, meningeal inflammation, fibrosis, cerebral and cerebellar tissues, ventricles with choroid plexuses, and gray matter heterotopias. Aberrant deep veins and ectopic dural venous sinuses are common findings. Most patients presenting with Chiari III malformation have an abnormal midbrain. Additionally, other anomalies of the brain have been reported in the literature, including scalloping of the posterior petrous pyramids and the clivus, overgrowth of the cerebellum, lack of the cerebellum, syringomyelia, creeping of the cerebellar hemispheres around the brainstem, and aplasia of the posterior falx cerebri. Brain parts occurring in the sac from most to least common include the cerebellum, occipital lobe, and parietal lobe. Occipital bone defects are seen with some but not all Chiari III malformations. Hydrocephalus in this group is not an essential finding but has been reported in the majority of cases. Additional ventricular abnormalities included septa in the ventricles, colpocephaly, and partial and complete agenesis of the corpus callosum. Syringomyelia is commonly present in association with Chiari III malformation. Seventy percent of patients with Chiari III malformation have incomplete fusion of the posterior arches of C1.

Chiari 3.5 Malformation

Three years after Chiari's description, Giuseppe Muscatello (1866–1951) (Privatdozent) of the University of Turin, while working with von Recklinghausen at the Pathological Institute in Strasbourg (France), reported a unique variant of the Chiari III malformation [37]. This was published in 1894 in *Langenbecks Archiv für klinische Chirurgie* with the title *Ueber die angeborenen Spalten des Schädels und der Wirbelsäule* (*About the Hereditary Clefts of the Skull and the Spine*). In this publication, Muscatello described a case of what he termed an encephalomyelocystocele. Due to the occipitocervical encephalocele, anomalous anatomy of the posterior cranial fossa (e.g., flattened brainstem, absent tentorium cerebelli), we consider this a unique variant of the Chiari III malformation, hence forward referred to as a Chiari 3.5 malformation (Fig. 2.19).

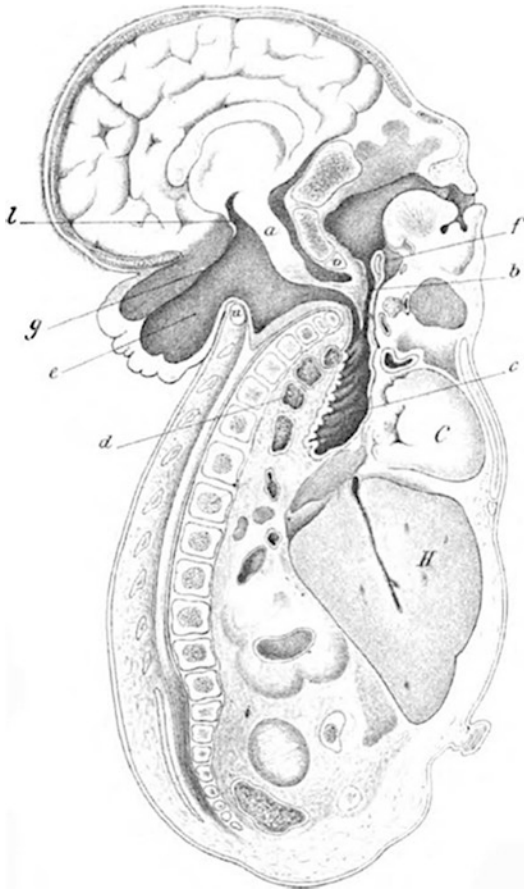

Fig. 2.19 Schematic drawing of the Chiari 3.5 malformation

Muscatello's Case Description

The patient was a premature 7-month-old female who lived for only 10 minutes after delivery. The length of the child from head to rump was 19 cm. No neck was observed and the face was flat and the nose compressed. The scalp mass was egg-shaped, covered with atrophic skin, and extended from the lower occipital to scapular regions (Fig. 2.19). The dolichocephalic-shaped skull was 101 mm × 72 mm with a large fontanel (50 mm × 30 mm). The mass had an irregular surface and was 32 mm long and 42 mm wide and had a height of 28 mm. The base of the skull was slightly kyphotic, and the spine was abbreviated and consisted of only 22 vertebral bodies (4 coccygeal, 5 sacral, 5 lumbar, and 8 thoracic vertebrae), which were mostly underdeveloped. Almost no muscles were identified around the neck, and the stomach and intestines were located in the thorax and posterior to the heart (posterior mediastinum). The dura mater did not extend into the spinal canal, and there were no signs of the tentorium cerebelli or the transverse sinuses. The cerebral hemispheres were 9.5 cm long and the cerebellum was grossly missing. The occipital mass has a sagittal diameter of 38 mm and, notably, is connected anteriorly with the stomach. The spinal canal ended at the third lumbar vertebral body (Fig. 2.19).

Histologically, Muscatello found that the connecting channel between the fourth ventricle and the esophagus showed the dorsal as well as the ventral sections of the channel wall in thin cuts. It was possible to recognize the structure of the esophagus with its normal components (mucosa and mucous glands, loose submucosa, smooth muscle fibers, and loose connective tissue with striated muscle) [37]. Directly abutting to the esophagus components, one can find tissue without ganglion cells, rich in vasculature, and with ecchymosis permeating the nerve tissue. It is remarkable that the mucous membrane settles like a blanket over the nerve tissue, becoming thinner and thinner until only one layer of epithelium can be appreciated.

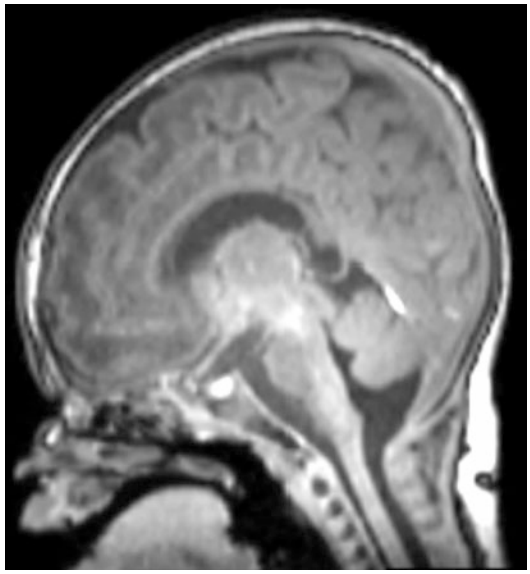

Fig. 2.20 Image of a patient described as having a Chiari IV malformation, although this is incorrect based on Chiari's original descriptions

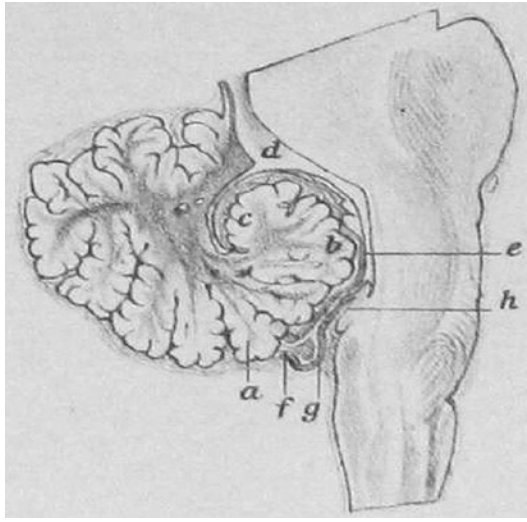

Fig. 2.21 Sagittal drawing of the cerebellum and brainstem from Chiari's original description of the Chiari IV malformation

Chiari IV Malformation

Four years after Chiari's 1891 publication, his second paper of such herniations described the type IV malformation in two patients (Figs. 2.20, 2.21, and 2.22) [2]. A translation of his description of this malformation is as follows:

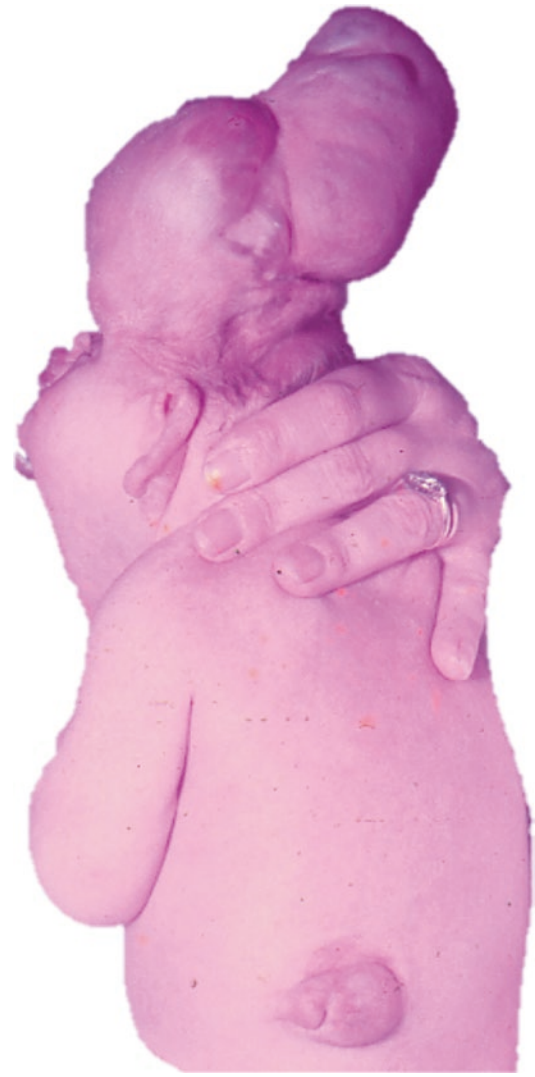

Fig. 2.22 Patient meeting criteria for the original description of the Chiari IV malformation with supratentorial herniation. Also note the myelomeningocele

> Fourth type
>
> Cerebellar hypoplasia without herniation of posterior fossa content into the spinal canal
>
> Here, I describe two cases of cerebellar changes secondary to congenital hydrocephalus of the cerebrum without herniation of posterior fossa contents into the spinal canal as encountered in the other types.

A. Significant hypoplasia of the entire cerebellum. Rolling of the interior vermis.

Indentation of the dorsal wall of the fourth ventricle.

Twenty-third case: Two-day-old girl. Department of Surgery at the Kaiser Franz Joseph pediatric hospital under Prof. Dr. Bayer. Dissection on March 19th, 1892 (30 hours post mortem).

Clinical diagnosis: Encephalocele occipitalis amputata. Encephalitis. Sclerema.

Medical history: **The encephalocele consists of a cylindrical, broad based, 6 cm long, and 3 cm wide skin sac**. The sac has an ulcerated opening measuring about 8 cm. Through this opening, another, 4 cm wide inner sac, similarly ulcerated at the end, protrudes. That second, inner sac is made up of meninges with longitudinally oriented folds, almost of the size of a little finger. The inner sac communicates with the intracranial compartment through a 1 cm^2 wide opening located just below the posterior fontanel. The outer sac is contingent with the scalp. In surgery the inner sac was disconnected and resected at the intracranial opening and closed with the excess skin overlying it. The patient passed 36 hours after surgery.

Pathological-anatomical diagnosis: Meningitis cerebralis suppurativa et suppuratio in ventriculiscerebri ex ulcerationehydrencephaloceles occipitalis (horas XXXVI ante mortem amputatae). Dilatatio congenita ventriculoriumcerebri. Pneumonia lobularisbilateralis. Sclerematextus adipose subcutanei.

Dissection of the central nervous system: The child's head is disproportionally large compared to its height (47 cm), just a little more narrow. Hair shaved. Inferior to the posterior fontanel there is a skin bulge measuring 6 cm × 3 cm × 2 cm with a 6 cm long closed incision at the top. The edges are edematous and erythematous.

The soft skull is ecchymotic, pale, in the area of the bulge edematous, serous, and purulent. Circumferentially the skull measures 27 cm. The sutures are split. The sagittal suture is 0.5 cm wide. The anterior fontanel is larger measuring 4 cm in length and 2.5 cm in width. The posterior fontanelle is normal in size. The skull bones are fairly rigid. In the squama ossis occipitalis, 2 cm inferior to the posterior fontanel, there is an opening of the size of the nail of a small finger. The opening is surrounded by the split of the processus sagittalis major of the pachymenix. Through that opening a hemorrhagic and necrotic mass of inner meninges and brain parenchyma are extruding. In the sinus durae matris there is dark, liquid, and also freshly coagulated blood. The sinus sagittalis major is split into two sinuses from the area of the posterior fontanel that diverge to form the sinus transversi. The tentorium cerebelli is narrow, the processus falciformis minor is absent, the posterior fossa is small. The inner surface of the skull base has deep impressiones digitatae. The foramen occipital magnum is remarkably narrow. The inner meninges are pale and infiltrated by serous and purulent liquid.

The gyri and sulci of the cerebrum appear normal. The lateral ventricles and third ventricle are enlarged and contain serous and purulent liquid. The brain matter is pale, moist, and soft. **Originating from the precuneus are two processes of brain matter that contain the occipital horns and plexus choroidei of the lateral ventricles and protrude through the previously mentioned opening**.

The cerebellum is only half the size of a normal cerebellum. It is 3.5 cm wide and 2 cm long. The largest diameter from the upper to the lower surface is 3 cm. It is asymmetric with the left hemisphere significantly smaller than the right. The lobi superiores, posteriores et inferiores are easily distinguished, the tonsils and flocculi are rudimentary. The inferior vermis is more prominent and the incisura marginalis posterior is absent. The pons and medulla oblongata are 14 and 11 mm long, respectively. Both are thin.

A median sagittal section of the cerebellum, pons, medulla oblongata, and upper cervical spinal cord (Figure 2.21) shows unusual rolling of the lower portion of the arbor vitae resulting in a deep location of the pyramis (a), high location of the uvula (b), and location of the nodulus (c) of the inferior vermis on the upper end of the rolling of the arbor vitae. The dorsal wall of the fourth ventricle (d) is bowed due to the rolling and the velum medullare posterius (e) is very long. The entry of the tela choroidea ventriculi IV is well demarcated (f) and at the usual location. The ponticuli (g) are longer and thicker, as is the velum medullare posterius. The corpora dentata cerebelli are smaller, otherwise normally shaped. The pons and medulla are normal.

The spinal cord is of dense consistency. The inner meninges of medulla oblongata, pons, and cerebellum are not purulent.

Microscopic examination of the encephalocele occipitalis, vermis, pons, medulla oblongata, corpus dentatum of the right cerebellar hemisphere, the fifth cervical segment, fifth and ninth thoracic segments, and third segment of the spinal cord is performed after solidification with liquor Mülleri.

The inner sac of the encephalocele has two layers. The outer layer is highly vascularized and hemorrhagic as are the inner meninges while the inner

layer is of sclerotic brain matter. The latter makes up the previously mentioned longitudinally oriented folds. The inner surface of the sac is lined with cylindrical epithelium.

The vermis, pons, and medulla oblongata are examined using the right half of the section. The vermis has normal texture. Its cortex has an external granular layer, a molecular layer, and an inner granular layer. There are numerous Purkinje cells. The medulla is mostly black on copper hematoxylin stain. The pons and medulla oblongata are normal. Only the pyramids are devoid of medullary substance. The fourth ventricle is lined with normal epithelium. The elongated velum medullare posterius and taenia plexus chorioidei ventriculi IV are sclerotic.

The corpus dentatum cerbelli has prominent folding and numerous multipolar ganglion cells. The medulla spinalis has a mild dilatation of the central canal lined with epithelium and the pyramidal tract is devoid of medullary substance [2].

Confusion

Due to the continued misuse of the term Chiari IV malformation, several reports have entirely misunderstood and misinterpreted the definition of this pathology and have therefore made incorrect statements about the malformation (Fig. 2.20). The already confused and incorrect use of the term Chiari IV malformation has been convoluted even more as some have reported a similarity between this malformation and the Dandy-Walker malformation or variant.

Since the original paper, the literature has used the term Chiari IV malformation incorrectly [38]. As Chiari depicted (Fig. 2.21) only the posterior cranial fossa contents in his 1895 tome, this may have resulted in many misinterpreting his findings and to propagate the idea that the main feature of the Chiari IV malformation is cerebellar hypoplasia. The primary feature of this malformation, from hence forward and in line with Chiari's original description, should be an occipital encephalocele with supratentorial contents. The other associated findings, based on the original description, should be the following:

- Splitting of the superior sagittal sinus around the occipital encephalocele.
- Hydrocephalus.
- Cerebellar hypoplasia but *not* aplasia.
- Absence of the falx cerebelli.
- Narrowed tentorium cerebelli.
- Small posterior cranial fossa.
- Narrow foramen magnum.
- Elongated inferior medullary velum.
- "Rolled" inferior vermis
- Indentation of the posterior wall of the fourth ventricle.

Chiari V Malformation

We previously reported a newborn with sacral myelomeningocele that was repaired on day 1 of life [39]. A head computed tomography (CT) revealed hydrocephalus, and this was shunted on day 4 of life with an increasing head circumference and tense and bulging anterior fontanelle. The patient developed difficulty with stridor, and MRI demonstrated absence of the cerebellum with herniation of the occipital lobes into and through the foramen magnum (Fig. 2.23). No cerebellum was present on any images. A tracheostomy was performed and the issues with stridor resolved. At 6 months old and on physical examination, he is awake. His eyes are open and

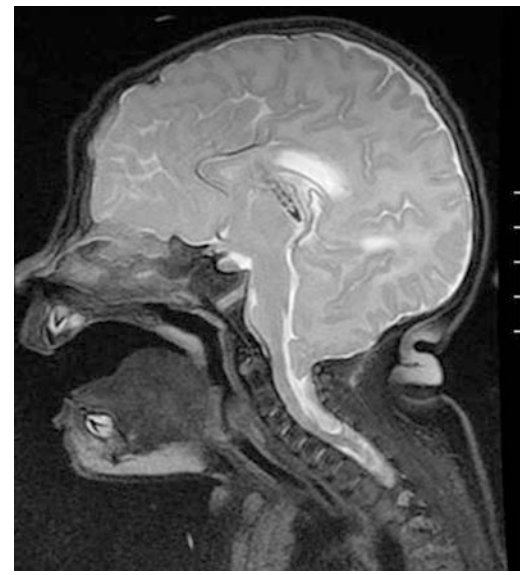

Fig. 2.23 Herniation of the occipital lobe through the foramen magnum representing the Chiari V malformation

his pupils are equal, round, and reactive to light. He tracks with his eyes and there is no nystagmus. His shunt and myelomeningocele closure sites are well healed. He does not sit on his own and continues to receive weekly physical and occupational therapy. He moves his upper extremities and lower extremities well. We believed that the case described was the first report of its kind and proposed the term Chiari V malformation be used to describe this phenomenon [39].

Conclusion

The older classifications of the Chiari malformations are still relevant but necessitate additional subclassifications and clarification of the original definitions, e.g., Chiari IV malformation. Knowledge of the newer classifications is required to improve patient treatment and outcomes. An improved understanding of their embryology and clinical manifestations will help in better categorizing these entities.

References

1. Chiari H. Ueber Veranderungen des Kleinhirnsinfolge von Hydrocephalie des Grosshirns. Med Wochenschr. 1891;17:1172–5.
2. Chiari H. Ueber Veranderungen des Kleinhirns, des Pons und der Medulla oblongata Infolge von congenitaler Hydrocephalie des Grosshirns. Denkschriften Kais Akad Wiss Math-Naturw. 1895;63:71–116.
3. Loukas M, Shayota BJ, Oelhafen K, Miller JH, Chern JJ, Tubbs RS, Oakes WJ. Associated disorders of Chiari Type I malformations: a review. Neurosurg Focus. 2011;31(3):E3.
4. Iskandar BJ, Hedlund GL, Grabb PA, Oakes WJ. The resolution of syringohydromyelia without hindbrain herniation after posterior fossa decompression. J Neurosurg. 1998;89:212–6.
5. Tubbs RS, Iskandar BJ, Bartolucci AA, Oakes WJ. A critical analysis of the Chiari 1.5 malformation. J Neurosurg. 2004;101:179–83.
6. Cesmebasi A, Loukas M, Hogan E, Kralovic S, Tubbs RS, Cohen-Gadol AA. The Chiari malformations: a review with emphasis on anatomical traits. Clin Anat. 2015;28:184–94.
7. Tubbs RS, Griessenauer CJ, Hendrix P, Oakes P, Loukas M, Chern JJ, Rozzelle CJ, Oakes WJ. Relationship between pharyngitis and peri-odontoid pannus: a new etiology for some Chiari I malformations? Clin Anat. 2015;28:602–7.
8. Homen E. ZurKenntnis der rachitischenDeformationen der Schadelbasis und der BasdenScadelhyperostosen. Dtsch Z Nervenheilkd. 1901;20:3–15.
9. Massimi L, Peppucci E, Peraio S, Di Rocco C. History of Chiari type I malformation. Neurol Sci. 2011;32(Suppl 3):S263–5.
10. Aboulezz AO, Sartor K, Geyer CA. Position of cerebellar tonsils in the normal population and in patients with Chiari malformation: a quantitative approach with MRimaging. J Comput Assist Tomogr. 1985;9:1033–6.
11. Barkovich AJ, Wippold FJ, Sherman JL, Citrin CM. Significance of cerebellar tonsillar position on MR. AJNR Am J Neuroradiol. 1986;7(5):795–9.
12. Smith BW, Strahle J, Bapuraj R, Muraszko KM, Garton HJL, Maher CO. Distribution of cerebellar tonsil position: implication in understanding Chiari malformation. J Neurosurg. 2013;119:812–9.
13. Bindal A, Dunsker S, Tew J. Chiari I malformation: classification and management. Neurosurgery. 1995;37(6):1069.
14. Tubbs RS, Beckman J, Naftel RP, Chern JJ, Wellons JC, Rozzelle CJ, Blount JP, Oakes WJ. Institutional experience with 500 cases of surgically treated pediatric Chiari malformation type I. J Neurosurg Pediatr. 2011;7:248–56.
15. Tubbs RS, Kirkpatrick CM, Rizk E, Chern JJ, Oskouian RJ, Oakes WJ. Do the cerebellar tonsils move during flexion and extension of the neck in patients with Chiari I malformation? A radiological study with clinical implications. Childs Nerv Syst. 2016;32(3):527–30.
16. Tubbs RS, Wellons JC, Oakes WJ. Asymmetry of tonsillar ectopia in Chiari malformation. Pediatr Neurosurg. 2002;37:199–202.
17. Kyoshima K, Kuroyanagi T, Oya F, Kamijo Y, El-Noamany H, Kobayashi S. Syringomyelia without hindbrain herniation: tight cisterna magna. Report of four cases and a review of the literature. J Neurosurg. 2002;96:239–49.
18. Newton EJ. Syringomyelia as a manifestation of defective fourth ventricular drainage. Ann R Coll Surg Engl. 1969;44:194–213.
19. Tubbs RS, Elton S, Grabb P, Dockery SE, Bartolucci AA, Oakes WJ. Analysis of the posterior fossa in children with the Chiari 0 malformation. Neurosurgery. 2001;48:1050–4. discussion 1054–5
20. Chern JJ, Gordon AJ, Mortazavi MM, Tubbs RS, Oakes WJ. Pediatric Chiari malformation Type 0: a 12-year institutional experience. J Neurosurg Pediatr. 2011;8:1–5.
21. Isik N, Elmaci I, Kaksi M, Gokben B, Isik N, Celik M. A new entity: Chiari zero malformation and its surgical method. Turk Neurosurg. 2011;21:264–8.
22. Sekula RF Jr, Jannetta PJ, Casey KF, Marchan EM, Sekula LK, McCrady CS. Dimensions of the posterior fossa in patients symptomatic for Chiari I mal-

formation but without cerebellar tonsillar descent. Cerebrospinal Fluid Res. 2005;2:11.
23. Markunas CA, Tubbs RS, Moftakhar R, Ashley-Koch AE, Gregory SG, Oakes WJ, Speer MC, Iskandar BJ. Clinical, radiological, and genetic similarities between patients with Chiari Type I and Type 0 malformations. J Neurosurg Pediatr. 2012;9:372–8.
24. Haddad F, Qaisi I, Joudeh N, Dajani H, Jumah F, Elmashala A, Adeeb N, Chern J, Tubbs RS. The newer classifications of the Chiari malformations with clarifications: an anatomical review. Clin Anat. 2018;31:314–22.
25. Lavarato L, Spallone A, Visocchi M. Surgical treatment of Chiari malformation in adults: comparison of surgical techniques described in the literature and our experience. Acta Neurochir Suppl. 2019;125:139–43.
26. Badie B, Mendoza D, Batzdorf U. Posterior fossa volume and response to suboccipital decompression in patients with Chiari I malformation. Neurosurgery. 1995;37:214.
27. Kim IK, Wang KC, Kim IO, Cho BK. Chiari 1.5 malformation: an advanced form of Chiari I malformation. J Korean Neurosurg Soc. 2010;48:375–9.
28. Capra V, De Marco P, Merello E, Baffico AM, Baldi M, Divizia MT, Gimelli S, Mallet D, Raso A, Mascelli S, Toma P, Rossi A, Pavanello M, Cama A, Magnani C. Craniosynostosis, hydrocephalus, Chiari I malformation and radioulnar synostosis: probably a new syndrome. Eur J Med Genet. 2009;52:17–22.
29. Deng X, Yang C, Gan J, Yang B, Wu L, Yang T, Xu Y. Chiari malformation type 1.5 in male monozygotic twins: case report and literature review. Clin Neurol Neurosurg. 2015;130:155–8.
30. Tubbs RS, McGirt MJ, Oakes WJ. Surgical experience in 130 pediatric patients with Chiari I malformations. J Neurosurg. 2003;99:291–6.
31. Tubbs RS, Wellons JC, Blount JP, Grabb PA, Oakes WJ. Inclination of the odontoid process in the pediatric Chiari I malformation. J Neurosurg. 2003;98:43–9.
32. Cinalli G, Chumas P, Arnaud E, Sainte-Rose C, Renier D. Occipital remodeling and suboccipital decompression in severe craniosynostosis associated with tonsillar herniation. Neurosurgery. 1998;42:66–71. discussion 71–63
33. Cinalli G, Spennato P, Sainte-Rose C, Arnaud E, Aliberti F, Brunelle F, Cianciulli E, Renier D. Chiari malformation in craniosynostosis. Childs Nerv Syst. 2005;21:889–901.
34. Scott WW, Fearon JA, Swift DM, Sacco DJ. Suboccipital decompression during posterior cranial vault remodeling for selected cases of Chiari malformations associated with craniosynostosis. J Neurosurg Pediatr. 2013;12:166–70.
35. Ömer N. Kisi MO, Gezercan Y, Erman T. Chiari malformation type 1.5-related syringomyelia: treatment options differentiate this new entity from classic tonsillar ectopia: case report. Neurosurg Quart. 2014;24:183–5.
36. Ivashchuk G, Loukas M, Blount JP, Tubbs RS, Oakes WJ. Chiari III malformation: a comprehensive review of this enigmatic anomaly. Childs Nerv Syst. 2015;31:2035–40.
37. Fisahn C, Shoja MM, Turgut M, Oskouian RJ, Oakes WJ, Tubbs RS. The Chiari 3.5 malformation: a review of the only reported case. Child's Nerv Syst. 2016;32:2317–19.
38. Tubbs RS, Demerdash A, Vahedi P, Griessenauer CJ, Oakes WJ. Chiari IV malformation: correcting an over one century long historical error. Childs Nerv Syst. 2016;32:1175–9.
39. Tubbs RS, Muhleman M, Loukas M, Oakes WJ. A new form of herniation: the Chiari V malformation. Childs Nerv Syst. 2012;28:305–7.
40. Chiari H. UeberVeranderungen des Kleinhirnsinfolge von Hydrocephalie des Grosshirns. Med Wochenschr. 1891;17:1172–5.

Newer Subsets: Chiari 1.5 and Chiari 0 Malformations

3

Rima S. Rindler and Joshua J. Chern

Introduction

A Chiari 1 malformation refers to cerebellar tonsillar descent inferior to the foramen magnum, often caused by bony morphological variants of the posterior fossa, skull base, and/or cervical spine. Specifically, it may be caused by a more acute angle of the base of the occipital bone, a more horizontal inclination of the clivus, or posterior tilting or invagination of the odontoid. These changes may decrease the volume of the posterior fossa and may lead to caudal descent of the tonsils and cervicomedullary compression at the foramen magnum. Additional anatomical findings led to creation of a separate class of Chiari malformations, named Chiari 1.5 malformation. This entity is defined as tonsillar ectopia with associated caudal descent of the brainstem through the foramen magnum. These patients present with classic Chiari 1 symptoms and may include additional symptoms related to brainstem compression as described below. Chiari 1.5 patients present at a younger age than Chiari 1 (fourth versus fifth decade of life, respectively [1]) but develop cervical syrinxes at the same rate. Some authors argue that Chiari 1.5 is just a subtype of Chiari 1 rather than a separate classification, as their presentation and operative outcomes are similar [1].

Chiari 0 is another defined, unique class of posterior fossa malformations. These patients develop idiopathic cervical syringomyelia without frank tonsillar herniation through the foramen magnum. It is a diagnosis of exclusion, wherein the etiology of the syrinx is determined not to have been caused by trauma, infection, spinal dysraphism, or tumor [2]. The putative mechanism for syrinx formation in this rare group is cerebrospinal fluid (CSF) flow disturbance due to crowding at the foramen magnum [3], an arachnoid web, compression by a ligamentous band, or a "tight cisterna magna" where cerebellar tonsils compact CSF outflow above the foramen magnum [4]. These patients usually respond to foramen magnum decompression and release of the offending obstruction, if found, with postoperative resolution of the syrinx. This is a very rare entity; in a group of more than 400 patients who underwent posterior fossa decompression between 1989 and 2010, only 15 cases (3.7%) fulfilled the criteria of Chiari 0 malformation [5]. Some authors argue that Chiari 0 is actually on a continuum of Chiari 1 malformation, and not a separate class [6].

This chapter will focus on the diagnosis and treatment options of the "newer" Chiari malformation classes.

R. S. Rindler
Department of Neurosurgery, Emory University School of Medicine, Atlanta, GA, USA

J. J. Chern (✉)
Department of Neurosurgery, Children's Healthcare of Atlanta, Emory University School of Medicine, Atlanta, GA, USA
e-mail: joshua.chern@choa.org

R. S. Tubbs et al. (eds.), *The Chiari Malformations*, https://doi.org/10.1007/978-3-030-44862-2_3

Clinical Presentation

Presenting symptoms of patients with Chiari 1.5 and Chiari 0 malformations are generally similar to other patients with Chiari 1 malformation [7–9]. These include occipital headaches that are Valsalva-induced and promptly resolve with rest, neck pain, paresthesias, dyspnea, swallowing difficulties, and gait changes. Cranial nerve dysfunction, just as diplopia due to divergence insufficiency, can occur in Chiari 1.5 [10]. Interestingly, clinical findings that are potentially attributable to brainstem compression are not found any more frequently in Chiari 1.5 compared to Chiari 1 [8]. Rarely, patients may present with inducible symptoms of vertebrobasilar insufficiency due to focal vascular compression [11]. Physical examination may be normal in the absence of a syrinx. Patients with a syrinx may develop dissociated sensory loss of pain and temperature with preservation of light touch and proprioception in the upper extremities in a cape-like distribution. This can be elicited in older children. As the syrinx progresses caudally, loss of the abdominal reflex can result. Rarely, symptoms progress to frank cervical myelopathy. Importantly, bowel and bladder symptoms are usually absent, as sphincter fibers are located at the periphery of the spinal cord and are relatively unaffected by the presence of a central cord syrinx. Rare findings include torticollis, weakness or myelopathy in the extremities, opisthotonos/irritability, and scoliosis [5]. Lower cranial nerve findings may include an absence of gag reflex, sleep apnea, and hoarseness. When oropharyngeal dysfunction is present, especially in patients under the age of 3 years, it should always prompt one to consider hindbrain herniation as a possible cause of brainstem compression [9].

Diagnosis and Management

Chiari malformations are most commonly diagnosed with magnetic resonance imaging (MRI) of the brain and spine. For any patient presenting with signs and symptoms concerning for craniocervical compression, non-contrast MRI of the brain and cervical spine is indicated. This is required to properly characterize the anatomy of the craniocervical junction, identify the presence or absence of tonsillar herniation, and elucidate potential causes of craniocervical compression or cerebrospinal fluid outflow obstruction. Importantly, other intracranial pathology, such as hydrocephalus or stigmata of idiopathic intracranial hypertension, should be ruled out as causes of cerebellar tonsillar herniation.

Chiari 1 malformation is classically defined as caudal descent of the cerebellar tonsils past the foramen magnum by more than 5 millimeters. This measurement is typically much more dramatic in patients with Chiari 1.5 malformations, which can be 12 mm or more in length [8]. There is an absence of tonsillar herniation in patients with Chiari 0 malformation.

Both the Chiari 1.5 and Chiari 0 malformations share the feature of a caudally displaced brainstem [3] (Figs. 3.1 and 3.2). The obex of the fourth ventricle, especially in Chiari 1.5, is often noted to be at or below the level of the foramen magnum (mean 14 mm below in one series [8], where it typically should reside 8–17 mm above the level of the foramen magnum in healthy patients) [7]. In the Chiari 0 population, the obex was found to be only 2 mm above the foramen magnum, or lower [3]. Naturally, the anteroposterior diameter of the cervicomedullary junction in the sagittal plane in these patients is slightly wider than average (13 mm in Chiari 0 versus 9.5 mm in controls), likely due to chronic caudal descent of the medulla oblongata, which is thicker than the spinal cord [3]. This is associated with a corresponding decreased width of the CSF spaces at the level of the foramen magnum in patients with Chiari 0 as compared to controls [2]. There is also an increase in the distance between the basion and opisthion in the midsagittal plane (34 vs. 28.6 mm in age-adjusted controls), indicating a larger-than-normal foramen magnum [3]. Other radiographic bony measurements of Chiari 1 with syrinx and Chiari 0 indicate that posterior fossa bones are underdeveloped and associated with skull base flattening, suggesting that a distorted posterior fossa may lead to foramen magnum and posterior fossa crowding in these patients [2].

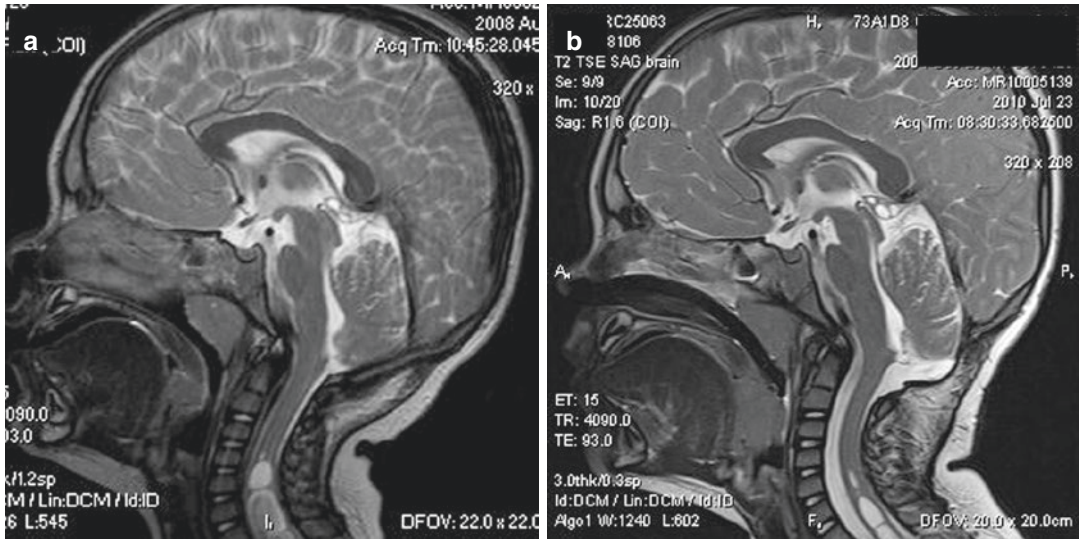

Fig. 3.1 Chiari 0 malformation. (**a**) Before and (**b**) after posterior fossa decompression. Notice the decompression at the cervicomedullary junction and decrease in the size of the syrinx

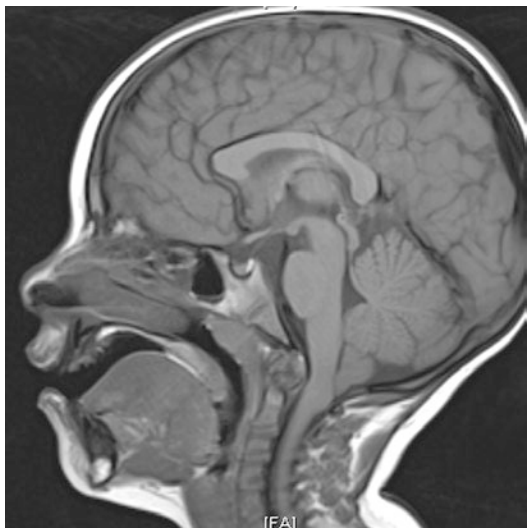

Fig. 3.2 Chiari 1.5 malformation. The position of the obex is below the level of the foramen magnum

Presence of a cervical spine syrinx is required for diagnosis of Chiari 0. Syrinxes in Chiari 1.5 (greater than or equal to 50% [8]) occur in similar frequency in patients with Chiari 1 malformations (50–70%). Syrinxes associated with Chiari malformations are thought to be a result of abnormal or obstruction of flow through the foramen magnum. When a syrinx is present, a complete brain and spine MRI with and without gadolinium contrast enhancement is required to characterize the extent of syringomyelia and to rule out intrinsic spinal cord neoplasm, tethered spinal cord, or spinal dysraphism as a cause of the syrinx [5]. A history of significant trauma, meningitis, arachnoiditis, and other explanations for syrinx development should be investigated [4, 5]. Syrinxes usually involve the cervicothoracic region. The size and length of the syrinx may range from a small cross-sectional area across a few spinal levels to a large, holocord syrinx.

CSF outflow obstruction at the foramen magnum may not be obvious if a normal anatomical morphology of the craniocervical junction is present on MRI. A cine flow study may be a useful adjunct for identifying a CSF outflow obstruction at the foramen magnum, especially in the presence of a cervical spine syrinx (i.e., Chiari 0 [6]). In one series, patients with Chiari 0 that lacked CSF flow through the foramen magnum on cine flow study showed restoration of flow after decompression [12]. Some clinicians believe that cine flow is not always accurate for identifying patients that may benefit from decompression [7]. Furthermore, intermittent and dynamic craniocervical compression due to craniocervical junction instability should be consid-

ered as an alternative explanation. Instability should be suspected in patients with large pannus formation posterior to the dens, as it is thought to represent ligamentous changes due to chronic hypermobility. Flexion and extension cervical radiographs are useful for evaluating this possibility. Thin-cut computed tomography (CT) of the craniocervical junction is necessary to examine the bony anatomy, if instability is present. Special attention is given to the location of the vertebral artery and its extracranial course for surgical planning purposes.

Accurate diagnosis of Chiari 1.5 and Chiari 0 is imperative for guiding management. Operative posterior fossa decompression should be considered for patients with credible signs and symptoms attributable to the presence of tonsillar ectopia and/or syringomyelia as defined above. Foramen magnum decompression should be considered before shunting an idiopathic cervical syrinx. It is also worth noting that very small syrinxes involving fewer than two spinal levels are commonly found incidentally and are asymptomatic. Close neurological and imaging follow-up of these patients, rather than posterior fossa decompression, is a reasonable approach.

Surgical Approach and Intraoperative Findings

A standard bony decompression of the foramen magnum with removal of the posterior arch of the atlas is the recommended operative approach to treat both Chiari 1.5 and 0 malformations [4, 5]. The patient is positioned prone on gel rolls with a head fixed in place in a flexed and capitally extended position with a three-point skull clamp. Midline dissection of the suboccipital musculature along the median raphe is essential to minimize postoperative pain and inadvertent vertebral artery injury. Care must be taken as one approaches the posterior C1 arch, as incomplete formation and C1 assimilation are sometimes encountered. Thickened bone at the foramen magnum and an upward lipping of the opisthion are also discovered in some patients. The size of the suboccipital craniectomy should be roughly 2.5 cm in width and height [7]. Excessive bony removal may result in cerebellar ptosis.

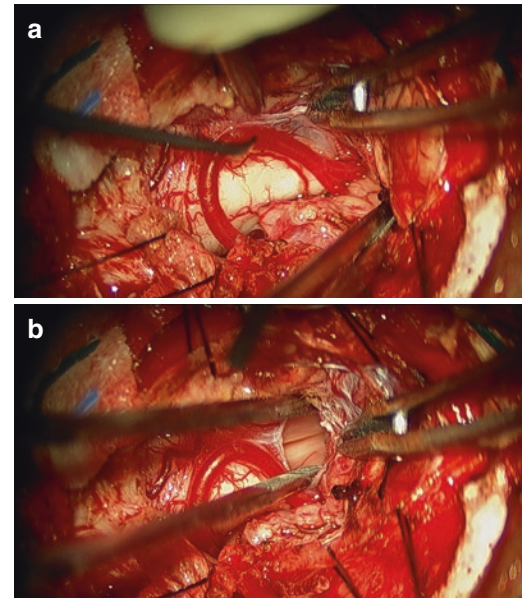

Fig. 3.3 Intraoperative finding of arachnoid veil over the fourth ventricular outlet in a Chiari 0 malformation patient (**a**) pre- and (**b**) post opening

Extra- and intradural decompression should be considered in cases of Chiari 1.5 and Chiari 0. Extradural compression can result from a small foramen magnum, thickened posterior lip of the occipital bone, or a taut atlantooccipital ligament. If an extradural offending agent in a patient with Chiari 1.5 is identified and adequately treated, intradural exploration may not be necessary. This can be confirmed by the use of intraoperative ultrasound to confirm CSF flow at the craniocervical junction represented by pulsations of the dentate ligament. In contrast, it is wise to conclusively rule out both intradural and extradural pathologies in Chiari 0 cases, as the suspected underlying etiology is CSF flow disturbances [7]. Unusual arachnoid adhesions or veils, scar tissue, and exaggerated tonsillar loops of PICA are all potential intradural causes of CSF flow obstruction (Fig. 3.3a, b) but are not found in every case [7]. If intradural exploration is pursued in Chiari 1.5 cases, extrapial cauterization of unilateral or bilateral, ectopic, cerebellar tonsils is an option.

It is important to minimize blood spillage into the subarachnoid space, as subarachnoid hemorrhage leads to inflammation that may further occlude free CSF flow in this region. All patients undergo duraplasty with autologous pericranium. This last maneuver is important to restore CSF flow around the craniocervical junction and facilitate watertight dural closure.

Clinical Outcomes

With proper patient selection, patients presenting with Chiari 1.5 or Chiari 0 malformations are expected to improve following operative decompression. Occipital headaches and neck pain usually improve rapidly, but other signs and symptoms, such as torticollis, paresthesias, and gait-related complaints, usually take weeks to months to improve. At long-term follow-up, 77.8% of patients significantly improved in Chiari 1.5, similar to Chiari 1 (81.7%) [1]. Associated hydrocephalus in Chiari 0 has a good chance of improvement without shunting [4].

Syrinxes often resolve in the months that follow decompression [5, 7]. In the Chiari 0 population, syrinx size was stable at 1 month postoperatively [12], and almost all decreased in size within 6–12 months (93.3% [7]), which is similar to Chiari 1 [9]. Scoliosis in Chiari 0 may stabilize with resolution of the syrinx and may even improve spontaneously over a period of months to years. However, this end result may be less successful in patients with Chiari 1.5 [8]; in one series, 13.6% of patients who presented with syringomyelia required repeated operation and was often associated with progressive scoliosis vs. 6.9% recurrence in Chiari 1 [8]. The relationship between symptom improvement and improvement in the size of the syrinx postoperatively is still not clear. In one study, symptoms often improved prior to improvement in syrinx size [12]. These numbers provide a good starting point for patient education.

Although it is reasonable to expect good surgical outcomes with Chiari 1.5 and Chiari 0 malformations, there remains clinical equipoise for how to treat patients who remain symptomatic after decompression surgery. The ideal postoperative recovery and waiting period for symptom or syrinx improvement are not established. Re-exploration after a certain observation period (around 6 months in our practice) and proceeding right to syringosubarachnoid or syringopleural shunting are both viable options [6, 13].

Conclusion

Patients with Chiari 1.5 malformations generally present similarly to Chiari 1 malformations and respond well to posterior fossa decompression, with the greatest difference being the presence of medullary herniation in Chiari 1.5 malformation. A separate entity, Chiari 0, is presumably a result of CSF flow abnormalities at the foramen magnum with the absence of tonsillar herniation. Foramen magnum decompression and elimination of any intradural outflow obstructions improve syrinx size and symptoms. Favorable clinical and radiologic responses are possible after restoring normal CSF flow dynamics.

References

1. Liu W, Wu H, Aikebaier Y, Wulabieke M, Paerhati R, Yang X. No significant difference between Chiari malformation type 1.5 and type I. Clin Neurol Neurosurg. 2017;157:34–9.
2. Bogdanov EI, Heiss JD, Mendelevich EG, Mikhaylov IM, Haass A. Clinical and neuroimaging features of "idiopathic" syringomyelia. Neurology. 2004;62:791–4.
3. Tubbs RS, Elton S, Grabb P, Dockery SE, Bartolucci AA, Oakes WJ. Analysis of the posterior fossa in children with the Chiari 0 malformation. Neurosurgery. 2001;48:1050–4.
4. Kyoshima K, Kuroyanagi T, Oya F, Kamijo Y, El-Noamany H, Kobayashi S. Syringomyelia without hindbrain herniation: tight cisterna magna. Report of four cases and a review of the literature. Neurosurgery. 2002;96:239–49.
5. Iskandar BJ, Hedlund GL, Grabb PA, Oakes WJ. The resolution of syringohydromyelia without hindbrain herniation after posterior fossa decompression. J Neurosurg. 1998;89:212–6.
6. Azahraa Haddad F, Qaisi I, Joudeh N, Dajani H, Jumah F, Elmashala A, et al. The newer classifications of the Chiari malformations with clarifications: an anatomical review. Clin Anat. 2018;31(3):314–22.

7. Chern JJ, Gordon AJ, Mortazavi MM, Tubbs RS, Oakes WJ. Pediatric Chiari malformation type 0: a 12-year institutional experience. J Neurosurg Pediatr. 2011;8:1–5.
8. Tubbs RS, Iskandar BJ, Bartolucci AA, Oakes WJ. A critical analysis of the Chiari 1.5 malformation. J Neurosurg Pediatr. 2004;101:179–83.
9. Greenlee JD, Donovan KA, Hasan DM, Menezes AH. Chiari I malformation in the very young child: the spectrum of presentations and experience in 31 children under age 6 years. Pediatrics. 2002;110:1212–9.
10. Strickland A, Baker CM, Siatkowski RM, Mapstone TB. Divergence insufficiency alleviated by posterior fossa decompression with duraplasty in a patient with Chiari type 1.5 malformation. J Neurosurg Pediatr. 2018;22(5):504–7.
11. Janjua MB, Ivasyk I, Greenfield JP. Vertebrobasilar insufficiency due to distal posterior inferior cerebellar artery compression in Chiari 1.5. World Neurosurg. 2017;4:1050.e1–e6. Epub 2017 Jun 3.
12. Ozsoy KM, Oktay K, Cetinalp NE, Gezercan Y, Erman T. The role of cine flow magnetic resonance imaging in patients with Chiari 0 malformation. Turk Neurosurg. 2018;28(2):251–6.
13. Shijman E, Steinbok P. International survey on the management of Chiari I malformation and syringomyelia. Childs Nerv Syst. 2004;20:341–8.

Part II

Embryology and Anatomy

4 Embryology of the Craniocervical Junction and Posterior Cranial Fossa

Mohammadali M. Shoja, Skyler Jenkins, and R. Shane Tubbs

Introduction

The notochord, primarily formed during embryogenesis, is the key initiator in stimulating neural tube development, sclerotogenesis, and paraxial mesoderm patterning [1–4]. Sensenig [5] described vertebral development as comprising three overlapping stages, which additionally incorporated bony elements in the occipital region that fuse early to form the basiocciput and exoccipiut. The first stage highlights the maturation of the notochord beginning the fourth week of embryogenesis. Specifics of notochordal development during early embryonic life are detailed and not the focus of review. The general aspects and features of notochordal development are schematized in Fig. 4.1 [6]. The second stage highlights the intense proliferation and migration of sclerotomic cells toward the notochord, formation of mesenchymal perinotochordal sclerotomes, expansion and patterning of the neural crest, and spinal nerve formation and occurs around the fifth and sixth weeks of gestation. The third and final stage consists of chondrification and ossification, starting around the middle of the sixth week.

Sclerotogenesis and Development of Vertebrae

Near the end of the fourth week of gestation, the primary sclerotomes are formed from the notochord-induced ventromedial migration of mesenchymal cells from the condensed paraxial mesoderm of the somites. These cells encircle the notochord to become the primary sclerotomes. These primary sclerotomes are grossly segmented following after the same pattern of the respective somites. With the rearrangement (or re-segmentation) of the primary sclerotomes, sclerotomal cells from differing somital origins pool together to form secondary sclerotomes with a segmentation pattern, which follows that in the final vertebrae [5]. Somitogenesis and the formation and rearrangement of primary sclerotomes all occur in a craniocaudal direction. Therefore, vertebral differentiation in the occipital and cervical regions precedes the development in the caudal region [5]. Along with sclerotomal rearrangement, a subpopulation of

M. M. Shoja
Division of General Surgery, Tabriz University of Medical Sciences, Tabriz, Iran

University of Illinois at Chicago, Metropolitan Group Hospitals, Chicago, IL, USA

S. Jenkins
Department of Anatomical Sciences, St. George's University School of Medicine, Grenada, West Indies

R. S. Tubbs (✉)
Department of Neurosurgery, Tulane University School of Medicine, New Orleans, LA, USA

Department of Neurosurgery and Ochsner Neuroscience Institute, Ochsner Health System, New Orleans, LA, USA

R. S. Tubbs et al. (eds.), *The Chiari Malformations*, https://doi.org/10.1007/978-3-030-44862-2_4

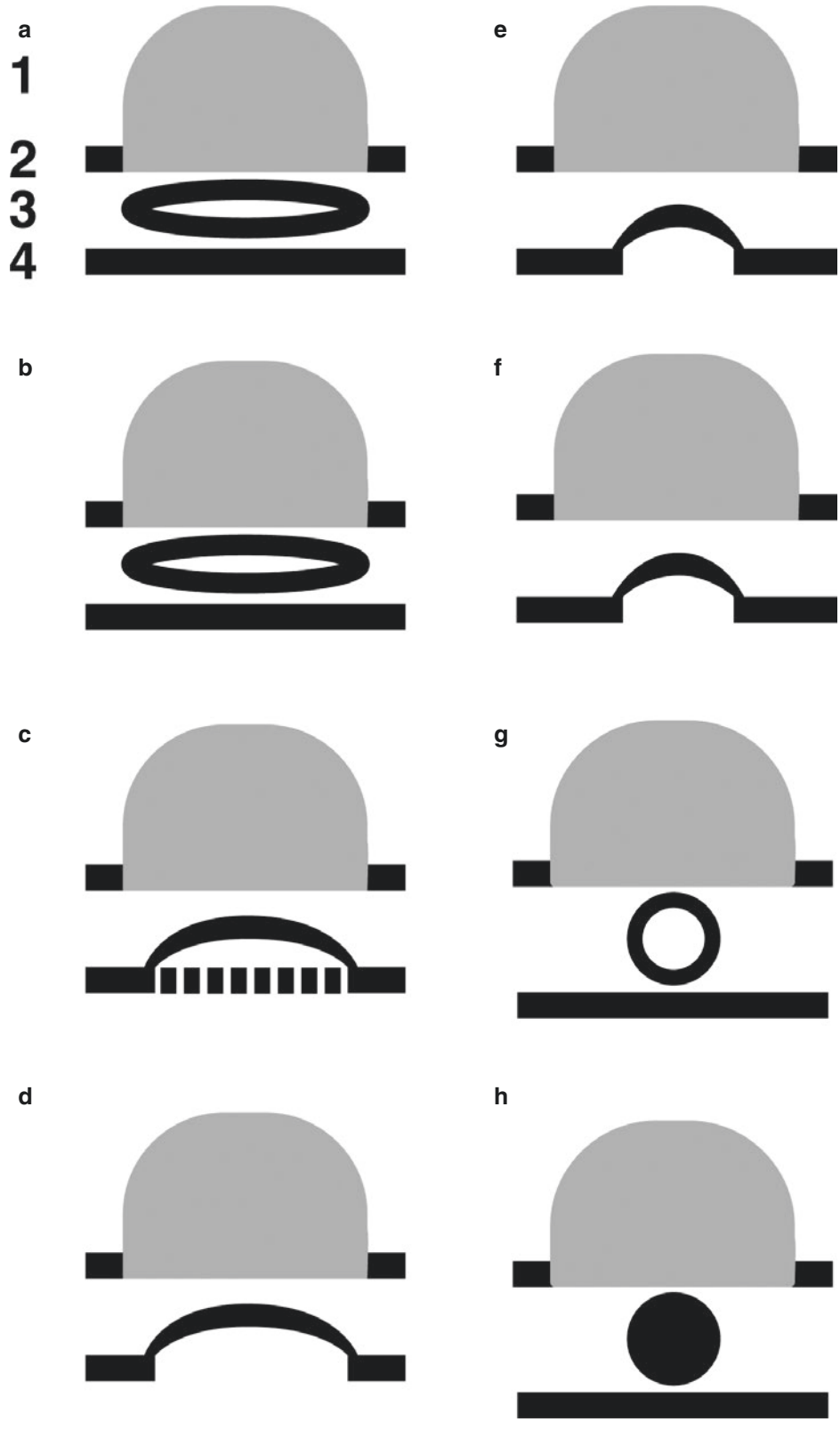
a
1
2
3
4
e
b
f
c
g
d
h

sclerotomes, which were derived from its densely packed cellular region, migrate dorsolaterally around the neural tube and between the spinal nerves and ganglia to establish the mesenchymal primordia of the vertebral arch [5]. The basic structure of the early vertebra is formed by the chondrification of the mesenchymal primordium of each vertebra and comprises a cartilaginous centrum (the future vertebral body) and a neural arch around the neural tube [5, 7]. It is crucial that the primary sclerotomes above and below the C2 vertebra adopt different rearrangement patterns in order to meet the anatomical and functional requirements of the craniovertebral junction above and the rest of vertebral column below.

The Development of Vertebrae Below C2

The fundamental concepts in vertebral development below the axis (C2 vertebra) were recognized over a century ago (cf. Robinson, 1918 [7]) and concluded in the seminal work of Sensenig in 1957 [5]. By the end of the first month of embryonic development, the notochord and neural tube are bounded by the skeletogenic mesodermal tissue composed of primary sclerotomes, which were derived from the ventromedial parts of somites that were found on either side of the neural tube. Dockter [8] explained that the cell distribution in each primary sclerotome is heterogeneous, with craniocaudal and mediolateral gradients. In addition, the caudal and lateral sclerotomal regions have a greater cell density than the cranial and medial regions. The initial segmentation of primary sclerotomes follows the somital pattern with re-segmentation occurring soon after. The spinal nerves and blood vessels emerge at the fissure of von Ebner, which separates the two halves of the primary sclerotomes on the lateral region. The secondary sclerotome is formed when the loosely cellular cranial half of each primary sclerotome combines with the densely cellular caudal half of the sclerotome above, corresponding to the future vertebra (Fig. 4.2). After dorsolateral migration of some of the sclerotomal cells, a dense lateral mass and a central mass (containing dense upper and loose lower regions) are apparent in each secondary sclerotome (Fig. 4.2). The dense lateral mass gives rise to the vertebral arch, comprised of the pedicle, articular facets, and lamina. The larger lower loose region within the central mass gives rise to the centrum (body) of the vertebra. The narrow band of densely cellular sclerotomal tissue retained between the centra of the secondary sclerotomes is sometimes referred to as the hypochordal bow [7, 9], perichordal disc [5], hypocentrum [10], or intercentrum [11]. In this review, the term "hypochordal bow" is preferred. It is believed that the hypochordal bow degenerates into the fibrous part of the intervertebral disc [7].

Development of the Craniocervical Junction

Ludwig [12], O'Rahilly and Müller [9], and Müller and O'Rahilly [13, 14] have contributed extensively to the current knowledge of craniovertebral junction development. The superior

Fig. 4.1 Schematized drawing of a transverse section through the midportion of the embryonic plate showing notochordal development and maturation. Upon formation of the primitive streak from the ectoderm on the dorsal midline of the embryonic plate, the mesodermal precursor cells originating from the primitive streak migrate between the ectoderm and endoderm (not shown here). The longitudinal midline condensation of the mesodermal cells forms the head process or notochordal plate in front of the primitive streak. (**a**) The notochordal plate (3) has a lumen, a floor next to the endoderm (4), and a roof next to the neural plate (1) of the ectoderm (2). (**b**) The floor of the notochordal plate fuses with the endoderm. (**c**, **d**) The floor then disappears, leaving the roof of the notochordal plate (known as the notochordal groove at this stage) attached to endoderm on either side. (**e**, **f**) The notochordal groove deepens and its margins approximate each other by the growth of the endoderm. (**g**) Following the fusion of the margin of the notochordal groove, the notochordal tube is formed and is liberated from the endoderm. (**h**) The lumen of the notochordal tube disappears and the tube solidifies to form the mature notochord. This description is based on Frazer [6]

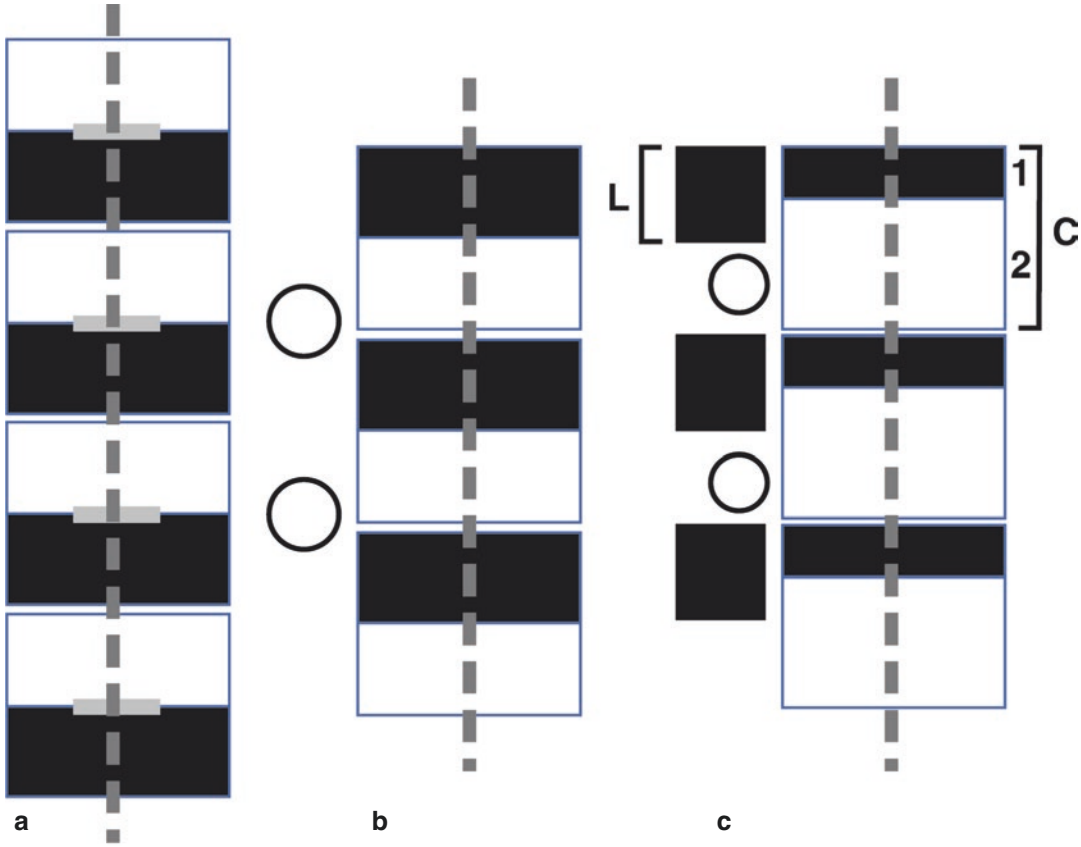

Fig. 4.2 Simplified model of the rearrangement of primary sclerotomes and development of vertebrae below C2. (**a**) Shows primary sclerotomes with loose upper (white) and dense lower (dark) regions partially separated by the fissures of von Ebner (gray horizontal bars). The longitudinal dashed line represents the notochord. (**b**) Shows the secondary sclerotomes following rearrangement. The circles represent the spinal root ganglia, nerves, and blood vessels emerging at the level of the loosely cellular region. (**c**) Shows the sclerotomic primordia of the vertebrae following dorsolateral migration of a subpopulation of cells from the dense region between the spinal root ganglia and nerves. At this stage, the central (C) and lateral (L) masses are discernible. The central mass is composed of the hypochordal bow (1) and centrum (2)

four somites, the occipital somites 1–4, are formed from the ventromedial migration of sclerotomal cells from somites 1 to 4 toward the cephalic notochord. This cellular migration gives rise to primary occipital sclerotomes 1–4 (O1–O4). The hypoglossal nerve rootlets course laterally between the hypochordal bows of the occipital sclerotomes, whereas the C1 spinal nerve courses between the hypochordal bows of O4 and sclerotome 5 (S5 or first cervical sclerotome). Initially, occipital sclerotomes 1–3 join to form the main portion of the mesenchymal basiocciput [9]. In an embryo of 9 mm crown-rump length, approximately the fifth week of gestation, the hypochordal bows of O4 (proatlas) and S5 (atlas) are distinct in the craniovertebral junction [12]. These hypochordal bows are ventral to the notochord [12]. The rostral O1–O3 hybrid and O4 join together in an embryo of 9–11 mm CRL (approximately the sixth week of gestation) to form a mesenchymal O1–O4 hybrid, which surrounds the cephalic end of the notochord [9]. This mesenchymal hybrid becomes chordal cartilage, later in gestation, after chondrification occurs. The hypochordal bow of O2 is small and disappears medially while fusing laterally with the hypochordal bow of O3. The dorsolateral extensions of the hypochordal bows of O2–O4 form the lateral masses. Further dorsal extension of these masses adds to the development of the exocciput, homologous to the neural arch of a typical vertebra. O3 forms the portion of the

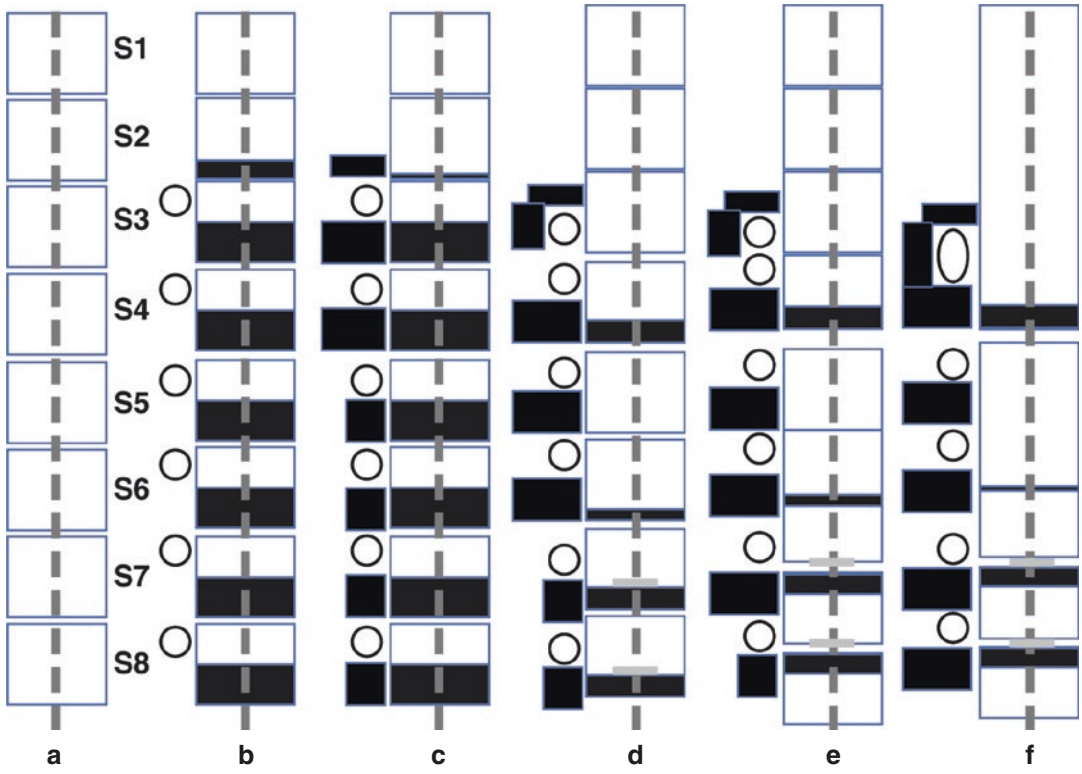

Fig. 4.3 A simplified model of craniovertebral junction and upper cervical vertebral development based on O'Rahilly and Müller [9], Müller and O'Rahilly [13], and Sensenig [5]. (**a**) With migration of ventromedial somital cells toward the notochord, segmented sclerotomes are formed. The longitudinal dashed lines represent the notochord. (**b**) The lower half of occipital sclerotomes 2, 3, and 4 and cervical sclerotomes undergo condensation (dark regions). Segmental ganglia and nerves, represented by circles, develop from the neural crest. (**c**) The cells from the caudal half of the sclerotome migrate dorsolaterally through the interganglionic space. Note the craniocaudal gradient in the development of the neural arches, with more dorsolateral extension of the hypochordal bows in the occipital region than in the cervical region. At this stage, the median (central) and lateral segments are established, roughly representing the centrum and neural arch of a developing vertebra. The median part of the hypochordal bow of S2 begins to disappear. The median segments of S3–S8 are still composed of dense caudal and loose rostral parts. (**d**) The dense caudal parts of the centra of S2 (or O2) and S5 (C1) disappear. The dense caudal parts of the other sclerotomes are now smaller. The fissures of von Ebner (horizontal gray bars) separate the caudal and loose rostral parts of S7 and S8 (C3 and C4, respectively). The median portion of the hypochordal bow of S3 disappears. The lateral mass derived from the hypochordal bow of S2 is fused with the hypochordal bow of S3 laterally, leaving the two hypoglossal nerve rootlets within in a single canal. (**e**) The rearrangement at the S7–S9 centra occurs in such a way that the dense caudal part of S7 joins the loose rostral part of S8 (S7–S8 fusion or future C3 vertebra) and the dense caudal part of S8 joins the loose upper part of S9 (S8–S9 fusion or future C4 vertebra). S9 is not shown in **a**–**d**. The centra of S1 to S4 fuse to form the basiocciput. The centra of S5 and S6 and the loose rostral part of the S7 centrum fuse to form the dens and body of the C2 vertebra. Note the hypochordal bows of S3 and S4 are fused laterally. (**f**) The final rearrangement of the occipitocervical junction is achieved. Note the hypoglossal nerve within the exocciput formed by fusion of the lateral bars (or extensions) of the hypochordal bows of O2–O4. The lateral bars of S7 and S8 form the neural arches of C3 and C4. Fusion of the upper dense parts of S7–S8 forms intervertebral disc C2–C3, and fusion of the upper dense parts of S8–S9 forms intervertebral disc C3–C4. The development of the remaining vertebrae is similar to that of the C3 and C4 vertebrae

exocciput rostral to the hypoglossal nerve and canal, whereas O4 forms the caudal portion. Ultimately, the lateral masses of S3 and S4 fuse to create a single exocciput ventral and dorsal to the hypoglossal canal. Loosely packed sclerotomal cells between the hypochordal bows of the proatlas and atlas, corresponding to the centrum of primary sclerotome 5, contribute to the occipital condyles laterally and the tip of the odontoid process of the axis medially [9, 13].

A simplified model of craniovertebral junction development is presented in Fig. 4.3. The hypo-

chordal bow of O3 degenerates except for its lateral projections. These projections are exaggerated by fusing with the hypochordal bow of O2 and contribute to the exoccipital. At 5 weeks of gestation, the hypochordal bow of O3 is noticed laterally superior and anterior to the hypochordal bow of O4 [9]. An osseous separation within the hypoglossal canal is formed by the medial remnant of the hypochordal bow of O3 [14]. The median part of the hypochordal bow of O4 remains as a continuous mass across the midline and begins fusing with the remainder of the basiocciput rostrally during the mesenchymal stage [9]. After chondrification, its fusion is completed, forming the basion. The hypochordal bow of S5 forms the anterior arch of the atlas and disappears from between the loosely packed regions of the S5 and S6 sclerotomes [14]. The lateral mass of S5 (C1) encompasses the odontoid process and forms the neural/posterior arch of the atlas [13, 14], whereas the lateral mass of S6 forms its neural arch.

Development of the Occipital Condyle

The occipital condyles arise from the anterolateral region of the foramen magnum and are two semilunar prominences with an inward concavity and outward convexity [10]. The condyles form a cartilaginous articular facet that is convex ventrodorsally and mediolaterally. They also have an osseous portion and are larger medially than laterally. During embryogenesis, the hypochordal bow of S4 and loosely packed region of S5 form the sclerotomic primordia of the occipital condyles. After chondrification in the occipital region, the basioccipital and exoccipital components are united, and the ossification centers appear independently within these segments. The anterior intraoccipital synchondrosis is formed from the fusion of the ventral and dorsal regions of the exoccipital and suboccipital ossification centers. This synchondrosis traverses the occipital condyle and is seen in children, corresponding to the unossified anterior intraoccipital synchondrosis [15]. This synchondrosis divides the condyle into a smaller, anterior basioccipital area and a larger, posterior exoccipital region [15]. The ossification of this synchondrosis occurs in a mediolateral direction [15], beginning at 1–2 years of age and is completed by 7–10 years of age [16]. After complete fusion, the occipital condyle presents as a single osseous prominence with a uniform articular facet. Sometimes, however, adults have a transverse division of the articular facet, resulting from maceration of its midportion [15].

A bony ridge ("prebasioccipital arch") sometimes connects the anterior ends of the occipital condyles in front of the anterior rim of the foramen magnum [17–21]. If the medial part of this ridge disappears, its lateral part will be retained unilaterally or bilaterally, forming the basilar process, which appears ridge-like or bumpy [18]. However, if the lateral part were to disappear, the medial part of the ridge could remain as a single median or two paramedian projections [18, 22]. These variants include the pseudocondylus tertius [18, 19] or precondylar process [22] and the true condylus tertius, which is found at the anterior rim of the foramen magnum [19, 20] (Fig. 4.4 [21, 23]). Both of these are derived from the hypochordal bow of the proatlas—remnants of the anterior arch of the proatlas [18]. The precondylar process is a continuation of the anterior end of the occipital condyle [18] and is positioned slightly anterior to the foramen magnum.

Proatlas Segmentation Malformation and Variable Manifestations of the Proatlas

The proatlas, found in some lower vertebrates but not normally in man, is a separate and unique atlas-like vertebra partitioned between the occipital bone and the atlas [24, 25]. Under normal conditions in man, it is formed from the failure of fusion of the hypochordal bow of S4 with the centrum of S5. It partially regresses and normally only contributes to the inferior portion of the basiocciput and the caudal part of the exoccipital. The centrum of S5 forms the apex of the dens, the medial portion of the apical ligament, and con-

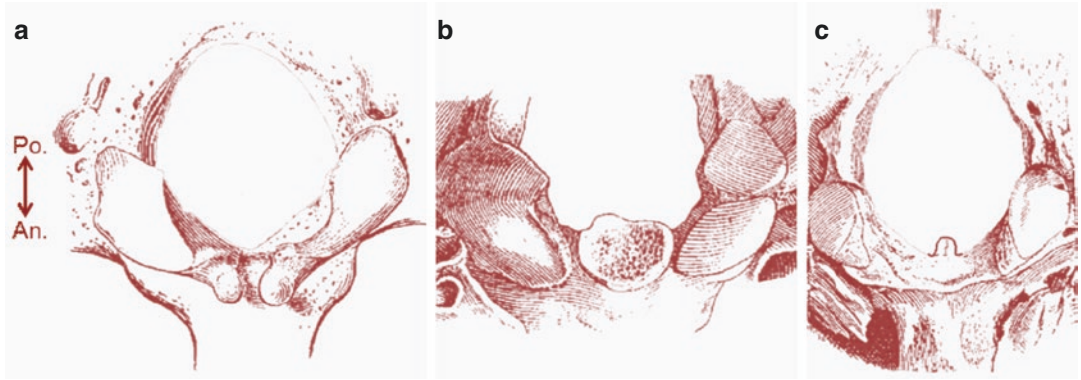

Fig. 4.4 The remnants of the anterior arch of the proatlas. (Reproduced from Oetteking B [21]. with permission from John Wiley and Sons). The arrow shows the orientation of the specimens: An., anterior; Po., Posterior. (**a**) Shows two basilar processes (the paramedian precondylar processes). (**b**) Shows a single large condylus tertius. (**c**) Shows a backward spur-like projection from the median portion of the anterior margin of the foramen magnum. Some advocate that this spur-like projection is not derived from the proatlas but represents ossification of the attachment of the apical ligament [21, 23]

tributes to the development of the lateral regions of the occipital condyles. This unique craniovertebral sclerotomal segmentation pattern dictates that the mesodermal constituents of the proatlas in man should be integrated into the occipital bone and axis. However, the craniovertebral junction may have anomalies and variations termed "proatlas segmentation failure or malformation" [26–28] if (1) the segmentation pattern of this junction is disordered; (2) the proatlas' mesodermal constituents are abnormally distributed; (3) the hypochordal bow of S4 hypertrophies or fails to regress partially; or (4) the centrum of S5 is abnormally liberated from the axis or fuses with the hypochordal bow of S4. The associated anomalies or variations are collectively referred to as "proatlas remnants" or "manifestations of the proatlas," which are grouped under a broader category of "manifestations of the occipital vertebrae" (Table 4.1) [7, 9, 14, 15, 17, 19, 21, 22, 27–56].

In an evolutionary sense, the proatlas segmentation malformation represents a phylogenetic regression in the ontogeny of the craniovertebral junction with an attempt to retain the proatlas and liberate it from the occipital region [47, 48]. To our knowledge, there has only been one reported case of a persistent proatlas as an additional atlas-like vertebra in the human species [57–59].

Due to the complicated developmental process, the anatomical presentations of proatlas segmentation malformation are variable with some being more relevant clinically. Less clinically relevant presentations include remnants forming the basilar and precondylar processes and prebasioccipital arch. The incidence of clinically significant anomalies is 1.4% and usually consists of lower brain stem compression [26], as well as anomalous bony excrescences around the foramen magnum [26, 47]. In such cases, the apex of the odontoid process is absent, and the basiocciput tends to be elongated, protruding posteroinferiorly into the foramen magnum [26, 29]. This protrusion is embryologically derived from the centrum of S5. Occasionally, the apex of the dens may be present but is typically small and malformed. In cases where there is no hypoplasia of the odontoid, the posteroinferiorly directed median bony projection at the anterior margin of the foramen magnum is the third occipital condyle (condylus tertius), which sometimes articulates with the apex of the dens or the anterior arch of the atlas [19]. As the notochord travels toward the back of the hypochordal bow of S4, the osseous anomalies in front of the apical ligament, such as the condylus tertius, represent the derivatives of the hypochordal bow. The apical ligament attaches to the basion over

Table 4.1 Some developmental anomalies and osseous variations of the occipital bone including manifestations of occipital vertebrae

Anomaly or variation	Description	Reference(s)
Canalis basilaris medianus	Postnatal remnant of the cephalic notochord; presents as a well-corticated longitudinal canal in the midline of the basiocciput	Madeline and Elster [32]
Median basioccipital raphe	Midline trace of the median fusion of the parachordal plates	Madeline and Elster [32]
Longitudinal basioccipital cleft	Partial midline cleft in the basiocciput; is reminiscent of midline fusion of the bilateral parachordal plates	Madeline and Elster [32]
Cruciform spheno-occipital synchondrosis	Longitudinal anterior basioccipital and postsphenoidal clefts in conjunction with unossified spheno-occipital synchondrosis	Madeline and Elster [32]
Transverse (coronal) basioccipital cleft	Results from retention of the segmented nature of the basioccipital primordium; can traverse the basiocciput partially or completely; can be an incomplete groove or a complete gap; is radiographically similar to the spheno-occipital synchondrosis but is actually filled with fibrous tissue not cartilage; very rare	Kruyff [33]; Johnson and Israel [34]; Prescher [19]
Basioccipital hypoplasia	A consequence of paraxial mesodermal insufficiency in the occipital region or premature closure of the spheno-occipital synchondrosis; associated with basilar invagination	Smoker [35]; Nishikawa et al. [36]; Noudel et al. [37]
Fossa navicularis	A shallow depression measuring ~3 × 5 mm on the undersurface of the anterior portion of the basiocciput	Cankal et al. [38]
Pharyngeal tubercle	A median tuberosity on the undersurface of the basiocciput about 1 cm anterior to the foramen magnum; is the point of attachment of the pharyngeal raphe; a tubercle of 1.5–2.0 cm diameter is radiographically apparent in 3.8% of cases	Robinson [7]; Hauser and De Stefano [39]; Finke [40]
Bipartite hypoglossal canal	Division of the hypoglossal canal by a bony spicule; is a remnant of the hypochordal bow of S3	O'Rahilly and Müller [9]; Müller and O'Rahilly [14]
Divided (bipartition of) occipital condyle	Partial or complete subdivision of the articular facet; can be unilateral or bilateral; associated with division of the superior articular facet of the atlas; has an incidence of ~5%	Tubbs et al. [41]; Kunicki and Ciszek [42]; Tillmann and Lorenz [15]
Condylar hypoplasia	Underdevelopment of the occipital condyles; associated with a more horizontal than oblique orientation of the atlanto-occipital joint and basilar invagination	Smoker [35]
Occipitocondylar hyperplasia	Hypertrophy of the occipital condyles; can cause cervicomedullary compression	Ohaegbulam et al. [43]; Halanski et al. [44]
Paracondylar (paramastoid or jugular) process	A pneumatized osseous process in the lateral condylar area (jugular process of the occipital bone) located between the occipital condyle and mastoid process at the point of insertion of the rectus capitis lateralis muscle; can be unilateral or bilateral; may or may not fuse with the transverse process of the atlas; has an incidence of 2–4%	Lang [45]; Tubbs et al. [41]; Anderson [46]; Taitz [17]; Prescher [19]
Lateral (transverse) process of the occipital condyle	Is homologous to the transverse process of the atlas arising from the its lateral mass; is a proatlas remnant	Stratemeier and Jensen [47]; Gladstone and Erichsen-Powell [48]
Prebasioccipital arch or anterior lip of the foramen magnum	A U-shaped ridge connecting the end of the occipital condyles; manifests as the ventral arch of the proatlas	Prescher [19]; Taitz [17]; Oetteking [21]
Basilar process	Lateral tubercle and the remains of the prebasioccipital arch; a proatlas remnant; is sometimes considered a variant of or the same as the precondylar process	Prescher [19]; Oetteking [21]

Table 4.1 (continued)

Anomaly or variation	Description	Reference(s)
Condylus tertius	A downward bony projection located just at the anterior margin of the foramen magnum; associated with an increased prevalence of os odontoideum; has an incidence of ~1%	Smoker [35]; Prescher [49]; Prescher [19]
Precondylar process or pseudocondylus tertius	A single median or two paramedian projection(s) from the inferior surface of the basiocciput located a few millimeters in front of the anterior margin of the foramen magnum; has an incidence of up to 25% in adults; is a proatlas remnant; is also regarded as an ossification in the median portion of the anterior atlanto-occipital membrane; unlike the condylus tertius, it contains a sagittal canal	Vasudeva and Choudhry [22]; Prescher [19]; Hauser and De Stefano [39]
Anteromedian tubercle of foramen magnum	A small median triangular tubercle projected horizontally backward from the anterior border of the foramen magnum; is distinct from the condylus tertius, which projects downward; can represent ossification of the attachment of the apical ligament	Lakhtakia et al. [50]; Prescher [19]; Oetteking [21]
Posterior lip of the foramen magnum	A bony ridge extending from the posterior end of one or both occipital condyle(s) along the posterior foraminal margin; does not fuse posteriorly; can be hypertrophied and manifest as the bony excrescences around the posterior margin of the foramen magnum; remnants of the dorsal arch of the proatlas	Gladstone and Erichsen-Powell [48]; Prescher [19]; Menezes and Fenoy [29]; Oetteking [21]
Kerckring or Kerckring-like ossicle(s)	A single median or paramedian ossicle at the lower edge of the supraocciput; there may be two paramedian ossicles, which then fuse to form a single median ossicle; appears in the fourth and fifth fetal months and usually fuses with the supraocciput before birth; rarely remains completely separated; although controversial, some have regarded it as a remnant of the proatlas	Piersol [51]; Le Double [52]; Caffey [53]; Madeline and Elster [32]
Accessory ossicle(s) of the innominate (posterior intraoccipital) synchondrosis	Is seen in 0.4% of newborns as one to four ossicles within the synchondrosis between the supraocciput and exocciput; can be large and protrude externally and internally; fuses with the supraocciput in the first year of life; the medially located ossicles can be considered as proatlas remnants	Caffey [53]
Persistent transverse occipital fissure/suture	A fissure/suture between the intermediate and interparietal parts of the occipital squamous; is sometimes misnamed the mendosal suture	Lochmuller et al. [54]; Nayak et al. [55]; Tubbs et al. [56]
Atlanto-occipital assimilation	Partial or complete fusion of the atlas and occipital bone along the margin of the foramen magnum; associated with basilar invagination	Smoker [35]

the condylus tertius [10]. Clinically significant variants of the proatlas remnants include (1) a triangular projection from the anterior margin of the foramen magnum, (2) a medial indentation from the occipital condyle and non-fusion, (3) inward displacement and hypertrophy of the condyle, (4) os terminale persistens (Fig. 4.5) [48, 60], and (5) os odontoideum [20, 26, 47]. Menezes [29] found that 8 out of 100 patients had clinically significant proatlas segmentation malformations with Chiari malformation and craniovertebral junction anomalies. Likewise, hindbrain herniation accompanied proatlas segmentation malformations in 33% of cases [26].

Ossification of the Atlas

The mesodermal primordium of the atlas is derived from the hypochordal bow of S5. Ganguly and Roy [10] believed that before the embryo attains a CRL of 30 mm (approximately the eighth gestational week), the precartilaginous proatlas is divided and its dorsal caudal half incorporates into the cartilaginous primordium of the atlas, while its ventral cranial part incorporates into the occipital cartilage at the anterior margin of the foramen magnum. Though other authors share this view [26, 61], its accuracy is uncertain. This uncertainty is due to the absence

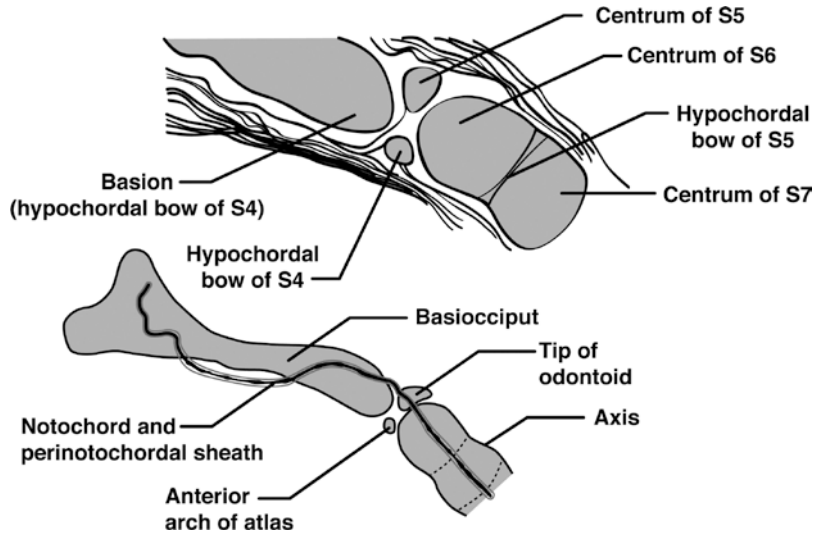

Fig. 4.5 Embryogenesis of the proatlas segmentation malformation—os terminale persistens (Bergman's ossicle) variant (after Gladstone and Erichsen-Powell [48]). The upper and lower images show the mesenchymal/chondrified and osseous stages of the craniocervical junction, respectively. In the upper image, a small segment of notochord (star) is shown traversing between the centra of S5 and S6. In the lower image, the original fetal position of the notochord is superimposed on the components of the craniocervical junction. Note that the hypochordal bow of S4 contributes to the basion and the centrum of S5 to the tip or apophysis of the odontoid. Normally, the centra of S5–S7 fuse to form the dens and body of the axis. Failure of fusion leads to the formation of an independent center for chondrification and ossification in the S5 centrum and results in the tip of the odontoid being isolated, giving rise to os terminale persistens. On the other hand, if mesenchymal fusion and chondrification of the dens occur normally, the apex of the odontoid can be separated from the body of the dens by an intervening synchondrosis derived from the vestigial remnant of the S5 hypochordal bow. This synchondrosis usually ossifies; however, failure of this ossification gives rise to os terminale persistens. The notochord has an S-shaped course through the basiocciput and passes through the os terminale persistens. It is located on the ventral surface of the basiocciput at its midportion and travels obliquely within its rostral and caudal parts [60]

of embryonic specimens relating to the 11–30 mm CRL, a major period in the development of the craniovertebral junction as presented by Ganguly and Roy [10]. During the fifth week of gestation, Macalister [62] showed that the ring of the atlas had been completely chondrified, and by the seventh week the right and left posterior bony hemi-arches are formed. These arches are formed from two ossification centers that appear at the root of the posterior arch close to the lateral masses and grow in a retrograde direction. This growth continues after birth until the right and left hemi-arches of the posterior arch fused and closed in the dorsomedian plane at 4 years of age. The bilateral ossification centers also extend forward into the lateral masses and outward into the transverse processes [62]. There is a delay in the ossification of the anterior arch, which commences during the first year of life. Initially, two unequally sized ossification centers appear in the median part of the cartilaginous anterior arch, which rapidly fuse to form a single dominant ossification center; this grows backward and laterally to join the lateral mass by the fifth year of age [62]. If there is failure in the development of the median ossification centers of the anterior arch, ossification will then proceed to the midline from the lateral masses of the atlas [63].

The Atlanto-Occipital Assimilation and Other Developmental Anomalies of the Atlas

One of the most common anomalies of the craniovertebral junction, with a prevalence of 0.5–3%, is the occipitalization of the atlas, or atlanto-occipital assimilation/fusion. This is a

process by which the atlas is either completely or partially fused with the occipital bone [64–67] and it appears to have a multifactorial causation, often aggregated in families [68]. The syndromic forms of atlanto-occipital assimilation have been associated with Klippel-Feil syndrome and DiGeorge syndrome [61, 66]. Embryologically, the assimilation takes place when the primordia of the atlas and occiput are still cartilaginous [62]; however, it may also occur during the early mesodermal stage. The anterior arch of the atlas fuses with the basion at the anterior margin of the foramen magnum, the posterior arch with the lower end of the supraocciput at the posterior margin of the foramen magnum, the superior articular facet with the occipital condyles anterolateral to the foramen magnum, and the transverse process of the atlas with the jugular process of the occipital bone [62, 63]. Atlanto-occipital assimilation results in a 15–35% reduction in the surface area of the foramen magnum [69] and is occasionally associated with os odontoideum and basilar invagination [66]. Animal models have shown that this atlanto-occipital assimilation may be related to aberrations in homeobox (*Hox*) gene expression, which code for transcription regulator proteins involved in patterning and determining the segmental fate of the axial skeleton in vertebrates [70–73]. In an evolutionary sense, and unlike the proatlas segmentation malformation, atlanto-occipital assimilation represents phylogenetic progression in the ontogeny of the craniovertebral junction with an attempt to integrate an additional vertebra into the occipital region [47, 48].

Other developmental anomalies of the atlas have been reported [20, 62, 63]. Defects—such as hypoplasia, dysplasia, agenesis, or clefts—in the anterior arch are less common than in the posterior arch. In a series of 21 patients with either confirmed or suspected Chiari I malformation, agenesis of the anterior or posterior arches of the atlas or variable degrees of atlanto-occipital assimilation were the most frequent osseous anomalies at the craniovertebral junction [74]. Menezes [29] found that atlanto-occipital assimilation was present in 92% of patients with Chiari malformation and concomitant craniovertebral junction anomalies [29]. These observations suggest that anomalies of the atlas are familiar in patients with hindbrain herniation and could indicate a common underlying ontogenetic error or could actually entail a cause-effect relationship.

Basicranial Development

The basicranium is composed of a flat anterior part and an oblique posterior part (clivus). The posterior part comprises basisphenoidal (anterosuperior) and basioccipital (posteroinferior) segments that are joined by an intervening spheno-occipital synchondrosis; the caudal portion of the synchondrosis is delineated by the rostral end of the notochord. The development of the basicranium proceeds in three stages: mesenchymal condensation, chondrification, and ossification [75, 76]. Once the mesenchymal (desmal or blastemal) basicranium is formed, chondrification and ossification take place in a posteroanterior direction, starting with the posterior cranial fossa and ending with the anterior fossa [75]. Chondrification and ossification take place at the same time in different locations. For example, chondrification of the anterior portion of the basicranium takes place while the posterior basicranium begins ossifying [75]. During the third month of gestation, chondrification is completed. The following relates to the posterior basicranium, which contributes to the formation of the posterior cranial fossa.

The segmented (sclerotomal) nature of the developing basiocciput has been studied in calves, in rats, and in humans (cf. Schäfer et al. [77]). The initial mesenchymal primordium of the basicranium was found to occur during the first month of gestation. Chondrification appears in the basioccipital region during the second month [77]. During the fifth week of gestation, two longitudinal cartilaginous plates (also referred to as parachordal plates) are formed on either side of the cephalic notochord [60, 75, 77]. Simultaneously, the cartilaginous otic capsule is also developing but is separate from the parachordal cartilage [75, 77]. The two parachordal plates fuse across the midline to form a single plate, known as the basal or chordal plate, surrounding the notochord [75, 77]. The cartilagi-

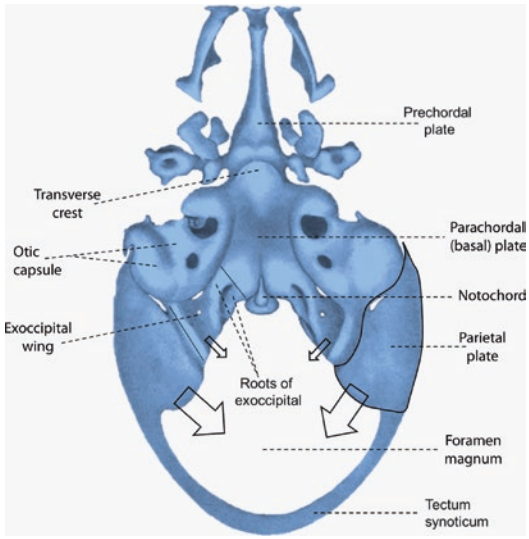

Fig. 4.6 Basichondrium of a 20 mm CRL embryo, approximately eighth week of fetal life. (Modified with permission from Kernan Jr. [79]). The foramen magnum is very large at this stage. The exocciput is shown between two solid lines on the left side. The territory of the parietal plate is marked on the right side. The parietal plate of the occipital bone is fused anteroinferiorly with the otic capsule and posteroinferiorly with the exocciput. It extends posteriorly as the tectum synoticum. The caudal portion of the prechordal cartilage contributes to the basisphenoid, whereas the anterior basicranium is developed from the rest of the prechordal cartilage and the appendages [78]

nous otic capsule is then incorporated into the basal plates laterally [77]. The segmented nature of the basiocciput begins to disappear during the late mesenchymal stage and is totally lost with fusion of the cartilaginous centers [77, 78]. The occipital plate, the cartilaginous primordium of the exocciput, is formed from the caudal division and dorsolateral extension of the basal cartilage in both a horizontal plane and on either side of the foramen magnum [77–79]. The hypoglossal nerve passes through a foramen in the cartilaginous exocciput. This foramen is large during the cartilaginous stage but becomes smaller with ossification. Anterior to the rostral end of the notochord, which also marks the rostral border of the parachordal plates, chondrification occurs in the prechordal cartilage and its appendages [78].

In an embryo of 20 mm CRL (eighth week of gestation), the basichondrocranium is composed of four regions: occipital, otic, orbitotemporalis, and ethmoidal [79]. Kernan studied the development of the basichondrocranium and found that its central portion is comprised of two continuous ventral and dorsal cartilaginous bars, the chordal and prechordal plate, respectively, marked by a transverse crest between them (Fig. 4.6) [78, 79]. The transverse crest is the primordium of the dorsum sellae. The cartilaginous otic capsule is fused with the lateral border of the basal plate, and the line of fusion is marked as the basicapsular commissure or sulcus. The caudal end of the basal plate marks the anterior margin of the foramen magnum. Ventrally, each exoccipital plate is composed of two cranial and caudal roots with an intervening foramen through which the hypoglossal nerve travels. These roots represent the pedicles (neural arches) of the occipital vertebrae. Dorsally, the two roots unite to form a single flat cartilaginous plate known as the exoccipital wing. Ventrally, the lateral border of the exoccipital plate is separated from the otic capsule by the jugular foramen and is dorsally fused with it at the capsulo-occipital commissure. At its posterior border, the exoccipital wing joins a thin plate of triangular cartilage known as the parietal plate of the occipital bone, the apex of which is pointed anteriorly toward the otic capsule. The superior border is free, whereas the inferior border of the parietal plate fuses with the otic capsule anteriorly and the exoccipital wing posteriorly. From the upper part of the posterior border of the parietal plate, a narrow band of cartilage extends from either plate dorsally and fuses with the contralateral counterpart to form a thin ribbon of cartilage known as the tectum synoticum of “Kernan” or tectum cranii anterius of “Fawcett” (Fig. 4.6) [78, 79]. At this stage, the basichondrocranium contains a very large foramen magnum.

The later stages in basichondrocranial development are prominently characterized by development in the posterior occipital region between the parietal plates and exoccipital wings of both sides. This region corresponds to the cartilaginous supraoccipital part of the occipital squamous bone. As indicated by the arrows in Fig. 4.6, the parietal plates (below the tectum synoticum) and exoccipital wings of the right and left sides extend dorsomedially. These ultimately fuse in the dorsal midline, forming the tectum posterius

of "Kernan" or tectum cranii posterius of "Fawcett"—a wide, trapezoidal cartilaginous plate posterior to the foramen magnum. Simultaneously, the tectum synoticum undergoes regression. This view has been supported by Levi [80], Macklin [81], and Kernan [79] and more recently by Müller and O'Rahilly [82]. With regression of the tectum synoticum, the parietal plate simultaneously shrinks [79]. The posterior aspect of the basichondrocranium and occipital region in a fetus of 43 mm CRL (approximately 12th week of fetal life) is shown in Fig. 4.7 [81]. The final fate of the parietal plate of the occipital bone is not well described in the literature; however, it is most likely retained as the mastoid fontanelle. This gives rise to the superolateral part of the cartilaginous supraoccipput next to the fontanelle. It has been shown that the mendosal fissure, which postnatally is connected to the mastoid fontanelle, is the remnant of the tectum synoticum of the parietal plate [83]. Figure 4.8 shows the mastoid fontanelle and its relationship to the supraoccipput and exoccipput at birth [83]. The different components of the posterior basichondrocranium and their relationships are schematized in Fig. 4.9.

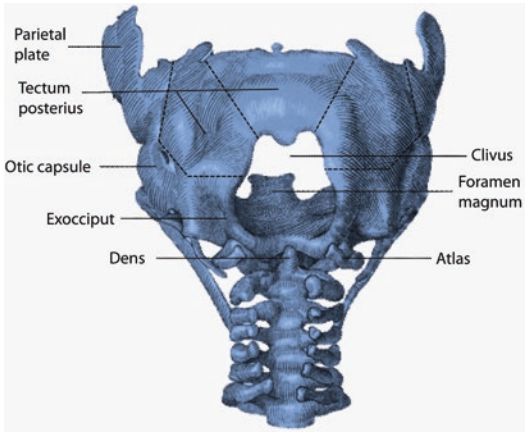

Fig. 4.7 The posteroinferior aspect of the basichondrocranium and occipital region of a 43 mm CRL fetus, ~12th week of fetal life. (Modified with permission from Macklin [81]) The tectum synoticum is regressed and the upper part of the posterior border of the parietal plates is free. The tectum posterius is derived from the parietal plates and exoccipital wings and is arbitrarily composed of two lateral pieces and a central piece (marked by dashed lines). At this stage, ossification progresses in the central part of the tectum posterius, the anterior (root) portion of the exocciput and the caudal portion of the basiocciput

The basichondrocranium is completely matured by the 14th week of gestation (Fig. 4.10 [84]) as several other centers undergo endochondral ossification [75, 77]. Ossification of the cartilaginous basicranium occurs sequentially and in a consistent direction [85]. The first ossification centers in the supraoccipital, exoccipital, and basioccipital regions appear in 30, 37 and 51 mm CRL embryos,

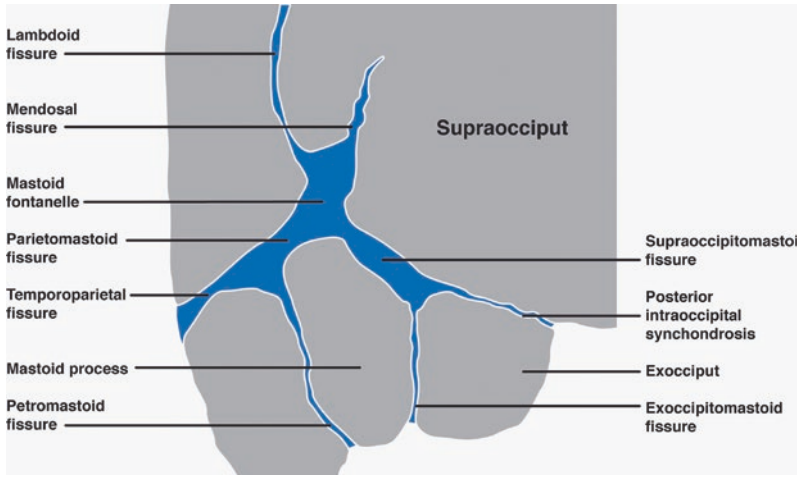

Fig. 4.8 Schema showing the mastoid fontanelle and its related cartilaginous fissures at birth. The fissures are replaced by the sutures in the adult skull. Some of these sutures are obliterated completely when the bones fuse. The mastoid fontanelle seems to be the remnant of the fetal parietal plate. The mendosal fissure is the remnant of the tectum synoticum [83]

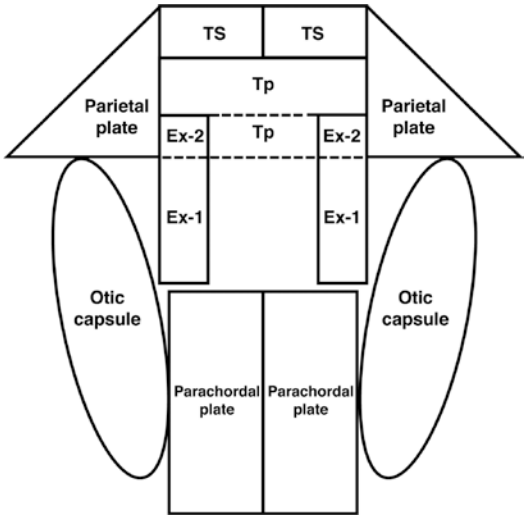

Fig. 4.9 A schematic drawing of the posterior basichondrocranium. The parachordal plates fuse to form a single basal plate. The exocciput is composed of a root (Ex-1) and a wing (Ex-2). The otic capsule is located lateral to the exocciput and basal plate. Note this schema is a simplified drawing and lacks some details of the anatomical relationships between the related parts. The tectum synoticum (TS), which is a temporary structure, originates from the upper part of the base of the parietal plate. The tectum posterius (TP) originates from the lower part of the base of the parietal plate and exoccipital wing

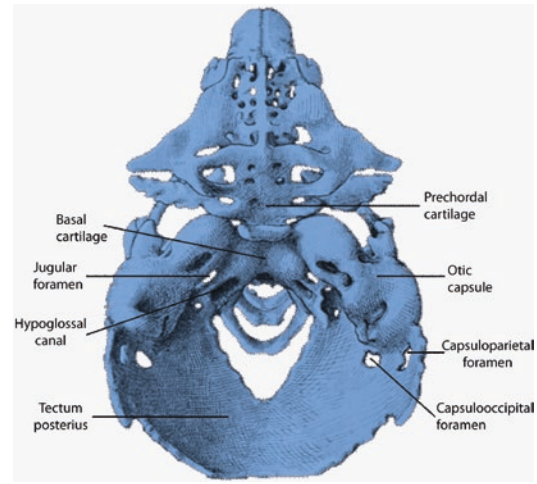

Fig. 4.10 The superior aspect of the basicranium in a fetus of 80 mm CRL, ~14th week of fetal life. (Reproduced with slight modifications from Hertwig [84]). The jugular foramen is located between the otic capsule and exocciput. Two other foramina are visible, one between the otic capsule and the tectum posterius (capsulo-occipital foramen) and one between the otic capsule and the parietal plate (capsuloparietal foramen). These foramina transmit emissary veins. They disappear or are retained as the mastoid foramina in adults

respectively [45]. There is one ossification center in the basioccipital and exoccipital segments; however, the supraoccipital segment develops from multiple ossification centers [86]. Radiographically, the ossified basiocciput is easily recognizable when the fetus attains a CRL of 80–100 mm [85], as is the basisphenoid and anterior basicranium in fetuses of 100 to 150 mm CRL [85]. During the second trimester, the rate of longitudinal growth of the posterior basicranium is approximately half of that of the anterior basicranium [87]. Details of the development of the anterior basicranium are beyond the scope of this review.

Contribution of Cells of Neural Crest Origin to the Basicranium

McBratney-Owen and colleagues [88] demonstrated, using a mouse model, that the basicranial mesenchyme, both rostral and caudal to the spheno-occipital synchondrosis, is derived from neural crest and mesoderm, respectively (Fig. 4.11). The spheno-occipital synchondrosis is initially of dual origin, its rostral half being from the neural crest-derived prechordal cartilage and its caudal half from the mesoderm-derived basiocciput [88]. After birth, the neural crest-derived cells in the synchondrosis vanish, and the synchondrosis becomes entirely mesodermal. Later, the mesoderm-derived osteoblasts are brought into the caudal basisphenoid through endochondral ossification of the spheno-occipital synchondrosis [88]. The boundary of the neural crest- and mesoderm-derived basicranium—only roughly correlating with the prechordal-chordal boundary—is ontogenetically and phylogenetically important as it marks the transition from the mesoderm-derived basicranium (posteriorly) to the neural crest-derived basicranium anteriorly. Since they contribute to the formation of the head including the basicranium, cells of neural crest origin could have been predominant in the evolution of vertebrates from chordate-like ancestors [89].

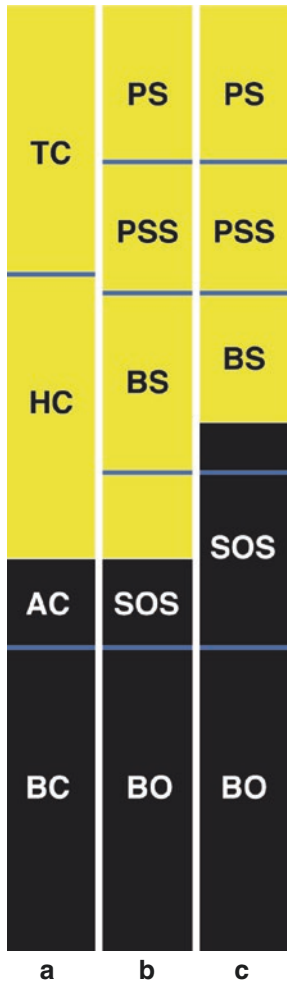

Fig. 4.11 Dynamic changes in the boundary of the neural crest- and mesoderm-derived basicranium based on a mouse model. (Adapted from [88]). AC, acrochordal cartilage; BC, basal cartilage; BO, basiocciput; BS, basisphenoid; HC, hypophyseal cartilage; PS, presphenoid; PSS, presphenoidal synchondrosis; TC, trabecular cartilage; SOS, spheno-occipital synchondrosis. (**a**) The fetal period. The acrochordal cartilage is the rostral part of the basal cartilage surrounding the tip of the notochord. The black region is a mesodermal derivative, and the yellow region is a neural crest derivative. (**b**) The early postnatal period; the spheno-occipital synchondrosis has a dual origin. (**c**) The late postnatal period. With apoptosis of neural crest cells and introduction of mesoderm-derived osteoblasts into the caudal basisphenoid, the mesoderm-neural crest boundary moves anteriorly. The entire spheno-occipital synchondrosis is now mesodermally derived

Development of the Occipital Bone

At birth, the occipital bone is comprised of a squamous portion, a basioccipital, and two exoccipital segments (Fig. 4.12) [51]. The developmental anatomy of the basioccipital and exoccipital segments has been discussed previously. The squamous portion has a dual developmental origin. It is derived from a lower cartilaginous plate (from the parietal plates and exoccipital wings) and an upper membranous part. The upper membranous part is composed of ribbon-like intermediate and triangular interparietal segments (Fig. 4.13) [90]. The membranous interparietal segment is formed by two symmetrical medial and lateral plates on either side of the midline. The medial plates are separated by a median fissure [90, 91]. Two ossification centers make up each plate and the intermediate segment [91]. At 12–15 weeks of gestation, the lateral plates of the membranous interparietal region grow medially and fuse together to form a single hybrid between the intermediate segment inferiorly and the medial plates of the interparietal segment superiorly [91, 92]. A transverse occipital fissure separates the intermediate from the interparietal segment. The lateral (mendosal) fissure is formed from the obliteration of the transverse fissure when the intermediate and interparietal segments fuse medially. This fissure is distinguishable at 16 weeks of gestation [91]. At this time, the median fissure mostly disappears as the two medial plates fuse [91].

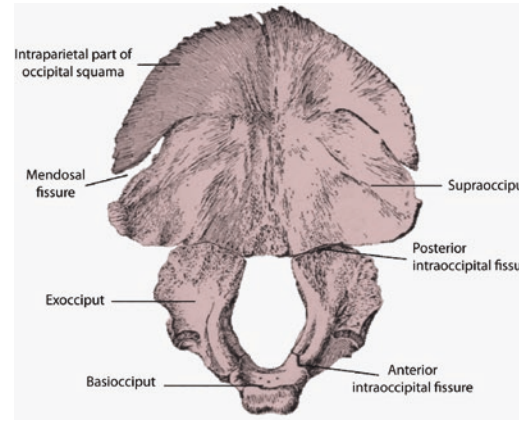

Fig. 4.12 The occipital bone at birth (after Piersol [51])

In a developed skull, the highest nuchal line signifies the border between the intermediate segment and interparietal bone, whereas the superior nuchal line represents the border

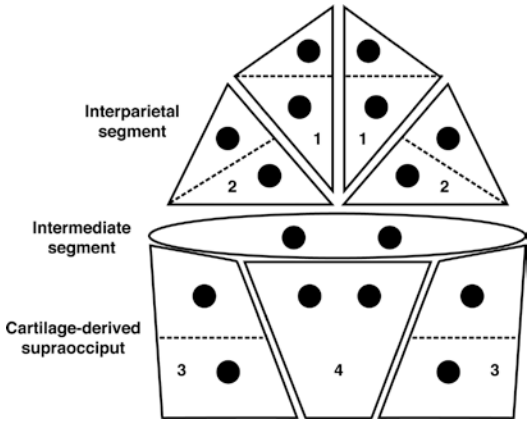

Fig. 4.13 A line diagram showing the different segments contributing to the development of the squamous portion of the occipital bone and their respective ossification centers. (**1**) Medial plates of the interparietal segment; (**2**) lateral plates of the interparietal segments; (**3**) lateral plates of the supraoccipital cartilage; (**4**) central plate of the supraoccipital cartilage. The intermediate segment and cartilage-derived supraocciput together form the supraoccipital part of the occipital squama. The ossification centers are indicated by black circles. The dashed lines represent the boundaries between them. The variable separation and fusion of the different plates and/or ossification centers can result in the formation of variant sutures and sutural (Inca) bones in the adult skull [90]

between the intermediate segment and the cartilage-derived supraocciput. Initially, the lateral fissure transforms into a suture (mendosal suture) at the lateral part of the highest nuchal line. The mendosal suture normally disappears with complete fusion of bones, between the second and fourth years of life. In approximately 16% of adult skulls, the mendosal suture persists due to the lack of complete fusion [56]. Very rarely, the entire transverse fissure/suture between the intermediate and interparietal segments can persist; this should not be confused with the mendosal suture [54]. The terms "fissure" and "suture" are often used interchangeably, depending on the author [93]. However, morphologically, they are different stages of the same structure. Ontogenetically, the fissure is replaced by the suture, which can be completely obliterated following ossification.

The appearance of ossification centers in the supraoccipital cartilage has long been controversial. According to Mall [86], two paramedian ossification centers appear in the 55-day-old embryo and quickly fuse into a single median center. Simultaneously, two new ossification centers appear lateral to the fusing paramedian centers, all fusing by day 57. On day 58, there is a single ossifying mass across the supraoccipital midline. As previously mentioned, the supraoccipital cartilage may be arbitrarily divided into a central plate and two lateral plates (Fig. 4.7). The paramedian centers occupy the central plate, and lateral centers occupy the upper parts of the lateral plates [94]. Srivastava [94] also mentions another independent ossification center in the lower part of the lateral plate of the supraoccipital cartilage on either side. The different segments and plates of the developing supraoccipital squama are schematized in Fig. 4.13 [90]. The rapid formation and fusion of the supraoccipital ossification centers could account for the discrepancies in the literature regarding the number and arrangement of those centers.

Basicranial Angle, Platybasia, and Basilar Kyphosis

The basal angle is formed between the axes of the anterior and posterior basicranium. The landmark for the basicranial hinge, around which the posterior basicranium rotates, is formed by the center of the pituitary fossa [95], tuberculum sellae [96, 97], or dorsum sellae [95]. The basion is invariably used as the inferior limit of the posterior basicranium [95–97], whereas the foramen cecum (nasion) [95, 97, 98] is used as the front limit of the anterior basicranium. Figure 4.14 shows different landmarks and methods used for measuring the basicranial angle [96]. The posterior basicranium retroflexes during the fetal period, increasing the basicranial angle [97–99]. This retroflexion moves the basion dorsally and superiorly, flattens the basicranium [99], and decreases the ventral depth of the posterior cranial fossa. There are two hypotheses about the mechanism of posterior basicranial retroflexion: (1) enlargement of the intracranial space and, more importantly, (2) the expansion of the developing upper airways, which can act from above and below to flatten the skull base [97, 99]. Excessive retroflexion of the posterior basicranium results in platybasia, whereas

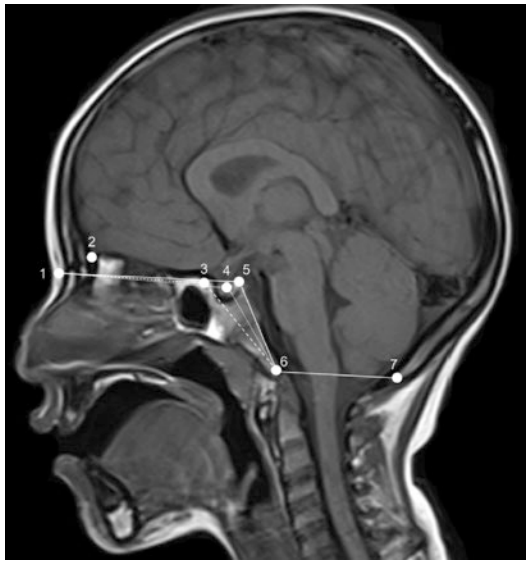

Fig. 4.14 Midsagittal magnetic resonance imaging of the head. The different landmarks used for measuring the basicranial angle are shown: 1, nasion; 2, foramen cecum; 3, tuberculum sellae; 4, center of pituitary fossa; 5, dorsum sellae; 6, basion; 7, opisthion. Note the opisthion-basion-tuberculum sellae angle is known as Boogard's angle. The size of the posterior cranial fossa decreases with an increase in Boogard's angle [96]

insufficient retroflexion results in basilar kyphosis. The normal angle varies slightly depending on the method and landmarks used for its measurement. An angle between 125° and 143° is generally considered normal [95]. A basicranial angle greater than 143° indicates platybasia. One less than 125° indicates basilar kyphosis [95]. Isolated and mild platybasia is asymptomatic and affects the posterior fossa volume insignificantly [100]. Moderate to severe platybasia is often associated with basilar invagination [35]. The basicranial angle is greater in patients with Chiari I malformation [96].

Basilar Invagination and Basilar Impression

Basilar invagination, one of the most common craniovertebral junction anomalies, occurs when the caudal part of the occipital bone is displaced inward and upward and the vertebral column and skull base abnormally approximate each other. The odontoid process herniates into the foramen magnum in severe cases [96]. Basilar invagination can be congenital or secondary to such conditions as Paget's disease, osteogenesis imperfecta, hyperparathyroidism, rickets, etc. [35]. The congenital forms are associated with hypoplasia of the atlas, basiocciput and/or occipital condyle, platybasia, and atlanto-occipital assimilation [35, 101] and have a higher incidence of hindbrain herniation [96, 101]. The secondary or acquired forms of basilar invagination are referred to as basilar impression [35]. These associations may not reflect a cause-effect relationship but may represent consequences of the same pathological mechanism. The craniocervical growth collision theory of Roth may present a potential embryological explanation for the occurrence of basilar invagination and associated anomalies. According to Roth [102], following an early embryonic period of predominant neural growth, the proliferation of skeletogenic tissue and vertebral growth ultimately overtake the growth of the spinal cord. Normally, the vertebral column grows in a cranio-caudal direction resulting in expansion of the vertebrae below the distal end of the spinal cord. If the distribution of skeletogenic tissue is reversed for any reason and vertebral growth occurs in a caudo-cranial direction, the growing vertebral column collides with the developing skull base [102]. This collision will push the posterior skull base and the margin of the foramen magnum upward, compressing the primordia of the occipital and cervical vertebrae against each other. This may potentially lead to abnormal segmentation at the craniovertebral junction, fusion of the atlas and occipital bones, platybasia, and prolapse of cervical vertebral column into the skull base.

There are several morphometric criteria for diagnosing basilar invagination [103]. Figure 4.15 shows some of the reference lines used for this purpose [103, 104]. Basilar invagination is divided into two groups. Group 1 is associated with Chiari I malformation, and Group 2 is not [105, 106]. According to Pearce [105], approximately 20% of patients with basilar invagination have Chiari malformation [105]. Pure basilar invagination has pyramidal motor and proprioceptive deficits, whereas basilar invagination with Chiari malformation usually presents chronically with cerebel-

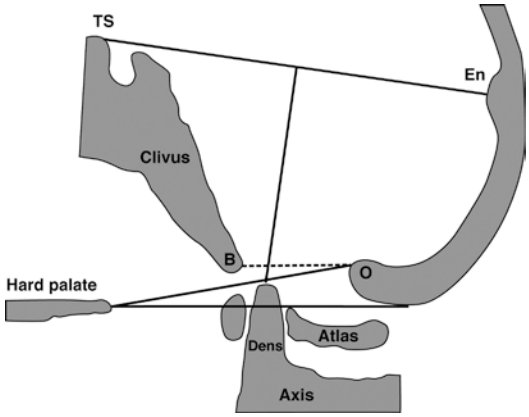

Fig. 4.15 Reference lines used for diagnosing basilar invagination. Chamberlain's line connects the posterior end of the hard palate to the opisthion (O). McGregor's line extends from the posterior end of the hard palate to the lowest point on the midline supraoccipital curve [103, 104]. Note the posterior margin of the foramen magnum is curved upward into the posterior cranial fossa, which is usually the case in basilar invagination. McRae's line extends from the basion (B) to the opisthion (O). Twining's line connects the tuberculum sellae (TS) and the endinion (En). The Klaus height index line represents a line perpendicular to Twining's line, which passes through the apex of the dens [103]. Normally, the apex of the dens should lie below McRae's line [104]. Severe basilar invagination is diagnosed when the odontoid process violates McRae's line. The diagnosis of basilar invagination is considered if the odontoid process extends beyond 5 mm and 7 mm above Chamberlain's and McGregor's lines, respectively [104]. A Klaus height index less than 30 mm indicates basilar invagination, and a value between 30 and 36 mm indicates a tendency toward basilar invagination [103]. These cutoff values of the diagnostic measurements differ between authors

lar and vestibular deficits [106, 107]. A familial form of basilar invagination has been reported, and an autosomal dominant pattern of inheritance with incomplete penetrance and variable expressivity was suggested for this case [108].

Shallowness of the Posterior Cranial Fossa in Chiari I Malformation

Various linear morphometric measurements have been defined to determine the dimensions and size of the posterior cranial fossa and occipital bone (Fig. 4.16) [109, 110]. Karagöz et al. [110] conducted a study to compare the depths of the posterior cranial fossa between patients over 15 years old with and without Chiari I malformations. It was concluded that the height of the supratentorial occipital region (H) was similar between the two groups [110]. However, the posterior fossa height or depth (h) was approximately 16% less among the Chiari 1 patients. This observation, confirmed by other studies [96, 111], implies that patients with Chiari I malformation have a shallow posterior fossa. As the supratentorial and infratentorial parts of the squamous occipital bone are composed of membranous and cartilaginous origins, respectively, the shallowness of the posterior fossa reflects an abnormality of the occipital squamous bone that is restricted to its cartilage-derived lower part.

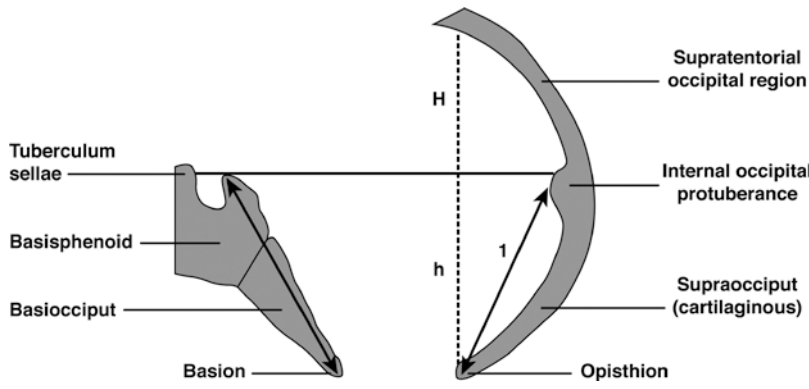

Fig. 4.16 Linear morphometry of the posterior cranial fossa and occipital bone. McRae's and Twining's lines are shown. A line perpendicular to Twining's line is drawn at one-quarter of its distance from the endinion (internal occipital protuberance) connecting the inner table of bones in the infra- and supra-tentorial compartments. The distances between Twining's line and the inner table of the skull in the supratentorial and infratemporal regions, respectively, indicate the depth of the posterior fossa in the supraoccipital region and the height of the supratentorial occipital region [109, 110]. The lengths of the supraocciput and clivus are represented by the two-headed arrows 1 and arrow parallel to the clivus, respectively

Underdevelopment of the Occipital Bone and Basioccipital Hypoplasia in Chiari I Malformation

The bulk of evidence indicates that the supraoccipital, exoccipital, and basioccipital segments of the occipital bone are underdeveloped and hypoplastic, to various degrees, in Chiari I malformation [112]. Nishikawa et al. [36] found, in a study of patients age 15 and older with Chiari I malformations, that the supraocciput and exoccipital heights (measured from the jugular tubercle to the atlanto-occipital joint) were ~20% lower in patients with Chiari I malformation as compared to control. In another study, Noudel et al. [37] compared the basioccipital lengths (measured from the spheno-occipital synchondrosis to the basion) among 17 patients with Chiari I malformation aged over 16 years with healthy controls. The basioccipital length was also lower among Chiari I patients. The association of a short clivus with Chiari I malformation has been confirmed by other studies [110, 113]. Severe basioccipital hypoplasia or dysgenesis is associated with basilar invagination [36]. Dysgenesis of the basiocciput can be associated with a normal-appearing basisphenoid [114]. Basioccipital dysgenesis (with scalloping, concavity, and thinness) has also been reported in the Chiari II malformation [96].

Nonlinear Nature of Occipital Bone Dysplasia in Chiari I Malformation

In order to elucidate the nature of occipital bone dysplasia in Chiari I malformation, a meta-analysis was performed. Figure 4.17 shows the results of this meta-analysis for four studies that reported the means and standard deviations of clival or supraoccipital length or size of the foramen magnum in adult patients with Chiari I malformation [110, 115–117]. Although there were significant reductions in the lengths of the supraocciput and clivus, the meta-analysis indicated that the overall size reduction is more prominent in the supraocciput than in the clivus. This is consistent with the observations by Nishikawa et al. [36] and Dagtekin et al. [118] on adult Chiari I patients in whom the supraocciput was significantly more underdeveloped than the clivus. The meta-analysis also indicated a tendency for the foramen magnum to widen anteroposteriorly. However, this increase in size of the foramen magnum was not proportionate to the growth retardation of the supraocciput and clivus. Overall, the meta-analysis showed nonlinear occipital bone dysplasia in Chiari I malformation with different parts of this bone being disproportionately affected.

To recap, the supraocciput develops through a morphologically complex process of chondrification and ossification. The chondrified supraocciput is derived from the parietal plate and exocciput, composed of lateral and central plates. The lateral plates ossify by two upper and lower ossification centers and the central plate by two centers that rapidly fuse. The parietal plate undergoes partial reversion during fetal life, rendering the upper part of the chondrified supraocciput derived from this plate also vulnerable to regression. This could potentially provide an embryological basis for the shortening of the supraocciput in Chiari malformation.

Midface Retrocession in Chiari Malformation

In an experimental fetal animal model of Chiari malformations and spinal dysraphism induced by a single maternal dose of vitamin A, Marin-Padilla and Marin-Padilla [119] noted that underdevelopment of the occipital bone and posterior cranial fossa causes the maxilla to take a more posterior position within the viscerocranium, leading to retrocession of the midface. In humans, a subtle midface retrocession may be related to a shorter length of Chamberlain's line. This shortening is present in patients with Chiari I malformation, reflecting a subtle abnormality in the midface [96]. In addition, patients with greater midface retrocession have smaller posterior fossae [96].

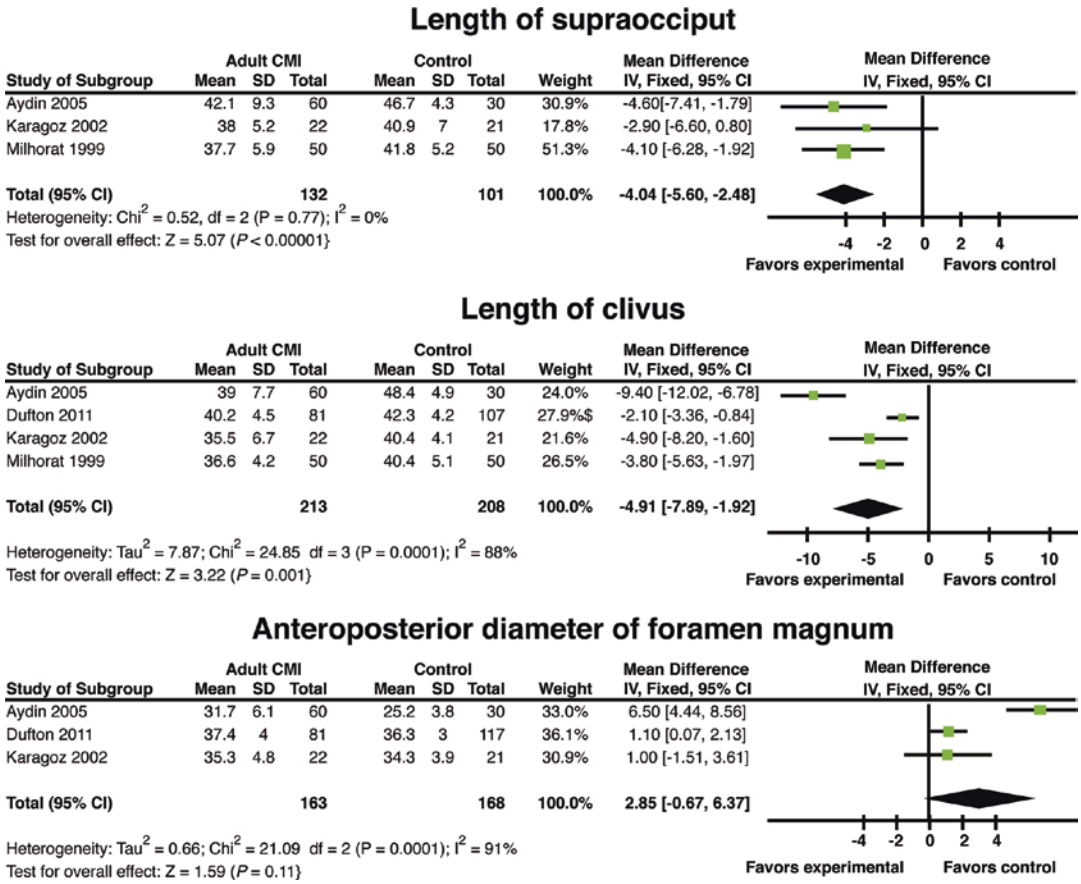

Fig. 4.17 Forest plots comparing the clival and supraoccipital lengths and anteroposterior diameter of the foramen magnum among adult patients with Chiari I malformation and controls. Homogeneity-based meta-analysis was performed using Review Manager Version 5 for Windows (Cochrane Collaboration and Update Software). Homogeneity between studies was assessed using the standard Cochran's Q and I^2 statistics. A fixed effect model (for a data set with nonsignificant heterogeneity) or random effect model (for a data set with significant heterogeneity) was used to merge odds ratio values and to estimate the overall effect size. Overall effect, odds ratios, and confidence intervals are presented

The Developmental Anatomy of the Cerebellum

Observations about the embryogenesis of the cerebellum began in late nineteenth to early twentieth centuries and helped form our current understanding. The following discussion is based on the studies of Bailey and Miller [120], Dow [121], Frazer [6], Hamilton et al. [122], Heisler [123], Hochstetter [124], Keibel and Mall [125], Keith [126], Minot [127], Patten [128], Piersol [51], and Stroud [129]. More recent observations have been obtained from in vitro and in vivo fetal sonography and magnetic resonance imaging [130–134].

The primary neural tube, which gives rise to the hindbrain, expands cranially to form three vesicles (the forebrain, midbrain, and hindbrain) separated by two constrictions (Fig. 4.18) [123]. The constriction between the midbrain and hindbrain is called the *isthmus* and appears even before the cranial closure of the neural tube [123]. Additional two constrictions appear in the region of the forebrain and hindbrain yielding a five-vesicle neural tube composed of the telencephalon, diencephalon, mesencephalon, metencephalon, and myelencephalon (Fig. 4.18). Transfer from a three-vesicle to a five-vesicle neural tube is associated with bend-

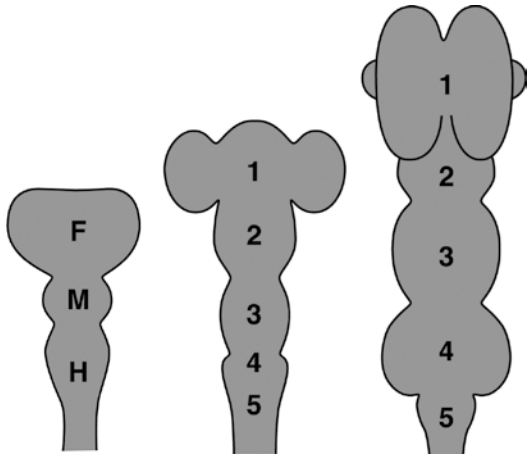

Fig. 4.18 Schema of the cranial neurocele at three-vesicle and five-vesicle stages. (Reproduced with slight modifications from Heisler [123]) Expansion of the cranial neurocele initially yields the forebrain (F), midbrain or mesencephalon (M), and hindbrain (H). With further subdivision, the telencephalon (1), diencephalon (2), mesencephalon (3), metencephalon (4), and myelencephalon (5) are formed

ing of the neural tube at three levels (midbrain, midportion of hindbrain, and cervicomedullary junction). In addition, there is a spatial change from a craniocaudal to ventrodorsal orientation of the vesicles [123].

The rhombencephalon (hindbrain) extends from the isthmus to the cervical flexure [127]. In the midportion of the rhombencephalon, the basal and alar plates lie in the same plane. Rostrally and caudally, the bilateral alar plates approximate each other in the dorsal midline (Fig. 4.19), attaining a dorsal position in much the same way as in the spinal cord [6]. Thus, the roof plate is wider in the midportion and narrower in the cranial and caudal portions of the rhombencephalon. Just beneath the isthmus and as a result of the rapid initial growth of the midbrain, the rostral ends of the right and left metencephalic alar plates, which are in close proximity in the dorsal midline, are pushed downward. This creates an internal bend in the metencephalic alar plate (Fig. 4.19). A medial portion, located rostrally, lies transversely beneath the isthmus. The lateral arms, located caudal to this bend, are initially longitudinally oriented [6].

During the fourth week of fetal life, the roof of the rhombencephalon is bounded laterally by the rhombic lip, inferiorly by the obex, and superiorly by the metencephalic alar plates [126]. Dorsal extension of the metencephalic alar plate over the roof plate forms a thickened metencephalic rhombic lip at the junction between the roof plate and the alar plates [122]. The metencephalic alar plates thicken and bulge internally toward the fourth ventricle and externally toward the cisterna magna to form the intraventricular and extraventricular parts of the cerebellar plates, respectively [122]. At this stage, the cerebellar plates have three topographically oriented layers from inside to out: the ependymal, mantle, and marginal [122]. Between the sixth and eighth weeks, the pontine flexure is maximized. The metencephalic rhombic lip and cerebellar plates, including the previously longitudinal arm caudal to its internal bend, are now in a transverse plane. At the second month, the growth of the intraventricular part dominates, owing to the proliferation of precursor neural cells (neuroblasts) in the subependymal region forming a mantle layer.

Several topographically distinguishable regions are formed due to the spatial and temporal heterogeneity of the growth of the cerebellar plates (and later, the primordium) (Fig. 4.19). Initially, the cerebellar plates grow in a transverse direction, expanding laterally [120], coinciding with the growth of the intraventricular part during early embryonic stages. The lateral parts of the cerebellar plates corresponding to the cerebellar peduncles grow more slowly than the medial parts [125]. During the third month, a single cerebellar primordium is formed from the fusion of the two transversely lying cerebellar plates [125]. These plates fuse externally, leaving the two intraventricular parts separate at the midline [120]. The cerebellar primordium is connected anteriorly to the roof of the midbrain and posteriorly to the choroid plexus of the fourth ventricle by two thin membranes: the anterior and posterior medullary vela. Subsequently, the cerebellar primordium grows mostly through longitudinal expansion of its extraventricular part [120]. The neuroblasts migrate from the metencephalic rhombic lip and

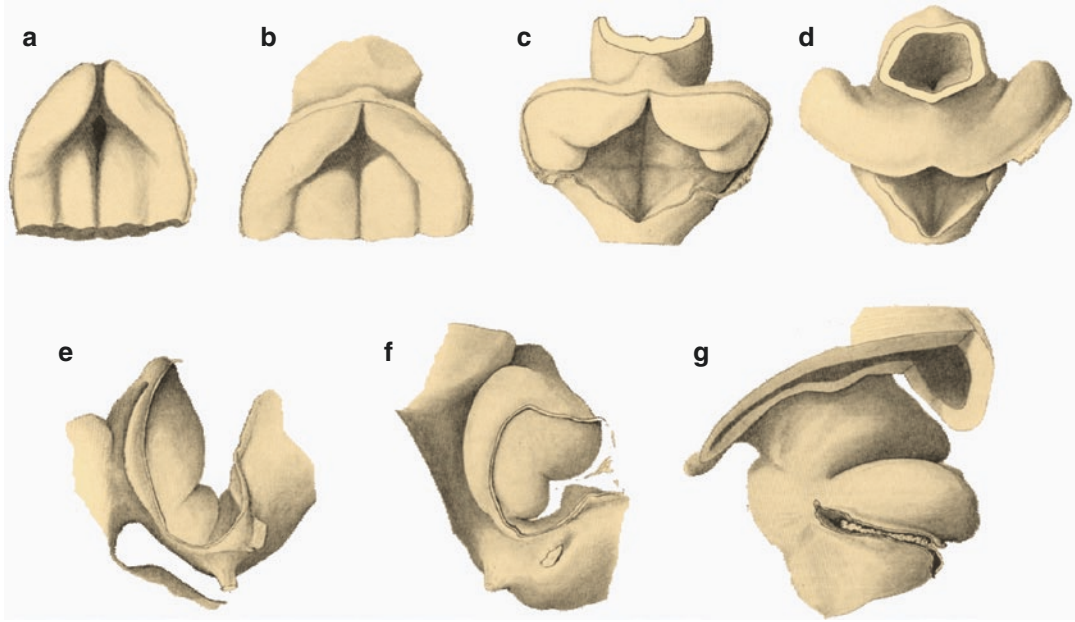

Fig. 4.19 Schema of the posterior (**a**–**d**) and lateral (**e**–**g**) views of the developing cerebellum (after Frazer [6] with slight modifications). (**a**) The right and left metencephalic alar plates approximate each other rostrally and are in an inverted V-shape position. (**b**) The enlarging mesencephalon pushes the metencephalic alar plates downward. This creates an internal bend in each alar plate, clearest in **c** and **f**. (c) The cerebellar plates are composed of longitudinal and transverse parts marked by the internal bend. The transverse parts begin to fuse rostrally and externally beneath the mesencephalic isthmus. (**d**) The dorsomedian fusion of the cerebellar plates progresses caudally. (**e**) The lateral view corresponding to **b** shows the intraventricular growth of the cerebellar plates at this stage. (**f**) The lateral view corresponding to **c** shows the transverse and longitudinal parts of the cerebellar plates. The internal bend is maximized. The extraventricular part of the cerebellum is enlarging. (**g**) The lateral view corresponding to **d** shows that the extraventricular part of the cerebellum has grown considerably. The longitudinal part of the cerebellum grows more slowly than the transverse part, and the intraventricular part of the cerebellum is now substantially regressed

mantle layer of the intraventricular part, contributing to the formation of cerebellar gray matter within the extraventricular part [122].

The development of cerebellar gray matter follows several stages: (1) first, the superficial cerebellar cortex is formed from neuroblast migration; (2) Purkinje cells are formed by a group of neuroblasts that stop superficial migration deep to the superficial cerebellar cortex; (3) neuroblasts of the superficial cerebellar cortex migrate deeply beneath the Purkinje cell layer; and (4) the remaining mantle zone neuroblasts form the deep cerebellar nuclei [122]. Ultimately, subependymal neuroblast proliferation ceases. This process of precursor neuronal cell migration and cessation of subependymal neuroblast proliferation is termed "eversion of the cerebellum," which is associated with the gradual disappearance of the intraventricular part of the cerebellar primordium [122] (Fig. 4.20). The eversion can be attributed to the shift in pattern of cerebellar growth pattern from intraventricular to predominantly extraventricular. The cerebellar primordium is mainly extraventricular in an 80 mm crown-rump length (CRL) embryo (the 14th week of fetal life) [122]. Despite the cessation of subependymal neuroblast proliferation, the metencephalic rhombic lip continues to generate new neuroblasts destined for the extraventricular part of the cerebellum [125]. The longitudinally growing extraventricular part then overlaps the superior and inferior medullary vela [120].

In summary, the transverse growth of the cerebellar plates precedes the longitudinal growth of

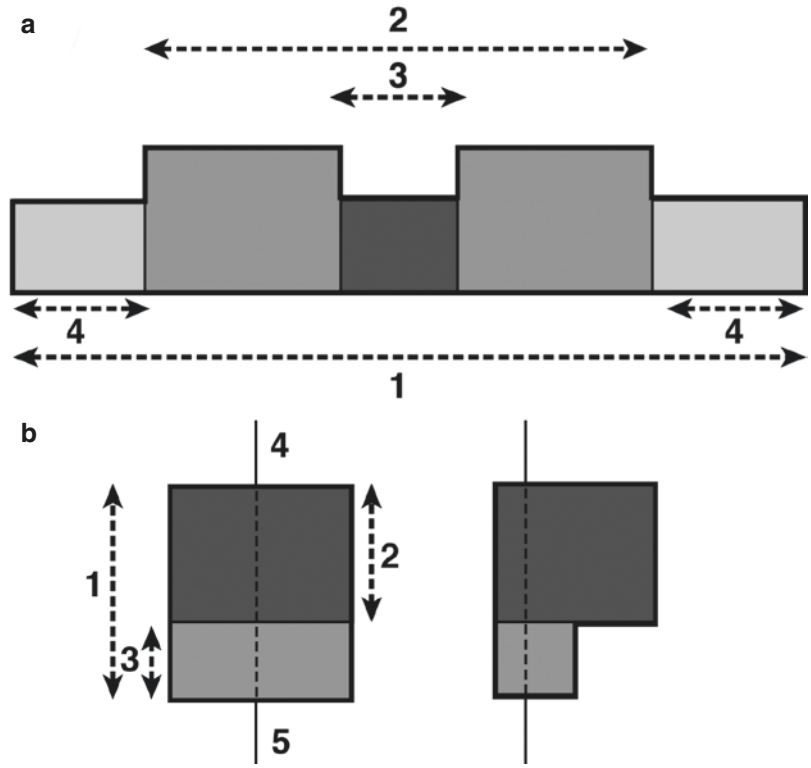

Fig. 4.20 Schematic representation of the heterogeneous growth of the cerebellar primordium. The transverse section (**a**) through the cerebellar primordium (1) shows a medial region (2) and two lateral arms (4). The medial region comprises a median vermis (3) and lateral (hemispheric) masses between the vermis and lateral arms. The lateral arms form the cerebellar peduncles [125]. The sagittal section (**b**) through the cerebellar primordium (1) shows the cranial and caudal parts derived from the metencephalic alar plates (2) and thickened rhombic lip (3), respectively. The superior and inferior medullary vela are attached to the cerebellar primordium and arbitrarily divide it into intra- and extraventricular parts marked by the dashed lines. As depicted here, the median vermis, lateral arms, and caudal region of the cerebellar primordium grow more slowly

the primordium, whereas the growth of the intraventricular part precedes that of the extraventricular part. The formation of a single cerebellar primordium marks a shift in the pattern of early cerebellar development and growth. During the second trimester, the longitudinal growth of the cerebellar primordium results in the appearance of several cortical sulci and fissures. The initial rapid transverse growth of the cerebellar plates (before fusion and during the second month of fetal life) continues more slowly in the cerebellar primordium during the third to fifth months. Between the fifth month of fetal life and predominantly during the third trimester, the cerebellum experiences its most rapid transverse growth compared to all other parts of the brain. The following is a discussion of the development of the vermis and cerebellar hemispheres.

Dorsomedian fusion of the cerebellar plates begins rostrally at the ninth week of fetal life, giving rise to the vermis [135]. The embryogenesis of the vermis has two stages. The anterior vermis forms first, following the rostral fusion of the extraventricular part of the cerebellar plates through their thickened rhombic lips. The anterior vermis is anatomically continuous with the germinating rhombic lip laterally and the rhombic roof inferiorly. Until the 18th week of gestation, the vermis covers only the rostral half of the fourth ventricle [130]. Between the 18th and 21st week, the vermis grows progressively in a caudal direction, closing the postero-

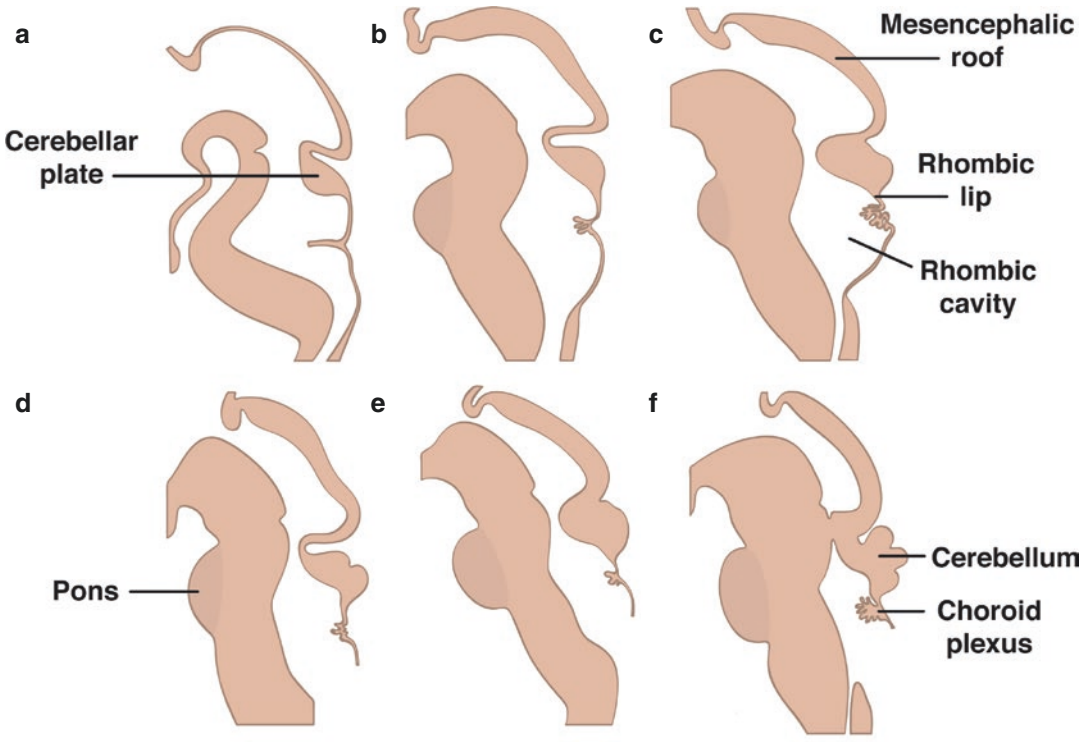

Fig. 4.21 Parasagittal sections through the midbrain/hindbrain showing the successive stages of cerebellar development and the process of cerebellar eversion. (Modified from Hochstetter [124].) The cerebellar primordium is mainly intraventricular in **a** and is extraventricular in **b**–**f**. The fusion of the cerebellar plates (not shown here) marks the transition from intraventricular to extraventricular development of the cerebellum. Note that the ventral pons, which contains corticopontocerebellar fibers, grows and the pontine flexure straightens concomitantly with development of the extraventricular cerebellum

inferior interhemispheric cleft until it entirely covers the fourth ventricle [130]. This growth takes place through specialization of the adjacent part of the rhombic roof and primarily by the growth of the rhombic lips toward the midline. Their fusion is favored by the mechanical effects of the transversely expanding lateral hemispheres. Once the vermis is completely closed, after the fifth month of fetal life, it continues to grow linearly in both longitudinal and anteroposterior directions. This growth is closely proportionate to the transverse growth of the cerebellum [134]. During the first half of fetal life, the vermis grows in a craniocaudal direction; however, during the second half, it grows circumferentially. This circumferential growth ultimately leaves two notches between the cerebellar hemispheres—an anterior and a posteroinferior one.

At the end of the third month, the cerebellum is dumbbell-shaped with two lateral masses and a relatively thin median vermis [126]. The cerebellar primordium comprises the metencephalic alar plates, which partially extend into the roof plate forming a thickened metencephalic rhombic lip. The metencephalic rhombic lip continues to yield neuroblasts, which migrate superficially to the cerebellar cortex [125]. As a result of the differential growth of the metencephalic alar plate and rhombic lip, three sulci successively appear between them, one in the median area (sulcus postnodularis) and two in the lateral areas (sulcus flocculares). These sulci (postnodularis and flocculares) later become continuous to form the posterolateral fissure, the first fissure to appear in the developing cerebellum [122]. It separates the flocculonodular lobe from the rest of the cerebellum (corpus cerebelli) [51]. In this way, the thick-

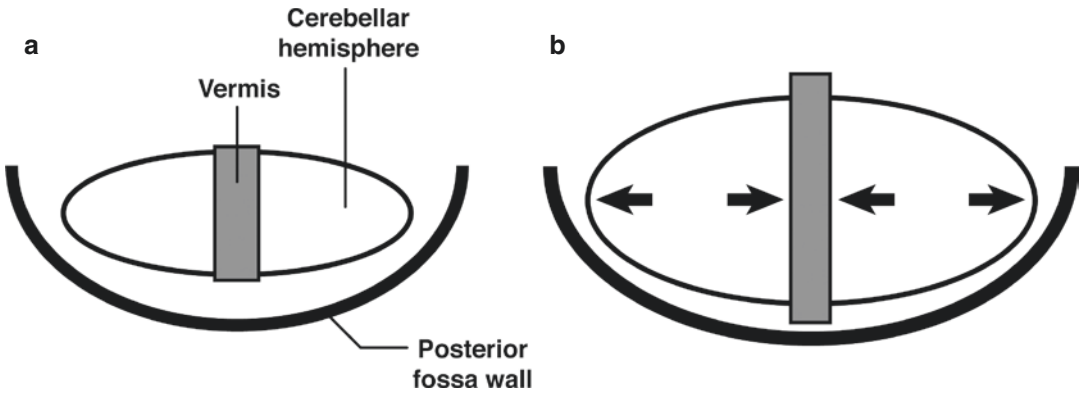

Fig. 4.22 Schema depicting the relative overcrowding of the posterior cranial fossa from the early (**a**) to the late (**b**) second trimester. Arrows indicate the conflict between the growing cerebellar hemispheres and the midline vermis and the wall of the posterior fossa. Slight degrees of overcrowding are favored because the transverse growth rate of the cerebellar hemispheres is greater than that of the posterior cranial fossa. Relative overcrowding is a normal event, beginning during the second trimester and continuing into the third trimester and early postnatal life. Exaggerated overcrowding as a result of a small posterior fossa can result in upward and downward herniation of the vermis

ened rhombic lip gives rise to the nodulus and flocculus (Fig. 4.21) [125].

During the fourth and fifth months, the cerebellar cortex grows rapidly in the longitudinal axis resulting in the appearance of several other transverse sulci or fissures and intervening lobules [125, 128]. This superficial longitudinal growth of the cerebellum commences in the median region (vermis) and proceeds, to a greater extent, in the lateral region (cerebellar hemispheres). The first fissure, appearing in the vermian region of the corpus cerebelli, is the fissura prima of Elliot-Smith or sulcus primarius of Bolk. This fissure separates the anterior and posterior cerebellar lobes during the fourth month of fetal life [51, 128, 133]. Initially, the growth rates and volumes of the anterior and posterior cerebellar lobes are proportionate and similar. However, beginning in week 16, the posterior lobe grows faster [133]. The minor cerebellar fissures appear until the seventh month of fetal growth [126].

The fourth month of fetal life is marked by cortical growth of the median vermis [125]. During this time, the lateral masses of the corpus cerebelli are smooth and further subdivide during the fifth month after the basic subdivision of the vermis [51, 125]. With the rapid longitudinal growth of the cerebellum within the posterior fossa during the second trimester, the cerebellar primordium gradually becomes wedge-shaped, with the apex backward because of mechanical factors [126]. However, the transverse growth is relatively slow, and the expanding lateral hemispheres roll in toward the midline, overlapping the vermis [125]. This results in the formation of a median longitudinal fissure between the two hemispheres. During the early second trimester, the transverse length of the cerebellum is approximately three times the longitudinal length of the vermis [133]. However, by the end of the second trimester, the transverse length is only double the longitudinal length of the vermis [133]. The rate of growth could have clinical implications such as relative posterior fossa overcrowding seen in two stages: (1) during the second trimester, the longitudinal growth of the vermis overrides the transverse growth of the cerebellar hemispheres, and (2) the cerebellar growth is faster than the expansion of the confined posterior cranial fossa. This overcrowding results in the compression and spreading out of the vermis sandwiched between the two cerebellar hemispheres. The mechanism is depicted in Fig. 4.22.

This overcrowding is further complicated by the rapid growth of the fetal cerebellum after 28 weeks of fetal life [132] and by the transverse growth of the cerebellar hemispheres during the

third trimester [134]. Near the end of pregnancy, wedging of the cerebellum becomes more evident due to the posterior fossa being more yielding anteroposteriorly than transversely. During this phase of growth, which is mainly due to the massive proliferation and migration of the cortical granule cells, the cerebellar volume increases ~2.8-fold [132]. The intracranial and cerebral volumes increase approximately twofold during the same period [132].

The embryogenesis of the cerebellar lobules is beyond the scope of the current review; however, the reader is referred to the review by Dow [121] for details of the ontogeny and phylogeny of cerebellar lobulation. Several different systems of nomenclature and subdivision have been proposed. Ingvar (cited by Dow [121]) noted that the most morphologically constant regions in the mammalian cerebellum are the region in front of the primary fissure and the one behind the prepyramidal fissure. However, the region between the primary and prepyramidal fissures is phylogenetically variable. This phylogenetically variable region of the cerebellum (the middle lobe of Ingvar) receives the corticopontocerebellar afferents and, according to Dow, should be designated the neocerebellum. Phylogenetically, the oldest part of the cerebellum is the archicerebellum, comprised of the flocculonodular lobe and the lingula. This is followed by the appearance of the paleocerebellum, which includes the anterior lobe (except lingula), pyramis, uvula, and paraflocculus. Lastly, the neocerebellum appears, composed of the rest of the cerebellum.

While the archicerebellum predominantly receives vestibular inputs, the paleocerebellum and neocerebellum receive spinal and cortical inputs, respectively. In lower primates, the paraflocculus is larger than the flocculus, projects between the latter and the lateral part of the corpus cerebelli, and is connected by a stalk to the uvula and pyramis [121, 129]. The parafloccculus is retained as a small and vestigial structure in humans [129] and is often referred to as an accessory parafloccculus [136]. It lies close to the flocculus and varies markedly in shape from a flat lamella to a rosette-like cluster of folia akin to the flocculus [137]. There are varying opinions as to the origin of the tonsils (the lowest part of the corpus cerebelli) in humans. Some state they are a downward extension of the middle lobe, anterior to the prepyramidal fissure, that becomes contiguous with the uvula. However, others believe that they represent the growth of the stalk of the paraflocculus, intervening between the uvula/pyramis and the vestigial parafloccculus [121].

Development of the Rhombic Roof

In human embryos and other mammals, Weed [138] identified an oval, thinned-out area of epithelial differentiation (the *area membranacea superior*) in the superior portion of the ependymal roof of the fourth ventricle (Fig. 4.23). The superior and inferior border of this area was continuous with the ependymal layer, while its lateral borders were flanked by a hypercellular region of ependyma on either side. With further development of the rhombencephalon and formation of the pontine flexure, the rhombic roof invaginated at the midpoint of its cephalo-caudal axis and further developed into the choroid plexus. At this stage, the area membranacea superior separated from the inferior portion of the rhombencephalic roof by the primordium of the choroid plexus. Shortly thereafter, the area membranacea superior in the human embryo was replaced by the growth of ependymal cells originating from its proliferative lateral borders. At the same time, the ependymal lining below the invaginated roof thinned out and underwent epithelial differentiation to form the area membranacea inferior (Fig. 4.23). The area membranacea inferior extended from the choroid plexus primordium superiorly to the obex inferiorly. The mesenchyme posterior to the area membranacea inferior is then broken down, retaining only a pial layer and arachnoid strands extending from the condensed mesenchymal layer of dura mater to the area membranacea inferior. The space between the dura and area membranacea inferior develops into the cisterna magna. The inferior membrane, which separates the fourth ventricle from the developing cisterna magna, bulges backward and is covered internally by a thin ependymal layer.

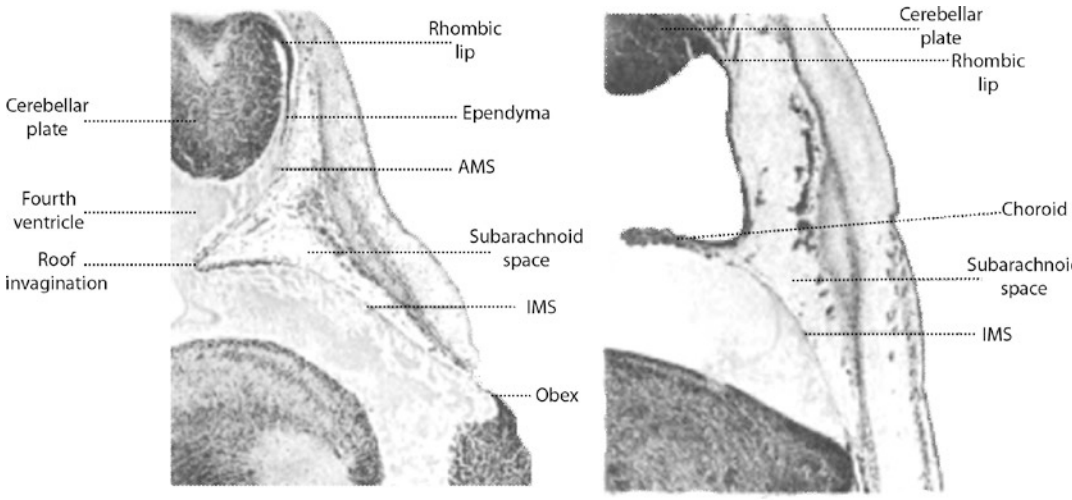

Fig. 4.23 Embryogenesis of the rhombic roof. (Reproduced with slight modifications from Weed [138]) AMS, area membranacea superior; AMI, area membranacea inferior. Note the developing cerebellum is mainly intraventricular at these stages

The embryonic fate of the saccular invagination (outpouching or diverticulum) at the caudal portion of the rhombic roof has been debated [139]. Blake [140] stated that the saccular invagination gradually becomes larger, ultimately disappearing in humans, leaving a remnant of the caudal sac retained at the margin of the foramen of Magendie [139]. Thus, in adults, the rhombic roof is made up of the inferior medullary velum, the tela choroidea, and the area membranacea inferior of Weed. The area membranacea inferior includes the foramen of Magendie at its middle section. The inferior medullary velum flanks the nodulus of the cerebellum [139] and is derived from the most caudal part of the metencephalic rhombic lip. The rostral part of the rhombic lip contributes to the flocculus.

Abnormal Cerebellar Development and Morphology Associated with Neural Tube Defects and the Chiari II Malformation

Prenatal Period

In twin embryos of 25 mm CRL (7–8 weeks), Padget [141] observed that one of the embryos had a lumbosacral spina bifida aperta, as well as a smaller posterior fossa and fourth ventricle (rhombic cavity). The cerebellar plates, which were intraventricular at this stage, were of similar size between the two embryos; however, they fused prematurely in the dysraphic embryo. Thus, due to the small posterior fossa, the transverse diameter of the intraventricular cerebellum in the dysraphic embryo was diminished during the late embryonic period. It can be posited that if the later longitudinal growth of the extraventricular cerebellum occurs about a restricted transverse axis, the disproportionate longitudinal expansion (especially of the midline vermis) would result in an upward or downward herniation.

Van Hoytema and van den Berg studied a later stage in cerebellar development using a fetus of 140 mm CRL with spina bifida aperta [142]. At this stage in normal fetuses, the rhombic roof perforates, allowing the cerebellum to inwardly rotate such that its caudal part (i.e., caudal vermis) turns into the fourth ventricle. However, in a fetus with spina bifida, the rhombic roof is thick, infiltrated by the choroid plexus, and only partially perforates. This partial perforation restricts the inward rotation of the caudal cerebellum. Therefore, the vermis is pulled inferiorly by its arachnoidal attachments to the overcrowded choroid plexus and thick rhombic roof [142]. Pilu et al. also found using ultrasound that in fetuses

older than 15 weeks with spina bifida, the transverse cerebellar diameter is substantially reduced and cisterna magna may be obliterated [143]. Taken together, the subnormal cerebellar development in fetuses with spina bifida is characterized by a tendency toward early fusion of the cerebellar plates, restricted transverse growth, and failure of inward rotation of the caudal cerebellum.

Postnatal Period

Salman et al. found that in pediatric patients with Chiari II malformation, the total and lateral (hemispheric) cerebellar volumes are reduced and the vermian volume is near normal; however, the midsagittal vermis area and longitudinal and anteroposterior diameters of the vermis are increased [144]. This implies that (1) the cerebellum in patients with Chiari II malformation is smaller (secondary to hypoplasia or atrophy), (2) the hypoplasia or atrophy predominantly affects the lateral cerebellar hemispheres, and (3) the elongation and expansion of the cerebellar vermis may result from side-to-side compression by the two cerebellar hemispheres in an unyielding posterior cranial fossa. Moreover, while the absolute and relative (i.e., fraction of total) volumes of the posterior cerebellar lobe are reduced in Chiari II malformation, the absolute and relative volumes of the anterior cerebellar lobe are increased [145]. This also implies that the overall reduction in size of the cerebellar hemispheres in Chiari II malformation is related to subnormal growth of the posterior cerebellar lobe. The enlarged anterior cerebellar lobe could be a secondary compensation for the compromised posterior lobe [145].

Rhombencephalosynapsis

Complete and partial rhombencephalosynapsis rarely occurs in association with the Chiari II malformation [146, 147]. Rhombencephalosynapsis is an uncommon anomaly in which the two cerebellar hemispheres are fused. In its most complete form, the vermis is fully absent, allowing a fusion, or opposition, of the two cerebellar hemispheres and the dentate nuclei [146]. In partial rhombencephalosynapsis, there is complete absence of the anterior vermis with a hypoplastic posterior vermis [147]. The developmental origin of this malformation is controversial. It has been mentioned that the cerebellar primordium demonstrates a heterogeneous pattern of growth following midline fusion of the cerebellar plates. Generally, the growth of the vermis is slower than that of the lateral hemispheres. This differential growth pattern makes the median-fused region (vermis) topographically distinct from the cerebellar hemispheres. Rhombencephalosynapsis is expected to occur if the growth of the vermis is either retarded, following the early fusion, or paradoxically enhanced to a level comparable to that of the cerebellar hemispheres. However, there is no direct evidence by which to assess this statement.

Agenesis or Occlusion of the Foramen of Magendie in Chiari I Malformation

In 1950, Gardner and Goodall reported 17 patients with Chiari I malformations with or without associated hydromyelia or basilar impression [148]. Each of the patients had an occluded foramen of Magendie due to atresia or to arachnoid adhesions between the impacted cerebellum and the medulla oblongata [148]. Release of the obstruction allowed for symptomatic relief. Gardner et al. [149] posited that the atresia or agenesis of the foramen of Magendie resulted from persisting remnants of the embryonic rhombic roof, which covers the foramen of Magendie. The rhombic roof may also occlude the foramina of Luschka laterally. Depending on the elasticity and permeability of this occluding membrane, a unified embryological theory was proposed for Chiari malformation, Dandy-Walker syndrome, arachnoid cysts of the cerebellum, and hydromyelia/syringomyelia. If the occluding membrane is impermeable, the anomaly is severe. If the membrane is elastic, the fourth ventricle bulges into the cisterna magna, resulting in Dandy-Walker syndrome, whereas an

inelastic membrane causes Chiari malformations. If the membrane is split, an arachnoid cyst appears between the two layers of the rhombic roof. Gardner et al. [149] proposed that occlusion of the foramen of Magendie is physiologically more significant than that of the foramina of Luschka. This is because the foramen of Magendie is located midline and dissipates the ventricular pulse wave into the subarachnoid space. However, these findings faced skepticism when subsequent studies showed occlusion of the foramen of Magendie in only a small proportion of Chiari I patients [150].

Development of the Tentorium Cerebelli

During the eighth week of fetal life, mesenchymal condensations of the cerebrocerebellar fissure, between the cerebellum and the occipital lobe of the cerebrum, form a small transverse fold on either side of the midbrain [75, 141, 151]. These tentorial folds attach laterally to the otic capsules [75] and are symmetrical. Initially, these folds are separate, transparent, and histologically composed of a central core of loosely packed mesodermal cells sandwiched between two layers of flattened mesodermal cells [151]. The tentorium cerebelli is formed, during the third month of fetal life, from the medial fusion of the bilateral tentorial folds dorsally. Once the dorsal tentorial fusion attains a considerable length (10 mm), the fusion is completed, leaving a notch (i.e., tentorial incisura) between the ventral non-united portions of the tentorium through which the midbrain traverses [151]. From this point, there is proportional growth of different regions of the tentorium, as well as replacement of loosely packed mesenchymal core by dense collagenous tissue [151]. Due to differential encephalization, the disproportionate growth of the cerebrum and cerebellum, the tentorium is subjected to continuous traction [75, 98]. This traction stretches the tentorial insertion over the otic capsules, resulting in enhanced bone deposition along its basicranial attachments. This corresponds to the crest of the petrous temporal bone, marking the boundary of the posterior and middle cranial fossa [75].

From an evolutionary point of view, the tentorial folds fuse relatively late in the evolution of mammals. The ratio of the length of the fused tentorium to that of the incisura (the tentorial index) is greater among higher mammals [152]. In addition, the human tentorium cerebelli has the largest surface area relative to body size among primates, and it is the most posteroinferiorly positioned [98, 151, 152]. In patients with Chiari II malformation, the tentorium is often dysplastic, its calvarial attachment is displaced inferiorly toward the foramen magnum, and the tentorial index is low [153, 154].

Posterior Cranial Fossa Volume and Its Determinants

Assuming the posterior cranial fossa is a triaxial ellipsoid, its volume can be estimated by the following formula:

$$V = \frac{1}{6}\pi xyz$$

where $\pi(pi)$ is a constant approximately equal to 3.14, and x, y, and z are, respectively, the width (maximum transverse diameter), length (distance from the dorsum sella to the internal occipital protuberance), and height (distance from the basion to the peak of the tentorium cerebelli corresponding to its ventral edge on the midsagittal plane) of the posterior cranial fossa [111]. Therefore, any factor affecting the width, length, and height of the posterior cranial fossa affects its volume proportionately. In accordance with this formula, the overcrowding of the posterior fossa, in patients with Chiari I malformations, may be related to the fossa's reduced height [96, 110, 111, 155]. The reduction in height is a consequence of supraoccipital and basioccipital hypoplasia, platybasia, and basilar invagination. In addition, the length of the fossa may be low or normal in pediatric patients [111, 156]; however, it is occasionally greater than normal in adult patients [110]. The elongation of the posterior fossa in adults with Chiari I malformations is hypothesized to be compensatory for the reduced height of the posterior fossa [110, 157]. In the studies of pediatric patients that measured the

width of the posterior fossa, both reduced and normal widths were reported [111, 156]. In comparison with a Chiari I malformation that has a slightly larger foramen magnum, a Chiari II malformation is associated with a substantially enlarged foramen magnum [158].

The boundary of the posterior cranial fossa is established by the end of the embryonic period. Initially, the posterior fossa is larger and partially opened posteriorly. During the third month, its posterior boundary is completed. Ventricular distension and cerebellar growth contribute to the growth of the posterior fossa during the embryonic period. Additionally, the volume of the fossa is reduced from the rotation of the tentorium and petrous bone during the second and third trimesters. This reduction in volume is compensated for by the growth of the basicranial synchondroses and upward reflection of the extensible tentorium. Hormonal factors are also crucial in the growth of the posterior fossa. Since the volume of the posterior fossa is dependent on many factors during the embryonic, fetal, and early postnatal periods, a disruption in these factors may lead to a smaller fossa with possible overcrowding and hindbrain herniation. These factors are subsequently discussed.

Ventricular Distension

McLone and Knepper [159] used a mouse embryo model with a caudal neural tube defect to examine the role of ventricular distention in expansion of the posterior cranial fossa. Due to cerebrospinal fluid draining through the neural tube defect, the cranial neurocoele, including the hindbrain vesicle, partially collapsed. The incomplete distension of the hindbrain vesicle leads to the formation of a small posterior fossa, due to the lack of adequate forces and mechanical induction necessary to expand the surrounding mesenchymal or chondrified primordium. McLone and Knepper [159] proposed that a decrease in ventricular distension caused the small posterior fossa in Chiari II malformation. However, ventricular distension is only one factor that influences the size of the posterior fossa, affecting its dimensions during the embryonic and early fetal periods. Therefore, antenatal repair of the neural tube defect between 19 and 25 weeks of gestation does not affect the overall posterior fossa size during the late fetal period [160].

Rotation of the Intracranial Attachment of the Tentorium Cerebelli

During the fetal period, the tentorium rotates backward and downward toward the foramen magnum [98]. This rotation ranges from 90° to 180°, mainly occurring in a fetus less than 160 mm CRL (before 22 weeks of fetal life). During this period, the otic capsule may be precartilaginous or cartilaginous [76, 161–164]. Differential encephalization (i.e., greater expansion of the cerebrum in relation to the cerebellar expansion) is the main factor influencing this rotation, ultimately determining the final intracranial-tentorial attachment [98, 162]. With the expansion of the supratentorial space and posteroinferior rotation of the tentorium, the infratentorial angle (the angle formed between the lines extending from the calvarial attachment of the tentorium to the center of the pituitary fossa and from the pituitary fossa to the basion) decreases by ~40% between 10 and 22 weeks and ~10% between 22 and 29 weeks of the fetal period [98]. The gradual cessation of tentorial rotation after 22 weeks of the fetal period corresponds to the ossification of the otic capsule. The posteroinferior tentorial rotation diminishes the volume of the posterior cranial fossa by reducing its height.

Rotation of the Otic Cartilage and Petrous Temporal Bone and Shift in the Pattern of Posterior Cranial Fossa Growth

By the end of third month of fetal life, the posterior cranial fossa is circular or funnel-shaped with its width and length nearly similar. During the second trimester, the width of the posterior

fossa grows more quickly than its length [87]. This transverse growth is concomitant with, and most likely favored by, the transverse growth of the cerebellum. However, during the late phase fetal development, the posterior fossa grows longitudinally with the expansion of the middle cranial fossa.

During the second half of fetal life, the otic cartilage and petrous temporal bone rotate backward [165] (Fig. 4.24). This rotation is temporally and mechanistically distinct from the tentorial rotation. While the latter ceases around 20–22 weeks of fetal life, the former becomes more prominent following this period. Posteroinferior tentorial rotation occurs on a vertical plane and around a horizontal axis. In contrast, the petrous bone rotates backward along a horizontal plane and around a vertical axis. This results from expansion of the floor of the middle cranial fossa, housing the temporal lobe of the cerebrum [165]. The squeezing of the posterior fossa tends to diminish its width along with the posterior rotation of the petrous bones. However, rapid anteroposterior elongation of the posterior fossa accommodates the growing cerebellum during the late fetal period [165].

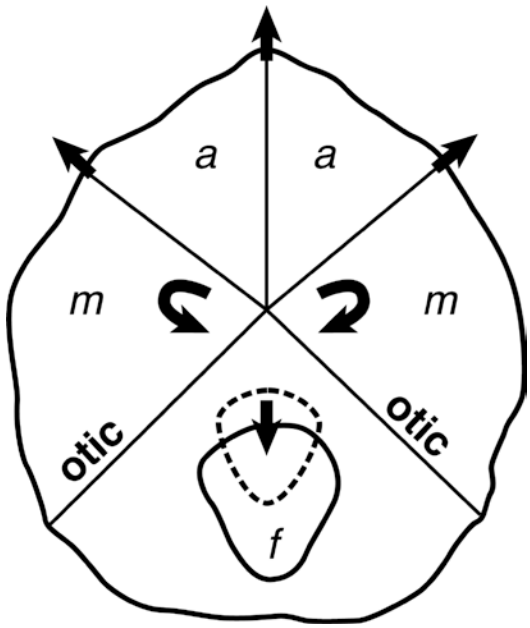

Fig. 4.24 The pattern of basicranial growth and rotation of the otic capsule (petrous temporal) during the second and third trimesters. (Reproduced with slight modifications with permission from Lee et al. [165]) Note that the anterior cranial fossa (*a*) extends forward, the middle cranial fossa (*m*) expands with backward rotation of the petrous, and the foramen magnum (*f*) enlarges and is displaced posteriorly with fetal growth

Growth of the Basicranial Synchondroses

During the fifth month of fetal life, the wall of the posterior cranial fossa is composed of several osseous segments (basiocciput anteriorly, supraoccipuut posteriorly, and exoccipuuts and portions of the petromastoid temporal bone laterally) joined by intervening synchondritic cartilages (Fig. 4.25) [75]. A synchondrosis is an area of quiescent chondrocytes surrounded by a pair of proliferating and hypertrophic cartilaginous growth plates [88]. The growth of synchondrosis results in the deposition of new bone at the flanking osseous segments and growth of the basicranium (Fig. 4.25). The petro-occipital and occipitomastoid synchondroses contribute to the transverse growth of the posterior fossa. The spheno-occipital, anterior and posterior intraoc-

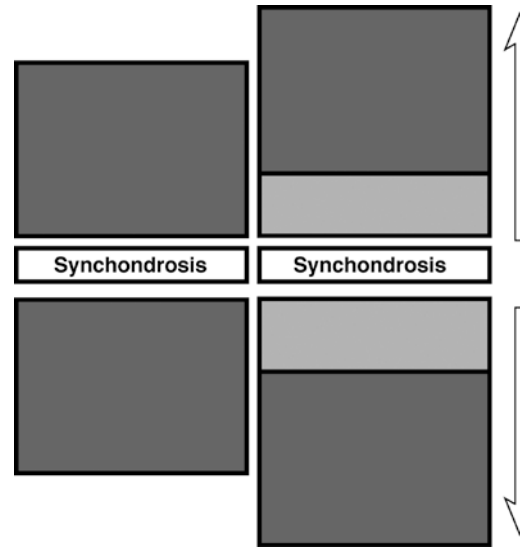

Fig. 4.25 Schema showing the growth of a synchondrosis with introduction of new bone into the flanking osseous segments and centrifugal displacement of those segments [75]

cipital, and occipitomastoid synchondroses contribute to its elongation [75]. This growth, beginning as early as the fourth to fifth month of fetal life [165], continues into postnatal life until the synchondroses become nonfunctional and are replaced by sutures. These sutures are then ossified and fully obliterated with the concomitant fusion of the adjacent bones [16]. The synchondroses show different rates of growth and timing for closure between genders [16]. Generally, the posterior intraoccipital synchondrosis is the first to close. This is followed by the closure of the anterior intraoccipital synchondrosis and then the petro-occipital, occipitomastoid, and spheno-occipital synchondroses [16]. Closure of the anterior and posterior intraoccipital and spheno-occipital synchondroses is usually later in males than females [16].

Histologically, the middle resting zone contains the precursor cells of proliferating chondrocytes and is maintained by bone morphogenetic protein 3 (BMP3) [166]. The maintenance of synchondrosis depends on the proliferation of chondrocytes [167] and the balance between the zones of proliferating and hypertrophied chondrocytes [168]. The phenotypic transition from proliferating to hypertrophic chondrocytes, and later to osteoblasts, occurs toward the chondro-osseous junction of the synchondrosis, resulting in the introduction of new bone around the synchondrosis [167]. Several mediators and signaling pathways control this transition. Fibroblast growth factor receptor isoform 3 (FGFR3) is expressed in the proliferating chondrocytes of the basicranial synchondroses [169]. In a mouse model, overactivation of FGFR3 signaling resulted in a rapid phenotypic transition and accelerated closure of the synchondroses [167]. BMP4 also exerts a biphasic effect on the basicranial synchondroses characterized by an early phase of enhanced proliferation of chondrocytes. This is followed by an accelerated phase of transition into the hypertrophic phenotype [168]. In humans, the spheno-occipital synchondrosis demonstrates a characteristically delayed postnatal closure. Its closure starts at 8 years of age and is almost complete in 50% and 95% of individuals by the ages of 14 and 16–18 years, respectively [16, 32]. Premature closure of the spheno-occipital synchondrosis is a suggested cause of clival hypoplasia (shortened clivus) in patients with Chiari I malformation [37].

Upward Reflection of the Tentorium Cerebellum

Although generally considered a stiff membrane, the dura mater has considerable viscoelastic properties [170, 171], enabling it to react to the tensions and forces applied to it with a rapid phase of expansion mediated by the elastic component and a slow phase mediated by the viscous component. In a cadaveric study, the dura mater had an extensibility of 10–30% [172]. Connective tissues containing collagen fibers and elastin may adapt to mechanical stresses through remodeling or changing the intermolecular crosslinks [173, 174]. These properties of the tentorium enable it to reflect upward and expand to compensate for the increased volume of the infratentorial contents. Although the short-term tentorial expansion is restricted by its viscoelasticity, remodeling of its fibers, as a result of prolonged stress, could lead to greater tentorial expansion in the long term.

Tentorial extensibility has important anatomical relevance. As mentioned earlier, a slight degree of overcrowding in the posterior cranial fossa is normal during fetal development. This overcrowding pushes the expanding tentorium upward. As the tentorium is peripherally attached to the inner surface of the occipital bone and the superior crest of the petrous bone and its attachments are fixed after the second trimester, tentorial expansion makes it concave downward. In the midsagittal plane, the ventral edge (apex) of the tentorium is the peak of this structure and is located above the upper level of the bony posterior fossa. Thus, the posterior fossa can be divided into two regions as shown in Fig. 4.26. Unlike the lower bony region, the upper tentorial region ought to be expansile owing to the extensibility of the tentorium. In adult patients with Chiari I malformation, the tentorial region expands to compensate for overcrowding of the posterior fossa [36].

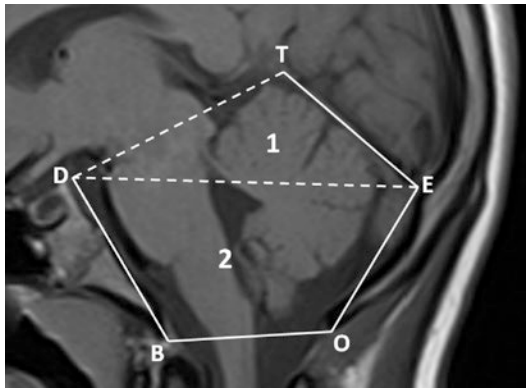

Fig. 4.26 A midsagittal plane of the posterior cranial fossa shows its division into tentorial (1) and bony (2) regions. B, basion; D, dorsum sellae; E, endinion; O, opisthion; T, apex or peak of the tentorium. The T-E-O angle is the tentorial angle; T-E-D, the angle of the tentorium to Twining's line; D-E-O, the supraoccipital angle; E-D-B, the clival angle; and D-B-O, Boogard's angle

Hormonal Influences

The basicranial synchondroses are homologous to the epiphyseal growth plates of the long bones. In experimental and human studies, endochondral and periosteal bone growth and bone turnover and remodeling are influenced by such hormones as tyroxine, cortisol, estrogen, testosterone, parathyroid hormone, growth hormone, and activated vitamin D (cholecalciferol) [175–181]. It is not yet clear the extent to which the posterior fossa reacts to these hormones. In vitro, hydrocortisone and parathyroid hormone dose-dependently enhance glycosaminoglycan synthesis by the chondrocytes derived from the spheno-occipital synchondrosis of the rabbit [182, 183]. In addition, hydrocortisone and cholecalciferol increase the proliferation of these chondrocytes [183, 184]. In patients with hypothyroidism, the spheno-occipital synchondrosis may remain open until the fourth decade of life [185]. In patients with growth hormone deficiency, the basiocciput is shorter than normal [185]. Finally, the posterior fossa was significantly smaller in a series of patients with rickets than in healthy controls, and ~30% of those patients had Chiari I malformation [186]. This data indirectly indicates that various hormones regulate posterior fossa growth. Further studies are required to elucidate this aspect of development and especially the role of sex hormones.

References

1. Dockter JL. Sclerotome induction and differentiation. Curr Top Dev Biol. 2000;48:77–127.
2. Christ B, Huang R, Scaal M. Formation and differentiation of the avian sclerotome. Anat Embryol (Berl). 2004;208:333–50.
3. Ebensperger C, Wilting J, Brand-Saberi B, Mizutani Y, Christ B, Balling R, Koseki H. Pax-1, a regulator of sclerotome development is induced by notochord and floor plate signals in avian embryos. Anat Embryol (Berl). 1995;191:297–310.
4. Fan CM, Tessier-Lavigne M. Patterning of mammalian somites by surface ectoderm and notochord: evidence for sclerotome induction by a hedgehog homolog. Cell. 1994;79:1175–86.
5. Sensenig EC. The early development of the human vertebral column. Contr Embryol Carneg Inst. 1957;33:21–41.
6. Frazer JE. A manual of embryology. New York: William Wood and Company; 1931. p. 142–63.
7. Robinson A, editor. Cunningham's textbook of anatomy. 5th ed. New York: William Wood and Company; 1918.
8. Dockter JL. Sclerotome induction and differentiation. In: Ordahl CP, editor. Somitogenesis: Part 2. San Diego: Academic Press; 2000b. p. 77–128.
9. O'Rahilly R, Müller F. The early development of the hypoglossal nerve and occipital somites in staged human embryos. Am J Anat. 1984;169:237–57.
10. Ganguly DN, Roy KK. A study on the craniovertebral joint in the man. Anat Anz Bd. 1964;114:433–52.
11. Bailey RW, Sherk HH, Dunn EJ, et al., editors. The cervical spine – the Cervical Spine Research Society. Philadelphia: JB Lippincott; 1983.
12. Ludwig KS. Die frühentwicklung des atlas und der occipitalwirbel beim menschen. Acta Anat (Basel). 1957;80:444–61.
13. Müller F, O'Rahilly R. Occipitocervical segmentation in staged human embryos. J Anat. 1994;185:251–8.
14. Müller F, O'Rahilly R. Segmentation in staged human embryos: the occipitocervical region revisited. J Anat. 2003;203:297–315.
15. Tillmann B, Lorenz R. The stress at the human atlanto-occipital joint. I. The development of the occipital condyle. Anat Embryol (Berl). 1978;153:269–77.
16. Madeline LA, Elster AD. Suture closure in the human chondrocranium: CT assessment. Radiology. 1995;196(3):747–56.

17. Taitz C. Bony observations of some morphological variations and anomalies of the craniovertebral region. Clin Anat. 2000;13:354–60.
18. Prescher A, Brors D, Adam G. Anatomic and radiologic appearance of several variants of the craniocervical junction. Skull Base Surg. 1996;6:83–94.
19. Prescher A. The craniocervical junction in man, the osseous variations, their significance and differential diagnosis. Ann Anat. 1997;179:1–19.
20. Pang D, Thompson DN. Embryology and bony malformations of the craniovertebral junction. Childs Nerv Syst. 2011;27:523–64.
21. Oetteking B. On the morphological significance of certain cranio-vertebral variations. Anat Rec. 1923;25:339–53.
22. Vasudeva N, Choudhry R. Precondylar tubercles on the basiocciput of adult human skulls. J Anat. 1996;188:207–10.
23. Tubbs RS, Grabb P, Spooner A, Wilson W, Oakes WJ. The apical ligament: anatomy and functional significance. J Neurosurg. 2000;92:197–200.
24. Rao PV. Median (third) occipital condyle. Clin Anat. 2002;15(2):148–51.
25. Scheuer L, Black SM. The juvenile skeleton. San Diego: Elsevier Academic Press; 2004. p. 195.
26. Menezes AH, Fenoy KA. Remnants of occipital vertebrae: proatlas segmentation abnormalities. Neurosurgery. 2009;64:945–53.
27. Goel A, Shah A. Unusual bone formation in the anterior rim of foramen magnum: cause, effect and treatment. Eur Spine J. 2010;19:S162–4.
28. Xu S, Pang Q, Zhang K, Zhang H. Two patients with proatlas segmentation malformation. J Clin Neurosci. 2010;17:647–8.
29. Menezes AH. Primary craniovertebral anomalies and the hindbrain herniation syndrome (Chiari I): data base analysis. Pediatr Neurosurg. 1995;23:260–9.
30. Csakany G. Proatlas manifestation as diagnostic problem [Hungarian]. Magy Radiol. 1957;9:216–20.
31. Denisov SD, Kabak SL. Rare case of manifestation of a proatlas [Russian]. Arkh Anat Gistol Embriol. 1984;86:75–7.
32. Madeline LA, Elster AD. Postnatal development of the central skull base: normal variants. Radiology. 1995b;196:757–63.
33. Kruyff E. Transverse cleft in the basi-occiput. Acta Radiol Diagn (Stockh). 1967;6:41–8.
34. Johnson GF, Israel H. Basioccipital clefts. Radiology. 1979;133:101–3.
35. Smoker WR. Craniovertebral junction: normal anatomy, craniometry, and congenital anomalies. Radiographics. 1994;14:255–77.
36. Nishikawa M, Sakamoto H, Hakuba A, Nakanishi N, Inoue Y. Pathogenesis of Chiari malformation: a morphometric study of the posterior cranial fossa. J Neurosurg. 1997;86(1):40–7.
37. Noudel R, Jovenin N, Eap C, Scherpereel B, Pierot L, Rousseaux P. Incidence of basioccipital hypoplasia in Chiari malformation type I: comparative morphometric study of the posterior cranial fossa. Clinical article. J Neurosurg. 2009;111(5):1046–52.
38. Cankal F, Ugur HC, Tekdemir I, Elhan A, Karahan T, Sevim A. Fossa navicularis: anatomic variation at the skull base. Clin Anat. 2004;17:118–22.
39. Hauser G, De Stefano GF. Epigenetic variants of the human skull. Stuttgart: Schweizerbartsche; 1989.
40. Finke J. On the incidence of the pharyngeal tubercle, a roentgenological variant at the base of the skull [German]. Dtsch Z Nervenheilkd. 1964;186:186–9.
41. Tubbs RS, Salter EG, Oakes WJ. Duplication of the occipital condyles. Clin Anat. 2005;18:92–5.
42. Kunicki J, Ciszek B. The clinical anatomy and the occipital condyle variants. Clin Anat. 2005;18:646–7.
43. Ohaegbulam C, Woodard EJ, Proctor M. Occipitocondylar hyperplasia: an unusual craniovertebral junction anomaly causing myelopathy. Case report. J Neurosurg. 2005;103:379–81.
44. Halanski MA, Iskandar B, Nemeth B, Noonan KJ. The coconut condyle: occipital condylar dysplasia causing torticollis and leading to c1 fracture. J Spinal Disord Tech. 2006;19:295–8.
45. Lang J. Skull base and related structures: atlas of clinical anatomy. 2nd ed. Stuttgart: Schattauer; 2001.
46. Anderson T. Paracondylar process: manifestation of an occipital vertebra. Int J Osteoarchaeo. 1996;l6:195–201.
47. Stratemeier PH, Jensen SR. Partial regressive occipital vertebra. Neuroradiology. 1980;19:47–9.
48. Gladstone RJ, Erichsen-Powell W. Manifestation of occipital vertebrae, and fusion of the atlas with the occipital bone. J Anat Physiol. 1915;49:190–209.
49. Prescher A. The craniocervical junctions and its variations. In: Voger R, Fanghanel J, Giebel J, editors. Aspects of teratology, volume 1 – proceedings on the 9th teratology symposium, Greifswald, August 30–September 1, 1995. Marburg: Tectum Verlag; 1996. p. 62–4.
50. Lakhtakia PK, Premsagar IC, Bisaria KK, Bisaria SD. A tubercle at the anterior margin of the foramen magnum. J Anat. 1991;177:209–10.
51. Piersol GA, editor. Human anatomy including structure and development and practical considerations. 6th ed. Philadelphia: J.B. Lippincott Company; 1918.
52. Le Double AF. Traité des variations des os du crane de l'homme, et de leur signification au point de vue de l'anthropologie zoologique. Paris: Vigot Freres; 1903.
53. Caffey J. On the accessory ossicles of the supraoccipital bone: some newly recognized roentgen features of the normal infantile skull. Am J Roentgenol Radium Therapy, Nucl Med. 1953;70:401–12.
54. Lochmuller CM, Marks MK, Mileusnic-Polchan D, Cogswell SC. Misidentification of a transverse occipital suture as a persistent mendosal suture. J Pediatr. 2011;159:876–7.
55. Nayak SR, Krishnamurthy A, Madhan Kumar SJ, Prabhu LV, Jiji PJ, Pai MM, Kumar A, Avadhani R. The mendosal suture of the occipital bone: occurrence in Indian population, embryology and clinical significance. Surg Radiol Anat. 2007;29:329–32.

56. Tubbs RS, Salter EG, Oakes WJ. Does the mendosal suture exist in the adult? Clin Anat. 2007;20:124–5.
57. Tsuang FY, Chen JY, Wang YH, Lai DM. Neurological picture. Occipitocervical malformation with atlas duplication. J Neurol Neurosurg Psychiat. 2011;82:1101–2.
58. Shoja MM, Loukas M, Tubbs RS. Persistence of proatlas in man (comment on "Occipitocervical malformation with atlas duplication"). J Neurol Neurosurg Psych. 2012.; http://jnnp.bmj.com/content/82/10/1101/reply. Accessed February 2017.
59. Shoja MM, Johal J, Oakes WJ, Tubbs RS. Embryology and pathophysiology of the Chiari I and II malformations: a comprehensive review. Clin Anat. 2017;2017
60. Gasser RF. Early formation of the basicranium in man. In: Bosma JF, editor. Symposium on development of the Basicranium. Bethesda: Department of Health, Education and Welfare. 1976. p. 29–43.
61. Menezes AH. Craniocervical developmental anatomy and its implications. Childs Nerv Syst. 2008;24:1109–22.
62. Macalister A. Notes on the development and variations of the atlas. J Anat Physiol. 1893;27:519–42.
63. Allen W. The varieties of the atlas in the human subject, and the homologies of its transverse processes. J Anat Physiol. 1879;14:18–27.
64. Bergman RA, Afifi AK, Miyauchi R. Cervical vertebrae. 1996, http://www.anatomyatlases.org/AnatomicVariants/SkeletalSystem/Text/CervicalVertebrae.shtml. Accessed February 2012.
65. Chopra JS, Sawhney IM, Kak VK, Khosla VK. Craniovertebral anomalies: a study of 82 cases. Br J Neurosurg. 1988;2:455–64.
66. Gholve PA, Hosalkar HS, Ricchetti ET, Pollock AN, Dormans JP, Drummond DS. Occipitalization of the atlas in children. Morphologic classification, associations, and clinical relevance. J Bone Joint Surg Am. 2007;89:571–8.
67. Kassim NM, Latiff AA, Das S, Ghafar NA, Suhaimi FH, Othman F, Hussan F, Sulaiman IM. Atlantooccipital fusion: an osteological study with clinical implications. Bratisl Lek Listy. 2010;111:562–5.
68. Kalla AK, Khanna S, Singh IP, Sharma S, Schnobel R, Vogel F. A genetic and anthropological study of atlanto-occipital fusion. Hum Genet. 1989;81:105–12.
69. Tubbs RS, Lancaster JR, Mortazavi MM, Shoja MM, Chern JJ, Loukas M, Cohen-Gadol AA. Morphometry of the outlet of the foramen magnum in crania with atlantooccipital fusion. J Neurosurg Spine. 2011;15:55–9.
70. Condie BG, Capecchi MR. Mice homozygous for a targeted disruption of Hoxd-3 (Hox-4.1) exhibit anterior transformations of the first and second cervical vertebrae, the atlas and the axis. Development. 1993;119:579–95.
71. Ferrier DE, Holland PW. Ancient origin of the Hox gene cluster. Nat Rev Genet. 2001;2:33–8.
72. Burke AC, Nelson CE, Morgan BA, Tabin C. Hox genes and the evolution of vertebrate axial morphology. Development. 1995;121:333–46.
73. Pourquié O, editor. Hox genes. San Diego: Academic Press; 2009.
74. Davies HW. Radiological changes associated with Arnold-Chiari malformation. Br J Radiol. 1967;40:262–9.
75. Friede H. Normal development and growth of the human neurocranium and cranial base. Scand J Plast Reconstr Surg. 1981;15(3):163–9.
76. Lemire RJ. Embryology of the skull. In: Cohen Jr MM, MacLean RE, editors. Craniosynostosis. Diagnosis, evaluation and management. 2nd ed. Oxford: Oxford University Press; 2000. p. 25–34.
77. Schäfer EA, Symington J, Bryce TH (eds). Quain's elements of anatomy, vol. 1: embryology. 11th ed. New York: Longmans, Green, and Co.; 1908.
78. Parsons FG. Skull. In: Encyclopedia Britannica, vol. 25, 11th ed. New York: Encyclopedia Britannica Company. 1911. p. 196–200.
79. Kernan JD Jr. The Chondrocranium of a 20 mm. Human Embryo. J Morphol. 1916;27:605–46.
80. Levi G. Beitrag lum studium der entwickelung des knorpeligen primordialcraniums des menschen. Arch Mikr Anat. 1900;55:341–414.
81. Macklin CC. The skull of a human fetus of 43 millimeters greatest length. Contri Embryol. 1921;48:57–103.
82. Müller F, O'Rahilly R. The human chondrocranium at the end of the embryonic period, proper, with particular reference to the nervous system. Am J Anat. 1980;159:33–58.
83. Niida S, Yamasaki A, Kodama H. Interference with interparietal growth in the human skull by the tectum synoticum posterior. J Anat. 1992;180:197–200.
84. Hertwig O. Handbuch Der Vergleichenden Und Experimentellen Entwicklungslehre Der Wirbeltiere, Band II, Teil 2. Jena: G. Fischer. 1906. p. 824.
85. Kjaer I. Ossification of the human fetal basicranium. J Craniofac Genet Dev Biol. 1990;10:29–38.
86. Mall FP. On ossification centers in human embryos less than one hundred days old. Am J Anat. 1906;5:433–58.
87. Jeffery N. A high-resolution MRI study of linear growth of the human fetal skull base. Neuroradiology. 2002;44:358–66.
88. McBratney-Owen B, Iseki S, Bamforth SD, Olsen BR, Morriss-Kay GM. Development and tissue origins of the mammalian cranial base. Dev Biol. 2008;322(1):121–32.
89. Gans C, Northcutt RG. Neural crest and the origin of vertebrates: a new head. Science. 1983;220:268–73.
90. Choudhary AK, Jha B, Boal DK, Dias M. Occipital sutures and its variations: the value of 3D-CT and how to differentiate it from fractures using 3D-CT? Surg Radiol Anat. 2010;32:807–16.
91. Srivastava HC. Ossification of the membranous portion of the squamous part of the occipital bone in man. J Anat. 1992;180:219–24.

92. Shapiro R, Robinson F. Embryogenesis of the human occipital bone. AJR Am J Roentgenol. 1976;126:1063–8.
93. Balboni AL, Estenson TL, Reidenberg JS, Bergemann AD, Laitman JT. Assessing age-related ossification of the petro-occipital fissure: laying the foundation for understanding the clinicopathologies of the cranial base. Anat Rec. 2005;282:38–48.
94. Srivastava HC. Development of ossification centres in the squamous portion of the occipital bone in man. J Anat. 1977;124:643–9.
95. Koenigsberg RA, Vakil N, Hong TA, Htaik T, Faerber E, Maiorano T, Dua M, Faro S, Gonzales C. Evaluation of platybasia with MR imaging. AJNR Am J Neuroradiol. 2005;26:89–92.
96. Schady W, Metcalfe RA, Butler P. The incidence of craniocervical bony anomalies in the adult Chiari malformation. J Neurol Sci. 1987;82(1–3):193–203.
97. Jeffery N. Cranial base angulation and growth of the human fetal pharynx. Anat Rec A Discov Mol Cell Evol Biol. 2005;284:491–9.
98. Jeffery N. Differential regional brain growth and rotation of the prenatal human tentorium cerebelli. J Anat. 2002b;200:135–44.
99. Jeffery N, Spoor F. Brain size and the human cranial base: a prenatal perspective. Am J Phys Anthropol. 2002;118:324–40.
100. Hodak JA, Mamourian A, Dean BL. Radiologic evaluation of the craniovertebral junction. In: Dickman CA, Spetzler RF, Sonntag VK, editors. Surgery of the craniovertebral junction. New York: Thiem; 1998.
101. Bares L. Basilar impression and the so-called 'associated anomalies'. Eur Neurol. 1975;13:92–100.
102. Roth M. Cranio-cervical growth collision: another explanation of the Arnold-Chiari malformation and of basilar impression. Neuroradiology. 1986;28:187–94.
103. Hinck VC, Hopkins CE, Savara BS. Diagnostic criteria of basilar impression. Radiology. 1961;76:572–85.
104. Smith JS, Shaffrey CI, Abel MF, Menezes AH. Basilar invagination. Neurosurgery. 2010;66:39–47.
105. Pearce JM. Platybasia and basilar invagination. Eur Neurol. 2007;58:62–4.
106. Goel A, Bhatjiwale M, Desai K. Basilar invagination: a study based on 190 surgically treated patients. J Neurosurg. 1998;88:962–8.
107. Caetano de Barros M, Farias W, Ataíde L, Lins S. Basilar impression and Arnold-Chiari malformation. A study of 66 cases. J Neurol Neurosurg Psychiatry. 1968;31:596–605.
108. Paradis RW, Sax DS. Familial basilar impression. Neurology. 1972;22:554–60.
109. Krogness KG. Posterior fossa measurements. I. The normal size of the posterior fossa. Pediatr Radiol. 1978;6(4):193–7.
110. Karagöz F, Izgi N, Kapíjcíjoğlu Sencer S. Morphometric measurements of the cranium in patients with Chiari type I malformation and comparison with the normal population. Acta Neurochir. 2002;144(2):165–71.
111. Greenlee J, Garell PC, Stence N, Menezes AH. Comprehensive approach to Chiari malformation in pediatric patients. Neurosurg Focus. 1999;6(6):e4.
112. Cesmebasi A, Loukas M, Hogan E, Kralovic S, Tubbs RS, Cohen-Gadol AA. The Chiari malformations: a review with emphasis on anatomical traits. Clin Anat. 2015;28:184–94.
113. Vega A, Quintana F, Berciano J. Basichondrocranium anomalies in adult Chiari type I malformation: a morphometric study. J Neurol Sci. 1990;99:137–45.
114. Shah A, Goel A. Clival dysgenesis associated with Chiari Type 1 malformation and syringomyelia. J Clin Neurosci. 2010;17:400–1.
115. Aydin S, Hanimoglu H, Tanriverdi T, Yentur E, Kaynar MY. Chiari type I malformations in adults: a morphometric analysis of the posterior cranial fossa. Surg Neurol. 2005;64:237–41.
116. Dufton JA, Habeeb SY, Heran MK, Mikulis DJ, Islam O. Posterior fossa measurements in patients with and without Chiari I malformation. Can J Neurol Sci. 2011;38(3):452–5.
117. Milhorat TH, Chou MW, Trinidad EM, Kula RW, Mandell M, Wolpert C, Speer MC. Chiari I malformation redefined: clinical and radiographic findings for 364 symptomatic patients. Neurosurgery. 1999;44:1005–17.
118. Dagtekin A, Avci E, Kara E, Uzmansel D, Dagtekin O, Koseoglu A, Talas D, Bagdatoglu C. Posterior cranial fossa morphometry in symptomatic adult Chiari I malformation patients: comparative clinical and anatomical study. Clin Neurol Neurosurg. 2011;113:399–403.
119. Marin-Padilla M, Marin-Padilla TM. Morphogenesis of experimentally induced Arnold–Chiari malformation. J Neurol Sci. 1981;50:29–55.
120. Bailey FR, Miller AM. Textbook of human embryology. 4th ed. New York: William Wood and Company; 1921. p. 495–500.
121. Dow RS. The evolution and anatomy of the cerebellum. Biol Rev. 1942;17:179–220.
122. Hamilton WJ, Boyd JD, Mossman HW. Human embryology. 2nd ed. Baltimore: The Williams & Wilkins Company; 1952. p. 285–9.
123. Heisler JC. A textbook of embryology. 3rd ed. Philadelphia: W.B. Saunders Company; 1907. p. 287–8.
124. Hochstetter F. Beitrage zur Entwicklungsgeschichte des menschlichen Gehirns: Teil I. Wien: Deuticke; 1919.
125. Keibel F, Mall FP. Manual of human embryology, vol. 2. Philadelphia: J.B. Lippincott Company; 1912. p. 67–74.
126. Keith A. Human embryology and morphology. 6th ed. Baltimore: The Williams and Wilkins Company; 1948. p. 138–46.
127. Minot CS. Human embryology. New York: William Wood and Company; 1892. p. 593–705.

128. Patten BM. Human embryology. 3rd ed. New York: McGraw-Hill Book Company; 1968. p. 280–2.
129. Stroud BB. The morphology of the ape cerebellum. Proc Ass Am Anat. 1897:107–26.
130. Babcook CJ, Chong BW, Salamat MS, Ellis WG, Goldstein RB. Sonographic anatomy of the developing cerebellum: normal embryology can resemble pathology. AJR Am J Roentgenol. 1996;166:427–33.
131. Chong BW, Babcook CJ, Pang D, Ellis WG. A magnetic resonance template for normal cerebellar development in the human fetus. Neurosurgery. 1997;41(4):924–8.
132. Limperopoulos C, Soul JS, Gauvreau K, Huppi PS, Warfield SK, Bassan H, Robertson RL, Volpe JJ, du Plessis AJ. Late gestation cerebellar growth is rapid and impeded by premature birth. Pediatrics. 2005;115(3):688–95.
133. Liu F, Zhang Z, Lin X, Teng G, Meng H, Yu T, Fang F, Zang F, Li Z, Liu S. Development of the human fetal cerebellum in the second trimester: a post mortem magnetic resonance imaging evaluation. J Anat. 2011;219:582–8.
134. Malinger G, Ginath S, Lerman-Sagie T, Watemberg N, Lev D, Glezerman M. The fetal cerebellar vermis: normal development as shown by transvaginal ultrasound. Prenat Diagn. 2001;21:687–92.
135. Lemire RJ, Looser JD, Leech RW, Alvord EC. Normal and abnormal development of the human nervous system. Hagerstown: Harper & Row; 1975.
136. Anthony TR. Neuroanatomy and the neurologic exam: a thesaurus of synonyms, similar-sounding non-synonyms, and terms of variable meaning. Boca Raton: CRC Press; 1994. p. 137.
137. Tagliavini F, Pietrini V. On the variability of the human flocculus and paraflocculus accessorius. J Hirnforsch. 1984;25:163–70.
138. Weed LH. The development of the cerebrospinal spaces in pig and in man. Contrib Embryol. 1917;5:1–116.
139. Wilson JT. On the nature and mode of origin of the foramen of Magendie. J Anat. 1937;71:423–8.
140. Blake JA. The roof and lateral recesses of the fourth ventricle, considered morphologically and embryologically. J Comp Neurol. 1900;10:79–108.
141. Padget DH. Development of so-called dysraphism; with embryologic evidence of clinical Arnold-Chiari and Dandy-Walker malformations. Johns Hopkins Med J. 1972;130(3):127–65.
142. van Hoytema GJ, van den Berg R. Embryological studies of the posterior fossa in connection with Arnold-Chiari malformation. Dev Med Child Neurol. 1966;11:61–76.
143. Pilu G, Romero R, Reece EA, Goldstein I, Hobbins JC, Bovicelli L. Subnormal cerebellum in fetuses with spina bifida. Am J Obstet Gynecol. 1988;158(5):1052–6.
144. Salman MS, Dennis M, Sharpe JA. The cerebellar dysplasia of Chiari II malformation as revealed by eye movements. Can J Neurol Sci. 2009;36(6):713–24.
145. Juranek J, Dennis M, Cirino PT, El-Messidi L, Fletcher JM. The cerebellum in children with spina bifida and Chiari II malformation: quantitative volumetrics by region. Cerebellum. 2010;9(2):240–8.
146. Sener RN, Dzelzite S. Rhombencephalosynapsis and a Chiari II malformation. J Comput Assist Tomogr. 2003;27(2):257–9.
147. Utsunomiya H, Takano K, Ogasawara T, Hashimoto T, Fukushima T, Okazaki M. Rhombencephalosynapsis: cerebellar embryogenesis. AJNR Am J Neuroradiol. 1998;19(3):547–9.
148. Gardner WJ, Goodall RJ. The surgical treatment of Arnold-Chiari malformation in adults; an explanation of its mechanism and importance of encephalography in diagnosis. J Neurosurg. 1950;7(3):199–206.
149. Gardner WJ, Abdullah AF, McCormack LJ. The varying expressions of embryonal atresia of the fourth ventricle in adults: Arnold-Chiari malformation, Dandy-Walker syndrome, arachnoid cyst of the cerebellum, and syringomyelia. J Neurosurg. 1957;14(6):591–605.
150. Tubbs RS, Smyth MD, Wellons JC 3rd, Oakes WJ. Arachnoid veils and the Chiari I malformation. J Neurosurg. 2004;100(5 Suppl Pediatrics): 465–7.
151. Klintworth GK. The ontogeny and growth of the human tentorium cerebelli. Anat Rec. 1967;158(4):433–41.
152. Klintworth GK. The comparative anatomy and phylogeny of the tentorium cerebelli. Anat Rec. 1968;160(3):635–42.
153. Peach B. Arnold-Chiari malformation: anatomic features of 20 cases. Arch Neurol. 1965;12:613–21.
154. Gardner WJ. The Dysraphic states. Amsterdam: Excerpta Medica; 1973.
155. Stovner LJ, Bergan U, Nilsen G, Sjaastad O. Posterior cranial fossa dimensions in the Chiari I malformation: relation to pathogenesis and clinical presentation. Neuroradiology. 1993;35:113–8.
156. Furtado SV, Reddy K, Hegde AS. Posterior fossa morphometry in symptomatic pediatric and adult Chiari I malformation. J Clin Neurosci. 2009;16:1449–54.
157. Nyland H, Krogness KG. Size of posterior fossa in Chiari type 1 malformation in adults. Acta Neurochir. 1978;40:233–42.
158. Burgener FA, Meyers SP, Tan RK, Zaunbauer W. Differential diagnosis in magnetic resonance imaging. New York: Thieme; 2002.
159. McLone DG, Knepper PA. The cause of Chiari II malformation: a unified theory. Pediatr Neurosci. 1989;15(1):1–12.
160. Grant RA, Heuer GG, Carrión GM, Adzick NS, Schwartz ES, Stein SC, Storm PB, Sutton LN. Morphometric analysis of posterior fossa after in utero myelomeningocele repair. J Neurosurg Pediatr. 2011;7(4):362–8.
161. Hochstetter F. Über die Entwicklung und Differenzierung de Hüllen des Menschlichen Hehirns. Morph Jahrb. 1939;83:359–494.

162. Spoor F, Zonneveld F. Comparative review of the human bony labyrinth. Am J Phys Anthropol. 1998;Suppl 27:211–51.
163. Butler H. The development of certain human dural venous sinuses. J Anat. 1957;91(4):510–26.
164. Moss ML, Noback CR, Robertson GG. Growth of certain human fetal cranial bones. Am J Anat. 1956;98(2):191–204.
165. Lee SK, Kim YS, Jo YA, Seo JW, Chi JG. Prenatal development of cranial base in normal Korean fetuses. Anat Rec. 1996;246(4):524–34.
166. Kettunen P, Nie X, Kvinnsland IH, Luukko K. Histological development and dynamic expression of Bmp2-6 mRNAs in the embryonic and postnatal mouse cranial base. Anat Rec A Discov Mol Cell Evol Biol. 2006;288(12):1250–8.
167. Matsushita T, Wilcox WR, Chan YY, Kawanami A, Bükülmez H, Balmes G, et al. FGFR3 promotes synchondrosis closure and fusion of ossification centers through the MAPK pathway. Hum Mol Genet. 2009;18(2):227–40.
168. Shum L, Wang X, Kane AA, Nuckolls GH. BMP4 promotes chondrocyte proliferation and hypertrophy in the endochondral cranial base. Int J Dev Biol. 2003;47(6):423–31.
169. Rice DP, Rice R, Thesleff I. Fgfr mRNA isoforms in craniofacial bone development. Bone. 2003;33(1):14–27.
170. Galford JE, McElhaney JH. A viscoelastic study of scalp, brain, and dura. J Biomech. 1970;3(2):211–21.
171. Twomey C, Tsui BC. Complications of epidural blockade. In: Finucane BT, editor. Complications of regional anesthesia. 2nd ed. New York: Springer. 2007. p. 167–94.
172. Kargapol'tseva GV. The strength and elasticity of the dura mater [Russian]. Vopr Neirokhir. 1975;1:53–4.
173. Lundon K. The effect of mechanical load on soft connective tissue. In: Hammer WI, editor. Functional soft-tissue examination and treatment by manual methods. Sudbury: Jones and Bartlett Publishers, Inc.; 2007. p. 15–30.
174. Alter MJ. Science of flexibility. 3rd ed. Champaign: Human Kinetics; 2004.
175. Raisz LG, Kream BE. Regulation of bone formation. N Engl J Med. 1983;309(1):29–35.
176. Raisz LG, Kream BE. Regulation of bone formation (second of two parts). N Engl J Med. 1983;309(2):83–9.
177. Raisz LG. Hormonal regulation of bone growth and remodelling. Ciba Found Symp. 1988;136:226–38.
178. Lombardi G, Di Somma C, Rubino M, Faggiano A, Vuolo L, Guerra E, Contaldi P, Savastano S, Colao A. The roles of parathyroid hormone in bone remodeling: prospects for novel therapeutics. J Endocrinol Invest. 2011;34(7 Suppl):18–22.
179. Ohlsson C, Bengtsson BA, Isaksson OG, Andreassen TT, Slootweg MC. Growth hormone and bone. Endocr Rev. 1998;19(1):55–79.
180. Wit JM, Camacho-Hübner C. Endocrine regulation of longitudinal bone growth. Endocr Dev. 2011;21:30–41.
181. Ahmed M, Sarwar M, Ahmed I, Qureshi GA, Makhdoom A, Parvez SH. Effect of carbimazole induced hypothyroidism and thyroxine replacement on the growth of the long bones in albino rats of different age groups. Neuro Endocrinol Lett. 2007;28(4):484–8.
182. Takano T, Takigawa M, Shirai E, Nakagawa K, Sakuda M, Suzuki F. The effect of parathyroid hormone (1-34) on cyclic AMP level, ornithine decarboxylase activity, and glycosaminoglycan synthesis of chondrocytes from mandibular condylar cartilage, nasal septal cartilage, and spheno-occipital synchondrosis in culture. J Dent Res. 1987;66(1):84–7.
183. Takigawa M, Takano T, Nakagawa K, Sakuda M, Suzuki F. Hydrocortisone stimulation of proliferation and glycosaminoglycan synthesis in rabbit craniofacial chondrocytes in vitro. Arch Oral Biol. 1988;33(12):893–9.
184. Takano-Yamamoto T, Soma S, Kyung HM, Nakagawa K, Yamashiro T, Sakuda M. Differential effects of 1 alpha, 25-dihydroxycholecalciferol and 24R,25-dihydroxycholecalciferol on the proliferation and the differentiated phenotype of rabbit craniofacial chondrocytes in primary culture. J Osaka Univ Dent Sch. 1992;32:51–9.
185. Tubbs RS, Wellons JC 3rd, Smyth MD, Bartolucci AA, Blount JP, Oakes WJ, Grabb PA. Children with growth hormone deficiency and Chiari I malformation: a morphometric analysis of the posterior cranial fossa. Pediatr Neurosurg. 2003;38(6):324–8.
186. Tubbs RS, Webb D, Abdullatif H, Conklin M, Doyle S, Oakes WJ. Posterior cranial fossa volume in patients with rickets: insights into the increased occurrence of Chiari I malformation in metabolic bone disease. Neurosurgery. 2004;55(2):380–3.

5 Embryology and Pathophysiology of the Chiari I and II Malformations

Mohammadali M. Shoja, R. Shane Tubbs, and W. Jerry Oakes

Although Chiari I and II malformations have hindbrain herniation into the upper cervical spinal canal, both are also often associated with other anomalies of the craniofacial skeleton, vertebral column, and central nervous system (CNS). Table 5.1 lists some of these associated anomalies [1–22]. The herniated hindbrain may include the medulla oblongata, fourth ventricle, and caudal vermis and cerebellar hemispheres (usually tonsils) to varying extents. An efficient theory with high explanatory power should be able to provide a rational basis for the occurrence of not only hindbrain herniation but also that of other associated anomalies. Currently, no single theory explains each of these malformations as the Chiari malformation seems to result from a heterogeneous spectrum of ontogenetic errors and pathological mechanisms, which share some common phenotypical presentations [23]. In this chapter, the theories pertinent to the embryology and pathophysiology of Chiari I and II malformations and their associated anomalies are discussed.

M. M. Shoja
Division of General Surgery, Tabriz University of Medical Sciences, Tabriz, Iran

University of Illinois at Chicago, Metropolitan Group Hospitals, Chicago, IL, USA

R. S. Tubbs (✉)
Department of Neurosurgery, Tulane University School of Medicine, New Orleans, LA, USA

Department of Neurosurgery and Ochsner Neuroscience Institute, Ochsner Health System, New Orleans, LA, USA

W. J. Oakes
Departments of Neurosurgery and Pediatrics, University of Alabama, Birmingham, AL, USA

Hydrocephalic Brain or Pressure Coning Theory

The question of whether hydrocephalus is the cause or effect of hindbrain herniation has been considered since Chiari's initial description and is complicated by the fact that hydrocephalus may occur without associated hindbrain herniation and vice versa [24]. Therefore, it is reasonable to assume that the developmental or postnatal factors leading to hydrocephalus and hindbrain herniation are mechanistically distinct but also partially overlap. A historical account of the discourses on the relationship between hydrocephalus and hindbrain herniation would best aid in clarifying this concept. In his classic paper of 1891, Hans Chiari wrote:

> Since giving more attention to these relationships [in both type I and II malformations], I have had the impression that the extension of the tonsils and medial side of the inferior lobes [of the cerebellum] *probably* always is the result of chronic and the very early onset of cerebral hydrocephalus. I have found it in a relatively large percentage of cases of chronic congenital hydrocephalus, but never without hydrocephalus or in cases of acute or later developing hydrocephalus. (Quoted from English translation of Radkowski [25])

R. S. Tubbs et al. (eds.), *The Chiari Malformations*, https://doi.org/10.1007/978-3-030-44862-2_5

Table 5.1 Some of the anomalies associated with Chiari malformation

Anomaly	Description	Reference(s)
Cranium bifidum	Is the cranial counterpart of spina bifida and is likewise comprised of occulta, cystica, and aperta variants	Padget, 1972 [1]; Ingraham and Scott, 1943 [2]; Anegawa et al., 1993 [3]
Lacunar skull	Is characterized by rounded (punched-out) defects in the inner table of the skull separated by whorl-like bony ridges	Ingraham and Scott, 1943 [2]; Peach, 1965 [4]
Platybasia	Flattening of the angle between the clivus and anterior basicranium; severe form is associated with basilar invagination	Schady et al., 1987 [5]; Smoker, 1994 [6]
Small posterior cranial fossa	Reduction in the size of posterior cranial fossa in relation to the cranial dimensions	Schady et al., 1987 [5]
Basilar invagination	Abnormal approximation of the odontoid process and skull base	Schady et al., 1987 [5]
Proatlas segmentation malformation	Most often present as osseous anomalies around the foramen magnum	Muhleman et al., 2012 [7]; Menezes, 1995 [8]
Atlanto-occipital assimilation	Partial or complete fusion of the atlas and occipital bone; is seen in about 8% of pediatric patients with Chiari I malformation	Tubbs et al., 2011 [9]
Klippel-Feil syndrome	Fusion of two or more cervical vertebrae; is seen in about 3% of patients with Chiari I malformation	Tubbs et al., 2011 [9]
Spina bifida	Is composed of spina bifida occulta, cystica, and aperta variants; the latter two are comprised of meningocele, meningomyelocele, myelocystocele, and myeloschisis; is often but not always associated with hydrocephalus and Chiari II malformation	Pooh and Pooh, 2011 [10]; Russell and Donald, 1935 [11]; Ingraham and Scott, 1943 [2]
Dysplastic tentorium cerebelli	Decreased length of the fused tentorium and increased length of the incisura	Peach, 1965 [4]
Low-lying tentorium cerebelli	Downward displacement of intracranial attachment of the tentorium; contribute to a small posterior cranial fossa	Gardner, 1973 [12]
Hypoplasia or absence of falx cerebri and falx cerebelli	Is related to overcrowding of the intracranial and posterior cranial fossae	Peach, 1965 [4]; Tubbs et al., 2002 [13]
Hydrocephalus	Often communicating; may be a primary event or secondary to hindbrain herniation	Ingraham and Scott, 1943 [2]
Microgyria	The cerebral gyri are smaller but numerous giving rise to a "wormy" appearance of the cerebral cortex	Ingraham and Scott, 1943 [2]
Gray matter heterotopia	Collection of neural cells in abnormal *locations within the white matter*; has been reported in patients with spina bifida and Chiari II malformation	Gilbert et al., 1986 [14]
Large massa intermedia	Excessive approximation and adhesion of the thalami and thickening of the interthalamic adhesion	Gardner, 1977 [15]; Naidich et al., 1980 [16]; Peach, 1965 [4]
Stenosis of the aqueduct of Sylvius	May be primary or secondary to midbrain compression by hydrocephalus or overcrowded brain	Masters, 1978 [17]; Russell and Donald, 1935 [11]
Tectal beaking	The quadrigeminal plate of the midbrain is fused into a conical mass, the apex of which projects between the cerebellar hemisphere	Peach, 1965 [4]
Dorsal wedging of the brain stem	Dorsal part of pons and/or upper medulla protrudes into the fourth ventricle	Lichtenstein, 1942 [18]
Imperforated rhombic roof	Primary agenesis or secondary occlusion of the outlets of the fourth ventricle by a fibrovascular membrane or arachnoid veil	Gardner, 1965 [19]; Tubbs et al., 2004 [20]

Table 5.1 (continued)

Anomaly	Description	Reference(s)
"Tight" cisterna magna	The cisterna magna is small or obliterated; is due to overcrowding of the posterior cranial fossa, downward displacement of cerebellum, fibrovascular adhesions of the meningeal layers, or dysgenesis during embryonic and early fetal periods	Gardner, 1973 [12]; Masters, 1978 [17]
Low-lying and obliterated fourth ventricle	The fourth ventricle is slit-like and compressed and partly or entirely extends below the foramen magnum	Russell and Donald, 1935 [11]
Upslanting cervical spinal nerves	Upper cervical spinal nerves with an ascending intradural course; these spinal nerves normally have a rather horizontal course	Barry et al., 1957 [21]
Syringomyelia	The cavitation within the spinal cord tissue; is more common in Chiari II than in Chiari I malformations	Josef and Fehlings, 2011 [22]
Hydromyelia	Dilated central canal	Ingraham and Scott, 1943 [2]

The presence of hydrocephalus was not appreciated by Arnold, but Chiari assumed that it might have been, in some cases, a transient event in the fetal period [26]. The hydrocephalic brain theory, later known as "pressure coning effect" [12], dominated the thoughts and still stands as a plausible—albeit not the sole—mechanism behind hindbrain herniation.

The validity of the pressure coning theory has been questioned by the forerunners of caudal traction, posterior fossa overcrowding, the so-called neural tube overgrowth theory, and inadequate ventricular distension theories (see below). It has been noted that only ~15% of patients with meningomyelocele had externally recognizable hydrocephalus at birth and that a majority of them develop hydrocephalus during the first 3 years of life [27], casting doubt on the presumed role of primary fetal hydrocephalus in Chiari II malformation. The idea that hydrocephalus and hindbrain herniation "may be causally independent of each other" was emphasized by Bell et al. [24]; in their study of 21 human fetuses with spina bifida, 3 of 12 fetuses with Chiari II malformation lacked hydrocephalus. Instead, hindbrain herniation was closely linked with the size and location of the spinal defect: "the more cephalad and extensive the spinal lesion, the more likely it was to be accompanied with Chiari II malformation" [24]. It also has been suggested that a high cerebrospinal fluid (CSF) flow rate through the fistulous communication between the neurocele and amniotic cavity at the level of neural tube defect may induce a high craniospinal pressure gradient (by reducing the pressure of the spinal neurocele without increasing the intracranial pressure), which by itself causes the hindbrain to herniate into the spinal canal [28]. The latter findings indicated that hindbrain herniation may be either a direct or an indirect consequence of the spina bifida defect, shedding light into the plausibility of other theories (e.g., caudal traction, posterior fossa overcrowding and inadequate ventricular distension, etc.), which are mechanistically favored by the spina bifida defect.

The findings of Bell et al. [24] and others could, however, by no means totally exclude the possibility that hydrocephalus is of a direct cause-and-effect relationship with hindbrain herniation at least in some cases. If one accepts the hydrocephalic brain theory, then an account of the etiologies of the *primary* fetal hydrocephalus would deem it inevitable. It has been suggested that CSF absorption pathways are underdeveloped in patients with spina bifida cystica [11]. Atresia of the aqueduct of Sylvius [11], cranial venous outflow insufficiency and venous blood backflow [29], lack of elasticity and reduced permeability of the embryonic rhombic roof [30], primary agenesis of the outlets of the fourth ventricle or occlusion of the rhombic roof foramina by a membrane [11, 19], hyperfunctioning choroid plexus of the lateral ventricles and

overproduction of CSF [15], and dysgenesis of the cisterna magna [15, 17] all hinder normal CSF balance and circulation and are among the known etiologies of primary fetal hydrocephalus in Chiari malformation. In the context of hydrocephalic brain theory, a differentiation should ideally be made between the factors initiating hydrocephalus and those maintaining or aggravating it once it develops. However, such a distinction remains arbitrary in the majority of cases as multiple interrelated anomalies often coexist at the same time in the same subject.

Ultimately, evidence exists for hydrocephalus being either a primary event causing hindbrain herniation (per hydrocephalic brain theory) or a secondary event caused by hindbrain herniation. This may in fact reflect the heterogeneous nature of the pathogenesis of hindbrain herniation across patients with or without spina bifida, and it is safe to assume that the relationship between hydrocephalus and hindbrain herniation is bidirectional, one causing or aggravating the other. Figure 5.1 shows a self-perpetuating cycle; irrespective of the factor(s) initiating the cycle, hydrocephalus reduces the compliance of the intracranial cavity [29]. Therefore, with slight elevation of the CSF and intracranial blood volumes, the intracranial pressure increases quickly, pushing the hindbrain down through the foramen magnum. Obstruction of CSF flow through the foramen magnum aggravates the hydrocephalus, and the cycle continues resulting in increasing hydrocephalus and hindbrain herniation [29]. If hindbrain herniation is the inciting event, then CSF flow blockage would secondarily lead to hydrocephalus, which by itself aggravates hindbrain herniation by increasing intracranial pressure. Several mechanisms have been recognized for CSF blockage in the Chiari malformation. Partial blockage of the foramen magnum with herniated hindbrain is commonly observed in patients with meningomyelocele and Chiari II malformation [11]. Usually, the outlet of the fourth ventricle is below the foramen magnum, and CSF drains into the spinal subarachnoid space. But because of partial blockage at the level of the foramen magnum, an accumulating amount of CSF does not circulate into the cranial subarachnoid space [11]. The spinal compartment has a capacity of CSF absorption that is only one-sixth that of the cranial compartment [31]. Although the dural sac of the spina bifida cystica has abnormally high absorptive capacity [32], this may not compensate for exclusion of the intracranial CSF absorption in severe cases of foramen magnum blockage. Thus, if the accumulated spinal CSF overwhelms the absorptive capacity of the spinal compartment, it reenters the ventricular cavity, leading to a communicating hydrocephalus [11], or penetrates into the substance of the spinal cord, leading to syringomyelia [33]. Alternatively, the outlets of the fourth ventricle may become secondarily obliterated between the impacted cerebellum and brain stem, causing a non-communicating hydrocephalus [2]. Mechanical irritation of the basal cistern can also induce an aseptic inflammatory reaction and fibrosis within the subarachnoid space, which hinders CSF circulation in the posterior cranial fossa [2].

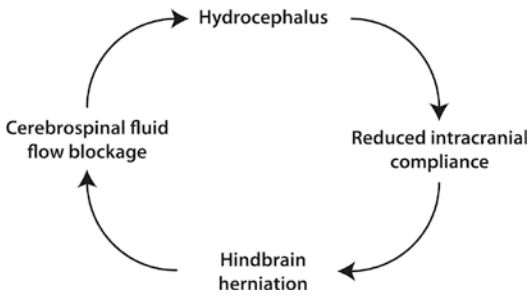

Fig. 5.1 The self-perpetuating cycle linking hydrocephalus with hindbrain herniation

External Compression Theory

The external compression theory was proposed by Cameron [34] to provide a mechanical basis for hindbrain herniation aside from hydrocephalus in the fetuses with spina bifida defect. Cameron believed that ontogenetically, the spina bifida cystica is, at the initial stage, an aperta (myeloschisis) lesion, later epithelialized to form a cystic lesion. Thus, in embryonic and early fetal life, there is a fistulous communica-

tion between the neurocele and amniotic cavity. Cameron [34] opined that increased intra-amniotic pressure (perhaps due to fetal and maternal maneuvers) is transmitted onto the developing skull, squeezing the cranial neurocele to drain out through the hydromyelic cord. Leakage of the neurocele fluid into the amniotic space and squeezing of the developing brain would thereby induce a Chiari II malformation and produce a variety of associated anomalies including stenosis of the aqueduct of Sylvius, hypoplasia of the falx cerebri, tectal beaking, large massa intermedia, etc. This theory, however, was refuted by Peach [35] on the grounds that according to Pascal's law, the pressure exerted by the amniotic fluid on the embryo or fetus is equal at the skull and defective spinal lesion. Thus, the intra-amniotic pressure cannot induce a pressure gradient between the cranial neurocele and the hydromyelic cord. Moreover, in a study of infants less than 3 months of age with lumbar meningomyelocele, about half of them were found to have amniotic fluid debris (squama, lanugo hair, and mucin) in the spinal cord tissues, central spinal cord canal, and spinal subarachnoid space, i.e., vernicomyelia [36]. The presence of vernicomyelia in meningomyelocele infants implies that the direction of flow between the amniotic cavity and neurocele is not always caudad and that a degree of rostral flow from the amniotic cavity to the neurocele also exists in some if not all of the affected fetuses [36].

Although the external compression theory has not been accepted, its invalidation does not contradict the hydrodynamic theory or other theories, which emphasize that hindbrain herniation is a consequence of neurocele fluid leaking through the defect in the neural tube. This leakage could instead be mechanically favored by a normally higher neurocele pressure than amniotic pressure in the embryonic and early fetal neural tube [15]. However, when the hindbrain herniates, the spinal compartment is isolated—partially or completely—from the cranial compartment and becomes in equilibrium with the amniotic cavity. As a result, a to-and-fro flow through the spina bifida defect is established: The in utero maneuvers compressing the head cause caudad egress of the fluid through the defect, while subsequent release of head compression causes the amniotic fluid to pass rostrad into the spinal compartment [36].

Crowding of the Posterior Fossa in Chiari Malformation

The phenomenon of posterior cranial fossa overcrowding is an integral part of the modified hydrodynamic theory of Gardner, occipital dysplasia theory, disorganized neural tube growth theory, and inadequate ventricular distension theory (see below). In fact, these theories have been proposed to explain the overcrowding phenomenon on the grounds of either a small posterior cranial fossa or increased size of the hindbrain (see below). Accordingly, normal growth of the posterior fossa brain within a confined, unyielding fossa or abnormally large size of the posterior fossa brain in an apparently normal fossa results in the state of "overcrowding." The overcrowded posterior fossa brain herniates upward through the tentorial incisura and downward through the foramen magnum and also hinders CSF circulation, leading to the hydrocephalus. A point of importance here is that the relative ratio of the posterior fossa brain volume to total fossa volume is above normal but less than one in this state, and overcrowding by no means indicates that the posterior fossa brain volume is greater than the total posterior fossa volume. In one study, the posterior fossa brain occupied 83.3% of the posterior fossa space in adult patients with Chiari I malformation and 79% of the fossa space in healthy individuals [37]. Whether such a degree of posterior fossa overcrowding (~5%) is by itself sufficient to cause hindbrain herniation or not is not clear. However, it is more likely that the overcrowding phenomenon works in concert with other factors to induce hindbrain herniation.

Hydrodynamic Theory

The hydrodynamic theory was suggested by Gardner et al. in 1957 [30], and in 1977 [15], he

modified it to explain the smallness of the posterior cranial fossa as well as formation of the neural tube defect in Chiari II malformation. Consulting the works of Weed [38], Padget [39], and Bering [40], Gardner [15] attested that (1) development of the area membranacea superior of Weed coincides with development of the posterior choroid plexus of the rhombic cavity, and that of the area membranacea inferior of Weed coincides with development of the anterior choroid plexus of the lateral ventricles; (2) the area membranacea superior and inferior filter the CSF out of the brain ventricles in normal fetuses; and (3) the anterior choroid plexus expands rapidly and out of proportion to the posterior choroid plexus; thus, the CSF pressure generated by the anterior choroid plexus in the supratentorial space overrides the pressure generated by the posterior choroid plexus, and this pressure gradient pushes the tentorium downward. If the second mechanism fails due to abnormal thickening or reduced permeability of the rhombic roof [30], then the CSF cannot egress from the ventricular cavity through the rhombic roof. If the third mechanism becomes exaggerated due to hyperfunctioning or markedly enlarged anterior choroid plexus [12, 15], the filtering capacity of the rhombic roof is overwhelmed, and the neural tube expands to a greater extent than normal. Under both these circumstances, a state of fetal hydrocephalus and hydromyelia ensues. The fetal hydromyelia leads to rupture of the weakest part of the closed neurocele in the caudal region (or occasionally in the cephalic region such as in the mesencephalon) leading to a variety of neural tube defects [15]. When the caudal neurocele opens, CSF drains out of the fourth ventricle through the hydromyelic central spinal cord canal and from the spina bifida defect into the amniotic cavity; this results in dissipation of the CSF pressure generated by the posterior choroid plexus within the infratentorial space. The supratentorial CSF pressure generated by the anterior choroid plexus and the hydrocephalic cerebrum push the tentorium downward to a greater extent than in normal, leading to a small posterior cranial fossa. Ultimately, the growing hindbrain herniates out of the small posterior fossa [15].

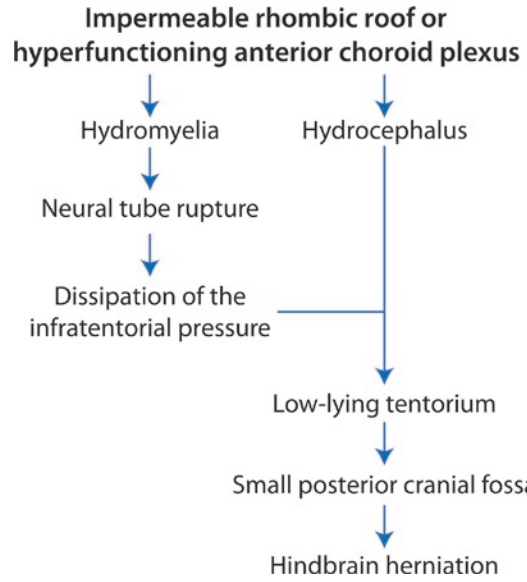

Fig. 5.2 A flow diagram depicting Gardner's hydrodynamic theory

The sequence of the events per Gardner's hydrodynamic theory (Fig. 5.2) occurs in the embryonic and early fetal period when the otic capsule is still cartilaginous and tentorial rotation is feasible. Gardner [19] outlined the differences in pathogenesis of the Chiari I and II malformations in an interesting manner: "if the size of the posterior fossa is severely reduced by this process, the cerebellar portion of the resulting hernia will consist of the earlier developing vermis (Chiari II); if its size is reduced to a lesser degree, the cerebellar hernia will consist of the later developing tonsils (Chiari I)."

Gardner [19] elaborated upon the hydrodynamic theory to explain the co-occurrence of hydromyelia and syringomyelia with Chiari malformation and hydrocephalus. He postulated that with any restriction in the outflow of the fourth ventricle, either due to complete or partial obstruction of the foramen of Magendie, the CSF pulse wave generated by the pulsating choroid plexus (synchronous with cardiac beat) cannot be dissipated at the level of the foramen of Magendie but is directed downward toward the obex of the medulla and central canal. The "water hammer effect" of the CSF pulse pressure causes funnel-shaped dilation at the obex, dilation of the central

canal, and/or hydrodissection of the lower medulla or spinal cord along the nerve fiber tracts. Notably, the foramen of Magendie was completely obliterated by an arachnoid veil in at least 30% of patients with syringomyelia and Chiari malformation examined by Gardner [19] and was also partially closed in more than 10% of patients.

Ultimately, in the hydrodynamic theory of Gardner, overdistension of the supratentorial ventricles and/or imperforation of the roof of the fourth ventricle is an inciting event, which independently leads to hydrocephalus, hydromyelia, and syringomyelia. The induction of hindbrain herniation is secondary to the *early fetal* hydrocephalus and growth of the hindbrain within a small posterior cranial fossa. Moreover, this theory maintains that the expansion of the syrinx is due to a pulsatile CSF flow wave (hammer effect), which is transmitted into the syrinx through a patent upper cervical central canal. Hence, it predicts that the syrinx should expand during cardiac systole and should constrict during diastole. The latter assumption has been invalidated by Oldfield et al. [33] who put forth another theory for the pathogenesis of the syringomyelia (see below).

Occipital Dysplasia Theory

The size of the posterior cranial fossa is determined by several factors effective in fetal and postnatal life, including (1) ventricular distension, (2) rotation of the intracranial attachment of the tentorium cerebelli, (3) rotation of the otic cartilage and petrous temporal bone, (4) growth of the basicranial synchondroses, (5) upward reflection of the tentorium cerebellum, and (6) various hormonal influences (see Chap. 4 "Embryology of the Craniocervical Junction and Posterior Cranial Fossa" for details). The occipital dysplasia theory implies that failure of the occipital bone to develop normally, primary axial skeletal defect, paraxial mesodermal insufficiency, or altered morphogenesis of the occipital bone gives rise to a small posterior cranial fossa and contributes to the overcrowding phenomenon.

This theory was emphasized by Marin-Padilla and Marin-Padilla [41] in an animal embryo model of Chiari I and II malformations induced by maternal administration of vitamin A and was later supported by the morphometric data obtained from patients with Chiari malformation. Marin-Padilla and Marin-Padilla's model expressed a constellation of craniofacial anomalies and dysraphic states. In this model, (1) there was a reduction in the length of the skull base essentially as a result of an underdeveloped occipital region; underdevelopment and shortening of the basiocciput were more pronounced in animal fetuses with a spina bifida defect (corresponding to Chiari II malformation) than in those without a spina bifida defect (corresponding to Chiari I malformation); (2) the odontoid process was apparently protruded into the posterior fossa with its tip located above the plane of the depressed basion of the underdeveloped basiocciput; and (3) shortening of the basiocciput resulted in a small posterior cranial fossa and subsequent compression of the brain stem and cerebellum and partial reduction in the ventricular size and slight compression of the aqueduct of Sylvius. Therefore, Marin-Padilla and Marin-Padilla [41] suggested that Chiari I and II malformations are "complex developmental disorders" or sequence anomalies initiated by "primary axial skeletal defects" (invariably involving the craniocervical junction and occipital region) leading to "secondary neurological anomalies."

The nature of occipital dysplasia leading to a small posterior cranial fossa in Chiari I malformation is already discussed (see Chap. 4 "Embryology of the Craniocervical Junction and Posterior Cranial Fossa"). In brief, the supraocciput is affected more than the basiocciput, the foramen magnum tends to enlarge, and the height of the posterior fossa is reduced. There may be a compensatory increase in the length of the posterior fossa in adults. Further studies comparing adult and pediatric patients are required to fully elucidate the dynamic and potentially age-related pattern of the occipital dysplasia in the Chiari I malformation. Patients with Chiari II malformation also have a small

posterior cranial fossa, but the pattern of occipital dysplasia shows some differences from that of the Chiari I malformation. A reduced clivus-supraocciput angle (the angle formed between the lines drawn along the axes of the clivus and supraocciput) has been reported among Chiari II patients [42]. The following equations reflect the morphological significance of the clivus-supraocciput angle:

$$\text{Basicranial angle} + \text{Clival angle} = 180^{\circ} \quad (5.1)$$

The clival angle is between Twining's line and axis of the clivus, and the basicranial angle is formed between the axis of the clivus and horizontal plane of the anterior basicranium.

$$\text{Supraoccipital angle} + \text{Clival angle} + \text{Clivus Supraocciput angle} = 180^{\circ} \quad (5.2)$$

The supraoccipital angle is between Twining's line and the axis of the supraocciput. Based on Eqs. 5.1 and 5.2, Eq. 5.3 can be obtained.

$$\text{Clivus Supraocciput angle} = \text{Basicranial angle} - \text{Supraoccipital angle} \quad (5.3)$$

Equation 5.3 indicates that a decrease in the clivus-supraocciput angle is associated with (and, in a mechanistic term, caused by) a reduction in the basicranial angle and an increase in the supraoccipital angle. Therefore, the clivus and supraocciput tend to lie perpendicular to Twining's line when the clivus-supraocciput angle is reduced. Figure 5.3 shows the three morphological changes in the posterior cranial fossa, which can potentially explain a reduced clivus-supraocciput angle. These include increased size of the foramen magnum as well as an increased height and reduced length of the posterior fossa. The possibility of an increase in the posterior fossa height in Chiari II malformation is not supported by the literature as the reduction in the posterior fossa volume is recognized as an etiopathogenic factor. Thus, a combination of increased foraminal size and reduced length of the posterior fossa can best explain the co-occurrence of small posterior fossa with the reduced clivus-supraocciput angle in the Chiari II malformation.

The Neural Tube Overgrowth or Disorganized Neural Tube Growth Theory

This theory was proposed by Barry, Patten, and Stewart [21] in an attempt to link the co-occurrence of neural tube non-closure, Chiari malformation, and other cerebral anomalies with an earlier observation by Patten [43] of a curious neural tube maldevelopment, the so-called overgrowth of the neural tube. The neuroepithelium in such cases was characterized by an enhanced growth, folding and refolding on itself and crowding into the apparently normal surrounding space and ventricular cavity [43]. Later, Patten [44] reported that a local overgrowth may lead to non-closure of the neural tube. Examining the fetuses with caudal neural tube defects and Chiari II malformation, Barry and colleagues observed that (1) the spinal cord segments immediately proximal to the defect were larger than normal; (2) the cerebrum and hindbrain were enlarged; and (3) the proximal cervical spinal cord segments were also larger but were compressed cephalocaudally [21]. They subsequently posited that the neural tube overgrowth phenomenon observed in the fetuses with spina bifida involves distant regions of the developing central nervous system as well and occurs before differential growth of the vertebral column begins. Such a phenomenon, Barry et al. [21] opined, leads to neural tube non-closure (spina bifida), downward displacement of the overgrown hindbrain into the cervical spinal canal (Chiari II malformation), and multiplicity of the cerebral cortical gyri (microgyria). In a rat fetal model of Chiari II malformation induced by maternal dose of ethylenthiourea, hydrocephalus was absent, but overgrowth of the neural tube was evident, indicating that Chiari malformation can develop without hydrocephalus and with crowding of the cranial space by the overgrown brain [45]. The neural overgrowth theory was faced with skepticism as the cerebellum in the Chiari II malformation has often been found atrophied and small postnatally. However, an unbiased revisit of this theory in the light of earlier accounts and most recent observations implies that this theory

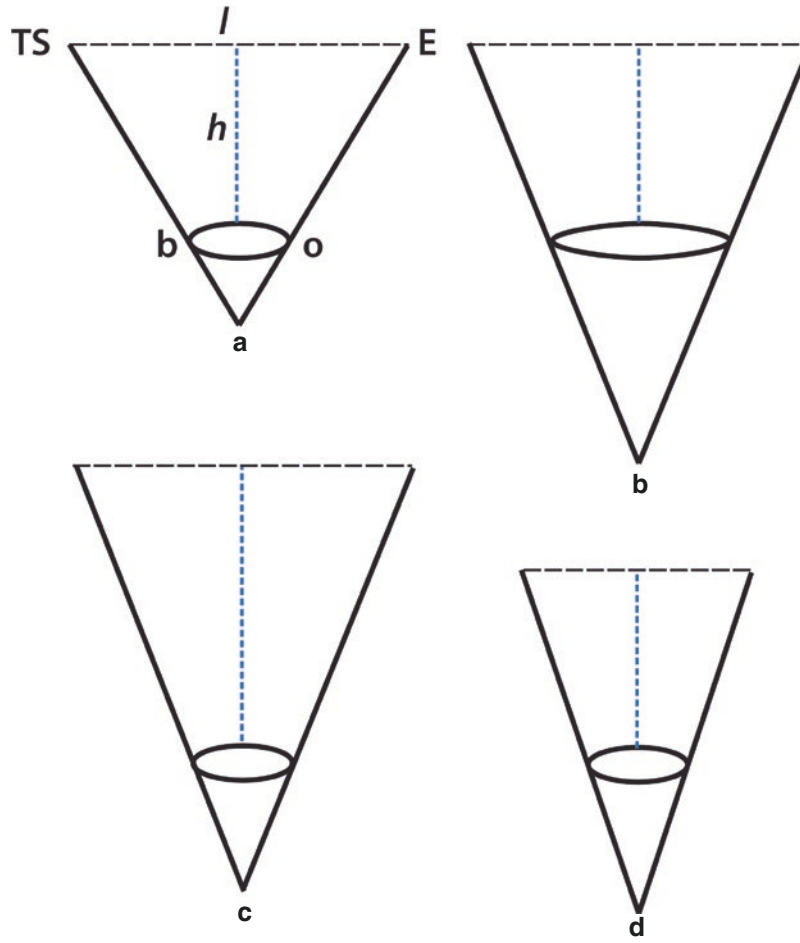

Fig. 5.3 Line diagrams showing the morphological implications of the reduced clivus-supraocciput angle in the posterior cranial fossa of patients with Chiari II malformation. *TS* tuberculum sellae, *E* endinion, *b* basion, o opisthion. *l* and *h* indicate the length and height of the bony posterior cranial fossa. The oval circle represents the foramen magnum. (**a**) Is the reference diagram representing the normal condition; (**b**), increase in the size of foramen magnum; (**c**), increase in the height of the posterior fossa; (**d**) decrease in the length of the posterior fossa

may indeed be relevant and has the power of explaining such associated anomalies as microgyria, neural dysgenesis, and gray matter heterotopia in the cerebrum and cerebellum of patients with Chiari II malformation. The so-called neural tube overgrowth theory is supported by findings that the brain in the Chiari II malformation is heavier than normal despite the presence of hydrocephalus [36].

Perhaps, the main barrier to the popularity of the neural overgrowth theory is its name, giving rise to a misunderstanding of its pathological nature. Barry and colleagues stated that this term is "a purely descriptive morphological term," thus testifying that it may or may not reflect the underlying histopathogenesis. Experimentally, this phenomenon can be induced by manipulation or extirpation of the notochord, hypoxia, and various non-specific chemical insults in animal embryos [46] and is characterized by disorganized neuroepithelial cell migration and formation of the rosette-like accumulation of cells within the overgrown regions [47] as well as shrinkage of the brain vesicles [48]. Splotch-delayed mouse embryos harboring Pax-3 gene mutation [49] are predisposed to neural tube defects and also demonstrate features of an overgrown neural tube [50]. The so-called overgrowth is associated with mesodermal insufficiency, notochordal abnormality, alterations in the neuroepithelial basal lamina, loss of cellular polarity, disorganized cell orientation, and increased neuroepithelial intercellular space rather than true neuroblast proliferation [51, 52]. Overgrowth of the neural tube in the chicken embryo overexpressing the forkhead transcription factor *FoxG1*

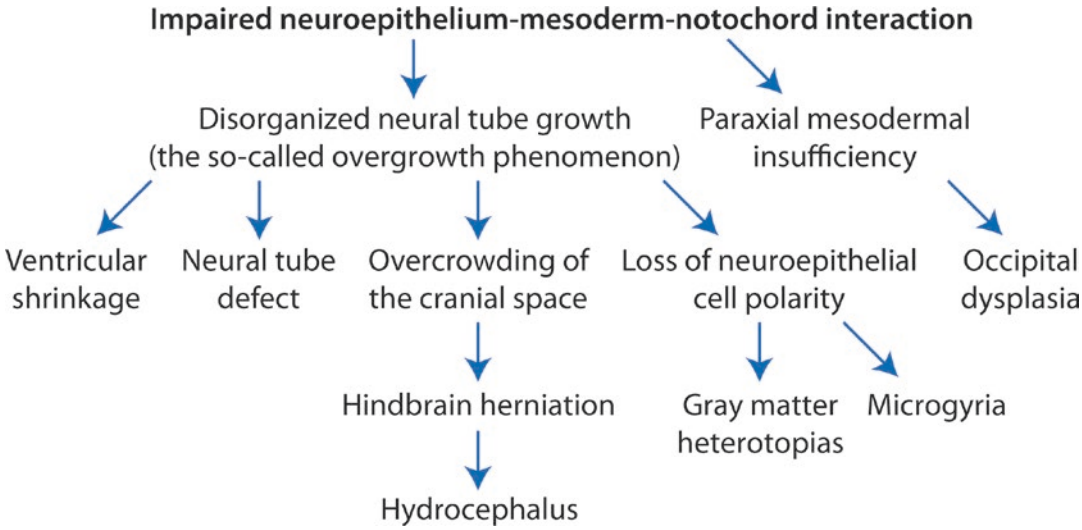

Fig. 5.4 The proposed sequence of events in the disorganized neural tube growth theory. In splotch-delayed animal models, impaired neuroepithelium-mesoderm-notochord interaction was associated with mesodermal insufficiency and disorganized neural tube growth [52]

is also associated with decreased neuroepithelial apoptosis mainly in the telencephalon and mesencephalon [53].

The data above imply that the phenomenon of "neural tube overgrowth" mentioned by Patten [43] and Barry et al. [21] is in fact a generalized disorder of neuroepithelial organization manifesting as an enlarged, folded, or crowded neural tube in the embryonic or early fetal periods. The manifestation of *disorganized neural tube growth* in late fetal and postnatal life, especially in connection with hindbrain development, remains to be elucidated in experimental studies or studies of aborted human fetuses. If *disorganized neural tube growth* is the underlying factor in the pathogenesis of a neural tube defect (as suggested by Patten [44]), one should look for distant abnormalities in the central nervous system derived from a fused but still disorganized neural tube in patients with a spina bifida defect. Barry et al. [21] proposed that such a pathological phenomenon leads to hindbrain enlargement and herniation and microgyria. It is not unlikely that the structures similar to rosette-like neuroepithelial cell accumulations seen in animal embryos with a disorganized neural tube give rise to the masses of gray matter heterotopia, which are often located periventricularly in patients with Chiari II malformation. There is no direct evidence in the literature as to whether the mesodermal and notochordal abnormalities seen in the experimental models of a disorganized neural tube also contribute to the constellation of axial skeletal anomalies and occipital dysplasia in human fetuses with Chiari II malformation. However, such a possibility is likely, and further studies should address this aspect of maldevelopment. Figure 5.4 shows the proposed sequence of events per the disorganized neural tube growth theory leading to hydrocephalus and hindbrain herniation [52].

Neuroschisis Theory

This theory was formulated by Padget [1] and, in fact, represented an early attempt to put forth the foundations of an inadequate ventricular distension theory and merge it with the disorganized neural tube growth theory. The neuroschisis or neural cleft is the splitting open of the neural plate. The mesencephalon is the most common site of the cleft. The irregular margins of the cleft are composed of pyknotic cells and occasionally tend to join in an end-to-end manner sometimes with an everted or inverted fusion of the cleft walls. A neuroschisis bleb is formed at the site of the cleft by escape of neurocele fluid into the surrounding mesoderm; this bleb is walled by a

membrane and mesoderm and is often covered by an intact cutaneous ectoderm (primitive skin), but occasionally the skin is also damaged and interrupted by pyknotic, degenerated cells. Padget [1] noted that the process of neuroschisis was associated with folding of irregularly widened neural tube walls into the neurocele cavity and secondary fusion of these folds as well as narrowing of the neurocele cavity. These features are reminiscent of disorganized neural tube growth and, according to Padget [1], are most prominent at the mesencephalon and hindbrain regions, which are relatively voluminous in normal embryos. Padget [1] added that narrowing of the neurocele cavity arises from abnormal folding and fusion of the neural tube walls and partial collapse of the neurocele following rupture of the neural clefts.

Padget [1] postulated that the neuroschisis blebs (1) may undergo healing with some scarring left at the site of the healed neuroschisis, (2) may remain intact as a loculated fluid collection with a mesodermal periphery, or (3) may rupture with eversion of the neural cleft margins, leading to the spectrum of cranium bifidum and spina bifida anomalies, respectively, comprising occulta, cystic, and aperta variants. Reduction in the size of the neurocele secondary to partial neurocele collapse and folding and fusion of the neural tube walls results in micrencephaly. Subsequently, a small posterior cranial fossa ensues as the neural tube folding process is more conspicuous in the voluminous mesencephalic and hindbrain regions of the embryonic neural tube. Neural wall folding and fusion at the mesencephalon lead to stenosis and forking of the aqueduct of Sylvius, and crowding of the meten-myelencephalic junction blocks the outlets of the fourth ventricle, leading to hydrocephalus. Subsequent development of the crowded cerebellum within a small posterior cranial fossa results in a Chiari malformation. Figure 5.5 shows the sequence of events proposed by the neuroschisis theory.

Cord Traction or Tethered Cord Theory

This theory was proposed by Penfield and Coburn [54] based on surgical and autopsy findings in an adult patient with hindbrain herniation and a history of operation for a thoracic meningomyelocele in childhood. At the level of the bifid vertebral arch, the dura mater and spinal cord were dorsally attached to the soft tissues by fibrous adhesions. The brain stem was elongated, and the lower brain stem and cerebellum were herniated downward through the foramen magnum. The cisterna magna was obliterated, and the space between the cerebellum and tentorium was enlarged to form a supracerebellar cisterna. The lower cranial nerves and cervical nerves demonstrated a prominent ascending course rather than their expected descending or horizontal course. The tip of the herniated cerebellum was firmly adherent to the spinal cord by meningeal adhesions, and upon release of these adhesions, the herniated cerebellum retracted upward for a significant distance. Penfield and Coburn [54] then proposed that spinal cord fixation at the level of the bifid vertebral arch produces traction on the cord during vertebral growth. This traction interrupts the normal ascent of the spinal cord and results in downward traction of the brain stem and spinal cord and nerves above the point of fixation.

Lichtenstein [18] expounded upon the cord traction theory to explain the co-occurrence of Chiari II malformation with hydrocephalus and syringomyelia. He posited that spinal cord stretching secondary to various dysraphic conditions results in hindbrain herniation early in life and spinal cord degeneration later in life. Secondary to spinal cord stretching, the brain stem is elongated. The medulla oblongata, fourth ventricle, choroid plexus, and vermis are pulled downward. Midbrain traction results in the elongation, flattening, and stenosis of the aqueduct of Sylvius, which subsequently leads to the hydrocephalus of the third and lateral ventricles. The herniated choroid plexus produces CSF. As the fourth ventricle is collapsed and restricted at the foramen magnum, the CSF escapes into the substance of the upper cervical spinal cord through a diverticulum or fissure along the intramedullary path of least resistance, leading to syringomyelia. Penfield and Coburn [54] and Lichtenstein [18] noted that with distal cord tethering, the fourth ventricle is obliterated by a wedge-shaped pro-

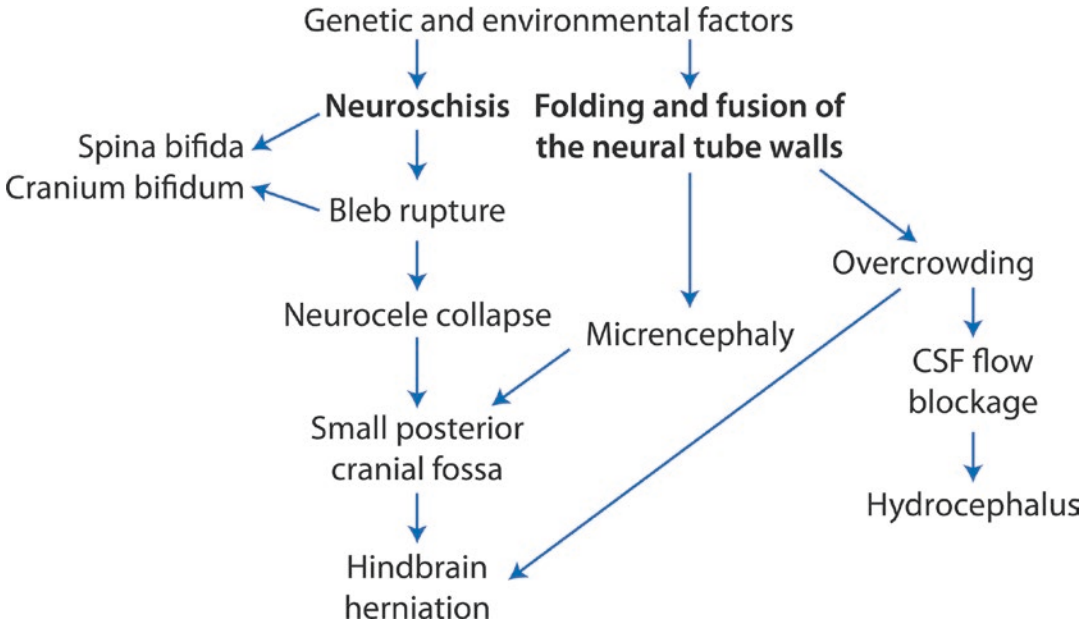

Fig. 5.5 The sequence of events in the neuroschisis theory of Padget leading to a neural tube defect, hindbrain herniation, and hydrocephalus

trusion of the upper medulla or pons into the ventricle. Such brain stem deformation also blocks the fourth ventricle leading to hydrocephalus. In order to explain this finding, Lichtenstein [18] proposed that the dorsal part of the spinal cord is often fixed in the midline in case of tethering. Thus, the ventral part of the spinal cord and hindbrain ascends to a greater extent than does the dorsal part. This results in a relative overcrowding of the ventral hindbrain, which wedges backward into the fourth ventricle.

Ultimately, the cord traction theory states that hindbrain elongation/herniation is due to impediment of normal ascent of the spinal cord during axial growth and subsequent downward pulling of the cord. Protracted spinal cord traction should be present since the fetal or early postnatal growth period to sufficiently interfere with spinal cord ascent and cause hindbrain herniation [55]. The spinal ascent is a passive process related to the disproportionate growth rates of the vertebral column and spinal cord. Failure of cord ascent is due to the fixation of the spinal cord against the elongating vertebral column. This theory is able to explain the occurrence of brain stem gross abnormality, stenosis of the aqueduct of Sylvius, hydrocephalus and syringomyelia in patients with spinal dysraphism, and a tethered cord. However, the validity of the caudal traction theory was doubted by Barry et al. [21] as they noted that the tension exerted by the anchorage of the spinal cord at the level of the spina bifida defect is dissipated within five spinal cord segments. The ascending course of the upper cervical spinal nerves attributed to caudal cord traction by Penfield and Coburn [54] and Lichtenstein [18] was instead attributed to the compression of the cervical cord by the enlarged and herniated hindbrain (Barry et al. [21]).

Developmental Arrest Theory

This theory was suggested by Daniel and Strich [56]. They postulated that hindbrain abnormalities in Chiari malformations are a consequence of failure in normal development of the pontine flexure. The pontine flexure together with the mesencephalic and cervical flexures develops late in the first month of embryonic life as the brain grows rapidly [57]. Therefore, the flexures reduce the length of the neural tube along the longitudinal axis of the body. According to Daniel and Strich [56], if the pontine flexure does not

develop, the vascularized rhombic roof fails to normally invaginate into the rhombic cavity. Therefore, it is retained as a thick fibrovascular band connecting the caudal vermis to the obex and dorsal medulla. The cerebellum wraps around the brain stem, and the elongated hindbrain herniates through the foramen magnum. In this theory, the elongated brain stem is a primary event central to the pathogenesis of Chiari malformation. In contrast, brain stem elongation is secondary to tethering of the cord in the caudal traction theory. This theory has major shortcomings. Firstly, formation of the pontine flexure is necessary for cerebellar anlages and primordium to come into a horizontal plane securing the normal development of the cerebellum in such a way that in the mature cerebellum, the vermis is located medially and the hemispheres laterally. If the pontine flexure does not develop normally, then it is reasonable to assume that the cerebellar anlages would retain a rather angular position. Therefore, in the mature cerebellum, the cerebellar vermis and hemispheres would, respectively, be superiorly and inferiorly positioned. This pattern is not appreciated in cases of Chiari malformation. Secondly, the fibrovascular adhesions between the cerebellum and medulla are in fact due to failure of the area membranacea inferior to differentiate and thin out. As a result, the choroid plexus does not normally grow into the rhombic cavity but infiltrates the thickened rhombic roof [58]. Finally, like the mesencephalic and cervical flexures, the pontine flexure straightens during brain development [57]. Although the pontine flexure initially leads to invagination of the rhombic roof, it could not be a main factor in maintaining the intraventricular position of the choroid plexus. Instead, it has been shown that intorsion of the choroid plexus is associated with inward rotation of the caudal vermis favored by regression of the area membranacea inferior and perforation of the rhombic roof [58].

Inadequate Ventricular Distension Theory

This theory was suggested by McLone and Knepper [59] and was based on the observation that the spinal neurocele undergoes a transient and partial collapse early in the developing embryo. McLone and Knepper [59] found a temporal association of this partial neurocele occlusion with distension of the cranial vesicles in a mouse embryo model. They attested that in the embryo with a neural tube defect, the occlusion process is defective in a way that the ventral portion of the spinal neurocele fails to collapse in the midline and the medial walls do not come into opposition. The latter results in less-than-normal distension of the cranial vesicles, which leads to the formation of a small posterior fossa from lack of the adequate forces necessary to expand the surrounding mesenchymal primordia of the chondrocranium. Subsequently, the development of the rhombencephalon in an inadequate and fixed space results in the downward displacement of the brain stem and cerebellum.

McLone [60] further expounded upon this theory in an attempt to link the co-occurrence of pan-brain and calvarial anomalies with the Chiari II malformation. Figure 5.6 shows the sequence of events led by an inadequate ventricular distension. Hydrocephalus is not a primary event in this theory, but is secondary to hindbrain herniation and overcrowding of the intracranial cavity resulting in blockade of CSF flow through the restricted foramen magnum and obliterated subarachnoid space as well as occlusion of the fourth ventricular outlet and aqueduct of Sylvius. The cortical dysplasia and gray matter heterotopias are attributed to lack of the inductive ventricular forces necessary for normal development and organization of the telencephalon. A large massa intermedia is due to abnormal approximation and fusion of the thalami in a collapsed third ventricle. McLone [60] also posited that normal orientation of calvarial ossifying collagen bundles requires distension of the lateral ventricles; the inadequate ventricular distension causes these ossifying bundles to abnormally whorl, leading to the appearance of the lacunar skull (craniolacunia). The inadequate ventricular distension theory has been supported by experimental data. In the fetal rat model of dysraphism induced by a midline dorsal incision deep into the medulla oblongata during late pregnancy, hindbrain herniation consistent with Chiari type II malforma-

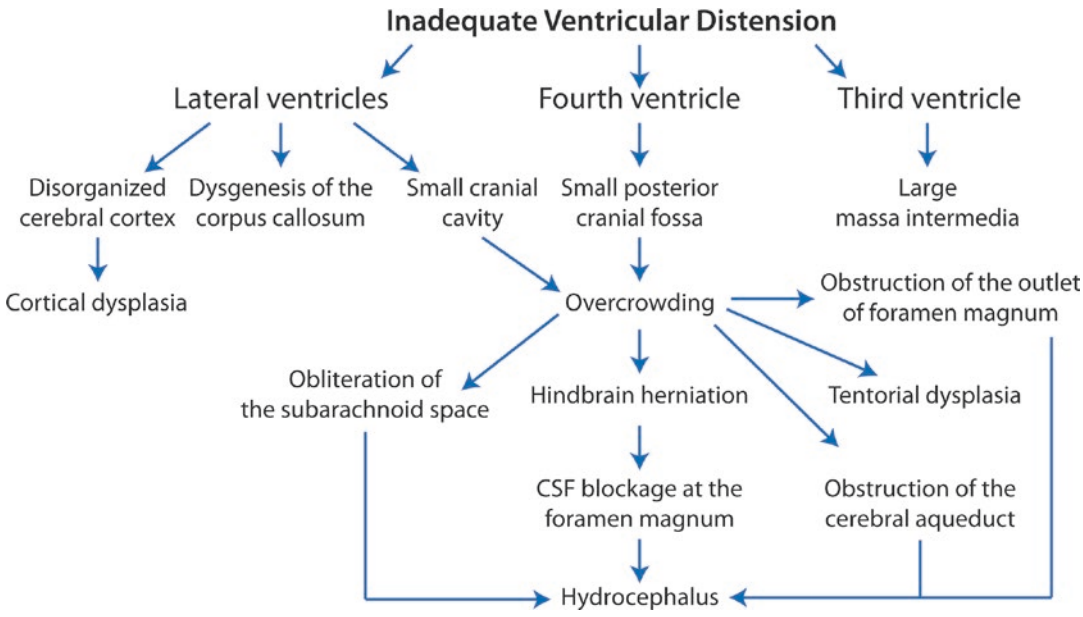

Fig. 5.6 A flow diagram showing the sequence of pathological events favored by inadequate distension of the lateral, third, and fourth ventricles

tion was noted in surviving animals [61]. This observation indicated that *significant* leakage of CSF distal to the brain stem is sufficient to result in hindbrain herniation. Although this theory explains the small posterior cranial fossa in Chiari II malformation, it fails to provide a clue to the pathoembryogenesis of Chiari I malformation.

Craniocervical Growth Collision or Caudocranial (Reversed) Vertebral Growth Theory

This theory, suggested by Roth [62], is pertinent to the pathogenesis of Chiari malformation in the case of lumbar tethering of the spinal cord such as observed in patients with a caudal meningomyelocele. Craniocervical growth collision theory claims that hindbrain herniation is essentially secondary to maldevelopment of the vertebral column. Roth maintained that:

1. The developing neurocele is always separated from the surrounding skeletogenic tissues (primordia of axial skeleton) as the subarachnoid space is apparent as early as when chondrification takes place.
2. The availability of space along the developing central nervous system determines the distribution of and relative quantity of the skeletogenic mesoderm.
3. With the onset of a neuro-vertebral growth differential, the relatively faster growth of the vertebral column overrides the growth of the spinal cord.
4. With upward retraction of the spinal cord, more space is available caudally for distribution of skeletogenic tissue; thus, the vertebral column grows caudally below the level of the spinal cord.

This pattern is referred to as cranio-caudal direction of vertebral growth, which, according to Roth, is a "basic growth law." With fixation of the spinal cord to the caudal vertebrae, upward ascent of the cord is restricted. Therefore, skeletogenic materials are distributed cranially, colliding with the developing skull base. This pattern is referred to as a caudocranial direction of vertebral growth (reversed cervical growth or reversal of cranio-caudal vertebral growth), which,

according to Roth, leads to the following abnormalities:

1. "Sucking up" of the hindbrain into the upper cervical spinal canal
2. Upward rather than downward slanting of the upper cervical spinal nerves, giving rise to the impression of a "cervico-cranial cauda equina"
3. Funneling of the upper cervical spinal canal and widening of the foramen magnum
4. Secondary hydrocephalus
5. Basilar invagination

Per this theory, the sequence of events leading to Chiari malformation begins with a primary neural tube defect, which then alters the development of the vertebral column, secondarily leading to the malformation of the hindbrain at the craniocervical junction. Although the craniocervical growth collision theory essentially associates Chiari malformation with dysraphism, Roth attempted to attribute the Chiari malformation of non-dysraphic states to a "genuine" (i.e., primary or intrinsic) abnormality of axial growth. Roth further mentioned the phenomenon of "postembryonic neural growth" (especially that of the cerebellum), which contributes to the pathogenesis of hindbrain herniation by caudal displacement of the growing neural tissue within the collided craniocervical junction. Not mentioned by Roth, however, is the adaptability of the craniocervical growth collision theory for explaining the occurrence of atlanto-occipital or cervical vertebral fusion in Chiari patients. These abnormalities may represent a reaction to the cranially directed colliding force stimulating abnormal osteogenesis and fixing the derivatives of the occipital and cervical somites.

Theory of "Suck and Slosh" Effect as the Cause of Origin and Expansion/Maintenance of a Spinal Cord Syrinx

This theory was formulated by Williams [63, 64] to provide a mechanism for formation and maintenance of communicating and non-communicating spinal cord syrinx seen with Chiari malformations. This theory maintains that under physiologic conditions and at rest, the pressure within the spinal canal is equal to the intracranial pressure. With maneuvers that increase thoracoabdominal pressure, the spinal CSF pressure initially goes up but soon equalizes with the intracranial pressure by the shift of CSF from the spinal to the intracranial compartment. Following the cessation of the straining maneuver, the spinal CSF pressure goes down, which also rapidly equalizes with the intracranial pressure by the shift of CSF between the two compartments. If the pressure within the spinal canal becomes substantially lower than the intracranial pressure for a prolonged time (the so-called phenomenon of craniospinal pressure dissociation), the relative negative pressure within the spinal cord tends to "suck" the CSF from the fourth ventricle down into the spinal cord central canal and tissues, leading to the formation of hydromyelia and syringomyelia. This "suck" effect occurs in Chiari patients and causes further downward displacement of the hindbrain through the foramen magnum. Once a significant hindbrain (tonsillar) herniation is established and the upper cervical spinal cord central canal is secondarily impacted at or below the level of the foramen magnum by the herniated tonsils, the anatomical communication between the fourth ventricle and syrinx closes off. Next, the maintenance or further expansion of the syrinx takes place by another mechanism, the so-called "slosh" effect. Accordingly, the fluctuation in the CSF pressure within the spinal subarachnoid space is transmitted to the spinal cord and the wall of the syrinx externally. The increased spinal CSF pressure compresses the syrinx leading to the egress of the intrasyrinx fluid rostral and/or caudal to the site of its maximum compression. This potentially forceful pulsatile and bidirectional movement of intrasyrinx fluid extends the syrinx at its proximal and distal ends without the need for any anatomical communication between the syrinx cavity and the intracranial ventricular system. Expansion and maintenance of the syrinx are further contributed to by the perivascular transport of spinal CSF into the syrinx cavity.

Thus, the "suck" effect is driven by the craniospinal pressure dissociation, and the "slosh" effect is driven by the isolated spinal CSF pressure fluctuation. In an attempt to explain the mechanism underlying the fluctuations in the spinal CSF pressure, Williams stressed that the spinal CSF pressure is mainly a result of extradural spinal venous pressure. Increases in the extradural spinal venous pressure with Valsalva maneuver lead to an increase in spinal CSF pressure. Following the cessation of the restraining maneuver, an abrupt increase in the spinal venous outflow leads to a rebound decrease in the spinal CSF pressure. In this way, fluctuations in the spinal CSF pressure reflect the pressure fluctuations of the spinal venous system. The mechanism behind the "suck" effect and craniospinal pressure dissociation is slightly more complex. In patients with hindbrain herniation not significant enough to cause impaction of the cord, the herniated hindbrain (tonsils) acts as a unidirectional valve. The CSF can move in an upward direction from the spinal to the cranial compartments; however, downward movement of CSF from the cranial to the spinal compartment is dampened by the synchronous downward movement of the herniated hindbrain and partial obstruction at or below the level of the foramen magnum. Such dampening of CSF flow in the craniospinal direction results in an aggravated and protracted (rebound) decline in spinal CSF pressure in relation to the intracranial pressure.

The "suck and slosh" effect of Williams is pervasive and can explain the occurrence of communicating and non-communicating syringomyelia as well as their temporal relationship. In this theory, the communicating syringomyelia is the precursor for the non-communicating syringomyelia, and temporally, these two are separated by the timing of *significant* hindbrain herniation through the foramen magnum. At first, the *internally* acting "suck" effect leads to formation of syringomyelia, and once a significant hindbrain herniation occurs, the syrinx is maintained or expanded by the *externally* acting "slosh" effect. However, this theory cannot explain and was not proposed to explain the events leading to the occurrence of initial hindbrain herniation, which are necessary to generate the "suck" effect. Notably, in patients with Chiari I malformation, syringomyelia is more commonly found in patients with moderate cerebellar herniation (9–14 mm) than in those with smaller or larger herniation [65]. Thus, it is reasonable to assume that the valve-like mechanism imposed by the herniated hindbrain is more efficient at the moderate degrees of herniation. While the smaller herniation may not be sufficient enough to induce a valve-like mechanism, the larger herniation hinders this mechanism by blocking the CSF flow through the foramen magnum in both upward and downward directions and eliminating the "suck" effect.

Exaggerated Spinal CSF Systolic Wave Theory of Syringomyelia

This theory proposed by Oldfield et al. [33] only deals with the pathogenesis of syringomyelia in patients with Chiari malformation. The theory stresses the earlier observations of du Boulay et al. [66, 67] that in normal individuals and during the cardiac systole, CSF moves downward from the cranial into the spinal subarachnoid space through the foramen magnum to accommodate for the increased intracranial blood volume. During diastole and when blood rushes out of the cranial cavity, the CSF flow is reversed back into the cranial subarachnoid space. This waveform or pulsatile flow of CSF across the foramen magnum is approximately ten times greater than the synchronous CSF flow through the fourth ventricle. In the cases examined by Oldfield et al. [33], they noted that the communication between the spinal syrinx and fourth ventricle (i.e., upper cervical spinal cord central canal) in Chiari I patients was invariably closed. Contrary to the prediction of Gardner's theory, they also noted that, in fact, the syrinx constricts during cardiac systole and expands during diastole. The systolic constriction of the syrinx was synchronous with the downward excursion of the herniated tonsils. The CSF "to-and-fro" flow between the cranial and spinal compartments was dampened as a result of partial occlusion of the

subarachnoid space at the level of the foramen magnum (secondary to hindbrain herniation). Based on these findings, Oldfield et al. [33] concluded that (1) the sudden, pistonlike excursion of the herniated tonsils transmits an accentuated pressure wave on the spinal CSF and creates an exaggerated CSF pulsatile pressure in the spinal canal during systole, (2) the exaggerated spinal CSF pulse pressure acts on the syrinx externally causing its compression, and (3) by diastole, the spinal CSF pressure suddenly ceases, leading to sudden expansion of the syrinx during diastole. Ultimately, Oldfield et al. [33] formulated a new theory to compensate for the inadequacy of Gardner's hydrodynamic theory of syringomyelia: The exaggerated CSF wave pressure during cardiac systole leads to a greater than normal passage of CSF along the perivascular spaces of the spinal cord into the cord substance. Intramedullary accumulation of CSF leads to the formation of syringomyelia. The pathophysiology of syringomyelia in Chiari I malformations is further discussed in Chap. 12 ("Research on the Pathophysiology of Chiari I-Related Symptoms and Syringomyelia, with Emphasis on Dynamic MRI Techniques").

Peri-Odontoid Pannus

We recently hypothesized that inflammatory reactions—e.g., pharyngitis in the peri-odontoid region—might result in inhibition of CSF flow at the craniocervical junction with resultant raised intracranial pressure [68]. Such raised pressure above the foramen magnum might then result in hindbrain herniation (Fig. 5.7). Our experience with the pediatric CIM has shown that almost 1 in 20 patients who present with symptoms is found to have a peri-odontoid pannus (Fig. 5.8).

These masses ranged in size from 4 to 11 mm in diameter (Fig. 5.8). Forty percent had a history of clinically significant pharyngitis or pharyngeal abscess. Pannus formation around the odontoid process resulted in ventral compression of the craniocervical junction in each of these patients. Highlighting the hypermobility that causes such lesions, following fusion, the pannus and symptoms in several patients were diminished.

Pharyngeal inflammatory conditions are known to cause disorders of the craniocervical junction. Non-traumatic atlanto-axial subluxation following an upper respiratory tract infection or surgical intervention in the head and neck region, also referred to as Grisel's syndrome, is the prime example. The syndrome is named after Pierre Grisel, a French ENT specialist who described three such cases of patients with pharyngitis associated with torticollis and atlanto-axial subluxation. It was Bell [69], however, who first reported a patient who suffered from pharyngitis that consequently died from spinal cord compression from atlanto-axial subluxation. His report underlines the potential consequences of this rare condition that affects primarily the pediatric population. Even though the precise pathogenesis of Grisel's syndrome remains unknown, the condition is attributed to spread of septic emboli from an infection nidus via the pharyngovertebral veins to the peri-odontoid vascular plexus, resulting in ligamentous laxity.

The vascular supply of the pharynx, peripharyngeal space, and odontoid process illustrate their close relationship. Parke [70] demonstrated that small venous branches drain the posterior nasopharyngeal region into two sets of pharyngovertebral veins. These pharyngovertebral veins pass through the upper posterior pharyngeal wall, penetrate the anterior atlanto-occipital membrane, and drain into the peri-odontoidal plexus, providing the anatomical correlate for the hematogenous spread of septic exudates thought to occur with Grisel's syndrome. The theory of direct spread of infectious material via the aforementioned route is complemented by Battiata and Pazos' [71] two-hit hypothesis. According to the hypothesis, patients with baseline laxity of the atlanto-axial joint (first hit), such as children or patients with Down syndrome, are more susceptible to muscle spasm that is triggered by inflammatory mediators transported to the cervical muscles by the pharyngovertebral venous plexus (second hit) and consequently develop Grisel's syndrome.

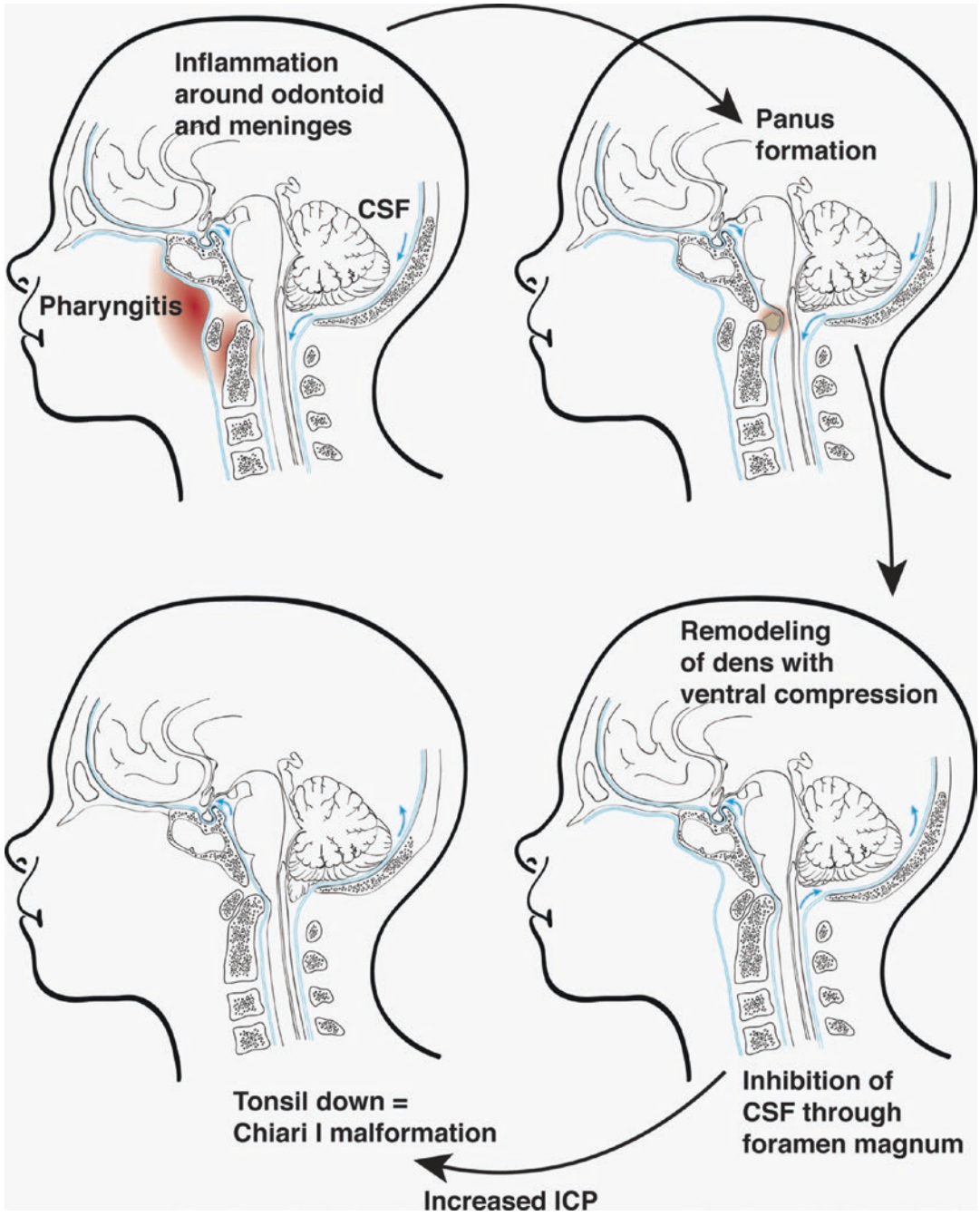

Fig. 5.7 Hypothetical process of peri-odontoid pannus formation with resultant Chiari I malformation

Chiari malformations are dynamic processes that may change with time. While they are generally considered a congenital condition, acquired Chiari malformation as a result of various causes is well described. The pathophysiology responsible for the development of a CIM seems to involve impaired CSF circulation out of the fourth ventricle and across the craniocervical junction. We hypothesize that inflammatory pharyngeal conditions attribute to the impendence of CSF circulation and to the formation and progression of CIM.

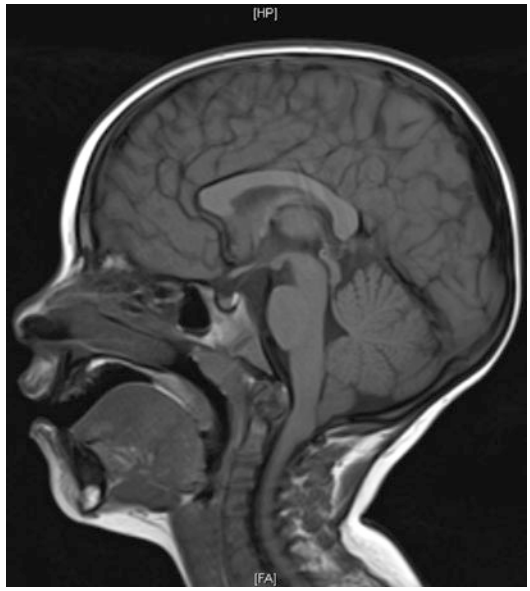

Fig. 5.8 MRI of patient with peri-odontoid process pannus and CIM

Abnormalities of the bony elements of the craniocervical junction are common in patients with CIM. Up to a quarter of all patients with CIM have an increased incidence of a retroflexed odontoid process. A smaller percentage have concomitant atlanto-occipital fusion and basilar invagination. Associated abnormalities of the craniocervical junction contribute to the impairment of CSF circulation, as evidenced by the observation that a higher grade of odontoid retroflexion is more frequently associated with syringomyelia and holocord syrinx [72].

Hypermobility of the occipitoatlantal and atlanto-axial joints is a well-established cause of retro-odontoid pannus formation in patients with hereditary connective tissue disorders. While those patients may be particularly susceptible, pannus formation is also frequently observed in CIM patients not possessing underlying connective tissue disorders. In patients with underlying

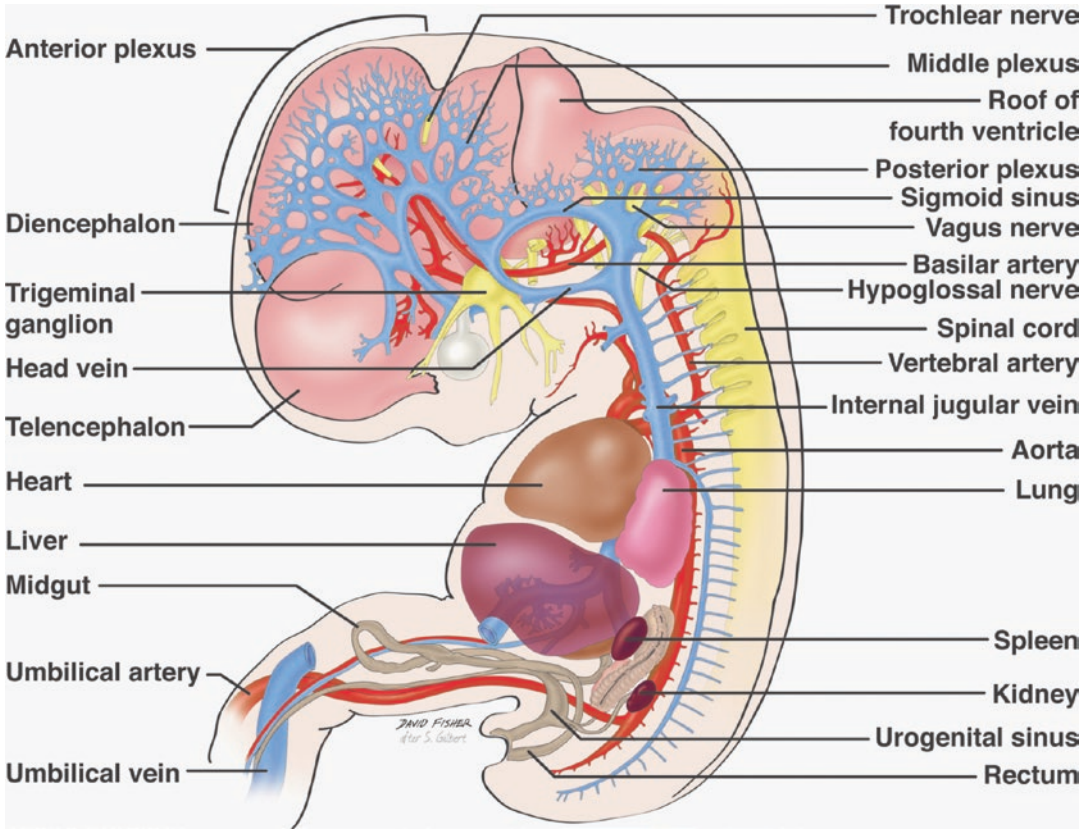

Fig. 5.9 Schematic drawing of the developing human and noting the complexity of the developing brain and posterior cranial fossa

craniocervical junction abnormalities, such as odontoid retroflexion and pre-existing CIM, acceleration of pannus formation may have profound radiographic and clinical consequences. One extreme example of an association of pharyngeal infection and CIM is a reported case of mononucleosis resulting in transient, highly symptomatic CIM that completely resolved with treatment of the infection [73].

Conclusion

The development of the hindbrain and craniocervical junction is a complicated process resulting in eloquent structures (Fig. 5.9). Derailment of this process can result in Chiari malformations. However, the exact reason for these hindbrain hernias remains elusive but is multifactorial.

References

1. Padget DH. Development of so-called dysraphism; with embryologic evidence of clinical Arnold-Chiari and Dandy-Walker malformations. Johns Hopkins Med J. 1972;130(3):127–65.
2. Ingraham FD, Scott HW. Spina bifida and cranium bifidum V. The Arnold-Chiari malformation: a study of 20 cases. N Engl J Med. 1943;229:108–14.
3. Anegawa S, Hayashi T, Torigoe R, Hashimoto T. Meningomyelocele associated with cranium bifidum: rare coexistence of two major malformations. Childs Nerv Syst. 1993;9(5):278–81.
4. Peach B. Arnold-Chiari malformation: anatomic features of 20 cases. Arch Neurol. 1965;12:613–21.
5. Schady W, Metcalfe RA, Butler P. The incidence of craniocervical bony anomalies in the adult Chiari malformation. J Neurol Sci. 1987;82(1–3):193–203.
6. Smoker WR. Craniovertebral junction: normal anatomy, craniometry, and congenital anomalies. Radiographics. 1994;14(2):255–77.
7. Muhleman M, Charran O, Matusz P, Shoja MM, Tubbs RS, Loukas M. The proatlas: a comprehensive review with clinical implications. Childs Nerv Syst. 2012;28(3):349–56.
8. Menezes AH. Primary craniovertebral anomalies and the hindbrain herniation syndrome (Chiari I): data base analysis. Pediatr Neurosurg. 1995;23(5):260–9.
9. Tubbs RS, Beckman J, Naftel RP, Chern JJ, Wellons JC 3rd, Rozzelle CJ, Blount JP, Oakes WJ. Institutional experience with 500 cases of surgically treated pediatric Chiari malformation type I. J Neurosurg Pediatr. 2011;7(3):248–56.
10. Pooh RK, Pooh KH. Fetal central nervous system. In: Kurjak A, Chervenak FA, editors. Donald school textbook of ultrasound in obstetrics & gynecology. 3rd ed. New Delhi: Jypee; 2011. p. 233–76.
11. Russell DS, Donald C. The mechanism of internal hydrocephalus in spina bifida. Brain. 1935;58:203–15.
12. Gardner WJ. The dysraphic states. Amsterdam: Excerpta Medica; 1973.
13. Tubbs RS, Dockery SE, Salter G, Elton S, Blount JP, Grabb PA, Oakes WJ. Absence of the falx cerebelli in a Chiari II malformation. Clin Anat. 2002;15(3):193–5.
14. Gilbert JN, Jones KL, Rorke LB, Chernoff GF, James HE. Central nervous system anomalies associated with meningomyelocele, hydrocephalus, and the Arnold-Chiari malformation: reappraisal of theories regarding the pathogenesis of posterior neural tube closure defects. Neurosurgery. 1986;18(5):559–64.
15. Gardner WJ. Hydrodynamic factors in Dandy-Walker and Arnold-Chiari malformations. Childs Brain. 1977;3(4):200–12.
16. Naidich TP, Pudlowski RM, Naidich JB. Computed tomographic signs of the Chiari II malformation. III: Ventricles and cisterns. Radiology. 1980;134(3):657–63.
17. Masters CL. Pathogenesis of the Arnold-Chiari malformation: the significance of hydrocephalus and aqueduct stenosis. J Neuropathol Exp Neurol. 1978;37(1):56–74.
18. Lichtenstein BW. Distant neuroanatomic complications of spina bifida (spinal dysraphism). Arch Neurol Psychiatr. 1942;47:195–214.
19. Gardner WJ. Hydrodynamic mechanism of syringomyelia: its relationship to myelocele. J Neurol Neurosurg Psychiatry. 1965;28:247–59.
20. Tubbs RS, Smyth MD, Wellons JC 3rd, Oakes WJ. Arachnoid veils and the Chiari I malformation. J Neurosurg. 2004;100(5 Suppl Pediatrics):465–7.
21. Barry A, Patten BM, Stewart BH. Possible factors in the development of the Arnold-Chiari malformation. J Neurosurg. 1957;14(3):285–301.
22. Josef V, Fehlings MG. Chiari malformations and syringomyelia. In: Goel A, Cacciola F, editors. The craniovertebral junction: diagnosis, pathology, surgical techniques. New York: Thieme; 2011.
23. Tubbs RS, Shoja MM, Ardalan MR, Shokouhi G, Loukas M. Hindbrain herniation: a review of embryological theories. Ital J Anat Embryol. 2008;113(1):37–46.
24. Bell JE, Gordon A, Maloney AF. The association of hydrocephalus and Arnold-Chiari malformation with spina bifida in the fetus. Neuropathol Appl Neurobiol. 1980;6(1):29–39.
25. Radkowski MA. (translator). Concerning alterations in the cerebellum resulting from cerebral hydrocephalus, 1891 by Hans Chiari [original article in German]. Pediatr Neurosci. 1987;13(1):3–8.
26. Koehler PJ, Greenblatt SH. The Chiari malformation. In: Koehler PJ, Bruyn GW, Pearce JMS, editors. Neurological eponyms. New York: Oxford University Press; 2000. p. 277–82.

27. Stein SC, Schut L. Hydrocephalus in myelomeningocele. Childs Brain. 1979;5(4):413–9.
28. Caviness VS. The Chiari malformations of the posterior fossa and their relation to hydrocephalus. Dev Med Child Neurol. 1976;18(1):103–16.
29. Williams H. A unifying hypothesis for hydrocephalus, Chiari malformation, syringomyelia, anencephaly and spina bifida. Cerebrospinal Fluid Res. 2008;5:7.
30. Gardner WJ, Abdullah AF, McCormack LJ. The varying expressions of embryonal atresia of the fourth ventricle in adults: Arnold-Chiari malformation, Dandy-Walker syndrome, arachnoid cyst of the cerebellum, and syringomyelia. J Neurosurg. 1957;14(6):591–605.
31. Pollay M. The function and structure of the cerebrospinal fluid outflow system. Cerebrospinal Fluid Res. 2010;7:9.
32. Penfield W, Cone W. Spina bifida and cranium bifidum: results of plastic repair of meningocele and myelomeningocele by a new method. JAMA. 1932;93:454–61.
33. Oldfield EH, Muraszko K, Shawker TH, Patronas NJ. Pathophysiology of syringomyelia associated with Chiari I malformation of the cerebellar tonsils. Implications for diagnosis and treatment. J Neurosurg. 1994;80(1):3–15.
34. Cameron AH. The Arnold-Chiari malformation and other neuro-anatomical malformations associated with spina bifida. J Pathol Bacteriol. 1957;73:195–211.
35. Peach B. The arnold-chiari malformation; morphogenesis. Arch Neurol. 1965;12:527–35.
36. Jacobs EB, Landing BH, Thomas W Jr. Vernicomyelia. Its bearing on theories of genesis of the Arnold-Chiari complex. Am J Pathol. 1961;39:345–53.
37. Nishikawa M, Sakamoto H, Hakuba A, Nakanishi N, Inoue Y. Pathogenesis of Chiari malformation: a morphometric study of the posterior cranial fossa. J Neurosurg. 1997;86(1):40–7.
38. Weed LH. The development of the cerebrospinal spaces in pig and in man. Contrib Embryol. 1917;5:1–116.
39. Padget DH. The development of the cranial venous system in man, from the viewpoint of comparative anatomy. Contrib Embryol. 1957;36:79–104.
40. Bering EA Jr. Choroid plexus and arterial pulsations of cerebrospinal fluid: demonstration of the choroid plexus as a cerebrospinal fluid pump. AMA Arch Neurol Psychiatry. 1955;73:165–72.
41. Marin-Padilla M, Marin-Padilla TM. Morphogenesis of experimentally induced Arnold – Chiari malformation. J Neurol Sci. 1981;50(1):29–55.
42. D'Addario V, Pinto V, Del Bianco A, Di Naro E, Tartagni M, Miniello G, Serio G. The clivus-supraocciput angle: a useful measurement to evaluate the shape and size of the fetal posterior fossa and to diagnose Chiari II malformation. Ultrasound Obstet Gynecol. 2001;18(2):146–9.
43. Patten BM. Overgrowth of the neural tube in young human embryos. Anat Rec. 1952;113(4):381–93.
44. Patten BM. Embryological stages in the establishing of myeloschisis with spina bifida. Am J Anat. 1953;93(3):365–95.
45. Hung CF. The relationship between hydrocephalus and Chiari type II malformation in the experimental rat fetuses with Arnold-Chiari malformation. Proc Natl Sci Counc Repub China B. 1986;10(2):118–26.
46. Bergquist H. Experiments on the 'overgrowth' phenomenon in the brain of chick embryos. J Embryol Exp Morphol. 1959;7:122–7.
47. Kallen B. Errors in the differentiation of the central nervous system. In: Vinken PJ, Bruyn GW, Klawans HL, editors. Handbook of clinical neurology – volume 50 of current clinical practice: malformations. Amsterdam: Elsevier; 1987. p. 19–48.
48. Jelinek R. A report to the so-called "overgrowth" of the neural tube [Czech]. Cesk Morfologie. 1961;9:151–61.
49. Vogan KJ, Epstein DJ, Trasler DG, Gros P. The splotch-delayed (Spd) mouse mutant carries a point mutation within the paired box of the Pax-3 gene. Genomics. 1993;17(2):364–9.
50. Moase CE, Trasler DG. Splotch locus mouse mutants: models for neural tube defects and Waardenburg syndrome type I in humans. J Med Genet. 1992;29(3):145–51.
51. O'Shea KS, Liu LH. Basal lamina and extracellular matrix alterations in the caudal neural tube of the delayed splotch embryo. Brain Res. 1987;465(1–2):11–20.
52. Yang XM, Trasler DG. Abnormalities of neural tube formation in pre-spina bifida splotch-delayed mouse embryos. Teratology. 1991;43(6):643–57.
53. Ahlgren S, Vogt P, Bronner-Fraser M. Excess FoxG1 causes overgrowth of the neural tube. J Neurobiol. 2003;57(3):337–49.
54. Penfield W, Coburn DF. Arnold-Chiari malformation and its operative treatment. Arch Neurol Psychiatr. 1938;40:328–36.
55. Tubbs RS, Loukas M, Shoja MM, Oakes WJ. Observations at the craniocervical junction with simultaneous caudal traction of the spinal cord. Childs Nerv Syst. 2007;23(4):367–9.
56. Daniel PM, Strich S. Some observations on congenital deformity of central nervous system known as Arnold-Chiari malformation. J Neuropath Exp Neurol. 1958;17:255–66.
57. Lang J. Skull base and related structures: atlas of clinical anatomy. 2nd ed. Stuttgart: Schattauer; 2001.
58. van Hoytema GJ, van den Berg R. Embryological studies of the posterior fossa in connection with Arnold-Chiari malformation. Dev Med Child Neurol. 1966;Suppl 11:61–76.
59. McLone DG, Knepper PA. The cause of Chiari II malformation: a unified theory. Pediatr Neurosci. 1989;15(1):1–12.
60. McLone DG. The Chiari II malformation of the hindbrain and the associated hydromyelia. In: Anson JA, Benzel EC, Awad IA, editors. Syringomyelia and the Chiari malformations. Park Ridge: The American

Association of Neurological Surgeons; 1997. p. 69–82.
61. Corti G, Manzur T, Nagle C, Martinez-Ferro M. Etiopathology of Arnold-Chiari malformation: a fetal rat model of dysraphism. Fetal Diagn Ther. 2010;28(1):28–33.
62. Roth M. Cranio-cervical growth collision: another explanation of the Arnold-Chiari malformation and of basilar impression. Neuroradiology. 1986;28(3):187–94.
63. Williams B. On the pathogenesis of syringomyelia: a review. J R Soc Med. 1980;73(11):798–806.
64. Williams B. Syringomyelia. Neurosurg Clin N Am. 1990;1(3):653–85.
65. Stovner LJ, Rinck P. Syringomyelia in Chiari malformation: relation to extent of cerebellar tissue herniation. Neurosurgery. 1992;31(5):913–7.
66. du Boulay GH. Pulsatile movements in the CSF pathways. Br J Radiol. 1966;39(460):255–62.
67. du Boulay G, O'Connell J, Currie J, Bostick T, Verity P. Further investigations on pulsatile movements in the cerebrospinal fluid pathways. Acta Radiol Diagn (Stockh). 1972;13:496–523.
68. Tubbs RS, Griessenauer CJ, Hendrix P, Oakes P, Loukas M, Chern JJ, Rozzelle CJ, Oakes WJ. Relationship between pharyngitis and peri-odontoid pannus: a new etiology for some Chiari I malformations? Clin Anat. 2015;28(5):602–7.
69. Bell C. The nervous system of the human body: embracing the papers delivered to the Royal Society on the subject of the nerves. London: Longman, Rees, Orme, Brown, and Green; 1830.
70. Parke WW, Rothman RH, Brown MD. The pharyngovertebral veins: an anatomical rationale for Grisel's syndrome. J Bone Joint Surg Am. 1984;66:568–74.
71. Battiata AP, Pazos G. Grisel's syndrome: the two-hit hypothesis–a case report and literature review. Ear Nose Throat J. 2004;83(8):553–5.
72. Tubbs RS, Wellons JC 3rd, Blount JP, Grabb PA, Oakes WJ. Inclination of the odontoid process in the pediatric Chiari I malformation. J Neurosurg. 2003;98:43–9.
73. Shokouhi G, Naghili B. Spontaneous resolution of acquired tonsillar herniation caused by isolated cerebellar tonsil inflammation: case report. Neurosurgery. 2005;56(5):E1158.

6 The Occipital Bone: Review of Its Embryology and Molecular Development

Stephen J. Bordes and R. Shane Tubbs

Embryology and Anatomy

Like that of other mammals, the human occipital bone is ontogenetically and functionally unique when compared to other bones of the cranium [1]. It is one of the first bones of the skull to develop and consists anatomically of four parts surrounding the foramen magnum: the basilar, squamous, and two condylar parts (Figs. 6.1, 6.2, and 6.3). The fusion of four primary cranial vertebrae creates the basilar part or basiocciput (Fig. 6.3), which unites with the basisphenoid at the sphenooccipital synchondrosis to form the clivus [2]. The supraoccipital, or squamous part [2], consists of right and left central segments. Right and left vertical sutures, which extend from the interparietal–supraoccipital suture to the posterior margin of the foramen magnum, separate these right and left central segments [2, 3]. Lateral and posterior walls of the posterior cranial fossa are formed by the central segment's inferior concave surface. Right and left portions [3] articulate with the inferior angle of the parietal bones superolaterally on either side at the lambdoid suture and the mastoid part of the temporal bone at the occipitomastoid suture [2].

Superoposteriorly, the occipital bone has an internal and external occipital protuberance in the region surrounding the torcular Herophili or confluence of sinuses. The occipital bone may have impressions of the inner table extending into the diploic space occupied in part by the arachnoid granulations [2]. The lateral borders of the foramen magnum are formed by the exoccipital or condylar part (Figs. 6.2 and 6.3). This part lies between the basiocciput and squamous part of the occipital bone, fusing with them in early life by synchondrosis [2].

The occipital bone has an intricate development as a result of dual origin from both membranous and cartilaginous components. Occipital development has been extensively studied, dating back to Ranke's 1913 account of the development of the membranous part of the squamous occipital bone with the development of two pairs of centers and an occasional third pair, known as the pre-interparietal [4]. In 1977, Srivastava confirmed the three pairs of centers previously described by Ranke in 1913 on the basis of anomalies observed in a large number of skulls [4]. The membranous part of the occipital bone consists of interparietal and pre-intraparietal elements [4]. Additionally, Srivastava and Standring considered that a separate bone at the posterior

S. J. Bordes
Department of Anatomical Sciences, St. George's University School of Medicine, St. George's, Grenada, West Indies

R. S. Tubbs (✉)
Department of Neurosurgery, Tulane University School of Medicine, New Orleans, LA, USA

Department of Neurosurgery and Ochsner Neuroscience Institute, Ochsner Health System, New Orleans, LA, USA

R. S. Tubbs et al. (eds.), *The Chiari Malformations*, https://doi.org/10.1007/978-3-030-44862-2_6

Fig. 6.1 Posterior view of the fetal skull noting the squama and foramen magnum. Also, note the developing occipital condyles

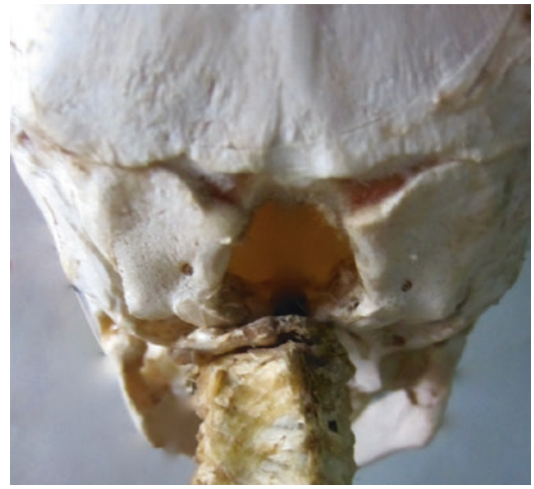

Fig. 6.2 Posterior view of the fetal skull noting the squama and foramen magnum. Also, note the developing occipital condyle articulating with the developing C1 vertebra on the left

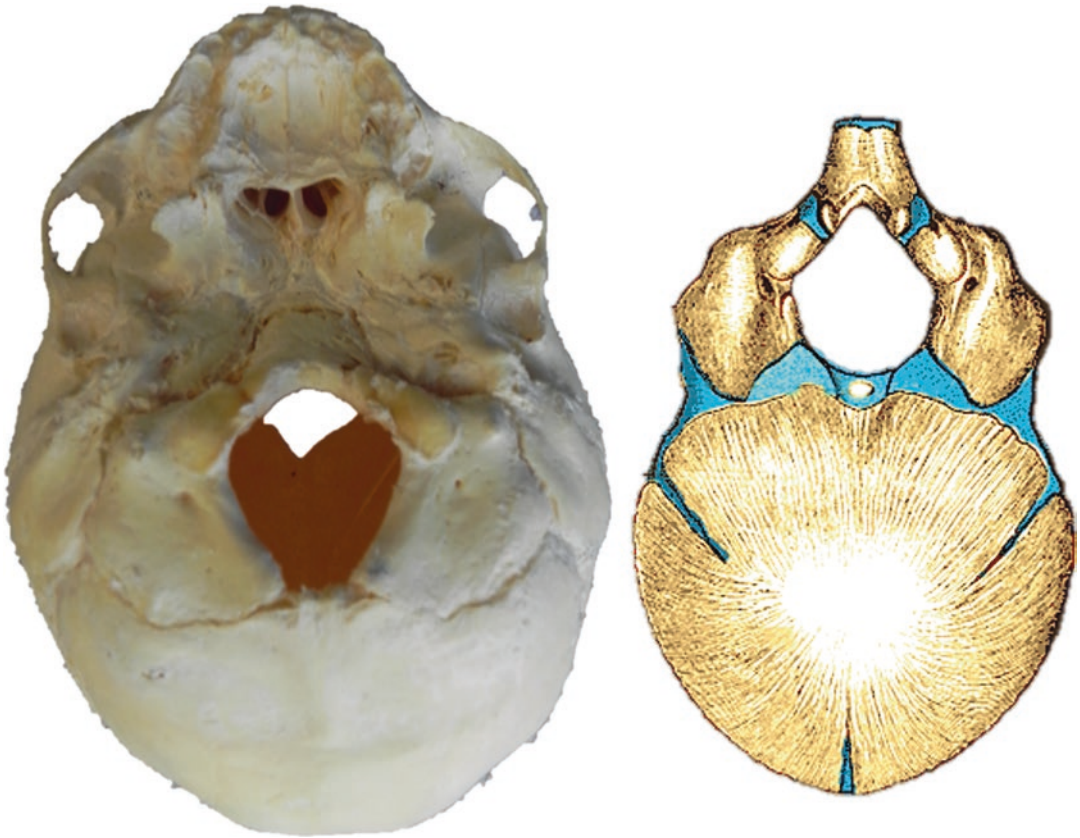

Fig. 6.3 Basilar view of the developing fetal skull base (left) and schematic drawing (right) of the occipital bone parts. Note Kerkring's bone located at the posterior aspect of the foramen magnum

fontanelle (lambda) might represent the preinterparietal element [4, 5].

In 1976, Shapiro and Robinson studied a total of 125 skulls from fetuses ranging from 8 to 40 weeks' gestation in an attempt to finally determine and chronologically document the embryogenesis of the occipital bone. They concluded that the occipital bone is formed from one membranous element and the four united primary cartilaginous centers laid down on the chondrocranium around the foramen magnum [6]. Endochondral bone arises from glycoprotein- and glycosaminoglycan-rich matrices that condense into cartilaginous anlage in the occipital part of the cranial base [1]. The basioccipital, the lateral or exoccipitals, and the supraoccipital (inferior squama below the suture) comprise the four cartilaginous portions. The mendosal suture (Fig. 6.3) is an accessory suture of the occipital bone located somewhat superior to the transverse sinus that develops in the region of the posterior lateral (mastoid) fontanelle, between the developing interparietal and supraoccipital bones, and runs horizontally from the medial portion of the lambdoid suture. Its fusion begins prior to birth and is completed between the second and fourth year of life [7]. The membranous component gives rise to the interparietal bone, the superior squama above the mendosal suture [6]. Fetuses, dated at 9 weeks of gestation in this study, were found to have single median ossification centers present in the cartilaginous basiocciput ventral to the notochord and in each lateral occipital cartilage around the hypoglossal canal. Additionally, the supraoccipital segment was ossified from a single focus in the tectum synoticum in all specimens. Further, coronal sections of these specimens revealed ossification in the membranous interparietal segment [6]. At 12 weeks' gestation, the interparietal and supraoccipital segments are fused in the midline but remained laterally separated by the mendosal sutures. Ossification in the supraoccipital segment was noted to be more advanced than in the interparietal segment [6]. At 14 weeks, the mendosal sutures reduced to narrow slits, and the interparietal and supraoccipital segments further united [6].

Basioccipital segment ossification proceeds laterally into the ventral portion of each condyle, while ossification of the lateral occipitals concurrently advances into the dorsal portion of the occipital condyles [6]. Shapiro and Robinson noticed a midline cleft in the inferior margin of the supraoccipital bone in a few fetal specimens. Such clefts may persist or subsequently fill with bone [6]. Less commonly, a small central bony projection, also known as Kerkring's bone or ossicle [6] (Fig. 6.3), is present on the inferior aspect of the supraoccipital segment [3]. At birth, basioccipital and lateral occipital bones are separated by a prominent synchondrosis on each side, which normally obliterates between 2 and 4 years of age. The innominate synchondrosis separates the lateral occipitals from the supraoccipital segment. Bony fusion of these segments takes place between 2 and 4 years of age [6]. At birth, the interparietal and supraoccipital segments are fused with the exception of lateral surfaces, which are separated by the mendosal sutures. These sutures were once thought to completely obliterate by the end of the second year of life [6]; however, Tubbs et al. showed remnants of these sutures in adults in recent years [8, 9].

Matsumura et al. conducted a different study to determine the progression of ossification in the development of the occipital bone. As a result, their study examined a total of 256 Japanese fetal skulls ranging from 3 to 6 months of age. Occipital squama observation of these specimens was performed using dissection microscopy, and celloidin-embedded sections were examined by light microscopy [10]. These authors found that a pair of small ossification centers was present in the supraoccipital cartilage of 3-month-old fetuses. These ossification centers quickly fused to form a single, solid bony plate, known as the supraoccipital bone, which had a smooth surface and no apparent bony trabecular structures [10]. Following the formation of the supraoccipital bone, a pair of primary interparietal ossification centers appeared in the membranous portion, rostral to the supraoccipital region. A group of threadlike ossification nuclei comprised each ossification center, which then rapidly grew and fused with one another to form mesh-like bone. As the mesh-like primary interparietal bone forms, primary centers extend downward and fuse with the upper edge of the supraoccipital bone [10].

During the third month, secondary interparietal ossification centers appeared anterior to the primary interparietal bone. The medial pair of these centers developed first followed by the lateral pair. These centers formed a meshwork of trabeculae, which rapidly fused with each other and/or the upper edge of the primary bone. Irregular areas of ossification were observed on the external surface of the supraoccipital bone at this stage of development. These granular and threadlike areas of ossification developed into a bony meshwork that fused with the lateral part of the primary interparietal bone on each side [10]. Ossification sites could be seen scattered throughout the external membranous tissue of the supraoccipital plate and occasionally connected to the supraoccipital bone by thin trabeculae [10]. In 4-month-old fetuses, irregular areas of ossification could be found on the internal surface of the supraoccipital bone. They were occasionally laterally fused with the trabeculae of the primary interparietal bone. These areas of ossification, however, were not fused with the medial portion of the interparietal part until the fifth month of gestation, at which time they developed a meshwork of thick bony trabeculae [10]. Secondary interparietal centers then formed a fan-shaped bone with a distinct border along the internal surface of the primary interparietal part. The root of the bone fused with the bony trabeculae along the midline and covered the internal surface of the supraoccipital bone [10]. By the fifth month of fetal gestation, all intramembranous ossification centers fused and formed a meshwork of trabeculae covering the external surface of the occipital squama in all specimens [10].

Molecular Associations

Skeletal development is an intricate process that requires stringent control of gene activation and suppression by a variety of transcription factors [11]. The development of the cranial bones relies on various signals from different regions of the brain. The occipital bone, in particular, is under direction of the rhombencephalon [12]. Precursor cells of the cranial vault are primarily located between the neural tube and surface ectoderm with its paraxial mesoderm of organized on a rostro-caudal axis [12]. The cephalic mesoderm constitutes the most rostral part of this domain with the remainder of paraxial mesoderm forming segmented somites. These somites are metameric units extending to the tip of the embryonic tail. The first four somites are occipital somites, since they fuse to form the occipital bone and posterior parts of the foramen magnum [12]. Sclerotomes migrate ventromedially and differentiate into vertebral bodies [13]. The basiocciput is derived from the first two occipital sclerotomes, while the exoccipital bone, which forms the jugular tubercles, seeks its origins from the third sclerotome [13].

The caudal, dense zone of the fourth occipital sclerotome combines with the loose, cranial half of the first cervical sclerotome to produce a transitional sclerotome called the proatlas [14]. While the proatlas may exist as its own separate entity in rare cases, it normally fuses with the upper three occipital sclerotomes contributing to parts of the basioccipital bone [14] and dorsal part of the foramen magnum [13]. The proatlas also gives rise to the anterior tubercle of the clivus, which is derived from the hypocentrum [13]. The lateral dense region of the proatlas becomes the exoccipitals, which later form the occipital condyles and the remainder of the anterolateral rim of the foramen magnum [14]. The neural arch segment of the proatlas differentiates into two separate regions. The ventral portion creates the anterior margin of the foramen magnum, the occipital condyle, and the midline third occipital condyle [13]. The fifth somite, also known as the first cervical somite, participates in the formation of the first cervical vertebra, which expresses *Hox d4* [12]. If one forces *Hox d4* expression in more rostral mesoderm, the supraoccipital and exoccipital bones transform into occipital vertebra [12].

The formation of the chordal part of the skull base is therefore dependent upon the influence of the notochord. This was demonstrated using a chick embryo in which the anterior notochord was removed. Hypoplasia of the basioccipital and basipostsphenoid bones resulted [12]. Such an outcome is furthered reinforced by *Bapx1* gene knockout studies in mice. The *Bapx1* is a vertebrate homologue of the drosophila *bagpipe* gene, which codes for the transcription factor of the NK2 family. *Bapx1* is expressed in the sclero-

tome, splanchnic mesoderm, limb, and Meckel's cartilage [12]. The *Bapx1*$^{-/-}$ mouse showed abnormal development of not only the axial skeleton but also the basioccipital and basipostsphenoid bones [12].

Lee et al. conducted an experiment to study aberrations of the skeletal system using the *Whsc1* gene (Wolf- Hirschhorn syndrome candidate 1), which encodes a histone H3 lysine 36 (H3K36) trimethyltransferase [11]. The study was conducted using E18.5 *Whsc1*$^{-/-}$ knockout mice, which were found to have significant ossification disruptions in cranial elements including the occipital and periotic bones [11]. Alkaline phosphatase (ALP) activity was measured and used as an early marker for osteoblast differentiation. In *Whsc1* deficiency, ALP activity is significantly decreased [11].

Mineralization abnormalities were examined in *Whsc1*$^{-/-}$ bone by a micro X-ray computed tomography (CT) system. The occipital bone, sternum, and clavicles exhibited signs of mineralization deficiency. These results demonstrated that *Whsc1* is involved in the regulation of skeletal development, primarily in the sternum and occipital bone [11]. However, gene expression of *Ocn*, a marker of mineralization, was not significantly altered in *Whsc1*$^{-/-}$ occipital bone and sternum. This suggests that *Whsc1* deficiency might also affect early commitment of the number of osteoprogenitors. As a result, *Whsc1* is essential in the regulation of skeletal development [11]. In an attempt to understand the genetic basis of the ossification deficiencies observed in the occipital bone and sternum of the *Whsc1* $^{-/-}$ embryos, expression levels of various genes in several bone tissues of E18.5 *Whsc1*$^{-/-}$ embryos were examined. In the occipital bone, *Whsc1* deficiency decreased expression of osteopontin (*Opn*) and collagen type 1a (*Col1A1*). Critical transcription factors for bone development, runt-related transcription factors 1 and 2 (*Runx1* and *Runx2*), were unaffected [11]. These results suggest that *Whsc1* plays a critical role in bone differentiation and is also necessary for osteoblast differentiation at least in the occipital bone and sternum [11]. In E18.5 *Whsc1*$^{-/-}$ embryos and newborns, significant disruptions in ossification were observed in the sternum and certain cranial bone elements, particularly involving the occipital bone [11].

In another knockout mouse experiment, transforming growth factor-beta (TGF-β) signaling was required in somite-derived bone structures, such as the supraoccipital bone and C1 vertebra. TGF-β(beta) signaling controls chondrocyte proliferation and prevents premature cartilage ossification. Loss of TGF-β(beta) signaling compromises the expression of *Msx2* during supraoccipital bone development, which is critical for somite-derived caudal skull development [15]. As a result, the TGF-β(beta)/*Msx2* signaling cascade was considered critical for the development of the cranial base [15].

Epigenetic factors play an important role in cranial development. Internal and external stimuli affect functional growth units [1]. Occipital bone development involves three distinct processes: cortical drift, appositional deposition, and sutural expansion. Together, these processes allow for anteroposterior, mediolateral, and superoinferior expansion [1]. Cortical drift occurs through a combination of osteoblastic and osteoclastic cellular activities, which are organized into various growth fields [1]. Bone remodeling, a process of deposition and resorption, is a major contributor as to the way in which bone grows, takes shape, and receives genetic instruction from both internal (e.g., genetic encoding) and external (e.g., bone strain) sources [1].

Osteoblastic and osteoclastic activities allow for cortical drift to occur throughout the entire basicranial portion of the occipital bone. In contrast, the neurocranium increases in size through the apposition of bone matrix from depositional growth fields, although some drift occurs within and immediately adjacent to these cranial sutures [1]. Bone remodeling processes can involve Haversian systems, pathological reconstruction, molecular biomechanics, and ontogenetics [1]. Ontogenetic growth remodeling is likely most important as it coordinates genetic and epigenetic input as bone develops from infancy throughout adulthood [1]. The external surface of the modern human occiput is depositional, unlike the endocranial side that is completely resorptive. A circumcranial line along the attachment of the tentorium cerebellum marks a critical reversal line in bone growth activity [1].

Chiari I Malformation

The supratentorial and infratentorial parts of the squamous occipital bone are composed of membranous and cartilaginous parts, respectively [16]. Such origins have bearing on many pathologies of the posterior cranial fossa including congenital hindbrain hernias such as the Chiari I malformation. The shallowness of the posterior cranial fossa in the Chiari I malformation may reflect an abnormality of the squamous bone that is restricted to its cartilage-derived lower part [16, 17]. In Chiari I malformation, the supraoccipital, exoccipital, and basioccipital segments can exhibit variable underdevelopment [16, 18, 19]. Occipital bone dysplasia is nonlinear in nature, and different parts of the occipital bone are disproportionately affected [16, 20]. Severe basioccipital hypoplasia or dysgenesis is usually associated with basilar invagination [16]. It has been postulated that partial reversion of the parietal plate during fetal life serves as an embryological basis for the shortening of the supraocciput in Chiari I malformations [16]. The upper part of the chondrified supraocciput that is derived from this plate is thus vulnerable to regression [16].

Conclusion

In the past, much controversy existed regarding the developmental process required for occipital bone formation. Meticulous experimentation and documentation of genes and molecular interactions have recently clarified many of these significant developmental questions.

References

1. Mowbray K. Surface bone histology of the occipital bone in humans and chimpanzees. Anat Rec. 2005;283B:14–22.
2. Jinkins JR. The Skull. Atlas of neuroradiologic embryology, anatomy, and variants. Philadelphia: Lipincott Williams and Wilkins; 2000. p. 63.
3. Srivastava HC. Development of ossification centers in the squamous portion of the occipital bone in man. J Anat. 1997;124:643–9.
4. Pal GP, Tamankar BP, Routal RV, Bhagwat SS. The ossification of the membranous part of the squamous portion of the occipital bone in man. J Anat. 1984;138:259–66.
5. Standring S. Gray's anatomy. 41st ed. Philadelphia: Elsevier; 2015.
6. Shapiro R, Robinson F. Embryogenesis of the human occipital bone. Am J Roentgenol. 1976;126:1063–8.
7. Nayak SR, Krishnamurthy A, Kumar AJ, Probhu L, Jiji P, Pai M, Kumar A, Avadhani R. The mendosal suture of the occipital bone: occurrence in Indian population, embryology and clinical significance. Surg Radiol Anat. 2007;29:329–32.
8. Tubbs RS, Salter EG, Oakes WJ. Does the mendosal suture exist in the adult? Clin Anat. 2007;20:124–5.
9. Gallagher E, Evans K, Hing A, Cunningham M. Bathrocephaly: a head shape associated with a persistent mendosal suture. Cleft Palate Craniofac J. 2013;50:104–8.
10. Matsumura G, England MA, Uchiumi T, Kodama G. The fusion of ossification centers in the cartilaginous and membranous parts of the occipital squama in human fetuses. J Anat. 1994;185:295–300.
11. Lee YF, Nimura K, Lo WN, Saga K, Kaneda Y. Histone H3 lysine 36 methyltransferase Whsc1 promotes the association of Runx2 and p300 in the activation of bone-related genes. PLoS One. 2014;9(9):e106661.
12. Tortori-Donati P, Rossi A. Embryology of the head and neck. Pediatric neuroradiology. Head, neck and spine. New York: Springer; 2005. p. 1257–64; 1271–1272.
13. Muhleman M, Charran O, Matusz P, Shoja MM, Tubbs S, Loukas M. The Proatlas: a comprehensive review with clinical implications. Childs Nerv Syst. 2012;28:349–56.
14. Pang D, Thompson DNP. Embryology and bony malformation of the craniovertebral junction. Child Nerv Syst. 2011;27:523–64.
15. Hosokawa R, Urata M, Han J, Zehnaly A, Bringas P, Nonaka K, Chai Y. TGF-β mediated Msx2 expression controls occipital somites derived caudal region of skull development. Dev Biol. 2007;310:140–53.
16. Shoja MM, Tubbs RS, Oakes WJ. Embryology of the craniocervical junction and posterior cranial fossa. The Chiari Malformations. New York: Springer; 2013. p. 13–54.
17. Graham JM. Lambdoidal craniosynostosis. Smith's recognizable patterns of human deformation. 3rd ed. Philadelphia: Saunders Elsevier; 2007. p. 204–9.
18. Tubbs RS, Cesmebasi A, Loukas M, Hogan E, Kralovic S, Cohen Gadol AA. The Chiari malformations: a review with emphasis on anatomical traits. Clin Anat. 2015;28:184–94.
19. Tubbs RS, Wellons JC, Smyth MD, Bartolucci AA, Blount JP, Oakes WJ, Grabb PA. Children with growth hormone deficiency and Chiari I malformation: a morphometric analysis of the posterior cranial fossa. Pediatr Neurosurg. 2003;38:324–8.
20. Huang MH, Gruss JS, Clarren SK, Mouradian WE, Cunningham ML, Roberts TS, Loeser JD, Cornell CJ. The differential diagnosis of posterior plagiocephaly: true lambdoid synostosis versus positional molding. Plast Recontr Surg. 1996;98:765–74.

The Proatlas

7

Stephen J. Bordes and R. Shane Tubbs

Introduction

The proatlas is a rare, vestigial bone formation that seldom persists in the form of bony remnants in humans [1]. The term "proatlas" stems from the field of comparative anatomy. It is considered to be a rudimentary or vestigial vertebral structure and can be found between the atlas and the occipital bone in nonhuman animals such as some rodents, reptiles, and dinosaurs [2].

In humans, the proatlas forms the occipital bone and the dorsal part of the foramen magnum after fusing with the upper three occipital sclerotomes (Fig. 7.1) [3–6]. As a result, it is not generally observed as a separate structure. However, there are instances in which proatlantal remnants have been noted in man. On occasion, additional vertebra will appear in front of the atlas, thus the term "proatlas" [3]. Although the proatlas hardly exists as its own entity, parts of it may be present due to failure of regression of embryonic structures. According to Wollin [7], the proatlas refers to a vertebra between the atlas and the occipital bone in reptiles. Subsequent studies have found evidence of this structure in fossils of dinosaurs [8–10]. Futhermore, proatlas elements still exist in some modern-day reptiles [3, 11]. In such lower vertebrates, the proatlas persists as a separate bone derived from the cranial half of the first cervical sclerotome [12, 13].

Usually, proatlas derivations can present in humans following incomplete structural regression. Bergman's tubercle, a small central ossicle between the tip of the odontoid process and the foramen magnum in man, may be analogous to the centrum of the proatlas in reptiles [7]. Humans are not the only mammals with these vestigial, proatlas-derived structures. White rats typically have an ossicle representing a fragmentary anterior arch of the proatlas located between the anterior arch of the atlas and the foramen magnum [3, 11]. The anterior arch of the proatlas may fuse with the anterior margin of the foramen magnum in birds. This results in the formation of the avian third or medial occipital condyle [7, 12]. A similar structure can exist in humans and is discussed later. Early vertebrates routinely possess a proatlas. Analogous structures are thought to form the apex of the dens, or the body of the proatlas, and regions of the occipital bone bordering the foramen magnum in higher mammals [10].

A number of theories have been put forth regarding the occasional occurrence of this additional vertebra in humans. It was previously believed that the presence of a proatlas, an addi-

S. J. Bordes
Department of Anatomical Sciences, St. George's University School of Medicine, St. George's, Grenada, West Indies

R. S. Tubbs (✉)
Department of Neurosurgery, Tulane University School of Medicine, New Orleans, LA, USA

Department of Neurosurgery and Ochsner Neuroscience Institute, Ochsner Health System, New Orleans, LA, USA

R. S. Tubbs et al. (eds.), *The Chiari Malformations*, https://doi.org/10.1007/978-3-030-44862-2_7

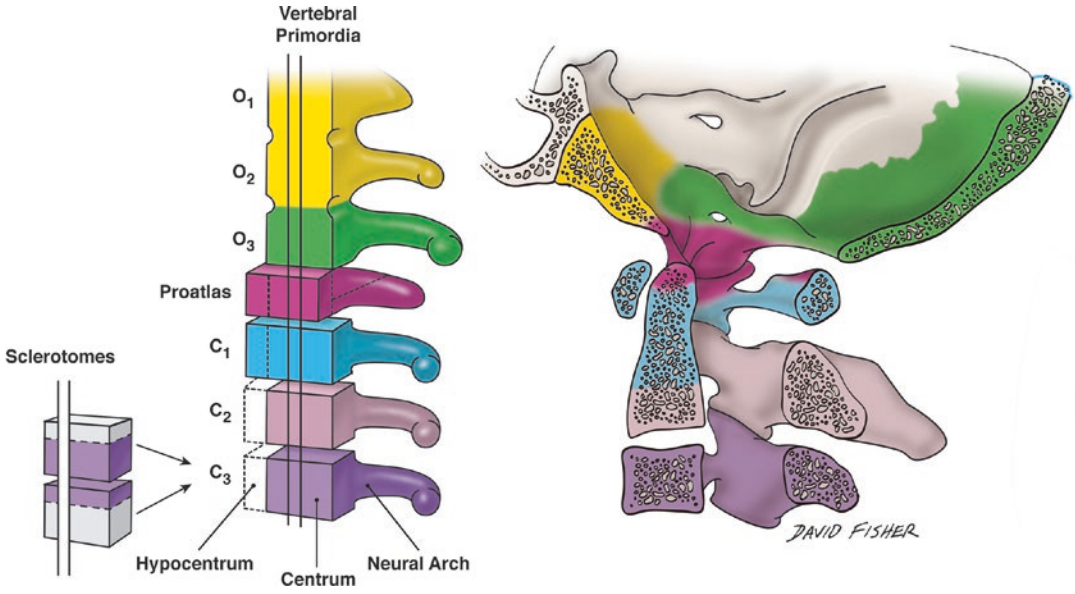

Fig. 7.1 Embryological derivations of the bony parts of the craniocervical junction

tional vertebral element, represented a lengthening vertebral column. However, Gladstone and Erichsen-Powell [3] opined that this lengthening takes place at the expense of the cranium by liberation of an occipital vertebra.

Zoologists might consider this a reversionary or regressive variation. As a result, the human proatlas could be viewed as an atavistic structure since the occipital bone is usually formed by incorporating vertebrae, which tend to exist separately in lower vertebrates, into the cranium of mammals (vide ante). However, another theory states that this variation does not represent a tendency to shorten the vertebral column. Gladstone and Erichsen-Powell [3] supported the notion that the presentation of such occipitoatlantal deviations represents a variation about a mean, with compensatory changes in other regions. Other speculations regarding these disparities in normal human vertebral column structure include arrest of development, intrauterine pressure, and prenatal disease [3].

Ontology and Normal Development

In the human embryo, 42 somites are present by the close of the fourth week of gestation [4–6, 14]. Each somite further differentiates, forming a sclerotome, dermatome, and myotome. As a result, there are four occipital somites in a human embryo and four corresponding sclerotomes. Sclerotomes migrate ventromedially and eventually form vertebral bodies [4–6].

Conventionally, the occipital bone and posterior parts of the foramen magnum are formed from the amalgam of the four occipital sclerotomes [3–6]. The basiocciput is derived from the first two occipital sclerotomes; and the third sclerotome forms the exoccipital bone, which produces the jugular tubercles.

The fourth occipital sclerotome forms a number of structures. The anterior tubercle of the clivus is derived from the hypocentrum of the proatlas. The terminal portion of the dens and the apical ligament is similarly formed from the centrum of this structure. In other words, the proatlas contributes to the apex of the odontoid process of the axis [15]. The neural arch segment of the proatlas differentiates into two separate regions. The ventral portion creates the anterior margin of the foramen magnum, the occipital condyle, and the midline third occipital condyle. The caudal portion gives rise to the superior portion of the posterior arch of the atlas and lateral atlantal masses. The lateral section of the proatlas condenses to produce the cruciate and alar ligaments [4–6].

The formation of structures in the craniocervical junction is directed by two families of developmental control genes. The homeobox (Hox) gene cluster on chromosome 6 and the paired box (Pax) genes on chromosome 2 are believed to play a crucial role in the development of cervical vertebrae [10].

Experimentation was carried out using transgenic mice with gain-of-function mutations following the introduction of Hox-1.1 genomic sequences under the control of a chicken β(beta)-actin promoter. Such mutations resulted in manifestations of the proatlas. Additionally, the basioccipital bone, atlas, and axis were malformed. The mice possessed craniofacial abnormalities and were nonviable after birth.

Mutations of the paired box-1 gene caused variations of the upper cervical vertebra, although these changes were not identical to those caused by altered homeobox genes [10]. Menezes [4–6, 16] claimed that variations of the craniocervical junction may be attributed to disruption of gene expression, as suggested by the aforementioned study on proatlas structural abnormalities.

One or more elements of the proatlas may fail to regress completely, which creates an "occipital vertebra" phenomenon (Fig. 7.2a, b) [17]. Generally, this occurs concurrently with a normal atlas [18, 19]. There is also a potential for partition of the upper joint facets into anterior and posterior segments upon failure of fusion of the posterior arch of the proatlas with the atlas [18]. The proatlas contributes to the lateral masses and part of the posterior arch of C1. The first spinal sclerotome completes the anterior and inferior aspect of the posterior atlas arch. Aplasia or hypoplasia of the atlas arch of C1 frequently manifests [20]. The structures created by variations of proatlas remnants include the basilar process, atlantic ponticles, craniocervical junction fusion anomalies, paracondyloid processes, a third occipital condyle, and partial regressive occipital vertebrae [1] (Figs. 7.1 and 7.2a,b).

A persistent hypochordal bow may be incorporated in the anterior foramen magnum as a prebasilar (hypochordal) arch, third occipital condyle (condylus tertius), or basilar processes [18, 21, 22]. The median occipital condyle is a rare structure created by the proatlas around the foramen magnum. The third condyle is produced by incomplete regression of the hypochordal arch of the occipital vertebra or proatlas [23]. As with other proatlas segmentation anomalies, this structure is formed from the first cervical sclerotome

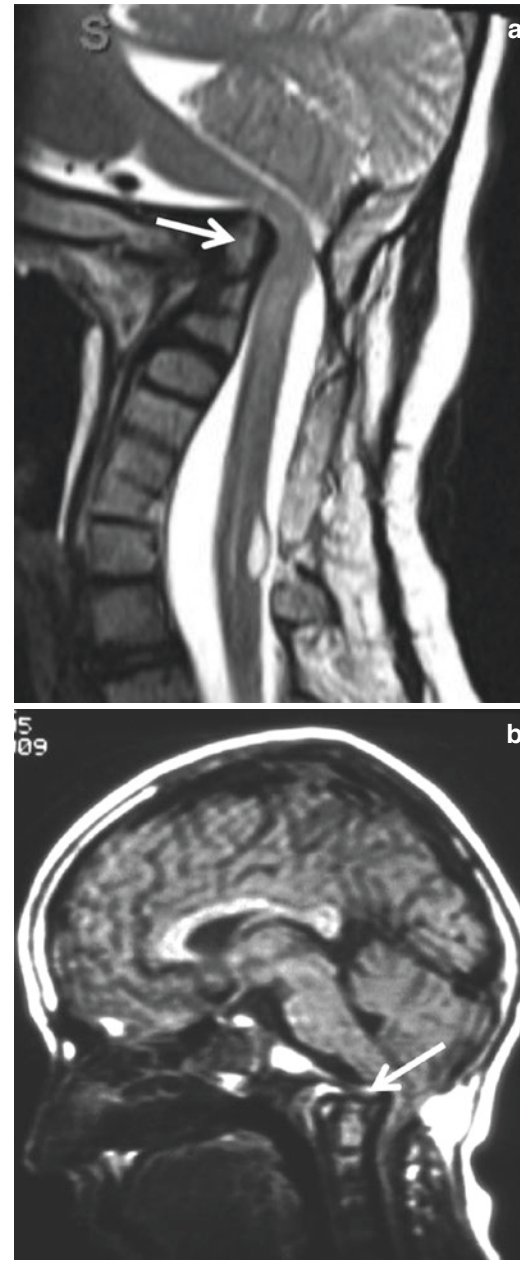

Fig. 7.2 (**a**, **b**) Imaging of patients with what are believed to be proatlantal remnants (arrows)

in lower vertebrates [12]. It is typically found on the anterior border of the foramen magnum and extends inferiorly and anteriorly from the inferior surface of the clivus. A case presented by Rao et al. [12] found the condylus tertius to be wider at its base and narrower toward its inferior surface. However, it is more common to find the median occipital condyle with a narrow base and wider inferior surface [23].

Condylus tertius in the midsagittal plane may restrict rotational movement of the head. This tends to occur when the median occipital condyles are well developed; otherwise, its placement causes few symptoms. The third condyle creates variable sites of attachment and location of the apical and alar ligaments of the dens, which are not currently known [12]. The associated ligamentous tissue may constrain flexion and extension of the head on the atlas. Furthermore, the area of the foramen magnum may be curtailed by atypical osseous formations from the arches of the proatlas. Consequently, patients present with compressive neurological symptoms [23].

Partial Regressive Occipital Vertebrae

A partial regressive occipital vertebra is another known variation. Partial regression creates enlarged condyles with transverse processes if the proatlas does not regress as expected when forming the occipital condyles. As a result, the craniocervical junction is displaced caudally. A partial regressive occipital vertebra can be palpated as a hard, nontender mass below the tip of the mastoid process [1]. These occipital vertebrae should be distinguished from assimilation of the atlas. Fusion of the C1 sclerotome with the proatlas causes this phenomenon. Occipital vertebrae do not feature a foramen between the occipital vertebra and skull base for passage of the vertebral artery. Atlas assimilation can be distinguished by the presence of such a fissure for passage of the vertebral artery and suboccipital nerve [20].

Bicornuate Dens and Ossiculum Terminale Persistens

Failure of midline fusion of the two paramedian ossification centers gives rise to a bicornuate dens. On AP open-mouth radiographs of the craniovertebral junction, this structural feature appears as a vertical radiolucent line through the dens. The ossiculum terminale, or third ossification center of the odontoid process, arises from the centrum of the proatlas [24]. This structure is usually fused to the dens by 12 years of age. A congenital anomaly, known as an ossiculum terminale persistens, arises when fusion does not occur. Such can be visualized as a small radiodense ossicle at the tip of the dens [20]. Although ossiculum terminale persistens and a bicornuate dens are interesting phenomena, they have little clinical significance. Despite this fact, it is crucial for neurosurgeons and radiologists to acknowledge such abnormalities in order to prevent misdiagnoses [20].

Clinical

Proatlas segmentation abnormalities usually result in neural compression and vascular compromise. Abnormal cerebrospinal fluid dynamics may result less commonly at the craniocervical junction. Other sequelae include hindbrain herniation, spastic quadriparesis, and lower cranial nerve abnormalities [25]. Chiari I malformation occurs in roughly one-third of cases. Proatlas segmentation abnormalities manifest around the posterior arch of C1 and foramen magnum [4–6].

Menezes [4–6] stated that patients with proatlas segmentation anomalies usually develop symptoms within the first two decades of life. Spastic quadriparesis is one of the most common neurological defects due to these abnormal bony masses. This condition is often misdiagnosed since trauma can precipitate the start of neurological symptoms. Oftentimes, patients exhibit restricted neck flexion, extension, and rotation [26].

Menezes and Fenoy [16] have presented and thoroughly described a number of instructive case studies of patients with proatlas anomalies. A variety of symptoms manifest in these patients; thus, it is not surprising for this condition to be misdiagnosed. Menezes [4–6] has proposed a number of surgical techniques to relieve the symptoms created by proatlas segmentation anomalies. Symptoms have been completely relieved in some cases.

References

1. Stratemeier PH, Jensen SR. Partial regressive occipital vertebra. Neuroradiology. 1980;19:47–9.
2. Morris P. Practical neuroangiography. Philadephia: Lippincott Williams & Wilkins; 2007. p. 124.
3. Gladstone RJ, Erichsen-Powell W. Manifestation of occipital vertebrae, and fusion of the atlas with the occipital bone. J Anat. 1915;50:190–209.
4. Menezes AH. Craniocervical developmental anatomy and its implications. Childs Nerv Syst. 2008;24:1109–22.
5. Menezes AH. Surgical approaches: postoperative care and complications "posterolateral-far lateral transcondylar approach to the ventral foramen magnum and upper cervical spinal canal". Childs Nerv Syst. 2008;24:1203–7.
6. Menezes AH. Surgical approaches: postoperative care and complications "transoral-transpalatopharyngeal approach to the craniocervical junction". Childs Nerv Syst. 2008;24:1187–93.
7. Wollin DG. The os odontoideum. Separate odontoid process. J Bone Joint Surg. 1963;45A:1459–71.
8. Hayek H. Über das Schicksal des proatlas und über die Entwicklung der Kopfgelenke bei Reptilien und Vögeln. Jahrbuch für Morphologie und mikroskopische Anatomie. 1924;53:137–63.
9. Jenkins FA. The evolution and development of the dens of the mammalian axis. Anat Rec. 1969;164:173–84.
10. Kessel M, Balling R, Gruss P. Variations of cervical vertebrae after expression of a Hox-1.1 transgene in mice. Cell. 1990;61:301–8.
11. Gadow FH. The evolution of the vertebral column: a contribution to the study of vertebrate phylogeny. London: Cambridge University Press; 1933. p. 93–4.
12. Rao PVVP. Median (third) occipital condyle. Clin Anat. 2002;15:148–51.
13. Shapiro R, Robinson F. Anomalies of the craniovertebral border. Am J Roentgenol. 1976;127:281–7.
14. Ganguly DN, Roy KKS. A study on the craniovertebral joint in man. Anat Anz. 1964;114:433–52.
15. Swischuk LE. Imaging of the cervical spine in children. New York: Springer; 2002.
16. Menezes AH. Remnants of occipital vertebrae: proatlas segmentation abnormalities. Neurosurgery. 2009;64:945–54.
17. Von Torklus D, Gehle W. The upper cervical spine. New York: Grune and Stratton; 1972. p. 23.
18. Hadley LA. Anatomico-roentgenographic studies of the spine. Springfield: Thomas; 1974. p. 79–83.
19. MacRae DL. Craniovertebral junction. Radiology of the skull and brain, Vol 1, Book 1. Saint Louis: Mosby; 1971. p. 264–6.
20. Dickman CA, Spetzler RF, Sonntag VKH. Surgery of the craniovertebral junction. New York: Thieme Medical Publishers; 1998.
21. Ingelmark BE. Über dascraniovertebrale Grenzgebiet beim Menschen. Acta Anat Suppl. 1947;4(6):5–113.
22. Prescher A, Brors D, Adam G. Anatomic and radiologic appearance of several variants of the craniocervical junction. Skull Base Surgery. 1996;6(2):83–94.
23. Lombardi G. The occipital vertebra. Am J Roentgenol. 1961;86:260–9.
24. Travan L, Sabbadini G, Saccheri P, Crivellato E. Unusual case of occipital vertebra in a medieval skeleton. Anat Sci Int. 2008;82:286–90.
25. Goel A, Shah A. Unusual bone formation in the anterior rim of foramen magnum: cause, effect and treatment. Eur Spine J. 2010;19(Suppl 2):S162–4.
26. Xu S, Pang Q, Zhang K, Zhang H. Two patients with proatlas segmentation malformation. J Clin Neurosci. 2009;17:647–8.

Development of the Atlas and Its Variations

8

R. Shane Tubbs

Introduction

Embryology and Molecular Development of the Atlas

Gastrulation involves the invagination of epiblastic cells from the embryonic plate through the primitive streak to form mesoderm on both sides of the neural plate, while cells from both sides of the dorsal lip of Hensen's node migrate through the primitive pit to integrate into the midline notochord. The embryonic plate thus elongates by new additions to its caudal aspect [1, 2]. The presomitic mesoderm (PSM) or segmental plate segregates into segmental clusters called somites, which eventually gives rise to the smooth muscle of the dermis, the axial musculature, the vertebral column, and support structures of the peripheral nervous system [2].

During segmentation, the caudal half of somite 5 and the cranial half of somite 6 combine to produce the first cervical sclerotome [2]. The hypochondral bow in occipital segment 5 gives rise to the anterior arch of the atlas, while the posterior arch of the atlas develops from sclerotome 5 [3]. Unlike in the more caudal sclerotomes where the intervertebral boundary zone (IBZ) ultimately becomes the anulus fibrosus and nucleus pulposus of an intervertebral disc, the dense zones of the first two cervical sclerotomes do not form true intervertebral discs and soon disappear [2, 3]. Their intervertebral boundary mesenchyme gradually turns into the upper and lower dental synchondroses, which cement the apical to the basal dens and the basal dens to the body of C2, respectively [2].

Somitogenesis involves the transformation of the loose mesenchymal cells of the PSM into tightly apposed epithelial cells with definite polarity and orientation. The first somite forms immediately caudal to the otic vesicle, followed by sequential transformation such that a new pair of somites is regularly added in a rostrocaudal direction [2].

The mechanism of metameric transformation of the PSM follows the "clock and wavefront" model. In this model, cells oscillate between a permissive and nonpermissive state for somite formation. These oscillations are phase-linked and controlled autonomously by a segmentation clock. Somite formation is triggered when cells of the rostral PSM while in the permissive phase are hit by a wavefront of maturation that slowly moves caudally along the embryonic axis [2, 4].

At the molecular level, the phasic oscillation of the segmentation clock is reflected by rhythmic expressions of cycling genes including the C-hairy1 family, which encode transcription factors such as

R. S. Tubbs (✉)
Department of Neurosurgery, Tulane University School of Medicine, New Orleans, LA, USA

Department of Neurosurgery and Ochsner Neuroscience Institute, Ochsner Health System, New Orleans, LA, USA

R. S. Tubbs et al. (eds.), *The Chiari Malformations*, https://doi.org/10.1007/978-3-030-44862-2_8

the split (HES) family and the glycosyl-transferase Lunatic Fringe that is tightly involved in the Notch signaling pathway [2]. A ligand (e.g., Delta) is bound to the surface Notch signaling receptor, whose intracellular domain (NICD) detaches from the cell membrane, enters the nucleus, and co-activates cycling genes of the C-hairy1 family to encode transcription factors such as HES, HER, HAIRY, and Lunatic Fringe. In chick embryos, Lunatic Fringe is known to recycle back to the cell surface where it enables the surface Notch signaling receptor to accept another ligand. The repetitive working of this simplified cycling gene model is the underlying mechanism of the oscillating segmentation clock [2].

In chick and mouse embryos, the maturation or determination wave is generated by expression of genes such as fibroblast growth factor 8, also known as FGF8 [2, 5]. The caudal domain of the PSM is very high in FGF8, which seems to actively maintain the mesenchymal identity of caudal PSM cells. The FGF gradient decreases toward the rostral axis so that FGF level is very low at the rostral domain of the PSM where somitogenesis is taking place. Thus, high concentration of FGF8 is expressed by newly formed PSM cells at Hensen's node, and low concentration is expressed in older PSM cells near the somitogenesis front. The limit between the high and low FGF8 domains near the site of active somitogenesis represents the somitogenesis wavefront [2]. Overexpression of FGF8 in this region inhibits somitogenesis, and the absence of FGF8 allows the PSM cells to become competent to respond to the clock signal and initiate somatic boundary formation [2, 6].

Cells from the ventromedial part of the somite lose their epithelial arrangement and migrate toward the notochord to form the mesenchymal sclerotomes, while cells from the dorsolateral part of the somite retain their epithelial arrangement to produce the dermomyotomes [2, 7]. While the anterior-posterior pattern of the somite appears to be determined very early, the dorsoventral values are not. If a somite is surgically rotated dorsoventrally by 180 degrees, sclerotomes still develop in the ventromedial position, while the dermomyotomes remain dorsolateral. It is thought that the dorsoventral differentiations of the somite depend on apositional instructions from the notochord, very likely through sonic hedgehog (Shh) expression [2, 8].

Resegmentation—the reshuffling of the early metameric boundaries between the somites during the development of the sclerotome—then ensues. It is believed to occur so that the later boundaries between the vertebral bodies do not match up with the original intersomitic clefts [2, 7]. After resegmentation, the human membranous axis consists of three median constituents that have been designated the apical dental segment from the caudal proatlas (fourth occipital sclerotome), the basal dental segment from the first cervical sclerotome, and the body of the axis from the second cervical sclerotome. These three constituents simultaneously chondrify around week 6 of gestation but remain segregated by the more cellular upper and lower dental synchondroses [2]. The apical ligament is almost certainly derived from the axial proatlas, while the alar and transverse atlantal ligaments are derived from the first cervical sclerotome in association with the basal dental segments [2, 3].

Ossification Patterns

The atlas usually forms from three primary ossification centers and no secondary ossification centers. The posterior arch arises from the lateral dense zone of the first cervical sclerotome [2]. In contrast, the anterior arch is formed from the hypochordal bow of the first cervical sclerotome [2]. Interestingly, this is the only area of the spine where the hypochordal bow or cells similar to it are involved in formation of the vertebral column [2]. In a radiographic study of 298 children, Karwacki and Schneider [9] found singular (66%), bipartite (29%), and multiple ossification centers (5%) (Fig. 8.1). The posterior arch usually fuses by 5 years of age, and the anterior arch typically fuses before 8 years of age [10]. The anterior and posterior ossification centers are separated by the right and left neurocentral synchondroses [10]. As the anterior and posterior ossification centers are separated by the neurocentral synchondroses, the two posterior ossification centers are separated by the posterior synchondrosis [10]. Fusion of the neurocentral synchondroses typically does not occur until age 5–8. In contrast, the poste-

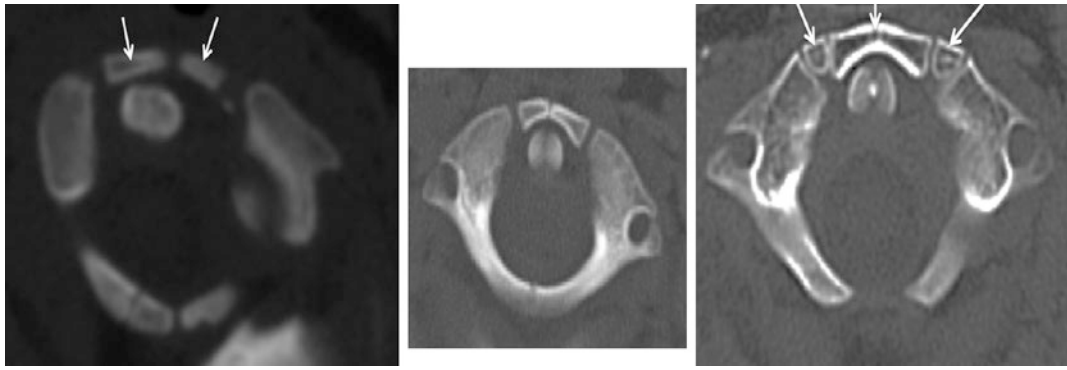

Fig. 8.1 Imaging noting variations in the ossification centers of the anterior and posterior arches of the atlas

rior synchondrosis shows fusion at age 3–5 [10]. The anterior arch of the C1 vertebra only shows progressive ossification in 20% of infants throughout months 6 through 24. Most infants have cartilaginous anterior arches [10]. Although the most common finding in the anterior arch is a single ossification center, in a study of 660 subjects, 27% showed multiple ossification centers (Fig. 8.2). This does not include the complete cartilaginous anterior arches or the neurocentral synchondroses [10]. From this study, it was discovered that the most common multiple ossification pattern was two ossification centers. Some less-common findings showed three ossification centers in 5% and four ossification centers in 4% [10]. Fusion and ossification of the anterior arch are typically complete by 6–8 years. In one study, 103 subjects were examined, and fusion or ossification was incomplete in 46% in the 80–90 months' age range [10]. From these data, it is suggested that ossification may take up to 90 months.

Overall, there are many patterns of C1 ossification. Up to 25% of children younger than 8 years show multiple ossification centers at the anterior arch of the atlas [10]. This process of anterior arch ossification can be delayed past 2 years of age in children. Incomplete ossification of the anterior arch of the atlas vertebra is not uncommon [10]. It is also shown that variant ossification patterns are more common in anterior arches as compared to posterior arches. A thorough understanding of ossification patterns is required in certain settings to accurately assess C1 fractures [10].

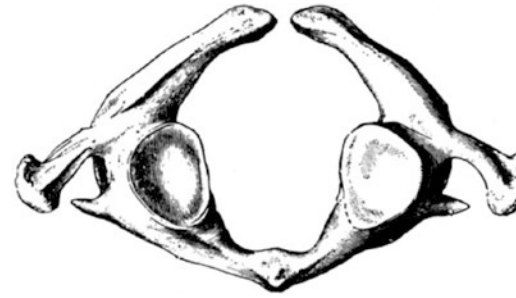

Fig. 8.2 Drawing of the bifid posterior arch of C1 and bilateral unfused transverse foramina

Anatomical Variations

Anterior/Posterior Arch Malfusion

Incomplete fusion of the anterior or posterior part of the atlantal ring is considered a variant of normal when seen outside of the adolescent period. Both the anterior and posterior arches may have facets that articulate with the foramen magnum. There are several cases in the literature that describe a congenital absence of the anterior portion of the ring of C1 [11]. This anomaly is quite rare and is estimated to occur in less than 0.1% of the population [12]. The anterior arch may be enlarged and accessory ossicles may be found near it. Congenital malformation or non-union of the posterior ring (Fig. 8.2) is more common and is seen in approximately 4% of the population. Combined non-union of both the anterior and posterior rings is described as a bipartite atlas [12, 13]. A bipartite atlas is felt to be of little clinical

significance, though there is a case report in the literature advocating cervical fusion in individuals with evidence of instability [14]. The posterior arch may have two instead of one tubercle, which can also be bifid, and ossicles may be found in the posterior atlanto-occipital membrane. Spina bifida of the posterior arch of C1 is typically an incidental, asymptomatic variation of the atlas.

Posterior Ponticulus/Arcuate Foramen

These sulci of the vertebral artery may have varying levels of surrounding ossification. In as many as 13.8% of individuals, there is a posterior bony spicule that projects from the superior articular process [15–17]. Such bony bridges are seen in some primates [18]. The atlas may even have a completely ossified arcuate foramen (Fig. 8.3). In such cases, the vertebral artery exits the transverse foramen, passes through the arcuate foramen, and then travels through the foramen magnum. A laterally placed ponticulus may form a lateral arcuate foramen that can coexist with the more posteriorly located foramen, resulting in a canal for the vertebral artery to travel through.

The retroarticular canal is formed from the posterior bridge of the atlas [19]. The posterior bridge is located behind the lateral mass of the posterior arch of the atlas [16]. More uncommonly than posterior bridges, lateral bridges may form complete foramina [20]. These complete foramina are also termed "supratransverse foramina" [16]. The retroarticular canal shows great variation in the superoinferior and anteroposterior diameters [21]. Some studies have shown differences in the retroarticular canal diameter based on individual, sex, and side [19, 22]. Additionally, the transverse foramen on the same side is found to be larger than the retroarticular canal itself [22]. With the transverse foramen being larger than the retroarticular canal, the vertebral artery is at risk of being compressed [18]. The side of the artery most vulnerable to the risk of compression is the left vertebral artery [18].

Fig. 8.3 Posterior ponticulus (arrow) of the atlas creating a bony foramen for the third part of the vertebral artery or the so-called arcuate foramen

Facet Asymmetry/Bipartition

Facet asymmetry is common on the superior aspect of the atlas, and, interestingly, the atlas may possess bipartite (bilobed) facets that articulate with the occipital condyles (Figs. 8.4 and 8.5) [23, 24]. This area of the atlas typically

Fig. 8.4 Asymmetry of the superior facets of C1

Fig. 8.5 Bilobed superior articular facets

has a reniform or kidney-shaped appearance. Billmann et al. [24] saw variation in the morphology of the lateral mass in 20.8% of specimens during a study of 500 atlases. Bipartition of the superior articular facets of C1 (*foveae articulares craniales atlantis*) was found both bilaterally (9.6%) and unilaterally (11.2%) [24].

Atlanto-Occipital Fusion

Assimilation of the atlas (occipitalization) is felt to be a distinct variant from the presence of an occipital vertebra (Fig. 8.6). Occipitalization is a congenital synostosis of the atlas to the occiput, which is a result of failure of segmentation and separation of the most caudal occipital sclerotome and the first cervical sclerotome during the first few weeks of fetal life. The degree of bony fusion between the atlas and occiput can vary; complete and partial assimilation have been described. In most cases assimilation occurs between the anterior arch of the atlas and the anterior rim of the foramen magnum and is associated with other skeletal malformations such as basilar invagination, occipital vertebra, spina bifida of the atlas, or Klippel-Feil syndrome. The incidence of atlanto-occipital fusion ranges from 0.14% to 0.75% of the population, both sexes being equally affected [5, 25, 26].

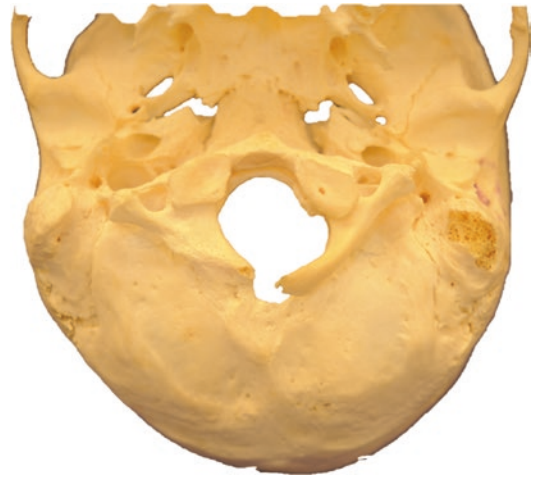

Fig. 8.6 Example of assimilation of the atlas. Also note the defect of the posterior arch

Klippel-Feil Syndrome

Neurologist Maurice Klippel and his resident Andre Feil described a case in which there was a congenital absence of the cervical vertebrae [27]. Congenital fusion of two or more cervical vertebrae is also commonly seen and is referred to as Klippel-Feil syndrome (Fig. 8.7). The classic triad of Klippel-Feil syndrome includes a short neck, low posterior hairline, and limited range of cervical motion. The majority of patients with a congenital fusion of the cervical vertebrae have a normal appearance, and fewer than 50% exhibit this classic triad [28].

Transverse Process/Epitransverse Process

The transverse process of the atlas may be bifid [26, 29]. The transverse foramen can be absent at C1 or be divided by a bony septum, thus separating the vertebral artery from the vertebral vein, or open anteriorly or posteriorly. When present, an epitransverse process extends from the transverse process of the atlas superiorly and can articulate with the paramastoid region

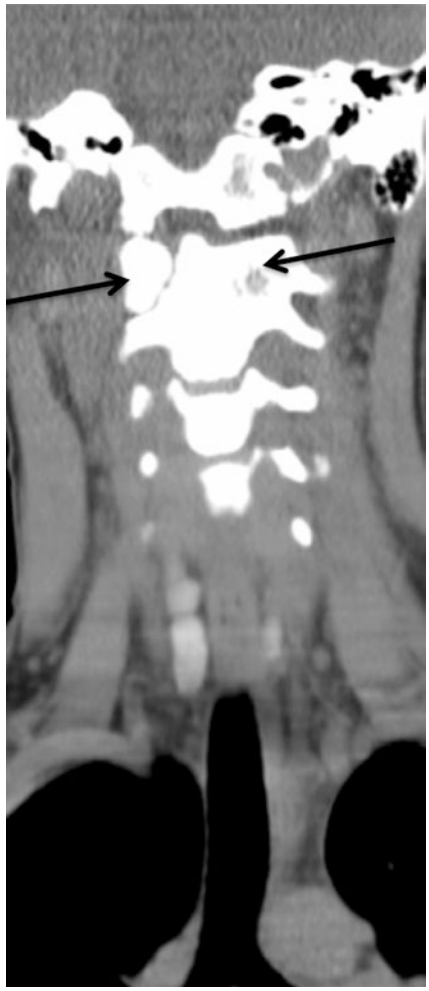

Fig. 8.7 Example of Klippel-Feil anomaly of C1 (arrows) and C2

Fig. 8.8 Schematic drawing of a left paramastoid process (left arrow) and right-sided epitransverse process of the atlas (right arrow). (After Allen [26])

of the occipital bone to form pseudoarthroses (Fig. 8.8) [26]. The transverse processes of C1 can be asymmetrical.

Absence/Hypoplasia

The atlas has been reported to be hypoplastic or altogether absent, which is rare [26, 30].

Stenosis

The vertebral foramen at C1 may be stenotic, and this is most often seen in patients with achondroplasia. However, Devi et al. described five male patients with symptomatic cervical stenosis secondary to C1 spina bifida [31]. The pathologic distinction in these cases was that the bifid posterior arch was imbricated anteriorly. This latter pathologic variant should be differentiated from the more common congenital non-union of the posterior arch of the atlas.

References

1. Dietrich S, Kessel M. The vertebral column. In: Thorogood P, editor. Embryos, genes and birth defects. Chichester: Wiley; 1997. p. 281–302.
2. Pang D, Thompson D. Embryology and bony malformations of the craniovertebral junction. Childs Nerv Syst. 2011;4:523–64.
3. Muller F, O'Rahilly R. Segmentation in staged human embryos: the occipito-cervical region revisited. J Anat. 2003;3:297–315.
4. Pourquie O. Vertebrate somitogenesis: a novel paradigm for animal segmentation? Int J Dev Biol. 2003;47:587–603.
5. Sawada A, Shinya M, Jiang YJ, Kawakami A, Kuroiwa A, Takeda H. Fgf/MAPK signaling is a crucial positional cue in somite boundary formation. Development. 2001;128:4873–80.
6. Dubrulle J, McGrew MJ, Pourquie O. FGF signaling controls somite boundary position and regulates segmentation clock control of spatiotemporal Hox gene activation. Cell. 2001;106:219–32.
7. Christ B, Wilting J. From somites to vertebral column. Ann Anat. 1992;174:23–32.
8. Koseki H, Wallin J, Wilting J, Mizutani Y, Kispert A, Ebensperger Cm Herrmann BG, Christ B, Balling R. A role for Pax-1 as mediator of notochordal signals during the dorsoventral specification of vertebrae. Development. 1993;119:649–60.
9. Karwacki GM, Schneider JF. Normal ossification patterns of atlas and axis: a CT study. AJNR Am J Neuroradiol. 2012;33:1882–7.
10. Junewick JJ, Chin MS, Meesa IR, Ghori S, Boynton SJ, Luttenton CR. Ossification patterns of the

atlas vertebra. AJR Am J Roentgenol. 2011;197:229–1234.
11. Thavarajah D, McKenna P. Congenital absence of the anterior arch of the atlas: a normal variant. Ann R Coll Surg Engl. 2012;94:208–9.
12. Petraglia AL, Childs SM, Walker CT, Hogg J, Bailes JE, Lively MW. Bipartite atlas in a collegiate football player – not necessarily a contraindication for return-to-play: a case report and review of the literature. Surg Neurol Int. 2012;3:126.
13. Jans C, Mahieu G, Van Riet R. Bipartite atlas mimicking traumatic atlantoaxial instability following a rugby tackle. BMJ Case Reports. 2009;2009:bcr0420091824.
14. Hu Y, Ma W, Xu R. Transoral osteosynthesis C1 as a function-preserving option in the treatment of bipartite atlas deformity: a case report. Spine. 2009;34:418–21.
15. Krishnamurthy A, Nayak SR, Khan S, Prabhu LV, Ramanathan LA, Ganesh Kumar C, Prasad SA. Arcuate foramen of atlas: incidence, phylogenetic and clinical significance. Romanian J Morphol Embryol. 2007;48:263–6.
16. Le Minor JM, Trost O. Bony ponticles of the atlas (C1) over the groove for the vertebral artery in humans and primates: polymorphism and evolutionary trends. Am J Phys Anthro. 2004;125:16–29.
17. Taitz C, Nathan H, Arensburg B. Anatomical observations of the foramina transversaria. J Neurol Neurosurg Psychiatry. 1978;41:170–6.
18. Karau B, Ogeng'o JA, Hasanali J, Odula PO. Morphometry and variations of bony ponticles of the atlas vertebrae (C1) in Kenyans. Int J Morphol. 2010;28:1019–24.
19. Mitchell J. The incidence and dimensions of the retroarticular canal of the atlas vertebra. Acta Anat. 1998a;163:113–20.
20. Mitchell J. The incidence of the lateral bridge of the atlas vertebra. J Anat. 1998b;193:283–5.
21. Paraskevas G, Papaziogas B, Tsonidis C, Kapetanos G. Gross morphology of the bridges over the vertebral artery groove on the atlas. Surg Radiol Anat. 2005;27:129–36.
22. Tubbs RS, Johnson PC, Shoja MM, Loukas M, Oakes WJ. Foramen arcuale: anatomical study and review of the literature. J Neurosurg Spine. 2007;6:31–4.
23. Bergman RA. Compendium of human anatomic variation: text, atlas, and world literature. Baltimore: Urban & Schwarzenberg; 1988.
24. Billmann F, Le Minor JM, Steinwachs M. Bipartition of the superior articular facets of the first cervical vertebra (atlas or C1): a human variant probably specific among primates. Ann Anat. 2007;189:79–85.
25. Cardoso AC, Fontes RB, Tan LA, Rhoton AL Jr, Roh SW, Fessler RG. Biomechanical effects of the transcondylar approach on the craniovertebral junction. Clin Anat. 2015;28:683–9.
26. Allen W. The varieties of the atlas in the human subject, and the homologies of its transverse processes. J Anat Physiol. 1879;14:18–27.
27. Klippel M, Feil A. The classic: a case of absence of cervical vertebrae with the thoracic cage rising to the base of the cranium (cervical thoracic cage). Clin Orthop. 1975;24:3–8.
28. Clark CR. The cervical spine. 4th ed. Philadelphia: Lippincott Williams & Wilkins; 2005. p. 198.
29. Adams MA, Lama P, Zehra U, Dolan P. Why do some intervertebral discs degenerate, when others (in the same spine) do not? Clin Anat. 2015;28:195–204.
30. Bergman RA, Afifi A, Miyauchi R. Cervical vertebrae. http://www.anatomyatlases.org/AnatomicVariants/SkeletalSystem/Text/CervicalVertebrae.shtml. Accessed 9 Sept 2019.
31. Devi BI, Shenoy SN, Panigrahi MK, Chandramouli BA, Das BS, Jayakumar PN. Anomaly of arch of atlas: a rare cause of symptomatic canal stenosis in children. Pediatr Neurosurg. 1997;26:214–8.

The Odontoid Process

9

R. Shane Tubbs

The odontoid process (Figs. 9.1, 9.2, and 9.3) was once thought to be a displaced body of the atlas but is now believed to have separated from the anterior part of the atlas between the sixth and seventh week of gestation and to have migrated caudally to fuse with the body of the axis [1]. This important structure has its origins from the axial portion of the occipital and upper two cervical sclerotomes: caudally from the atlas and cephalically from the axis, formed from two separate ossification centers that fuse in the midline by the seventh month of gestation (Fig. 9.4). A secondary ossification center appears at the apex of the odontoid process (ossiculum terminale) between ages 3 and 6 years and usually fuses by the beginning of puberty [2]. The tip of the odontoid process is originally laid out as the central part of the atlas and then fuses caudally with the cephalic portion of the body of the axis in the evolution of the development of the vertebral column. This process of fusion completes at about the third or fourth year of life of a child [3]. Until then, the junction of the odontoid tip and the axis is a cartilaginous physis. The odontoid process itself possesses two lateral primary ossification centers and an apical secondary ossification center. The axis has four articular processes like the rest of the vertebrae—a pair of spherical convex-shaped superior and a pair of flat and sagittally aligned inferior articular processes that are individually connected through a long pars interarticularis. Unlike all other vertebral segments, the superior and inferior articular processes of the axis are completely offset from one another in the sagittal plane, thus placing a high strain on the pars interarticularis. This in turn requires integrity of the axis ring structure for proper cranio-cervical mechanical function and in turn places a focal point of stress concentration on the narrow waist of the odontoid as anchoring pivot for the atlantoaxial articulation (Fig. 9.5). This complex arrangement allows for the substantial rotating ability of the head and the quick turn ability of the upper cervical spine. The two primary ossification centers of the odontoid appear in utero and usually fuse in the midline by the eighth month of fetal life [4]. This medially fused primary ossification center then coalesces with the body of the axis by the 6th year of life forming a line usually seen on radiographs until the 11th year of life. This line can be radiographically mistaken for a fracture and remains throughout life in about one-third of individuals. This area of fusion between the odontoid process and the body of the axis is referred to as the subdental synchondrosis (Fig. 9.6) [4]. Fusion between the secondary ossification center and the rest of the odontoid process usually occurs

R. S. Tubbs (✉)
Department of Neurosurgery, Tulane University School of Medicine, New Orleans, LA, USA

Department of Neurosurgery and Ochsner Neuroscience Institute, Ochsner Health System, New Orleans, LA, USA

R. S. Tubbs et al. (eds.), *The Chiari Malformations*, https://doi.org/10.1007/978-3-030-44862-2_9

Fig. 9.1 Right lateral view of the C2 vertebra

Fig. 9.2 Left lateral view of the C2 vertebra

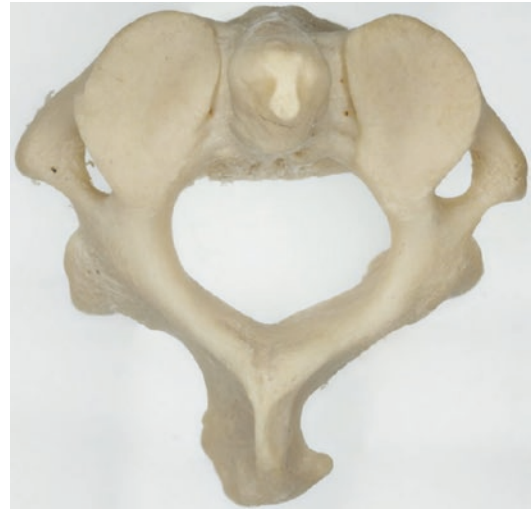

Fig. 9.3 Superior view of the C2 vertebra

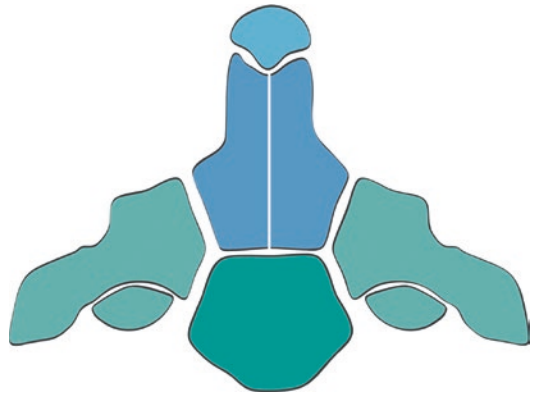

Fig. 9.4 Ossification centers of the C2 vertebra

by the age of 12 years. The loose prevertebral zone of the first cervical sclerotomes gives rise to the basal segment of the odontoid process, and that of the second cervical sclerotomes becomes the body of the axis. In essence, after resegmentation, the odontoid process is composed of the apical dental segment from the caudal proatlas, the basal dental segment from the first cervical sclerotomes, and the body of the axis from the second cervical sclerotomes. Chondrification of the respective components occurs simultaneously at various periods during gestation starting around 6 weeks and fusion beginning at birth up until the fifth to sixth postnatal year of life, although ossi-

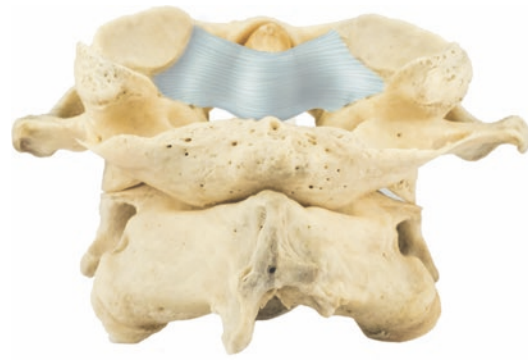

Fig. 9.5 Posterior view of the median atlanto-axial joint. Note the position of the transverse ligament

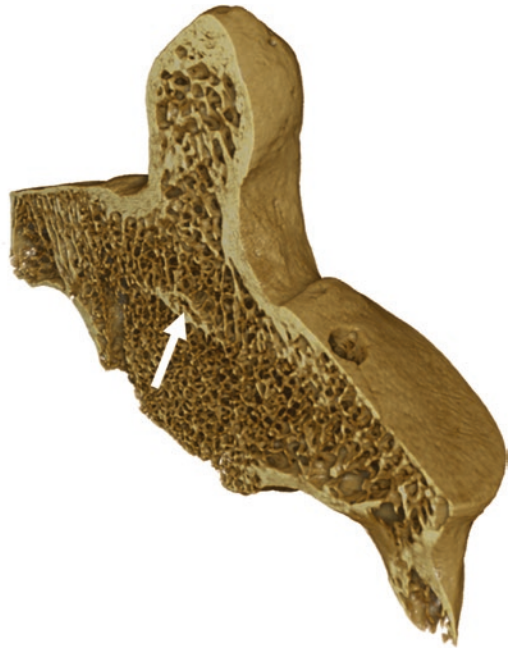

Fig. 9.6 Microcomputed tomography (CT) noting the subdental synchondrosis (*arrow*)

fication of the dental tip and bony fusion of the upper synchondrosis are not completed until adolescence. The base of the odontoid process is separated during development by an embryologic remnant of the C1–C2 intervertebral disc—a cartilaginous disc that may remain until old age [5]. At birth, the neurocentral syndrochondrosis, an epiphyseal growth plate, separates the body of the axis from the odontoid process. These cartilaginous articulations are named the dentocentral (separating the odontoid process from the body) and the neurocentral synchondrosis (separating the odontoid process and body from neural arches) [4]. Synchondroses among the neural arches, body, and odontoid process fuse at 3–6 years of age. After the age of 6 years, the odontoid process fuses with the body and the neural arches. In adults, the remnant of the dentocentral synchondrosis can be imagined by magnetic resonance images (MRI) as a hypointense ring between the inferior end of the odontoid and the superior roof of the body of C2. This structure is located in the cancellous bone and should be accepted as the inferior border of the odontoid process in adults. The anatomical level of the dentocentral synchondrosis is well below from the superior articulating facets and the indentation of the transverse ligament to the posterior aspect of the odontoid process.

Morphometry

The fully formed odontoid process is toothlike/peg shaped with a curved superior surface and deviates slightly to the left or right in approximately 14–26% of the population [4]. It ranges from 15.5 mm (±1.8 mm) in males and 14.6 mm (±1.5) in females, with an anteroposterior diameter of 10.3 (±0.7) in males and 9.6 (±0.9 mm) in females, respectively [4]. According to Lang, the mean transverse diameter of the odontoid process was 11.21 mm as opposed to 10.5 and 9.8 mm in Japanese males and females, respectively, and the mean height was 15.7 mm compared to 17.9 and 16.5 mm in Japanese men and women [6]. The sagittal and transverse diameters are approximately 10.5 and 10 mm, respectively. The anterior articular surface of the dens is circular or elliptical in shape and is roughly 10 × 9 mm [6]. Tubbs et al., in their study on inclination of the odontoid process in pediatric Chiari I malformation, showed that the posterior angulation (retroflexion) of the odontoid process can be affected by sex, with females having higher angulation grades (Fig. 9.7) [7].

Variations

Absent or Hypoplastic Odontoid Process

Complete absence or aplasia of the odontoid process is a very rare occurrence and is seen in some patients with collagenopathy syndromes such as spondyloepiphyseal and spondylometaplasial dysplasia [8]. This is manifested as an odontoid process with excessive dysplasia that does not reach the upper edge of the anterior atlantic arch

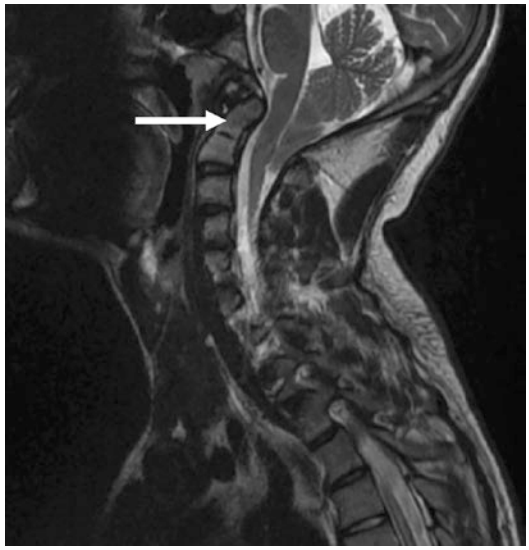

Fig. 9.7 Magnetic resonance imaging (MRI) noting a retroflexed odontoid process (*arrow*) in a patient with Chiari I malformation

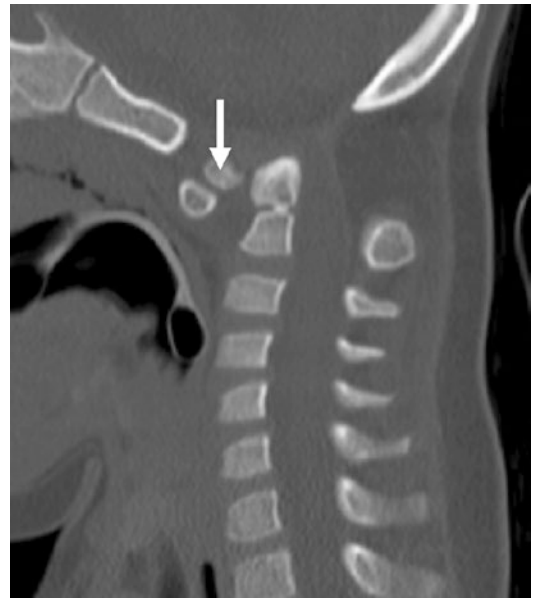

Fig. 9.8 Computed tomography (CT) noting an os odontoideum (*arrow*)

[9]. The cruciate and alar ligaments are therefore not adhered and, thus, unable to contribute to the stability of the joint. Agenesis of the apical segment is the most common variety of odontoid process anomalies. Partial absence or hypoplasia of the odontoid is usually associated with spondyloepiphyseal dysplasia, mucopolysaccharidoses, and metatropic dwarfism. The presence of this anomaly predisposes the craniovertebral junction (CVJ) to dislocation and cord compression due to the absence of the apical and alar ligaments.

Os Odontoideum

Os odontoideum (Fig. 9.8) represents the separation of the odontoid tip, a derivative of the fourth occipital sclerotomes (the proatlas), from the body of C2, with a smooth and separate caudal portion of the odontoid process. It is a rare radiographic diagnosis, most of the time found incidentally [10]. The debate about the true etiology of this anomaly being either congenital or acquired remains unresolved. Proponents of the acquired theory posit that having the neurocentral synchondrosis below the level of the superior articulating facet, with the separation of the odontoid process in this anomaly occurring above the plane of the superior articulating facet, makes a developmental cause unlikely.

Conversely, the incidence of this anomaly in identical twins and people with familial relations also weakens the prior injury argument [10]. Currently upheld views state that due to posttraumatic effects on the nonhealed odontoid, the neurocentral syndrochondrosis as well as disruption in blood supply to the midportion thereby results in the failure of the odontoid fracture to remodel and unite. This leads to a potentially unstable CVJ, especially the atlanto-axial joint, leading to possible dislocation and neurological deficits. Depending on the actual location of nonunion, this can be divided into orthotopic and dystopic variants [4, 8, 11]:

1. Orthotopic os odontoideum—This is the part of the odontoid process that moves with the anterior arch of the atlas, situated in an anatomical position [8, 10, 11].
2. Dystopic os odontoideum—This part of the odontoid process (ossicle) lies near the basion and fuses with the clivus near the foramen magnum, and movement is in concert with the clivus. This kind of anomaly results in hypo-

plasia of the posterior arch of the atlas and hypertrophy of the anterior arch and is also referred to as ossiculum avis, which is attachment of the apical dental segment to the basiocciput, as opposed to being fused to the main dental stem.

The genesis of os odontoideum is thought to be related to prior injury to the odontoid process but may also be developmental. The pathological ramifications range from mild neck pain to acute quadriplegia, chronic myelopathy, or sudden death [10]. Os odontoideum has a 6% incidence in children with Down syndrome [4] and is seen in Morquio syndrome, spondyloepiphyseal dysplasia, Klippel-Feil anomaly, and Laron syndrome.

Ossiculum Terminale

An ossiculum terminale, or Bergmann's ossicle, refers to the unfused and detached apical (terminal) dental segment, leading to a shortened pivotal segment and predisposing to atlantoaxial subluxation and high cord compression. It is derived from the centrum of the fourth occipital sclerotome. Fusion is usually complete by age 12 [9].

Dens Bicornis

A bifid odontoid process, or dens bicornis, is an extremely rare entity. It manifests as the presence of a partition from the lower synchondrosis to the tip of the odontoid process. The absence of midline integration of the primary ossification centers, which is responsible for this phenomenon, occurs early on in development, most likely during the mesenchymal prevertebral stage or at chondrification. This leads to an unstable CVJ as a result of a very hypoplastic central pivot. In many bifid cases, the hypoplastic odontoid process is aggravated by an ossiculum terminale, negating any possibility for transverse and alar ligament anchorage.

Inclination of the Odontoid Process

An anteverted odontoid process, which can bend over the anterior arch of the atlas, is a rare occurrence, and its incidence is currently unknown. It is thought to result from the traction of the apical ligament on the tip of the odontoid process during the early process of development of the craniovertebral junction when the apical ligament is less rudimentary [7, 12]. Studies have shown anteversion angles to have a range of 60–105° with a mean of 95° [13]. However, the odontoid may also be retroflexed, and this has been found to be more common in individuals with the Chiari I malformation (Fig. 9.7) [14].

Malposition of the Odontoid Process

The odontoid process can be dramatically posteriorly positioned and, in some rare cases, may be located anterior to the anterior arch of the atlas.

Duplicated Odontoid Process

This anomaly is extremely rare and tends to occur in the presence of duplicated pituitary gland [15]. Results from faulty interactions among the notochord, prechordal plate, and surface endoderm [13, 16], with evidence of bony discontinuity of the posterior arch of C1, and a hypertrophied anterior arch are seen on CT [17]. The duplication possibly results from a lack of fusion of ossification centers, but definite etiologic factors are currently unknown.

Fused Nonseparated Odontoid Process to the Anterior Arch of the Atlas

This extremely rare variant has been posited to be a segmentation defect in the sclerotomes of the first cervical somite [18]. This defect causes the abnormal placement of the ossification centers or a complete absence of the ossification center hindering appropriate fusion of the said centers leading to abnormal movement in the midline, creating the appearance of a fissure in the anterior arch of the atlas. There is restriction in neck movement with or without accompanying neck pain [6, 19].

Dolicho-Odontoid

The dolicho (long)-odontoid process is a rare variant with scant reports found in the literature [20]. This anomaly has been described as hyperplasia and distortion of the odontoid tip with lateral or posterior deviation.

Acquired Forms of Odontoid Dysplasia

There are a large number of secondary forms of odontoid variations brought about by trauma and metabolic, neoplastic, and inflammatory and other arthritic conditions [21–25]. These are too numerous to present in this context, but all can have significant adverse effects on the function of the cranio-cervical junction and may lead to challenges in diagnosis as they can lead to considerable morphologic distortions on odontoid imaging. Again, a sound knowledge of the basic anatomic odontoid variants and dysplasia is helpful in this context to allow for a sound differentiation of acquired versus congenital variants and their respective preferred treatment.

Conclusion

The integrity of the odontoid process is critical for the stability and proper function of the atlantoaxial articulation and to assure integrity of the enclosed vulnerable neurovascular structures of the cranio-cervical region. Therefore, a sound understanding of this region's osseous development, both in normal and in variant forms, as well as its phenotypical morphology is a prerequisite for the diagnosis and treatment of patients presenting with disorders affecting the craniocervical spine.

References

1. Kyoshima K, Kakizawa Y, Tokushige K, Akaishi K, Kanaji M, Kuroyanagi T. Odontoid compression of the brainstem without basilar impression—odontoid invagination. J Clin Neurosci. 2005;12:565–9.
2. Kim DH, Betz RR, Huhn SL, Newton PO. Cervical spine development. Surgery of the pediatric spine. New York: Thieme; 2008. p. 95–6.
3. Francis S, Isamu N. Malformation of the odontoid process: report of a case and clinical survey. Calif Med. 1957;86:394–8.
4. Cramer GD, Darby SA. The anatomy of the odontoid process. Clinical anatomy of the spine, spinal cord and ANS. 3rd ed. St Louis: Mosby; 2013.
5. Jinkins R. Atlas of neuroradiologic embryology, anatomy, and variants. Philadelphia: Lippincott Williams and Wilkins; 2000. p. 542.
6. Lang J. Skull base and related structures: atlas of clinical anatomy. 2nd ed. Stuttgart: Schattauer Verlag; 2001. p. 289–306.
7. Tubbs RS, Wellons JC 3rd, Blount JP, Grabb PA, Oakes WJ. Inclination of the odontoid process in the pediatric Chiari I malformation. J Neurosurg Spine. 2003;98(1 Suppl):43–9.
8. Dachling P, Dominic NPT. Embryology and bony malformations of the craniovertebral junction. Childs Nerv Syst. 2011;7:523–64.
9. Thamburaj VA. Neurodevelopmental disorders: craniovertebral junction abnormalities. In: Textbook of contemporary neurosurgery. New Delhi: Jaypee Brothers Med. Publ.; 2012. p. 446–54.
10. Kilmo P Jr, Coon V, Brockmeyer D. Incidental os odontoideum: current management strategies. Neurosurg Focus. 2011;31(6):1–6.
11. Shenglin W, Chao W. Familial dystopic os odontoideum: a report of three cases. J Bone Joint Surg. 2011;93:e44.
12. Vijayasaradhi M, Phaniraj GL, Kumar B. Anteverted odontoid: a rare congenital bony anomaly of craniovertebral junction. Neurol India. 2010;58:490–2.
13. Usta Y, Sakha F, WhiteWL LAS, Knecht L. Duplicated pituitary gland and odontoid process. A case report. Neuroradiol J. 2012;3:360–3.
14. Tubbs RS, Cesmebasi A, Loukas M, Hogan E, Kralovic S, Cohen-Gadol A. The Chiari malformations: a review with emphasis on anatomical traits. Clin Anat. 2015;28:184–94.
15. Dilettoso S, Uccello M, Dilettoso A, Gelardi S, Dilettoso B. Duplicated odontoid process and atlas cleft associated to Klippel-Feil syndrome. Spine J. 2012;12:449–50.
16. Tubbs RS, Hallock JD, Radcliff V, et al. Ligaments of the craniocervical junction. A review. J Neurosurg Spine. 2011;14:697–709.
17. Garant M, Oudjhane K, Sinsky A, O'Gorman AM. Duplicated odontoid process: plain radiographic and CT appearance of a rare congenital anomaly of the cervical spine. AJNR. 1997;18:1719–20.
18. Tubbs RS, Oakes WJ, Grabb PA. Nonseparated odontoid process fused to an atlantal hemiarch. Pediatr Neurosurg. 2004;40:141–2.
19. Perez-Vallina JR, Riano-Galan I, Cobo-Ruisanchez A, Orejas-Rodriguez-Arango G, Lopez-Muniz C, Fernandez-Martinez JM. Congenital anomaly of craniovertebral junction: atlas odontoid process fusion with C1 anterior arch cleft. J Spinal Disord Tech. 2002;15(1):84–7.
20. Prokesch RW, Chocholka P, Bader TW, Ba-Ssalamah A, Trattnig S. Dolichoodontoid. A rare cranio-cervical anomaly—MRI finding. Eur J Radiol. 2000;33:38–40.
21. Bambakidis NC, Dickman CA, Spetzler RF, Sonntag VKH. The axis, associated anomalies, and injuries. Surgery of the craniovertebral junction. 2nd ed. New York: Thieme; 2012.
22. Combalia A. The axis vertebrae. Milan: Springer; 2013. p. 2–19.

23. Gilroy AM, Macpherson BR, Ross LM, Schuenke M, Schulte E, Schumacher U. Atlas of anatomy. New York: Thieme; 2012. p. 112.
24. Tubbs SR, Grabb P, Spooner A, Wilson W, Oakes JW. The apical ligament: anatomy and functional significance. J Neurosurg. 2000;92:197–200.
25. Tubbs RS, Griessenauer CJ, Hendrix P, Oakes P, Loukas M, Chern JJ, Rozzelle CJ, Oakes WJ. Relationship between pharyngitis and peri-odontoid pannus: a new etiology for some Chiari I malformations? Clin Anat. 2015;28:602–7.

10 Surgical Anatomy of the Craniocervical Junction Relevant to Chiari Malformations

R. Shane Tubbs

The anatomy of the juncture between the skull base and the upper cervical spine is complex and compact. Superiorly, the posterior cranial fossa houses not only the derivatives of the rhombencephalon (hindbrain) but also vessels that serve this structure, its outgrowths (lower cranial nerves), meninges with their vascular and nervous supply, and cerebrospinal fluid (CSF) within the ventricle and related subarachnoid spaces and cisterns. As the anatomy of the posterior cranial fossa is rich, the present chapter will focus on the specific and germane morphology related to approaches to the posterior fossa for Chiari malformations. As by definition this embryologic derailment extends into the upper cervical region; the anatomy of the craniocervical junction will be focused on from a surgical perspective [1–5].

Soft Tissues of the Posterior Craniocervical Junction

Advancing through the soft tissues overlying the craniocervical junction, a standard midline incision through the skin advances through the tela subcutanea and then the upper fibers of the trapezius muscle inserting on either side of the occipital bone near the most posterior aspect of the external occipital protuberance referred to as the inion. Deep to the trapezius muscle is the splenius capitis muscle, which has a fiber course that is opposite to that of the overlying upper fibers of the trapezius muscle (Fig. 10.1). The splenius capitis arises from the lower half of the nuchal ligament and spinous processes of the last cervical and upper three to four thoracic vertebrae and attaches to the mastoid process and lateral aspect of the superior nuchal line. Below the splenius capitis lies the semispinalis capitis muscle (Fig. 10.1), which at this point is composed of vertical fibers traveling cephalad to insert onto the occipital bone between the superior and inferior nuchal lines. Along with their bony attachments, the above-noted muscles also travel along and attach to the midline nuchal ligament, which is a continuation of the supraspinous ligament of the thoracic spine. As the deepest muscular layer, the suboccipital muscles are four in number. Of these the suboccipital triangle is composed of the rectus capitis major and inferior capitis inferior and superior (Fig. 10.1). The rectus capitis minor is found just medial to the rectus capitis major attaching the posterior tubercle of the atlas to the occiput. For the suboccipital triangle muscles, the rectus capitis major travels between the occiput and spinous process of C2. The superior oblique arises from the transverse process of the atlas and inserts onto the occiput. The inferior

R. S. Tubbs (✉)
Department of Neurosurgery, Tulane University School of Medicine, New Orleans, LA, USA

Department of Neurosurgery and Ochsner Neuroscience Institute, Ochsner Health System, New Orleans, LA, USA

R. S. Tubbs et al. (eds.), *The Chiari Malformations*, https://doi.org/10.1007/978-3-030-44862-2_10

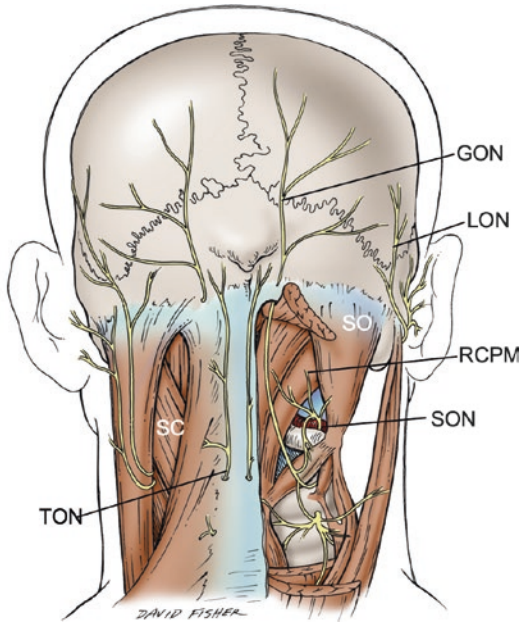

Fig. 10.1 Posterior craniocervical junction noting the third occipital (TON), greater occipital (GON), and lesser occipital nerves (LON). Also note the splenius capitis (SC), superior oblique (SO), and rectus capitis posterior major (RCPM) muscles. The suboccipital nerve (SON) is seen emerging below the horizontal segment of the vertebral artery

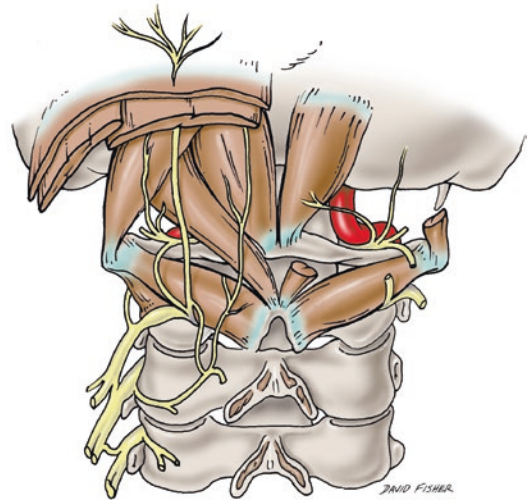

Fig. 10.2 Deeper view of Fig. 10.1 illustrating the positions of the muscles of the suboccipital region and their relationships to regional nerves. Note the position of the vertebral artery in the depths of the suboccipital triangle as it courses on C1 vertebra

oblique originates from the spinous process of C2 and attaches to the transverse process of the atlas. Except for the trapezius, which receives its innervation via the accessory nerve, the other above-noted muscles are all innervated by adjacent dorsal rami of spinal nerves. In unison, the trapezius, splenius capitis, and semispinalis capitis aid in extending the neck. The suboccipital triangle muscles and rectus capitis posterior minor, although theoretically these may move the atlas and axis, practically may act more as proprioceptive structures. This assumption is strengthened by the fact that many of these small muscles are removed with posterior fossa decompression, and in our experience no patient has ever complained of a functional deficit postoperatively that would be related.

Cervical Nerves

With midline dissection of the suboccipital region, one often encounters the third occipital nerve (Fig. 10.1). One of many nerves in this region, the third occipital nerve is a derivative of the dorsal ramus of the third spinal nerve. Like the majority of other spinal nerves, the third spinal nerve divides into lateral and medial branches, the latter of which ramifies into deep and superficial divisions. The superficial medial branch (the third occipital nerve) curves around the dorsolateral surfaces of the C2-C3 facet joint, which it innervates. The third occipital nerve then courses under the inferior capitis oblique muscle and supplies the semispinalis capitis and travels deeply along the muscle before sending a communicating branch to the greater occipital nerve. At the level of the superior surface of the second cervical spinal process, the third occipital nerve turns dorsally and pierces the semispinalis capitis, splenius capitis, and trapezius muscles. After exiting these overlying muscles, the nerve becomes cutaneous and supplies a small area near the inion.

About 3 cm lateral to the inion, one finds the greater occipital nerve (Figs. 10.1 and 10.2), which is a branch of the medial division of the dorsal ramus of the second spinal nerve. As does the third occipital nerve, the greater occipital nerve emerges below the inferior capitis oblique

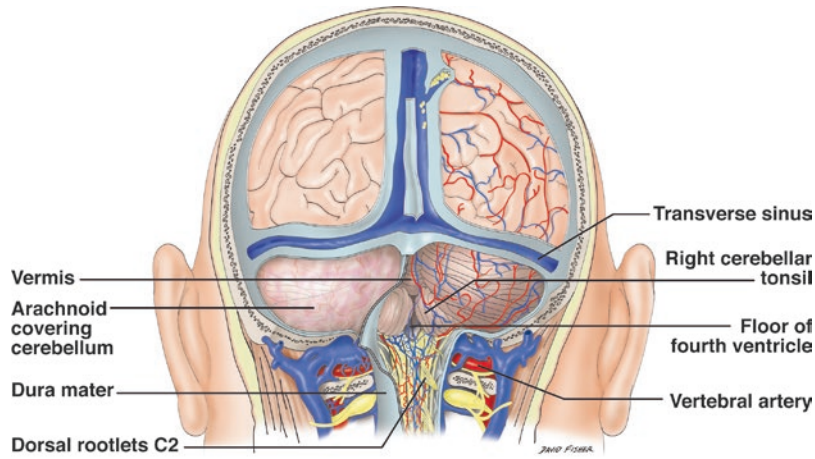

Fig. 10.3 Schematic drawing of the posterior head and craniocervical junction. Both extradural and intradural views of the cerebellum are seen. Note the avascular floor of the fourth ventricle deep to the cerebellar tonsils, which here are not herniated through the foramen magnum in order to illustrate the upper brain stem

muscle to ascend up through the soft tissues of the suboccipital region (semispinalis, splenius capitis, semispinalis capitis, and trapezius muscles) before it exits lateral to the inion to travel parallel to the occipital artery, which is usually lateral to it, and innervate skin anteriorly to at least the vertex of the skull. The greater occipital nerve will usually communicate medially with branches of the third occipital nerve and laterally with branches of the lesser occipital nerve. This latter nerve is unusual compared to the other nerves supplying the suboccipital and occipital regions in that it is derived from the ventral ramus of the second and third cervical nerves (i.e., the cervical plexus) and does not innervate the muscles that it travels by as does the third and greater occipital nerves. The lesser occipital nerve (Fig. 10.1) can be found approximately 7 cm lateral to the inion and branches into medial and lateral parts at approximately a midpoint between the inion and an intermastoid line.

Upper Cervical Spine Vasculature

Vascularly, in this region, and from superficial to deep, one finds branches to the overlying skin and muscles derived from the transverse cervical branch of the thyrocervical trunk (arising from the first segment of the subclavian artery, i.e., portion medial to the anterior scalene muscle, which supplies the trapezius muscle, branches of the occipital artery, a posterior branch of the external carotid artery, muscular branches of the vertebral artery, the first branch of the subclavian artery, and segmental branches feeding spinal nerve segments). Anastomoses are usually strong between the descending branch of the occipital artery and the vertebral arteries. The third part of the vertebral artery can be localized as one of the contents of the suboccipital triangle (Figs. 10.2 and 10.3). This horizontal or pre-intracranial segment of the artery and the suboccipital nerve (dorsal ramus of C1) are both found in this geometrically arranged region with the nerve being located inferior to the artery at the posterior arch of the atlas, which is in the floor of this triangle (Fig. 10.2). Regionally, accompanying veins are found, as is the deep cervical vein, which travels at the level of and lateral to the semispinalis cervicis muscle and feeds into the suboccipital venous plexus, which has been compared to the cavernous sinus in regard to its composition. This plexus has rich connections with the vertebral venous plexus.

Posterior Cranial Fossa

The posterior cranial fossa is limited inferiorly by the occipital and sphenoid bones. The posterior aspect of the temporal bones makes up the lateral walls of the posterior cranial fossa. Overlying these bones making up the inferolat-

eral walls is a layer of dura mater, which extends superiorly to form one of the many intracranial dural specializations, the tentorium cerebelli, which acts as the non-ridged roof of the posterior cranial fossa.

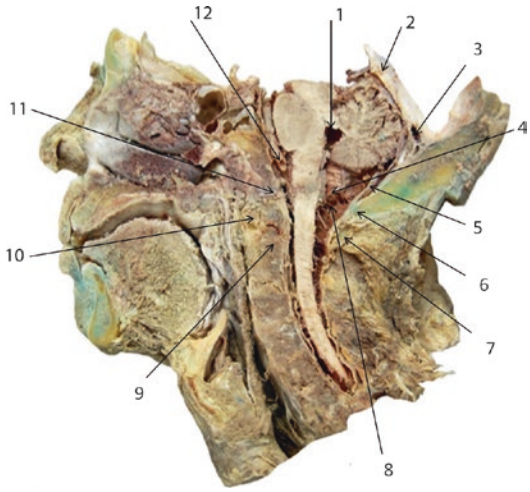

Fig. 10.4 Midsagittal transection through the head of an adult male cadaver. Note the (1) fourth ventricle, (2) tentorium cerebelli, (3) torcular Herophili, (4) right cerebellar tonsil, (5) dura mater underlying the occipital bone, (6) Opisthion, (7) posterior arch of C1, (8) arachnoid trabeculae of the cisterna magna, (9) odontoid process, (10) anterior arch of C1, (11) basion, and (12) left vertebral artery in cross section and just prior to contributing to the basilar artery

Venous Sinuses

The most valve lacking vertebral venous plexus (Batson's) communicates superiorly with the marginal sinus. This sinus encircles the foramen magnum and receives, among others, the basilar venous plexus anteriorly, veins traveling through the hypoglossal canal laterally, and the occipital sinus posteriorly. This latter sinus will often be encountered in midline decompression of the posterior fossa and is usually enlarged in children. Superiorly, it joins the torcular Herophili (Figs. 10.4 and 10.5). Interestingly, in the upright position, most intracranial blood travels via the marginal sinus and then into the vertebral venous plexus and through the internal jugular veins in recumbence. The basilar venous plexus also communicates with the inferior petrosal sinus that then drains into the internal jugular vein either intra- or extracranially. The superior petrosal sinus unites the cavernous sinus anteriorly to the transverse sinus posteriorly and runs in the attached edge of the tentorium cerebelli, which will often house several venous lakes (tentorial sinuses). The paired transverse sinuses connect venous blood flowing into the torcular Herophili from, for example, the superior sagittal and straight sinuses to the sigmoid sinuses, which after a short course drain into the superior jugular bulb.

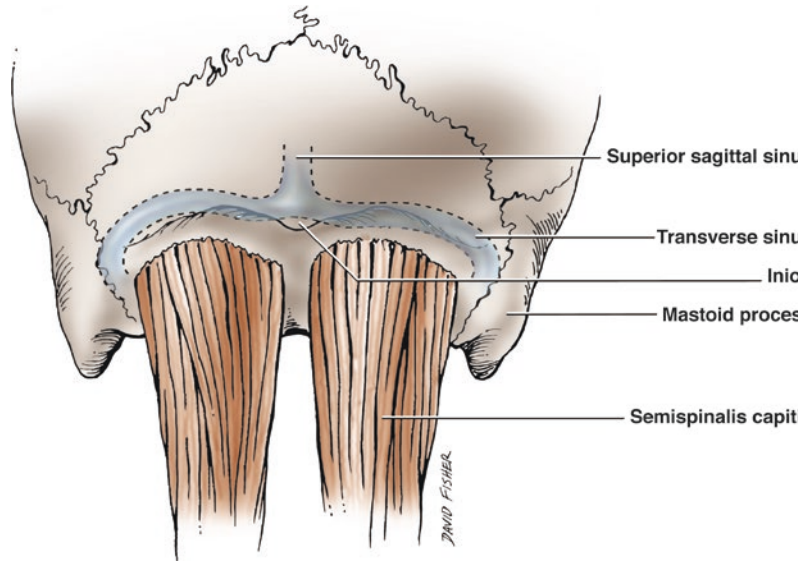

Fig. 10.5 Schematic drawing of the posterior occiput and attachment of the semispinalis capitis muscle. Note the position of the inion and transverse sinuses, the latter of which are uniting near the midline torcular Herophili

Dural Innervation

The innervation of the dura mater of the posterior fossa is important as many pain symptoms found in patients with Chiari malformations can be explained due to irritation of such nerves. The dura mater of the cranium is a two-layered membrane that is derived from neural crest cells. However, the spinal dura mater is a single layer and is derived from paraxial mesoderm. This difference in derivation helps one understand the varied innervation pattern seen between posterior fossa and cervical dura mater. In the cervical spine as well as the remaining spinal dura, the recurrent nerve of Luschka (recurrent meningeal or sinuvertebral nerve) segmentally innervates the dura mater. These meningeal branches arise from the spinal nerves and enter the intervertebral foramen to innervate the dura as well as the adjacent annulus fibrosis, periosteum, and posterior longitudinal ligament.

The dura mater of the posterior cranial fossa receives multiple nerves that contribute to its innervation. Branches have been found to arise from the facial, glossopharyngeal, vagus, and hypoglossal nerves. The majority of fibers from the hypoglossal nerve are thought to arise from the upper cervical nerves.

Once overlying muscles have been dissected away, the posterior atlanto-occipital membrane can be observed (Figs. 10.6 and 10.7). This structure is often thickened in the Chiari malformation and travels between the posterior arch of C1 to the posterior aspect of the occiput. A venous plexus may be found within this membrane, and the third part of the vertebral artery will pierce it prior to traversing the dura mater to enter the posterior fossa.

Posterior Aspect of the Atlas

The posterior arch of the atlas is easily seen with its midline posterior tubercle for the attachment of the rectus capitis posterior minor (Figs. 10.1, 10.2, and 10.3). The posterior arch may be bifid or assimilated to the occiput (atlanto-occipital fusion). Lateral on the posterior arch, the horizontal segment of the vertebral artery (Fig. 10.8), following leaving the transverse foramen of the

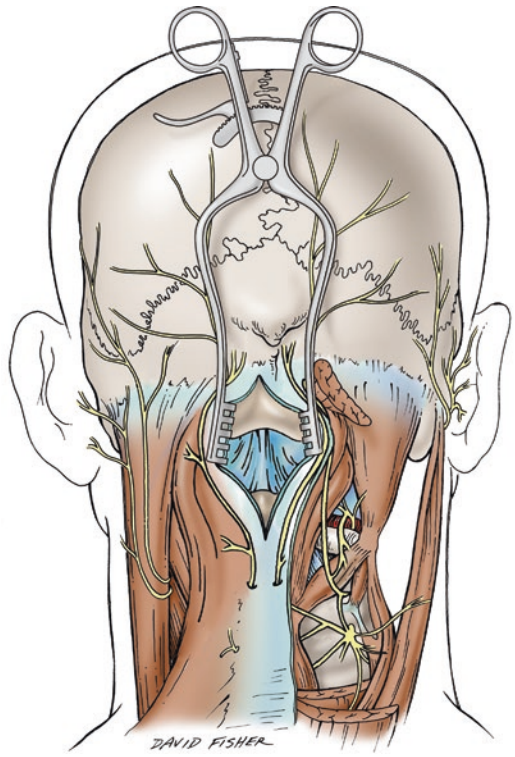

Fig. 10.6 Drawing of a deeper dissection (compare to Fig. 10.1) noting the posterior atlanto-occipital membrane

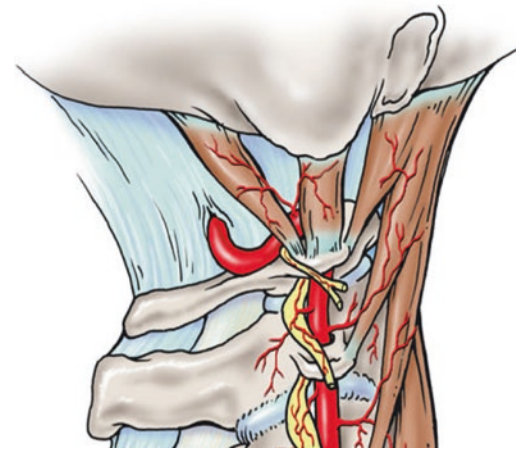

Fig. 10.7 Lateral view of the third and fourth parts of the vertebral artery, with the latter piercing the posterior atlanto-occipital membrane

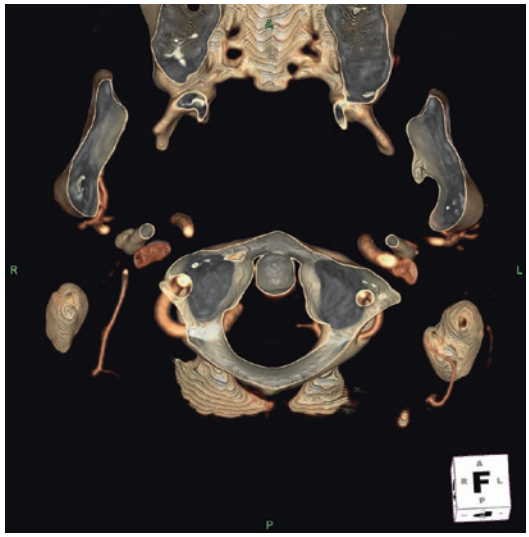

Fig. 10.8 Three-dimensional computed tomography angiogram noting the relationship of the V3 segment of the vertebral artery to the posterior arch of the atlas

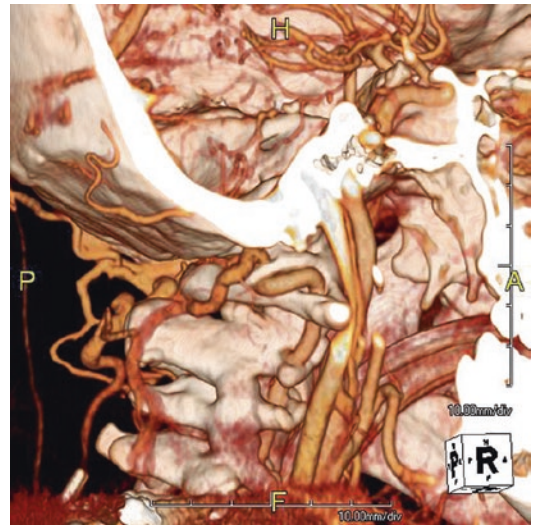

Fig. 10.9 Three-dimensional computed tomography angiogram noting a right-sided arcuate foramen with the V3 segment of the vertebral artery coursing through it

atlas, courses around the superior articular process to pierce the posterior atlanto-occipital membrane. A bony foramen (arcuate foramen) may be found at this location (Fig. 10.9). The periosteum along the anterior surface of the posterior arch of the atlas may be thickened in the Chiari malformations.

Intradural Anatomy of the Craniocervical Junction

First Denticulate Ligament

Intradurally at the craniocervical junction and from a posterior perspective, some of the lower cranial nerves and upper cervical nerves are observed. A good landmark for these structures is the first denticulate ligament, which is a pial extension from the C1 segment of the spinal cord to the inner aspect of the intracranial dura mater. Superiorly, this ligament attaches near the entrance of the third part of the vertebral artery, and inferiorly, it separates the vertebral artery and ventral rootlets of the upper cervical spinal nerves anteriorly from the dorsal rootlets of the upper cervical spinal nerves and spinal accessory nerve posteriorly. Of note, the dorsal roots are not always present nor are the dorsal root ganglia of C1. The ventral root of the C1 spinal nerve is often connected to the spinal accessory nerve via a communicating branch (nerve of McKenzie).

Accessory Nerve

Although variation exists, the spinal accessory nerve arises from the upper five or so cervical spinal cord segments, and connections between the nerve and especially the dorsal rootlets of the upper cervical spinal cord segments are common. The spinal part of the accessory nerve will ascend from the spinal cord to enter the foramen magnum and near the jugular foramen and unite with its cranial part to exit the skull (Figs. 10.10 and 10.11). The spinal portion will continue out to innervate the sternocleidomastoid and trapezius muscles. Although controversial, many opine that the cranial roots of the accessory nerve send their fibers to the vagus nerve (internal ramus or pars vagalis) and, specifically, its recurrent laryngeal branch to innervate the laryngeal muscles (less the cricothyroid muscle) and laryngeal mucosa below the vocal cords. Innervation of

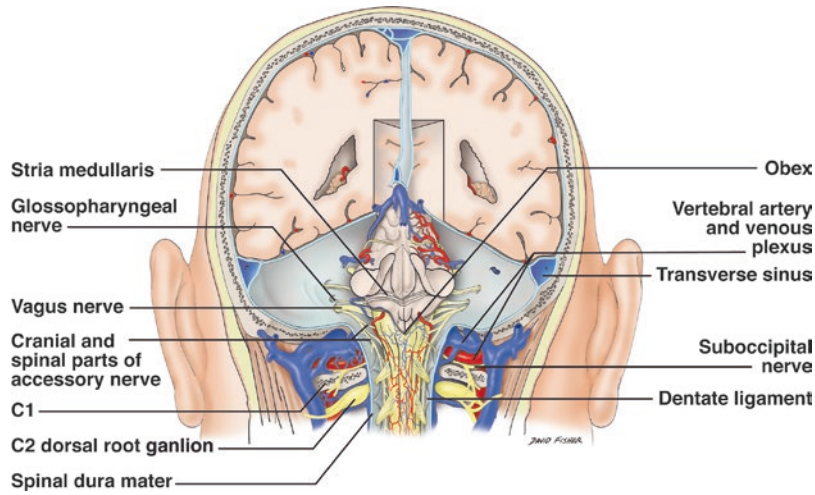

Fig. 10.10 Deeper dissection of Fig. 10.3

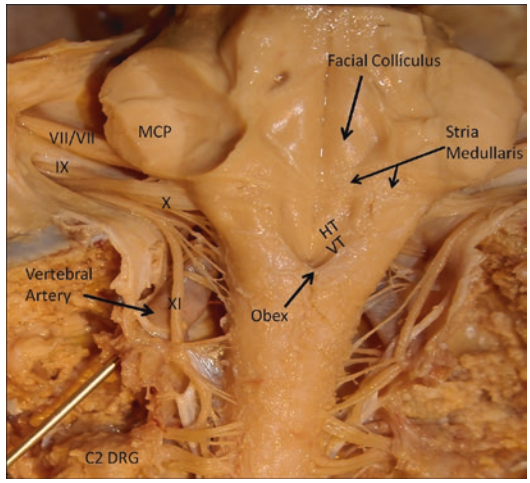

Fig. 10.11 Posterior craniocervical junction of a cadaver following the removal of the cerebellum. Note the floor of the fourth ventricle with the facial colliculus, stria medullaris. In the lower half of the floor, note the hypoglossal trigone (HT) and vagal trigone (VT). The obex marks the lowest part of the brain stem. On the left side, the middle cerebellar peduncle (MCP), cranial nerves VII-XI, and dorsal root ganglion (DRG) of C2 are seen

palatal muscles may also occur via the cranial rootlets of the accessory nerve.

Hypoglossal Nerve

Just superior to the uppermost attachment of the intracranial and first denticulate ligament is the hypoglossal nerve, which will innervate three of the four extrinsic tongue muscles (hyoglossus, styloglossus, and genioglossus). Also, as mentioned above, fibers from the upper cervical nerves will travel along the hypoglossal nerve to terminate on posterior fossa dura mater and thus provide some of its innervation.

First Spinal Nerve

The C1 nerve (Fig. 10.2), as mentioned previously, travels posteriorly to innervate the muscles of the suboccipital triangle including the rectus capitis posterior minor and overlying semispinalis capitis muscle. This nerve, in general, does not have a cutaneous distribution. Anteriorly, the ventral ramus of the C1 spinal nerve contributes to the cervical plexus and travels along the hypoglossal nerve to terminate on the thyrohyoid and geniohyoid muscles.

Posterior Spinal Artery

The posterior spinal arteries arise from the vertebral arteries and travel around the brain stem and then inferiorly along the posterolateral surface of the cervical spinal cord. They are distinct single vessels only at their origin and distally become irregular anastomosing channels, retaining to a large degree their embryonic plexiform pattern. The posterior spinal arteries are largest in the cervical and lumbar regions.

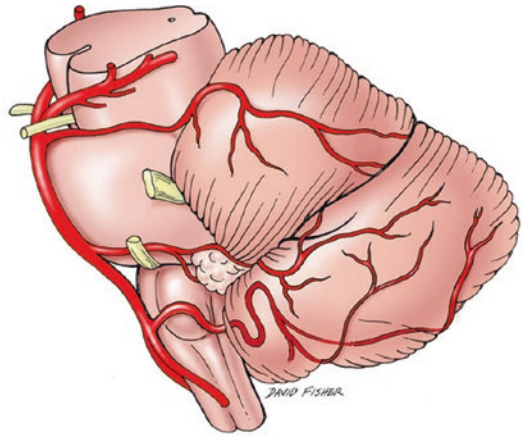

Fig. 10.12 Schematic drawing of the lateral brain stem and cerebellum. Note the course of the posterior inferior cerebellar artery (PICA) from the vertebral artery at its confluence into the basilar artery. The various segments of PICA are shown as it passes by the brain stem and then along the cerebellar hemisphere

Posterior Inferior Cerebellar Artery

An important artery of the posterior fossa, especially in regard to the Chiari malformation is the posterior inferior cerebellar artery (PICA), which arises from the vertebral artery near the vertebrobasilar junction and travels inferiorly toward the foramen magnum (Fig. 10.12). Occasionally, PICA may extend extracranially, especially in the hindbrain hernias. Once it reaches its lowest point, PICA recurs (caudal loop) around the cerebellar tonsil. PICA then ascends to its superiormost point (cranial loop) and travels inferolateral to course over the convexity of the cerebellar hemisphere. Along its course, PICA supplies the lower medulla oblongata, choroid plexus, posterior fossa dura, fourth ventricle, cerebellar tonsils, vermis, and inferolateral hemisphere. PICA can be divided into five segments:

1. An *anterior medullary segment*, which is often absent (i.e., PICA does not originate anterior to the medulla oblongata), extends from the origin of PICA to the inferior olive.
2. A *lateral medullary segment* that extends from the inferior olive to the origins of the lower cranial nerves.
3. A *posterior medullary segment* (tonsillomedullary segment) begins where the PICA passes posterior to the lower cranial nerves and ends where the ascending vessel reaches the midlevel of the medial surface of the tonsil. It passes immediately posterior to the roof of the lower half of the fourth ventricle. All medullary segments give rise to perforating branches, which if injured, are the reason nuclear dysfunction occurs (e.g., Wallenberg syndrome).
4. A *supratonsillar segment* (telovelotonsillar segment) begins at the midportion of the tonsil, includes the cranial loop, and ends where the PICA exits the fissures between the vermis, tonsil, and cerebellar hemisphere to reach the suboccipital surface. This is the most complex of the PICA segments.
5. *Cortical segments* (hemispheric segment) supply such areas as the midline vermis and tonsils. The PICA often bifurcates into medial and lateral trunks where the vessel emerges onto the inferior cortical surface. The medial trunk gives rise to vermian and tonsillar branches, and the lateral trunk gives rise to hemispheric branches.

Variations of PICA are common such as it arising from the basilar artery. For example, PICA may be found to arise extradurally in up to 20% of cases and may be duplicated in up to 5%. The vertebral artery may terminate (approximately 0.2%) as PICA, and PICA may be absent or hypoplastic and may share a common origin with the anterior inferior cerebellar artery.

Cerebellar Tonsils

The cerebellar tonsils (Figs. 10.13 and 10.14) are normally found several millimeters above the foramen magnum and are often asymmetric between left and right sides. These structures are connected to the cerebellum along their upper lateral surface by the so-called tonsillar peduncle. Laterally, the cerebellar tonsils are covered by the biventral lobule. The cerebellomedullary fissure separates the tonsil from the posterior surface of the medulla oblongata. The space that separates the left and

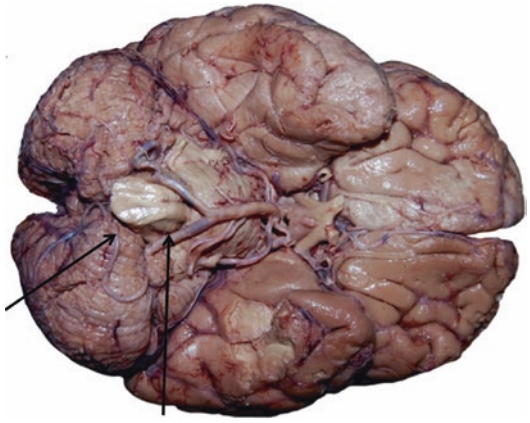

Fig. 10.13 The basilar surface of the brain illustrating the left vertebral artery (right arrow) and the tonsillar segment of PICA (left arrow)

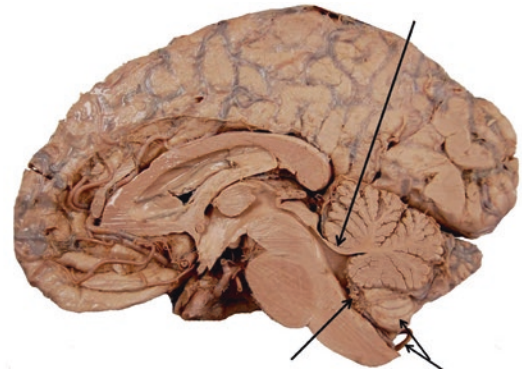

Fig. 10.14 Mid-sagittal section of the brain noting the superior medullary velum (upper arrow), choroid plexus of the fourth ventricle and attached to the inferior medullary velum (left lower arrow), and the right cerebellar tonsil and PICA (right lower arrows)

right tonsils across the midline is referred to as the vallecula. At its superior pole, each tonsil's anterior surface faces the nodule, inferior medullary velum, and tela choroidea. This superior pole of the tonsil, which faces the uvula medially, is separated from the aforementioned structures by an extension of the cerebellomedullary fissure known as the telovelotonsillar cleft.

Retrotonsillar Veins

The superior retrotonsillar vein originates from the superior pole of the cerebellar tonsil and travels posteriorly to unite with the inferior retrotonsillar vein, which arises near the inferior pole of the tonsil to course superiorly. Together, these vessels form the inferior vermian vein, which therefore drains the medial and lateral surfaces of the tonsils. The inferior vermian vein may drain into the tentorial or transverse sinuses or into the torcular Herophili.

Fourth Ventricle

Communicating superiorly with the cerebral aqueduct and inferiorly with the subarachnoid space, the fourth ventricle lies just posterior to the pons and medulla oblongata. The fourth ventricle can be described as a gable-roofed chamber with a diamond-shaped floor. The gables are directed lateralward and are prolonged in tunnel-like extensions around the restiform body. The long axis of the ventricular floor is parallel with the spinal cord and extends from the superior extremity of the pons to the middle of the medulla. The fourth ventricle (Figs. 10.11 and 10.14) is lined with ependyma, which is complete throughout, except in the roof of the inferior part, where below the inferior medullary velum only the epithelial layer is present. The choroid plexus of the fourth ventricle invaginates the roof epithelium and hangs from the roof into the lateral recesses and the inferior part of the ventricular cavity. Its roof is composed of the superior and inferior medullary vela, which come into contact at the fastigium (Fig. 10.14). The superior medullary velum is partially concealed by the lingula of the cerebellum, and its proximal portion acts as a bridge for the crossing of the fibers from the contralateral trochlear nerve nucleus. The inferior medullary velum is smaller and gives rise to the tuft of choroid plexus found within the fourth ventricle. Specifically, the tela choroidea, which is a fold of pia mater and related ependyma related to the inferior medullary velum, gives rise to the choroid plexus here and is the basis for the so-called telovelar approach to the fourth ventricle. The tela choroidea turns inferiorly from the telovelar junction around the superior pole of the tonsils to attach to the infero-

lateral edges of the fourth ventricular floor termed the taeniae. Superiorly, the taeniae travel lateral over the inferior cerebellar peduncles and travel horizontally along the inferior aspect of the lateral recesses. Branches of PICA supply the choroid plexus of the fourth ventricle. Specifically, these are derived from the telovelotonsillar segment of this vessel.

The floor of the fourth ventricle (rhomboid fossa) contains multiple landmark structures formed due to underlying bulging of various tracts and nuclei. Dividing the fossa into an upper and lower half, the stria medullaris of the fourth ventricle represents fibers connecting arcuate nuclei to the middle cerebellar peduncle. Above this horizontal marker is the facial colliculus, which represents the underlying motor nuclei of the facial and abducens nerves. Vertically, the left and right sides of the rhomboid fossa are divided by the median fissure, and on either side of this fissure and extending cephalad from the facial colliculus is the medial eminence. Lateral to the facial colliculus is the fovea superior that represents the remnant of the sulcus limitans, which more or less differentiates medial motor nuclei from lateral sensory nuclei. The sulcus limitans represents the embryologic border between the alar (sensory) and basal (motor) plates. The upper aspect of the fossa above the facial colliculus contains the locus ceruleus and may have a darkened appearance. This nucleus is a site of norepinephrine production. Laterally, at the junction of the upper and lower half of the rhomboid fossa, the dorsal cochlear and vestibular nuclei are found in the so-called acoustic area. The lateral recesses of the acoustic areas (foramina of Luschka) allow for CSF egress and may allow for a tuft of choroid plexus (basket of Luschka) from the fourth ventricle to protrude out into the cerebellopontine angle. In the lower half of the fossa, a collection of underlying nuclei forms two V-shaped trigones, the hypoglossal and vagal, representing the nuclei of the vagus and hypoglossal nerves. The obex (Latin for "barrier"), which is a small fold of tissue at the lower dorsal fourth ventricular wall, marks the lower level of the fourth ventricle and is found, on average, 12 mm above the foramen magnum. Arachnoid webs have been observed at the level of the obex that occlude the foramen of Magendie. The obex is inferiorly displaced with both the Chiari 0 and 1.5 malformations. The edges of the V-shaped lower half of the rhomboid fossa are termed the calamus scriptorius due to their resemblance to a writing pen, and just inside this edge are the nuclei related to the emetic response termed the area postrema. The "closed" (i.e., non-ventricular) posterior aspect of the medulla demonstrates additional external landmarks including the clava (gracile tubercle), located just inferior to the obex and off the midline from the dorsal median sulcus, which is formed by the underlying funiculus gracilis carrying proprioceptive fibers. Lateral to the clava and separated by the dorsal intermediate sulcus is the cuneate tubercle, which also carries proprioceptive fibers. Lateral to the cuneate tubercle and marking the position of the spinal tract and nucleus of the trigeminal nerve is the tuberculum trigeminum (cinereum). Ventral to the tuberculum trigeminum and not seen with a direct posterior view of the posterior brain stem is the site of emergence of the rootlets of the cranial part of the accessory, vagus, and glossopharyngeal nerves (Figs. 10.10 and 10.11).

The foramen of Magendie is a median aperture resting at the inferior aspect of the fourth ventricle and with the laterally positioned foramina of Luschka, allows CSF egress from the fourth ventricle into the cisterna magna and cervical subarachnoid space. The foramen of Magendie may be stenotic or imperforate as it is in other mammals. Interestingly, neither the foramen of Magendie nor the foramina of Luschka are lined with ependyma.

References

1. Brennan PA, Standring SM, Wiseman SM. Gray's surgical anatomy. Philadelphia: Elsevier; 2020.
2. Hollinshead WH. Anatomy for surgeons. Volume 1: The head and neck. New York: Hoeber-Harper; 1968.
3. Lang J. Clinical anatomy of the posterior cranial fossa and its foramina. New York: Thieme; 1991.
4. Rhoton AL. Cranial anatomy and surgical approaches. Congress of Neurological Surgeons: Schaumburg; 2003.
5. Standring S. Gray's anatomy. 42nd ed. Philadelphia: Elsevier; 2020.

Part III

Pathology

Pathology of Chiari I and II Malformations

11

Lucy B. Rorke-Adams

More than 100 years ago, Hans Chiari wrote two papers describing four types of cerebellar malformations, all of which currently bear his name [1, 2]. He was primarily interested in the relationship between hydrocephalus and abnormalities of the cerebellum, although only type II is most consistently associated with ventricular enlargement.

This chapter will focus on pathological features of Chiari I and II, as these are relevant to neurosurgeons. Types III and IV are rare, and, while some features of type III may be ameliorated by surgery [3], type IV, which is partial or complete aplasia of the cerebellum, is not a treatable condition.

Chiari I

What is currently referred to as Chiari I malformation consists of clinical and pathological features that do not match Chiari's original description [4]. In the 1891 paper, he basically described chronic herniation of the cerebellar tonsils in a 17-year-old girl who also had mild enlargement of the third and lateral ventricles, unassociated with a large head. Viewed from a distance, it would appear that this case was simply an example of chronic tonsillar herniation secondary to increased intracranial pressure, a concept unknown at that time, but only discerned 6–8 years later by Cushing [5] and Collier [6].

In view of what Chiari described, no other abnormalities beyond tonsillar herniation and hydrocephalus, it is clear that the association of these coexisting conditions as a specific malformation is incorrect.

Nevertheless, there is a clinical-pathological condition most common among older children and young adults currently called Chiari I malformation. Tonsillar herniation is one component, but it does not include ventricular dilatation (Fig. 11.1). However, it is associated with a variety of clinical symptoms and anatomical abnormalities, such as platybasia [7], basilar impression

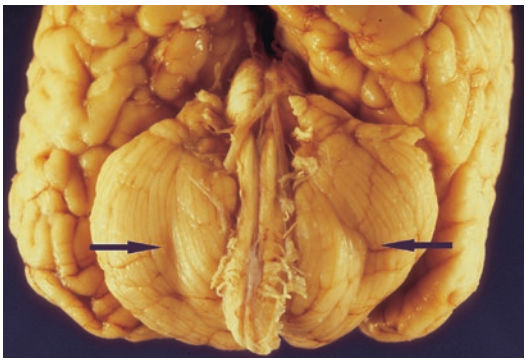

Fig. 11.1 Chiari I defect characterized by striking herniation of cerebellar tonsils into upper cervical canal. Note the ridges separating tonsils and adjacent cerebellar tissue produced by bony rim of the foramen magnum (arrows)

L. B. Rorke-Adams (✉)
Department of Pathology, The Children's Hospital of Philadelphia, Philadelphia, PA, USA

R. S. Tubbs et al. (eds.), *The Chiari Malformations*, https://doi.org/10.1007/978-3-030-44862-2_11

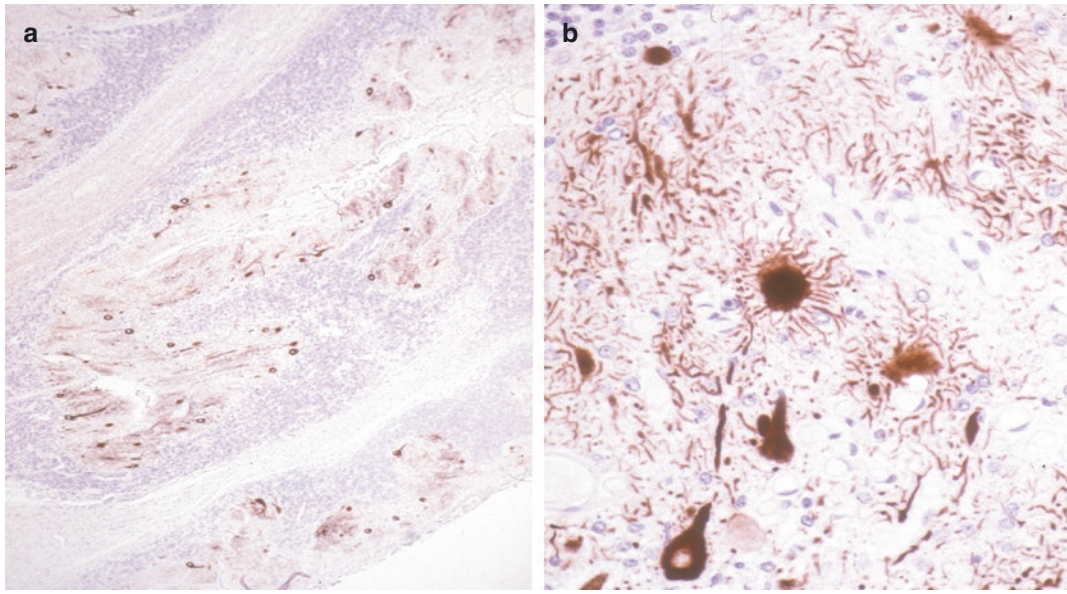

Fig. 11.2 (**a**) Photomicrographs of dysplastic cerebellar tonsils from surgical specimen of child with Chiari I defect. Immunoperoxidase preparation for NFP ×250. (**b**) Higher magnification of (**a**) showing dysplastic anatomy and bizarre Purkinje cells. Immunoperoxidase preparation for NFP ×400

[8], or simply a posterior fossa that is smaller than normal [9, 10]. Occasionally, the foramen magnum is larger than normal, or there are other anomalies of the occipital bone or rostral cervical vertebrae [11].

Additionally, aside from the tonsillar herniation, there may be syringomyelia, especially in older individuals [12, 13], or aberrant dorsal angulation of rostral cervical roots [14]. The chronically herniated tonsils may be sclerotic [4] or be composed of frankly malformed tissue [14]. Among the cerebellar malformations, which may be confined to the tonsils or more widespread, are nonspecific foliar (cortical) dysplasia (Fig. 11.2) or hypertrophy of the cerebellar cortex of the type described by Lhermitte and Duclos [15]. This rare condition straddles the divide between malformation and neoplasia. Pathological features are those of a malformation primarily affecting the granule cell layer, whereas clinically it may present as a space-occupying lesion [16].

It should be emphasized that the clinical and pathological features of what is currently called Chiari I malformation do not match Chiari's original description, but are instead a more complex combination of posterior fossa, cerebellar, and spinal cord abnormalities.

Chiari II

Of the four entities bearing Chiari's name, type II is the most severe and complex. There is a vast literature dealing with all aspects of this disorder, including who described what and when, along with issues of nomenclature. A detailed, scholarly review of the historical evolution of Chiari II malformation may be found elsewhere [17, 18]. Here, only key aspects will be noted before focusing upon the pathological features.

The central nervous system (CNS) components of Chiari II malformation were actually described first by Cleland in 1883 [19]. As noted previously, Chiari's detailed observations appeared in two papers published in 1891 and 1896 [1, 2], respectively. Subsequently, the name of Arnold was united with Chiari's, even though he (Arnold) made no substantial contribution to either clinical or pathological features of the dis-

order [20], and Cleland's contribution was lost to the vicissitudes of history.

Currently, Chiari II malformation is often diagnosed on ultrasound monitoring of a pregnancy; otherwise, it is known to be present due to the patient's myelomeningocele. This diagnosis carries with it a substantial number of abnormalities involving all parts of the nervous system, including the skull, spine, and dura mater as well. Contributions to this wealth of information have come from neurosurgeons, radiologists, pathologists, and embryologists.

Presentation of the major pathological features will be separated by structures affected, although this is artificial and, in some instances, cannot be done with precision.

Bone

Skull

Squamous bones – (membranous) Aside from sutural separation in infants whose hydrocephalus is not treated, the major abnormality is a condition in which bone is irregularly thinned, the thinned areas being separated by ridges (Fig. 11.3). Originally named Lückenschädel (i.e., lacunar skull), it was suggested that pulsation of underlying gyri were responsible for the defect, but it is now clear that this is a primary bone lesion and present in at least 80% of affected babies at birth [21]. It is a consequence of the lack of ossification of the inner table of the skull [22].

Basicranium (endochondral bones) Of the bony components of the skull base, those forming the posterior fossa are primarily affected. In general, the volume is reduced, but additional deformities include a short and dorsal concave clivus, scalloping of the petrosal bone with a foreshortened internal acoustic meatus, and an enlarged foramen magnum (Fig. 11.4) [23].

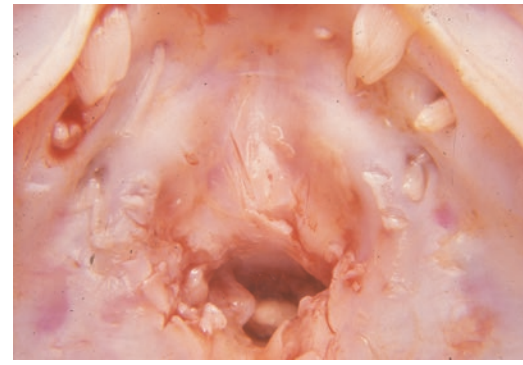

Fig. 11.4 Hypoplastic posterior fossa. Note the steep angle of the clivus and overgrowth of the bone forming the foramen magnum

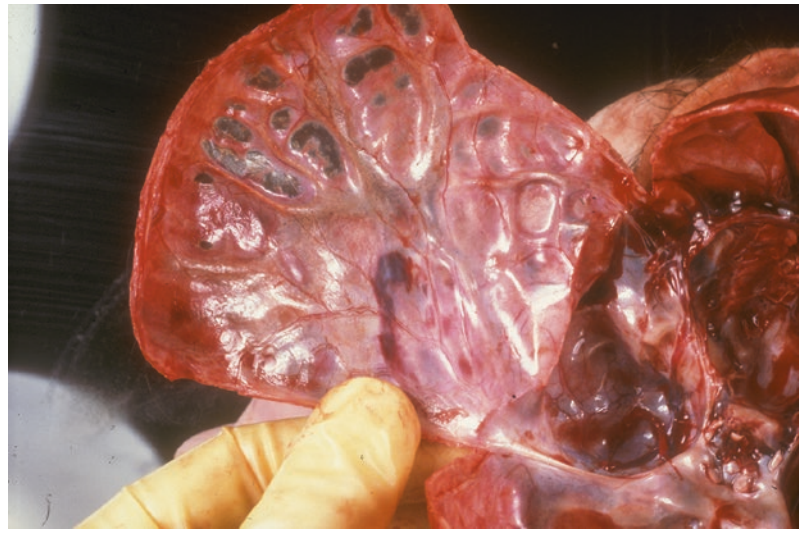

Fig. 11.3 Left parietal bone displaying ridges separating multiple patches of thinned bone characteristic of "Lückenschädel"

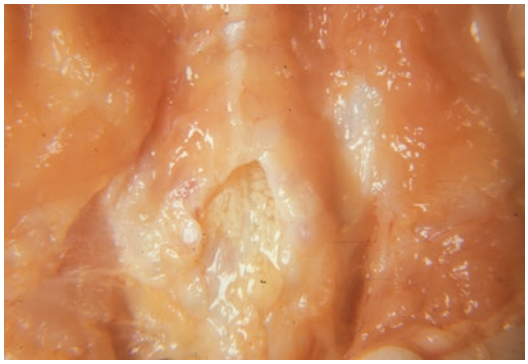

Fig. 11.5 Spina bifida occulta. Note the absence of fusion of sacral laminae

Vertebral Column

The vertebral column is always dysraphic in individuals with Chiari II anomaly. Dysraphism refers to imperfect midline closure of the spinolaminar arch, extent of the defect varying considerably in severity. Least severe is a simple bony defect, generally at the caudal end, spina bifida occulta, unassociated with neural or mesenchymal components, and hence not relevant here (Fig. 11.5).

Of major clinical concern is spina bifida aperta, in which the bone anomaly is associated with a wide range of mesenchymal and neural malformations (Fig. 11.6). Although the dysraphic defect may occur at any level, it is most common in the lumbosacral region. In general, there is a correlation between the vertebral level affected and the extent of neurological deficit; more rostral defects (e.g., involving thoracic vertebrae) are associated with more severe neurological deficits than sacral dysraphism.

Most frequently, the bony defect consists of lack of formation/fusion of laminar processes, but occasionally a hypoplastic laminar process (spur) may curve inward to separate neural tissue, i.e., split cord malformation.

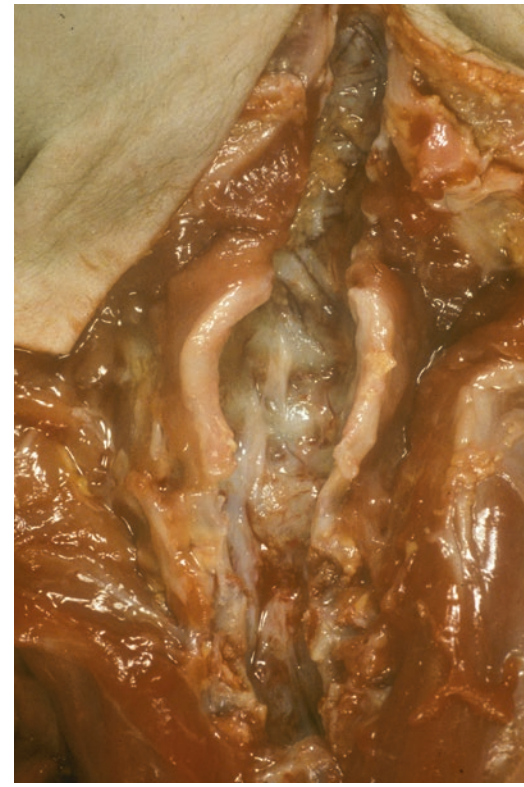

Fig. 11.6 Spina bifida aperta. Note the total absence of laminae and round edges of the bone allowing exposure of intraspinal contents

Mesodermal Component

Dura Mater

Cranial

Dural abnormalities of the cranium largely involve the falx cerebri, tentorium cerebella, and venous sinuses of the posterior fossa. The tentorium may be absent or hypoplastic, leading to a lateral-low insertion causing vertical orientation of the straight sinuses and a low position of the torcular [22].

In individuals with hypoplasia or aplasia of the falx cerebri, there is interdigitation of medial cerebral gyri (Fig. 11.7).

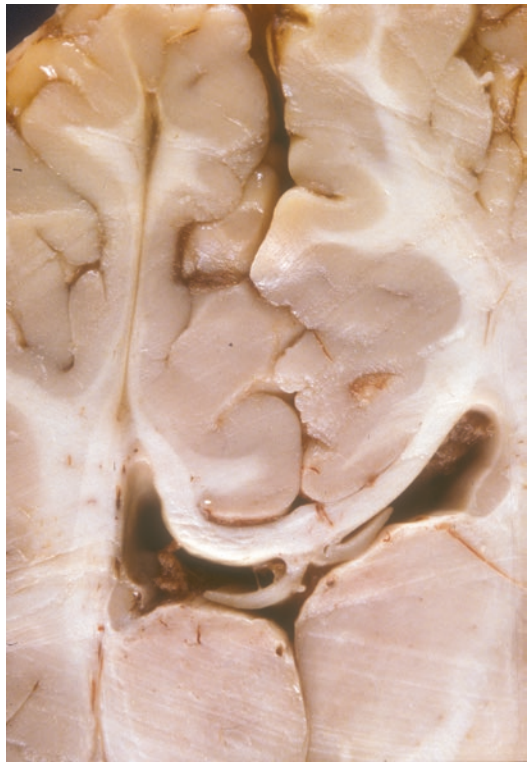

Fig. 11.7 Interdigitation of medially placed cerebral hemispheric gyri in partial agenesis of the falx cerebri

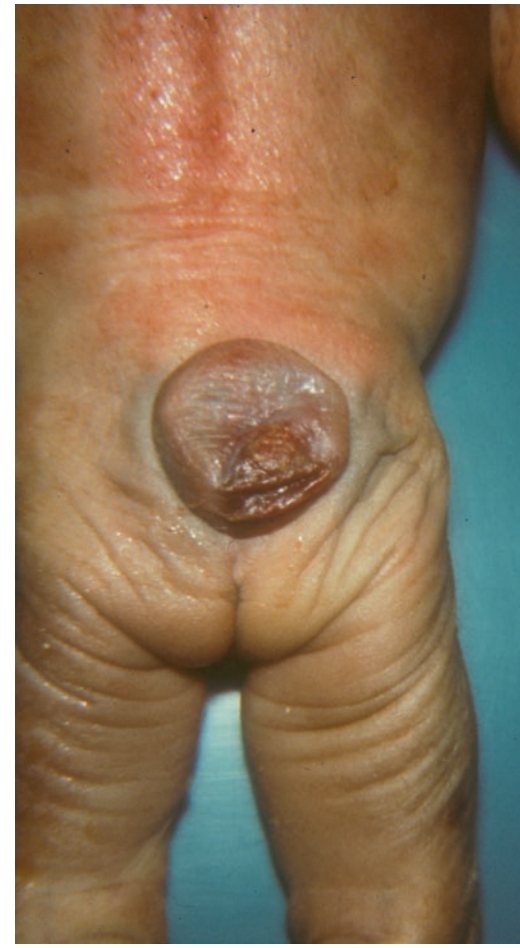

Fig. 11.8 Back of infant with lumbosacral meningomyelocele showing characteristic partially redundant sac

Spinal

Dural abnormalities are a constant feature in the region of spina bifida aperta. It may be absent altogether, allowing exposure of neural elements, but more often there is a complete or incomplete dural sac that, along with overlying epithelium, plus or minus dermis, protects the neural elements (Figs. 11.8 and 11.9). Dura and arachnoid herniated through the boney defect, and with or without a covering of intact or ulcerated skin, forms the sac, which is a hallmark of the condition. A placode of neural tissue is attached to the undersurface (Fig. 11.10). See below.

Mesenchymal Tissue

Closure of the head and tail ends of the neural tube requires involvement of the epithelial, neural, and mesenchymal tissue; hence if the process does not proceed normally, the resulting defect contains a disordered combination of all of these elements. A primary mesenchymal component consists of an excessive number of blood vessels, the structure of which, for the most part, is normal; but because of their abundance, the lesion as a whole is referred to as the "area cerebrovasculosa" if at the head end or the "area medullovasculosa" if at the caudal end. Aside from dysplastic neural tissue and a prominent vascular component, there is disordered fibrous or fibrofatty tissue and often hamartomatous nests/bundles of smooth muscle.

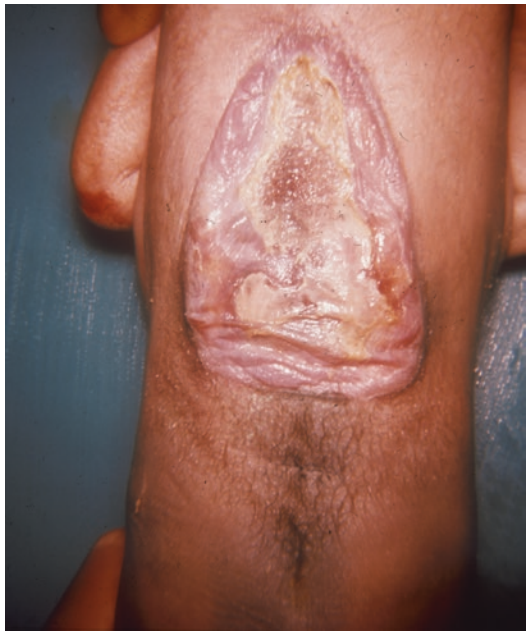

Fig. 11.9 Large thoracolumbar complex meningomyelocele with incomplete formation of the sac. Note the abnormal hirsutism of the skin caudal to the defect

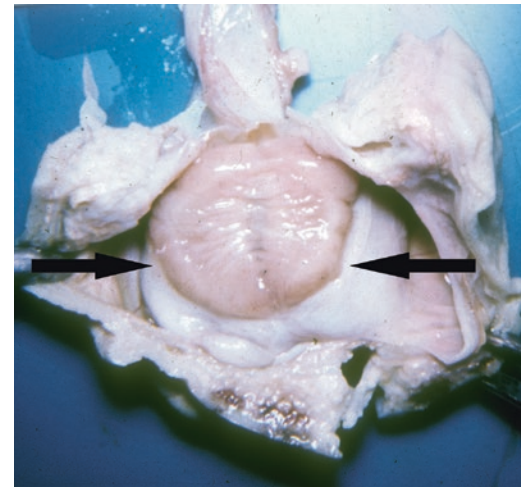

Fig. 11.10 Sac has been opened to expose large neural placode at caudal end of the cord

Pathology of the Sac

Pathological features of the spinal defect are variable, ranging from total exposure of neural tissue (i.e., no covering sac) to one that is covered by apparently normal skin (Figs. 11.8 and 11.9). In most instances, however, there is a balloon-like protuberance continuous with normal adjacent skin, but which consists of an attenuated layer of intact or ulcerated epithelium. This generally has a reddish color and a somewhat folded redundant character. When the sac is opened, the bony defect is exposed along with the herniated neural contents. These include spinal roots (including filum terminale) and dysplastic neural tissue plastered on the undersurface of the sac, the so-called "neural placode" (Figs. 11.10 and 11.11). This varies in size and complexity. There may also be excessive fatty tissue, i.e., a lipoma.

Microscopic features that are most characteristic display a transition from normal skin to the sac consisting of attenuated, intact, or ulcerated and/or inflamed squamous epithelium. Underlying dermis may/may not be present, but dermal appendages are almost always absent (Figs. 11.12 and 11.13). Heterotopic, dysplastic neural tissue consisting of glia, with or without neurons, may be located superficially or in deeper layers (Figs. 11.14, 11.15, and 11.16). Ependymal cells are a common component and are typically arranged in strips similar to a ventricular lining (Fig. 11.17). Small nerve roots or twiglets are often present as well. These are located within the sac and in deeper tissues. The sac is lined by arachnoid and fibrous tissue, presumably dura, although it does not look like normal spinal dura. Occasionally, abortive dorsal root ganglia are found as well. Associated and generally intermixed with these tissues is an excessive number of blood vessels, typically of small to medium diameter; vascular walls are usually normal although occasionally they may exhibit structural defects (Fig. 11.18).

A curious component of the dysplastic tissues in these specimens is a scattering of irregular bundles or strands of smooth muscle (Fig. 11.19). Dysplastic striated muscle is much less frequently observed.

Size and complexity of the neural placode is variable. It may be large and consist of dysplastic

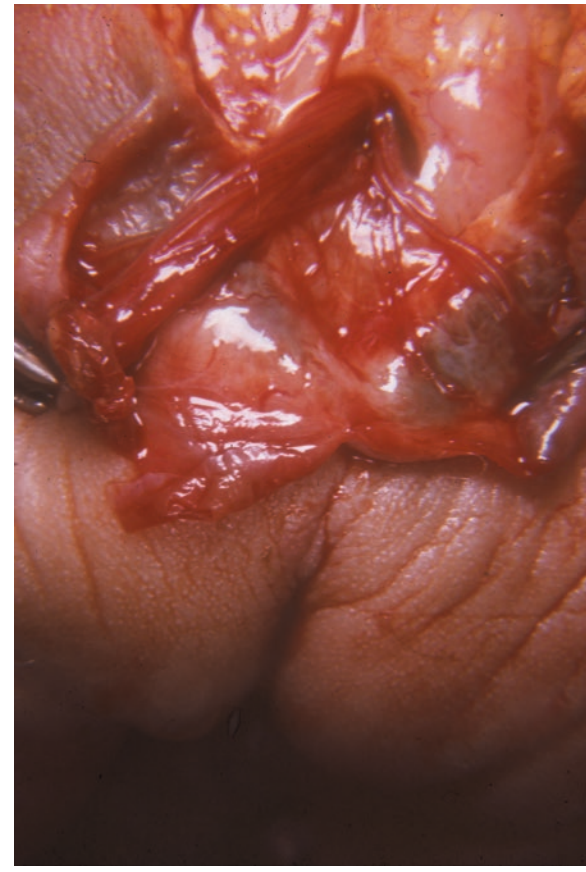

Fig. 11.11 Sac of infant pictured in Fig. 11.8 has been opened to display roots of cauda equina and filum, which are attached to the undersurface of the sac

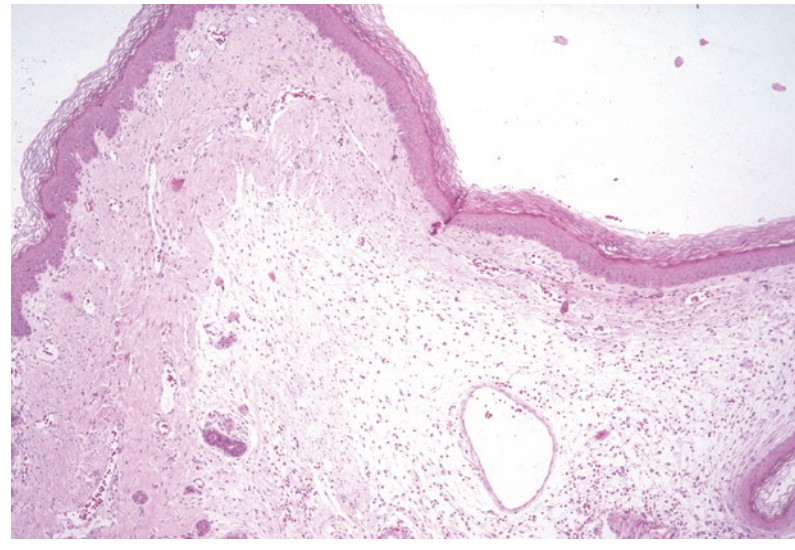

Fig. 11.12 Photomicrograph of intact epithelial covering of the sac. Note the underlying loose mesenchymal tissue and absence of dermal appendages. H&E ×100

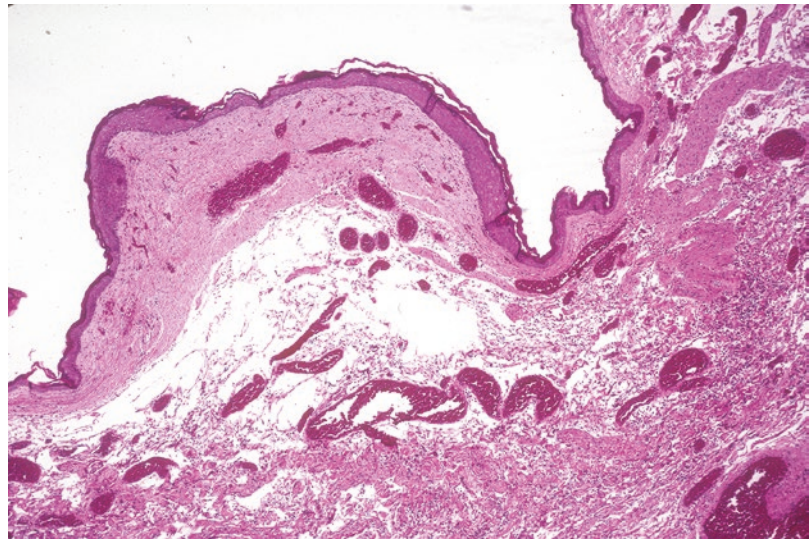

Fig. 11.13 Photomicrograph of sac and contents containing dense and loose connective tissue and abundant blood vessels. H&E ×100

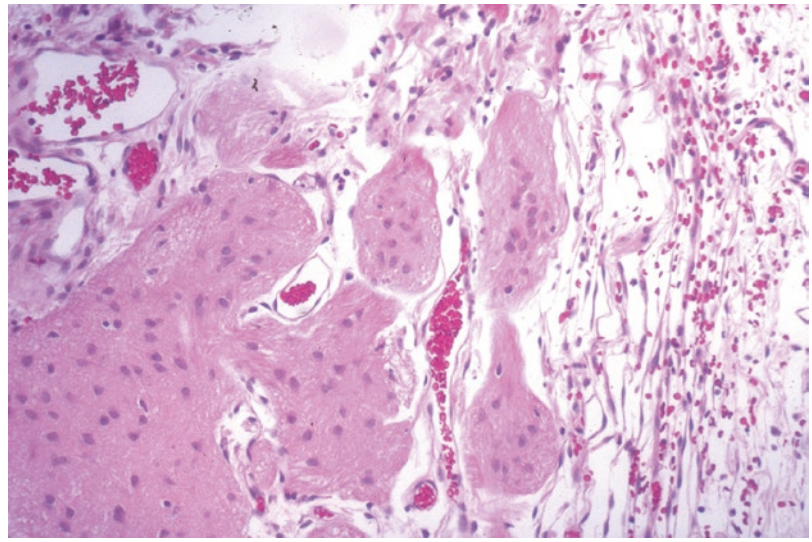

Fig. 11.14 Nests of dysplastic glial islands within sac. H&E ×250

neuronal and glial tissue that includes ependyma. Recognizable spinal cord, well-formed or dysplastic, a split cord (Fig. 11.20), and duplication or even triplication of the cord are also possibilities. Excessive fat may be associated with the abnormal spinal cord (Fig. 11.21).

An uncommon lesion consists of a dilated sac lined by ependyma, i.e., myelocystocele. This represents distension of an extreme hydromyelic condition; hence nerve roots are present in the outer walls of the cyst. This lesion may be associated with a defect in one or more vertebral bodies [24].

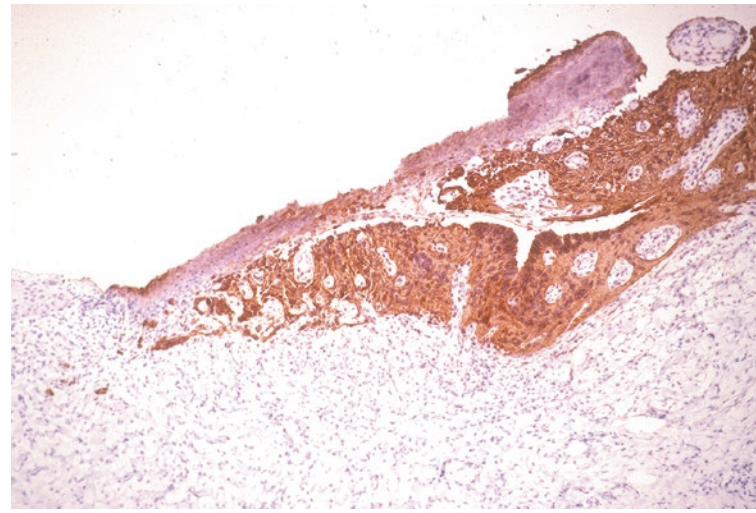

Fig. 11.15 Large strips of glial tissue along the surface of myelocele sac. Immunoperoxidase preparation for GFAP ×100

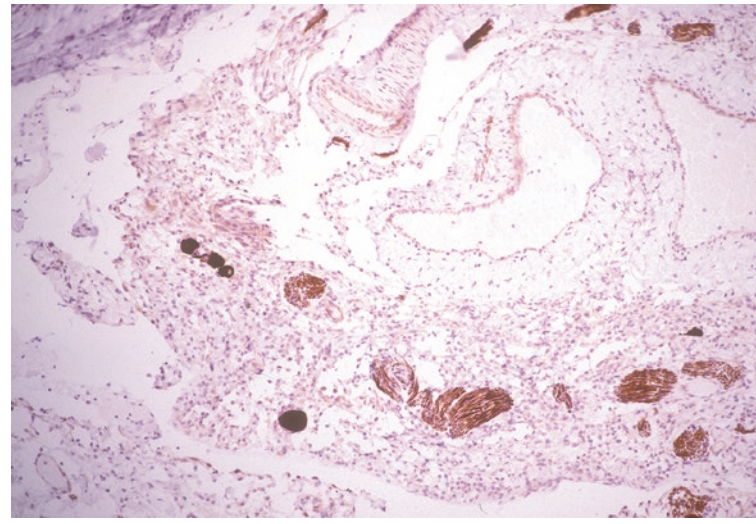

Fig. 11.16 Scattered nests of neuropil containing neurons within myelocele sac. Immunoperoxidase preparation for NFP ×100

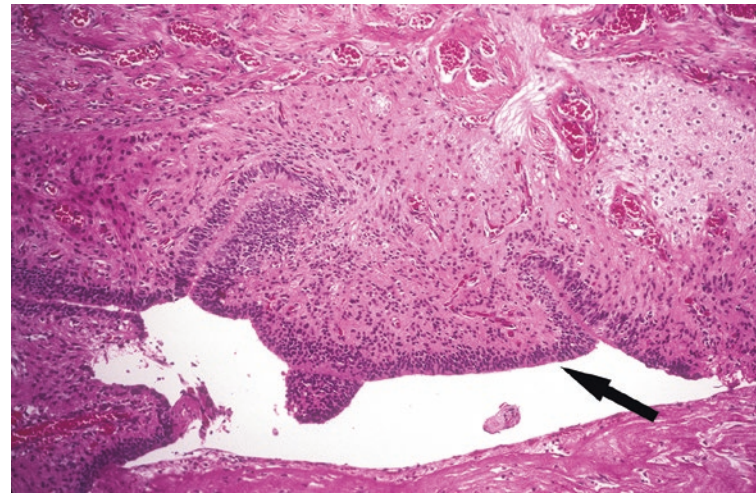

Fig. 11.17 Cavity in myelocele sac lined by ependyma below which is the glial tissue. H&E ×250

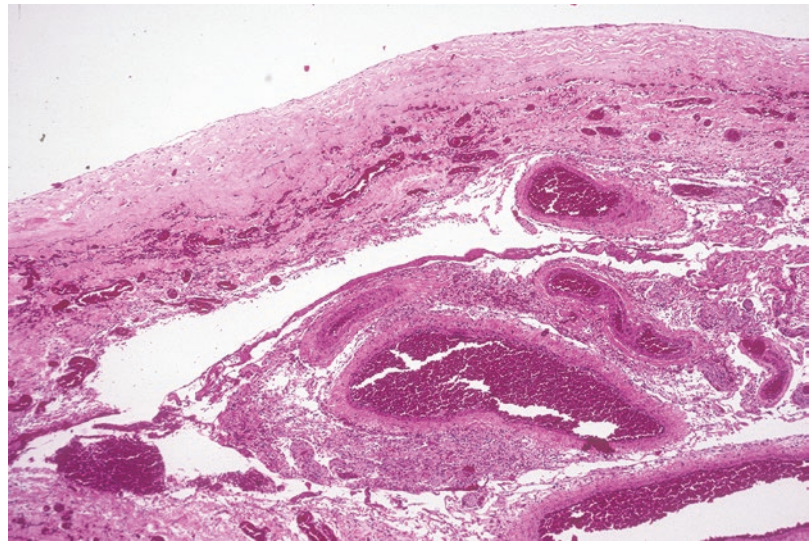

Fig. 11.18 Portion of myelocele sac containing many blood vessels of variable size. H&E ×250

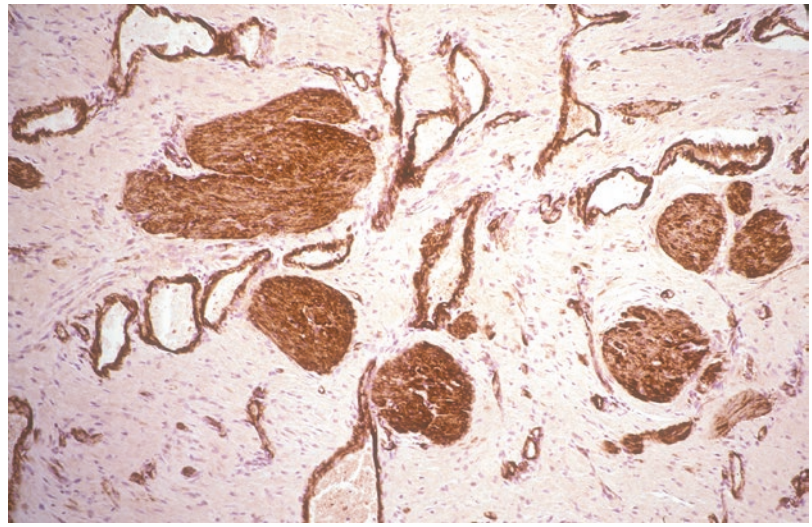

Fig. 11.19 Nests of smooth muscle in myelocele sac. Immunoperoxidase preparation for SMA ×250

Brain Abnormalities Associated with Chiari II Defect

A staggering number of lesions comprise the pathologic spectrum of Chiari II and involve all levels of the neuraxis. Thus, although attention has been focused on the cerebellar and brain stem defects, dysplastic development of the CNS is wide-ranging. One textbook account lists 10 involving the cerebrum, 12 in brain stem, 7 cerebellar, and 10 spinal, aside from those involving the dura (5) and skull and spine (11). Associated abnormalities of other organs are also described [17].

Clearly, all possible defects do not simultaneously affect all infants, but a sufficient number are found in combination in any given child to lead to significant clinical neurological deficit, only some of which can be treated surgically.

Gross abnormalities found in the cerebrum include polygyria, polymicrogyria, subependy-

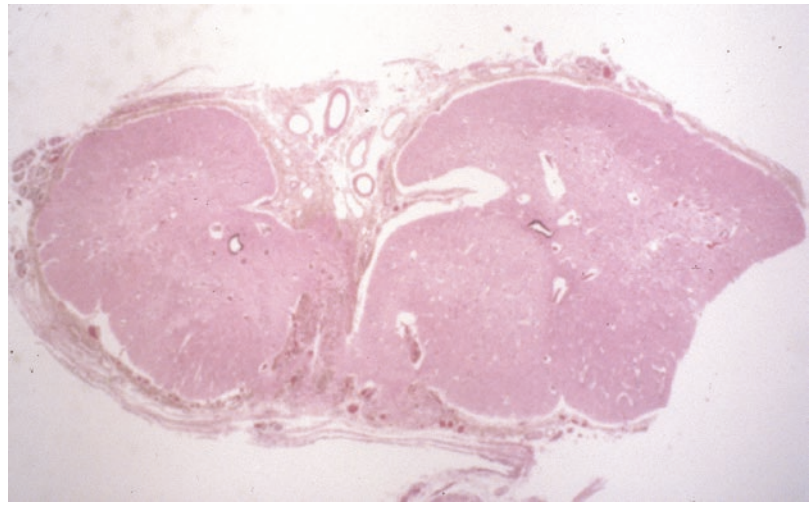

Fig. 11.20 Split cord associated with split cord malformation. Note the central incomplete cleft and small central canal in each hemisection. H&E ×40

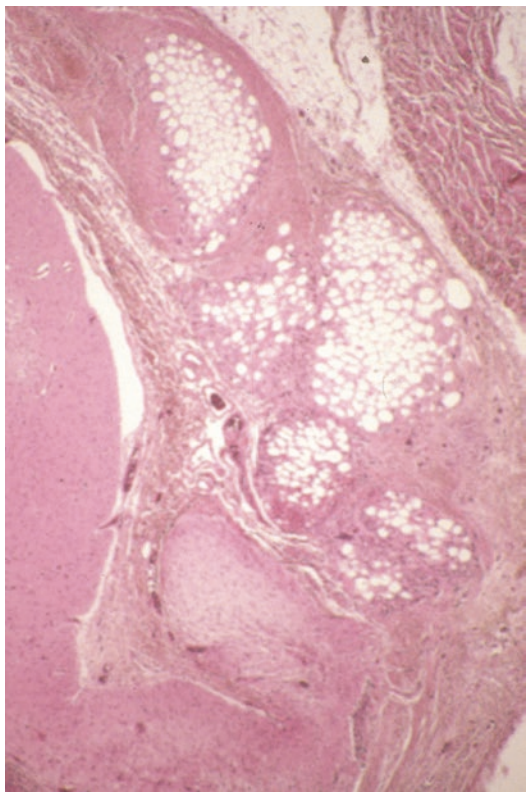

Fig. 11.21 Prominent fat deposits in mesenchymal tissue adjacent to dysplastic spinal cord in left field. Dura is located on right side. H&E ×100

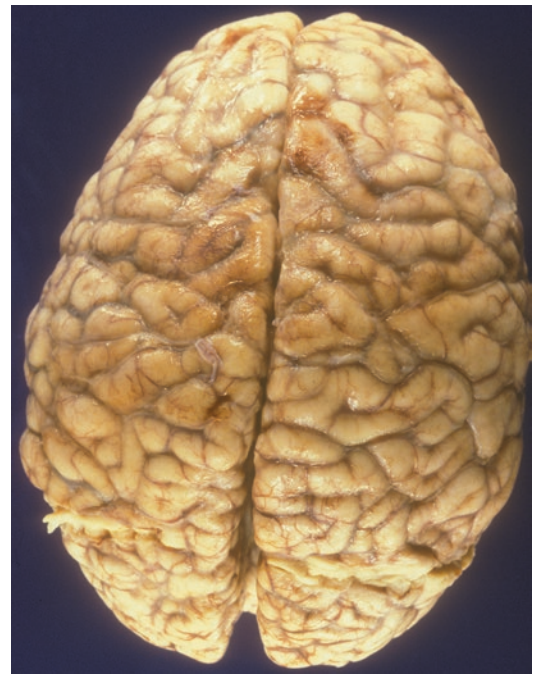

Fig. 11.22 Cerebrum of child with Chiari II malformation displaying polygyria. In this situation there appears to be an excessive number of gyri, but the cortex has a normal six-layered architecture

mal heterotopic nodules, maldevelopment of basal ganglia, and agenesis of the corpus callosum; rarely the olfactory bulbs and tracts are agenetic (Figs. 11.22, 11.23, and 11.24). Aside from these, a host of associated abnormalities has been described in individual cases.

In contrast, most defects of the cerebellum and brain stem, which initially captured the attention of Cleland and Chiari, are not primary malformations, but are consequent to the bony

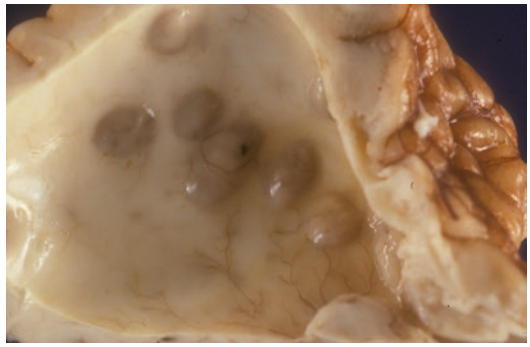

Fig. 11.23 Dilated ventricle containing multiple subependymal heterotopias

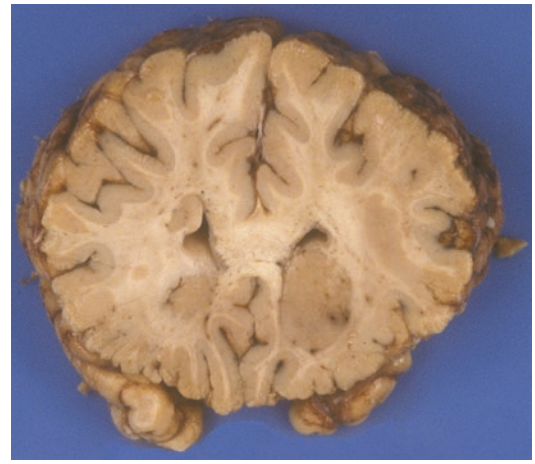

Fig. 11.24 Coronal section of cerebrum at level of corpus striatum. Note dysplasia of striatal nuclei on left and periventricular heterotopia on same side

defects of the posterior fossa, foramen magnum, and tentorial hypoplasia.

Those involving the cerebellum consist of both caudal and rostral herniation of the vermis often in combination with overall hypoplasia. Cerebellar tissue that descends into the spinal canal is vermian but in some instances may also include tonsils. The herniated cerebellum forms a peg on the surface of the spinal cord (Fig. 11.25). It is sometimes difficult to separate the cerebellar from the spinal tissues, as fibrotic leptomeninges may bind them together. In rare cases, a frank cerebellar malformation, rhombencephalosynapsis, may be present. In this defect, the cerebellar hemispheres and dentate nuclei are fused, as the entire vermis is absent.

As the posterior fossa is hypoplastic, herniation of superior vermis rostrally encroaches into the cranial cavity, especially if the tentorium is ill-formed.

Herniated cerebellar folia are often necrotic/sclerotic as the blood supply is compromised secondary to the corking effect caused by herniation of the soft tissue through the bony ring of the foramen magnum or, if rostral, by the rigid leaves of the tentorium (Fig. 11.26).

The majority of brain stem defects are also secondary to inadequate space in the posterior fossa. The brain stem is elongated hence has a smaller transverse diameter than normal. A beak-shaped deformity of the quadrigeminal plate is often present (Fig. 11.27). The displaced brain stem structures carry with them the aqueduct, fourth ventricle, and outlet foramina of the fourth ventricle—namely, the foramina of Luschka and Magendie.

Displacement of the brain stem into the cervical spinal canal also leads to elongation and rostral orientation of the cranial and cervical spinal nerve roots (Fig. 11.25b).

Microscopic abnormalities are found at all levels. Aside from those in spinal cord associated with the meningomyeloceles, there may be hydromyelia and/or syringomyelia at levels rostral to the sac and its anomalous contents.

Brain stem lesions include syringobulbia, hypoaplasia of olivary nuclei, hypoplasia of cranial nerve nuclei, and hypoplasia of tegmental or basal pontine nuclei [25]. Microscopic dysplasias are commonly found in cerebella of individuals of any age but are most abundant in infants [26] and have also been identified in these cases but they have no established clinical significance.

On the other hand, remarkable are relatively common dysplasias of cerebral cortex with or without subependymal or white matter heterotopias [25]. These fall into the general category of migration disorders about which there is a wealth of information relating these to a variety of gene defects [27].

In view of the common association of hydrocephalus with Chiari II, it is of importance to examine the morphological foundation for this

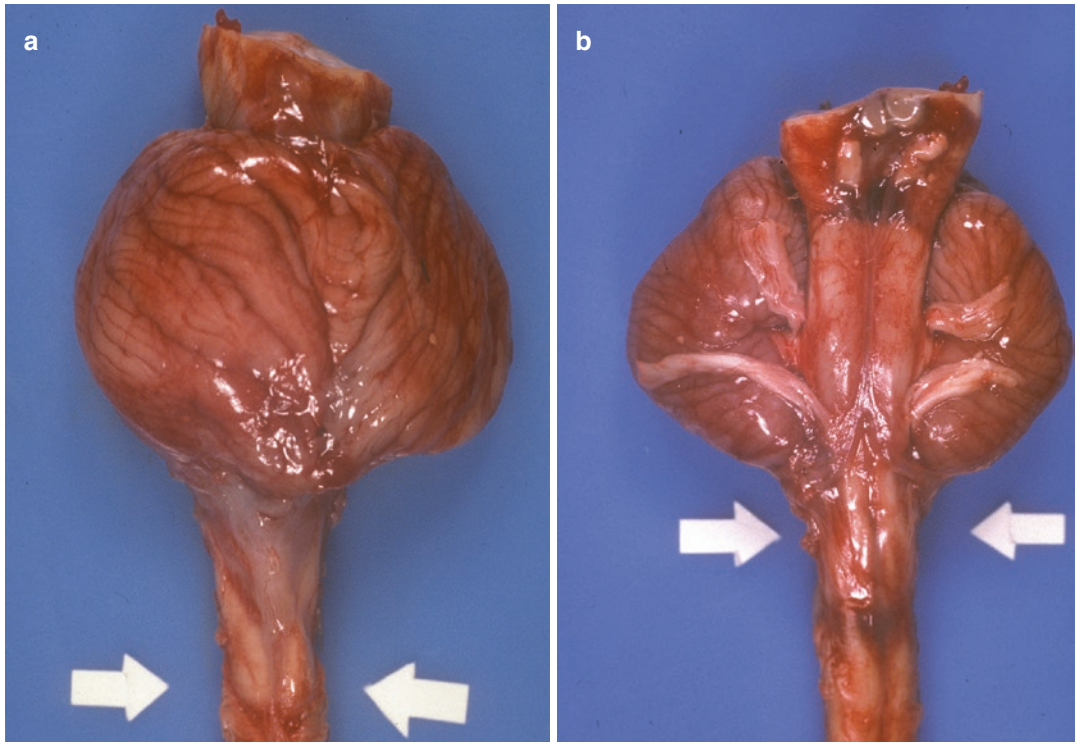

Fig. 11.25 (**a**) Dorsal view of the cerebellum and spinal cord of infant with Chiari II malformation. Note the tongue of vermis that obscures several levels of cervical cord (arrows). (**b**) Ventral view of the same specimen displaying elongated, compressed brain stem, which exhibits a redundant fold over the ventral aspect of the cervical cord (arrows). Note the cephalad orientation of nerve roots

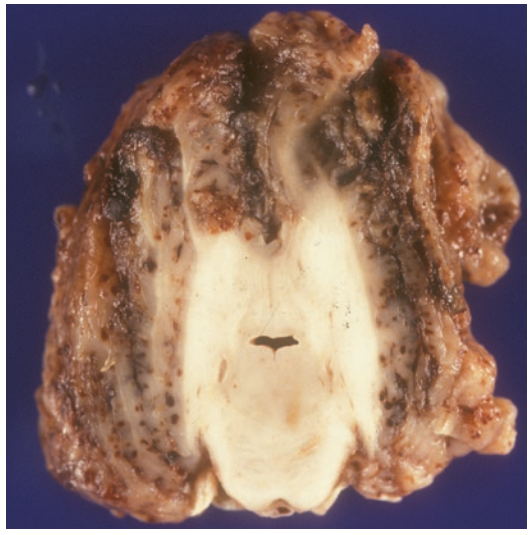

Fig. 11.26 Transverse section through midpons and cerebellum showing compression of pons and fourth ventricle and hemorrhagic necrosis of cerebellum consequent to compromise of vascular flow

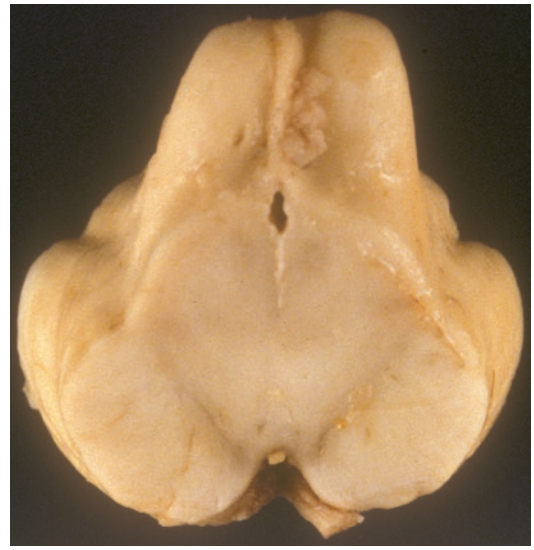

Fig. 11.27 Beaking of collicular plate of infant with Chiari II defect

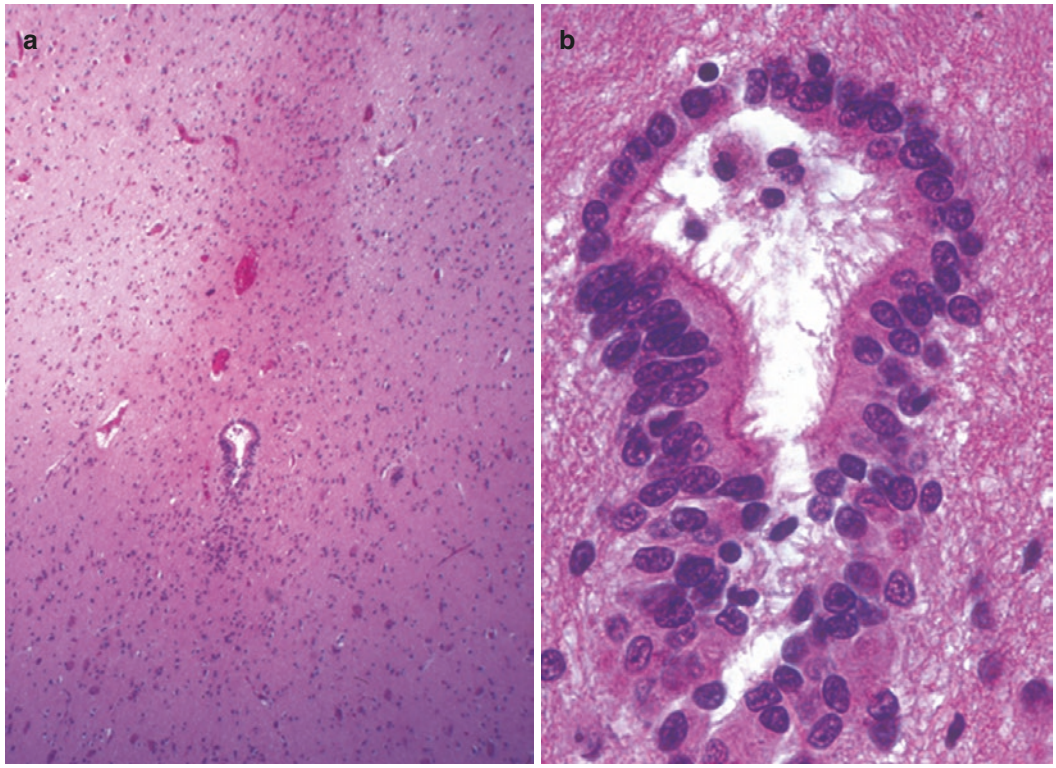

Fig. 11.28 (**a**) Transverse section of the midbrain through level of aqueduct. Note the isolated tiny channel in the center of field. H&E ×40. (**b**) High magnification of hypoplastic aqueduct shown in (**a**). Note the normally formed structure with tiny lumen. H&E ×400

phenomenon. One obvious explanation is obstruction of the fourth ventricular outlet foramina consequent to the corking effects caused by herniation of brain stem and cerebellum into the upper cervical canal.

However, the flow of cerebrospinal fluid may be impeded rostral to these foramina. For example, crowding of posterior fossa structures may be sufficiently severe to produce stenosis of the fourth ventricle.

The most common problematic region, however, is the aqueduct of Sylvius in the midbrain. Major contributions to elucidation of the pathoanatomy have been made by Russell [28] and Alvord [29], in particular, and much of this discussion is based upon their studies.

The aqueduct is not a straight tube but is slightly curved along its path from the posterior third ventricle to the iter at the level of the rostral pons. Its length and transverse diameter naturally change from infancy to adulthood. Suffice it to say that even a small deviation from normal may produce impedance to flow. Aqueductal abnormalities associated with inadequate flow have been separated into hypoplasia, forking, and stenosis.

Stenosis is basically an acquired condition consequent to inflammation.

The other two, namely, hypoplasia and forking, however, are commonly found in this condition and regarded as malformations, although Williams has suggested that they are produced by compression of enlarged ventricles [30]. Hypoplasia refers to a mean diameter below the lower limit of normal range. In practice, it is a qualitative judgment on the part of a radiologist evaluating this region by magnetic resonance

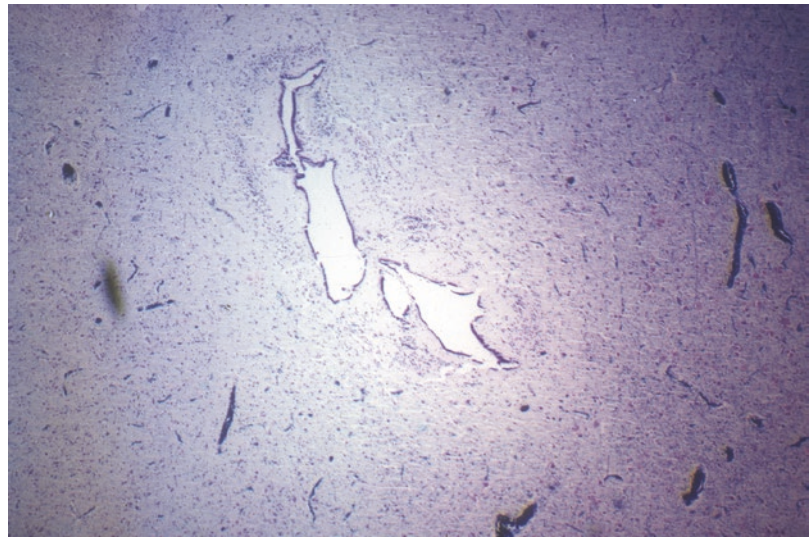

Fig. 11.29 Transverse section through the midbrain showing forking defect. Note two separate channels separated by normal neural tissue. H&E ×250

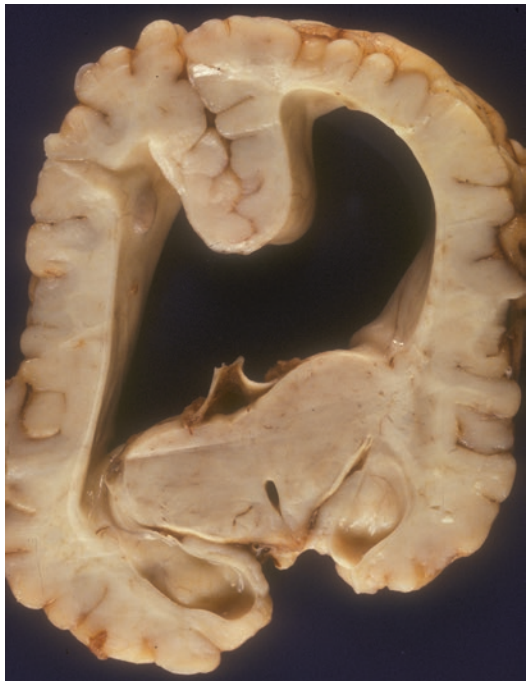

Fig. 11.30 Coronal section through the cerebrum of infant with Chiari II defect in which foramina of Monro are absent, the third ventricle is hypoplastic, thalami are almost totally fused, and lateral ventricles are massively enlarged

imaging (MRI) or a pathologist who examines the midbrain tissue postmortem (Fig. 11.28).

The forking defect consists of two or more ependymal canals in the midline (of the midbrain) separated by normal neural tissue. The dorsal channel tends to be larger and may be branched, whereas the ventral channel is simply a slit-like opening. One or the other of these channels communicates with the ventricle, whereas the others have blind pouches (Fig. 11.29).

Rarely, obstruction of CSF flow is caused by atresia of the foramina of Monro (Fig. 11.30) or hypoplasia of the third ventricle (Fig. 11.31). In these defects, the thalami are fused, and ventricular dilatation is confined to the lateral ventricles.

Reflections on the Basic Nature of Chiari I and II

This brief review of the pathological features of Chiari I and II forces the conclusion that the cerebellar component of each is, in most cases, not a primary malformation of this part of the brain, but is secondary to a malformation of bones forming the posterior fossa.

With the exception of cases in which there is cerebellar hypoplasia or rhombencephalosynapsis, frankly dysplastic cerebellar tonsils, or Lhermitte-Duclos malformation, the herniation and associated foliar sclerosis are clearly a consequence of inadequate space and other abnormalities of the posterior fossa. Specifically, the malformation in Chiari I in most cases is not a primary cerebellar defect, but a consequence of the bone abnormalities of the posterior fossa.

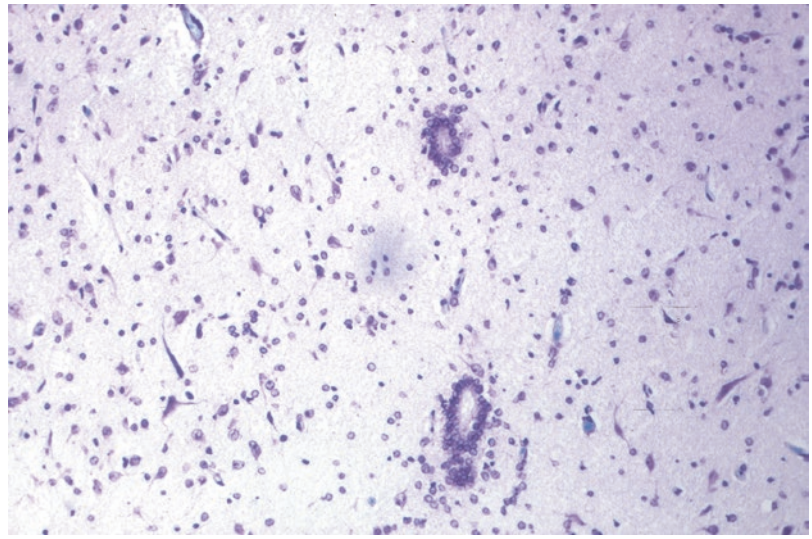

Fig. 11.31 Two small ependymal canals are the only evidence of the third ventricle in infant with Chiari II defect

The constellation of abnormalities at all levels of the neuraxis associated with Chiari II presents a more complex problem. Critical consideration of the diverse lesions allows separation into those which qualify as primary developmental defects and a second group of lesions that arise consequent to those malformations.

Primary malformations include the following: (1) skull defects of both membranous and endochondral bones; (2) spinal dysraphism involving bone, other mesenchymal, and neural tissues; (3) brain stem neuronal aplasia/hypoplasia; (4) agenesis of corpus callosum; and (5) cerebral migration disorders. Whether aqueductal/third ventricular hypoplasia/atresia is developmental or acquired abnormalities is unclear.

Acquired abnormalities include the following: (1) rostral and caudal herniation of brain stem and cerebellum, (2) syringobulbia/myelia, (3) cerebellar sclerosis, (4) infarction of cerebellum and/or brain stem, and (5) hydrocephalus.

Under the circumstances, it seems that the essential basis for Chiari I consists of abnormalities of the skull not cerebellar development. Many of the cerebellar defects associated with Chiari II are also consequent to hypoplasia of the posterior fossa, but this is a considerably more complex developmental disorder that affects all levels of the neuraxis. Thus, to focus strictly on the cerebellar component is misleading.

References

1. Chiari H. Ueber Veränderungen des Kleinhirns infolge von Hydrocephalie des Grosshirns. Deutsche Mediziner Wochenschrift. 1891;17:1172–5.
2. Chiari H. Veränderungen des Kleinhirns, des Pons und der Medulla oblongata in Folge von congenitaler Hydrocephalie des Grosshirns. Denkschrift Akad Wiss Wien. 1896;63:71–116.
3. Garg K, Malik N, Jaiswol AK, Behari S. Chiari III malformation with hypertelorism and microcephaly in a neonate: case report and a review of the literature. J Pediatr Neurosci. 2008;31:169–71.
4. Friede RL. Developmental neuropathology. 2nd ed. Berlin: Springer; 1989. p. 271–3.
5. Cushing H. Some experimental and clinical observations concerning states of increased intracranial tension. Am J Med Sci. 1902;124:375–400.
6. Collier J. The false localizing signs of intracranial tumour. Brain. 1904;27:490–508.
7. Spillane JD, Pallis C, Jones AM. Developmental abnormalities in the region of the foramen magnum. Brain. 1957;80:11–48.
8. Sandbank U. Le syndrome d'Arnold-Chiari. Contribution Clinique et neuro-pathologique par l' etude de quatre cas infantiles. Rev Neurol (Paris). 1955;93:529–63.
9. Nyland H, Krogness KG. Size of posterior fossa in Chiari type I malformation in adults. Acta Neurochir. 1978;40:233–42.

10. Trigylidas T, Baronia B, Vassilyadi M, et al. Posterior fossa dimension and volume estimates in pediatric patients with Chiari I malformations. Childs Nerv Syst. 2008;24:329–36.
11. List CF. Neurological syndrome accompanying developmental anomalies of occipital bone, atlas and axis. Arch Neurol Psychiatr. 1941;45:577–616.
12. Mohr PD, Strang FA, Sambrook MA, et al. The clinical and surgical features of 40 patients with primary cerebellar ectopia (adult Chiari malformation). Q J Med. 1977;181:85–96.
13. Shady W, Metcalfe RA, Butler P. The incidence of cranio-cervical bony anomalies in the adult Chiari malformation. J Neurol Sci. 1987;82:193–203.
14. Harding BN, Copp AJ. Malformations. In: Love S, Louis DN, Ellison DW, editors. Greenfield's neuropathology. 8th ed. London: Hodder Arnold; 2008. p. 365.
15. Lhermitte J, Duclos P. Sur un ganglioneurome diffus du cortex du cervelet. Bull Assoc Fr Etud Cancer. 1920;9:99–107.
16. Van Calenbergh F, Vantomme N, Flamen P, et al. Lhermitte-Duclos disease: C-methionine positron emission tomography data in 4 patients. Surg Neurol. 2006;65:293–6.
17. Shaw C-M, Alvord EC Jr. Hydrocephalus. In: Duckett S, editor. Pediatric neuropathology. Baltimore: Williams and Wilkins; 1995. p. 168–78.
18. Brocklehurst G. Spina bifida. In: Vinken PJ, Bruyn GW, editors. Handbook of clinical neurology, Vol 32. Congenital malformation of the spine and spinal cord. Amsterdam: North Holland Publishing Co; 1978. p. 519–78.
19. Cleland J. Contribution to the study of spina bifida, encephalocele, and anencephalus. J Anat Physiol. 1883;17:257–92.
20. Arnold J. Myelocele, Transportation von Gewebskeimen und Sympodie. Beitr Path Anat. 1894;16:1–28.
21. Tajima M, Yamada MB, Kageyama N. Cranio-lacunca in newborn with myelomeningocele. Childs Brain. 1977;3:297–303.
22. Chen C-Y, Zimmerman RA. Congenital brain anomalies. In: Zimmerman RA, Gibby WA, Carmody RF, editors. Neuroimaging clinical and physical principles. New York: Springer; 1997. p. 1279.
23. Chen C-Y, Zimmerman RA. Congenital brain anomalies. In: Zimmerman RA, Gibby WA, Carmody RF, editors. Neuroimaging clinical and physical principles. New York: Springer; 1997. p. 500.
24. Chen C-Y, Zimmerman RA. Congenital brain anomalies. In: Zimmerman RA, Gibby WA, Carmody RF, editors. Neuroimaging clinical and physical principles. New York: Springer; 1997. p. 1274.
25. Gilbert JN, Jones KL, Rorke LB, et al. Central nervous system anomalies associated with meningomyelocele, hydrocephalus, and the Arnold-Chiari malformation: reappraisal of theories regarding the pathogenesis of posterior neural tube closure defects. Neurosurgery. 1986;18:559–64.
26. Rorke LB, Fogelson MH, Riggs HE. Cerebellar heterotopia in infancy. Dev Med Child Neurol. 1968;10:644–50.
27. Rorke LB. A perspective: the role of disordered genetic control in neurogenesis in the pathogenesis of migration disorders. J Neuropathol Exp Neurol. 1994;53:105–17.
28. Russell DS. Observations on the pathology of hydrocephalus. Medical Research Council Special Report Series No. 265. London: Her Majesty's Stationery Office, 4th impression (1949); 1968.
29. Alvord EC Jr. Observations on the pathology of hydrocephalus. In: Fields WS, Desmond MM, eds. Springfield: Charles C. Thomas; 1961:343.
30. Williams B. Is aqueduct stenosis a result of hydrocephalus? Brain. 1973;96:399–412.

12 Research on the Pathophysiology of Chiari I-Related Symptoms and Syringomyelia, with Emphasis on Dynamic MRI Techniques

Joyce Koueik, Bryn A. Martin, and Bermans J. Iskandar

Introduction

Much of the Chiari literature is riddled with questions, but scarcely any answers have emerged since the time of Gardner and Williams. What causes a Chiari I malformation? If it is a mesodermal problem resulting in abnormal bone development, then why do acquired Chiari malformations exist? How important is the cerebellar tonsil morphology? If the tonsils are considered essential for a diagnosis of a Chiari I malformation, then what explains the Chiari 0? Why do symptoms arise in some patients but not in others, although the magnetic resonance images (MRI) seem identical? And why does syringomyelia exist in some but not in others? Which is the best surgical Chiari decompression technique? How wide should the decompression be? Should the tonsils be reduced? Why are some of the symptoms typical and others "crazy"? Why do children fare better than adults? Why are some Chiari malformations inherited and others not?

Serious multidisciplinary research efforts should be undertaken if any of these questions is to be answered. Research from the Bernard Williams days was limited to clinical observations, basic mechanical modeling, and invasive techniques of cranial and spinal pressure monitoring [1, 2]. The advent of MRI, computer technology, and molecular biology has radically changed both perspective and prospects. Pathophysiological theories can now be tested, not just hypothesized. Invasive procedures have been, for all practical purposes, replaced with noninvasive technology. Probably the most important—certainly the most used—of these technologies is the ability to track cerebrospinal fluid (CSF) flow through dynamic MRI, quantify it, and analyze it using software programs. In this chapter, we will not address research on the embryology or pathophysiology of the Chiari malformation itself, as this is covered elsewhere in the text. Instead, we will review research efforts that ask how the Chiari malformation causes clinical problems and syringomyelia. Such efforts have been productive, in large part, due to collaborative efforts among neurosurgeons, radiologists, engineers, and physicists. The chapter starts with an overview of previously proposed theories of syringomyelia formation and concludes with an examination of present-day tools used to explore the pathogenesis of

J. Koueik
Department of Neurological Surgery, University of Wisconsin Hospital and Clinics, Madison, WI, USA

B. A. Martin
Department of Biological Engineering, University of Idaho, Neurophysiological Imaging and Modeling Laboratory, Moscow, ID, USA

B. J. Iskandar (✉)
Department of Neurological Surgery, Pediatric Neurosurgery, University of Wisconsin, Madison, WI, USA
e-mail: iskandar@neurosurgery.wisc.edu

R. S. Tubbs et al. (eds.), *The Chiari Malformations*, https://doi.org/10.1007/978-3-030-44862-2_12

clinical (symptoms and signs) and imaging (syringomyelia) findings in patients with the Chiari I malformation. This will consist primarily of a review of dynamic MRI flow imaging, followed by a brief overview of other propitious research efforts aimed at understanding this enigmatic anomaly.

Proposed Theories of Syringomyelia Formation

Gardner's Hydrodynamic/Water-Hammer Theory

In 1959, Gardner and Angel suggested that syringomyelia forms because of a persistent opening of the central canal at the obex, in the setting of a closed fourth ventricular outlet foramina [3]. This hypothesis was the basis upon which plugging of the obex was suggested as part of the treatment for syringomyelia. Subsequently, Gardner expanded on his theory to propose that syringomyelia is a result of direct transmission of a CSF pulse through the obex in a "water-hammer" fashion [4, 5]. The theory is based on Bering's assumption that during embryological development, pulsations from the choroid plexus contribute to the expansion of the neural tube. Gardner proposed that these pulsations also help with the development of the arachnoid pathways and suggested that a balance exists between the pulsatile flow in the supratentorial and fourth ventricular choroid plexus. When this balance is disturbed, overactive supratentorial pulsations may result in tentorial migration and the development of a Chiari I malformation. In turn, compression by the posterior fossa structures leads to closure of the fourth ventricular outlet foramina, which forces CSF through the opening at the obex and into the central canal. Gardner proposed that the obstruction would first result in distension of the central canal (hydromyelia), after which the fluid would rupture into the substance of the spinal cord (syringomyelia).

Inconsistencies of Gardner's Theory

Gardner's theory could not explain the following observations [6]: First, if one were to assume that the pathophysiology of syringomyelia is invariable regardless of etiology, the hydrodynamic theory cannot explain cyst formation secondary to trauma, arachnoiditis, tethered cord, etc. Second, this single theory of pathogenesis at the foramen magnum does not account for the syrinx septations that are often evident on MRI. Third, West and Williams [7] showed using ventricular contrast studies that the obex is actually patent in only 10% of patients, thus refuting Gardner's hypothesis. Furthermore, Milhorat and colleagues have suggested that central canal ependymitis can cause an obstruction that results in dilatation of the central canal cephalad to the obstruction. This is based on the observation that CSF can be produced by the ependymal lining of the central canal and the still unproven assumption that CSF normally flows through the central canal [8, 9].

Williams' Modifications of Gardner's Hydrodynamic Theory: The Suck Effect Theory

Based on manometric observations in normal subjects and Chiari I patients, Williams devised a theory that examined syringomyelia from another perspective [10]. Similar to Gardner, he postulated an obstruction at the foramen magnum. However, he theorized that the Chiari I malformation was an acquired anomaly that results from excessive molding of the head, perhaps during delivery through the birth canal, which then causes hindbrain adhesions and related outlet obstruction. In support of this claim, he showed using ventricular contrast that posterior fossa arachnoiditis correlates strongly with a history of difficult birth [7]. Williams hypothesized that hindbrain adhesions can result in transient pressure differentials between the cranial and spinal compartments due to epidural venous congestion, particularly during Valsalva maneuvers (coughing, sneezing, and straining). This, in turn, causes a delay of caudad CSF flow while maintaining normal craniad flow, and as a result, fluid is "sucked from the ventricle into the central canal." Williams provided human manometric measurements demonstrating these pressure dif-

ferentials and showing pressure equilibration postoperatively [11]. However, although this theory is more compelling than Gardner's, it fails to provide an adequate explanation of syringomyelia from other etiologies, and as with Gardner's theory, it assumes a patent opening between the fourth ventricle and central canal [12].

Perivascular Cerebrospinal Fluid Dissection Theory

In an attempt to provide a more unified view of syringomyelia regardless of etiology, Ball and Dayan hypothesized that the impact of the tonsils on the posterior fossa structures results in distortion of the subarachnoid space, which then allows CSF to dissect into the perivascular (Virchow-Robin) spaces and subsequently into the spinal cord parenchyma [13]. Aboulker [14] had a similar theory but thought that CSF dissection occurred via the dorsal roots with extension into the spinal cord.

Oldfield et al. expounded on the perivascular CSF dissection theory by providing favorable observations using various imaging studies [15–17]. They showed that rostrocaudal movement of the spinal cord results in CSF dissection in the subarachnoid space and documented such movement both intraoperatively using ultrasonography, as well as on dynamic MRI studies. Unlike Williams' theory, in which the CSF dissection is driven by Valsalva maneuvers, Oldfield et al. proposed that normal CSF pulsations provide a more or less continuous reason for fluid to enter the spinal cord. They specified that the displaced cerebellar tonsils act like a piston as they are propelled caudally with systole, thus creating a pressure wave within the entrapped subarachnoid space and syrinx. One might consider as supportive evidence of the perivascular CSF dissection mechanism, and specifically Oldfield's piston effect theory, the recent observation of a "presyrinx state," in which spinal cord edema precedes syringomyelia [18, 19]. In addition, animal studies have provided evidence that such fluid flow between the subarachnoid space and the central canal does occur under specific experimental conditions [20, 21], and intraoperative ultrasonic studies have proven the occurrence of cardiac cycle-driven syrinx wall pulsations, which in turn decrease after dural expansion. Furthermore, more recent controversial research emerged, which hypothesizes that resonance between the subarachnoid space and syrinx fluid may be the driving force that causes fluid to enter a syrinx cavity [22]. Yet, the evidence remains incomplete, and others have presented arguments against the piston effect theory, namely, that the mechanism also relies on CSF being forced from the subarachnoid space into the spinal cord, and the exposure of the spinal cord to an outside force would be expected to crush rather than expand a syrinx [12].

Intramedullary Pulse Pressure Theory

Based on animal experiments, Greitz's group developed a theory that suggests that the fluid within a syrinx derives from extracellular fluid forced into the spinal cord from a high-pressure microcirculation rather than high-pressure CSF from the spinal cord subarachnoid space [12, 23, 24]. Specifically, they state that when the subarachnoid space is obstructed from any cause (Chiari I, tumor, arachnoiditis, etc.), there is significant decrease in pressure transmission to the distal CSF spaces and concomitant increased transmission of the systolic CSF pulse pressure into spinal cord parenchyma close to the obstruction. This imbalance of pressures between the spinal cord and subarachnoid space leads to distention of the spinal cord just below the blockage [12, 23, 24]. Furthermore, part of the systolic CSF pulse pressure is "reflected" into the spinal cord at the site of obstruction, also distending the spinal cord above the blockage [12, 25]. The repeated mechanical distention of the cord results in dilatation of the central canal and accumulation of extracellular fluid (of vascular origin) that ultimately coalesces into cavities [12, 23, 24].

In spite of tremendous advancements in technology and considerable effort by many researchers, no single theory has so far definitively solved the enigma of Chiari-related syringomyelia formation.

Cerebrospinal Fluid Flow Studies of the Foramen Magnum

Chiari Symptoms: A Functional Problem?

It has been suggested that the onset of symptoms and the formation of syringomyelia in the case of Chiari I malformation are related, directly or indirectly, to dynamic processes in foramen magnum physiology that are not reflected on static imaging studies. More specifically, it is becoming evident that the extent of tonsillar herniation and size of the posterior fossa (both quantifiable on standard MRI) are not sufficient criteria for determining the symptomatic state of the Chiari patient. Rather, a more "functional" mechanism is at play. Possibilities include subtle chronic craniocervical instability, CSF flow perturbance (central theme of this chapter), cardiac-induced neural tissue deformation, and potentially other craniocervical junction stresses that are yet elusive.

Early Work

A variety of methods have been used to study CSF flow abnormalities with no clear anatomical correlates on static MR imaging. Early on, measurements were made using invasive means. Foremost are the studies by Williams in the late 1970s [26, 27], in which he calculated pressure differentials across the foramen magnum by simultaneously measuring intracranial and intraspinal pressures under a variety of clinical conditions. This allowed the study of pressure gradients at that location and showed that correction of the pressure dissociation is often associated with marked clinical improvement. Such techniques were found to support surgical indications while also providing a means of postoperative evaluation. However, with the advent of MRI, noninvasive approaches have been developed that allow quantification of CSF flow at the foramen magnum and elsewhere in the craniospinal axis.

Cine Magnetic Resonance Imaging

The idea that craniocervical hydrodynamics are altered in patients with Chiari I malformation and the possibility that partial CSF flow obstruction via tonsillar herniation and a small posterior fossa plays a role in the pathophysiology of this entity have guided most of the work in dynamic imaging. Initial applications of MRI to CSF dynamic studies started in the early 1990s. The term *cine* MRI (Fig. 12.1) applies to this modality that evaluates dynamic processes that occur over the cardiac cycle (usually through blood and CSF) rather than static anatomic structures (the brain, dura, bone, etc.) [28].

Early gated spin-echo MRI sequences were used in healthy volunteers to study the movement of the intracranial components and the pulsatile dynamics inside the cranial vault. Early evidence suggested that brain motion occurs in a funnel-shaped fashion as explained by the following: Blood influx into the cranial cavity during systole causes pulsatile propagation of ventricular compression and CSF displacement to the spinal canal, which leads to a complex interplay between the cranial contents—the brain and CSF, both of which are vented through the foramen magnum [29]. When healthy volunteers were studied using cardiac-gated cine MRI, a clear relationship between the cardiac cycle and CSF flow termed "flow-void sign" was detected, which consisted of an area of decreased signal related to CSF flow during systole [30].

Heterogeneity of Cerebrospinal Fluid Flow at the Foramen Magnum

In the early 1990s, Armonda et al. conducted one of the first studies, in which cine MRI results in healthy control subjects were compared to those of Chiari I patients, before and after surgery. The authors studied CSF velocity and flow direction in four particular regions in the craniocervical junction by examining the CSF velocity profile over the cardiac cycle. They found that normal subjects had a short period of CSF flow in the

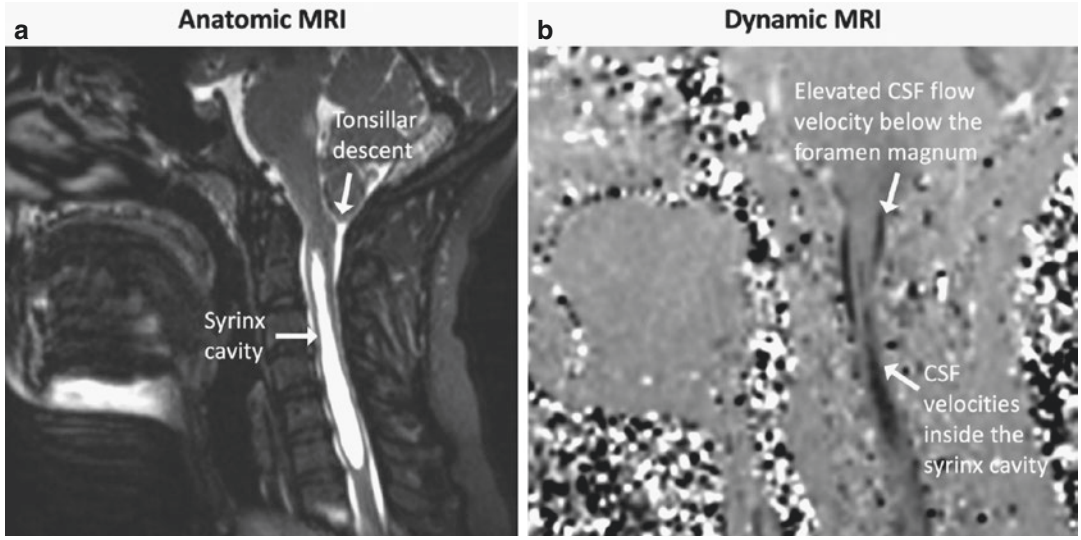

Fig. 12.1 Example of anatomic and quantitative cine MRI from a Chiari malformation patient with syringomyelia. (**a**) Anatomic MRI showing tonsillar descent below the foramen magnum and syrinx cavity within the cervical spinal cord. (**b**) Corresponding dynamic high-speed (128 frames/cardiac cycle [28]) sagittal PC MRI showing hyperdynamic CSF velocities (dark-colored pixels) posterior to the spinal cord below the foramen magnum and hyperdynamic CSF velocities within the syrinx cavity. Maximum CSF velocities encoded to 10 cm/s (black pixels represent craniocaudal-directed CSF velocities)

cranial direction followed by a sustained period of flow in the caudal direction. Conversely, subjects with tonsillar herniation had decreased velocity and obstructed CSF flow pattern with a longer craniad flow phase. In turn, postoperative changes in velocity seemed to mirror those of normal subjects. As the resistance to CSF flow decreased by elimination of the tonsillar herniation, an increase in magnitude and duration of caudad CSF velocity on MRI was observed, accompanied in some cases by syrinx resolution and symptomatic improvement [31].

Combining Invasive and Noninvasive Techniques

Accordingly, it became evident that while static MRI sequences allowed the characterization of anatomical differences between normal controls and Chiari subjects (diameter of the CSF pathways ventral and dorsal to the neural elements at the foramen magnum, syrinx dimensions, size of the lateral ventricles, any evidence of connection between the syrinx and the fourth ventricle, size of the posterior fossa, as well as cerebellar morphology including tonsillar size and displacement), dynamic assessment via phase-contrast imaging provided information that correlates the anatomy with the physiology [32]. This was particularly true with regard to movement of fluid within a syrinx, as well as movement of CSF at the foramen magnum and in the subarachnoid space both ventral and dorsal to the spinal cord [33]. By combining these noninvasive parameters with intraoperative CSF pressure analyses, Heiss et al. [33] were able to experimentally confirm previous hypotheses that tonsillar impaction in a smaller posterior fossa seems to cause partial intermittent occlusion of the subarachnoid space at the foramen magnum. In turn, this occlusion creates a pressure wave that propagates in the spinal subarachnoid space to compress the spinal cord and cause a syrinx to enlarge with every heartbeat. After posterior fossa decompression, craniocervical CSF flow increases, while peak CSF pulse pressure decreases [34], correlating with an eventual decrease in syrinx size [33].

These findings were supported by subsequent in vitro studies conducted by Martin et al. with a flexible spinal cord model that contained a syrinx cavity and an external subarachnoid space stenosis [35].

Cardiac Gating to Improve Magnetic Resonance Signal

Early motion-sensitive MRI techniques (primarily developed for blood flow applications) were plagued by variable signal loss within the cardiac cycle. This was rectified by the addition of cardiac gating. Since CSF flow is pulsatile and synchronous with the cardiac cycle, these technical improvements increased image sensitivity of CSF as well [36]. Cardiac gating was initially applied to routine spin-echo and gradient-echo MRI, which displayed CSF motion as decreased signal intensity resulting from dephasing and washout of moving spins [37].

Cardiac-Gated Phase-Contrast Magnetic Resonance Imaging

Phase-contrast MRI (PC MRI) is a dynamic imaging technique in which signal contrast is generated between flowing and stationary nuclei by sensitizing the phase of transverse magnetization to the velocity of motion. Two data sets with opposite sensitization are acquired. For stationary nuclei, the net phase is zero, which eliminates their signal in the final image, leaving only the residual signal from flowing CSF. The resultant signal contains information that can generate velocity data according to an intensity grayscale. Quantitative CSF velocity and qualitative flow information can be obtained by merging information from two series, usually axial and sagittal planes [38]. Further detailed result analysis using complex cardiac gating can be provided to increase sensitivity.

In spite of the many studies that have used PC MRI to quantify CSF velocities as a potential diagnostic indicator of symptomatic Chiari malformation, it is not yet considered a standard diagnostic procedure. A focus of investigations has been on the magnitude of peak CSF velocities that occur near the foramen magnum since this is the region of tonsillar obstruction and surgical treatment. A number of investigations have shown CSF velocities to be elevated in Chiari malformation patients compared to controls [39, 40], while others showed a reduction or relatively little alterations in CSF velocities compared to controls [41, 42]. Additionally, some studies showed CSF velocities to decrease post-suboccipital decompression surgery [43], and others showed CSF velocities to increase postsurgery [44]. Possible reasons for these discrepancies were discussed in several publications [45] such as the impact of phase-averaging of CSF velocities, spatial resolution of PC MRI sequence including in-plane pixel size and slice thickness, slice location selection relative to the foramen magnum, and eddy current artifacts. Researchers used in vitro models and found PC MRI to potentially have a significant degree of error for velocity detection [46]. In combination, these findings indicate that PC MRI of Chiari malformation shows promise but is sensitive to the methods for which it is applied.

Four-Dimensional Phase-Contrast Magnetic Resonance Imaging

Due to single-slice analysis, two-dimensional (2D) PC MRI has significant limitations. The introduction of four-dimensional phase-contrast MRI (4D PC MRI) technology now allows volumetric assessment of three-dimensional (3D) CSF flow velocities at the foramen magnum and in the spinal canal. This can be obtained with 1-millimeter isotropic resolution in a clinically relevant time frame but requires more sophisticated post-processing software to analyze the 3D velocity field results (Fig. 12.2) [45]. Bunck et al. showed that using single-slice 2D PC MRI, slice location selection could miss the exact location of elevated CSF velocities in Chiari malformation [47]. They showed that usage of 4D PC MRI allowed interrogation of the entire subarachnoid space volume near the craniovertebral junction, and this resulted in detection of more elevated

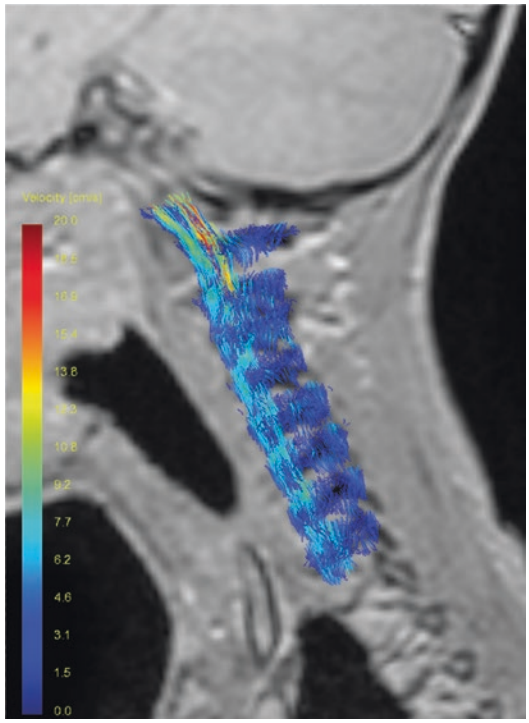

Fig. 12.2 Example of 4D PC MRI measurement of CSF velocities near the foramen in a pediatric Chiari malformation patient. 3D measurement of CSF flow velocities by 4D phase-contrast MRI in a 5-year-old Chiari patient with mild tonsillar descent [45] showing regions of elevated CSF flow velocities on the anterior side of the spinal cord originating from the pontine cistern. (Image courtesy of Alexander Bunck, MD). Full video description is viewable at https://www.youtube.com/watch?v=egjCp5IHXh8. Creative Commons Attribution license

CSF velocities near the point of obstruction [48, 49]. These findings were further supported in research by Yiallourou et al. [45]. As this technique becomes more available and robust, researchers will be better able to study and understand the complex nature of CSF physiology and pathophysiology at the craniocervical junction and in syrinx cavities.

Cerebrospinal Fluid Flow Dynamics and Symptoms

Several cine MRI investigators have proposed that the added value of flow studies is that symptoms may be more related to the degree of CSF obstruction than the degree of tonsillar herniation, which would potentially aid in the selection of patients who are likely to benefit from surgical correction [38, 49]. Unfortunately, although several attempts have been made to determine the differences in flow parameters between symptomatic and asymptomatic Chiari I patients, flow perturbation at the foramen magnum has been unable to fully account for the significant differences in symptomatic states often observed between patients with nearly identical tonsillar anatomy [50]. Another significant factor is that there may be considerable subjectivity in reading cine MRIs. In a 2007 study, in which several neuroradiologists were asked to evaluate the same flow images in a blinded fashion, the authors found that the readers were more likely to agree on the presence of abnormal foramen magnum flow in symptomatic patients than in asymptomatic patients (76% vs. 62%) [51]. However, agreements between pairs of readers were rather low, ranging between 44% and 63%. Of course, one would expect little disagreement when the tonsillar anatomy is very abnormal or nearly normal, with flow that is either severely restricted or near normal, respectively. In such situations, anatomical images clearly reflect the lack or presence of pathology, making flow analysis a less useful adjunct. Accordingly, most disagreements seem to occur in "gray zone" cases, i.e., in patients with moderate flow perturbation. To date, unfortunately, MRI flow analysis has been unsuccessful at separating symptomatic and asymptomatic patients under these conditions [51]. Similar investigations have been conducted to analyze CSF flow in syringomyelia. Although useful information was obtained with regard to flow velocities around the cyst cavity, these studies lacked impact on understanding the pathophysiology of the anomaly or determining the need for surgery [47, 52, 53].

Measuring Intracranial Compliance on Magnetic Resonance Imaging

The utility of PC MRI in the postoperative assessment of the Chiari I patient is illustrated in the

work of Alperin et al., who aimed to visualize and quantify pulsatile blood and CSF flow in the craniospinal region in an effort to derive a system that determines both intracranial compliance (ICC) and intracranial pressure (ICP) before and after posterior fossa decompression. Preliminary data suggested that intracranial compliance, as measured by these investigators, is diminished in Chiari I patients compared to healthy volunteers. Additional research is needed before this effort can result in the identification of an important diagnostic tool for guiding the treatment of patients with the Chiari I malformation [34].

Analyzing Flow Velocity Voxel by Voxel: Bidirectional Flow and Velocity Jets

Analytical techniques using computer algorithms based on cardiac-gated PC MRI images can be used to generate spatial and temporal velocity plots that illustrate the qualitative and quantitative characteristics of particular regions. In a 2004 study, our group analyzed voxel-by-voxel the velocity of CSF throughout the cardiac cycle in both systole and diastole, and corresponding surface contour and time-course color plots were displayed. This work showed that, in Chiari I patients, there was a preponderance of regional flow jets with significant elevations in flow velocity (Fig. 12.3). These jets, which occurred primarily anterior to the spinal cord, comprised only a small percentage of the voxels, which meant that the average flow velocity across the foramen magnum was normal. In addition, select regions within the foramen magnum of Chiari I patients exhibited synchronous bidirectional flow, i.e., CSF that travels simultaneously in the cranial and caudal directions. Such bidirectional flow was absent in volunteer subjects [54, 55]. Similar findings of flow jets were also found in other studies [40, 45, 51]. An excess of 50 qualitative and quantitative parameters was designed to assess the temporal and spatial heterogeneity within the foramen, of which 4 were found to be particularly useful in separating Chiari patients from control subjects. Still, our studies have not so far been able to identify parameters that specifically distinguish between symptomatic and asymptomatic states within the Chiari I population.

Computational Fluid Dynamics

Over the past decade, a number of physicists and engineers in the fields of biomechanics and fluid dynamics showed interest in developing other modern noninvasive methodologies to study Chiari I and syringomyelia. This recent surge in enthusiasm among nonclinicians seems to have resulted largely from a serious effort by the Chiari and syringomyelia societies (The American Syringomyelia and Chiari Alliance Project, The Chiari and Syringomyelia Foundation, Conquer Chiari, and others) to enlarge the scope of research to specialists outside of neurosurgery by providing grant money and forums for discussion. This culminated in several multidisciplinary research conferences, including the CSF Hydrodynamics Symposium held in Zurich (2011), New York (2013), Amiens, France (2015), and Atlanta (2017). These were organized and attended almost exclusively by engineers and physicists. Since that time, the group has formed the CSF Dynamics Society (www.csfdynamics.org). A major part of this effort was spent on applying principles of computational fluid dynamics (CFD) to the Chiari and syringomyelia pathologies (as well as hydrocephalus). This consists of hydrodynamic modeling of the anatomic region of interest (e.g., foramen magnum) and the prediction of physical interactions between its components (Fig. 12.4) [56].

CFD allows detailed quantification of CSF dynamics based on subject-specific anatomical and flow data obtained from MRI measurements. Quantities provided by CFD include CSF jet velocities, flow patterns, and other temporal and spatial parameters that can be considered in combination with anatomical and clinical variations (Chiari I, syringomyelia, and others) [57–59]. The CFD method applies equations from fluid dynamics to simulate CSF flow under normal and pathologic conditions, to provide detailed tempo-

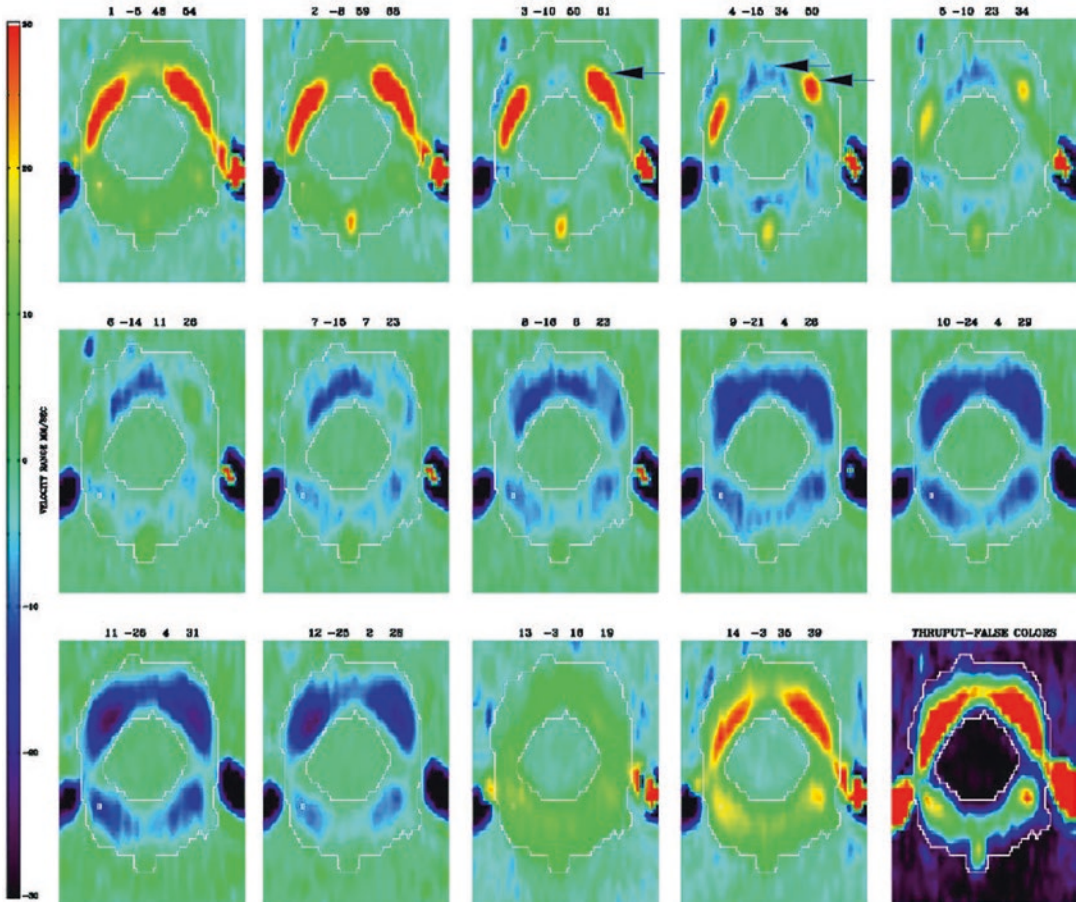

Fig. 12.3 Example of CSF flow velocity plots. Color plot of CSF flow velocity in the foramen magnum of a child with Chiari I malformation. The velocities are color coded and displayed in consecutive images representing 14 time points during the cardiac cycle (last plot represents the throughput). Note that there is a predominance of cephalad flow in seven of the images and caudad flow in the other seven images. This color plot of velocities displays the cephalad velocities in green, yellow, and red, with green being slowest and red being fastest; caudad flow is displayed with light blue, deep blue, and violet/black, with light blue being slowest and violet/black fastest. In children, Chiari I malformation jets (single arrow) of elevated velocities occur in the anterior quadrants of the foramen magnum (note the red color for velocities nearing 10 cm/second). Finally, note the bidirectional flow evident in some of the images (double arrows), in which cephalad and caudad velocities coexist at one time point. Such bidirectionality of flow was not present in healthy (control) subjects

ral and spatial resolution about CSF flow [60, 61]. Such modeling technology can be individualized to the patient's specific parameters [62–64] and could potentially greatly advance the noninvasive armamentarium aimed at improving treatment and surgical planning for Chiari, syringomyelia, and other CSF dyanmics pathologies. Recent studies using patient-specific modeling attempt to compare CFD measurements from patient simulations and healthy subject simulations [50, 65]. Impedance to CSF motion (unsteady resistance) in Chiari I malformation was investigated with promising results utilizing computational fluid dynamics modeling based on subject-specific MRI measurements [50]. The results showed that CSF flow impedance in Chiari I malformation patients presurgery ($n = 17$) was greater than controls (458 ± 62 vs. 237 ± 11 dyn/cm^5, $p < 0.002$) [65] and decreased post-decompression surgery compared to presur-

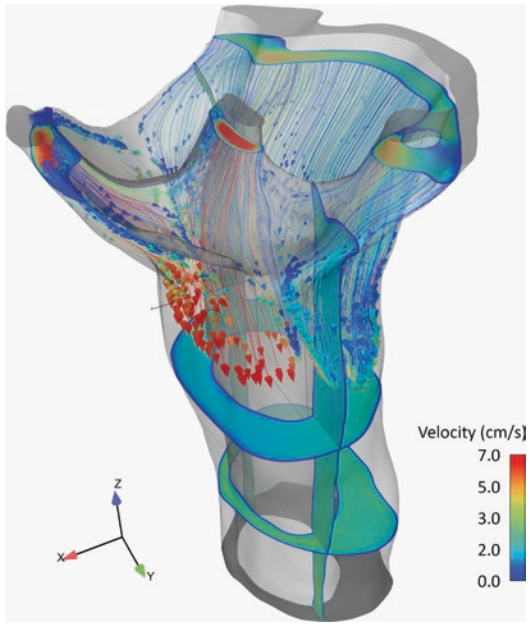

Fig. 12.4 Example of computational fluid dynamics simulation of CSF that included both fluid and tonsillar pulsations with each cardiac beat. CFD simulation based on in vivo MRI measurements from an adult-age Chiari patient with mild tonsillar descent below the foramen magnum [56]. (Figure left, posterior CSF space; right, anterior; arrows show direction and magnitude of velocity streamlines). Full video description is viewable at https://www.youtube.com/watch?v=KHqtsRuHTIk

gery (82 dyn/cm^5 average decrease, $p = 0.016$). However, postsurgery impedance remained greater on average than controls ($p = 0.004$).

Cardiac-Induced Neural Tissue Motion and Deformation

CSF pulses around the brain with each cardiac cycle due to the underlying arterial expansion that occurs within the relatively rigid surrounding structures (skull and meninges). Thus, an alternative dynamic method to help quantify alterations present in Chiari I malformations is to quantify neural tissue motion rather than CSF surrounding the tissue. Motion of the brain tissue can be quantified in terms of bulk motion using PC MRI-derived velocities that are integrated over a region of interest (i.e., cerebellar tonsils or medulla). A PC MRI study conducted by our group supported that bulk spinal cord motion is a diagnostic indicator of symptomatic Chiari I malformation and spinal cord motion decreases post-decompression surgery [66]. Three other publications had similar results, further adding confidence that tissue deformation could be an important biomarker for Chiari I [67–69]. Additionally, Hoffman et al. [70] and Pujol et al. [71] used PC MRI to quantify bulk spinal cord and cerebellar tonsil motion and found that the motion index was elevated in Chiari I malformation patients compared to controls. Similarly, Alperin et al. [72] found spinal cord motion at C2 was elevated. Cousins et al. [73], and another study by our research group [45], also found a similar trend of elevated tissue motion in Chiari patients versus controls.

In addition to bulk motion of the neural tissue, it is possible to obtain a measurement of neural tissue deformation or tension/compression acting on the tissue using displacement encoding with stimulated echoes (DENSE) MRI [74]. Pahlavian et al. and Soellinger et al. used the DENSE technique to quantify the 2D displacement and strain field acting on the brain tissue in healthy subjects within specific regions of interest [75, 76]. In principle, this technique can be used to quantify strain and displacement fields in Chiari I malformation patients, but at present this work has not yet been published.

Conclusions

It is becoming evident that the simple descent of cerebellar tonsils below the foramen magnum may not be sufficient in creating a pathophysiological disturbance that fully explains Chiari I symptoms and syrinx formation. Syringomyelia can develop as a result of foramen magnum abnormalities without obvious tonsillar herniation. In addition, mere tonsillar descent can create flow alterations at the foramen magnum without the onset of either symptoms or syringomyelia. Meaningful advances in research aimed at improving patient care require close correla-

tion between symptom states and imaging advancements. This requires inderdisciplinary research between radiologists, medical physicists/engineers, and neurosurgeons. Novel imaging and simulation tools aimed to improve diagnosis and treatment will derive from these efforts.

References

1. Williams B. Cerebrospinal fluid pressure-gradients in spina bifida cystica, with special reference to the Arnold-Chiari malformation and aqueductal stenosis. Dev Med Child Neurol Suppl. 1975;35:138–50.
2. Williams B. On the pathogenesis of syringomyelia: a review. J R Soc Med. 1980;73(11):798–806.
3. Gardner WJ, Angel J. The mechanism of syringomyelia and its surgical correction. Clin Neurosurg. 1958;6:131–40.
4. Gardner WJ. Syringomyelia. Surg Neurol. 1977;7(6):370.
5. Gardner WJ, McMurray FG. "Non-communicating" syringomyelia: a non-existent entity. Surg Neurol. 1976;6(4):251–6.
6. Pillay PK, Awad IA, Hahn JF. Gardner's hydrodynamic theory of syringomyelia revisited. Cleve Clin J Med. 1991;59(4):373–80.
7. West RJ, Williams B. Radiographic studies of the ventricles in syringomyelia. Neuroradiology. 1980;20(1):5–16.
8. Batzdorf U. Chiari I malformation with syringomyelia. Evaluation of surgical therapy by magnetic resonance imaging. J Neurosurg. 1988;68(5):726–30.
9. Milhorat TH, Kotzen RM. Stenosis of the central canal of the spinal cord following inoculation of suckling hamsters with reovirus type I. J Neurosurg. 1994;81(1):103–6.
10. Williams B. The distending force in the production of "communicating syringomyelia". Lancet. 1969;2(7613):189–93.
11. Williams B. A demonstration analogue for ventricular and intraspinal dynamics (DAVID). J Neurol Sci. 1974;23(3):445–61.
12. Rusbridge C, Greitz D, Iskandar BJ. Syringomyelia: current concepts in pathogenesis, diagnosis, and treatment. J Vet Intern Med. 2006;20(3):469–79.
13. Ball MJ, Dayan AD. Pathogenesis of syringomyelia. Lancet. 1972;2(7781):799–801.
14. Aboulker J. Syringomyelia and intra-rachidian fluids. V. Syringomyeliac cavities with low power. Neurochirurgie. 1979;25(Suppl 1):38–54.
15. Lonser RR, Heiss JD, Oldfield EH. Syringomyelia, hemangioblastomas, and Chiari I malformation. Case illustration. J Neurosurg. 1999;90(1):169.
16. Oldfield EH, Muraszko K, Shawker TH, Patronas NJ. Pathophysiology of syringomyelia associated with Chiari I malformation of the cerebellar tonsils. Implications for diagnosis and treatment. J Neurosurg. 1994;80(1):3–15.
17. Oldfield EH. Syringomyelia. J Neurosurg. 2001;95(1 Suppl):153–5.
18. Fischbein NJ, Dillon WP, Cobbs C, Weinstein PR. The "presyrinx" state: a reversible myelopathic condition that may precede syringomyelia. AJNR Am J Neuroradiol. 1999;20(1):7–20.
19. Levy EI, Heiss JD, Kent MS, Riedel CJ, Oldfield EH. Spinal cord swelling preceding syrinx development. Case report. J Neurosurg. 2000;92(1 Suppl):93–7.
20. Stoodley MA, Brown SA, Brown CJ, Jones NR. Arterial pulsation-dependent perivascular cerebrospinal fluid flow into the central canal in the sheep spinal cord. J Neurosurg. 1997;86(4):686–93.
21. Stoodley MA, Jones NR, Brown CJ. Evidence for rapid fluid flow from the subarachnoid space into the spinal cord central canal in the rat. Brain Res. 1996;707(2):155–64.
22. Egnor M, Rosiello A, Zheng L. A model of intracranial pulsations. Pediatr Neurosurg. 2001;35(6):284–98.
23. Greitz D. Unraveling the riddle of syringomyelia. Neurosurg Rev. 2006;29(4):251–63; discussion 64.
24. Josephson A, Greitz D, Klason T, Olson L, Spenger C. A spinal thecal sac constriction model supports the theory that induced pressure gradients in the cord cause edema and cyst formation. Neurosurgery. 2001;48(3):636–45; discussion 45–6.
25. Carpenter PW, Berkouk K, Lucey AD. Pressure wave propagation in fluid-filled co-axial elastic tubes. Part 2: mechanisms for the pathogenesis of syringomyelia. J Biomech Eng. 2003;125(6):857–63.
26. Williams B. Cerebrospinal fluid pressure changes in response to coughing. Brain. 1976;99(2):331–46.
27. Williams B. Chronic herniation of the hindbrain. Ann R Coll Surg Engl. 1981;63(1):9–17.
28. Kalata W, Martin BA, Oshinski JN, Jerosch-Herold M, Royston TJ, Loth F. MR measurement of cerebrospinal fluid velocity wave speed in the spinal canal. IEEE Trans Biomed Eng. 2009;56(6):1765–8.
29. Greitz D, Wirestam R, Franck A, Nordell B, Thomsen C, Stahlberg F. Pulsatile brain movement and associated hydrodynamics studied by magnetic resonance phase imaging. The Monro-Kellie doctrine revisited. Neuroradiology. 1992;34(5):370–80.
30. Citrin CM, Sherman JL, Gangarosa RE, Scanlon D. Physiology of the CSF flow-void sign: modification by cardiac gating. AJR Am J Roentgenol. 1987;148(1):205–8.
31. Armonda RA, Citrin CM, Foley KT, Ellenbogen RG. Quantitative cine-mode magnetic resonance imaging of Chiari I malformations: an analysis of cerebrospinal fluid dynamics. Neurosurgery. 1994;35(2):214–23; discussion 23–4.
32. Shaffer N, Martin B, Loth F. Cerebrospinal fluid hydrodynamics in type I Chiari malformation. Neurol Res. 2011;33(3):247–60.
33. Heiss JD, Patronas N, DeVroom HL, Shawker T, Ennis R, Kammerer W, et al. Elucidating the

pathophysiology of syringomyelia. J Neurosurg. 1999;91(4):553–62.
34. Alperin N, Sivaramakrishnan A, Lichtor T. Magnetic resonance imaging-based measurements of cerebrospinal fluid and blood flow as indicators of intracranial compliance in patients with Chiari malformation. J Neurosurg. 2005;103(1):46–52.
35. Martin BA, Labuda R, Royston TJ, Oshinski JN, Iskandar B, Loth F. Spinal subarachnoid space pressure measurements in an in vitro spinal stenosis model: implications on syringomyelia theories. J Biomech Eng. 2010;132(11):111007.
36. Nitz WR, Bradley WG Jr, Watanabe AS, Lee RR, Burgoyne B, O'Sullivan RM, et al. Flow dynamics of cerebrospinal fluid: assessment with phase-contrast velocity MR imaging performed with retrospective cardiac gating. Radiology. 1992;183(2):395–405.
37. Connor SE, O'Gorman R, Summers P, Simmons A, Moore EM, Chandler C, et al. SPAMM, cine phase contrast imaging and fast spin-echo T2-weighted imaging in the study of intracranial cerebrospinal fluid (CSF) flow. Clin Radiol. 2001;56(9):763–72.
38. Battal B, Kocaoglu M, Bulakbasi N, Husmen G, Tuba Sanal H, Tayfun C. Cerebrospinal fluid flow imaging by using phase-contrast MR technique. Br J Radiol. 2011;84(1004):758–65.
39. Shah S, Haughton V, del Rio AM. CSF flow through the upper cervical spinal canal in Chiari I malformation. AJNR Am J Neuroradiol. 2011;32(6):1149–53.
40. Struck AF, Haughton VM. Idiopathic syringomyelia: phase-contrast MR of cerebrospinal fluid flow dynamics at level of foramen magnum. Radiology. 2009;253(1):184–90.
41. Krueger KD, Haughton VM, Hetzel S. Peak CSF velocities in patients with symptomatic and asymptomatic Chiari I malformation. AJNR Am J Neuroradiol. 2010;31(10):1837–41.
42. Wang CS, Wang X, Fu CH, Wei LQ, Zhou DQ, Lin JK. Analysis of cerebrospinal fluid flow dynamics and morphology in Chiari I malformation with cine phase-contrast magnetic resonance imaging. Acta Neurochir. 2014;156(4):707–13.
43. Dolar MT, Haughton VM, Iskandar BJ, Quigley M. Effect of craniocervical decompression on peak CSF velocities in symptomatic patients with Chiari I malformation. AJNR Am J Neuroradiol. 2004;25(1):142–5.
44. McGirt MJ, Atiba A, Attenello FJ, Wasserman BA, Datoo G, Gathinji M, et al. Correlation of hindbrain CSF flow and outcome after surgical decompression for Chiari I malformation. Childs Nerv Syst. 2008;24(7):833–40.
45. Yiallourou TI, Kroger JR, Stergiopulos N, Maintz D, Martin BA, Bunck AC. Comparison of 4D phase-contrast MRI flow measurements to computational fluid dynamics simulations of cerebrospinal fluid motion in the cervical spine. PLoS One. 2012;7(12):e52284.
46. Wentland AL, Wieben O, Korosec FR, Haughton VM. Accuracy and reproducibility of phase-contrast MR imaging measurements for CSF flow. AJNR Am J Neuroradiol. 2010;31(7):1331–6.
47. Bunck AC, Kroeger JR, Juettner A, Brentrup A, Fiedler B, Crelier GR, et al. Magnetic resonance 4D flow analysis of cerebrospinal fluid dynamics in Chiari I malformation with and without syringomyelia. Eur Radiol. 2012;22(9):1860–70.
48. Bunck AC, Kroger JR, Juttner A, Brentrup A, Fiedler B, Schaarschmidt F, et al. Magnetic resonance 4D flow characteristics of cerebrospinal fluid at the craniocervical junction and the cervical spinal canal. Eur Radiol. 2011;21(8):1788–96.
49. McGirt MJ, Nimjee SM, Fuchs HE, George TM. Relationship of cine phase-contrast magnetic resonance imaging with outcome after decompression for Chiari I malformations. Neurosurgery. 2006;59(1):140–6; discussion -6.
50. Martin BA, Kalata W, Shaffer N, Fischer P, Luciano M, Loth F. Hydrodynamic and longitudinal impedance analysis of cerebrospinal fluid dynamics at the craniovertebral junction in type I Chiari malformation. PLoS One. 2013;8(10):e75335.
51. Hofkes SK, Iskandar BJ, Turski PA, Gentry LR, McCue JB, Haughton VM. Differentiation between symptomatic Chiari I malformation and asymptomatic tonsilar ectopia by using cerebrospinal fluid flow imaging: initial estimate of imaging accuracy. Radiology. 2007;245(2):532–40.
52. Brugieres P, Idy-Peretti I, Iffenecker C, Parker F, Jolivet O, Hurth M, et al. CSF flow measurement in syringomyelia. AJNR Am J Neuroradiol. 2000;21(10):1785–92.
53. Mauer UM, Gottschalk A, Mueller C, Weselek L, Kunz U, Schulz C. Standard and cardiac-gated phase-contrast magnetic resonance imaging in the clinical course of patients with Chiari malformation Type I. Neurosurg Focus. 2011;31(3):E5.
54. Iskandar BJ, Quigley M, Haughton VM. Foramen magnum cerebrospinal fluid flow characteristics in children with Chiari I malformation before and after craniocervical decompression. J Neurosurg. 2004;101(2 Suppl):169–78.
55. Quigley MF, Iskandar B, Quigley ME, Nicosia M, Haughton V. Cerebrospinal fluid flow in foramen magnum: temporal and spatial patterns at MR imaging in volunteers and in patients with Chiari I malformation. Radiology. 2004;232(1):229–36.
56. Heidari Pahlavian S, Yiallourou T, Tubbs RS, Bunck AC, Loth F, Goodin M, et al. The impact of spinal cord nerve roots and denticulate ligaments on cerebrospinal fluid dynamics in the cervical spine. PLoS One. 2014;9(4):e91888.
57. Clarke EC, Fletcher DF, Stoodley MA, Bilston LE. Computational fluid dynamics modelling of cerebrospinal fluid pressure in Chiari malformation and syringomyelia. J Biomech. 2013;46(11):1801–9.

58. Lloyd RA, Fletcher DF, Clarke EC, Bilston LE. Chiari malformation may increase perivascular cerebrospinal fluid flow into the spinal cord: a subject-specific computational modelling study. J Biomech. 2017;65:185–93.
59. Stoverud KH, Langtangen HP, Ringstad GA, Eide PK, Mardal KA. Computational investigation of cerebrospinal fluid dynamics in the posterior cranial fossa and cervical subarachnoid space in patients with Chiari I malformation. PLoS One. 2016;11(10):e0162938.
60. Hentschel S, Mardal KA, Lovgren AE, Linge S, Haughton V. Characterization of cyclic CSF flow in the foramen magnum and upper cervical spinal canal with MR flow imaging and computational fluid dynamics. AJNR Am J Neuroradiol. 2010;31(6):997–1002.
61. Loth F, Yardimci MA, Alperin N. Hydrodynamic modeling of cerebrospinal fluid motion within the spinal cavity. J Biomech Eng. 2001;123(1):71–9.
62. Linge SO, Mardal KA, Haughton V, Helgeland A. Simulating CSF flow dynamics in the normal and the Chiari I subarachnoid space during rest and exertion. AJNR Am J Neuroradiol. 2013;34(1):41–5.
63. Linge SO, Mardal KA, Helgeland A, Heiss JD, Haughton V. Effect of craniovertebral decompression on CSF dynamics in Chiari malformation type I studied with computational fluid dynamics: laboratory investigation. J Neurosurg Spine. 2014;21(4):559–64.
64. Stoverud KH, Mardal KA, Haughton V, Langtangen HP. CSF flow in Chiari I and syringomyelia from the perspective of computational fluid dynamics. Neuroradiol J. 2011;24(1):20–3.
65. Shaffer N, Martin BA, Rocque B, Madura C, Wieben O, Iskandar BJ, et al. Cerebrospinal fluid flow impedance is elevated in Type I Chiari malformation. J Biomech Eng. 2014;136(2):021012.
66. Lawrence BJ, Luciano M, Tew J, Ellenbogen RG, Oshinski JN, Loth F, et al. Cardiac-related spinal cord tissue motion at the foramen magnum is increased in patients with Type I Chiari malformation and decreases postdecompression surgery. World Neurosurg. 2018;116:e298–307.
67. Alperin N, Loftus JR, Bagci AM, Lee SH, Oliu CJ, Shah AH, et al. Magnetic resonance imaging-based measures predictive of short-term surgical outcome in patients with Chiari malformation Type I: a pilot study. J Neurosurg Spine. 2017;26(1):28–38.
68. Holdsworth SJ, Rahimi MS, Ni WW, Zaharchuk G, Moseley ME. Amplified magnetic resonance imaging (aMRI). Magn Reson Med. 2016;75(6):2245–54.
69. Leung V, Magnussen JS, Stoodley MA, Bilston LE. Cerebellar and hindbrain motion in Chiari malformation with and without syringomyelia. J Neurosurg Spine. 2016;24(4):546–55.
70. Hofmann E, Warmuth-Metz M, Bendszus M, Solymosi L. Phase-contrast MR imaging of the cervical CSF and spinal cord: volumetric motion analysis in patients with Chiari I malformation. AJNR Am J Neuroradiol. 2000;21(1):151–8.
71. Pujol J, Roig C, Capdevila A, Pou A, Marti-Vilalta JL, Kulisevsky J, et al. Motion of the cerebellar tonsils in Chiari type I malformation studied by cine phase-contrast MRI. Neurology. 1995;45(9):1746–53.
72. Alperin N, Loftus JR, Oliu CJ, Bagci AM, Lee SH, Ertl-Wagner B, et al. Magnetic resonance imaging measures of posterior cranial fossa morphology and cerebrospinal fluid physiology in Chiari malformation type I. Neurosurgery. 2014;75(5):515–22; discussion 22.
73. Cousins J, Haughton V. Motion of the cerebellar tonsils in the foramen magnum during the cardiac cycle. AJNR Am J Neuroradiol. 2009;30(8):1587–8.
74. Aletras AH, Ding S, Balaban RS, Wen H. DENSE: displacement encoding with stimulated echoes in cardiac functional MRI. J Magn Reson. 1999;137(1):247–52.
75. Pahlavian SH, Oshinski J, Zhong X, Loth F, Amini R. Regional quantification of brain tissue strain using displacement-encoding with stimulated echoes magnetic resonance imaging. J Biomech Eng. 2018;140(8)1–13.
76. Soellinger M, Rutz AK, Kozerke S, Boesiger P. 3D cine displacement-encoded MRI of pulsatile brain motion. Magn Reson Med. 2009;61(1):153–62.

The Chiari Malformations and Hydrocephalus

13

Robert P. Naftel, James M. Johnston, and John C. Wellons III

Introduction and Historical Background

The association of hydrocephalus and the Chiari malformations has been described from the time of Hans Chiari's initial report in 1891 [1]. The pathophysiology of Chiari-associated hydrocephalus has nonetheless been controversial, with several hypotheses proposed to explain its pathophysiology. In his original manuscript, Chiari postulated that tonsillar herniation resulted from supratentorial pressure due to concomitant hydrocephalus [1], suggesting that brain herniation was in fact secondary to intrinsic hydrocephalus. This initial explanation was cogent and quite popular and still provides the rationale for cerebrospinal fluid (CSF) diversion as a primary treatment of Chiari-associated hydrocephalus. The Dutch surgeon van Houweninge Graftdijk proposed a converse theory in 1932 [2], whereby the foramina of the fourth ventricle, herniated into the upper spinal canal, act as a valvular obstruction and precipitate hydrocephalus. He advocated surgical correction of the hindbrain herniation in order to widen the space and allow for better flow of CSF. More recent advances in cranial imaging and volumetric analysis have provided some detail to this theory, linking tonsillar herniation to a disorder of the paraxial mesoderm with underdevelopment of the occipital somites and secondary hypoplasia of the occipital bone, leading to overcrowding of the vascular and neural structures within the posterior cranial fossa [3, 4]. This combination of factors may lead to impaired CSF absorption and flow due to hindbrain distortion, decreased cisterns, and anomalies of the venous circulation, resulting in hydrocephalus. Whether hydrocephalus is the cause of or the result of hindbrain herniation is quite relevant, as it may dictate the surgeon's approach to a management strategy that is perceived to lead to the best clinical outcome for each individual patient. Given the wide range of hindbrain anomalies that fall under the Chiari rubric, each Chiari subtype will be discussed separately.

R. P. Naftel (✉)
Department of Neurological Surgery, Monroe Carell Jr Children's Hospital at Vanderbilt/Vanderbilt University, Nashville, TN, USA
e-mail: robert.p.naftel@vumc.org

J. M. Johnston
Division of Pediatric Neurosurgery, Department of Neurosurgery, University of Alabama at Birmingham, Children's of Alabama, Birmingham, AL, USA

J. C. Wellons III
Department of Neurological Surgery, Division of Pediatric Neurosurgery, Monroe Carell Jr Children's Hospital at Vanderbilt/Vanderbilt University, Nashville, TN, USA

R. S. Tubbs et al. (eds.), *The Chiari Malformations*, https://doi.org/10.1007/978-3-030-44862-2_13

Chiari I

Epidemiology and Clinical Presentation

Reported incidence rates of hydrocephalus in cases of Chiari I malformation (CMI) range from 0% to 9.6% [4–6], and it may often be associated with concomitant syringomyelia [4]. In addition to classic hindbrain symptoms of CMI, symptoms of hydrocephalus and resultant elevated intracranial pressure (ICP) may include headaches, vomiting, papilledema, and enlarging head circumference in infants. Magnetic resonance imaging (MRI) is the modality of choice for diagnosis of Chiari and associated syringomyelia. In patients being considered for endoscopic third ventriculostomy (ETV), MRI also provides necessary anatomic detail of the third ventricle, basilar artery, and prepontine space (Fig. 13.1). Threshold values of ventricular enlargement necessary for a diagnosis of hydrocephalus are not well defined in the literature, making clinical diagnosis of elevated ICP a crucial component of the decision-making process.

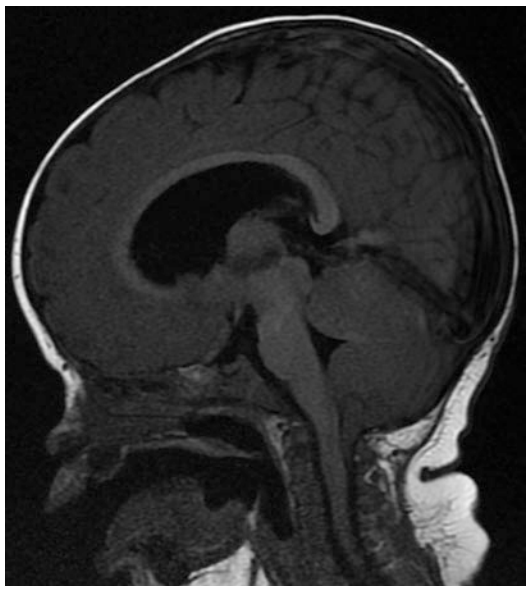

Fig. 13.1 Chiari I malformation with hydrocephalus. Sagittal T1-weighted magnetic resonance imaging demonstrates caudal displacement of the cerebellar tonsils and ventricular enlargement

Management and Outcomes

As mentioned before, some controversy exists regarding whether hydrocephalus should be considered the cause of the CMI hindbrain herniation or rather the effect of obstruction at the level of the fourth ventricular outlet or even abnormal CSF absorption at the level of the posterior fossa cisterns [3]. This controversy notwithstanding, it is generally accepted that in cases of CMI, hydrocephalus should be treated before consideration is given to suboccipital decompression [7–10]. On a population-level analysis of CMI decompression, preexisting hydrocephalus was the only comorbidity that significantly associated with surgical morbidity after decompression [11]. However, from this administrative data, determining how the hydrocephalus had been diagnosed and treated is not possible.

Ventriculoperitoneal shunt (VPS) placement has long been the mainstay of treatment for CMI-associated hydrocephalus. While there are no published studies looking specifically at the durability of VPS for CMI-associated hydrocephalus, the complication and infections rate for shunt placement are not insignificant, especially in the pediatric population [12, 13].

Recent studies have reported relative success of ETV in the management of CMI-related hydrocephalus [14–25]. The two largest series reported an 87–94% (28 of 31) early success rate, with two failures due to late (>1 year) stoma closure and in one case of a previously shunted patient [23, 24]. Together, the 2 series reported no mortality or clinically significant complications and syringomyelia resolution or improvement in 8 of 11 patients. Of note, despite similar success rates in the management of hydrocephalus, the two groups reported very different rates of patients going on to require subsequent posterior fossa decompression for persistent CMI symptomatology (0 vs. 37.5%). Whether this was due to different mean ages of their populations (15.2 vs. 31.9) or criteria for operative decompression is unclear. Nonetheless, both groups advocate ETV as the procedure of choice in the management of hydrocephalus associated with CMI, both for

hydrocephalus control and treatment of hindbrain herniation symptoms, including syringomyelia.

Postoperative Development of Hydrocephalus

A small subset (0.8–7%) of patients has developed hydrocephalus after CMI decompression [6, 26–28]. These patients may present with ventricular dilation, persistent CSF leak/pseudomeningocele, worsening tonsillar herniation, or elevated intracranial pressure. The vast majority of these patients are treated with shunting compared to ETV. Risk factors in single-center studies include high blood loss, young age, and the presence of a fourth ventricular web [26]. All reported cases occurred after duraplasty. In many cases there is an associated development of subdural hygromas that are believed to be associated with the development of hydrocephalus [27, 28]. Treatment options have included wound revision, CSF diversion, and acetazolamide to corticosteroids, but with the low number of patients reported and lack of uniformity of the cases, standard treatments have not been defined.

Chiari II Malformation

Epidemiology and Clinical Presentation

The Chiari II malformation (CMII) almost always occurs in patients born with neural tube defects, most commonly myelomeningocele or encephalocele. Criteria for diagnosis include the elongation and caudal migration of the cerebellar vermis, brain stem, and fourth ventricle into the upper cervical canal, as well as a host of other cerebral anomalies (Fig. 13.2). Associated findings may include tectal beaking, basilar invagination, colpocephaly, low-lying torcular, skull anomalies, and syringomyelia (40–95%) [29]. Incidence of clinical hydrocephalus requiring CSF diversion varies from 40% in prenatally closed groups [30] to 52–90% in postnatally closed series [31–37]. This wide variation in reported incidence is likely a reflection of different patient populations, health systems, and criteria for diagnosis and intervention.

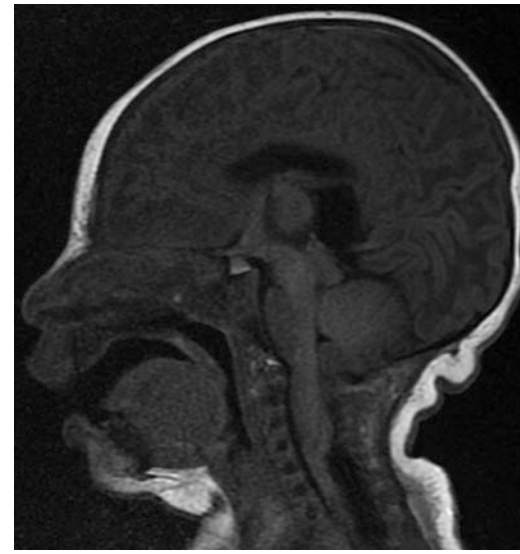

Fig. 13.2 Chiari II malformation with hydrocephalus. Sagittal T1-weighted magnetic resonance imaging demonstrates elongation and caudal displacement of the cerebellar vermis and brain stem into the upper cervical canal, tectal beaking, and low-lying torcular

Symptoms of hydrocephalus in infants with CMII may include bulging fontanelle, split cranial sutures, and leakage from the myelomeningocele closure site. Of note, hydrocephalus may also worsen symptoms referable to the CMII, including lower cranial neuropathies, swallowing dysfunction, and stridor. Numerous methods exist to quantify ventriculomegaly, including calculation of the ratio of biventricular diameter to biparietal diameter [38] frontal-occipital horn ratio, and ventricular index—though no published studies to date have clearly delineated the best measure.

Management and Outcomes

As in CMI, the management of hydrocephalus or verification of a working shunt should always precede suboccipital decompression, even in the setting of brain stem symptomatology (i.e., stridor, dysphagia, sleep apnea) or worsening syringomyelia. Criteria for CSF diversion have

historically been somewhat variable, though efforts have been made to standardize indications to better compare outcomes across multiple institutions [30]. Traditionally, ventriculoperitoneal shunting has been the most common procedure used for the treatment of hydrocephalus associated with CMII and myelomeningocele (MMC). However, in a review of the literature, Tamburrini et al. noted that there was an overall reduction in the number of patients with MMC who were being treated for hydrocephalus, and in those who are treated, there was a trend toward performing more ETVs rather than shunts [39]. Shunt complication rates and death in children with myelomeningocele may be higher than in children requiring shunts for other reasons [40–43]. Some authors have suggested that infective complications of shunting may have a greater impact on cognitive development than the hydrocephalus [44] and that children with MMC who do not require shunt placement have better survival [45, 46] and higher IQ [47] than those who have undergone shunt placement [48]. These studies are limited by their retrospective nature and potential bias, and prospective studies are required to elucidate the appropriate threshold for intervention given the known risks of shunting. In children with mild ventriculomegaly and no signs or symptoms of increased intracranial pressure, potentially improved brain development must be weighed against the known risks of CSF diversion in this population. In children from the Management of Myelomeningocele Study (MOMS), 30-month neurocognitive testing showed no difference among patients who were treated for hydrocephalus, those who were diagnosed with hydrocephalus but not treated, and those not meeting criteria for hydrocephalus diagnosis [49]. Prenatal closure of the MMC was associated with lower incidence of hydrocephalus treatment and reduction in CMII presence (64% vs. 98%) and severity [50]. Further analysis established that ventricle size (atrial diameter) at the time of prenatal closure is predictive of developing hydrocephalus (<10 mm, 20%; 10–15 mm, 45%; >15 mm, 79%). This was different than the postnatal closure cohort (<10 mm, 79%; 10–15 mm, 86%; >15 mm, 87%) [51]. Additionally, for those who do go on to develop hydrocephalus in the prenatal cohort, there is a delay in their need for treatment [52]. This is advantageous because with older age comes less complications in shunting and increased likelihood of ETV or ETV with choroid plexus cauterization (CPC) success [53, 54].

Endoscopic third ventriculostomy has become an alternative to ventriculoperitoneal shunting in children with myelomeningocele [55–60], with acknowledged lower success rates in infants and children with a previously placed shunt [57–59, 61]. The addition of CPC to ETV has also been investigated, based on extensive experience with children in developing countries [62–65], where cost and medical access preclude ventriculoperitoneal shunt placement. Long-term follow-up in this cohort demonstrated similar neurocognitive outcomes in the ETVCPC and shunt groups [63]. In North America, myelomeningocele has been found to be the most successful etiology for ETVCPC with success rates at 1 year of 48%, 62%, 100%, and 100% for age categories <1 month, 1–5 months, 6–11 months, and ≥1 year, respectively [53].

Chiari III

Chiari III malformation (CMIII) is an extremely rare entity characterized by herniation of the posterior fossa contents through a low occipital and/or upper cervical osseous defect [1, 66, 67], estimated to account for 0.64–4% of all Chiari malformations [68, 69]. Published series report an incidence of hydrocephalus of 88% [29, 66, 67]. Associated hydrocephalus has traditionally been managed with ventriculoperitoneal shunt placement, and the rarity of CMIII limits the availability of published data regarding long-term shunt survival or alternative CSF diversion.

Pseudotumor Cerebri and the Chiari Malformation

Tonsillar descent secondary to lumboperitoneal shunting for pseudotumor cerebri (PTC) is quite common [70] and will not be treated further here. However, there has been much disagree-

ment regarding the nature of the association between PTC and primary Chiari malformation. PTC classically presents with headaches, visual changes, elevated intracranial pressure measured on lumbar puncture (LP) in the lateral decubitus position, and no evidence of hydrocephalus or intracranial pathology. It is most often observed in obese women of childbearing age, though it can also be seen secondary to certain medications (tetracycline, minocycline, vitamin A, corticosteroids, lithium, and oral contraceptives) and in the setting of venous sinus thrombosis [71]. The source of the controversy lies in two observations. First, several groups have described an increased prevalence of cerebellar ectopia in patients with PTC. Sinclair described a series of 156 cases of PTC noting an overall incidence of 2.7%, significantly higher than the 0.77% rate previously reported in the general population [72]. Banik observed a 24% rate of inferior tonsillar displacement in patients with PTC, with 10% fulfilling criteria for Chiari malformation (>5 mm) [73]. Of note, all patients with tonsillar descent were female and obese.

Second, several groups have described the effectiveness of CSF shunting in patients with recurrent Chiari symptoms following posterior fossa decompression. Fagan reported a series of 15 patients with post-Chiari PTC, defined as recurrence of Chiari-like symptoms after decompression, elevated lumbar CSF pressure in the absence of meningitis or ventriculomegaly, and transient resolution of symptoms following lumbar CSF drainage [74]. All patients were evaluated with CSF flow studies at the foramen magnum as well as lumbar puncture to rule out infection/aseptic meningitis and to evaluate intracranial pressure. Those found to have increased ICP underwent lumboperitoneal shunting, with significant symptom resolution in 7/9 (78%) pediatric patients and in 0/6 adult patients [74]. Bejjani reported a series of six adult patients with similar recurrence of Chiari-like symptoms following posterior fossa decompression and found significant improvement in all following either shunting or repeat LP with acetazolamide [75].

Whether the association is real or coincidental is unclear. Some authors argue that they are two pathophysiologically distinct entities with overlapping clinical presentation, specifically headaches and tonsillar descent [76]. Others suggest that the entities may actually share a similar pathophysiology, namely, increased intracranial contents, engorged brain with venous hypertension, decreased intracranial volume, and mechanical obstruction of CSF outflow at the foramen magnum with a common end result of altered compliance and disturbed neural hydrodynamics [73, 75, 77]. Definitive resolution of the issue will require more detailed imaging and prospective studies of larger populations.

Practically speaking, given the similar demographics, clinical presentation, and increased incidence of tonsillar ectopia in patients with pseudotumor cerebri, it is critical that the neurosurgeon strives to differentiate these two groups during clinical evaluation prior to surgery for optimal outcome. Patients with atypical headaches, obesity, relevant medication exposure, visual changes, and papilledema should be most closely examined to better differentiate between the two diagnoses. Detailed fundoscopic exam, MRI cine studies to visualize CSF flow at the foramen magnum, and lumbar puncture may be considered in these complex patients to evaluate intracranial pressure and also determine if the patient responds symptomatically to CSF drainage. Those patients with evidence of intracranial hypertension and symptomatic improvement following lumbar puncture will benefit from CSF diversion instead of posterior fossa decompression.

A Special Note About Predicting Success of Endoscopic Third Ventriculostomy in Chiari I and II

Populations

Major factors that predict the success of ETV include age, etiology of hydrocephalus, and the presence or absence of a shunt preoperatively [78–90]. In 2009, Kulkarni et al. used these factors to develop a model to predict the probability of ETV success in the treatment of childhood hydrocephalus: the Endoscopic Third Ventriculostomy Success Score (Fig. 13.3) [59].

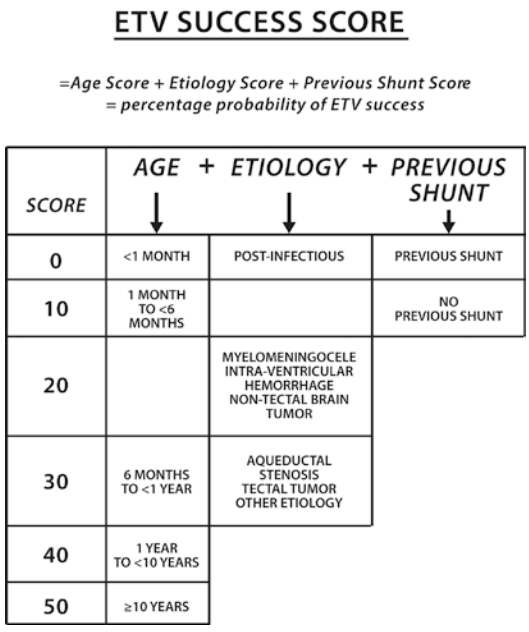

Fig. 13.3 The ETV Success Score predicts the likelihood of successful endoscopic third ventriculostomy at 6 months after the procedure. (Reprinted with permission from Kulkarni et al. [59])

By assigning a score to age range, etiology, and shunt history, an overall score is calculated that predicts the likelihood of successful ETV at 6 months post procedure and was found to closely approximate success. Since that time, there have been several publications using the ETVSS. The Canadian Pediatric Neurosurgery Study Group evaluated a multicenter cohort of children newly diagnosed with hydrocephalus and evaluated the risk of failure between ETV and VPS for high-, moderate-, and low-ETVSS groups [91]. For all groups, the risk of ETV failure became progressively lower compared with shunt failure with increasing time from surgery. In the high-ETVSS group, the risk of ETV failure was lower than shunt failure soon after surgery. For all the rest, the risk of ETV failure only became lower than shunt failure 3–6 months out from surgery. Kulkarni, Riva-Cambrin, and Browd then applied the ETVSS to several well-known published series of patients on whom ETV was performed for various reasons. The overall mean predicted ETVSS was 58%, and the actual ETV success rate was 59%, showing excellent predictive capability of the model [57]. Two articles were published in November of 2011 in the *Journal of Neurosurgery: Pediatrics* intended to further validate the ETVSS [56, 92]. Both single institution series showed excellent predictive capability of the ETVSS in separate analyses.

As reviewed earlier, hydrocephalus related to the CMI is relatively rare. Therefore, ETVs for hydrocephalus due to CMI make up only a small part of most single-center and multicenter ETV series. Within the etiology portion of the ETVSS, the same predictive capability is apportioned to CMI ("other") as those etiologies that traditionally have a high rate of success: aqueductal stenosis and tectal tumors. Despite the initial success in published series reviewed above, this may very well be an overestimation of the capability of ETV to adequately treat hydrocephalus in patients with CMI, or this may be clinically accurate. Additional series continue to accrue [23, 24], and future adjustments to the model may be necessary.

Performance of an ETV for hydrocephalus related to spina bifida, however, is becoming more common. Based on the current ETVSS model, there is less likelihood of success in patients with this etiology than with CMI. Due to the large number of patients with post-infectious hydrocephalus, Warf, Mugamba, and Kulkarni modified the existing ETVSS in order to apply it to children seen at the CURE Children's Hospital of Uganda (CCHU) [89]. As a result, the CCHU ETVSS for use in the field predicted ETV success to a much higher degree by taking into consideration age, etiology, and the degree of choroid plexus cauterization (CPC). A substantial number of ETVs in this population were performed with choroid plexus cauterization. In a very interesting finding and one that was independent of CPC and age, regression analysis revealed that the odds of ETV success were 2.25 times greater in spina bifida patients compared with other etiologies. In his US series, Warf et al. found that the ETVSS underestimated his success rate; however, in Hydrocephalus Clinical Research Network studies, ETVSS has been predictive of ETVCPC success [53, 54]. Further validation studies may shed more light on this relationship.

Conclusion

The Chiari malformations have long been associated with hydrocephalus. Controversy remains, however, regarding which entity precedes the other, though most authors agree the pathophysiology is multifactorial. Though hydrocephalus is relatively rare in the setting of the CMI, most agree that CSF diversion should be performed prior to suboccipital decompression. In addition to traditional shunting, emerging data suggest that ETV is effective in a large majority of these patients and may improve hindbrain compression symptoms and syringomyelia. Hydrocephalus is much more common in the CMII-myelomeningocele population, though controversy remains regarding the proportion of these patients that will ultimately require CSF diversion. As in the Chiari I population, adequate CSF drainage should be ensured prior to surgical decompression, even in the setting of hindbrain compression symptoms or syringomyelia. Though traditional shunting remains the most common treatment for these patients, ETV has become more common, especially in experienced centers when combined with choroid plexus cauterization when applicable. Prospective studies of both entities continue, examining diagnostic criteria, neuropsychological outcomes, and preferred CSF diversion technique in these challenging populations.

References

1. Chiari H. Uber Veranderungen des Kleingirns infolge von Hydrocephalie des Grosshirns. Detsch Med Wochenschr. 1891;17:1172–5.
2. van Houweninge Graftdijk C. Over hydrocephalus. Leiden: Eduard Ijdo; 1932.
3. Di Rocco C, Frassanito P, Massimi L, Peraio S. Hydrocephalus and Chiari type I malformation. Childs Nerv Syst. 2011;27(10):1653–64.
4. Milhorat TH, Chou MW, Trinidad EM, Kula RW, Mandell M, Wolpert C, et al. Chiari I malformation redefined: clinical and radiographic findings for 364 symptomatic patients. Neurosurgery. 1999;44(5):1005–17.
5. Badie B, Mendoza D, Batzdorf U. Posterior fossa volume and response to suboccipital decompression in patients with Chiari I malformation. Neurosurgery. 1995;37(2):214–8.
6. Tubbs RS, Beckman J, Naftel RP, Chern JJ, Wellons JC 3rd, Rozzelle CJ, et al. Institutional experience with 500 cases of surgically treated pediatric Chiari malformation Type I. J Neurosurg Pediatr. 2011;7(3):248–56.
7. Osuagwu FC, Lazareff JA, Rahman S, Bash S. Chiari I anatomy after ventriculoperitoneal shunting: posterior fossa volumetric evaluation with MRI. Childs Nerv Syst. 2006;22(11):1451–6.
8. Grabb PA, Mapstone TB, Oakes WJ. Ventral brain stem compression in pediatric and young adult patients with Chiari I malformations. Neurosurgery. 1999;44(3):520–7. discussion 7–8
9. Schijman E, Steinbok P. International survey on the management of Chiari I malformation and syringomyelia. Childs Nerv Syst. 2004;20(5):341–8.
10. Tubbs RS, Lyerly MJ, Loukas M, Shoja MM, Oakes WJ. The pediatric Chiari I malformation: a review. Childs Nerv Syst. 2007;23(11):1239–50.
11. Greenberg JK, Olsen MA, Yarbrough CK, Ladner TR, Shannon CN, Piccirillo JF, et al. Chiari malformation Type I surgery in pediatric patients. Part 2: complications and the influence of comorbid disease in California, Florida, and New York. J Neurosurg Pediatr. 2016;17(5):525–32.
12. Drake JM, Kestle JR, Milner R, Cinalli G, Boop F, Piatt J Jr, et al. Randomized trial of cerebrospinal fluid shunt valve design in pediatric hydrocephalus. Neurosurgery. 1998;43(2):294–303. discussion −5
13. Vernet O, Rilliet B. Late complications of ventriculoatrial or ventriculoperitoneal shunts. Lancet. 2001;358(9293):1569–70.
14. Decq P, Le Guerinel C, Sol JC, Brugieres P, Djindjian M, Nguyen JP. Chiari I malformation: a rare cause of noncommunicating hydrocephalus treated by third ventriculostomy. J Neurosurg. 2001;95(5):783–90.
15. Ersahin Y, Gokcay A. Acquired Chiari I malformation changes postendoscopic third ventriculostomy. Pediatr Neurosurg. 2002;36(1):54.
16. Fukuhara T, Vorster SJ, Luciano MG. Risk factors for failure of endoscopic third ventriculostomy for obstructive hydrocephalus. Neurosurgery. 2000;46(5):1100–9. discussion 9–11
17. Kandasamy J, Kneen R, Gladstone M, Newman W, Mohamed T, Mallucci C. Chiari I malformation without hydrocephalus: acute intracranial hypertension managed with endoscopic third ventriculostomy (ETV). Childs Nerv Syst. 2008;24(12):1493–7.
18. Metellus P, Dufour H, Levrier O, Grisoli F. Endoscopic third ventriculostomy for treatment of noncommunicating syringomyelia associated with a Chiari I malformation and hydrocephalus: case report and pathophysiological considerations. Neurosurgery. 2002;51(2):500–3. discussion 3–4
19. Mohanty A, Suman R, Shankar SR, Satish S, Praharaj SS. Endoscopic third ventriculostomy in the management of Chiari I malformation and syringomyelia associated with hydrocephalus. Clin Neurol Neurosurg. 2005;108(1):87–92.

20. Nishihara T, Hara T, Suzuki I, Kirino T, Yamakawa K. Third ventriculostomy for symptomatic syringomyelia using flexible endoscope: case report. Minim Invasive Neurosurg. 1996;39(4):130–2.
21. Suehiro T, Inamura T, Natori Y, Sasaki M, Fukui M. Successful neuroendoscopic third ventriculostomy for hydrocephalus and syringomyelia associated with fourth ventricle outlet obstruction. Case report. J Neurosurg. 2000;93(2):326–9.
22. Teo C, Nakaji P, Serisier D, Coughlan M. Resolution of trigeminal neuralgia following third ventriculostomy for hydrocephalus associated with Chiari I malformation: case report. Minim Invasive Neurosurg. 2005;48(5):302–5.
23. Massimi L, Pravata E, Tamburrini G, Gaudino S, Pettorini B, Novegno F, et al. Endoscopic third ventriculostomy for the management of Chiari I and related hydrocephalus: outcome and pathogenetic implications. Neurosurgery. 2011;68(4):950–6.
24. Hayhurst C, Osman-Farah J, Das K, Mallucci C. Initial management of hydrocephalus associated with Chiari malformation Type I-syringomyelia complex via endoscopic third ventriculostomy: an outcome analysis. J Neurosurg. 2008;108(6):1211–4.
25. Buxton N, Jaspan T, Punt J. Treatment of Chiari malformation, syringomyelia and hydrocephalus by neuroendoscopic third ventriculostomy. Minim Invasive Neurosurg. 2002;45(4):231–4.
26. Guan J, Riva-Cambrin J, Brockmeyer DL. Chiari-related hydrocephalus: assessment of clinical risk factors in a cohort of 297 consecutive patients. Neurosurg Focus. 2016;41(5):E2.
27. Zakaria R, Kandasamy J, Khan Y, Jenkinson MD, Hall SR, Brodbelt A, et al. Raised intracranial pressure and hydrocephalus following hindbrain decompression for Chiari I malformation: a case series and review of the literature. Br J Neurosurg. 2012;26(4):476–81.
28. Vivas AC, Shimony N, Jackson EM, Xu R, Jallo GI, Rodriguez L, et al. Management of hydrocephalus and subdural hygromas in pediatric patients after decompression of Chiari malformation type I: case series and review of the literature. J Neurosurg Pediatr. 2018;22(4):426–38.
29. Soleau S, Tubbs RS, Oakes JW. Chiari malformations. In: Albright AL, Pollack IF, Adelson PD, editors. Principles and practice of pediatric neurosurgery. 2nd ed. New York: Thieme; 2008. p. 217–32.
30. Adzick NS, Thom EA, Spong CY, Brock JW 3rd, Burrows PK, Johnson MP, et al. A randomized trial of prenatal versus postnatal repair of myelomeningocele. N Engl J Med. 2011;364(11):993–1004.
31. Arynchyna A, Shannon C, Ditty B, Oakes JW, Blount J, Wellons J. Applying the MOMS Shunting Criteria to a Single Institutional Experience. AANS/CNS Section on Pediatric Neurological Surgery; November 29; Austin, Texas; 2011.
32. Chakraborty A, Crimmins D, Hayward R, Thompson D. Toward reducing shunt placement rates in patients with myelomeningocele. J Neurosurg Pediatr. 2008;1(5):361–5.
33. Bowman RM, McLone DG, Grant JA, Tomita T, Ito JA. Spina bifida outcome: a 25-year prospective. Pediatr Neurosurg. 2001;34(3):114–20.
34. Rintoul NE, Sutton LN, Hubbard AM, Cohen B, Melchionni J, Pasquariello PS, et al. A new look at myelomeningoceles: functional level, vertebral level, shunting, and the implications for fetal intervention. Pediatrics. 2002;109(3):409–13.
35. Swank M, Dias L. Myelomeningocele: a review of the orthopaedic aspects of 206 patients treated from birth with no selection criteria. Dev Med Child Neurol. 1992;34(12):1047–52.
36. Talamonti G, D'Aliberti G, Collice M. Myelomeningocele: long-term neurosurgical treatment and follow-up in 202 patients. J Neurosurg. 2007;107(5 Suppl):368–86.
37. Dias M, McLone DG. Myelomeningocele. In: Albright AL, Pollack IF, Adelson PD, editors. Principles and practice of pediatric neurosurgery. 2nd ed. New York: Thieme; 2008. p. 338–66.
38. O'Hayon BB, Drake JM, Ossip MG, Tuli S, Clarke M. Frontal and occipital horn ratio: a linear estimate of ventricular size for multiple imaging modalities in pediatric hydrocephalus. Pediatr Neurosurg. 1998;29(5):245–9.
39. Tamburrini G, Frassanito P, Iakovaki K, Pignotti F, Rendeli C, Murolo D, et al. Myelomeningocele: the management of the associated hydrocephalus. Childs Nerv Syst. 2013;29(9):1569–79.
40. Steinbok P, Irvine B, Cochrane DD, Irwin BJ. Long-term outcome and complications of children born with meningomyelocele. Childs Nerv Syst. 1992;8(2):92–6.
41. Acakpo-Satchivi L, Shannon CN, Tubbs RS, Wellons JC 3rd, Blount JP, Iskandar BJ, et al. Death in shunted hydrocephalic children: a follow-up study. Childs Nerv Syst. 2008;24(2):197–201.
42. Iskandar BJ, Tubbs S, Mapstone TB, Grabb PA, Bartolucci AA, Oakes WJ. Death in shunted hydrocephalic children in the 1990s. Pediatr Neurosurg. 1998;28(4):173–6.
43. Tuli S, Drake J, Lamberti-Pasculli M. Long-term outcome of hydrocephalus management in myelomeningoceles. Childs Nerv Syst. 2003;19(5–6):286–91.
44. McLone DG. Central nervous system infections as a limiting factor in the intelligence of children with myelomeningocele. Pediatrics. 1982;70(3):338–42.
45. Davis BE, Daley CM, Shurtleff DB, Duguay S, Seidel K, Loeser JD, et al. Long-term survival of individuals with myelomeningocele. Pediatr Neurosurg. 2005;41(4):186–91.
46. Tuli S, Tuli J, Drake J, Spears J. Predictors of death in pediatric patients requiring cerebrospinal fluid shunts. J Neurosurg. 2004;100(5 Suppl Pediatrics):442–6.
47. Mapstone TB, Rekate HL, Nulsen FE, Dixon MS Jr, Glaser N, Jaffe M. Relationship of CSF shunting and IQ in children with myelomeningocele: a retrospective analysis. Childs Brain. 1984;11(2):112–8.
48. Mataro M, Poca MA, Sahuquillo J, Cuxart A, Iborra J, de la Calzada MD, et al. Cognitive changes after cere-

brospinal fluid shunting in young adults with spina bifida and assumed arrested hydrocephalus. J Neurol Neurosurg Psychiatry. 2000;68(5):615–21.
49. Houtrow AJ, Burrows PK, Thom EA. Comparing neurodevelopmental outcomes at 30 months by presence of hydrocephalus and shunt status among children enrolled in the MOMS trial. J Pediatr Rehabil Med. 2018;11(4):227–35.
50. Adzick NS. Fetal myelomeningocele: natural history, pathophysiology, and in-utero intervention. Semin Fetal Neonatal Med. 2010;15(1):9–14.
51. Tulipan N, Wellons JC 3rd, Thom EA, Gupta N, Sutton LN, Burrows PK, et al. Prenatal surgery for myelomeningocele and the need for cerebrospinal fluid shunt placement. J Neurosurg Pediatr. 2015;16(6):613–20.
52. Moldenhauer JS, Soni S, Rintoul NE, Spinner SS, Khalek N, Martinez-Poyer J, et al. Fetal myelomeningocele repair: the post-MOMS experience at the Children's Hospital of Philadelphia. Fetal Diagn Ther. 2015;37(3):235–40.
53. Riva-Cambrin J, Kestle J, Rozzelle CJ, Naftel RP, Alvey J, Reeder R, et al. Predictors of ETV+CPC success in a North American setting: a Hydrocephalus Clinical Research Network study. JNS Peds. 2019; 8(2):128–38.
54. Kulkarni AV, Riva-Cambrin J, Rozzelle CJ, Naftel RP, Alvey JS, Reeder RW, et al. Endoscopic third ventriculostomy and choroid plexus cauterization in infant hydrocephalus: a prospective study by the Hydrocephalus Clinical Research Network. J Neurosurg Pediatr. 2018;21(3):214–23.
55. Kadrian D, van Gelder J, Florida D, Jones R, Vonau M, Teo C, et al. Long-term reliability of endoscopic third ventriculostomy. Neurosurgery. 2008;62(Suppl 2):614–21.
56. Naftel RP, Reed GT, Kulkarni AV, Wellons JC. Evaluating the Children's Hospital of Alabama endoscopic third ventriculostomy experience using the Endoscopic Third Ventriculostomy Success Score: an external validation study. J Neurosurg Pediatr. 2011;8(5):494–501.
57. Kulkarni AV, Riva-Cambrin J, Browd SR. Use of the ETV Success Score to explain the variation in reported endoscopic third ventriculostomy success rates among published case series of childhood hydrocephalus. J Neurosurg Pediatr. 2011;7(2):143–6.
58. Kulkarni AV, Drake JM, Kestle JR, Mallucci CL, Sgouros S, Constantini S. Predicting who will benefit from endoscopic third ventriculostomy compared with shunt insertion in childhood hydrocephalus using the ETV Success Score. J Neurosurg Pediatr. 2010;6(4):310–5.
59. Kulkarni AV, Drake JM, Mallucci CL, Sgouros S, Roth J, Constantini S. Endoscopic third ventriculostomy in the treatment of childhood hydrocephalus. J Pediatr. 2009;155(2):254–9.e1.
60. Drake JM, Kulkarni AV, Kestle J. Endoscopic third ventriculostomy versus ventriculoperitoneal shunt in pediatric patients: a decision analysis. Childs Nerv Syst. 2009;25(4):467–72.
61. Kulkarni AV, Warf BC, Drake JM, Mallucci CL, Sgouros S, Constantini S. Surgery for hydrocephalus in sub-Saharan Africa versus developed nations: a risk-adjusted comparison of outcome. Childs Nerv Syst. 2010;26(12):1711–7.
62. Warf BC. Hydrocephalus associated with neural tube defects: characteristics, management, and outcome in sub-Saharan Africa. Childs Nerv Syst. 2011;27(10):1589–94.
63. Warf B, Ondoma S, Kulkarni A, Donnelly R, Ampeire M, Akona J, et al. Neurocognitive outcome and ventricular volume in children with myelomeningocele treated for hydrocephalus in Uganda. J Neurosurg Pediatr. 2009;4(6):564–70.
64. Warf BC, Campbell JW. Combined endoscopic third ventriculostomy and choroid plexus cauterization as primary treatment of hydrocephalus for infants with myelomeningocele: long-term results of a prospective intent-to-treat study in 115 East African infants. J Neurosurg Pediatr. 2008;2(5):310–6.
65. Warf BC. Endoscopic third ventriculostomy and choroid plexus cauterization for pediatric hydrocephalus. Clin Neurosurg. 2007;54:78–82.
66. Castillo M, Quencer RM, Dominguez R. Chiari III malformation: imaging features. AJNR Am J Neuroradiol. 1992;13(1):107–13.
67. Isik N, Elmaci I, Silav G, Celik M, Kalelioglu M. Chiari malformation type III and results of surgery: a clinical study: report of eight surgically treated cases and review of the literature. Pediatr Neurosurg. 2009;45(1):19–28.
68. Cama A, Tortori-Donati P, Piatelli GL, Fondelli MP, Andreussi L. Chiari complex in children--neuroradiological diagnosis, neurosurgical treatment and proposal of a new classification (312 cases). Eur J Pediatr Surg. 1995;5(Suppl 1):35–8.
69. Dyste GN, Menezes AH, VanGilder JC. Symptomatic Chiari malformations. An analysis of presentation, management, and long-term outcome. J Neurosurg. 1989;71(2):159–68.
70. Chumas PD, Armstrong DC, Drake JM, Kulkarni AV, Hoffman HJ, Humphreys RP, et al. Tonsillar herniation: the rule rather than the exception after lumboperitoneal shunting in the pediatric population. J Neurosurg. 1993;78(4):568–73.
71. Degnan AJ, Levy LM. Pseudotumor cerebri: brief review of clinical syndrome and imaging findings. AJNR Am J Neuroradiol. 2011;32(11):1986–93.
72. Meadows J, Kraut M, Guarnieri M, Haroun RI, Carson BS. Asymptomatic Chiari Type I malformations identified on magnetic resonance imaging. J Neurosurg. 2000;92(6):920–6.
73. Banik R, Lin D, Miller NR. Prevalence of Chiari I malformation and cerebellar ectopia in patients with pseudotumor cerebri. J Neurol Sci. 2006;247(1):71–5.
74. Fagan LH, Ferguson S, Yassari R, Frim DM. The Chiari pseudotumor cerebri syndrome: symptom recurrence after decompressive surgery for Chiari malformation type I. Pediatr Neurosurg. 2006;42(1):14–9.

75. Bejjani GK, Cockerham KP, Rothfus WE, Maroon JC, Maddock M. Treatment of failed adult Chiari malformation decompression with CSF drainage: observations in six patients. Acta Neurochir. 2003;145(2):107–16. discussion 16
76. Sinclair N, Assaad N, Johnston I. Pseudotumour cerebri occurring in association with the Chiari malformation. J Clin Neurosci. 2002;9(1):99–101.
77. Bejjani GK. Association of the Adult Chiari Malformation and Idiopathic Intracranial Hypertension: more than a coincidence. Med Hypotheses. 2003;60(6):859–63.
78. Warf BC. Hydrocephalus in Uganda: the predominance of infectious origin and primary management with endoscopic third ventriculostomy. J Neurosurg. 2005;102:1–15.
79. Balthasar AJ, Kort H, Cornips EM, Beuls EA, Weber JW, Vles JS. Analysis of the success and failure of endoscopic third ventriculostomy in infants less than 1 year of age. Childs Nerv Syst. 2007;23:151–5.
80. Boschert J, Hellwig D, Krauss JK. Endoscopic third ventriculostomy for shunt dysfunction in occlusive hydrocephalus: long-term follow up and review. J Neurosurg. 2003;98:1032–9.
81. Buxton N, Macarthur D, Robertson I, Punt J. Neuroendoscopic third ventriculostomy for failed shunts. Surg Neurol. 2003;60:201–3. discussion 3–4
82. Drake JM. Endoscopic third ventriculostomy in pediatric patients: the Canadian experience. Neurosurgery. 2007;60:881–6. discussion 881–6
83. Elgamal EA, El-Dawlatly AA, Murshid WR, El-Watidy SM, Jamjoom ZA. Endoscopic third ventriculostomy for hydrocephalus in children younger than 1 year of age. Childs Nerv Syst. 2010;27(1):111–6.
84. Hader WJ, Walker RL, Myles ST, Hamilton M. Complications of endoscopic third ventriculostomy in previously shunted patients. Neurosurgery. 2008;63:ONS168–74; discussion ONS74–5.
85. Marton E, Feletti A, Basaldella L, Longatti P. Endoscopic third ventriculostomy in previously shunted children: a retrospective study. Childs Nerv Syst. 2010;26:937–43.
86. Navarro R, Gil-Parra R, Reitman AJ, Olavarria G, Grant JA, Tomita T. Endoscopic third ventriculostomy in children: early and late complications and their avoidance. Childs Nerv Syst. 2006(22):506–13.
87. Ogiwara H, Dipatri AJ Jr, Alden TD, Bowman RM, Tomita T. Endoscopic third ventriculostomy for obstructive hydrocephalus in children younger than 6 months of age. Childs Nerv Syst. 2010;26:343–7.
88. Siomin V, Cinalli G, Grotenhuis A, Golash A, Oi S, Kothbauer K, Weiner H, Roth J, Beni-Adani L, Pierre-Kahn A, Takahashi Y, Mallucci C, Abbott R, Wisoff J, Constantini S. Endoscopic third ventriculostomy in patients with cerebrospinal fluid infection and/or hemorrhage. J Neurosurg. 2002;97:519–24.
89. Warf BC, Mugamba J, Kulkarni AV. Endoscopic third ventriculostomy in the treatment of childhood hydrocephalus in Uganda: report of a scoring system that predicts success. J Neurosurg Pediatr. 2010;5:143–8.
90. Wellons JC 3rd, Tubbs RS, Banks JT, Grabb B, Blount JP, Oakes WJ, Grabb PA. Long-term control of hydrocephalus via endoscopic third ventriculostomy in children with tectal plate gliomas. Neurosurgery. 2002;51:63–7. discussion 7–8
91. Kulkarni AV, Drake JM, Kestle JR, Mallucci CL, Sgouros S, Constantini S, Canadian Pediatric Neurosurgery Study Group. Predicting who will benefit from endoscopic third ventriculostomy compared with shunt insertion in childhood hydrocephalus using the ETV success score. J Neurosurg Pediatr. 2010;6:310–5.
92. Durnford AJ, Kirkham FJ, Mathad N, Sparrow OC. Endoscopic third ventriculostomy in the treatment of childhood hydrocephalus: validation of a success score that predicts long-term outcome. J Neurosurg Pediatr. 2011;8(5):489–93.

14 Cerebellar Tonsillar Ischemia and Cysts in the Chiari I Malformation

R. Shane Tubbs and Joshua J. Chern

Introduction

A feature that has been observed in some patients with Chiari I malformation (CM I) is the presence of a degenerative cyst at the tip of the cerebellar tonsil. The premise is that the herniated tonsil is put under stress in its aberrant location under, for example, the posterior arch of the atlas and that this leads to ischemia.

In 1995, Koga et al. reported on the degenerative changes of the cerebellar tonsils in four CM I patients. The histopathological examination revealed loss of both Purkinje and granular cells with axonal degeneration and chromatolysis. When compared to a control sample, all four patients had less than a quarter of the normal number of Purkinje cells [1]. Another study by Pueyrredon et al. was conducted to determine the pathological changes seen in the cerebellar tonsils among 43 CM I patients [2]. In 29 patients, Purkinje cell loss associated with Bergman gliosis and loss of the granular layer was observed. There were six patients who showed anoxic neuronal changes, fibrosis, and gliosis with the presence of Rosenthal fibers. The level of descent of the cerebellar tonsils did not demonstrate any histological difference. The results supported the assumption that some CM I patients have pathological degeneration of the cerebellar tonsils that can be attributed to their descent through a very narrow space, which results in some disturbance of the blood supply that leads to ischemia [2].

Using magnetic resonance imaging (MRI), intraoperative ultrasound, operative findings, and histopathological examination, Stevenson et al. identified three cases of CM I with cystic degeneration of the cerebellar tonsils [3]. Their findings were based on a database review of 440 CM I patients. It was noted that preoperative MRI missed this finding in all but one patient. On microscopic examination, there was Purkinje cell loss associated with granular layer loss and areas of gliosis; there were no neoplastic changes in any of the three specimens [3].

As this phenomenon has not been adequately investigated, the following prospective radiological, surgical, and histological study was performed to better determine the etiology of such lesions of the cerebellar tonsils in patients with CM I.

R. S. Tubbs (✉)
Department of Neurosurgery, Tulane University School of Medicine, New Orleans, LA, USA

Department of Neurosurgery and Ochsner Neuroscience Institute, Ochsner Health System, New Orleans, LA, USA

J. J. Chern
Department of Neurosurgery, Children's Healthcare of Atlanta, Emory University School of Medicine, Atlanta, GA, USA

R. S. Tubbs et al. (eds.), *The Chiari Malformations*, https://doi.org/10.1007/978-3-030-44862-2_14

Ischemic or Cystic Lesions on Cerebellar Tonsils in Chiari I Patients

Previously, we reviewed 340 children with CM I aged 3 to 18 years (155 males/46% and 185 females/54%) for ischemic or cystic lesions of the herniated cerebellar tonsils on preoperative MRI. Presentations were varied, but the most common were Valsalva-induced headache and scoliosis. Of this cohort, if ischemia or cystic lesions were noted preoperatively or at operation, these patients were placed into a separate database for study. Patients confirmed to have ischemia or cystic change of the tonsillar tips at operation and, when these lesions were thought to occlude the fourth ventricular outlet [4], had tissue from these resected areas sent for routine histological analysis. Out of 340 patients, 10 (2.9%; 6 girls and 4 boys) were found to have signal changes on MRI consistent with ischemia (Fig. 14.1) or cysts (Fig. 14.2) in the cerebellar tonsils. Of these, seven lesions were found in the right cerebellar tonsil and three in the left cerebellar tonsil. Of the 340 patients with Chiari I malformation, 67 (20%) patients underwent posterior fossa decompression for symptoms. Of these 67 patients, cerebellar tonsillar ischemia was observed in 7 (10.4%) (5 right sides and 2 left sides), and cerebellar tonsillar cysts were seen in 4 (6%) (1 left side and 3 right sides). Four of the seven operative patients had cerebellar tonsillar ischemia and concomitant syringomyelia [5] and, as part of their posterior fossa decompression, underwent subpial dissection of some cerebellar tonsil to ensure cerebrospinal fluid (CSF) egress from the fourth ventricle to the cervical subarachnoid space. This transected tissue was sent for histological analysis. Likewise, of the four operative patients found to have tonsillar cysts, three also had concomitant syringomyelia and cerebellar tonsillar cysts and underwent subpial dissection of some cerebellar tonsil to ensure CSF egress from the fourth ventricle to the cervical subarachnoid space. This transected tissue was also sent for histological analysis. Three of the four patients found to have intraoperative tonsillar cysts were noted to have tonsillar ischemic changes on preoperative imaging in this same region, indicating a transformation from ischemic tonsil to cystic tonsil. One patient was included in both groups, as at operation the right

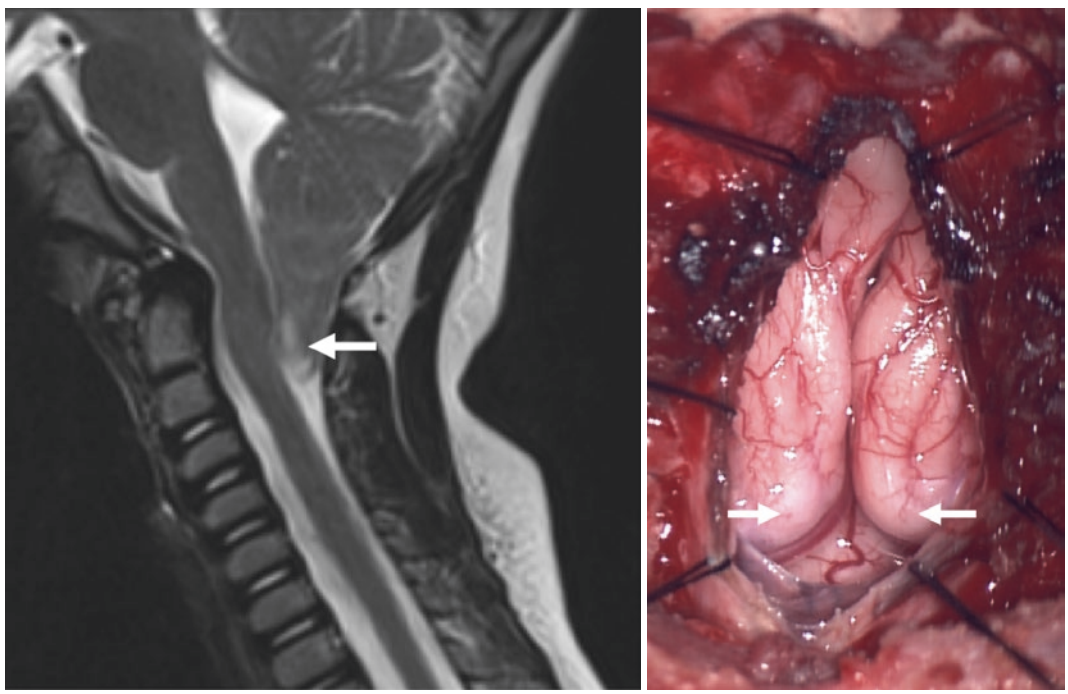

Fig. 14.1 Midline sagittal T2-weighted MRI illustrating cerebellar tonsillar ischemia (arrow) and as viewed at operation (arrows)

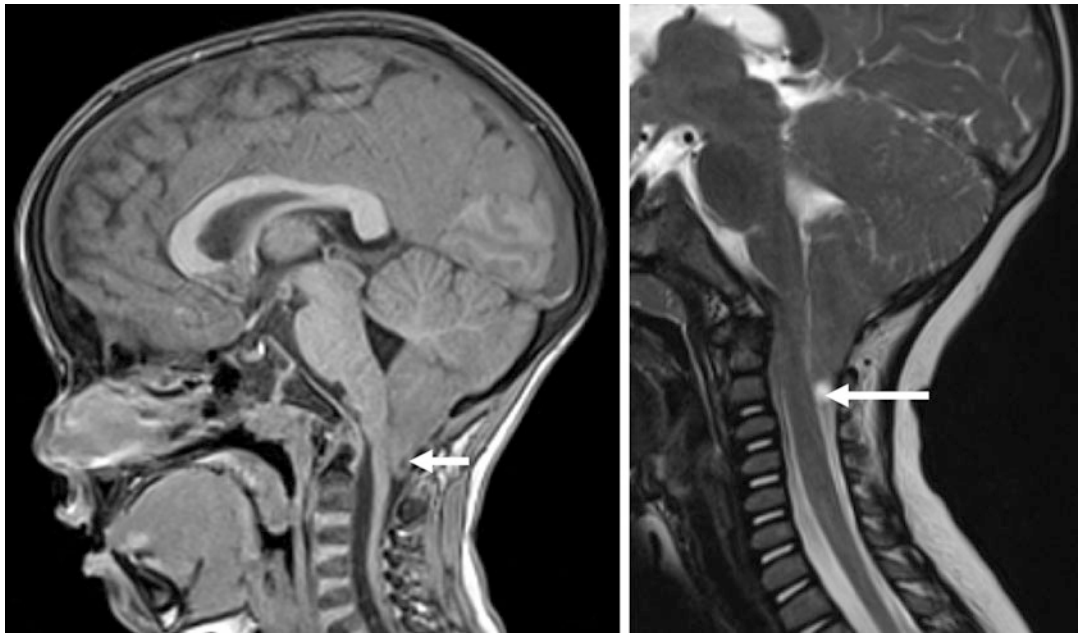

Fig. 14.2 Midline sagittal T1- (left) and T2-weighted (right) MRI illustrating cerebellar tonsillar cysts (arrows)

cerebellar tonsil had both an ischemic area and adjacent cystic area (Fig. 14.3). For both ischemic and cystic cerebellar tonsils, histologically, the tissue demonstrated loss of Purkinje cells with concomitant Bergmann gliosis (Fig. 14.4). The ischemic and cystic tissues were virtually the same, histologically. Interestingly, on imaging, one patient was initially found to have no cerebellar tonsillar ischemia or cyst. At 8 months' follow-up, tonsillar ischemia was noted on imaging, and at 2 years' follow-up, the ischemia evolved to a tonsillar cyst.

Our prospective study found that cerebellar tonsillar ischemia and cysts can be observed preoperatively on MRI. These pathological entities, if not seen on imaging, are often then appreciated at surgery. Radiologically, these were shown in several cases to be directly related; i.e., ischemic tonsils evolved to cystic tonsils. Histologically, the two tissues were nearly identical, and this again reinforces the notion that they lie along a continuum. In CM I patients, the cerebellar tonsils are believed to be exposed to two forms of brain injury: poor blood supply leading to ischemia and continuous pressure resulting from the

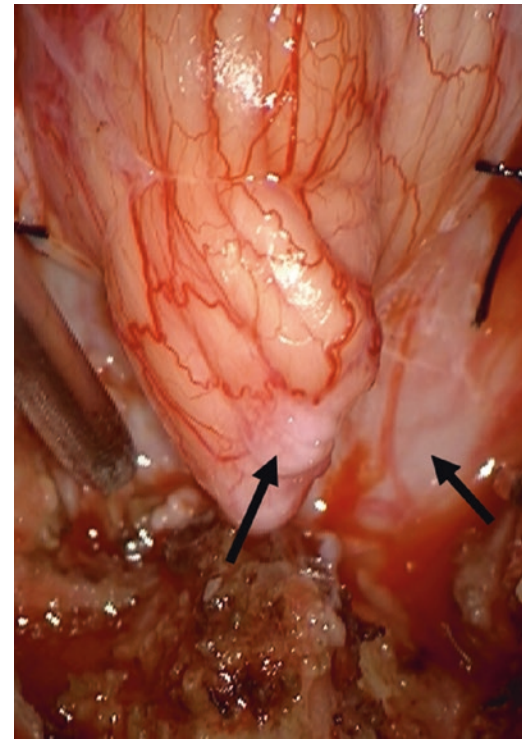

Fig. 14.3 Operative image of the left cerebellar tonsil illustrating ischemic changes (arrow) and the right demonstrating cystic changes (arrow)

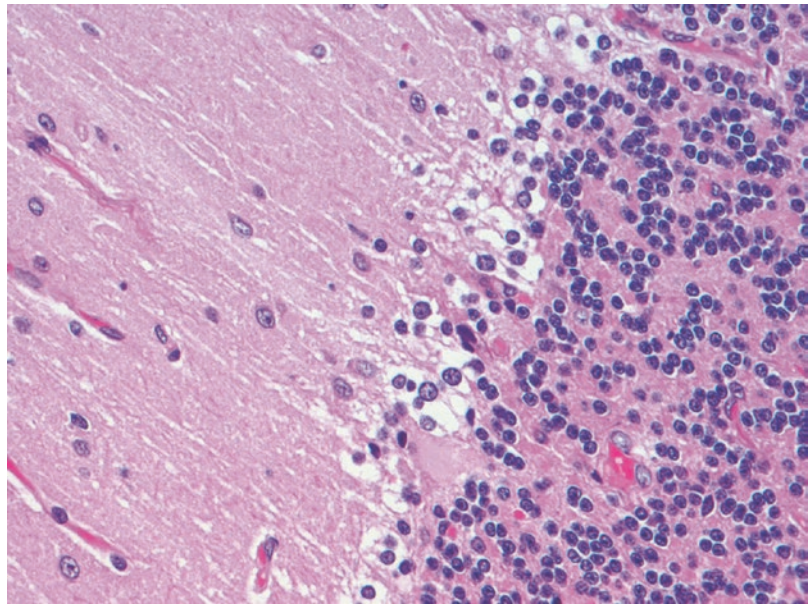

Fig. 14.4 Histological findings of cerebellar tonsillar ischemia with loss of Purkinje cells and concomitant Bergmann gliosis

pulsating CSF. Both theories are directly attributed to the location of the cerebellar tonsils in a very narrow space [2]. Another factor playing a role in the degeneration of the cerebellar tonsils is how Purkinje cells react to ischemia and anoxia; the deficiency in Aldolase C and EAAT4 makes it difficult for the Purkinje cells to overcome excessive synaptic impulses from the inferior olivary nucleus. It has also been suggested that Purkinje cells are vulnerable to ischemia due to their diminished ability to store glutamate and due to the difficulty to produce energy in the lack of oxygen [6]. Other studies suggested that mild to moderate brain trauma might be the cause of gliosis and Purkinje cell loss, which might endorse the pulsating CSF theory as the cause of injury [7, 8]. Another possible cause for Purkinje cell loss is excitotoxicity, which is explained by the distinctive configuration of the Purkinje cells receiving parallel fibers from the granular cells and climbing fibers from the inferior olivary nucleus, both of which are excitatory. Excessive synaptic impulses from both afferent fibers can cause death of the Purkinje cells [9].

After Purkinje cell death and the loss of the granular cell layer accompanied by the formation of Bergmann gliosis, the degeneration of the cerebellar tonsils into an avascular cystic mass could be explained. For reference, Go et al. made an extensive review of the different types of intracranial cysts based on their appearance on MRI and whether the fluid is CSF-like or not [10]. Taken together, cerebellar tonsillar ischemia and cysts are on a continuum and represent chronic compression of this herniated part of the cerebellum.

References

1. Koga H, Mukawa J, Nakata M, Miyazato H, Ishikawa Y, Sakuta O, Hokama A, Terada Y. Histopathological analysis of herniated cerebellar tonsils resected from the patients with Chiari type I malformation with syringomyelia. No To Shinkei. 1995;47:1075–9.
2. Pueyrredon F, Spaho N, Arroyave I, Vinters H, Lazareff J. Histological findings in cerebellar tonsils of patients with Chiari type I malformation. Childs Nerv Syst. 2007;23:427–9.

3. Stevenson CB, Leach JL, Gupta A, Crone KR. Cystic degeneration of the cerebellar tonsils in pediatric patients with Chiari Type I malformation: clinical article. J Neurosurg Pediatr. 2009;4:557–63.
4. Rhoton AL Jr. Cerebellum and fourth ventricle. Neurosurgery. 2000;47:S7–S27.
5. Jacob RP, Rhoton AL Jr. The Chiari I malformation. In: Anson JA, Benzel EC, Awad IA, editors. Syringomyelia and the Chiari malformations. Park Ridge: AANS; 1997. p. 51–67.
6. Welsh JP, Yuen G, Placantonakis DG, Vu TQ, Haiss F, O'Hearn E, Moliver ME, Aicher SA. Why do Purkinje cells die so easily after global brain ischemia? Aldolase C, EAAT4, and the cerebellar contribution to posthypoxic myoclonus. Adv Neurol. 2002;89:331–59.
7. Allen G, Chase T. Induction of heat shock proteins and motor function deficits after focal cerebellar injury. Neuroscience. 2001;102:603–14.
8. Fukuda K, Aihara N, Sagar S, Sharp F, Pitts L, Honkaniemi J. Purkinje cell vulnerability to mild traumatic brain injury. J Neurotrauma. 1996;5:255–65.
9. Potts MB, Adwanikar H, Noble-Haeusslein LJ. Models of traumatic cerebellar injury. Cerebellum. 2009;8:211–21.
10. Go KG, Hew JM, Kamman RL, Molenaar WM, Pruim J, Blaauw EH. Cystic lesions of the brain. A classification based on pathogenesis, with consideration of histological and radiological features. Eur J Radiol. 1993;17:69–84.

Syringomyelia and the Chiari Malformations

15

Esther Beeson Dupépé, Kathrin Zimmerman, and Brandon G. Rocque

Introduction

Syringomyelia is a tubular fluid-filled cavity within the spinal cord parenchyma that spans more than one spinal segment [1–3]. Although most commonly associated with the Chiari malformations, there are a variety of etiologies associated with the development of syringomyelia including other congenital conditions and inflammatory or post-traumatic etiologies following injury to the brain or spine [2, 4–6]. Surgical intervention is considered for progressive syringomyelia that causes neurological deficits; however, the surgical management can be variable, and some have proposed tailoring treatment decisions to the underlying pathology [2]. In this chapter, we review the epidemiology, pathophysiology, treatment options, and prognosis of syringomyelia in patients with Chiari malformations.

Background and Terminology

In classic Greek mythology, Syrinx was a water nymph who was turned into a hollow reed to escape the god Pan who later turned the hollow reed into a musical flute [1, 2]. In 1827, the term syringomyelia was first used by D'Angers and today is used to refer to a tubular fluid-filled cavity within the spinal cord parenchyma that spans more than one spinal segment [1–3].

In its simplest form, syringomyelia is a tubular cavity within the spinal cord parenchyma [1]. In contrast to syringomyelia, which refers to a cystic dilation within the spinal cord parenchyma and inconsistently involves the central canal, *hydromyelia* refers to a cystic dilation of the central canal [1]. Because it is often impossible to determine if fluid in the spinal cord is truly a dilation of the central canal or external to the canal, the term *hydrosyringomyelia* has been used to describe the phenomenon, in an attempt to be rigorously correct. Despite these semantic distinctions, these terms are used somewhat interchangeably. Rostral extension of syringomyelia into the brainstem is termed *syringobulbia*. This most commonly involves the medulla, but the pons or midbrain may also be involved in severe cases [1].

E. B. Dupépé
Department of Neurological Surgery, St. Louis Children's Hospital, Washington University School of Medicine, St. Louis, MO, USA

K. Zimmerman
Department of Neurosurgery, Division of Pediatric Neurosurgery, University of Alabama at Birmingham, Birmingham, AL, USA

B. G. Rocque (✉)
Department of Neurosurgery, University of Alabama at Birmingham, Children's of Alabama, Birmingham, AL, USA
e-mail: brandon.rocque@childrensal.org

R. S. Tubbs et al. (eds.), *The Chiari Malformations*, https://doi.org/10.1007/978-3-030-44862-2_15

Pathology

Neuropathology

Findings at autopsy of the typical syrinx associated with Chiari malformations include an expanded or enlarged spinal cord that can fill the spinal canal and is described as tense [1, 2] and is absent of leptomeningeal thickening [7]. The syrinx skips the first cervical segment and is usually largest in the cervical segment but can extend caudally to the level of the conus in the most severe cases [2, 7]. The syrinx cavity is filled with clear fluid similar to cerebrospinal fluid (CSF) or extracellular fluid [1, 8, 9].

Morphology can be that of a simple cyst cavity or can be more complex, multiple, and possibly multiloculated [1]. However, when the septations that appear on imaging to cordon a syrinx into distinct fluid cavities have been explored using endoscopy, they have been found to be incomplete, allowing fluid to move from one cavity to another [2]. In Chiari I, the syrinx cavity may appear as a focal dilatation of the central canal within the cervical region that is discontinuous with the fourth ventricle, but in Chiari II, these fluid spaces can communicate; hence they are occasionally termed *communicating syringomyelia* [10]. The cyst cavity seen in the Chiari malformations will involve the dorsal aspect of the anterior horns, cross midline, and extend to the posterior horns in the transverse section [2, 7]. With enlargement, the lateral and posterior columns are thinned with preservation of the anterior horn cells ventrally and destruction of the anterior spinal commissure [2, 7]. Syrinx cavities are observed to communicate with the subarachnoid space, typically noted at the dorsal root entry zone [1, 10, 11]. Dissection into the spinal cord parenchyma is usually noted to be dorsolateral [1, 11, 12].

Pathophysiology

The underlying pathophysiology leading to syringomyelia formation has not been definitively established. However, several theories have been proposed that vary depending on the underlying associated etiology [13–15].

In the Chiari malformations, *hydrodynamic theories* center on a disruption of CSF flow at the craniocervical junction but diverge from each other on a proposed mechanism for syrinx formation. Gardner, Williams, and Oldfield have each proposed a variation of a theory centrally focused on pressure differences in the intracranial and spinal subarachnoid spaces [1]. In the late 1950s, Gardner and Angel first proposed a mechanism for syrinx formation in the context of fourth ventricular outlet obstruction due to a persistent opening of the central canal at the level of the obex [16, 17]. Gardner later described a "water hammer" effect of CSF pulsation at the obex as the driving mechanism for syrinx formation. In his model, hydromyelia and syringomyelia represent a progression from an initially enlarged central canal to eventual dissection into the spinal cord parenchyma [18].

Gardner was the first to observe a relationship between Chiari I malformations and syringomyelia [9]. He expanded on this concept to propose an imbalance of choroid plexus pulsations between the supratentorial and fourth ventricles underlying tentorial migration and the pathogenesis of Chiari malformations with subsequent fourth ventricular outlet obstruction due to underdevelopment of the foramen of Luschka and Magendie. Gardner's theory is limited by an inability to account for syringomyelia formation without underlying pathology at the craniocervical junction and experimental evidence that the obex is patent in a minority of patients [19, 20]. Additionally, his theory necessitates the existence of hydrocephalus for some period of time, even if transient [1].

Williams proffered a modernized version of the hydrodynamic theory that focused on the subarachnoid space and a more relative obstruction leading to CSF pressure disassociations. This theory accounts for the absence of hydrocephalus in many patients with Chiari I malformation by focusing on a relative increase in intracranial versus spinal CSF pressures. The theory holds that unidirectional impedance of CSF flow in the caudal direction due to arachnoid adhesions and asso-

ciated venous congestion leads to a valve-like effect exacerbated by Valsalva maneuvers [21, 22]. Williams was able to provide manometric pressure recordings demonstrating a craniospinal pressure differential supporting his theory [23, 24]. Ball and Dayan proposed that distortion of the subarachnoid spaces from the impact of the cerebellar tonsils on the structures of the posterior fossa leads to CSF tracking along the perivascular Virchow-Robin spaces ultimately into the spinal cord parenchyma [25]. Like Gardner's theory, these modified hydrodynamic theories do not account for syringomyelia associated with other etiologies.

Oldfield and others have proposed a relationship between the cardiac cycle and syrinx formation from the "piston effect" of the cerebellar tonsils at the foramen magnum that leads to pressure waves causing CSF to dissect into the spinal cord parenchyma along perivascular spaces [26, 27]. Furthermore, Oldfield proposes that the impact of the cerebellar tonsils at the level of the foramen magnum is the underlying pathophysiology driving formation of Chiari I malformations and the progressive development of syringomyelia, suggesting that Chiari I malformation is an acquired and not congenital phenomenon [27].

Venous congestion secondary to epidural venous compression has also been proposed as the driving pathophysiology for syrinx development. Here an increase in hydrostatic pressure within the valveless venous system of the spinal cord would lead to fluid transudation and increased interstitial fluid that precedes cyst expansion [2]. Levine has proposed a mechanical stress component associated with an obstructive lesion resulting in differential venous pressures and collapse in relation to the lesion. Mechanical stress and breakdown of the blood spinal barrier lead to fluid transudation within the damaged spinal cord [15]. Postural changes in posterior fossa contents have also been proposed as the etiology for syrinx formation and a rationale for posterior fossa decompression [28]. Bony abnormalities at the craniocervical junction have been associated with syringomyelia formation in pediatric patients, supporting blockage or obstruction at the level of the foramen magnum as a contributing pathology [29].

In summary, there are a number of theories about the pathogenesis of syringomyelia, but there remains no accepted consensus.

Classification

Syringomyelia is almost always a secondary finding, caused by an underlying pathology, which provides a scheme for classification. There are a variety of observed etiologies, including but not limited to post-traumatic etiologies, associated with tethered cord, tumors or vascular malformations, post-infectious arachnoiditis, and, of course, Chiari malformation. Distinguishing the underlying etiology as the basis for a classification system also provides a framework for determining clinical management and types of surgical intervention to be considered. Our review here focuses on the relationship of syringomyelia with the Chiari malformations.

Typical Presentation and Clinical Syndromes

Syringomyelia is often discovered during evaluation for scoliosis or incidentally during imaging performed for symptoms that are not referable to the spinal cord. However, in some cases, syringomyelia itself can be symptomatic. Segmental neurological deficits can be observed. The most common is sensory loss. In small syringes, only the anterior spinal cord is involved, leading to loss of pain and temperature sensation, with sparing of light touch and proprioception. This is known as dissociated sensory loss. If syringomyelia expands eccentrically or asymmetrically, one side may be more affected than the other (Figs. 15.1, 15.2, and 15.3). With larger syringes, a cape-like distribution of sensory loss can be seen.

Motor symptoms from syringomyelia tend to follow a pattern similar to central cord syndrome. Since motor fibers to intrinsic hand muscles are located most centrally, they are affected first, followed by those to the forearm, hand, and shoulder. Muscle stretch reflexes may be decreased due to anterior horn cell dysfunction or

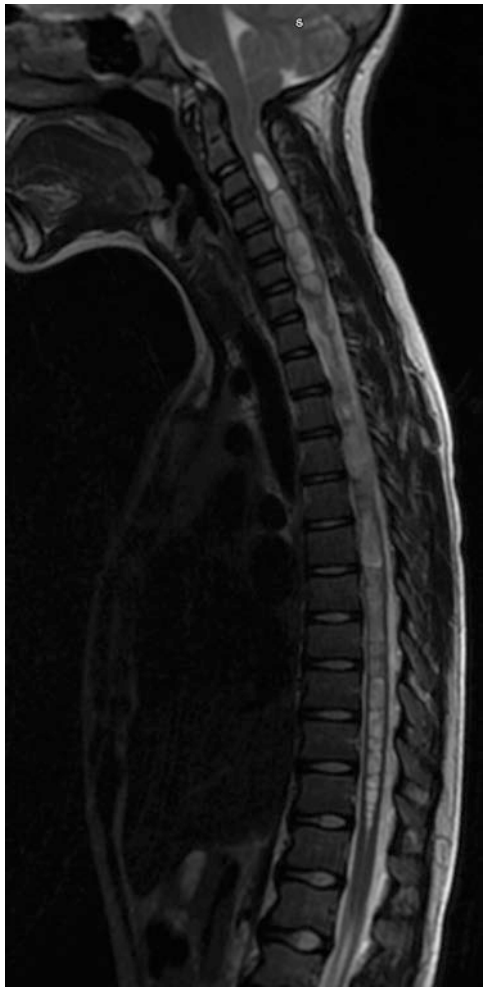

Fig. 15.1 Sagittal, T2-weighted magnetic resonance image (MRI) noting a holocord syrinx

increased due to stretching of corticospinal tracts. Horner syndrome is present in some cases due to disruption of the thoracic intermediolateral cell column. Bladder impairment is often a late finding. Paraparesis, Brown-Sequard syndrome, muscular atrophy, or cranial nerve palsies can also be seen [10].

Scoliosis is commonly seen in association with syringomyelia. It is assumed that this occurs because of asymmetric weakness of paraspinal muscles due to unilateral anterior horn cell dysfunction. Thresholds for treatment of scoliosis

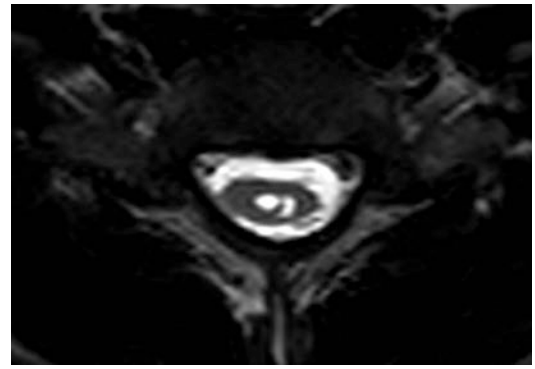

Fig. 15.2 Axial magnetic resonance image (MRI) of Fig. 15.1

vary depending on patient age and underlying conditions. Detailed discussion of these issues is beyond the scope of this chapter. However, in mild scoliosis associated with syringomyelia, treatment of the syrinx may arrest progression of the scoliosis. However, when scoliosis is more severe, the curve may progress regardless of syrinx treatment.

Surgical Management

As a general rule, treatment of progressive symptomatic syringomyelia should be aimed at the primary pathology causing syrinx formation. For example, a syrinx that is predominately in the distal spinal cord in a patient with myelomeningocele would likely best be treated by spinal cord untethering, whereas a syrinx associated with a Chiari I malformation would best be treated by Chiari decompression. However, the presence of a syrinx in itself is not always an indication for surgical intervention. Risks and benefits of surgery should always be considered. A small, idiopathic syrinx without associated symptoms may be followed clinically with serial imaging with consideration for surgery if progressive enlargement is observed, especially if attributable neurological symptoms develop, whereas a large syrinx or one with associated neurological deficits warrants more immediate surgical treatment.

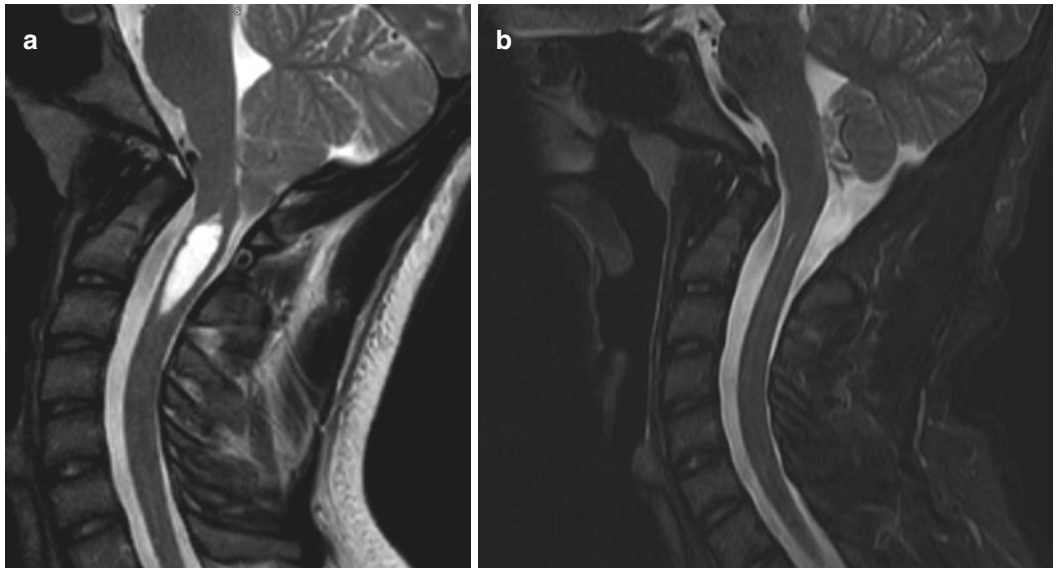

Fig. 15.3 Sagittal, T2-weighted magnetic resonance image (MRI) of patient with isolated cervical syrinx (**a**) preoperative and (**b**) postoperative

Chiari and Syringomyelia

The presence of a syrinx in the setting of Chiari I malformation is often considered an indication for surgical intervention. Syringomyelia secondary to Chiari I malformation carries a high risk for progression of symptoms or development of new neurological deficits [30, 31].

Surgical Techniques

In the presence of Chiari I malformation, it is most commonly assumed that the Chiari I is the cause of the syrinx. Therefore, posterior fossa decompression is the treatment of choice. In its simplest form, this consists of a craniectomy at the foramen magnum with C1 laminectomy. Many surgeons also perform expansile duraplasty, and some also advocate for resection or reduction of the cerebellar tonsils.

Variations of posterior fossa decompression range from bone-only decompression (craniectomy with or without C1 laminectomy) to the addition of tonsillar resection after duraplasty [32]. Of note, whether or not to open the dura has been the subject of much debate with techniques described to augment surgical decision-making, e.g., intraoperative ultrasonography [33, 34]. Unfortunately, available literature addressing this technical question is limited by surgeon preference and selection bias [35]. There is a prospective randomized clinical trial underway to address this particular question [36].

Some patients with Chiari I malformation have accompanying ventral abnormalities at the foramen magnum, including platybasia or basilar invagination. These individuals may be at higher risk for persistence or progression of syringomyelia after standard posterior fossa decompression. Some authors consider presence of these conditions to be evidence of craniocervical instability and therefore advocate occipito-cervical fusion in addition to standard posterior fossa decompression [37–39]. The clival basal angle, Grabb's line (pB-C2), and Wackenheim's line can be used as measures to help identify frank instability during preoperative workup [40]. Details of the surgical approach to posterior fossa decompression are covered at length in other chapters of this book.

The term "Chiari 0 malformation" has been used to describe patients with syringomyelia and posterior fossa crowding but with tonsils in a normal position. These patients have syringomyelia

without any evidence of an underlying condition. In well-selected patients with Chiari 0, syringomyelia may resolve after posterior fossa decompression [40, 41]. Detailed discussion of this entity is also covered elsewhere.

Outcomes

In general patients do well with surgery directed at their primary pathology. Improvement or resolution of their syringomyelia is observed on postoperative imaging over time, and neurological symptoms stabilize. In some cases, neurological symptoms can also improve, though this is not always the case [42, 43]. In patients with persistent postoperative syringomyelia, re-exploration with re-establishment of flow of CSF pathways has been shown to result in favorable outcomes [44]. In reviews of adult and pediatric patients, those most likely to respond well to surgery presented with headache or cervical pain, sleep apnea, or scoliosis less than 30°. Poor outcome was more likely observed in patients with preoperative neurological symptom duration greater than 2 years, evidence of muscular atrophy, cerebellar signs (ataxia or nystagmus), and dorsal column dysfunction [45, 46]. Additionally, an eccentric location of the syringomyelia cavity compared to the more common central location may be associated with less improvement, although overall favorable response and decrease in syrinx size are still observed [47].

Syrinx Shunting

Direct treatment of syringomyelia, using fenestration or shunting, is controversial. As noted, syringomyelia is most commonly treated by addressing what is thought to be the underlying pathology, such as a Chiari I malformation. However, in some cases, for example, an idiopathic syrinx with progressive symptoms, direct treatment of the syrinx is indicated. Some surgeons will also advocate for direct treatment of syringomyelia when the syrinx is not improved after what is considered to be an adequate posterior fossa decompression [48–50].

Syrinx fenestration is rarely advocated. It is presumed that a surgical fenestration will close spontaneously and thus that this procedure will have limited benefit. Syrinx shunting is performed through a standard laminotomy or laminectomy. Dural opening is performed in the usual fashion, typically in the midline. Midline myelotomy is then performed and a catheter placed into the syrinx [49–56]. Alternatively, if the syrinx is eccentric, myelotomy may be performed at the location where the spinal cord is thinnest or through the dorsal root entry zone. The proximal catheter placed into the syrinx may be a lumbar shunt catheter, a simple tube, or T-shaped. There are several options for placing the distal catheter. Most simply, the distal catheter is placed in the spinal subarachnoid space through the same incision, thus creating a syringo-subarachnoid shut. In this case, care must be taken to place the distal catheter in the subarachnoid space, not into the subdural space. A valve is not required for a syringo-subarachnoid shunt. Alternatively, the distal catheter may be placed in the pleura or peritoneum. If placed outside the central nervous system, a valve is typically used.

Conclusion

Syringomyelia is a pathologic accumulation of fluid within the substance of the spinal cord. It may lead to progressive neurological deficits. Treatment of syringomyelia is directed at resolving the underlying condition. In the presence of Chiari I malformation, posterior fossa decompression is the first-line therapy.

References

1. Harrison DK. Chapter 9: Pathology of syringomyelia due to Chiari malformation. In: Tubbs RS, Oakes WJ, editors. The Chiari malformations. New York: Springer; 2013. p. 121–5.
2. Iskandar BJ, Rocque BG, Medow JE. Chapter 31: Syringomyelia and hydromyelia. In: Albright AL, Pollack IF, Adelson PD, editors. Principles and practice of pediatric neurosurgery. 3rd ed. New York: Thieme; 2015.
3. Milhorat TH, Miller JI, Johnson WD, Adler DE, Heger IM. Anatomical basis of syringomyelia occurring with hindbrain lesions. Neurosurgery. 1993;32(5):748–54; discussion 754.

4. Batzdorf U. Syringomyelia, Chiari malformations, and hydromyelia. 4th ed. Philadelphia: WB Saunders; 1996.
5. Williams B. Surgical Management of non-hindbrain-related and Posttraumatic Syringomyelia. Philadelphia: WB Saunders; 1995.
6. Yamada S. Tethered cord syndrome in children and adults. 2nd ed. New York: Thieme Medical Publishers; 2010. 264 p.
7. Greenfield J, Graham D, Lantos P. Greenfield's neuropathology. 7th ed. London/New York: Arnold; 2002.
8. Ellertsson AB. Syringomyelia and other cystic spinal cord lesions. Acta Neurol Scand. 1969;45(4):403–17.
9. Gardner WJ. Hydrodynamic mechanism of syringomyelia: its relationship to myelocele. J Neurol Neurosurg Psychiatry. 1965;28(3):247–59.
10. Milhorat TH, Capocelli AL, Anzil AP, Kotzen RM, Milhorat RH. Pathological basis of spinal cord cavitation in syringomyelia: analysis of 105 autopsy cases. J Neurosurg. 1995;82(5):802–12.
11. Milhorat TH, Kotzen RM, Anzil AP. Stenosis of central canal of spinal cord in man: incidence and pathological findings in 232 autopsy cases. J Neurosurg. 1994;80(4):716–22.
12. Milhorat TH. Classification of syringomyelia. Neurosurg Focus. 2000;8(3):E1.
13. Ellertsson AB, Greitz T. The distending force in the production of communicating syringomyelia. Lancet Lond Engl. 1970;1(7658):1234.
14. Levine DN. The pathogenesis of normal pressure hydrocephalus: a theoretical analysis. Bull Math Biol. 1999;61(5):875–916.
15. Levine DN. The pathogenesis of syringomyelia associated with lesions at the foramen magnum: a critical review of existing theories and proposal of a new hypothesis. J Neurol Sci. 2004;220(1–2):3–21.
16. Gardner WJ, Angel J. The mechanism of syringomyelia and its surgical correction. Clin Neurosurg. 1958;6:131–40.
17. Gardner WJ, Angel J. The cause of syringomyelia and its surgical treatment. Cleve Clin Q. 1958;25(1):4–8.
18. Gardner WJ. Syringomyelia. Surg Neurol. 1977;7(6):370.
19. Pillay PK, Awad IA, Hahn JF. Gardner's hydrodynamic theory of syringomyelia revisited. Cleve Clin J Med. 1992;59(4):373–80.
20. West RJ, Williams B. Radiographic studies of the ventricles in syringomyelia. Neuroradiology. 1980;20(1):5–16.
21. Godzik J, Kelly MP, Radmanesh A, Kim D, Holekamp TF, Smyth MD, et al. Relationship of syrinx size and tonsillar descent to spinal deformity in Chiari malformation Type I with associated syringomyelia. J Neurosurg Pediatr. 2014;13(4):368–74.
22. Williams B. Pathogenesis of syringomyelia. Acta Neurochir. 1993;123(3–4):159–65.
23. Williams B. The distending force in the production of communicating syringomyelia. Lancet. 1970;296(7662):41–2.
24. Williams B. A demonstration analogue for ventricular and intraspinal dynamics (DAVID). J Neurol Sci. 1974;23(3):445–61.
25. Ball M, Dayan A. Pathogenesis of syringomyelia. Lancet. 1972;300(7781):799–801.
26. Oldfield EH, Muraszko K, Shawker TH, Patronas NJ. Pathophysiology of syringomyelia associated with Chiari I malformation of the cerebellar tonsils. Implications for diagnosis and treatment. J Neurosurg. 1994;80(1):3–15.
27. Oldfield EH. Pathogenesis of Chiari I – pathophysiology of syringomyelia: implications for therapy: a summary of 3 decades of clinical research. Neurosurgery. 2017;64(CN_suppl_1):66–77.
28. Rai SKR, Rai PSK. Volume change theory for syringomyelia: a new perspective. Asian J Neurosurg. 2015;10(4):245–51.
29. Gad KA, Yousem DM. Syringohydromyelia in patients with Chiari I malformation: a retrospective analysis. AJNR Am J Neuroradiol. 2017;38(9):1833–8.
30. Rocque BG, George TM, Kestle J, Iskandar BJ. Treatment practices for Chiari malformation Type I with syringomyelia: results of a survey of the American Society of Pediatric Neurosurgeons: clinical article. J Neurosurg Pediatr. 2011;8(5):430–7.
31. Strahle J, Smith BW, Martinez M, Bapuraj JR, Muraszko KM, Garton HJL, et al. The association between Chiari malformation Type I, spinal syrinx, and scoliosis. J Neurosurg Pediatr. 2015;15(6):607–11.
32. Guyotat J, Bret P, Jouanneau E, Ricci AC, Lapras C. Syringomyelia associated with type I Chiari malformation. A 21-year retrospective study on 75 cases treated by foramen magnum decompression with a special emphasis on the value of tonsils resection. Acta Neurochir. 1998;140(8):745–54.
33. Milhorat TH, Bolognese PA. Tailored operative technique for Chiari type I malformation using intraoperative color Doppler ultrasonography. Neurosurgery. 2003;53(4):899–905; discussion 905–906.
34. Yundt KD, Park TS, Tantuwaya VS, Kaufman BA. Posterior fossa decompression without duraplasty in infants and young children for treatment of Chiari malformation and achondroplasia. Pediatr Neurosurg. 1996;25(5):221–6.
35. Lu VM, Phan K, Crowley SP, Daniels DJ. The addition of duraplasty to posterior fossa decompression in the surgical treatment of pediatric Chiari malformation Type I: a systematic review and meta-analysis of surgical and performance outcomes. J Neurosurg Pediatr. 2017;20(5):439–49.
36. Posterior fossa decompression with or without duraplasty for Chiari Type I malformation with syringomyelia. ClinicalTrials.gov. Cited 2019 Feb 11. Available from: https://clinicaltrials.gov/ct2/show/NCT02669836
37. Menezes AH. Primary craniovertebral anomalies and the hindbrain herniation syndrome (Chiari I): data base analysis. Pediatr Neurosurg. 1995;23(5):260–9.
38. Menezes AH. Craniovertebral junction abnormalities with hindbrain herniation and syringomyelia:

regression of syringomyelia after removal of ventral craniovertebral junction compression. J Neurosurg. 2012;116(2):301–9.
39. Bollo RJ, Riva-Cambrin J, Brockmeyer MM, Brockmeyer DL. Complex Chiari malformations in children: an analysis of preoperative risk factors for occipitocervical fusion. J Neurosurg Pediatr. 2012;10(2):134–41.
40. Browd SR, Buckley RT, Ellenbogen RG. Chiari Malformations and Syringomyelia. In: Steinmetz MP, Benzel EC, editors. Benzel's spine surgery. 4th ed. Philadelphia: Elsevier; 2016. p. 1436–44.
41. Chern JJ, Gordon AJ, Mortazavi MM, Tubbs RS, Oakes WJ. Pediatric Chiari malformation Type 0: a 12-year institutional experience: clinical article. J Neurosurg Pediatr. 2011;8(1):1–5.
42. Tubbs RS, Beckman J, Naftel RP, Chern JJ, Wellons JC, Rozzelle CJ, et al. Institutional experience with 500 cases of surgically treated pediatric Chiari malformation Type I. J Neurosurg Pediatr. 2011;7(3):248–56.
43. Tubbs RS, McGirt MJ, Oakes WJ. Surgical experience in 130 pediatric patients with Chiari I malformations. J Neurosurg. 2003;99(2):291–6.
44. Heiss JD, Suffredini G, Smith R, DeVroom HL, Patronas NJ, Butman JA, et al. Pathophysiology of persistent syringomyelia after decompressive craniocervical surgery. J Neurosurg Spine. 2010;13(6). Available from: https://www.ncbi.nlm.nih.gov/pmc/articles/PMC3822767/.
45. Dyste GN, Menezes AH, VanGilder JC. Symptomatic Chiari malformations. An analysis of presentation, management, and long-term outcome. J Neurosurg. 1989;71(2):159–68.
46. Nagib MG. An approach to symptomatic children (ages 4–14 years) with Chiari type I malformation. Pediatr Neurosurg. 1994;21(1):31–5.
47. Adeeb N, Mortazavi MM, Shoja MM, Tubbs RS, Oakes WJ, Rozzelle CJ. A single-center experience with eccentric syringomyelia found with pediatric Chiari I malformation. Childs Nerv Syst. 2012;28(11):1937–41.
48. Hida K, Iwasaki Y, Koyanagi I, Sawamura Y, Abe H. Surgical indication and results of foramen magnum decompression versus syringosubarachnoid shunting for syringomyelia associated with Chiari I malformation. Neurosurgery. 1995;37(4):673–8; discussion 8–9.
49. Isu T, Iwasaki Y, Akino M, Abe H. Syringosubarachnoid shunt for SYRINGOMYELIA associated with Chiari I malformation (Type I). Acta Neurochir. 1990;107:152–60.
50. Tognetti F, Calbucci F. Syringomyelia: syringosubarachnoid shunt versus posterior fossa decompression. Acta Neurochir. 1993;123:196–797.
51. Barbaro NM, Wilson CB, Gutin PH, Edwards MS. Surgical treatment of syringomyelia. Favorable results with syringoperitoneal shunting. J Neurosurg. 1984;61(3):531–8.
52. Batzdorf U, Klekamp J, Johnson JP. A critical appraisal of syrinx cavity shunting procedures. J Neurosurg. 1998;89(3):382–8.
53. Edgar RE. Surgical management of spinal cord cysts. Paraplegia. 1976;14(1):21–7.
54. Padovani R, Cavallo M, Gaist G. Surgical treatment of syringomyelia: favorable results with syringosubarachnoid shunting. Surg Neurol. 1989;32(3):173–80.
55. Tator CH, Meguro K, Rowed DW. Favorable results with syringosubarachnoid shunts for treatment of syringomyelia. J Neurosurg. 1982;56(4):517–23.
56. Vernet O, Farmer JP, Montes JL. Comparison of syringopleural and syringosubarachnoid shunting in the treatment of syringomyelia in children. J Neurosurg. 1996;84(4):624–8.

16 Non-hindbrain-Related Syringomyelia

Jörg Klekamp

The term syringomyelia was introduced by Ollivier D'Angers in 1827 [1] for cystic cavitations of the spinal cord. Syringomyelia describes a progressive accumulation of fluid inside the spinal cord. Up to this day, no pathophysiological concept for the development of syringomyelia is generally accepted [2]. However, with the advent of modern imaging techniques in the 1970s and 1980s, it became clear that a syrinx is always associated with other pathologies in the spinal canal or craniocervical junction. This observation has changed treatment concepts for these patients in a fundamental way. If the associated pathology can be treated successfully, no further measures for the syrinx are needed. It is now widely accepted that syringomyelia is related to intramedullary tumors or pathologies that cause a disturbance of cerebrospinal fluid (CSF) flow or spinal cord tethering [2, 3]. Table 16.1 gives an overview on the different pathologies related to syringomyelia in the author's series.

Currently, syringomyelia is considered as an accumulation of extracellular fluid of the spinal cord [3, 4]. In case of intramedullary tumors, it is generally believed that alterations of the blood-spinal cord barrier play a major role [5]. But this may not be the only mechanism. It is noteworthy that infiltrating intramedullary tumors rarely produce syringomyelia, whereas a syrinx is a common feature of displacing neoplasms [6]. More information is available on the effects of CSF flow obstructions on the spinal cord from animal [7] as well as computer models [8]. The subarachnoid space pressure is increased above the obstruction inducing changes of extracellular fluid distribution in the spinal cord [7], which may then lead to syringomyelia [3, 4]. Increased flow in the perivascular spaces has been implicated for this effect [3, 7, 9–12]. If flow capacities in the extracellular space are exceeded, there appears to be an evolution from spinal cord

Table 16.1 Pathologies associated with syringomyelia

Diagnosis	Total	Syringomyelia
Craniocervical junction	971	677
Chiari I	856	607 (70.9%)
Chiari II	54	28 (51.9%)
Foramen magnum arachnoiditis	34	34 (100%)
Posterior fossa tumors—Chiari I	13	3 (23.1%)
Posterior fossa arachnoid cysts—Chiari I	14	5 (35.7%)
Spinal canal	2897	1077
Posttraumatic syringomyelia	177	177
Non-traumatic arachnopathies	429	429
Intramedullary tumors	391	183 (46.8%)
Extramedullary tumors	971	117 (12.0%)
Extradural tumors	600	22 (3.7%)
Tethered cord syndromes	264	84 (31.8%)
Degenerative disc disease	65	65

J. Klekamp (✉)
Department of Neurosurgery, Christliches Krankenhaus Quakenbrück, Quakenbrück, Lower Saxony, Germany
e-mail: j.klekamp@ckq-gmbh.de

R. S. Tubbs et al. (eds.), *The Chiari Malformations*, https://doi.org/10.1007/978-3-030-44862-2_16

edema (i.e., the so-called presyrinx state) to syringomyelia [13]. Intramedullary neoplasms and cord tethering may alter extracellular fluid movements to similar effects. Once syringomyelia has developed, the increased intramedullary pressure [14] and fluid movements inside the syrinx [15, 16] may lead to spinal cord damage [17–19] and progressive neurological symptoms.

Diagnosis

In patients with Chiari malformations, CSF flow can be compromised by cerebellar tonsils filling the space of the cisterna magna, by arachnoid scarring in the foramen magnum area, and by obstruction of the foramen of Magendie. In posttraumatic syringomyelia, CSF flow obstruction may be caused by arachnoid scarring at the trauma level and narrowing of the spinal canal due to posttraumatic stenosis or kyphosis. Furthermore, posttraumatic cord tethering may contribute to syrinx development.

In the absence of a craniocervical malformation, an intramedullary tumor, a tethered cord syndrome, or a history of spinal trauma, syringomyelia is still considered idiopathic by many physicians. However, these patients have to be evaluated very carefully for radiological and clinical signs of arachnoid pathologies in the spinal canal causing CSF flow obstructions. The syrinx starts at the level of obstruction and expands from there. If the syrinx expands in a rostral direction, the obstruction will be found at the caudal end of the syrinx and vice versa. This also implies that the obstruction will most likely be found close to the largest diameter of the syrinx [2] (Fig. 16.1).

Due to the pulsatile movements of arachnoid septations, webs, or cysts, standard magnetic resonance imaging (MRI) may not always be able to demonstrate an arachnopathy directly. With a history of spinal meningitis or subarachnoid hemorrhage [20], the often quite extensive arachnopathy is rather easy to diagnose on MRI [21] (Fig. 16.2). Many arachnopathies, however, are quite discrete and extend over a few millimeters only. Cardiac gated cine MRI should be employed for such instances to study spinal CSF flow to identify areas of flow obstruction that may correspond to such circumscribed arachnoid pathologies [16, 21] (Fig. 16.1). Sometimes significant flow signals can also be detected in the syrinx itself. In such cases, the highest flow velocities in the syrinx can be expected adjacent to the arachnoid scarring (Fig. 16.1). The spinal cord should be studied with thin axial slices in T2 over the entire extent of the syrinx to search for areas of cord compression, displacement, or adhesion to the dura [21–23] (Figs. 16.1, 16.2, and 16.3). In the sagittal plane, the contour of the cord may appear distorted in areas of arachnoid scarring. Constructive interference in steady state (CISS) sequences can be used not only for the demonstration of the syrinx [24] but may also be helpful to detect arachnoid webs, scars, and cysts, because this technique is less susceptible to CSF flow artifacts [24]. Primary arachnopathies—i.e., unrelated to trauma or any other disease process—will almost always be found in the thoracic spine posterior to the spinal cord [21, 25]. Myelography and postmyelographic computed tomography (CT) are alternative methods to demonstrate arachnoid pathologies but have a lower sensitivity.

The sequence of events leading to a syrinx has implications not only for the neuroradiological appearance as just described but also for the evolution of clinical symptoms. The syrinx develops as a consequence of events that are set off by a pathology leading to CSF flow obstruction. Therefore, the first neurological symptoms in the patient's history are generally caused by this underlying pathology rather than the syrinx. In other words, a carefully taken clinical history can provide clues to the underlying pathology. If neurological signs spread to other parts of the body in an ascending pattern, the cause of the syrinx will be located at the lower pole of the syrinx and vice versa similar to the radiological evolution [2]. Apart from trauma, arachnoid scarring may be related to infection [26], hemorrhage [20], irritation by old contrast agents such as pantopaque [27], or surgery, to mention a few [21].

It is always puzzling that patients may harbor a huge syrinx and yet have just minor symptoms with exactly the opposite observation for some smaller syrinx cavities associated with major

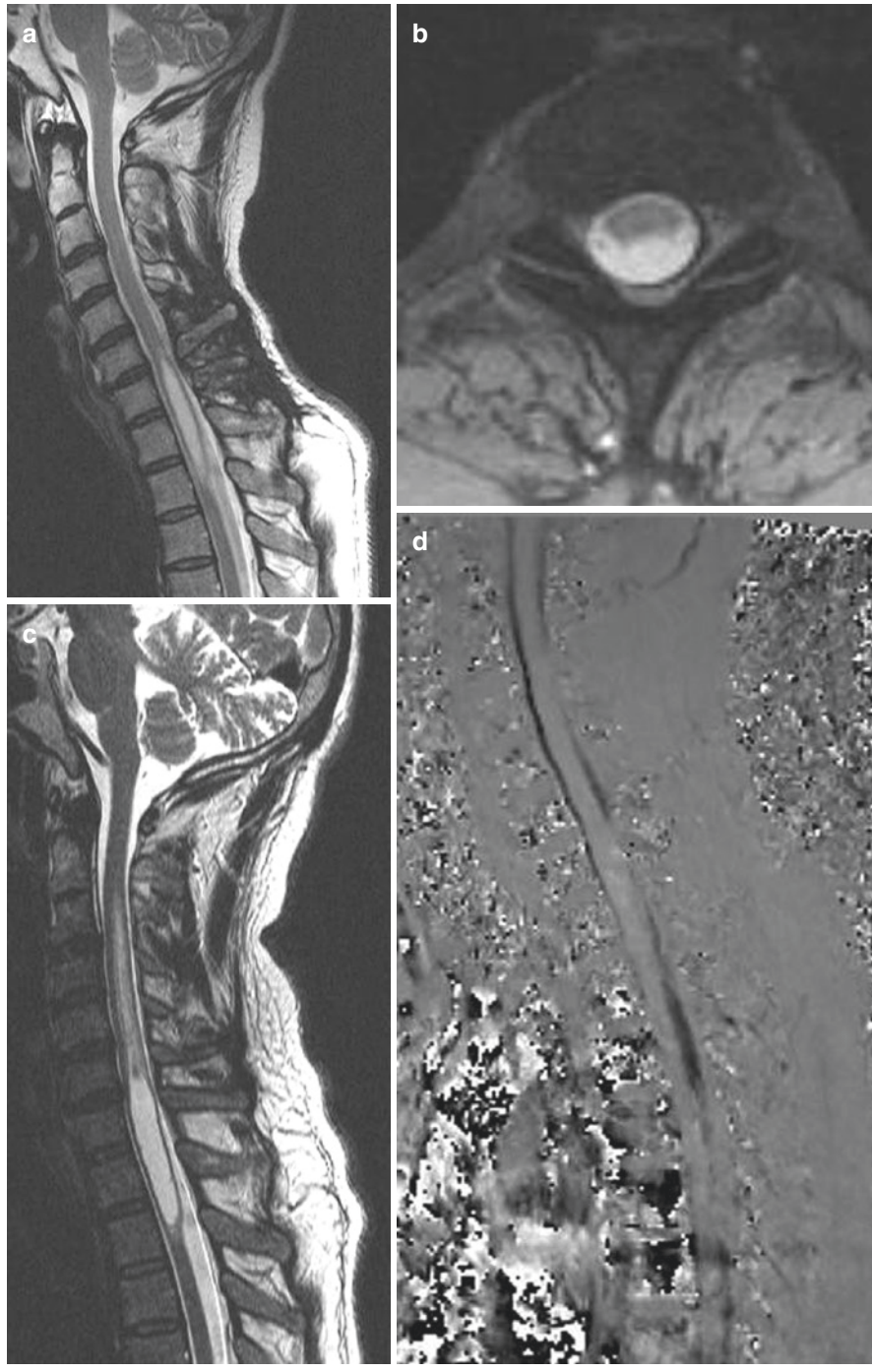

Fig. 16.1 (**a**) This sagittal T2-weighted MRI shows a syrinx extending from C6 to Th2 in a 43-year-old neuroradiologist with pain, sensory deficits, and dysesthesias in his left arm. Next to the lower pole, the spinal cord appears slightly indented. (**b**) The axial scan right below the syrinx demonstrates a slight posterior compression of the cord. (**c**) Two years later, the sagittal scan demonstrates the edema extending to C3 with increased diameter of the syrinx C6 to Th2. (**d**) The cine MRI shows a diminished CSF flow posteriorly across the syrinx and at Th2. (**e**) After decompression at Th2, the postoperative MRI demonstrates complete resolution of the syrinx and edema with no further compression of the cord in the axial scan (**f**). Postoperatively, the patient reported no change with 2 years of follow-up

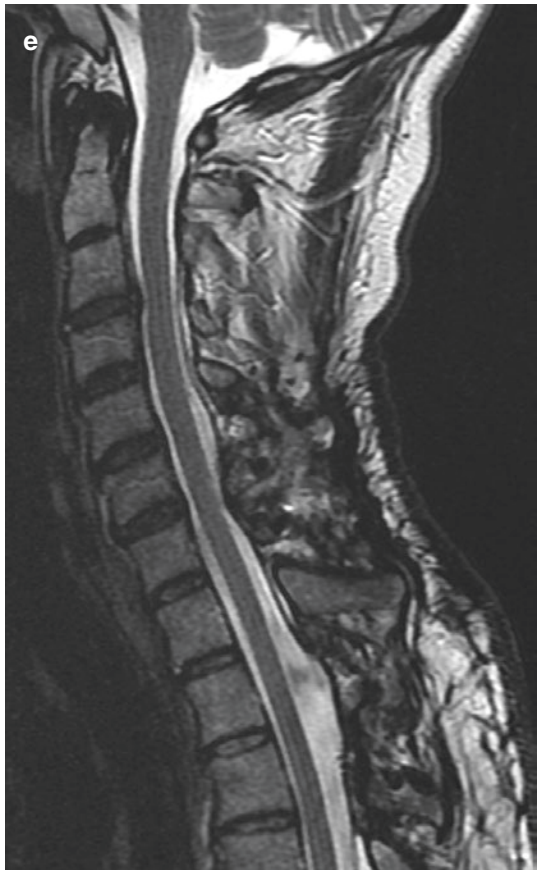

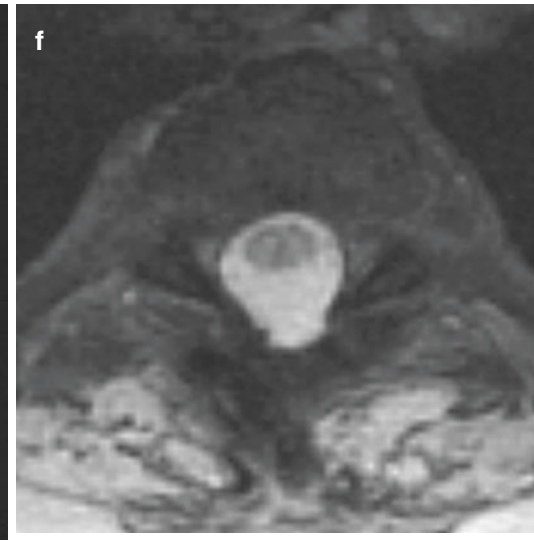

Fig. 16.1 (continued)

neurological deficits. One explanation for this paradox may be that a great deal of the clinical problems are related to the underlying disease process causing the syrinx rather than to the syrinx itself [2, 28]. This holds particularly for patients with extensive arachnopathies completely encircling the spinal cord after multiple surgeries, subarachnoid hemorrhages, or spinal meningitis [21, 25]. Similarly, a syrinx associated with a tethered cord or an intramedullary tumor will almost never become symptomatic as signs of cord compression and tethering dominate the clinical picture [2].

The classical symptoms of syringomyelia are a dissociated sensory loss with loss of sensation for temperature and pain but preserved sensation for light touch. Pain related to syringomyelia is either permanent or aggravated by maneuvers such as coughing and sneezing and perceived in dermatomes corresponding to the syrinx. Late symptoms of syringomyelia are muscle atrophies corresponding to damage of anterior horn cells or trophic changes leading to skin and joint damages, particularly in the shoulder and elbow [2, 28].

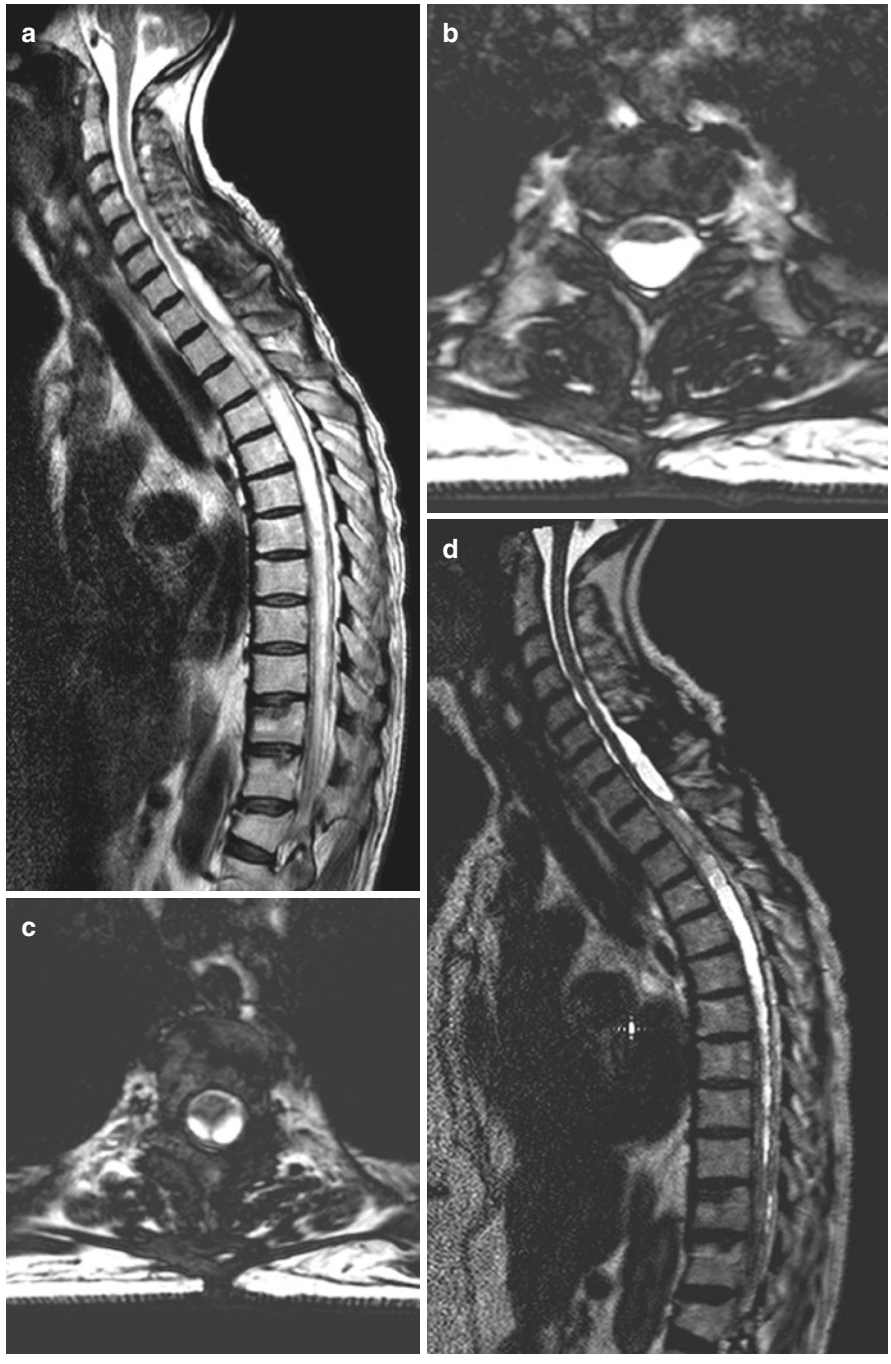

Fig. 16.2 (**a**) The sagittal T2-weighted MRI shows a syrinx Th2 to Th12 related to an extensive postmeningitic arachnopathy extending from C7 downward, causing compression of the cervical cord as demonstrated in the axial scan (**b**) in a 67-year-old woman with progressive paraparesis making her wheelchair dependent after unsuccessful fenestration of arachnoid septations in the cervicothoracic region in another institution. (**c**) The posterior median arachnoid septum appears thickened. (**d**) Thin sagittal slices in T2 demonstrate arachnoid septations, cysts, and adhesions between the cord and dura from C7 downward throughout the entire thoracic canal. The postoperative sagittal (**e**) and axial (**f**) MRIs show the decompression of the spinal cord after fenestration of arachnoid septations and cysts in the cervicothoracic area. The patient reported postoperative improvement of sensory functions, dysesthesias, pain, and motor weakness but was still left confined to a wheelchair

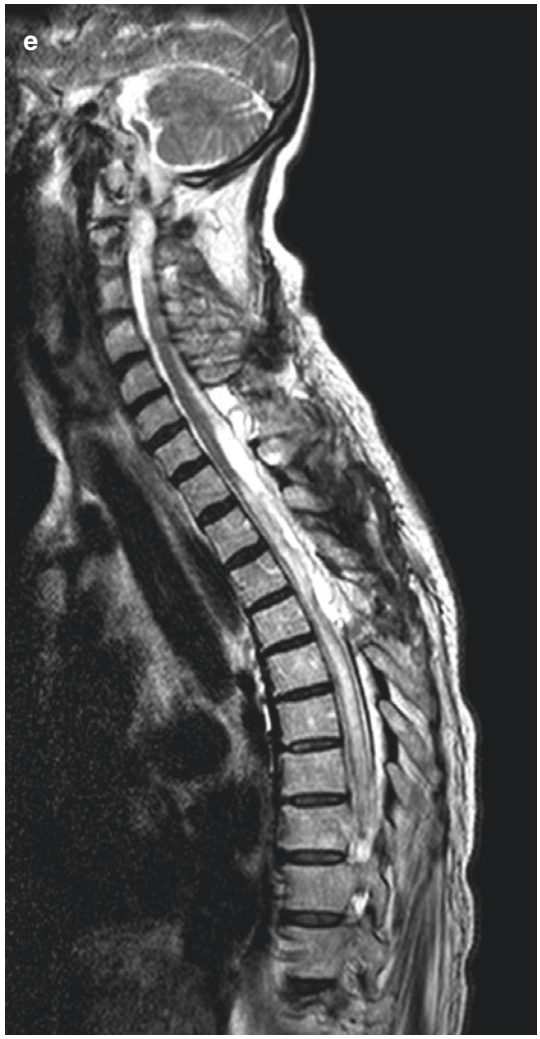

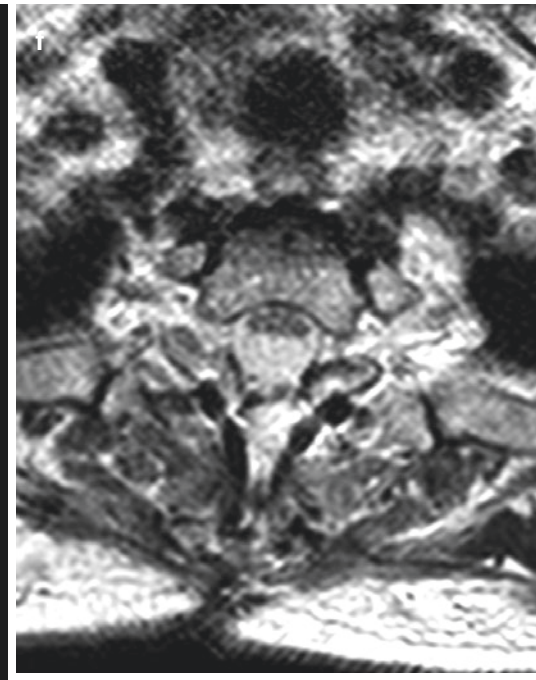

Fig. 16.2 (continued)

Management

About 71.1% of patients with a Chiari I malformation developed a syrinx in the author's series. No other pathology causes syringomyelia in such a high proportion (Table 16.1). For syringomyelia associated with intramedullary tumors and Chiari I malformation, the rates for postoperative syrinx resolution are above 80%, provided the tumor is removed and all components contributing to CSF flow obstruction in Chiari malformations have been surgically addressed, respectively.

Successful treatment of syringomyelia related to spinal rather than craniocervical CSF flow obstructions is much more challenging. The underlying causes are more difficult to identify and to deal with surgically. For spinal arachnopathies, surgery should be reserved for patients with progressive symptoms. Nevertheless, treating the cause of the syrinx with arachnolysis and duraplasty is rewarded by considerably better results compared to syrinx shunting procedures [25, 28–32].

Neuropathic pain and dysesthesias, particularly those of burning character, may be major

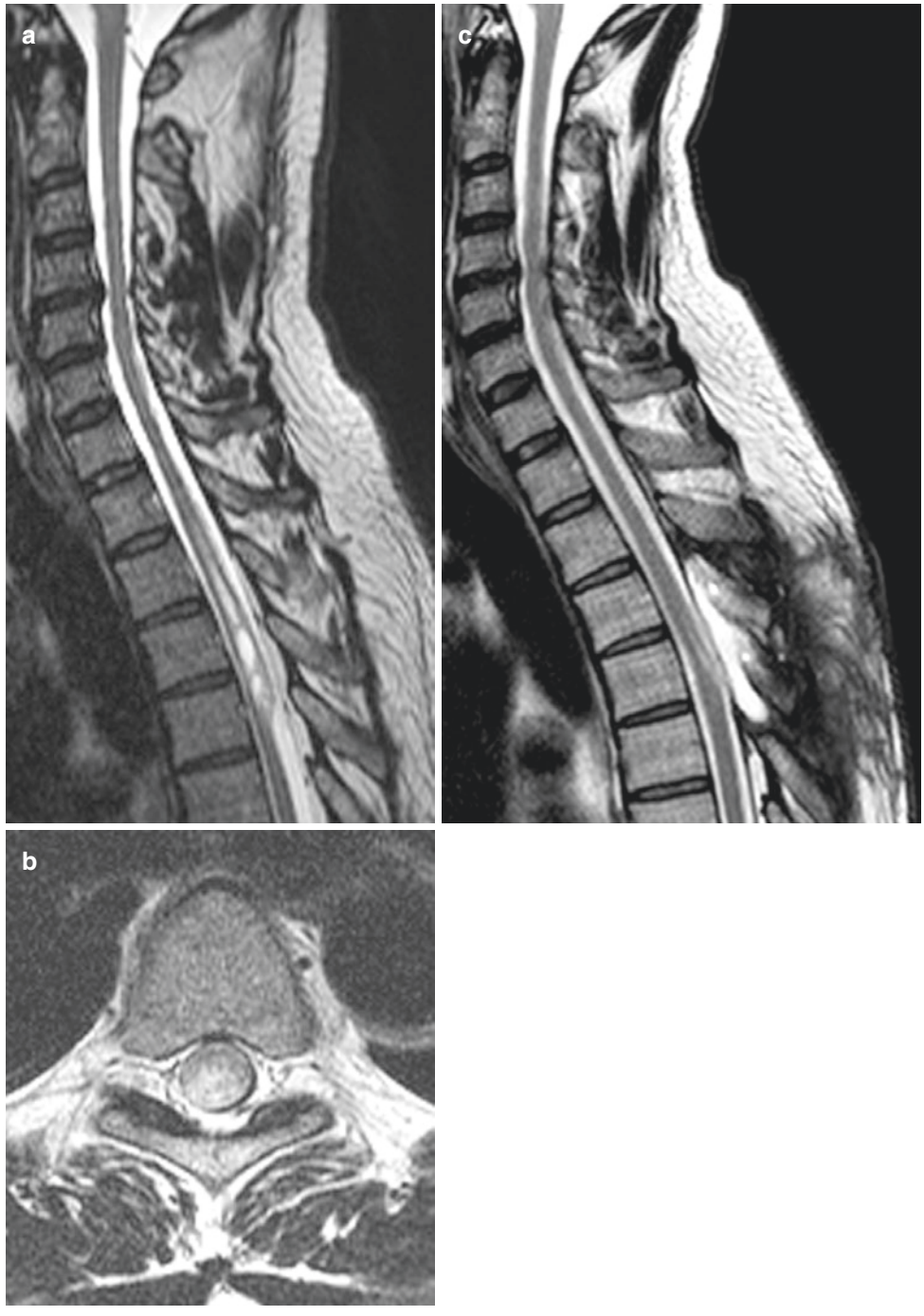

Fig. 16.3 (**a**) The sagittal T2-weighted MRI shows a posttraumatic syrinx Th2–Th4 in a 46-year-old man 16 months after suffering an incomplete cord injury at Th4 with sensory but no motor deficits. The cyst caliber is largest at the lower pole. (**b**) At Th4/Th5 the axial scan reveals an area of cord compression by a cystic posttraumatic arachnopathy at this level. (**c**) After decompression at Th3 and Th4, the postoperative MRI demonstrates a complete resolution of the syrinx. Postoperatively, symptoms remained unchanged for 14 months

clinical problems. Even though these may improve with successful treatment of the syrinx, this is never certain. Therefore, the decision for or against surgery should be based on the course of neurological signs and symptoms rather than pain syndromes alone.

In general, surgery can be recommended for patients with arachnoid scarring limited to about 2–3 spinal segments in the posterior section of the subarachnoid space [21, 25] (Figs. 16.1 and 16.3). All operations are performed in prone position. Laminotomies are recommended to reinsert the lamina at the end of the operation with titanium miniplates. After exposure of the dura, the extent of the arachnoid pathology can be visualized with ultrasound. The syrinx can be visualized. Pulsations of syrinx fluid and CSF may become visible. Sometimes, arachnoid septations can be seen. Most importantly, the safest spot for opening of the dura can be chosen with this technique. As contamination of the CSF with blood may cause inflammatory reactions of the arachnoid, great care is taken to achieve good hemostasis. For this purpose, the entire surgical field is covered by moist cottonoids, which keep soft tissues moist and soak up any minor bleeding. Then the dura is opened under the operating microscope in the midline without opening of the arachnoid. Once the dura is held open with sutures, the arachnoid pathology can be studied, and adequate exposure cranially and caudally is ensured in order to gain access to normal and unaffected subarachnoid space on either end. Obviously, any surgeon should be familiar with the normal anatomy of the spinal subarachnoid space [33]. The posterior subarachnoid space is divided in two halves by a posterior longitudinal arachnoid septum. This septum extends between the outer arachnoid layer and an intermediate layer on the cord surface. The insertion on the cord surface is related to the midline dorsal vein. Further strands of arachnoid may be encountered in the posterior and—to a lesser degree—lateral subarachnoid space. Another landmark is the dentate ligaments, which originate from the spinal cord pia mater, run between posterior and anterior nerve roots, and insert close to the dural nerve root sleeve. With a microdissector, arachnoid and dura can be separated from each other without any problem in areas without arachnoid scarring, i.e., at either end of the exposure. In the area of scarring, sharp dissection with microscissors is usually required to achieve this. At the level of CSF flow obstruction, the arachnoid may become densely adherent to the cord surface. With opening of the rostral and caudal subarachnoid space, CSF flushes into the surgical field, and often the cord, which was distended by the syrinx, starts to pulsate, and the syrinx may collapse at this point. The arachnoid scar can be resected layer by layer leaving a last sheath on the cord surface to avoid injury to the cord or surface vessels. This last layer resembles the intermediate arachnoidal layer mentioned previously. In this way, a free CSF passage in the posterior subarachnoid space can be created in every patient across the region of the arachnopathy. Dissection is then continued laterally on either side toward the dentate ligaments. This leads to complete untethering of the cord in the majority of cases. No dissection should be performed anteriorly of the dentate ligaments to avoid injuries to motor pathways and anterior spinal cord vessels. Closing the microsurgical part of the operation, an expansile duraplasty is inserted with a tight running suture and finally lifted up with tenting sutures on either side. To avoid scar formation and tethering between duraplasty and spinal cord, alloplastic material for duraplasty should be preferred, i.e., Gore-Tex® (W.L. Gore & Associates GmbH, Putzbrunn, Germany). Special attention is finally paid to a good, tight closure of the muscle layer to prevent any CSF from entering the epifascial space [25, 29]. In patients who have been operated before, as in patients with posttraumatic syringomyelia who underwent spinal instrumentation, for instance, a lumbar drain is placed prophylactically if the soft tissue appears scarred and sparsely vascularized.

Considerable experience is needed to be successful with this surgical technique. The more focused the surgery, the less scarring may result. If unnecessary steps are taken, such as a too extensive dura opening, or the surgical field is contaminated with considerable amounts of blood, postoperative scarring may counterbalance completely the effect of surgery. On the other hand, if the dura opening is not extensive enough to gain access to the normal subarachnoid space above and below the level of scarring, the

procedure is insufficient. As always, it is the right measure that counts and determines whether an operation will be successful.

For patients with more extensive arachnopathies after meningitis, multiple intradural surgeries, or spinal subarachnoid hemorrhage, surgery can rarely provide a sustained normal CSF passage [21, 25, 28]. Axial MRIs taken over the entire area of the arachnopathy may be evaluated in such instances for evidence of cord compression. Quite often, pouches and cysts have formed causing profound cord compression over a few spinal segments. Such compressions can be treated surgically by wide fenestration of the corresponding arachnoid membranes in individual cases (Fig. 16.2). Such an operation can improve neurological symptoms related to the cord compression for some time, but it will neither influence the syrinx nor the further neurological progress in the long term [21].

For patients, in whom the cause of syringomyelia is not amenable to surgery, thecoperitoneal shunts have been introduced, which drain CSF from the subarachnoid space above the level of obstruction to the peritoneal cavity [34–38]. For cavities extending into the cervical cord, ventriculoperitoneal shunts have been used for the same purpose [39, 40]. However, these shunts have their problems. There is little experience concerning the correct pressure settings other than to set them as low as possible avoiding signs of overdrainage or low intracranial pressure. Ten patients in the author's series were treated with low-pressure shunts of 4 cm H_2O opening pressure. In one patient, this low pressure was still not low enough, so that the valve was removed leaving the patient with a valveless drain. One patient developed a low-pressure syndrome including subdural effusions requiring surgery so that the shunt needed to be removed despite a good effect on the syrinx. Overall, about half of the patients benefitted from thecoperitoneal shunts for at least 4 years in the author's series (Fig. 16.4).

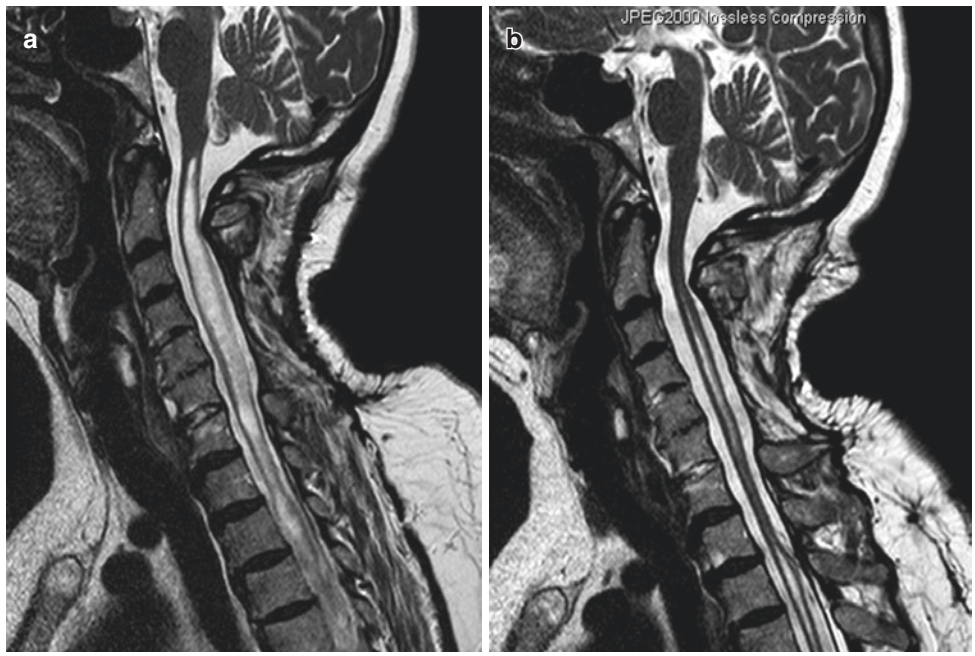

Fig. 16.4 (**a**) The sagittal T2-weighted MRI shows a posttraumatic syringomyelia extending from the injury level at Th12 up to the foramen magnum in a 61-year-old woman 40 years after the accident. In the previous 5 years, she underwent two attempts to improve CSF flow at the level of her incomplete cord lesion. Due to severe adhesions between the conus and dura, the posttraumatic tethering could not be completely resolved, and postoperative arachnoid scarring obstructed the subarachnoid space within weeks of these attempts. Furthermore, a posterior decompression and fusion of her cervical spine had been performed to eliminate any further cervical cord damage from her multilevel cervical stenosis. (**b**) Four years after placement of a thecoperitoneal shunt at the level of Th1/Th2, the syrinx is still considerably decreased in size with sustained resolution of neurological symptoms in her right arm and hand

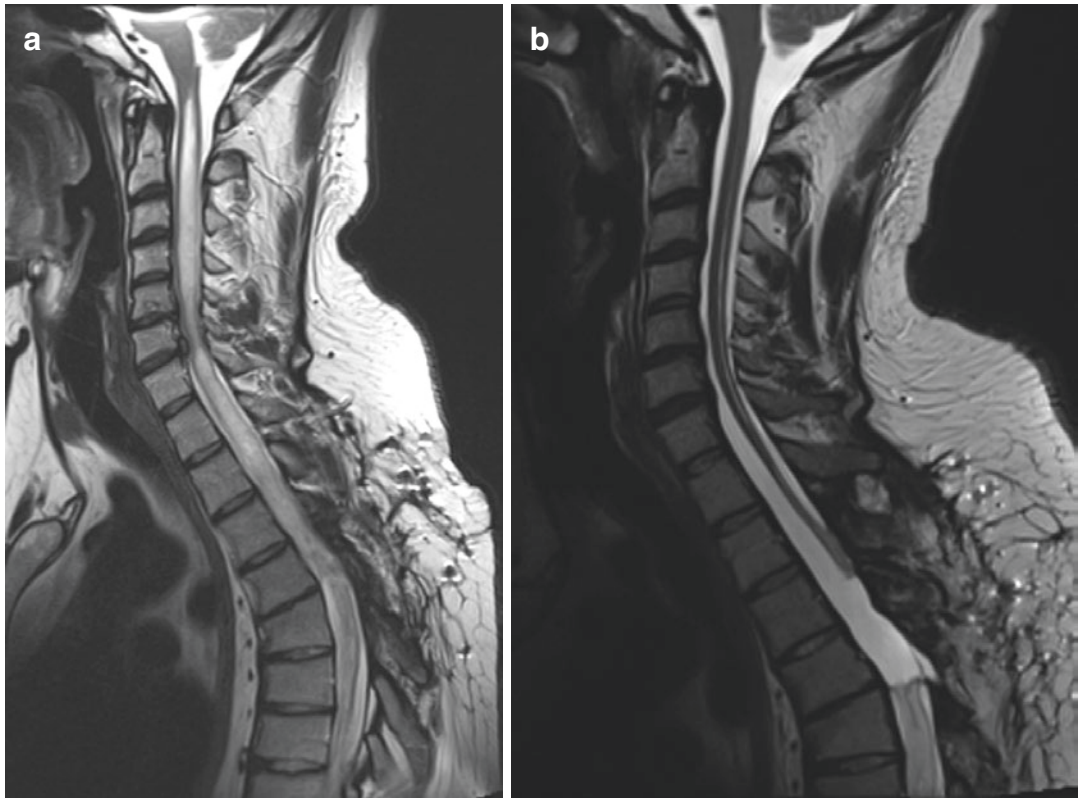

Fig. 16.5 (**a**) The sagittal T2-weighted MRI shows a posttraumatic syringomyelia C2 to Th6 14 years after a motorcycle accident resulting in complete paraplegia with an injury level at Th4/Th5. One year previously, an attempt to improve CSF flow at Th4/Th5 with untethering of the cord was undertaken, which led to a short-lived resolution of the syrinx. With reappearance of the syrinx, the patient requested a revision fearing permanent neurological deficits in his upper extremities. A cordectomy at Th4 was undertaken. (**b**) The postoperative MRI shows a complete resolution of the cervical syrinx and decrease in size below that level. The dissociated sensory loss in his right arm improved during a follow-up of 14 months

For patients with a complete cord lesion, cordectomy is a very effective form of treatment for syringomyelia [29, 41–46]. All 17 patients treated in this manner in the author's series improved neurologically with permanent resolution of the syrinx (Fig. 16.5). However, the psychological burden for a patient to accept this operation should not be underestimated. Most patients prefer to undergo a decompression first. After all, this operation does provide good results for the majority of patients [45]. Patients will accept a cordectomy, however, if the ascending neurology cannot be arrested by decompression or shunting procedures and the neurological progress threatens important functions such as respiratory or hand muscles.

Results

Concentrating on patients with syringomyelia related to spinal arachnopathies, 177 patients with posttraumatic arachnoid scarring and 429 patients with non-traumatic arachnopathies were encountered in the author's series. Reserving surgery for patients with progressive neurological symptoms and refusal of surgery by some patients led to 119 operations for 92 patients with post-

Table 16.2 Operations for patients with spinal arachnopathies

Type of surgery	Posttraumatic arachnopathies 92 patients	Non-traumatic arachnopathies 135 patients	All 227 patients
Arachnolysis + duraplasty	86	139	225
Cordectomy	16	1	17
Thecoperitoneal shunt	4	6	10
Ventral fusion	5	4	9
Posterior decompression	7	4	11
Opiate pump	1	–	1

traumatic and 154 operations for 135 patients with non-traumatic arachnopathies (Table 16.2). Overall, 225 decompressions aiming at improving CSF flow and decompressing the spinal cord by arachnolysis and duraplasty were performed, while 17 patients with complete paraplegias underwent cordectomies and 10 thecoperitoneal shunts were placed. One patient received an opiate pump for his neuropathic pain syndrome. Twenty operations dealt with degenerative diseases of the cervical spine.

Concentrating on the 225 decompressions with arachnolysis and duraplasty, complications were observed after 59 operations (26.0%); the commonest were urinary tract infections (8%), wound infections (6%), hemorrhages (5%), and CSF fistulas (3%). Permanent surgical morbidity defined as a permanent neurological worsening within 1 month after surgery occurred in 19 patients, i.e., 8.4%. A postoperative decrease of the syrinx was observed in 76%, and 21% showed no postoperative change, while 4% increased further despite surgery. After 3 months, 49% considered their condition improved, 42% as unchanged, and 9% as worsened. Looking at individual symptoms revealed postoperative improvements for sensory deficits and pain, whereas motor weakness, gait, and sphincter functions were left unchanged. Long-term results were determined with Kaplan-Meier statistics to determine the rates for progression-free survival after surgery. Overall, 63% of all patients undergoing a decompression with arachnolysis and duraplasty for traumatic or non-traumatic arachnopathies regardless of etiology remained in an unchanged or improved neurological status for at least 5 years after surgery. This rate was reduced to 48% after 10 years.

However, not all patients with spinal arachnopathies are good candidates for this type of surgery, while others respond particularly well. Looking at subgroups revealed good long-term results for patients with focal non-traumatic arachnopathies not exceeding two spinal segments operated first time and for posttraumatic patients who had not conceded a spinal cord injury with their accident (Table 16.3). For these subgroups, significantly higher progression-free survival rates for 10 years of 76% and 89%, respectively, were determined. Patients with an incomplete cord injury or those requiring a revision, on the other hand, were the most difficult to treat. The risk of further spinal cord damage in these patients is very real so that intraoperative compromises were often required, especially when trying to dissect dense adhesions between the spinal cord and dura. For patients with extensive arachnopathies after meningitis or intradural hemorrhages, the surgical concept of establishing a permanently improved CSF passage cannot be generally recommended. For such patients, a causative treatment leading to a better outcome compared to the natural history is not available. Symptomatic treatment with thecoperitoneal shunts offers better results in such patients although they address the syrinx only and leave impaired spinal cord blood flow due to the arachnoiditis untreated. The same applies to syrinx shunts, which, according to the author's experience, provide less favorable results compared to thecoperitoneal shunts.

Table 16.3 Progression-free survival for patients with spinal arachnopathies

Patient group	5 years	10 years	*P*
All arachnopathies	63%	48%	
Non-traumatic Focal—first surgery	86%	76%	0.001
Non-traumatic Focal—revision surgery	44%	–	
Non-traumatic Focal	80%	72%	<0.0001
Non-traumatic Extensive	29%	23%	
Non-traumatic All	63%	55%	
Posttraumatic No cord injury	89%	89%	0.03
Posttraumatic Incomplete cord injury	53%	19%	
Posttraumatic Complete cord injury	63%	46%	
Posttraumatic All	62%	36%	

Conclusion

The diagnosis of syringomyelia should be reserved for patients with a space-occupying intramedullary cyst of progressive character and differentiated from such entities such as a dilatation of the central canal or myelomalacia [2, 28, 47, 48]. Syringomyelia is not a disease in its own right but a manifestation of a disorder of the spinal canal or craniocervical junction that has either resulted in an obstruction of CSF flow or spinal cord tethering or is associated with an intramedullary tumor [2]. Management of patients with syringomyelia requires the correct diagnosis of the underlying disorder and the successful treatment of it. The long-term prognosis depends on the treatability of the underlying disorder. Whenever this can be achieved, no further surgical measures for the syrinx are required [2].

References

1. Olivier A, Tran Quan VAN. A case of monstrous posttraumatic hypertrophy of the foot, of true syringomyelic type. J Radiol Electrol Arch Electr Medicale. 1955;36(9–10):808–10.
2. Klekamp J. How should syringomyelia be defined and diagnosed? World Neurosurg. 2018;111:e729–e45.
3. Klekamp J. The pathophysiology of syringomyelia - historical overview and current concept. Acta Neurochir. 2002;144(7):649–64.
4. Greitz D. Unraveling the riddle of syringomyelia. Neurosurg Rev. 2006;29(4):251–63; discussion 64.
5. Lohle PN, Wurzer HA, Hoogland PH, Seelen PJ, Go KG. The pathogenesis of syringomyelia in spinal cord ependymoma. Clin Neurol Neurosurg. 1994;96(4):323–6.
6. Klekamp J, Samii M. Surgery of spinal tumors. Heidelberg: Springer Verlag; 2007.
7. Klekamp J, Völkel K, Bartels CJ, Samii M. Disturbances of cerebrospinal fluid flow attributable to arachnoid scarring cause interstitial edema of the cat spinal cord. Neurosurgery. 2001;48(1):174–85; discussion 85-86.
8. Bilston LE, Fletcher DF, Stoodley MA. Focal spinal arachnoiditis increases subarachnoid space pressure: a computational study. Clin Biomech (Bristol, Avon). 2006;21(6):579–84.
9. Brodbelt AR, Stoodley MA, Watling AM, Tu J, Jones NR. Fluid flow in an animal model of post-traumatic syringomyelia. Eur Spine J. 2003;12(3):300–6.
10. Bilston LE, Fletcher DF, Brodbelt AR, Stoodley MA. Arterial pulsation-driven cerebrospinal fluid flow in the perivascular space: a computational model. Comput Methods Biomech Biomed Engin. 2003;6(4):235–41.
11. Stoodley MA, Gutschmidt B, Jones NR. Cerebrospinal fluid flow in an animal model of noncommunicating syringomyelia. Neurosurgery. 1999;44(5):1065–75; discussion 75-6.
12. Stoodley MA, Jones NR, Yang L, Brown CJ. Mechanisms underlying the formation and enlargement of noncommunicating syringomyelia: experimental studies. Neurosurg Focus. 2000;8(3):E2.
13. Fischbein NJ, Dillon WP, Cobbs C, Weinstein PR. The "presyrinx" state: a reversible myelopathic condition that may precede syringomyelia. AJNR Am J Neuroradiol. 1999;20(1):7–20.
14. Milhorat TH, Capocelli AL Jr, Kotzen RM, Bolognese P, Heger IM, Cottrell JE. Intramedullary pressure in syringomyelia: clinical and pathophysiological correlates of syrinx distension. Neurosurgery. 1997;41(5):1102–10.
15. Tobimatsu Y, Nihei R, Kimura T, Suyama T, Tobimatsu H. A quantitative analysis of cerebrospinal fluid flow in posttraumatic syringomyelia. Nippon Seikeigeka Gakkai Zasshi. 1991;65(8):505–16.
16. Aghakhani N, Baussart B, David P, Lacroix C, Benoudiba F, Tadie M, et al. Surgical treatment of posttraumatic syringomyelia. Neurosurgery. 2010;66(6):1120–7; discussion 7.
17. Goldstein B, Hammond MC, Stiens SA, Little JW. Posttraumatic syringomyelia: profound neuronal loss, yet preserved function. Arch Phys Med Rehabil. 1998;79(1):107–12.

18. Squier MV, Lehr RP. Post-traumatic syringomyelia. J Neurol Neurosurg Psychiatry. 1994;57(9):1095–8.
19. Reddy KK, Del Bigio MR, Sutherland GR. Ultrastructure of the human posttraumatic syrinx. J Neurosurg. 1989;71(2):239–43.
20. Eneling J, Bostrom S, Rossitti S. Subarachnoid hemorrhage-associated arachnoiditis and syringomyelia. Clin Neuroradiol. 2011;22(2):169–73.
21. Klekamp J. A new classification for pathologies of spinal meninges-part 2: primary and secondary intradural arachnoid cysts. Neurosurgery. 2017;81(2):217–29.
22. Inoue Y, Nemoto Y, Ohata K, Daikokuya H, Hakuba A, Tashiro T, et al. Syringomyelia associated with adhesive spinal arachnoiditis: MRI. Neuroradiology. 2001;43(4):325–30.
23. Falci SP, Indeck C, Lammertse DP. Posttraumatic spinal cord tethering and syringomyelia: surgical treatment and long-term outcome. J Neurosurg Spine. 2009;11(4):445–60.
24. Hirai T, Korogi Y, Shigematsu Y, Sugahara T, Takahashi M, Ushio Y, et al. Evaluation of syringomyelia with three-dimensional constructive interference in a steady state (CISS) sequence. J Magn Reson Imaging. 2000;11(2):120–6.
25. Klekamp J. Treatment of syringomyelia related to nontraumatic arachnoid pathologies of the spinal canal. Neurosurgery. 2013;72(3):376–89; discussion 89.
26. Kaynar MY, Kocer N, Gencosmanoglu BE, Hanci M. Syringomyelia--as a late complication of tuberculous meningitis. Acta Neurochir. 2000;142(8):935–8; discussion 8-9.
27. Kubota M, Shin M, Taniguchi M, Terao T, Nakauchi J, Takahashi H. Syringomyelia caused by intrathecal remnants of oil-based contrast medium. J Neurosurg Spine. 2008;8(2):169–73.
28. Klekamp J, Samii M. Syringomyelia - diagnosis and treatment. Heidelberg: Springer Verlag; 2001.
29. Klekamp J. Treatment of posttraumatic syringomyelia. J Neurosurg Spine. 2012;17(3):199–211.
30. Klekamp J, Batzdorf U, Samii M, Bothe HW. Treatment of syringomyelia associated with arachnoid scarring caused by arachnoiditis or trauma. J Neurosurg. 1997;86(2):233–40.
31. Morisako H, Takami T, Yamagata T, Chokyu I, Tsuyuguchi N, Ohata K. Focal adhesive arachnoiditis of the spinal cord: imaging diagnosis and surgical resolution. J Craniovertebr Junction Spine. 2011;1(2):100–6.
32. Parker F, Aghakhani N, Tadie M. Non-traumatic arachnoiditis and syringomyelia. A series of 32 cases. Neurochirurgie. 1999;45(Suppl 1):67–83.
33. Nicholas DS, Weller RO. The fine anatomy of the human spinal meninges. A light and scanning electron microscopy study. J Neurosurg. 1988;69(2):276–82.
34. Suzuki S, Chiba Y, Hidaka K, Nishimura S, Noji M. A new operative technique of posttraumatic syringomyelia: thecoperitoneal shunt. No Shinkei Geka. 1998;26(6):541–6.
35. Vassilouthis J, Papandreou A, Anagnostaras S. Thecoperitoneal shunt for post-traumatic syringomyelia. J Neurol Neurosurg Psychiatry. 1994;57(6):755–6.
36. Vengsarkar US, Panchal VG, Tripathi PD, Patkar SV, Agarwal A, Doshi PK, et al. Percutaneous thecoperitoneal shunt for syringomyelia. Report of three cases. J Neurosurg. 1991;74(5):827–31.
37. Lam S, Batzdorf U, Bergsneider M. Thecal shunt placement for treatment of obstructive primary syringomyelia. J Neurosurg Spine. 2008;9(6):581–8.
38. Oluigbo CO, Thacker K, Flint G. The role of lumboperitoneal shunts in the treatment of syringomyelia. J Neurosurg Spine. 2010;13(1):133–8.
39. Williams B, Sgouros S, Nenji E. Cerebrospinal fluid drainage for syringomyelia. Eur J Pediatr Surg. 1995;5(Suppl 1):27–30.
40. Piatt JH Jr. Progressive syringomyelia controlled by treatment of associated hydrocephalus in an infant with birth injury. Case Rep J Neurosurg. 2005;103(2 Suppl):198–202.
41. Laxton AW, Perrin RG. Cordectomy for the treatment of posttraumatic syringomyelia. Report of four cases and review of the literature. J Neurosurg Spine. 2006;4(2):174–8.
42. Sgouros S, Williams B. Management and outcome of posttraumatic syringomyelia. J Neurosurg. 1996;85(2):197–205.
43. Williams B. Post-traumatic syringomyelia, an update. Paraplegia. 1990;28(5):296–313.
44. Kasai Y, Kawakita E, Morishita K, Uchida A. Cordectomy for post-traumatic syringomyelia. Acta Neurochir. 2008;150(1):83–6; discussion 6.
45. Gautschi OP, Seule MA, Cadosch D, Gores M, Ewelt C, Hildebrandt G, et al. Health-related quality of life following spinal cordectomy for syringomyelia. Acta Neurochir. 2011;153(3):575–9.
46. Ewelt C, Stalder S, Steiger HJ, Hildebrandt G, Heilbronner R. Impact of cordectomy as a treatment option for posttraumatic and non-posttraumatic syringomyelia with tethered cord syndrome and myelopathy. J Neurosurg Spine. 2010;13(2):193–9.
47. Roser F, Ebner FH, Sixt C, Hagen JM, Tatagiba MS. Defining the line between hydromyelia and syringomyelia. A differentiation is possible based on electrophysiological and magnetic resonance imaging studies. Acta Neurochir. 2010;152(2):213–9; discussion 9.
48. Holly LT, Batzdorf U. Slitlike syrinx cavities: a persistent central canal. J Neurosurg Spine. 2002;97(2):161–5.

Chiari and Scoliosis

17

Vijay M. Ravindra and Douglas L. Brockmeyer

Epidemiology

Chiari malformation type I (CMI), which is characterized by downward displacement of the cerebellar tonsils at least 5 mm below the foramen magnum [1], is an abnormality of hindbrain development that is frequently associated with syringomyelia and scoliosis [2, 3]. Scoliosis occurs at a higher rate in CMI patients than in those in the general population, and scoliosis is often the sole presenting symptom [4–6]. The overall incidence of scoliosis is 2–4%, but among patients with CMI, the incidence ranges from 13% to 36% [3, 6–10]. In patients with a syrinx, the prevalence rises to 53–85% [11–14]. There are some controversial and conflicting reports on the association between CMI and thoracolumbar scoliosis in the absence of a syrinx [14–16]; despite this, there are numerous reports describing the relationship between syringomyelia, with or without CMI, and scoliosis [5, 7, 11, 17–19].

V. M. Ravindra
Department of Neurosurgery, University of Utah, Clinical Neurosciences Center, Salt Lake City, UT, USA

D. L. Brockmeyer (✉)
Department of Neurosurgery, Primary Children's Hospital, University of Utah, Salt Lake City, UT, USA
e-mail: douglas.brockmeyer@hsc.utah.edu; neuropub@hsc.utah.edu

Pathophysiology

The underlying pathogenesis and association between CMI and thoracolumbar scoliosis are not well understood. It was hypothesized by Huebert and Mackinnon [20] in 1969 that scoliosis in the setting of syringomyelia is a result of destruction of medial nuclei cells in the spinal cord by the enlarging syrinx resulting in progressive denervation of truncal musculature. Over time, this causes worsening spinal deformity.

The pathophysiology for Chiari-related scoliosis—which is distinctly different from adolescent idiopathic scoliosis, infantile scoliosis, and juvenile idiopathic scoliosis—differs from other forms of scoliosis (Fig. 17.1). Characteristic features of CMI-related scoliosis are described as "atypical findings" including a higher incidence of left thoracic curves, a left apical curve, juvenile onset before age 11 years, neurological deficits, and kyphotic deformity associated with the curve and rapid curve progression [5, 21–23].

Treatment

The treatment for CMI with or without the presence of syringomyelia is suboccipital decompression with or without duraplasty (Fig. 17.2). Patients with concomitant syringomyelia are more likely to undergo surgical decompression than those with CMI without

R. S. Tubbs et al. (eds.), *The Chiari Malformations*, https://doi.org/10.1007/978-3-030-44862-2_17

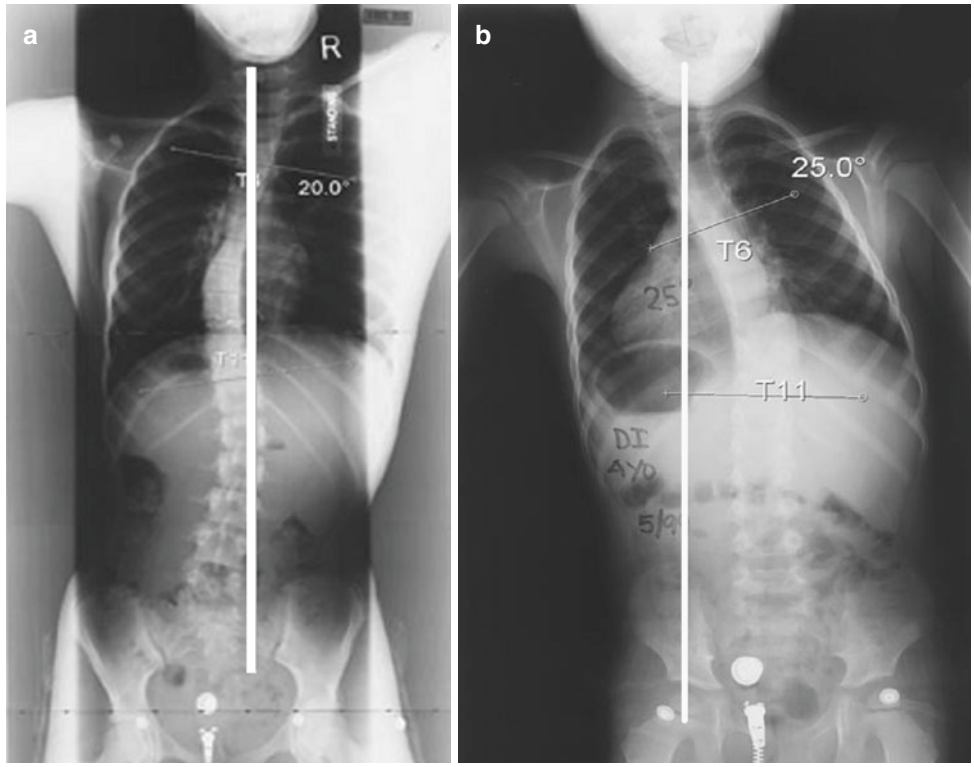

Fig. 17.1 Radiographs showing patients with idiopathic (**a**) and Chiari (**b**) scoliotic curves

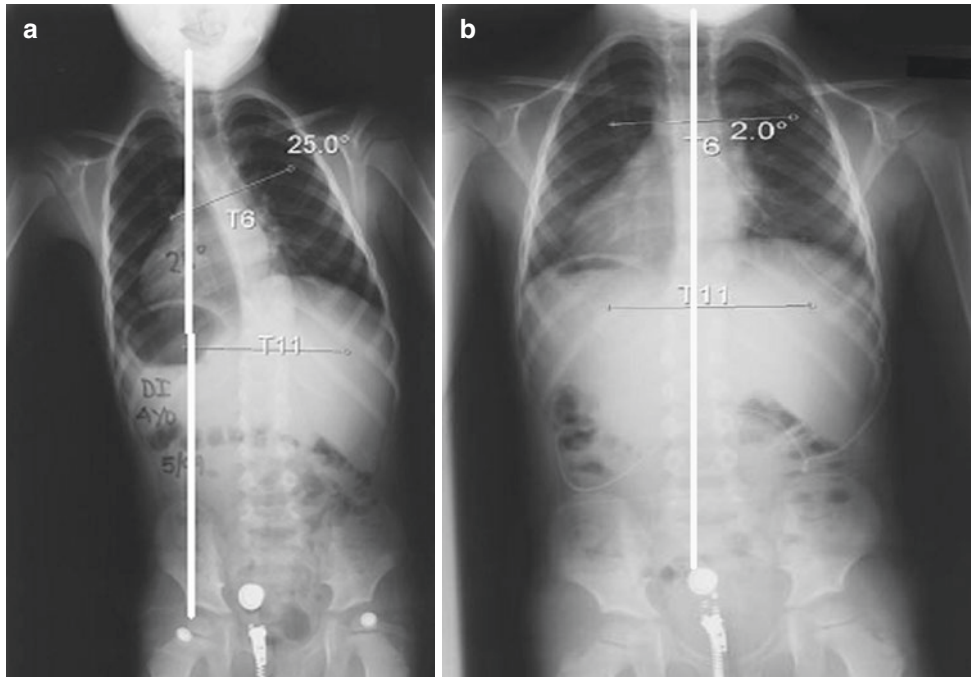

Fig. 17.2 Radiograph showing a patient with Chiari with scoliosis before (**a**) and after (**b**) surgery

syringomyelia [4–6, 24]. There are varying reports of rates of improvement or halting progression of scoliosis after suboccipital decompression. Approximately 50% (range 18–70%) of patients with Chiari-related scoliosis may require thoracolumbar spinal fusion despite having previously had suboccipital decompression [3, 7–9, 11, 18, 21, 25–33].

Previously published risk factors for progression of scoliosis after suboccipital decompression include older age at presentation, greater degree of initial scoliosis indicated by Cobb angle, location of the curve/level of the spinal deformity, and less syrinx resolution after suboccipital decompression [7, 15, 19, 21, 31, 34]. However, two of these variables—age at decompression and pre-decompression curve severity—are the most commonly cited predictors of thoracolumbar deformity progression [7, 11, 26–29, 34–37].

In 2012, Hwang et al. [21] performed a meta-analysis of pediatric CMI-associated scoliosis and discovered that age and posterior fossa decompression were two factors associated with improvement or stabilization of thoracolumbar curvature. The authors also reported the significant limitations of the literature, including inconsistent reporting of radiologic parameters at presentation and during follow-up across studies, which are both prohibitive to definitive associations.

Surgical Interventions

Surgical intervention for Chiari malformation with or without syringomyelia includes suboccipital decompression with or without duraplasty. Currently, no evidence exists to indicate whether the addition of duraplasty contributes to improvement of scoliotic curvature over time, but future endeavors may focus on this.

With respect to surgical correction of the thoracolumbar scoliosis, the decision to offer correction with posterior spinal fusion is often undertaken by a multidisciplinary team comprising orthopedic surgeons and neurosurgeons. Common indications for deformity correction in the setting of Chiari-related scoliosis include progressive and painful deformity, to improve sitting balance, worsening pulmonary function, increased symptoms from curvature particularly that exceeds 45–50 degrees in children ≥10 years of age, or significant deterioration in the child's functionality [38–40].

Uncovering the Relationship

Dauser et al. [41] initially described the observation and subsequent association between Chiari malformation and scoliosis. Previous reports have suggested that patients with CMI and scoliosis of 30–40 degrees would eventually require spinal deformity correction after suboccipital decompression for treatment of CMI [6, 7, 9, 11, 28, 36, 42].

In addition to CMI, CM 1.5 has been described to describe herniation of brainstem contents into the foramen magnum. Bollo et al. [43] stressed the importance of the clivo-axial angle (CXA) for the evaluation of alignment in patients with Chiari malformation. They found that basilar invagination, Chiari 1.5, and a clivo-axial angle (CXA) <125 degrees together were risk factors for requiring occipitocervical fusion.

Using a cohort of 23 children with long-term follow-up, Ravindra et al. [44] performed a retrospective review of the long-term behavior of the scoliotic curve and the necessity of correcting deformity in CMI patients. Eleven of the 23 patients required deformity correction at an average of 88.3 ± 15.4 months after suboccipital decompression and duraplasty, including 7 (30%) in whom the need for fusion developed more than 5 years after surgery. On univariate analysis, the authors found that a lower CXA, a pBC2 > 9 mm, and a higher initial Cobb angle were associated with the need for thoracolumbar fusion. Lower CXA was independently associated on multivariable modeling with a need for delayed thoracolumbar fusion. This was the first study to describe Chiari-level parameters and the influence on thoracolumbar deformity progression. This information may support the hypothesis that cervical alignment is affected by thoracolumbar alignment

and vice versa [45], indicating that detailed imaging and analysis of global parameters are warranted.

Severity of Curvature

In 2003, Tubbs et al. [6] reviewed the cases of 16 patients and found that suboccipital decompression alone did not resolve curvature >40 degrees. This is parallel to the findings by Ghanem et al. [18], who discovered that patients who presented with a ≥40-degree curve all needed deformity correction. Going even further, Zhu et al. [42] reported that a 44.5-degree threshold was specific for progression of the scoliotic curve in the setting of CM and scoliosis.

Using data from the Park-Reeves Syringomyelia Research Consortium, which is a large multicenter retrospective and prospective registry of pediatric patients with CMI and syrinx (≥3 mm in axial width), Taiwo et al. [46] studied 47 patients with CMI, syrinx, and scoliosis (coronal curve ≥10 degrees) in patients who underwent posterior fossa decompression and 1 year of follow-up imaging (mean follow-up 1.9 years). Ten patients (21%) had stable curves, with 18 (38%) showing improvement (>5 degrees) and 19 (40%) displaying progression of the curve (>5 degrees) during the study period. Younger age at diagnosis of CMI was associated with scoliosis improvement; for those with curves 35 degrees or less, 17% of patients <10 years had curve progression compared with 54% of those ≥10 years ($p = 0.03$). Interestingly, baseline tonsil position, syrinx characteristics, and craniocervical junction metrics were not associated with changes in scoliosis curvature after suboccipital decompression. To date, this is the most comprehensive prospectively collected data discussing the influence of Chiari malformation and scoliosis, and it solidifies the findings of previous reports.

Similar to the findings of Strahle et al. [46], Mackel et al. [29] observed that greater curve severity in patients >10 years was associated with an increased need for fusion after posterior fossa decompression surgery, with patients with curves >35 degrees at greater risk for requiring fusion/correction surgery. Notably, this study included only patients with CMI and excluded patients with Chiari 1.5.

There are some reports that do not support curve magnitude as a strong predictor of outcome after suboccipital decompression, including a meta-analysis that concluded that curve magnitude is not associated with post-decompression curve changes [21, 30, 31].

Age as a Protective Factor

Several reports have discussed age as a protective factor against progression of scoliosis in the setting of CMI. Sengupta et al. [31] found that presentation at <10 years of age offered a 71% chance of avoiding a need for deformity correction. Similarly, Brockmeyer et al. [9] found a 91% rate of avoidance of fusion in patients <10 years of age, and Flynn et al. [26] reported a 70% avoidance rate of fusion in a similar cohort. In a study of 54 patients, Zhu et al. [42] proposed a cutoff of 10.5 years of age for improvement or stabilization versus progression after suboccipital decompression. Navarro et al. [47], however, did not find an association of age of decompression and requiring deformity correction. In the series by Muhonen et al. [30], scoliosis after decompression resolved in all children <10 years, including some with curves that exceeded 40 degrees.

Future Directions

Each of the previously referenced studies highlights the need for large multi-institutional efforts to fully elucidate the long-term effects of CMI on thoracolumbar scoliosis. The role of CMI-related imaging parameters (i.e., craniocervical junction metrics) specifically may enhance the knowledge of the relationship as well. With the information presented in this chapter, we advise extended follow-up of 5+ years for patients with Chiari malformation and scoliosis [44].

Conclusion

Chiari-related scoliosis is a well-known and described phenomenon. It is also clear that younger children with curves less than <35 degrees may benefit from suboccipital decompression to halt curve progression. Knowledge of the natural history of this phenomenon as well as emphasis not only on characteristics of the spinal deformity but also on the craniocervical junction will enhance the care and management of these patients. Future multicenter, long-term natural history studies are needed to fully understand this phenomenon further.

Acknowledgments The authors thank Kristin Kraus, MSc, for editorial assistance with this chapter.

References

1. Milhorat TH, Chou MW, Trinidad EM, Kula RW, Mandell M, Wolpert C, et al. Chiari I malformation redefined: clinical and radiographic findings for 364 symptomatic patients. Neurosurgery. 1999;44(5):1005–17.
2. Hankinson T, Tubbs RS, Wellons JC. Duraplasty or not? An evidence-based review of the pediatric Chiari I malformation. Childs Nerv Syst [Review]. 2011;27(1):35–40.
3. Tubbs RS, Beckman J, Naftel RP, Chern JJ, Wellons JC 3rd, Rozzelle CJ, et al. Institutional experience with 500 cases of surgically treated pediatric Chiari malformation Type I. J Neurosurg Pediatr. 2011;7(3):248–56.
4. Dure LS, Percy AK, Cheek WR, Laurent JP. Chiari type I malformation in children. J Pediatr. 1989;115(4):573–6.
5. Emery E, Redondo A, Rey A. Syringomyelia and Arnold Chiari in scoliosis initially classified as idiopathic: experience with 25 patients. Eur Spine J. 1997;6(3):158–62.
6. Tubbs RS, McGirt MJ, Oakes WJ. Surgical experience in 130 pediatric patients with Chiari I malformations. J Neurosurg. 2003;99(2):291–6.
7. Bhangoo R, Sgouros S. Scoliosis in children with Chiari I-related syringomyelia. Childs Nerv Syst. 2006;22(9):1154–7.
8. Attenello FJ, McGirt MJ, Atiba A, Gathinji M, Datoo G, Weingart J, et al. Suboccipital decompression for Chiari malformation-associated scoliosis: risk factors and time course of deformity progression. J Neurosurg Pediatr. 2008;1(6):456–60.
9. Brockmeyer D, Gollogly S, Smith JT. Scoliosis associated with Chiari 1 malformations: the effect of suboccipital decompression on scoliosis curve progression: a preliminary study. Spine [Evaluation Studies]. 2003;28(22):2505–9.
10. Strahle J, Muraszko KM, Kapurch J, Bapuraj JR, Garton HJ, Maher CO. Chiari malformation Type I and syrinx in children undergoing magnetic resonance imaging. J Neurosurg Pediatr. 2011;8(2):205–13.
11. Eule JM, Erickson MA, O'Brien MF, Handler M. Chiari I malformation associated with syringomyelia and scoliosis: a twenty-year review of surgical and nonsurgical treatment in a pediatric population. Spine [Case Reports Review]. 2002;27(13):1451–5.
12. Hida K, Iwasaki Y, Koyanagi I, Abe H. Pediatric syringomyelia with chiari malformation: its clinical characteristics and surgical outcomes. Surg Neurol [Case Reports Research Support, Non-US Gov't]. 1999;51(4):383–90; discussion 90-1.
13. Isu T, Iwasaki Y, Akino M, Abe H. Hydrosyringomyelia associated with a Chiari I malformation in children and adolescents. Neurosurgery [Case Reports]. 1990;26(4):591–6; discussion 6-7.
14. Strahle J, Smith BW, Martinez M, Bapuraj JR, Muraszko KM, Garton HJ, et al. The association between Chiari malformation Type I, spinal syrinx, and scoliosis. J Neurosurg Pediatr. 2015;15(6):607–11.
15. Godzik J, Dardas A, Kelly MP, Holekamp TF, Lenke LG, Smyth MD, et al. Comparison of spinal deformity in children with Chiari I malformation with and without syringomyelia: matched cohort study. Eur Spine J. 2016;25(2):619–26.
16. Zhu Z, Yan H, Han X, Jin M, Xie D, Sha S, et al. Radiological features of scoliosis in Chiari I malformation without syringomyelia. Spine. 2016;41(5):E276–81.
17. Zhu Z, Sha S, Chu WC, Yan H, Xie D, Liu Z, et al. Comparison of the scoliosis curve patterns and MRI syrinx cord characteristics of idiopathic syringomyelia versus Chiari I malformation. Eur Spine J. 2016;25(2):517–25.
18. Ghanem IB, Londono C, Delalande O, Dubousset JF. Chiari I malformation associated with syringomyelia and scoliosis. Spine. 1997;22(12):1313–7; discussion 8.
19. Ozerdemoglu RA, Transfeldt EE, Denis F. Value of treating primary causes of syrinx in scoliosis associated with syringomyelia. Spine. 2003;28(8):806–14.
20. Huebert HT, MacKinnon WB. Syringomyelia and scoliosis. J Bone Joint Surg Br. 1969;51(2):338–43.
21. Hwang SW, Samdani AF, Jea A, Raval A, Gaughan JP, Betz RR, et al. Outcomes of Chiari I-associated scoliosis after intervention: a meta-analysis of the pediatric literature. Childs Nerv Syst [Meta-Analysis Research Support, Non-US Gov't]. 2012;28(8):1213–9.
22. Schwend RM, Hennrikus W, Hall JE, Emans JB. Childhood scoliosis: clinical indications for magnetic resonance imaging. J Bone Joint Surg Am. 1995;77(1):46–53.
23. Spiegel DA, Flynn JM, Stasikelis PJ, Dormans JP, Drummond DS, Gabriel KR, et al. Scoliotic curve

patterns in patients with Chiari I malformation and/or syringomyelia. Spine. 2003;28(18):2139–46.
24. Rocque BG, George TM, Kestle J, Iskandar BJ. Treatment practices for Chiari malformation type I with syringomyelia: results of a survey of the American Society of Pediatric Neurosurgeons. J Neurosurg Pediatr. 2011;8(5):430–7.
25. Farley FA, Puryear A, Hall JM, Muraszko K. Curve progression in scoliosis associated with Chiari I malformation following suboccipital decompression. J Spinal Disord Tech. 2002;15(5):410–4.
26. Flynn JM, Sodha S, Lou JE, Adams SB Jr, Whitfield B, Ecker ML, et al. Predictors of progression of scoliosis after decompression of an Arnold Chiari I malformation. Spine. 2004;29(3):286–92.
27. Krieger MD, Falkinstein Y, Bowen IE, Tolo VT, McComb JG. Scoliosis and Chiari malformation Type I in children. J Neurosurg Pediatr. 2011;7(1):25–9.
28. Lee S, Wang KC, Cheon JE, Phi JH, Lee JY, Cho BK, et al. Surgical outcome of Chiari I malformation in children: clinico-radiological factors and technical aspects. Childs Nerv Syst [Research Support, Non-US Gov't]. 2014;30(4):613–23.
29. Mackel CE, Cahill PJ, Roguski M, Samdani AF, Sugrue PA, Kawakami N, et al. Factors associated with spinal fusion after posterior fossa decompression in pediatric patients with Chiari I malformation and scoliosis. J Neurosurg Pediatr. 2016;25(6):737–43.
30. Muhonen MG, Menezes AH, Sawin PD, Weinstein SL. Scoliosis in pediatric Chiari malformations without myelodysplasia. J Neurosurg [Case Reports]. 1992;77(1):69–77.
31. Sengupta DK, Dorgan J, Findlay GF. Can hindbrain decompression for syringomyelia lead to regression of scoliosis? Eur Spine J [Clinical Trial]. 2000;9(3):198–201.
32. Sha S, Zhu Z, Lam TP, Sun X, Qian B, Jiang J, et al. Brace treatment versus observation alone for scoliosis associated with Chiari I malformation following posterior fossa decompression: a cohort study of 54 patients. Eur Spine J. 2014;23(6):1224–31.
33. Yeom JS, Lee CK, Park KW, Lee JH, Lee DH, Wang KC, et al. Scoliosis associated with syringomyelia: analysis of MRI and curve progression. Eur Spine J. 2007;16(10):1629–35.
34. Attenello FJ, McGirt MJ, Garces-Ambrossi GL, Chaichana KL, Carson B, Jallo GI. Suboccipital decompression for Chiari I malformation: outcome comparison of duraplasty with expanded polytetrafluoroethylene dural substitute versus pericranial autograft. Childs Nerv Syst [Comparative Study Research Support, Non-US Gov't]. 2009;25(2):183–90.
35. Albert GW, Menezes AH, Hansen DR, Greenlee JD, Weinstein SL. Chiari malformation Type I in children younger than age 6 years: presentation and surgical outcome. J Neurosurg Pediatr. 2010;5(6):554–61.
36. Brockmeyer DL. Editorial. Chiari malformation Type I and scoliosis: the complexity of curves. J Neurosurg Pediatr [Comment Editorial]. 2011;7(1):22–3; discussion 3-4.
37. Nagib MG. An approach to symptomatic children (ages 4-14 years) with Chiari type I malformation. Pediatr Neurosurg. 1994;21(1):31–5.
38. McCarthy RE. Management of neuromuscular scoliosis. Orthop Clin North Am [Review]. 1999;30(3):435–49, viii.
39. Herring J. Disorders of the brain. In: Herring J, editor. Tachjian's pediatric orthopaedics. Philadelphia: W.B. Saunders; 2002. p. 1121–248.
40. Lonstein JE, Akbarnia A. Operative treatment of spinal deformities in patients with cerebral palsy or mental retardation. An analysis of one hundred and seven cases. J Bone Joint Surg Am [Research Support, Non-US Gov't]. 1983;65(1):43–55.
41. Dauser RC, DiPietro MA, Venes JL. Symptomatic Chiari I malformation in childhood: a report of 7 cases. Pediatr Neurosci [Case Reports]. 1988;14(4):184–90.
42. Zhu Z, Wu T, Zhou S, Sun X, Yan H, Sha S, et al. Prediction of curve progression after posterior fossa decompression in pediatric patients with scoliosis secondary to Chiari malformation. Spine Deform. 2013;1(1):25–32.
43. Bollo RJ, Riva-Cambrin J, Brockmeyer MM, Brockmeyer DL. Complex Chiari malformations in children: an analysis of preoperative risk factors for occipitocervical fusion. J Neurosurg Pediatr. 2012;10(2):134–41.
44. Ravindra VM, Onwuzulike K, Heller RS, Quigley R, Smith J, Dailey AT, et al. Chiari-related scoliosis: a single-center experience with long-term radiographic follow-up and relationship to deformity correction. J Neurosurg Pediatr. 2018;21(2):185–9.
45. Smith JS, Shaffrey CI, Bess S, Shamji MF, Brodke D, Lenke LG, et al. Recent and emerging advances in spinal deformity. Neurosurgery. 2017;80(3S):S70–85.
46. Taiwo R, Averill C, Torner J, Shannon C, Wellons J III, Bonfield C, et al. Radiologic and clinical associations with scoliosis outcomes after posterior fossa decompression patients with Chiari malformation and syrinx from the Park-Reeves Syringomyelia Research Consortium. J Neurosurg Pediatr. In press.
47. Navarro R, Olavarria G, Seshadri R, Gonzales-Portillo G, McLone DG, Tomita T. Surgical results of posterior fossa decompression for patients with Chiari I malformation. Childs Nerv Syst. 2004;20(5):349–56.

18 Associated Bony Malformations and Instability in the Chiari I Malformation

Arnold H. Menezes

Introduction

The morphology of the craniovertebral junction (CVJ) and the explanation of variations in the axis and occipital bone are subjects that have engaged the attention of comparative anatomists and evolutionary biologists for the last two centuries [1]. Improvements in neurodiagnostic imaging have shown the frequent occurrence of patterns of various combinations of both nervous system and osseous abnormalities at the craniocervical junction and have suggested an interrelationship. A database analysis of 2100 symptomatic patients referred to this author with primary CVJ abnormalities (1977–1994) identified 100 patients with the hindbrain herniation syndrome [2]. Atlas assimilation was the common bony anomaly in these 100 patients with basilar invagination in 92, and 20 showed paramesial invagination. Of these 100 patients, 66 had cervical C2-C3 vertebral segmentation defects, and syringohydromyelia was evident in 46 individuals. A proatlas segmentation abnormality was present in eight. A common finding of atlas assimilation and Chiari malformation in the 92 patients showed that 70 of them had a shortened clivus with condylar hypoplasia. The posterior fossa was reduced in its vertical height and was further compromised by the basilar invagination, which was present in the majority of individuals.

Incidence of Bony Anomalies Associated with Chiari I Malformation

In a comprehensive review of 364 symptomatic patients with Chiari I malformation, Milhorat et al. found associated syringohydromyelia in 65% of cases, scoliosis in 42%, an abnormal retroflexed odontoid process in 26%, and basilar invagination in 12% [3]. This is a series that was not skewed to bony abnormalities at the craniocervical junction. In contrast, this author reviewed our Chiari I malformation database, which was different from the craniovertebral junction database, in 2005 [4]. A total of 639 patients had undergone an operative procedure for a Chiari I malformation; 276 of these had craniovertebral junction bony abnormalities of which 41 were reducible and 46% had syringohydromyelia. There were 363 patients who did not have a bony abnormality at the craniocervical junctionc. The incidence of instability in these patients was 8% and 67% had syringohydromyelia.

In a study "based on 190 surgically treated patients with basilar invagination," Goel et al. [5] grouped these into those who did have a Chiari I malformation and those who did not have a Chiari malformation. Of the 190 patients with

A. H. Menezes (✉)
Department of Neurosurgery, University of Iowa Hospitals and Clinics, Iowa City, IA, USA
e-mail: arnold-menezes@uiowa.edu

R. S. Tubbs et al. (eds.), *The Chiari Malformations*, https://doi.org/10.1007/978-3-030-44862-2_18

basilar invagination, 88 did not have a Chiari malformation, 102 patients had a Chiari I malformation associated with the basilar invagination, and 50% had a syrinx. Perrini et al. reviewed their surgical management of craniovertebral junction malformations and recognized 34 adult patients in a 7-year span who underwent operation [6]. This was for basilar invagination, and 13 of the 34 had an associated Chiari I malformation. Of these, three had a syrinx. In a long-term follow-up of Chiari-related syringomyelia in adults, Aghakhani et al. analyzed 157 surgically treated cases of Chiari-related syrinx and found that only 11 of the 157 (7%) had basilar invagination or "platybasia" and basilar impression [7]. Thus the incidence of a Chiari I malformation having craniovertebral junction bony abnormalities is between 7% and 11% [1, 8]. On the other hand, the incidence of craniovertebral junction bony abnormalities having a hindbrain herniation present is between 33% and 38% [9].

Table 18.1 refers to the associated bony anomalies with the Chiari I malformation in whom instability may be present at the craniocervical junction. In this author's series, these can be conveniently divided into those of congenital origin, the developmental, and the acquired [8, 10].

Table 18.1 The Chiari malformations: associated bony anomalies/instability

Congenital	Developmental	Acquired
Proatlas segmentation failures (dorsal, ventral, lateral)	Atlas assimilation with segmentation failure C2-C3	Basilar impression with bone softening states
Condylar hypoplasia	Basilar invagination	Os odontoideum
Hypoplastic clivus		Chiari secondary to craniofacial dysostosis and Klippel-Feil syndrome
Retroflexed odontoid		Ehlers-Danlos syndrome, Marfan's syndrome Chiari with instability secondary to holocord syrinx and repeated operations Morquio's disease Taybi-Rubinstein syndrome

Instability with the Chiari I Malformation

The preceding chapters have dealt with the symptomatology and the diagnostic imaging recommended for patients with the Chiari malformations. The symptoms of craniovertebral junction instability in patients with the Chiari I malformation with or without syringohydromyelia have headaches as their main symptom. This was present in 82% of patients whose headaches were worse with exertion or standing [11]. These seem to be relieved by lying down or supporting their head. The common thread of complaint was a feeling of "heaviness in the head" and "I feel that I have to support my head." This is translated into holding or supporting the head even in a sitting position. The headaches usually are centered in the base of the skull at the junction with the cervical spine. They may project upward but usually are associated with a feeling of nausea unless lying down. Numbness in the scalp or the face was present in 34% and torticollis in 15% [11]. Vasomotor instability presented as extreme dizziness and nausea with the headaches and a feeling of impending crisis with exertion. They had relief of these headaches with head support using brace, collar, or cervical traction.

The diagnosis of the craniovertebral bony abnormalities and instability is dependent on complete imaging of the CVJ with preoperative computed tomography (CT) and magnetic resonance imaging (MRI) studies [12, 13]. A three-dimensional reconstruction of the craniocervical region is made to define the surgical anatomy as well as the bony abnormalities [14]. Also, dynamic MRI in both the flexed and extended position is obtained to evaluate the extent of ventral and dorsal cervicomedullary compression, respectively, and is a key component in determining reducibility of the abnormality. Stabilization is of paramount

importance for reducible lesions at the craniocervical junction in order to maintain the neural decompression [13]. Irreducible lesions require a decompression at the site of compression. This may be in the form of cervical traction and followed by appropriate decompression and fusion.

Table 18.2 outlines the indications for craniocervical junction fusions in patients with the Chiari I malformation [11]. For ease of recognition, these have been divided into:

A. Bony abnormalities with reducible compression on the cervicomedullary junction. Into this category would fall the reducible basilar invagination as well as patients in whom cervical traction can be obtained intraoperatively with documentation with intraoperative CT.
B. Previous ventral cervicomedullary decompression, such as after the resection of clivus-odontoid for bony decompression of the cervicomedullary junction.
C. Innate occipitocervical instability in situations such as Noonan's syndrome.
D. Musculoligamentous instability. This category is quite significant and the table is self-explanatory.

Table 18.2 Indications for craniocervical junction fusions in patients with Chiari malformation I/syringohydromyelia for the years 1996–2010

Indications for CCJ fusions in patients with CMI/SHM 1996–2010 355 (2.5–86 years old) 128 (36%) <16 years old
A. CCJ abnormalities with reducible compression of CMJ (25%), e.g., atlas assimilation with reducible atlantoaxial dislocation. Reducible basilar invagination
B. Previous ventral cervicomedullary decompression (44%), e.g., after transoral resection of bony compression of CMJ
C. Occipitocervical instability with CMI/SHM with bony abnormalities (26%), e.g., Noonan's syndrome
D. Musculoligamentous instability (15%), e.g.: 1. Neurogenic: syrinx in upper cervical cord 2. Pathologic states: Ehlers-Danlos syndrome, Down syndrome 3. After repeated posterior fossa procedures secondary to muscle dehiscence, fibrotic scar

CJJ craniocervical junction, *CMI* Chiari malformation I, *SHM* syringohydromyelia, *CMJ* cervicomedullary junction

Implications of Bony Abnormalities in the Chiari I Malformation and Craniocervical Instability

Once a bony abnormality is detected at the craniocervical junction, it is important to decide whether this is playing a part in the patient's symptoms within the sphere of the Chiari I malformation. A ventral or lateral compression of the cervicomedullary junction or the medulla that reduces with dynamic positions of the head should be documented with MRI. If this is a reducible situation whereby the neural compression is relieved off the bony mass, then a dorsal posterior fossa decompression procedure should be completed with an occipitocervical fusion [1, 15, 16]. In individuals below the age of 15, the author has performed intraoperative crown halo traction under general anesthesia using muscle relaxation and changing head position with traction so as to allow for relief of the bony compression [17]. This has to be documented with intraoperative CT. Furthermore, it should be documented both in the supine and in the prone positions into which the patient would be placed for the definitive procedure. If the lesion is irreducible, then the ventral or lateral compression must first be relieved and followed by a dorsal procedure for the Chiari malformation and fusion. It is critical to differentiate between distraction and reduction [16–18]. A reducible situation implies relief of neural compression with restoration of anatomical alignment [13]. Mere distraction does not provide reduction. This author has shown that atlas assimilation or "occipitalization of the atlas" is the most common bony abnormality. This, when present, is usually associated with a hypoplastic clivus. In a publication by Gholve et al., 30 children were identified with "occipitalization of the atlas" and were carefully studied; 57% had a C1-C2 instability and "most had congenital C2-C3 fusion" [19]. In our series, atlas assimilation was encountered in 550 of 6000 patients in the craniovertebral junction database [1, 14, 20]. Hindbrain herniation occurred in 38%. The situation was compounded by failure of segmentation of the second and third cervical vertebrae. In this situation of atlas assimilation,

segmentation failure of C2 and C3, atlantoaxial instability occurs as a result of abnormal loads placed on patent motion segments. Initially, the instability is reducible, and through a series of events with pannus formation around the odontoid process, the lesion becomes irreducible [2]. This then results into upward migration of the odontoid process by the time the child is between 14 and 15 years of age [1]. The bony abnormality is then an irreducible basilar invagination. Thus a child who is being evaluated for atlantoaxial dislocation is more likely than a full-grown adult to have a reducible atlantoaxial dislocation or a reducible basilar invagination. It is critical that an operative procedure that relies on posterior decompression for "hindbrain herniation" addresses the potential instability so that unfortunate results either in a short-term or a long-term basis are avoided.

Basilar invagination is commonly associated with an abnormal odontoid process invaginating into the posterior fossa. Of significance is the fact that the body of the axis becomes elongated and the true odontoid process is small. Of greater significance is the abnormal clivus-odontoid articulation. The resultant abnormal clivus-canal angle produces a ventral indentation of the pons, medulla, or cervicomedullary junction. As has been described before, the ability to reduce invagination is related to age in the presence of atlas assimilation. Reduction of the bony abnormality with traction or distraction can result in improvement of the craniocervical relationship and relief of compression on the cervicomedullary junction. This has been documented with postoperative imaging. On the other hand, an irreducible lesion will require decompression first. Restoration of posterior fossa volume by bony decompression, whether by traction or surgical resection, has been shown to produce upward migration of the tonsils and relief of the syrinx when present [21]. This phenomenon in the reverse, with reduction of posterior fossa volume, has led to severe hindbrain herniation in patients with osteogenesis imperfecta and related osteochondrodystrophies [10, 18, 20–23]. This same mechanism may be present in patients with os odontoideum who develop a secondary "Chiari I malformation."

Craniocervical instability with Chiari I malformation and syringohydromyelia for all the reasons documented in Table 18.2 will require treatment [11]. A properly fitting brace, such as the "Aspen or Miami J collar," can be both diagnostic and therapeutic. If the patient has relief of symptoms, it would imply that a fusion would be beneficial in the long-term. Below the age of 7, the author prefers to use a bony fusion alone. Beyond that age, it is possible to use rigid fixation using plates and screws depending on the size of the bony anatomy.

Illustrative Cases

Case 1

A 3-year-old presented with headaches when he was playing, episodic emesis, and coughing. He was diagnosed as having gastroesophageal reflux. On examination, the main findings were absence of a gag reflex and significantly abnormal hyperactive deep tendon reflexes in the upper and lower extremities. He walked with an extremely broad-based gait. MRI revealed atlas assimilation with segmentation failure of C2 and C3 vertebral bodies and gross atlantoaxial instability. The odontoid process indented into the pontomedullary junction (Fig. 18.1). The cervicomedullary buckle was seen at the mid-C2-C3 level, and a hindbrain herniation was evident. This was relieved with the patient being in extension, and the predental interval became normal. At posterior fossa decompression, the assimilated atlas was resected. A dorsal occipitocervical fusion was made using full-thickness rib grafts between the occiput and C2. He was maintained postoperatively in an occipitocervical-molded shell brace for 6 months. His symptoms resolved. This is an example of a reducible craniocervical bony abnormality.

Case 2

A 12-year-old girl presented with occipital and frontal headaches, difficulty swallowing, a lisping speech, and ataxic gait. She had a reduced gag reflex and decreased sensation to the back of the

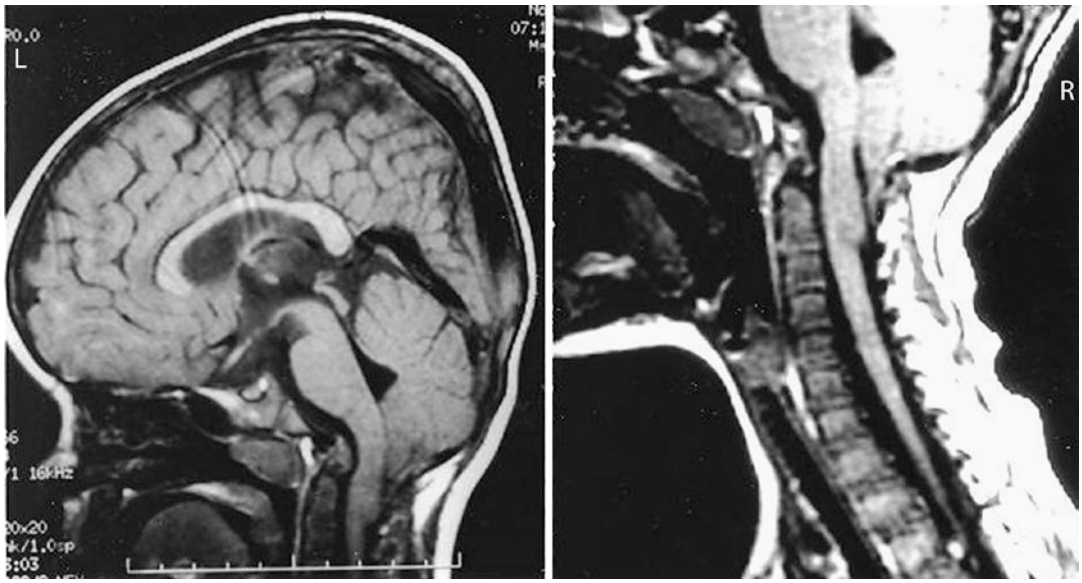

Fig. 18.1 Composite of midsagittal T1-weighted MRI of craniocervical region in flexion (L) and extension (R). There are atlas assimilation, segmentation failure of C2-C3 vertebral bodies, and gross atlantoaxial instability. The odontoid indentation into the ventral medulla corrects in extension. There is hindbrain herniation

tongue with partial atrophy. The deep tendon reflexes were grossly exaggerated. She was ataxic in neutral position. MRI and 3D CT of the craniocervical junction revealed a proatlas segmentation abnormality as visualized in Fig. 18.2a, b. A cervicothoracic syrinx was also identified. She underwent ventral transpalatopharyngeal decompression of the ventral medulla and a posterior dorsal occipitocervical fusion. Her symptoms resolved. This is an example of an irreducible ventral bony abnormality associated with the Chiari I malformation.

Case 3

This 28-year-old had a history of unrelenting "migraine headaches" and a choking sensation with swallowing. She noticed diminished dexterity in her hands and decreased sensation in her face. On examination, she had a partial glossopharyngeal and vagus nerve palsy with gross hyperreflexia and reduced pain sensation in her face down to the mid-neck on the right. Imaging demonstrated atlas assimilation with a short abnormal clivus and an acute angle to the clivus-canal junction (Fig. 18.3). She had basilar invagination, Chiari I malformation, and ventral cervicomedullary compression. The craniovertebral junction abnormality was irreducible and required transpalatopharyngeal resection of the clivus-odontoid process. She was noted to be extremely unstable intraoperatively, and a dorsal occipitocervical fusion was performed. She recovered the cranial nerve deficits and facial sensation.

Case 4

A 14-year-old boy with osteogenesis imperfecta presented with difficulty swallowing and weakness in his hands. MRI confirmed the severe "secondary basilar invagination" or basilar impression with marked crowding of the posterior fossa structures and clivus-canal angle of nearly 90 degrees. There were tonsillar descent and ventral compression of the medulla (Fig. 18.4). He responded to a high transpalatopharyngeal approach with decompression of the medulla and a dorsal posterior fossa decompression with fusion. This is an example of a secondary appearance of the Chiari I malformation as a result of marked reduction in the posterior fossa volume.

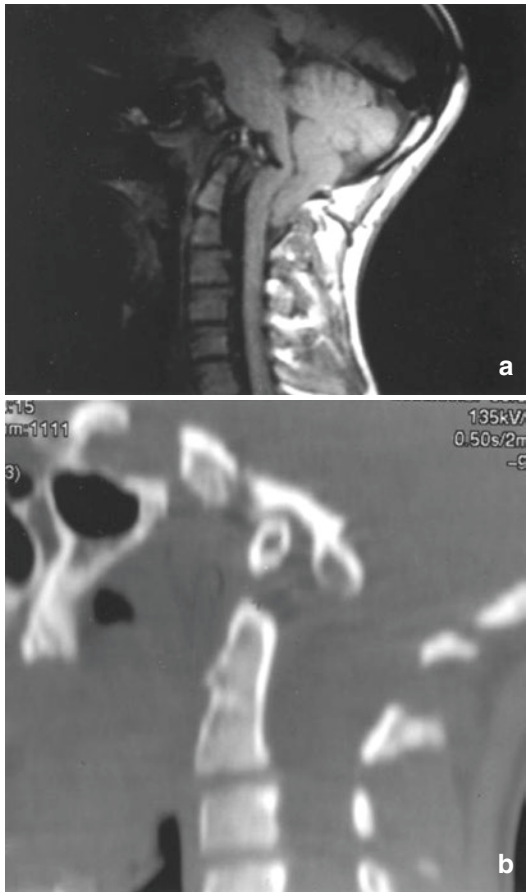

Fig. 18.2 (**a**) Midsagittal T1-weighted MRI of brain and cervical cord. Note the tonsil descent, ventral bony abnormality indenting into the medulla oblongata. (**b**) Midsagittal 2D CT reconstruction of craniovertebral junction reveals the proatlas abnormality as an extension of the clivus

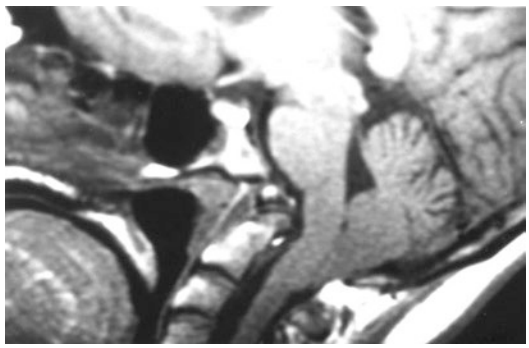

Fig. 18.3 Midsagittal T1-weighted MRI of cervicomedullary junction (CMJ). There is basilar invagination, atlas assimilation, short clivus, reduced clivus-canal angle, and ventral CMJ compression with Chiari I malformation

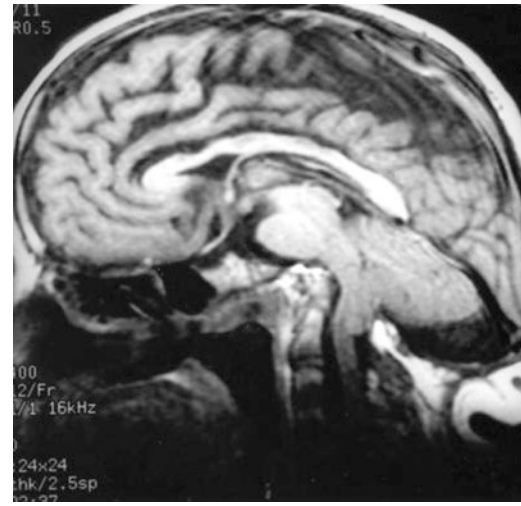

Fig. 18.4 Midsagittal T1-weighted MRI of brain in a 14-year-old with osteogenesis imperfecta. There is severe basilar impression and upward location of the cervical spine with marked reduction in posterior fossa volume and tonsillar herniation

Case 5

This 10-year-old presented with exertional headaches as well as a feeling of being unable to support her head. She had difficulty swallowing solids and had a slow, wide-based abnormal gait. Her cervical muscles were weak. MRI showed a clivus-canal angle of 92 degrees in flexion, which changed to 127 degrees in extension (which would be considered as being normal) (Fig. 18.5a). She responded to cervical traction, and using an Aspen cervical brace, her headaches were relieved though the rest of the neurological symptoms persisted. The high cervical syrinx was noted. She underwent intraoperative crown halo cervical traction, posterior fossa and foramen magnum decompression with intradural procedure, shrinkage of the cerebellar tonsils, and cervical fascia duraplasty. An occipitocervical fusion completed the operative procedure. Her postoperative MRI shows (Fig. 18.5b) the maintenance of the normal clivus-odontoid angle and disappearance of the cervical syrinx. She is 4 years following her operative procedure and is doing well.

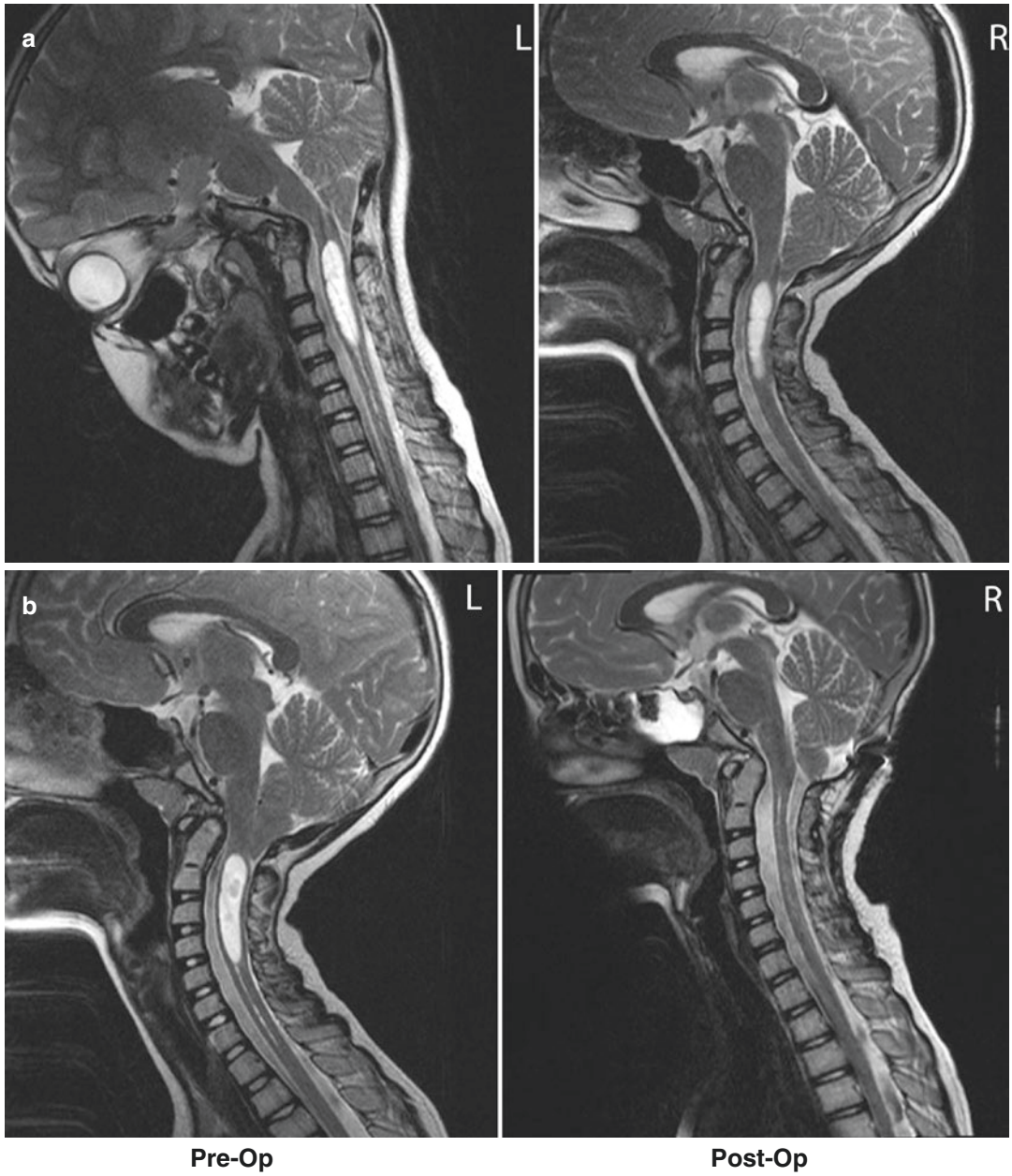

Fig. 18.5 (**a**) Composite of midsagittal T1-weighted MRI in flexion (L) and extension (R). The clivus-odontoid angle of 92 degrees (L) changes to 127 degrees (R) in extension. This signifies craniocervical instability. Note the CM1 with high cervical cord syrinx. "Valsalva-type headaches" were present together with a feeling of a "heavy head." She had weak cervical musculature. (**b**) Composite of T2-weighted MRI of the brain and cervical cord, preoperative (L) and postoperative (R). She underwent posterior fossa decompression with duraplasty and occipitocervical (O-C2-C3) fusion. The tonsils have ascended and the syrinx is not seen

References

1. Menezes AH. Developmental abnormalities of the craniovertebral junction. In: Winn HR, editor. Youmans neurological surgery. Philadelphia: WB Saunders; 2004. p. 3331–45.
2. Menezes AH. Primary craniovertebral anomalies and the hindbrain herniation syndrome (Chiari I): data base analysis. Pediatr Neurosurg. 1995;23:260–9.
3. Milhorat TH, Chou MW, Trinidad EM, Kula RW, Mandell M, Wolpert C, et al. Chiari I malformation redefined: clinical and radiographic findings for 364 symptomatic patients. Neurosurgery. 1999;44:1005–17.
4. Menezes AH, Greenlee JDW, Donovan KA. Honored guest presentation: lifetime experiences and where we are going. Chiari I with syringomyelia – controversies and development of decision tree. Clin Neurosurg. 2005;52:297–305.
5. Goel A, Bhatjiwale M, Desai K. Basilar invagination: a study based on 190 surgically treated patients. J Neurosurg. 1998;88:962–8.
6. Perrini P, Benedetto N, Guidi E, Di Lorenzo N. Transoral approach and its superior extensions to the craniovertebral junction malformations: surgical strategies and results. Spine. 2009;64(5 Suppl 2):331–42.
7. Aghakhani N, Parker F, David P, Morar S, Lacroix C, Benoudiba F, et al. Long-term follow-up of Chiari-related syringomyelia in adults: analysis of 157 surgically treated cases. Neurosurgery. 2009;64:308–15.
8. Menezes AH. Craniocervical developmental anatomy and its implications. Childs Nerv Syst. 2008;24:1109–22.
9. Menezes AH. Craniovertebral junction database analysis: incidence, classification presentation and treatment algorithms. Childs Nerv Syst. 2008;24:1101–8.
10. Sawin PD, Menezes AH. Basilar invagination in osteogenesis imperfecta and related osteochondrodysplasias: medical and surgical management. J Neurosurg. 1997;86:950–60.
11. Fenoy AJ, Menezes AH, Fenoy KA. Craniocervical junction fusions in patients with hindbrain herniation and syringohydromyelia. J Neurosurg Spine. 2008;9:1–9.
12. Menezes AH. Current opinions for treatment of symptomatic hindbrain herniation or Chiari type I malformation. World Neurosurg. 2011;75:226–8.
13. VanGilder JC, Menezes AH, Dolan KD. The Craniovertebral junction and its abnormalities. Mount Kisco/New York: Futura Publishing; 1987.
14. Menezes AH, Fenoy KA. Remnants of occipital vertebrae: Proatlas segmentation abnormalities. Neurosurgery. 2009;64:945–54.
15. Grabb PA, Mapstone TB, Oakes WJ. Ventral brain stem compression in pediatric and young adults with Chiari I malformations. Neurosurgery. 1999;44:520–8.
16. Jian FZ, Chen Z, Wrede KH, Samii M, Ling F. Direct posterior reduction and fixation for the treatment of basilar invagination with atlantoaxial dislocation. Neurosurgery. 2010;66:678–87.
17. Dahdaleh NS, Dlouhy BJ, Menezes AH. Application of neuromuscular blockade and intraoperative 3D imaging in the reduction of basilar invagination. J Neurosurg Pediatr. 2012;9(2):119–24.
18. Botelho RV, Neto EB, Patriota GC, Daniel JW, Dumont PA, Rotta JM. Basilar invagination: craniocervical instability treatment with cervical traction and occipitocervical fixation. J Neurosurg Spine. 2007;7:444–9.
19. Gholve PA, Hosalkar HS, Ricchetti ET, Pollock AN, Dormans JP, Drummond DS. Occipitalization of the atlas in children. Morphologic classification, associations, and clinical relevance. J Bone Joint Surg Am. 2007;89(3):571–8.
20. Stovwer LJ, Bergan U, Nilsen G, Sjaastad O. Posterior cranial fossa dimensions in the Chiari I malformation: relation to pathogenesis and clinical presentation. Neuroradiology. 1993;35:113–8.
21. Menezes AH. Craniovertebral junction abnormalities with hindbrain herniation and syringomyelia: regression of syringomyelia after removal of ventral craniovertebral junction compression. J Neurosurg. 2012;116(2):301–9.
22. Kohno K, Sakaki S, Shiraishi T, Matsuoka K, Okamura H. Successful treatment of adult Arnold-Chiari malformation associated with basilar impression and syringomyelia by the transoral anterior approach. Surg Neurol. 1990;33:284–7.
23. Nishikawa M, Sakamoto H, Hakuba A, Nakanishi N, Inoue Y. Pathogenesis of Chiari malformation: a morphometric study of the posterior cranial fossa. J Neurosurg. 1997;86:40–7.

Ventral Decompression for Chiari Malformations

19

Akal Sethi, Thomas Ridder, and Todd C. Hankinson

Introduction

This chapter describes and encapsulates the clinical appearance and treatment options for ventral brain stem compression (VBSC) in Chiari malformation, type I (CMI) and associated craniocervical pathologies [1]. For the purposes of this chapter, the term CMI will include entities that are commonly referred to as complex Chiari malformation and Chiari malformation type 1.5.

Ventral Brain Stem Compression

Background

Prior to the advent of modern imaging, VBSC tended to be a postmortem diagnosis [2, 3]. It is most commonly associated with inflammatory conditions such as rheumatoid arthritis, trauma, and neoplastic processes but is also associated with CMI. Initial treatments of VBSC included posterior fossa decompression alone, but were advanced to include anterior decompressive techniques. Kanavel, in 1917, published a technique paper on the transoral approach to remove a bullet lodged between the clivus and the atlas [4]. Anterior approaches to VBSC have been improved with advances in neuroimaging as well as transnasal endoscopy.

Factors that contribute to the decision regarding the potential operative management of VBSC include (1) patient age, (2) symptoms, (3) reducibility of the compressive lesion, and (4) underlying pathology.

Ventral Brain Stem Compression in Chiari Malformations, Type I

CMI is reported in up to 1–5% of all craniocervical imaging studies [5]. However, VBSC is far less common. One series reported rates of retroflexed dens at 26% and presence of basilar invagination at 12% in symptomatic Chiari patients [6–8]. Grabb et al., in their 1999 study, classified the presence of VBSC in young Chiari patients with a measurement of the line perpendicular to the basion-C2 (B-C2) line, termed the

A. Sethi
Department of Neurosurgery, University of Colorado, Aurora, CO, USA

T. Ridder
Pediatric and Adult Neurosurgery, Children's Hospital Colorado – Colorado Springs/UCHealth Brain and Spine, Colorado Springs, CO, USA

T. C. Hankinson (✉)
Departments of Neurosurgery and Pediatrics, Children's Hospital Colorado/University of Colorado School of Medicine, Aurora, CO, USA
e-mail: Todd.Hankinson@childrenscolorado.org

R. S. Tubbs et al. (eds.), *The Chiari Malformations*, https://doi.org/10.1007/978-3-030-44862-2_19

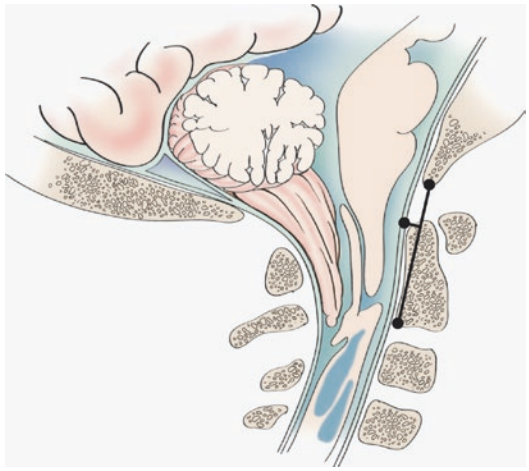

Fig. 19.1 Drawing illustrating the pB-C2 line connecting the basion to the posterior body of C2. A line drawn perpendicular to this indicates the amount of ventral compression

pB-C2 (Fig. 19.1) [9, 10]. All patients with a pB-C2 of less than 9 mm were successfully treated with posterior fossa decompression alone, whereas a minority of patients with a pB-C2 of greater than 9 mm required occipitocervical fixation with or without ventral decompression.

Diagnosis of Ventral Brainstem Compression

Clinical Examination

Patients with CMI and VBSC present with a wide range of symptoms within the context of Chiari symptomatology. This can range from the classic posterior occipital headache and neck pain to long tract signs and cranial neuropathies. Furthermore, the onset can be insidious or rapidly progressive. Numerous studies have examined the specific symptoms of VBSC in CMI [11–18]. Menezes et al. state that these patients are more likely to have long tract signs, cranial neuropathies, brain stem dysfunction, and myelopathy [18, 19]. Additionally, their series identified patients with facial pain, facial hypalgesia, and urinary incontinence at rates of 3.6%, 7.1%, and 16.7%, respectively (Table 19.1).

Table 19.1 Signs and symptoms of craniocervical abnormalities with VBSC

Signs and symptoms of craniovertebral anomalies associated with ventral brain stem compression
Posterior occipital headache or neck pain
Myelopathy or quadraparesis
Basilar migraines
Lower cranial neuropathies (e.g., dysphagia, aspiration pneumonia, and diminished gag reflex)
Facial pain
Urinary frequency or incontinence
Ataxia
Nystagmus (downbeat and lateral gaze)
Central sleep apnea
Sensory disturbances (posterior column dysfunction)
Hearing loss or tinnitus

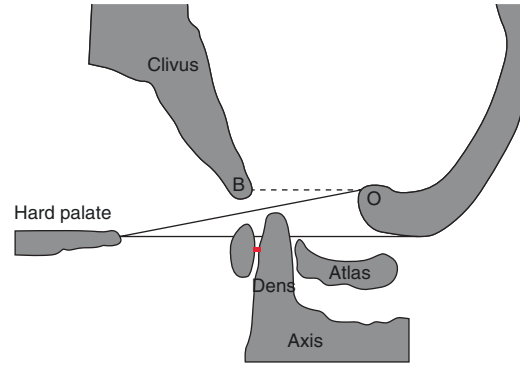

Fig. 19.2 Commonly used measurements of the craniocervical junction. B basion, O opisthion. Dotted line between B and O is McRae's line. The line between O and the hard palate is Chamberlain's line, and the line between the hard palate and inferior occiput is McGregor's line. The short red line between the posterior aspect of the anterior arch of C1 and the anterior aspect of the dens is the atlantodental interval (ADI)

Radiographic Evaluation

Most patients will have undergone cranial imaging prior to neurosurgical consultation for CMI and VBSC. Magnetic resonance imaging (MRI) should be performed in the setting of any concern for symptoms of either aforementioned pathology. CMI is traditionally diagnosed by cerebellar tonsillar herniation of greater than 5 mm below the McRae line (defined by the line drawn from the basion to the opisthion) (Fig. 19.2). When identified, additional MRI of the spine should be performed to assess for syrinxes and scoliosis (Fig. 19.3). VBSC may prompt additional imaging

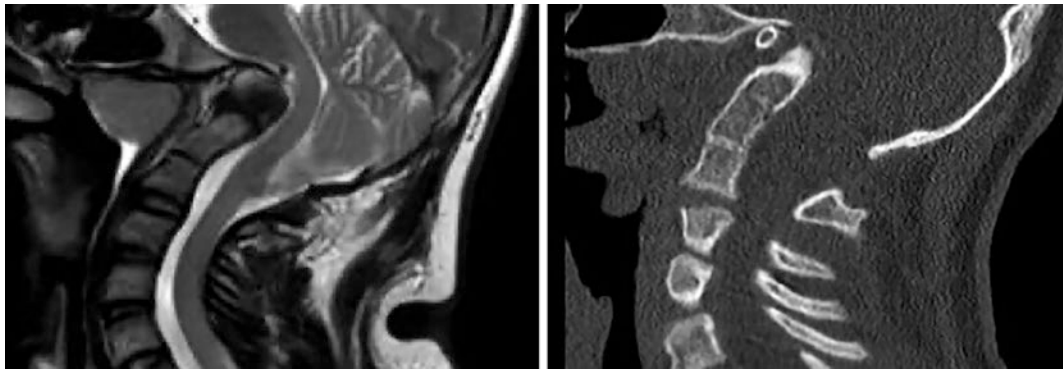

Fig. 19.3 Sagittal T2-weighted magnetic resonance imaging (MRI) scan and Sagittal CT images at presentation, demonstrating CMI with BI and substantial VBSC. There is no syringomyelia

of the craniocervical junction including noncontrast computed tomography (CT) for osseous evaluation and flexion extension X-rays to ascertain for pathologic motion. Prior to operative intervention for patients with significant VBSC, vascular imaging may be useful in determining the course of the vertebral and carotid arteries, as they are more likely to be aberrant in this context.

Craniovertebral measurements such as the pB-C2 line, the clivoaxial angle (CXA), and others are also useful parameters in the assessment of ventral compression. While none of these has been established as a standardized tool, Bollo and colleagues identified a clivoaxial angle of <125° as a risk factor for the need for occipitocervical fusion [20], and data from the Park-Reeves Syringomyelia Research Consortium and Pediatric Craniocervical Society indicate that pB-C2 can be assessed with good inter-rater reliability using MRI or CT [21].

Treatment of Ventral Brainstem Compression in Chiari Malformations, Type I

Conservative Management

Operative intervention for CMI and VBSC shares similar indications. Without the aforementioned symptoms of cervical headaches, neck pain, cranial neuropathies, brain stem dysfunction, or long tract signs, non-operative treatment is usually warranted. Careful neurologic examination throughout the entire spectrum of cervical motion looking for both long tract signs and brain stem dysfunction should be performed on every patient. In the absence of findings, flexion-extension films should be obtained to elucidate any pathologic motion. Clinical and radiographic follow-up should be determined on a patient-specific basis and may include adjunctive tests, such as ophthalmological or sleep study evaluation.

Operative Management

Symptomatic patients with CMI and VBSC should be strongly considered for operative intervention. In many cases, posterior fossa decompression or posterior fossa decompression and occipitocervical fusion will relieve symptoms that results from VBSC. As such, direct ventral approaches are only rarely required in this population of patients. When they are necessary, the most common approaches to ventral craniocervical pathology include the transoral and transnasal techniques. In the authors' institution, such approaches are performed in conjunction with the otolaryngology service.

Transoral Approach

Traditionally, the transoral approach provides excellent exposure of the ventral craniocervical junction, the C1-2 complex, and lower third of the clivus in an extradural fashion without the need for brain retraction. Morbidity associated

with the approach derives from tongue and pharyngeal retraction, which can result in prolonged intubation. In rare circumstances, the combination of the preoperative neurological compromise with the operative irritation may necessitate a gastrostomy or tracheostomy.

Positioning and Setup

After oral fiber-optic intubation, the patient is positioned supine and fixed in the Mayfield head holder with the neck slightly extended. Pin fixation allows for intraoperative navigation, which is preferred. Corticosteroid cream can be applied to the tongue to reduce postoperative swelling per anesthesia preference. There are multiple transoral retractor systems, such as the Dingman or Spetzler-Sonntag. The uvula and soft palate can be retracted superiorly by a narrow retractor blade or stitch and rarely need to be divided for exposure. The tongue is moved inferiorly with a wide retractor blade, with the endotracheal tube preferably along the side of the mouth to help reduce postoperative swelling. Guards can be placed to protect the teeth as well. The lateral walls of the oropharynx are moved laterally with blades. Once the retractor is fixed, it is imperative to ensure the tongue is not compressed against the teeth. Such compression can lead to highly morbid lingual edema or necrosis. Once proper position is ensured, the blades are prepped with Betadine solution. The surgeon is positioned at the head of the patient and uses an operating microscope.

Incision and Dissection

The posterior wall of the pharynx can be injected with local anesthetic with epinephrine per surgeon preference. The incision should be made along the anterior tubercle of C1, which can be palpated, but is also easily identified with navigation. The incision can be made with a scalpel or low-power monopolar cautery in the median raphe between the pharyngeal muscles, and extends down to the anterior tubercle of C1 through the anterior longitudinal ligament. The exposure is then carried in a superoinferior fashion to expose from the lower third of the clivus to the C2 body, as needed. Bleeding is minimized with subperiosteal dissection of the longus colli muscles and is further minimized with retraction.

Removal of C1 Arch and Dens

The anterior arch of C1 is removed with a combination of a high-speed drill and bone-biting instruments. This is usually removed to a width just lateral to the dens. There can be a significant amount of soft tissue/pannus present between the anterior arch and the dens. This can be removed safely with bone-biting instruments. Once the borders of the dens are delineated, careful ligamentous dissection is necessary to identify and release the apical and alar ligaments. The dens is meticulously drilled away until a thin rim of dorsal cortical bone remains. The remaining bone is carefully dissected free and removed. As needed, underlying soft tissue and posterior longitudinal ligament/tectorial membrane are also removed, recognizing that the underlying dura may be attenuated or, especially in the case of reoperation, absent. The superior tip of the dens can be difficult to identify and remove once the inferior portion has been removed, but the smooth superior cupula should be identified and removed in order to assure adequate decompression. If needed, the inferior third of the clivus can be drilled or rongeured away in a similar fashion. Once bony removal is complete, dural pulsatility should be observed to confirm adequate decompression.

Closure

There have been several different closure techniques described for the transoral approach [19, 22–24]. Both the muscle and mucosal layers should be approximated with interrupted 3-0 Vicryl sutures, ensuring not to necrose the delicate mucosa. Fibrin glue can be used in the presence of a cerebrospinal fluid (CSF) leak.

Endoscopic Transnasal Approach

The endoscopic transnasal approach has been widely used to access lesions in the sella turcica and with this experience has been expanded to reach the craniocervical junction and lower clivus as well. One cadaveric study demonstrated a better exposure with the endoscopic compared to the microscopic transoral approach [25]. An experienced otolaryngologist is an invaluable

member of the operative team when these approaches are employed. In the authors' institution, this approach is generally preferred to the transoral approach due to the decreased trauma to the oropharynx and resultant minimization of postoperative swelling, thereby allowing for earlier extubation and enteral nutrition.

Endoscopic Endonasal Approach

Similar to the transoral approach, the patient is positioned supine with the head fixed in pin fixation and the neck slightly extended. The head may be slightly rotated toward the surgeon. The inferior turbinate can be resected or lateralized depending on the size of the working channel. After a posterior nasal septectomy enlarges the choana, the adenoids are removed with a microdebrider. Subsequently, the posterior nasopharynx is incised from the clivus to the body of C2 in a longitudinal fashion, taking care to stay in the midline with the lateral borders being the tori of the Eustachian tubes. The underlying longus capitis muscles are dissected in a subperiosteal fashion and retracted laterally. The anterior tubercle of C1 is palpated and confirmed with neuronavigation. Removal of the arch of C1 and dens is carried out as previously described.

Closure

With the transnasal approach, closure of the posterior nasopharynx is usually undertaken with fibrin glue. In the setting of a CSF leak, the defect is addressed in a similar manner to endoscopic transsphenoidal procedures, which include rotation of a nasal septal flap and dural/fat grafts as preferred.

Order of Surgery

Most patients with CMI will be sufficiently treated with posterior fossa decompression alone without the need for a ventral decompression [26]. Even patients with CMI and VBSC most often do not require ventral decompression. Furthermore, patients with VBSC do not always require posterior fusion, although fusion can help alleviate symptoms of VBSC without the need for a ventral approach [9]. Due to the success with posterior approaches alone even in the setting of VBSC, most surgeons prefer to proceed with posterior fossa decompression with or without occipitocervical fusion, keeping in mind that fusion can limit the positioning of the neck during a ventral approach, if needed. There have been no studies to analyze the best sequence of procedures or predictive scoring system to ascertain the need for ventral decompression; however, the surgeon must use the available tools to make the best clinical decision.

Conclusion

In summary, VBSC can be associated with CMI malformations and should be looked for closely on preoperative films or at the initial consultation. Here, in this chapter, we present the morphology and incidence of VBSC as well as associated symptoms. Both the transoral and the endoscopic endonasal approaches are valid surgical options for refractory VBSC; however, most are adequately decompressed from a traditional posterior suboccipital craniectomy and C1 laminectomy with or without expansile duraplasty.

References

1. Bhangoo RS, Crockard HA. Transmaxillary anterior decompression in patients with severe basilar impression. Clin Orthop. 1999;359:115–25.
2. Caetano de Barros M, Farias W, Ataíde L, Lins S. Basilar impression and Arnold-Chiari malformation: a study of 66 cases. J Neurol Neurosurg Psychiatry. 1968;31:596–605.
3. Dyste GN, Menezes AH. Presentation and management of pediatric Chiari malformations without myelodysplasia. Neurosurgery. 1988;23:589–97.
4. Choi D, Crockard HA. Evolution of transoral surgery: three decades of change in patients, pathologies, and indications. Neurosurgery. 2013;73(2):296–303 [discussion: 303–4].
5. Elster AD, Chen MY. Chiari I malformations: clinical and radiologic reappraisal. Radiology. 1992;183:347–53.
6. Milhorat TH, Chou MW, Trinidad EM, Kula RW, Mandell M, Wolpert C, et al. Chiari I malformation redefined: clinical and radiographic findings for 364 symptomatic patients. Neurosurgery. 1999;44:1005–17.

7. Pillai P, Baig MN, Karas CS, Ammirati M. Endoscopic image-guided transoral approach to the craniovertebral junction: an anatomic study comparing surgical exposure and surgical freedom obtained with the endoscope and the operating microscope. Neurosurgery. 2009;64(5 Suppl 2):437–42 [discussion: 442–4].
8. Menezes AH. Craniovertebral junction abnormalities with hindbrain herniation and syringomyelia: regression of syringomyelia after removal of ventral craniovertebral junction compression. J Neurosurg. 2012;116(2):301–9.
9. Grabb PA, Mapstone TB, Oakes WJ. Ventral brain stem compression in pediatric and young adult patients with Chiari I malformations. Neurosurgery. 1999;44(3):520–7 [discussion: 527–8].
10. Greenberg JK, Yarbrough CK, Radmanesh A, Godzik J, Yu M, Jeffe DB, et al. The Chiari severity index: a preoperative grading system for chiari malformation type 1. Neurosurgery. 2015;76(3):279–85.
11. Greenlee JDW, Donovan KA, Hasan DM, Menezes AH. Chiari I malformation in the very young child: the spectrum of presentations and experience in 31 children under age 6 years. Pediatrics. 2002;110(6):1212–9.
12. McGirt MJ, Attenello FJ, Atiba A, Garces-Ambrossi G, Datoo G, Weingart JD, et al. Symptom recurrence after suboccipital decompression for pediatric Chiari I malformation: analysis of 256 consecutive cases. Childs Nerv Syst. 2008;24:1333–9.
13. Meadows J, Kraut M, Guarnieri M, Haroun RI, Carson BS. Asymptomatic Chiari Type I malformations identified on magnetic resonance imaging. J Neurosurg. 2000;92(6):920–6.
14. Mendes GA, Dickman CA, Rodriguez-Martinez NG, Kalb S, Crawford NR, Sonntag VK, et al. Endoscopic endonasal atlantoaxial transarticular screw fixation technique: an anatomical feasibility and biomechanical study. J Neurosurg Spine. 2015;22(5):470–7.
15. Menezes AH. Acquired abnormalities of the craniovertebral junction. In: Winn HR, editor. Youman's neurological surgery. Philadelphia: Saunders; 2003. p. 4569–85.
16. Tubbs RS, Beckman J, Naftel RP, Chern JJ, Wellons JC 3rd, Rozzelle CJ, et al. Institutional experience with 500 cases of surgically treated pediatric Chiari malformation type I. J Neurosurg Pediatr. 2011;7:248–56.
17. Yu Y, Hu F, Zhang X, Ge J, Sun C. Endoscopic transnasal odontoidectomy combined with posterior reduction to treat basilar invagination: technical note. J Neurosurg Spine. 2013;19(5):637–43.
18. Menezes AH. Craniovertebral junction database analysis: incidence, classification, presentation, and treatment algorithms. Childs Nerv Syst. 2008;19(10):1101–8.
19. Menezes AH. Decision making. Childs Nerv Syst. 2008;24(10):1147–53.
20. Bollo RJ, Riva-Cambrin J, Brockmeyer MM, Brockmeyer DL. Complex Chiari malformations in children: an analysis of preoperative risk factors for occipitocervical fusion. J Neurosurg Pediatr. 2012;10(2):134–41.
21. Hankinson TC, Tuite GF, Moscoso DI, Robinson LC, Torner JC, Limbrick DD Jr, et al. Analysis and interrater reliability of pB-C2 using MRI and CT: data from the Park-Reeves Syringomyelia Research Consortium on behalf of the Pediatric Craniocervical Society. J Neurosurg Pediatr. 2017;20(2):170–5.
22. Dlouhy BJ, Dahdaleh NS, Menezes AH. Evolution of transoral approaches, endoscopic endonasal approaches, and reduction strategies for treatment of craniovertebral junction pathology: a treatment algorithm update. Neurosurg Focus. 2015;38(4):E8.
23. Henn JS, Lee MC, Rhoton AL. Transoral approach to the craniocervical junction and upper cervical spine. In: Surgical anatomy and techniques of the spine. 1st ed. Philadelphia: Elsevier; 2006. p. 3–12.
24. Singh H, Harrop J, Schiffmacher P, Rosen M, Evans J. Ventral surgical approaches to craniovertebral junction chordomas. Neurosurgery. 2010;66(3 Suppl):96–103.
25. Hickman ZL, McDowell MM, Barton SM, et al. Transnasal endoscopic approach to the pediatric craniovertebral junction and rostral cervical spine: case series and literature review. Neurosurg Focus. 2013;35(2):E14.
26. Ridder T, Anderson RE, Hankinson H. Ventral decompression in chiari malformation, basilar invagination and related disorders. Neurosurg Clin N Am. 2015;26:571–8.

Chiari I Malformation and Craniosynostosis

20

Mehmet Turgut and R. Shane Tubbs

Introduction

Chiari malformation type I (CM I), downward herniation of one or both cerebellar tonsils to more than 3–5 mm below the basion-opisthion line through the foramen magnum (FM) into the upper cervical spinal canal, is a dynamic disease [1–10]. Craniosynostosis—the premature fusion of one or more sutures in the vault or base of the cranium restricting cranial growth perpendicular to the affected suture associated with compensatory overgrowth of the other patent sutures—is one of the major neurosurgical problems in children and can result from genetic mutations, mechanical causes such as intrauterine compression, metabolic causes, or teratogens [4, 11–13]. The incidence of craniosynostosis ranges from 1/2100 to 1/8750 live births [14–17]. It has been reported that craniosynostosis is an isolated condition in 85% of patients and part of a complex condition in the remaining 15% [18, 19]. Clinically, in patients where compensation does not provide sufficient space for the growth of the brain, craniosynostosis leads to characteristic deformities of the skull with various functional results like increased intracranial pressure (IICP), visual and auditory impairment, and cognitive deficits [5, 12, 13, 20, 21].

In recent years, with the advent of magnetic resonance imaging (MRI), increasing numbers of patients have been diagnosed as CM I, and the association CM I together with craniosynostosis is a major neurosurgical concern in children. Etiologically, it has been suggested that underdevelopment of the occipital bone and hindbrain structures, including the cerebellum and brain stem, and/or craniocephalic disproportion in patients with craniosynostosis, could cause an inadequate posterior cranial fossa volume (PFV) and inferior displacement of the tentorium cerebelli and the torcular Herophili, resulting in the development of CM I [7, 22–26]. Other causes could include congenital anomalies of the hindbrain structures, hydrocephalus, venous hypertension, or decreased PFV in bone disorders such as osteopetrosis [27–30]. Depending on the degree of compression of the spinal cord and/or brain stem by the herniated cerebellar tonsils, clinical findings ranging from simple headache localized in the suboccipital region and neck pain to life-threatening neurological deficits (i.e., weakness and/or dysfunctions of the lower cranial nerves) have been reported, although some patients with CM I and craniosynostosis are asymptomatic [8, 22, 31, 32].

M. Turgut (✉)
Department of Neurosurgery, Aydın Adnan Menderes University School of Medicine, Efeler, Aydın, Turkey

R. S. Tubbs
Department of Neurosurgery, Tulane University School of Medicine, New Orleans, LA, USA

Department of Neurosurgery and Ochsner Neuroscience Institute, Ochsner Health System, New Orleans, LA, USA

R. S. Tubbs et al. (eds.), *The Chiari Malformations*, https://doi.org/10.1007/978-3-030-44862-2_20

There is a close relationship between CM I associated with craniosynostosis and disorders such as congenital anomalies of the brain stem and cerebellum, ventricular dilatation and hydrocephalus, IICP, and venous hypertension. Importantly, the herniated cerebellar tonsils become repositioned into the posterior cranial fossa, and the symptoms of patients with CM I will reverse when the associated pathologies such as craniosynostosis and hydrocephalus are treated appropriately [33–37].

History

CM I, which manifests with brain tissue protruding into the spinal canal, was first defined by Cleland in 1883 in a pediatric patient with hydrocephalus, spina bifida, and involvement of the brain stem and cerebellum [38, 39]. Chiari then reported a case with congenital CM I resulting from fetal hydrocephalus [40]. However, the association between CM I and craniosynostosis was first reported by Saldino et al. in a pediatric patient with Pfeiffer syndrome in 1972, and during subsequent years further cases have been reported owing to the increased use of MRI in pediatric neurosurgery [28, 41–43]. In 1995, Cinalli et al. published a clinical series of 95 craniosynostosis patients with a high frequency of CM I [22]. The association between CM I and craniosynostosis, syndromic multisutural or nonsyndromic monostutural, has now been described by many authors in clinical practice, as reported as follows in detail.

Pathogenesis

Genetic Mutations

Some authors have suggested that iatrogenic factors such as exposure to certain teratogens, shunting of hydrocephalus in the early postnatal period, and radiotherapy application for craniofacial tumors in infants can cause monosutural or multisutural synostosis, albeit rarely [14]. However, it is now widely accepted that monosutural synostosis is caused by idiopathic defective dural mesenchymal signaling in most patients [14], while syndromic multisutural synostoses are related to genetic disorders or metabolic causes [14]. Only 1/4 of all craniosynostosis cases are syndromic multisutural; mutations in the FGFR genes are held responsible for the development of craniosynostoses in various syndromes such as Crouzon, Apert, Pfeiffer, Muenke, and Saethre-Chotzen [44–47]. Specifically, mutations of the genes involved in endochondral ossification during skull base development are located on FGFR1 for Pfeiffer syndrome; on FGFR2 for Apert, Crouzon, and Pfeiffer; and on FGFR3 for Crouzon syndrome [48–52]. In addition, mutations involving the genes modulating normal cranial development such as *TWIST1*, *MSX2,* and *RAB23* have been reported [45, 53]. Fujisawa et al. suggested that mutations over exons IIIa and IIIc of the FGFR2 gene contribute to the development of CM I in children with Crouzon syndrome [44].

Craniosynostosis

Most patients with craniosynostosis have multisutural involvement, nonsyndromic or syndromic, frequently associated with CM I; in contrast, the prevalence of CM I in patients with monosutural craniosynostosis is only 5.0% in the current literature [4, 5, 19, 21, 42, 54–56]. It has been reported that CM I is frequent in patients with sagittal synostosis (Fig. 20.1), which is the

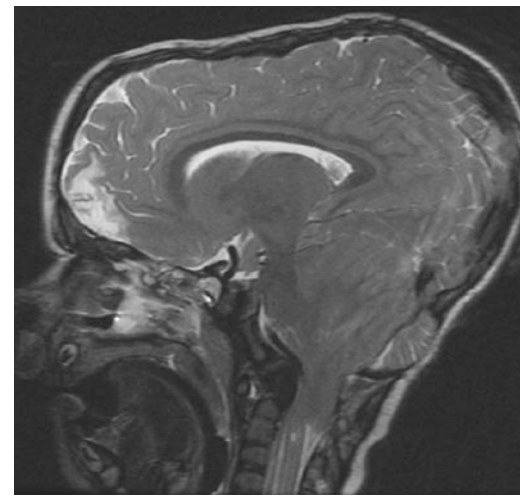

Fig. 20.1 MRI noting a CM I in a male patient with sagittal synostosis

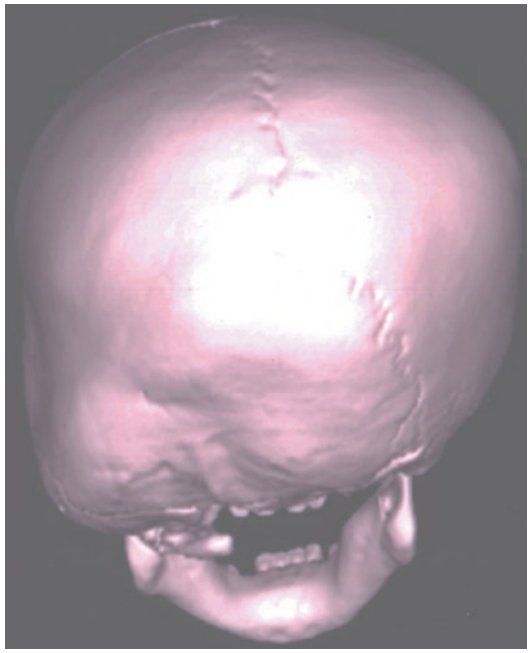

Fig. 20.2 3D reconstruction of the skull in a child with left-sided lambdoidal synostosis who was found to have a CM I

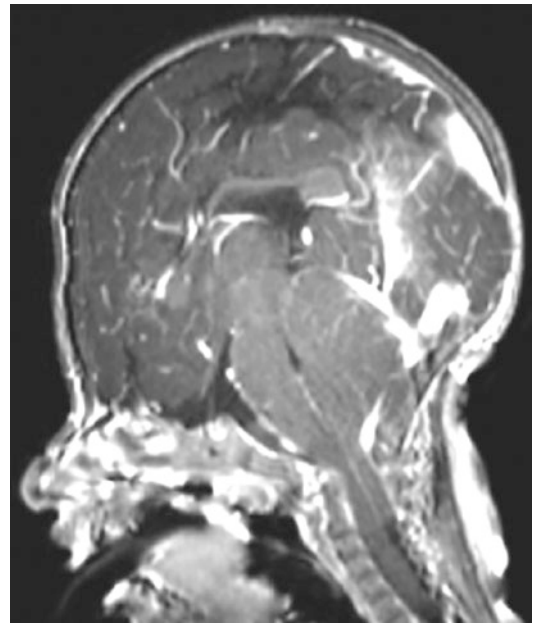

Fig. 20.3 MRI noting a CM I in a child with bilateral coronal synostosis

most common type of craniosynostosis, and most of the involved sutures are located in the posterior part of the cranium such as the lambdoid suture (Fig. 20.2); or patients have bilateral coronal synostosis (Fig. 20.3), associated or not with the closure of synchondroses in the cranial base [4, 5, 22, 56, 57]. In 2011, Strahle et al. found CM I in five of nine patients with nonsyndromic isolated lambdoid synostosis [56]. However, Leikola et al. found no patients with isolated lambdoid synostosis associated with CM I in their series [54], and Engel et al. reported only one patient with lambdoid synostosis associated with CM I in their series [57]. On the other hand, association of CM I with monosutural craniosynostoses involving cranial sutures at locations other than the lambdoid suture, such as sagittal, coronal, or metopic sutures, is extremely rare [54, 56, 57]. In contrast, Tubbs et al. found a 30% incidence of CM I in trigonocephaly related to a reduced anterior cranial fossa volume (AFV) due to closure of the metopic suture; the explanation is unclear [21]. Interestingly, asymmetrical herniation of the cerebellar tonsils has also been observed in patients with CM I associated with monosutural craniosynostosis [24, 58, 59]. In particular, Karppinen et al. observed that the right cerebellar tonsil is more inferiorly located in most patients, predominantly on the synostotic suture side in asymmetric craniosynostosis cases [58]. More importantly, it has been suggested that CM I is not present at birth in craniosynostosis patients but develops following premature closure of the lambdoid suture and/or sutures of cranial base in the first 6 months of age [22].

In patients with craniosynostosis, the following related parameters should be kept in mind for the occurrence of CM I:

1. *Type and number of involved cranial sutures:* It is well known that CM I is rarely associated with nonsyndromic monosutural synostosis and most of these patients are asymptomatic. In a review of 29 children of CM I who operated for craniosynostosis, Strahle et al. observed that involvement of the lambdoid suture (lambdoid synostosis) was more frequently associated with CM I [56]. These authors reported that 55.6% and 57.1% of

patients with monosutural and syndromic multisutural synostosis involving the lambdoid suture, respectively, had CM I, compared with only 0–10.5% of all other synostosis patients [56]. Similarly, Fearon et al. reported a 60% incidence of involvement of the lambdoid suture together with CM I [60]. Engel et al. also reported that only 1 child with lambdoid synostosis among 89 with craniosynostosis was associated with CM I [57]. Thus, it is clear that synostosis of the lambdoid suture is very important for the development of CM I, though other factors also play a role in the development of this condition. However, in a review of 124 children with monosutural synostosis, Leikola et al. found only 7 cases (5.6%) associated with CM I, 5 with sagittal synostosis, and 2 with coronal synostosis [54]. In another clinical series with monosutural synostosis, a higher prevalence (9%) of CM I was reported [61]. Interestingly, Tubbs et al. reported 30% of CM I in 50 pediatric patients with simple metopic ridges, not trigonocephaly [21].

2. *Age of patient:* The age range in the nonsyndromic monosutural craniosynostosis series of Leikola and colleagues with higher prevalence of CM I was 33.5–37.7 months [61], although the mean age in the series of Engel et al. with lower incidence of CM I was 11.6 months, suggesting that CM I is part of the natural history of craniosynostosis if it is not corrected by surgical intervention [25, 57]. In another series, two patients of uncorrected sagittal synostosis were associated with the development of CM I, syringomyelia, and hydrocephalus in later life [55].
3. *Intracranial volume:* In the past, it was believed that craniosynostosis affected the growth of the brain negatively by reducing the intracranial volume (ICV) [4, 62]. However, this concept has changed because it has been found that ICV is within normal limits in most patients with craniosynostosis owing to compensatory growth along unaffected sutures, despite the fused sutures [63–67], whereas the total volume of the ventricles is related to the presence of CM I [11]. Interestingly, in patients with Apert syndrome, the values of ICV tend to be higher than normal despite the involvement of multiple sutures in these cases, possibly because compensatory skull growth allows the brain to grow normally [11, 63, 65–67]. Sgouros et al. suggested that newborns with craniosynostosis are born with a small ICV but achieve normal volume by the age of 6 months [65]. In clinical practice, only patients with pansynostosis developed microcephaly and a small ICV due to advanced restriction of skull growth [65–67].
4. *Posterior cranial fossa volume and cerebellum volume:* Many volumetric studies of craniosynostosis patients are related to the anterior part of the skull [68], but similar studies for the posterior fossa are lacking. As expected, there is an inverse relationship between the degree of tonsillar herniation and the PFV [69]. However, it is not clear whether CM I is related to a restricted PFV in craniosynostosis patients [65–67, 70, 71]. In craniosynostosis patients with CM I, both PFV and cerebellum volume (CV) are similar to those in control subjects, but the ratio of CV/PFV is significantly higher than in controls, suggesting that the posterior fossa is overcrowded [70, 71]. Therefore, the presence of a high CV/PFV ratio should be accepted as a facilitating factor for the development of CM I. However, CV/PFV ratios in children with craniosynostosis associated with CM I fall within the control group range [70, 71]. Therefore, it has been suggested that these volumetric data are of minor significance for the etiology of CM I [70, 71]. It is not possible to predict which patients with craniosynostosis will have a greater tendency to develop CM I on the basis of CV/PFV ratios alone [70, 71]. Hence, the focus of treatment for patients with craniosynostosis should be the vault of the cranium, instead of the posterior fossa, and on other parameters related to the development of IICP [70, 71]. Accordingly, Tubbs et al. suggested that the cranial abnormality with a reduced AFV causes CM I, although it is usually due to a reduction in PFV with disproportionate growth of hind-

brain structures including the cerebellum and brain stem [21].

5. *Diameter of foramen magnum:* Leikola et al. reported that the anteroposterior diameter of the FM is lower in pediatric patients with nonsyndromic monosutural craniosynostosis associated with CM I than in controls [72, 73].
6. *Cerebrospinal fluid circulation:* Apart from a decreased PFV, dynamic factors regarding cerebrospinal fluid (CSF) circulation such as an IICP and venous hypertension are considered responsible for the development of CM I in patients with craniosynostosis [26, 70, 71, 74–78]. de Jong et al. suggested a strong correlation between the presence of CM I and total ventricle volume because reduced outflow of CSF due to CM I and IICP could increase the ventricular volume [11].
7. *Obstruction of upper airway:* Upper airway obstruction in patients with craniosynostosis could contribute to the development of IICP as a result of CO_2 retention and hypoxia during sleep [4]. In cases with craniosynostosis associated with CM I, obstructive sleep apnea can develop due to craniofacial hypoplasia, while central sleep apnea can develop due to compression of the brain stem [4].

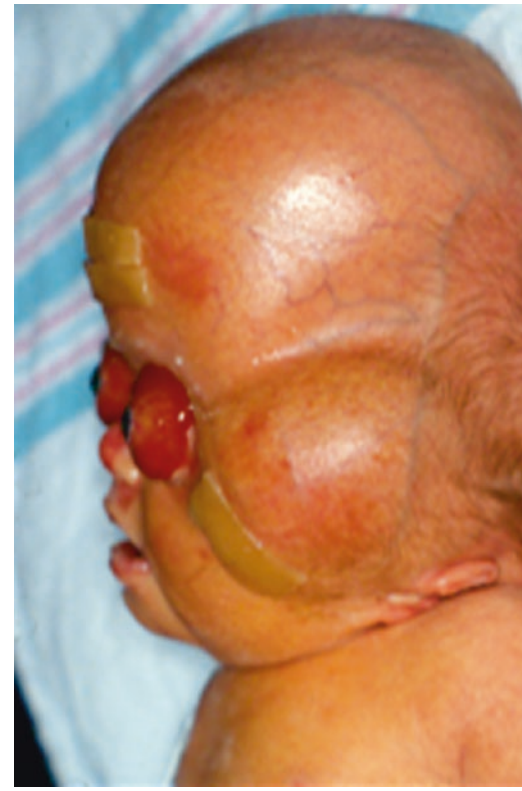

Fig. 20.4 Patient with Kleeblattschädel or cloverleaf deformity of the skull and found to have a CM I on MRI

Syndromic Craniosynostoses

In a review of 95 patients with syndromic craniosynostosis, Cinalli et al. found a high incidence of CM I in both syndromic craniosynostosis: 100% in Kleeblattschädel or cloverleaf deformity (Fig. 20.4), 70% in Crouzon syndrome, and 50% in Pfeiffer syndrome (Fig. 20.5) and multisutural craniosynostosis (75% in oxycephaly or pansynostosis) [22]. Many clinical studies reported high incidence values for CM I as 50% in Pfeiffer syndrome, 70% in Crouzon syndrome [22], 75% in nonsyndromic oxycephaly [79], and 100% in Kleeblattschädel or cloverleaf deformity [80, 81]. Furthermore, CM I was found in Seckel syndrome [82], Antley-Bixler syndrome [83], Shprintzen-Goldberg syndrome [84], and patients with nonsyndromic complex craniosynostosis such as lambdoid synostosis. Many authors have confirmed these findings [5, 28, 34, 56, 57, 79, 80, 85–88]. Therefore, all patients with syndromic multisutural craniosynostosis should be investigated for CM I [11]. On the other hand, CM I has been reported in only 1.9% of children with Apert syndrome (Fig. 20.6), because closure of the lambdoid suture (60 months) is late in Apert syndrome but very early (21 months) in Crouzon syndrome [22]. Importantly, earlier synostosis of the lambdoid suture is accepted as one of the most important indicators of the development of CM I in patients with Crouzon and Pfeiffer syndromes, in contrast to those with Apert syndrome, in which lambdoid suture synostosis occurs later [22].

In the vast majority of these children, the sutures of the facial skeleton and skull base are also involved, but there are anatomical differences between Apert syndrome and Crouzon syndrome in both the cranial base and the posterior cranial fossa [89]: the spheno-occipital, petro-occipital, and occipital synchondroses fuse between 12 and 48 months in Apert syndrome,

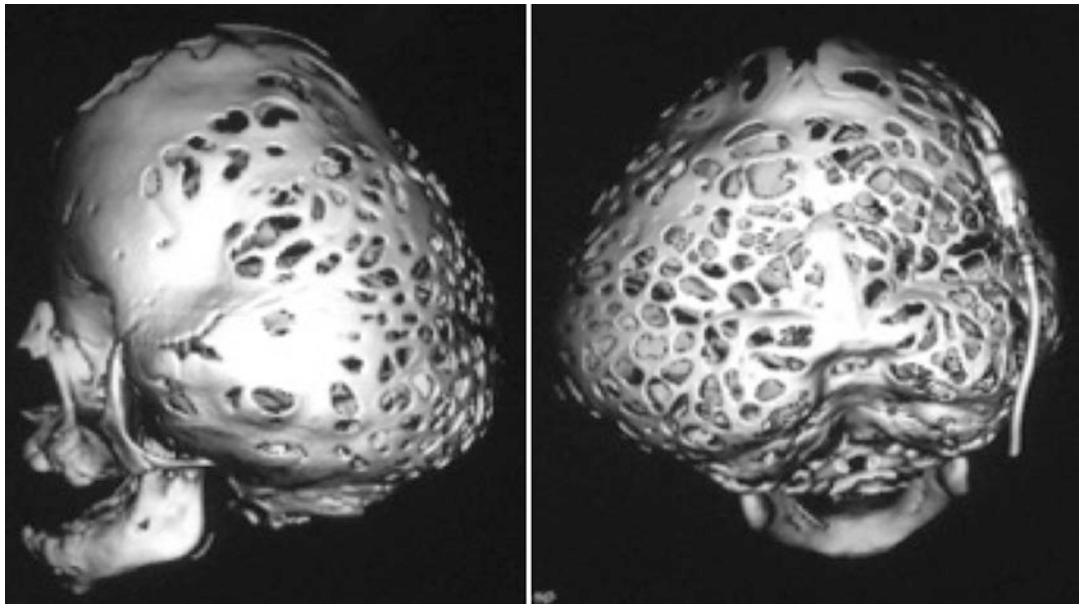

Fig. 20.5 Patient with Pfeiffer syndrome type II who was found to have a CM I on MRI

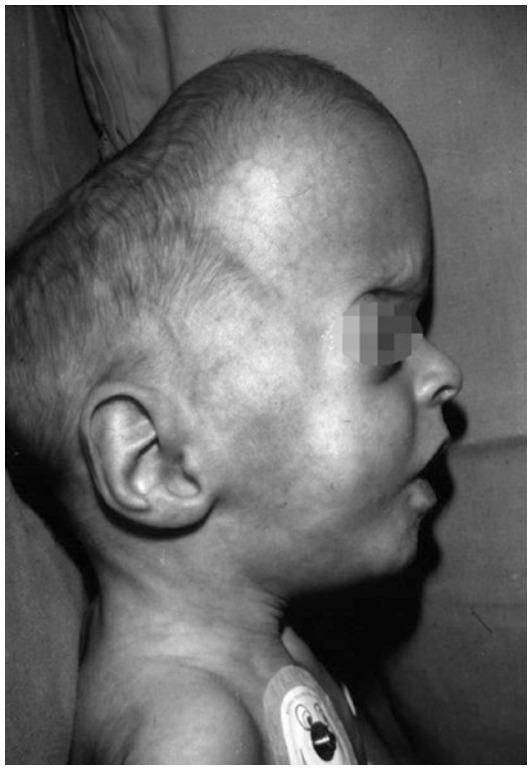

Fig. 20.6 Patient with Apert syndrome found to have a CM I on MRI

while they are fused in Crouzon syndrome patients during the first year of life. As a result, the posterior cranial fossa is larger in Apert syndrome than in Crouzon syndrome [65–67, 90, 91]. Thus, premature closure of the sutures in the cranial base before 6 months of age is critical for the development of CM I, though it is not present at birth. In these patients, stenosis of the jugular foramen develops as a result of the closure of the sutures in the skull base, with consequent venous hypertension, compression of the venous sinuses including the transverse sinus and sigmoid sinus, crowding of the posterior cranial fossa, and the development of hydrocephalus.

In patients with complex or syndromic craniosynostoses, the following synchondroses of the skull base and a small FM are present [50, 92–95]:

1. *Spheno-occipital synchondrosis (SOS)*: The premature fusion of SOS is observed in patients with Apert [96], Crouzon, and Pfeiffer [52] syndromes.
2. *Intra-occipital synchondrosis (IOS)*: The IOS fuses prematurely in Crouzon, Pfeiffer, and Apert syndromes [50, 70, 71, 92].

Crouzon Syndrome

Crouzon syndrome, also called craniofacial dysostosis, named by French neurosurgeon Octave Crouzon (1874–1938) in 1912, is an autosomal dominant disorder with a prevalence of 1/25,000–1/50,000 characterized by early ossification of the coronal sutures, called brachycephaly [97]. It is well known that this is the most common syndromic craniosynostosis, and there is progressive involvement of other cranial sutures in later life [22]. Etiologically, the development of CM I in Crouzon syndrome patients is possibly owing to the premature fusion of bilateral coronal and lambdoid sutures along, very early, with the sagittal suture (6 and 21 months, respectively), in addition to mutation of the FGFR2 gene [22, 44]. The incidence of CM I has been reported as 32%, 50%, and 73% in patients with Crouzon syndrome by de Jong et al. [11], Francis et al. [28], and Cinalli et al. [22], respectively. Because of premature fusion of multiple calvarial and skull base sutures within the first year of life, there are abnormal head shape, proptosis, mandibular prognathism, maxillary hypoplasia, hypertelorism, airway obstruction, mental retardation, epileptic seizure, agenesis of the corpus callosum, and ventriculomegaly in the vast majority of CM I patients associated with craniosynostosis [44], while hydrocephalus is observed in only 50% of all these patients; syndactyly is not encountered in Crouzon syndrome [22, 24]. In Crouzon syndrome patients, hydrocephalus and CM I with/without syringhydromyelic cavitation are related to underdevelopment of the posterior cranial fossa, lambdoid suture synostosis, and jugular foramen stenosis [22, 28].

The surgical management of patients with CM I associated with Crouzon syndrome consists of cranial vault remodeling with or without adequate decompression of the posterior fossa or FM [34, 56]. As a general rule, the conservative approach is reserved for patients with CM I who are not symptomatic or associated with spinal syringomyelia [56, 98, 99]. In addition, Strahle et al. reported that herniation of the tonsilla cerebelli in patients with CM I associated with Crouzon syndrome regressed with cranial vault remodeling alone, without decompression of the posterior cranial fossa or FM [56, 98, 99]. Moreover, they stressed the importance of avoiding dural opening and removal of the posterior arch of C1 in those patients because of the high risk of venous bleeding due to abnormal venous sinuses and increased venous hypertension during the infratentorial cranial expansion procedure [56, 98, 99]. Lastly, it is important that all CM I patients are examined for the syndromic craniosynostosis of Crouzon syndrome before posterior fossa or FM decompression are considered as a treatment option.

Apert Syndrome

Apert syndrome, also called as acrocephalosyndactyly type I, the most commonly observed syndromic craniosynostosis, is generally sporadic with older parental age, although it could be autosomal dominant in some patients [100]. It has been reported that the cranial vault synostosis involving the coronal suture occurs at a median 5 months and then 51 and 60 months for the sagittal and lambdoid sutures, respectively, in Apert syndrome patients [22, 90]. Nevertheless, in Apert syndrome, the sagittal suture is patent, and the value of the posterior cranial fossa volume is higher than that of normal individuals [91]. The incidence of CM I is only 2–8% of all Apert syndrome patients, and the incidence of IICP is low owing to an increased ICV, despite the increased volume of the ventricles [22, 65–67]. In addition to craniosynostosis, there are clinical findings such as hypoplasia of the midface, severe syndactyly of all four extremities, mental deficiency, corpus callosum agenesis, ventriculomegaly, and brain anomalies involving the olfactory bulbs, limbic lobes, gray matter, and white matter, though hydrocephalus is very rare in Apert syndrome [101–104]. Interestingly, lambdoid synostosis and CM I are rarer in patients with Apert syndrome (1.9%) than in Crouzon syndrome despite severe craniosynostosis [22].

Pfeiffer Syndrome

Pfeiffer syndrome, also called acrocephalosyndactyly type V, is classified into three subtypes: (1) type I, the classical autosomal dominant, a mild form of craniosynostosis with bicoronal

synchondrosis, brachycephaly, ventriculomegaly, hypertelorism, mental deficiency, and mild syndactyly; and (2 and 3) types II and III, sporadic and severe forms of craniosynostosis with proptosis, hydrocephalus, central nervous system involvement, congenital heart disease, and bad prognosis [105, 106]. In Pfeiffer syndrome patients, the CM I and hydrocephalus are caused by underdevelopment of the posterior cranial fossa and compression of the hindbrain including the cerebellum and brain stem in the FM [104].

Saethre-Chotzen Syndrome

Saethre-Chotzen syndrome, also called acrocephalosyndactyly type III, is characterized by brachycephaly, hypoplasia of the maxilla, late closing fontanels, shallow orbits with eyelid ptosis, flat forehead, facial asymmetry, and low-set hairline due to craniosynostosis involving the metopic, coronal, or lambdoid sutures [106]. Clinically, there are also prominent ear crus, gyrus abnormalities and cortical atrophy, and mild syndactyly with only cutaneous involvement of the second and third fingers as well as the third and fourth toes; mental deficiency is very rare [24, 106].

Muenke Craniosynostosis

Muenke craniosynostosis, also called FGFR3-associated coronal synostosis, a rare autosomal dominant disease, is characterized by early closure of the coronal suture, hypoplasia of the maxilla, hypertelorism, ptosis, and mild mental retardation; brain malformation and ventriculomegaly are very rare [24, 106].

Carpenter Syndrome

Carpenter syndrome, also called acrocephalopolysyndactyly type II, a rare autosomal recessive disease, is characterized by acrocephaly, syndactyly and polydactyly of the hands and the feet, ventriculomegaly, corpus callosum agenesis, mental retardation, hypogonadism, and obesity [106].

Other Syndromes

CM I has also been found in Seckel syndrome [82], Antley-Bixler syndrome [83], Shprintzen-Goldberg syndrome [84], and nonsyndromic complex craniosynostosis with involvement of the lambdoid suture. Similarly, CM I and hydrocephalus can develop in Kleeblattschädel or cloverleaf deformity after remodeling surgery for craniosynostosis [43]. However, most such cases present with multisutural craniosynostosis, syndromic or nonsyndromic, as a common feature, associated with involvement of the posterior aspect of the skull.

Nonsyndromic Monosutural Craniosynostoses

CM I associated with nonsyndromic monosutural synostosis is rare, with an incidence of 5.6% [5, 21, 54]. Interestingly, a higher incidence of CM I in association with anterior nonsyndromic monosutural craniosynostoses such as oxycephaly has been reported [79]. The incidence of CM I in sagittal synostosis is reportedly higher than that of coronal synostosis, related to its being the most common type of craniosynostosis [54]. The pathogenic mechanisms underpinning the association of CM I with nonsyndromic monosutural sagittal synostosis could be related to the compensatory growth pattern of sagittal synostoses, the increased head circumference resulting in craniocephalic disproportion, or an unrecognized underlying common genetic alteration for both sagittal synostosis and CM I [55]. Leikola et al. found no association between nonsyndromic metopic synostosis and CM I [54], but Tubbs et al. suggested a high (30%) incidence of CM I in these patients [21].

Lambdoid Synostosis

Embryologically, the cranium starts to develop about the fifth month of intrauterine life, while the posterior portion of the skull develops in neonates [32]. Anatomically, each lambdoid suture connects with the posterior part of the sagittal suture and the ipsilateral parietomastoid and occipitomastoid sutures of the cranial base [32]. The posterior fontanel, which is the junction between the lambdoid and sagittal sutures, closes shortly after birth [32]. However, the development of the lambdoid suture is maximal during the first 3 months of age, related to growth of the cerebellum during infancy [22, 32].

Craniosynostosis involving the lambdoid suture, unilateral or bilateral, is uncommon, with an incidence of 1–5% of all patients [14, 32]. A unilateral premature fusion, unilateral lambdoid synostosis, causes posterior plagiocephaly, which is more frequently caused by positional problems called positional plagiocephaly [12]. Ipsilateral occipital flattening, contralateral compensatory bossing of the parietal and frontal bones, a unilateral small posterior cranium, and moving of the ear inferoposteriorly are observed radiologically, resulting in a head wider posteriorly than anteriorly, called "trapezoid configuration" [12, 14, 32, 107]. On the other hand, both lambdoid sutures fuse prematurely in 15% of all cases of lambdoid synostoses. This is observed in patients with turricephaly, also known as oxycephaly, or the syndromic synchondroses including Apert or Pfeiffer syndromes, characterized by widening and flattening of the entire occipital region, a small posterior cranial fossa due to underdevelopment of the occipital bone, and compensatory growth at the bregma with elongation of the vertex and displacement of both ears anteriorly and inferiorly [12, 19, 22, 32, 108–110].

In clinical practice, lambdoid synostosis is diagnosed by physical examination alone, although three-dimensional (3D) computed tomography (CT) scanning could be necessary for definitive diagnosis [32, 60]. The goal of the surgical intervention is to increase the ICV for enough brain growth and to obtain a normal skull shape [32]. Surgical intervention is indicated without delay if there are symptoms related to IICP, CM I, or the calvarial deformity [32]. It is now widely accepted that the optimal age for surgical correction of craniosynostosis is between 10 and 12 months of age to preclude recurrence after surgery [32]. In such patients, therefore, a preoperative MRI is necessary to exclude the associated diagnosis of a CM I [60]. Surgically, many techniques have been defined for correcting lambdoid synostosis, but the occipital advancement technique provides the optimal outcome for these patients [111, 112]. A large bone flap is surgically removed from the superior part of the posterior cranium, another flap is removed from the inferior part of the posterior cranium, and then the hair ties are rotated 180 degrees, and the upper bone flap is inverted for correction of the deformity [32].

Sagittal Synostosis

Synostosis of the sagittal suture is characterized by a deformity with narrow cranium, frontal and occipital bulging, and flat vertex owing to loss of cranial convexity, known as scaphocephaly [12]. This is the most common type of craniosynostosis, 40–60% of all cases; 80% of these are isolated, with a male predominance possibly due to androgens on sutural osteogenesis [14]. In such patients, the skull grows at patent coronal, metopic, and lambdoid sutures, causing frontal bossing with hypotelorism [14].

CM I is usually associated with syndromic sagittal synostosis, though a few reports of nonsyndromic isolated sagittal suture synostosis with CM I have been published [56]. Suggested mechanisms regarding the development of CM I in patients with sagittal synostosis are (1) compensatory growth in patients with sagittal synostosis occurring at the coronal and lambdoid sutures, which are perpendicular to the axis of the fused sagittal suture, resulting in inferior displacement of the tentorium cerebelli and the torcular Herophili, a reduced PFV, and development of CM I; (2) the craniocephalic disproportion in patients with sagittal synostosis, the ICV being insufficient for brain growth; and (3) a genetic etiology underpinning both the sagittal synostosis and CM I, suggesting that patients with sagittal synostosis have a risk of developing CM I later in life [55]. Clinically, these patients present with symptoms and signs of IICP or venous hypertension because of jugular foramen stenosis and/or hydrocephalus. CM I with sagittal synostosis is frequently diagnosed in infant patients and treated by only supratentorial cranial vault expansion with or without decompression of the posterior cranial fossa or FM [56].

Coronal Synostosis

Coronal synostosis is caused by restriction of skull growth in the anterior-posterior direction, which is perpendicular to the coronal suture, associated with compensatory overgrowth in the parietal

direction, which is perpendicular to the open sagittal suture [12]. Unicoronal synostosis, called anterior plagiocephaly, occurs in 20–30% of all patients with synostoses and is characterized by shallowness of the ipsilateral anterior fossa of the cranial cavity, bossing of the contralateral frontal bone, facial asymmetry, and "harlequin appearance" due to elevation of the roof and lateral wall of the ipsilateral orbit and the lesser wing of the sphenoid [12]. On the other hand, bicoronal synostosis, called brachycephaly, observed in syndromic craniosynostoses such as Pfeiffer, Apert, and Crouzon syndromes, is characterized by restriction of skull growth in the anterior-posterior direction with shortening of the anterior cranial fossa, widening of the biparietal dimension of the skull, bilateral "harlequin eye" deformity in both orbits, and hypertelorism [12]. Clinically, coronal synostosis has more involvement of craniofacial appearance than those involving the other sutures owing to skull base involvement, and there are hypertropia, amblyopia, and astigmatism [14].

Metopic Synostosis

Embryologically, the metopic suture, which is visible during the second trimester, differs from the other sutures; its closure begins in the third trimester and is frequently complete by postnatal ninth month of the life [14]. Premature fusion of the metopic suture, called trigonocephaly, is characterized by a prominent ridge, also called as "omega-shaped notch"; a small and narrow anterior cranial fossa; hypotelorism; ethmoidal hypoplasia; parieto-occipital bossing owing to constriction of the frontal bones; and upward-slanting of the orbital roof known as "quizzical eye appearance" [12]. Metopic synostosis accounts for less than 10% of craniosynostoses; the condition is isolated in 2/3 of all patients, while 1/3 are syndromic with associated brain abnormalities. There is a male predominance, possibly attributable to the effect of androgens on sutural osteogenesis [12].

Other Patterns

Prominent features of the craniosynostosis patterns (described below) differ according to the combination of sutures, and they frequently form part of a clinical syndrome [12]. Also, they have other associated structural or functional abnormalities in addition to those of craniosynostosis [12].

Pansynostosis

Pansynostosis, the cloverleaf deformity of the skull, known as turricephaly or oxycephaly or Kleeblattschädel or a tower-like skull, is the most frequent and severe form of craniosynostosis [12]. It is characterized by fusion of all cranial sutures including the sagittal, coronal, and lambdoid sutures; bulging of the temporal regions; proptosis; and involvement of the second and eighth cranial nerves [12].

Z-Shaped Craniosynostosis

Z-shaped craniosynostosis is characterized by fusion of unilateral coronal, contralateral lambdoid, and sagittal suture located between these.

Mercedes Benz Pattern Craniosynostosis

Mercedes Benz synostosis, called anterior turricephaly, is characterized by synostosis of the sagittal and bilateral lambdoid sutures (trisutural fusion), a diminished posterior skull height and width, and occipital flattening [12, 14, 113]. In 2/3 of these patients, there is CM I requiring surgical decompression due to the development of syringomyelia or severe neurological symptoms such as apnea [113]. In such children, a remodeling procedure for posterior part of the cranial vault is performed at 8–10 months of age [32]. Surgically, the primary goal is to provide sagittal lengthening in addition to widening and elevation of the posterior part of the cranium to alleviate the IICP and esthetic problems [32, 112]. The FM is enlarged simultaneously because of the high risk of development of CM I [32]. Therefore, preoperative MRI is useful for patients with Mercedes Benz synostosis, while overnight sleep study and spinal MRI are recommended for diagnosing central sleep apnea and syringomyelia in patients with CM I [32].

Various Conditions Mimicking Craniosynostosis

Metopic Ridge

Metopic ridge, which is generally accepted as a normal variant of the closure of metopic suture, is present in about 5% of normal children before

18 months of age, and it is very important to differentiate this ridge from metopic synostosis [12, 114]. Infants with metopic ridge have none of the characteristic features of metopic synostosis given above [12, 114]. It has been reported that CM I associated with metopic ridges in children is caused by a decrease in the AFV [21].

Positional Plagiocephaly

Positional plagiocephaly, a preferential head positioning on only one side during sleep, leads in asymmetrical and unilateral flattening of the occipital bone [12]. Importantly, the lambdoid suture is open (nonsynostotic). The condition is treated conservatively, in contrast to lambdoid synostosis, which requires surgical correction [12]. Nevertheless, positional plagiocephaly is rarely associated with acquired CM I, possibly due to fetal hydrocephalus, hypoplasia of the occipital bone, and reduced PFV [7, 22]. In such cases, gradual tonsillar ascent and resolution of CM I after surgical reconfiguration of the posterior cranial vault, resulting in an increase in the PFV in comparison with the CV, has been reported in some patients [115, 116].

Osteopetrosis

Osteopetrosis, an inherited autosomal recessive disorder, is characterized by failure of osteoclasts to resorb bone, causing excessive bone deposition and thickening of the calvarium and skull base including the cranial foramina, resulting in various cranial and intracranial manifestations of the disease [117, 118]. It is rarely reported in patients with craniosynostosis associated with CM I [72, 73, 118, 119]. Clinically, patients with osteopetrosis have skeletal fragility, hematopoietic insufficiency, and cranial nerve entrapment syndromes involving the second, fourth, seventh, and eighth cranial nerves [120–123]. In managing osteopetrosis patients with craniosynostosis and CM I, the posterior cranial fossa should be decompressed first [119].

Congenital Anomalies of the Brain Stem and Cerebellum

In craniosynostosis patients with CM I, various abnormalities of the brain have been reported such as agenesis of the septum pellucidum or corpus callosum, ventriculomegaly, agenesis of the temporal lobe, and vascular malformations [5, 11]. Radiologically, an elongated and straightened brain stem, a beaked tectal plate of the midbrain, and a vertically oriented tentorium are noted [27]. The possible effects of congenital anomalies of the brain stem and cerebellum and in the development of CM I in patients with craniosynostosis are controversial [22].

Ventricular Dilatation and Hydrocephalus

Ventricular dilatation and hydrocephalus are extremely rare in patients with nonsyndromic monosutural craniosynostosis (e.g., sagittal craniosynostosis), although it is frequent in syndromic multisutural craniosynostosis [25, 81, 124, 125]. The association between hydrocephalus and craniosynostosis is 0.14–12% (Table 20.1) [6, 28, 81, 124–129]. Cinalli and Sainte-Rose reported only 2 cases with ventricular dilatation in a series of 1387 patients with

Table 20.1 Incidence of ventriculomegaly/hydrocephalus in patients with syndromic craniosynostosis (%). Modified from [4]

Author(s), year [reference number]	Crouzon syndrome	Apert syndrome	Pfeiffer syndrome
Noetzel et al., 1985 [128]	33% (17%)	NS	0% (40%)
Murovic et al., 1993 [127]	NS	48% (12%)	NS
Hanieh & David, 1993 [126]	NS	92% (8%)	NS
Moore & Hanieh, 1994 [6]	NS	NS	27% (64%)
Proudman et al., 1995 [125]	63% (9%)	NS	NS
Renier et al., 1996 [129]	NS	35% (8%)	NS
Cinalli et al., 1998 [81]	16% (26%)	NS	0% (28%)
Collmann et al., 2005 [124]	35% (16%)	67% (4%)	20% (60%)

NS not stated

craniosynostosis [81]. Collmann et al. then reported a total of 30 cases with ventricular dilatation in a series of 300 patients with craniosynostosis; only 1 of those patients presented with CM I [124]. CM I is observed in most children affected by hydrocephalus, and this high incidence suggests a relationship between those two entities in craniosynostosis [4, 5, 22, 81, 124]. It has been suggested that ventricular dilatation and hydrocephalus could be due to the crowding of the posterior fossa, mechanical obstruction of the CSF pathway at the level of the FM, or venous hypertension related with stenosis of the jugular foramen [25, 28, 81, 124].

Clinically, symptoms and signs of CM I in patients with craniosynostosis can differ depending on the severity of herniation of the tonsilla cerebelli and compression of the brain stem [4]. Moreover, 1/3 of all patients with CM I associated with craniosynostosis have a syringomyelia [5]. Therefore, MRI of both brain and spine is necessary to reveal such an abnormality in these patients [98].

Surgically, an endoscopic third ventriculostomy (ETV) can be used for hydrocephalus associated with craniosynostosis; ventriculoperitoneal (VP) shunting is the most common mode of treatment [55, 130]. Unfortunately, it has been reported that decompression of the posterior fossa or FM often fails to provide normal CSF circulation in these cases [124]. It is also important to know that ventriculomegaly and hydrocephalus in Apert syndrome has a nonprogressive feature and a conservative approach is sufficient.

Venous Hypertension

Pathophysiologically, CSF reabsorption as a possible etiological factor in CM I is related to the difference between CSF pressure and venous pressure in the sagittal sinus [5]. A higher CSF pressure develops due to venous hypertension caused by stenosis of the jugular foramen, collateral circulation, and brain compliance, as well as FGFR2 or FGFR3 mutations [131].

Increased Intracranial Pressure

In children with craniosynostosis, an IICP is observed as a result of decreased ICV, depending on the number of cranial sutures involved [132]; 50% of syndromic synostosis patients with multisuture involvement, but only 20% of patients with nonsyndromic monosutural synostosis, show increased ICP (Table 20.2) [30, 132–135]. However, in some craniosynostosis cases, IICP has been observed despite a normal ICV, possibly due to abnormal circulation of the CSF, hydrocephalus, upper airway obstruction, or intracranial venous congestion as a result of an impaired venous drainage [4, 135]. Thompson et al. suggested that IICP is more common in children with craniosynostosis, if a midline suture such as the sagittal or metopic suture is involved, because they can easily impair the CSF absorption via arachnoid granulations owing to compression of the superior sagittal sinus, in contrast to a single coronal suture [135]. Interestingly, there is also dilation of subarachnoid spaces underlying the synostotic cranial sutures, coronal or lambdoid, in infants with craniosynostosis as a result of continuous brain pulsations [135].

Clinically, the most common IICP-related nonspecific symptoms and signs in patients with craniosynostosis are headache, nausea, vomiting,

Table 20.2 Incidence of IICP in patients with syndromic craniosynostosis (%)

Author(s), year [reference number]	Crouzon syndrome	Apert syndrome	Pfeiffer syndrome
Renier et al., 1982 [133]	100%	50%	NS
Thompson et al., 1995 [135]	65%	38%	60%
Taylor et al., 2001 [30]	50%	71%	75%
Tamburrini et al., 2004 [134]	100%	100%	67%

Modified from [4]
NS not stated, *IICP* increased intracranial pressure

irritability, bulging anterior fontanelle, papilledema, optic atrophy and blindness, somnolence, apathy, poor feeding, and impaired intelligence [4, 136]. In such patients, visual evoked potentials can be used to detect IICP in the early period [4].

Natural History

Cinalli et al. suggested that 2/3 of patients with CM I may be asymptomatic throughout life, while 1/3 become symptomatic [22]. In 2008, Novegno et al. reported that 13 of 22 children with CM I were asymptomatic over the follow-up period, and only 4 showed a decrease, 1 with complete spontaneous resolution, and 3 with improvement in their CM Is [8]. Aitken et al. then reported that 19 of 51 children with CM I were asymptomatic on presentation and new neurological deficits developed in only 4 of those cases [31]. Massimi et al. also reported that the majority of 16 asymptomatic children with CM I on presentation were stable; only 3 of them developed new neurological symptoms, and radiological regression of the tonsilla cerebelli was noted in only 1 case during follow-up [36]. Similarly, Saletti et al. reported that 58% of 65 patients were asymptomatic [137].

Imaging Findings

As a general rule, clinical examination is the first step in evaluating patients with CM I and craniosynostosis, and the classic finding in all forms of craniosynostoses is an abnormal skull shape. Imaging studies including ultrasonography (US), X-ray, CT with 3D reformatted images, MRI, CT or MR venography or angiography, and nuclear medicine brain imaging are necessary for the correct diagnosis, surgical intervention, and follow-up of these patients [14, 22].

Ultrasonography

US, a radiation-free technique, is the best choice for diagnosing craniosynostosis in children before 1 year of age [138]. In a US study, the following findings are observed: (1) loss of the hypoechoic gap between hyperechoic bony structures; (2) irregular and thickened margin related with inner suture; (3) loss of a beveled bony edge near the suture; and (4) loss of symmetry of fontanel [138].

X-ray

X-ray of the skull is useful for most patients with a prematurely fused suture [12]. In such an X-ray, the following are observed: perisutural sclerosis, bridging, or loss of the suture and secondary signs of IICP including a "beaten-copper appearance" in severe cases [12].

Computed Tomography

Today, 3D CT is the primary radiological technique for correct diagnosis and treatment of patients with craniosynostosis, in particular the syndromic and multisutural types [12].

Magnetic Resonance Imaging

In infants with craniosynostosis, an MRI study in combination with US is the best choice for diagnosing associated congenital cerebral anomalies such as CM I and hydrocephalus, as noted previously, and to identify the cranial sutures [12, 139]. In clinical practice, therefore, MRI is recommended only for patients with syndromic craniosynostosis or with lambdoid synostosis or bilateral coronal synostosis before surgical intervention for craniosynostosis [57, 61]. Furthermore, it is the gold standard for evaluating patients with craniosynostosis associated with CM I [22]. Most recently, Eley et al. suggested a novel 3D MRI technique (black bone MRI) for identifying the affected fused sutures [140]. Therefore, 3D MRI is expected to become an alternative to X-ray of the skull and 3D CT in the future [12].

Computed Tomography or Magnetic Resonance Angiography/Venography

In patients with syndromic craniosynostosis and/or hydrocephalus, a preoperative angio-MRI to demonstrate the venous circulation of the posterior cranial fossa is suggested because of the high potential for a venous abnormality [22].

Surgical Treatment of CM I Associated with Craniosynostosis

It is now widely accepted that decompression of the posterior fossa or FM for CM I is indicated if the condition is symptomatic or associated with a syringomyelia due to mechanical blockage of free CSF flow at the cranio-spinal FM level [141, 142]. However, the treatment of choice for CM I in patients with craniosynostosis remains controversial [4]. In CM I cases associated with craniosynostosis, the clinical and radiological findings and the age of the patient at the time of initial diagnosis are important for deciding the appropriate treatment. Many authors have recommended decompressive surgery of the posterior fossa or FM prior to craniosynostosis correction as the treatment of choice for all patients of CM I with craniosynostosis [5, 143, 144]. There is still no consensus about the management of CM I associated with craniosynostosis. Some authors have suggested that prophylactic decompression of CM I can be accomplished "simultaneously" at the time of surgery for craniosynostosis in patients less than 1 year old [22, 56, 81, 98, 99], while others suggest that a supratentorial cranial expansion results in resolution of an acquired CM I [145]. Thus, simultaneous decompression is not indicated for all patients with craniosynostosis. However, some authors have suggested that cranial vault remodeling procedure should be the first surgical stage to stop the progression of CM I in patients with craniosynostosis [5, 25].

A surgical technique composed of remodeling of the posterior cranium and suboccipital decompression has been suggested for newborns with CM I associated with severe overcrowding of the FM [80]. Technically, the patient is in prone position with the neck in flexion, and the scalp flap is reflected to expose the FM. The posterior fossa is then dissected extradurally following the removal of both parietal bones and the occipital bone; lastly, occipital bone fragments are repositioned [80]. It is very important to remember that the risk of severe bleeding is high during dissection at the level of the FM owing to the collateral circulation.

Importantly, if CM I in a patient with craniosynostosis is associated with hydrocephalus, IICP caused by the hydrocephalus should be resolved before decompression of CM I or correction of the craniosynostosis [4]. In such patients, hydrocephalus should be managed as a first step, and ETV can be considered as a valid alternative to VP shunt [146]. On the other hand, in children without ventricular dilatation or hydrocephalus, a cranial vault expansion should be considered in the first years of life [147]. Treatment of hydrocephalus with shunts or ETV should be discussed in detail before cranial vault remodeling to preclude a subsequent worsening of the hydrocephalus and IICP [25]. In some cases with craniosynostosis, ventricular dilatation can develop after cranial vault remodeling [81]. As a rule, hydrocephalus treatment should be considered a priority if the condition coexists with CM I and craniosynostosis [148]. ETV, which offers a lower risk of skull growth impairment and infection than the shunt, can be used to treat hydrocephalus before cranial vault remodeling and suboccipital decompression [25]. However, Di Rocco et al. suggested that "early" management of hydrocephalus is not recommended in craniosynostosis patients with cephalocranial disproportion because of the potential for further aggravation of the impaired growth of the skull as a result of inserting a CSF shunt device. A posterior cranial vault expansion with/without simultaneous decompression of the posterior cranial fossa instead of VP shunting is advised in such patients [77]. There is no doubt that craniostenosis associated with CM I and hydrocephalus has a poor prognosis owing to IICP [149].

In particular, when the lambdoid sutures are involved, occipital cranial vault expansion and

remodeling providing enlargement of the posterior cranial fossa should be considered to decompress the dural sinuses, and a midline suboccipital craniectomy without duraplasty should be added if there is a CM I [65–67]. Among the different techniques for expansion of the posterior cranial vault, free bone flaps are preferred in the newborn period of life because they make it possible, with no technical difficulty, to avoid dissection of the bone from the dural sinuses [65–67].

As a general rule, surgical correction of the cranial deformity in the prone position that necessitates a prolonged neck hyperextension during surgery is contraindicated in patients with craniosynostosis, in particular in the presence of CM I [22]. Technically, a "staged" repair of the malformation is suggested in such patients because a one-step procedure is performed in the "modified prone position" with hyperextension of the neck, which can lead to compression of the spinal cord and brain stem [143, 150]. Moreover, it has been suggested that early remodeling of the posterior cranium before that of the anterior can be useful for preventing IICP [22].

In asymptomatic patients with craniosynostosis, "observation" alone is sufficient if CM I is diagnosed in children after the first years of life, although decompressive craniectomy of the FM with/without duroplasty should be considered if there are clinical symptoms during the first year [22]. Recently, it has been suggested that decompression of the posterior fossa or FM should be reserved for symptomatic patients or those associated with syringomyelia because of the possibility of spontaneous CM I improvement following cranial vault remodeling [25]. Thus, the only treatment of asymptomatic cases of CM I associated with nonsyndromic monosutural craniosynostosis should be cranial vault remodeling without suboccipital decompression [25, 72, 73]. Interestingly, Levitt et al. reported a CM I patient with cervical syringomyelia in a patient with syndromic multisutural craniosynostosis, which was managed solely with posterior cranial vault correction surgery [34]. As expected, it has been suggested that posterior occipital cranial vault expansion to relieve IICP is more effective for craniosynostosis patients with CM I than anterior fronto-orbital advancement [22, 72, 73]. Unfortunately, the management of craniosynostosis patients with CM I is complicated because of the potential for failure of the treatment and even a worsening of clinical findings if an appropriate treatment is not used [77].

Outcome

Early treatment of syndromic multisutural craniosynostosis is very important to avoid both the development of associated CM I and the risk of IICP. Da Costa et al. reported that patients with craniosynostosis have a risk of central nervous system injury associated with impairment of cognitive functions caused by IICP, hydrocephalus, and developmental cerebral malformations [151]. Even nonsyndromic monosutural synostosis is associated with mild neuropsychological deficits [152, 153]. However, patients with syndromic multisutural synostosis have a significantly higher frequency of neurocognitive and developmental disabilities than those with nonsyndromic monosutural craniosynostosis or the normal population [7, 151]. It is expected that surgical cranial expansion can rapidly improve the intellectual and behavioral dysfunctions in children with CM I associated with craniosynostosis [154–156]. In a recent study, it has been demonstrated that cranial reconstruction also has a useful effect on neuropsychological development in children with CM I associated with craniosynostosis [4]. Undoubtedly, no surgical intervention can cure this disorder, but appropriate treatment of patients with craniosynostosis associated with CM I will relieve most of the neurocognitive symptoms [4].

Conclusion

CM I is a common associated entity in patients with syndromic multisuture craniosynostoses, characterized by early fusion of lambdoid sutures and cranial base synchondroses including Crouzon syndrome during the first 2 years [22]. Today, simultaneous or consecutive cranial vault remodeling and suboccipital decompression are

standard treatments for craniosynostosis associated with CM I [80]. However, it is widely accepted that a cranial vault expansion or remodeling procedure should be done before suboccipital decompression in patients with combined craniosynostosis and CM I [5]. Further study is clearly needed.

References

1. Aboulezz AO, Sartor K, Geyer CA, Gado MH. Position of cerebellar tonsils in the normal population and in patients with Chiari malformation: a quantitative approach with MR imaging. J Comput Assist Tomogr. 1985;9:1033–6.
2. Barkovich AJ, Wippold FJ, Sherman JL, Citrin CM. Significance of cerebellar tonsillar position on MR. AJNR Am J Neuroradiol. 1986;7:795–9.
3. Chern JJ, Gordon AJ, Mortazavi MM, Tubbs RS, Oakes WJ. Pediatric Chiari malformation type 0: a 12-year institutional experience. J Neurosurg Pediatr. 2011;8:1–5.
4. Choi JW, Lim SY, Shin HJ. Craniosynostosis in growing children: pathophysiological changes and neurosurgical problems. J Korean Neurosurg Soc. 2016;59:197–203.
5. Cinalli G, Spennato P, Sainte-Rose C, Arnaud E, Aliberti F, Brunelle F, Cianciulli E, Renier D. Chiari malformation in craniosynostosis. Childs Nerv Syst. 2005;21:889–901.
6. Moore MH, Hanieh A. Hydrocephalus in Pfeiffer syndrome. J Clin Neurosci. 1994;1:202–4.
7. Nishikawa M, Sakamoto H, Hakuba A, Nakanishi N, Inoue Y. Pathogenesis of Chiari malformation: a morphometric study of the posterior cranial fossa. J Neurosurg. 1997;86:40–7.
8. Novegno F, Caldarelli M, Massa A, Chieffo D, Massimi L, Pettorini B, Tamburrini G, Di Rocco C. The natural history of the Chiari type I anomaly. J Neurosurg Pediatr. 2008;2:179–87.
9. Oakes W, Tubbs R. Chiari malformations. In: Winn HR, editor. Youman's neurological surgery. Philadelphia: Saunders; 2004. p. 3347–61.
10. Van den Broek MJ, Arbues AS, Chalard F, Pinto Da Costa NM, Trang H, Dorfmuller G, Evrard PP, Husson I, Servais LJ. Chiari type I malformation causing central apnoeas in a 4-month-old boy. Eur J Paediatr Neurol. 2009;13:463–5.
11. de Jong T, Rijken BF, Lequin MH, van Veelen ML, Mathijssen IM. Brain and ventricular volume in patients with syndromic and complex craniosynostosis. Childs Nerv Syst. 2012;28:137–40.
12. Kim HJ, Roh HG, Lee IW. Craniosynostosis: updates in radiologic diagnosis. J Korean Neurosurg Soc. 2016;59:219–26.
13. Slater BJ, Lenton KA, Kwan MD, Gupta DM, Wan DC, Longaker MT. Cranial sutures: a brief review. Plast Reconstr Surg. 2008;121:170e–8e.
14. Blaser SI, Padfield N, Chitayat D, Forrest CR. Skull base development and craniosynostosis. Pediatr Radiol. 2015;45(Suppl 3):S485–96.
15. Boulet SL, Rasmussen SA, Honein MA. A population-based study of craniosynostosis in metropolitan Atlanta, 1989-2003. Am J Med Genet A. 2008;146A:984–91.
16. Sharma VP, Fenwick AL, Brockop MS, McGowan SJ, Goos JA, Hoogeboom AJ, Brady AF, Jeelani NO, Lynch SA, Mulliken JB, Murray DJ, Phipps JM, Sweeney E, Tomkins SE, Wilson LC, Bennett S, Cornall RJ, Broxholme J, Kanapin A, 500 Whole-Genome Sequences (WGS500) Consortium, Johnson D, Wall SA, van der Spek PJ, Mathijssen IM, Maxson RE, Twigg SR, Wilkie AO. Mutations in TCF12, encoding a basic helix-loop-helix partner of TWIST1, are a frequent cause of coronal craniosynostosis. Nat Genet. 2013;45:304–7.
17. Wilkie AO, Byren JC, Hurst JA, Jayamohan J, Johnson D, Knight SJ, Lester T, Richards PG, Twigg SR, Wall SA. Prevalence and complications of single-gene and chromosomal disorders in craniosynostosis. Pediatrics. 2010;126:e391–400.
18. Kirmi O, Lo SJ, Johnson D, Anslow P. Craniosynostosis: a radiological and surgical perspective. Semin Ultrasound CT MR. 2009;30:492–512.
19. Nagaraja S, Anslow P, Winter B. Craniosynostosis. Clin Radiol. 2013;68:284–92.
20. Gault DT, Renier D, Marchac D, Jones BM. Intracranial pressure and intracranial volume in children with craniosynostosis. Plast Reconstr Surg. 1992;90:377–81.
21. Tubbs RS, Elton S, Blount JP, Oakes WJ. Preliminary observations on the association between simple metopic ridging in children without trigonocephaly and the Chiari I malformation. Pediatr Neurosurg. 2001;35:136–9.
22. Cinalli G, Renier D, Sebag G, Sainte-Rose C, Arnaud E, Pierre-Kahn A. Chronic tonsillar herniation in Crouzon's and Apert's syndromes: the role of premature synostosis of the lambdoid suture. J Neurosurg. 1995;83:575–82.
23. Jane JA, Persing JA. Neurosurgical treatment of craniosynostosis. In: Cohen Jr MM, editor. Craniosynostosis: diagnosis, evaluation, and management. New York: Raven Press; 1986. p. 249–320.
24. Raybaud C, Di Rocco C. Brain malformation in syndromic craniosynostoses, a primary disorder of white matter: a review. Childs Nerv Syst. 2007;23:1379–88.
25. Sgulò FG, Spennato P, Aliberti F, Di Martino G, Cascone D, Cinalli G. Contemporary occurrence of hydrocephalus and Chiari I malformation in sagittal craniosynostosis. Case report and review of the literature. Childs Nerv Syst. 2017;33:187–92.

26. Stovner LJ, Bergan U, Nilsen G, Sjaastad O. Posterior cranial fossa dimensions in the Chiari I malformation: relation to the pathogenesis and clinical presentation. Neuroradiology. 1993;35:113–8.
27. Carmel PW. Comment on Venes JL: Arnold–Chiari malformation in an infant with Kleeblattschädel: an acquired deformity? Neurosurgery. 1988;23:362.
28. Francis PM, Beals S, Rekate HL, Pittman HW, Manwaring K, Reiff J. Chronic tonsillar herniation and Crouzon's syndrome. Pediatr Neurosurg. 1992;18:202–6.
29. Rengachary SS, Blount J, Heros D, Bowers S, Truwit C. Craniocephalic disproportion with increased intracranial pressure and brain herniation: a new clinical syndrome in anemic patients: report of two cases. Neurosurgery. 1997;41:297–304.
30. Taylor WJ, Hayward RD, Lasjaunias P, Britto JA, Thompson DN, Jones BM, Evans RD. Enigma of raised intracranial pressure in patients with complex craniosynostosis: the role of abnormal intracranial venous drainage. J Neurosurg. 2001;94:377–85.
31. Aitken LA, Lindan CE, Sidney S, Gupta N, Barkovich AJ, Sorel M, Wu YW. Chiari type 1 malformation in a pediatric population. Pediatr Neurol. 2009;40:499–54.
32. Rhodes JL, Tye GW, Fearon JA. Craniosynostosis of the lambdoid suture. Semin Plast Surg. 2014;28:138–43.
33. Hayhurst C, Osman-Farah J, Das K, Mallucci C. Initial management of hydrocephalus associated with Chiari malformation type I-syringomyelia complex via endoscopic third ventriculostomy: an outcome analysis. J Neurosurg. 2008;108:1211–12114.
34. Levitt MR, Niazi TN, Hopper RA, Ellenbogen RG, Ojemann JG. Resolution of syndromic craniosynostosis-associated Chiari malformation type I without suboccipital decompression after posterior cranial vault release. J Neurosurg Pediatr. 2012;9:111–5.
35. Massimi L, Novegno F, di Rocco C. Chiari type I malformation in children. Adv Tech Stand Neurosurg. 2011;37:143–211.
36. Massimi L, Pravatà E, Tamburrini G, Gaudino S, Pettorini B, Novegno F, Colosimo C Jr, Di Rocco C. Endoscopic third ventriculostomy for the management of Chiari and related hydrocephalus: outcome and pathogenetic implications. Neurosurgery. 2011;68:950–6.
37. Tubbs RS, Oakes WJ. The Chiari malformations. New York: Springer; 2013.
38. Cleland J. Contribution to the study of spina bifida, encephalocele, and anencephalus. J Anat Physiol. 1883;17:257–92.
39. Schijman E. History, anatomic forms, and pathogenesis of Chiari I malformations. Child Nerv Syst. 2004;20:323–8.
40. Chiari H. Über Veränderungen des Kleinhirns in folge von Hydrocephalie des Grosshirns. Dtsch Med Wochenschr. 1891;17:1172–11725.
41. Frim DM, Jones D, Goumnerova L. Development of symptomatic Chiari malformation in a child with craniofacial dysmorphism. Pediatr Neurosurg. 1990;16:228–31.
42. Saldino RM, Steinbach HL, Epstein CJ. Familial acrocephalosyndactyly (Pfeiffer syndrome). Am J Roentgenol Radium Therapy, Nucl Med. 1972;116:609–22.
43. Venes JL. Arnold-Chiari malformation in an infant with Kleeblattschädel: an acquired deformity? Neurosurgery. 1988;23:360–2.
44. Fujisawa H, Hasegawa M, Kida S, Yamashita J. A novel fibroblast growth factor receptor 2 mutation in Crouzon syndrome associated with Chiari Type I malformation and syringomyelia. J Neurosurg. 2002;97:396–400.
45. Johnson D, Wilkie AO. Craniosynostosis. Eur J Hum Genet. 2011;19:369–76.
46. Park WJ, Meyers GA, Li X. Novel FGFR2 mutations in Crouzon and Jackson–Weiss syndromes show allelic heterogeneity and phenotypic variability. Hum Mol Genet. 1995;4:1229–33.
47. Reardon W, Winter RM, Rutland P. Mutations in the fibroblast growth factor receptor 2 gene cause Crouzon syndrome. Nat Genet. 1994;8:98–103.
48. Hermann CD, Lee CS, Gadepalli S, Lawrence KA, Richards MA, Olivares-Navarrete R, Williams JK, Schwartz Z, Boyan BD. Interrelationship of cranial suture fusion, basicranial development, and resynostosis following suturectomy in twist1(+/−) mice, a murine model of Saethre-Chotzen syndrome. Calcif Tissue Int. 2012;91:255–66.
49. McGrath J, Gerety PA, Derderian CA, Steinbacher DM, Vossough A, Bartlett SP, Nah HD, Taylor JA. Differential closure of the spheno-occipital synchondrosis in syndromic craniosynostosis. Plast Reconstr Surg. 2012;130:681e–9e.
50. Rijken BF, Lequin MH, de Rooi JJ, van Veelen ML, Mathijssen IM. Foramen magnum size and involvement of its intraoccipital synchondroses in Crouzon syndrome. Plast Reconstr Surg. 2013;132:993e–1000e.
51. Saarimaki-Vire J, Peltopuro P, Lahti L, Naserke T, Blak AA, Weisenhorn DMV, Yu K, Ornitz DM, Wurst W, Partanen J. Fibroblast growth factor receptors cooperate to regulate neural progenitor properties in the developing midbrain and hindbrain. J Neurosci. 2007;27:8581–92.
52. Tahiri Y, Paliga JT, Vossough A, Bartlett SP, Taylor JA. The spheno-occipital synchondrosis fuses prematurely in patients with Crouzon syndrome and Midface hypoplasia compared with age- and gender-matched controls. J Oral Maxillofac Surg. 2013;72:1173–9.
53. Coussens AK, Hughes IP, Wilkinson CR, Morris CP, Anderson PJ, Powell BC, van Daal A. Identification of genes differentially expressed by prematurely fused human sutures using a novel in vivo–in vitro approach. Differentiation. 2008;76:531–45.
54. Leikola J, Koljonen V, Valanne L, Hukki J. The incidence of Chiari malformation in nonsyndromic, single suture craniosynostosis. Childs Nerv Syst. 2010;26:771–4.

55. Pouratian N, Sansur CA, Newman SA, Jane JA Jr, Jane JA Sr. Chiari malformations in patients with uncorrected sagittal synostosis. Surg Neurol. 2007;67:422–7.
56. Strahle J, Muraszko KM, Buchman SR, Kapurch J, Garton HJ, Maher CO. Chiari malformation associated with craniosynostosis. Neurosurg Focus. 2011;31:E2.
57. Engel M, Castrillón-Oberndorfer G, Hoffmann J, Orakcioglu B, Rohde S, Seeberger R, Freudlsperger C. Chiari malformation in nonsyndromal single craniosynostosis-much ado about nothing? Acta Neurochir. 2012;154:1803–7.
58. Karppinen A, Koljonen V, Valanne L, Leikola J. Asymmetric laterality of Chiari type I malformation in patients with non-syndromic single-suture craniosynostosis. Acta Neurochir. 2012;154:2103–7.
59. Tubbs RS, Wellons JC 3rd, Oakes WJ. Asymmetry of tonsillar ectopia in Chiari I malformation. Pediatr Neurosurg. 2002;37:199–202.
60. Fearon JA, Singh DJ, Beals SP, Yu JC. The diagnosis and treatment of single-sutural synostoses: are computed tomographic scans necessary? Plast Reconstr Surg. 2007;120:1327–31.
61. Hukki A, Koljonen V, Karppinen A, Valanne L, Leikola J. Brain anomalies in 121 children with nonsyndromic single suture craniosynostosis by MR imaging. Eur J Paediatr Neurol. 2012;16:671–5.
62. Dufresne CR, McCarthy JG, Cutting CB, Epstein FJ, Hoffman WY. Volumetric quantification of intracranial and ventricular volume following cranial vault remodeling: a preliminary report. Plast Reconstr Surg. 1987;79:24–32.
63. Gosain AK, McCarthy JG, Glatt P, Staffenberg D, Hoffmann RG. A study of intracranial volume in Apert syndrome. Plast Reconstr Surg. 1995;95:284–95.
64. Mardini S, See LC, Lo LJ, Salgado CJ, Chen YR. Intracranial space, brain, and cerebrospinal fluid volume measurements obtained with the aid of three-dimensional computerized tomography in patients with and without Crouzon syndrome. J Neurosurg. 2005;103(3 Suppl):238–46.
65. Sgouros S, Hockley AD, Goldin JH, Wake MJ, Natarajan K. Intracranial volume change in craniosynostosis. J Neurosurg. 1999;91:617–25.
66. Sgouros S, Natarajan K, Hockley AD, Goldin JH, Wake M. Skull base growth in childhood. Pediatr Neurosurg. 1999;31:259–68.
67. Sgouros S, Natarajan K, Hockley AD, Goldin JH, Wake M. Skull base growth in craniosynostosis. Pediatr Neurosurg. 1999;31:281–93.
68. Posnick JC, Lin KY, Jhawar BJ, Armstrong D. Apert syndrome: quantitative assessment by CT scan of presenting deformity and surgical results after first-stage reconstruction. Plast Reconstr Surg. 1994;93:489–97.
69. Thompson DN, Harkness W, Jones BM, Hayward RD. Aetiology of herniation of the hindbrain in craniosynostosis. An investigation incorporating intracranial pressure monitoring and magnetic resonance imaging. Pediatr Neurosurg. 1997;26:288–95.
70. Rijken BF, Lequin MH, van der Lijn F, van Veelen-Vincent ML, de Rooi J, Hoogendam YY, Niessen WJ, Mathijssen IM. The role of the posterior fossa in developing Chiari I malformation in children with craniosynostosis syndromes. J Craniomaxillofac Surg. 2015;43:813–9.
71. Rijken BF, Lequin MH, van Veelen ML, de Rooi J, Mathijssen IM. The formation of the foramen magnum and its role in developing ventriculomegaly and Chiari I malformation in children with craniosynostosis syndromes. J Craniomaxillofac Surg. 2015;43:1042–8.
72. Leikola J, Haapamäki V, Karppinen A, Koljonen V, Hukki J, Valanne L, Koivikko M. Morphometric comparison of foramen magnum in non-syndromic craniosynostosis patients with or without Chiari I malformation. Acta Neurochir. 2012;154:1809–13.
73. Leikola J, Hukki A, Karppinen A, Valanne L, Koljonen V. The evolution of cerebellar tonsillar herniation after cranial vault remodeling surgery. Childs Nerv Syst. 2012;28:1767–71.
74. Aydin S, Hanimoglu H, Tanriverdi T, Yentur E, Kaynar MY. Chiari type I malformations in adults: a morphometric analysis of the posterior cranial fossa. Surg Neurol. 2005;64:237–41.
75. Barkovich AJ, Raybaud C. Pediatric neuroimaging. 5th ed: Lippincott Williams and Wilkins. ISBN/ISSN: 9781605477145; 2011.
76. Dagtekin A, Avci E, Kara E, Uzmansel D, Dagtekin O, Koseoglu A, Talas D, Bagdatoglu C. Posterior cranial fossa morphometry in symptomatic adult Chiari I malformation patients: comparative clinical and anatomical study. Clin Neurol Neurosurg. 2011;113:399–403.
77. Di Rocco C, Frassanito P, Massimi L, Peraio S. Hydrocephalus and Chiari type I malformation. Childs Nerv Syst. 2011;27:1653–64.
78. Furtado SV, Reddy K, Hegde AS. Posterior fossa morphometry in symptomatic pediatric and adult Chiari I malformation. J Clin Neurosci. 2009;16:1449–54.
79. Renier D, Cinalli G, Lajeunie E, Arnaud E, Marchac D. Oxycephaly, a severe craniosynostosis. Apropos of a series of 129 cases (in French). Arch Pediatr. 1997;4:722–9.
80. Cinalli G, Chumas P, Arnaud E, Sainte-Rose C, Renier D. Occipital remodeling and suboccipital decompression in severe craniosynostosis associated with tonsillar herniation. Neurosurgery. 1998;42:66–73.
81. Cinalli G, Sainte-Rose C, Kollar EM, Zerah M, Brunelle F, Chumas P, Arnaud E, Marchac D, Pierre-Kahn A, Renier D. Hydrocephalus and craniosynostosis. J Neurosurg. 1998;88:209–14.
82. Hopkins TE, Haines SJ. Rapid development of Chiari I malformation in an infant with Seckel syndrome and craniosynostosis. Case report and review of the literature. J Neurosurg. 2003;98:1113–5.
83. Chang YT, Tsai FJ, Shen WC, Lin HC, Peng CT, Tsai CH. Antley–Bixler syndrome associated with Arnold–Chiari malformation. Acta Paediatr. 2000;89:737–9.

84. Greally MT, Carey JC, Milewicz DM, Hudgins L, Goldberg RB, Shprintzen RJ, Cousineau AJ, Smith WL Jr, Judisch GF, Hanson JW. Shprintzen-Goldberg syndrome: a clinical analysis. Am J Med Genet. 1998;19:202–12.
85. Fearon JA, Rhodes J. Pfeiffer syndrome: a treatment evaluation. Plast Reconstr Surg. 2009;123:1560–9.
86. Hayward R, Gonsalez S. How low can you go? Intracranial pressure, cerebral perfusion pressure, and respiratory obstruction in children with complex craniosynostosis. J Neurosurg. 2005;102(1 Suppl):16–22.
87. Mulliken JB, Steinberger D, Kunze S, Müller U. Molecular diagnosis of bilateral coronal synostosis. Plast Reconstr Surg. 1999;104:1603–15.
88. Shigeta H, Sakai K. Chiari malformation (chronic tonsillar herniation) and syringomyelia in Crouzon's syndrome. Childs Nerv Syst. 1996;21:395–401.
89. Kreiborg S. Postnatal growth and development of the craniofacial complex in premature craniosynostosis. In: Cohen Jr MM, editor. Craniosynostosis: diagnosis, evaluation, and management. New York: Raven; 1986. p. 157–89.
90. Kreiborg S, Marsh JL, Cohen MM Jr, Liversage M, Pedersen H, Skovby F, Børgesen SE, Vannier MW. Comparative three-dimensional analysis of CT-scans of the calvaria and cranial base in Apert and Crouzon syndromes. J Craniomaxillofac Surg. 1993;21:181–8.
91. Richtsmeier JT. Comparative study of normal, Crouzon and Apert craniofacial morphology using finite element scaling analysis. Am J Phys Anthropol. 1987;74:473–93.
92. Coll G, Arnaud E, Selek L, Brunelle F, Sainte-Rose C, Collet C, Di Rocco F. The growth of the foramen magnum in Crouzon syndrome. Childs Nerv Syst. 2012;28:1525–35.
93. Di Rocco F, Dubravova D, Ziyadeh J, Sainte-Rose C, Collet C, Arnaud E. The foramen magnum in isolated and syndromic brachycephaly. Childs Nerv Syst. 2014;30:165–72.
94. Madeline LA, Elster AD. Postnatal development of the central skull base: normal variants. Radiology. 1995;196:757–63.
95. Madeline LA, Elster AD. Suture closure in the human chondrocranium: CT assessment. Radiology. 1995;196:747–56.
96. Mikulis DJ, Diaz O, Egglin TK, Sanchez R. Variance of the position of the cerebellar tonsils with age: preliminary report. Radiology. 1992;183:725–8.
97. Crouzon LE. Dysostose cranio-faciale hereditaire (Hereditary cranio-facial dysostose) Bulletin de la Societe des Medecins des Hopitaux Paris. 1912;33:545–55.
98. Strahle J, Muraszko KM, Kapurch J, Bapuraj JR, Garton HJ, Maher CO. Chiari malformation type I and syrinx in children undergoing magnetic resonance imaging. J Neurosurg Pediatr. 2011;8:205–13.
99. Strahle J, Muraszko KM, Kapurch J, Bapuraj JR, Garton HJ, Maher CO. Natural history of Chiari malformation type I following decision for conservative treatment. J Neurosurg Pediatr. 2011;8:214–21.
100. Cohen MM Jr, Kreiborg S, Lammer EJ, Cordero JF, Mastroiacovo P, Erickson JD, Roeper P, Martinez-Frias ML. Birth prevalence study of the Apert syndrome. Am J Med Genet. 1992;42:655–9.
101. Cohen MM Jr, Kreiborg S. The central nervous system in the Apert syndrome. Am J Med Genet. 1990;35:36–45.
102. Lajeunie E, Cameron R, El Ghouzi V, de Parseval N, Journeau P, Gonzales M, Delezoide AL, Bonaventure J, Le Merrer M, Renier D. Clinical variability in patients with Apert's syndrome. J Neurosurg. 1999;90:443–7.
103. Patton MA, Goodship J, Hayward R, Lansdown R. Intellectual development in Apert's syndrome: a long term follow-up of 29 patients. J Med Genet. 1988;25:164–7.
104. Tokumaru AM, Barkovich AJ, Ciricillo SF, Edwards MSB. Skull base and calvarial deformities: association with intracranial changes in craniofacial syndromes. Am J Neuroradiol. 1996;17:619–30.
105. Cohen MM Jr. Pfeiffer syndrome update, clinical subtypes, and guidelines for differential diagnosis. Am J Med Genet. 1993;45:300–7.
106. Jones KL. Smith's recognizable pattern of human malformation. 6th ed. Philadelphia: Elsevier Saunders; 2006.
107. Huang MH, Gruss JS, Clarren SK, Mouradian WE, Cunningham ML, Roberts TS, Loeser JD, Cornell CJ. The differential diagnosis of posterior plagiocephaly: true lambdoid synostosis versus positional molding. Plast Reconstr Surg. 1996;985:765–74.
108. Delashaw JB, Persing JA, Jane JA. Cranial deformation in craniosynostosis. A new explanation. Neurosurg Clin N Am. 1991;2:611–20.
109. Leboucq N, Montoya P, Martinez Y, Castan P, Bourbotte G. Lambdoid craniosynostosis. A 3D-computerized tomographic approach. J Neuroradiol. 1993;20:24–33.
110. Vander Kolk CA, Carson BS. Lambdoid synostosis. Clin Plast Surg. 1994;21:575–84.
111. Goodrich JT, Argamaso R. Lambdoid stenosis (posterior plagiocephaly) and craniofacial asymmetry: long-term outcomes. Childs Nerv Syst. 1996;12:720–6.
112. Zöller JE, Mischkowski RA, Speder B. Preliminary results of standardized occipital advancement in the treatment of lambdoid synostosis. J Craniomaxillofac Surg. 2002;30:343–8.
113. Rhodes JL, Kolar JC, Fearon JA. Mercedes Benz pattern craniosynostosis. Plast Reconstr Surg. 2010;125:299–304.
114. Weinzweig J, Kirschner RE, Farley A, Reiss P, Hunter J, Whitaker LA, Bartlett SP. Metopic synostosis: defining the temporal sequence of normal suture fusion and differentiating it from synostosis on the basis of computed tomography images. Plast Reconstr Surg. 2003;112:1211–8.

115. Briganti F, Leone G, Briganti G, Orefice G, Caranci F, Maiuri F. Spontaneous resolution of Chiari type 1 malformation. A case report and literature review. Neuroradiol J. 2013;26:304–9.
116. Waldau B, Domeshek LF, Leigh FA, Lum KC, Fuchs HE, Marcus JR, Mukundan S, Grant GA. Spontaneous resolution of a 13-mm Chiari malformation type I in relation to differential growth of the posterior fossa volume. J Neurosurg Pediatr. 2009;3:110–4.
117. Cure JK, Key LL, Goltra DD, VanTassel P. Cranial MR imaging of osteopetrosis. Am J Neuroradiol. 2000;21:1110–5.
118. Dlouhy BJ, Menezes AH. Osteopetrosis with Chiari I malformation: presentation and surgical management. J Neurosurg Pediatr. 2011;7:369–74.
119. Jamjoom AA, Jamjoom BA, Waliuddin AR, Jamjoom AB. Lessons from a case of osteopetrosis oxycephaly and Chiari type I malformation: a case report. Cases J. 2009;2:6787.
120. Dowlati D, Winston KR, Ketch LL, Quinones R, Giller R, Frattini A, van Hove J. Expansion cranioplasty with jackscrew distracters for craniosynostosis and intracranial hypertension in transplanted osteopetrosis. Pediatr Neurosurg. 2007;43:102–6.
121. Krimmel M, Niemann G, Will B, Reinert S. Surgical correction of craniosynostosis in malignant osteopetrosis. J Craniofac Surg. 2004;15:218–20.
122. Kulkarni ML, Marakkanavar SN, Sushanth S, Pradeep N, Ashok C, Balaji MD, Sajith KP, Srinivas G. Osteopetrosis with Arnold Chiari malformation type I and brain stem compression. Indian J Pediatr. 2007;74:412–5.
123. Stark Z, Savarirayan R. Osteopetrosis. Orphanet J Rare Dis. 2009;4:5.
124. Collmann H, Sörensen N, Krauss J. Hydrocephalus in craniosynostosis: a review. Childs Nerv Syst. 2005;21:902–12.
125. Proudman TW, Clark BE, Moore MH, Abbott AH, David DJ. Central nervous system imaging in Crouzon's syndrome. J Craniofac Surg. 1995;6:401–5.
126. Hanieh A, David DJ. Apert's syndrome. Childs Nerv Syst. 1993;9:289–91.
127. Murovic JA, Posnick JC, Drake JM, Humphreys RP, Hoffman HJ, Hendricks EB. Hydrocephalus in Apert syndrome: a retrospective review. Pediatr Neurosurg. 1993;19:151–5.
128. Noetzel MJ, Marsh JL, Palkes H, Gado M. Hydrocephalus and mental retardation in craniosynostosis. J Pediatr. 1985;107:885–92.
129. Renier D, Arnaud E, Cinalli G, Sebag G, Zerah M, Marchac D. Prognosis for mental function in Apert's syndrome. J Neurosurg. 1996;85:66–72.
130. Yadav YR, Parihar V, Pande S, Namdev H, Agarwal M. Endoscopic third ventriculostomy. J Neurosci Rural Pract. 2012;3:163–73.
131. Robson CD, Mulliken JB, Robertson RL, Proctor MR, Steinberger D, Barnes PD, McFarren A, Muller U, Zurakowski D. Prominent basal emissary foramina in syndromic craniosynostosis: correlation with phenotypic and molecular diagnoses. Am J Neuroradiol. 2000;21:1707–17.
132. Eide PK, Helseth E, Due-Tønnessen B, Lundar T. Changes in intracranial pressure after calvarial expansion surgery in children with slit ventricle syndrome. Pediatr Neurosurg. 2001;35:195–204.
133. Renier D, Sainte-Rose C, Marchac D, Hirsch JF. Intracranial pressure in craniostenosis. J Neurosurg. 1982;57:370–7.
134. Tamburrini G, Di Rocco C, Velardi F, Santini P. Prolonged intracranial pressure (ICP) monitoring in non-traumatic pediatric neurosurgical diseases. Med Sci Monit. 2004;10:MT53–63.
135. Thompson DN, Harkness W, Jones B, Gonsalez S, Andar U, Hayward R. Subdural intracranial pressure monitoring in craniosynostosis: its role in surgical management. Childs Nerv Syst. 1995;11:269–75.
136. Bannink N, Joosten KF, van Veelen ML, Bartels MC, Tasker RC, van Adrichem LN, van der Meulen JJ, Vaandrager JM, de Jong TH, Mathijssen IM. Papilledema in patients with Apert, Crouzon, and Pfeiffer syndrome: prevalence, efficacy of treatment, and risk factors. J Craniofac Surg. 2008;19:121–7.
137. Saletti V, Esposito S, Frittoli M, Valentini LG, Chiapparini L, Bulgheroni S, Riva D. Neurological pictures in paediatric Chiari I malformation. Neurol Sci. 2011;32(Suppl 3):295–8.
138. Soboleski D, Mussari B, McCloskey D, Sauerbrei E, Espinosa F, Fletcher A. High-resolution sonography of the abnormal cranial suture. Pediatr Radiol. 1998;28:79–82.
139. Kotrikova B, Krempien R, Freier K, Mühling J. Diagnostic imaging in the management of craniosynostoses. Eur Radiol. 2007;17:1968–78.
140. Eley KA, Watt-Smith SR, Sheerin F, Golding SJ. "Black Bone" MRI: a potential alternative to CT with three-dimensional reconstruction of the craniofacial skeleton in the diagnosis of craniosynostosis. Eur Radiol. 2014;24:2417–26.
141. Heiss JD, Patronas N, DeVroom HL, Shawker T, Ennis R, Kammerer EA, Talbot T, Morris J, Eskioglu E, Oldfield E. Elucidating the pathophysiology of syringomyelia. J Neurosurg. 1999;91:553–62.
142. Zhang Y, Zhang N, Qiu H, Zhou J, Li P, Ren M, Shen G, Chen L, Zhou C, Yang D, Liu Y, Mao Y, Gu X, Zhao Y. An efficacy analysis of posterior fossa decompression techniques in the treatment of Chiari malformation with associated syringomyelia. J Clin Neurosci. 2011;18:1346–9.
143. Sgouros S, Goldin JH, Hockley AD, Wake MJ. Posterior skull surgery in craniosynostosis. Childs Nerv Syst. 1996;12:727–33.
144. Wall SA, Goldin JH, Hockley AD, Wake MJ, Poole MD, Briggs M. Fronto-orbital re-operation in craniosynostosis. Br J Plast Surg. 1994;47:180–4.
145. Di Rocco C, Velardi F. Acquired Chiari type I malformation managed by supratentorial cranial enlargement. Childs Nerv Syst. 2003;19:800–7.

146. Di Rocco F, Jucà CE, Arnaud E, Renier D, Sainte-Rose C. The role of endoscopic third ventriculostomy in the treatment of hydrocephalus associated with faciocraniosynostosis. J Neurosurg Pediatr. 2010;6:17–22.
147. Hoffman HJ, Hendrick EB. Early neurosurgical repair in craniofacial dysmorphism. J Neurosurg. 1979;51:796–803.
148. Tubbs RS, Lyerly MJ, Loukas M, Shoja MM, Oakes WJ. The pediatric Chiari I malformation: a review. Childs Nerv Syst. 2007;23:1239–50.
149. Renier D, Lajeunie E, Arnaud E, Marchac D. Management of craniosynostosis. Childs Nerv Syst. 2000;16:645–58.
150. Pollack IF, Losken HW, Hurwitz DJ. A combined frontoorbital and occipital advancement technique for use in total calvarial reconstruction. J Neurosurg. 1996;84:424–9.
151. Da Costa AC, Walters I, Savarirayan R, Anderson VA, Wrennall JA, Meara JG. Intellectual outcomes in children and adolescents with syndromic and non-syndromic craniosynostosis. Plast Reconstr Surg. 2006;118:175–81.
152. Kapp-Simon KA, Speltz ML, Cunningham ML, Patel PK, Tomita T. Neurodevelopment of children with single suture craniosynostosis: a review. Childs Nerv Syst. 2007;23:269–81.
153. Speltz ML, Kapp-Simon KA, Cunningham M, Marsh J, Dawson G. Single-suture craniosynostosis: a review of neurobehavioral research and theory. J Pediatr Psychol. 2004;29:651–68.
154. Inagaki T, Kyutoku S, Seno T, Kawaguchi T, Yamahara T, Oshige H, Yamanouchi Y, Kawamoto K. The intracranial pressure of the patients with mild form of craniosynostosis. Childs Nerv Syst. 2007;23:1455–9.
155. Knight SJ, Anderson VA, Spencer-Smith MM, Da Costa AC. Neurodevelopmental outcomes in infants and children with single-suture craniosynostosis: a systematic review. Dev Neuropsychol. 2014;39:159–86.
156. Shimoji T, Shimabukuro S, Sugama S, Ochiai Y. Mild trigonocephaly with clinical symptoms: analysis of surgical results in 65 patients. Childs Nerv Syst. 2002;18:215–24.

Part IV

Epidemiology, Natural History, and Genetics

Epidemiology of Chiari I Malformation

21

John D. Heiss and Davis P. Argersinger

Introduction

Epidemiology is defined as "the branch of medicine which deals with the incidence, distribution, and possible control of diseases and other factors relating to health" [1]. A determination of the incidence and distribution of Chiari I malformation (CM I) therefore depends on the criteria one uses to characterize the "disease" of CM I. Disease can be defined as "a disorder of structure or function in a human, animal, or plant, especially one that produces specific symptoms or that affects a specific location and is not simply a direct result of physical injury" [2]. Based on that definition, one could describe the disease of CM I simply as a disorder of hindbrain structure, as seen on magnetic resonance imaging (MRI), or could in addition require specific symptoms to be manifested. On the other hand, because the epidemiology of CM I is not well established, one could look at the epidemiology of CM I both from the perspective of (1) prototypical MRI characteristics alone and (2) MRI characteristics that must be accompanied by distinctive clinical criteria. This two-pronged approach would not preclude longitudinal evaluation of presently asymptomatic people with MRI findings of CM I (incidental CM I) who may later develop typical symptoms of CM I. In addition, comparison of the determinants that predominate in symptomatic versus asymptomatic people with CM I could reveal insights into possible environmental events that could trigger the onset of symptomatic CM I. The ultimate goal would be to design interventions to reduce the occurrence of symptomatic CM I in the population [3].

Epidemiology of Rare Diseases

There are several ways to measure the frequency of a disease such as Chiari I malformation (CM I) in a population [4]. The *incidence rate* of CM I is the number of new cases per unit of person-time at risk. The *cumulative incidence* refers to the proportion of people who develop CM I during a specified period of time. The *period prevalence* is the proportion of individuals in a stable population who have CM I during a specific period of time. *Point prevalence* is the proportion of individuals in a population who have CM I at a specific time. *Lifetime prevalence* is a measure of current cases of CM I and cases of CM I that have previously occurred, including those that have been treated [4]. The *case fatality rate* for CM I refers to the proportion of deaths caused by CM I in a population of patients with CM I.

J. D. Heiss (✉) · D. P. Argersinger
Surgical Neurology Branch, National Institute of Neurological Disorders and Stroke, National Institutes of Health, Bethesda, MD, USA
e-mail: heissj@ninds.nih.gov

R. S. Tubbs et al. (eds.), *The Chiari Malformations*, https://doi.org/10.1007/978-3-030-44862-2_21

Symptomatic CM I appears to be a rare condition [5]. A rare (or orphan) disease is generally considered to have a prevalence of fewer than 200,000 affected individuals in the United States [6]. Research studies of a rare disease do not usually include a population of patients that is sufficiently large to allow determinations of the incidence or prevalence of a disorder [7]. Most rare diseases do not recognize geographical or political borders [7]. Of the more than 7000 conditions that are considered rare diseases, a majority are inherited, but many others are acquired and are related to environmental factors [7]. Expression of a rare disease often varies between patients [7]. Diagnostic delays occur frequently in patients with CM I and other rare diseases [8].

Prevalence of Chiari I Malformation

A population-based retrospective cohort study was conducted in Northern California by searching for the diagnosis of CM I in radiology reports over a 2-year period (January 1997–December 1998) [9]. Clinical follow-up was 6.4 ± 4.1 years. From an overall population of 741,815 children under age 20 within Kaiser Northern California (a medical insurance plan), 5248 (0.71%) underwent head and spine MRI scans during the 2-year period. Radiographic diagnosis of CM I required ≥5 mm of tonsillar ectopia. Of the 5248 children scanned, 51 (0.97%) were identified as having a radiographic diagnosis of CM I, with ectopia ranging from 5 to 32 mm (median: 7 mm). Patients who previously had been diagnosed with CM I apparently were not excluded from evaluation, so the incidence rate of radiographic CM I in this pediatric population could not be determined. The study instead measured period prevalence, which was 0.0068% (0.68 per 10,000) over the 2-year period. Of the 51 children with radiographic CM I, 32 (63%) were symptomatic. The most common symptoms were headache (55%), neck pain (12%), vertigo (8%), sensory changes (6%), and ataxia or poor coordination (6%). The period prevalence of symptomatic CM I in the pediatric population was therefore 0.0043% (0.43 per 10,000) over the 2-year period. Of the 51 children with radiographic CM I, 6 had syringomyelia (12%), giving a period prevalence of CM I-syringomyelia of 0.00081% (0.81 per 100,000). Of the six patients with syringomyelia, five received surgical decompression with significant reduction in syrinx size after surgery. Only three children with CM I without syringomyelia underwent suboccipital decompression, which initially relieved their daily intractable headaches, although one patient had recurrence of headaches beginning 1 year after surgery. In the follow-up period, 4 of the 19 originally asymptomatic patients (21%) developed symptoms, with headaches being present in 3 (16%) and tremor and poor coordination in 2 (11%) [9]. No cases of syringomyelia developed in the follow-up period. Interestingly, of the 19 patients with tonsillar ectopia of 2–4 mm, 14 (74%) had headaches, characterized as severe in 3, occipital in 2, and Valsalva-related in 1. The true period prevalence of radiographic CM I in the pediatric population is undoubtedly higher than the numbers noted above, because the entire population did not undergo MRI scanning but only the subset of the population who experienced symptoms that prompted MRI scanning of the head or neck. In addition, the development of symptoms in previously asymptomatic patients indicates that period prevalence of symptomatic CM I will increase as the period of observation increases. Finally, prevalence figures in this study did not include patients with CM I who had previously been treated.

The study reported by Aitken and colleagues confirms the general impression among clinicians that the prevalence of CM I diagnosed by radiographic criteria is considerably higher than that of CM I diagnosed by radiographic criteria and accompanied by typical clinical signs and symptoms [9]. The radiographic diagnosis of CM I in that study was defined as ≥5 mm of tonsillar ectopia [9]. Studies based on the amount of tonsillar ectopia indicate that the normal range (mean ± 2 standard deviations) of the cerebellar tonsils ascends with age, so 6 mm of ectopia exceeds the normal range in the first decade, 5 mm is abnormal in the second and third decades, and 4 mm is abnormal in the fourth to eighth

decades of life [10]. Using these standards, the period prevalence of CM I in children would be lower than reported in the Aitken study because children with 5–5.9 mm of ectopia in the first decade of life would be diagnosed as normal rather than having CM I.

In a study of incidental findings on brain and spine imaging in children, Maher and Piatt reported that as many as 3.6% of children undergoing MRI of the brain or cervical spine have CM I per the imaging criteria of ≥5 mm of tonsillar ectopia [11]. However, it is quite possible that the prevalence of CM I in children is in fact lower than the figure reported in this study, as the threshold of normal tonsillar ectopia compared to classification as CM I is higher (≥6 mm) in the pediatric population as described above.

After excluding patients with posterior fossa disease, supratentorial tumors, hydrocephalus, increased intracranial pressure, and diffuse or focal atrophy, Mikulis and colleagues studied a population of 221 randomly selected outpatients (age range: 5 months to 89 years). The upper limit of normal (>2 standard deviations above the mean) for tonsillar ectopia in this population was slightly greater in younger than older people [10]. If the position of the cerebellar tonsils relative to the foramen magnum assumes a normal distribution, about 2.3% of these outpatients would exceed a threshold of 2 standard deviations above the mean. In contrast, if an upper threshold of 3 standard deviations above the mean were applied, only 0.14% of the population would exceed this range. Applying this more rigid standard of 3 standard deviations above the mean to the data reported by Mikulis results in similar values to the 2 standard deviation threshold, with the upper limit of tonsillar ectopia being 8 mm in the first decade and 5 mm in the second to eighth decades [10]. This study did not report if any subject with tonsillar ectopia had symptoms related to CM I. The value of 5 mm of tonsillar ectopia corresponds to a threshold for the diagnosis of CM I established in a previous study [12].

The proportion of the population that has MRI findings compatible with the diagnosis of CM I far exceeds the proportion of the population with symptoms of CM I. One study found that 0.9% of normal adults undergoing MRI studies of the brain had tonsillar herniation extending more than 5 mm below the foramen magnum (Fig. 21.1) [13–15]. People who have MRI findings of CM I but are asymptomatic are given the diagnosis of "incidental Chiari I malformation." When symptomatic rather than normal subjects undergo MRI scanning, radiographic findings of CM I similar to those observed in the study of normal subjects often are cited as the cause of symptoms. In a retrospective review of more than 22,000 hospitalized patients, only 14% of patients with radiographic findings of CM I were thought to be clinically asymptomatic [16]. In another retrospective series of 68 patients with MRI findings of CM I, 30% of patients were asymptomatic. However, in this study it was apparent that the amount of tonsillar ectopia correlated with symptom production, as ectopia over 12 mm was always associated with symptoms [14]. Symptomatic CM I patients in one study had a mean tonsillar ectopia of 13 mm, although symptoms were reported with as little as 3 mm of ectopia [12]. In patients with lesser degrees of tonsillar ectopia, symptoms can be associated with narrowing of the CSF space posterior to the cerebellar tonsils, molding of the cerebellar tonsils, and/or syringomyelia [17].

The prevalence of CM I in the general population is uncertain. One can estimate the prevalence of syringomyelia associated with CM I by multiplying the prevalence of syringomyelia in an English city (8.4 cases per 100,000 people) [18] by the proportion of patients who have syringomyelia due to the CM I (estimated to be about 70%) [19]. This calculation would give a prevalence of Chiari I-related syringomyelia (CM I-syringomyelia) of 5.9 cases per 100,000 people. The same method can be applied to a retrospective study of 1.3 million people in northern New Zealand that identified all cases of syringomyelia diagnosed between 1961 and 2003. The prevalence of syringomyelia in 2003 in all ethnic groups was 8.2/100000 population [20], which is remarkably similar to the figure of 8.4 cases/100,000 population reported for an English city 40 years previously [18]. Syringomyelia in

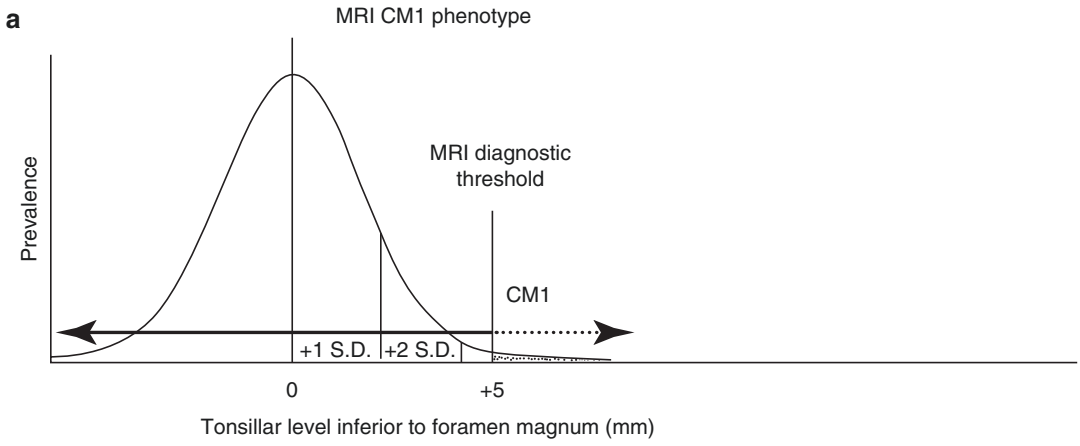

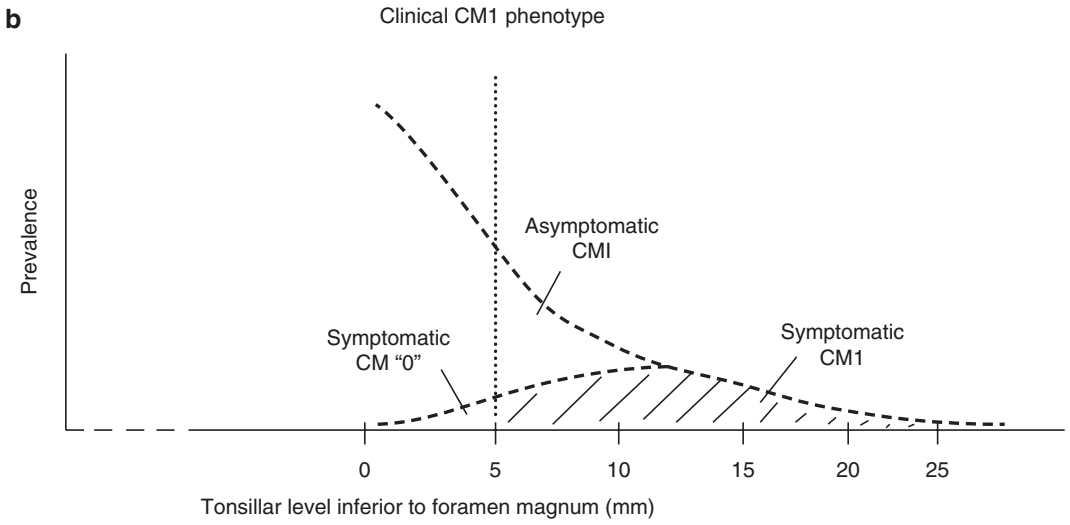

Fig. 21.1 Drawings describe different ways to define Chiari I malformation (CM I). In (**a**), the threshold for the diagnosis of CM I on magnetic resonance imaging (MRI) scans is usually 5 mm, although this number can be modified slightly to conform to age-based norms. In (**b**), the population of patients with symptomatic CM I is marked by the angled lines in the area under the curve. The drawing reflects the finding that virtually all subjects with 12 mm of more of tonsillar ectopia are symptomatic [14]. The prevalence of MRI-diagnosed CM I in normal adults is 0.009 (0.9%) [13]. The prevalence of symptomatic CM I in the population is uncertain. The prevalence of symptomatic Chiari type 0 malformation (CM "0") is probably quite low based on the small number of cases reported in the clinical literature [15]

New Zealand was associated with CM I in 64.3% of cases, giving a prevalence of CM I-syringomyelia of 5.4 cases per 100,000 people, which is again very similar to the findings of Brewis [18, 20]. These prevalence values that include both the adult and pediatric populations are much greater than the 2-year period prevalence in pediatric patients of 0.8 cases per 100,000 that was reported by Aitken and colleagues [9]. This difference in the prevalence of CM I-syringomyelia in the pediatric and total population is consistent with the observation that symptomatic CM I and syringomyelia most commonly present in adulthood [21].

In a review of demographics, operative treatment, and outcomes of pediatric and adult CM I

surgical series from 1965 to 2013, Arnautovic and colleagues reviewed 145 operative series of patients with CM I, primarily from the United States and Europe [22]. Of the 145 series reviewed, most were published in the United States (67), followed by Great Britain (14), Italy (11), Japan (8), France (8), Spain (5), Germany (5), Turkey (5), Brazil (4), China (3), Canada (3), India (2), Poland (2), Belgium (2), Russia (1), Puerto Rico (1), Egypt (1), Ireland (1), Australia (1), and Saudi Arabia (1). The distribution of CM I studies by continent of publication was as follows: North America (49%), Europe (37%), Asia (10%), South America (1%), Africa (1%), and Australia (1%). The median number of patients in each operative series was 31 (range: 4–585), with a mean study time of 10 years (range: 1–23), including a total of 8605 patients: 2351 adult (27%), 2583 pediatric (30%), and 3671 unknown (sex not reported) (43%) [22]. There were 1608 patients in the adult-only series: 913 women (57%), 543 men (34%), and 152 (9%) of unknown sex. There were 2302 patients in the pediatric-only series: 635 girls (28%), 578 boys (25%), and 1089 (47%) of unknown sex. In total, CM I in females was more prevalent than in males (57% vs. 43%, respectively). The median ages of adult and pediatric patients in the series were 40.5 years and 8 years, respectively. Of the 8605 patients in the review, 4144 (48%) had CM I-associated syringomyelia. The incidence of syringomyelia ranged from 20% to 100% in the adult series and 12–100% in the pediatric series [22]; 69% of patients in the adult series had a syrinx, compared to 40% of patients in the pediatric series. The incidence of CM I-associated syringomyelia reported in this study is similar to that reported by Milhorat and colleagues, as described below [17]. The results of the comprehensive review by Arnautovic and colleagues ultimately support what has been reported in earlier studies by Aitken and Milhorat [9, 17]. Arnautovic reported a prevalence of CM I ranging 0.5–3.5% in the general population, from 0.56% to 0.77% in MRI studies, and 0.62% in anatomical brain-dissection studies [22].

Milhorat reported that 65% of his CM I patients undergoing surgery had accompanying syringomyelia [17]. The prevalence of all cases of CM I (CM I-syringomyelia plus CM I without syringomyelia) can be calculated by dividing the prevalence of CM I-syringomyelia by 0.65. Assuming a prevalence of CM I with syringomyelia of 5.9 cases per 100,000 population [18], one would estimate a prevalence of CM I of 9.1 cases per 100,000 people. However, based on Aitken's study, it is clear that symptomatic patients with CM I-syringomyelia are much more likely to undergo surgery than patients with CM I without syringomyelia. An estimate of the prevalence of symptomatic CM I in the general population would be about 36 cases per 100,000 people if one assumed that CM I with syringomyelia accounts for only 19% of all cases of symptomatic CM I [9].

The Role of Non-genetic Factors in the Development of Chiari I Malformation

Non-genetic factors appear to affect the development of CM I. One traditional method to measure the influence of non-genetic factors on the development of CM I would be to evaluate siblings with identical genomic DNA (i.e., monozygotic twins or monozygotic triplets) to see if they differed in the extent of their tonsillar ectopia and symptomatology. Because these monozygotic siblings had identical genomic DNA sequences, differences in phenotype would presumably be related to non-genetic factors. A first example of differences in phenotype is a report of adult monozygotic triplet sisters in which only the proband met the radiographic criteria for diagnosing CM I [23]. The amount of tonsillar ectopia in the proband was not given in this report but appeared to be about 15–20 mm in an MRI scan shown in a figure in the article. Tonsillar ectopia of 4 mm and 2.5 mm in the asymptomatic siblings was considered to be variable expression of tonsillar ectopia. The authors made the case that the triplets demonstrated 100% concordance for tonsillar ectopia with variable expression. However, if the triplets were evaluated using the accepted threshold of 5 mm of tonsillar ectopia for diag-

nosing CM I, only one would be diagnosed as being affected by CM I and the other two would be considered to be unaffected (Fig. 21.2) [23–27]. Despite all three have the same genomic DNA sequence, only one developed CM I. Even acknowledging that each triplet had some degree of tonsillar ectopia, the disparity in the amounts of ectopia among the triplets is striking and cannot be explained in terms of their identical inherited genomic DNA. Compression of the retrocerebellar cerebrospinal fluid space was evident in the MRI scans of the triplets, and it is likely that their common genomic sequences resulted in a smaller-than-normal posterior fossa in all of them. In this example, pre- and postnatal environmental, nutritional, and epigenetic

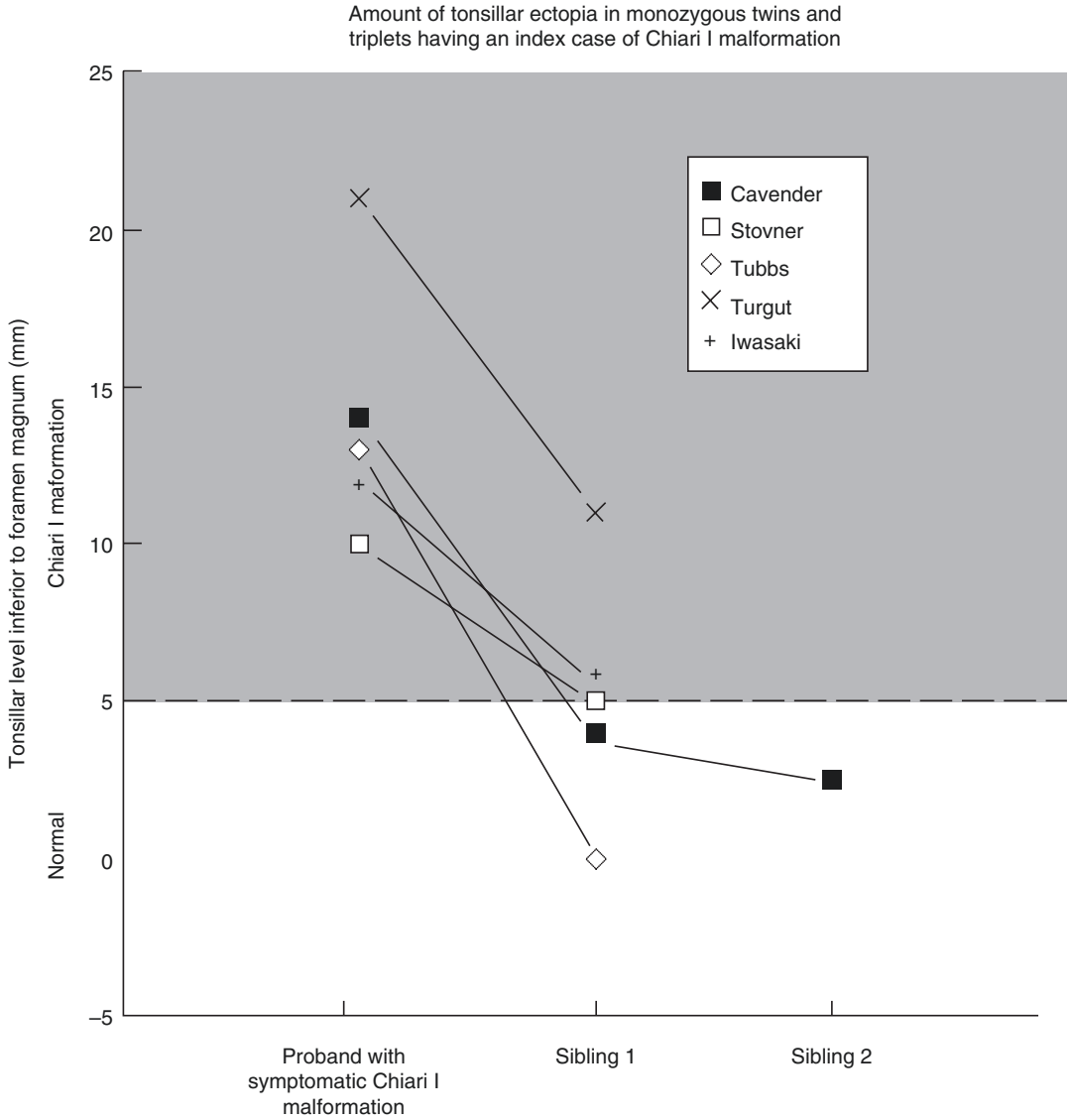

Fig. 21.2 This graph compares the amount of tonsillar ectopia in monozygous twins and triplets from reports in the medical literature in which tonsillar ectopia was measured [23–27]. All probands presented with symptomatic CM I. Their monozygous siblings had lesser amounts of tonsillar ectopia and were asymptomatic, with the exception of Sibling 1, reported by Tubbs et al. who had symptomatic syringomyelia

influences on an identical substrate of genomic DNA led to the development of CM I in the proband and lesser degrees of tonsillar ectopia in the others [28].

In another report, Stovner and colleagues reported monozygotic twin sisters with 5 mm and 10 mm of tonsillar ectopia. The twin with 10 mm of tonsillar ectopia also had syringomyelia. Their mother had 8 mm of tonsillar ectopia [25]. In another study, CM I was diagnosed in monozygotic twin sisters and in the daughter of one of the twins. Although measurements of tonsillar ectopia were not given, imaging suggested that the amount of tonsillar ectopia was similar in the twins [29]. Affected family members had occipital dysplasia and overcrowding of the posterior fossa structures, suggesting that occipital dysplasia was the heritable condition and that CM I developed in response to reduced posterior fossa volume [29].

The complexity of factors involved in the development of CM I is apparent in another report describing 11-year-old monozygotic twin boys who had syringomyelia. One twin had CM I with 13 mm of tonsillar ectopia and associated scoliosis. The other twin did not have any (0 mm) tonsillar ectopia but had findings of lower extremity hyperreflexia, "jumpy legs," syringomyelia, shortening of the basiocciput, and inferior displacement of the obex [26]. Review of the birth history revealed that the twin with CM I had a cephalic presentation, whereas his brother had a breech presentation. Posterior fossa decompression and duraplasty was performed in both twins and resulted in reduction in syrinx diameter and clinical stabilization in both. Both twins shared findings of syringomyelia and abnormal development of the inferior part of the posterior fossa [26]. However, the disparity in the amount of tonsillar ectopia in the twins cannot be explained on the basis of their common genomic DNA sequence.

A report of 26-year-old, identical twin brothers from Turkey provides further evidence of the amount of variation in tonsillar ectopia and symptoms that can be seen in identical twins. The proband had a 6-year history of headache exacerbated by coughing and the Valsalva maneuver, gait disturbance, and 21 mm of tonsillar ectopia. The other brother was asymptomatic and had 11 mm of tonsillar ectopia [27]. These twins were concordant for having radiographic CM I but discordant for symptoms.

Iwasaki reported monozygotic twins in which the proband had an uneventful and healthy childhood before developing pain and numbness in the left arm that began at the age of 16 years [24]. Symptoms progressed for 10 years until she was diagnosed by MRI with CM I (12 mm of tonsillar ectopia) and cervicothoracic syringomyelia at the age of 26. The asymptomatic twin had 6 mm of tonsillar ectopia. Review of birth records revealed that the affected twin was delivered first and suffered from coiling of the umbilical cord and neonatal asphyxia. In contrast, the unaffected twin was born uneventfully [24]. Neonatal asphyxia is a possible non-genetic factor that could have influenced the development of CM I and syringomyelia in the proband, although this report stated that she otherwise developed normally [30].

Phenotypic differences in monozygous twins and triplets identified in the studies mentioned above have been used in this chapter and in other studies to make the case that environmental factors play a role in the development of CM I. In most cases, the mechanisms by which environmental factors influence a complex disease such as CM I have not been obvious. Recently, epigenetics has been used to explain how phenotypic differences between monozygous twins become more pronounced with age. Age-related differences in the content and genomic distribution of 5-methylcytosine DNA and histone acetylation are thought to result in gene expression being modulated differently in monozygous twins [28]. Environmental factors such as smoking, physical activity, and diet have been proposed to influence epigenetic modifications, but it has also been suggested that epigenetic changes simply occur as a result of normal aging. Fraga and colleagues reported that one-third of monozygous twins harbored epigenetic differences in DNA methylation and histone modification. Differences in the placenta and amniotic sac between the monozy-

gous twins are also postulated to play a role in creating phenotypic discordance between monozygous twins [28].

Non-genetic Factors Associated with the Development of Chiari I Malformation

Gender

In reports of adult patients with CM I from the United States and Europe, there is usually a female preponderance. In a cohort of 364 symptomatic patients in the United States with CM I, defined in this series as tonsillar herniation of >3 mm below the foramen magnum, there were 275 (76%) females and 89 (24%) males. Age of onset of symptoms was 24.9 ± 15.8 years (mean ± standard deviation) [17]. In a review of 145 surgical series, Arnautovic et al. reported that CM I in females was more prevalent than in males in their study (57% vs. 43%) [22]. Elster et al. reported 42 females (62%) and 26 males (38%) in a series of 68 pediatric and adult patients with CM I [14]. In a surgical series of 157 patients with CM I-syringomyelia conducted in France, 53% were female and 47% were male [31]. However, in the Republic of Tatarstan in the Russian Federation, males are affected more often than females (see below). The prevalence of CM I in the pediatric population does not appear to be related to gender. In a surgical series of 130 pediatric patients in the United States with CM I, 53% were males and 47% were females [32].

Birth Injury

Williams reported that there was an association between difficult birth and the later development of CM I-related syringomyelia. Syringomyelia was more likely to develop in a first-born child, heavy birth-weight babies, and those in whom forceps were used. Williams believed that a difficult birth causes the cerebellar tonsils to engage in the foramen magnum and could also cause basal arachnoiditis [33]. Hida supported the view that adverse events during delivery were associated with CM I-related syringomyelia. In his study, abnormal presentation, the use of forceps, neonatal asphyxia, and birth injury were much more frequently reported in patients with CM I-related syringomyelia compared to normal subjects [30].

History of Trauma

In Milhorat's report, 89 patients (24%) cited trauma as the precipitating event [17]. In a retrospective Canadian study of 85 patients with symptomatic CM I, 12.9% reported a history of minor head or neck trauma preceding the onset of symptoms [34]. In a case report by Spina and colleagues, a 6-month-old child presented with sudden onset of coughing, dysphagia, and vomiting after an accidental fall from a bed. An MRI scan revealed 8 mm of tonsillar ectopia in the context of a small posterior fossa [35].

Ethnic Factors

The prevalence of syringomyelia, including CM I-related syringomyelia, was evaluated in the population of northern New Zealand, which consisted of 1.3 million people in 2001. The ethnic makeup of the population was 11.7% Pacific people, 12.5% Maori, and 75.5% Caucasians or others. Pacific people (18.4/100,000) and Maori (15.4/100,000) had a higher prevalence of syringomyelia than Caucasians (5.4/100,000) [20]. In addition, Pacific people were more likely to have syringomyelia associated with CM I (87.5%) than Maori (53.6%) and Caucasians (58.8%). The prevalence of CM I-syringomyelia in Pacific people was 16.1/100,000, in Maori was 8.2/100,000, and in Caucasians was 3.2/100,000. In northern New Zealand, CM I-syringomyelia was therefore found to be five times more prevalent in Pacific people and more than 2 1/2 times more prevalent in the Maori than in Caucasians. Female-to-male ratios were similar in the Pacific people (55:45) and Maori (50:50), but females (69:31) predominated in the Caucasians. The

authors of this study speculated that ethnic variations in the size of the posterior fossa and of cerebrospinal fluid flow in the foramen magnum may underlie the differences in the prevalence of syringomyelia among the ethnic groups [20].

The period prevalence of CM I in four northern districts of the Republic of Tatarstan in the Russian Federation was 275 per 100,000 inhabitants in a recent study [36]. Tatars are the predominant ethnic group in that region and make up 84% of affected patients. Unlike in the adult population of the United States, males in that population were affected (88%) much more often than females (12%). The affected males are predominantly manual laborers who perform agricultural work [37]. Patients in that population usually develop syringomyelia in association with reduced volume of the posterior fossa, which in about one-half of cases is also associated with CM I [38, 39]. A study of the genetics of CM I in Tatarstan is currently being conducted [40].

Ethnic factors also affect the presentation and severity of CM I characteristics and symptoms. In a recent study of racial, socioeconomic, and gender disparities in the presentation, treatment, and outcomes of CM I, Krucoff and colleagues found that the mean tonsillar depth in African Americans (n = 67) was 11.6 mm, compared to 9.4 mm in white subjects (P = 0.003) [41]. The study also reported that CM I-syringomyelia was found in 37.3% of African American subjects, compared to 21.5% of white subjects (P = 0.009). Additionally, white patients presented with a higher frequency of back pain, ataxia, and syncope, whereas African American patients presented with worse lower extremity weakness, along with greater tonsillar ectopia and syringomyelia [41], as described above.

Reduced Intracranial Volume

CM I is not associated with an underlying disease and is considered primary in most patients, although a majority of patients have underdevelopment of the posterior fossa of unknown etiology [42]. Processes that reduce the volume of the inferior part of the posterior fossa will result in deformation of the hindbrain and the development of idiopathic CM I [42–44]. Factors that reduce the supratentorial volume can also influence the development of CM I. For example, the incidence of CM I by MRI criteria in children diagnosed with non-syndromic, single-suture craniosynostosis was 5.6% in Finland [45]. Additional disease mechanisms contributing to the presence of CM I are discussed below.

Increased Brain Volume or Intracranial Pressure

Hydrocephalus was included in Chiari's original description of his type 1 malformation [46] and in Milhorat's series was present in 9% of patients with CM I-syringomyelia and 3% of patients with CM I alone [17]. Treatment of associated hydrocephalus usually reduces the amount of cerebellar ectopia [47]. In the Netherlands, the prevalence of CM I by MRI criteria in patients with pseudotumor cerebri was found to be 10% (7/68) [48]. All patients with idiopathic intracranial hypertension and Chiari I malformation were overweight or obese women.

Secondary Chiari I Malformation

Though not the subject of this chapter, CM I can occur in the context of genetic disorders of abnormal skull bone development, including Apert syndrome, Crouzon syndrome, and achondroplasia. In a study of the role of craniosynostosis syndromes in the development of CM I, of the 39 patients with Apert syndrome, 5 had tonsillar herniation (13%) and 3 had CM I (8%) [49]. Of the 56 patients with Crouzon syndrome, 18 (32%) had tonsillar herniation and 11 had CM I (20%). Several reports have described achondroplasia associated with brainstem displacement or tonsillar herniation [50, 51], though no comprehensive review reporting the relationship between achondroplasia and CM I has been published. It is plausible that some cases diagnosed as primary CM I could be secondary to undetected reduced intrathecal pressure or intracranial sinus obstruction.

Furthermore, symptoms in primary CM I could be triggered by a secondary etiology such as a decreased rate of CSF absorption that is insufficient to enlarge the cerebral ventricles or cause symptomatic hydrocephalus.

Conclusion

Epidemiological studies are sorely needed in Chiari I malformation and most rare diseases. The prevalence of CM I in the general population of the United States or any other country has not been determined with any certainty. The uncertain clinical implication of tonsillar ectopia that lies just outside the normal range reinforces the need for better criteria for the radiographic diagnosis of CM I.

The development of symptoms of CM I generally correlates with the amount of tonsillar ectopia, but lesser degrees of tonsillar ectopia can sometimes create symptomatic CM I (or CM zero) and syringomyelia by critically narrowing the posterior CSF space, especially if accompanied by arachnoidal scaring [15, 52]. MRI remains the primary diagnostic tool for CM I, but as described above, the relationship between tonsillar ectopia and its corresponding symptoms remains unclear, which may re-introduce the question of how CM I is truly defined, especially when considering an incidental versus non-incidental CM I diagnosis.

Nonetheless, the studies discussed in this chapter collectively describe the primary epidemiological characteristics of CM I available in the literature today. A retrospective study of the prevalence of CM I in children has been conducted in northern California. The prevalence of CM I associated with syringomyelia has also been evaluated in the entire population of northern New Zealand. These studies provide some insight into the prevalence of CM I in those populations. The vast difference in the degree of tonsillar ectopia among monozygotic twins and triplets suggests that factors other than genomic DNA play a large role in the development of CM I. Several factors that influence the development of CM I and the onset of symptoms have been described, including female gender in American and European adults and a history of trauma. The reports of ethnic differences in the prevalence of CM I suggest the need for additional studies to discover if differences arise from genetic or environment factors, or a combination of both.

Better understanding of the prevalence of Chiari I malformation, the factors that influence its development or symptomatology, and the criteria by which CM I is diagnosed in both the adult and pediatric populations may lead to interventions that could reduce the disease burden of Chiari I malformation.

References

1. Anonymous. Epidemiology. Oxford dictionaries online. Oxford: Oxford University Press; 2012.
2. Anonymous. Disease. Oxford dictionaries online. Oxford: Oxford University Press; 2012.
3. Merrill RM. Introduction to epidemiology. 5th ed. Sudbury: Jones and Bartlett Publishers; 2010.
4. Posada de la Paz M, Villaverde-Hueso A, Alonso V, Janos S, Zurriaga O, Pollan M, et al. Rare diseases epidemiology research. In: Posada de la Paz M, Groft SC, editors. Rare diseases epidemiology. Advances in experimental medicine and biology, vol. 686. Dordrecht: Springer Science+Business Media B.V.; 2010. p. 17–39.
5. Groft SC, Brooks PJ, Demory M, Eckstein DJ, Eddy M, Ferguson J, et al. Chiari malformation type 1. Bethesda: Office of Rare Diseases Research, National Institutes of Health; 2012. Available from: http://rarediseases.info.nih.gov/GARD/Condition/9230/Chiari_malformation_type_1.aspx.
6. Groft SC, Brooks PJ, Demory M, Eckstein DJ, Eddy M, Ferguson J, et al. Rare diseases and related terms. Bethesda: Office of Rare Diseases Research, National Institutes of Health; 2012. Available from: http://rarediseases.info.nih.gov/RareDiseaseList.aspx?PageID=1.
7. Groft SC, Posada de la Paz M. Rare diseases–avoiding misperceptions and establishing realities: the need for reliable epidemiological data. In: Posada de la Paz M, Groft SC, editors. Rare diseases epidemiology. Advances in experimental medicine and biology, vol. 686. Dordrecht: Springer Science+Business Media B.V.; 2010. p. 3–13.
8. Pillay PK, Awad IA, Little JR, Hahn JF. Surgical management of syringomyelia: a five year experience in the era of magnetic resonance imaging. Neurol Res. 1991;13(1):3–9.
9. Aitken LA, Lindan CE, Sidney S, Gupta N, Barkovich AJ, Sorel M, et al. Chiari type I malformation in a pediatric population. Pediatr Neurol. 2009;40(6):449–54.

10. Mikulis DJ, Diaz O, Egglin TK, Sanchez R. Variance of the position of the cerebellar tonsils with age: preliminary report. Radiology. 1992;183(3):725–8.
11. Maher CO, Piatt JH Jr, Section on Neurologic Surgery, American Academy of Pediatrics. Incidental findings on brain and spine imaging in children. Pediatrics. 2015;135(4):e1084–96.
12. Barkovich AJ, Wippold FJ, Sherman JL, Citrin CM. Significance of cerebellar tonsillar position on MR. AJNR Am J Neuroradiol. 1986;7(5):795–9.
13. Vernooij MW, Ikram MA, Tanghe HL, Vincent AJ, Hofman A, Krestin GP, et al. Incidental findings on brain MRI in the general population. N Engl J Med. 2007;357(18):1821–8.
14. Elster AD, Chen MY. Chiari I malformations: clinical and radiologic reappraisal. Radiology. 1992;183(2):347–53.
15. Tubbs RS, Elton S, Grabb P, Dockery SE, Bartolucci AA, Oakes WJ. Analysis of the posterior fossa in children with the Chiari 0 malformation. Neurosurgery. 2001;48(5):1050–4; discussion 4–5.
16. Meadows J, Kraut M, Guarnieri M, Haroun RI, Carson BS. Asymptomatic Chiari type I malformations identified on magnetic resonance imaging. J Neurosurg. 2000;92(6):920–6.
17. Milhorat TH, Chou MW, Trinidad EM, Kula RW, Mandell M, Wolpert C, et al. Chiari I malformation redefined: clinical and radiographic findings for 364 symptomatic patients. Neurosurgery. 1999;44(5):1005–17.
18. Brewis M, Poskanzer DC, Rolland C, Miller H. Neurological disease in an English city. Acta Neurol Scand. 1966;S24:1–89.
19. Klekamp J, Batzdorf U, Samii M, Bothe HW. The surgical treatment of Chiari I malformation. Acta Neurochir. 1996;138(7):788–801.
20. Brickell KL, Anderson NE, Charleston AJ, Hope JK, Bok AP, Barber PA. Ethnic differences in syringomyelia in New Zealand. J Neurol Neurosurg Psychiatry. 2006;77(8):989–91.
21. Boman K, Iivanainen M. Prognosis of syringomyelia. Acta Neurol Scand. 1967;43(1):61–8.
22. Arnautovic A, Splavski B, Boop FA, Arnautovic KI. Pediatric and adult Chiari malformation type I surgical series 1965–2013: a review of demographics, operative treatment, and outcomes. J Neurosurg Pediatr. 2015;15(2):161–77.
23. Cavender RK, Schmidt JH 3rd. Tonsillar ectopia and Chiari malformations: monozygotic triplets. Case report. J Neurosurg. 1995;82(3):497–500.
24. Iwasaki Y, Hida K, Onishi K, Nanba R. Chiari malformation and syringomyelia in monozygotic twins: birth injury as a possible cause of syringomyelia–case report. Neurol Med Chir (Tokyo). 2000;40(3):176–8.
25. Stovner LJ, Cappelen J, Nilsen G, Sjaastad O. The Chiari type I malformation in two monozygotic twins and first-degree relatives. Ann Neurol. 1992;31(2):220–2.
26. Tubbs RS, Wellons JC, Blount JP, Oakes WJ. Syringomyelia in twin brothers discordant for Chiari I malformation: case report. J Child Neurol. 2004;19(6):459–62.
27. Turgut M. Chiari type I malformation in two monozygotic twins. Br J Neurosurg. 2001;15(3):279–80.
28. Fraga M, Ballestar E, Paz M, Ropero S, Setien F, Ballestar M, et al. Epigenetic differences arise during the lifetime of monozygotic twins. Proc Natl Acad Sci U S A. 2005;102(30):10604–9.
29. Atkinson JL, Kokmen E, Miller GM. Evidence of posterior fossa hypoplasia in the familial variant of adult Chiari I malformation: case report. Neurosurgery. 1998;42(2):401–3. discussion 4
30. Hida K, Iwasaki Y, Imamura H, Abe H. Birth injury as a causative factor of syringomyelia with Chiari type I deformity. J Neurol Neurosurg Psychiatry. 1994;57(3):373–4.
31. Aghakhani N, Parker F, David P, Morar S, Lacroix C, Benoudiba F, et al. Long-term follow-up of Chiari-related syringomyelia in adults: analysis of 157 surgically treated cases. Neurosurgery. 2009;64(2):308–15; discussion 15.
32. Tubbs RS, McGirt MJ, Oakes WJ. Surgical experience in 130 pediatric patients with Chiari I malformations. J Neurosurg. 2003;99(2):291–6.
33. Williams B. Difficult labour as a cause of communicating syringomyelia. Lancet. 1977;2(8028):51–3.
34. Wan MJ, Nomura H, Tator CH. Conversion to symptomatic Chiari I malformation after minor head or neck trauma. Neurosurgery. 2008;63(4):748–53; discussion 53.
35. Spina A, Boari N, Gagliardi F, Donofrio CA, Mortini P. Sudden onset of Chiari malformation type 1 in a young child after trauma. Childs Nerv Syst. 2015;31(9):1589–94.
36. Bogdanov EI, Faizutdinova AT, Mendelevich EG, Sozinov AS, Heiss JD. Epidemiology of symptomatic Chiari malformation in tatarstan: regional and ethnic differences in prevalence. Neurosurgery. 2019;84(5):1090–7.
37. Bogdanov EI, Mendelevich EG. Syrinx size and duration of symptoms predict the pace of progressive myelopathy: retrospective analysis of 103 unoperated cases with craniocervical junction malformations and syringomyelia. Clin Neurol Neurosurg. 2002;104(2):90–7.
38. Bogdanov EI, Heiss JD, Mendelevich EG. The post-syrinx syndrome: stable central myelopathy and collapsed or absent syrinx. J Neurol. 2006;253(6):707–13.
39. Bogdanov EI, Heiss JD, Mendelevich EG, Mikhaylov IM, Haass A. Clinical and neuroimaging features of "idiopathic" syringomyelia. Neurology. 2004;62(5):791–4.
40. Heiss JD, Oldfield EH, Zhuang Z, Lubensky I, Patronas N, Smith R, et al. Genetic analysis of the Chiari I malformation; 2000. Available from: http://clinicaltrials.gov/ct2/show/NCT00004738?term=chiari+AND+genetics&rank=2.
41. Krucoff MO, Cook S, Adogwa O, Moreno J, Yang S, Xie J, et al. Racial, socioeconomic, and gender disparities in the presentation, treatment, and outcomes

of adult Chiari I malformations. World Neurosurg. 2017;97:431–7.
42. Nyland H, Krogness KG. Size of posterior fossa in Chiari type 1 malformation in adults. Acta Neurochir. 1978;40(3–4):233–42.
43. Nishikawa M, Sakamoto H, Hakuba A, Nakanishi N, Inoue Y. Pathogenesis of Chiari malformation: a morphometric study of the posterior cranial fossa. J Neurosurg. 1997;86(1):40–7.
44. Noudel R, Jovenin N, Eap C, Scherpereel B, Pierot L, Rousseaux P. Incidence of basioccipital hypoplasia in Chiari malformation type I: comparative morphometric study of the posterior cranial fossa. Clinical article. J Neurosurg. 2009;111(5):1046–52.
45. Leikola J, Koljonen V, Valanne L, Hukki J. The incidence of Chiari malformation in nonsyndromic, single suture craniosynostosis. Childs Nerv Syst. 2010;26(6):771–4.
46. Harding BN, Copp AJ. Malformations. In: Graham DI, Lantos PL, editors. Greenfield's neuropathology. 1. 7th ed. London: Arnold; 2002. p. 357–483.
47. Decq P, Le Guerinel C, Sol JC, Brugieres P, Djindjian M, Nguyen JP. Chiari I malformation: a rare cause of noncommunicating hydrocephalus treated by third ventriculostomy. J Neurosurg. 2001;95(5):783–90.
48. Banik R, Lin D, Miller NR. Prevalence of Chiari I malformation and cerebellar ectopia in patients with pseudotumor cerebri. J Neurol Sci. 2006;247(1):71–5.
49. Rijken BF, Lequin MH, Van Veelen ML, de Rooi J, Mathijssen IM. The formation of the foramen magnum and its role in developing ventriculomegaly and Chiari I malformation in children with craniosynostosis syndromes. J Craniomaxillofac Surg. 2015;43(7):1042–8.
50. Nakai T, Asato R, Miki Y, Tanaka F, Matsumoto S, Konishi J. A case of achondroplasia with downward displacement of the brain stem. Neuroradiology. 1995;37(4):293–4.
51. Yundt KD, Park TS, Tantuwaya VS, Kaufman BA. Posterior fossa decompression without duraplasty in infants and young children for treatment of Chiari malformation and achondroplasia. Pediatr Neurosurg. 1996;25(5):221–6.
52. Kyoshima K, Kuroyanagi T, Oya F, Kamijo Y, El-Noamany H, Kobayashi S. Syringomyelia without hindbrain herniation: tight cisterna magna. Report of four cases and a review of the literature. J Neurosurg. 2002;96(2 Suppl):239–49.

Natural History of Chiari Malformations

22

Cormac O. Maher

Introduction

For any medical condition or imaging finding, an understanding of the natural history of the condition is a prerequisite to successful clinical decision-making. In order to properly determine the best course for our patients, we must know the relative efficacy of surgical treatment versus "conservative" management. Although patients with Chiari malformation type I (CM I) are frequently referred for evaluation, many aspects of CM I natural history remain unsolved. As a result, there are no universally accepted criteria for selecting surgical versus non-surgical management of patients with CM I. Surveys of pediatric neurosurgeons have consistently found significant differences of opinion regarding surgical indications [1–3]. In a 2004 survey, Schijman et al. [3] found that 8% of pediatric neurosurgeons would recommend surgical treatment for an asymptomatic patient with CM I and 75% would recommend surgical treatment for an asymptomatic child if a spinal cord syrinx was present [3]. That survey also found that most neurosurgeons (77%) predicted that an asymptomatic child would likely have symptoms in the future [3].

A principal cause for these uncertain surgical indications is lack of understanding of the fundamentals of this condition, including its prevalence and natural history. Most reported series of CM I describe outcomes of patients who have been selected for surgery. These reports provide little or no insight into the natural history of this condition. Nevertheless, some progress is being made. In this chapter, we discuss our current understanding of this complex topic. The natural history of scoliosis in individuals with CM I is an important topic covered elsewhere in this volume.

Chiari Prevalence

There are a number of published reports of spontaneous improvement [4–11] and spontaneous worsening [12–15] in patients with CM I. In order to place these reports into their proper context, it is necessary to have an accurate estimate of the population prevalence of CM I.

Most centers use 5 mm of tonsillar descent below the foramen magnum as the imaging criterion for defining CM I [16–19]. This relatively arbitrary definition is based on older studies reporting that tonsillar descent more than 3 mm below the foramen magnum was rare in normal adults [16, 17]. Analyses of large numbers of patients undergoing imaging for a variety of indications have estimated that between 0.24% and

C. O. Maher (✉)
Department of Neurosurgery, University of Michigan, Ann Arbor, MI, USA
e-mail: cmaher@med.umich.edu

R. S. Tubbs et al. (eds.), *The Chiari Malformations*, https://doi.org/10.1007/978-3-030-44862-2_22

3.6% of the population have at least 5 mm of tonsillar descent below the foramen magnum [19–24]. Differences in these estimates may have resulted from varying sensitivity in CM I detection as well as the different populations that were analyzed. Theoretically, true population prevalence of an imaging finding or disease can only be calculated by screening every member of a population of interest with a tool that is both completely sensitive and completely specific. Since such an approach is not practical, prevalence is usually estimated by other means. One technique that has been employed involves reviewing imaging studies obtained from normal volunteers or those screened for reasons other than the disease of interest. This technique is subject to some negative selection bias in that those with disease symptoms may be excluded from such a study. In addition, this technique may be insensitive for discovering common imaging findings that were not an object of the original study. Several groups have reported on various intracranial findings in normal adult volunteers [25–27]. Although each of these studies was small, a combined meta-analysis by Morris et al. [28] found CM I in 71 of 15,559 (0.24%) magnetic resonance imaging (MRI) studies from combined data of multiple reports in adults. The sensitivity for detecting CM I in each of these studies and the subsequent meta-analysis is not clear, and in some reports contained in that meta-analysis, no cases of CM I were found [25]. Given these concerns about the sensitivity of CM I detection, it is possible that the estimated prevalence of CM I reported by those studies may be less than the true population prevalence.

Other groups have attempted to estimate CM I prevalence by reviewing consecutive imaging studies performed for any clinical indication, looking specifically for CM I. Meadows et al. [22] found CM I in 0.8% of those undergoing MRI at a single referral center. All age groups were included in that analysis, but children comprised a relatively small proportion of their subjects. The report by Meadows et al. [22] is remarkable for the relatively few asymptomatic cases of CM I (14%) discovered on imaging. More recently, Aitken et al. [20] found CM I in 1% of 5248 children undergoing brain or spine MRI—a prevalence estimate similar to that of Vernooij et al. [19] (0.9%) in their recent analysis of normal adults over the age of 45. We recently studied a large group of children undergoing MRI at our institution and found that 3.6% met imaging criteria for CM I [23]. In our study, the prevalence of CM I in those undergoing MRI did not vary significantly by age or gender. The currently available reports on CM I prevalence vary substantially with respect to the proportion of asymptomatic or incidental CM I in each group. Aitken et al. [20] reported that only 19% of findings in their group were thought to be incidental or asymptomatic. By contrast, compared to prior reports, we found a higher percentage of asymptomatic cases (68%) at the time of CM I diagnosis, probably reflecting differences in the relative sensitivity of CM I diagnosis, especially in asymptomatic cases. It is possible that the finding of a larger number of asymptomatic CM I cases reflects a greater sensitivity for detection of CM I and is one factor contributing to higher prevalence estimates. If that is the case, then the higher prevalence estimates with a higher percentage of asymptomatic cases are more likely to reflect the true population prevalence of CM I than those studies with a greater proportion of asymptomatic cases. Finally, it is worth noting that the largest study in children has found a higher prevalence estimate than the largest study comprised mostly of adults, suggesting a need for age-group specific prevalence analyses in the adult age range [22, 23].

Natural History of Chiari

The degree of cerebellar tonsillar descent is not always stable over time. Gradual ascent of cerebellar tonsils has been associated with normal childhood development [29]. This normal ascent should be considered in any interpretation of the natural history of CM I. Furthermore, improvement or worsening of tonsillar descent over time may result from changes in the skull or, less likely, cerebellar morphology [30]. There is no convincing evidence to suggest that spinal tethering or caudal traction plays any role in CM

I pathogenesis in most cases [31–33], although there may be some rare exceptions to this rule [11, 34]. Growth in height during childhood, therefore, does not appear to be an important factor in clinical or imaging progression. Spinal cerebrospinal fluid (CSF) leaks or drainage infrequently causes progressive tonsillar descent but is not a cause of tonsillar descent in the vast majority of cases [35–37].

There are several reported cases of CM I that experienced spontaneous improvement in cerebellar tonsillar descent [4, 5, 7–9, 38, 39]. Since a finding of CM I is relatively common on intracranial imaging, case reports or even small case series of spontaneous improvement or worsening do not provide any real insight into CM I natural history. Any attempt to consider the natural history of CM I will need to account for selection bias in the decision to pursue surgical treatment. The patients followed in most natural history analyses have been selected for non-surgical management. Therefore, any conclusions derived from these asymptomatic or minimally symptomatic patients should not be applied to symptomatic patients who are ordinarily considered good surgical candidates. It seems likely that the natural history is worse for more symptomatic patients for whom surgery is more frequently offered. Furthermore, any natural history analyses of patients selected for surgery are biased by a presumed preferential inclusion of those who are presumed to have an unfavorable natural course [40]. Based on results of the best currently available natural history studies, there is no basis for making any assumptions about the natural history of patients who meet our usual surgical criteria [41–43].

Recently, several groups have reported on CM I natural history in selected groups of patients who were managed without surgery [15, 41–44]. Any attempt to analyze changes in CM I symptoms over time will necessarily require some subjective determinations of CM I symptoms. CM I symptoms can be notoriously protean and may overlap with other neurological conditions, making it difficult to precisely identify those patients with symptomatic CM I [23, 45]. In general, patients with headaches are considered symptomatic if the headaches have at least some of the features considered compatible with CM I headaches, including a tussive component, short duration, and a lack of migrainous features. Other symptoms typically assigned to CM I include sleep apnea, swallowing difficulty, scoliosis, and motor or sensory disturbances in the extremities of patients with spinal syrinx. Although there are case reports of sudden symptomatic presentation [46–58], the onset of symptoms of CM I is usually gradual [41–43, 59, 60]. In the series reported by Aitken et al. [20], 4 of 19 patients with incidental CM I (21%) developed at least 1 CM I symptom over an interval of over 6 years. In most cases, the new symptoms were headaches only. They found that no imaging characteristics were predictive of new symptoms. Novegno et al. [42] reported on a series of 22 patients with CM I for whom non-surgical management was recommended. Over a mean follow-up interval of almost 6 years, they found that 5 patients had symptomatic worsening and 3 of these required surgery, while 17 of their patients remained asymptomatic or their symptoms improved [42]. They concluded that a conservative approach to asymptomatic or minimally symptomatic CM I could be justified based on their data. Benglis et al. [41] recently reported on a larger series of 124 patients with CM I who were followed without surgery for a mean of 2.8 years. None of the patients in that series had new neurological deficits at follow-up. Finally, in our own series of 147 patients followed after an initial decision for non-surgical management, 90% remained asymptomatic or minimally symptomatic over an interval greater than 6 years [43]. In addition, six patients who were symptomatic at presentation were not symptomatic at last follow-up. Each of these studies followed patients for several years, but further study will be required before any conclusions can be drawn for determining the need for surgery over the lifetime of a patient.

Gender appears to be an important factor in CM I presentation. Some groups have reported a female predominance for those undergoing surgical treatment of CM I, but this has not been a universal finding [21, 22, 42, 61–63]. There is now evidence that CM I as an imaging finding

has an equal gender distribution [23] but that girls appear more likely to present for medical attention of a CM I [21, 62, 64, 65]. In our own survey of all symptomatic and asymptomatic children who underwent imaging at our institution, a higher proportion of girls with CM I (41%) were considered to be symptomatic compared to boys (22%), although the prevalence on imaging did not differ according to gender [23]. Girls are also more likely to have an associated spinal syrinx and more likely to have associated scoliosis compared to boys [23]. As a result, girls appear to be more likely to present for neurosurgical treatment, probably explaining the female predominance in some surgical series [21, 62, 64, 65].

In series comprised mostly of children, older age is often associated with symptomatic presentation of CM I. Aitken et al. [20] found that older age at the time of diagnosis was predictive of having neurological symptoms associated with CM I. This is also supported by a comparison of pediatric and adult case series with respect to symptomatic presentation. In general, higher rates of symptomatic presentation and syrinx have been reported in series consisting mainly of adults compared to pediatric cases [21–24, 66]. In our own pediatric series [23], as well as in several prior reports on CM I in children [20, 42, 67, 68], patients who were symptomatic at presentation were older at the time of CM I diagnosis compared to children who were asymptomatic. In contrast to pediatric case series, surgical series that focused on adults have generally reported that symptomatic presentation most often occurs in the third decade or early in the fourth decade of life [62, 69, 70]. This finding, combined with the data from pediatric population studies, implies that patients are most likely to present during late childhood and young adulthood. Symptomatic presentation during late adulthood may occur but is relatively unusual.

The presence of symptoms does not always correlate with the perceived need for surgical treatment. Occasionally, patients and surgeons may elect to manage even a symptomatic CM I without surgery if the symptoms are mild. In our own series of 147 patients followed after an initial decision for non-surgical management, 14 (9%) patients ultimately underwent surgery for CM I at some point during a 6-year follow-up interval [43]. The most common reasons for surgical treatment during the follow-up interval were medically refractory and persistent headaches, sleep apnea, and changes in a syrinx. For these 14 patients, the mean time to surgery after CM I diagnosis was 2 years. In some cases, patients were initially recommended for non-surgical management and then later underwent Chiari decompression despite a lack of any new symptoms or radiological findings. In these cases, the decision to offer surgery was made because symptoms had persisted despite conservative management. There was no significant difference in initial tonsillar herniation in the group that ultimately underwent surgery compared with those individuals who did not undergo surgery. In addition, there were no significant differences in change in CSF flow at the foramen magnum between the group that underwent surgery and the group that did not have surgery. These results are similar to reported rates of surgical treatment in the series by Novegno et al. [42] (14%) as well as Benglis et al. [41] (4%). Although the decision to pursue surgical treatment is necessarily based on subjective and difficult-to-quantify criteria, it is clear that surgery is rarely required for patients for whom an initial decision to pursue non-surgical treatment has been made.

Although changes in patient symptoms or neurological examination have been the primary focus of most efforts at understanding CM I natural history, changes in tonsillar descent over time have also been noted. In our recent natural history analysis, there was no change in mean cerebellar tonsillar herniation for the group as a whole over a mean imaging follow-up of almost 4 years, although spontaneous worsening and improvement were seen in some cases. Interval improvement in the amount of tonsillar descent was seen in 31% of patients, and 5% had a follow-up MRI with less than 5 mm tonsillar descent and were no longer considered to have a CM I according to the usual definition (Fig. 22.1). An increase in tonsillar herniation of at least 4 mm was seen in 4% of patients. We attempted to identify factors that were predictive of a change in the degree of tonsillar descent. Gender was not predictive of change in tonsillar descent. Advancing age, however, was associated with a decrease in the

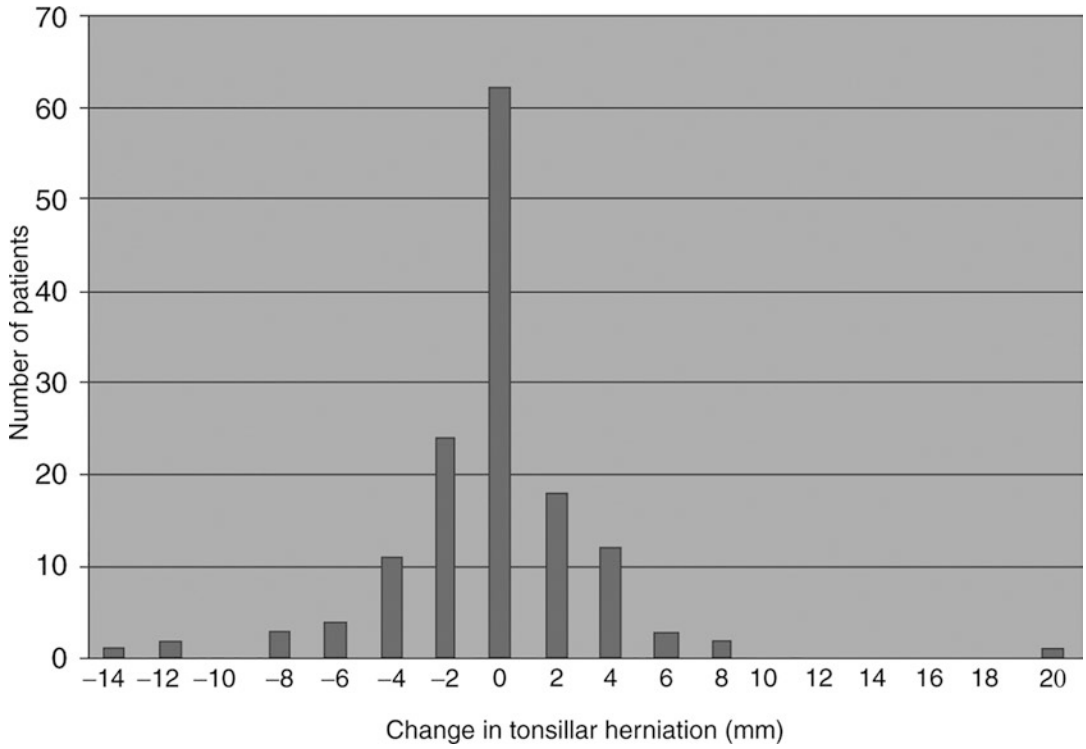

Fig. 22.1 Bar graph illustrating change in tonsillar herniation in 147 patients with CM I

amount of tonsillar herniation. Patients between 0 and 6 years of age at the time of CM I diagnosis had a mean increase in tonsillar herniation of 0.63 mm. In contrast, patients between 6 and 12 years of age at time of CM I diagnosis had a mean decrease in tonsillar herniation of 0.53 mm, and those between 12 and 18 years of age at time of CM I diagnosis had a mean decrease in tonsillar herniation of 1.24 mm. Our results, like those of Novegno et al. [42] and Benglis et al. [41], support a generally benign natural history for those patients with CM I who meet the usual criteria for conservative management.

Natural History of Chiari I-Associated Syrinx

CM I is known to cause spinal cord syrinx in some patients [14, 44, 71–78]. Most surgical series report that between 60% and 85% of CM I patients have an associated syrinx [59, 62, 79]. Since the presence of a syrinx is an indication for surgery at many centers, reported surgical series tend to overestimate the frequency that syrinx occurs in patients with CM I [1–3]. Analyses of imaging databases generally have shown that syringes are less frequently associated with CM I than have been reported in surgical series. A syrinx was found in 12% of patients with CM I in the imaging series reported by Aitken et al. [20] and in 23% of CM I patients in our own series [23]. As with CM I in general, the natural history of spinal syrinx associated with CM I has not been studied until recently. There are several case reports of both spontaneous improvement and worsening in individuals with CM I and spinal syrinx (Figs. 22.2 and 22.3) [6–9]. The tendency to treat CM I surgically when a syrinx is present has made any larger natural history analysis of this subgroup particularly challenging [44, 73].

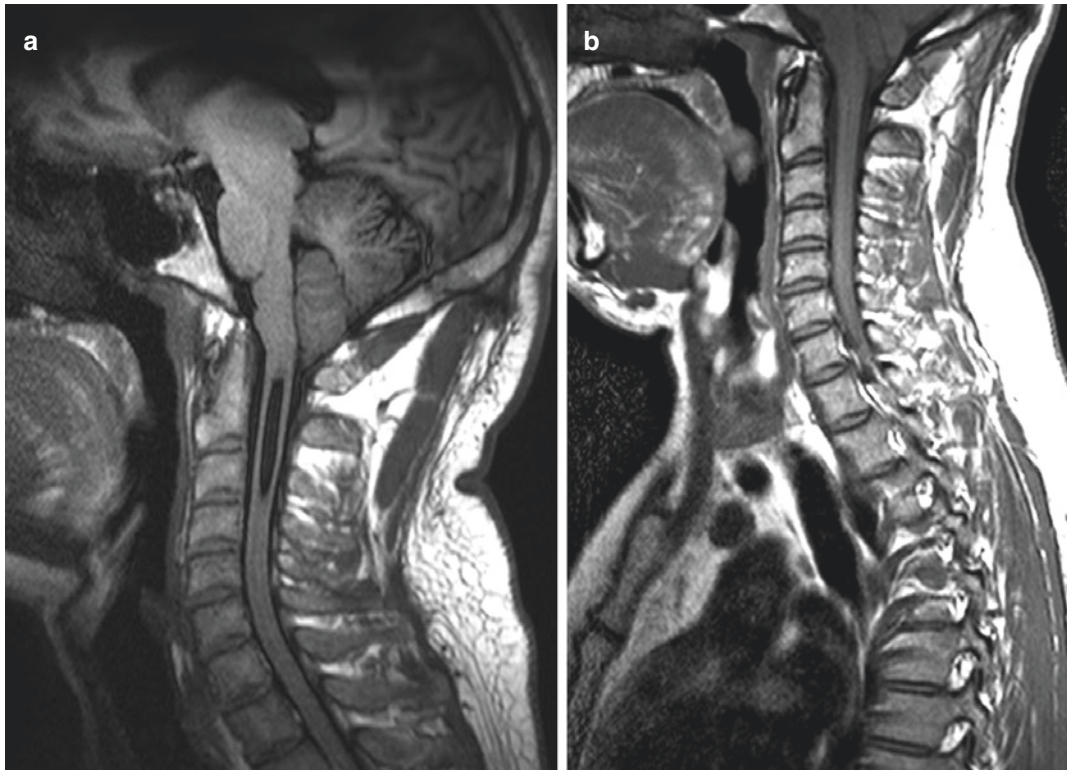

Fig. 22.2 (**a**) Sagittal T1-weighted magnetic resonance image (MRI) of a "normal volunteer" for an MRI research study demonstrating a CM I as well as a cervical spine syrinx. The patient was evaluated by a neurosurgeon but elected follow-up without surgical treatment. (**b**) Six months later, another sagittal T1-weighted MRI demonstrates substantial resolution of cervical spine syrinx. Such cases illustrate that spontaneous resolution may be rare but is not impossible

Syrinx formation appears to be a rare event in patients with CM I over short follow-up intervals. Benglis et al. [41] identified no new syrinx formation among 124 patients with CM I that were followed for almost 3 years. In our own recent natural history analysis, syrinx formation occurred in 5% of the 148 patients with CM I who were followed without surgery over an imaging follow-up duration of nearly 4 years. The mean time interval to syrinx development was 28 months [43]. Of the seven new syringes, two developed from a previously identified pre-syrinx state (T2-hyperintensity on MRI without cavitation) [80–82], three developed from what had been considered a dilated central canal of less than 3 mm in diameter, and only two patients had previously normal spine MRIs. In patients with CM I, age appears to be a relevant factor in spinal syrinx formation. In our analysis, although the prevalence of CM I in those undergoing MRI did not vary significantly by age, spinal syrinx was more commonly found in older children with CM I [23]. Syringes were much less common during the first years of life but appear to become increasingly common until 5 years of age. It was not unusual for a younger child with CM I but no syrinx on presentation to develop a syrinx over the follow-up interval. This finding supports our current understanding of the causal relationship between the CM I and spinal syrinx and suggests some potential utility for spine imaging follow-up in those children diagnosed with CM I at a very young age. Development of a syrinx later in childhood is certainly possible but was noted less frequently. In contrast to CM I alone, CM I with syrinx was more common in girls compared with

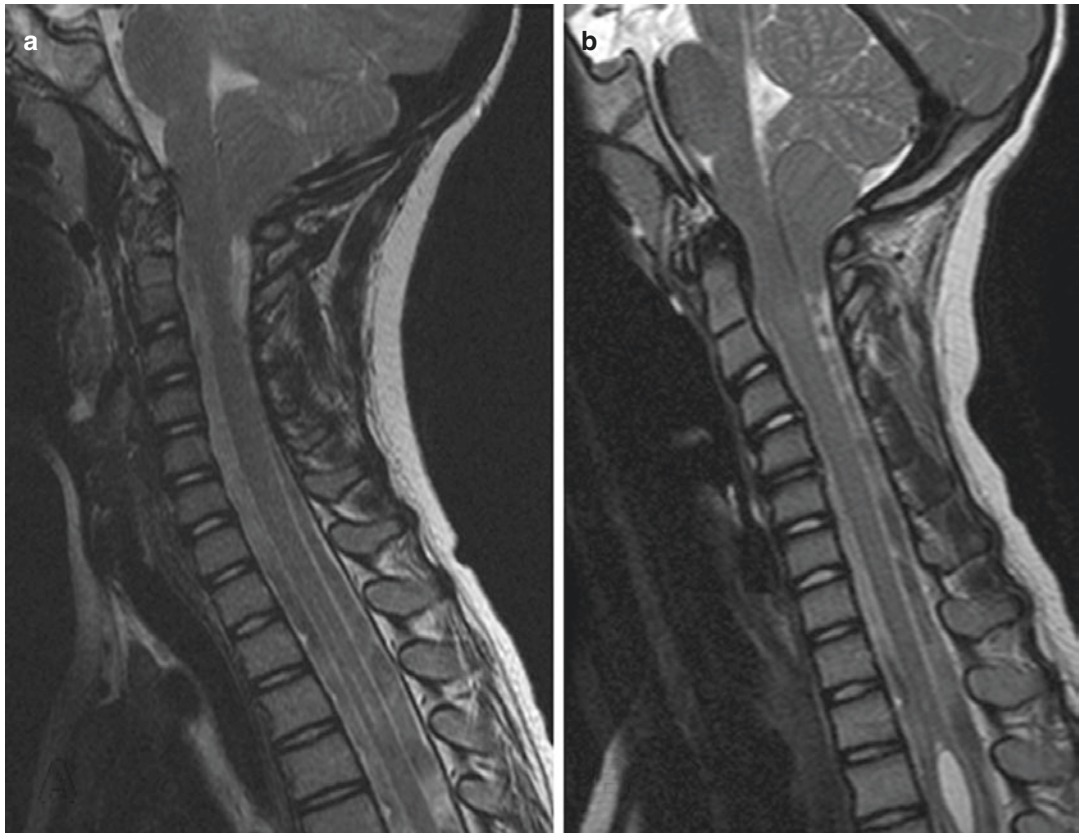

Fig. 22.3 (**a**) Sagittal T2-weighted MRI of a young boy with incidental discovery of CM I on imaging. (**b**) The patient was followed without surgery, and MRI obtained 4 years later shows formation of a new spinal syrinx

boys and more common in those with greater degrees of tonsillar descent [23].

Syrinx was more likely to be found in those with more severe CSF flow alterations at the foramen magnum. Over half of patients with significantly abnormal tonsillar pulsations had a syrinx compared with 13% of patients with normal CSF flow at the foramen magnum. Patients with basilar invagination were also more likely to have an associated syrinx. The relevance of the degree of tonsillar herniation and the likelihood of syrinx formation is controversial. Although some have suggested that an intermediate degree of tonsillar herniation (between 9 mm and 14 mm) is more likely to be associated with syrinx than lesser or greater degrees of tonsillar descent [83], this proposition is no longer widely supported. Most studies have shown that syrinx is associated with a greater amount of tonsillar herniation (Fig. 22.4) [21, 23, 84]. Taking these known risk factors into account, it is possible to justify following those with abnormal CSF flow, younger age, and more severe degrees of tonsillar descent with more frequent clinical or imaging assessments.

Spinal syringes in patients with CM I follow a varied and unpredictable natural course. In addition to reports showing stability of syrinx over time, there have been reported cases of regression and complete resolution of syrinx, as well as many instances of symptomatic and imaging progression [6, 8–10, 85, 86]. In the report by Benglis et al. [41], seven patients were followed for spinal syrinx in addition to the CM I. None of these patients had a change in imaging appearance or new neurological deficit over the 3-year follow-up interval. These findings are supported by our

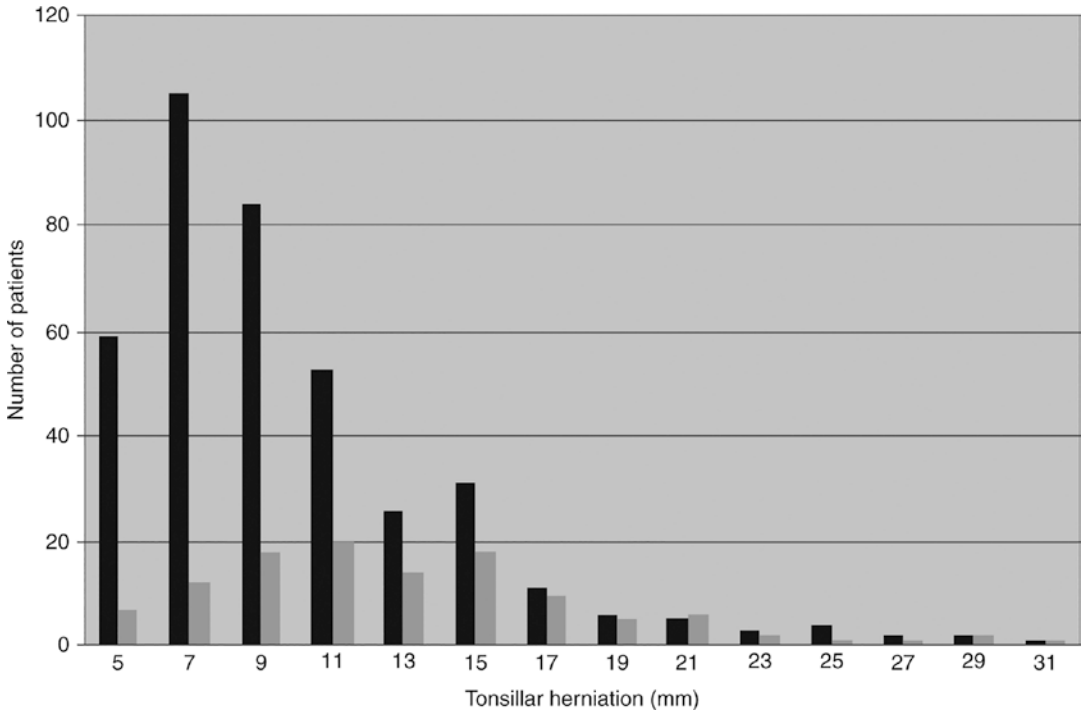

Fig. 22.4 Bar graph illustrating the number of patients with CM I alone (black bars) versus those with both CM I and syrinx (gray bars), according to the measurement (in mm) of tonsillar descent below the foramen magnum. Those with greater amounts of tonsillar decent were more likely to have an associated syrinx

recent natural history analysis [43]. Although it has generally been our practice to recommend surgical treatment for a CM I associated with a spinal syrinx, we identified 13 patients in our series who were known to have a spinal cord syrinx at the time of CM I diagnosis that were managed without surgery. Of the 13 patients with a syrinx at time of CM I diagnosis, 6 were unchanged in size, 5 were smaller, and 2 were larger on follow-up MRI after a period of conservative management (Fig. 22.5). Of the five patients with spontaneous improvement in syrinx size, three demonstrated complete syrinx resolution on follow-up MRI. Patients with syrinx progression (mean age 6.7 years) or regression (mean age 5.6 years) were younger compared with those whose syrinx remained stable (mean age 11.6 years). Patients with new syrinx formation over the follow-up interval had a mean initial tonsillar herniation of 13.5 mm. Those patients with larger syringes on follow-up imaging had a greater mean initial tonsillar herniation (14.5 mm) compared with those patients with stable (8.6 mm) or decreased (8.6 mm) syrinx size. In other series, it has been suggested that surgery may not be necessary in all cases of CM I and syrinx [44, 73]. Nishizawa et al. [44] reported on nine adult patients with incidental CM I and syrinx, only one of which required surgery over a 10-year follow-up interval. They reported no significant change in the MRI characteristics for eight of their nine patients over the follow-up interval. Although the extant literature suggests an unpredictable course for spinal syrinx in those patients with CM I, it is worth remembering that in each of the available natural history studies, patients were selected for non-surgical treatment. It is possible, therefore, that the true natural history for all patients with syrinx and CM I is worse than predicted by outcomes in these series. Future studies will be required before strong recommendations can be made for changing decisions to pursue surgery for patients with spinal syrinx.

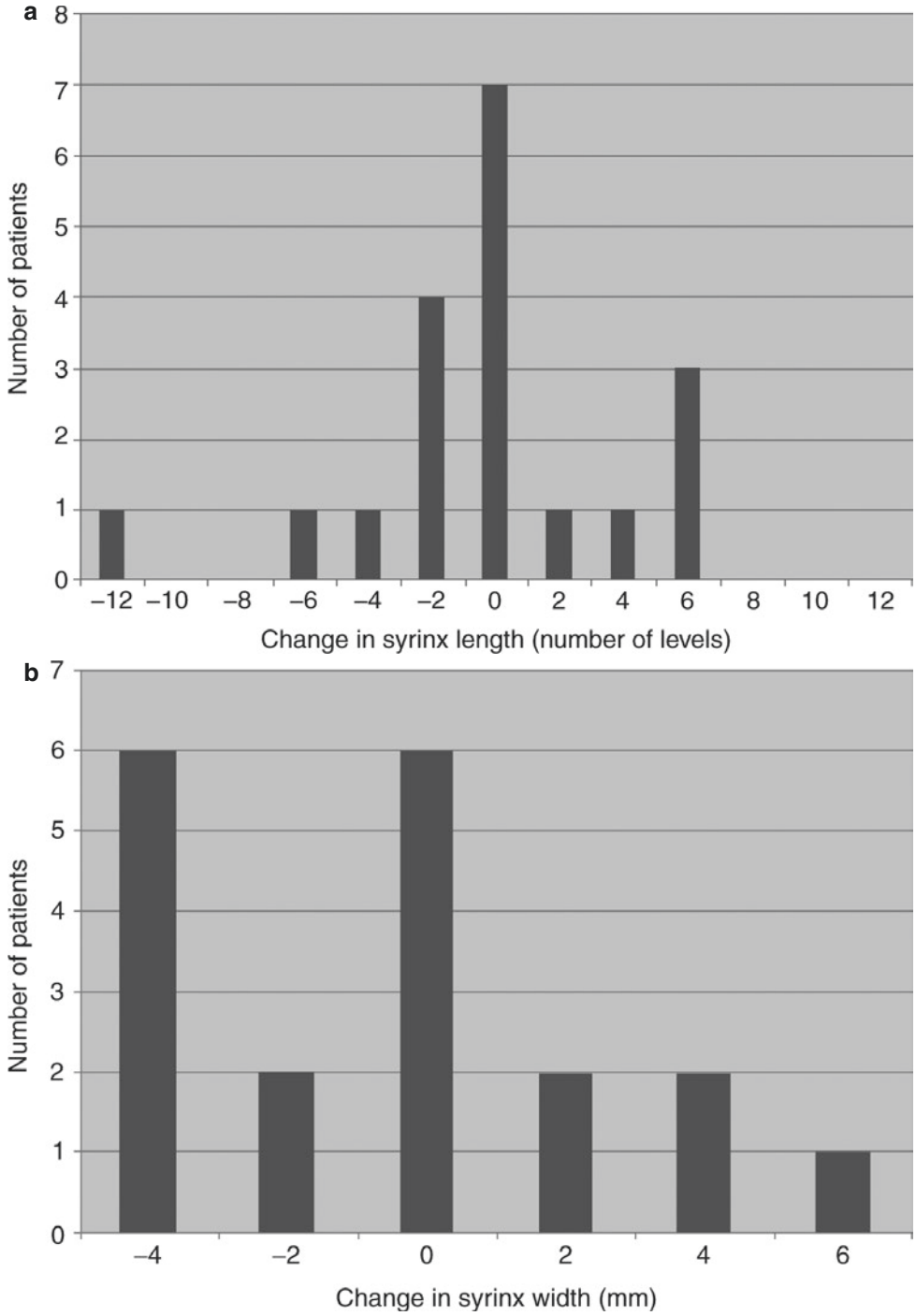

Fig. 22.5 (**a**) Bar graph depicting change in syrinx length by number of levels in patients with spinal cord syrinx at any time over duration of follow-up. (**b**) Bar graph depicting change in syrinx width (mm) in patients with syrinx at any time over duration of follow-up

Prediction of Injury Related to Chiari I

The extent to which physicians should limit sports participation or other activities of patients with CM I found on imaging has been an area of ongoing debate. In the survey by Schijman and Steinbok [3], only 19% of neurosurgeons would prohibit contact sport participation for an asymptomatic child with 9 mm of tonsillar descent, and 46% recommended no restrictions of any kind. Nevertheless, there are many case reports of individual patients with CM I who presented with acute injury or new neurological symptoms following a traumatic event [58, 87–91]. In some of these case reports, there was no connection made between the CM I and the injury, except that the injury occurred in a patient with CM I found on imaging. It is impossible to exclude a coincidental co-occurrence in some of these cases. The relative value of these reports in guiding clinical decision-making can only be understood in the context of the prevalence of CM I in the population. If CM I is relatively more common than previously believed, then it follows that it also is less likely to present with acute worsening following injury than had been feared in the past. There is now reason to believe that this is the case. In my own practice, I generally do not restrict the activities of children with CM I found on imaging if a decision for non-surgical management has been made. Further study of this vexing issue is underway at multiple centers.

Conclusion

Progress has been made in our understanding of the natural history of CM I. Nevertheless, two significant blind spots remain in our understanding of this issue. Since patients who are normally deemed good surgical candidates are treated surgically, there is very little available information on the true natural history of this subgroup of patients. We may infer certain aspects of their natural history from that of the non-operative cohort, but this comparison is inexact. Obviously, any analysis of the natural history of a group of patients who are normally considered good surgical candidates will be difficult to perform. The other remaining blind spot results from our need for longer clinical and imaging follow-up in our natural history analyses. The mean duration of clinical follow-up for most studies cited in this chapter is between 3 and 6 years. This follow-up interval may be insufficient to capture all cases of clinical or radiographic deterioration that could be seen over longer follow-up intervals. Further study on patients over longer time intervals will be necessary in order to define the natural history of CM I over the lifetime of individuals with this diagnosis. Despite these limitations, the available natural history data does help to clarify the natural history of CM I for that subgroup of CM I patients who are considered to be asymptomatic or minimally symptomatic and without neurological deficits.

Acknowledgments The author would like to thank Holly Wagner for providing editorial assistance.

References

1. Haines SJ, Berger M. Current treatment of Chiari malformations types I and II: a survey of the Pediatric Section of the American Association of Neurological Surgeons. Neurosurgery. 1991;28(3):353–7.
2. Haroun RI, Guarnieri M, Meadow JJ, Kraut M, Carson BS. Current opinions for the treatment of syringomyelia and chiari malformations: survey of the Pediatric Section of the American Association of Neurological Surgeons. Pediatr Neurosurg. 2000;33(6):311–7.
3. Schijman E, Steinbok P. International survey on the management of Chiari I malformation and syringomyelia. Childs Nerv Syst. 2004;20(5):341–8.
4. Avellino AM, Britz GW, McDowell JR, Shaw DW, Ellenbogen RG, Roberts TS. Spontaneous resolution of a cervicothoracic syrinx in a child. Case report and review of the literature. Pediatr Neurosurg. 1999;30(1):43–6.
5. Klekamp J, Iaconetta G, Samii M. Spontaneous resolution of Chiari I malformation and syringomyelia: case report and review of the literature. Neurosurgery. 2001;48(3):664–7.
6. Kyoshima K, Bogdanov EI. Spontaneous resolution of syringomyelia: report of two cases and review of the literature. Neurosurgery. 2003;53(3):762–9.
7. Olivero WC, Dinh DH. Chiari I malformation with traumatic syringomyelia and spontaneous resolution: case report and literature review. Neurosurgery. 1992;30(5):758–60.
8. Sun JC, Steinbok P, Cochrane DD. Spontaneous resolution and recurrence of a Chiari I malformation and

associated syringomyelia. Case report. J Neurosurg. 2000;92(2 Suppl):207–10.
9. Sun PP, Harrop J, Sutton LN, Younkin D. Complete spontaneous resolution of childhood Chiari I malformation and associated syringomyelia. Pediatrics. 2001;107(1):182–4.
10. Tokunaga M, Minami S, Isobe K, Moriya H, Kitahara H, Nakata Y. Natural history of scoliosis in children with syringomyelia. J Bone Joint Surg Br. 2001;83(3):371–6.
11. Waldau B, Domeshek LF, Leigh FA, Lum KC, Fuchs HE, Marcus JR, et al. Spontaneous resolution of a 13-mm Chiari malformation type I in relation to differential growth of the posterior fossa volume. J Neurosurg Pediatr. 2009;3(2):110–4.
12. Elliott R, Kalhorn S, Pacione D, Weiner H, Wisoff J, Harter D. Shunt malfunction causing acute neurological deterioration in 2 patients with previously asymptomatic Chiari malformation type I. Report of two cases. J Neurosurg Pediatr. 2009;4(2):170–5.
13. Hopkins TE, Haines SJ. Rapid development of Chiari I malformation in an infant with Seckel syndrome and craniosynostosis. Case report and review of the literature. J Neurosurg. 2003;98(5):1113–5.
14. Lipson AC, Ellenbogen RG, Avellino AM. Radiographic formation and progression of cervical syringomyelia in a child with untreated Chiari I malformation. Pediatr Neurosurg. 2008;44(3):221–3.
15. Massimi L, Caldarelli M, Frassanito P, Di Rocco C. Natural history of Chiari type I malformation in children. Neurol Sci. 2011;32(Suppl 3):275–7.
16. Aboulezz AO, Sartor K, Geyer CA, Gado MH. Position of cerebellar tonsils in the normal population and in patients with Chiari malformation: a quantitative approach with MR imaging. J Comput Assist Tomogr. 1985;9(6):1033–6.
17. Barkovich AJ, Wippold FJ, Sherman JL, Citrin CM. Significance of cerebellar tonsillar position on MR. AJNR Am J Neuroradiol. 1986;7(5):795–9.
18. Rekate HL. Natural history of the Chiari type I anomaly. J Neurosurg Pediatr. 2008;2(3):177–8.
19. Vernooij MW, Ikram MA, Tanghe HL, Vincent AJ, Hofman A, Krestin GP, et al. Incidental findings on brain MRI in the general population. N Engl J Med. 2007;357(18):1821–8.
20. Aitken LA, Lindan CE, Sidney S, Gupta N, Barkovich AJ, Sorel M, et al. Chiari type I malformation in a pediatric population. Pediatr Neurol. 2009;40(6):449–54.
21. Elster AD, Chen MY. Chiari I malformations: clinical and radiologic reappraisal. Radiology. 1992;183(2):347–53.
22. Meadows J, Kraut M, Guarnieri M, Haroun RI, Carson BS. Asymptomatic Chiari type I malformations identified on magnetic resonance imaging. J Neurosurg. 2000;92(6):920–6.
23. Strahle J, Muraszko KM, Kapurch J, Bapuraj JR, Garton HJ, Maher CO. Chiari malformation type I and syrinx in children undergoing magnetic resonance imaging. J Neurosurg Pediatr. 2011;8(2):205–13.
24. Wu YW, Chin CT, Chan KM, Barkovich AJ, Ferriero DM. Pediatric Chiari I malformations: do clinical and radiologic features correlate? Neurology. 1999;53(6):1271–6.
25. Katzman GL, Dagher AP, Patronas NJ. Incidental findings on brain magnetic resonance imaging from 1000 asymptomatic volunteers. JAMA. 1999;282(1):36–9.
26. Weber F, Knopf H. Cranial MRI as a screening tool: findings in 1,772 military pilot applicants. Aviat Space Environ Med. 2004;75(2):158–61.
27. Yue NC, Longstreth WT Jr, Elster AD, Jungreis CA, O'Leary DH, Poirier VC. Clinically serious abnormalities found incidentally at MR imaging of the brain: data from the Cardiovascular Health Study. Radiology. 1997;202(1):41–6.
28. Morris Z, Whiteley WN, Longstreth WT Jr, Weber F, Lee YC, Tsushima Y, et al. Incidental findings on brain magnetic resonance imaging: systematic review and meta-analysis. BMJ. 2009;339:b3016.
29. Mikulis DJ, Diaz O, Egglin TK, Sanchez R. Variance of the position of the cerebellar tonsils with age: preliminary report. Radiology. 1992;183(3):725–8.
30. Luciano MG. Chiari malformation: are children little adults? Neurol Res. 2011;33(3):272–7.
31. Tubbs RS, Elton S, Bartolucci AA, Grabb P, Oakes WJ. The position of the conus medullaris in children with a Chiari I malformation. Pediatr Neurosurg. 2000;33(5):249–51.
32. Tubbs RS, Hill M, Loukas M, Shoja MM, Oakes WJ. Volumetric analysis of the posterior cranial fossa in a family with four generations of the Chiari malformation type I. J Neurosurg Pediatr. 2008;1(1):21–4.
33. Tubbs RS, Loukas M, Shoja MM, Oakes WJ. Observations at the craniocervical junction with simultaneous caudal traction of the spinal cord. Childs Nerv Syst. 2007;23(4):367–9.
34. Sgouros S. Acquired Chiari I malformation in a child with corrected diastematomyelia disappeared after thickened filum division. Pediatr Neurosurg. 2010;46(5):402–5.
35. Atkinson JL, Weinshenker BG, Miller GM, Piepgras DG, Mokri B. Acquired Chiari I malformation secondary to spontaneous spinal cerebrospinal fluid leakage and chronic intracranial hypotension syndrome in seven cases. J Neurosurg. 1998;88(2):237–42.
36. Padmanabhan R, Crompton D, Burn D, Birchall D. Acquired Chiari 1 malformation and syringomyelia following lumboperitoneal shunting for pseudotumour cerebri. J Neurol Neurosurg Psychiatry. 2005;76(2):298.
37. Tubbs RS, Law C, Oakes WJ, Grabb PA. Acquired Chiari I malformation following baclofen pump placement in a child. Case report. J Neurosurg. 2004;101(2 Suppl):211–3.
38. Guillen A, Costa JM. Spontaneous resolution of a Chiari I malformation associated syringomyelia in one child. Acta Neurochir. 2004;146(2):187–91.
39. Jack CR Jr, Kokmen E, Onofrio BM. Spontaneous decompression of syringomyelia: magnetic reso-

nance imaging findings. Case report. J Neurosurg. 1991;74(2):283–6.
40. Furtado SV, Thakar S, Hegde AS. Correlation of functional outcome and natural history with clinicoradiological factors in surgically managed pediatric Chiari I malformation. Neurosurgery. 2011;68(2):319–28.
41. Benglis D Jr, Covington D, Bhatia R, Bhatia S, Elhammady MS, Ragheb J, et al. Outcomes in pediatric patients with Chiari malformation type I followed up without surgery. J Neurosurg Pediatr. 2011;7(4):375–9.
42. Novegno F, Caldarelli M, Massa A, Chieffo D, Massimi L, Pettorini B, et al. The natural history of the Chiari type I anomaly. J Neurosurg Pediatr. 2008;2(3):179–87.
43. Strahle J, Muraszko KM, Kapurch J, Bapuraj JR, Garton HJ, Maher CO. Natural history of Chiari malformation type I following decision for conservative treatment. J Neurosurg Pediatr. 2011;8(2):214–21.
44. Nishizawa S, Yokoyama T, Yokota N, Tokuyama T, Ohta S. Incidentally identified syringomyelia associated with Chiari I malformations: is early interventional surgery necessary? Neurosurgery. 2001;49(3):637–41.
45. Grazzi L, Usai S. Headache and Chiari malformation in young age: clinical aspects and differential diagnosis. Neurol Sci. 2011;32(Suppl 3):299–301.
46. Alvarez D, Requena I, Arias M, Valdes L, Pereiro I, De la Torre R. Acute respiratory failure as the first sign of Arnold-Chiari malformation associated with syringomyelia. Eur Respir J. 1995;8(4):661–3.
47. Bullock R, Todd NV, Easton J, Hadley D. Isolated central respiratory failure due to syringomyelia and Arnold-Chiari malformation. BMJ. 1988;297(6661):1448–9.
48. Fish DR, Howard RS, Wiles CM, Simon L. Respiratory arrest: a complication of cerebellar ectopia in adults. J Neurol Neurosurg Psychiatry. 1988;51(5):714–6.
49. Hamlat A, Helal H, Carsin-Nicol B, Brassier G, Guegan Y, Morandi X. Acute presentation of hydromyelia in a child. Acta Neurochir. 2006;148(10):1117–21.
50. Quebada PB, Duhaime AC. Chiari malformation type I and a dolichoodontoid process responsible for sudden cardiorespiratory arrest. Case report. J Neurosurg. 2005;103(6 Suppl):567–70.
51. Stephany JD, Garavaglia JC, Pearl GS. Sudden death in a 27-year-old man with Chiari I malformation. Am J Forensic Med Pathol. 2008;29(3):249–50.
52. Tomaszek DE, Tyson GW, Bouldin T, Hansen AR. Sudden death in a child with an occult hindbrain malformation. Ann Emerg Med. 1984;13(2):136–8.
53. Tsara V, Serasli E, Kimiskidis V, Papagianopoulos S, Katsaridis V, Fylaktakis M, et al. Acute respiratory failure and sleep-disordered breathing in Arnold-Chiari malformation. Clin Neurol Neurosurg. 2005;107(6):521–4.
54. Wellons JC 3rd, Tubbs RS, Bui CJ, Grabb PA, Oakes WJ. Urgent surgical intervention in pediatric patients with Chiari malformation type I. Report of two cases. J Neurosurg. 2007;107(1 Suppl):49–52.
55. Yoshikawa H. Sudden respiratory arrest and Arnold-Chiari malformation. Eur J Paediatr Neurol. 2003;7(4):191.
56. Zager EL, Ojemann RG, Poletti CE. Acute presentations of syringomyelia. Report of three cases. J Neurosurg. 1990;72(1):133–8.
57. Ziegler DK, Mallonee W. Chiari-1 malformation, migraine, and sudden death. Headache. 1999;39(1):38–41.
58. Kurup H, Lawrence T, Hargreaves D. Transient quadriparesis following neck injury: presentation of a Chiari I malformation. Eur J Orthop Surg Traumatol. 2005;15:319–21.
59. Tubbs RS, Beckman J, Naftel RP, Chern JJ, Wellons JC 3rd, Rozzelle CJ, et al. Institutional experience with 500 cases of surgically treated pediatric Chiari malformation type I. J Neurosurg Pediatr. 2011;7(3):248–56.
60. Tubbs RS, Lyerly MJ, Loukas M, Shoja MM, Oakes WJ. The pediatric Chiari I malformation: a review. Childs Nerv Syst. 2007;23(11):1239–50.
61. Guo F, Wang M, Long J, Wang H, Sun H, Yang B, et al. Surgical management of Chiari malformation: analysis of 128 cases. Pediatr Neurosurg. 2007;43(5):375–81.
62. Milhorat TH, Chou MW, Trinidad EM, Kula RW, Mandell M, Wolpert C, et al. Chiari I malformation redefined: clinical and radiographic findings for 364 symptomatic patients. Neurosurgery. 1999;44(5):1005–17.
63. Zhang ZQ, Chen YQ, Chen YA, Wu X, Wang YB, Li XG. Chiari I malformation associated with syringomyelia: a retrospective study of 316 surgically treated patients. Spinal Cord. 2008;46(5):358–63.
64. Krieger MD, McComb JG, Levy ML. Toward a simpler surgical management of Chiari I malformation in a pediatric population. Pediatr Neurosurg. 1999;30(3):113–21.
65. Saez RJ, Onofrio BM, Yanagihara T. Experience with Arnold-Chiari malformation, 1960 to 1970. J Neurosurg. 1976;45(4):416–22.
66. Dones J, De Jesus O, Colen CB, Toledo MM, Delgado M. Clinical outcomes in patients with Chiari I malformation: a review of 27 cases. Surg Neurol. 2003;60(2):142–8.
67. Genitori L, Peretta P, Nurisso C, Macinante L, Mussa F. Chiari type I anomalies in children and adolescents: minimally invasive management in a series of 53 cases. Childs Nerv Syst. 2000;16(10–11):707–18.
68. Navarro R, Olavarria G, Seshadri R, Gonzales-Portillo G, McLone DG, Tomita T. Surgical results of posterior fossa decompression for patients with Chiari I malformation. Childs Nerv Syst. 2004;20(5):349–56.
69. Aghakhani N, Parker F, David P, Morar S, Lacroix C, Benoudiba F, et al. Long-term follow-up of Chiari-

related syringomyelia in adults: analysis of 157 surgically treated cases. Neurosurgery. 2009;64(2):308–15.
70. Aydin S, Hanimoglu H, Tanriverdi T, Yentur E, Kaynar MY. Chiari type I malformations in adults: a morphometric analysis of the posterior cranial fossa. Surg Neurol. 2005;64(3):237–41.
71. Armonda RA, Citrin CM, Foley KT, Ellenbogen RG. Quantitative cine-mode magnetic resonance imaging of Chiari I malformations: an analysis of cerebrospinal fluid dynamics. Neurosurgery. 1994;35(2):214–24.
72. Blagodatsky MD, Larionov SN, Manohin PA, Shanturov VA, Gladyshev YV. Surgical treatment of "hindbrain related" syringomyelia: new data for pathogenesis. Acta Neurochir. 1993;124(2–4):82–5.
73. Bogdanov EI, Mendelevich EG. Syrinx size and duration of symptoms predict the pace of progressive myelopathy: retrospective analysis of 103 unoperated cases with craniocervical junction malformations and syringomyelia. Clin Neurol Neurosurg. 2002;104(2):90–7.
74. Cahan LD, Bentson JR. Considerations in the diagnosis and treatment of syringomyelia and the Chiari malformation. J Neurosurg. 1982;57(1):24–31.
75. Eule JM, Erickson MA, O'Brien MF, Handler M. Chiari I malformation associated with syringomyelia and scoliosis: a twenty-year review of surgical and nonsurgical treatment in a pediatric population. Spine (Phila Pa 1976). 2002;27(13):1451–5.
76. Hida K, Iwasaki Y, Koyanagi I, Abe H. Pediatric syringomyelia with chiari malformation: its clinical characteristics and surgical outcomes. Surg Neurol. 1999;51(4):383–91.
77. Oldfield EH, Muraszko K, Shawker TH, Patronas NJ. Pathophysiology of syringomyelia associated with Chiari I malformation of the cerebellar tonsils. Implications for diagnosis and treatment. J Neurosurg. 1994;80(1):3–15.
78. Pujol J, Roig C, Capdevila A, Pou A, Marti-Vilalta JL, Kulisevsky J, et al. Motion of the cerebellar tonsils in Chiari type I malformation studied by cine phase-contrast MRI. Neurology. 1995;45(9):1746–53.
79. Menezes AH. Chiari I malformations and hydromyelia–complications. Pediatr Neurosurg. 1991;17(3):146–54.
80. Fischbein NJ, Dillon WP, Cobbs C, Weinstein PR. The "presyrinx" state: a reversible myelopathic condition that may precede syringomyelia. AJNR Am J Neuroradiol. 1999;20(1):7–20.
81. Goh S, Bottrell CL, Aiken AH, Dillon WP, Wu YW. Presyrinx in children with Chiari malformations. Neurology. 2008;71(5):351–6.
82. Levy EI, Heiss JD, Kent MS, Riedel CJ, Oldfield EH. Spinal cord swelling preceding syrinx development. Case report. J Neurosurg. 2000;92(1 Suppl):93–7.
83. Stovner LJ, Rinck P. Syringomyelia in Chiari malformation: relation to extent of cerebellar tissue herniation. Neurosurgery. 1992;31(5):913–7.
84. Pillay PK, Awad IA, Little JR, Hahn JF. Symptomatic Chiari malformation in adults: a new classification based on magnetic resonance imaging with clinical and prognostic significance. Neurosurgery. 1991;28(5):639–45.
85. Sudo K, Doi S, Maruo Y, Tashiro K, Terae S, Miyasaka K, et al. Syringomyelia with spontaneous resolution. J Neurol Neurosurg Psychiatry. 1990;53(5):437–8.
86. Sudo K, Tashiro K, Isu T. Spontaneous drainage in syringomyelia. J Neurosurg. 1994;80(5):950–1.
87. Bunc G, Vorsic M. Presentation of a previously asymptomatic Chiari I malformation by a flexion injury to the neck. J Neurotrauma. 2001;18(6):645–8.
88. Callaway GH, O'Brien SJ, Tehrany AM. Chiari I malformation and spinal cord injury: cause for concern in contact athletes? Med Sci Sports Exerc. 1996;28(10):1218–20.
89. Harrell BR, Barootes BG. The type I Chiari malformation in a previously asymptomatic college athlete: addressing the issue of return to athletic participation. Clin J Sport Med. 2010;20(3):215–7.
90. Riviello JJ Jr, Marks HG, Faerber EN, Steg NL. Delayed cervical central cord syndrome after trivial trauma. Pediatr Emerg Care. 1990;6(2):113–7.
91. Wan MJ, Nomura H, Tator CH. Conversion to symptomatic Chiari I malformation after minor head or neck trauma. Neurosurgery. 2008;63(4):748–53.

Genetics of the Chiari I and II Malformations

23

Christina A. Markunas, Allison E. Ashley-Koch, and Simon G. Gregory

Introduction

Chiari malformations are considered to be genetically complex with multiple genetic and environmental factors potentially contributing to disease development. As a result, the genetic dissection of Chiari malformations is expected to be challenging. The substantial genetic heterogeneity is likely reflected in the observed phenotypic heterogeneity. Therefore, an important first step is to accurately define the phenotype. Misclassification of patients can result in inclusion of unknown disease subtypes with distinct genetic etiologies, as well as individuals with different diseases or even without disease, all of which will negatively impact the ability to localize "Chiari genes." Identification of subgroups of patients with similar clinical characteristics should reduce the phenotypic heterogeneity and ultimately genetic heterogeneity, as well. This approach may lead to improved power to identify Chiari genes. Often the next step to genetic dissection of a complex disorder is to determine if sufficient evidence exists to support a genetic component for the disease. Researchers often look for familial aggregation of the disease, disease concordance between twins, animal models of the disease where a gene has been identified, as well as co-occurrence of the disease with known genetic syndromes. Importantly, it is the preponderance of evidence from multiple well-designed studies that provide the strongest support.

Once sufficient genetic evidence exists, experimental design follows and depends on a variety of factorsc, including the main goal of the study, disease prevalence, proportion of sporadic versus familial cases, age of disease onset, disease-specific mortality, and practical considerations such as personnel and financial resources. Population ascertainment is a key component of study design that demands a great deal of time and planning to ensure enrollment criteria are met (e.g., disease phenotype criteria and clinical exclusion criteria at the personal and family history level). Once study participants are enrolled, data generation, analysis, and validation (test findings using another method or technique), replication (test findings in a separate study population), and interpretation of findings usually follow. This entire process can take even a large research team many years to complete and can cost anywhere from tens of thousands to millions of dollars.

C. A. Markunas
Behavioral Health Research Division, RTI International, Durham, NC, USA

A. E. Ashley-Koch (✉)
Departments of Medicine, and Biostatistics and Bioinformatics, Duke Molecular Physiology Institute, Durham, NC, USA
e-mail: allison.ashleykoch@duke.edu

S. G. Gregory
Department of Neurology, Duke Molecular Physiology Institute, Durham, NC, USA

R. S. Tubbs et al. (eds.), *The Chiari Malformations*, https://doi.org/10.1007/978-3-030-44862-2_23

Given that genetic studies expend tremendous financial and personnel resources, much of what is currently known about the genetics of Chiari relates to the collection of data supporting a genetic contribution to the disease, as this is one of the first steps to complete before embarking on more costly genetic studies. There are several lines of evidence including twin studies, familial aggregation, co-occurrence with known genetic syndromes, as well as previous genetic studies that suggest a genetic component in at least a subset of Chiari I malformation cases, while our understanding of the genetic causes of Chiari II malformation is more limited. As such, the focus of this chapter will be primarily on the genetics of Chiari I malformation but will conclude with a brief discussion of Chiari II malformation genetics at the end of the chapter.

Chiari I Malformation

Twin Studies

Twin studies allow researchers to identify the genetic contribution for a disease by comparing the concordance of disease between monozygotic twins (share 100% of their genome) to dizygotic twins (share on average 50% of their genome). This approach helps establish if a disease is at least due in part to genetic causes. However, there are several important factors to consider in terms of the design and interpretation of twin studies, especially in the context of complex disease; these include (1) whether a common pre- and postnatal environment were shared between the twins, (2) what additional factors might explain discordance between monozygotic twins (e.g., epigenetic factors or modifications to the genome that do not change the underlying DNA sequence but may affect things such as gene expression), and (3) if the dizygotic twins are of the same sex. The latter point is particularly important in the context of Chiari malformation, as females appear to be three times more likely to be affected with Chiari I malformation than males [1].

The largest Chiari I malformation twin study to date compared three sets of monozygotic twins (two sets of sisters, one set of brothers) to three sets of dizygotic twins (three sets of sisters) and found a higher concordance between monozygotic twins compared to dizygotic twins [2]. Multiple reports have also described concordance between single sets of monozygotic twins [3–9] and one set of monozygotic triplets [10]. In general, twins were concordant with respect to the Chiari I malformation diagnosis, although they were sometimes discordant in terms of other factors, including the presence of syringomyelia, age of onset, extent of tonsillar herniation, and symptom severity. Discordance with respect to the Chiari I malformation diagnosis between monozygotic twins was noted in at least three studies [3, 8, 10]; however, these differences can likely be attributed to the absence of standardized classification of Chiari malformation patients and our current poor understanding on how best to define the disorder, for example: (1) Iwasaki and colleagues [8] described one twin sister as having Chiari I malformation and the other as having mild tonsillar ectopia (6 mm herniation); (2) Tubbs and colleagues [3] reported a set of twin brothers, one diagnosed with Chiari I malformation and the other with Chiari 0 malformation; and (3) Cavender and colleagues [10] described monozygotic female triplets, one of which was diagnosed with Chiari I malformation, and the other two were diagnosed with varying degrees of tonsillar ectopia (4 and 2.5 mm herniation).

Familial Aggregation

Familial aggregation or clustering refers to the identification of families where multiple members are affected with the disease of interest. It is important to keep in mind that the observation of multiple affected individuals in a family does not mean that the disease is genetic. One must also consider that this observation is due to chance or environmental causes. In the case of Chiari I malformation, there are an overwhelming number of reports of familial clustering [1, 5, 6, 9, 11–23] that in combination with other observations (e.g., results from the twin studies, frequent observations that multiple family generations are

affected with the disease, many families contain even more than two affected family members, and many families appear to be spread out geographically) makes it less likely to be observed by chance or solely due to an environmental factor(s). There have also been multiple reports of familial syringomyelia, some of which have Chiari I malformation (reviewed in Ref. [20]).

In addition to family studies, several studies have provided estimates of the proportion of patients with a positive family history for Chiari I malformation. In a seminal paper by Milhorat and colleagues, it was reported that out of a cohort of 364 symptomatic patients, 43 (12%) had at least 1 close relative with Chiari I malformation with or without syringomyelia or idiopathic syringomyelia [1]. Additionally, 72 patients (20%) were reported as having at least 1 close relative with a similar symptomology without an official Chiari I malformation diagnosis [1]. In a large retrospective review of 500 Chiari I pediatric surgical patients, only 3% of patients had a positive family history for Chiari I malformation [24]. When interpreting these results, it is important to note that these studies are based on highly selected samples of patients and, in the absence of neuroimaging on all family members, it is difficult to obtain accurate diagnoses.

Although a proper segregation analysis has not been conducted previously for Chiari malformation, the mode of inheritance has been suggested to be either autosomal dominant (vertical inheritance, with male-to-male transmission) with reduced penetrance (disease appears to be transmitted through "unaffected" relatives) or autosomal recessive (horizontal inheritance) [1]; however, Chiari malformation is likely to be more complex and influenced by multiple genetic, epigenetic, and environmental factors.

Heritability

Heritability refers to the proportion of phenotypic variation in a population that is attributable to genetic variation among individuals. In other words, if something is found to be significantly heritable, it is likely to have a genetic component. Heritability estimates of the posterior fossa are especially important to the genetics of Chiari malformation as the posterior fossa is compromised in many Chiari I malformation patients and is likely to play an important role in the development of the malformation in at least some patients [25].

Heritability has been previously estimated for various components of the posterior fossa using 99 individuals from 35 Chiari I malformation families [23]. In this study, posterior fossa measurements were taken from pre-surgical magnetic resonance images (MRIs) from both affected and unaffected family members. Out of the 11 measurements examined, the posterior fossa volume ($H^2r = 0.96$, $p = 0.0035$) and basal angle ($H^2r = 0.51$, $p = 0.0144$) were significantly heritable in the families. The clivus ($H^2r = 0.39$, $p = 0.0542$) and the supraoccipital bone ($H^2r = 0.28$, $p = 0.0685$) were also nearing significance. These results were based on a small sample size, so additional heritability studies are needed to try and separate the various genetic and environmental components contributing to the observed trait variation.

Co-occurrence with Known Genetic Syndromes

Another important tool that geneticists use to determine that a disease has a genetic component is to determine if a disease co-occurs with another syndrome with a known genetic basis. If the two diseases co-occur more often than would be expected by chance, then this would suggest that the diseases may be related and perhaps share an underlying genetic risk. For example, if two diseases are independent and both occur at a population frequency of 0.10, one would expect the diseases to co-occur at a frequency of 0.01 (0.10×0.10) in the population. In selected populations, such as a cohort of Chiari patients, the prevalence of another disease in that cohort therefore needs to be higher than that observed in the general population for it to represent a potentially meaningful association.

Although more than 20 genetic syndromes have been previously described as co-occurring with Chiari I malformation [2], many of these are based on single-case reports in the literature, and more data are needed in order to rule out spurious associations. Examples of the more commonly associated genetic syndromes include Ehlers-Danlos syndrome [26–29], Marfan syndrome [26, 30–32], Klippel-Feil syndrome [1, 24, 33–43], growth hormone deficiency [24, 40, 44–50], Paget's disease [51–53], craniosynostosis [54, 55], Goldenhar syndrome [56–58], Williams syndrome [59–61], Kabuki syndrome [62, 63], hypophosphatemic rickets [64, 65], and neurofibromatosis type I [66, 67]. In some of these reports, authors hypothesize that the Chiari I malformation is "acquired," occurring secondarily to the primary genetic syndrome [30, 36, 52]. In addition, there have also been multiple reports of Chiari I malformation co-occurring with other diseases or syndromes in patients where chromosomal aberrations or genetic defects have been identified. These include a 16p11.2 rearrangement [68], 17p13.3 deletion distal to PAFAH1B1 [69], FOXP1 haploinsufficiency [70], 5p13.3–13.2 deletion [71], germline-activating mutation in TSHR [72], and pentasomy 49,XXXXY [73], among others.

Genetic Studies

Genetic studies can encompass a wide range of study designs depending on the research goal. These may vary by scale (e.g., candidate gene versus whole-genome studies), the type of data generated (e.g., genotype versus gene expression data), as well as the analysis conducted (e.g., association versus linkage). As the development of new genetic techniques and technologies has increased over the years, it has become increasingly feasible to conduct large-scale genetic screens within reasonable time frames and financial constraints. However, regardless of time and money, a separate barrier to genetic research is the ability to ascertain a large enough study population that meets enrollment criteria. Consequently, very few genetic screens have been conducted for Chiari malformations to date, but data from ongoing studies, including the authors' own, will improve this number in coming years.

As mentioned previously, there are multiple varieties of genetic studies that can be employed to detect a genetic component for a disease. One of the first reported genetic studies for Chiari was conducted in 1982 and was a candidate gene association analysis of the human leukocyte antigen (HLA) locus [74]. HLA-A, HLA-B, and HLA-C antigen frequencies were compared between 53 patients with syringomyelia, 40 of whom had a Chiari anomaly (type not specified), and 500 pooled controls. After correction for multiple testing, a significant increase of HLA-A9 was observed in patients with syringomyelia (corrected $p = 0.007$). When restricted to the Chiari cases, an increased frequency was still observed but did not remain significant after correction (uncorrected $p = 0.0038$; corrected $p = 0.11$). Authors suggested that perhaps there is an association between the HLA locus and the development of syringomyelia or Chiari malformation.

Another type of genetic screen that can be carried out is a candidate gene sequencing study. In this type of study, investigators select a gene based on biological relevance, perhaps in combination with positional information, and then sequence that gene in a number of cases and controls to identify DNA sequence changes (mutations and/or polymorphisms) that may be associated with the disease. The first candidate gene sequencing study for Chiari I malformation was published in 2003 [2]. Speer and colleagues investigated an excellent biological candidate gene, Noggin, which is known to play an important role in development. Thirty-three cases of nonsyndromic Chiari I were screened for mutations in the coding region and part of the 3′ and 5′ untranslated region by first using pooled samples and denaturing high-performance liquid chromatography, followed by Sanger sequencing to validate potential mutations. No mutations were identified in the 33 Chiari I cases, leading researchers to conclude that Noggin mutations are unlikely to represent a common etiology of Chiari I malformation.

A whole-genome linkage study is another type of genetic screen. The goal of this analysis is to identify regions of the genome that segregate with the disease in families or show excess sharing across affected family members. The only whole-genome linkage screen published to date for Chiari malformation consisted of 23 Caucasian multiplex (two or more affected individuals) families containing 67 sampled individuals affected with Chiari I malformation with or without syringomyelia [23]. Individuals were genotyped using the whole-genome Affymetrix 10K SNP Chip (TGen, Phoenix, AZ). Both parametric and nonparametric 2-point and multipoint linkage analyses were conducted. Significant evidence for linkage was identified on regions of chromosomes 9 and 15. Biologically plausible candidate genes within these intervals were explored, and in particular, the authors discussed the gene, Fibrillin-1, located on chromosome 15 due to its role in Marfan syndrome, ectopia lentis, and Shprintzen-Goldberg syndrome; however, sequencing studies to identify causal DNA mutations were not performed.

Chiari II Malformation

While little is known about the genetics of Chiari I malformation, even less is known about the genetics of Chiari II malformation. To our knowledge, there have been no reports of twin studies and only one possible report of familial Arnold-Chiari malformation (unspecified type) occurring in sisters [75]. The sisters were both described as having Arnold-Chiari malformation, myelomeningocele, and hydrocephalus, among other findings [75]. There have been multiple reports of Chiari II malformation co-occurring with known genetic syndromes, including trisomy 18 [76], Kousseff syndrome [77], lathosterolosis [78], Klippel-Feil syndrome [79–81], Duchenne muscular dystrophy [82], spondyloepiphyseal dysplasia tarda [83], velocardiofacial syndrome [84], and osteogenesis imperfecta [85]. While this may lend some limited support to a genetic etiology, with the exception of Klippel-Feil syndrome, these all appear to be single-case reports; thus we are unable to rule out the fact that these diseases co-occurred due to chance or that the association is due to another nongenetic reason.

It is widely believed that all patients with myelomeningocele have a Chiari II malformation [86, 87]. Neural tube defects (NTDs), such as myelomeningocele, are thought to be influenced by genetic as well as environmental factors. While multiple studies have been published on the genetics of NTDs [88], one study reported that while screening patients with NTDs for mutations in the candidate gene, VANGL1, a missense mutation was identified in a sporadic case with myelomeningocele, Chiari II malformation, hydrocephalus, tethered cord, club feet, scoliosis, and kyphosis [89]. Kibar and colleagues also identified two additional VANGL1 missense mutations in familial cases, one of which was also described as having myelomeningocele, but there was no mention of a Chiari II malformation diagnosis [89].

There have been no genetic screens conducted to date for Chiari II malformation specifically; however, there have been a few reports focusing on the expression of candidate genes in the ependyma of Chiari II patients, two of which focused primarily on hydrocephalus [84, 90, 91]. One study in particular found that ependymal vimentin was overexpressed only in regions of dysgenesis in Chiari II malformation fetuses and young infants [84]. Vimentin is a cytoskeletal protein that forms intermediate filaments in multiple cells belonging to the immature nervous system [92]. It was suggested that the upregulation of vimentin occurred secondarily in response to aberrant expression of another gene [84]. Although many theories have been proposed regarding the pathogenesis of Chiari II malformation [87, 93], some genetic hypotheses exist including Williams' hypothesis that both genetics and environment play a role in the underdeveloped posterior fossa or vertebral dysgenesis, which results in altered cerebrospinal fluid (CSF) pressure and Chiari II malformation and spina bifida [94], as well as Sarnat's hypothesis that a genetic mutation perhaps in the HOX, WNT, or PAX gene families may be responsible for the rhombomeric segmentation defect as well as the underdevelopment of the posterior fossa [84].

Conclusion

The accumulation of data over the years has established that there is a preponderance of evidence supporting a genetic contribution to at least a subset of Chiari I malformation patients, and the field is at a point where significant progress is being made in this area of research. Although there is strong evidence that genetics play an important role in the development of at least certain forms of Chiari malformation, Chiari malformation is likely to have a multifactorial etiology, influenced by genetic, epigenetic, as well as environmental factors. While it is important not to discount these other nongenetic contributions to disease, there are many potential benefits of genetic research. Future genetic analyses will likely result in the identification of a gene or genes that increase susceptibility to Chiari malformation that may later be translated into a genetic test resulting in more accurate and quicker diagnoses. This can be especially useful for complex diseases, such as Chiari malformation, where the symptoms are vague and not unique to a disorder, resulting in slow diagnoses and even misdiagnoses [1].

Understanding the genetics of a disease can provide more information on the underlying disease mechanism and can also indicate which specific biological processes play a role in disease development. There is also the exciting potential for the development of new therapies and treatments targeting identified genes or pathways that are dysregulated, which may ultimately provide patients with alternative treatment options to surgery.

References

1. Milhorat TH, Chou MW, Trinidad EM, Kula RW, Mandell M, Wolpert C, et al. Chiari I malformation redefined: clinical and radiographic findings for 364 symptomatic patients. Neurosurgery. 1999;44(5):1005–17.
2. Speer MC, Enterline DS, Mehltretter L, Hammock P, Joseph J, Dickerson M, et al. Chiari type I malformation with or without syringomyelia: prevalence and genetics. J Genet Couns. 2003;12:297–311.
3. Tubbs RS, Wellons JC 3rd, Blount JP, Oakes WJ. Syringomyelia in twin brothers discordant for Chiari I malformation: case report. J Child Neurol. 2004;19(6):459–62.
4. Turgut M. Chiari type I malformation in two monozygotic twins. Br J Neurosurg. 2001;15(3):279–80.
5. Stovner LJ, Cappelen J, Nilsen G, Sjaastad O. The Chiari type I malformation in two monozygotic twins and first-degree relatives. Ann Neurol. 1992;31(2):220–2.
6. Atkinson JL, Kokmen E, Miller GM. Evidence of posterior fossa hypoplasia in the familial variant of adult Chiari I malformation: case report. Neurosurgery. 1998;42(2):401–3; discussion 4.
7. Solth A, Barrett C, Holliman D, Mitchell P. Chiari malformation in female monozygotic twins. Br J Neurosurg. 2010;24(5):607–8.
8. Iwasaki Y, Hida K, Onishi K, Nanba R. Chiari malformation and syringomyelia in monozygotic twins: birth injury as a possible cause of syringomyelia – case report. Neurol Med Chir (Tokyo). 2000;40(3):176–8.
9. Szewka AJ, Walsh LE, Boaz JC, Carvalho KS, Golomb MR. Chiari in the family: inheritance of the Chiari I malformation. Pediatr Neurol. 2006;34(6):481–5.
10. Cavender RK, Schmidt JH 3rd. Tonsillar ectopia and Chiari malformations: monozygotic triplets. Case report. J Neurosurg. 1995;82(3):497–500.
11. Gimenez-Roldan S, Benito C, Mateo D. Familial communicating syringomyelia. J Neurol Sci. 1978;36(1):135–46.
12. Coria F, Quintana F, Rebollo M, Combarros O, Berciano J. Occipital dysplasia and Chiari type I deformity in a family. Clinical and radiological study of three generations. J Neurol Sci. 1983;62(1–3):147–58.
13. George S, Page AB. Familial Arnold-Chiari type I malformation. Eye (Lond). 2006;20(3):400–2.
14. Herman MD, Cheek WR, Storrs BB. Two siblings with the Chiari I malformation. Pediatr Neurosurg. 1990;16(3):183–4.
15. Mavinkurve GG, Sciubba D, Amundson E, Jallo GI. Familial Chiari type I malformation with syringomyelia in two siblings: case report and review of the literature. Childs Nerv Syst. 2005;21(11):955–9.
16. Schanker BD, Walcott BP, Nahed BV, Kahle KT, Li YM, Coumans JV. Familial Chiari malformation: case series. Neurosurg Focus. 2011;31(3):E1.
17. Stovner LJ, Sjaastad O. Segmental hyperhidrosis in two siblings with Chiari type I malformation. Eur Neurol. 1995;35(3):149–55.
18. Tubbs RS, Hill M, Loukas M, Shoja MM, Oakes WJ. Volumetric analysis of the posterior cranial fossa in a family with four generations of the Chiari malformation type I. J Neurosurg Pediatr. 2008;1(1):21–4.
19. Weisfeld-Adams JD, Carter MR, Likeman MJ, Rankin J. Three sisters with Chiari I malformation with and without associated syringomyelia. Pediatr Neurosurg. 2007;43(6):533–8.
20. Yabe I, Kikuchi S, Tashiro K. Familial syringomyelia: the first Japanese case and review of the literature. Clin Neurol Neurosurg. 2002;105(1):69–71.

21. Zakeri A, Glasauer FE, Egnatchik JG. Familial syringomyelia: case report and review of the literature. Surg Neurol. 1995;44(1):48–53.
22. Speer MC, George TM, Enterline DS, Franklin A, Wolpert CM, Milhorat TH. A genetic hypothesis for Chiari I malformation with or without syringomyelia. Neurosurg Focus. 2000;8(3):E12.
23. Boyles AL, Enterline DS, Hammock PH, Siegel DG, Slifer SH, Mehltretter L, et al. Phenotypic definition of Chiari type I malformation coupled with high-density SNP genome screen shows significant evidence for linkage to regions on chromosomes 9 and 15. Am J Med Genet A. 2006;140(24):2776–85.
24. Tubbs RS, Beckman J, Naftel RP, Chern JJ, Wellons JC 3rd, Rozzelle CJ, et al. Institutional experience with 500 cases of surgically treated pediatric Chiari malformation type I. J Neurosurg Pediatr. 2011;7(3):248–56.
25. Noudel R, Jovenin N, Eap C, Scherpereel B, Pierot L, Rousseaux P. Incidence of basioccipital hypoplasia in Chiari malformation type I: comparative morphometric study of the posterior cranial fossa. Clinical article. J Neurosurg. 2009;111(5):1046–52.
26. Milhorat TH, Bolognese PA, Nishikawa M, McDonnell NB, Francomano CA. Syndrome of occipitoatlantoaxial hypermobility, cranial settling, and chiari malformation type I in patients with hereditary disorders of connective tissue. J Neurosurg Spine. 2007;7(6):601–9.
27. Castori M, Camerota F, Celletti C, Danese C, Santilli V, Saraceni VM, et al. Natural history and manifestations of the hypermobility type Ehlers-Danlos syndrome: a pilot study on 21 patients. Am J Med Genet A. 2010;152A(3):556–64.
28. Jacome DE. Blepharoclonus and Arnold-Chiari malformation. Acta Neurol Scand. 2001;104(2):113–7.
29. Jacome DE. Headache in Ehlers-Danlos syndrome. Cephalalgia. 1999;19(9):791–6.
30. Puget S, Kondageski C, Wray A, Boddaert N, Roujeau T, Di Rocco F, et al. Chiari-like tonsillar herniation associated with intracranial hypotension in Marfan syndrome. Case report. J Neurosurg. 2007;106(1 Suppl):48–52.
31. Braca J, Hornyak M, Murali R. Hemifacial spasm in a patient with Marfan syndrome and Chiari I malformation. Case report. J Neurosurg. 2005;103(3):552–4.
32. Owler BK, Halmagyi GM, Brennan J, Besser M. Syringomyelia with Chiari malformation; 3 unusual cases with implications for pathogenesis. Acta Neurochir. 2004;146(10):1137–43; discussion 43.
33. Khan AA, Bhatti SN, Khan G, Ahmed E, Aurangzeb A, Ali A, et al. Clinical and radiological findings in Arnold Chiari malformation. J Ayub Med Coll Abbottabad. 2010;22(2):75–8.
34. Samartzis D, Shen FH, Herman J, Mardjetko SM. Atlantoaxial rotatory fixation in the setting of associated congenital malformations: a modified classification system. Spine (Phila Pa 1976). 2010;35(4):E119–27.
35. Perrini P, Rawlinson A, Cowie RA, King AT. Acute external hydrocephalus complicating craniocervical decompression for syringomyelia-Chiari I complex: case report and review of the literature. Neurosurg Rev. 2008;31(3):331–5.
36. Abel TJ, Chowdhary A, Gabikian P, Ellenbogen RG, Avellino AM. Acquired chiari malformation type I associated with a fatty terminal filum. Case report. J Neurosurg. 2006;105(4 Suppl):329–32.
37. Kagawa M, Jinnai T, Matsumoto Y, Kawai N, Kunishio K, Tamiya T, et al. Chiari I malformation accompanied by assimilation of the atlas, Klippel-Feil syndrome, and syringomyelia: case report. Surg Neurol. 2006;65(5):497–502; discussion 502.
38. Cakmakkaya OS, Kaya G, Altintas F, Bakan M, Yildirim A. Anesthetic management of a child with Arnold-Chiari malformation and Klippel-Feil syndrome. Paediatr Anaesth. 2006;16(3):355–6.
39. Konstantinou DT, Chroni E, Constantoyiannis C, Dougenis D. Klippel-Feil syndrome presenting with bilateral thoracic outlet syndrome. Spine (Phila Pa 1976). 2004;29(9):E189–92.
40. Tubbs RS, McGirt MJ, Oakes WJ. Surgical experience in 130 pediatric patients with Chiari I malformations. J Neurosurg. 2003;99(2):291–6.
41. Ulmer JL, Elster AD, Ginsberg LE, Williams DW 3rd. Klippel-Feil syndrome: CT and MR of acquired and congenital abnormalities of cervical spine and cord. J Comput Assist Tomogr. 1993;17(2):215–24.
42. Ritterbusch JF, McGinty LD, Spar J, Orrison WW. Magnetic resonance imaging for stenosis and subluxation in Klippel-Feil syndrome. Spine (Phila Pa 1976). 1991;16(10 Suppl):S539–41.
43. Woosley RE, Whaley RA. Use of metrizamide in computerized tomography to diagnose the Chiari I malformation. J Neurosurg. 1982;56(3):373–6.
44. Gupta A, Vitali AM, Rothstein R, Cochrane DD. Resolution of syringomyelia and Chiari malformation after growth hormone therapy. Childs Nerv Syst. 2008;24(11):1345–8.
45. Hilal L, Hajaji Y, Vie-Luton MP, Ajaltouni Z, Benazzouz B, Chana M, et al. Unusual phenotypic features in a patient with a novel splice mutation in the GHRHR gene. Mol Med. 2008;14(5–6):286–92.
46. Murphy RL, Tubbs RS, Grabb PA, Oakes WJ. Chiari I malformation and idiopathic growth hormone deficiency in siblings: report of three cases. Childs Nerv Syst. 2007;23(10):1221–3.
47. Tubbs RS, Wellons JC 3rd, Smyth MD, Bartolucci AA, Blount JP, Oakes WJ, et al. Children with growth hormone deficiency and Chiari I malformation: a morphometric analysis of the posterior cranial fossa. Pediatr Neurosurg. 2003;38(6):324–8.
48. Hamilton J, Chitayat D, Blaser S, Cohen LE, Phillips JA 3rd, Daneman D. Familial growth hormone deficiency associated with MRI abnormalities. Am J Med Genet. 1998;80(2):128–32.
49. Hamilton J, Blaser S, Daneman D. MR imaging in idiopathic growth hormone deficiency. AJNR Am J Neuroradiol. 1998;19(9):1609–15.

50. Marwaha R, Menon PS, Jena A, Pant C, Sethi AK, Sapra ML. Hypothalamo-pituitary axis by magnetic resonance imaging in isolated growth hormone deficiency patients born by normal delivery. J Clin Endocrinol Metab. 1992;74(3):654–9.
51. Otsuka F, Inagaki K, Suzuki J, Ogura T, Makino H. Skull Paget's disease developing into Chiari malformation. Endocr J. 2004;51(3):391–2.
52. Richards PS, Bargiota A, Corrall RJ. Paget's disease causing an Arnold-Chiari type 1 malformation: radiographic findings. AJR Am J Roentgenol. 2001;176(3):816–7.
53. Iglesias-Osma C, Gomez Sanchez JC, Suquia Mugica B, Querol Prieto R, de Portugal Alvarez J. Paget's disease of bone and basilar impression associated with an Arnold-Chiari type-1 malformation. An Med Interna. 1997;14(10):519–22.
54. Sandberg DI, Navarro R, Blanch J, Ragheb J. Anomalous venous drainage preventing safe posterior fossa decompression in patients with chiari malformation type I and multisutural craniosynostosis. Report of two cases and review of the literature. J Neurosurg. 2007;106(6 Suppl):490–4.
55. Strahle J, Muraszko KM, Buchman SR, Kapurch J, Garton HJ, Maher CO. Chiari malformation associated with craniosynostosis. Neurosurg Focus. 2011;31(3):E2.
56. Menezes AH, Vogel TW. Specific entities affecting the craniocervical region: syndromes affecting the craniocervical junction. Childs Nerv Syst. 2008;24(10):1155–63.
57. Mesiwala AH, Shaffrey CI, Gruss JS, Ellenbogen RG. Atypical hemifacial microsomia associated with Chiari I malformation and syrinx: further evidence indicating that Chiari I malformation is a disorder of the paraaxial mesoderm. Case report and review of the literature. J Neurosurg. 2001;95(6):1034–9.
58. Sze RW, Gruss JS, Cunningham ML. Unilateral aplasia of the middle cranial fossa floor in atypical hemifacial microsomia. AJNR Am J Neuroradiol. 2001;22(7):1434–7.
59. Pober BR, Filiano JJ. Association of Chiari I malformation and Williams syndrome. Pediatr Neurol. 1995;12(1):84–8.
60. Mercuri E, Atkinson J, Braddick O, Rutherford MA, Cowan FM, Counsell SJ, et al. Chiari I malformation in asymptomatic young children with Williams syndrome: clinical and MRI study. Eur J Paediatr Neurol. 1997;1(5–6):177–81.
61. Ferrero GB, Biamino E, Sorasio L, Banaudi E, Peruzzi L, Forzano S, et al. Presenting phenotype and clinical evaluation in a cohort of 22 Williams-Beuren syndrome patients. Eur J Med Genet. 2007;50(5):327–37.
62. Ciprero KL, Clayton-Smith J, Donnai D, Zimmerman RA, Zackai EH, Ming JE. Symptomatic Chiari I malformation in Kabuki syndrome. Am J Med Genet A. 2005;132A(3):273–5.
63. McGaughran J, Aftimos S, Jefferies C, Winship I. Clinical phenotypes of nine cases of Kabuki syndrome from New Zealand. Clin Dysmorphol. 2001;10(4):257–62.
64. Kuether TA, Piatt JH. Chiari malformation associated with vitamin D-resistant rickets: case report. Neurosurgery. 1998;42(5):1168–71.
65. Caldemeyer KS, Boaz JC, Wappner RS, Moran CC, Smith RR, Quets JP. Chiari I malformation: association with hypophosphatemic rickets and MR imaging appearance. Radiology. 1995;195(3):733–8.
66. Tubbs RS, Rutledge SL, Kosentka A, Bartolucci AA, Oakes WJ. Chiari I malformation and neurofibromatosis type 1. Pediatr Neurol. 2004;30(4):278–80.
67. Hara H, Arakawa H. Coexistence of neurofibromatosis 1 and Chiari type I malformation: an unusual association. J Dermatol. 2005;32(1):34–7.
68. Schaaf CP, Goin-Kochel RP, Nowell KP, Hunter JV, Aleck KA, Cox S, et al. Expanding the clinical spectrum of the 16p11.2 chromosomal rearrangements: three patients with syringomyelia. Eur J Hum Genet. 2011;19(2):152–6.
69. Schiff M, Delahaye A, Andrieux J, Sanlaville D, Vincent-Delorme C, Aboura A, et al. Further delineation of the 17p13.3 microdeletion involving YWHAE but distal to PAFAH1B1: four additional patients. Eur J Med Genet. 2010;53(5):303–8.
70. Carr CW, Moreno-De-Luca D, Parker C, Zimmerman HH, Ledbetter N, Martin CL, et al. Chiari I malformation, delayed gross motor skills, severe speech delay, and epileptiform discharges in a child with FOXP1 haploinsufficiency. Eur J Hum Genet. 2010;18(11):1216–20.
71. Bayrakli F, Bilguvar K, Ceyhan D, Ercan-Sencicek AG, Cankaya T, Bayrakli S, et al. Heterozygous 5p13.3-13.2 deletion in a patient with type I Chiari malformation and bilateral Duane retraction syndrome. Clin Genet. 2010;77(5):499–502.
72. Bertalan R, Sallai A, Solyom J, Lotz G, Szabo I, Kovacs B, et al. Hyperthyroidism caused by a germline activating mutation of the thyrotropin receptor gene: difficulties in diagnosis and therapy. Thyroid. 2010;20(3):327–32.
73. Raven R, Bingham PM, Graupman P. Pentasomy 49,XXXXY associated with a Chiari type 1 malformation and cervical syrinx. Pediatr Neurosurg. 2007;43(1):47–9.
74. Newman PK, Wentzel J, Foster JB. HLA and syringomyelia. J Neuroimmunol. 1982;3(1):23–6.
75. Lindenberg R, Walker BA. Arnold-Chiari malformation in sibs. Birth Defects Orig Artic Ser. 1971;7(1):234–6.
76. Case ME, Sarnat HB, Monteleone P. Type II Arnold-Chiari malformation with normal spine in trisomy 18. Acta Neuropathol. 1977;37(3):259–62.
77. Maclean K, Field MJ, Colley AS, Mowat DR, Sparrow DB, Dunwoodie SL, et al. Kousseff syndrome: a causally heterogeneous disorder. Am J Med Genet A. 2004;124A(3):307–12.
78. Rossi M, D'Armiento M, Parisi I, Ferrari P, Hall CM, Cervasio M, et al. Clinical phenotype of lathosterolosis. Am J Med Genet A. 2007;143A(20):2371–81.

79. Tassabehji M, Fang ZM, Hilton EN, McGaughran J, Zhao Z, de Bock CE, et al. Mutations in GDF6 are associated with vertebral segmentation defects in Klippel-Feil syndrome. Hum Mutat. 2008;29(8):1017–27.
80. Royal SA, Tubbs RS, D'Antonio MG, Rauzzino MJ, Oakes WJ. Investigations into the association between cervicomedullary neuroschisis and mirror movements in patients with Klippel-Feil syndrome. AJNR Am J Neuroradiol. 2002;23(4):724–9.
81. Erbengi A, Oge HK. Congenital malformations of the craniovertebral junction: classification and surgical treatment. Acta Neurochir. 1994;127(3–4):180–5.
82. Seemann N, Campbell C, Hammond R, Prasad C. 9 year old girl with progressive weakness. Brain Pathol. 2010;20(1):255–6.
83. Gripp KW, Scott CI Jr, Nicholson L, Magram G, Grissom LE. Chiari malformation and tonsillar ectopia in twin brothers and father with autosomal dominant spondylo-epiphyseal dysplasia tarda. Skelet Radiol. 1997;26(2):131–3.
84. Sarnat HB. Regional ependymal upregulation of vimentin in Chiari II malformation, aqueductal stenosis, and hydromyelia. Pediatr Dev Pathol. 2004;7(1):48–60.
85. Imagama S, Wakao N, Kitoh H, Matsuyama Y, Ishiguro N. Factors related to surgical outcome after posterior decompression and fusion for craniocervical junction lesions associated with osteogenesis imperfecta. Eur Spine J. 2011;20(Suppl 2):S320–5.
86. Stevenson KL. Chiari type II malformation: past, present, and future. Neurosurg Focus. 2004;16(2):E5.
87. Juranek J, Salman MS. Anomalous development of brain structure and function in spina bifida myelomeningocele. Dev Disabil Res Rev. 2010;16(1):23–30.
88. Au KS, Ashley-Koch A, Northrup H. Epidemiologic and genetic aspects of spina bifida and other neural tube defects. Dev Disabil Res Rev. 2010;16(1):6–15.
89. Kibar Z, Torban E, McDearmid JR, Reynolds A, Berghout J, Mathieu M, et al. Mutations in VANGL1 associated with neural-tube defects. N Engl J Med. 2007;356(14):1432–7.
90. Takano T, Becker LE. Overexpression of nestin and vimentin in the ependyma of spinal cords from hydrocephalic infants. Neuropathol Appl Neurobiol. 1997;23(1):3–15.
91. Takano T, Rutka JT, Becker LE. Overexpression of nestin and vimentin in ependymal cells in hydrocephalus. Acta Neuropathol. 1996;92(1):90–7.
92. Sarnat HB. Histochemistry and immunocytochemistry of the developing ependyma and choroid plexus. Microsc Res Tech. 1998;41(1):14–28.
93. Tubbs RS, Shoja MM, Ardalan MR, Shokouhi G, Loukas M. Hindbrain herniation: a review of embryological theories. Ital J Anat Embryol. 2008;113(1):37–46.
94. Williams H. A unifying hypothesis for hydrocephalus, Chiari malformation, syringomyelia, anencephaly and spina bifida. Cerebrospinal Fluid Res. 2008;5:7.

Part V

Diagnostics

Electrophysiological Diagnostics in Chiari Malformation

24

Florian Roser, Marina Liebsch, and Luigi Rigante

Introduction

One of the hallmark signs of Chiari malformation are the various degrees of herniation of the cerebellar tonsils below the foramen magnum. Additionally, up to 60% of patients with Chiari type 1 malformation harbor a cervical syringomyelia, with some of these suffering from concomitant hydrocephalus, and a substantial number of them present altered electrophysiological parameters and concomitant symptoms before any surgical intervention [1–3]. The most prevalent theory regarding the pathophysiological mechanism for the development of a syrinx in Chiari malformations is the presence of increased transmural flow of cerebrospinal fluid, which causes spinal cord swelling that subsequently coalesces into a syrinx [3]. Due to its anatomical location within the spinal cord, a centromedullary syndrome with predominant symptoms of dissociated pain and thermal sensory impairment clinically characterizes syringomyelia. Later in the course of the disease with distension of descending pathways, segmental weakness, atrophy, upper motor neuron syndrome (motor pathways), and autonomic dysfunctions (anterolateral column) may occur.

With the improvement of imaging resolution and the more frequent use of magnetic resonance (MR) imaging in the last decades, patients with subtle and diffuse pain symptoms due to small syrinx cavities increasingly present to neurosurgical care. Patients with a patent central canal (hydromyelia) do not share progressive clinical nor radiological characteristics of patients harboring a true syringomyelia [4]. No neurological deficits come along with patients affected by hydromyelia, who mainly present with diffuse pain, different from neuropathic pain in dissociative syndromes. The use of diffusion tensor imaging (DTI) in hydromyelia demonstrates intact white matter fiber tracts around and beyond the cavity, consistent with preserved electrophysiological values [5].

As the underlying pathology in subtle cases is difficult to assess, electrophysiological diagnostics help in distinguishing between a physiologically patent central canal (hydromyelia) and a developing syringomyelia at an early stage with possible functional alterations of the spinothalamic tract [3]. Further on, indication for surgical treatment of Chiari malformation varies but certainly depends on the patients' clinical signs and symptoms,

F. Roser (✉) · L. Rigante
Department of Neurosurgery, Cleveland Clinic Abu Dhabi, Abu Dhabi, United Arab Emirates

Cleveland Clinic Lerner College of Medicine of Case Western Reserve University, Cleveland, OH, USA
e-mail: roserf@clevelandclinicabudhabi.ae

M. Liebsch
Department of Neurosurgery, University Hospital Tübingen, Tübingen, BW, Germany

R. S. Tubbs et al. (eds.), *The Chiari Malformations*, https://doi.org/10.1007/978-3-030-44862-2_24

especially in the presence of syringomyelia, which most often is chronic and might lead to significant neurological deficit if untreated. Several electrodiagnostic findings associated with syringomyelia have been recently documented, playing an important role in the quantification of deficits induced by the spinal cord cavity. Both somatosensory evoked potentials (SSEPs) and motor evoked potentials (MEPs) after noninvasive electrical or magnetic stimulation of the motor cortex are sensitive tools for the detection of morphological and functional lesions of spinal cord pathways. Moreover, cutaneous (CSP), mixed nerve (MNSP), and cortical silent periods (CoSP) have all presented alterations in syringomyelia. As SSEP and MEP monitoring reflects nerve fibers' integrity of the dorsal column and corticospinal tract, respectively, a small syrinx at the initial stage might not have the morphological impact to alter these pathways. When recording silent periods, alterations of the spinothalamic pathways become obvious also at the subclinical stage. According to Rexed, pain-conducting (mechanical and thermal) A∂-fibers enter the spinal cord via the dorsal root entry zone mainly in laminae I and V. The second-order neuron crosses the midline in close proximity to the central canal (within 2–3 segments) and finally ascends as the spinothalamic tract. The presence of an inhibitory interneuron connecting the A∂-fibers to the α(alpha)-motoneuron leads to a physiological reflex, which can be measured as the silent period, resulting in a suppression of the electromyography (EMG) signal in a voluntarily contracted muscle (Figs. 24.1 and 24.2).

Although the application of intraoperative neurophysiological monitoring (IOM) during surgery of the cervical spine and spinal cord has been well documented, the use of IOM during surgeries for Chiari malformation remains controversial [6, 7]. IOM might prevent further neurological deficits due to microsurgical manipulation at the cranio-cervical junction and determine the extent of decompression [8]. Even though IOM is routinely used in pediatric patients, there are only a few reports of the application of IOM in adult patients as suboccipital decompression is considered to carry a low risk for neurological morbidity, when presenting mostly due to dural opening and

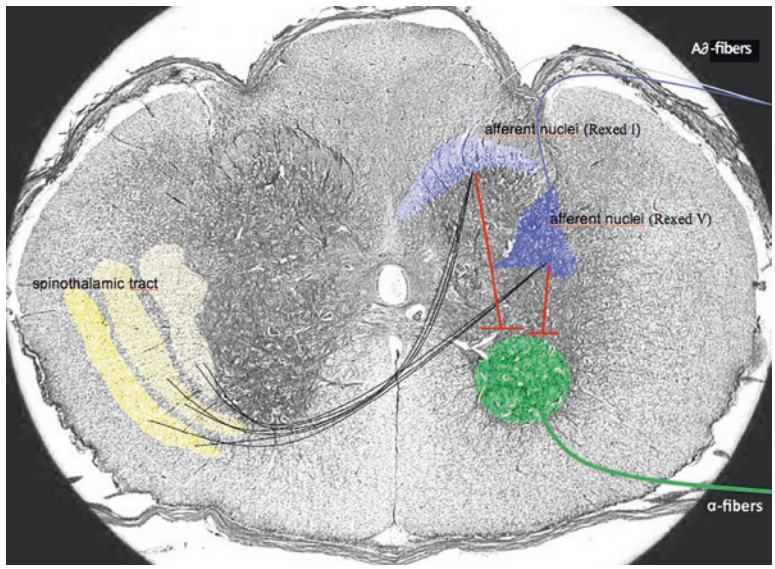

Fig. 24.1 Anatomical physiology of silent period generation (transverse section of cervical spinal cord, myelin staining). Mechanical and thermal pain-conducting A∂-fibers enter the spinal cord via the dorsal root entry zone mainly in laminae I and V of Rexed. The second-order neuron crosses the midline in close proximity to the central canal (within 2–3 segments) and finally ascends as the spinothalamic tract. Inhibitory interneurons connecting the A∂-fibers to the α(alpha)-motoneuron leads to a physiological reflex resulting in a suppression of the electromyography (EMG) signal in a voluntarily contracted muscle (silent period)

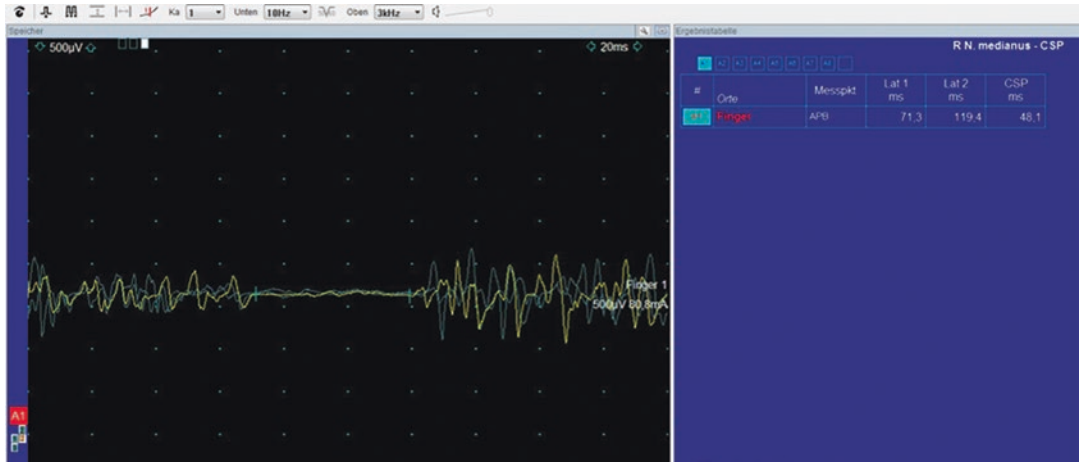

Fig. 24.2 Electromyography (EMG) signal suppression at abductor pollicis brevis muscle recording from right median nerve stimulation at the wrist (silent period) due to the inhibitory interneuron connecting the A∂-fibers to the α(alpha)-motoneuron

cerebrospinal fluid (CSF) leakage or to attempts to reduce the syrinx cavity [1, 9–11].

Preoperative Diagnostics

Comprehensive preoperative electrophysiological assessment with SSEP, MEP, and silent periods (CSP, MNSP, CoSP) should be performed to differentiate between Chiari malformation-related syringomyelia and patent central canal (hydromyelia) as an incidental finding or prior to surgery as a baseline study.

Surgical candidates receive an equivalent preoperative electrophysiological evaluation 1 day before the surgery. SSEP are measured (band-pass filter: 10–1000 Hz) after stimulation of the medial (M-SSEP) and tibialis nerves (T-SSEP) by surface electrodes on the wrist or ankle using square-wave electrical impulses. A high current amplitude (16–40 mA) sufficient enough to elicit a moderate twitch of the target muscle and a low duration of stimulus (0.2 ms) are used. Recording electrodes are placed in the parietal area at C3′, C4′, CZ′, and FZ according to the international 10/20 system. A minimum of two series of up to 500 sweeps are amplified, averaged, and superimposed to ensure reproducibility. The N_{20} and P_{40} peaks are used to determine the latency and amplitude of the responses. The preoperative MEP recordings are recorded at rest after transcranial magnetic stimulation (MAGSTIM© 200 MonoPulse, 1.5 T Magstim Ltd.) and a slight facilitation of the indicated muscle. Stimulus intensity is set at 80% of stimulator output (20–3000 Hz filter, superposition of 7–8 stimuli).

Silent periods are only assessed preoperatively or at postoperative follow-up as they require voluntary isometric muscle activation by the patient. CoSP are derived by recording MEP responses from the abductor pollicis brevis (APB) muscle with stimulation of the contralateral cortex. Stimulus intensity is set at 80% with five repeated stimuli. Median nerve stimulation (MNSP) at the wrist or cutaneous nerve stimulation at the tip of the index finger (CSP) with square-wave pulses of 0.1 ms and an intensity of 25 times the sensory threshold (max 100 mA) are applied to evoke a silent period in the volitionally activated APB muscle. Recordings are obtained using surface electrodes placed over the belly and tendon of the target muscle, which contracts isometrically on command with submaximal force. During the preoperative assessment, auditory feedback to the patient is given to achieve near maximal force (80%) (Fig. 24.3). The silent period is defined as the depression or absence (silent period) of voluntary activity in the EMG following a stimulus. Sensitivity on the screen is set up to 500 mcV/div and 20 ms/div for CSP/MNSP as well as 50 ms/div for CoSP. Ten repeating stimuli are applied for MNSP (0.2 ms duration), while three stimuli for

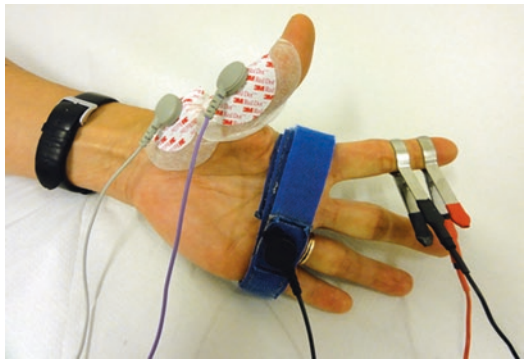

Fig. 24.3 Setup for silent period recording. Median nerve stimulation (MNSP) at the wrist and nociceptive cutaneous nerve stimulation at the tip of the index finger (CSP) with square-wave pulses of 0.1 ms and 80–100 mA intensity (circa 25 times the sensory threshold). Auditory feedback provided to the patient is given to achieve near maximal force (80%) during abductor pollicis brevis muscle recording

CSP. Stimuli intensity is adjusted according to the tolerance of the patient but is applied at 20 times the sensory threshold (80–100 mA) (Fig. 24.2).

Intraoperative Neurophysiological Monitoring

Total intravenous anesthesia (TIVA) is induced with sufentanil, an initiation bolus of propofol, and a bolus of rocuronium for intubation only and then maintained with a continuous infusion of remifentanil and propofol.

Multimodal SSEP and MEP monitoring is continuously performed by an experienced electrophysiological team and appropriate equipment (e.g., Endeavor CR, Viasys Healthcare, Madison, WI). Baseline studies are obtained prior to positioning the patient prone and thereafter.

Intraoperative MEP differ from preoperative setting. They are recorded at the hand and foot muscles after cortical stimulation at C1/C2 for lower and C3/C4 position for upper limbs with an anodal monopolar high-frequency train of five stimuli and an interstimulation interval of 2–4 ms. Voltage of more than 20% above the stimulation threshold is required (filter 150–3000 Hz). As latencies are largely depending on temperatures of the patient's body, the most important values intraoperatively are amplitudes. Therefore, the baseline amplitude at dural opening to the amplitude of the end of surgery is compared. Metrics of SSEP and MEP after positioning (baseline) and after closure of the dura (final) are noted for further analysis. Stimulation intensity for SSEP and MEP is maintained at a constant level throughout the surgery to compare amplitude changes, and evoked potentials are continuously monitored. Final-to-baseline MEP and SSEP amplitude and latency ratios are calculated. Left- and right-sided data are pooled for statistical evaluation (Fig. 24.4).

Discussion

Electrophysiological Diagnostics in Syringomyelia

The clinical course of syringomyelia is variable and usually characterized by slowly progressive neurological deficits, beginning with protopathic pain and dissociative symptoms. Typically, this is followed by motor weakness and spinal ataxia due to alteration of corticospinal and sensory pathways. Altered electrophysiological recording in syringomyelia may be explained by ischemic events in the spinal cord, first in the watershed areas of the intermediate gray substance and later in the central gray matter of the dorsal horns. Centromedullary diseases lead to alterations of spinothalamic pathways by loss of inhibitory interneurons with unbalanced overexpressed excitatory motor neurons' function [12, 13]. Electrophysiological studies are an essential component of clinical diagnostics in syringomyelia. Both SSEP and MEP monitoring provide quantification and segmental orientation of morphological and functional lesions of the spinal cord and dorsal column pathways; however, interpretation of the results remains controversial [14–18]. Additionally, due to an increase in the excitability of spinal motor neurons, patients with syringomyelia show a large variation of spontaneous EMG-like activity [13].

The most common SSEP abnormality described in these patients is the attenuation or absence of N_{13} with a normal N_{20} potential, a parameter reported

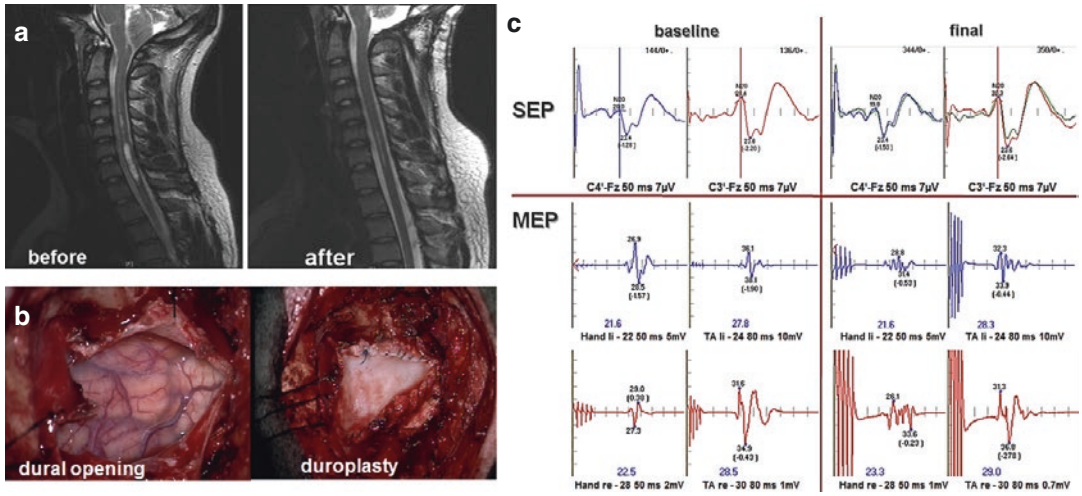

Fig. 24.4 (**a**) T2-weighted sagittal magnetic resonance imaging of the cranio-cervical junction in a patient with a Chiari type 1 malformation with syringomyelia before and after surgery. (**b**) Intraoperative imaging of the suboccipital decompression after dural opening (left) and duraplasty (right). (**c**) Surgery was accompanied by continuous somatosensory evoked potential (SSEP) and motor evoked potential (MEP) monitoring

in spinal cord lesions involving the gray matter but sparing the dorsal column [18–22]. Such findings can be detected even in patients with subclinical dysfunctions of the dorsal column pathways [19, 20, 23]. Although it has been proven that SSEPs do not reflect spinothalamic pathways [18, 24, 25], correlation of N_{13} absence after pain stimuli with clinical loss of pain and temperature sensation has been described [26, 27]. The demonstrated SSEP sensitivity and specificity for centromedullary symptoms such as hypalgesia (0–40%) or hyperesthesia (25–75%) is 54% and 81%, respectively [20, 28]. Conversely, several authors also described physiological SSEPs in syringomyelia [29], pathological results in very small syrinx cavities [17], and no correlation to neurological status [30, 31].

MEP recordings showed pathological results in clinically intact patients but otherwise a good correlation to motor deficits [31–33].

Activation of cutaneous fibers following sensory nerve stimulation can produce transient suppression of ongoing EMG activity, known as the "silent period" [12, 34]. Most investigators agree that the afferent impulses generating silent periods are carried by slow-conducting δ(delta)-fibers, and the latency of response indicates an inhibitory spinal reflex [35, 36]. Using H-reflexes, F-waves, and MEP to assess motor neuron excitability, studies have shown that motor neurons are inhibited during the time period that CSP occurs. Maximal inhibition occurs early in the CSP, caused by postsynaptic inhibition of motor neurons by spinal inhibitory interneurons [37, 38]. Silent period testing is likely to reveal conduction abnormalities in these small sensory fibers missed by routine nerve conduction studies (SSEP/MEP), which detect conduction via large myelinated fibers. The anatomic pathway of small myelinated pain-conducting fibers that cross the midline closer to the central canal than the major ascending and descending pathways, where most syrinx cavities arise, provides further evidence that alteration of silent periods is likely to occur before changes in sensory-motor conduction studies. Syringomyelia can cause abolition of silent periods through lesions of the dorsal horn of the spinal cord or dilatation of the central canal in centric syrinx cavities [39–41]. Since the duration of the silent period exceeds the time period of the inhibitory effect by *gamma-aminobutyric acid* (GABA) or glycine transmission, other inhibitory mechanisms must exist such as cutaneous modulation of cortical excitability elicited by powerful electrical stimuli or propriospinal Ib-inhibitory interneurons with

postsynaptic inhibition on alpha-motoneurons [36, 42–45] (Figs. 24.1 and 24.2).

Kaneko and co-workers conducted electrophysiological testing using silent periods in five patients with syringomyelia and reported a 100% sensitivity and specificity for the CSP in upper extremities with sensory loss, but not in asymptomatic upper limbs. CMAP, F-waves, and MEP were still preserved in these upper extremities, demonstrating that the efferent arc of the CSP was intact [39]. Kofler et al. also described a high sensitivity (95%) for the tested silent periods compared to SSEP in syringomyelia patients ($n = 8$). Moreover, the silent periods showed pathological abnormalities, whereas SSEP monitoring was within normal limits [28]. Stetkarova and colleagues found similar results with shortened CSP on the affected compared to the unaffected side in four patients with syringomyelia. Each patient had unilateral pain and temperature loss and relatively normal SSEP and MEP. The sensitivity of CSP in these cases was calculated as 100% [46]. However, it is worth recognizing that data in the literature differ considerably in the utilized conduction parameters, and no information regarding normal baseline values and limits are provided. In addition, the number of syringomyelia patients examined was relatively low.

Moreover, the CoSP is an expression of the inhibitory effect of the transcranial magnetic stimulation of the motor cortex and is independent from the elicited response, suggesting primary cranial generation and involvement of spinal mechanisms [35, 41, 47]. Evidence has been given for the existence of supraspinal inhibition due to intracortical inhibitory interneurons, as MEP and CoSP are variably changed in different cortical and subcortical lesions [48–50]. CoSP can be used for prediction of recovery in deficient motor systems poststroke and assessment of callosal function [12, 51]. Our published case series study demonstrated how CoSP correlates well to motor deficits and has higher specificity compared to MEP in syringomyelia (86% vs. 72%), although this result was not statistically significant. To date, a specific definition for a pathologic silent period has not been reported yet. Statements vary from completely suppressed EMG or shortening to incomplete suppression of voluntary muscle activity [13, 28, 35, 41]. We defined the silent period as pathologic if the duration was shorter or the latency was longer than the standard deviation (SD) of the normal baseline. In addition, the silent period was defined as pathologic if either the latency or duration parameters were abnormal [3]. Early onset and long duration of a SP, however, were interpreted as physiological fast conduction and longer suppression of EMG. Sensitivity and specificity were evaluated for each cardinal symptom. Due to the variable prevalence of these symptoms, positive and negative predictive values differ considerably. A positive predictive value of 0.63 was obtained in CSP for pain, and a negative predictive value for the symptom "paresis" was 0.83–0.94 in all conduction studies (CSP, MNSP, CoSP). Data recorded demonstrates significantly higher sensitivity and specificity for the symptom "pain" in CSP recordings compared with (EMG/MEP) recordings (48% vs. 26%, $p = 0.023$; 88% vs. 65%, $p = 0.0059$). This was also true for "dissociative symptoms" in MNSP recordings compared with (EMG/MEP) recordings (38% vs. 33% sensitivity and 78% vs. 71% specificity, $p < 0.018$). Although sensitivity and specificity in all SP showed higher values, the difference was not statistically significant. This may be due to the rare occurrence of the symptoms [3].

From our experience, a combination of several electrophysiological parameters, including silent periods, are useful to distinguish syringomyelia from a patent central canal (hydromyelia). We base our decision to operate on a patient with syringomyelia on several elements. MRI is in fact invaluable in the detection of focal arachnoid scarring causing CSF disturbance, which is an indication for surgery. In addition, the patient must show appropriate neurological symptoms for the level of the syrinx cavity over a certain period of time. Finally, electrophysiological diagnosis must correlate with the clinical and investigative findings [3].

Electrophysiological Diagnostics in Chiari Malformation

Suboccipital decompression under IOM is a safe and effective surgery to treat Chiari I malformations, with an overall low complication rate and no neurological deterioration [52]. Sala et al.

reported a series of 132 adult patients who underwent surgery for Chiari I or II malformations, and surgical complications were observed in 7.8% of the patients [53]. In contrast, Klekamp reported a complication rate of 21.8% with a permanent surgical morbidity of 3.2% in 359 patients undergoing suboccipital decompression without IOM [1]. No differences were found between adult and pediatric patients. Sindou et al. reported no neurological aggravation in 44 adult cases [46]. Notably, several patients showed an intraoperative latency prolongation of >10% and/or a >50% amplitude reduction, which were associated with the appearance of postoperative neurological deficits [54]. However, as we did not observe any clinical correlates in the few cases where these changes occurred in our cohort, we considered them as false positive and influenced not only by surgical maneuvers such as CSF drainage, opening of fourth ventricle, and relief of syrinx cavity but also by several covariates not directly related to the surgeon's intervention (i.e., anesthesia, blood pressure, temperature, positioning, electrode impedances) [52]. As the baseline and final recordings are instantaneous values of the current electrophysiological status, changes in the covariates will cause false-positive or false-negative recordings. Hence, the continuous real-time evaluation and interpretation of potentials are crucial in IOM.

As no significant changes in IOM during positioning or intradural exploration in adult patients with syringomyelia were detected [3], the question arises whether IOM should be a prerequisite during Chiari surgery at all. Although used routinely in pediatric patients [10, 11, 55], there are only a few reports on the IOM application in adult patients undergoing Chiari surgery [52]. Anderson et al. showed the highest improvement of conduction times of brainstem auditory evoked potentials (BAEP) after suboccipital decompression in pediatric patients [8, 9]. Only 20% of the patients required further duraplasty [11]. Additionally, Chen et al. described an improvement of SSEP latencies after decompression and durotomy [10]. Therefore, IOM certainly influences surgical decision-making, whether to perform duraplasty or not, in the pediatric population. However, to date, no evidence is available on electrophysiological changes in adults. Furthermore, the available data do not establish whether an improvement in electrophysiological parameters during surgery indicates postoperative symptom improvement. This information will influence the ongoing controversial discussions on the preferred surgical approach to Chiari malformations in adults (only bony cranio-cervical decompression, duraplasty, or even an inspection of the obex in all cases) [1, 56–58].

Any manipulation of the spinal cord (e.g., positioning or microsurgical manipulation) in patients with Chiari malformation can potentially further damage spinal cord function. The rationale for using SSEP IOM is to prevent new neurological deficits during suboccipital decompression. In our experience, deterioration of the SSEP and/or MEP necessitating an adaptation of the positioning is extremely rare [52].

In our published series of 38 consecutive cases of patients with Chiari type 1, deterioration of SSEP parameter during positioning was documented only in 2 cases (5%) followed by an adjustment of the positioning by the surgeon [52]. There were no significant differences in the absolute baseline and final latencies of M-SSEPs ($p = 0.9085$) and T-SSEPs ($p = 0.4613$), as well as the final-to-baseline SSEP latency ratios ($p = 0.5659$). An increase of >10% in four recordings of the final-to-baseline M-SSEP and T-SSEP latency ratios was recorded in three patients; none of these patients developed new postoperative deficits. Likewise, there were no significant differences of the absolute baseline and final amplitudes of the M-SSEPs ($p = 0.2397$) and T-SSEPs ($p = 0.1440$) nor of the final-to-baseline SSEP amplitude ratios ($p = 0.4778$). Two patients presented >50% SSEP amplitude reduction during surgery; however, none of them developed new postoperative deficits. In contrast, an intraoperative SSEP amplitude increase indicated a more favorable outcome, with improvements in the symptoms of dysesthesia and ataxia/gait disturbance specifically noticed at the follow-up visits [52]. During a mean follow-up period of 22.4 ± 20.3 months, 92.6% of the symptoms improved or remained stable, while 8.1% patients presented a relapse of syringomyelia-related symptoms after 25.7 ± 7.6 months [52] (Fig. 24.5).

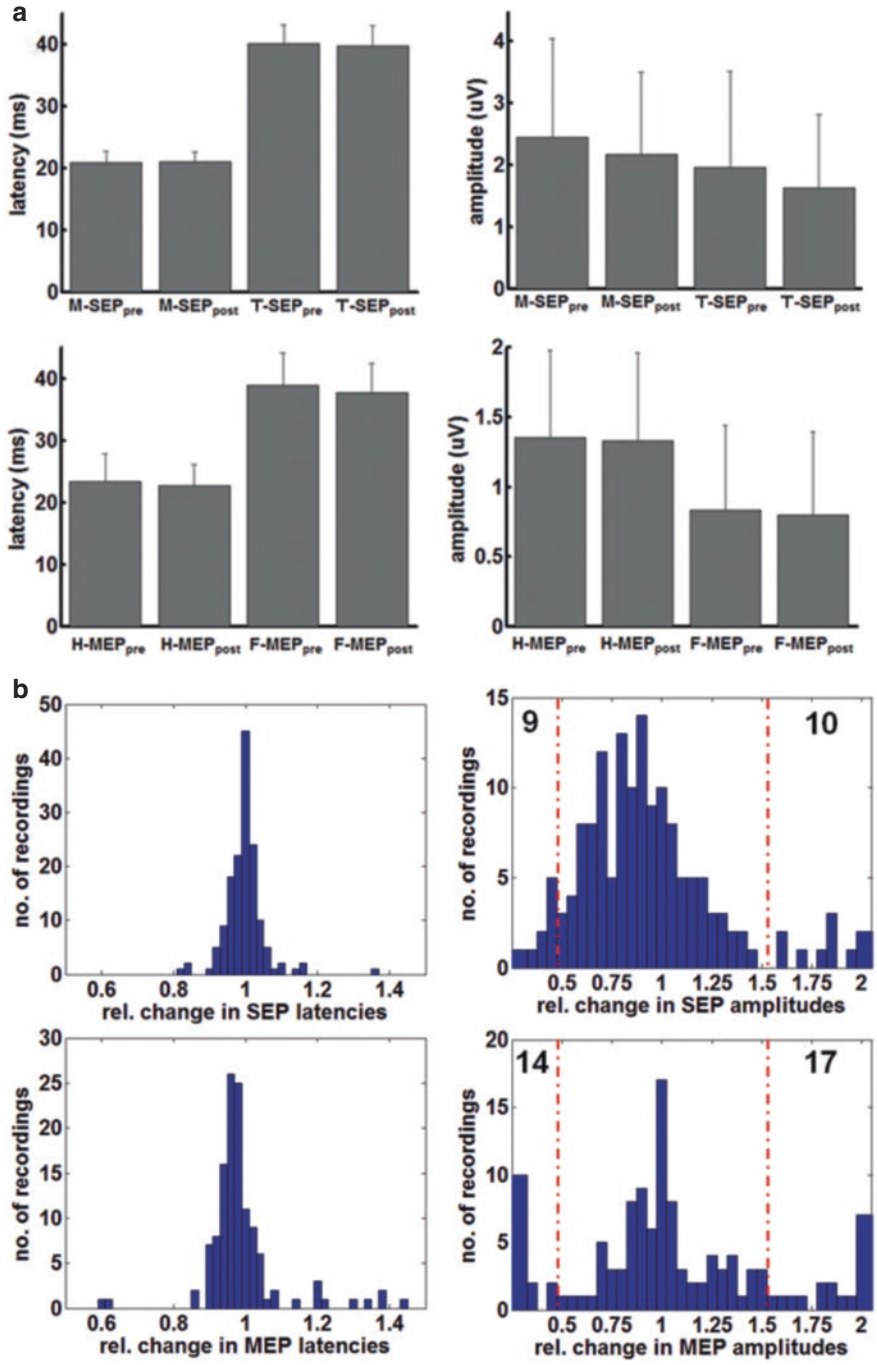

Fig. 24.5 (**a**) Bars represent absolute amplitudes and latencies (mean ± SD) of M-SSEPs, T-SSEPs, H-MEPs, and F-MEPs recorded during baseline and after surgery ($p > 0.05$, Student's t-test). (**b**) The final-to-baseline ratios of the SSEP/MEP amplitudes and latencies of the upper and lower extremities were pooled, and their distributions were plotted in histograms. Dashed red lines indicate >50% decreases or increases of the amplitudes compared with baseline. Abbreviations: *F-MEP* MEP of the tibialis anterior muscle, *H-MEP* MEP of the abductor digiti minimi muscle, *SD* standard deviation, *SSEP* somatosensory evoked potential, *M-SSEP* SSEP of the medial nerve, *T-SSEP* SSEP of the tibialis nerve

In contrast to our data, Danto et al. reported significant changes in SSEPs, mainly related to positioning, in 32% of 500 patients who underwent surgery for Chiari malformations [59]. Even though these findings could be attributed to the unique characteristics of the patient's cohort, we did not experience comparable alterations in our series, although a significant number of our patients presented with syringomyelia and preoperative alteration of electrophysiological parameters [3, 52]. This could be attributed to the neurosurgeon's experience in positioning the patient and the identification of high-risk patients with preoperative electrophysiological recordings, which could guide the surgeon to take special precautions during positioning. However, it should always be considered that there is no reliable relation between the extra- and intraoperative baseline measurements as multiple covariates influence the recordings (e.g., anesthesia, blood pressure, temperature, positioning, electrode impedance). In this respect, only one of the patients who showed electrophysiological changes during positioning in Danto's series was considered at high risk and underwent preoperative electrophysiological evaluation [59].

As for the SSEP recording, there was a deterioration of the MEP parameters during positioning in 2/33 cases (5%) for which data of continuous monitoring of the upper (H-MEP) and lower extremities (L-MEP) were available in our published series [52]. There were no significant differences in the absolute baseline and final latencies of H-MEPs (p = 0.4126) and L-MEPs (p = 0.2167), as well as the final-to-baseline MEP latency ratio (p = 0.2175). Neither of the two patients who presented a MEP latency increase >10% during surgery developed new postoperative deficits. In contrast, a MEP latency decrease indicated a more favorable outcome, with an improvement in pain symptoms specifically observed during follow-up visits in these patients. Similarly, there was no significant difference of either the absolute baseline and final amplitudes of H-MEPs (p = 0.8427) and L-MEPs (p = 0.7466) or the final-to-baseline MEP amplitude ratios (p = 0.1610). None of the patients who presented a MEP amplitude reduction of >50% during surgery developed new postoperative deficits [52] (Fig. 24.5).

Conclusion

There is evidence of electrophysiological data in the adult population available indicating that an improvement in the intraoperative evoked potentials is associated with a favorable clinical outcome. Our surgical experience indicates that IOM is not a prerequisite for a safe suboccipital decompression during the primary treatment of Chiari I malformations in adults when performed by an experienced team using standardized positioning, surgical approach, and technique. In this situation, the advantages of IOM need to be weighed against its disadvantages. On the one hand, there is continuous feedback about the functional state of the patient; on the other hand, IOM means increase of costs, consumption of considerable resources and time, and potential distraction of the surgeon by false-positive recordings. We still recommend IOM to prevent neurological injury during positioning, for surgeons at the beginning of their learning curve, in institutions with low case-volume of Chiari malformation, and in cases involving complex cranio-cervical malformations, re-explorations in scarred medullary junctions, or known cranio-cervical junction instabilities [55, 59, 60]. In general, ethical implications are an issue when conducting studies on the use of IOM in spinal cord surgery. However, as evidence of safe suboccipital decompression with nonsignificant changes in electrophysiological parameters exists, a prospective randomized trial may be ethically feasible to further characterize the advantages of IOM in this specific subtype of cranio-cervical surgery.

References

1. Klekamp J. Surgical treatment of Chiari I malformation – analysis of intraoperative findings, complications, and outcome for 371 foramen magnum decompressions. Neurosurgery. 2012;71:365–80; discussion 380.

2. Leis AA, Kofler M, Ross MA. The silent period in pure sensory neuronopathy. Muscle Nerve. 1992;15:1345–8.
3. Roser F, Ebner FH, Liebsch M, Dietz K, Tatagiba M. A new concept in the electrophysiological evaluation of syringomyelia. J Neurosurg Spine. 2008;8:517–23.
4. Sigal R, Denys A, Halimi P, Shapeero L, Doyon D, Boudghene F. Ventriculus terminalis of the conus medullaris: MR imaging in four patients with congenital dilatation. AJNR Am J Neuroradiol. 1991;12:733–7.
5. Roser F, Maier G, Ebner FH, Tatagiba M, Naegele T, Klose U. Fractionated anisotropy (FA-) levels derived from diffusion tensor imaging in cervical syringomyelia. Neurosurgery. 2010;67:901–5.
6. Epstein NE, Danto J, Nardi D. Evaluation of intraoperative somatosensory-evoked potential monitoring during 100 cervical operations. Spine (Phila Pa 1976). 1993;18:737–47.
7. Kombos T, Suess O, Da Silva C, Ciklatekerlio O, Nobis V, Brock M. Impact of somatosensory evoked potential monitoring on cervical surgery. J Clin Neurophysiol. 2003;20:122–8.
8. Anderson RC, Dowling KC, Feldstein NA, Emerson RG. Chiari I malformation: potential role for intraoperative electrophysiologic monitoring. J Clin Neurophysiol. 2003;20:65–72.
9. Anderson RC, Emerson RG, Dowling KC, Feldstein NA. Improvement in brainstem auditory evoked potentials after suboccipital decompression in patients with chiari I malformations. J Neurosurg. 2003;98:459–64.
10. Chen JA, Coutin-Churchman PE, Nuwer MR, Lazareff JA. Suboccipital craniotomy for Chiari I results in evoked potential conduction changes. Surg Neurol Int. 2012;3:165.
11. Zamel K, Galloway G, Kosnik EJ, Raslan M, Adeli A. Intraoperative neurophysiologic monitoring in 80 patients with Chiari I malformation: role of duraplasty. J Clin Neurophysiol. 2009;26:70–5.
12. Gelfan S, Tarlov IM. Interneurones and rigidity of spinal origin. J Physiol. 1959;146:594–617.
13. Nogues MA, Stalberg E. Electrodiagnostic findings in syringomyelia. Muscle Nerve. 1999;22:1653–9.
14. Barker A, Jalinous S, Freeston I. Non-invasive magnetic stimulation of the human motor cortex. Lancet. 1985;1:1106–7.
15. Masur H, Klostermann F, Oberwittler C, Papke K. Somatosensory evoked potentials after magnetic stimulation at different points of the body in normal subjects and in patients with syringomyelia. Funct Neurol. 1996;11:253–9.
16. Masur H, Oberwittler C. SEPs and CNS magnetic stimulation in syringomyelia. Muscle Nerve. 1993;16:681–2.
17. Masur H, Oberwittler C, Fahrendorf G, Heyen P, Reuther G, Nedjat S, et al. The relation between functional deficits, motor and sensory conduction times and MRI findings in syringomyelia. Electroencephalogr Clin Neurophysiol. 1992;85:321–30.
18. Restuccia D, Mauguiere F. The contribution of median nerve SEPs in the functional assessment of the cervical spinal cord in syringomyelia. A study of 24 patients. Brain. 1991;114(Pt 1B):361–79.
19. Jabbari B, Geyer C, Gunderson C, Chu A, Brophy J, McBurney JW, Jonas B. Somatosensory evoked potentials and magnetic resonance imaging in syringomyelia. Electroencephalogr Clin Neurophysiol. 1990;77:277–85.
20. Morioka T, Kurita-Tashima S, Fujii K, Nakagaki H, Kato M, Fukui M. Somatosensory and spinal evoked potentials in patients with cervical syringomyelia. Neurosurgery. 1992;30:218–22.
21. Stöhr M, Buettner UW, Riffel B, Koletzki E. Spinal somatosensory evoked potentials in cervical cord lesions. Electroencephalogr Clin Neurophysiol. 1982;54:257–65.
22. Urasaki E, Wada S, Kadoya C, Matsuzaki H, Yokota A, Matsuoka S. Absence of spinal N13-P13 and normal scalp far-field P14 in a patient with syringomyelia. Electroencephalogr Clin Neurophysiol. 1988;71:400–4.
23. Veilleux M, Stevens JC. Syringomyelia: electrophysiologic aspects. Muscle Nerve. 1987;10:449–58.
24. Noel P, Desmedt JE. Somatosensory cerebral evoked potentials after vascular lesions of the brain-stem and diencephalon. Brain. 1975;98:113–28.
25. Schieppati M, Ducati A. Effects of stimulus intensity, cervical cord tractotomies and cerebellectomy on somatosensory evoked potentials from skin and muscle afferents of cat hind limb. Electroencephalogr Clin Neurophysiol. 1981;51:363–72.
26. Iragui VJ. The cervical somatosensory evoked potential in man: far-field, conducted and segmental components. Electroencephalogr Clin Neurophysiol. 1984;57:228–35.
27. Jeanmonod D, Sindou M, Mauguiere F. Intraoperative spinal cord evoked potentials during cervical and lumbo-sacral microsurgical DREZ-tomy (MDT) for chronic pain and spasticity (preliminary data). Acta Neurochir Suppl (Wien). 1989;46:58–61.
28. Kofler M, Kronenberg MF, Brenneis C, Felber A, Saltuari L. Cutaneous silent periods in intramedullary spinal cord lesions. J Neurol Sci. 2003;216:67–79.
29. Forcadas I, Hurtado P, Madoz P, Zarranz JJ. Somatosensory evoked potentials in syringomyelia and the Arnold-Chiari anomaly. Clinical and imaging correlations. Neurologia. 1988;3:172–5.
30. Elster AD, Chen MY. Chiari I malformations: clinical and radiologic reappraisal. Radiology. 1992;183:347–53.
31. Hort-Legrand C, Emery E. Evoked motor and sensory potentials in syringomyelia. Neurochirurgie. 1999;45(Suppl 1):95–104.
32. Cristante L, Herrmann HD. Surgical management of intramedullary spinal cord tumors: functional outcome and sources of morbidity. Neurosurgery. 1994;35:69–74; discussion 74–66.
33. Emery E, Hort-Legrand C, Hurth M, Metral S. Correlations between clinical deficits, motor and

sensory evoked potentials and radiologic aspects of MRI in malformative syringomyelia. 27 Cases. Neurophysiol Clin. 1998;28:56–72.
34. Leis AA. Conduction abnormalities detected by silent period testing. Electroencephalogr Clin Neurophysiol. 1994;93:444–9.
35. Leis AA. Cutaneous silent period. Muscle Nerve. 1998;21:1243–5.
36. Uncini A, Kujirai T, Gluck B, Pullman S. Silent period induced by cutaneous stimulation. Electroencephalogr Clin Neurophysiol. 1991;81:344–52.
37. Floeter MK. Cutaneous silent periods. Muscle Nerve. 2003;28:391–401.
38. Inghilleri M, Berardelli A, Cruccu G, Manfredi M. Silent period evoked by transcranial stimulation of the human cortex and cervicomedullary junction. J Physiol. 1993;466:521–34.
39. Kaneko K, Kawai S, Fuchigami Y, Morita H, Ofuji A. Cutaneous silent period in syringomyelia. Muscle Nerve. 1997;20:884–6.
40. Kaneko K, Kawai S, Taguchi T, Fuchigami Y, Yonemura H, Fujimoto H. Cortical motor neuron excitability during cutaneous silent period. Electroencephalogr Clin Neurophysiol. 1998;109:364–8.
41. Stetkarova I, Kofler M, Leis AA. Cutaneous and mixed nerve silent periods in syringomyelia. Clin Neurophysiol. 2001;112:78–85.
42. Alstermark B, Lundberg A, Sasaki S. Integration in descending motor pathways controlling the forelimb in the cat. 10. Inhibitory pathways to forelimb motoneurones via C3-C4 propriospinal neurones. Exp Brain Res. 1984;56:279–92.
43. Burke D, Gracies JM, Mazavet D, Meunier S, Pierrot-Deseilligny E. Convergence of descending and various peripheral inputs onto common propriospinal-like inputs in man. J Physiol. 1992;449:655–71.
44. de Noordhout A, Rothwell JC, Day BL, Dressler D, Nakashima K, Thompson PD, Marsden CD. Effect of digital nerve stimuli on responses to electrical or magnetic stimulation of the human brain. J Physiol. 1992;447:535–48.
45. Fuhr P. Motor evoked potentials. Physiology, indications, safety aspects. Schweiz Rundsch Med Prax. 1992;81:1489–94.
46. Sindou M, Chávez-Machuca J, Hashish H. Craniocervical decompression for Chiari type I-malformation, adding extreme lateral foramen magnum opening and expansile duroplasty with arachnoid preservation. Technique and long-term functional results in 44 consecutive adult cases – comparison with l. Acta Neurochir. 2002;144:1005–19.
47. Fuhr P, Agostino R, Hallett M. Spinal motor neuron excitability during the silent period after cortical stimulation. Electroencephalogr Clin Neurophysiol. 1991;81:257–62.
48. Brasil-Neto JP, Cammarota A, Valls-Sole J, Pascual-Leone A, Hallett M, Cohen LG. Role of intracortical mechanisms in the late part of the silent period to transcranial stimulation of the human motor cortex. Acta Neurol Scand. 1995;92:383–6.
49. Cantello R. Prolonged cortical silent period after transcranial magnetic stimulation in generalized epilepsy. Neurology. 2002;58:1135; author reply 1135.
50. Roick H, von Giesen HJ, Benecke R. On the origin of the postexcitatory inhibition seen after transcranial magnetic brain stimulation in awake human subjects. Exp Brain Res. 1993;94:489–98.
51. van Kuijk AA, Pasman JW, Geurts AC, Hendricks HT. How salient is the silent period? The role of the silent period in the prognosis of upper extremity motor recovery after severe stroke. J Clin Neurophysiol. 2005;22:10–24.
52. Roser F, Ebner FH, Liebsch M, Tatagiba MS, Naros G. The role of intraoperative neuromonitoring in adults with Chiari I malformation. Clin Neurol Neurosurg. 2016;150:27–32.
53. Sala F, Squintani G, Tramontano V, Coppola A, Gerosa M. Intraoperative neurophysiological monitoring during surgery for Chiari malformations. Neurol Sci. 2011;32(Suppl 3):S317–9.
54. Nuwer MR, Emerson RG, Galloway G, Legatt AD, Lopez J, Minahan R, et al. Evidence-based guideline update: intraoperative spinal monitoring with somatosensory and transcranial electrical motor evoked potentials. J Clin Neurophysiol. 2012;29:101–8.
55. Anderson RC, Emerson RG, Dowling KC, Feldstein NA. Attenuation of somatosensory evoked potentials during positioning in a patient undergoing suboccipital craniectomy for Chiari I malformation with syringomyelia. J Child Neurol. 2001;16:936–9.
56. Durham SR, Fjeld-Olenec K. Comparison of posterior fossa decompression with and without duraplasty for the surgical treatment of Chiari malformation type I in pediatric patients: a meta-analysis. J Neurosurg Pediatr. 2008;2:42–9.
57. Haroun RI, Guarnieri M, Meadow JJ, Kraut M, Carson BS. Current opinions for the treatment of syringomyelia and chiari malformations: survey of the Pediatric Section of the American Association of Neurological Surgeons. Pediatr Neurosurg. 2000;33:311–7.
58. Schijman E, Steinbok P. International survey on the management of Chiari I malformation and syringomyelia. Childs Nerv Syst. 2004;20:341–8.
59. Danto J, Milhorat T, Hertzberg H, Bolognese P, Conlon J, Korn A. The neurophysiological intraoperative monitoring of Chiari malformation surgery. Riv Med. 2006;12:51–4.
60. Deinsberger W, Christophis P, Jödicke A, Heesen M, Böker DK. Somatosensory evoked potential monitoring during positioning of the patient for posterior fossa surgery in the semisitting position. Neurosurgery. 1998;43:36–40; discussion 40–42.

Radiology

25

Abby E. Deans and A. James Barkovich

Magnetic resonance imaging (MRI) is the mainstay of imaging for diagnosis and characterization of the Chiari malformations.

Chiari I

The Chiari I malformation is a very misunderstood condition. As illustrated by Chiari's initial paper, it is not a brain malformation; it is a disorder caused by *compression* of neural structures (usually the cerebellar tonsils, upper cervical spinal cord, or medulla oblongata, which have been either pushed or pulled downward) near the craniocervical junction by the surrounding bone and consequent alteration of cerebrospinal fluid (CSF) flow through the foramen magnum. The mere presence of low cerebellar tonsils does not constitute the Chiari I disorder; low tonsils are common and usually asymptomatic. When clinical signs and symptoms develop, the responsible compression is caused by a downward push or a downward pull. The push may result from a small posterior fossa as in genetic craniofacial syndromes such as Crouzon syndrome [1–3], from increased pressure due to abnormal CSF flow or resorption [4] or from an intracranial mass (usually in the posterior fossa). The pull is typically from low infratentorial/spinal CSF pressure due to a CSF leak [5, 6] or a lumboperitoneal [7] or even an intracranial [8] shunt. Foramen magnum crowding from either a push or a pull will result in altered CSF flow and craniospinal pressure dissociation; this condition, in turn, can cause intraspinal edema ("presyrinx" [9]) or frank syringohydromyelia.

The imaging study of choice to evaluate patients with cerebellar ectopia is MRI. Sagittal and axial T1- and T2-weighted MRI with images no thicker than 3 mm should be obtained in all patients. The images should include the entire brain and skull, as it is important to look for hydrocephalus, masses, malformations, deformities, or evidence of high or low intracranial pressure. The cervical spine should also be evaluated down to C6–C7 to look for associated spinal cord edema or syringohydromyelia; as it may be difficult to differentiate a syrinx from edema on T2 sagittal images, axial T1 images are useful for confirmation. If the anatomic images are suggestive of cerebellar ectopia, cardiac-gated phase contrast images should be obtained in order to determine the effects of the ectopia upon CSF flow at and around the foramen magnum.

A. E. Deans
Department of Radiology and Biomedical Imaging, University of California, San Francisco, San Francisco, CA, USA

A. J. Barkovich (✉)
Departments of Radiology, Neurology, Pediatrics and Neurosurgery, University of California, San Francisco, San Francisco, CA, USA
e-mail: James.barkovich@ucsf.edu

R. S. Tubbs et al. (eds.), *The Chiari Malformations*, https://doi.org/10.1007/978-3-030-44862-2_25

The key anatomic imaging finding on MRI of these malformations is tonsillar ectopia with compressed ("peg-like" or "pointed") cerebellar tonsils and nearly complete effacement of CSF at the foramen magnum or C1 level (Fig. 25.1a). In general, if the tonsils are displaced 5 mm or more below a line drawn from the bottom tip of the basion to the bottom tip of the opisthion (Fig. 25.1b), they are too low and are probably compressed [10]. Children may have slightly greater ectopia of cerebellar tissue without compression and, therefore, without symptoms [11]. However, measurements are less important than the actual appearance of the structures. Notably, most patients with borderline low-lying tonsils are asymptomatic, and the measurement of tonsillar ectopia alone (without tonsil compression or subarachnoid space effacement) should not necessarily instigate further workup. In addition to the pointed appearance of the inferior tonsils and effacement or obliteration of the CSF space in the caudal posterior fossa, foramen magnum, and C1 level, syrinx or presyrinx in the cervical spinal cord (Fig. 25.1a, b) should raise suspicion for compression of the subarachnoid spaces or tumor. Tumor can usually be confidently diagnosed by the finding of an intramedullary mass effect that enhances after administration of para-

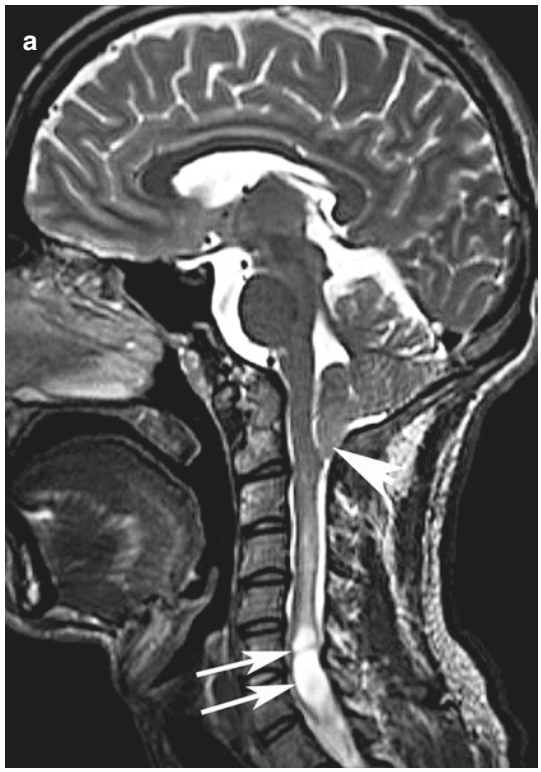

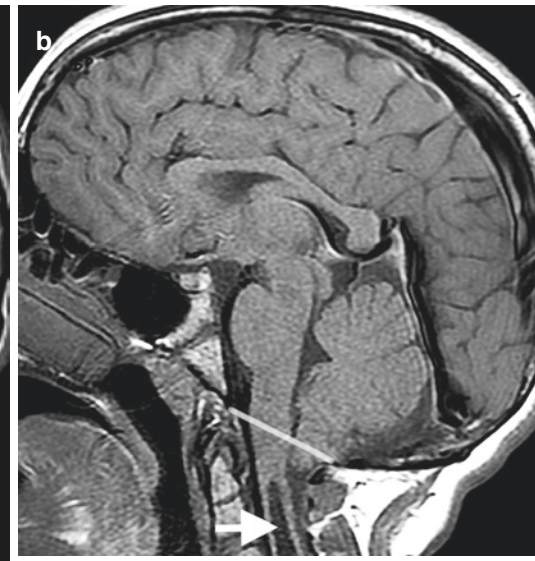

Fig. 25.1 (**a**) Sagittal T2-weighted MRI of the brain and cervical spine demonstrating findings of Chiari I with cervical ectopia of the cerebellar tonsils with compressed, "pointed" or "peg-like," morphology (arrow) and effacement of CSF spaces at the level of the foramen magnum and upper cervical spinal canal. This patient was found to have a lower cervical syrinx (double arrow) at presentation. (**b**) In another patient, more subtle findings of slightly low position of the cerebellar tonsils, 6 mm below a line drawn from the basion to the opisthion, with slightly compressed morphology and effacement of CSF at the foramen magnum. Associated finding of cervical syrinx (arrow) suggests narrowing of subarachnoid spaces at the foramen magnum/C1 levels, which could be further evaluated with phase contrast CSF flow imaging to identify region of obstruction to CSF flow

magnetic contrast. If no tumor is found, cardiac-gated, phase contrast CSF flow studies can be used to look for alteration of CSF dynamics. Although described further elsewhere, a brief description of CSF flow studies deserves mention here given the importance of these studies for diagnosis in Chiari I. Normal studies demonstrate craniocaudal CSF flow (white CSF) during cardiac systole, which lasts about 40% of the cardiac cycle [12], and the lower brain stem and cerebellar tonsils move slightly downward. During cardiac diastole (60% of cycle), CSF moves rostrally and is black; the brain stem and tonsils move slightly upward [12]. When the CSF flow is impaired by cerebellar tissue in the foramen magnum, the amount of CSF seen in motion ventral and dorsal to the brain stem and craniocervical junction is reduced (Fig. 25.2a, b), CSF systole is shortened, diastole is prolonged, and movement of the brain stem and tonsils is increased [13, 14]. When flow studies demonstrate prolonged CSF diastole at the foramen magnum with increased downward motion of the cerebellar tonsils and brain stem, it is strong evidence of impaired CSF flow.

Any cause of restriction of CSF flow at the foramen magnum/C1/C2 levels can cause clinical symptoms or syrinx formation. Imaging is important to differentiate among these different causes, as the treatments might be very different. If a "slumping brain" is seen (Fig. 25.3a–d), with pachymeningeal enhancement (Fig. 25.3b), the brain stem slumping against the clivus, enlarged dural venous sinuses and pituitary gland (Fig. 25.3a), or a low third ventricle floor, intracranial hypotension should be strongly suspected, and a search for the CSF leak should be sought [5, 6]. In the case of primary mesenchymal disorders or premature suture fusion resulting in a small skull base, the head is typically brachycephalic (Fig. 25.4a), and early closure of the sutures can be identified; in this situation, it is useful to perform an MR venogram to look for restriction of venous outflow at the undersized jugular foramina and, more importantly, extensive collateral venous flow via emissary veins in the occipital region [1, 15]. The imaging study might also show hydrocephalus or a posterior fossa mass causing cerebellar herniation through the foramen magnum. In patients with diseases of bone, basilar invagination (Fig. 25.4b) may result in tonsillar herniation. Younger people with mesenchymal abnormalities resulting in a small skull base or a flattened chondrocranium

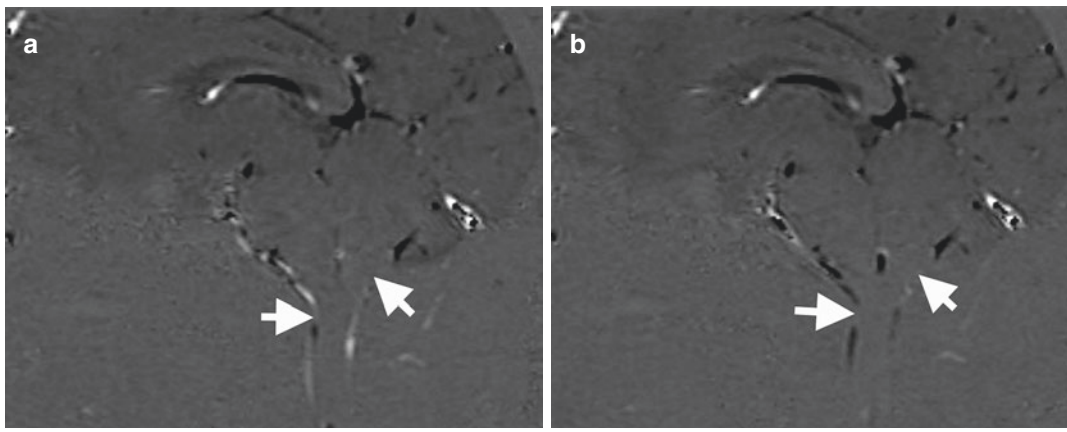

Fig. 25.2 Cardiac-gated phase contrast CSF flow imaging demonstrates obstructed CSF flow at the foramen magnum in a patient with platybasia (same patient as in Fig. 25.4c). (**a**) Decreased CSF flow anterior to the medulla and absent flow posterior to the cerebellar tonsils (arrows) in CSF systole (white CSF) and (**b**) absent flow both anteriorly and posteriorly (arrows) during CSF diastole (black CSF)

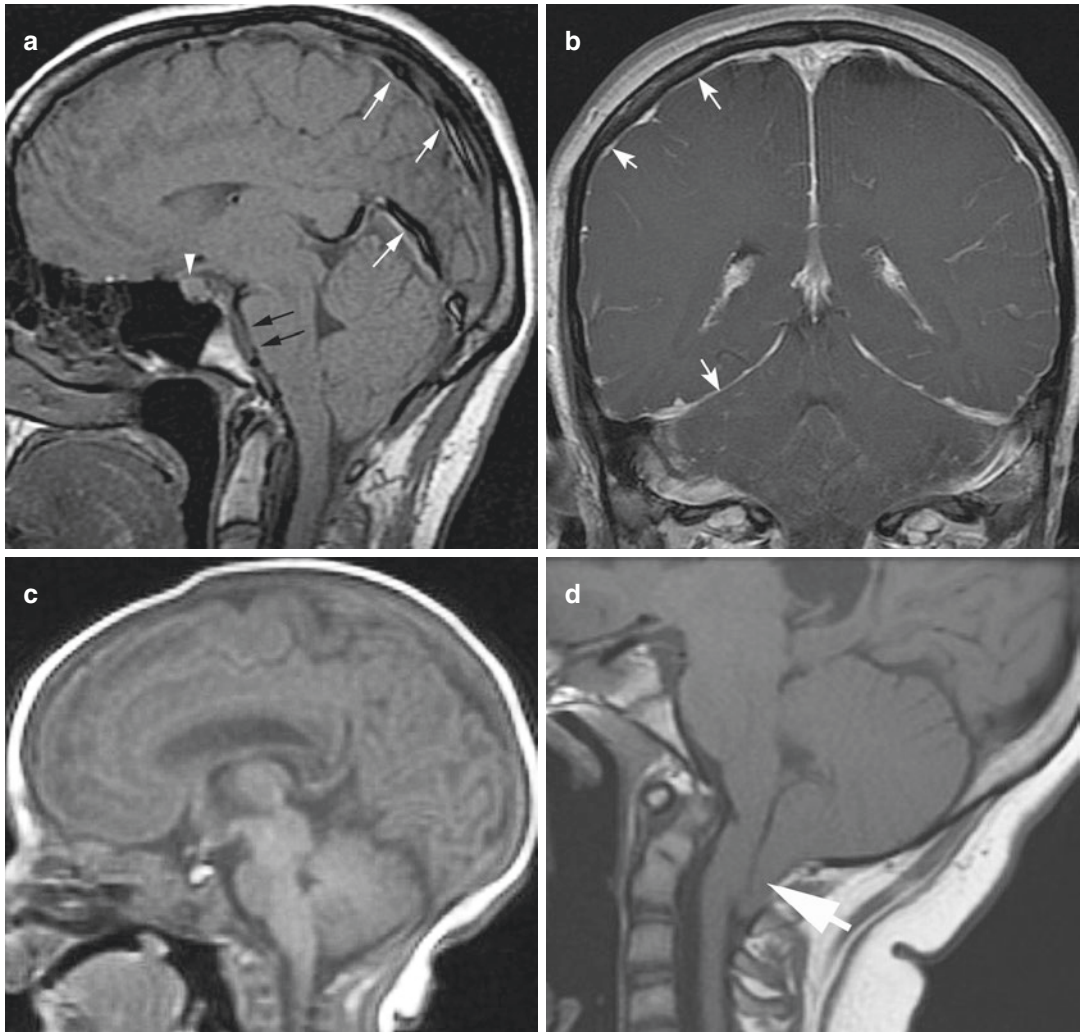

Fig. 25.3 Cervical ectopic location of the cerebellar tonsils can result from a downward pull as in the setting of (**a**) spontaneous intracranial hypotension (SIH) from spinal CSF leak. Findings of SIH on sagittal MRI include tonsillar ectopia, enlarged dural venous sinuses (arrow) and pituitary gland (arrowhead), compression of pons against clivus (black arrows), and (**b**) diffuse pachymeningeal enhancement (white arrows) on post-gadolinium T1-weighted MRI sequences. Cerebellar herniation can also result from a downward push from hydrocephalus. (**c**) Normal cerebellar location and morphology in a neonate who later developed hydrocephalus with (**d**) subsequent progressive downward herniation of the cerebellar tonsils (arrow) and symptomatic foramen magnum compression by age 11 years

(platybasia) can result in herniation of cerebellar structures (Fig. 25.4c). Any of these conditions can cause occipital headaches and alteration of CSF flow resulting in syringohydromyelia. In fact, even in the absence of tonsillar herniation, patients with clinical history strongly suggestive of CSF obstruction at the level of the foramen magnum or posterior fossa with syringohydromyelia (the "Chiari 0 malformation" [16]) may benefit from evaluation with cardiac-gated phase contrast CSF flow imaging to look for flow or pulsation abnormalities as decompression or targeted shunt placement may provide symptomatic relief.

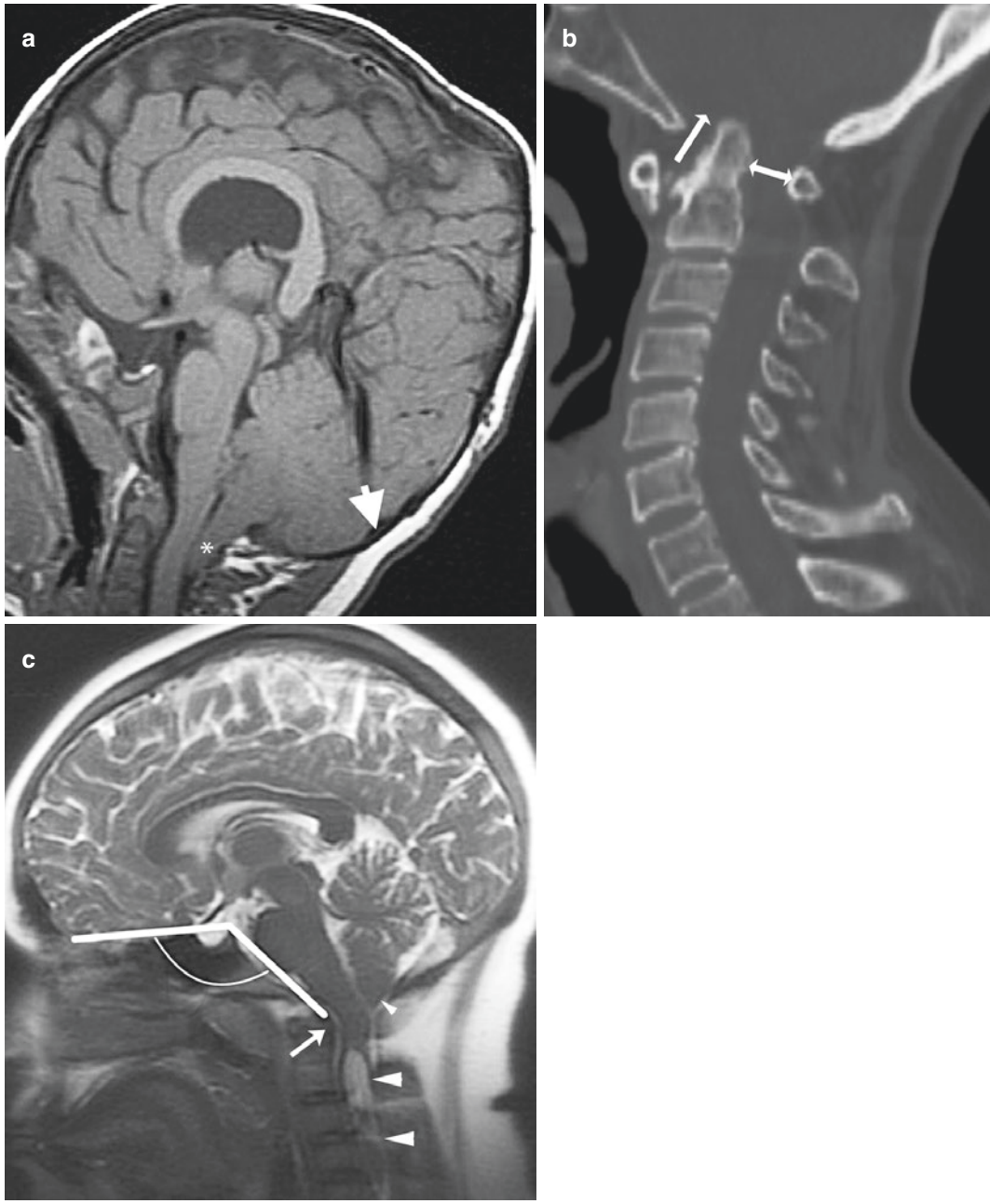

Fig. 25.4 Chiari I malformation can also be seen in the setting of small posterior fossa from other causes. (**a**) Early fusion of cranial sutures in Crouzon syndrome results in brachycephaly, arched morphology of the corpus callosum, and small posterior fossa with low torcular attachment (arrow) and cervical ectopia of the cerebellar tonsils (∗) to the level of C2. (**b**) Basilar invagination as shown on this sagittal CT of the cervical spine demonstrating upward displacement of C2 (arrow) superiorly through the foramen magnum, resulting in foramen magnum and upper cervical stenosis (double-headed arrow) with tonsillar compression. (**c**) Platybasia is often seen in association with posterior angulation of the dens (arrow) or basilar invagination which exacerbates foramen magnum stenosis. Note pointed morphology of the cerebellar tonsils (small arrowhead), effacement of CSF at the foramen magnum, and cervical syringomyelia (large arrowheads) suggesting compression at the foramen magnum

Chiari II

For assessment of the Chiari II malformation, the complex set of posterior fossa, and supratentorial abnormalities seen in the setting of myelomeningocele (MMC), MRI again forms the diagnostic mainstay. However, prenatal screening ultrasound is often where the brain and spine abnormalities in the Chiari II malformation complex are identified initially and deserves discussion in this setting. Subsequent fetal MRI is indicated for further characterization and identification of associated findings. The appearance of myelomeningocele and the Chiari II malformation on prenatal imaging will be commensurate to the relatively early developmental stage, with abnormalities often progressing on follow-up studies.

Fetal Ultrasound

Fetal screening ultrasound protocols [17] include an evaluation of the nuchal translucency late in the first trimester, which includes a limited evaluation of anatomy, followed by a full anatomic evaluation at 18–20 weeks. Therefore, findings suggestive of Chiari II and myelomeningocele are generally first visualized in this period. Maternal serum screening tests or amniocentesis, performed within the same period, revealing elevated alpha-fetoprotein in the setting of open neural tube defect can also be the referring indication for fetal brain and spine MRI.

Screening fetal ultrasound examination [17] includes evaluation of the brain and spine. Evaluation of the brain will include axial view of the fetal head through the level of the thalami and cavum septum pellucidum for measurement of biparietal diameter and head circumference, axial view through the posterior fossa, and axial view through the cerebral lateral ventricles. Evaluation of the spine includes longitudinal (sagittal) and axial views through the cervical, thoracic, lumbar, and sacral spine. Nearly universally, fetuses with Chiari II malformation will demonstrate bilaterally flattened or slightly collapsed appearance of the frontal calvarium on axial views through the supratentorial brain, the so-called "lemon sign" (Fig. 25.5a), and effaced cisterna magna with anterior wrapping of the cerebellar hemispheres, the so-called "banana sign" (Fig. 25.5b) [18], or nonvisualization of the cerebellum. Other findings that are suggestive of Chiari II malformation include decreased biparietal diameter [19], with a majority of cases demonstrating measurements below the fifth percentile and ventriculomegaly [20, 21]. Axial views of the normal fetal spine will demonstrate a complete vertebral ring surrounding the spinal canal and intact layer of skin dorsally. In the setting of spina bifida, the posterior vertebrae have a U- or V-shaped configuration with splaying of the vertebral pedicles (Fig. 25.5c), absence of spinous processes, and disruption of the normal overlying integument (Fig. 25.5d), often with associated focal kyphoscoliosis. When any of these findings are identified, referral for fetal brain and spine MRI is appropriate to confirm these abnormalities and to identify any additional abnormalities that may not have been apparent on ultrasound.

Fetal and Postnatal Magnetic Resonance Imaging

Although fetal MRI has been performed for more than 20 years, it has become more technically feasible in the past decade through advancements in MRI coil design and development of real-time imaging using fast T2-weighted MRI sequences, called single-shot fast spin echo (SSFSE) or half Fourier acquisition single-shot turbo spin echo (HASTE). The subsecond image acquisition minimizes image artifact due to fetal or maternal motion, obviating the need for fetal sedation. MRI at 1.5 T is generally believed to be safe for the fetus throughout gestation, without any risk of teratogenic or developmental consequences [22, 23]. However, second trimester scan acquisition, often after 22 weeks gestation, yields optimal image quality due to increased fetal size and decreased motion. Standard fetal brain MRI protocol at our institution includes a large field of view localizer to visualize the position of the fetus and location of the placenta in the uterus, followed by sagittal, coronal, and axial sequences with respect to fetal brain with 3 mm slice thickness separated by a 2–3 mm interslice gap. The images are acquired in at least two sets to guarantee that the entire brain is visualized; the purpose

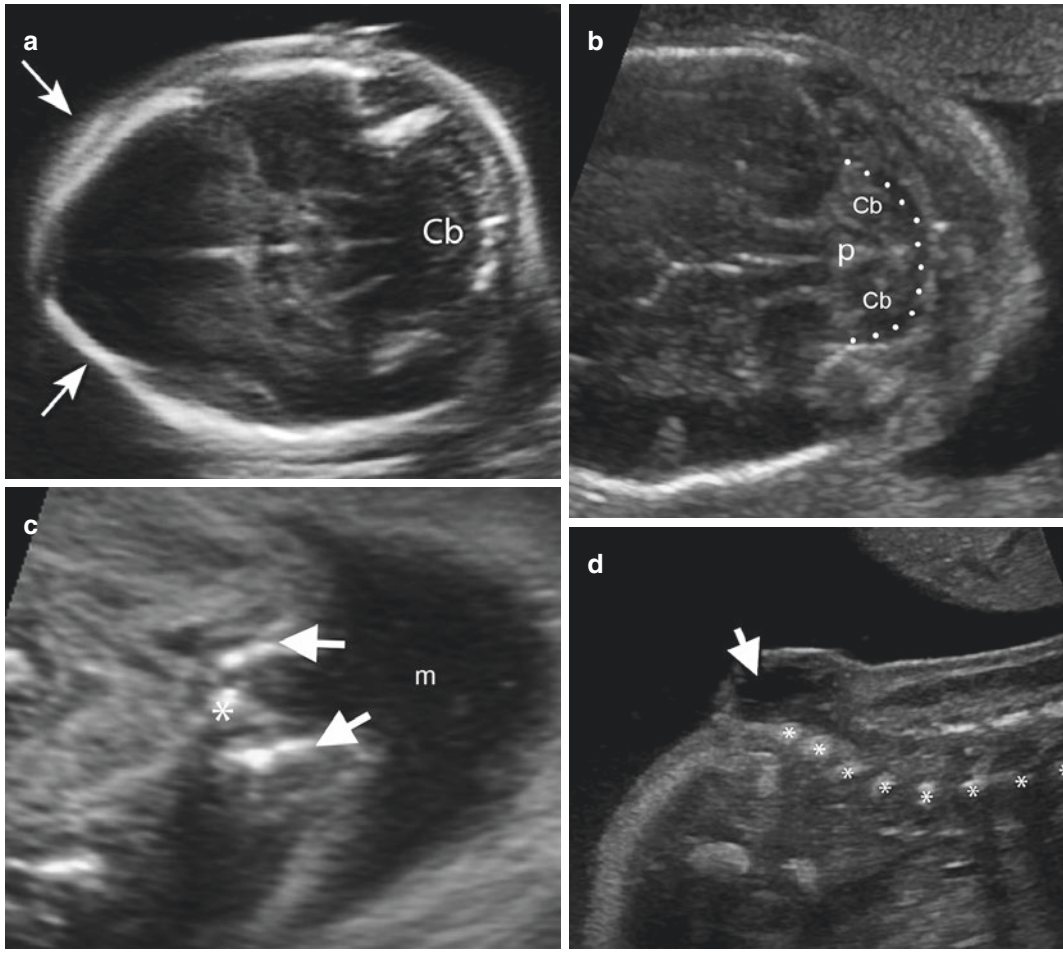

Fig. 25.5 Chiari II malformation and myelomeningocele are often first identified on prenatal ultrasound. (**a**) Flattened or collapsed appearance (arrows) of bilateral frontal calvaria at fetal ultrasound at 18-week gestational age, the so-called lemon sign, is thought to be secondary to insufficient distension of the cerebral ventricles due to CSF leakage from the myelomeningocele (Cb designates cerebellum). (**b**) Small posterior fossa with obliteration of the cisterna magna and wrapping of the cerebellar hemispheres (Cb) laterally around the pons ("p") and midbrain, the so-called banana sign. (**c**) Evaluation of the fetal spine in the transverse (axial) plane demonstrates spina bifida defect in the sacral spine with splaying of the bright vertebral pedicles (arrows), absent spinous process, and large anechoic dorsal meningocele (m). (**d**) Longitudinal (sagittal) view of the lumbosacral spine (vertebral bodies denoted by ∗ in **c** and **d**) shows dorsal sacral myelomeningocele (arrow)

of the gap is to avoid saturation effects that result from exciting the protons in a single slice before they are completely relaxed from excitation of the previous section [24]. Evaluation of the fetal spine includes sagittal and axial T2-weighted sequences with 2 mm slice thickness and no gap between slices. Each subsequent sequence is localized based on the most recent prior slice to adjust for fetal motion.

In the fetus with suspected Chiari II/myelomeningocele (Fig. 25.6a–d), fetal MRI is essential to confirm the level and extent of the myelomeningocele defect (Fig. 25.6b), the severity of posterior fossa abnormalities (Fig. 25.6a), and the presence and extent of associated supratentorial brain abnormalities (Fig. 25.6c), which are often occult on ultrasound. Complete characterization of findings facilitates prognostication for optimal pregnancy and postnatal management, including consideration of termination or planning for fetal myelomeningocele surgical closure where possible.

After delivery, MRI is the study of choice for children with myelomeningocele. Three-

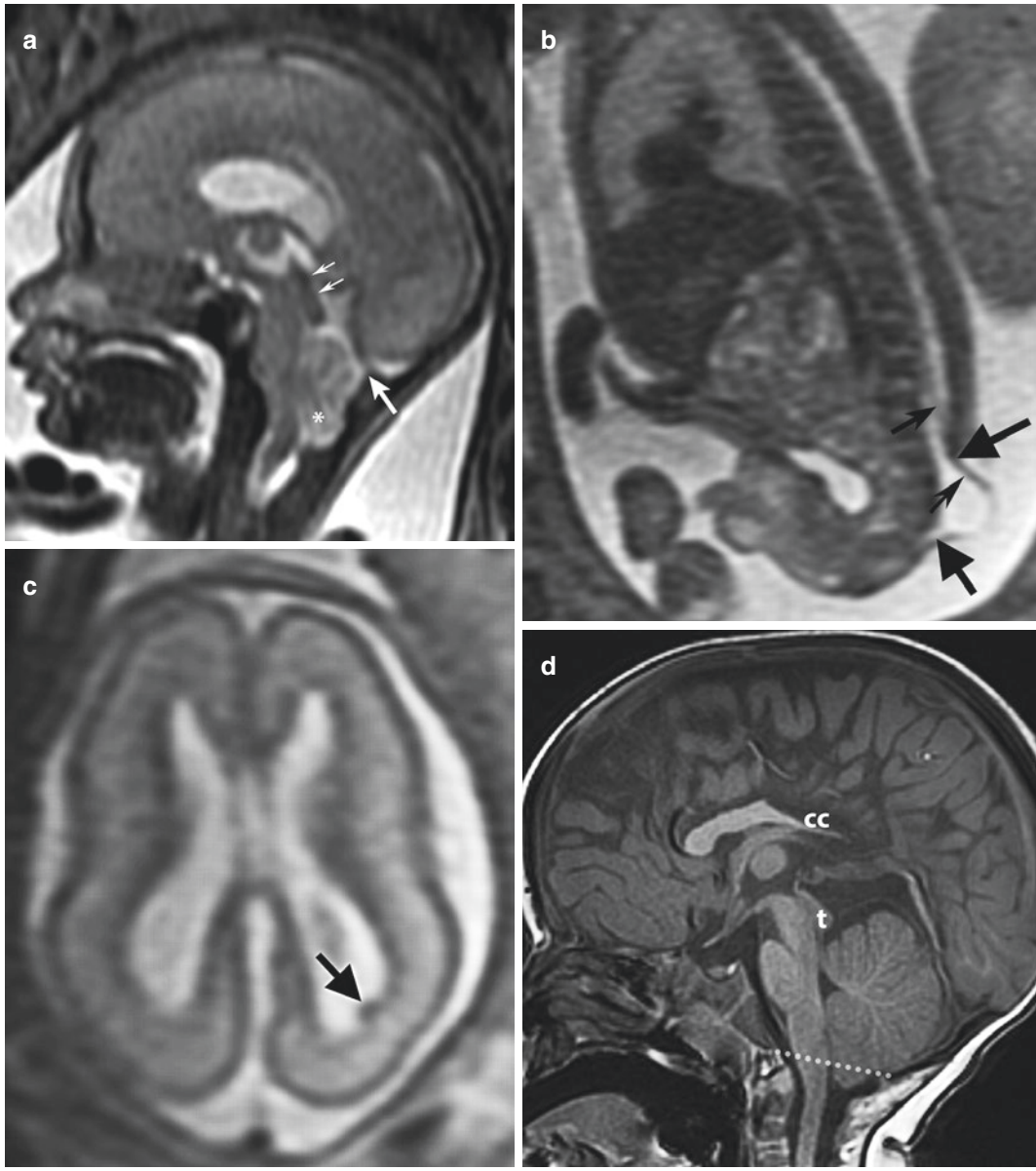

Fig. 25.6 Fetal MRI of Chiari II malformation/myelomeningocele. (**a**) Sagittal T2-weighted fetal MRI at 25 weeks gestation shows small posterior fossa with steep tentorium, narrow and low fourth ventricle, low torcular Herophili (large arrow), and elongated midbrain tectum (small arrows), with cervical ectopia of the developing inferior cerebellum (∗) consistent with severe Chiari II malformation. (**b**) Spine views show lumbosacral myelomeningocele (large arrows) and tethered cord (small arrows). (**c**) Axial view through the lateral ventricles demonstrates periventricular nodular heterotopia in the atrium (arrow). (**d**) Following prenatal myelomeningocele repair, mild findings of Chiari II malformation at 12-month postnatal age include borderline low, rounded cerebellar tonsils and mild posterior inferior stretching of the tectum (t). Note dysgenetic corpus callosum (cc)

dimensional (3D) spoiled gradient-echo acquisitions (SPGR, MP-RAGE) in the brain are best acquired in the sagittal plane and reformatted in thin (1–2 mm) coronal and axial sections. Axial and coronal T2-weighted images (either 2D acquisition with thickness of 3 mm or less or 3D volumetric acquisition with reformations in three orthogonal planes) are useful supplemental sequences. For spine imaging, it is essential to acquire sagittal and axial T1- and T2-weighted

sequences. If kyphoscoliosis is present, the imaging planes should be angled such that the sagittal images are parallel to and axial images perpendicular to each straight section of spine.

MRI of the brain has identical findings whether performed in the fetus, neonate, infant, or child, although subtle anomalies—such as anomalies of the cerebral cortex and smaller commissures—are easier to detect in the larger brains [25]. The posterior fossa is small with little or no CSF space. The tentorium cerebelli has a low attachment and steep orientation (Figs. 25.6a and 25.7a), causing the straight sinus to have a nearly vertical course to the torcular Herophili. The cerebellum nearly fills the small posterior fossa with hemispheres wrapping laterally around the midbrain (Fig. 25.7b). As a result of the CSF leakage through the open spina bifida in utero, a rostro-caudal pressure gradient acts upon the posterior fossa structures, resulting in the characteristic downward displacement of portions of the cerebellum, midbrain, and fourth ventricle. The fourth ventricle is small and narrowed in its rostro-caudal dimension (a normal-sized or enlarged fourth ventricle should raise the possibility of an isolated ventricle) (Fig. 25.7c). The pons may be pushed against the clivus, and the pressure of the hindbrain structures on the skull base can cause concave erosive changes upon that structure. The foramen magnum and tentorial incisura are enlarged due to the chronic herniation of the cerebellum through these structures. The cerebellar hemispheres and vermis are often very small, possibly due to chronic ischemia from compression (Fig. 25.7d). The inferior colliculi are often enlarged and stretched in an inferior and dorsal direction, while the superior colliculi are small, resulting in the "beaked tec-

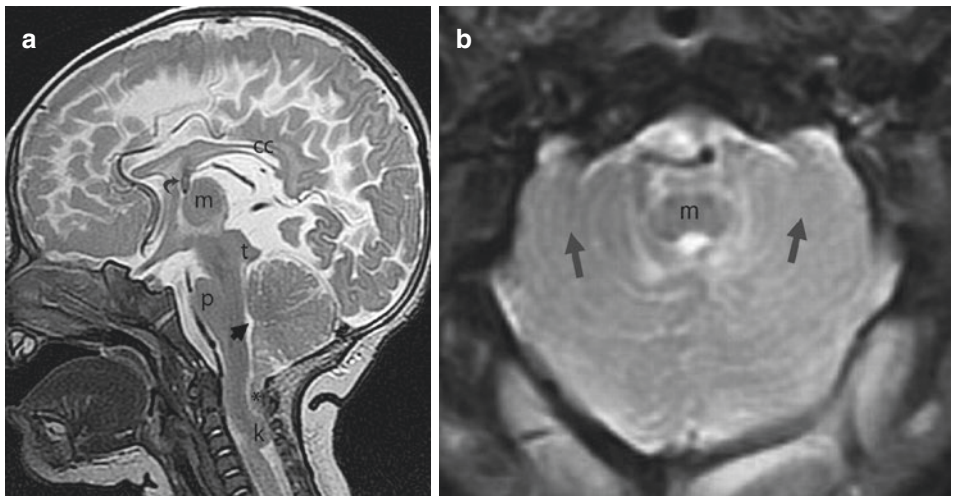

Fig. 25.7 Chiari II malformation. (**a**) Sagittal T2-weighted MRI from an 8-year-old patient born with myelomeningocele demonstrates many of the findings of the Chiari II malformation including small posterior fossa with low tentorial attachment and steep tentorial angle, with downward shift of posterior fossa contents including cerebellum (with herniation ∗ into the cervical canal), pons (p), and medulla. The fourth ventricle (large arrow) is effaced and low. There is a characteristic cervicomedullary kink (k) at the C4 level. The midbrain tectum (t) is posteriorly and inferiorly stretched or "beaked." The massa intermedia (m) is enlarged. The corpus callosum (cc) is thin in the posterior body and splenium. This patient has a ventriculoperitoneal shunt (curved arrow) for treatment of hydrocephalus. (**b**) Axial T2-weighted view through the posterior fossa demonstrates wrapping of the cerebellar hemispheres anteriorly (arrows) around the medulla (m) with effacement of the posterior fossa CSF space. (**c**) In a T1 sagittal image of a different patient, fourth ventricular enlargement (arrow) suggests isolated fourth ventricle. This patient has a cervical syrinx (double arrow), which resolved after shunting the fourth ventricle. (**d**) Severe Chiari II malformation; sagittal T1 image in a different patient shows very small posterior fossa, near absence of the cerebellum (minimal residual, likely cerebellar, tissue is noted by the arrow), and tiny pons. Stenogyria, or increased number of small gyri, is apparent in the occipital cortex (double arrow) most likely due to shunting of severe hydrocephalus and paucity of subcortical white matter. (**e**) Periventricular nodular heterotopia (arrow) and decreased posterior cerebral white matter are common associated supratentorial abnormalities, (**f**) as are dysplastic medial temporal lobes (arrows) with herniation across midline (∗)

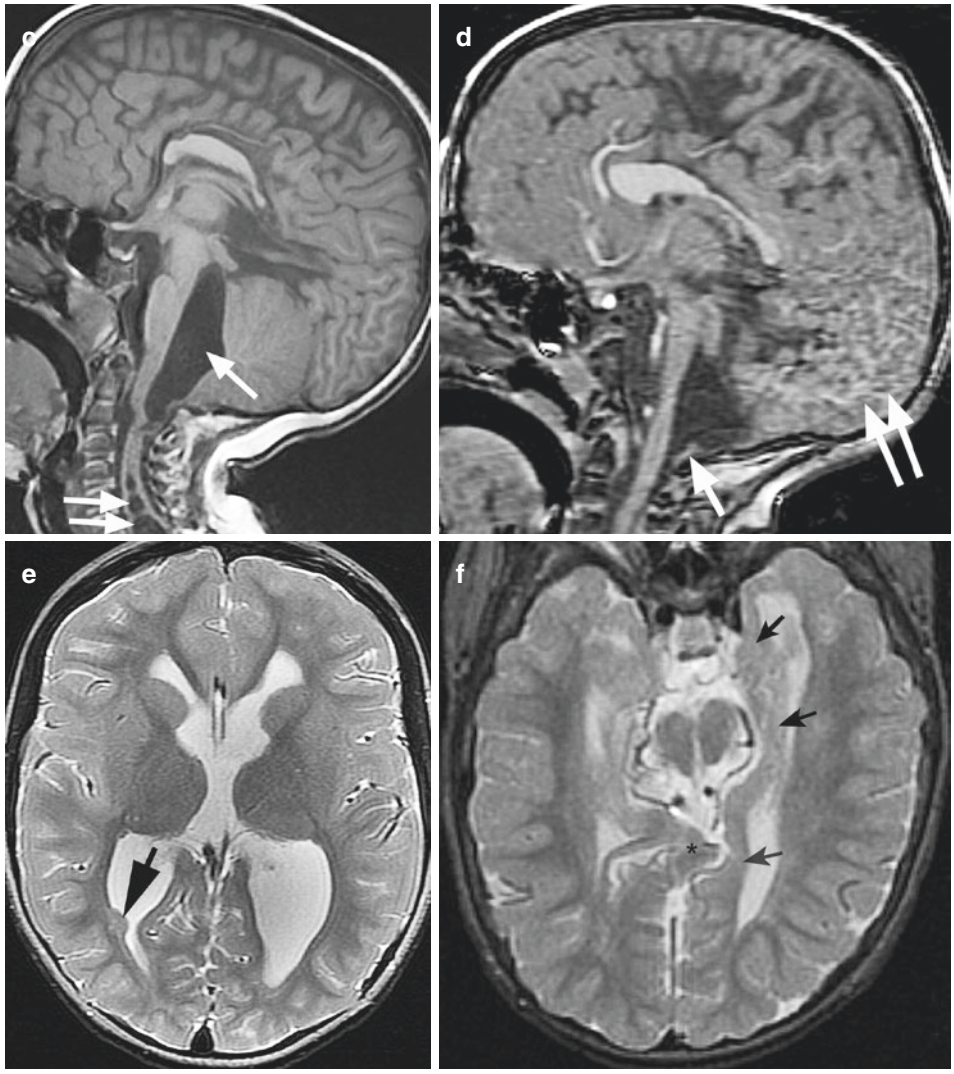

Fig. 25.7 (continued)

tum" appearance (Fig. 25.7a, c, d). The supratentorial vault is small, again, most likely due to inadequate ventricular distension earlier in gestation; however, disproportionate ventricular dilation is common from narrowing of the aqueduct, posterior fossa crowding, or perhaps lack of dampening of CSF pulsations in the spine because the foramen magnum is occluded [26].

Supratentorial anomalies are common, although it is not known whether they are genetic, a result of chronic hydrocephalus, or a result of the effects of chronic intracranial hypotension upon the developing brain [27]. Complete evaluation of the supratentorial brain is indicated, therefore, in all affected patients. Anomalies of the cerebral commissures are very common. The anterior commissure is in a low position (halfway between the optic chiasm and the foramen of Monro) in 40%. The corpus callosum has a very variable appearance. Most typically, it is thin in the posterior aspects (posterior body and splenium), similar to what is seen associated with other causes of congenital hydrocephalus (Fig. 25.7a). However, ~30% have frank hypogenesis with absent splenium, absent rostrum, and a small posterior callosal body [28]. The cerebral white matter often has diminished volume posteriorly, particularly in patients with

abnormalities of the corpus callosum [28]. It is not known whether this is a result of congenital hydrocephalus, cerebral dysgenesis related to callosal hypogenesis or dysgenesis, or a combination of the two factors. In about 10%, white matter volume is severely diminished globally. Gray matter heterotopias are identified in 15–20% of affected individuals (Fig. 25.7e), typically two to three nodules in the periventricular region, with the trigones/occipital horns the most common locations, followed by the frontal horns [28]. Anomalies of sulcation are commonly identified. A condition called "stenogyria" (narrow gyri), in which too many small gyri are seen on the cerebral surface but histology is normal (Fig. 25.7d), is the most common abnormality, seen in about 70% [28]. It is believed to be the result of cerebral decompression by shunting after the cortex has been stretched by hydrocephalus. Polymicrogyria has been described sin humans with MMC [29], but the series was one of very severely affected patients who died before the age of 2 years; it is very uncommonly detected by neuroimaging. In addition, a sheep model of myelomeningocele showed a "cobblestone-like" cortical malformation, perhaps resulting from disruption of the leptomeninges in utero [27]. The posteromedial temporal lobe, in particular the posterior limbic lobe, is nearly always abnormal (Fig. 25.7f), with cortical thinning, diminution of underlying white matter, and resultant huge supravermian/quadrigeminal plate/interhemispheric cisterns [28, 30]. Occasional aberrant gyri extend into this enlarged cistern, often crossing the midline. Again, the causes of these findings—fetal/neonatal hydrocephalus versus genetic versus compression of the structures in utero versus disruption of meninges during development as a result of the chronic CSF leak—are not known [30], and these abnormalities are not always evident prenatally [25].

Evaluation of the spinal cord differs on the fetal exam as compared to the postnatal (postsurgical) MRI. The purpose of the fetal spine MRI is to identify and characterize the MMC and its levels and to look for associated spine anomalies. The spinal defect is evidenced as splayed pedicles and dorsally open neural tube with variable herniation of the neural plate beyond the spinal canal into the amniotic space (myelocele to myelomeningocele spectrum). Adjacent levels will show lack of mesenchymal tissues, bony posterior elements, and fat, interposed between the spinal canal and the surface. Severity of intracranial abnormalities, necessity of CSF shunting, and clinical prognosis are correlated with more rostral location [31]. The recent multicenter randomized trial comparing prenatal to postnatal surgical closure of myelomeningocele [32] and preceding animal studies [33] demonstrated decreased severity of the Chiari II malformation on follow-up MRI (Fig. 25.6a vs. d), decreased necessity of CSF shunting, and improved early functional outcomes following prenatal repair of thoracic and lumbar myelomeningocele. Fetal MRI will likely remain an invaluable tool for characterization of MMC and Chiari II for purposes of pregnancy management and prenatal treatment.

After repair of the myelomeningocele, fetal imaging to assess the state of the hydrocephalus is best performed via ultrasound. After birth, imaging of the spine is usually performed if progressive lower extremity or bladder/bowel function is observed. Potential causes that need to be excluded include hydrocephalus, syringohydromyelia, development of congenital or acquired inclusion masses such as epidermoids, or retethering of the spinal cord at the site of MMC repair. Hydrocephalus and syringohydromyelia are best diagnosed by comparing the MRI to prior studies to look for increasing size of the lateral ventricles or the central canal of the spinal cord. Epidermoids are usually round or lobulated masses that are hyperintense on T2-weighted images (Fig. 25.8a) and hypointense on T1-weighted MRI images (Fig. 25.8b). They do not enhance after contrast administration (Fig. 25.8c). If diffusion-weighted imaging can be performed, the epidermoids will be seen as very hyperintense on diffusion-weighted images (Fig. 25.8d). Retethering of the cord as the cause of symptoms is really a diagnosis of exclusion because all repaired MMCs appear attached to dura or scar tissue at the level of the repair (Fig. 25.8a); the cord does not ascend after MMC repair. A diagnosis of retethering as the cause of symptoms cannot be made, therefore, until all other potential causes have been excluded.

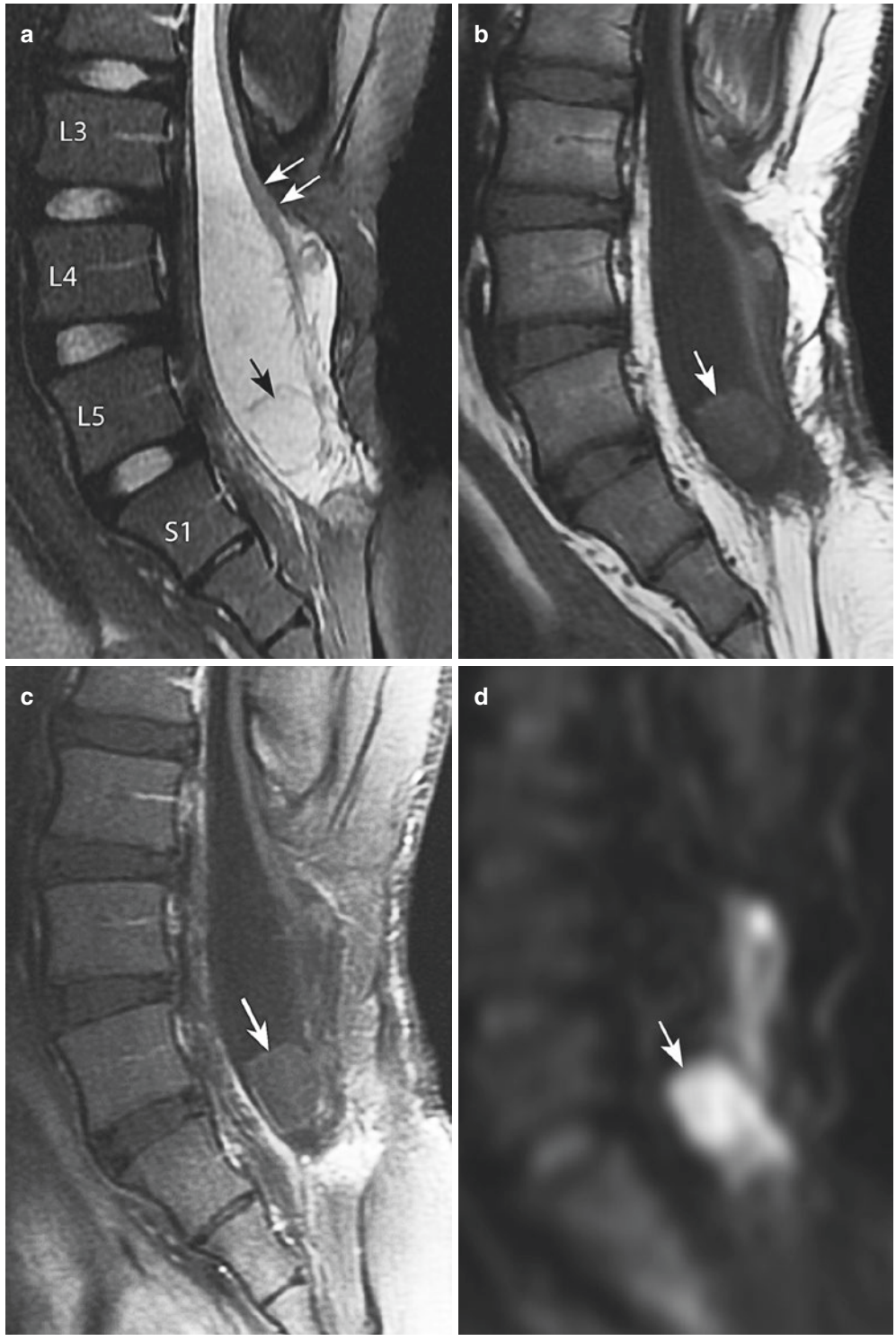

Fig. 25.8 Complications post-myelomeningocele repair. (**a**) Mass (black arrow in **a**, white arrow in **b**–**d**) within the inferior thecal sac at the S1 level is T2 hyperintense, (**b**) T1 hypointense, (**c**) and non-enhancing and (**d**) demonstrates reduced diffusion (hyperintense on diffusion-weighted image), consistent with epidermoid. Note the persistent low position of the conus medullaris (caudal-most spinal cord, double arrow in **a**). The cord does not ascend following repair

Chiari III

The much more rare Chiari III malformation is also best evaluated with MRI, which can characterize the contents of the occipito-cervical encephalocele and associated brain and spine abnormalities. Low-dose computed tomography (CT) may also be helpful to visualize the bony cervical and/or occipital cranial defects. The MRI protocol for evaluation of the Chiari III malformation is the same as for the Chiari II malformation, including multiplanar sequences through the head and spine for evaluation of the Chiari III malformation and associated abnormalities. The purpose of imaging is to define the contents of the encephalocele, including volume of herniated cerebellum and/or brainstem, meninges, and CSF (Fig. 25.9a). MR venography is also indicated to assess the location of the dural venous sinuses with respect to the mass

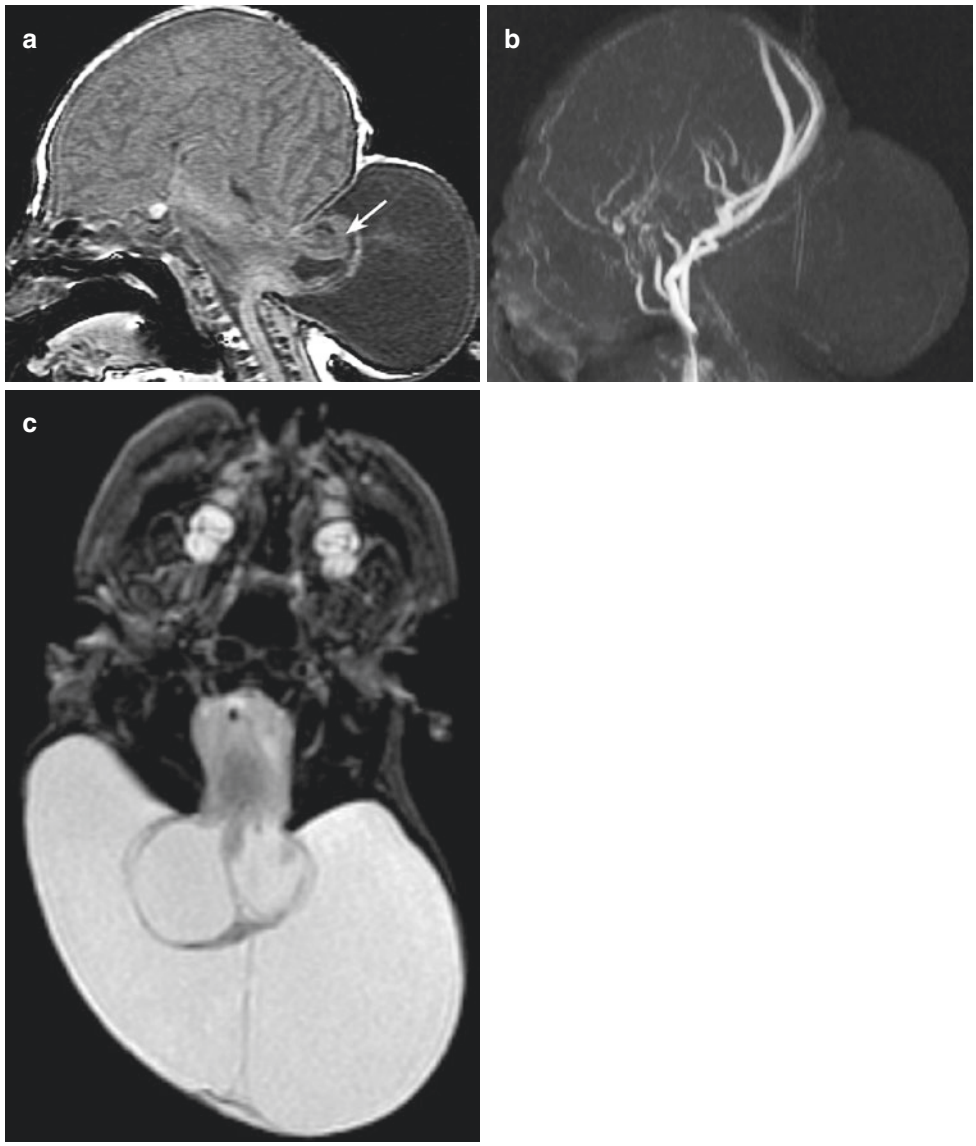

Fig. 25.9 Chiari III malformation. (**a**) Occipital encephalocele with atrophy and herniation of posterior fossa contents as well as part of the occipital lobe (arrow). (**b**) MR venography for surgical planning demonstrates that dural venous sinuses are not included in this large mass. (**c**) Axial T2 image shows dysplastic brain stem and cerebellar tissue herniating into larger cystic area

(Fig. 25.9b). These findings are essential for surgical planning and may be helpful for prognostication. Complete evaluation of the supratentorial brain and spinal cord is indicated due to frequent association with callosal abnormalities, gray matter heterotopia, syringohydromyelia, or tethered cord (Fig. 25.9c).

References

1. Cinalli G, Spennato P, Sainte-Rose C, Arnaud E, Aliberti F, Brunelle F, et al. Chiari malformation in craniosynostosis. Childs Nerv Syst. 2005;21(10):889–901.
2. Stovner LJ, Bergan U, Nilsen G, Sjaastad O. Posterior cranial fossa dimensions in the Chiari I malformation: relation to pathogenesis and clinical presentation. Neuroradiology. 1993;35(2):113–8.
3. Vega A, Quintana F, Berciano J. Basichondrocranium anomalies in adult Chiari type I malformation: a morphometric study. J Neurol Sci. 1990;99(2–3):137–45.
4. Banik R, Lin D, Miller NR. Prevalence of Chiari I malformation and cerebellar ectopia in patients with pseudotumor cerebri. J Neurol Sci. 2006;247(1):71–5.
5. Atkinson JL, Weinshenker BG, Miller GM, Piepgras DG, Mokri B. Acquired Chiari I malformation secondary to spontaneous spinal cerebrospinal fluid leakage and chronic intracranial hypotension syndrome in seven cases. J Neurosurg. 1998;88(2):237–42.
6. Fishman RA, Dillon WP. Dural enhancement and cerebral displacement secondary to intracranial hypotension. Neurology. 1993;43(3 Pt 1):609–11.
7. Chumas PD, Armstrong DC, Drake JM, Kulkarni AV, Hoffman HJ, Humphreys RP, et al. Tonsillar herniation: the rule rather than the exception after lumboperitoneal shunting in the pediatric population. J Neurosurg. 1993;78(4):568–73.
8. Martinez-Lage JF, Ruiz-Espejo AM, Almagro MJ, Alfaro R, Felipe-Murcia M, Lopez-Guerrero AL. CSF overdrainage in shunted intracranial arachnoid cysts: a series and review. Childs Nerv Syst. 2009;25(9):1061–9.
9. Fischbein NJ, Dillon WP, Cobbs C, Weinstein PR. The "presyrinx" state: a reversible myelopathic condition that may precede syringomyelia. AJNR Am J Neuroradiol. 1999;20(1):7–20.
10. Barkovich AJ, Wippold FJ, Sherman JL, Citrin CM. Significance of cerebellar tonsillar position on MR. AJNR Am J Neuroradiol. 1986;7(5):795–9.
11. Elster AD, Chen MY. Chiari I malformations: clinical and radiologic reappraisal. Radiology. 1992;183(2):347–53.
12. Enzmann DR, Pelc NJ. Normal flow patterns of intracranial and spinal cerebrospinal fluid defined with phase-contrast cine MR imaging. Radiology. 1991;178(2):467–74.
13. Armonda RA, Citrin CM, Foley KT, Ellenbogen RG. Quantitative cine-mode magnetic resonance imaging of Chiari I malformations: an analysis of cerebrospinal fluid dynamics. Neurosurgery. 1994;35(2):214–23; discussion 23–4.
14. Pujol J, Roig C, Capdevila A, Pou A, Marti-Vilalta JL, Kulisevsky J, et al. Motion of the cerebellar tonsils in Chiari type I malformation studied by cine phase-contrast MRI. Neurology. 1995;45(9):1746–53.
15. Sandberg DI, Navarro R, Blanch J, Ragheb J. Anomalous venous drainage preventing safe posterior fossa decompression in patients with chiari malformation type I and multisutural craniosynostosis. Report of two cases and review of the literature. J Neurosurg. 2007;106(6 Suppl):490–4.
16. Chern JJ, Gordon AJ, Mortazavi MM, Tubbs RS, Oakes WJ. Pediatric Chiari malformation type 0: a 12-year institutional experience. J Neurosurg Pediatr. 2011;8(1):1–5.
17. Anonymous. AIUM practice guideline for the performance of obstetric ultrasound examinations. J Ultrasound Med. 2010;29(1):157–66.
18. Van den Hof MC, Nicolaides KH, Campbell J, Campbell S. Evaluation of the lemon and banana signs in one hundred thirty fetuses with open spina bifida. Am J Obstet Gynecol. 1990;162(2):322–7.
19. Nicolaides KH, Campbell S, Gabbe SG, Guidetti R. Ultrasound screening for spina bifida: cranial and cerebellar signs. Lancet. 1986;2(8498):72–4.
20. Nishikawa M, Sakamoto H, Hakuba A, Nakanishi N, Inoue Y. Pathogenesis of Chiari malformation: a morphometric study of the posterior cranial fossa. J Neurosurg. 1997;86(1):40–7.
21. Ghi T, Pilu G, Falco P, Segata M, Carletti A, Cocchi G, et al. Prenatal diagnosis of open and closed spina bifida. Ultrasound Obstet Gynecol. 2006;28(7):899–903.
22. Kanal E, Borgstede JP, Barkovich AJ, Bell C, Bradley WG, Felmlee JP, et al. American College of Radiology White Paper on MR safety. AJR Am J Roentgenol. 2002;178(6):1335–47.
23. Levine D, Barnes PD, Robertson RR, Wong G, Mehta TS. Fast MR imaging of fetal central nervous system abnormalities. Radiology. 2003;229(1):51–61.
24. Barkovich AJ, Raybaud C. Pediatric neuroimaging. 5th ed. Philadelphia: Wolters Kluwer Health/Lippincott Williams & Wilkins; 2011.
25. Glenn OA, Barkovich AJ. Magnetic resonance imaging of the fetal brain and spine: an increasingly important tool in prenatal diagnosis, part 1. AJNR Am J Neuroradiol. 2006;27(8):1604–11.
26. Greitz D. Radiological assessment of hydrocephalus: new theories and implications for therapy. Neurosurg Rev. 2004;27(3):145–65; discussion 66–7.
27. Encinas JL, Garcia-Cabezas MA, Barkovich J, Fontecha CG, Peiro JL, Soto GM, et al. Maldevelopment of the cerebral cortex in the surgically induced model of myelomeningocele: implications for fetal neurosurgery. J Pediatr Surg. 2011;46(4):713–22.

28. Miller E, Widjaja E, Blaser S, Dennis M, Raybaud C. The old and the new: supratentorial MR findings in Chiari II malformation. Childs Nerv Syst. 2008;24(5):563–75.
29. Gilbert JN, Jones KL, Rorke LB, Chernoff GF, James HE. Central nervous system anomalies associated with meningomyelocele, hydrocephalus, and the Arnold-Chiari malformation: reappraisal of theories regarding the pathogenesis of posterior neural tube closure defects. Neurosurgery. 1986;18(5):559–64.
30. Juranek J, Salman MS. Anomalous development of brain structure and function in spina bifida myelomeningocele. Dev Disabil Res Rev. 2010;16(1):23–30.
31. Chang CK, Wong TT, Huang BS, Chan RC, Yang TF. Spinal dysraphism: a cross-sectional and retrospective multidisciplinary clinic-based study. J Chin Med Assoc. 2008;71(10):502–8.
32. Adzick NS, Thom EA, Spong CY, Brock JW 3rd, Burrows PK, Johnson MP, et al. A randomized trial of prenatal versus postnatal repair of myelomeningocele. N Engl J Med. 2011;364(11):993–1004.
33. Bouchard S, Davey MG, Rintoul NE, Walsh DS, Rorke LB, Adzick NS. Correction of hindbrain herniation and anatomy of the vermis after in utero repair of myelomeningocele in sheep. J Pediatr Surg. 2003;38(3):451–8; discussion 451−8.

26

Measurement of the Volume of the Posterior Cranial Fossa Using MRI

Niyazi Acer, Mehmet Turgut, Seher Yilmaz, and Hatice Susar Güler

Introduction

The posterior cranial fossa (PCF) volume is a useful diagnostic parameter for many clinical diseases, including Chiari malformation type I (CM I), craniosynostosis, intracranial hypotension, and various intracranial pathologies [1]. Recently, advanced automated and semiautomated segmentation programs have been developed for calculating PCF volume [2–5]. volBrain and MRICloud offer web-based volume calculation via automatic analysis of magnetic resonance imaging (MRI) brain data. Technically, they use an anonymized MRI brain volume in the Neuroimaging Informatics Technology Initiative and hdr format and produce a PDF (portable document file) and text report with the volumes of the main intracranial cavities and tissues, i.e., cerebrospinal fluid (CSF), gray matter (GM), and white matter (WM), and of brain substructures such as the cerebral hemispheres, cerebellum, and brain stem [6–8].

Clinically, quantification of the PCF volume is important for tonsillar herniation in CM I, defined as overcrowding that occurs because the PCF is small [9, 10]. Manual measurement of PCF volume was laborious, but the Cavalieri method on computed tomography (CT) scans and MRI showed that the PCF is significantly smaller in CM I than controls [11–13]. Accurate quantification of PCF volume is therefore critical for diagnosis.

Nowadays, it is widely accepted that overcrowding of the hindbrain associated with CM I can be due to underdevelopment of the PCF, as demonstrated by CT and MRI studies. Many previous morphometrical studies focusing on the bony part of the PCF supported this hypothesis [14]. This chapter reviews brain segmentation methods tailored toward PCF volumetry. Its main purpose is to collate information about PCF volume and its clinical implications.

Posterior Cranial Fossa

It is now well known that the PCF is a compact and hard field with low compliance. Anatomically, it is bounded by the dorsum sellae and the basilar part of the occipital bone anteriorly, petromastoid parts of the temporal bone laterally, the tentorium cerebelli superiorly, and the occipital bone posteroinferiorly. It is important to know that the dural venous sinuses, the trans-

N. Acer (✉)
Department of Anatomy, Erciyes University School of Medicine, Kayseri, Turkey

M. Turgut
Department of Neurosurgery, Aydın Adnan Menderes University School of Medicine, Efeler, Aydın, Turkey

S. Yilmaz · H. S. Güler
Department of Anatomy, Bozok University School of Medicine, Yozgat, Turkey

R. S. Tubbs et al. (eds.), *The Chiari Malformations*, https://doi.org/10.1007/978-3-030-44862-2_26

verse, sigmoid, and occipital sinuses, traverse the PCF. It has been reported that the cerebral aqueduct is a constricted passage for CSF drainage, and any obturation involving this structure can cause hydrocephalus with a major increase in intracranial pressure [15]. Various pathologies of the PCF such as intracranial tumors, aneurysms, arachnoid/epidermoid cysts, and hemifacial spasms and craniocervical abnormalities such as Arnold Chiari malformation (ACM) and Dandy Walker malformation can compress the brain stem, and surgical decompression may then be warranted [5, 16]. Even a minor increase in PCF volume (e.g., because of a tumor or hematoma) can result in a prominent increase in intracompartmental pressure, leading to life-threatening brain stem compression. The PCF is the broadest of the three cranial fossae and the deepest of all, including the brain stem, cerebellum, and lower six cranial nerves. The cerebellum is located within the PCF, behind the pons and the medulla oblongata. The great foramen is centrally indwelling in the PCF. The PCF is bounded by a deep trough containing the transverse and sigmoid sinuses. It is separated from the overlying cerebrum by an appendage of dura mater and the tentorium [17].

In recent years, most neuroscientists have focused on the role of the cerebellum in processing speed and cognitive efficiency as well as in balance and posture [18]. It is now certain that the cerebellum is important for many functions other than the coordination of action; it is also involved in regulating cognition and emotion [19–21].

Diverse Imaging Methods for Diagnosis and Examination of the Posterior Cranial Fossa

Ultrasound

Ultrasound (US) scanning is accepted as a safe, accurate, noninvasive method for examining the fetus. Many types of neurological malformation such as hydrocephalus, anencephaly, and myelomeningocele can now be diagnosed by US [17, 22].

Plain X-Ray of the Skull

Plain skull X-ray is the primary imaging modality. Radiologically, various abnormalities including chronic intracranial hypertension, calcification, and skull fractures can easily be demonstrated using this technique [17].

Computed Tomography Scanning

CT scanners have been used in clinical practice since 1972. Because of the possible hazards associated with radiation exposure, some experts prefer not to use CT scanning. However, modalities such as CT angiography and CT venography in neuroradiology are the best choices in clinical practice. Today, CT is preferred for patients with PCF masses who frequently present with nausea, vomiting, ataxia, and other signs of intracranial hypertension. In particular, it is widely used for evaluating various neurological emergencies including hemorrhage, hydrocephalus, and herniation syndromes because it is rapid and cheap [17, 23].

Magnetic Resonance Imaging

MRI has been used since 1980 to visualize any anomaly or pathology in the PCF, brain stem, and cerebellum. Clinically, various lesions of the PCF, congenital diseases, vascular lesions, WM diseases, and inflammatory lesions can be demonstrated by MRI [17].

Morphometric Measurement of Posterior Cranial Fossa

The linear measurements of the PCF are often approximated using linear markers measured using mid-sagittal T1-weighted MRI [24, 25].

Allen et al. [26] found the midsagittal plane by these means. The criteria verifying the midsagittal section are as follows: the sulcus corporis callosi separating the corpus callosum from the gyrus cinguli; the aqueductus cerebri between the tegmentum and the tectum; a visible "V" from the fornix of the fourth ventricle; and a non-visible hemispherium cerebelli [26]. In midsagittal sections of the T1 images, Taştemur et al. [25] applied measurements identical to those they used in the sagittal plane. They took measurements identical to those they used in the transverse plane on sections where the cranium was largest in the T2 images [25]. All the morphometric measurements were obtained using syngo fastView software. Taştemur et al. [25] used various measurement points for the cerebrum, cerebellum, cranium, and cranial fossa. Specifically, the anthropometric points were taken as references on the sagittal and axial T1 and T2 images [25] (Figs. 26.1, 26.2, and 26.3).

The lengths were measured on the midsagittal T1-weighted images so that the sizes of the PCF and the cranium could be determined [25, 27, 28] (Figs. 26.2 and 26.3).

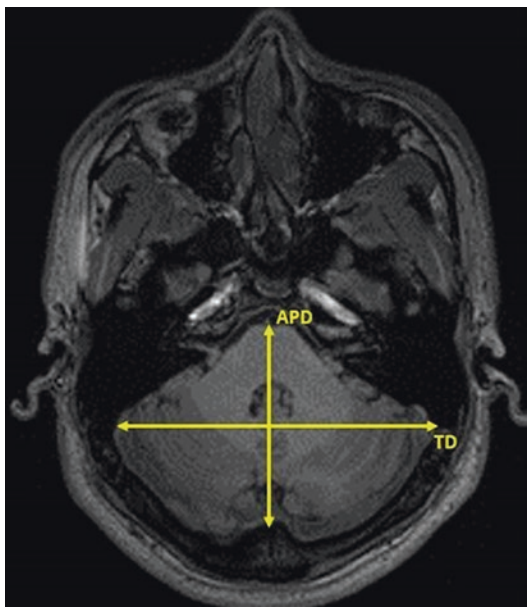

Fig. 26.1 Measurement of anteroposterior and transverse diameters of posterior cranial fossa. APD – anteroposterior diameter, TD – transverse diameter

Automated Imaging Methods for the Posterior Cranial Fossa and Techniques for Substructures

Several software tools have been developed recently for automatic determination of the volumes of brain substructures such as cerebellum, medulla, pons, and others. Here we describe the web-based volume measurement techniques volBrain and MRICloud [8].

volBrain

The volBrain system is rooted in providing automatic segmentations of several brain structures from T1-weighted MRI images [6, 8].

The preprocessing step includes normalizing and registering into the Montreal Neurological Institute (MNI) space. The first preprocessing step is denoizing using the adaptive non-local mean filter [29, 30]. This is followed by an affine registration to MNI space using the Advanced Normalization Tools algorithm [31]. Normalization is finally completed [29].

After this preprocessing, MRI images are segmented at different scales using non-local patch-based multi-atlas methods [6]. First, the intracranial cavity is extracted by Non-local Intracranial Cavity Extraction [32]. This step is followed by extraction of the hemispheres based on Non-local Automatic Brain Hemisphere Segmentation [33]. Brain tissues are also classified using a procedure described by Manjón et al. [29]. Afterward, eight subcortical structures are segmented by the method described by Coupé et al. [6]. Volumes of various intracranial structures such as the cerebrum, cerebellum, and brain stem and some subcortical structures such as the caudate nucleus, putamen, thalamus, amygdala, hippocampus, globus pallidus, and nucleus accumbens have been measured using volBrain [8]. As a rule, all structure segmentations are based on expert volBrain definitions with the exception of the hippocampus, which is segmented following the European Alzheimer's Disease Consortium protocol [34]. From a tech-

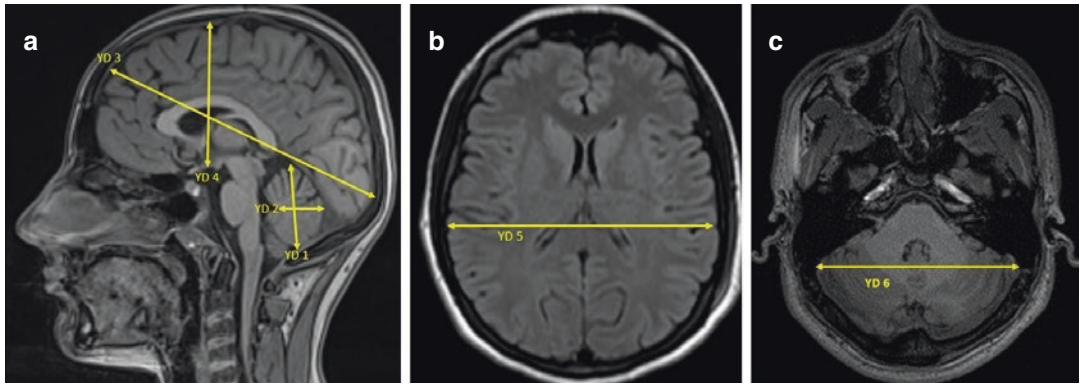

Fig. 26.2 MRI of a patient with a CM I. (**a**) Measurements of the cerebrum and cerebellum on the T1 midsagittal section. YD1 = Distance between the lowest and highest points of the cerebellum, YD2 = distance between the most posterior point of the fourth ventricle and the most salient point of the posterior cerebellum, YD3 = distance between the polus frontalis and the polus occipitalis (the longest anteroposterior diameter of the cerebrum), YD4 = distance between the highest point of the cerebrum and the corpus mamillare. (**b**) Measurement of the cerebrum on the axial section. YD5 = Lateral distance between the points most remote from each other in the cerebral hemispheres. (**c**) Measurement of the cerebellum on the axial section. YD6 = Lateral distance between the points most remote from each other in the cerebellar hemispheres

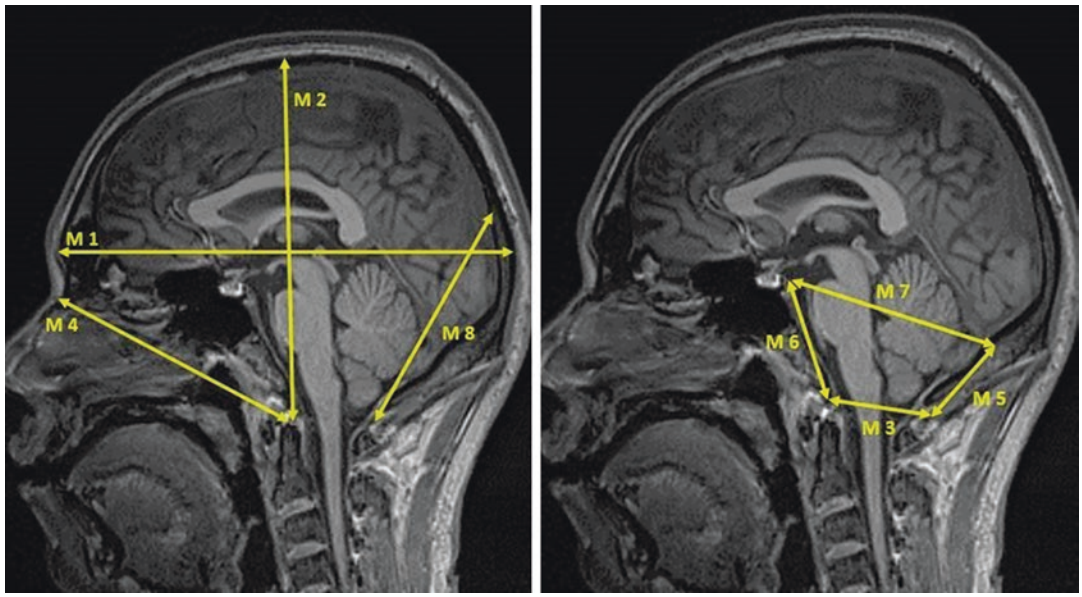

Fig. 26.3 The sizes of the cranium and the posterior cranial fossa. M1 = Distance between the glabella and the opisthocranion (maximum cranial length), M2 = distance between the basion and the vertex (maximum cranial height), M3 = distance between the basion and the opisthion (foramen magnum sagittal diameter), M4 = distance between the nasion and the basion (cranium base length), M5 = distance between the opisthion and the protuberentia occipitalis interna (supraocciput), M6 = distance between the basion and the dorsum sellae top edge (clivus length), M7 = distance between the dorsum sellae and the protuberentia occipitalis interna, M8 = distance between the opisthion and the lambda

nical point of view, it is important to know that all the processes used are completed within around 12 minutes [35].

After the process is finished, an email is received and a package can be downloaded including image files and two comma-separated values (CSV) in PDF files. These reports provide all the volumetric values calculated from the segmentations. The PDF files include patient information, details of brain tissues such as WM and GM, volumes of subcortical structures such as (thalamus, globus pallidus, caudate, and hippocampus), and asymmetry indexes [36]. The brain parcellation maps are illustrated in Fig. 26.4.

MRICloud

Mori et al. [37] have developed image analysis tools for brain MRI. They produced DtiStudio in 2001 [37, 38]. Users can now obtain a single-subject atlas containing at least 286 brain regions to produce automated brain segmentation [38, 39].

Using MRICloud, the T1-weighted images can be segmented using an online website (www.mricloud.org) [7, 40]. Segmentation accuracy with multi-atlas fusion has been validated in comparison to single atlas approaches [41]. The whole brain was segmented into 289 structures including the cerebellum, brain stem, fourth ventricle, etc. [40]. Volumes of posterior cranial structures were obtained on the basis of the T1 segmentation (Fig. 26.5).

Arnold Chiari Malformation

Hans Chiari (1851–1916) defined variations in hindbrain malformations in autopsy studies, 4 types of ACM in total: types 1, 2, 3, and 4 [42]. In 1894, Julius Arnold (1835–1915) also described a malformation in neonates in which the fourth ventricle and cerebellum were herniated through the foramen magnum (FM) while sparing the medulla. It is now well known that ACM is a set of congenital conditions involving an anatomical defect in the base of the skull, because of which the cerebellum and the brain stem herniate through the FM into the cervical spinal canal. The ACMs are described in terms of increasing degrees of hindbrain herniation [42, 43].

Tonsillar herniation related to ACMs generally occurs without hydrocephalus according to MRI [42–44]. Many types of ACM are known, but CM I is the most common [45]. CM I malformation is described as a peg-like herniation of the tonsilla cerebelli of at least 3 mm through the FM. It is common in adults and usually develops during the second or third decade of life, while CM2 is more common in the pediatric population and is often associated with spinal dysraphism [42, 43, 46]. Even today there is no consensus about the etiology of ACM, and there are several hypotheses concerning its pathogenesis. It is believed to be due to a defect in the sclerotomes during development of the occipital bone, resulting in a PCF that is too small to accommodate the cerebellum. Among the subtypes of ACM, CM I is outstanding owing to the intensity of its ACM symptoms, but it can be asymptomatic [9]. Clinical symptoms in patients with CM I include suboccipital or retro-orbital headache, double vision, blurred vision, photophobia, diplopia, and vertigo [1, 47].

Anatomically, the extent of tonsillar herniation is ascertained by measuring the length of the tonsilla cerebelli, which remains below a line drawn between the basion and the opisthion. Herniations with a length of tonsilla cerebelli extending >3–5 mm from the level of the FM to the canalis vertebralis are considered to be CM I [16] (Fig. 26.6).

Manual delineation of the PCF in MRI was used for image intensity-based segmentation of brain tissue and CSF followed by assessment of the effects of age and sex on PCF volume in healthy subjects. Men had larger PCF and hindbrain volumes than women, whereas women

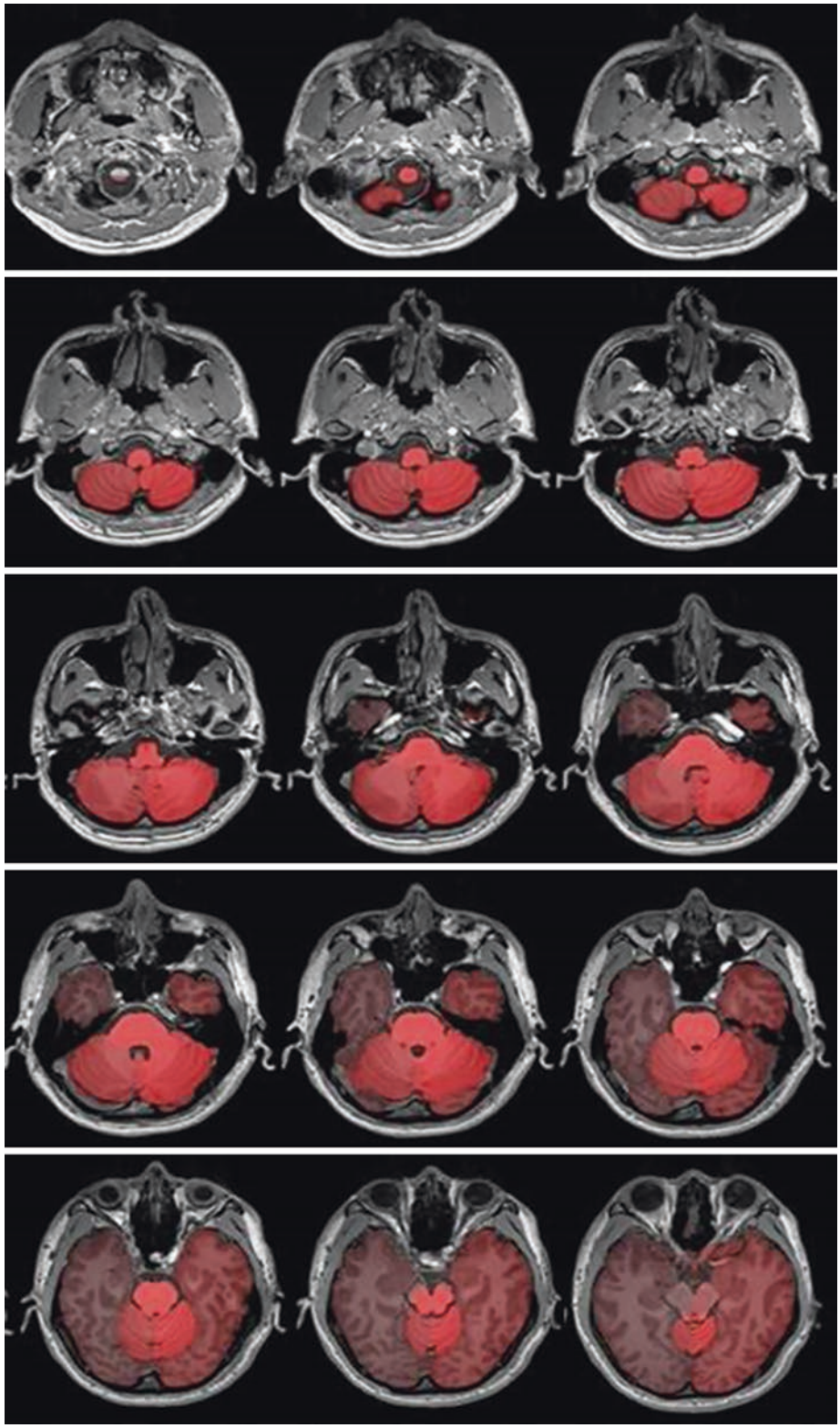

Fig. 26.4 Automated imaging of the posterior cranial fossa using volBrain

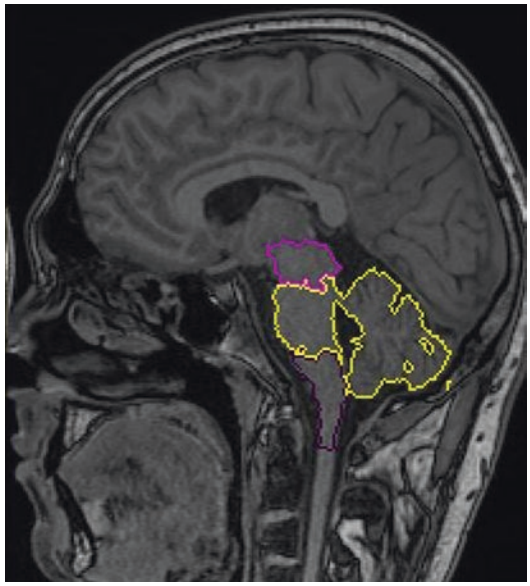

Fig. 26.5 Automated parcellation of the posterior cranial fossa structures using MRICloud

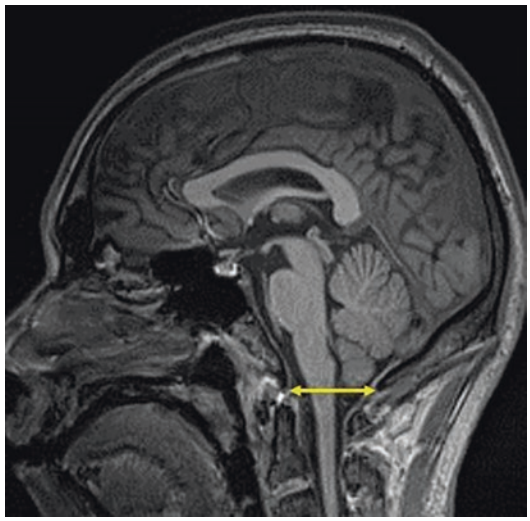

Fig. 26.6 MRI of a patient with CM I. The cerebellar tonsils are below the line (shown in yellow) marking the connection of the skull and spine

demonstrated more crowdedness; this could explain the greater frequency of CM I in women. According to imaging data, especially MRI images gathered over the last several decades, CM I is also associated with a smaller-than-normal PCF [5, 12, 18, 28, 48]. Therefore, the etiology of CM I still remains unclear. One hypothesis suggested to explain this form of hindbrain herniation is that a smaller-than-normal PCF predisposes a normal-sized cerebellum to traverse the FM during development [12]. Today, considering the differences in treatment, further types of ACM have been added to the definitions such as type 0, type 1.5, and type 3.5 [45, 49].

Discussion

MRI has become an important diagnostic and investigative tool in brain research because it is essential study for quantitative estimation of volumes of brain structures in the PCF. This quantitative information offers researchers the chance to investigate the potential relationship between neuroanatomical changes and some neurological and neuropsychiatric diseases [50]. Some software tools have been developed recently to obtain some or all of these volumetric measurements automatically using different strategies such as the Statistical Parametric Mapping, FreeSurfer, FMRIB Software Library (FSL), OsiriX, MRI Studio, etc. The FSL package and FreeSurfer are freely available for obtaining more specific volume measurements [51].

In the past, volumes of the PCF, the hindbrain, and the fourth ventricle were measured using the automated atlas-based method [2, 24, 51, 52]. Here we have discussed in detail some methodological approaches to calculating the PCF volume using atlas-based automated segmentation and grid-based volume estimation techniques.

Recently, Lirng et al. [1] and Khalsa et al. [43] developed a semiautomated segmentation program. Khalsa et al. [43] used it to compare the pre- and postoperative volumes of the PCF in pediatric patients with CM I. Lirng et al. calculated a PCF crowdedness index [1]. Ertekin et al. [11] and Vurdem et al. [13] used stereological methods for their studies. In contrast, Iqbal et al. [53] used an ellipsoid formula to calculate the volume of the PCF from CT images. Ulutabanca et al. [5] used OsiriX for the same purpose.

Several studies have revealed associations between ACM and cerebellar volume, showing that both cerebellum and PCF volumes are relevant

Table 26.1 Literature review of volumetric studies of the posterior cranial fossa

Author(s) and year	Imaging type	Number of people	Technique used	PCF volume (cm^3)	PCF volume	Result
Vurdem et al. (2012) [13]	MRI	Control ($N = 25$) CM I ($N = 30$)	Stereological study	Control = 165.57 CM I = 146.01	Decreased	CM I was significantly smaller
Furtado et al., (2010) [27]	MRI and CT	CM I ($N = 21$)	Linear measurements	NA	NA	
Bagci et al. (2013) [2]	MRI	Control ($N = 3$) CM I ($N = 14$)	Atlas-based automated and manual	Patient = 151–172 Control = 186–207	Decreased	Automated method and manual delineation were similar
Lirng et al. (2009) [1]	MRI	52 healthy volunteers Men ($N = 24$) Women ($N = 28$)	Semiautomated magnetic resonance	Men = 200.7 Women = 178.5	NA	Women had a more crowded PCF than men
Iqbal et al. (2018) [53]	CT	Patient ($N = 100$)	Linear measurements, cross-sectional	Men = 159.66 Women = 154.50	NA	PCF and FM were larger in males than females
Urbizu et al. (2012) [54]	MRI	Patient ($N = 50$) Control ($N = 50$)	Morphometric measurements made on mid-sagittal	Patient PCF area (cm^2) = 33.7 Control = 37.8	Decreased	PCF area lower in patients
Ertekin et al. (2017) [11]	CT	Retrospective ($N = 339$)	Stereological study	Men = 244.89 Women = 228.24	NA	Volume of PCF greater in males than females

Abbreviations: *CT* computed tomography, *MRI* magnetic resonance imaging, *PCF* posterior cranial fossa, *CM I* Chiari malformation type I, *FM* foramen magnum, *NA* not available

to such diseases [2, 12, 13]. Importantly, the vast majority of these studies used T1-weighted volumetric MRI data with 1 mm isotropic resolution and reported a smaller PCF volume (Table 26.1) [1, 2, 11–13, 27, 53, 54]. Bagci et al. [2] used 3 T scanner data from 14 CM I patients and three healthy subjects and found that none of the PCF linear landmarks were significantly associated with PCF volume. Vurdem et al. [13] compared MRI images from 25 control subjects and 30 CM I patients and found the PCF volumes were significantly smaller in the patients than the controls. Iqbal et al. [53] used CT scans of suspected head injury patients collected retrospectively. They measured the height and volume of the PCF and the anteroposterior, transverse diameter, and surface area of the FM [53]. The dimensions of the PCF and FM did not differ significantly among the various age groups, and almost all of them were larger in males than females [53, 55, 56]. Ulutabanca et al. [5] used CT scans to measure the PCF and FM. Their study revealed that the PCF was transformed to a narrow funnel shape [5]. They measured the lengths of the clivus, FM, and supraocciput and found a volume difference between CM I patients and normal controls [5, 55, 56]. Some studies used the Cavalieri method for volumetric measurements [27, 46, 56] of the PCF in 21 patients with CM I, matched with an equal number of pediatric controls, using MRI. They computed the ratio of PCF volume to intracranial volume in pediatric patients with CM I, adult patients with CM I, and a pediatric control group [46], using simple mathematical formulae to calculate spheroidal volume [11].

Conclusion

The true success of web-based volumetric tools such as volBrain and MRICloud depends on their role in producing volumetric information using

MRI data and on their free availability. These methods provide very useful data about PCF volume. Quantification of PCF volume can be helpful in differential diagnosis of herniation of the tonsilla cerebelli and prediction of surgical outcomes for CM I patients. Volume measurements can help pediatric neurosurgeons both in selecting patients for surgery and in evaluating any surgical technique used to treat various malformations of the PCF.

References

1. Lirng JF, Fuh JL, Chen YY, Wang SJ. Posterior cranial fossa crowdedness is related to age and sex: a magnetic resonance volumetric study. Acta Radiol. 2005;46:737–42.
2. Bagci AM, Lee SH, Nagornaya N, Green BA, Alperin N. Automated posterior cranial fossa volumetry by MRI: applications to Chiari malformation type I. AJNR Am J Neuroradiol. 2013;34:1758–63.
3. Cabezas M, Oliver A, Llado X, Freixenet J, Cuadra MB. A review of atlas-based segmentation for magnetic resonance brain images. Comput Methods Prog Biomed. 2011;104:e158–77.
4. Fischl B, Salat DH, Busa E, Albert M, Dieterich M, Haselgrove C, Van Der Kouwe A, Killiany R, Kennedy D, Klaveness S, Montillo A, Makris N, Rosen B, Dale AM. Whole brain segmentation: automated labeling of neuroanatomical structures in the human brain. Neuron. 2002;33:341–55.
5. Ulutabanca H, Acer N, Küçük A, Doğan S, Tümtürk A, Kurtsoy A, Sağiroğlu A, Bilgen M. Chiari type I malformation with high foramen magnum anomaly. Folia Morphol (Warsz). 2015;74:402–6.
6. Coupé P, Manjón JV, Fonov V, Pruessner J, Robles M, Collins DL. Patch-based segmentation using expert priors: application to hippocampus and ventricle segmentation. NeuroImage. 2011;54:940–54.
7. Ma J, Ma HT, Li H, Ye C, Wu D, Tang X, Miller M, Mori S. Fast atlas pre-selection procedure for multi-atlas based brain segmentation. Conf Proc IEEE Eng Med Biol Soc. 2015;2015:3053–6.
8. Manjon JV, Coupé P. volBrain: an online MRI brain volumetry system. Front Neuroinform. 2016;10:1–14.
9. Nishikawa M, Sakamoto H, Hakuba A, Nakanishi N, Inoue Y. Pathogenesis of Chiari malformation: a morphometric study of the posterior cranial fossa. J Neurosurg. 1997;86:40–7.
10. Noudel R, Gomis P, Sotoares G, Bazin A, Pierot L, Pruvo JP, Bordet R, Roche PH. Posterior fossa volume increase after surgery for Chiari malformation type I: a quantitative assessment using magnetic resonance imaging and correlations with the treatment response. J Neurosurg. 2011;115:647–58.
11. Ertekin T, Degermenci M, Ucar I, Sagiroglu A, Atay E, Susar H. The intracranial and posterior cranial fossa volumes and volume fractions in children: a stereological study. Int J Morphol. 2017;35:1465–72.
12. Milhorat TH, Chou MW, Trinidad EM, Kula RW, Mandel M, Wolpert C, Speer MC. Chiari I malformation redefined: clinical and radiographic findings for 364 symptomatic patients. Neurosurgery. 1999;44:1005–17.
13. Vurdem ÜE, Acer N, Ertekin T, Savranlar A, Inci MF. Analysis of the volumes of the posterior cranial fossa, cerebellum, and herniated tonsils using the stereological methods in patients with Chiari type I malformation. ScientificWorldJournal. 2012;2012:616934.
14. Enver IB, Aisylu TF, Elena GM, Alexey SS, John DH. Epidemiology of symptomatic Chiari malformation in Tatarstan: regional and ethnic differences in prevalence. Neurosurgery. 2019;84(5):1090–7.
15. Rolls ET, Joliot M, Tzourio-Mazoyer N. Implementation of a new parcellation of the orbitofrontal cortex in the automated anatomical labeling atlas. NeuroImage. 2015;122:1–5.
16. Vogl TJ, Harth M. "Neuro imaging of the posterior fossa", pp. 1–15. 2011. Retrieved from https://pdfs.semanticscholar.org/5f8d/0abf76715d2dfadca3fc943da1beba32acb1.pdf.
17. Grassi W, Filippucci E. A brief history of ultrasound in rheumatology: where we were. Clin Exp Rheumatol. 2014;32(1 Suppl 80):S3–6.
18. Wang SH, Kloth AD, Badura A. The cerebellum, sensitive periods, and autism. Neuron. 2014;83:518–32.
19. Ailion AS, King TZ, Wang L, Fox ME, Mao H, Morris RM, Crosson B. Cerebellar atrophy in adult survivors of childhood cerebellar tumor. J Int Neuropsychol Soc. 2016;22:501–11.
20. Baillieux H, De Smet HJ, Paquier PF, De Deyn PP, Marien P. Cerebellar neurocognition: insights into the bottom of the brain. Clin Neurol Neurosurg. 2008;110:763–73.
21. Eccles JC, Ito M, Szentagothai J. The cerebellum as a neuronal machine. Berlin, Heidelberg, New York: Springer; 1967. pp. 335. 62s
22. Odaci E, Bahadir A, Yildirim Ş. Volume estimation using the Cavalieri principle on computerized tomography and magnetic resonance images and its clinical application: review. Türkiye Klinikleri J Med Sci. 2005;25:421–8.
23. Apolito G, Calandrelli R, Gaudino S, Tumino M, Pedone L, Colosimo C. Posterior fossa morphometry and volumetric analysis in three different groups of pediatric patients: congenital Chiari type 1 malformation, posterior craniosynostosis and Costello syndrome. Presented in ECR 2014, Poster No.: C-0685, EPOS. 2014). pp. 1–19. https://doi.org/10.1594/ecr2014/C-0685.
24. Alperin N, Loftus JR. MRI measures of posterior cranial fossa morphology and CSF physiology in Chiari malformation type I. Neurosurgery. 2014;75:515–22.

25. Taştemur Y, Sabanciogullari V, İsmail S, Sönmez M, Çimen M. The relationship of the posterior cranial fossa, the cerebrum, and cerebellum morphometry with tonsiller herniation. Iran J Radiol. 2017;14(1):24436.
26. Allen LS, Richey MF, Chai YM, Gorski RA. Sex differences in the corpus callosum of the living human being. J Neurosci. 1991;11:933–42.
27. Furtado SV, Thakre DJ, Venkatesh PK, Reddy K, Hegde AS. Morphometric analysis of foramen magnum dimensions and intracranial volume in pediatric Chiari I malformation. Acta Neurochir (Wien). 2010;152:221–7.
28. Sekula RF, Jannetta PJ, Casey KF, Marchan EM, Sekula LK, McCrady CS. Dimensions of the posterior fossa in patients symptomatic for Chiari I malformation but without cerebellar tonsillar descent. Cerebrospinal Fluid Res. 2005;2:11.
29. Manjón JV, Tohka J, Robles M. Improved estimates of partial volume coefficients from noisy brain MRI using spatial context. NeuroImage. 2010;53:480–90.
30. Tustison NJ, Avants BB, Cook PA, Zheng Y, Egan A, Yushkevich PA, Gee JC. N4ITK: improved N3 bias correction. IEEE Trans Med Imaging. 2010;29:1310–20.
31. Avants BB, Tustiso NJ, Song G, Cook PA, Klein A, Gee JC. A reproducible evaluation of ANTs similarity metric performance in brain image registration. NeuroImage. 2011;54:2033–44.
32. Manjón JV, Eskildsen SF, Coupé P, Romero JE, Collins DL, Robles M. Nonlocal intracranial cavity extraction. Int J Biomed Imaging. 2014;2014:820205.
33. Romero JE, Manjón JV, Tohka J, Coupé P, Robles M. NABS: non-local automatic brain hemisphere segmentation. Magn Reson Imaging. 2015;33:474–84.
34. Boccardi M, Bocchetta M, Morency FC, Collins DL, Nishikawa M, Ganzola R, Grothe MJ, Wolf D, Redolfi A, Pievani M, Antelmi L, Fellgiebel A, Matsuda H, Teipel S, Duchesne S, Jack CR Jr, Frisoni GB. EADC-ADNI Working Group on the harmonized protocol for manual hippocampal segmentation and for the Alzheimer's disease neuroimaging initiative, 2015. Training labels for hippocampal segmentation based on the EADC-ADNI harmonized hippocampal protocol. Alzheimers Dement. 2014;11:175–83.
35. Huhtaniska S, Jääskeläinen E, Heikka T, Moilanen JS, Lehtiniemi H, Tohka J, Manjón JV, Coupé P, Björnholm L, Koponen H, Veijola J, Isohanni M, Kiviniemi V, Murray GK, Miettunen J. Long-term antipsychotic and benzodiazepine use and brain volume changes in schizophrenia: the Northern Finland Birth Cohort 1966 study. Psychiatry Res Neuroimaging. 2017;266:73–82.
36. Tzourio-Mazoyer N, Landeau B, Papathanassiou D, Crivello F, Etard O, Delcroix N, Mazoyer B, Joliot M. Automated anatomical labeling of activations in SPM using a macroscopic anatomicalparcellation of the MNI MRI single-subject brain. NeuroImage. 2002;15:273–89.
37. Jiang H, van Zijl PC, Kim J, Pearlson GD, Mori S. DtiStudio: resource program for diffusion tensor computation and fiber bundle tracking. Comput Methods Prog Biomed. 2006 Feb;81(2):106–16.
38. Oishi K, Faria A, Jiang H, Li X, Akhter K, Zhang J, Hsu JT, Miller MI, van Zijl PC, Albert M, Lyketsos CG, Woods R, Toga AW, Pike GB, Rosa-Neto P, Evans A, Mazziotta J, Mori S. Atlas-based whole brain white matter analysis using large deformation diffeomorphic metric mapping: application to normal elderly and Alzheimer's disease participants. NeuroImage. 2009;46:486–99.
39. Ceritoglu C, Oishi K, Li X, Chou MC, Younes L, Albert M, Lyketsos C, Van Zijl PCM, Miller MI, Mori S. Multi-contrast large deformation diffeomorphic metric mapping for diffusion tensor imaging. NeuroImage. 2009;47:618–27.
40. Djamanakova A, Tang X, Li X, Faria AV, Ceritoglu C, Oishi K, Hillis AE, Albert M, Lyketsos C, Miller MI, Mori S. Tools for multiple granularity analysis of brain MRI data for individualized image analysis. NeuroImage. 2014;101:168–76.
41. Artaechevarria X, Munoz-Barrutia A, Ortiz-de-Solorzano C. Combination strategies in multi-atlas image segmentation: application to brain MR data. IEEE Trans Med Imaging. 2009;28:1266–77.
42. Chiari H. Über veränderungen des kleinhirns, des pons und der medulla oblongata in folge von congenitaler hydrocephalie des grosshirns (concerning changes in the cerebellum, pons, and medulla oblongata due to hydrocephalus of the cerebrum). Denkschr Akad Wissensch. 1896;63:71–116.
43. Khalsa SSS, Siu A, Freitas TA, Cappuzzo JM, Myseros JS, Magge SN, Oluigbo CO, Keating RF. Comparison of posterior fossa volumes and clinical outcomes after decompression of Chiari malformation type I. J Neurosurg Pediatr. 2017;19:511–7.
44. Badie B, Mendoza D, Batzdorf U. Posterior fossa volume and response to suboccipital decompression in patients with Chiari I malformation. Neurosurgery. 1995;37:214–8.
45. Fisahn C, Shoja MM, Turgut M, Oskouian RJ, Oakes WJ, Tubbs RS. The Chiari 3.5 malformation: a review of the only reported case. Childs Nerv Syst. 2016;32:2317–9.
46. Furtado SV, Reddy K, Hegde AS. Posterior fossa morphometry in symptomatic pediatric and adult Chiari I malformation. J Clin Neurosci. 2009;16:1449–54.
47. Aasef GS, Fatema FG. Neuro-ophthalmology of type 1 Chiari malformation. Expert Rev Ophthalmol. 2015;10:351–7.
48. Karagoz F, Izgi N, Kapicioglu Sencer S. Morphometric measurements of the cranium in patients with Chiari type I malformation and comparison with the normal population. Acta Neurochir. 2002;144:165–71.
49. Işik N. Chiari malformation and syringomyelia. Turk Neurosurg. 2013;23:185–94.
50. Acer N, Dolu N, Zararsiz G, Dogan MS, Gümüş K, Özmen S, Kara AY, Soysal H, Per H, Bilgen M. Anatomical characterization of ADHD using an atlas-based analysis: a diffusion tensor imaging study. Eurobiotech J. 2017;1:46–56.

51. Jenkinson M, Beckmann CF, Behrens TE, Woolrich MW, Smith SM. FSL. NeuroImage. 2012;62:782–90.
52. Tubbs RS, Lyerly MJ, Loukas M, Shoja MM, Oakes WJ. The pediatric Chiari I malformation: a review. Childs Nerv Syst. 2007;23:1239–50.
53. Iqbal S, Robert AP, Mathew D. Computed tomographic study of posterior cranial fossa, foramen magnum, and its surgical implications in Chiari malformations. Asian J Neurosurg. 2018;1:428–34.
54. Urbizu A, Poca MA, Vidal X, Rovira A, Sahoqulllo J, Macaya A. MRI-based morphometric analysis of posterior cranial fossa in the diagnosis of Chiari malformation type I. J Neuroimaging. 2007;24:250–6.
55. Hwank HS, Moon JG, Kim CH, Oh SM, Song JH, Jeong JH. The comparative morphometric study of the posterior cranial fossa: what is effective approaches to the treatment of Chiari malformation type 1? J Korean Neurosurg Soc. 2013;54:405–10.
56. Trigylidas T, Baronia B, Vassilyadi M, Ventureyra EC. Posterior fossa dimension and volume estimates in pediatric patients with Chiari I malformations. Childs Nerv Syst. 2008;24:329–36.

27 Intraoperative Ultrasound in Chiari Type I Malformation

Roger Schmidt Brock, Mario Augusto Taricco, Matheus Fernandes de Oliveira, Marcelo de Lima Oliveira, Manoel Jacobsen Teixeira, and Edson Bor-Seng-Shu

Introduction

Chiari malformation type I (CM I) is a congenital disease characterized by herniation of the cerebellar tonsils 5 mm below the foramen magnum. The usual prevalence is approximately 8 per 1000 live births. It is generally understood as a congenital error during mesodermic phase segmentation in craniocervical junction, generating shallow bony posterior fossa and overcrowding of neural posterior fossa content [1–10].Additionally, the overcrowding of posterior fossa impairs cerebrospinal fluid (CSF) circulation. In many CM I cases, it is possible to see CSF circulation disturbances, which might reflect in patient clinical picture demanding specific treatment.

CM I may also occur secondary to increased intracranial pressure in the presence of hydrocephalus, space-occupying lesions in the posterior fossa, and downward movement of brain structures caused by decreased intracranial pressure due to a CSF fistula [11–14].

Many patients are asymptomatic, but some may experience progressive neurological symptoms of muscle weakness; impairments in balance, coordination, and sensitivity; difficulty swallowing; and headache and disabling neck pain, especially on exertion. These symptoms are caused by direct compression of the cerebellum, spinal cord, and brainstem structures, which often leads to the formation of a syringomyelic cavity with involvement of the spinal tracts and cell bodies of neurons in the gray columns of the spinal cord. The pathophysiology is related to CSF flow changes at the craniovertebral junction (CVJ). The presence of these symptoms impairs quality of life and ultimately requires surgical treatment [15–21].

R. S. Brock · M. A. Taricco
Department of Neurosurgery, Hospital das Clínicas, University of São Paulo, DFV Neurology and Neurosurgery Service S/C Ltda, Bela Vista, São Paulo, Brazil

M. F. de Oliveira (✉)
Department of Neurosurgery, Hospital das Clínicas, University of São Paulo, DFV Neurology and Neurosurgery Service S/C Ltda, Hospital do Servidor Público Estadual de São Paulo, São Paulo, Brazil
e-mail: roger@dfvneuro.com.br

M. de Lima Oliveira
Department of Neurology, Hospital das Clínicas, University of São Paulo, São Paulo, Brazil

M. J. Teixeira
Department of Neurology, Division of Neurosurgery, Hospital das Clínicas, University of São Paulo, University of São Paulo School of Medicine, São Paulo, Brazil

E. Bor-Seng-Shu
Laboratory for Neurosonology and Cerebral Hemodynamics, Division of Neurological Surgery, Hospital das Clínicas, São Paulo University Medical School, São Paulo, Brazil

R. S. Tubbs et al. (eds.), *The Chiari Malformations*, https://doi.org/10.1007/978-3-030-44862-2_27

Cerebrospinal Fluid Hydrodynamics Applied to Chiari I

The most accepted theory is based on hydrodynamics proposed by Gardner in 1965 [22], which reveals a CSF pulse during the embryonic development with fundamental roles in neural tube expansion, pathway development, and brain conformation. Hyperactivity of the fourth ventricle pulsatility displaces superiorly the posterior fossa and results in malformations such as Dandy-Walker [22]. Conversely, imbalance in favor of supratentorial hyperactivity would result in migration of the cerebellum tent, causing a small posterior fossa formation with the genesis of CM I [22]. In 1981, Williams demonstrated a pressure gradient experiment between the subarachnid space and intraventricular surgery by measuring the concomitant pressures in patients with CM I [23].

The CSF total volume is 120–150 ml in an adult. Its production depends mainly on the choroid plexus and the ependymal lining of the ventricles, also occurring in the brain parenchyma, the spinal cord, and the central canal of the spinal cord.

It has two components: mass or circulatory flow and pulsatile flow. The mass flow originates by the variation of the hydrostatic pressure between the ventricles and the subdural space due to the reabsorption of the liquor by the arachnoid granulations. The pulsatile flow occurs bidirectionally and is generated by pulsations related to the cardiac cycle of the choroid plexus and the arteries located in the subarachnoid space [15–21].

In patients with CM I, the tonsils are impacted in the foramen magnum, obstructing the free movement of the cerebrospinal fluid that occurs during systole through it. This occlusion results in reduced complacency in the subarachnoid space [15–21]. In this altered scenario, the tonsils act like a piston over the clogged cystic space, producing an increase in intrathecal pressure and an increase in pulse pressure [1–10]. In a vicious circle, increased pressure gradient, associated with increased cerebrospinal complacency and increased resistance to CSF, eventually altered the elasticity of neural tissue, its permeability, and water content. This pressure increase leads to the genesis of suboccipital headache and other symptoms in patients with or without syringomyelia. In addition, the incomplete development of the fourth ventricle output would lead to the latter's communication with the central canal of the spinal cord. This obstruction would favor the water hammer mechanism in the central canal of the medulla and development of syringomyelia [1–10]. Such morphofunctional phenomena can be evaluated statically and dynamically with the use of ultrasound.

Treatment of Chiari Malformation

Asymptomatic or oligosymptomatic patients may be followed and treated just when symptoms happen, especially those related to headache, cervical pain, nausea, and dizziness. Analgesics, nonsteroidal anti-inflammatories (NSAIDs), and antidepressants may be employed [9–11, 15].

When patients become persistently symptomatic, the recommended treatment consists of posterior fossa decompression (PFD), alleviation of posterior fossa overcrowding,and reestablishment of adequate CSF flow [24–38]. However, the optimal technique is still controversial.

The extent of bone decompression, dural opening, resection of arachnoid adhesions, coagulation, and even resection of the cerebellar tonsils remain subjects of controversy among specialists. Recently, lessinvasive methods with bone decompression alone have been reported with good results [39]. A recent meta-analysis revealed that bony decompression with dural opening was superior to decompression alone, but without statistical significance [40]. On the other hand, complications related to CSF fistula were more common and severe in patients submitted to dural opening. Thus, decompression alone may probably be the best strategy considering treatment success and side effects. Nevertheless, in cases harboring syringomyelia, success rate is higher when dural opening is performed [40].

The advent of intraoperative ultrasonography (USG) has allowed identification of

craniovertebral junction (CVJ) anatomy and CSF dynamics and CVJ structures with real-time images. It is possible to use intraoperative USG in patients with CM I as a method for selection of candidates for PFD with bone removal alone. Below we describe our experience.

Ultrasound: Technique and Indications

History and Literature Review

Ultrasonography has been used with neurosurgical aims for several diseases, including cranial and spinal tumors, vascular neurosurgery, and many others [41]. The advent of intraoperative ultrasonography (USG) has allowed identification of CVJ anatomy and CSF dynamics and CVJ structures with real-time images.

Intraoperative USG was used by Oldfield [9, 10] to demonstrate partial occlusion of the subarachnoid space and CSF flow changes in the CVJ in patients with CM I and syringomyelia. The authors observed that expansion of the brain parenchyma occurs during systole and imposes a downward force at the junction, manifested by an abnormal piston motion of the cerebellar tonsils, suggesting that pathophysiology and CSF dynamics in patients with MC can be examined sonographically in real time.

Isu [28] used intraoperative USG to determine the need to remove the outer layers of the dura and to obtain adequate decompression, succeeding in six of seven patients studied. Hida et al. used this technique to confirm the presence of pulsatile flow in the CVJ in 33 patients with adult CM I and syringomyelia and determine the extent of surgical treatment required [42]. Finally, Yeh indicated that bone-only decompression could be ideal for a particular group of patients and that these patients could be identified with the use of intraoperative USG [37].

Milhorat [15, 18] performed decompression and duraplasty in 315 patients and identified better prognoses and more favorable results in patients with a peak CSF flow velocity in the range of 3–5 cm/s, bidirectional movement, and fluctuations arising from cardiac and ventilatory movements. Cui et al. [17] used USG to assess the presence and rate of flow in 20 patients undergoing PFD. Based on this literature, with a view to achieving the best possible outcomes in our patients, we chose a CSF flow rate (Vf) value of 3 cm/s as our threshold for performing duraplasty [39, 40].

McGirt [32–34] conducted a magnetic resonance imaging (MRI)-based CSF flow study and found that preoperative abnormalities in CSF flow correlated with better prognosis after decompression. They consider that the change in CSF flow is mainly responsible for the onset of symptoms in patients with CM I and is the determining factor in the success of surgery; therefore, we adopted measurement of CSF flow rate as an indicator of the need for duraplasty [32–34].

Technique

Intraoperative USG is then performed to determine the retrocerebellar space, cisterna magna, and CSF flow through the foramen magnum in the retrocerebellar space. At our facility, a two-dimensional (2D) USG system (MicroMaxx Sonosite, Bothell, WA) with high- and low-frequency transducers (13–6 MHz and 04.08 MHz, respectively) is used.

USG allows identification of the anatomical structures of the CVJ (Fig. 27.1). With the system in B-scan mode, the craniocaudal (A), anteroposterior (B), and lateral (C) dimensions of the cisterna magna are measured (Fig. 27.2). Three different images are obtained in each plane, and the mean of the three resulting measurements is taken into account for analysis. CSF flow measurement is performed with the system in Doppler mode, with the transducer placed in longitudinally in a window parallel to CSF flow at the level of the foramen magnum. The average speed is determined by the formula:

$$\frac{\left(V_{max} + 2 \times V_{min}\right)}{3}$$

Three measurements are obtained, and the weighted average of the three is defined as the

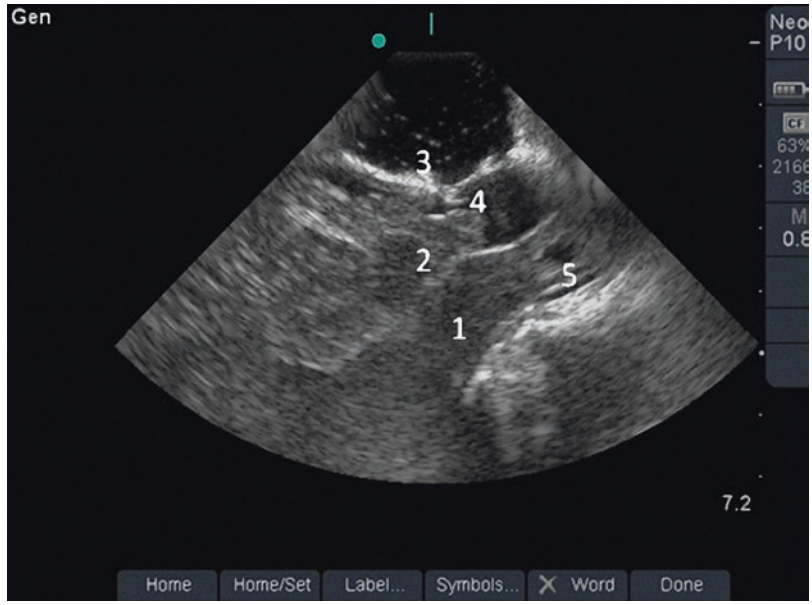

Fig. 27.1 Image of intraoperative ultrasonography anatomical identification. (1) Brainstem; (2) cerebellar tonsils; (3) dura; (4) retrocerebellar space; (5) spinal cord with syringomyelic cavity

CSF flow rate (Vf) through the foramen magnum (Fig. 27.3).

A Vf value of 3 cm/s was adopted as the threshold for opening the dura and performing duraplasty. This was the lowest Vf value found in the literature for patients who achieved a good outcome after PFD [15, 18]. After bone decompression and dural delamination, CSF flow was measured, and if Vf was equal to or greater than 3 cm/s, the procedure was completed without dural opening. If the Vf was less than 3 cm/s, then a Y-shaped dural opening was fashioned, and, under microscopy, arachnoid membrane adhesions were dissected, and the foramen of Magendie was opened to communicate the subdural space to the fourth ventricle. No tonsillar coagulation was performed in the present sample.

Experience

Using a prospective design, we collected demographic, clinical, and sonographic data from 49 consecutive adult patients who had received a diagnosis of CM and underwent decompressive surgery of the posterior fossa [39].

We perform surgery in prone position, with the head slightly bent and held in a skull clamp. A midline skin incision is made extending from the external occipital protuberance to the height of the fourth or fifth spinous process of the cervical vertebra. If needed, in patients lacking proper CSF flow, the incision is extended 3 cm to harvest pericranium grafts for duraplasty. This is followed by a suboccipital craniectomy 3–4 cm in diameter with removal of the posterior arch of C1 (Fig. 27.4) [39]. If needed, we perform dural opening, posterior fossa decompression, and arachnoid debridement. We also look for tonsillar hypertrophy or ptosis; however, we do not perform routine tonsillectomy unless there is clear and voluminous hypertrophy or ptosis (Fig. 27.5).

A CSF flow >3 cm/s was measured in 36 of the 49 patients (73.46%). These patients were thus enrolled in the bone-only decompression (BOD) group and did not undergo duraplasty. In the other 13 patients (26.53%), CSF flow through the retrocerebellar space was measured as <3 cm/s, and dural opening with duraplasty (DD) was performed. Nine patients were lost to follow-up;thus 40 patients were included for sta-

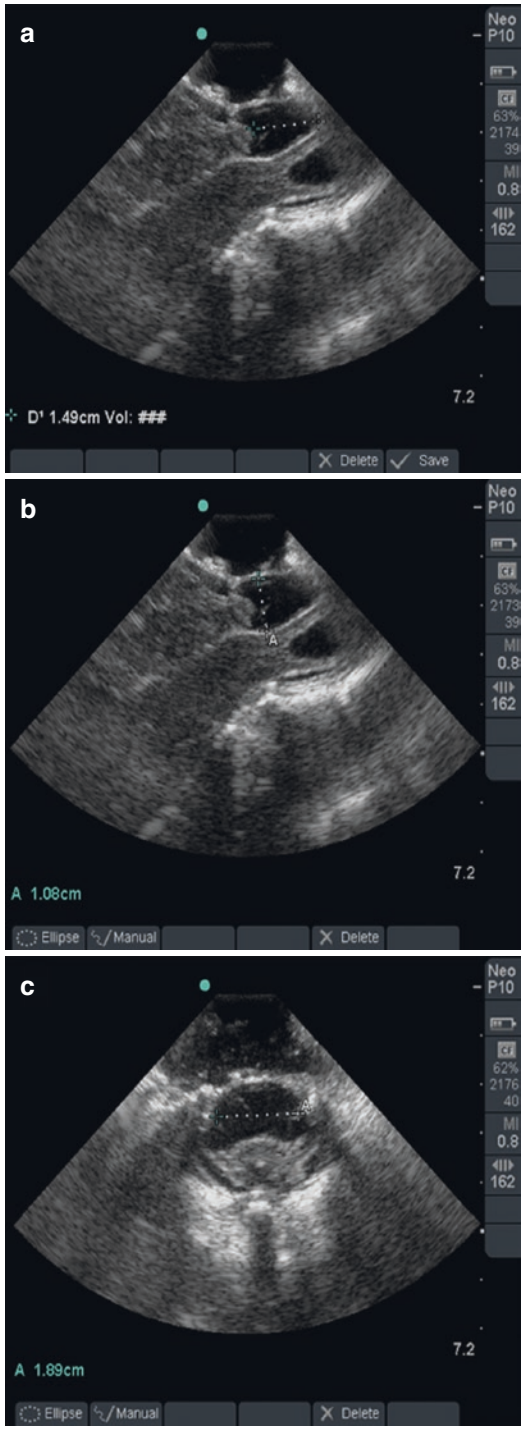

Fig. 27.2 Measures of retrocerebellar space. (**a**) Diameter skull, flow; (**b**) anteroposterior diameter; (**c**) lateral-lateral diameter

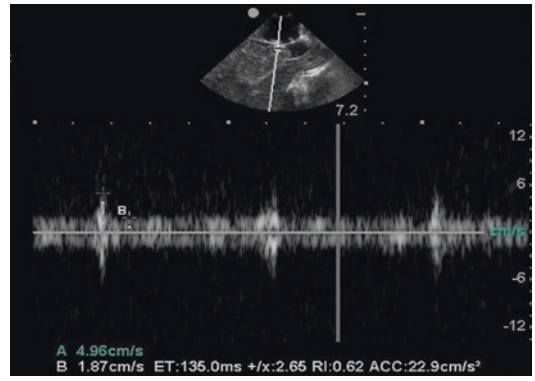

Fig. 27.3 Measurement of the CSF flow rate by retrocerebellar space. $V_{med} = (V_{max} + 2 \times V_{min}) / 3$

tistical analysis: 30 in the BOD group and 10 in the DD group [39].

Concomitant syringomyelia and basilar invagination (type B) were present in 47% and 49% of patients, respectively. The distribution of these findings between the two groups of patients was 44% and 53% in the BOD group and 54% and 38% in the DD group [39].

There was no significant difference in retrocerebellar space dimensions between the two groups ($P = 0.825$). The mean craniocaudal dimension (A) was 1.43 ± 0.64 in the BOD group and 1.48 ± 0.62 in the DD group. Measurement B, corresponding to the lateral-lateral diameter, averaged 0.61 ± 0.29 in the BOD group and 0.71 ± 0.49 in the DD group, with no significant difference ($P = 0.312$). Anteroposterior diameter (C) was also similar between groups, averaging 1.24 ± 0.31 in the BOD group and 1.23 ± 0.48 in the DD group ($P = 0.925$) [39].

The only parameter that differed significantly between groups was, as expected, the CSF flow rate. The average flow velocity (V) was 6.02 ± 3.07 cm/s in the BOD group and 1.73 ± 0.92 cm/s in the DD group ($P < 0.01$). These results are consistent with previous studies that failed to identify preoperative morphological changes that might indicate the presence or absence of adequate CSF flow [39].

There was no significant difference between the BOD and DD groups in terms of headache

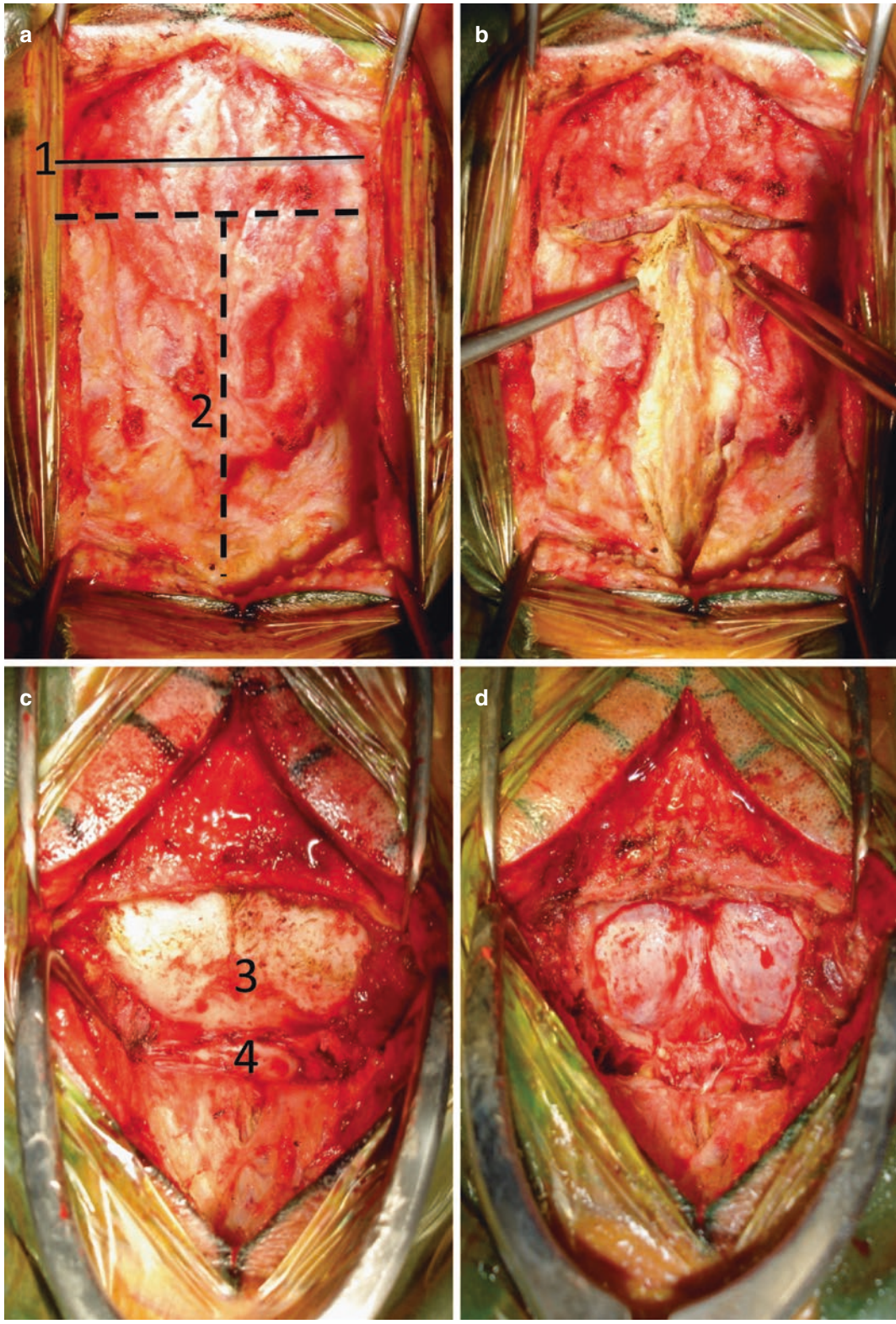

Fig. 27.4 (**a**) Exposure of muscle fascia,(1) superior nuchal line, (2) linea alba, surgical incision; (**b**) opening and muscle dissection; (**c**) bone exposure, (3) occiput; (4) posterior arch of C1; (**d**) dural exposure after suboccipital craniectomy and removal of the C1 posterior arch

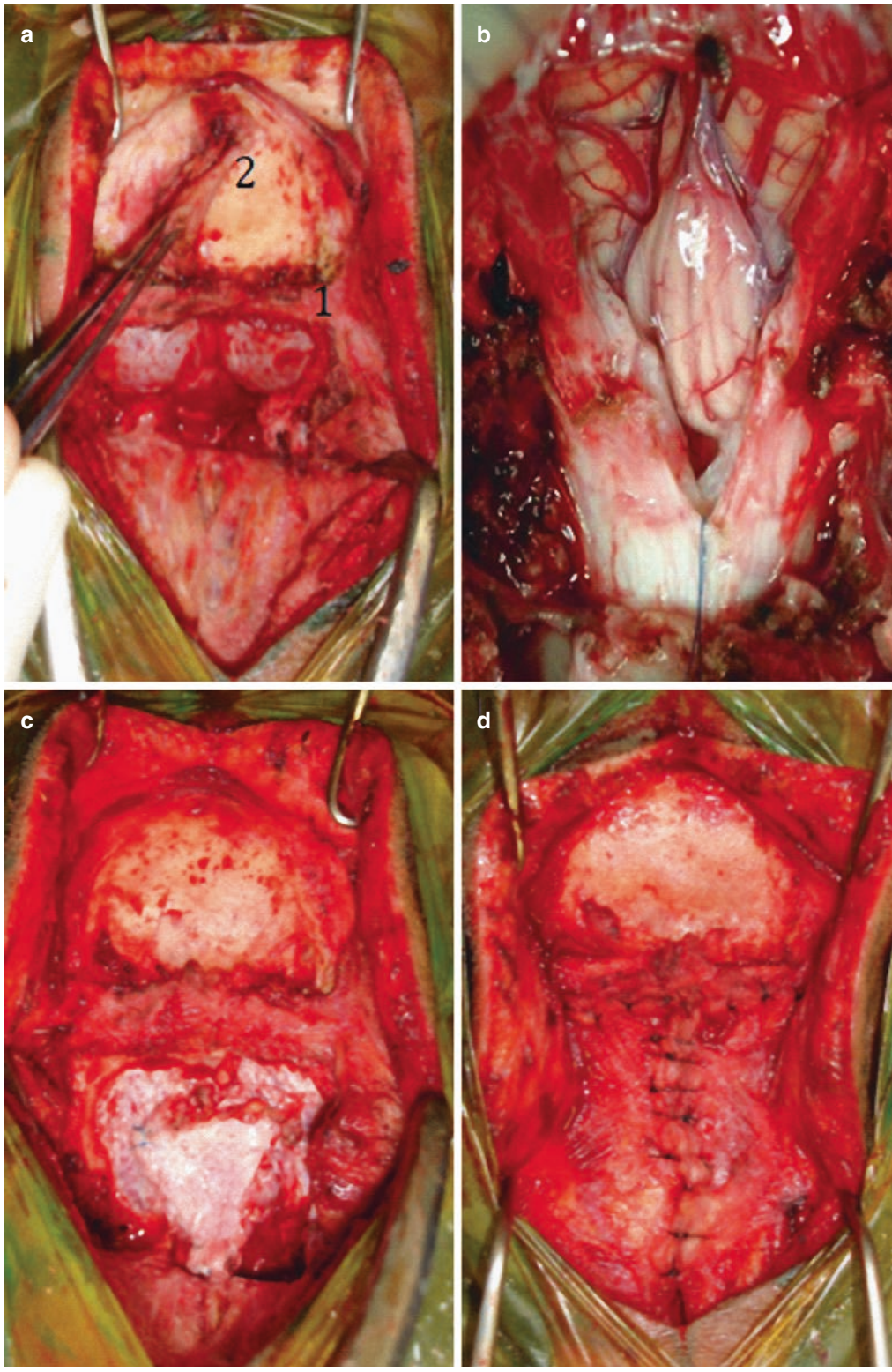

Fig. 27.5 (**a**) Dural exposure; (**b**) dural decompression and dissection of arachnoid; (**c**) lock with duraplasty; (**d**) closure of muscle fascia maintaining muscle insertion

scores (P = 0.589). After surgery, headache improved in both groups. Improvements in perception of overall health were also observed in both groups at 1-year follow-up [39].

Questions have been raised regarding the validity of intraoperative measurements obtained with the patient in the prone position. Bond [16], using MRI with intraoperative flow study, noted substantial differences between measurements performed in the prone and orthostatic positions, with improvement in CSF flow obtained in 93% of patients only with proper positioning. However, our USG evaluation was performed in one standard position (prone), avoiding the higher potential for complications described with the semi-sitting position. Thus, we believe that our USG technique is an effective adjunct measure that can optimize the surgical approach while maintaining a safe position for the patient [16].

We observed no between-group differences in need for reintervention in our sample (16% in the BOD group vs. 20% in the DD group). Indications for reintervention were worsening of neurological status and recurrence of symptoms after surgery. Headache is the symptom most likely to recur, due to its multifactorial origin and to the difficulty of establishing a clinical relationship with the condition in question. Only one patient in the BOD group required reintervention due to persistent, severe symptoms and did not experience further improvement after duraplasty. In the DD group, two patients required reoperation due to neurological worsening, in one case due to cerebellar ptosis [39].

In our sample, three of ten patients (30%) in the DD group had complications after dural opening: one developed a CSF fistula (10%), one developed pseudomeningocele (10%), and one had cerebellar ptosis (10%)—the last requiring surgery. We did not observe perioperative complications related to surgery in the BOD group [39].

Therefore, our results showed no significant difference between adult patients with CM I who underwent bone-only decompression of the posterior fossa (BOD) and those who underwent PFD with duraplasty (DD) regarding postoperative quality of life, improvement of headache and neck pain, or reoperation rate. This suggests that measurement of CSF flow via intraoperative USG was an effective method for the selection of patients who would benefit from less-aggressive surgery.

Conclusion

Ultrasound use is practical, inexpensive, and valuable in patients undergoing treatment for Chiari 1 malformation. Real-time evaluation of CSF flow in cisterna magna allows the best choice for surgical approach (extradural versus intradural) and immediate assessment of post decompression status. Thus, ultrasound in experienced hands may increase the surgical success rate while decreasing potential surgical complications. One must remember that ultrasound is operator dependent, with results depending on the level of experience of the practitioner. However, ultrasound for Chiari 1 malformation surgery demands a small learning curve to reach optimal results.

References

1. Bejjani GK. Definition of the adult Chiari malformation: a brief historical overview. Neurosurg Focus. 2001;11(1):E1.
2. Botelho RV, Bittencourt LR, Rotta JM, Tufik S. A prospective controlled study of sleep respiratory events in patients with craniovertebraljunction malformation. J Neurosurg. 2003;99(6):1004–9.
3. Goel A. Basilar invagination, Chiari malformation, syringomyelia: a review. Neurol India. 2009;57(3):235–46.
4. Goel A. Is Chiari malformation nature's protective “air-bag”? Is its presence diagnostic of atlantoaxialinstability? J Craniovertebr Junction Spine. 2014;5(3):107–9.
5. Heiss JD, Patronas N, DeVroom HL, Shawker T, Ennis R, Kammerer W, Eidsath A, Talbot T, Morris J, Eskioglu E, Oldfield EH. Elucidating the pathophysiology of syringomyelia. J Neurosurg. 1999;91(4):553–62.
6. Strahle J, Smith BW, Martinez M, Bapuraj JR, Muraszko KM, Garton HJ, Maher CO. The association between Chiari malformation Type I, spinal syrinx, and scoliosis. J Neurosurg Pediatr. 2015;15(6):607–11.
7. Markunas CA, Soldano K, Dunlap K, Cope H, Asiimwe E, Stajich J, Enterline D, Grant G, Fuchs

H, Gregory SG, Ashley-Koch AE. Stratified whole genome linkage analysis of Chiari type I malformation implicates knownKlippel-Feil syndrome genes as putative disease candidates. PLoS One. 2013;8(4):e61521.
8. Menezes AH. Primary craniovertebral anomalies and the hindbrain herniation syndrome (Chiari I): database analysis. Pediatr Neurosurg. 1995;23(5): 260–9.
9. Oldfield EH, Muraszko K, Shawker TH, Patronas NJ. Pathophysiology of syringomyelia associated with Chiari I malformation of the cerebellar tonsils: implications for diagnosis and treatment. J Neurosurg. 1994;80(1):3–15.
10. Oldfield EH, Muraszko K, Shawker TW, Patronas NJ. Pathophysiology of syringomyelia associated with Chiari I malformation of the cerebellar tonsils: implications for diagnosis and treatment. J Neurosurg. 2004;80(1):3–15.
11. Nishikawa M, Sakamoto H, Hakuba A, Nakanishi N, Inoue Y. Pathogenesis of Chiari malformation: a morphometric study of the posterior cranial fossa. J Neurosurg. 1997;86(1):40–7.
12. Alperin N, Sivaramakrishnan A, Lichtor T. Magnetic resonance imaging-based measurements of cerebrospinal fluid and blood flow as indicators of intracranial compliance in patients with Chiari malformation. J Neurosurg. 2005;103(1):46–52.
13. Meadows J, Kraut M, Guarnieri M, Haroun RI, Carson BS. Asymptomatic Chiari Type I malformations identified on magnetic resonance imaging. J Neurosurg. 2000;92(6):920–6.
14. Barkhof F, Kouwenhoven M, Scheltens P, Sprenger M, Algra P, Valk J. Phase-contrast cine MR imaging of normal aqueductal CSF flow. Effect of aging and relation to CSF void on modulus MR. Acta Radiol. 1994;35(2):123–30.
15. Milhorat TH, Chou MW, Trinidad EM, Kula RW, Mandell M, Wolpert C, Speer MC. Chiari I malformation redefined: clinical and radiographic findings for 364symptomatic patients. Neurosurgery. 1999;44(5):1005–17.
16. Bond AE, Jane JA Sr, Liu KC, Oldfield EH. Changes in cerebrospinal fluid flow assessed using intraoperative MRI during posterior fossadecompression for Chiari malformation. J Neurosurg. 2015;122(5):1068–75.
17. Cui LG, Jiang L, Zhang HB, Liu B, Wang JR, Jia JW, Chen W. Monitoring of cerebrospinal fluid flow by intraoperative ultrasound inpatients with Chiari I malformation. Clin Neurol Neurosurg. 2011;113(3):173–6.
18. Milhorat TH, Bolognese PA. Tailored operative technique for Chiari type I malformation usingintraoperative color Doppler ultrasonography. Neurosurgery. 2003;53(4):899–905. discussion 905–6
19. Sakushima K, Hida K, Yabe I, Tsuboi S, Uehara R, Sasaki H. Different surgical treatment techniques used by neurosurgeons and orthopedists for syringomyelia caused by Chiari I malformation in Japan: clinical article. J Neurosurg Spine. 2013;18(6):588–92.
20. Taricco MA, Pereira WC. Tratamento cirúrgico da siringomielia associada à malformaçäo de Chiari do tipo I. Arq. bras. neurocir. 1997;16(2):47–60.
21. Fan T, Zhao H, Zhao X, Liang C, Wang Y, Gai Q. Surgical management of Chiari I malformation based on different cerebrospinal fluid flow patterns at the cranial-vertebral junction. Neurosurg Rev. 2017;40(4):663–70.
22. Koyanagi I, Houkin K. Pathogenesis of syringomyelia associated with Chiari type 1 malformation: review ofevidences and proposal of a new hypothesis. Neurosurg Rev. 2010;33(3):271–84. discussion 284–5
23. Gardner WJ. Hydrodynamic mechanism of syringomyelia: its relationship to myelocele. J Neurol Neurosurg Psychiatry. 1965;28:247–59.
24. Williams B. Simultaneous cerebral and spinal fluid pressure recordings. Cerebrospinal dissociation with lesions at the foramen magnum. Acta Neurochir. 1981;59:123–42.
25. Durham SR, Fjeld-Olenec K. Comparison of posterior fossa decompression with and without duraplasty for the surgical treatment of Chiari malformation Type I in pediatric patients: a meta-analysis. J Neurosurg Pediatr. 2008;2(1):42–9.
26. Greenberg JK, Milner E, Yarbrough CK, Lipsey K, Piccirillo JF, Smyth MD, Park TS, Limbrick DD Jr. Outcome methods used in clinical studies of Chiari malformation Type I: a systematic review. J Neurosurg. 2015;122(2):262–72.
27. Hankinson T, Tubbs RS, Wellons JC. Duraplasty or not? An evidence-based review of the pediatric Chiari I malformation. Childs Nerv Syst. 2011;27(1):35–40.
28. Isu T, Sasaki H, Takamura H, Kobayashi N. Foramen magnum decompression with removal of the outer layer of the dura as treatment forsyringomyelia occurring with Chiari I malformation. Neurosurgery. 1993;33(5):845–9. discussion 849–50
29. Kalb S, Perez-Orribo L, Mahan M, Theodore N, Nakaji P, Bristol RE. Evaluation of operative procedures for symptomatic outcome afterdecompression surgery for Chiari type I malformation. J Clin Neurosci. 2012;19(9):1268–72.
30. Klekamp J. Surgical treatment of Chiari I malformation–analysis of intraoperative findings, complications, and outcome for 371 foramen magnum decompressions. Neurosurgery. 2012;71(2):365–80. discussion 380
31. Lee A, Yarbrough CK, Greenberg JK, Barber J, Limbrick DD, Smyth MD. Comparison of posterior fossa decompression with or without duraplasty in children withType I Chiari malformation. Childs Nerv Syst. 2014;30(8):1419–24.
32. McGirt MJ, Atiba A, Attenello FJ, Wasserman BA, Datoo G, Gathinji M, Carson B, Weingart JD, Jallo GI. Correlation of hindbrain CSF flow and outcome after surgical decompression for Chiari Imalformation. Childs Nerv Syst. 2008;24(7):833–40.
33. McGirt MJ, Attenello FJ, Atiba A, Garces-Ambrossi G, Datoo G, Weingart JD, Carson B, Jallo GI. Symptom

recurrence after suboccipital decompression for pediatric Chiari I malformation: analysis of 256 consecutive cases. Childs Nerv Syst. 2008;24(11):1333–9.
34. McGirt MJ, Attenello FJ, Datoo G, Gathinji M, Atiba A, Weingart JD, Carson B, Jallo GI. Intraoperative ultrasonography as a guide to patient selection for duraplasty aftersuboccipital decompression in children with Chiari malformation Type I. J Neurosurg Pediatr. 2008;2(1):52–7.
35. Munshi I, Frim D, Stine-Reyes R, Weir BK, Hekmatpanah J, Brown F. Effects of posterior fossa decompression with and without duraplasty on Chiari malformation-associated hydromyelia. Neurosurgery. 2000;46(6):1384–9. discussion 1389–90
36. Mutchnick IS, Janjua RM, Moeller K, Moriarty TM. Decompression of Chiari malformation with and without duraplasty: morbidity versus recurrence. J Neurosurg Pediatr. 2010;5(5):474–8.
37. Yeh DD, Koch B, Crone KR. Intraoperative ultrasonography used to determine the extent of surgery necessary duringposterior fossa decompression in children with Chiari malformation type I. J Neurosurg. 2006;105(1 Suppl):26–32.
38. Karras CL, Jamshidi AO, Prevedello DM. Short comings of intraoperative ultrasound in Chiari type 1 decompression and call for routine use of duraplasty. J Neurosurg Sci. 2018;62(2):221–3.
39. Brock RS, Taricco MA, de Oliveira MF, de Lima Oliveira M, Teixeira MJ, Bor-Seng-Shu E. Intraoperative ultrasonography for definition of less invasive surgical technique in patients with Chiari type I malformation. World Neurosurg. 2017;101:466–75.
40. de Oliveira Sousa U, de Oliveira MF, Heringer LC, Barcelos ACES, Botelho RV. The effect of posterior fossa decompression in adult Chiari malformation and basilar invagination: a systematic review and meta-analysis. Neurosurg Rev. 2018;41(1):311–21.
41. Dohrmann GJ, Rubin JM. Use of ultrasound in neurosurgical operations: a preliminary report. Surg Neurol. 1981;16(5):362–6.
42. Hida K, Iwasaki Y, Koyanagi I, Sawamura Y, Abe H. Surgical indication and results of foramen magnum decompression versus syringosubarachnoid shunting for syringomyelia associated with Chiari I malformation. Neurosurgery. 1995;37(4):673–8. discussion 678–9

Advanced Imaging of Chiari I Malformations

28

Rami W. Eldaya, Jennifer M. Strahle, and Manu S. Goyal

Background

In 1891 Hans Chiari, an Austrian pathologist, detailed three separate morphological abnormalities of the posterior fossa, including Chiari type I malformation (CM I), characterized by descent of part of the cerebellum and brain stem through the foramen magnum [1, 2]. Since then, extensive attention has been given to Chiari type I malformation given its relatively common prevalence and simple diagnosis on magnetic resonance imaging (MRI) [3–5]. The diagnosis of Chiari type I malformation can be made on routine brain or cervical spine MRI by establishing the caudal position of the cerebellar tonsils below the foramen magnum [6–8].

MRI has contributed to the significant increase in the diagnosis of Chiari type I malformation with a reported incidence of 1–3.6% in children undergoing MR imaging [9, 10]. The increase in identification of Chiari I malformation on routine MRI not only has resulted in increased diagnosis rates but has also allowed for increased understanding of the pathophysiology of this condition. It has also identified a subset of patients diagnosed with Chiari type I malformation, up to 35–68%, that are nevertheless asymptomatic, raising the question about the diagnosis itself and its appropriate management in this subgroup [9, 10].

The pathophysiology of Chiari type I malformation is complex and heterogeneous but can be summarized as a discrepancy between the content (hindbrain) and container (posterior fossa) [11, 12]. This discrepancy is due to a deformation of the involved structures and results in hindbrain and tonsillar descent through the foramen magnum. This concept is supported by the fact that longitudinal studies have shown that Chiari type I malformation can develop postnatally and increase or regress in patients over time [11–17].

Standard MRI sequences can establish the diagnosis of CM I rather easily and detect associated skull base, craniocervical junction, and cervical osseous deformities. Furthermore, spine MRI can detect associated syringomyelia and scoliosis reliably [10, 18–20]. However, some patients

Electronic Supplementary Material The online version of this chapter (https://doi.org/10.1007/978-3-030-44862-2_28) contains supplementary material, which is available to authorized users.

R. W. Eldaya (✉)
Department of Neuroradiology, Mallinckrodt Institute of Radiology, Bames Jewish Hospital, Washington University School of Medicine, St. Louis, MO, USA
e-mail: rami.eldaya@wustl.edu

J. M. Strahle
Department of Neurosurgery, Washington University School of Medicine, Orthopedic Surgery and Pediatrics, Washington University School of Medicine, St. Louis Children's Hospital, St. Louis, MO, USA

M. S. Goyal
Department of Neuroradiology, Mallinckrodt Institute of Radiology, Washington University School of Medicine, St. Louis, MO, USA

R. S. Tubbs et al. (eds.), *The Chiari Malformations*, https://doi.org/10.1007/978-3-030-44862-2_28

with syringomyelia or low tonsil position may be asymptomatic (up to 68% with tonsil position 5–10 mm below the foramen magnum), while others with minimal tonsillar descent can be markedly symptomatic (3 to 4 mm below the foramen magnum) [6, 9, 17, 21]. These findings argue that while standard MRI can diagnose CM I reliably, it remains neither sensitive nor specific for predicting symptoms [22, 23]. This is further validated by the recently published international survey on the management of CM I (published in 2018) [24]. Despite the increased understanding of CM I pathophysiology and symptomatology progression, the role of standard MRI in treatment decisions, while important, has not changed significantly from the prior survey (performed in 2003) [25].

The development of advanced sequences in MRI has expanded the role of MRI in disease assessment. Advanced MR imaging in CM I aims to improve the assessment of the severity of the disease and its effects on cerebrospinal fluid (CSF) dynamics [11, 26] in order to predict and correlate patient's symptoms with the deformity. The establishment of such correlation in addition to assessment of CSF flow dynamics by advanced imaging helps determine the likelihood that surgical treatment with posterior fossa decompression will improve the patient's symptoms. This and other advanced imaging are also used to further improve our understanding of the pathophysiology of CM I.

Advanced imaging techniques frequently used to assess patients with CM I include:

- CSF flow imaging at the foramen magnum using cardiac-gated phase-contrast MRI.
- Cerebellar tonsillar pulsatility at the foramen magnum using cardiac-gated cine MRI.

Additional advanced imaging techniques that have been primarily used in research studies to assess CM I and have shown promise in further assessing the disease include:

- Quantitative volumetrics of the posterior fossa and biometrics of the skull base.
- Diffusion tensor imaging (DTI) of the posterior fossa and spinal cord.

This chapter will detail the former two and supplement the discussion of both with images and videos. A short discussion of the latter two techniques will be included.

Radiological Diagnosis of Chiari I

MRI is the imaging modality of choice for the diagnosis of CM I. Standard T1 and T2 sequences can readily detect the location of the tonsils and its relationship to the foramen magnum. The line of McRae, extending from the basion to the opisthion, can be assumed to represent the plane of the foramen magnum. The radiological definition of Chiari I malformation, the position of the cerebellar tonsils with respect to the foramen magnum, was first established in the mid-1980s with the location of the cerebellar tonsils in normal pediatric population noted to be variable and ranges from 8 mm above to 5 mm below the foramen magnum [6, 19, 27, 28]. However, given the weak correlation between tonsillar position and symptoms, there has been considerable variation across studies on the criteria for CM I [6, 9, 11, 12, 21, 28]. The simplest and most widely used criteria are:

- Tonsil position of one or both tonsils 5 mm or more below the foramen magnum is considered diagnostic of CM I.
- Tonsil position of both tonsils less than 3 mm below the foramen magnum is considered normal.
- Tonsil position between 3 to 5 mm is debatable, with some considering it to be diagnostic of CM I if both tonsils are below 3 mm [11, 12], whereas others label such tonsil position as normal.

In addition to tonsil position, morphologic appearance of the tonsils varies from a rounded appearance to a pointed "peg-like" appearance often associated with crowding of the foramen magnum [11, 12], which is best appreciated on sagittal images [29]. Asymmetry in tonsil position is not uncommon (15% of cases), and when present, the right tonsil is lower than the left in approximately 75% of cases [28].

Coronal images are used to detect such asymmetry [11].

Spine MRI can reliably detect the presence of syringomyelia. CM I is the most common cause of syringomyelia in the pediatric population, with the prevalence of syringomyelia ranging from 20% to 70% of patients with CM I [10, 30, 31]. MRI of the spine also determines the location, extent, size, and appearance of the syrinx. The most common location for CM I-associated syrinxes is within the mid cervical to upper thoracic spine, with the C4 to C6 levels being the most commonly involved regions [11, 32, 33]. In addition, CM I-associated syrinxes are usually greater than 5 mm in width [33]. MRI of the spine can also reliably and readily detect the presence and severity of associated spinal deformities, in particular scoliosis. Scoliosis has been associated with CM I and can be seen in up to 20% of patients with this diagnosis and as high as 60% in patients with associated syringomyelia [34].

Lastly, conventional MRI can also detect associated craniocervical abnormalities, skull base abnormalities, and the less commonly associated hydrocephalus.

Advanced Imaging

Cerebrospinal Fluid Flow Imaging

Standard MRI is sufficient to diagnose CM I. However, it does not accurately predict symptoms nor surgical success. Functional sequences such as CSF flow imaging can provide additional physiologic information that can aid in understanding symptomology and pathophysiology and help predict the potential benefit of surgery [35, 36].

Although CSF circulation remains incompletely understood and is more complex than previously thought, CSF flow across the foramen magnum is an established route of CSF circulation and is synchronous with the cardiac and respiratory cycles [37]. The flow of CSF from the foramen magnum into the spinal subarachnoid space is essential to maintain normal intracranial pressure throughout the cardiac cycle. As blood flows into the brain, the rigid skull limits brain tissue expansion. In order to accommodate for increased blood volume during systole, CSF flows from the brain into the spinal subarachnoid space, thereby helping to maintain normal intracranial pressure (Monro-Kellie doctrine). In diastole, CSF returns to the cranial cavity to, again, help maintain intracranial pressure. Cerebellar tonsillar displacement into the foramen magnum alters the bidirectional CSF flow and velocity across the foramen that in turn subjects the tonsils to forces of CSF pulsation. This may result in further displacement of the tonsils caudally and altering the rounded shape of the tonsils into a more pointed "peg-like" appearance, which may further restrict CSF flow [38–40]. This alteration of CSF flow at the foramen magnum has been identified more commonly in symptomatic patients, in particular with patients presenting with occipital headaches [30, 41]. The alteration of CSF flow is also present more frequently in patients with syringomyelia than in patients without syringomyelia [42]. This latter finding has led to theories suggesting that alteration/elevation of CSF flow velocity at the foramen magnum could represent the mechanism of syrinx formation [42–44]. However, at this point the association between syrinx formation and altered CSF flow at the foramen magnum is still evolving.

Analysis of CSF flow across the foramen magnum can be assessed using a combination of phase-contrast and cardiac-gated MR imaging. Phase-contrast MR sequence, a flow-sensitive sequence, allows detection of phase shifts in moving protons proportional to their velocity [45–49]. Cardiac gating allows for synchronization of acquired images with the cardiac cycle. This is achieved by automated QRS wave detection and recording of multiple cardiac cycles simultaneously with image acquisitions. Subsequently, multiple cardiac cycles are averaged, and the MR data is correlated/reordered to match the cardiac cycle [50–52]. The combination of both acquisition techniques allows for analysis of CSF flow direction, velocity, amplitude, pulsatility, magnitude, and wave form throughout the cardiac cycle.

Prior to the acquisition of cardiac-gated phase-contrast MRI, specific setup is required that includes the following [26]:

- Electrocardiogram or peripheral pulse monitoring is needed to successfully achieve cardiac gating. The former is more robust in detection of cardiac contraction and flow pulsatility. However, peripheral pulse gating can be used and is often adequate for cine CSF flow studies.
- Prior to acquisition of phase-contrast MRI, the anticipated maximum CSF flow velocity VENC (velocity encoding) should be set. Optimal signal is usually acquired at VENC equal to or slightly more than the maximum CSF flow velocity [48]. Based on this requirement and the typical normal CSF flow velocity, the VENC is usually set between 5 and 10 cm/s. However, the VENC should be adjusted in cases of altered CSF flow. In cases of increased CSF velocity at the foramen magnum, aliasing is typically visualized. In such cases the VENC should be increased, and acquisition of the images should be repeated. Alternatively, if the velocity of CSF flow is low, the VENC should be decreased, or else a weak signal would be acquired [53].
- Phase-contrast MRI is typically acquired in two planes: axial and sagittal. This allows for both flow quantification and qualitative assessment.

Assessment of CSF flow across the foramen magnum includes the presence of flow, direction of flow, flow waveform, uniformity of flow, and velocity of flow. Conventionally, caudal CSF flow is represented as shades of white or bright signal, and cranial flow is represented as shades of black or dark signal on phase-contrast MRI. Velocity can be quantified by placing a region of interest at the desired location, typically anterior or posterior to the cervicomedullary junction, at or inferior to the foramen magnum. The velocity of flow is dependent on the dimensions of the foramen magnum. Normally, CSF bidirectional flow should be equivalent anterior and posterior to the spinal cord in either direction. The flow should be low in velocity without aliasing with relatively similar low peak velocity in systole and diastole [39]. However, processes narrowing the foramen magnum, such as tonsillar crowding, will likely impede CSF flow and result in compensatory increased velocity [11, 26]. CM I patients may demonstrate one or multiple of several CSF flow abnormalities at the foramen magnum such as (Figs. 28.1, 28.2, 28.3, 28.4, 28.5, 28.6, 28.7, and 28.8, Videos 28.1, 28.2, 28.3, 28.4, 28.5, 28.6, 28.7, and 28.8):

- *Increased systolic and diastolic velocity* – Haughton et al. showed an average peak systolic velocity of 2.4 cm/s and average peak diastolic velocity of 2.8 cm/s in normal volunteers with both velocities elevated in symptomatic CM I patients at 3.1 cm/s and 4.0 cm/s, respectively, with peak systolic velocities significantly higher than those of normal volunteers [39]. Multiple other studies have also documented elevation of both systolic and diastolic velocities with reported averaged peak velocities as high as 11 cm/s [43, 44, 54].
- *Nonuniformity* – Nonuniform flow can be noted and is likely secondary to mechanical obstruction throughout the cardiac cycle. This is more frequently seen in the axial plane [26].
- *Variation between anterior and posterior flow* – In normal individuals, minimal CSF flow variations occur along the anterior and posterior subarachnoid spaces at the foramen magnum [54]. However, in Chiari I patients, lack of uniformity of CSF flow is common and frequently demonstrates a progressive pattern [39, 43, 44, 54–57].
- *Synchronous bidirectional flow* – Simultaneous caudal and cephalad flow has been noted in CM I patients but not in healthy volunteers and can occur in up to 25% of the cardiac cycle [54, 58]. This can potentially explain the persistent aliasing in some cases despite increasing the VENC.

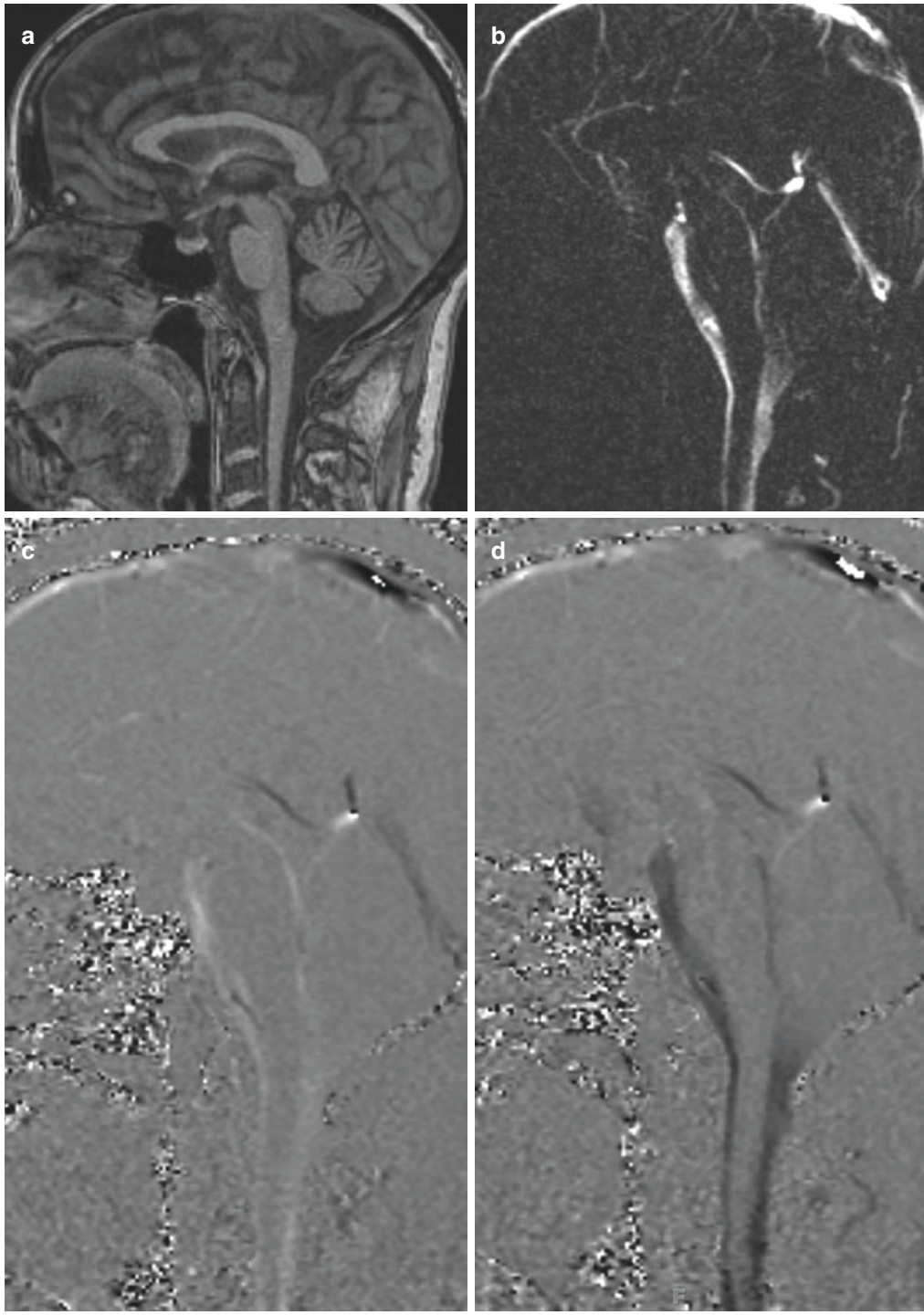

Fig. 28.1 Normal subject with normal flow at the foramen magnum. (**a**) Sagittal T1 view of the brain demonstrating normal position of the cerebellar tonsils in a normal subject. (**b**) Sagittal second phase-contrast image with a velocity encoding (VENC) of 10 showing normal flow at the foramen magnum anteriorly and posteriorly. (**c**, **d**) Midsagittal image from cine phase-contrast study with a VENC of 10 showing normal bidirectional flow at the foramen magnum anteriorly and posteriorly (Supplement Video 28.1 demonstrates the normal flow through the cardiac cycle)

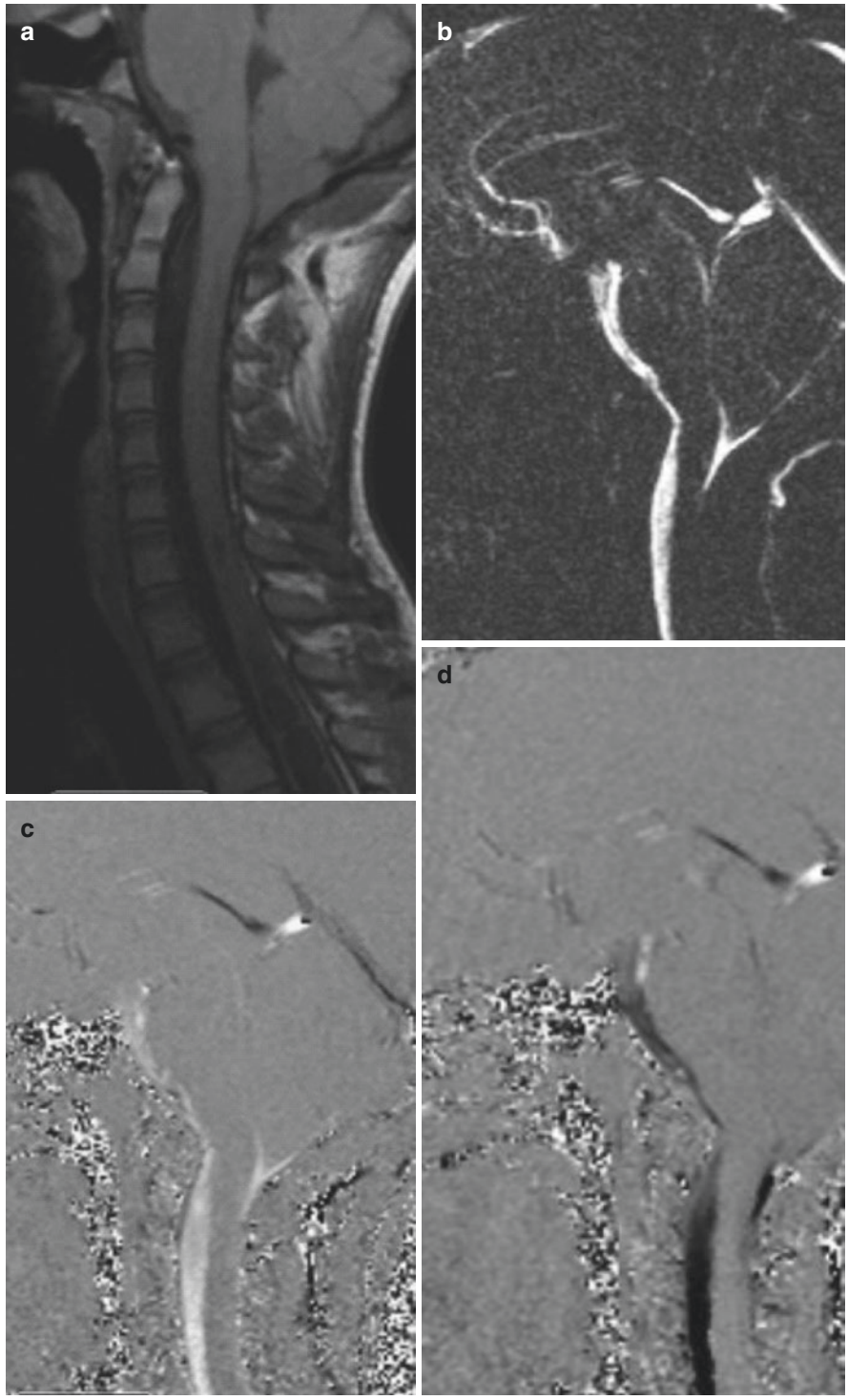

Fig. 28.2 Chiari I deformity patient with normal flow at the foramen magnum. (**a**) Sagittal T1 view of the brain showing Chiari I deformity with peg-like shape of the tonsils and approximately 10 mm cerebellar tonsillar ectopia. (**b**) Sagittal second phase-contrast image with a velocity encoding (VENC) of 10 showing normal flow at the foramen magnum anteriorly and posteriorly. (**c**, **d**) Midsagittal image from cine phase-contrast study with a VENC of 10 showing normal bidirectional flow at the foramen magnum anteriorly and posteriorly (Supplement Video 28.2 demonstrates the normal flow through the cardiac cycle)

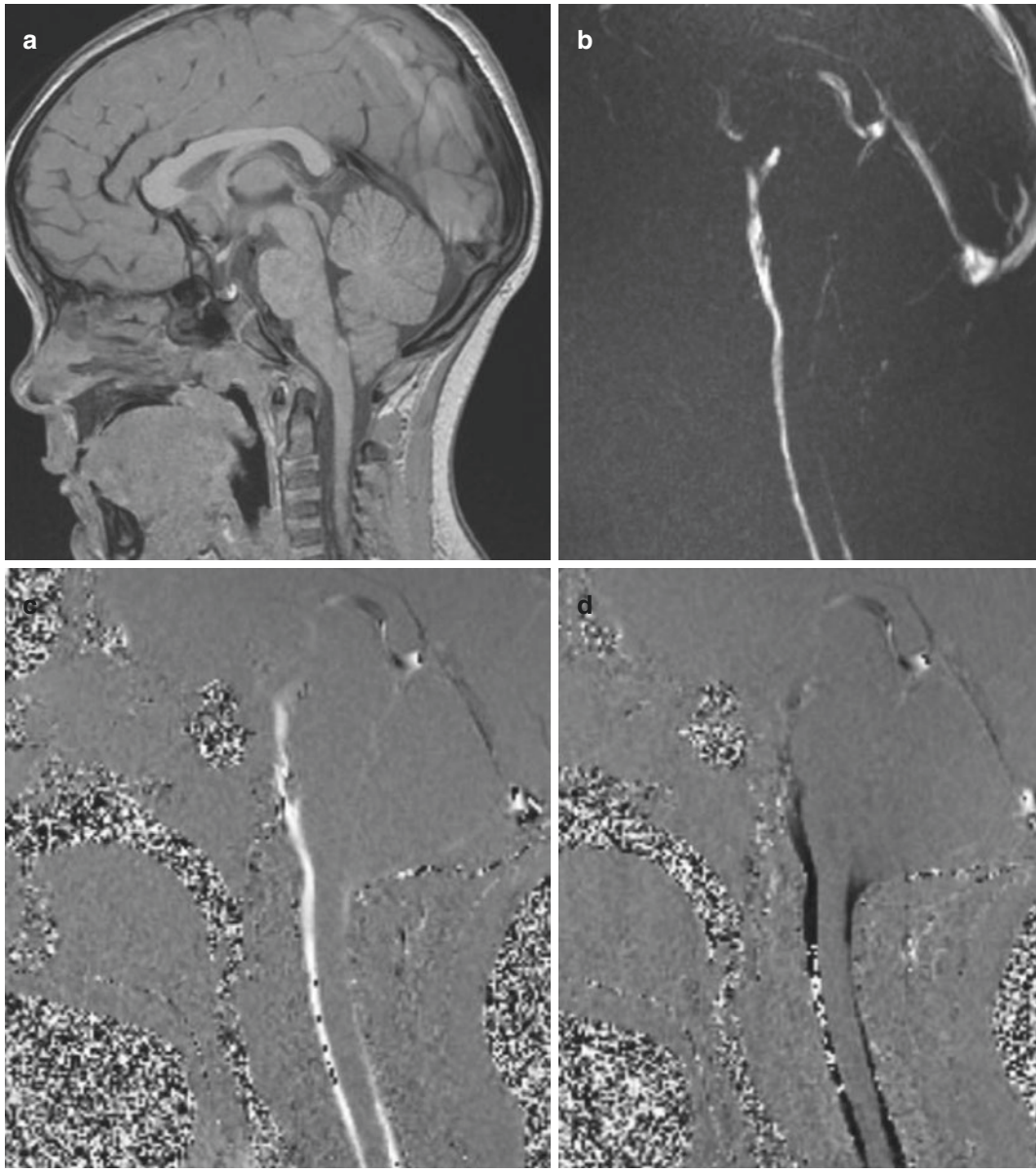

Fig. 28.3 Chiari I deformity patient with mildly abnormal flow study. (**a**) Sagittal T1 view of the brain showing Chiari I deformity with peg-like shape of the tonsils and approximately 7 mm cerebellar tonsillar ectopia. (**b**) Sagittal second phase-contrast image with a velocity encoding (VENC) of 10 showing normal flow anteriorly at the foramen magnum with mildly decreased, but present, flow posteriorly at the foramen magnum. (**c**, **d**) Midsagittal image from cine phase-contrast study with a VENC of 10 showing normal flow at the foramen magnum anteriorly with decreased but present flow posteriorly (Supplement Video 28.3 demonstrates flow in this patient through the cardiac cycle)

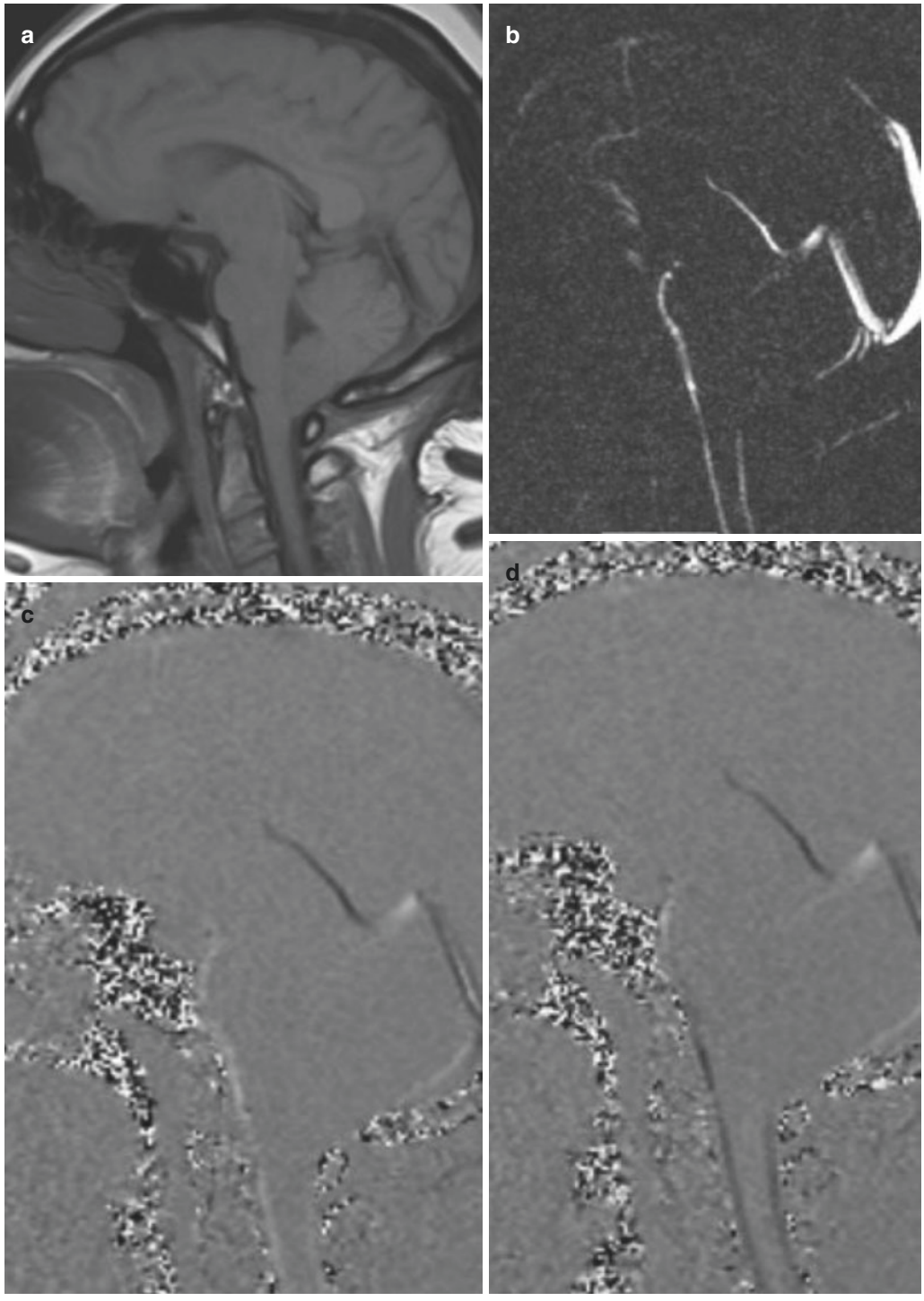

Fig. 28.4 Chiari I deformity patient with absent flow posteriorly. (**a**) Sagittal T1 view of the brain showing Chiari I deformity with peg-like shape of the tonsils and approximately 8 mm cerebellar tonsillar ectopia. (**b**) Sagittal second phase-contrast image with a velocity encoding (VENC) of 10 showing normal flow anteriorly at the foramen magnum with absent flow posteriorly at the foramen magnum. (**c**, **d**) Midsagittal image from cine phase-contrast study with a VENC of 10 showing normal bidirectional flow at the foramen magnum anteriorly with absent flow posteriorly (Supplement Video 28.4 demonstrates flow in this patient through the cardiac cycle)

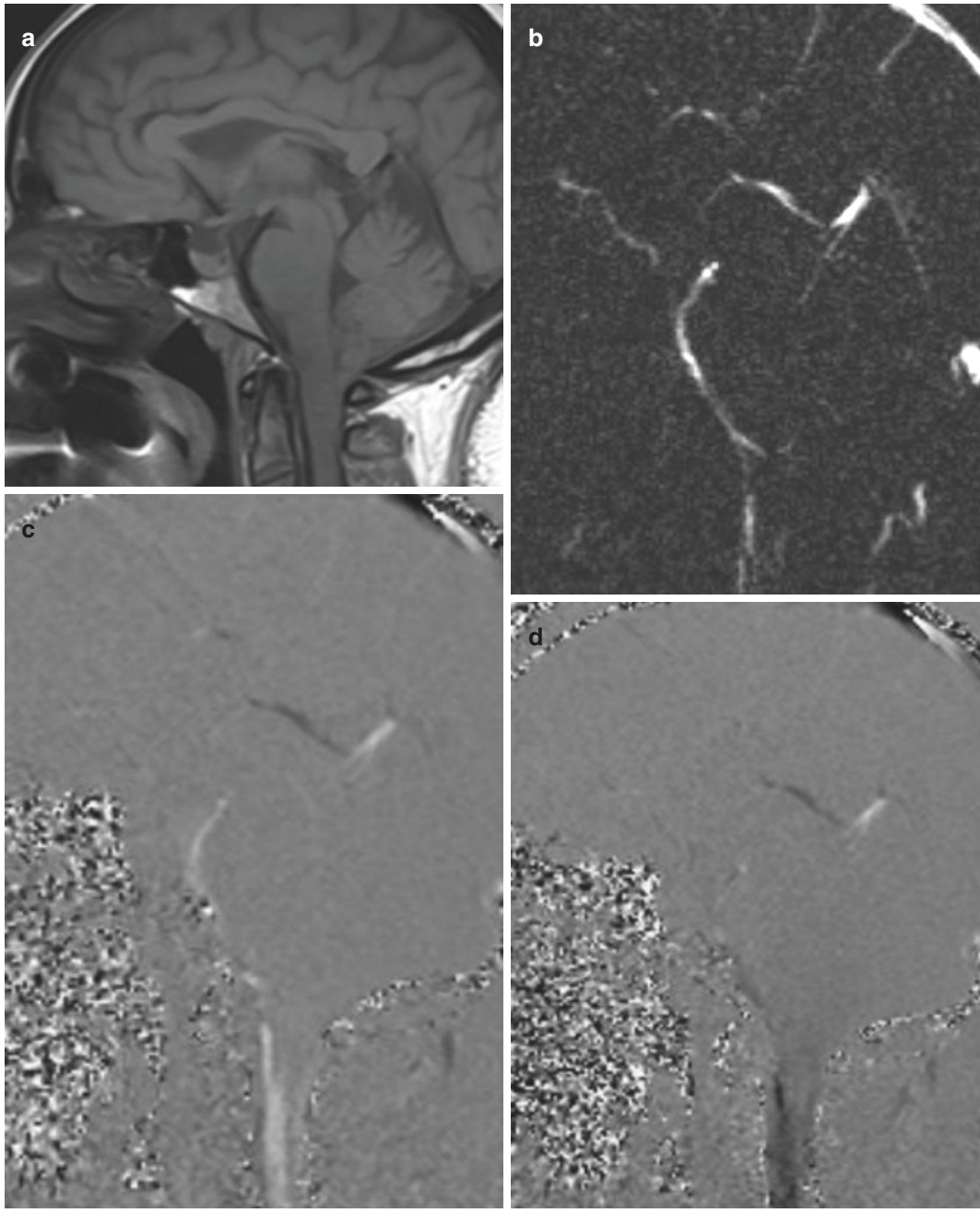

Fig. 28.5 Chiari I deformity patient with decreased flow anteriorly and absent flow posteriorly. (**a**) Sagittal T1 view of the brain showing Chiari I deformity with peg-like shape of the tonsils and approximately 11 mm cerebellar tonsillar ectopia. (**b**) Sagittal second phase-contrast image with a velocity encoding (VENC) of 10 showing decreased flow anteriorly at the foramen magnum with absent flow posteriorly at the foramen magnum. (**c**, **d**) Midsagittal image from cine phase-contrast study with a VENC of 10 showing decreased bidirectional flow at the foramen magnum anteriorly with absent flow posteriorly (Supplement Video 28.5 demonstrates flow in this patient through the cardiac cycle)

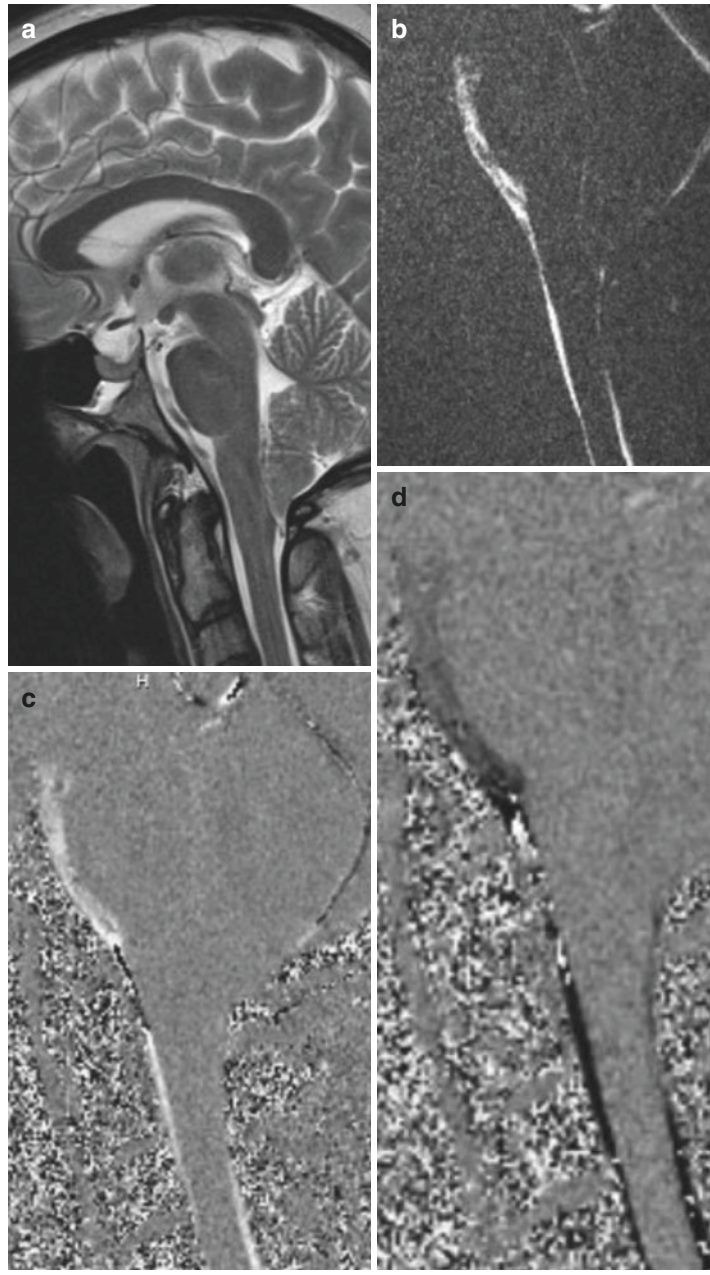

Fig. 28.6 Chiari I deformity patient with absent flow posteriorly and complex flow anteriorly. (**a**) Sagittal T2 view of the brain showing Chiari I deformity with peg-like shape of the tonsils and approximately 10 mm cerebellar tonsillar ectopia. (**b**) Sagittal second phase-contrast image with a velocity encoding (VENC) of 5 (VENC 10 not shown but demonstrates similar appearance) showing normal flow anteriorly at the foramen magnum with absent flow posteriorly at the foramen magnum, failing to show the complex flow anteriorly in this patient. (**c**, **d**) Midsagittal image from cine phase-contrast study with a VENC of 5 showing aliasing at the foramen magnum anteriorly with absent flow posteriorly. The aliasing could be related to elevated peak velocities anteriorly (a common finding in Chiari I deformity patients) or complex simultaneous cranial and caudal flow (see text for details). (**e**, **f**) Midsagittal image from cine phase-contrast study with a VENC of 10 showing near complete resolution of the aliasing anteriorly suggesting that the majority of the aliasing was secondary to elevated peak velocities. Small residual aliasing is noted and could relate to either elevated peak velocities or complex simultaneous cranial and caudal flow. Note persistent absent flow posteriorly (Supplement Video 28.6 demonstrates flow in this patient through the cardiac cycle at both VENC of 5 and 10)

Fig. 28.6 (continued)

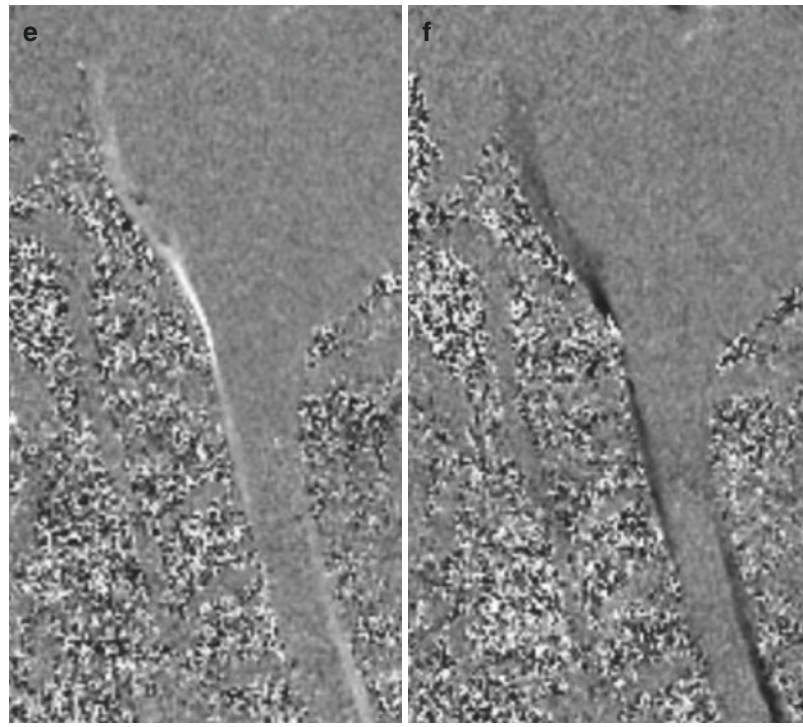

Tonsillar Motion Imaging

Standard MRI sequences can reliably detect the location of the tonsils in CM I. However, such sequences cannot assess real-time motion of the tonsils and such motion correlation with symptoms or contribution to the disease pathophysiology. The utilization of cardiac-gated balanced steady-state MR sequences (at our institution cardiac-gated cine true fast imaging with steady-state precession [true FISP]), initially developed for cardiac imaging, has allowed for identification of pulsatile motion of brain structures throughout the cardiac cycle and for visualization of the cerebellar tonsils throughout the cardiac cycle [59, 60].

Normally, there is slight movement of the brain and spinal cord throughout the cardiac cycle. Initially, there is minimal anteroposterior and caudal displacement of the brain, including the tonsils and brain stem, followed by the spinal cord in systole, which in turn is followed by cephalad motion to previous position throughout the remaining cardiac cycle [26, 59–62].

Increased pulsatile craniocaudal and anteroposterior displacement of the cerebellar tonsils and upper spinal cord has been documented in patients with CM I [47, 63–66] (Video 28.9). This finding is detected on both visual assessment and quantitative assessment [59, 64, 67–69]. Furthermore, the velocity of tonsillar motion was noted to be ten times greater in CM I patients [47]. The increased pulsatility of tonsils in CM I patients has been attributed to CM I-specific symptoms, in particular cough-strain headaches [47, 66, 70]. The association between the degree of cerebellar tonsillar pulsatility and syringomyelia is unclear with conflicting data. A study of 11 patients reports a greater degree of cerebellar tonsillar motion in patients with syringomyelia compared to those without (22% greater tonsillar motion in patients with syringomyelia) [59]. Another study showed increased tonsillar pulsatility in CM I patients when compared to controls, but no significant difference in the degree of pulsatility in CM I patients with and without syrinx [66].

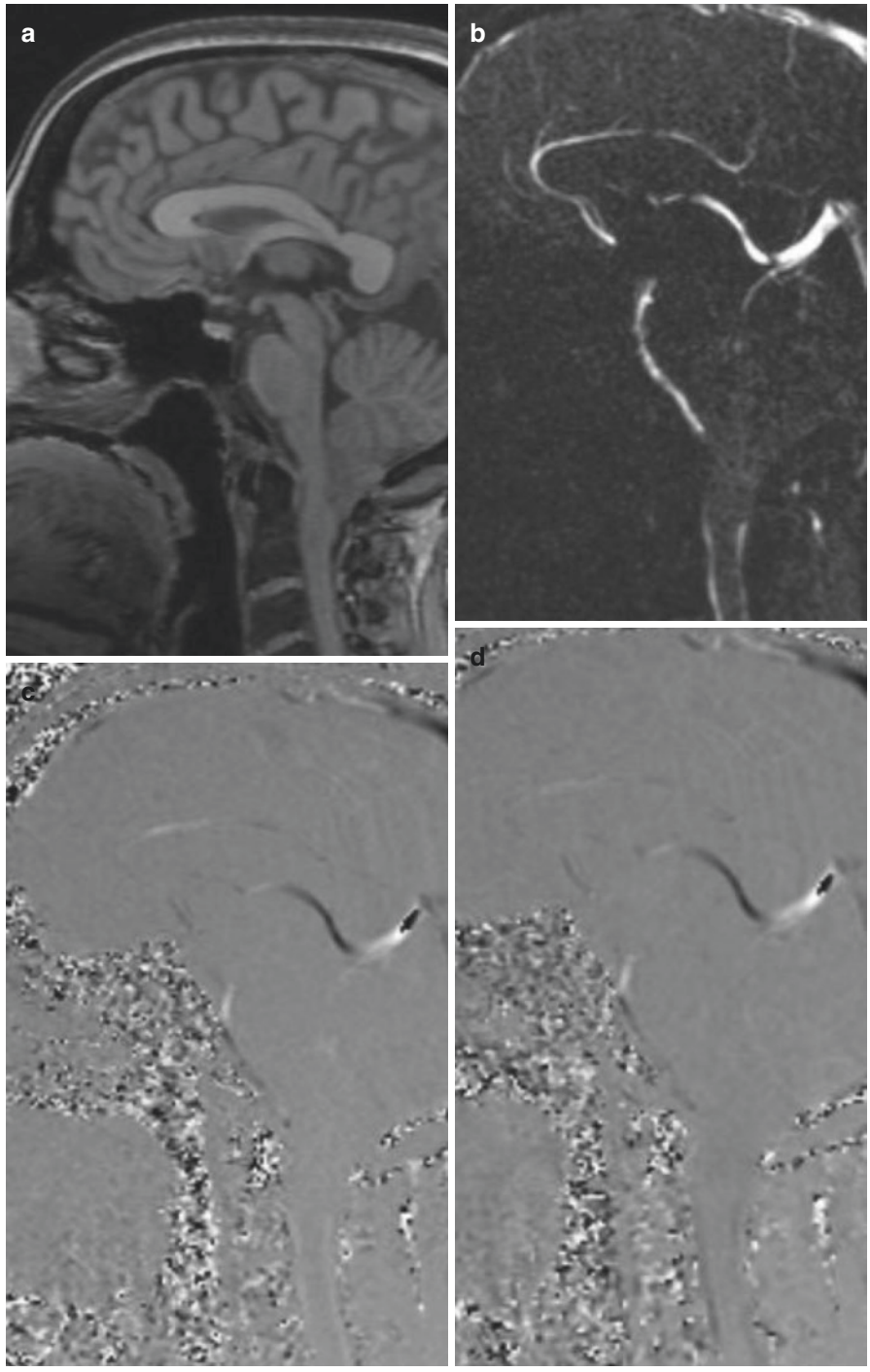

Fig. 28.7 Chiari I deformity patient with absent flow anteriorly and posteriorly. (**a**) Sagittal T1 view of the brain showing Chiari I deformity with peg-like shape of the tonsils and approximately 14 mm cerebellar tonsillar ectopia. (**b**) Sagittal second phase-contrast image with a velocity encoding (VENC) of 10 showing absent flow anteriorly and posteriorly at the foramen magnum. (**c**, **d**) Midsagittal image from cine phase-contrast study with a VENC of 10 showing absent bidirectional flow at the foramen anteriorly and posteriorly (Supplement Video 28.7 demonstrates flow in this patient through the cardiac cycle)

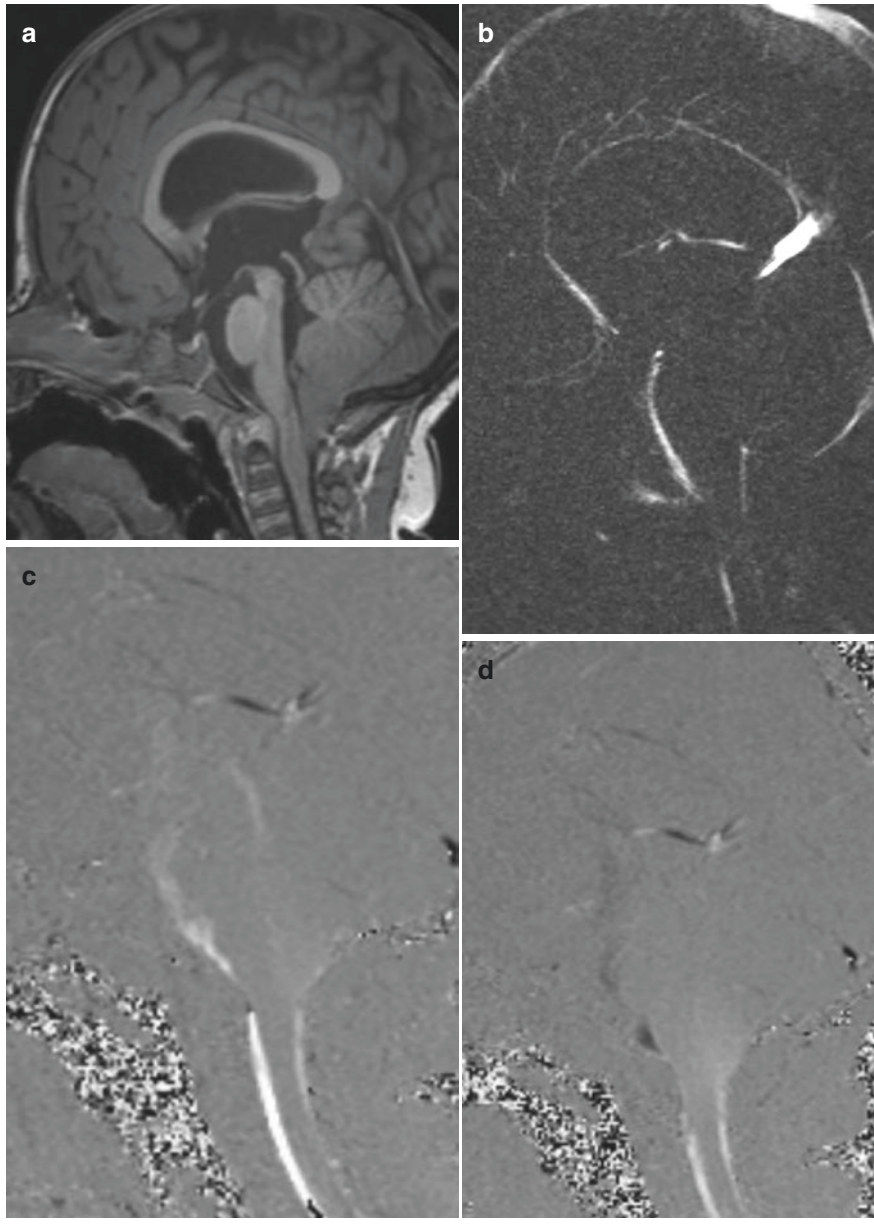

Fig. 28.8 Cerebellar tonsillar pulsatility in a patient with Chiari I deformity resulting in transient flow obstruction at the foramen magnum. (**a**) Sagittal T1 view of the brain showing Chiari I deformity with peg-like shape of the tonsils and approximately 13 mm cerebellar tonsillar ectopia. (**b**) Sagittal second phase-contrast image with a velocity encoding (VENC) of 10 showing absent flow anteriorly and posteriorly at the foramen magnum secondary to tonsillar pulsatility. (**c**–**f**) Midsagittal image from different cine phase-contrast study with a VENC of 10 at different points of the cardiac cycle showing abnormal bidirectional flow at the foramen anteriorly and posteriorly (**c**, **e**) with transient obstruction secondary to significant tonsillar pulsatility (**d**, **f**). (**g**) Sagittal T2 view showing changes of postoperative decompression. (**h**) Sagittal second phase-contrast image with a VENC of 10 showing marked improved flow anteriorly and posteriorly at the foramen magnum. (**i**, **j**) (Supplement Video 28.8 demonstrates flow in this patient through the cardiac cycle.) Midsagittal image from cine phase-contrast study with a VENC of 10 showing marked improvement of flow at the foramen magnum anteriorly and posteriorly (Supplement Video 28.8 detailed these findings in pre- and postoperative setting with pre- and postoperative true-FISP videos demonstrating the degree of tonsillar pulsatility)

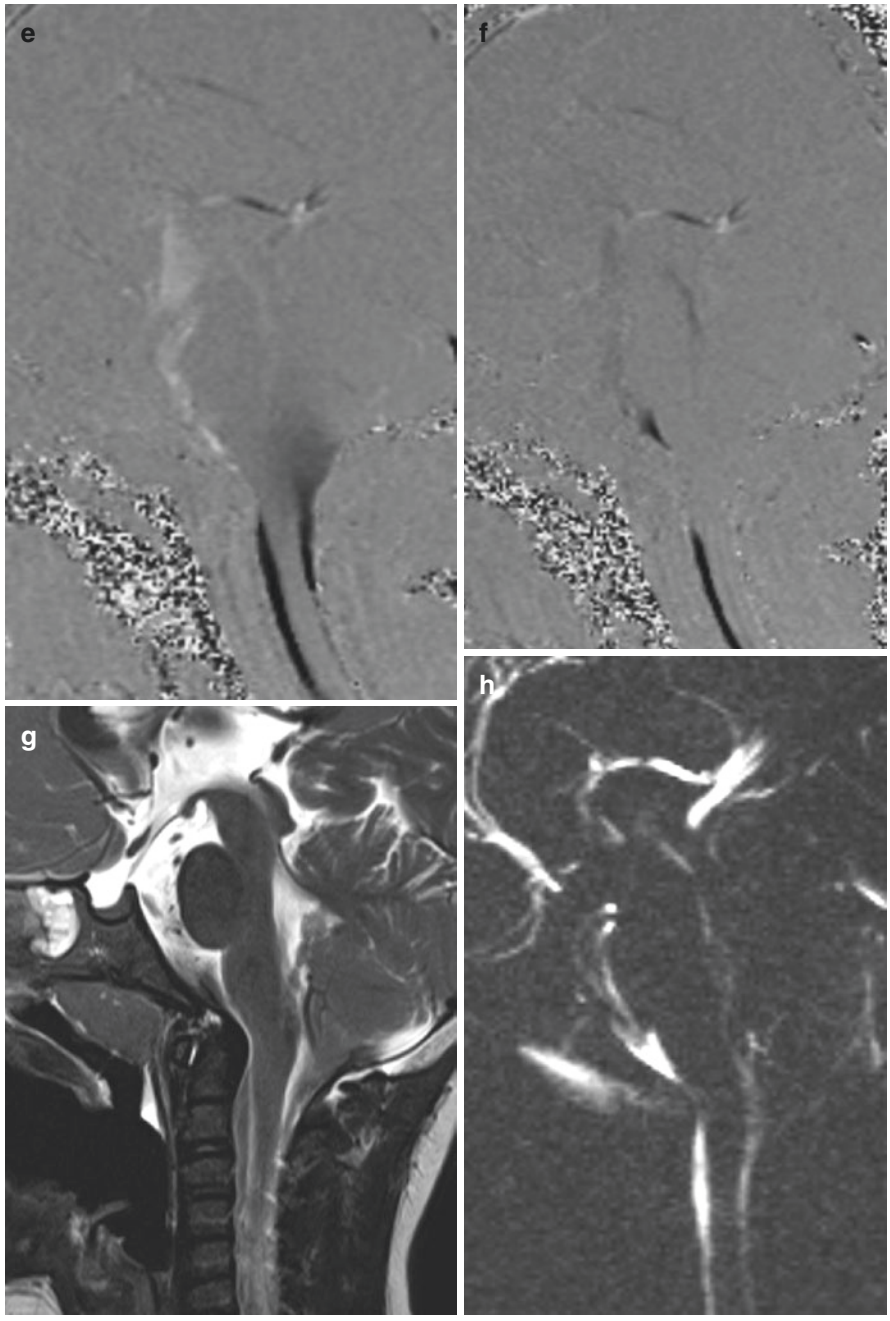

Fig. 28.8 (continued)

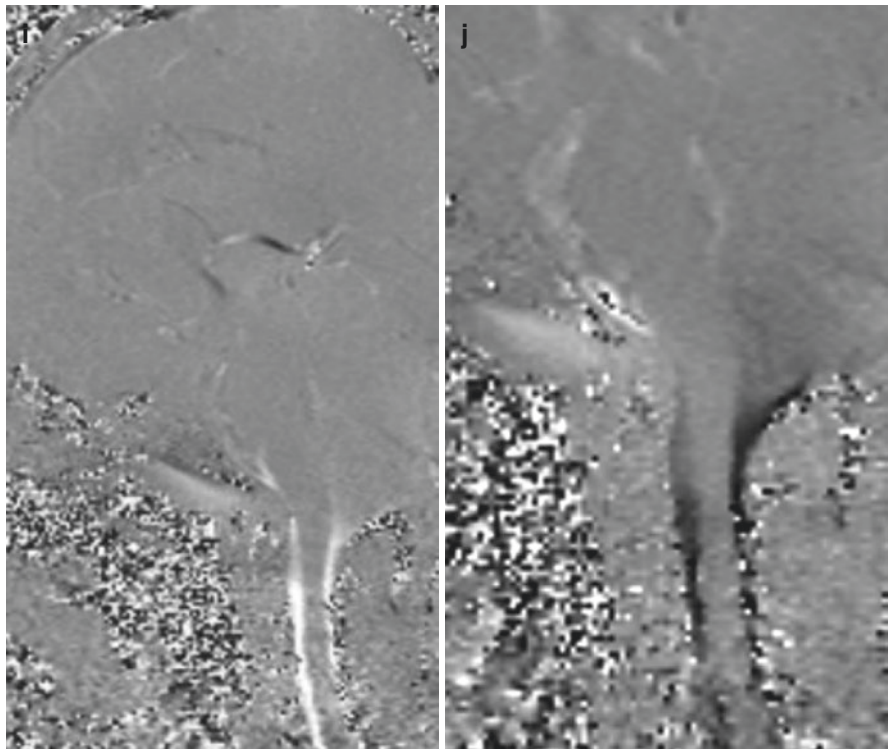

Fig. 28.8 (continued)

Diffusion Tensor Imaging

Diffusion tensor imaging (DTI) has been extensively studied in other neurological disorders such as multiple sclerosis, Alzheimer's, neuropsychiatric disorders, trauma, and neurodevelopmental disorders [71–79]; however, it has only been recently utilized in the assessment of CM I. DTI assesses microstructural tissue properties and has been widely utilized for understanding white matter integrity. DTI has the advantage of detecting pathological white matter changes early in the disease process, before structural MRI changes are apparent. Furthermore, white matter changes can be quantitatively assessed with DTI through fractional anisotropy (FA) and mean diffusivity (MD) [71–79].

The preliminary application of DTI in CM I patients has been promising with studies demonstrating abnormalities in the brain and spinal cord, in the case of an associated syrinx. Kumar et al. detected reduced FA values and increased MD values in the corpus callosum, fornix, and cingulum [80] in patients with CM I compared to age-matched control groups. Additional DTI studies suggest changes in the middle cerebellar peduncle through differences in axial diffusivity between symptomatic and asymptomatic pediatric patients with CM I in addition to patients with or without a syrinx [81]. Furthermore, Abeshaus

et al. showed normalization of FA in the middle cerebellar peduncles after surgery [82].

DTI is a promising quantitative tool in further investigating the relationship of syringomyelia and CM I. DTI has already demonstrated correlation between FA values and somatosensory symptoms in patients with syringomyelia in general [83]. More recently, Yan et al. showed decreased FA value of the spinal cord at the level of the syringomyelia in patients with CM I when compared to controls [84]. Changes in FA values were also noted to significantly relate to the syrinx size and appearance of neurological signs/symptoms.

Posterior Fossa Morphometry/ Volumetry

A common finding in CM I is a small overcrowded posterior fossa [85–88]. A low tonsil position has been hypothesized to be partially explained by the discrepancy in the size of the small container (posterior cranial fossa) and content (hindbrain tissue) [88]. Multiple linear measurements, including basal angle, clival line, supraoccipital line, dense inclination, and Twining's line, have been shown to be abnormal in CM I patients [89–93] but fail to predict symptoms in these patients [94]. These measurements have been used in multiple studies to estimate the volume of the posterior cranial fossa; however, they have been shown to be poor predictors of actual volume [95, 96]. Recent advancement in imaging analysis software has allowed a more accurate measurement of the posterior cranial fossa [95–97]. Advancement in applications of artificial intelligence may further simplify and enhance the ability to accurately measure the posterior fossa volume and potentially clarify the interplay between the small posterior fossa volume and CM I pathogenesis.

Prediction and Assessment of Postoperative Outcome

The aforementioned advanced imaging techniques not only expand our understanding of the pathophysiology of CM I but are emerging as tools for prediction and assessment of postoperative outcome. In the preoperative setting, such imaging may aid in selecting patients who are more likely to respond favorably to surgery. In the postoperative setting, advanced imaging can assess the response of specific parameters, such as CSF flow or tonsillar motion, to surgical intervention when compared to preoperative imaging.

Outcomes after posterior fossa decompression for CM I are dependent on multiple factors such as patient selection, surgical technique, presenting symptoms, associated craniocervical junction pathology, syrinx, and postoperative course/complications [11]. Therefore, it is not uncommon for some patients to have persistent symptoms after surgery. CSF flow imaging can serve as an aid to select patients who are more likely to respond to surgical treatment, as one of the main goals of surgical intervention is to establish adequate CSF flow at the level of the foramen magnum. Preoperative CSF flow studies, as discussed earlier, can confidently establish flow or lack of flow at the foramen magnum and thus indicate patients who are more likely to benefit from decompressive surgery [92]. McGirt et al. demonstrated that abnormal CSF flow on flow studies on preoperative scans was associated with improved response to hindbrain decompression, while patients with normal CSF were up to 4.8 times more likely to experience postsurgical symptomatic recurrence [98]. This is especially true in patients with combined preoperative ventral and dorsal CSF flow abnormalities with up to 2.6-fold reduction in the risk of postoperative symptom recurrence. Postoperative CSF flow studies can assess for reestablished CSF flow at the foramen magnum.

The change in tonsillar pulsatility, assessed on cardiac-gated true-FISP MRI, can also be assessed on postoperative imaging. As discussed previously, tonsillar pulsatility is markedly increased in Chiari I patients with specific symptoms attributed to it [47, 66, 70]. Quantitative and qualitative assessment of tonsillar pulsatility after decompressive surgery has documented a decrease in tonsillar motion in comparison with preoperative imaging [32, 66]. However, despite the significant decrease in tonsillar motion, it does not achieve the very low pulsatility seen

in controls [66]. This finding on postoperative imaging is nonetheless encouraging and could potentially serve as a marker for surgical success, but prospective studies are needed to establish its predictive capacity for surgical success.

Assessment of CM I operative outcome by DTI is still primarily a research tool. The few DTI studies assessing the white matter tracks post-decompressive surgery are promising. Abeshaus et al. showed increased FA values within the middle cerebellar peduncles postoperatively [77]. Krishna et al. showed that the FA values were significantly higher in the anterior brainstem in patients with CM I and that the FA values normalize after decompressive surgery [99]. Both of these studies suggest that DTI can play a promising role in the assessment of decompressive surgery on the brain microstructural integrity. However, further research is needed in this field to fully understand the clinical significance of such findings.

Posterior fossa morphometry and volumetry have consistently shown a decrease in the volume of the posterior fossa in patients with CM I [87, 95, 97]. Postoperative assessment of the posterior fossa volumes has documented an increase in the posterior fossa volume, a finding that has been associated with greater likelihood of symptomatic relief with improvement in headaches, tonsillar descent, syringomyelia, and cervicomedullary kinking [97]. In a case series of 11 symptomatic CM I patients, Noudel et al. showed that postoperative posterior fossa volume increase in all 11 patients was associated with symptomatic recovery in patients with posterior fossa volume increases of 15%. Partial symptomatic recovery was noted in patients with posterior fossa volume increases of 7% [100]. Both studies not only highlight the role of MR volumetry in pre- and postoperative setting but also suggest that in the preoperative setting, it can help individualize the surgical approach and craniotomy size [100].

Conclusion

CM I is a common disease in the pediatric and adult populations. Despite it being first described in the 1890s, many aspects of this heterogeneous disease have only been recently understood or are still in need of further analysis. Advanced MR imaging has played an integral role in understanding the disease's pathophysiology and postoperative assessment. CSF flow and tonsillar pulsatility imaging are now routinely used across imaging centers to help identify symptomatic patients and predict decompressive surgery response. Other emerging techniques such as DTI and posterior fossa volumetry have been validated in research studies to complement existing tools in assessing Chiari type I patients and show promise as useful imaging techniques to predict symptoms and response to surgical treatment.

References

1. Chiari H. Über Veränderungen des Kleinhirns, des Pons und der Medulla oblongata infolge von congenitaler Hydrocephalie des Grosshirns. Denkschr der Kais Akad Wiss Wien mathnaturw 1896;63:71–116. (partially translated in Tubbs et al. (2016) Child Nerv Syst 32:1175–9).
2. Chiari H. Uber Veranderungen des Kleinhirns infolge von Hydrocephalie des Grosshirns. Dtsch med Wochenschr. 1891;17:1172–5 (translated by MARadkowski (1987) Pediatr Neurosci 13:3–8).
3. Drue LS, Percy AK, Cheek WR, Laurent JP. Chiari type I malformation in children. J Pediatr. 1989;115:573–6.
4. Wu YW, Chin CT, Chan KM, Barkovich AJ, Ferriero DM. Pediatric Chiari I malformations: do clinical and radiologic features correlate? Neurology. 1999;53:1271–6.
5. Schwedt TJ, Guo Y, Rothner AD. "Benign" imaging abnormalities in children and adolescents with headache. Headache. 2006;46:387–98.
6. Barkovich A, Wippold FJ, Sherman JL, Citrin CM. Significance of cerebellar tonsillar position on MR. AJNR Am J Neuroradiol. 1986;7(5):795–9.
7. Ishikawa M, Kikuchi H, Fujisawa I, Yonekawa Y. Tonsillar herniation on magnetic resonance imaging. Neurosurgery. 1988;22(1):77–81.
8. Spinos E, Laster DW, Moody DM, Ball MR, Witcofski RL, Kelly DL Jr. MR evaluation of Chiari I malformations at 0.15 T. AJNR Am J Neuroradiol. 1985;6(2):203–8.
9. Aitken LA, Lindan CE, Sidney S, Gupta N, Barkovich AJ, Sorel M, et al. Chiari type I malformation in a pediatric population. Pediatr Neurol. 2009;40(6):449–54.
10. Strahle J, Muraszko KM, Kapurch J, Bapuraj JR, Garton HJ, Maher CO. Chiari malformation type I and syrinx in children undergoing magnetic resonance imaging. J Neurosurg Pediatr. 2011;8(2):205–13.

11. Poretti A, Ashmawy R, Garzon-Muvdi T, Jallo GI, Huisman TA, Raybaud C. Chiari I deformity in children: Pathogenetic, clinical, neuroimaging, and management aspects. Neuropediatrics. 2016;47: 293–307.
12. Raybaud C, Jallo GI. Chiari I deformity in children: etiopathogenesis and radiological diagnosis. In: Manto M, Husiman TAGM, editors. Handbook of clinical neurology, vol 155. Elsevier. 2018. p. 24–48.
13. Castillo M, Wilson JD. Spontaneous resolution of a Chiari I malformation: MR demonstration. AJNR Am J Neuroradiol. 1995;16:1158–60.
14. Novegno F, Caldarelli M, Massa A, Chieffo D, Massimi L, Pettorinin B, et al. The natural history of the Chiari type 1 anomaly. J Neurosurg Pediatr. 2008;2:179–87.
15. Huang PH, Constantini S. "Acquired" Chiari I malformation case report. J Neurosurg. 1994;80:1099–102.
16. Leon TJ, Kuhn EN, Arynchyna AA, Smith PB, Tubbs RS, Johnston JM, et al. Patients with "benign" Chiari I malformations require surgical decompression at a low rate. J Neurosurg Pediatr. 2019;23(4):498–506.
17. Strahle J, Muraszko KM, Kapurch J, Bapuraj JR, Garton HJ, Maher CO. Natural history of Chiari malformation type I following decision for conservative treatment. J Neurosurg Pediatr. 2011;8(2):214–21.
18. Caldarelli M, Di Rocco C. Diagnosis of Chiari I malformation and related syringomyelia: radiological and neurophysiological studies. Childs Nerv Syst. 2004;20(5):332–5.
19. Chiapparini L, Saletti V, Solero CL, Bruzzone MG, Valentini LG. Neuroradiological diagnosis of Chiari malformations. Neurol Sci. 2011;32(3):283–6.
20. Elster AD, Chen M. Chiari I malformations: clinical and radiologic reappraisal. Radiology. 1992;183(2):347–53.
21. Hekman KE, Aliaga L, Straus D, Luther A, Chen J, Sampat A, et al. Positive and negative predictors for good outcome after decompressive surgery for Chiari malformation type 1 as scored on the Chicago Chiari outcome scale. Neurol Res. 2012;34(7):694–700.
22. Godzik J, Kelly MP, Radmanesh A, Kim D, Holekamp TF, Smyth MD, et al. Relationship of syrinx size and tonsillar descent to spinal deformity in Chiari malformation type I with associated syringomyelia. J Neurosurg Pediatr. 2014;13(4):368–74.
23. Yarbrough CK, Greenberg JK, Smyth MD, Leonard JR, Park TS, Limbrick DD Jr. External validation of the Chicago Chiari outcome scale. J Neurosurg Pediatr. 2014;13(6):679–84.
24. Singhal A, Cheong A, Steinbok P. International survey on the management of Chiari 1 malformation and syringomyelia: evolving worldwide opinions. Childs Nerv Syst. 2018;34:1177–82.
25. Schijman E, Steinbok P. International survey on the management of Chiari I malformation and syringomyelia. Childs Nerv Syst. 2004;20(5):341–8.
26. Fakhri A, Shah MN, Goyal MS. Advanced imaging of Chiari 1 malformations. Neurosurg Clin N Am. 2015;26:519–26.
27. Aboulezz AO, Sartor K, Geyer CA, Gado MH. Position of cerebellar tonsils in the normal population and in patients with Chiari malformation: a quantitative approach with MR imaging. J Comput Assist Tomogr. 1985;9(6):1033–6.
28. Smith BW, Strahle J, Bapuraj JR, Muraszko KM, Garton HJL, Maher CO. Distribution of cerebellar tonsil position: implications for understanding Chiari malformation. J Neurosurg. 2013;119(3): 812–9.
29. Tubbs RS, Beckman J, Naftel RP, Chern JJ, Wellons JC 3rd, Rozzelle CJ, et al. Institutional experience with 500 cases of surgically treated pediatric Chiari malformation type I. J Neurosurg Pediatr. 2011;7(3):248–56.
30. Tubbs RS, Lyerly MJ, Loukas M, Shoja MM, Oakes WJ. The pediatric Chiari I malformation: a review. Childs Nerv Syst. 2007;23(11):1239–50.
31. Milhorat TH, Chou MW, Trinidad EM, Kula RW, Mandell M, Wolpert C, et al. Chiari I malformation redefined: clinical and radiographic findings for 364 symptomatic patients. Neurosurgery. 1999;44(5):1005–17.
32. Radmanesh A, Greenberg JK, Chatterjee A, Smyth M, Limbrick DD, Sharma A. Tonsillar pulsatility before and after surgical decompression for children with Chiari malformation type 1: an application for true fast imaging with steady state precession. Neuroradiology. 2015;57(4):387–93.
33. Strahle J, Muraszko KM, Garton HJL, Smith BW, Starr J, Kapurch JR, et al. Syrinx location and size according to etiology: identification of Chiari-associated syrinx. J Neurosurg Pediatr. 2015;16(1):1–9.
34. Kelly MP, Guillaume T, Lenke LG. Spinal deformity associated with Chiari malformation. Neurosurg Clin N Am. 2015;26(4):579–85.
35. McGirt MJ, Nimjee SM, Floyd J, Bulsara KR, George TM. Correlation of cerebrospinal fluid flow dynamics and headache in Chiari I malformation. Neurosurgery. 2005;56(4):716–21.
36. Hofkes SK, Iskandar BJ, Turski PA, Gentry LR, McCue JB, Haughton VM. Differentiation between Symptomatic Chiari I Malformation and Asymptomatic Tonsilar Ectopia by Using Cerebrospinal Fluid Flow Imaging: Initial Estimate of Imaging Accuracy. Radiology. 2007;245(2): 532–40.
37. Haughton V, Mardal KA. Spinal fluid biomechanics and imaging: an update for neuroradiologists. AJNR Am J Neuroradiol. 2014;35(10):1864–9.
38. Quigley MF, Iskandar B, Quigley ME, Nicosia M, Haughton V. Cerebrospinal fluid flow in foramen magnum: temporal and spatial patterns at MR imaging in volunteers and in patients with Chiari I malformation. Radiology. 2004;232(1):229–36.
39. Haughton VM, Korosec FR, Medow JE, Dolar MT, Iskandar BJ. Peak systolic and diastolic CSF velocity in the foramen magnum in adult patients with Chiari I malformations and in normal control participants. AJNR Am J Neuroradiol. 2003;24:169–76.

40. Buell TJ, Heiss JD, Oldfield EH. Pathogenesis and cerebrospinal fluid hydrodynamics of the Chiari I malformation. Neurosurg Clin N Am. 2015;26:495–9.
41. Hofkes S, Iskandar BJ, Turski PA, Gentry LR, McCue JB, Haughton VM. Differentiation between symptomatic Chiari I malformation and asymptomatic tonsillar ectopia by using cerebrospinal fluid imaging: initial estimate of the imaging accuracy. Radiology 2007;45:532–540.
42. Pinna G, Alessandrini F, Alfieri A, Rossi M, Bricolo A. Cerebrospinal fluid dynamic study in Chiari I malformation: implications for syrinx formation. Neurosurg Focus. 2003;8:E3.
43. Hiess JD, Patronas N, DeVroom HL, Shawker T, Ennis R, Kammerer W, et al. Elucidating the pathophysiology of syringomyelia. J Neurosurg. 1999;91(4):553–63.
44. Oldfield EH, Muraszko K, Shawker TH, Patronas NJ. Pathophysiology of syringomyelia associated with Chiari I malformation of the cerebellar tonsils. Implications for diagnosis and treatment. J Neurosurg. 1994;80(1):3–15.
45. Bhadelia RA, Bogdan AR, Wolpert SM. Cerebrospinal fluid flow waveforms: analysis in patients with Chiari I malformation by means of gated phase-contrast MR imaging velocity measurements. Radiology. 1995;196:195–202.
46. Enzmann DR, Pelc NJ. Normal flow patterns of intracranial and spinal cerebrospinal fluid defined with phase-contrast cine MR imaging. Radiology. 1991;178(2):467–74.
47. Wolpert SM, Bhadelia RA, Bogdan AR, Cohen AR. Chiari I malformations: assessment with phase-contrast velocity MR. AJNR Am J Neuroradiol. 1994;15(7):1299–308.
48. Battal B, Kocaoglu M, Bulakbasi N, Husmen G, Tuba SH, Tayfun C. Cerebrospinal fluid flow imaging by using phase-contrast MR technique. Turk Neurosurg. 2014;84(1004):758–65.
49. Hofmann E, Warmuth-Metz M, Bendszus M, Solymosi L. Phase-contrast MR imaging of the cervical CSF and spinal cord: volumetric motion analysis in patients with Chiari I malformation. AJNR Am J Neuroradiol. 2000;21(1):151–8.
50. Mauer UM, Gottschalk A, Mueller C, Weselek L, Kunz U, Schulz C. Standard and cardiac-gated phase-contrast magnetic resonance imaging in the clinical course of patients with Chiari malformation type I. Neurosurg Focus. 2011;31(3):E5.
51. Connor SE, O'Gorman R, Summers P, Simmons A, Moore EM, Chandler C, Jarosz JM. SPAMM, cine phase contrast imaging and fast spin-echo T2-weighted imaging in the study of intracranial cerebrospinal fluid (CSF) flow. Clin Radiol. 2001;56(9):763–72.
52. Nitz WR, Bradley WG Jr, Watanabe AS, Lee RR, Burgoyne B, O'Sullivan RM, Herbst MD. Flow dynamics of cerebrospinal fluid: assessment with phase-contrast velocity MR imaging performed with retrospective cardiac gating. Radiology. 1992;183(2):395–405.
53. Saloner D. The AAPM/RSNA physics tutorial for residents. An introduction to MR angiography. Radiographics. 1995;15(2):453–65.
54. Quigley MF, Iskander B, Quigley MA, Nicosia M, Haughton V. Cerebrospinal fluid flow in the foramen magnum: temporal and spatial patterns at MR imaging in volunteers and in patients with Chiari I malformation. Radiology. 2004;232:229–36.
55. Brugieres P, Idy-Peretti I, Iffenecker C, Parker F, Odile J, Hurth M, et al. CSF flow measurement in syringomyelia. AJNR Am J Neuroradiol. 2000;21:1785–92.
56. Armonda RA, Citrin CM, Foley KT, Ellenbogen RG. Quantitative cinemode magnetic resonance imaging of Chiari I malformations: an analysis of cerebrospinal fluid dynamics. Neurosurgery. 1994;35:214–24.
57. Bhadelia RA, Bogdan AR, Wolpert SM, Lev S, Appignani BA, Heilman CB. Cerebrospinal fluid flow waveforms: analysis in patients with Chiari I malformation by means of gated phase-contrast MR imaging velocity measurements. Radiology. 1995;196:195–202.
58. Alperin NJ, Lee SH, Loth F, Raksin PB, Lichtor T. MR-intracranial pressure (ICP): a method to measure intracranial elastance and pressure noninvasively by means of MR imaging—baboon and human study. Radiology. 2000;217:877–85.
59. Cousins J, Haughton V. Motion of the cerebellar tonsils in the foramen magnum during the cardiac cycle. AJNR Am J Neuroradiol. 2009;30(8):1587–8.
60. Hentschel S, Mardal KA, Lovgren AE, Linge S, Haughton V. Characterization of cyclic CSF flow in the foramen magnum and upper cervical spinal canal with MR flow imaging and computational fluid dynamics. AJNR Am J Neuroradiol. 2010;31(6):997–1002.
61. Maier SE, Hardy CJ, Jolesz FA. Brain and cerebrospinal fluid motion: real-time quantification with M-mode MR imaging. Radiology. 1994;193:477–83.
62. Poncelet BP, Wedeen VJ, Weisskoff RM, Cohen MS. Brain parenchyma motion: measurement with cine echo-planar MR imaging. Radiology. 1992;185:645–51.
63. Ventureyra EC, Aziz HA, Vassilyadi M. The role of cine flow MRI in children with Chiari I malformation. Childs Nerv Syst. 2003;19(2):109–13.
64. Pujol J, Roig C, Capdevila A, Pou A, Marti-Vilalta JL, Kulisevsky J, et al. Motion of the cerebellar tonsils in Chiari type I malformation studied by cine phase-contrast MRI. Neurology. 1995;45(9):1746–53.
65. Terae S, Miyasaka K, Abe S, Abe H, Tashiro K. Increased pulsatile movement of the hindbrain in syringomyelia associated with the Chiari malformation: cine-MRI with presaturation bolus tracking. Neuroradiology. 1994;36:125–9.
66. Leung V, Magnussen JS, Stoodley M, Bilston LE. Cerebellar and hindbrain motion in Chiari malformation with and without syringomyelia. J Neurosurg Spine. 2016;24:546–55.
67. Sharma A, Parsons MS, Pilgram TK. Balanced steady-state free-precession MR imaging for measur-

ing pulsatile motion of the cerebellar tonsils during the cardiac cycle: a reliability study. Neuroradiology. 2012;54(2):133–8.
68. Radmanesh A, Greenberg JK, Chatterjee A, Smyth MD, Limbrick DD, Sharma A. Tonsillar pulsatility before and after surgical decompression for children with Chiari malformation type 1: an application for true fast imaging with steady state precession. Neuroradiology. 2015;57:387–93.
69. Bunck AC, Kröger JR, Jüttner A, Brentrup A, Fiedler B, Schaarschmidt F, et al. Magnetic resonance 4D flow characteristics of cerebrospinal fluid at the craniocervical junction and the cervical spinal canal. Eur Radiol. 2011;21:1788–96.
70. Bhadelia R, Frederick E, Patz S, Dubey P, Erbay SH, Do-Dai D, et al. Cough-associated headache in patients with Chiari I malformation: CSF flow analysis by means of cine phase-contrast MR imaging. AJNR Am J Neuroradiol. 2011;32(4):739–42.
71. Basser PJ, Mattiello J, LeBihan D. Estimation of the effective self-diffusion tensor from the NMR spin echo. J Magn Reson B. 1994;103(3):247–54.
72. Basser PJ, Mattiello J, LeBihan D. MR diffusion tensor spectroscopy and imaging. Biophys J. 1994;66(1):259–67.
73. Le Bihan D, Mangin JF, Poupon C, Clark CA, Pappata S, Molko N, et al. Diffusion tensor imaging: concepts and applications. J Magn Reson Imaging. 2001;13(4):534–46.
74. Sundgren PC, Dong Q, Gómez-Hassan D, Mukherji SK, Maly P, Welsh R. Diffusion tensor imaging of the brain: review of clinical applications. Neuroradiology. 2004;46(5):339–50.
75. Ciccarelli O, Catani M, Johansen-Berg H, Clark C, Thompson A. Diffusion-based tractography in neurological disorders: concepts, applications, and future developments. Lancet Neurol. 2008;7(8):715–27.
76. Yamada K, Sakai K, Akazawa K, Yuen S, Nishimura T. MR tractography: a review of its clinical applications. Magn Reson Med Sci. 2009;8(4):165–74.
77. Voineskos AN, Rajji TK, Lobaugh NJ, Miranda D, Shenton ME, Kennedy JL, et al. Age-related decline in white matter tract integrity and cognitive performance: a DTI tractography and structural equation modeling study. Neurobiol Aging. 2012;33(1):21–34.
78. White T, Nelson M, Lim KO. Diffusion tensor imaging in psychiatric disorders. Top Magn Reson Imaging. 2008;19(2):97–109.
79. Shimony JS, Sheline YI, D'Angelo G, Epstein AA, Benzinger TL, Mintun MA, et al. Diffuse microstructural abnormalities of normal-appearing white matter in late life depression: a diffusion tensor imaging study. Biol Psychiatry. 2009;66(3):245–52.
80. Kumar M, Rathore RK, Srivastava A, Yadav SK, Behari S, Gupta RK. Correlation of diffusion tensor imaging metrics with neurocognitive function in Chiari I malformation. World Neurosurg. 2011;76(1–2):189–94.
81. Eshetu T, Meoded A, Jallo GI, Carson BS, Huisman TA, Poretti A. Diffusion tensor imaging in pediatric Chiari type I malformation. Dev Med Child Neurol. 2014;56(8):742–8.
82. Abeshaus S, Friedman S, Poliachik S, Poliakov A, Shaw DWW, Ojemann J, et al. Diffusion tensor imaging changes with decompression of Chiari I malformation. Neurosurgery. 2012;71:E578.
83. Hatem SM, Attal N, Ducreux D, Gautron M, Parker F, Plaghki L, et al. Assessment of spinal somatosensory systems with diffusion tensor imaging in syringomyelia. J Neurol Neurosurg Psychiatry. 2009;80(12):1350–6.
84. Yan H, Zhu Z, Liu Z, Zhang X, Sun X, Sha S, et al. Diffusion tensor imaging in cervical syringomyelia secondary to Chiari I malformation: preliminary results. Spine. 2015;40(7):E381–7.
85. Nishikawa M, Sakamoto H, Hakuba A, Nakanishi N, Inoue Y. Pathogenesis of Chiari malformation: a morphometric study of the posterior cranial fossa. J Neurosurg. 1997;86(1):40–7.
86. Milhorat TH, Chou MW, Trinidad EM, Kula RW, Mandell M, Wolpert C, et al. Chiari I malformation redefined: clinical and radiographic findings for 364 symptomatic patients. Neurosurgery. 1999;44(5):1005–17.
87. Karagoz F, Izgi N, Kapijcijoglu Sencer S. Morphometric measurements of the cranium in patients with Chiari type I malformation and comparison with the normal population. Acta Neurochir. 2002;144(2):165–71.
88. Milhorat TH, Nishikawa M, Kula RW, Dlugacz YD. Mechanisms of cerebellar tonsil herniation in patients with Chiari malformations as guide to clinical management. Acta Neurochir. 2010;152(7):1117–27.
89. Besachio DA, Khaleel Z, Shah L. Odontoid process inclination in normal adults and in an adult population with Chiari malformation type I. J Neurosurg Spine. 2015;23:701–6.
90. Noudel R, Jovenin N, Eap C, Scherpereel B, Pierot L, Rousseaux P. Incidence of basioccipital hypoplasia in Chiari malformation type I: comparative morphometric study of the posterior cranial fossa. Clinical article. J Neurosurg. 2009;111(5):1046–52.
91. Markunas CA, Enterline DS, Dunlap K, Soldano K, Cope H, Stajich J, et al. Genetic evaluation and application of posterior cranial Fossa traits as Endophenotypes for Chiari type I malformation. Ann Hum Genet. 2014;78:1–12.
92. Smoker WRK. Craniovertebral junction: Normal anatomy, craniometry, and congenital anomalies. Radiographics. 1994;14:255–77.
93. Vega A, Quintana F, Berciano J. Basichondrocranium anomalies in adult Chiari type I malformation: amorphometric study. J Neurol Sci. 1990;99(2–3):137–45.
94. Khalsa SSS, Geh N, Martin BA, Allen PA, Strahle J, Loth F, et al. Morphometric and volumetric comparison of 102 children with symptomatic and asymptomatic Chiari malformation type I. J Neurosurg Pediatr. 2018;21(1):65–71.

95. Alperin N, Loftus JR, Oliu CJ, Bagci A, Lee SH, Ertl-Wagner B, et al. MR measurement of the posterior cranial morphology and CSF physiology in Chiari malformation type I. Neurosurgery. 2014;75:515–22.
96. Bagci AM, Lee SH, Nagornaya N, Green BA, Alperin N. Automated posterior cranial Fossa Volumetry by MRI: applications to Chiari malformation type I. AJNR Am J Neuroradiol. 2013;34(9):1758–63.
97. Khalsa SSS, Siu A, DeFreitas TA, Cappuzzo JM, Myseris JS, Magge SN, et al. Comparison of posterior fossa volumes and clinical outcomes after decompression of Chiari malformation type I. J Neurosurg Pediatr. 2017;19:511–7.
98. McGirt MJ, Nimjee SM, Fuchs HE, George TM. Relationship of cine phase-contrast magnetic resonance imaging with the outcome after decompression for Chiari I malformations. Neurosurgery. 2006;59(1):140–6.
99. Krishna V, Sammartino F, Yee P, Mikulis D, Walker M, Elias G, et al. Diffusion tensor assessment of microstructural brainstem integrity in Chiari malformation type I. J Neurosurg. 2016;125(5):1112–9.
100. Noudel R, Gomis P, Sotoares G, Bazin A, Pierot L, Pruvo JP, et al. Posterior fossa volume increase after surgery for Chiari malformation type I: a quantitative assessment using magnetic resonance imaging and correlations with the treatment response. J Neurosurg Pediatr. 2017;19(5):511–7.

Part VI

Clinical Presentations

29 Clinical Presentation of Pediatric Chiari I Malformations

Curtis J. Rozzelle

Introduction

The clinical presentation of pediatric Chiari I malformations differs somewhat from that of adult patients, especially for those presenting very early in life. Chiari I malformations in childhood typically present with symptoms and signs attributable to cerebrospinal fluid (CSF) flow impairment, compression of neural elements, and/or syringomyelia. Perhaps due to differences in age, children present with a shorter duration of symptoms at diagnosis than adults [1]. This chapter will enumerate the commonly described and generally accepted clinical sequelae of these pathological mechanisms in infancy, childhood, and adolescence. The more esoteric and controversial clinical presentations associated with Chiari I in children are addressed elsewhere in this text. It is also worth noting here that reviewing the literature on this topic reveals a dramatic shift in presentations over time. Prior to the introduction and widespread availability of magnetic resonance image (MRI) scanning, diagnosis was rarely made prior to the onset of significant neurologic morbidity. This chapter reflects a greater emphasis on more contemporary literature reports from the MRI era.

C. J. Rozzelle (✉)
Department of Neurosurgery, University of Alabama at Birmingham, Birmingham, AL, USA
e-mail: Curtis.Rozzelle@childrensal.org

Symptoms and Signs

The most common presenting symptom is pain, reported in 60–70% of patients [2, 3]. It is typically non-dermatomal and localized to the occipital or cervical region. Occipital headache/neck pain is the most common presentation in every contemporary pediatric Chiari I series, accounting for 40–60% [3–7]. The pain is often precipitated or exacerbated by a Valsalva maneuver, suggesting CSF flow impairment as the pathophysiology (Table 29.1). Besides cough, sneeze, or defecation, Valsalva-inducing activities in children may include screaming, running, or repetitive jumping, such as on a trampoline. In nonverbal children, pain may be manifested as irritability, opisthotonos, incessant crying, or failure to thrive. Other symptoms include nonradicular pain in the shoulder, back, chest, and extremities that may be described as deep and burning; weakness and/or altered sensation in the extremities; clumsiness; dysphagia; dysarthria; hiccoughs; severe snoring; and drop attacks. Cerebellovestibular problems have also been cited.

Cephalgia localized beyond the occipital-cervical region and global headache correlates poorly with Chiari I malformation improvement following decompression. Every published series assessing the value of neuroimaging in the evaluation of pediatric headache recommends no

R. S. Tubbs et al. (eds.), *The Chiari Malformations*, https://doi.org/10.1007/978-3-030-44862-2_29

Table 29.1 Signs and symptoms of Chiari type I malformations

Impaired cerebrospinal fluid pressure/flow dynamic
High cervical or occipital pain or dysesthesia, especially with Valsalva
Hydrocephalus
Syringomyelia
Upper extremity weakness or atrophy
Lower extremity spasticity
Scoliosis, particularly single left thoracic curve
Hemiparesis
Dissociated or suspended sensory loss (pain and temperature)
Absent superficial abdominal reflexes
Direct neural compression
Clumsiness or truncal and appendicular ataxia
Dysphagia
Dysarthria
Hoarseness
Hiccoughs
Apnea
Nystagmus
Recurrent aspiration
Hyper- or hyporeflexia
Babinski response
Oscillopsia
Esotropia
Sinus bradycardia
Trigeminal or glossopharyngeal neuralgia
Opisthotonos
Severe snoring
Drop attacks
Glossal atrophy
Facial sensory loss

imaging for children with common headache syndromes and normal neurological exam findings. The reported incidence of Chiari I malformation requiring a "change in management" in children diagnosed with migraine, tension-type, and/or chronic daily headache and a normal neurological exam ranges from 0% to 1.4% [8–10]. This incidence range is exceeded by the 3.6% Chiari I detection rate reported in a review of 14,116 pediatric patients undergoing brain or cervical spine MRI for all indications [11]. Furthermore, a reported series of Chiari I patients analyzing the relationships between headache location, CSF flow dynamics on cine MRI, and headache response to Chiari decompression concluded that non-occipital "headaches are not pathologically or causatively associated with the Chiari I malformation in the vast majority of patients" [12]. Taken together, multiple lines of evidence support a recommendation for medical management of neurologically normal children with Chiari I malformations and "non-Chiari" headache types.

Signs seen in Chiari I malformation are variable but include upper motor neuron changes in the legs, with spasticity, exaggerated deep tendon reflexes, and upgoing toes. The upper extremities may have evidence of lower motor neuron injury, with loss of muscle bulk, diminished or absent reflexes, and fasciculations. Sensory loss is classically described as suspended and dissociated. This non-dermatomal loss involves pain and temperature but spares light touch and proprioception. Ataxia, irregular respirations, and lower cranial nerve dysfunction may also be seen.

Pediatric type I malformations often present with progressive scoliosis attributable to an associated syrinx. Syringomyelia is reportedly present in 5.6–57% of pediatric Chiari I patients, and scoliosis is reported in 18–22%, although syringomyelia and scoliosis do not always present together [3, 11, 13]. While the typical finding in idiopathic scoliosis is a right curve, the configuration reportedly associated with syringomyelia is levoscoliosis with a single curve [14]. MRI studies of 68 children presenting with left thoracic curves revealed Chiari I in 40% and syringomyelia in 29% [15]. Children presenting with scoliosis should be examined carefully for any neurologic abnormalities. The absence of superficial abdominal reflexes ipsilateral to the convexity appears to be a strong indicator of syringomyelia [16]. A relatively high incidence (19%) of intraspinal pathology, including syringomyelia, is reported in children presenting with idiopathic scoliosis before 11 years of age [17]. MRI screening of idiopathic scoliosis in neurologically normal adolescents, however, yields a low incidence of Chiari I, likely approaching the prevalence in the general population [11, 18]. Pediatric scoliosis associated with syringomyelia and Chiari I often stabilizes or improves following surgical decompression of the foramen magnum. Significant improvement in the scoliotic

curve is reported in 38% to 73%, while improvement or stabilization (combined) occurs in 62–91% [19–21]. Factors reportedly associated with continued scoliosis progression following decompression include age greater than 10 years, female sex, and more sever scoliosis at presentation (e.g., larger curves, double curves, kyphosis, and rotation) [19, 21, 22].

Prior to general availability of MRI, pediatric Chiari I malformations frequently presented with evidence of moderate to severe brain stem/cranial nerve/spinal cord dysfunction. Earlier detection with MRI appears to have significantly reduced the frequency of these presentations. Lower cranial nerve dysfunction may be manifested as vocal cord paralysis, dysarthria, soft palate weakness, glossal atrophy, cricopharyngeal achalasia, absent gag reflex, and facial sensory loss. The most common manifestation of medullary dysfunction in these patients is sleep apnea/vocal cord paralysis [23, 24]. Sleep apnea at presentation is reported in 12.9% [11] and is seen more frequently in children younger than 6 years compared to older children [25]. Nystagmus is another presenting sign that is classically the downbeat type and increased on lateral gaze [26]. This variety of nystagmus is specific for pathologic conditions involving the cervicomedullary junction. Other less common cranial nerve signs are esotropia, sinus bradycardia, oscillopsia, trigeminal and glossopharyngeal neuralgia, and sensorineural hearing loss [27–32].

Associated Conditions

Syringomyelia and scoliosis, as previously described, are by far the most common conditions associated with pediatric Chiari I malformation. Other associated spinal anomalies frequently reported in surgical series are retroversion of the odontoid process/platybasia/basilar invagination (12–24%), occipitoatlantal fusion/assimilation of the atlas (8%), hemivertebra/butterfly vertebra (2.4–4%), and Klippel-Feil anomaly (2.7–3%) [1, 3, 5, 11]. The presence of odontoid retroversion, basilar invagination, or platybasia is associated with greater tonsillar descent, while only basilar invagination correlates with syringomyelia [11].

Familial incidence of Chiari I malformation ranges from 3% to 12% with both autosomal dominant and recessive patterns reported [3, 5]. The prevalence of associated hydrocephalus in children diagnosed with Chiari I by MRI criteria is 8.3% and reportedly ranges from 10% to 31% in surgically treated series [1, 3, 11, 25, 33]. Neurofibromatosis type I is associated with pediatric Chiari I in up to 5% [3, 34] and idiopathic growth hormone deficiency in 4.2% [3].

Natural History

The natural history of pathological (i.e., symptomatic) Chiari I malformation is poorly understood and likely to remain so because surgical intervention is indicated and typically initiated in a timely fashion. However, recent reports have illuminated the natural history of Chiari I presenting with minimal or no symptoms in neurologically normal children. Collectively, these multi-year observational studies suggest that pediatric Chiari I subsequently followed up without surgery remains asymptomatic or improves clinically in 77–94% [13, 35, 36]. Imaging evidence of progressive tonsillar descent, new syrinx formation, or syrinx enlargement is reported in 4.5–10.2% [35, 36]. Conversely, resolution of previously diagnosed tonsillar herniation exceeding 5 mm is observed in up to 5%, and syrinx resolution occurred in up to 15% of those presenting with syringomyelia [35, 36]. A natural history study of untreated syringomyelia in children with trivial or no symptoms followed with serial MRI found progression in only 2 of 17 individuals (12%) and diminished syrinx size in 8 (47%) [37]. Nonsurgical management and longitudinal observation of otherwise normal children with asymptomatic or oligosymptomatic Chiari I appears to be a relatively safe treatment option. Repeat MRI is warranted to investigate new or progressive symptoms in this patient population, while serial imaging absent new complaints or findings appears likely to identify progression prompting a change in treatment for a small minority.

Indications for Treatment

In light of the generally benign natural history of pediatric Chiari I absent syringomyelia, occipito-cervical pain, or neurologic compromise attributable to cervicomedullary dysfunction, the malformation's mere presence does not equate to an indication for surgical decompression. Likewise there is no Chiari I imaging feature, such as extent of tonsillar herniation, which necessitates decompression (although extent of herniation correlates with clinical features that are indications for treatment). Serial observation with or without surveillance imaging is most appropriate for children whose Chiari I malformations do not require treatment.

Widely accepted indications for surgical decompression include (1) occipito-cervical pain triggered or aggravated by Valsalva, (2) cervical and/or thoracic syringomyelia with or without scoliosis, or (3) neurologic dysfunction that localizes to the cervicomedullary region, lower cranial nerves, or cerebellum. Because other headache types are not associated with Chiari I malformation, they should not be considered an indication for surgery.

References

1. Dyste GN, Menezes AH. Presentation and management of pediatric Chiari malformations without myelodysplasia. Neurosurgery. 1988;23(5):589–97.
2. Iskandar B, Oakes WJ. Chiari malformation and syringomyelia. In: Albright AL, Pollack IF, Adelson PD, editors. Principles and practice of pediatric neurosurgery. New York: Thieme; 1999. p. 165–87.
3. Tubbs RS, Beckman J, Naftel RP, Chern JJ, Wellons JC 3rd, Rozzelle CJ, et al. Institutional experience with 500 cases of surgically treated pediatric Chiari malformation Type I. J Neurosurg Pediatr. 2011;7(3):248–56.
4. Furuya K, Sano K, Segawa H, Ide K, Yoneyama H. Symptomatic tonsillar ectopia. J Neurol Neurosurg Psychiatry. 1998;64(2):221–6.
5. Milhorat TH, Chou MW, Trinidad EM, Kula RW, Mandell M, Wolpert C, et al. Chiari I malformation redefined: clinical and radiographic findings for 364 symptomatic patients. Neurosurgery. 1999;44(5):1005–17.
6. Park JK, Gleason PL, Madsen JR, Goumnerova LC, Scott RM. Presentation and management of Chiari I malformation in children. Pediatr Neurosurg. 1997;26(4):190–6.
7. Wu YW, Chin CT, Chan KM, Barkovich AJ, Ferriero DM. Pediatric Chiari I malformations: do clinical and radiologic features correlate? Neurology. 1999;53(6):1271–6.
8. Alehan FK. Value of neuroimaging in the evaluation of neurologically normal children with recurrent headache. J Child Neurol. 2002;17(11):807–9.
9. Lewis DW, Dorbad D. The utility of neuroimaging in the evaluation of children with migraine or chronic daily headache who have normal neurological examinations. Headache. 2000;40(8):629–32.
10. Schwedt TJ, Guo Y, Rothner AD. "Benign" imaging abnormalities in children and adolescents with headache. Headache. 2006;46(3):387–98.
11. Strahle J, Muraszko KM, Kapurch J, Bapuraj JR, Garton HJ, Maher CO. Chiari malformation Type I and syrinx in children undergoing magnetic resonance imaging. J Neurosurg Pediatr. 2011;8(2):205–13.
12. McGirt MJ, Nimjee SM, Floyd J, Bulsara KR, George TM. Correlation of cerebrospinal fluid flow dynamics and headache in Chiari I malformation. Neurosurgery. 2005;56(4):716–21; discussion −21.
13. Benglis D Jr, Covington D, Bhatia R, Bhatia S, Elhammady MS, Ragheb J, et al. Outcomes in pediatric patients with Chiari Malformation Type I followed up without surgery. J Neurosurg Pediatr. 2011;7(4):375–9.
14. Isu T, Chono Y, Iwasaki Y, Koyanagi I, Akino M, Abe H, et al. Scoliosis associated with syringomyelia presenting in children. Childs Nerv Syst. 1992;8(2):97–100.
15. Wu L, Qiu Y, Wang B, Zhu ZZ, Ma WW. The left thoracic curve pattern: a strong predictor for neural axis abnormalities in patients with "idiopathic" scoliosis. Spine (Phila Pa 1976). 2010;35(2):182–5.
16. Zadeh HG, Sakka SA, Powell MP, Mehta MH. Absent superficial abdominal reflexes in children with scoliosis. An early indicator of syringomyelia. J Bone Joint Surg Br. 1995;77(5):762–7.
17. Lewonowski K, King JD, Nelson MD. Routine use of magnetic resonance imaging in idiopathic scoliosis patients less than eleven years of age. Spine (Phila Pa 1976). 1992;17(6 Suppl):S109–16.
18. Maiocco B, Deeney VF, Coulon R, Parks PF, Jr. Adolescent idiopathic scoliosis and the presence of spinal cord abnormalities. Preoperative magnetic resonance imaging analysis. Spine (Phila Pa 1976). 1997;22(21):2537–41.
19. Brockmeyer D, Gollogly S, Smith JT. Scoliosis associated with Chiari 1 malformations: the effect of suboccipital decompression on scoliosis curve progression: a preliminary study. Spine (Phila Pa 1976). 2003;28(22):2505–9.
20. Hida K, Iwasaki Y, Koyanagi I, Abe H. Pediatric syringomyelia with chiari malformation: its clinical characteristics and surgical outcomes. Surg Neurol. 1999;51(4):383–90. discussion 90–1
21. Muhonen MG, Menezes AH, Sawin PD, Weinstein SL. Scoliosis in pediatric Chiari malformations without myelodysplasia. J Neurosurg. 1992;77(1):69–77.

22. Flynn JM, Sodha S, Lou JE, Adams SB Jr, Whitfield B, Ecker ML, et al. Predictors of progression of scoliosis after decompression of an Arnold Chiari I malformation. Spine (Phila Pa 1976). 2004;29(3):286–92.
23. Ruff ME, Oakes WJ, Fisher SR, Spock A. Sleep apnea and vocal cord paralysis secondary to type I Chiari malformation. Pediatrics. 1987;80(2):231–4.
24. Wynn R, Goldsmith AJ. Chiari type I malformation and upper airway obstruction in adolescents. Int J Pediatr Otorhinolaryngol. 2004;68(5):607–11.
25. Nagib MG. An approach to symptomatic children (ages 4–14 years) with Chiari type I malformation. Pediatr Neurosurg. 1994;21(1):31–5.
26. Cogan DG. Down-beat nystagmus. Arch Ophthalmol. 1968;80(6):757–68.
27. Gingold SI, Winfield JA. Oscillopsia and primary cerebellar ectopia: case report and review of the literature. Neurosurgery. 1991;29(6):932–6.
28. Lewis AR, Kline LB, Sharpe JA. Acquired esotropia due to Arnold-Chiari I malformation. J Neuroophthalmol. 1996;16(1):49–54.
29. Rosetti P, Ben Taib NO, Brotchi J, De Witte O. Arnold Chiari Type I malformation presenting as a trigeminal neuralgia: case report. Neurosurgery. 1999;44(5):1122–3. discussion 3–4
30. Sclafani AP, DeDio RM, Hendrix RA. The Chiari-I malformation. Ear Nose Throat J. 1991;70(4):208–12.
31. Selmi F, Davies KG, Weeks RD. Type I Chiari deformity presenting with profound sinus bradycardia: case report and literature review. Br J Neurosurg. 1995;9(4):543–5.
32. Yglesias A, Narbona J, Vanaclocha V, Artieda J. Chiari type I malformation, glossopharyngeal neuralgia and central sleep apnoea in a child. Dev Med Child Neurol. 1996;38(12):1126–30.
33. Dyste GN, Menezes AH, VanGilder JC. Symptomatic Chiari malformations. An analysis of presentation, management, and long-term outcome. J Neurosurg. 1989;71(2):159–68.
34. Galarza M, Martinez-Lage JF, Ham S, Sood S. Cerebral anomalies and Chiari type 1 malformation. Pediatr Neurosurg. 2010;46(6):442–9.
35. Novegno F, Caldarelli M, Massa A, Chieffo D, Massimi L, Pettorini B, et al. The natural history of the Chiari type I anomaly. J Neurosurg Pediatr. 2008;2(3):179–87.
36. Strahle J, Muraszko KM, Kapurch J, Bapuraj JR, Garton HJ, Maher CO. Natural history of Chiari malformation type I following decision for conservative treatment. J Neurosurg Pediatr. 2011;8(2):214–21.
37. Singhal A, Bowen-Roberts T, Steinbok P, Cochrane D, Byrne AT, Kerr JM. Natural history of untreated syringomyelia in pediatric patients. Neurosurg Focus. 2011;31(6):1–5.

Benign Chiari I Malformation

30

Elizabeth N. Alford, Kathrin Zimmerman, and Brandon G. Rocque

Chiari I malformation (CM I) is increasingly discovered on head and/or neck imaging obtained for routine screening, after head trauma or for workup of common symptoms, such as headache. Large studies have found a 0.24–3.6% prevalence of CM I in the general population [1–8]. As described in detail in Chap. 29, CM I classically causes a Valsalva-induced, or tussive, occipital headache. It can also be associated with cranial nerve and brain stem dysfunction, including derangement in extraocular movements, dysphagia, dysphonia, and central sleep apnea. Associated imaging findings include syringomyelia, hydrocephalus, and spinal cord signal change. However, many patients with anatomic findings consistent with CM I lack these classic signs and symptoms.

Evaluating and managing patients with CM I that lack classical symptoms and imaging findings can be challenging. While it has been presumed that these patients have a low risk of becoming symptomatic, there are limited data to verify this presumption. To study this population, it is important first to define precisely this group of patients. A *benign Chiari I malformation* is a CM I with minimal or no classical symptoms at presentation and no imaging evidence of syringomyelia, hydrocephalus, or spinal cord signal change. In other words, a benign CM I is one that lacks a classical indication for surgical decompression.

Early surveys on surgical indications in CM I found widely disparate indications for surgical decompression [9, 10]. One survey found that only 8% of surveyed neurosurgeons would recommend surgery for an asymptomatic patient with CM I, but 75% would recommend surgery for an asymptomatic patient with syringomyelia [10]. Studies such as these identified a need for long-term follow-up studies of benign or asymptomatic CM I. The majority of published literature concerning benign CM I come from prospective and retrospective observational studies of patients initially managed nonoperatively. As such, all evidence is, at best, Level II or III. Some of these studies, including those that will be discussed later, include a mix of patients with syringomyelia, hydrocephalus, and benign CM I.

It is estimated that 37–45.4% of all CM I is benign at presentation (Table 30.1) [7, 11–17], though studies have reported estimated prevalence as low as 25% [14] and as high as 70% [11, 15]. However, each of these studies uses slightly

E. N. Alford
Department of Neurosurgery, University of Alabama at Birmingham, Birmingham, AL, USA

K. Zimmerman · B. G. Rocque (✉)
Department of Neurosurgery, Division of Pediatric Neurosurgery, University of Alabama at Birmingham, Birmingham, AL, USA
e-mail: brandon.rocque@childrensal.org

R. S. Tubbs et al. (eds.), *The Chiari Malformations*, https://doi.org/10.1007/978-3-030-44862-2_30

Table 30.1 Estimated prevalence of benign Chiari I (CM I) in the literature

	Benign CM I	*n*	Prevalence (%)
Novegno et al. [14]	22	94	23.4
Strahle et al. [7]	147	267–509	28.8–55.1
Pomeraniec et al. [15]	70	95–116	60.3–73.7
Wu et al. [17]	28	49	57
Benglis et al. [11]	124	178	69.7
Whitson et al. [16]	83	228	36
Chavez et al. [12]	236	345	68.4
Leon et al. [13]	427	1030–1284	33.3–41.5
Total	1037	2286–2803	37–45.4

different inclusion criteria, and some studies include patients with hydrocephalus and syringomyelia. No true population-based studies have been performed to estimate the prevalence of benign CM I; the best available estimates derive from comprehensive institutional cohorts.

Benign Chiari I in the Pediatric Population

Five studies have reported cohorts of pediatric patients with CM I initially managed nonoperatively; however, these studies also included patients with syringomyelia and/or hydrocephalus. Massimi et al. reported a cohort of 16 asymptomatic patients with CM I, which also included 2 patients with syringomyelia and 5 patients with mild ventriculomegaly [18]. Overall, 3 of 16 had worsening clinical status (18.8%), and 2 underwent surgical intervention (12.5%). Excluding patients who presented with syrinx or hydrocephalus, 0 of 9 patients with benign CM I clinically worsened or required surgical intervention.

Novegno et al. published a similar cohort of 22 patients initially managed nonoperatively with mean follow-up of 6 years [14]. This cohort included five patients with hydrocephalus, one of whom also had syringomyelia. Excluding the patients who presented with hydrocephalus and syringomyelia, 3 of the remaining 17 (17.6%) had worsening clinical symptoms, only 1 (5.9%) of whom required posterior fossa decompression.

According to a cohort of 70 patients reported by Pomeraniec et al. [15], the overwhelming majority of CM I patients (92.9%) managed nonoperatively do not experience clinical or radiological progression during follow-up of 5.8 years. Two patients (2.9%) developed new syringomyelia during the follow-up period.

Benglis et al. reviewed 124 patients with CM I who were managed nonoperatively and followed for a mean 2.8 years [11]. Seven patients (5.6%) had a syrinx at presentation, all of which remained stable on follow-up imaging. In the remaining patients, no new syringomyelia developed during the follow-up period. During the observed follow-up, 16 patients (12.9%) had new or worsened symptoms, but none underwent surgical intervention. One of the patients with new/worsened symptoms had a syrinx at presentation that remained radiographically stable.

Strahle et al. identified a cohort of 147 patients at their institution with CM I managed nonoperatively (mean follow-up: 4.6 years) [7]. Thirteen patients had syringomyelia at time of CM I diagnosis (8.8%). Of the 147 patients, 9 developed new symptoms attributed to the CM I during the follow-up interval. During this time, development of a spinal cord syrinx occurred in eight patients; five of these patients had a prior diagnosis of a presyrinx state or a dilated central canal. Fourteen patients underwent surgical treatment for CM I (9.5%). Two patients who underwent surgery had a syrinx at presentation. Excluding the patients who presented with syrinx, 12/134 (9.0%) ultimately underwent surgical decompression, at a median of 1.24 years from initial evaluation.

Only two published studies have focused exclusively on benign CM I. Whitson et al. described a cohort of 55 patients with benign CM I; no patient developed new syringomyelia and 3 patients (5.5%) underwent posterior fossa decompression during the course of the study [16]. In the largest available study, Leon et al. reported a cohort of 427 patients with benign CM

Table 30.2 Reported rates of new syrinx development, clinical worsening, and posterior fossa decompression in pediatric patients with benign Chiari I

	n	New syrinx, *n* (%)	Clinical worsening, *n* (%)	Posterior fossa decompression, *n* (%)
Massimi et al. [18][a]	9	1 (11.1%)	0 (0%)	0 (0%)
Novegno et al. [14][a]	17	1 (5.9%)	3 (17.6%)	1 (5.9%)
Killeen et al. [19]	21	–	1 (4.8%)	–
Whitson et al. [16]	55	0 (0%)	–	3 (5.5%)
Pomeraniec et al. [15][a]	70	2 (2.9%)	5 (7.1%)	–
Benglis et al. [11][a]	117	0 (0%)	15 (12.8%)	0 (0%)
Strahle et al. [7][a]	134	7 (5.2%)	9 (6.7%)	12 (9.0%)
Leon et al. [13]	427	5 (1.2%)	–	15 (3.5%)
Total		16/829 (1.9%)	33/368 (9.0%)	31/759 (4.1%)

[a]Original publication included patients with syrinx and/or hydrocephalus, which are excluded here

I followed for a median of 2.1 years [13]. Fifteen patients underwent surgical intervention (3.5%) and 5 patients developed a new syrinx (1.2%). Using Kaplan-Meier survival analysis, 5–7% of patients required posterior fossa decompression at 5–10 years.

Taking all these studies together (Table 30.2), 1.9% of patients with benign CM I develop a new syrinx during follow-up, 9.0% experience clinical worsening, and 4.1% undergo posterior fossa decompression [7, 11, 13–16, 18, 19].

Benign Chiari I in the Adult Population

Literature focusing on benign CM I in the adult population is even scarcer. Killeen et al. describe a cohort of 76 adult and pediatric patients, 8 of whom underwent posterior fossa decompression (10.5%) [19]. Only 4.8% of pediatric patients experienced clinical worsening, while 25.5% of adult patients worsened, and 10.6% of adult patients had both improvement and worsening (in different clinical aspects). Langridge et al. reported a systematic review of 15 articles that reviewed nonoperative management of both symptomatic and asymptomatic patients with CM I; however, not all patients included in this systematic review met criteria for benign CM I [20]. Nevertheless, Langridge found that 93.3% of asymptomatic patients remained asymptomatic, even if syringomyelia was present. Among symptomatic patients, 27–47% had symptom improvement at 15 months.

Imaging Findings in Benign Chiari I

Mean reported tonsillar position among CM I patients initially managed nonoperatively ranges from 8.35 to 11.2 mm below the foramen magnum [7, 11, 15, 18]. A 2015 review of the literature found reports of 78 patients with nonoperative CM I followed with serial imaging [16]. Within this cohort, 10 patients (12.8%) had increase in tonsillar descent, 51 (65.4%) had decrease in tonsillar descent, and 17 (21.8%) had normalization of tonsil position [16]. Most of these were single case reports or reports of small case series that demonstrated improvement or normalization in tonsil position. It is less likely that case reports or series of CM I patients with stable tonsil position or increased descent of the tonsils below the foramen magnum would be published, since such findings would not be surprising. Therefore, the significant rate (87.2%) of improvement of tonsil position in this cohort should be interpreted cautiously, as it may reflect publication bias. In contrast, serial imaging of a cohort of 52 consecutive patients found that tonsil position remained stable in 50% of patients, increased in 12%, was reduced in 26%, and resolved in 12%. Radiographic changes did not correlate with neurologic exam changes or symptom development [16] Strahle et al. reported that while there was no significant change over time in mean tonsillar position overall, 45 patients (31%) had improvement in tonsillar position, 7 patients (4.8%) had normalization of tonsil position, and 6 patients (4%) had a descent in tonsillar

position of at least 4 mm [7]. Furthermore, Strahle et al. found no significant differences in initial cerebellar tonsillar herniation or CSF flow at the foramen magnum in those who ultimately underwent surgery compared with those who did not [7].

Evaluation and Management

Benign CM I appears to be relatively common among all CM I and demonstrates a favorable clinical course. Upon initial presentation, a patient with a suspected benign CM I should be assessed with magnetic resonance imaging (MRI) of the brain and cervical spine without contrast to evaluate for findings such as hydrocephalus, syrinx, etc. Some clinicians favor complete spinal axis imaging to evaluate for tethered spinal cord, occult dysraphism, and other findings. However, the diagnostic yield and cost-effectiveness of such imaging is not well characterized.

Patients with benign CM I and their families should be appropriately counseled about the expected clinical course of benign CM I. Based on the current literature, the overall rate of symptomatic worsening is about 9%, while 4% go on to need posterior fossa decompression and 1.9% develop a syrinx. Especially in benign CM I, it should be stressed that posterior fossa decompression be reserved for patients who develop signs or symptoms of CM I. In the authors' practice, patients with benign CM I are followed with serial MRI cervical spine without contrast. Provided that appropriate imaging is performed upon initial assessment, surveillance imaging of the brain, thoracic, and lumbar spine is not necessary. There are few published data to direct frequency of follow-up. In our practice, for a clinically stable patient, clinical and radiographic follow-ups are performed 1 year after initial evaluation. The follow-up interval is doubled after each subsequent visit (e.g., 2 years, 4 years, 8 years). However, if a patient develops new focal signs or symptoms, appropriate diagnostic workup and clinical evaluation should be pursued.

Conclusion

Benign CM I is one in which the patient lacks classic symptoms at presentation and has no radiographic evidence of hydrocephalus, syrinx, or spinal cord signal change. The published data on benign CM I are limited and come primarily from retrospective cohort studies. Additionally, studies often combine benign CM I with other nonoperatively managed CM I, restricting the generalizability of the findings. Studies with very-long-term follow-up (10–15 years or more) are lacking, as are studies of benign CM I in the adult population. Further analysis of imaging findings in CM I may help identify patients at higher risk of developing symptoms or syrinx. There is significant opportunity to systematically study this population and improve our understanding of benign CM I and its clinical course.

Benign CM I is relatively common, comprising ~40% of all CM I, and demonstrates a favorable clinical course. Clinical deterioration, development of syrinx, and need for posterior fossa decompression are uncommon events in benign CM I. Therefore, conservative management with clinical and radiographic surveillance is most appropriate.

References

1. Aitken LA, Lindan CE, Sidney S, Gupta N, Barkovich AJ, Sorel M, et al. Chiari type I malformation in a pediatric population. Pediatr Neurol. 2009;40:449–54.
2. Barkovich AJ, Wippold FJ, Sherman JL, Citrin CM. Significance of cerebellar tonsillar position on MR. AJNR Am J Neuroradiol. 1986;7:795–9.
3. Kahn EN, Muraszko KM, Maher CO. Prevalence of Chiari I malformation and Syringomyelia. Neurosurg Clin N Am. 2015;26:501–7.
4. Meadows J, Kraut M, Guarnieri M, Haroun RI, Carson BS. Asymptomatic Chiari Type I malformations identified on magnetic resonance imaging. J Neurosurg. 2000;92:920–6.
5. Morris Z, Whiteley WN, Longstreth WT, Weber F, Lee Y-C, Tsushima Y, et al. Incidental findings on brain magnetic resonance imaging: systematic review and meta-analysis. BMJ. 2009;339:b3016.
6. Nishizawa S, Yokoyama T, Yokota N, Tokuyama T, Ohta S. Incidentally identified syringomyelia associated with Chiari I malformations: is early

interventional surgery necessary? Neurosurgery. 2001;49:637–40; discussion 640–1.
7. Strahle J, Muraszko KM, Kapurch J, Bapuraj JR, Garton HJL, Maher CO. Natural history of Chiari malformation Type I following decision for conservative treatment. J Neurosurg Pediatr. 2011;8:214–21.
8. Vernooij MW, Ikram MA, Tanghe HL, Vincent AJPE, Hofman A, Krestin GP, et al. Incidental findings on brain MRI in the general population. N Engl J Med. 2007;357:1821–8.
9. Haines SJ, Berger M. Current treatment of Chiari malformations types I and II: a survey of the Pediatric Section of the American Association of Neurological Surgeons. Neurosurgery. 1991;28:353–7.
10. Schijman E. History, anatomic forms, and pathogenesis of Chiari I malformations. Childs Nerv Syst ChNS Off J Int Soc Pediatr Neurosurg. 2004;20:323–8.
11. Benglis D, Covington D, Bhatia R, Bhatia S, Elhammady MS, Ragheb J, et al. Outcomes in pediatric patients with Chiari malformation Type I followed up without surgery. J Neurosurg Pediatr. 2011;7:375–9.
12. Chavez A, Roguski M, Killeen A, Heilman C, Hwang S. Comparison of operative and non-operative outcomes based on surgical selection criteria for patients with Chiari I malformations. J Clin Neurosci Off J Neurosurg Soc Australas. 2014;21:2201–6.
13. Leon TJ, Kuhn EN, Arynchyna AA, Smith BP, Tubbs RS, Johnston JM, et al. Patients with "benign" Chiari I malformations require surgical decompression at a low rate. J Neurosurg Pediatr. 2019;23(4):498–506.
14. Novegno F, Caldarelli M, Massa A, Chieffo D, Massimi L, Pettorini B, et al. The natural history of the Chiari type I anomaly. J Neurosurg Pediatr. 2008;2:179–87.
15. Pomeraniec IJ, Ksendzovsky A, Awad AJ, Fezeu F, Jane JA. Natural and surgical history of Chiari malformation Type I in the pediatric population. J Neurosurg Pediatr. 2016;17:343–52.
16. Whitson WJ, Lane JR, Bauer DF, Durham SR. A prospective natural history study of nonoperatively managed Chiari I malformation: does follow-up MRI surveillance alter surgical decision making? J Neurosurg Pediatr. 2015;16:159–66.
17. Wu YW, Chin CT, Chan KM, Barkovich AJ, Ferriero DM. Pediatric Chiari I malformations: do clinical and radiologic features correlate? Neurology. 1999;53:1271–6.
18. Massimi L, Caldarelli M, Frassanito P, Di Rocco C. Natural history of Chiari type I malformation in children. Neurol Sci Off J Ital Neurol Soc Ital Soc Clin Neurophysiol. 2011;32(Suppl 3):S275–7.
19. Killeen A, Roguski M, Chavez A, Heilman C, Hwang S. Non-operative outcomes in Chiari I malformation patients. J Clin Neurosci Off J Neurosurg Soc Australas. 2015;22:133–8.
20. Langridge B, Phillips E, Choi D. Chiari malformation type 1: a systematic review of natural history and conservative management. World Neurosurg. 2017;104:213–9.

Unusual Presentations of the Chiari I Malformation

31

Christopher M. Bonfield
and Elizabeth Tyler-Kabara

Introduction

Chiari first described the Chiari malformations in 1891 after a series of observations in autopsies. These malformations may be associated with a small or shallow posterior fossa, variable skull base dysplasia, and decreased cerebrospinal fluid in the posterior fossa.

Although presenting symptoms are variable, Chiari I malformations (CM I) most commonly present with exertional occipital headaches and neck pain. This pain can be dull and persistent, but is usually associated with Valsalva maneuvers such as exercise, laughing, sneezing, bearing-down, or coughing. In infants, these headaches may present simply as irritability. It is thought that the cerebellar tonsils are impacted at the level of the foramen magnum during the Valsalva maneuver, thus causing the headaches.

Cerebellar tonsil herniation can also cause compression of the medulla and lower cranial nerves leading to neurologic symptoms as well. Syringomyelia, which is often associated with CM I, can result in neurologic sequelae. This spectrum of symptoms includes extremity weakness, sensory deficits, and abnormal reflexes. Lower cranial nerve compression can result in vocal cord paralysis, tongue weakness, aspiration, hoarseness, nystagmus, palatal weakness, and sleep apnea. Scoliosis is also commonly associated with patients who have CM I and a syrinx.

Although the majority of patients with CM I present with the symptoms listed above, there have been reports in the literature of more unusual presentations. This chapter will review the less common and more unusual presentations of CM I.

Unusual Presentations of Chiari I

As mentioned, cranial nerve deficits such as tinnitus can be a presenting symptom of CM I. However, these are generally limited to the lower cranial nerves and usually follow a subacute to chronic course. In 2008, Heuer et al. reported a case of a 5-year-old female with hearing loss as the only presentation of CM I [1]. The patient did not have a syrinx. Hearing loss can sometimes be seen in the constellation of CM I symptoms, but in this case, it was the only symptom of an otherwise asymptomatic CM I. Also,

C. M. Bonfield (✉)
Department of Neurological Surgery, Vanderbilt University Medical Center, Nashville, TN, USA
e-mail: chris.bonfield@vumc.org

E. Tyler-Kabara
Department of Neurological Surgery, Department of Bioengineering, Department of Physical Medicine and Rehabilitation, Neural Enhancement Laboratory, University of Pittsburgh School of Medicine, McGowan Institute for Regenerative Medicine, UPMC Children's Hospital of Pittsburgh, Pittsburgh, PA, USA

R. S. Tubbs et al. (eds.), *The Chiari Malformations*, https://doi.org/10.1007/978-3-030-44862-2_31

three adult patients with isolated asymmetric sensorineural hearing loss resulting from CM I improved after treatment of the CM I [2]. Cranial nerve neuralgias have also been reported. Papanastassiou et al. described a 63-year-old male with CM I and a syrinx who presented with chronic face pain and trigeminal neuralgia [3]. The patient failed numerous other treatments, but improved with posterior fossa decompression. Likewise, an 8-year-old with CM I and syrinx suffered from glossopharyngeal neuralgia [4]. This also improved after CM I treatment. Another pediatric patient had the acute onset of vocal cord paralysis with a concomitant CM I [5].

Brain stem and cerebellar dysfunction is due to the compression of the medulla and tonsils at the level of the foramen magnum. Selmi et al. described an adult with CM I who presented with sinus bradycardia for which a cardiac etiology was not found [6]. Syncope is another rare presentation of CM I. In 1982, a report illustrated three cases of CM I with associated syrinx, all presenting with syncope [7]. These patients varied in age from 20 to 52 years of age. Such "drop attacks" may be secondary to medullary decompression and the resultant dysautonomia. A patient was also reported to have vertigo as the only presenting symptom of CM I with syrinx, with other causes unable to be found [8]. We treated a 7-year-old with unilateral hearing loss and vertigo-associated vomiting and a CM I without syrinx. At 2-year follow-up, her vertigo was resolved and her hearing loss has stabilized.

Infants can often have respiratory compromise with severe CM II. However, it is rare for this to occur in CM I or older patients. Alvarez et al. and Bokinsky et al. published reports of CM I resulting in acute respiratory failure [9, 10]. The patient's ages were 38 and 18 years old, respectively, and both had a concomitant syrinx. In 2004, a 22-month-old presented after multiple episodes of apnea. He was found to have a CM I, and after decompression he had no further episodes of apnea before being lost to follow-up a year later. Even more devastating, in 1993, Martinot et al. reviewed two pediatric cases (aged 4 and 13) who suffered sudden death, with postmortem evaluation only revealing CM I as the likely cause of death [11]. One patient had a syrinx and the other did not.

Although the mechanism is not clear and such an association may be incidental, there have been rare reports of endocrinologic dysfunction as a result of CM I. A 6-year-old girl was reported to present with profound hypoglycemia and CM I [12]. Furthermore, a young boy presented with precocious puberty in association with CM I [13].

Patients with CM I can also have ophthalmologic symptoms, most commonly nystagmus resulting from cerebellar compression. However, more unusual reports are found in the literature. Gingold et al. described a 41-year-old female with oscillopsia and CM I [14]. Acute acquired comitant esotropia resulting from CM I has been reported. These reports describe 11 patients ranging from 5 to 36 years old, both male and female, and both with and without an associated syrinx [15–19].

Unusual nonspecific symptoms are also described in case reports. Unrelenting and chronic hiccups were the presenting symptom of a 19-year-old male with CM I [20]. Eleven patients, with ages ranging from 18 months to 5 years, had their developmental delay (including seizures, motor retardation, and delayed speech) attributed to CM I [21]. Furthermore, Hudgins reported two children with paroxysmal rage as the presenting symptom of CM I [22]. The behavior troubles improved after treatment.

Extremity motor and sensory deficits are commonly seen in CM I. These are mostly caused by an expanding syrinx in the cervical or thoracic spinal cord and follow a progressive and subacute or chronic course. However, acute neurologic deficits may rarely be the presenting symptom of CM I. Most of these reports involve a traumatic event preceding the onset of symptoms. Yarbrough et al. reported multiple deficits with acute onset in the pediatric population with CM I and syrinx [5]. A 13-year-old female presented with the acute onset of upper and lower extremity paresthesias. After jumping on a trampoline, a 13-year-old female experienced right-sided

hemianesthesia. A 12-year-old female suffered the acute onset of quadriparesis after a fall. Likewise, after a fall, a 10-year-old male had lower extremity paraparesis. A football injury resulted in upper extremity paresthesias in a 14-year-old male with CM I. Another report of a football injury resulting in transient quadriparesis in an 8-year-old boy with CM I without a syrinx was reported by Callaway et al. [23].

Peripheral nerve syndromes have also been described as presenting symptoms of CM I. A 24-year-old male presented with ulnar nerve neuropathy at the elbow from CM I and syrinx [24]. Similarly, a 26-year-old female had a CM I with syrinx with carpal tunnel syndrome as the only symptom [25].

In 2008, Laufer et al. reported isolated dorsiflexion weakness in a 5-year-old male and plantar flexion weakness in a 9-year-old girl [26]. In both cases, weakness was the only presenting symptom, and both patients also had an associated syrinx.

Single case reports also exist for the coexistence of CM I and hypertension [27] hyperhidrosis [28], hemifacial spasm [29], and chronic emesis [30]. Each of these symptoms resolved following posterior fossa decompression, lending credence to a cause and effect. Lastly, some have suggested CM I may be at the root of some patients with autism although this neuroanatomic connection is not clear [31].

Conclusion

With the widespread use of magnetic resonance imaging (MRI), CM I is being diagnosed more often and at earlier ages. It is important to remember the more common symptoms that present with CM I and syrinx. However, if other etiologies are not found, especially in a patient with sensory or motor deficits or brain stem and lower cranial nerve symptoms, one might consider evaluating for CM I. In the end, unusual presentations may be found in patients with CM I, but as these may be incidental, the clinical evaluation should be even more stringent.

References

1. Heuer GG, Gabel B, Lemberg PS, Sutton LN. Chiari I malformation presenting with hearing loss: surgical treatment and literature review. Childs Nerv Syst. 2008;24(9):1063–6.
2. Hendrix RA, Bacon CK, Sclafani AP. Chiari-I malformation associated with asymmetric sensorineural hearing loss. J Otolaryngol. 1992;21:102–7.
3. Papanastassiou AM, Schwartz RB, Friedlander RM. Chiari I malformation as a cause of trigeminal neuralgia: case report. Neurosurgery. 2008;63(3):E614–5; discussion E615.
4. Yglesias A, Narbona J, Vanaclocha V, et al. Chiari type I malformation, glossopharyngeal neuralgia and central sleep apnoea in a child. Dev Med Child Neurol. 1996;38:1126–30.
5. Yarbrough CK, Powers AK, Park TS, Leonard JR, Limbrick DD, Smyth MD. Patients with Chiari malformation Type I presenting with acute neurological deficits: case series. J Neurosurg Pediatr. 2011;7(3):244–7.
6. Selmi F, Davies KG, Weeks RD. Type I Chiari deformity presenting with profound sinus bradycardia: case report and literature review. Br J Neurosurg. 1995;9:543–5.
7. Hampton F, Williams B, Loizou LA. Syncope as a presenting feature of hindbrain herniation with syringomyelia. J Neurol Neurosurg Psychiatry. 1982;45:919–22.
8. Titlic M, Jukic I, Tonkic A, Buca A, Dolic K. Vertigo associated with Chiari I malformation and syringomyelia. Bratisl Lek Listy. 2008;109(4):168–70.
9. Alvarez D, Requena I, Arias M, Valdés L, Pereiro I, De la Torre R. Acute respiratory failure as the first sign of Arnold-Chiari malformation associated with syringomyelia. Eur Respir J. 1995;8(4):661–3.
10. Bokinsky GE, Hudson LD, Weil JV. Impaired peripheral chemosensitivity and acute respiratory failure in Arnold-Chiari malformation and syringomyelia. N Engl J Med. 1973;288(18):947–8.
11. Martinot A, Hue V, Leclerc F, Vallee L, Closset M, Pruvo JP. Sudden death revealing Chiari type 1 malformation in two children. Intensive Care Med. 1993;19:73–4.
12. Rekate HL, Nadkarni TD, Teaford PA, Wallace D. Brainstem dysfunction in chiari malformation presenting as profound hypoglycemia: presentation of four cases, review of the literature, and conjecture as to mechanism. Neurosurgery. 1999;45(2):386–91.
13. Interlici S, Montanari E, Conrieri M, Peretta P, Genitori L, Benso L. A patient with early puberty associated with Chiari 1 malformation. J Pediatr Endocrinol Metab. 2000;13(Suppl 1):849–51.
14. Gingold SI, Winfield JA. Oscillopsia and primary cerebellar ectopia: case report and review of the literature. Neurosurgery. 1991;29:932–6.

15. Hentschel SJ, Yen KG, Lang FF. Chiari I malformation and acute acquired comitant esotropia: case report and review of the literature. J Neurosurg. 2005;102(4 Suppl):407–12.
16. Weeks CL, Hamed LM. Treatment of acute comitant esotropia in Chiari I malformation. Ophthalmology. 1999;106(12):2368–71.
17. Bixenman WW, Laguna JF. Acquired esotropia as initial manifestation of Arnold–Chiari malformation. J Pediatr Ophthalmol Strabismus. 1987;24:83–6.
18. Lewis AR, Kline LB, Sharpe JA. Acquired esotropia due to Arnold–Chiari I malformation. J Neuroophthalmol. 1996;16:49–54.
19. Passo M, Shults WT, Talbot T, Palmer EA. Acquired esotropia. A manifestation of Chiari I malformation. J Clin Neuroophthalmol. 1984;4:151–4.
20. Loft LM, Ward RF. Hiccups. A case presentation and etiologic review. Arch Otolaryngol Head Neck Surg. 1992;118:1115–9.
21. Brill CB, Gutierrez J, Mishkin MM. Chiari I malformation: association with seizures and developmental disabilities. J Child Neurol. 1997;12:101–6.
22. Hudgins RJ. Paroxysmal rage as a presenting symptom of the Chiari I malformation. Report of two cases. J Neurosurg. 1999;91:328–9.
23. Callaway GH, O'Brien SJ, Tehrany AM. Chiari I malformation and spinal cord injury: cause for concern in contact athletes? Med Sci Sports Exerc. 1996;28:1218–20.
24. Scelsa SN. Syringomyelia presenting as ulnar neuropathy at the elbow. Clin Neurophysiol. 2000;111(9):1527–30.
25. Ziadeh MJ, Richardson JK. Arnold-Chiari malformation with syrinx presenting as carpal tunnel syndrome: a case report. Arch Phys Med Rehabil. 2004;85(1):158–61.
26. Laufer I, Engel M, Feldstein N, Souweidane MM. Chiari malformation presenting as a focal motor deficit. Report of two cases. J Neurosurg Pediatr. 2008;1(5):392–5.
27. Tubbs RS, Wellons JC, Blount JP, Oakes WJ, Grabb PA. Cessation of chronic hypertension after posterior fossa decompression in a child with Chiari I malformation. Case report. J Neurosurg. 2004;100:194–6.
28. Stovner LJ, Sjaastad O. Segmental hyperhidrosis in two siblings with Chiari type I malformation. Eur Neurol. 1995;35:149–55.
29. Mukerji N, Newman P, Nath FP. Hemifacial spasm as a feature of Chiari malformation: case report. Neurosurgery. 2010;67:E1826–30.
30. Mortazavi MM, Tubbs RS, Harmon D, Oakes WJ. Chronic emesis due to compression of the area postrema by the posterior inferior cerebellar artery: resolution following microvascular decompression. J Neurosurg Pediatr. 2010;6:583–5.
31. Zeegers M, Van Der Grond J, Durston S, Nievelstein RJ, Witkamp T, Van Daalen E, Buitelaar J, Engeland HV. Radiological findings in autistic and developmentally delayed children. Brain and Development. 2006;28:495–9.

Clinical Presentation of Adult Chiari I

32

Ulrich Batzdorf

Chiari malformations presenting in adults have generally been referred to as Chiari I malformations. They may present in a variety of ways, probably related to differences in the anatomical abnormalities in the individual patient leading to the clinical diagnosis of Chiari malformation. This may vary from a relatively small posterior fossa to associated bony anomalies such as basilar impression or platybasia. Patients with membrane formation at the outlets of the fourth ventricle similar to those described by Gardner [1], or arachnoid membranes within the cisterna magna, may demonstrate a similar effect on cerebrospinal fluid (CSF) circulation as do impacted cerebellar tonsils [2] and may have certain features in common with patients who have tonsil descent. Some of these patients may also develop syringomyelia [2], and these were subsequently labeled "Chiari 0." Based on imaging criteria, a subgroup of Chiari patients has been defined who have descent of the brainstem as well as the cerebellar tonsils, through the foramen magnum. This group has been named Chiari 1.5. No specific clinical characteristics have been associated with this group [3]. Recognition of Chiari 1.5 is, however, of clinical importance. Many of these patients are included among the so-called complex Chiari cases, which often require more than the standard posterior fossa decompression procedure [4]. Other examples of complex Chiari cases include patients with retroflexed odontoid and scoliosis. In addressing the symptoms with which patients may present, it is also evident that some symptoms, such as generalized headache or fatigue, are not specific for Chiari malformation and are not uncommon in the general population. One can also surmise that there are individuals with low-lying cerebellar tonsils who remain asymptomatic throughout their lifetime [5].

It is, of course, important to distinguish symptoms due to the Chiari malformation per se from those that are due to coexisting syringomyelia. It is beyond the scope of this chapter to deal in detail with the clinical presentation of syringomyelia. Symptoms of spinal cord dysfunction, notably upper limb atrophy and sensory deficits as well as lower extremity and gait problems, are typical of syringomyelia. Spasticity and leg weakness in patients with syringomyelia, sometimes in combination with sensory impairment, may cause balance problems indistinguishable from those seen with Chiari malformation alone. Postural hypotension may be seen with syringomyelia due to loss of autonomic input and may also be seen in patients who have only a Chiari malformation. In part related to limitations in diagnostic imaging, earlier reviews of Chiari malformation tended not to separate symptoms due to Chiari malformation from those due to syringomyelia [6–9].

U. Batzdorf (✉)
Department of Neurosurgery, David Geffen School of Medicine at UCLA, Los Angeles, CA, USA
e-mail: UBatzdorf@mednet.ucla.edu

R. S. Tubbs et al. (eds.), *The Chiari Malformations*, https://doi.org/10.1007/978-3-030-44862-2_32

Age of Onset

Considering that the anatomical variants leading to Chiari malformation are present in early childhood, if not at birth, the reasons for onset of symptoms in adults, often in their 20s or 30s, are not entirely clear. It seems logical to assume that normal activities such as coughing and straining may result in an incremental downward creep of the tonsils and brainstem, until a point is reached at which CSF circulation is compromised. Accidental events such as jarring of the head may play a role in precipitating symptoms in some adults [10–12].

A review of the literature makes it clear that a listing of symptoms and findings in order of frequency of occurrence cannot be made, inasmuch as patient populations differ in different clinics and observations differ for different authors. Overall, the most commonly reported symptoms and findings for patients with Chiari malformation are listed in Table 32.1. Other frequently mentioned symptoms of unclear physiological basis include fatigue, memory impairment, and what has been called "brain fog."

There have been a number of comprehensive analyses of presenting symptoms and findings in patients with Chiari malformation. The most comprehensive is that of Milhorat et al. [12], summarized in Table 32.2.

Dyste, Menezes, and VanGilder [13] reported the glossopharyngeal and vagus nerves to be the most commonly involved cranial nerves, as demonstrated by an abnormal gag reflex, 15/50; 13/50 had trigeminal hypesthesia, 9 had unilateral hypoglossal involvement, and a few had facial weakness and abducens weakness on one side.

Table 32.1 The most common symptoms and findings for Chiari malformation

Symptoms	Findings
Headache	Nystagmus
Exertional	Impaired spontaneous venous pulsations
Others	Extraocular muscle palsy
Visual symptoms	Papilledema (rare)
Blurred vision	Gag reflex loss
Double vision	Hoarseness
Hearing-related symptoms	Facial sensation impairment
Tinnitus	Tongue atrophy (mostly unilateral)
Hearing impairment	Balance impairment—truncal
Balance difficulties	

Table 32.2 Presenting symptoms and findings in patients with Chiari malformation, according to Milhorat et al. [12]

Ocular disturbances	97/126 patients
Otoneurological disturbances	89/26 patients
Lower cranial nerve, brainstem, and cerebellar disturbances	69/126 patients

Pathophysiology of Symptoms and Findings

It is helpful to try to consider symptoms related to Chiari Malformation under the following broad categories:

I. Symptoms due to interference with normal CSF circulation.
II. Symptoms due to pontomedullary (brainstem) compression; cerebellar symptoms.
III. Symptoms due to downward descent of the cerebellar tonsils and traction on cranial nerves.

Symptoms Related to Interference with Normal Cerebrospinal Fluid Circulation

Strain-related headaches are the classical and pathognomonic manifestation of impaired transmission of the normal fluctuations in CSF pulsations at or near the foramen magnum. This may result from descent of the cerebellar tonsils into the foramen magnum or membranous occlusion of the CSF cisterns at or near the level of the foramen magnum. Brief transient increases in intracranial pressure with dural distention are believed to be the cause of these headaches. Occasionally patients also

complain of seemingly strain-related symptoms involving the upper extremities, and it may be relevant to invoke the mechanism suggested by Bell [14]. Coughing, straining, and other similar Valsalva-type activities may be cited by patients. Shouting or even blowing into a wind instrument has also been mentioned by patients as provoking such headaches. These headaches are typically brief in duration, lasting only seconds or minutes, are mostly localized to the suboccipital or upper cervical area, and may occur many times during the day. Such headaches are present in 80% to 100% of published cases [10, 12]. The exertional aspect of the headache is characteristic and helps to distinguish this classical symptom from other more common types of headache.

Patients may also complain of less typical headache, such as suboccipital pain, generalized headache, or retro-orbital headache. These are often considerably longer in duration. Other explanations have been offered for these types of headaches, including altered brain tissue compliance [15]. It should be recognized that patients with Chiari malformation may also have other types of headache and it is not uncommon to find patients with unrelated but coexisting migraine headache.

Patients with "Chiari 0" malformation, that is, obstruction of the CSF pathways at the level of the foramen magnum without tonsillar descent, might be expected to show some symptoms of this type, although manifestations of syringomyelia appear to dominate in reports [2].

Changes in CSF dynamics have also been cited as possibly affecting perilymph dynamics and thereby accounting for various otological symptoms, such as tinnitus, hearing impairment, and even dizziness [12].

Findings related to this transient increase in intracranial volume are the obliteration of normal spontaneous venous pulsations on funduscopic examination in the sitting position. Since other factors, including purely technical ones, may affect the identification of such spontaneous venous pulsations, their presence is often considered more significant as a negative finding. Rarely one may detect papilledema.

Brainstem and Cerebellar Symptoms

Visual and balance disturbances including blurred vision and occasionally double vision are among the most common presentations of Chiari malformation in adults. Patients may be aware of the nystagmoid motion of their eyes, and nystagmus is reported to be present in up to 70% of Chiari patients in some series [16] and 35% in others [17]. Downbeat nystagmus is said to be characteristic of abnormalities at the cervical-medullary junction [18]. Special testing may be helpful in defining the type of nystagmus [17]. Double vision is considered to be due to impaired conjugate eye movements [13]. This may result from impaired function of brainstem nuclei or their connections. Traction on cranial nerves—particularly trochlear and abducens but also oculomotor—has also been invoked.

Impaired balance may result from traction and distortion of cerebellar pathways due to hindbrain descent and may be seen as frequently as in 40% of patients [8]. It is usually seen as truncal imbalance, rather than appendicular incoordination, and patients may have difficulty with gait, tandem gait, and tandem Romberg stance. Dizziness and balance problems were encountered in almost 60% of patients in one reported series [10]. "Dizziness" reported by patients may be positionally related, raising questions of positional vertigo in the differential diagnosis. Tinnitus has also been cited by a number of authors [12, 16, 18]. The mechanisms are not entirely clear, inasmuch as tinnitus might result from transmitted alterations in CSF fluid dynamics to the inner ear (see above) or downward traction on the eighth nerve complex.

Swallowing difficulties, particularly of liquids, are a not-infrequent complaint, ranging from 6% to 45% of patients [12, 13, 19]. Impairment of the gag reflex is frequently noted but can be related to other factors, possibly including the effects of medication, and this finding does not correlate closely with swallowing complaints. Hoarseness is less common but more specifically related to involvement of lower cranial nerve function. Facial pain in tri-

geminal distribution has been attributed to involvement of the spinal nucleus of the fifth nerve. Trigeminal area pain and findings of sensory loss in trigeminal distribution have been reported by a number of authors [12, 13, 19, 20]. Unilateral tongue atrophy has occasionally been noted [13, 16].

The entire range of autonomic symptoms must also be considered in this category. Up to 10% of patients have such symptoms, including drop attacks [12, 16, 18], bradycardia [21], dyspnea, syncopal episodes [22–24], and palpitations. Various forms of sleep disturbances are not uncommonly reported by patients with Chiari malformation. This includes central sleep apnea [25]. These disturbances may be related to brainstem compression involving the respiratory centers or reticular activating system [6]. Other mechanisms to explain sleep disturbances have also been proposed, including stretching of the lower cranial nerves by downward descent of the brainstem and abnormal chemoreceptor sensitivity. Patients with abnormal respiratory response to carbon dioxide have been reported [7]. Vocal cord paralysis and impaired diaphragmatic innervation may contribute to altered sleep patterns in these patients. Sleep studies may be of help in identifying patterns of a specific sleep disorder. Impotence has been reported particularly in patients with Chiari malformation and associated basilar invagination [23].

Syncope may be encountered in relation to coughing or other Valsalva-type maneuvers as well as with head movements and may be due to momentary increased brainstem compression with briefly increased tonsillar descent or possibly to brief vascular compression [22]. Profound sinus bradycardia has been documented in at least one instance and could be the underlying mechanism for a number of symptoms, including transient loss of consciousness and some instances of dizziness [21]. Death, attributed to respiratory distress, syncope, and respiratory arrest, has been cited, and there have been isolated reports of sudden death [26, 27].

Symptoms Due to Downward Descent of the Cerebellar Tonsils and Traction on the Cranial Nerves

It is difficult to know the precise mechanism by which some "brainstem" symptoms are produced and indeed different mechanisms may interact to produce certain symptoms in any one patient. Thus hoarseness and swallowing problems might arise either from brainstem compression or from traction on the lower cranial nerves, particularly cranial nerves IX and X. The possible contribution of traction on these nerves to sleep-related problems has been cited above. Involvement of the hypoglossal nerve with tongue fasciculations and atrophy has also been reported [8, 13, 19, 20] as noted above. Penfield and Coburn's [28] autopsy description provides excellent detail of the extent of cranial nerve stretching as well as stretching of the upper cervical nerve roots.

Frontal or generalized headaches encountered in Chiari malformation patients have been attributed to a variety of mechanisms (see above), including cervicogenic etiologies. Frontal headaches may also arise from direct compression of the second spinal nerve, as proposed by Kerr [29].

Chiari Malformation as Manifestation of Other Diseases

Crowding of the posterior fossa may result from bony thickening, including the occipital bone, as seen in hypophosphatemic rickets. Caldemeyer et al. [30] report Chiari malformation in 7 of 16 patients with this metabolic disorder. Flattening of the posterior fossa by thick bone characterized this subtype of patients (five of seven), and two patients with severe bone thickening also had syringomyelia. Four of seven had ventriculomegaly. There did not appear to be any specific clinical features of Chiari malformation that distinguished this group of patients. Tubbs et al. [31] established that the posterior fossa volume in children with rickets was significantly smaller

than in age-matched controls, presumably also true for rickets patients who reach adult age.

Bony encroachment of the foramen magnum may also be seen in patients with Paget's disease. Flattening of the foramen magnum with reduction of its anteroposterior diameter in conjunction with basilar invagination has been described [32]. Seen in as many as one-third of patients with Paget's disease, it may lead to alterations in CSF flow at the level of the foramen magnum that give rise to symptoms of Chiari malformation and may also be associated with the development of syringomyelia [33].

In both the aforementioned conditions, there may be narrowing of the spinal canal due to bony thickening, which may contribute to the development of myelopathy. This includes those patients who also have syringomyelia.

Early closure of the lambdoidal sutures in patients is the likely explanation for a relatively small posterior fossa and the high incidence of tonsillar ectopia (73%) [34]. Although the study was performed in children, adults with Crouzon's disease presumably are similarly involved.

Similar bony changes of a small, shallow posterior fossa, leading to symptoms of Chiari malformation, may be seen in achondroplastics [35, 36].

Based on imaging criteria, an association of hereditary connective tissue disorders (HCTD) and Chiari I malformation was reported by one group of investigators [37]. These patients presented with symptoms of Chiari malformation, and evidence for connective tissue disorder was sought subsequently. Cranio-cervical stability needs particular attention in HCTD patients. Royo-Salvador et al. [38] reported an association between Chiari malformation and tethering of the spinal cord at the level of the filum terminale in a small group of adult patients. The concept remains controversial in spite of a larger and more recent study [39]. Some of these patients had symptoms suggesting cauda equina abnormalities. Filum tethering may be verified by comparing prone and supine magnetic resonance imaging (MRI) studies of the cauda equina.

Secondary Chiari Malformations

At first glance the fact that cerebellar tonsillar descent may occur with both increased and decreased intracranial pressures may seem contradictory. These patients fall into two main categories: (1) idiopathic intracranial hypertension (IIH) (pseudotumor cerebri) and (2) undiagnosed or occult cerebrospinal fluid leaks at the spinal level. The importance of this subgroup of patients lies in the fact that both conditions may be easily missed. Patients with IIH may undergo posterior fossa decompression because of descended cerebellar tonsils, only to have acute or subacute postoperative problems related to their elevated intracranial pressure. Patients with an occult CSF leak may have little or only transient relief of their symptoms following posterior fossa decompressive surgery. This form of secondary tonsillar descent may also be encountered in patients who have undergone lumboperitoneal shunting. Clinically it is often manifested by headache related to upright posture and relieved when the patient lies down. Although first recognized in children who underwent such shunting [40], it was also observed in adults who had undergone lumboperitoneal shunts and may even be accompanied by syringomyelia [41]. Secondary Chiari malformation has also been reported in association with cerebrospinal fluid leaks [42]. In our own experience, pseudotumor cerebri was encountered in 2 of 177 patients, and an occult CSF leak in 1 of 177 patients.

Both problems can be diagnosed preoperatively, provided consideration is given to these diagnoses in the preoperative assessment. Preoperative intracranial pressure measurements [43] are the most conclusive way to make the diagnosis and avoid problems. Consideration should be given to such a study in selected patients with a high level of suspicion, even though it is invasive.

Differential Diagnosis

Other causes of headache, even of strain-related headache, need to be considered in the differential diagnosis. Nystagmus and imbalance have sometimes led to concern about a diagnosis of multiple sclerosis. Syringobulbia may produce many of the brainstem symptoms and signs seen with Chiari malformation [44].

The most difficult situation arises in patients with borderline descent of the cerebellar tonsils who have some symptoms such as headache and other symptoms not uncommon in the general population. Imaging studies that show somewhat low-lying cerebellar tonsils but without narrowing of the subarachnoid spaces may be interpreted as a borderline Chiari malformation by a radiologist, giving rise to patient concerns. Many patients then also read about this entity, so that it may become difficult to obtain a patient history "uncontaminated" by other inputs.

In spite of our increased awareness of the disease entity and alertness to a variety of presentations seen in patients with Chiari malformation, it is unfortunately far too common to encounter patients whose symptoms have been passed off, sometimes for years, before the correct diagnosis is established. This problem may be aggravated by very rigid adherence to imaging-derived measurements, which may also completely overlook patients with membranous occlusion at the foramen magnum without tonsillar descent (Chiari 0 malformation) [2] who present with at least some typical Chiari malformation symptoms.

References

1. Gardner WJ, Abdullah AF, McCormack LJ. The varying expressions of embryonal atresia of the fourth ventricle in adults. J Neurosurg. 1957;14:591–605.
2. Iskandar BJ, Hedlund GL, Grabb PA, Oakes WJ. The resolution of syringohydromyelia without hindbrain herniation after posterior fossa decompression. J Neurosurg. 1998;80:212–6.
3. Tubbs SR, Iskandar BJ, Bartolucci AA, Oakes WJ. A critical analysis of the Chiari 1.5 malformation. J Neurosurg Ped. 2004;101:179–83.
4. Brockmeyer DL. The complex Chiari: issues and management strategies. Neurol Sci. 2011;32(Suppl 3): S347.
5. Meadows J, Kraut M, Guarnieri M, Haroun RI, Carson BC. Asymptomatic Chiari Type I malformations identified on magnetic resonance imaging. J Neurosurg. 2000;92:920–6.
6. Gagnadoux F, Meslier N, Svab I, Menei P, Racineux JL. Sleep-disordered breathing in patients with Chiari malformation: improvement after surgery. Neurology. 2006;66:136–8.
7. Nogués M, Gené R, Benarroch E, Leiguarda R, Calderón C, Encabo H. Respiratory disturbances during sleep in syringomyelia and syringobulbia. Neurology. 1999;52:1777–83.
8. Paul KS, Lye RH, Strang F, Dutton J. Arnold-Chiari malformation. J Neurosurg. 1983;58:183–7.
9. Saez RJ, Onofrio BM, Yanagihara T. Experience with Arnold-Chiari malformation, 1960 to 1970. J Neurosurg. 1976;45:416–22.
10. Ellenbogen RG, Armonda RA, Shaw DWW, Winn HR. Toward a rational treatment of Chiari I malformation and syringomyelia. Neurosurg Focus. 2000;8(3):Article 6, 1–10.
11. Mampalam TJ, Andrews BT, Gelb D, Ferriero D, Pitts LH. Presentation of Type I Chiari malformation after head trauma. Neurosurgery. 1988;23(6):760–2.
12. Milhorat TH, Chou MW, Trinidad EM, Kula RW, Mandell M, Wolpert C, et al. Chiari I malformation redefined: clinical and radiographic findings for 364 symptomatic patients. Neurosurgery. 1999;44:1005–17.
13. Dyste GN, Menezes AH, VanGilder JC. Symptomatic Chiari malformations. An analysis of presentation, management, and long-term outcome. J Neurosurg. 1989;71:159–68.
14. Bell HS. Paralysis of both arms from injury of the upper portion of the pyramidal decussation: "cruciate paralysis". J Neurosurg. 1970;33:376–80.
15. Bejjani GK, Cockerham KP. Adult Chiari Malformation. Contemp Neurosurg. 2001;23(26):1–7.
16. Dobkin BH. The adult Chiari malformation. Bull Los Angel Neurol Soc. 1977;42(1):23–7.
17. Kumar A, Patni AH, Charbel F. The Chiari malformation and the Neurotologist. Otol Neurotol. 2002;23:727–35.
18. Menezes AH, Smoker WRK, Dyste GN. Syringomyelia, Chiari malformations, and hydromyelia. Chapter 46. In: Youmans JR, editor. Neurological surgery. 3rd ed. Philadelphia: WB Saunders Co.; 1990. p. 1421–59.
19. Foster JB, Hudgson P. The clinical features of communicating Syringomyelia. In: Barnett HJM, Foster JB, Hudgson P, editors. Syringomyelia. London: WB Saunders Co; 1973. p. 16–29.
20. Mohr PD, Strang FA, Sambrook MA, Boddie HG. The clinical and surgical features in 40 patients with primary cerebellar ectopia (adult Chiari malformation). Quart J Med (New Series). 1977;46:85–96.
21. Selmi F, Davies KG, Weeks RD. Type I Chiari deformity presenting with profound sinus bradycardia: case report and literature review. Brit J Neurosurg. 1995;9:543–5.

22. Weig SG, Buckthal PE, Choi SK, Zellem RT. Recurrent syncope as the presenting symptom of Arnold-Chiari malformation. Neurology. 1991;41:1673–4.
23. Goncalves da Silva JA, de Farias Britto JC, Virgolino da Nóbrega P. Neurovegetative Störungen bei 230 Fällen basilärer Impression und Arnold-Chiarischer Miβbildung. Neurochirurgia. 1992;35:183–8.
24. Tubbs RS, Iskandar BJ, Bartolucci AA, Oakes WJ. A critical analysis of the Chiari 1.5 malformation. J Neurosurg (Ped 2). 2004;101:179–83.
25. Levitt P, Cohn MA. Sleep apnea and the Chiari I malformation: case report. Neurosurgery. 1988;23:508–10.
26. Friede RL, Roessmann U. Chronic tonsillar herniation. Acta Neuropathol. 1976;34:219–35.
27. Williams B. Chronic herniation of the hindbrain. Ann R Coll Surg Engl. 1981;63(1):9–17.
28. Penfield W, Coburn DF. Arnold-Chiari malformation and its operative treatment. Arch Neurol Psychiatr. 1938;40:328–36.
29. Kerr FWL. A mechanism to account for frontal headache in cases of posterior-fossa tumors. J Neurosurg. 1961;18:605–9.
30. Caldemeyer KS, Boaz JC, Wappner RS, Moran CC, Smith RR, Quets JP. Chiari I malformation: association with hypophosphatemic rickets and MR imaging appearance. Radiology. 1995;195:733–8.
31. Tubbs RS, Webb D, Abdullatif H, Conklin M, Doyle S, Oakes WJ. Posterior cranial fossa volume in patients with rickets: insights into the increased occurrence of Chiari I malformation in metabolic bone disease. Neurosurgery. 2004;55:380–4.
32. Schmidek HH. Neurologic and neurosurgical sequelae of Paget's disease of bone. Clin Orthop. 1977;127:70–7.
33. Elisevich K, Fontaine S, Bertrand G. Syringomyelia as a complication of Paget's disease. J Neurosurg. 1987;66:611–3.
34. Cinalli G, Renier D, Sebag G, Sainte-Rose C, Arnaud E, Pierre-Kahn A. Chronic tonsillar herniation in Crouzon's and Apert's syndromes: the role of premature synostosis of the lambdoid suture. J Neurosurg. 1995;83:575–82.
35. Nakai T, Asato R, Miki Y, Tanaka F, Matsumoto S, Konishi J. A case of achondroplasia with downward displacement of the brain stem. Neuroradiology. 1995;37:293–4.
36. Ryken TC, Menezes AH. Cervicomedullary compression in achondroplasia. J Neurosurg. 1994;81:43–8.
37. Milhorat TH, Bolognese PA, Nishikawa M, McDonnell NB, Francomano CA. Syndrome of occipitoatlantoaxial hypermobility, cranial settling, and Chiari malformation Type I in patients with hereditary disorders of connective tissue. J Neurosurg Spine. 2007;7:601–9.
38. Royo-Salvador MB, Solé-Lienas J, Doménech JM, González-Adrio R. Results of section of the filum terminale in 20 patients with syringomyelia, scoliosis and Chiari malformation. Acta Neurochir. 2005;147(5):513–23.
39. Milhorat TH, Bolognese PA, Nishikawa M, Francomano CA, McDonnell NB, Roonprapunt C, et al. Association of Chiari malformation type I and tethered cord syndrome: preliminary results of sectioning filum terminale. Surg Neurol. 2009;72:20–35.
40. Hoffman HJ, Tucker WS. Cephalocranial disproportion. A complication of the treatment of hydrocephalus in children. Childs Brain. 1976;2:167–76.
41. Welch K, Shillito J, Strand R, Fischer EG, Winston KR. Chiari I "malformations" – an acquired disorder? J Neurosurg. 1981;55:604–9.
42. Samii C, Möbius E, Weber W, Heienbrok HW, Berlit P. Pseudo Chiari type I malformation secondary to cerebrospinal fluid leakage. J Neurol. 1999;246:162–4.
43. Bergsneider M, Yang I, Hu X, McArthur DL, Cook SW, Boscardin WJ. Relationship between valve opening pressure, body position and intracranial pressure in normal pressure hydrocephalus: paradigm for selection of programmable valve pressure setting. Neurosurgery. 2004;55:851–3.
44. Jonesco-Sisesti N. Syringobulbia. A contribution to the pathophysiology of the brainstem. Translated by Ross RT (ed). New York: Praeger Publishers; 1986.

33 Acute and Sudden Presentations of the Chiari Malformations

Jacob K. Greenberg and Matthew D. Smyth

Introduction

Chiari malformation type 1 (CM I) is typically defined by descent of the cerebellar tonsils ≥5 mm below the foramen magnum [1]. The widespread availability and utilization of magnetic resonance imaging (MRI) have revealed the notable prevalence of this radiologic diagnosis, seen in approximately 1–4% of MRI studies [1, 2]. Indeed, diagnosis of CM I is a common reason for elective pediatric neurosurgical referral, where providers evaluate for the presence of diverse signs or symptoms that may warrant neurosurgical intervention [3]. While CM I symptoms, such as headaches and cerebellar dysfunction, classically present in a slowly progressive fashion, rarely CM I patients can present with the abrupt onset or worsening of neurological deficits [4, 5].

These acute presentations can range from motor or sensory deficits to severe respiratory dysfunction or even death [5]. While the incidence of such abrupt presentations is unknown, there have been growing reports of these cases over the past four decades, providing an evolving perspective on this important subset of CM I patients. Given the relative rarity of this presentation, data on this topic has largely derived from individual case reports and small case series that provide a limited perspective on this condition. In this chapter we attempt to summarize those individual reports, which are presented in Table 33.1 [4, 6–49]. In doing so, we hope to provide an overview on the following topics pertaining to the sudden onset of neurological deficits related to CM I: presenting characteristics; the significance of comorbidities, such as syringomyelia or hydrocephalus; the role of trauma and sports participation; and, finally, the treatment and prognosis of these patients.

Clinical Presentations

While found in patients of all ages, CM I has a largely bimodal distribution, often presenting in both children and middle-age adults [50, 51]. The MRI prevalence of CM I is higher in children (up to 3.6%) [1] than adults (less than 1%) [2, 52], though limited administrative data suggest that more adults undergo surgery for symptomatic disease [50, 51]. In the current review, 66% of the cases of rapid-onset neurological deficits from CM I were diagnosed in children younger than 18 years. In the general CM I population, males represent about 50% of pediatric and 20% of adult patients undergoing CM I surgery [50, 51]. By comparison, males comprised 53% of patients with abrupt symptom development, including 57% of adults. While not conclusive,

J. K. Greenberg (✉) · M. D. Smyth
Department of Neurological Surgery, Washington University School of Medicine, St. Louis, MO, USA
e-mail: jacobgreenberg@wustl.edu

R. S. Tubbs et al. (eds.), *The Chiari Malformations*, https://doi.org/10.1007/978-3-030-44862-2_33

Table 33.1 Summary of reported cases of acute neurological deficits in patients with CM I

Series	Age (years)	Sex	Presentation	Syrinx	Preceding trauma	Treatment	Outcome
Tomaszek et al., 1984 [6]	3	M	Fall, followed by emesis, restlessness and fever, and ultimately apnea	No	Yes	None	Death
Bresnan et al., 1987 [7]	17	F	Sudden-onset numbness, weakness, emesis, diplopia, rotary nystagmus, right tongue deviation, and hyperreflexia. Preceded by 1 year of right leg numbness and recent spinal manipulation	Yes	Yes	Cervical laminectomy, myelotomy, and syringo-subarachnoid stenting with duraplasty	Partial resolution
Dong, 1987 [8]	8	M	Torticollis and hyperreflexia within 24 hrs of tonsillectomy	Yes	No	Chiari decompression+ ventricular drainage	Partial resolution
Vlcek and Ito, 1987 [9]	2	M	Gait unsteadiness, paraparesis, urinary retention, and hyperreflexia after a fall	No	Yes	Chiari decompression	Complete resolution
Bullock et al., 1988 (#1) [10]	26	F	2 weeks of dyspnea followed by lethargy and cyanosis, hyperreflexia, and bilateral diaphragm paralysis	Yes	No	Chiari decompression with syrinx aspiration	Partial resolution
Bullock et al., 1988 (#2) [10]	58	F	2 days of confusion, fall with minor head trauma, and decreased ventilatory status	Yes	Yes	Chiari decompression	Partial resolution
Mampalam et al., 1988 [11]	13	F	MVC with transient cardiac arrest followed by intubation for stridor, loss of gag reflex, and cranial nerve X and XI palsies	No	Yes	None	Partial resolution
Riviello et al., 1990 [12]	2	F	Tetraparesis and respiratory failure after a fall off a horse	No	Yes	None	Partial resolution
Martinot et al., 1993 (#1) [13]	13	F	Sudden dyspnea, followed 7 months later by dyspnea and cardiac arrest	No	No	None	Death
Martinot et al., 1993 (#2) [13]	4	F	Cardiac arrest	Yes	No	None	Death
Bondurant and Oro, 1993 [14]	2	M	Rapidly progressive tetraparesis after a fall, followed by respiratory distress and urinary retention	Yes	Yes	None	Partial resolution
Zager et al., 1990 (#1) [15]	32	F	Progressive facial and arm pain, followed by sudden headache, vertigo, sensory changes, nystagmus, dysmetria, cranial nerve X palsy, weakness, and urinary retention	Yes	No	Chiari decompression	Partial resolution
Zager et al., 1990 (#2) [15]	48	F	Sudden dyspnea and vocal cord paralysis 9 years after Chiari decompression; hand weakness and impaired sensation	Yes	No	T1 laminectomy and myelotomy, syringo-subarachnoid shunt	Partial resolution

Table 33.1 (continued)

Series	Age (years)	Sex	Presentation	Syrinx	Preceding trauma	Treatment	Outcome
Kanev et al., 1994 [16]	13	F	Acute-onset diplopia with left-gaze paralysis	Yes	No	Chiari decompression	Complete recovery
Alvarez et al., 1995 [17]	38	M	Respiratory failure; cranial nerve IX, X, and XII palsies; muscular atrophy; and hyperreflexia	Yes	No	Chiari decompression	Partial resolution
James, 1995 [18]	25	M	Punched in the head, followed by cardiac arrest and death	Yes	Yes	None	Death
Callaway et al., 1996 [19]	8	M	Hit the head during a football tackle followed by transient paresthesias	No		Chiari decompression	Resolution
Jackson and Penrose-Stevens, 1997 [20]	23	F	Nystagmus, cranial nerve VI palsy, dysphonia, dysphagia, quadriparesis, and hyperreflexia along with meningitis	Yes	No	Chiari decompression + EVD	Partial resolution
Wolf et al., 1998 (#1) [21]	71	M	Sudden death from presumed minor trauma	No	Yes	None	Death
Wolf et al., 1998 (#2) [21]	22	M	Sudden death following syncope and minor head trauma	No	Yes	None	Death
Weeks et al., 1999 [22]	14	M	Diplopia, esotropia	No	No	Strabismus correction, Chiari decompression	Complete resolution
Ziegler and Mallonee, 1999 [23]	17	M	Pulmonary failure and death. History of hemibody numbness, headache, and previous Chiari decompression	Yes	No	None	Death
Bunc and Vorsic, 2001 [24]	35	F	Rapidly worsening head/neck pain, paresthesias, gait ataxia, and hoarseness with cranial nerve IX and X palsies 5 months after an MVC	No	Yes	Chiari decompression	Partial resolution
Gentry et al., 2001 [25]	38	M	Months of dyspnea, subacute numbness, dysphagia, and ataxia, with acute respiratory distress	Yes	No	Chiari decompression	Partial resolution
Defoort-Dhellemmes et al., 2002 [26]	9	M	Diplopia, headache, hyperreflexia, and esotropia	No	No	Chiari decompression	Partial resolution
Yoshikawa et al., 2003 [27]	7	M	Acute respiratory distress	No	No	None	Complete resolution
Kurup et al., 2005 [28]	17	M	Acute tetraparesis after football tackle	No	Yes	None	Complete resolution
Quebada and Duhaime, 2005 [29]	11	F	Hit in the head with baseball and fall, followed by respiratory arrest and upper extremity weakness	No	Yes	Chiari decompression	Partial resolution

(continued)

Table 33.1 (continued)

Series	Age (years)	Sex	Presentation	Syrinx	Preceding trauma	Treatment	Outcome
Tsara et al., 2005 [30]	32	M	Acute respiratory failure, with cranial nerve IX–XII palsies. Mild numbness, weakness, and hyperreflexia	Yes	No	Chiari decompression	Persistent symptoms
Bhangoo et al., 2006 (#1) [31]	7	M	6 weeks of lethargy with acute respiratory depression	Yes	No	Chiari decompression	Partial resolution
Bhangoo et al., 2006 (#2) [31]	13	F	Worsening of chronic hemiparesis, acute respiratory depression; initially asymptomatic ventriculomegaly	Yes	No	Chiari decompression	Partial resolution
Pilon et al., 2007 [32]	30	F	2 weeks of blurry vision and bilateral cranial nerve VI palsies	Yes	No	Chiari decompression	Partial resolution
Wellons et al., 2007 (#1) [33]	16	M	Headache, neck pain, dysphagia, hemiparesis, respiratory distress, and hyperreflexia	No	No	Chiari decompression	Partial resolution
Wellons et al., 2007 (#2) [33]	7	M	Hemiparesis, hypesthesia, hyperreflexia, and anisocoria	Yes	No	Chiari decompression	Partial resolution
Kandasamy et al., 2008 [34]	14	M	Visual disturbance, headache, and tinnitus. Opening pressure 47 on lumbar puncture	Yes	No	ETV	Complete resolution
Stephany et al., 2008 [35]	27	M	Months of falls and intermittent apnea, 2 weeks of headache, and then sudden death	No	No	None	Death
Elliott et al., 2009 (#1) [36]	16	M	Tetraparesis, urinary retention, and cranial nerve VI palsy; history of shunted hydrocephalus	No	No	Chiari decompression + shunt revision	Partial resolution
Elliot et al., 2009 (#2) [36]	14	M	Cranial nerve VI, VII, and X palsies, ataxia; history of shunted hydrocephalus	Yes	No	Chiari decompression + shunt revision	Partial resolution
McMillan et al., 2011 (#1) [37]	5	F	Foot drop with diminished sensation	Yes	No	Chiari decompression	Partial resolution
McMillan et al., 2011 (#2) [37]	4	F	Foot drop with diminished sensation	Yes	No	Chiari decompression	Complete resolution
Massimi et al., 2011 (#1) [38]	38	M	Acute respiratory failure and enlargement of known syrinx, hydrocephalus; intubation for surgery 5 days earlier	Yes	Yes	ETV	Complete resolution
Massimi et al., 2011 (#2) [38]	1	M	Hemiparesis, partial Horner's sign, dysphagia, 1 day after minor head trauma	No	Yes	Chiari decompression	Complete resolution
Massimi et al., 2011 (#3) [38]	2	M	Tetraparesis, hypesthesia, respiratory failure after flexion/extension neck injury	Yes	Yes	Chiari decompression	Partial resolution

Table 33.1 (continued)

Series	Age (years)	Sex	Presentation	Syrinx	Preceding trauma	Treatment	Outcome
Yarbrough et al., 2011 (#1) [4]	12	F	Quadriparesis	Yes	Yes	Chiari decompression	Complete resolution
Yarbrough et al., 2011 (#2) [4]	13	F	Paresthesias	Yes	No	Chiari decompression	Complete resolution
Yarbrough et al., 2011 (#3) [4]	3	M	Vocal cord paresis	No	No	Chiari decompression	Complete resolution
Yarbrough et al., 2011 (#4) [4]	14	M	Paresthesias, head injury during football	Yes	Yes	Chiari decompression	Complete resolution
Yarbrough et al., 2011 (#5) [4]	10	M	Paraparesis after a fall	Yes	Yes	Chiari decompression	Complete resolution
Yarbrough et al., 2011 (#6) [4]	13	F	Right hemianesthesia after a trampoline flip	Yes	Yes	Chiari decompression	Complete resolution
Pettorini et al., 2011 [39]	15	F	Headache, left hand paresthesias, blurry vision, and presumed idiopathic intracranial hypertension	No	No	Chiari decompression + EVD	Complete resolution
Carew et al., 2012 (#1) [40]	1	M	Respiratory distress, drooling, and tetraparesis; hydrocephalus	Yes	No	Chiari decompression + EVD	Complete resolution
Carew et al., 2012 (#2) [40]	19 mo	F	Truncal ataxia and quadriceps weakness	No	No	Chiari decompression	Complete resolution
Oishi et al., 2013 [41]	11	F	Dysesthesia and spastic monoparesis, decreased gag reflex; history of hydrocephalus s/p ETV	No	No	Chiari decompression	Complete resolution
Schneider et al., 2013 [42]	19	F	Tetraparesis, generalized paresthesias, and neck pain	Yes	No	Chiari decompression	Near resolution
Zhang et al., 2013 [43]	17	F	Sudden death after head trauma	No	Yes	None	Death
Roohi et al., 2014 [44]	29	M	Acute on chronic worsening headache, stable hydrocephalus	No	None	None	Death
Wang et al., 2014 (#1) [45]	47	F	Acute quadriplegia and loss of gag/cough reflex 3 days after developing meningitis, progressive tonsillar herniation on MRI	No	No	Chiari decompression	Complete resolution
Wang et al., 2014 (#1) [45]	23	M	Fall and head trauma followed by transient quadriplegia, paresthesias, dysphagia, and gait dysfunction	No	Yes	Chiari decompression	Complete resolution
Spina et al., 2015 [46]	6 mo	M	Dysphagia, lethargy after a fall	No	Yes	None	Complete resolution

(continued)

Table 33.1 (continued)

Series	Age (years)	Sex	Presentation	Syrinx	Preceding trauma	Treatment	Outcome
Ulutabanca et al., 2015 [47]	47	M	Numbness, dysphagia, ataxia, hyperreflexia, and cranial nerve VI palsy after tooth extraction	Yes	No	Chiari decompression	Complete resolution
Miranda et al., 2016 [48]	3	M	Hemiparesis, drooling, incontinence	Yes	No	Chiari decompression	Complete resolution
Woodward and Adler, 2018 [49]	41	M	Paraparesis, apnea, C4 sensory level after a hit to the face	No	Yes	Chiari decompression	Partial resolution

MVC motor vehicle collision, *EVD* extraventricular drain, *ETV* endoscopic third ventriculostomy, *MRI* magnetic resonance imaging

these findings suggest that children and males may have a relatively increased susceptibility to the sudden development of neurological deficits.

In the general CM I population, occipital and/or cervical pain is the most common clinical presentation reported in a number of large clinical series [53, 54]. The comparatively piecemeal reporting of sudden-onset CM I deficits in case reports and small case series limits the extent to which the prevalence of specific presentations can be reliability estimated. Nonetheless, among the 62 cases identified in this review, motor deficits appeared particularly common, occurring in 48% of patients. This substantially exceeds the approximately 10% prevalence of such deficits reported by Tubbs and colleagues in their series of 500 CM I patients [55]. Significant respiratory impairment was noted in 31% of reports compared to a 1% rate of dyspnea in the Tubbs series. Aside from respiratory distress, cranial nerve dysfunction—including hoarseness, dysphagia, and loss of a gag reflex—was seen in 35% of patients compared to 10% reported by Tubbs and colleagues. Hyperreflexia was also noted in at least 23% of patients. A variety of less common findings were also seen, including gait ataxia, urinary retention, and torticollis. In addition, two patients developed symptoms in the context of acute meningitis [20, 45].

Notably, we identified ten reported cases of sudden death likely attributed to CM I. Preceding trauma was noted in five of these cases [6, 18, 21], and some degree of preexisting symptoms were likely present in at least three cases [23, 35, 44]. One of these patients also had hydrocephalus, further complicating the picture [21, 44]. Death from CM I is likely to be related to severe brainstem compression. Given the brainstem's integral role in controlling respiratory function (Fig. 33.1 [56]), pulmonary failure is an important cause of death in CM I. In these cases, medullary or pontine dysfunction may impair the body's normal respiratory drive, or death may result from vocal cord dysfunction from vagal nerve or nucleus involvement. In cases of a cervical spinal cord syrinx, diaphragm paralysis due to phrenic nerve dysfunction is another possible cause of respiratory distress in CM I [10]. In rare instances, impaired peripheral chemosensitivity from glossopharyngeal nerve involvement has been implicated as a cause of respiratory failure in patients with CM I and syringomyelia [30]. Aside from primary pulmonary failure, sudden death due to CM I may also relate to cardiac dysfunction due to vagal nucleus or other brainstem injuries, which are known to occur in CM I patients [4, 53]. The presence of hydrocephalus, as was the case in one CM I patient with sudden death, creates an additional mechanism for brainstem injury [21, 44].

We also identified several reports of unusual clinical events in patients with CM I that were

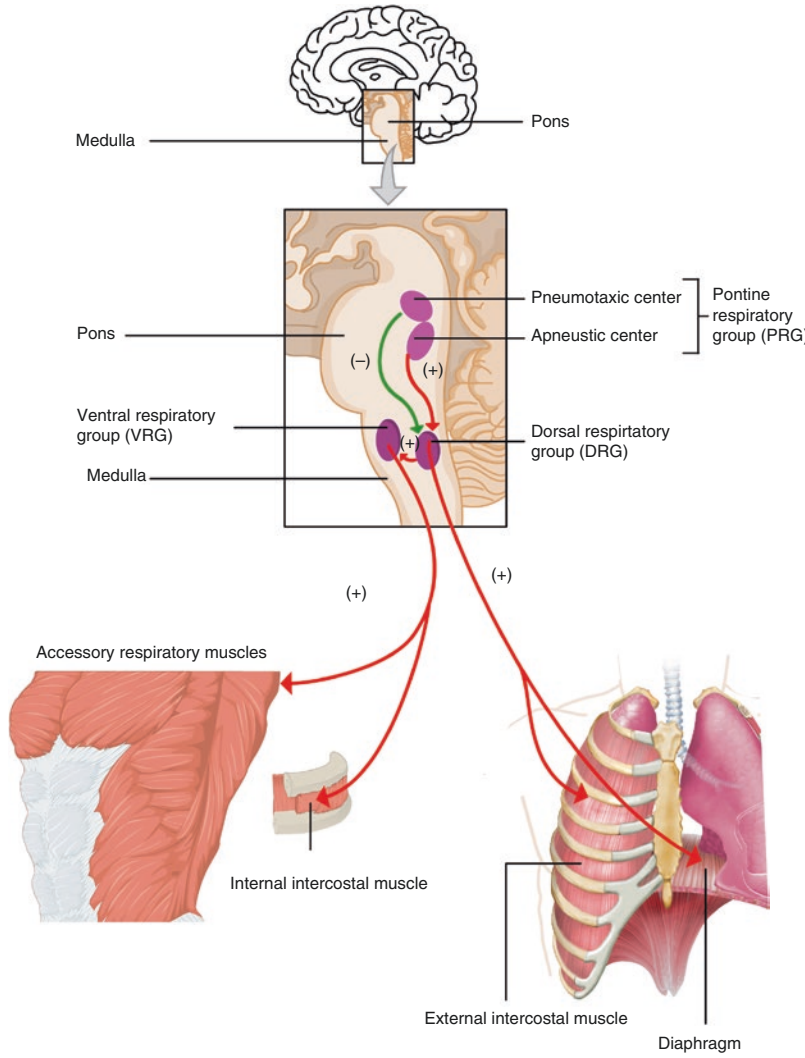

Fig. 33.1 A diagram demonstrating the brainstem's control over respiratory function. (Reproduced with permission from the textbook *Anatomy & Physiology*, published by OpenStax with a Creative Commons license (https://creativecommons.org/licenses/by/4.0/) [56]. Access for free at http://cnx.org/contents/14fb4ad7-39a1-4eee-ab6e-3ef2482e3e22@6.27)

not clearly attributable to their CM I pathology. For example, one child had sudden respiratory arrest with spontaneous resolution and was subsequently found to have CM I on MRI [27]. Another published report described ventricular fibrillation arrest with successful resuscitation following sudden head movement while showering [57]. While we attempted to exclude cases where CM I seemed unlikely to have been involved, such instances are inherently ambiguous, and caution should be taken when implicating CM I as the cause of these unexplained events.

Comorbid Conditions

The exact incidence of syringomyelia in CM I is unknown. Estimates of syrinx prevalence in the general CM I literature range from 12% [58]

to 85% [59], though most larger series report a range of 20–30% [1, 50–52]. In the current series of 62 reviewed cases, 55% had syringomyelia. This finding suggests that while the presence of a syrinx might confer a slightly increased risk, it is not a prerequisite for the development of abrupt neurological deficits.

In the current series, 13% of patients also had a diagnosis of ventriculomegaly or hydrocephalus, which is slightly higher than the 8–10% rate reported in large series of CM I patients [1, 55]. The relationship between hydrocephalus and CM I is complex and varies among patients. In some cases, the CM I is simply a reflection of raised intracranial pressure from obstructive hydrocephalus and possible shunt malfunction [60, 61]. We generally did not include these cases in our series. Often, the relationship is less clear. While some patients respond to treatment of hydrocephalus alone [38], others appeared to be symptomatic from both problems, requiring treatment for both hydrocephalus and CM I to achieve significant neurological improvement [36]. Finally, in rare circumstances, CM I can be associated with raised intracranial pressure without radiological evidence of hydrocephalus [39]. In at least one such instance, symptoms resolved after treatment with endoscopic third ventriculostomy (ETV) alone [34]. These diverse cases emphasize the importance of recognizing hydrocephalus and CM I as separate but often related entities that must each be addressed appropriately in patients with rapid-onset disease.

Aside from syringomyelia and hydrocephalus, patients in the current series were found to have a number of rarer comorbid conditions, including Noonan syndrome [38], basilar impression [17], Klippel-Feil syndrome [17], and an arachnoid cyst [38]. CM I is also known to be associated with other conditions, such as craniosynostosis, which may affect presentations and treatment strategies in some cases [62]. While the scarcity of these conditions limits the evaluation of their significance, such factors could be relevant to the presentations of specific patients.

The Role of Head and Neck Trauma

The extent to which CM I patients have a unique susceptibility to head trauma has been a long-standing question in the neurosurgical literature [11, 63–66]. In the current series of 62 patients, 42% had some form of head trauma noted preceding the onset of their symptoms. Of those with head trauma, 42% also had a syrinx. While some of these cases involved convincing episodes of trauma [4, 9, 11, 29], in other instances the instigating injury was quite minor [38] or was temporally removed from the development of clinical symptoms [24].

In the broader neurosurgical literature, several studies have examined the risk of sports participation in CM I patients. Strahle and colleagues prospectively followed 328 CM I patients who participated in 4641 sports seasons, including 205 patients who played contact sports [65]. Meehan and colleagues surveyed CM I patients regarding their participation in 1627 athletic seasons, including 191 seasons of collision sports [66]. Although each study reported one patient with potential injury-related paresthesias, no cases of sports-related motor weakness or other neurological deficits were noted. Based on these results and the cases identified in this review, we recognize that CM I may confer a slightly increased risk of a catastrophic injury after trauma, but the magnitude of this risk remains exceedingly small. Furthermore, many CM I patients with sudden death or neurological deficits do not have preceding trauma. Consequently, in our own practice, we typically permit asymptomatic CM I patients without a syrinx to return to play but caution patients with CM I and a syrinx to avoid contact sports until treatment, given the theoretical concern for significant injury with head trauma.

Treatment and Clinical Outcome

Patients with CM I who develop sudden- or rapid-onset neurological deficits require urgent evaluation commensurate to the severity of the patient's clinical presentation. As previously noted, 16% of patients in the current series died due to complications related to CM I, with respiratory failure implicated as an important etiology. Furthermore, of those patients who did not die, 33% were found to have some form of respiratory dysfunction, emphasizing the need for physicians to closely attend to airway concerns in CM I patients. In particular all patients with significant or progressive respiratory concerns should receive close hemodynamic monitoring, and physicians should consider the need for early endotracheal intubation in severe cases.

Once acute cardiopulmonary concerns have been addressed, attention should be directed to definitive treatment for acutely symptomatic patients. The optimal surgical approach for treatment of CM I remains a source of controversy. While posterior fossa decompression has been generally accepted as the standard-of-care first-line treatment [67], many questions remain, including the degree of bony removal and the need for dural augmentation [67, 68]. Those questions are addressed in more detail elsewhere in this book, and the results of an ongoing randomized trial will also provide more conclusive evidence regarding the need for duraplasty.

In the current series, 68% of patients were treated with some variation of a standard Chiari decompression. Other surgical treatments employed included cervical myelotomy and syringo-subarachnoid stenting [69], syrinx aspiration [10], and ventricular drainage [8]. These alternatives to a standard decompression all occurred during or before 1990. Among patients where hydrocephalus or elevated intracranial pressure was thought to contribute to the patient's symptoms, endoscopic third ventriculostomy was performed in two cases [34, 70]: shunt revision in two cases [36] and external ventricular drain placement in three cases [31, 39, 40]. At least one patient with initially asymptomatic ventriculomegaly required a delayed shunt several months after initial treatment [31]. Excluding patients who died suddenly, 12% were managed with observation or other nonsurgical interventions only.

While physicians must address associated pathologies, such as symptomatic hydrocephalus or spinal cord compression, posterior fossa decompression and C1 laminectomy, with or without dural augmentation, should be the mainstay treatment for acutely symptomatic CM I patients. For patients with relatively mild symptoms, such as new numbness without a motor deficit, extradural decompression is reasonable and is often the initial intervention in our practice. However, given the possibility of superior outcomes, we recommend posterior fossa decompression with dural augmentation for patients with severe symptoms, including vocal cord dysfunction, respiratory distress, or motor deficits [4]. We generally reserve other treatments, such as syrinx fenestration and shunting, for treatment-resistant or otherwise unique cases.

There is sparse evidence guiding the timing of surgical treatment for cases of CM I with sudden neurological deterioration. Nonetheless, we generally recommend treating such patients in an expedited manner, with urgent decompression considered for patients with severe symptoms, such as progressive motor or cranial nerve dysfunction. In addition, while some authors reported relative improvement without surgical intervention [11, 12, 14], we generally recommend surgical treatment for patients who have developed significant symptoms from CM I, even if there is temporary improvement.

Rapidly progressive symptoms in CM I can cause severe dysfunction and even death, emphasizing the importance of early diagnosis and intervention. Nonetheless, excluding those who die suddenly, most patients who obtain appropriate treatment will show significant improvement if not complete symptom resolution. In the current

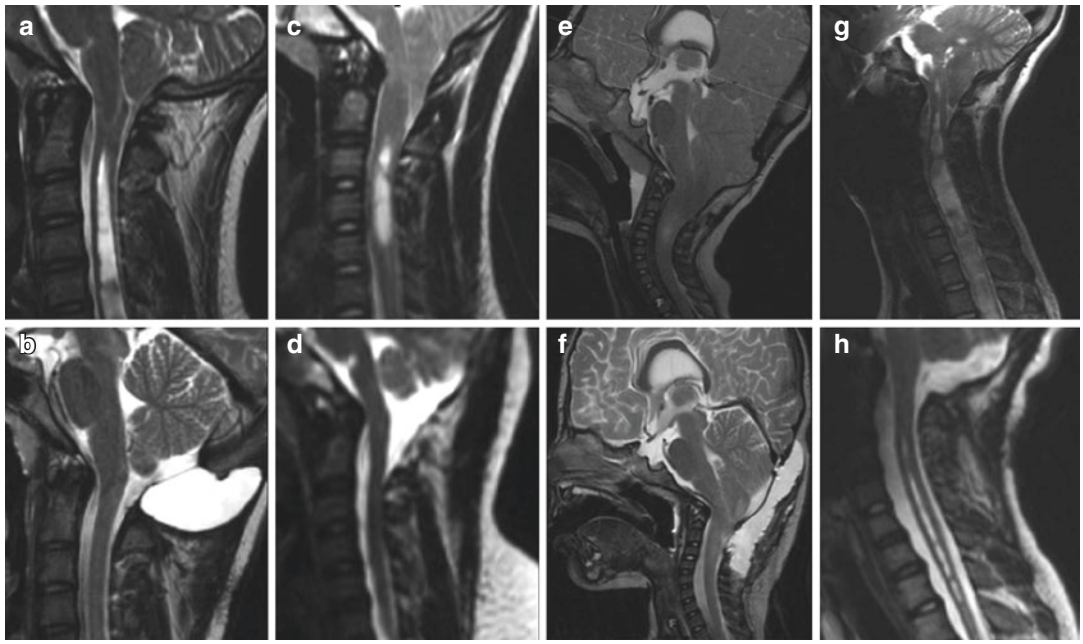

Fig. 33.2 Sagittal cut MRI images before (**a**, **c**, **e**, **g**) and after (**b**, **d**, **f**, **h**) CM I decompression in patients with acute neurological deficits. Postoperative imaging demonstrates a smaller or resolved syrinx. (Reproduced with permission from Yarbrough et al. [4])

series, 44% of patients experienced complete and 39% had partial resolution of symptoms. While complete information on syrinx response to treatment was not available, representative pre- and posttreatment MRI images are shown in Fig. 33.2 [4]. These results suggest that early intervention may in fact lead to better outcomes for patients with rapidly progressive deficits than those who have experienced more prolonged dysfunction related to syringomyelia or syringobulbia [3, 71].

Conclusion

While CM I is typically a slowly progressive disease that often presents with pain and headaches [55], an important minority of patients present with sudden- or rapid-onset neurological deficits. These patients often have motor deficits, respiratory compromise, and other cranial nerve abnormalities and may even present with sudden death. Comorbid syringomyelia and hydrocephalus may influence presentation, particularly in those with acute post-traumatic sensorimotor deficits. While patients with rapid clinical presentations are at risk for severe cardiopulmonary decline or significant neurological compromise, they often respond well to early surgical intervention. Consequently, it is essential that both neurosurgeons and non-neurosurgeons recognize the unique characteristics of this subset of CM I patients to enable early diagnosis and proper management.

References

1. Strahle J, Muraszko KM, Kapurch J, Bapuraj JR, Garton HJ, Maher CO. Chiari malformation Type I and syrinx in children undergoing magnetic resonance imaging. J Neurosurg Pediatr. 2011;8(2):205–13.
2. Meadows J, Kraut M, Guarnieri M, Haroun RI, Carson BS. Asymptomatic Chiari Type I malformations identified on magnetic resonance imaging. J Neurosurg. 2000;92(6):920–6.
3. Greenberg JK, Yarbrough CK, Radmanesh A, Godzik J, Yu M, Jeffe DB, et al. The Chiari severity index: a preoperative grading system for Chiari malformation type 1. Neurosurgery. 2015;76(3):279–85; discussion 85.

4. Yarbrough CK, Powers AK, Park TS, Leonard JR, Limbrick DD, Smyth MD. Patients with Chiari malformation Type I presenting with acute neurological deficits: case series. J Neurosurg Pediatr. 2011;7(3):244–7.
5. Massimi L, Della Pepa GM, Caldarelli M, Di Rocco C. Abrupt clinical onset of Chiari type I/syringomyelia complex: clinical and physiopathological implications. Neurosurg Rev. 2012;35(3):321–9; discussion 9.
6. Tomaszek DE, Tyson GW, Bouldin T, Hansen AR. Sudden death in a child with an occult hindbrain malformation. Ann Emerg Med. 1984;13(2):136–8.
7. Bresnan MJ, Shoukimas GM, Hedley-Whyte ET. Case 3-1987. N Engl J Med. 1987;316(3):150–7.
8. Dong ML. Arnold-Chiari malformation type I appearing after tonsillectomy. Anesthesiology. 1987;67(1):120–2.
9. Vlcek BW, Ito B. Acute paraparesis secondary to Arnold-Chiari type I malformation and neck hyperflexion. Ann Neurol. 1987;21(1):100–1.
10. Bullock R, Todd NV, Easton J, Hadley D. Isolated central respiratory failure due to syringomyelia and Arnold-Chiari malformation. Br Med J. 1988;297(6661):1448–9.
11. Mampalam TJ, Andrews BT, Gelb D, Ferriero D, Pitts LH. Presentation of type I Chiari malformation after head trauma. Neurosurgery. 1988;23(6):760–2.
12. Riviello JJ Jr, Marks HG, Faerber EN, Steg NL. Delayed cervical central cord syndrome after trivial trauma. Pediatr Emerg Care. 1990;6(2):113–7.
13. Martinot A, Hue V, Leclerc F, Vallee L, Closset M, Pruvo JP. Sudden death revealing Chiari type 1 malformation in two children. Intensive Care Med. 1993;19(2):73–4.
14. Bondurant CP, Oro JJ. Spinal cord injury without radiographic abnormality and Chiari malformation. J Neurosurg. 1993;79(6):833–8.
15. Zager EL, Ojemann RG, Poletti CE. Acute presentations of syringomyelia. Report of three cases. J Neurosurg. 1990;72(1):133–8.
16. Kanev PM, Getch CC, Jallo J, Faerber EN. Cerebral syrinx with Chiari I malformation. Pediatr Neurosurg. 1994;20(3):214–6.
17. Alvarez D, Requena I, Arias M, Valdes L, Pereiro I, De la Torre R. Acute respiratory failure as the first sign of Arnold-Chiari malformation associated with syringomyelia. Eur Respir J. 1995;8(4):661–3.
18. James DS. Significance of chronic tonsillar herniation in sudden death. Forensic Sci Int. 1995;75(2–3):217–23.
19. Callaway GH, O'Brien SJ, Tehrany AM. Chiari I malformation and spinal cord injury: cause for concern in contact athletes? Med Sci Sports Exerc. 1996;28(10):1218–20.
20. Jackson RM, Penrose-Stevens A. Meningococcal meningitis with Arnold-Chiari malformation. J Infect. 1997;35(1):90–2.
21. Wolf DA, Veasey SP 3rd, Wilson SK, Adame J, Korndorffer WE. Death following minor head trauma in two adult individuals with the Chiari I deformity. J Forensic Sci. 1998;43(6):1241–3.
22. Weeks CL, Hamed LM. Treatment of acute comitant esotropia in Chiari I malformation. Ophthalmology. 1999;106(12):2368–71.
23. Ziegler DK, Mallonee W. Chiari-1 malformation, migraine, and sudden death. Headache. 1999;39(1):38–41.
24. Bunc G, Vorsic M. Presentation of a previously asymptomatic Chiari I malformation by a flexion injury to the neck. J Neurotrauma. 2001;18(6):645–8.
25. Gentry JB, Gonzalez JM, Blacklock JB. Respiratory failure caused by Chiari I malformation with associated syringomyelia. Clin Neurol Neurosurg. 2001;103(1):43–5.
26. Defoort-Dhellemmes S, Denion E, Arndt CF, Bouvet-Drumare I, Hache JC, Dhellemmes P. Resolution of acute acquired comitant esotropia after suboccipital decompression for Chiari I malformation. Am J Ophthalmol. 2002;133(5):723–5.
27. Yoshikawa H. Sudden respiratory arrest and Arnold-Chiari malformation. Eur J Paediatr Neurol. 2003;7(4):191.
28. Kurup H, Lawrence T, Hargreaves D. Transient Quadriparesis following neck injury: presentation of a Chiari 1 malformation. Eur J Orthop Surg Traumatol. 2005;15(4):319–21.
29. Quebada PB, Duhaime AC. Chiari malformation Type I and a dolichoodontoid process responsible for sudden cardiorespiratory arrest. Case report. J Neurosurg. 2005;103(6 Suppl):567–70.
30. Tsara V, Serasli E, Kimiskidis V, Papagianopoulos S, Katsaridis V, Fylaktakis M, et al. Acute respiratory failure and sleep-disordered breathing in Arnold-Chiari malformation. Clin Neurol Neurosurg. 2005;107(6):521–4.
31. Bhangoo R, Sgouros S, Walsh AR, Clarke JR. Hindbrain-hernia-related syringomyelia without syringobulbia, complicated by permanent nocturnal central hypoventilation requiring non-invasive ventilation. Childs Nerv Syst. 2006;22(2):113–6.
32. Pilon A, Rhee P, Newman T, Messner L. Bilateral abducens palsies and facial weakness as initial manifestations of a Chiari 1 malformation. Optom Vis Sci. 2007;84(10):936–40.
33. Wellons JC 3rd, Tubbs RS, Bui CJ, Grabb PA, Oakes WJ. Urgent surgical intervention in pediatric patients with Chiari malformation type I. report of two cases. J Neurosurg. 2007;107(1 Suppl):49–52.
34. Kandasamy J, Kneen R, Gladstone M, Newman W, Mohamed T, Mallucci C. Chiari I malformation without hydrocephalus: acute intracranial hypertension managed with endoscopic third ventriculostomy (ETV). Childs Nerv Syst. 2008;24(12):1493–7.
35. Stephany JD, Garavaglia JC, Pearl GS. Sudden death in a 27-year-old man with Chiari I malformation. Am J Forensic Med Pathol. 2008;29(3):249–50.
36. Elliott R, Kalhorn S, Pacione D, Weiner H, Wisoff J, Harter D. Shunt malfunction causing acute neurological deterioration in 2 patients with previously

asymptomatic Chiari malformation Type I. report of two cases. J Neurosurg Pediatr. 2009;4(2):170–5.
37. McMillan HJ, Sell E, Nzau M, Ventureyra EC. Chiari 1 malformation and holocord syringomyelia presenting as abrupt onset foot drop. Childs Nerv Syst. 2011;27(1):183–6.
38. Massimi L, Della Pepa GM, Tamburrini G, Di Rocco C. Sudden onset of Chiari malformation Type I in previously asymptomatic patients. J Neurosurg Pediatr. 2011;8(5):438–42.
39. Pettorini BL, Gao A, Rodrigues D. Acute deterioration of a Chiari I malformation: an uncommon neurosurgical emergency. Childs Nerv Syst. 2011;27(6):857–60.
40. Carew CL, Prasad A, Tay KY, de Ribaupierre S. Unusual presentation of Chiari I in toddlers: case reports and review of the literature. Childs Nerv Syst. 2012;28(11):1965–70.
41. Oishi M, Hayashi Y, Kita D, Fukui I, Shinohara M, Heiss JD, et al. Rapidly progressing monoparesis caused by Chiari malformation type I without syringomyelia. Surg Neurol Int. 2013;4:79.
42. Schneider B, Birthi P, Salles S. Arnold-Chiari 1 malformation type 1 with syringohydromyelia presenting as acute tetraparesis: a case report. J Spinal Cord Med. 2013;36(2):161–5.
43. Zhang J, Shao Y, Qin Z, Liu N, Zou D, Huang P, et al. Sudden unexpected death due to Chiari type I malformation in a road accident case. J Forensic Sci. 2013;58(2):540–3.
44. Roohi F, Gropen T, Kula RW. Sudden unexpected nocturnal death in Chiari type 1 malformation and potential role of opioid analgesics. Surg Neurol Int. 2014;5:17.
45. Wang H, Wang B, Normoyle K, Farahvar A, Olivero W. Chiari I malformation with acute brain stem compression syndromes requiring emergency neurosurgical intervention: report of two cases. J Neurol Disord. 2014;2(5):177.
46. Spina A, Boari N, Gagliardi F, Donofrio CA, Mortini P. Sudden onset of Chiari malformation type 1 in a young child after trauma. Childs Nerv Syst. 2015;31(9):1589–94.
47. Ulutabanca H, Kucuk A, Tumturk A, Bicer E, Oral S, Koc R. Chiari malformation Type 1 associated with syringomyelia which clinical symptoms occuring during tooth extraction. Erciyes Tıp Dergisi/Erciyes Med J. 2015;37(10).
48. Miranda SP, Kimmell KT, Silberstein HJ. Acute presentation of Chiari I malformation with hemiparesis in a pediatric patient. World Neurosurg. 2016;85:366.e1–4.
49. Woodward JA, Adler DE. Chiari I malformation with acute neurological deficit after craniocervical trauma: case report, imaging, and anatomic considerations. Surg Neurol Int. 2018;9:88.
50. Greenberg JK, Ladner TR, Olsen MA, Shannon CN, Liu J, Yarbrough CK, et al. Complications and resource use associated with surgery for Chiari malformation Type 1 in adults: a population perspective. Neurosurgery. 2015;77:261.
51. Greenberg JK, Olsen MA, Yarbrough CK, Ladner TR, Shannon CN, Piccirillo JF, et al. Chiari malformation Type I surgery in pediatric patients. Part 2: complications and the influence of comorbid disease in California, Florida, and New York. J Neurosurg Pediatr. 2016;17(5):525–32.
52. Kahn EN, Muraszko KM, Maher CO. Prevalence of Chiari I malformation and syringomyelia. Neurosurg Clin N Am. 2015;26(4):501–7.
53. Rozzelle CJ. Clinical presentation of pediatric Chiari I malformations. In: Tubbs RS, Oakes WJ, editors. The Chiari malformations. New York: Springer New York; 2013. p. 247–51.
54. Batzdorf U. Clinical presentation of the adult Chiari I malformation. In: Tubbs RS, Oakes WJ, editors. The Chiari malformations. New York: Springer New York; 2013. p. 253–9.
55. Tubbs RS, Beckman J, Naftel RP, Chern JJ, Wellons JC 3rd, Rozzelle CJ, et al. Institutional experience with 500 cases of surgically treated pediatric Chiari malformation Type I. J Neurosurg Pediatr. 2011;7(3):248–56.
56. OpenStax. Anatomy & Physiology: OpenStax CNX; Jul 30, 2014.
57. Alegre S, Garcia-Rubira JC, Patrignani G. Cardiac arrest in a 31-year-old man because of the Arnold-Chiari malformation. Int J Cardiol. 1994;46(3):286–8.
58. Aitken LA, Lindan CE, Sidney S, Gupta N, Barkovich AJ, Sorel M, et al. Chiari Type I malformation in a pediatric population. Pediatr Neurol. 2009;40(6):449–54.
59. Menezes AH. Chiari I malformations and hydromyelia--complications. Pediatr Neurosurg. 1991;17(3):146–54.
60. Milhorat TH, Bolognese PA, Black KS, Woldenberg RF. Acute syringomyelia: case report. Neurosurgery. 2003;53(5):1220–1; discussion 1-2.
61. Di Rocco C, Frassanito P, Massimi L, Peraio S. Hydrocephalus and Chiari type I malformation. Childs Nerv Syst. 2011;27(10):1653–64.
62. Cinalli G, Spennato P, Sainte-Rose C, Arnaud E, Aliberti F, Brunelle F, et al. Chiari malformation in craniosynostosis. Childs Nerv Syst. 2005;21(10):889–901.
63. Haroun RI, Guarnieri M, Meadow JJ, Kraut M, Carson BS. Current opinions for the treatment of syringomyelia and chiari malformations: survey of the Pediatric Section of the American Association of Neurological Surgeons. Pediatr Neurosurg. 2000;33(6):311–7.
64. Kirschen MP, Illes J. Ethical implications of an incidentally discovered asymptomatic Chiari malformation in a competitive athlete. Continuum (Minneapolis, Minn). 2014;20(6 Sports Neurology):1683–7.
65. Strahle J, Geh N, Selzer BJ, Bower R, Himedan M, Strahle M, et al. Sports participation with Chiari I malformation. J Neurosurg Pediatr. 2016;17(4):403–9.
66. Meehan WP 3rd, Jordaan M, Prabhu SP, Carew L, Mannix RC, Proctor MR. Risk of athletes with Chiari malformations suffering catastrophic injuries during sports participation is low. Clin J Sport Med. 2015;25(2):133–7.

67. Oaks WJ. Treatment of the pediatric Chiari I malformation. In: Tubbs RS, Oakes WJ, editors. The Chiari malformations. New York: Springer New York; 2013. p. 307–13.
68. Lee A, Yarbrough CK, Greenberg JK, Barber J, Limbrick DD, Smyth MD. Comparison of posterior fossa decompression with or without duraplasty in children with Type I Chiari malformation. Childs Nerv Syst. 2014;30(8):1419–24.
69. Anonymous. Case records of the Massachusetts General Hospital. Weekly clinicopathological exercises. Case 3-1987. A 17-year-old girl with numbness of the right leg and the recent onset of vertigo and right-sided weakness. N Engl J Med. 1987;316(3):150–7.
70. Massimi L, Pravata E, Tamburrini G, Gaudino S, Pettorini B, Novegno F, et al. Endoscopic third ventriculostomy for the management of Chiari I and related hydrocephalus: outcome and pathogenetic implications. Neurosurgery. 2011;68(4):950–6.
71. Ranalli NJ, Limbrick DD, Park TS. Outcomes for the surgical management of Chiari I and Chiari II malformations. In: Tubbs RS, Oakes WJ, editors. The Chiari malformations. New York: Springer New York; 2013. p. 333–44.

Associated Disorders of Chiari Type I Malformations

34

R. Shane Tubbs and W. Jerry Oakes

Introduction

Chiari postulated that the cerebellar herniation might have been due to hydrocephalus with the three different types representing various degrees of disease progression [1]. In ensuing years, Chiari's mechanism of pathogenesis would be disproven as the primary cause of Chiari malformation type I (CM I). Among the classifications, however, no current consensus exists for the exact pathogenesis or treatment regime for all [2]. Many have formed theories such as the hindbrain dysgenesis and developmental arrest theory, caudal traction theory, small posterior fossa/hindbrain overgrowth theory, hydrocephalus and hydrodynamic theory of Gardner, and the lack of embryological ventricular distention theory, yet no single theory has been able to prove a single pathway in the pathogenesis of CM I [3–15]. This chapter will discuss the conditions associated with CM I in order to potentially shed light on how the pathophysiological mechanism of one condition, no matter how remote, might lead to the development of CM I. Many of these associations are summarized in Table 34.1. It should be noted that many of these associations may be incidental with an asymptomatic hindbrain hernia being identified due to testing for other pathologic entities, e.g., endocrinopathies.

R. S. Tubbs (✉)
Department of Neurosurgery, Tulane University School of Medicine, New Orleans, LA, USA

Department of Neurosurgery and Ochsner Neuroscience Institute, Ochsner Health System, New Orleans, LA, USA

W. J. Oakes
Departments of Neurosurgery and Pediatrics, University of Alabama, Birmingham, AL, USA

Pathophysiology

Small Posterior Cranial Fossa

Morphometric studies by authors such as Schady [16] and Milhorat [8] have provided evidence that the volume of the posterior cranial fossa in CM I patients was less than the controls. Furthermore, Badie [3] discovered the ratio of posterior fossa volume to supratentorial space ratio was significantly lower in symptomatic CM I patients compared to control patients. Marin-Padilla and Marin-Padilla [17] added to the understanding of this anatomical pathology by inducing underdevelopment of the basi-occiput and posterior fossa in hamsters through high doses of vitamin A. In doing so, these authors demonstrated how impairing posterior fossa development could induce caudal displacement of the cerebellum. Others, however, have challenged this proposition with studies showing no difference in posterior fossa volume in this group [18]. Additional morphological findings in CM I may include an underdeveloped supraocciput and

R. S. Tubbs et al. (eds.), *The Chiari Malformations*, https://doi.org/10.1007/978-3-030-44862-2_34

Table 34.1 Disorders associated with Chiari type I malformations

Craniosynostosis
Antley-Bixler syndrome
Apert's syndrome
Crouzon's syndrome
Jackson-Weiss syndrome
Kleeblattschädel syndrome
Loeys-Dietz syndrome type I
Seckel syndrome
Shprintzen-Goldberg syndrome
Endocrinology
Achondroplasia
Acromegaly
Growth hormone deficiency
Hyperostosis
Craniometaphyseal dysplasia
Erythroid hyperplasia
Osteopetrosis
Paget's disease
Bone mineral deficiency
Familial vitamin D-resistant rickets
Cutaneous disorders
Acanthosis nigricans
Blue rubber bleb nevus syndrome
Giant congenital melanocytic nevi
Leopard syndrome
Macrocephaly-cutis marmoratatelangiectatica congenita
Neurofibromatosis type I
Phacomatosis pigmentovascularis type II
Waardenburg syndrome
Spinal defects
Atlantoaxial assimilation
Basilar impression
Caudal regression syndrome
Klippel-Feil syndrome
Lipomeningomyelocele
Odontoid retroflexion
Spondyloepiphyseal dysplasia
Space-occupying lesions
Others
Beckwith-Wiedemann syndrome
CHERI
Cloacal exstrophy
Costello syndrome
Cystic fibrosis
Ehlers-Danlos syndrome
Fabry disease
Kabuki syndrome
Pierre Robin syndrome
Situs inversus
Williams-Beuren syndrome

exocciput, large foramen magnum, short clivus, and longer anterior cranial fossa [19–22]. Therefore, while it may be a common school of thought, a smaller posterior fossa does not necessarily lead to CM I.

Hydrocephalus

Hans Chiari's aforementioned original theory regarding the causative association between hydrocephalus and hindbrain herniation has not allowed for an all-encompassing explanation into the pathophysiology of CM I. Nonetheless, hydrocephalus is seen in approximately 4–18% of CM I patients [3, 14]. Tubbs et al. in a review of 500 patients treated between 1989 and 2010 demonstrated that 9.8% of patients had concomitant hydrocephalus [23]. These patients all required cerebrospinal fluid (CSF) diversion in addition to an operative posterior fossa decompression. The association is likely secondary to fourth ventricular outflow tract obstruction or concurrent aqueductal stenosis. As a result, endoscopic third ventriculostomy has been used with success in this patient population.

Craniosynostosis

Craniosynostosis and CM I is a well-documented association first noted by Saldino [24] in which certain cases will have abnormalities in the skull base with subsequent decreased posterior fossa volume and tonsillar herniation. More specifically, this most often occurs when the lambdoid sutures fuse too early in skull development, which is representative of 1% of all types of craniosynostosis [25]. Synostosis can exist solitarily or as part of a syndrome such as Crouzon's (72.7%), Apert's (1.9%), Pfeiffer's (50%), and Kleeblattschädel syndromes (100%) [26, 27]. Additional studies estimated the Crouzon's syndrome association to be as high as 70% [28]. Moreover, CM I is now thought to be associated with Pfeiffer type II [29], Jackson-Weiss [30], Seckel [31], Antley-Bixler [32], and Shprintzen-Goldberg syndromes [33] as well. In each of these associated syndromes, CM I is not present at birth because the lambdoid suture has not yet fused. The incidence and severity, however, have been correlated to the time of closure [34, 35]. Therefore, the higher incidence of CM I in Crouzon's syndrome patients can be explained by the median fusion time of 6 and 21 months as compared to that of Apert's syndrome at 51 and

60 months of age [26]. Normally, the skull continues to expand along with brain growth until the age of 16 years [36].

Although lambdoid synostosis is the most common type of craniosynostosis to be associated with CM I, evidence of additional premature suture closures leading to CM I is growing. In utero synostosis of the sagittal and coronal sutures, for example, can force neural growth posteriorly and inferiorly as is present in the association with Loeys-Dietz syndrome [37]. As a result, the attachment of the tentorium cerebelli is displaced toward the foramen magnum with subsequent reduction in posterior fossa size and development of CM I [27]. Additionally, Tubbs et al. [38] reported a 30% incidence of CM I associated with simple metopic ridging without signs of trigonocephaly. Tubbs et al. [38] hypothesized this was the result of a decrease in anterior cranial fossa volume and that the incidence of metopic ridging in this population may be overestimated.

Endocrinopathy

Reduced posterior fossa volume is also seen in other medical conditions, including those involved in cell signaling. For example, growth hormone deficiency (GHD) has been linked to CM I with 5–20% of GHD patients [39, 40]. This endocrine deficiency in children is thought to be a physiological mechanism for insufficient development of the posterior fossa with resultant tonsillar herniation [41]. While the posterior fossa volume of GHD patients has not been found to be significantly smaller, research has shown certain bony structures to be underdeveloped similar to those commonly seen in CM I patients [41]. Additionally, somatotropin replacement therapy in patients with GHD and CM I has resulted in improvement of tonsillar herniation with stabilization in syrinx size in some patients [22]. Conclusive evidence, however, of the pathophysiological mechanism and possible treatments is yet to be determined.

Acromegaly has also been implicated as an endocrine-related disorder causing CM I that also fits in the category of hyperostosis. In this scenario, an excessive amount of growth hormone is thought to thicken the bones of the posterior fossa resulting in CM I. CM I has also been seen in patients with achondroplasia because of the small, shallow posterior cranial fossa present in these patients [42].

Hyperostosis

When hyperostosis affects the posterior fossa, it can lead to CM I. Paget's disease of the skull is one example in which exaggerated bone turnover leads to thickening and deformation of bones. When this process takes place in the skull, it can compromise the posterior fossa and in a few cases has been reported to result in CM I. Both Iglesias [43] and Richards [44] have described cases of this association.

Cases of CM I relating to craniometaphyseal dysplasia are rare but have nonetheless been reported. Craniometaphyseal dysplasia, similar to the other types of hyperostosis, can manifest with CM I due to abnormal bone formation and progressive thickening. Of the few cases, Sewell [45] documented cervicomedullary compression as well. CM I secondary to osteopetrosis [46] and erythroid hyperplasia [47] has been documented but is also considered to be exceptionally rare.

Bone Mineral Deficiency

In regard to bone mineral deficiencies, familial vitamin D-resistant rickets has also been coupled with CM I at 44% [48], thought to be due to overcrowding of the posterior fossa. In this condition, bony overgrowths and calvarial thickening as a result of low serum phosphate have been proposed to be the attributing factor. Further studies, however, have not found a difference in rachitic patients' posterior fossa volume, and thus the pathophysiological mechanism remains unknown [49]. Kuether [50] suggested in a case study that CM I development from rickets is due to foramen magnum stenosis. Renier, interestingly, discovered that among 129 patients with oxycephaly, 15% suffered from rickets [51].

Cutaneous Disorders

Although it may not be considered a traditional association, cutaneous disorders are frequently reported to occur in conjunction with CM I. One such disorder is neurofibromatosis type I, in which a relationship as high as 8% has been reported [52]. Some investigators have hypothesized that mesodermal deficiency arrests posterior cranial fossa development, which is also proposed to occur in cutaneous disorders such as neurofibromatosis type I [8].

Equally mysterious is CM I's association with macrocephaly-cutis marmoratatelangiectatica congenita (M-CMTC) [53]. M-CMTC is characterized by benign spider nevus-like telangiectasias and superficial ulcerations, but little is known about the pathology. Hence, no mechanism has been suggested for the association.

Several other cutaneous disorders have been advocated as being involved in CM I, including Leopard syndrome [54], blue rubber bleb nevus syndrome [55], giant congenital melanocytic nevi [56], phacomatosis pigmentovascularis type II [57], acanthosis nigricans [58], and Waardenburg syndrome variants [59]. These are all based on scarce case reports and thus may have occurred coincidentally with CM I.

Spinal Defects

Not all causes of CM I have been shown to be directly related to the posterior fossa and skull base. A few disorders, such as spondyloepiphyseal dysplasia [60], caudal regression syndrome [61], Klippel-Feil syndrome, atlantoaxial assimilation, basilar impression, and odontoid retroflexion in which the vertebral column is the site of deformation, are also associated with CM I. Little is known about the pathophysiology of these spinal deformities, but it is thought that difficulty in equilibrating the dynamic CSF pulse pressure induced by the Valsalva maneuver is responsible for the CM I presentation.

Lipomeningomyelocele has been shown to be coupled with CM I in as many as 3–6% of patients [62, 63]. It has been postulated that a decrease in intracranial nervous tissue and CSF due to the lipomeningomyelocele removes the expansile pressure of the brain on the skull, thus causing the posterior fossa to be smaller and less developed [64].

Space-Occupying Lesions

To this point, all mentioned associated disorders have been congenital, but acquired methods of CM I manifestation also exist. This category includes both space-occupying lesions and cerebrospinal fluid leaks. Space-occupying lesions within the posterior cranial fossa can be caused by a variety of disorders ranging from brain tumors to hematomas. These can include supratentorial [65] and infratentorial [66] lesions. The multitude of potential space-occupying lesions is vast and will not be discussed further.

Not Otherwise Specified

A case of Beckwith-Wiedemann syndrome in association with CM I has been reported. Tubbs et al. [61] hypothesized the pathological mechanism responsible for the CM I to be hemihypertrophy involvement of the skull. Costello syndrome has also been recognized as presenting with concomitant CM I, although it too is described as having a low-frequency association [66]. Hemihypertrophy [67] and GHD [68] have been reported in both Costello syndrome patients and CM I and thus may be the common factor. Furthermore, an association with Marfan syndrome is commonly recognized due to intracranial hypotension [69]. Additionally, associations with Williams-Beuren syndrome have been found with morphometric analyses suggesting a diminished posterior fossa leading to CM I [70, 71]. Finally, associations with disorders such as cystic fibrosis [72], Pierre Robin syndrome [73, 74], Ehlers-Danlos syndrome [75], Fabry disease [76], Kabuki syndrome [77], situs inversus [78], CHERI [79], and cloacal exstrophy [80] have been made with no clear pathophysiological mechanism yet identified.

Conclusion

There exist a plethora of diseases affiliated with CM I, many of which have been mentioned in this article and certainly more to be discovered in the future. While the final outcome of CM I may be the same, the strength of the correlation and pathophysiological mechanisms of each differs greatly, and some may be spurious associations. Thus, the need for additional genetic research and investigation of CM I continues.

References

1. Loukas M, Noordeh N, Shoja MM, Pugh J, Oakes WJ, Tubbs RS. Hans Chiari (1851-1916). Childs Nerv Syst. 2007;24:407–9.
2. Tubbs RS, Lyerly MJ, Loukas M, Shoja MM, Oakes WJ. The pediatric Chiari I malformation: a review. Childs Nerv Syst. 2007;23:1239–50.
3. Badie B, Mendoza D, Batzorf U. Posterior fossa volume and response to suboccipital decompression in patients with Chiari I malformation. Neurosurgery. 1995;37:214–8.
4. Elster AD, Chen MY. Chiari I malformations: clinical and radiologic reappraisal. Radiology. 1992;183:347–53.
5. Gardner WJ. Hydrodynamic mechanism of syringomyelia: its relationship to myelocele. J Neurol Neurosurg Psychiatry. 1965;28:691–6.
6. Levy WJ, Mason L, Hahn JF. Chiari malformation presenting in adults: a surgical experience in 127 cases. Neurosurgery. 1983;12:377–90.
7. Meadows J. Asymptomatic Chiari type I malformations identified on magnetic resonance imaging. J Neurosurg. 2000;92:920–6.
8. Milhorat TH, Chou MW, Trinidad EM, Kula RW, Mandell M, Wolpert C, et al. Chiari I malformations redefined: clinical and radiographic findings for 364 symptomatic patients. Neurosurgery. 1999;44:1005–17.
9. Nohria V, Oakes WJ. Chiari I malformation: a review of 43 patients. Pediatr Neurosurg. 1990;16:222–7.
10. Oakes WJ. Chiari malformations, hydromyelia, syringomyelia. In: Wilkins RH, Rengachary SS, editors. Neurosurgery. New York: McGraw-Hill; 1996. p. 3593–616.
11. Oakes WJ. The Chiari malformations of the child. In: Menezes AH, Sonntag VKH, editors. Principles of spinal surgery. New York: McGraw-Hill; 1996. p. 379–94.
12. Paul KS, Lye RH, Strang FA, Dutton J. Arnold-Chiari malformation. Review of 71 cases. J Neurosurg. 1983;58:183–7.
13. Rinaldi F, Cioffi FA, Columbano L, Krasaqakis G, Bernini FP. Tethered cord syndrome. J Neurosurg Sci. 2005;49:131–5.
14. Tubbs RS, Oakes WJ. Costello syndrome and Chiari I malformation: Apropos of a case with a review of the literature regarding a potential association. J Child Neurol. 2003;18:496–8.
15. Tubbs RS, Wellons JC 3rd, Oakes WJ. Asymmetry of tonsillar ectopia in Chiari I malformation. Pediatr Neurosurg. 2002;37:199–202.
16. Schady W, Metcalfe RA, Butler P. The incidence of craniocervical bony anomalies in the adult Chiari malformation. J Neurol Sci. 1987;82:193–203.
17. Marin-Padilla M, Marin-Padilla TM. Morphogenesis of experimentally induced Arnold-Chiari malformation. J Neurol Sci. 1981;50:29–55.
18. Vega A, Quintana F, Berciano J. Basichondrocranium anomalies in adult Chiari type I malformation: a morphometric study. J Neurol Sci. 1990;82:193–203.
19. Cesmebasi A, Loukas M, Hogan E, Kralovic S, Shoja M, Tubbs RS, Cohen-Gadol A. The Chiari malformations: a review with emphasis on anatomical traits. Clin Anat. 2015;28(2):184–94.
20. Oakes WJ, Tubbs RS. Chiari malformations. In: Winn HR, editor. Youmans neurological surgery. 5th ed. Philadelphia: Elsevier; 2004. p. 3347–61.
21. Sgouros S, Kountouri M, Natarajan K. Skull base growth in children with Chiari malformation type I. J Neurosurg. 2007;107:188–92.
22. Wellons JC III, Tubbs RS, Oakes WJ. Chiari malformations and syringohydromyelia. In: Rengachary SS, Ellenbogen RG, editors. Principles of neurosurgery. Edinburgh: Elsevier Mosby; 2005. p. 181–95.
23. Tubbs RS, Beckman J, Naftel RP, Chern JJ, Wellons JC 3rd, Rozzelle CJ, et al. Institutional experience with 500 cases of surgically treated pediatric Chiari malformation Type I. J Neurosurg Pediatr. 2011;7:248–56.
24. Saldino RM, Steinbach HL, Epstein CJ. Familial acrocephalosyndactyly (Pfeiffer syndrome). Am J Roentgenol. 1972;116:609–22.
25. Harwood-Nash DC. Coronal synostosis. In: Rogers LF, editor. Disorders of the head and neck syllabus second series. Reston: American College of Radiology; 1977.
26. Cinalli G, Renier D, Sebag G, Sainte-Rose C, Arnaud E, Pierre-Kahn A. Chronic tonsillar herniation in Crouzon's and Apert's syndromes: the role of premature synostosis of the lambdoid suture. J Neurosurg. 1995;83:575–82.
27. Cinalli G, Spennato P, Sainte-Rose C, Arnaud E, Aliberti F, Brunelle F, et al. Chiari malformation in craniosynostosis. Childs Nerv Syst. 2005;21:889–901.
28. Shigeta H, Sakai K. [Chiari malformation (chronic tonsillar herniation) and syringomyelia in Crouzon's syndrome] (in Japanese). Nerv Syst Child. 1996;21:395–401.
29. Ranger A, Al-Hayek A, Matic D. Chiari type I malformation in an infant with type II Pfeiffer syndrome:

further evidence of acquired pathogenesis. J Craniofac Surg. 2010;21:427–31.
30. Park WJ, Meyers GA, Li X. Novel FGFR2 mutations in Crouzon and Jackson–Weiss syndromes show allelic heterogeneity and phenotypic variability. Hum Mol Genet. 1995;4:1229–33.
31. Hopkins TE, Haines SJ. Rapid development of Chiari I malformation in an infant with Seckel syndrome and craniosynostosis. Case report and review of the literature. J Neurosurg. 2003;98:1113–5.
32. Chang YT, Tsai FJ, Shen WC, Lin HC, Peng CT, Tsai CH. Antley–Bixler syndrome associated with Arnold–Chiari malformation. Acta Paediatr. 2000;89:737–9.
33. Greally MT, Carey JC, Milewicz DM, Hudgins L, Goldberg RB, Shprintzen RJ, et al. Shprintzen-Goldberg syndrome: a clinical analysis. Am J Med Genet. 1998;19:202–12.
34. Kreiborg S, Marsh JL, Cohen MM Jr, Liversage M, Pedersen H, Skovby F, et al. Comparative three-dimensional analysis of CT-scans of the calvaria and cranial base in Apert and Crouzon syndromes. J Cranio-Maxillofacial Surg. 1993;21:181–8.
35. Richtsmeier JT, Lele S. Analysis of craniofacial growth in Crouzon syndrome using landmark data. J Craniofac Genet Dev Biol. 1990;10:39–62.
36. Moore KL, Persaud TVN. Before we are born: essentials of embryology and birth defects. 7th ed. Philadelphia: Saunders Elsevier Inc.; 2008. p. 233.
37. Rodrigues VJ, Elsayed S, Loeys BL, Dietz HC, Yousem DM. Neuroradiologic manifestations of loeys-dietz syndrome type I. Am J Neuroradiol. 2009;30:1614–9.
38. Tubbs RS, Elton S, Blount JP, Oakes WJ. Preliminary observations on the association between simple metopic ridging in children without trigonocephaly and the Chiari I malformation. Pediatr Neurosurg. 2001;35:136–9.
39. Hamilton J, Chitayat D, Blaser S, Cohen LE, Phillips JA 3rd, Daneman D. Familial growth hormone deficiency associated with MRI abnormalities. Am J Med Genet. 1998;80:128–32.
40. Tubbs RS, Wellons JC 3rd, Oakes WJ, Blount JP. Reformation of the posterior atlanto-occipital membrane following posterior fossa decompression with subsequent constriction at the craniocervical junction. Pediatr Neurosurg. 2003;38:219–21.
41. Tubbs RS, Wellons JC 3rd, Smyth MD, Bartolucci AA, Blount JP, Oakes WJ, et al. Children with growth hormone deficiency and Chiari I malformation: a morphometric analysis of the posterior cranial fossa. Pediatr Neurosurg. 2003;38:324–8.
42. Nakai T, Asato R, Miki Y, Tanaka F, Matsumoto S, Konishi J. A case of achondroplasia with downward displacement of the brain stem. Neuroradiology. 1995;37:293–84.
43. Iglesias-Osma C, Gomez Sanchez JC, Suquia Mugica B, Querol Prieto R, de Portugal Alvarez J. Paget's disease of bone and basilar impression associated with an Arnold-Chiari type I malformation [in Spanish]. Ann Med Int. 1997;14:519–22.
44. Richards PS, Bargiota A, Corrall RJ. Paget's disease causing an Arnold-Chiari type I malformation: radiographic findings. Am J Roentgenol. 2001;176:816–7.
45. Sewell MD, Akram H, Wadley J. Foramen magnum decompression and expansile duroplasty for acquired Chiari type I malformation in craniometaphyseal dysplasia. Br J Neurosurg. 2008;22:83–5.
46. Kulkarni ML, Marakkanavar SN, Sushanth S, Pradeep N, Ashok C, Balaji MD, et al. Osteopetrosis with Arnold Chiari malformation type I and brainstem compression. Indian J Pediatr. 2006;74:412–5.
47. Rengachary SS, Blount J, Heros D, Bowers S, Truwit C. Craniocephalic disproportion with increased intracranial pressure and brain herniation: a new clinical syndrome in anemic patients: report of two cases. Neurosurgery. 1997;41:297–303.
48. Caldemeyer KS, Boaz JC, Wappner RS, Moran CC, Smith RR, Quets JP. Chiari I malformation: association with hypophosphatemic rickets and MR imaging appearance. Radiology. 1995;195:602–4.
49. Tubbs RS, Webb D, Abdullatif H, Conklin M, Doyle S, Oakes WJ. Posterior cranial fossa volume in patients with rickets: insights into the increased occurrence of Chiari I malformation in metabolic bone disease. Neurosurgery. 2004;55:380–4.
50. Kuether TA, Piatt JH. Chiari malformation associated with vitamin D-resistant rickets: case report. Neurosurgery. 1998;42:1168–71.
51. Renier D, Cinalli G, Lajeunie E, Arnaud E, Marchac D. Oxycephaly, a severe craniosynostosis: apropos of a series of 129 cases [in French]. Arch Pediatr. 1997;4:722–9.
52. Tubbs RS, Rutledge SL, Kosentka A, Bartolucci AA, Oakes WJ. Chiari I malformation and neurofibromatosis type I. Pediatr Neurol. 2004;30:278–80.
53. Tubbs RS, Smyth MD, Wellons JC, Blount JP, Oakes WJ. Cutaneous manifestations and the Chiari I malformation. Pediatr Neurol. 2003;29:250–2.
54. Agha A, Hashimoto K. Multiple lentigines (leopard) syndrome with Chiari I malformation. J Dermatol. 1995;22:520–3.
55. Kunishige M, Azuma H, Masuda K, Shigekiyo T, Arii Y, Kawai H, et al. Interferon alpha-2a therapy for disseminated intravascular coagulation in a patient with blue rubber bleb nevus syndrome. Angiology. 1997;48:273–7.
56. Frieden IJ, Williams ML, Barkovich AJ. Giant congenital melanocytic nevi: brain magnetic resonance findings in neurologically asymptomatic children. J Am Acad Dermatol. 1994;31:423–9.
57. Du LC, Delaporte E, Catteau B, Destee A, Piette F. Phacomatosispigmentovascularis type II. Eur J Dermatol. 1998;8:569–72.
58. Martinez-Perez D, Vander Woude DL, Barnes PD, Scott RM, Mulliken JB. Jugular foraminal stenosis in Crouzon syndrome. Pediatr Neurosurg. 1996;25:252–5.
59. Nye JS, Hayes EA, Amendola M. Myelocystocelecloacal exstrophy in a pedigree with mitochondrial 12S rRNA mutation, aminoglycoside-induced deaf-

ness, pigmentary disturbances, and spinal anomalies. Teratology. 2000;61:165–71.
60. Gripp KW, Scott CI Jr, Nicholson L, Magram G, Grissom LE. Chiari malformation and tonsillar ectopia in twin brothers and father with autosomal dominant spondylo-epiphyseal dysplasia tarda. Skelet Radiol. 1997;26:131–3.
61. Tubbs RS, Oakes WJ. Beckwith-Wiedemann syndrome in a child with Chiari I malformation: case report. J Neurosurg. 2005;103:172–4.
62. Byrne RW, Hayes EA, George TM, McLone DG. Operative resection of 100 spinal lipomas in infants less than 1 year of age. Pediatr Neurosurg. 1995;23:182–7.
63. Grijalvo CA, Bank WO, Balériaux D, Imaña FJ, Szliwowski HB, Brotchi J. Lipomyeloschisis associated with thoracic syringomyelia and Chiari I malformation. Neuroradiology. 1993;35:375–7.
64. Tubbs RS, Wellons JC 3rd, Oakes WJ. Occipital encephalocele, lipomyelomeningocele, and Chiari I malformation: case report and review of the literature. Childs Nerv Syst. 2003;19:50–3.
65. Onesti ST, Ashkenazi E, Miller AM, Michelsen WJ. Resolution of acquired tonsillar herniation after resection of supratentorial meningioma. Case illustration. J Neurosurg. 1997;86:572.
66. Tokime T, Okamoto S, Yamagata S, Konishi T. Syringomyelia associated with a posterior fossa cyst. Illustration of two cases. J Neurosurg. 1997;86:907.
67. Ringrose RE, Jabbour JT, Keele DK. Hemihypertrophy. Pediatrics. 1965;36:434–48.
68. Legault L, Gagnon C, Lapointe N. Growth hormone deficiency in Costello syndrome: a possible explanation for the short stature. J Pediatr. 2001;138:151–2.
69. Puget S, Kondageski C, Wray A, Boddaert N, Roujeau T, Di Rocco F, et al. Chiari-like tonsillar herniation associated with intracranial hypotension in marfan syndrome. Case report. J Neurosurg. 2007;106:48–52.
70. Ferrero GB, Biamino E, Sorasio L, Banaudi E, Peruzzi L, Forzano S, et al. Presenting phenotype and clinical evaluation in a cohort of 22 Williams-Beuren syndrome patients. Eur J Med Genet. 2007;50:327–37.
71. Pober BR, Filiano JJ. Association of Chiari I malformation and Williams syndrome. Pediatr Neurol. 1995;12:84–8.
72. Needleman JP, Panitch HB, Blerbrauer KS, Schldlow DV. Chiari type I malformation in children and adolescents with cystic fibrosis. Pediatr Pulmonol. 2000;30:490–2.
73. Lee J, Hida K, Seki T, Kitamura J, Iwasaki Y. Pierre-Robin syndrome associated with Chiari type I malformation. Childs Nerv Syst. 2003;19:380–3.
74. Tubbs RS, Oakes WJ. Chiari I malformation, caudal regression syndrome, and pierre robin syndrome: a previously unreported combination. Childs Nerv Syst. 2006;22:1507–8.
75. Milhorat TH, Bolognese PA, Nishikawa M, McDonnell NB, Francoman CA. Syndrome of occipitoatlantoaxial hypermobility, cranial settling, and Chiari malformation type I in patients with hereditary disorders of connective tissue. J Neurosurg Spine. 2007;7:601–9.
76. Germain DP, Benistan K, Halimi P. Chiari type I malformation in four unrelated patients affected with fabry disease. Eur J Med Genet. 2006;49:419–25.
77. Ciprero KL, Clayton-Smith J, Donnai D, Zimmerman RA, Zackai EH, Ming JE. Symptomatic Chiari I malformation in Kabuki syndrome. Am J Med Genet A. 2005;132A:273–5.
78. Serarslan Y, Melek IM, Duman T, Eraslan T, Akdemir G, Yalcin F. The co-occurrence of Chiari type I malformation with syringomyelia and total situs inversus. Med Sci Monit. 2007;13:110–3.
79. Haapanen ML. CHERI: time to identify the syndrome? J Craniofac Surg. 2007;18:369–73.
80. Tubbs RS, Smyth MD, Oakes WJ. Chiari malformation and cloacal exstrophy: report of a patient with both defects of blastogenesis. Am J Med Genet A. 2003;119:231–3.

35 Association Between Fibromyalgia, Chronic Fatigue, and the Chiari I Malformation

Richard G. Ellenbogen and David F. Bauer

Patients with fibromyalgia (FM), chronic fatigue (CF), and Chiari malformation type I (CM I) can have overlapping symptoms, including headaches, vertigo, tremors, and gait instability (Table 35.1) [1, 2]. Authors have proposed that cervical stenosis may be the cause of many of these symptoms in patients with FM, although data are limited on the effectiveness of posterior fossa or cervical decompression in patients with FM or CF [3–7]. In this chapter, we will review current evidence on the possible association between FM, CF, and CM I.

Fibromyalgia

Fibromyalgia is characterized by chronic pain with widespread muscle aches and pains, general fatigue, sleep disturbances, and neurological complaints [8, 9]. Often the diagnosis is made using the 1990 American College of Rheumatology classification criteria for the diagnosis of FM [2]. This criteria includes chronic, widespread pain

Table 35.1 Adjusted value for headache characteristics according to fibromyalgia status, adjusted for age, sex, and race

Characteristic	Fibromyalgia (n = 176)	Healthy (n = 67)	P
Localized to back of head, %	61	13	<.01
Starts in back of head and radiates, %	55	10	<.01
Temporal/side of head, %	68	19	<.01
Frontal, %	74	33	<.01
Behind eyes, %	76	26	<.01
Lateralized/one side, %	53	11	<.01
Generalized/all over, %	55	22	<.01
Neck pain, %	92	25	<.01
Throbbing and constant, %	70	33	<.01
Nonthrobbing, occasional headache, mean n (SD)/wk	2.1 (2.5)	0.4 (2.8)	<.01
Grade,[a] mean (SD)	5.9 (2.3)	3.6 (2.6)	<.01
Made worse by, %			
Normal activity	59	24	<.01
Lying down	13	3	.09
Standing	48	9	<.01
Head down	46	14	<.01
Coughing	59	22	<.01
Straining	70	25	<.01
Sneezing	52	20	<.01
Playing sports	62	27	<.01
Exercise	74	30	<.01

Reproduced with permission from Watson et al. [1]
[a]Range, 1–10: 1 = not bad to 10 = terrible, severe

R. G. Ellenbogen
Department of Neurological Surgery, University of Washington Medicine Neuroscience Institute, Seattle, WA, USA

D. F. Bauer (✉)
Department of Surgery, Division of Neurosurgery, Dartmouth-Hitchcock Medical Center, Lebanon, NH, USA

R. S. Tubbs et al. (eds.), *The Chiari Malformations*, https://doi.org/10.1007/978-3-030-44862-2_35

for at least 3 months' duration, involving the upper and lower body, right and left sides, and axial skeleton. Patients often have allodynia and hyperalgesia arising from muscles and joints. Common pain sites include the neck, back, shoulders, pelvic girdle, and hands, although other sites may be involved [10]. Diagnostic criteria include pain arising from at least 11 of 18 tender points on digital examination. These points are digitally palpated with about 4 kg per unit area of force, and bilateral points include under the lower sternocleidomastoid muscles, second costochondral junction, 2 cm distal to the lateral epicondyle, prominence of the greater trochanter, medial fat pad of the knee, insertion of the suboccipital muscle, mid-upper trapezius muscle, origin of the supraspinatus muscle, and upper outer quadrant of the buttock (see Fig. 35.1) [11]. This criteria provides a sensitivity of nearly 88% and specificity of 81% in distinguishing FM, and consequently this criteria is still used by many clinicians to make the diagnosis. In 2010, the American College of Rheumatology created preliminary diagnostic criteria for diagnosis of FM and the measurement of symptom severity. As a screening test, this criteria includes the use of a Widespread Pain Index and Symptom Severity Scale that can be completed without a patient examination [12]. Fibromyalgia affects 2% of the US general population, and approximately six million people suffer from FM in the United States alone [13–15]. Patients are more commonly women, and symptoms usually appear between 20 and 55 years of age. Other common diagnostic features include fatigue, sleep disturbances, stiffness, paresthesias, headaches, Raynaud's-like symptoms, depression, and anxiety. Currently, there is no accepted mechanism for the development of FM, although many possible abnormalities and mechanisms have been proposed [16–21]. There are other systemic diseases that have overlap of symptoms with FM. These diseases include hypothyroidism, systemic lupus erythematosus, and malignancies. Patients diagnosed with FM often report the onset of symptoms after a motor vehicle collision, surgery, or other trauma [22–24]. Fibromyalgia is 13

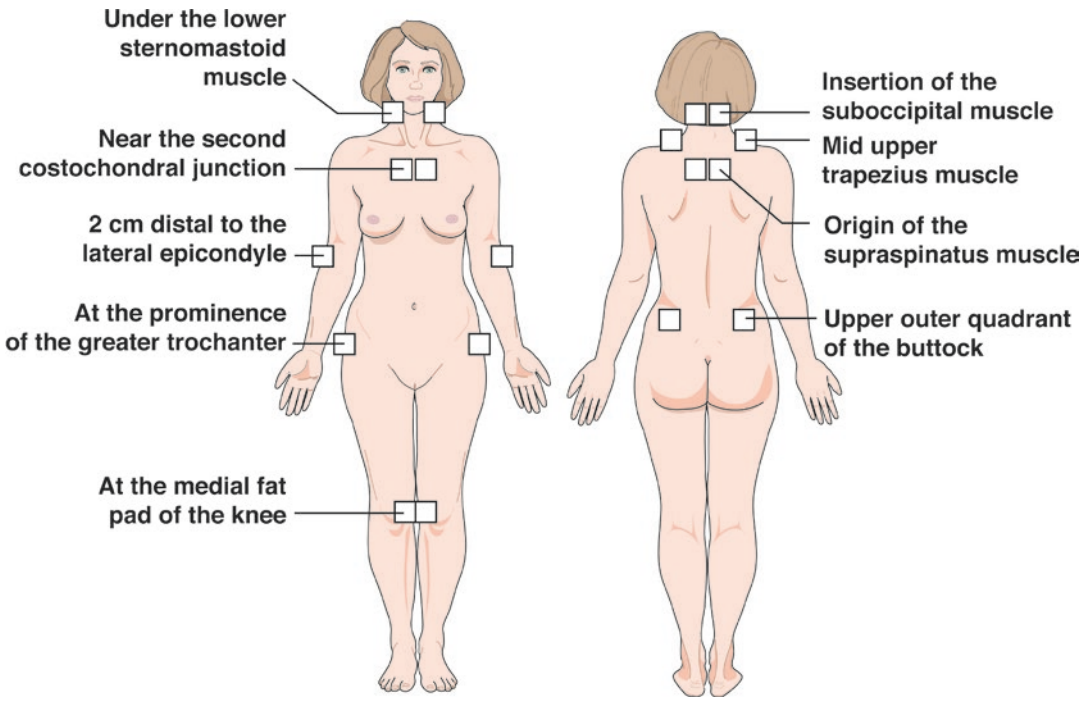

Fig. 35.1 Diagram of tender/trigger points used to diagnose fibromyalgia. (Adapted from [11])

times more common after neck injuries than after injuries to the lower extremities. Patients with FM also exhibit more neurologic signs and symptoms than control subjects, despite lack of imaging abnormalities in these patients. These include greater dysfunction of the glossopharyngeal and vagus nerves; more sensory, motor, and gait abnormalities; and more neurologic symptoms such as photophobia, poor balance, weakness, and tingling [12, 13]. Management of FM can be difficult. Medical therapy includes amitriptyline, cyclobenzaprine, tramadol, serotonin reuptake inhibitors, and pregabalin. Nonmedical therapies include cardiovascular exercise, cognitive behavioral therapy, patient education, biofeedback, and hypnotherapy [25].

Chronic Fatigue

CF is a condition characterized by a constellation of symptoms of at least 6 months' duration including severe, medically unexplained mental and physical fatigue, sleep disturbances, poor concentration, and flulike symptoms [26]. It is estimated that between 0.5% and 2.5% of the general population has CF, and associated physical and psychosocial disability has been thought to lead to high direct and indirect medical and societal costs. Many patients with CF have overlapping symptoms with FM. Patients with CF may have multiple tender points on examination, and it can often be difficult in these patients to differentiate between a diagnosis of FM and CF. There have been purported links between a diagnosis of CF and chronic Epstein-Barr virus infection, chronic Lyme disease, total allergy syndrome, multiple chemical sensitivity syndrome, and chronic candidiasis, but none of these etiologic agents have been scientifically linked to CF [27]. Current revised US Centers for Disease Control (CDC) criteria for CF includes new onset of unexplained, persistent, or relapsing fatigue, not a result of ongoing exertion, not alleviated by rest, resulting in substantial reduction in occupational, educational, social, or personal activities. In addition, patients must have four or more additional symptoms during a period of at least 6 months of fatigue. These symptoms include impairment in short-term memory or concentration, sore throat, tender cervical or axillary nodes, muscle pain, multijoint pain without redness or swelling, headaches of a new pattern or severity, unrefreshing sleep, and post-exertional malaise lasting >24 hours [28]. Treatment options for CF are limited. Meta-analysis has shown only cognitive behavioral therapy, and graded exercise treatment are effective treatments for CF.

Chiari Malformation Type I

Chiari I malformation is a hindbrain malformation characterized by downward extension of the cerebellar tonsils below the foramen magnum [29]. Magnetic resonance imaging (MRI) often reveals a full posterior fossa, and flow studies often document poor flow of cerebrospinal fluid (CSF) around the cerebellum and brainstem [30–35]. Up to 80% of CM I patients have comorbid syringomyelia, and there is a female predominance with this disorder [36]. Approximately 25% of patients diagnosed with CM I cite acute head trauma or birth trauma as a precipitating event [31]. While the most reliable symptom in patients with CM I is often a reproducible Valsalva-induced headache, some patients present with complaints similar to FM such as malaise, tremor, and vertigo [1].

Recent uncontrolled case series documented CM I in 4–20% of FM patients, with 46–71% exhibiting spinal canal stenosis or cervical compression after flexion/extension of the cervical spine [3–7, 36–38]. Non-randomized studies have shown that posterior fossa decompression with possible cervical laminectomy reduced fatigue and pain in FM patients with presumed CM I; however, a retrospective study has shown no correlation between cervical stenosis and FM [3–5]. Only one prospective, randomized study has been published looking at the association between FM and CM I [1]. This study, level II medical evidence, demonstrated no correlation between FM and CM I.

For example, Heffez et al. published two studies evaluating FM and CM I [3]. In 2004, they

retrospectively evaluated 278 adult patients with a clinical diagnosis of FM. These patients were 87% female, and they had symptoms predominantly of neck and back pain, fatigue, cognitive impairment, gait instability, grip weakness, paresthesia, vertigo, and numbness. Eighty-eight percent of patients reported worse symptoms with neck extension, 45% of patients had a cervical canal diameter <10 mm, and 20% of patients had tonsillar ectopia >5 mm. The authors concluded that FM symptoms may be secondary to CM I and cervical stenosis.

In 2008, Heffez et al. published a nonrandomized, prospective, case-control study comparing outcomes of craniocervical decompression verses nonoperative management of 40 operated and 31 non-operated patients with FM [5]. They reported an improvement in surgically treated patients at 1 year in physical and mental quality of life, anxiety, and depression. In the study, the authors noted that they chose patients from a larger cohort based on their prompt return of surveys sent to them over a year-long period. They did not describe complications or long-term outcomes.

In 2008, Holman et al. published a retrospective study evaluating "positional cervical cord compression" in patients with FM [37]. Seventy patients seen over a 2-month period in their clinic were evaluated with dynamic MRI, and 52 of them had cervical cord compression based on this study. The author posed that cervical cord irritation may be the cause of FM in these patients.

Watson et al. published the only prospective, randomized study of the relationship between CM I and FM [1]. This cohort study provides the only level II evidence on this subject. The authors prospectively obtained MRI studies of 176 participants with FM and 67 pain- and fatigue-free control subjects. Imaging was obtained of the brain and upper cervical spine. Chiari I malformation was defined as inferior extension of cerebellar tonsils greater than or equal to 5 mm below the basion-opisthion line of the foramen magnum or tonsillar ectopia 3–5 mm below the basion-opisthion line plus abnormalities of CSF flow, posterior fossa volume, or hindbrain or cervical spinal cord movement. Morphometric measurements were obtained of posterior-fossa volumes, and cerebrospinal fluid flow was evaluated with flow-sensitized phase-contrast gradient echo MRI (Table 35.2) [1]. The primary outcome was the frequency of CM I in participants with FM compared to healthy controls. The patients with FM were predominantly female (93% vs 54% in the control group). Patients in the FM group had

Table 35.2 Adjusted magnetic resonance imaging requirements (means and 95% confidence intervals) according to fibromyalgia statuses, adjusted for age, sex, and race

Measurement	Fibromyalgia (n = 176)	Healthy (n = 67)	P
Tonsillar position,[a] mm	−0.71 (−1.08, −0.34)	0.00 (−0.66, 0.66)	.09
Posterior fossa volume, cm3			
Total volume	189 (187–192)	192 (188–197)	.31
Brain volume	163 (160–165)	165 (161–169)	.30
Cerebrospinal fluid volume	27 (26–28)	27 (25–29)	.80
Ratio of brain to cerebrospinal volume	6.5 (6.2–6.7)	6.4 (5.9–6.8)	.72
Cerebrospinal fluid maximum systolic velocity, cm/s			
C2 anterior region	2.63 (2.52–2.73)	2.51 (2.32–2.70)	.33
C2 posterior region	2.29 (2.19–2.39)	2.28 (2.10–2.45)	.91
Foramen magnum anterior region	2.37 (2.23–2.51)	2.17 (1.92–2.42)	.19
Pulsatile tissue velocity motion, cm/s			
C2 spinal cord pulsatile motion	0.74 (0.72–0.77)	0.67 (0.62–0.72)	<.05
Foramen magnum pulsatile motion	0.76 (0.72–0.81)	0.66 (0.58–0.73)	<.05

Reproduced with permission from Watson et al. [1]
[a]Negative values indicate millimeters above the foramen magnum; positive values position below the foramen magnum

more pain, fatigue, and sleep disturbances than controls. Mean tonsillar position and the prevalence of CM I were similar in the FM and control groups. No association was found between FM and CM I in this study.

Conclusion

In conclusion, the overlap of symptoms between FM, CF, and CM I understandably has led to a search for an association between these entities. While there are a few retrospective, non-randomized studies that support an association between FM and CM I, there is one prospective, randomized, high-quality cohort study demonstrating no association between FM and CM I. No evidence supports routine use of static MRI to evaluate FM or CF patients. However, despite lack of current evidence, it is likely that future large prospective trials may bring more evidence to this topic.

References

1. Watson NF, Buchwald D, Goldberg J, Maravilla KR, Noonan C, Guan Q, et al. Is Chiari I malformation associated with fibromyalgia? Neurosurgery. 2011;68(2):443–8; discussion 8-9.
2. Wolfe F, Smythe HA, Yunus MB, Bennett RM, Bombardier C, Goldenberg DL, et al. The American College of Rheumatology 1990 criteria for the classification of Fibromyalgia. Report of the Multicenter Criteria Committee. Arthritis Rheum. 1990;33(2):160–72.
3. Heffez DS, Ross RE, Shade-Zeldow Y, Kostas K, Shah S, Gottschalk R, et al. Clinical evidence for cervical myelopathy due to Chiari malformation and spinal stenosis in a non-randomized group of patients with the diagnosis of fibromyalgia. Eur Spine J. 2004;13(6):516–23.
4. Clauw DJ, Petzke F, Rosner MJ, Bennett RM. Prevalence of Chiari malformation and cervical spine stenosis in Fibromyalgia. Arth Rheum. 2000;43:S173.
5. Heffez DS, Ross RE, Shade-Zeldow Y, Kostas K, Morrissey M, Elias DA, et al. Treatment of cervical myelopathy in patients with the fibromyalgia syndrome: outcomes and implications. Eur Spine J. 2007;16(9):1423–33.
6. Wilke WS. Can fibromyalgia and chronic fatigue syndrome be cured by surgery? Cleve Clin J Med. 2001;68(4):277–9.
7. Burton T. High hopes: surgery on the skull for chronic fatigue?. Wall Street J. 1999(A8).
8. Powers R. Fibromyalgia: an age-old malady begging for respect. J Gen Intern Med. 1993;8(2):93–105.
9. Watson NF, Buchwald D, Goldberg J, Noonan C, Ellenbogen RG. Neurologic signs and symptoms in fibromyalgia. Arthritis Rheum. 2009;60(9):2839–44.
10. Bennett RM. Clinical manifestations and diagnosis of fibromyalgia. Rheum Dis Clin N Am. 2009;35(2):215–32.
11. Goldenberg DL. Diagnostic and therapeutic challenges of fibromyalgia. Hosp Pract (Off Ed). 1989;24(9A):39–52.
12. Wolfe F. New American College of Rheumatology criteria for fibromyalgia: a twenty-year journey. Arthr Care Res (Hoboken). 2010;62(5):583–4.
13. Wolfe F, Ross K, Anderson J, Russell IJ, Hebert L. The prevalence and characteristics of fibromyalgia in the general population. Arthritis Rheum. 1995;38(1):19–28.
14. Wolfe F. The clinical syndrome of fibrositis. Am J Med. 1986;81(3A):7–14.
15. Wolfe F, Cathey MA. Prevalence of primary and secondary fibrositis. J Rheumatol. 1983;10(6):965–8.
16. Crofford LJ, Pillemer SR, Kalogeras KT, Cash JM, Michelson D, Kling MA, et al. Hypothalamic-pituitary-adrenal axis perturbations in patients with fibromyalgia. Arthritis Rheum. 1994;37(11):1583–92.
17. Buchwald D, Pearlman T, Kith P, Katon W, Schmaling K. Screening for psychiatric disorders in chronic fatigue and chronic fatigue syndrome. J Psychosom Res. 1997;42(1):87–94.
18. Bou-Holaigah I, Calkins H, Flynn JA, Tunin C, Chang HC, Kan JS, et al. Provocation of hypotension and pain during upright tilt table testing in adults with fibromyalgia. Clin Exp Rheumatol. 1997;15(3):239–46.
19. Leventhal LJ. Management of fibromyalgia. Ann Intern Med. 1999;131(11):850–8.
20. Ablin J, Neumann L, Buskila D. Pathogenesis of fibromyalgia - a review. Joint Bone Spine. 2008;75(3):273–9.
21. Bradley LA. Pathophysiologic mechanisms of fibromyalgia and its related disorders. J Clin Psychiatry. 2008;69(Suppl 2):6–13.
22. Salit IE. Precipitating factors for the chronic fatigue syndrome. J Psychiatr Res. 1997;31(1):59–65.
23. Buskila D, Neumann L. Fibromyalgia syndrome (FM) and nonarticular tenderness in relatives of patients with FM. J Rheumatol. 1997;24(5):941–4.
24. Buskila D, Neumann L, Vaisberg G, Alkalay D, Wolfe F. Increased rates of fibromyalgia following cervical spine injury. A controlled study of 161 cases of traumatic injury. Arthritis Rheum. 1997;40(3):446–52.
25. Goldenberg DL, Burckhardt C, Crofford L. Management of fibromyalgia syndrome. JAMA. 2004;292(19):2388–95.
26. Luyten P, Van Houdenhove B, Pae CU, Kempke S, Van Wambeke P. Treatment of chronic fatigue syndrome: findings, principles and strategies. Psychiatry Investig. 2008;5(4):209–12.

27. Baker R, Shaw EJ. Diagnosis and management of chronic fatigue syndrome or myalgic encephalomyelitis (or encephalopathy): summary of NICE guidance. BMJ. 2007;335(7617):446–8.
28. Fukuda K, Straus SE, Hickie I, Sharpe MC, Dobbins JG, Komaroff A. The chronic fatigue syndrome: a comprehensive approach to its definition and study. International Chronic Fatigue Syndrome Study Group. Ann Intern Med. 1994;121(12):953–9.
29. Ball WS Jr, Crone KR. Chiari I malformation: from Dr Chiari to MR imaging. Radiology. 1995;195(3):602–4.
30. Barkovich AJ, Wippold FJ, Sherman JL, Citrin CM. Significance of cerebellar tonsillar position on MR. AJNR Am J Neuroradiol. 1986;7(5):795–9.
31. Ellenbogen RG, Armonda RA, Shaw DW, Winn HR. Toward a rational treatment of Chiari I malformation and syringomyelia. Neurosurg Focus. 2000;8(3):E6.
32. Enzmann DR, Pelc NJ. Brain motion: measurement with phase-contrast MR imaging. Radiology. 1992;185(3):653–60.
33. Mayhew TM, Olsen DR. Magnetic resonance imaging (MRI) and model-free estimates of brain volume determined using the Cavalieri principle. J Anat. 1991;178:133–44.
34. Wolpert SM, Bhadelia RA, Bogdan AR, Cohen AR. Chiari I malformations: assessment with phase-contrast velocity MR. AJNR Am J Neuroradiol. 1994;15(7):1299–308.
35. Hofmann E, Warmuth-Metz M, Bendszus M, Solymosi L. Phase-contrast MR imaging of the cervical CSF and spinal cord: volumetric motion analysis in patients with Chiari I malformation. AJNR Am J Neuroradiol. 2000;21(1):151–8.
36. Milhorat TH, Chou MW, Trinidad EM, Kula RW, Mandell M, Wolpert C, et al. Chiari I malformation redefined: clinical and radiographic findings for 364 symptomatic patients. Neurosurgery. 1999;44(5):1005–17.
37. Holman AJ. Positional cervical spinal cord compression and fibromyalgia: a novel comorbidity with important diagnostic and treatment implications. J Pain. 2008;9(7):613–22.
38. Thimineur M, Kitaj M, Kravitz E, Kalizewski T, Sood P. Functional abnormalities of the cervical cord and lower medulla and their effect on pain: observations in chronic pain patients with incidental mild Chiari I malformation and moderate to severe cervical cord compression. Clin J Pain. 2002;18(3):171–9.

Symptoms of the Chiari II Malformation

36

Jeffrey P. Blount

Introduction

The Chiari II malformation (CM II) is perhaps the single most important component of an open myelomeningocele (MMC). The symptoms of a CM II arise from variable degrees of brainstem compromise and most commonly manifest as elements of bulbar failure but may involve the long tracts and sensorium as well. Whether this compromise in function arises as a result of brainstem dysfunction inherent to the dysraphic state or as a result of physical compression from a physically constricted posterior fossa remains an active area of debate. Complications related to the CM II are protean, but symptomatic CM II is the most common cause of death in infants less than 2 years who are born with a MMC [1–5]. Symptoms associated with the CM II are variable but are age specific in their presentation (Table 36.1). They can be subtle and are rarely intuitive to the uninitiated. The extent to which an intervention can reverse the course of a symptomatic CM II varies, but early detection and intervention offers a greater likelihood of recovery than an intervention undertaken once severe symptoms or a profound deficit have occurred. Detection of a symptomatic CM II may allow intervention and potentially prevent progression to an irreversible neurologic insult or death. As such it is imperative that those providing care to children with open neural tube defects be aware, watchful, and sensitive to the symptoms of the CM II.

Table 36.1 Symptoms of Chiari II malformation by age

Neonatal/infant	Older child/teen or adult
Stridor	Neck pain/occipital headache
Weak/absent/silent cry	Upper extremity dysfunction Spasticity Sensory impairment
Fatigue/lethargy or listlessness	Dysphonia
Poor control of oral secretions	Progressive difficulty with swallowing
Poor feeding	Sleep disorders Central sleep apnea Obstructive sleep apnea (if obese)
Nasal regurgitation of secretions	Dysconjugate gaze/diplopia
Reduced or absent gag reflex	Facial asymmetry
Poor head control	
Opisthotonus	
Emaciation	
Recurring bouts of aspiration	
Dysconjugate gaze	

J. P. Blount (✉)
Department of Neurosurgery, Children's of Alabama, University of Alabama at Birmingham, Birmingham, AL, USA
e-mail: Jeffrey.blount@childrensal.org

R. S. Tubbs et al. (eds.), *The Chiari Malformations*, https://doi.org/10.1007/978-3-030-44862-2_36

Symptoms and Signs of Chiari II in the Neonate and Infant

Stridor

Approximately one-third of infants born with MMC will develop symptoms of brainstem and lower cranial nerve (CN) failure before the age of 5 years, and up to one-third of these patients will expire as a consequence of symptomatic CM II. The symptoms in the neonate arise from progressively severe compromise of brainstem and lower cranial nerve function. This disproportionately impacts the laryngeal muscles, resulting in abductor paralysis of the cords and progressive airway obstruction. Impaired non-laminar airflow across the larynx results in stridor, which is the hallmark symptom of symptomatic CM II in the newborn [1–3, 6, 7]. Stridor is a high-pitched repetitive sound that can be clearly observed to arise from the throat of an affected infant. It often is worsened with inspiration or crying and may be associated with back arching or opisthotonus [7, 8]. In the child without a neural tube defect, it may be seen as a result of laryngomalacia, epiglottitis, an ingested foreign body, or as a complication of a severe upper respiratory infection or croup. However in a child with MMC, it must be considered as pathognomonic of symptomatic CM II and warrants urgent intervention [2, 5, 9, 10]. The child exhibiting stridor may show a wide range of overall clinical wellness. A newborn is often listless from progressive work of breathing, but occasionally the child may look well and have stridor as the singular indication of impaired brainstem function and impending peril [3, 8, 11]. Stridor is rarely observed immediately after birth in the child with MMC but rather tends to onset insidiously and often precipitously in the weeks following [8, 11]. Regardless of the associated symptoms, stridor must be interpreted as a neurosurgical emergency in the neonate or infant with hydrocephalus and MMC [10–12].

The pathophysiology of stridor associated with the CM II is incompletely understood, but the preferential impairment of abduction may be related to or potentiated by a rostral-caudal somatotopic organization of the cell bodies that respectively serve abduction and adduction within the nucleus ambiguus of the medulla [8, 13]. The nucleus ambiguus provides innervation to laryngeal, pharyngeal, and esophageal skeletal muscle that is branchiomerically derived. The most rostral components serve motor function of the larynx via glossopharyngeal motor fibers. More caudal nuclei serve motor function via vagal special visceral efferent fibers. Volitional control of the larynx is highly complex, but laryngeal function can be summarized to occur via four paired and one unpaired muscle groups. The paired muscles include the cricothyroids, cricoarytenoids, lateral cricoarytenoids, and thyroarytenoids, and the unpaired muscles include the arytenoids. The most rostral cell bodies within the nucleus ambiguus project to the cricothyroids, which provides tensor and adductor function. Cell bodies found slightly more caudally within the nucleus ambiguus project to the posterior cricoarytenoids and provide abductor function to the vocal cords. The most caudal cell bodies project to the arytenoids, which also provide adductor function. Thus, there is a somatotopic organization that may contribute to differential vulnerability to insult or stress in the nuclei that regulate adduction and abduction [5, 8, 13].

There is also some experimental evidence that there is differential susceptibility to injury or stress between fibers supplying adductor and abductor functions of the larynx and that those supplying abduction are more sensitive or vulnerable to injury. This may further contribute to abduction failure with brainstem shift or compromise. The caudal descent of the brainstem in CM II may contribute to the overall stretch upon exiting fibers, and those subserving abduction may be preferentially compromised [8, 13].

Controversy exists as to whether the primary insult to make the CM II symptomatic is related primarily to compression and downward traction on the brainstem and lower CN or is a manifestation of primary dysgenesis [14]. This is an important practical issue as it directs a rational clinical response. If the primary issue is that the congenitally malformed nuclei are vulnerable and sensitive to stress, then the appropriate clinical intervention is treating hydrocephalus and

normalizing intracranial pressure, because insufficiently treated hydrocephalus is a great stressor to a compromised nervous system [4, 5, 12, 15]. By contrast, if compression is the primary mediator of the pathophysiology, then the appropriate surgical response would be posterior fossa decompression via sub-occipital craniectomy and cervical laminectomy [15, 16]. While both interventions have been shown to have clinical benefit, a convincing propensity of clinical experience over time has supported shunt insertion and exploration as the first clinical intervention [2, 6, 8–12, 15, 17]. Shunt exploration should take place promptly regardless of the computed tomography (CT) findings. Absence of ventriculomegaly should not prevent shunt exploration and restoration of normal shunt function [10, 17, 18]. Endoscopic third ventriculostomy with choroid plexus coagulation (ETV/CPC) has gained favor as an effective treatment for hydrocephalus in infants with MMC [2, 19]. At present there are no specific papers that specifically address the efficacy of ETV/CPC in arresting stridor. Consistent favorable outcomes in ETV/CPC suggest that it is effective, but close monitoring of stridor and a low threshold to revert back to the time-proven intervention of ventricular shunting in the presence of persisting stridor appear prudent.

Impaired Airway Protection

Impaired airway protection is another important symptom of the CM II in the neonate [2, 6, 9, 15]. Impaired airway protection may not have the striking clinical finding expression as stridor and often requires a keen sensitivity and sense of awareness of risk for these infants. Affected infants will characteristically show pooling of secretions, which are audible when they cry and occasionally visible as they escape the mouth [16]. Nasal regurgitation, coughing, and choking are frequent, and pharyngeal suctioning yields large volumes of secretions. Most importantly, these children can progress readily to aspiration pneumonia, which can become a ready portal to more generalized infection and sepsis [16, 17].

Listlessness

Listlessness is often seen as a manifestation of a symptomatic CM II [1, 2, 6, 14]. It is grouped here along with the other respiratory manifestations of CM II in the infant as it is thought most frequently to arise as a result of progressive fatigue of breathing against an elevated resistance brought about by laryngeal compromise. As such, it is a very important comorbidity to stridor that can be a harbinger of impending collapse of the struggling infant. However, there are likely to be other contributors to listlessness in the infant with symptomatic CM II. Dysautonomias can potentially contribute to alterations and impairments of perfusion contributing to pallor. Impaired descending tract function may contribute to hypotonia. Impaired airway protection leads to a constant exposure to aspiration pneumonia and an elevated metabolic demand of constant low-grade inflammation or infection. The relatively underdeveloped, emaciated muscle mass of the affected infant provides no significant margin of reserve for such stresses and further contributes to overall risk within these young, fragile newborns [1, 2, 9, 10, 18].

Gastrointestinal Symptoms

A variety of gastrointestinal (GI) symptoms may also be evident in the infant with symptomatic CM II. These include impaired swallowing, impaired airway protection, reduced gastric emptying, and impaired bowel motility that is thought to arise from a primary gastrointestinal dysautonomia [2, 6, 11, 12]. Gastrointestinal issues of neurologic origin in MMC affect the upper part of the digestive system early in life (dysphagia, pharyngoesophageal dysmotility, etc.), while issues arising from the lower digestive tract (constipation, incontinence, etc.) plague later in life. Swallowing is frequently impaired by pharyngoesophageal dysmotility and/or an impaired or absent gag reflex. Progressive weight loss may lead to emaciation despite prolonged feeding times. The pathophysiology of these findings is not known in detail but, like respiratory issues, is

likely related to impaired medullary and vagus nerve function.

Symptom Patterns

Other symptoms can occur in the infant with a symptomatic CM II, but those bulbar functions surrounding the respiratory system (airway preservation and protection) and GI system (secretion management, catabolism/emaciation) predominate. The clinical profiles are variable, but distinct patterns of symptom evolution in newborns can be discerned. The first is that of the progressively and profoundly ill neonate who classically/characteristically has a fairly high (thoracolumbar to high lumbar) spinal defect/placode. These infants classically have nearly immediate hydrocephalus (occasionally with severe intrauterine macrocephaly) and early stridor and poor secretion management with choking, gurgling, and nasal regurgitation [4, 12, 20]. This more involved form of symptomatic CM II is often modestly or minimally responsive to intervention, and these children often succumb from primary and consumptive brainstem collapse despite aggressive treatment of hydrocephalus and posterior fossa decompression and airway support with tracheostomy. Recognition of this scenario can be helpful as it allows guided counseling of the family and care team toward a more palliative course of comfort support and respect for the dignity of the infant rather than a series of invasive and fruitless interventions that hold minimal hope of reversing or impacting the overall situation. In general, the younger the infant and the more severe the hydrocephalus and stridor at the time of prognosis, the more ominous is the scenario [4].

The second and more common scenario in the symptomatic infant is that of the otherwise adjusted infant with MMC/CM II who is noted to progressively develop stridor. Stridor often develops insidiously but precipitously in such children. It may be readily overlooked by parents because it is not intuitive that abnormal respiratory sounds may be the harbinger of an important brainstem problem that represents a neurosurgical emergency.

Symptoms of Chiari II in the Older Child and Adult

The manifestations of CM II in the older child and adult are less common and differ from those in the newborn and infant. They are more insidious in onset and less acutely threatening to the survival of the affected patient [2, 6, 10, 18].

Hand Dysfunction

The most common observed symptom of CM II in an older child or adult is progressive dysfunction of the hands. Classically, this follows a pattern of cervical myelopathy in which tone in the extremities progressively increases and coordination progressively falters. Associated sensory symptoms may be potentiated by associated syringomyelia. A cervical or thoracic syrinx occurs in up to 40% of patients who have MMC and CM II [9]. Its classic manifestation is a suspended sensory loss involving a cape-like distribution over the shoulders and arms. Involvement of the cervical spinal cord impairs the crossing fibers that mediate pain and temperature in the hands and lead to variable but often progressive hand sensory loss. Subtle sensory change can occur, yet what is most commonly observed clinically is a progressive difficulty with delicate hand tasks that has both a sensory and motor component. Such changes often must be actively pursued and directly inquired about by the clinician to be revealed. Practical contemporary tasks such as manipulation of a cell phone is a useful screening task in detecting subtle decline in hand coordination [2, 6, 11, 12].

Sleep Abnormalities

Sleep abnormalities are an important group of symptoms related to CM II in teens and adults. Central sleep apnea results from impaired neurologic respiratory drive during sleep and may arise from any condition that adversely affects brainstem function such as the CM II [3, 21].

Central sleep apnea may also be seen in premature infants and patients suffering brainstem strokes or other insults and as a complication of advanced cardiopulmonary disease. Obstructive sleep apnea occurs when the tongue and muscles of the soft palate, pharynx, and larynx relax and allow physical compromise of the airway. Obesity is a known independent risk factor for obstructive sleep apnea and is a common comorbidity in the MMC community. As such, many patients with MMC are at risk of both central and obstructive sleep apnea. Recent studies have indicated that more than 50% of patients with CM II have clinically significant sleep apnea syndrome and that the presence of CM II is an independent predictor of the severity of the sleep apnea. Typically, a patient suffering from sleep apnea will undergo transient spells of respiratory cessation until the systemic shortage of ventilation and oxygenation elicits an alarm startle arousal response that results in transient wakefulness (for which the patient is usually amnestic) and the restoration of breathing. The most feared complication of this syndrome in the CM II is the failure of such a startle arousal, which can lead to prolonged respiratory impairment and progressive respiratory embarrassment and culminate in respiratory arrest. Mortality in patients with MMC/CM II is estimated at 1% per year, of which a significant percent are victims who are simply found deceased in bed [5, 10, 12]. Symptoms of the CM II may be central to the tragic course of events in these unfortunate victims.

Ataxia

A less common but important symptom of CM II that may be seen in the older child or adult is ataxia. Ataxia is widely described in summary chapters and reviews about CM II, but the underlying evidence and documentation for this finding are relatively sparse. Certainly, there are sufficient abnormalities in the posterior fossa and brainstem to provide an anatomic rationale for these changes. By definition in CM II, the vermis is caudally displaced and elongated. Appendicular ataxia may be a component of collective brainstem and cerebellar dysfunction that is seen as upper extremity dysfunction, which is common in adults with CM II. Similarly truncal ataxia has been described but not comprehensively studied nor reviewed.

Impact of Recent Treatment Modalities on Chiari II

Results of a randomized, multicenter trial comparing prenatal and postnatal closure of MMC were published in March 2011 [22]. This landmark paper was the culmination of the MOMS (Management of Myelomeningocele Study). Women who met strict inclusion criteria and agreed to participate were randomized to either prenatal or postnatal closure of their infants' MMC. Better outcomes in multiple domains were seen for patients who underwent intrauterine closure of their MMC. Prenatal closure was associated with a decreased need for a CSF shunt (primary outcome measure) and a reduced incidence of radiologically determined CM II (secondary measure). At 12 months follow-up, approximately two-thirds (64%) of the patients treated with prenatal closure had a radiologically evident CM II, whereas 96% of the postnatal group had a CM II. The extent of brainstem kink and elongation of the fourth ventricle was also reduced in the prenatal group. The infant fatalities in the prenatal group were due to prematurity or stillbirth, while those in the postnatal treatment group died from symptoms and signs of CM II. Maternal and fetal morbidity was higher in the prenatal group as well [22]. Whether the advantages seemingly conferred by prenatal closure will persist over time remains to be seen. Concern over this, other limitations of the study and concern over other potential morbidities have generated significant controversy around the study results. Yet, the potential improvement in reducing symptomatic CM II may prove to be the greatest overall contribution of prenatal closure of MMC.

CM II symptom outcomes should be central in the assessment of other experimental modalities

for treating MMC and its associated comorbidities as well. Due to the considerable problems associated with VP shunts, several groups are attempting to decrease the frequency with which shunts are placed. One such approach is to relax the criteria for placement of a VP shunt [2] and another is to treat the hydrocephalus with an endoscopic third ventriculostomy and choroid plexus coagulation (ETV-CPC) [19]. As above, the role for ETV-CPC seems to be gradually increasing in the management of hydrocephalus associated with MMC. Traditionally, a shunt needs to be placed in approximately 85% of patients with a MMC, yet these novel approaches have reduced the need for a shunt to 50–60% and 35%, respectively [2, 19]. Long-term follow-up with regard to development of symptoms of CM II will be important in the analysis of these promising results.

Conclusion

The CM II is a complex anomaly of brainstem caudal displacement and malfunction that is of profound significance to the patient with a myelomeningocele. Symptoms are age related and localize predominantly to the bulbar musculature. In the neonate, symptoms of stridor, weak or even silent cry, poor control of oral secretions with nasal regurgitation, and risk for aspiration pneumonia are present and are often progressively associated with fatigue and listlessness that may portend an ominous prognosis. Recognition and timely intervention (hydrocephalus treatment initially followed by consideration for posterior fossa decompression if still symptomatic) provide the best opportunity to stabilize or reverse the findings and optimize outcomes.

Despite maximum treatment, some youngsters (particularly those with high neural tube defects, severe hydrocephalus, and early, pronounced stridor) may not respond to treatment and may succumb to their disease.

Older children and adults usually manifest symptoms of progressive upper extremity dysfunction. Sensory loss is common, and either a myelopathic or ataxia pattern of motor impairment may be observed. Failure to recognize and intervene virtually assures progression of deficit, which is likely irreversible. A high index of suspicion and a proactive, assertive surgical approach likely serve the patient and family optimally.

References

1. Bell WO, Charney EB, Bruce DA, Sutton LN, Schut L. Symptomatic Arnold-Chiari malformation: review of experience with 22 cases. J Neurosurg. 1987;66(6):812–6.
2. Bowman RA, McLone DG, Grant JA, Tomita T, Ita JA. Spina Bifida outcome: a 25 year perspective. Pediatr Neurosurg. 2001;34:114–20.
3. Dauvilliers Y, Stal V, Abril B, Coubes P, Bobin A, Touchon J, Escourrou P, Parker F, Bourgio P. Chiari II malformation and sleep related breathing disorders. J Neurol Neurosurg Psychiatry. 2007;78(12):1344–8.
4. McDowell MM, Blatt JE, Deibert CF, Zwagerman NT, Tempel ZJ, Greene S. Predictors of mortality in children with myelomeningocele and symptomatic Chiari II malformation. J Neurosurg Pediatr. 2018;21(6):587–96.
5. Tubbs RS, Oakes WJ. Treatment and management of the Chiarii~~r~~ II malformation: an evidence based review of the literature. Childs Nerv Syst. 2004;6:375–81.
6. Dyste GN, Menezes AH, VanGilder JC. Symptomatic Chiari malformations: an analysis of presentation, management, and long-term outcome. J Neurosurg. 1989;71(2):159–68.
7. McLone DG, Knepper DA. The cause of the Chiari II malformation- a unified hypothesis. Pediatr Neurosurg. 1989;15:1–12.
8. Choi SS, Tran LP, Zaizai GH. Airway abnormalities in patients with Arnold Chiari malformations. Otolaryngol Head Neck Surg. 1999;121(6):720–4.
9. Rahman M, Perkins LA, Pinkus D. Aggressive surgical management of patients with Chiari II malformation and brainstem malfunction. Pediatr Neurosurg. 2009;45:337.
10. Stevenson K. Chiari II malformation; past, present and future. Neurosurg Focus. 2004;16(2):E5.
11. Ocal E, Irwin B, Cochrane D, Singhal A, Steinbok P. Stridor at birth predicts poor outcome in neonates with myelomeningocele. Childs Nerv Syst. 2011;28:265.
12. Shoja MM, Johal J, Oakes WJ, Tubbs RS. Embryology and pathophysiology of the Chiari I and II malformations: a comprehensive review. J Clin Anat. 2018;31(2):202–15.
13. Kirsch KM, Duncan BR, Black FO, Sears JC. Laryngeal palsy in association with myelomeningocele, hydrocephalus, and the Arnold-Chiari malformation. J Neurosurg. 1968;28(3):207–14.

14. Paul KS, Lye RH, Strang FA. Dutton J:Arnold-Chiari malformation: review of 71 cases. J Neurosurg. 1983;58(2):183–7.
15. Piatt J. Treatment of myelomeningocele: a review of outcomes and continuing neurosurgical considerations among adults: a review. J Neuro Surg Pediatr. 2010;6(6):515–25.
16. Pollack IF, Pang D, Albright AL, Krieger D. Outcome following hindbrain decompression of symptomatic Chiari malformations in children previously treated with myelomeningocele closure and shunts. J Neurosurg. 1992;77(6):881–8.
17. Rauzzino M, Oakes WJ. Chiari 2 and syringomyelia. Neurosurg Clin N Am. 1995;6(2):293–9.
18. Talamanti G, D'Albierti G, Collace M. Myelomeningocele: long-term neurosurgical treatment and follow-up in 202 patients. J Neurosurg Pediatr. 2007;107(5):368–86.
19. Warf BC, Campbell JW. Combined endoscopic third ventriculostomy and choroid plexus coagulation as primary treatment of hydrocephalus for infants with myelomeningocele: long term results of a prospective intent to treat study in 115 East African infants. J Neurosurg Pediatr. 2008;2(5):310–6.
20. Teo C, Parker EC, Aureli S, Boop FA. Chiari II malformation; a surgical series. Pediatr Neurosurg. 1997;27(5):223–9.
21. Luigetti M, Losurdo A, Dittoni S, Testani E, Colcchio S, et al. Improvement of obstructive sleep apneas caused by hydrocephalus associated with Chiari malformation Type II following surgery: case report. J Neurosurg. 1993;78(4):568–73.
22. Adzick NS, Thom EA, Spong CY, Brock JW, Burrows MS, Johnson MP, et al. A randomized trial of prenatal versus postnatal repair of Myelomeningocele. N Engl J Med. 2011;364(11):993–1004.

Part VII

Treatment, Outcomes, and Complications

Treatment of the Pediatric Chiari I Malformation

37

W. Jerry Oakes

Surgical intervention for a pediatric Chiari malformation type I (CM I) is a simple and usually uncomplicated procedure. The more difficult portion of the care is deciding which patients will benefit and how likely that benefit is to occur. The procedure has generated significant controversy as to the extent of the surgery and the exact details that make up each step in the decompression. In general, the purpose of the procedure is to relieve compression at the craniocervical junction and reestablish free cerebrospinal fluid (CSF) egress from the fourth ventricular outlets.

Other aspects of the surgery have been judged to be sufficiently important that this book has devoted separate chapters to them (treatment of hydrocephalus and a discussion of dural opening). This chapter plans simply to outline what is done at the author's institution and attempt to justify why we take the steps we do. Although the chapter will mention alternative techniques, short of a randomized trial, the opinions expressed are solely ours based on our experience [1]. Because other chapters deal with the presentation and evaluation, little will be mentioned concerning those subjects.

We would comment that the presence of a syrinx seems to be a reasonable justification for surgical intervention even with the understanding that some patients with a syrinx will have spontaneous resolution [2]. The decision to recommend surgery rests on the remote likelihood of syrinx resolution contrasted with the risk of developing an irreversible neurological deficit developing due to delayed surgical intervention.

The type of headache that responds to intervention is also worthy of mention. The three headache characteristics that predictably yield a satisfactory outcome are (1) occipital or high cervical pain, (2) reproducibly brought on with some type of Valsalva maneuver, and (3) relatively short duration (few seconds/minutes). With these three characteristics present, the likelihood of relieving the pain is quite high (>95% in our experience). As soon as the headache description deviates from these characteristics, the rate of surgical success falls precipitously, and reoperation because of a lack of headache relief is illogical and unjustified. We have rarely seen it necessary to reoperate on patients because of a return of the characteristic Chiari-type headache.

Surgical Procedure

Once a decision for surgical intervention is made and the risks are accepted by the family, the patient is brought to the operating room and positioned prone with the neck flexed (Fig. 37.1). Pin fixation is used and the head of the bed is elevated 30 degrees to decrease venous pressure. Even

W. J. Oakes (✉)
Departments of Neurosurgery and Pediatrics, University of Alabama, Birmingham, AL, USA
e-mail: Jerry.Oakes@childrensal.org

R. S. Tubbs et al. (eds.), *The Chiari Malformations*, https://doi.org/10.1007/978-3-030-44862-2_37

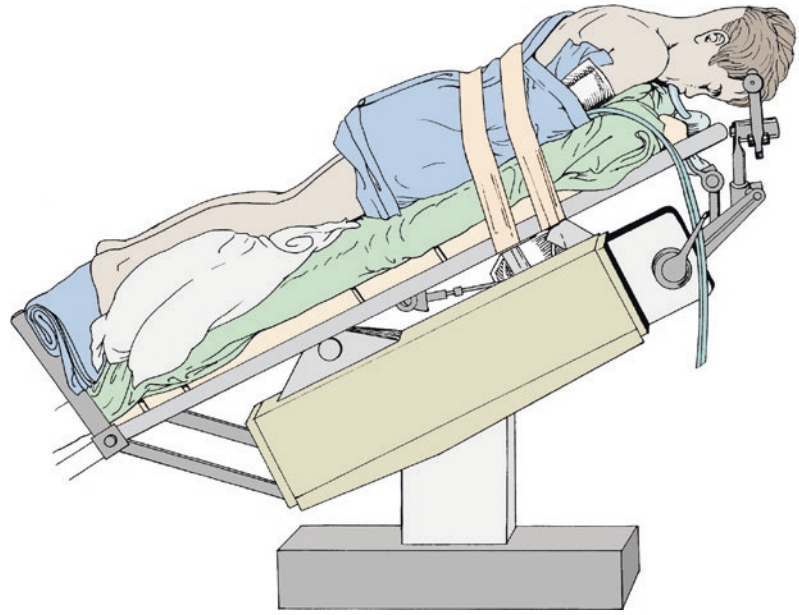

Fig. 37.1 Positioning for posterior fossa decompression for patients with Chiari malformation

small infants may have the judicious application of pin fixation with minimal pressure to ensure maintenance of a flexed position.

The area of the foramen magnum is exposed through a midline incision from a point just below the external occipital protuberance to the spinous process of C-2. I have rarely found it necessary to expose or remove any of C-2 even in the presence of significant caudal displacement of the cerebellar tonsils. In avoiding C-2 removal, we have not seen the development of postoperative kyphosis, which is a serious and difficult-to-treat postoperative complication. The relative avascular midline of the cervical musculature is easily divided and retracted to expose the area of the foramen magnum and dorsal arch of C-1 (Fig. 37.2).

One should keep in mind that this is a midline operation and that there is no need for significant lateral exposure. Especially in the presence of major bony anomalies of the craniocervical junction, the course of the vertebral artery laterally around C-1 is less predictable [3]. The extent of the bony opening need not be wider than the width of the spinal cord. One can easily judge this because the dura begins to become vertical in its orientation. In patients below 2 years of age, this is usually 22–25 mm. Bone at the foramen magnum may be removed with a high-speed drill or craniotome and rongeurs. The width of the foramen magnum opening again is to the point where the dura begins to course vertically. The height rarely needs to be greater than 20–25 mm. By avoiding excessive bony removal, the serious complication of cerebellar slump may be avoided.

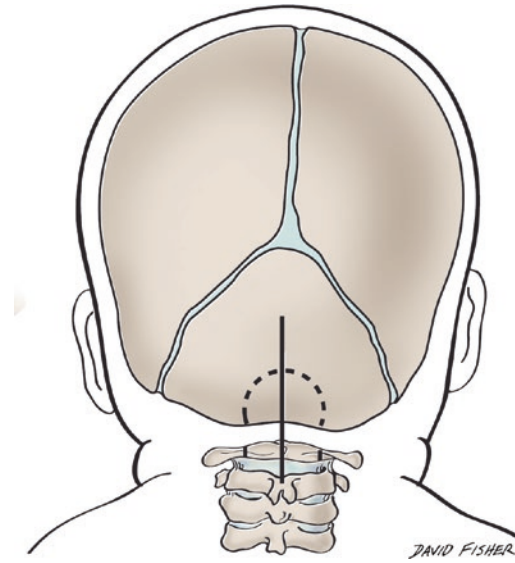

Fig. 37.2 Schematic drawing of the posterior craniocervical junction noting skin incision and areas of bony removal

In select patients, with significant side-to-side compression at the foramen magnum, a portion of the medial condyle may be removed to provide additional room laterally at the point of maximum compression. This situation is seen most commonly in patients with achondroplasia or other similar syndromes. The surgeon should remind himself that the pathology in this condition is in the area of the foramen magnum and not more cephalad in the posterior fossa. The various techniques of replacing bone or other physical restraints exactly where the intradural contents had been compressed seem counterintuitive and unnecessary.

The dorsal arch of C-1 is removed with rongeurs. The lateral and anterior ligaments connecting C-1 to the remainder of the spine can easily be overpowered by a surgeon with significant leverage and a mechanical advantage. This is especially true in young infants and should be avoided. Bony removal should be done with crisp side-to-side bites, and never place an instrument under the posterior arch of C1 where the intradural contents are crowded.

At this point, the surgeon has a choice to close or proceed on to a dural opening. I would agree that the majority of patients with symptomatic CM I will improve by simple bony decompression. However, a significant percentage of patients (6–10%) [4] will have intradural pathology not allowing free egress of CSF out of the fourth ventricular outlets. This is the group that will need an intradural exploration for the opening of these channels, and bony decompression alone will not suffice. The trade-off is the likelihood of creating a large inflammatory response from blood spilled into the subarachnoid space versus the likelihood of finding a fourth ventricular veil or some other obstruction to CSF egress [4]. I would argue that most skilled neurosurgeons can open and graft the dura of the posterior fossa with a very low morbidity and mortality, well less than 6–10%, and therefore dural opening should proceed.

To open the dura at the craniocervical junction, start caudally at the exposed dura. At the level of C-1, the leaves of the dura are generally fused and bleeding is more easily controlled. As you work cephalad, especially in young infants, a marginal or occipital sinus may be encountered. Unfortunately, this is exactly at the point of maximum compression and near the opening of the fourth ventricle. This venous sinus can be dealt with by staying extra-arachnoidal during the initial opening to help avoid subarachnoid blood spillage and working slowly and methodically keeping the leaves of the dura approximated. This can be accomplished with bipolar coagulation and Weck clips or simply by suturing the edge of the dura on each side as it is opened. The dura is opened the vertical length of the bony exposure (Fig. 37.3).

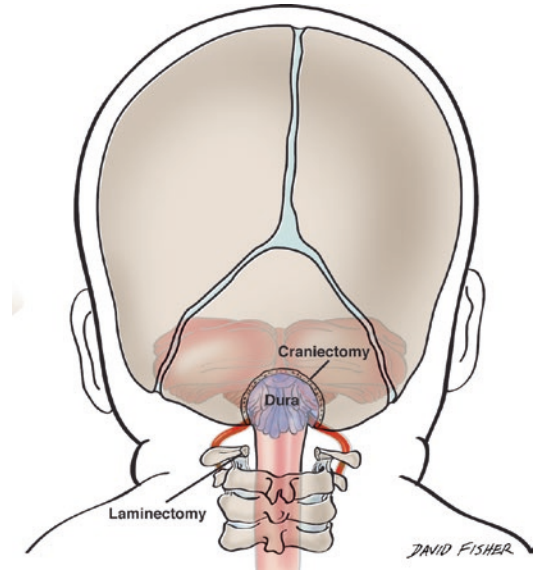

Fig. 37.3 Schematic drawing illustrating regional anatomy and intradural contents

If the point of maximum compression still appears constricted, a horizontal T incision at the point of maximum compression can expand the dural opening more. This may even be done bilaterally.

The arachnoid is opened as a separate layer and clipped to the dura in an attempt to avoid the uncommon complication of acute hydrocephalus from a CSF subdural effusion occurring postoperatively [5].

The tonsils are separated and, if present, the outlet veil is lysed. For initial procedures without life-threatening symptoms or without a huge

syrinx, I generally do not advise burning or shrinking one or both tonsils. Care is taken to manipulate the pial surface of the tonsil minimally, especially the medial surface where adhesions can reestablish fourth ventricular outlet occlusion. If a decision is made to decrease the volume of cerebellar tonsil over the ventricular outlet, the pia should be coagulated on the dorsal tonsillar surface and the removal done from within the pia (Fig. 37.4). This minimizes scarring across the outlet postoperatively.

There are numerous graft materials one can choose from for the dural closure. Not closing the dura and allowing blood and other irritative fluids to react within the subarachnoid space defeat the goal of establishing free and easy egress of CSF out of the fourth ventricle. Of all of the graft materials, the one that has the highest likelihood of being sterile and not causing some type of reaction is the patient's own tissue. A convenient place to harvest a piece of appropriate graft material is the periosteum over the posterior skull. I generally do this through a separate incision. A usual graft size is 4 × 1 ½ cm and it is sewn in place with an attempted watertight closure. The remainder of the closure is routine.

The patient is nursed in an intensive care unit overnight and is generally available for discharge home in 2–3 days. Steroids are not given, and postoperative chemical meningitis almost never occurs with a good dural closure. Blood transfusion is almost never needed, and pain management is adequate with alternating ibuprofen and acetaminophen with something being given every 3–4 hours [6]. With experience, the procedure can routinely be done in less than 90 minutes.

Postoperative complications will be covered in a separate chapter, but acute hydrocephalus may be seen in as many as 3% of patients. This problem appears to be lessened by clipping the arachnoid to the dura [1]. Acute medullary compromise may occur when there is significant anterior or ventral compression [7]. In those patients that violate a line drawn from the basion to the posterior inferior aspect of the C-2 vertebral body by more than 9–10 mm, acute ventral compression is possible (Fig. 37.5). Preparing the family and patient for this possibility is

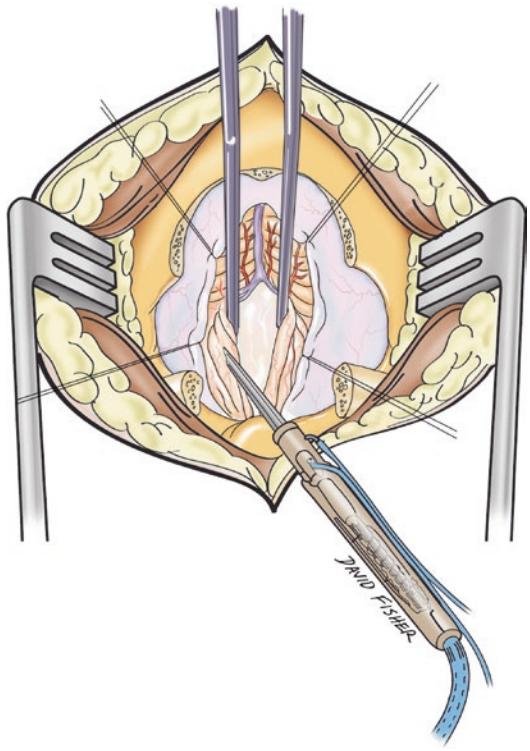

Fig. 37.4 Schematic drawing illustrating subpial resection of the cerebellar tonsil

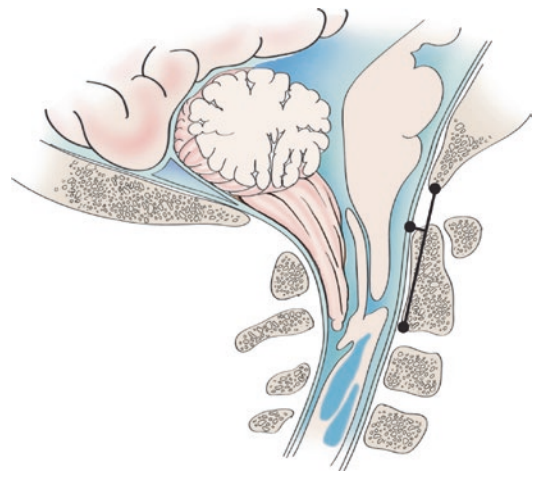

Fig. 37.5 "Rule of 9 mm." Patients may be in danger of postoperative decline when the perpendicular distance (to anterior dura mater) from a line connecting the basion to the posterior aspect of the base of C2 vertebra exceeds 9 mm. This reflects the degree of retroflexion of the odontoid process

important. In our experience, this does not occur without significant medullary symptoms preoperatively. Postoperative pseudomeningoceles are generally handled conservatively, and with time, most will resolve spontaneously. Large syringes associated with longstanding neurological dysfunction may resolve more slowly if not incompletely.

In summary, CM I decompression is a safe and effective procedure for appropriately selected patients. Syrinxes are likely to resolve or, if small, not progress. Occipital headache associated with Valsalva is predicatively relieved immediately and does not recur. Serious complications are rare. Avoiding subarachnoid blood and other subarachnoid irritants enhance recovery and free CSF egress from the fourth ventricular outlets.

References

1. Tubbs RS, Beckman J, Naftel RP, Chern JJ, Wellons JC 3rd, Rozzelle CJ, Blount JP, Oakes WJ. Institutional experience with 500 cases of surgically treated pediatric Chiari malformation Type I. J Neurosurg Pediatr. 2011;7(3):248–56.
2. Doughty KE, Tubbs RS, Webb D, Oakes WJ. Delayed resolution of Chiari I-associated hydromyelia after posterior fossa decompression: case report and review of the literature. Neurosurgery. 2004;55:711.
3. Tubbs RS, Smyth MD, Wellons JC 3rd, Oakes WJ. Distances from the atlantal segment of the vertebral artery to the midline in children. Pediatr Neurosurg. 2003;39:330–4.
4. Tubbs RS, Smyth MD, Wellons JC 3rd, Oakes WJ. Arachnoid veils and the Chiari I malformation. J Neurosurg. 2004;100(5 Suppl Pediatrics):465–7.
5. Elton S, Tubbs RS, Wellons JC 3rd, Blount JP, Grabb PA, Oakes WJ. Acute hydrocephalus following a Chiari I decompression. Pediatr Neurosurg. 2002;36:101–4.
6. Smyth MD, Banks JT, Tubbs RS, Wellons JC 3rd, Oakes WJ. Efficacy of scheduled nonnarcotic analgesic medications in children after suboccipital craniectomy. J Neurosurg. 2004;100(2 Suppl Pediatrics):183–6.
7. Grabb PA, Mapstone TB, Oakes WJ. Ventral brain stem compression in pediatric and young adult patients with Chiari I malformations. Neurosurgery. 1999;44:520–7.

Treatment of the Adult Chiari I Malformation

38

Panagiotis Mastorakos and John D. Heiss

History of Treatment of Chiari I Malformation

In clinical practice and in this chapter, Chiari I malformation (CM I) refers to a symptomatic condition associated with caudal location of the cerebellar tonsils and inferior part of the medulla, without displacement of the fourth ventricle [1, 2]. The first posterior fossa decompression for a patient with Chiari II malformation was performed by van Houweninge Graftdijk [3]. This was followed by a report of posterior fossa decompression for Chiari I malformation in five patients by McConnell and Parker [4]. Several authors over the following decade reported their experiences using craniocervical decompression to treat the Chiari I malformation [5, 6]. In 1950, James Gardner and associates at the Cleveland Clinic recognized the association of the Chiari I malformation with syringomyelia [7]. They postulated that the outlets of the fourth ventricle were occluded by the Chiari I malformation and that a "water-hammer" pulsation was directed from the fourth ventricle, through the obex, and into the central canal of the spinal cord, leading to pulsatile expansion of the central canal to form a syrinx. To reverse this process, Gardner performed a surgical procedure that (1) removed the bone from the posterior aspect of the foramen magnum, (2) opened the fourth ventricle to the subarachnoid space, and (3) "plugged the obex" [7]. His immediate postoperative results in 74 patients were as follows: 52 improved, 11 unchanged, 6 worse, and 5 dead [8]. Later Levy et al. compared craniovertebral decompression and opening of the fourth ventricle with and without obex plugging at the Cleveland Clinic [9] and found no differences in outcome. Plugging the obex could be complicated by damage to the hypoglossal and vagal nuclei and permanent neurologic deficits [10]. In the 1970s, Logue introduced a less invasive alternative to Gardner's procedure. His procedure consisted of simple bony decompression and expansion of the dura with a tissue graft and avoidance of opening of the arachnoid membrane and entrance into the subarachnoid space or fourth ventricle. They performed a clinical study comparing Gardner's procedure with their procedure of simple decompression and duraplasty and demonstrated that there was no difference in syrinx resolution between the procedures, although Gardner's operation resulted in a higher complication rate [8, 11]. Since then, some investigators have

Electronic Supplementary Material The online version of this chapter (https://doi.org/10.1007/978-3-030-44862-2_38) contains supplementary material, which is available to authorized users.

P. Mastorakos · J. D. Heiss (✉)
Surgical Neurology Branch, National Institute of Neurological Disorders and Stroke, National Institutes of Health, Bethesda, MD, USA
e-mail: heissj@ninds.nih.gov

R. S. Tubbs et al. (eds.), *The Chiari Malformations*, https://doi.org/10.1007/978-3-030-44862-2_38

Table 38.1 Comparison of outcomes after posterior fossa decompression (PFD) and posterior fossa decompression and duraplasty (PFDD) in patients with CM I

Outcome	PFDD (%)	PFD (%)
Adults[a]		
Clinical improvement	29/33 (88%)	37/45 (87%)
Decrease in syrinx size	14/14 (100%)	21/33 (64%)
Additional surgery	0/33 (0%)	1/11 (9%)
Complications	14/33 (42%)	4/45 (9%)
Pediatric[b]		
Clinical improvement	44/56 (79%)	51/79 (65%)
Decrease in syrinx size	40/46 (87%)	9/16 (56%)
Additional surgery	3/143 (2%)	15/119 (13%)
Complications	28/135 (22%)	3/111 (3%)

[a]Data are by combining the results of the reports by Chauvet, Isu, Kotil, and Romero [15, 17–19]
[b]From meta-analysis by Durham and Fjeld-Olenec [16]

advocated a decompressive procedure that opens the arachnoid membrane, removes or shrinks the inferior portion of the cerebellar tonsils, and attempts to enlarge the cerebrospinal fluid (CSF) pathways beyond what is achievable with bony decompression and duraplasty alone [12, 13]. Syringomyelia resolves following this latter procedure in about 80% of cases, which is like the results reported for simple decompression and duraplasty with preservation of the arachnoid membrane and tonsils [12–14]. More recently, less invasive surgical treatments have been investigated for Chiari I malformation with and without syringomyelia, ranging from simple bony decompression to bony decompression and partial incision of the dura (Table 38.1) [15–19].

Patient Selection for Operative Treatment

Chiari I malformation is usually not associated with an underlying disease and is considered primary in most patients, although a majority of patients have underdevelopment of the posterior fossa of unknown etiology [20]. Secondary causes should be considered during evaluation of a patient with CM I because if they are present, their treatment might make craniocervical decompression unnecessary. Such underlying conditions include craniosynostosis [21], hydrocephalus [22–26], intracerebral hypotension resulting from a spinal CSF fistula [27–31], pseudotumor cerebri, intracranial tumors, and acromegaly [32–35]. In addition, basilar invagination and instability or hypermobility at the craniocervical junction are causes for failure of craniocervical decompression craniectomy and should be excluded before performing a posterior decompression alone [36–38].

The decision to surgically decompress the craniocervical junction is based primarily on clinical, not radiologic, findings. It is imperative to avoid surgical treatment based primarily on magnetic resonance imaging (MRI) findings of Chiari I malformation in a patient with a history and neurological examination that suggests another cause for their symptoms. The proportion of the population that has MRI scan findings compatible with the diagnosis of CM I far exceeds the proportion with symptoms of CM I. One study found that 0.9% of normal adults undergoing MRI studies of the brain had tonsillar herniation extending more than 5 mm below the foramen magnum [39]. Therefore, the simple presence of 5 or more millimeters of tonsillar ectopia is not adequate justification for craniocervical decompression of any type. Vigilance in patient selection for surgical treatment includes evaluating for the presence of an associated syrinx, which confirms that the Chiari I malformation is causing critical compression of the CSF pathways at the foramen magnum. In patients with CM I without syringomyelia, the decision to operate is straightforward if subjects have cerebellar or medullary signs and symptoms or downbeat nystagmus. Suboccipital and cough headache are also reliable symptoms of CM I. Certain radiologic findings that support critical impaction of the tonsils at the craniocervical junction include (1) tonsils that are peg shaped, instead of rounded [2, 40], (2) narrowed CSF pathways at the foramen magnum as seen on anatomic and phase-contrast cine MRI [41, 42], and (3) tonsillar ectopia over 12 mm [43].

For subjects with CM I and syringomyelia or CM I alone with neurological signs, it is essential

that surgical treatment be rendered expeditiously, as delay in treatment may lead to further neurologic deficit or irreversible losses in neurological function [44]. Before surgery, it is essential to counsel patients with Chiari I malformation, syringomyelia, and neurologic deficit that craniocervical decompression, if successful, will result in stabilization of the associated myelopathy and that objective improvement may occur but is less common [13, 45]. In addition, based on the type of decompression that is being performed, it is necessary to explain the most frequent side effects of that form of treatment and the likelihood of additional surgical treatment in case the initial surgical procedure is unsuccessful. Patients should also be counseled about the fact that in rare cases the clinical symptoms may worsen even after successful surgical treatment and radiological resolution of the syrinx [46]. Patients with CM I without syringomyelia should be counseled that medullary or cerebellar symptoms would be expected to improve but that complete recovery does not occur in all cases. Cough headache improves or resolves completely after surgery in most patients [40, 47, 48].

Selection of the Optimal Operative Treatment

One of the goals of operative therapy is to provide consistently successful treatment while at the same time limiting surgical complications and morbidity. Some studies define surgical success solely on a clinical basis in terms of symptomatic improvement or neurologic outcome. Imaging after surgery is either not performed or not considered pertinent if signs and symptoms are stable. Other studies evaluate surgical success not only in terms of clinical outcome but also considering the effects of surgery on neural anatomy and physiology, seeking to confirm enough enlargement of the intradural volume at the foramen magnum to relieve pressure on the medulla and ectopic cerebellar tonsils, reduction in syrinx diameter, and restoration of CSF movement across the foramen magnum. In a congenital disease whose time course is usually slowly progressive, the long-term outcome of surgery may be prognosticated better if these anatomic and physiologic metrics are used to supplement findings of the patient's history and examination during the first year after surgery. Long-term follow-up of patients has been performed in many craniocervical decompression studies that include exposure of the extra-arachnoidal or intra-arachnoidal spaces. Most of these studies evaluated outcomes retrospectively, but a few of them have been prospective studies [40, 42, 48]. More recent modifications of the craniocervical decompression method, including bony decompression alone or with dural scoring, have generally had shorter follow-up after surgery than older, more invasive, methods. A prospective study in pediatric patients with Chiari I and syringomyelia is the first one to offer long-term outcome for bony decompression alone or with dural scoring [49]. A neurosurgeon must decide on the type of craniocervical decompression to perform based on (1) the reported short- and long-term clinical and radiologic outcomes from the various types of decompression procedures, (2) the pathophysiology of Chiari I malformation, and (3) personal experience [50]. The goal is to select the method that provides permanent, curative therapy, while minimizing injury to neural and soft tissue structures.

Rationale for Using Craniocervical Decompression and Duraplasty for All Patients with Symptomatic Chiari I or Symptomatic Chiari I with Syringomyelia

Although there is increasing evidence that bony decompression alone might be adequate treatment for at least some patients with CM I, especially those without syringomyelia, these studies must be viewed cautiously, as the evaluation of treatment outcome in patients with CM I without syringomyelia is often subjective and follow-up is usually short. Radiologic confirmation of surgical success or failure in patients without syringomyelia is not as straightforward as when syrinx size is used as a radiologic marker. Anatomic

MRI rarely demonstrates expansion of the CSF pathways at the foramen magnum after bony craniocervical decompression alone. Bony decompression alone in patients with CM I with syringomyelia results in a lower rate of syrinx resolution than does bony decompression and expansile duraplasty, which demonstrates that in many cases of CM I, bony decompression alone does not expand CSF pathways at the foramen magnum sufficiently to relieve the encroachment of the cerebellar tonsils on the CSF pathways (Table 38.1). Bony decompression alone in patients with CM I without syringomyelia would, similarly, produce less decompression of the neural elements than would decompression and duraplasty or bony decompression and partial-thickness dural incision. For these reasons and for those listed in the paragraphs that follow, we favor using a decompressive procedure that expands the CSF pathways and intradural volume more than that provided by bony decompression alone.

One can speculate about why syringomyelia only develops in some patients with Chiari I malformation. Clinical research in patients with CM I with syringomyelia has shown that these patients have narrowing of the CSF pathways that prevents normal CSF flow across the foramen magnum during the cardiac cycle. In this setting, expansion of the brain during cardiac systole cannot be compensated normally by the rapid flow of CSF into the spinal canal during systole. In lieu of CSF movement, the cerebellar tonsils and medulla descend every time the brain expands during cardiac systole. The resultant up-and-down motion of the cerebellar tonsils during the cardiac cycle acts as a piston on the spinal subarachnoid space, creating enlarged CSF pressure waves that drive CSF into the spinal cord to form a syrinx. After the syrinx forms, the spinal subarachnoid pressure waves propel the syrinx fluid, leading to syrinx expansion and clinical progression (Fig. 38.1) [40, 42]. This physiologic process usually takes years to create a symptomatic syrinx, perhaps explaining why syringomyelia does not usually affect patients until the age of 20–50 years. The reason that syringomyelia does not develop in other patients with CM I may be because (1) syringomyelia has not had enough time to develop, (2) the encroachment on the CSF pathways is not severe enough to produce the above mechanism of syrinx development and progression, or (3) the encroachment on the CSF pathways is more severe than in patients with CM I-syringomyelia, preventing the piston motion of the tonsils and medulla. Because all patients with symptomatic CM I have critical compression of the neural elements and/or the CSF pathways at the foramen magnum, the procedures to treat CM I alone, or CM I with syrinx, have identical endpoints in that the surgical decompression must sufficiently expand the intradural space at the foramen magnum to effectively decompress the neural elements and CSF pathways. On the other hand, patients with radiologic findings of minimal ectopia, minimal narrowing of the CSF pathways, and atypical symptoms may not be having symptoms referable to CM I but have symptoms due to another condition. In the absence of syringomyelia, we do not recommend surgical decompression, even minimally invasive procedures, for patients who do not have symptoms that can be clearly related to the Chiari I malformation.

Rationale for Using Less Invasive Forms of Craniocervical Decompression for Patients with Symptomatic Chiari I or Symptomatic Chiari I with Syringomyelia

The goal of surgery in patients with Chiari I malformation is to provide enough subarachnoid space at the level of the foramen magnum to relieve the impaction of the cerebellar tonsils in the foramen magnum and reverse the symptoms and signs of the Chiari I malformation. Development of a strategy of surgery, then, might ask how much additional space is required at the level of the foramen magnum for successful reversal of the pathophysiology. Certain observations suggest that the additional space required is very small. For instance, Chiari I malformations in young children occasionally reverse without treatment as the skull grows faster than the brain in

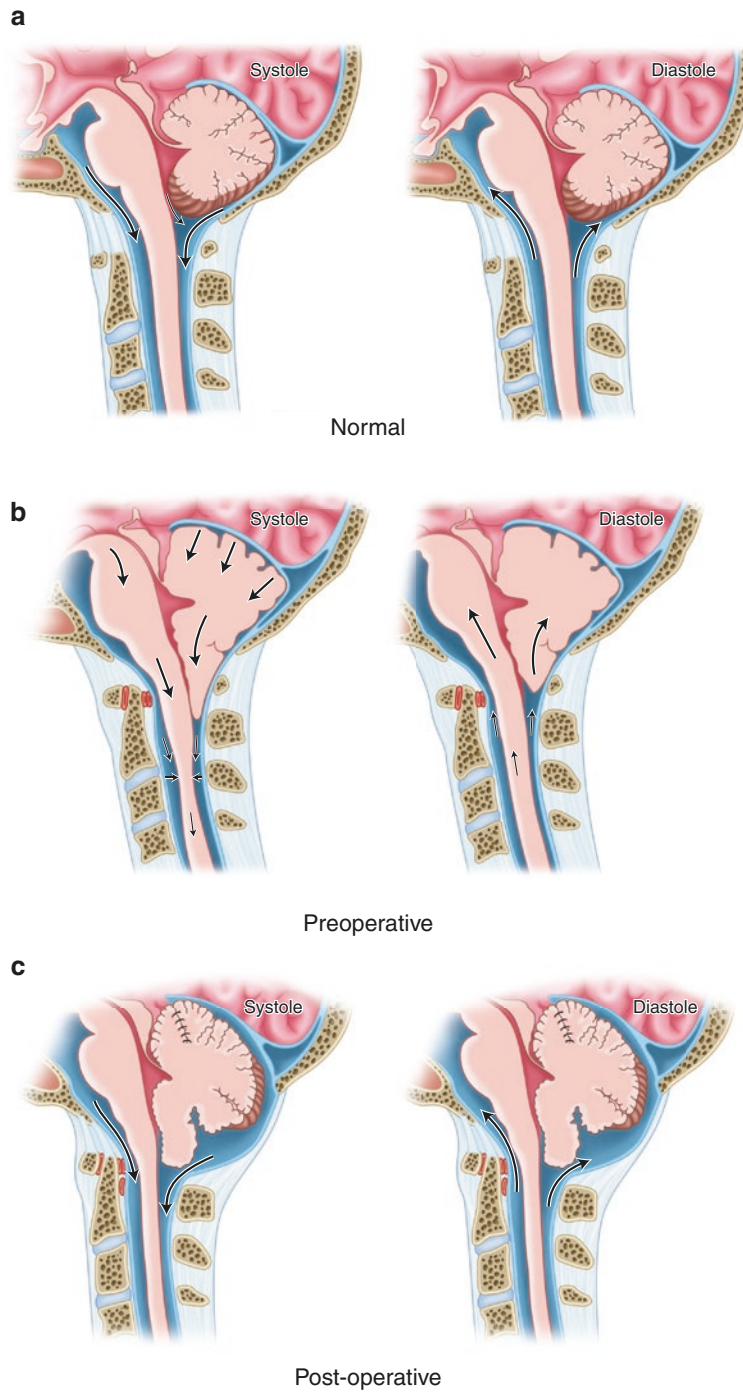

Fig. 38.1 (**a**) Illustration showing normal anatomy and flow of cerebrospinal fluid (CSF) in the subarachnoid space at the foramen magnum during the cardiac cycle. (**b**) Impaction of the cerebellar tonsils in the foramen magnum results in obstructed flow of CSF in the subarachnoid space at the foramen magnum and in the cerebellar tonsils acting as a piston on the cervical subarachnoid space, creating cervical subarachnoid pressure waves that compress the spinal cord from without, propagating syrinx fluid movement. (**c**) Relief of the obstruction of the subarachnoid space at the foramen magnum reverses the mechanism of the impaction of the cerebellar tonsils and of progression of syringomyelia. (Reproduced with permission from Heiss et al. [40], https://thejns.org/view/journals/j-neurosurg/91/4/article-p553.xml)

early childhood [51]. There are also indications that reversal of a very slight increase in thickness of the soft tissues at the level of the foramen magnum associated with acromegaly is sufficient for a Chiari I malformation to reverse after elimination of the excess growth hormone [32, 33]. Thus, the extra room required at the foramen magnum for successful surgery may be a millimeter or even a

fraction of a millimeter, and it may not require much surgery to provide this.

The argument for using either bony decompression alone (without a dural incision) or bony decompression combined with a partial-thickness dural incision as the initial procedure of choice is that it reduces the risk of complications associated with opening the dura and arachnoid, it is usually successful, the patient has a more comfortable postoperative course, and it saves healthcare costs [49]. For instance, in one study of pediatric patients, those undergoing PFDD (posterior fossa decompression and duraplasty) required increased healthcare services than patients with PFD (posterior fossa decompression alone). Patients in whom PFDD was performed were in the operating room 74 minutes longer than those receiving a PFD (201 ± 34 min compared with 127 ± 25 min; $p = 0.0001$)—a 59% increase [52]. Mutchnick et al. also found that morbidity was increased in the patients with PFDD; patients who underwent PFDD used low-grade narcotics, intravenous narcotics, muscle relaxants, and antiemetic medications at greater rates and longer than patients with PFD. Patients who underwent PFDD stayed in the hospital longer (4.0 vs. 2.7 days, $p = 0.0001$), and the average cost per patient undergoing PFDD was almost twofold greater than patients treated with PFD [52]. Similarly, in a recent meta-analysis comparing the two approaches in the pediatric population, PFDD was associated with a 60-minute-longer operation and 0.7-day-longer mean hospital stay. PFDD was associated with increased postoperative complications (OR: 1.71, 95% CI: 1.41–2.08) in the form of CSF leak and meningitis. In this cohort there was greater symptomatic improvement with PFDD (OR: 2.13; 95% CI: 1.31–3.45), but no difference in need for reoperation [53].

Although, in general, the surgical approaches of either bony decompression alone (without a dural incision) or bony decompression combined with a partial-thickness dural incision have been successful in 80–90% of patients, 10–20% of patients will require additional surgery (Table 38.1). There is substantially more information comparing the outcome of these procedures in children than there is in adults. Note that in patients with syringomyelia—the group with the most objective measure of successful surgery—PFD alone had much lower likelihood of resulting in a response of the syrinx (64% in adults, 56% in children) compared to patients who received PFDD (100% in adults, 87% in children). See Table 38.1. Almost no adults who received PFDD required additional surgery compared to 9% of the patients who were treated with PFD. Recent long-term follow-up of pediatric patients who underwent PFD demonstrated improvement of preoperative clinical symptoms in 58% of cases, with 7% of patients requiring repeat surgery [49].

As surgical therapy has evolved in the MRI era, an era in which the outcome of surgery is easier to assess and can be assessed with higher resolution, it has become apparent that simply performing the bone decompression alone or combining the bone decompression with superficially opening the dura (partial thickness) or removing the outer layer of the dura is successful in most patients. The arguments for using this approach as the initial procedure are that it reduces the morbidity of the procedure, it is usually successful, and these features outweigh the disadvantages of knowing that further surgery to open the dura will be required in 10–20% of patients treated in this fashion. On the other hand, those favoring PFDD discuss the value of having the capacity to visually assess the subarachnoid space to examine for a subarachnoid abnormality (arachnoiditis, dural or arachnoid band, arachnoid cyst) after opening the dura, whether the arachnoid is left intact or not, and argue that the consistency of success and a single operation outweighs the disadvantages associated with the greater incidence of complications and additional surgery later.

Ideally, there would be a method of determining during surgery the least amount of surgery that each individual patient requires to open the subarachnoid space at the foramen magnum. That is, it would be valuable if it could be determined during surgery if removal of bone alone, removal of bone combined with a partial-thickness opening of the dura, or bone removal and open-

ing the dura, but not the arachnoid, is sufficient in individual patients, so that the surgery could stop at the least stage that is likely to be successful. Intraoperative ultrasound has been used for this purpose to examine the distance between the inner layer of the dura and the posterior edge of the cerebellar tonsils, to assess the pulsatility of the cerebellar tonsils and the spinal cord surrounding a syrinx, and to see if bony decompression or partial-thickness dural incision provided the extra space needed [17, 40, 42, 54], although its value has not been established for this purpose.

Surgical Management

As mentioned in the discussions above, a surgical procedure for CM I should relieve the impaction of the cerebellar tonsils and the obstruction to the free pulsatile flow of CSF across the foramen magnum [40, 42]. In fact, clinical improvement in patients with CM I correlates with postsurgical enlargement of the subtonsillar and retrotonsillar cisterns [55]. A surgical method should be chosen that is extensive enough to target and eliminate the pathophysiologic process of the disorder. If it has equal or superior effectiveness, therapy associated with lesser risk should be selected in preference to treatment options associated with greater risk. Further, therapy with less invasion of the central nervous system (CNS) is preferable to options of equal effectiveness with more CNS invasion.

We advocate choosing between the two least invasive procedures that effectively expand the volume of the foramen magnum beyond bony decompression alone, either selecting simple craniocervical decompression and duraplasty without opening the arachnoid membrane (Fig. 38.2) or decompression of the bone of the posterior lip of the foramen magnum and removal of the posterior arch of C1, and occasionally part of C2, with a partial-thickness dural incision.

Patients are positioned in the prone position on silicone gel pads that support the chest and pelvis and that allow the abdomen to hang freely. The neck is flexed slightly. The head is held with the three-pin Mayfield head holder (OMI Inc., Cincinnati, OH).

A midline skin incision is made extending from above the inion to the level of the C2 spinous process. For duraplasty, a triangular pericranial graft is obtained from the occipital area measuring 4–5 cm in length and width. We free the skin margins from the deep fascia and open the fascia in a Y-shaped incision [56]. The Y-shaped incision is preferred to a linear fascial incision because its closure suspends the suboccipital muscles and prevents them from recessing against the dural graft.

Enough bone should be removed at the foramen magnum to completely decompress the entire posterior surface of the cerebellar tonsils, usually 2 cm deep and 2.5–3.0 cm from side to side. Cervical laminectomy extends inferiorly to the tips of the cerebellar tonsils; removal of the posterior arch of C1, and occasionally at least the superior part of the lamina of C2, is required.

After suboccipital craniectomy and laminectomy, but before opening the dura, ultrasound imaging is performed to assess if bony decompression is adequate to relieve impaction of the cerebellar tonsils and to search for bands and membranes within the cisterna magna and upper cervical subarachnoid space (Figs. 38.3, 38.4 and Video 38.1a, 38.1b).

The dura is opened in the midline at the C1 level with care to avoid injury to the underlying arachnoid (Fig. 38.5 and Video 38.2). For duraplasty, the incision is carried superiorly and split just below the foramen magnum to create a Y-shaped dural opening [56]. The cisterna magna expands immediately in almost all cases. Leakage of CSF through a small hole in the cisterna magna is not uncommon and has not resulted in inferior outcomes. The dura is retracted with 4–0 multifilament nylon sutures. A pattern of the size and shape of the opening for the dural graft is created by cutting a cottonoid to the same shape and size; the cottonoid is then used to determine the size and shape of the pericranial graft. The pericranial autograft is sutured to the durotomy margins with a running 4–0 multifilament nylon suture. The graft expands the volume of the posterior fossa and provides a biological membrane that con-

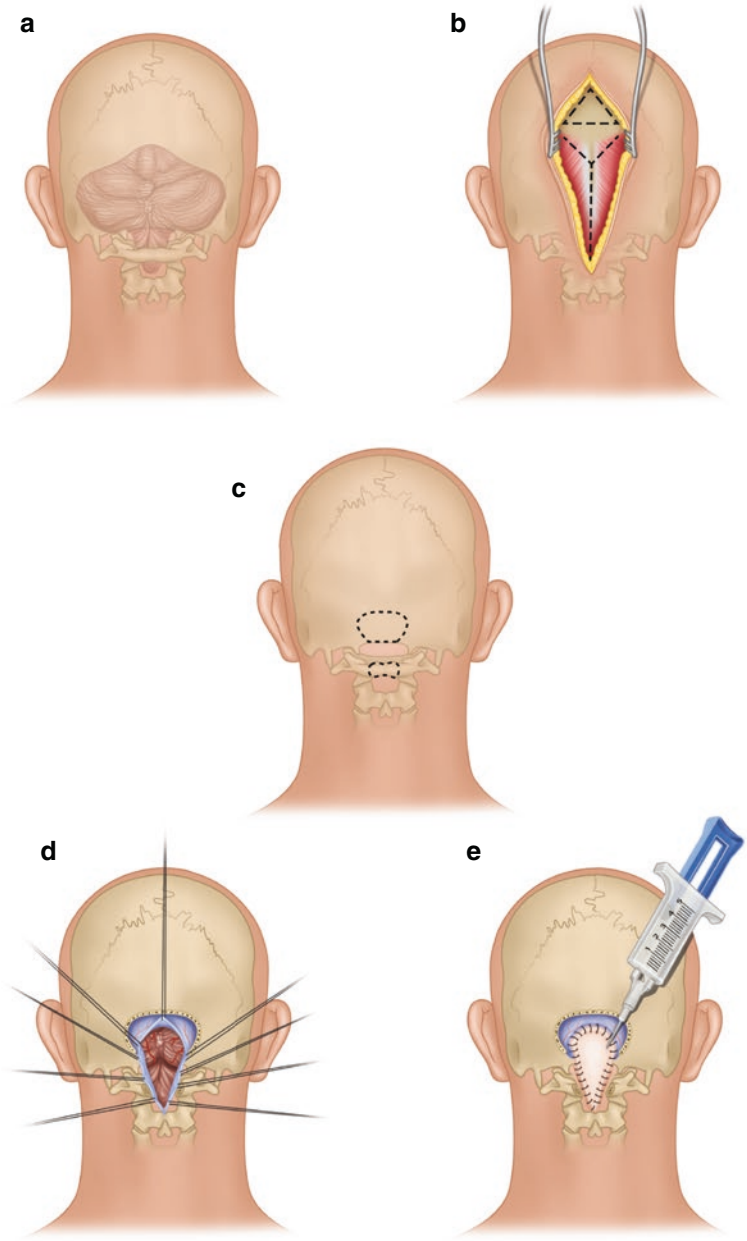

Fig. 38.2 Drawings describe decompression and duraplasty for Chiari I malformation. (**a**) The anatomic extent of the underlying cerebellum is seen through the transparent posterior fossa bone and dura. (**b**) The skin, fascial, and pericranial incisions are shown. (**c**) Bone removal includes the suboccipital bone at the foramen magnum, the dorsal arch of C1, and occasionally the superior part of the lamina of C2 if the tonsils protrude to this level. (**d**) The dura has been opened while preserving the arachnoid. (**e**) A pericranial graft has been sutured to the surrounding durotomy to create an expansile duraplasty. Fibrin glue is applied to augment closure of the suture line

tains the CSF and prevents adhesions to the cerebellum by the suboccipital musculature. Autologous pericranium is preferred to other graft material because it seals better to the surrounding dura and is not immunogenic.

Almost all patients respond to decompressive surgery [40, 45]. In rare patients, opening the dura will not result in expansion of the cisterna magna with CSF, signaling that bands or membranes are binding the arachnoid to the cerebellum and spinal cord. This contingency requires opening of the arachnoid of the cisterna magna, cutting the bands or membranes, and tacking the arachnoid to the durotomy margin. In the unusual patient in whom the syrinx fails to resolve after decompressive surgery, it is because the pathophysiologic mechanism has not been eliminated [57]; in these cases a second operation usually resolves syringomy-

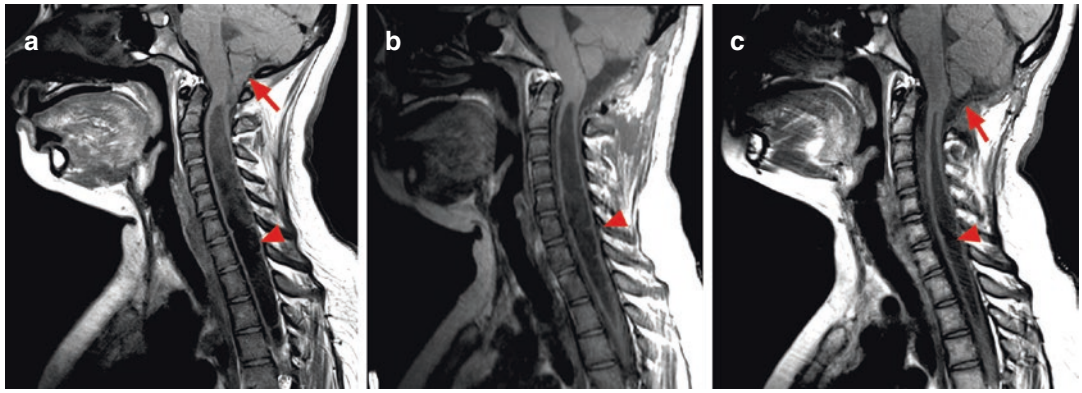

Fig. 38.3 T1-weighted magnetic resonance imaging (MRI) of the cervical spine in the midsagittal plane in a young woman with a 7-month history of cough headache and more recent onset of nystagmus, bilateral upper extremity dissociated sensory loss, and ataxia. Before craniocervical decompression and duraplasty, (**a**) a Chiari I malformation (arrow) and large-diameter syrinx (arrow head) are seen. (**b**) The syrinx diameter decreases progressively at 1 week. (**c**) Three months after surgery (arrow head), CSF is clearly seen posterior and inferior to the cerebellar tonsils (arrow), whose shape has begun to change from a pointed (**a**, arrow) to a rounded shape (**c**, arrow) as a result of no longer being impacted into the foramen magnum with each pulse. Headache, nystagmus, and ataxia resolved, and upper extremity sensation improved after surgery

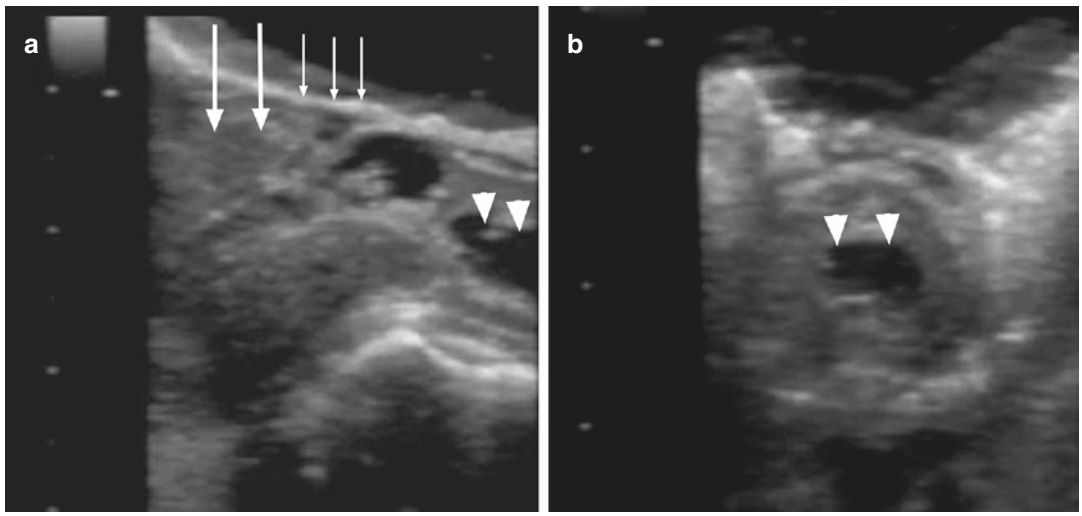

Fig. 38.4 (See also Videos 38.1a, b). (**a**) Sagittal and (**b**) axial intraoperative ultrasonographic images of the craniocervical junction were obtained on the patient described in Fig. 38.3 after bony decompression of the foramen magnum and laminectomy of C1. The dorsal dura (thin arrows) is superficial to the cerebellar tonsils (thick arrows), which have a pointed shape because of their pulsatile impaction into the foramen magnum. The syrinx is shown by arrowheads in (**a**) and (**b**)

elia by correcting conditions that prevented the subarachnoid space posterior to the cerebellar tonsils from expanding, such as inadequate bone removal or an extradural pseudocyst [57–61]. In the rare patient with severe primary or secondary arachnoiditis, syringomyelia cannot be treated successfully using an approach that opens CSF pathways at the foramen magnum. Syrinx shunts are an option but carry risks of neurologic deficits developing from their placement (20%) or delayed cord tethering, occlusion and malfunction over time, and foreign body-related infection [12, 62–

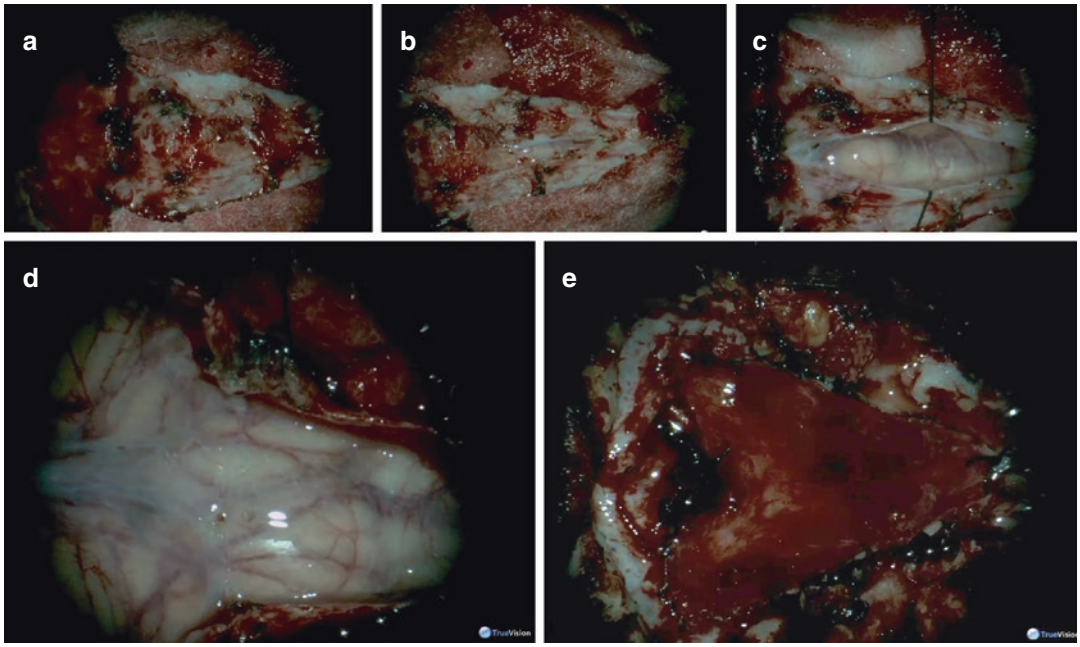

Fig. 38.5 (See also Video 38.2). Operative photographs were taken sequentially after suboccipital craniectomy, and C1 laminectomy was performed on the patient described in Fig. 38.3 with Chiari I malformation and syringomyelia. In each photograph, left is cephalad and right is caudal. (**a**) The dura in the upper cervical spinal canal is almost translucent in this case. (**b**) The spinal dura is opened in the midline while preserving the underlying arachnoid membrane. (**c**) The dural opening is elongated exposing the caudal aspect of the left cerebellar tonsil. (**d**) The inferior part of the cerebellar hemispheres, the cisterna magna, and the upper spinal canal are exposed; the arachnoid remains intact. (**e**) A triangular piece of autologous pericranium has been sutured to the surrounding dura to create an expansile duraplasty

65]. Because of these risks, in patients with Chiari I and syringomyelia, syrinx shunts should only be used in cases of syringomyelia that cannot be treated using an approach that opens CSF pathways at the foramen magnum.

In recent years, it has become apparent that simply performing the bone decompression and superficially opening the dura (partial thickness) or removing the outer layer of the dura results in resolution of the syrinx in most patients, with 10–35% failing to respond. The argument of using this approach as the initial procedure is that it reduces the risk of a pseudomeningocele associated with opening the dura and arachnoid, it is usually successful, and these features outweigh the disadvantages of knowing that further surgery to open the dura will be required more often in patients treated in this fashion (Table 38.1) [66].

In contrast to this trend toward less invasive approaches, Batzdorf et al. suggest that opening of the arachnoid allows identification of arachnoid strands, some of which could prevent ascent of the tonsils. They also found that cerebellar tonsil reduction opens the passage from the fourth ventricle immediately and prevents reapposition [55]. However, these additional steps may not benefit most patients and may be detrimental by increasing surgical morbidity, postsurgical scarring, and the complications of arachnoiditis [40, 57]. Jia et al. demonstrated that posterior fossa decompression combined with the resection of tonsils was associated with longer operation times and increased incidence of postoperative dizziness and headache without having overall better outcomes compared to PFDD [67].

Complication Avoidance

The most frequent cause of surgical failure is inadequate removal of bone at the foramen magnum, which results in persistent compression of the cerebellar tonsils and CSF pathways [57, 68, 69]. Another frequent reason for failure is the development of a persistent leak of CSF through the dural graft that results in the formation of a pseudomeningocele dorsal to the dural graft; the pseudomeningocele presses the dural graft anteriorly and creates adhesions between the graft and the underlying cerebellum that obliterates the dorsal CSF pathway [70]. Maintaining the arachnoid membrane during craniocervical decompression prevents CSF leakage and provides an additional biological barrier to scar formation between the graft or duraplasty suture line and the underlying neural elements. Cerebrospinal leakage through the skin should not occur if the dural closure and the fascial closure are secure, except for cases in which hydrocephalus or pseudotumor cerebri is present. Hydrocephalus and pseudotumor cerebri should be assessed for before surgery because syringomyelia may improve after ventricular shunting in patients with associated hydrocephalus, and decompressive surgery at the foramen magnum is rarely successful and uncomplicated in patients with a Chiari I malformation caused by high intracranial pressure [71, 72]. Leakage of CSF through the skin incision is treated initially with skin sutures. If CSF leakage persists, a computed tomography (CT) scan should be obtained to evaluate for hydrocephalus and extradural hematoma. External drainage of CSF and/or reoperation to replace or repair the dural graft may be required. Excessive drainage of lumbar CSF may increase tonsillar ectopia [73]. Treatment should be prompt because development of meningitis or graft infection may lead to surgical failure from secondary arachnoiditis at the surgical site.

Postoperative Care

The patient is observed overnight after surgery in the intensive care unit (ICU) for changes in neurological status and is given a level of narcotic analgesia that allows participation in hourly neurological examinations. Rarely, hydrocephalus may develop and is signaled by persistent lethargy. An urgent head CT scan should be performed in such patients and treatment of hydrocephalus rendered. After leaving the ICU, most patients report symptoms of pain and local muscle spasm for 1–2 weeks after surgery, which are relieved with a regimen of narcotic analgesic, muscle relaxant, and nonsteroidal anti-inflammatory drugs (NSAIDs). All patients receive deep-vein thrombosis (DVT) prophylaxis including (1) sequential compression stockings (SCS) beginning before induction of anesthesia and continuing throughout hospitalization when the patient is in bed and (2) low-dose subcutaneous heparin.

The results of surgical therapy of syringomyelia can be evaluated noninvasively using MRI. Clinical stabilization or improvement after treatment follows reduction in syrinx diameter [74]. MRI scans of the cervical spine and posterior fossa should be performed at 3–12 months after surgery to evaluate if CSF pathways have been restored at the foramen magnum and if the syrinx is becoming progressively smaller (Fig. 38.3). Elimination of the active pathophysiologic process causing the syringomyelia is demonstrated by collapse of a syrinx and reduction in the spinal cord edema as seen on MRI [44, 45, 75, 76].

Patients may desire additional treatment because of symptoms of myelopathy that persist after surgery. Neuropathic pain often continues after surgery, despite successful surgery and collapse of the syrinx. Various medications from the antidepressant (amitriptyline) and antiepileptic groups (gabapentin) may be tried to control this symptom, but the need for chronic treatment may require consultation with a pain-control specialist. Craniocervical decompression and duraplasty should be revised only if the syrinx maintains its size or enlarges after surgery and neurologic deficits progress. Symptomatic hydrocephalus, if present, should be treated.

Procedures for Chiari I malformation that effectively open the CSF pathways to provide

normal pulsatile flow across the subarachnoid space at the foramen magnum provide effective and lasting treatment of syringomyelia with low morbidity (Figs. 38.1 and 38.2). After successful craniocervical decompression surgery for Chiari I and syringomyelia, the cerebellar tonsils lose their conical shape, the CSF pathways expand at the foramen magnum, and the syrinx decreases to less than 50% of its presurgical diameter—although it may take several months for the collapse of the syrinx to occur [45].

Conclusion

Chiari I malformation is not a primary neural malformation but rather a secondary malformation that results from deformation of the neural elements in response to reduced volume of the inferior part of the posterior fossa [20, 77, 78] and impaction of the cerebellar tonsils into the foramen magnum with every heartbeat [40, 42]. Because of this, a surgical procedure that expands the volume of the foramen magnum relieves compression on the neural elements and CSF pathways and opens the obstruction to the free pulsatile flow of CSF during the cardiac cycle. Medullary and cerebellar symptoms usually improve after decompression of CM I. Syringomyelia and cough headache reliably resolve following restoration of normal CSF flow at the foramen magnum.

Acknowledgments This chapter is an updated version of the one authored by Dr. Heiss and the late Edward H. Oldfield, MD, in the first edition of this book.

References

1. Chiari H. Über Veränderungen des Kleinhirns infolge von congenitaler Hydrocephalie des Grosshirns (concerning changes in the cerebellum due to hydrocephalus of the cerebrum). Dtsch Med Wochenschr. 1891;17:1172–5.
2. Harding BN, Copp AJ. Malformations. In: Graham DI, Lantos PL, editors. Greenfield's neuropathology. 1. 7th ed. London: Arnold; 2002. p. 357–483.
3. Mortazavi MM, Tubbs RS, Hankinson TC, Pugh JA, Cohen-Gadol AA, Oakes WJ. The first posterior fossa decompression for Chiari malformation: the contributions of Cornelis Joachimus van Houweninge Graftdijk and a review of the infancy of "Chiari decompression". Childs Nerv Syst. 2011;27(11):1851–6.
4. McConnell AA, Parker HL. A deformity of the hindbrain associated with internal hydrocephalus. Its relation to the Arnold-Chiari malformation. Brain. 1938;61:415–29.
5. Adams RD, Schatzki R, Scovill WB. The Arnold-Chiari malformation. Diagnosis, demonstration by intraspinal Lipiodol and successful surgical treatment. N Engl J Med. 1941;225:125–31.
6. Bucy PC, Lichtenstein BW. Arnold-Chiari deformity in an adult without obvious cause. J Neurosurg. 1945;2:245–50.
7. Gardner WJ, Goodall RJ. The surgical treatment of Arnold-Chiari malformation in adults; an explanation of its mechanism and importance of encephalography in diagnosis. J Neurosurg. 1950;7(3):199–206.
8. Gardner WJ. Hydrodynamic mechanism of syringomyelia: its relationship to myelocele. J Neurol Neurosurg Psychiatry. 1965;28:247–59.
9. Levy WJ, Mason L, Hahn JF. Chiari malformation presenting in adults: a surgical experience in 127 cases. Neurosurgery. 1983;12(4):377–90.
10. Pillay PK. Thecoperitoneal shunting for syringomyelia. J Neurosurg. 1991;75(5):835–6.
11. Logue V, Edwards M. Syringomyelia and its surgical treatment--an analysis of 75 patients. J Neurol Neurosurg Psychiatry. 1981;44(4):273–84.
12. Barbaro NM. Surgery for primarily spinal syringomyelia. In: Batzdorf U, editor. Syringomyelia: current concepts in diagnosis and treatment. Baltimore: Williams & Wilkins; 1991. p. 183–98.
13. Klekamp J, Batzdorf U, Samii M, Bothe HW. The surgical treatment of Chiari I malformation. Acta Neurochir. 1996;138(7):788–801.
14. Villa A, Imperato A, Maugeri R, Visocchi M, Iacopino DG, Francaviglia N. Surgical treatment in symptomatic Chiari malformation Type I: a series of 25 adult patients treated with cerebellar tonsil shrinkage. Acta Neurochir Suppl. 2019;125:125–31.
15. Chauvet D, Carpentier A, George B. Dura splitting decompression in Chiari type 1 malformation: clinical experience and radiological findings. Neurosurg Rev. 2009;32(4):465–70.
16. Durham SR, Fjeld-Olenec K. Comparison of posterior fossa decompression with and without duraplasty for the surgical treatment of Chiari malformation Type I in pediatric patients: a meta-analysis. J Neurosurg Pediatr. 2008;2(1):42–9.
17. Isu T, Sasaki H, Takamura H, Kobayashi N. Foramen magnum decompression with removal of the outer layer of the dura as treatment for syringomyelia occurring with Chiari I malformation. Neurosurgery. 1993;33(5):844–9; discussion 9-50.

18. Kotil K, Ton T, Tari R, Savas Y. Delamination technique together with longitudinal incisions for treatment of Chiari I/syringomyelia complex: a prospective clinical study. Cerebrospinal Fluid Res. 2009;6:7.
19. Romero FR, Pereira CAdB. Suboccipital craniectomy with or without duraplasty: what is the best choice in patients with Chiari type 1 malformation? Arq Neuropsiquiatr. 2010;68(4):623–6.
20. Nyland H, Krogness KG. Size of posterior fossa in Chiari type 1 malformation in adults. Acta Neurochir. 1978;40(3–4):233–42.
21. Cinalli G, Spennato P, Sainte-Rose C, Arnaud E, Aliberti F, Brunelle F, et al. Chiari malformation in craniosynostosis. Childs Nerv Syst. 2005;21(10):889–901.
22. Buxton N, Jaspan T, Punt J. Treatment of Chiari malformation, syringomyelia and hydrocephalus by neuroendoscopic third ventriculostomy. Minim Invasive Neurosurg. 2002;45(4):231–4.
23. Decq P, Le Guerinel C, Sol JC, Brugieres P, Djindjian M, Nguyen JP. Chiari I malformation: a rare cause of noncommunicating hydrocephalus treated by third ventriculostomy. J Neurosurg. 2001;95(5):783–90.
24. Hayhurst C, Osman-Farah J, Das K, Mallucci C. Initial management of hydrocephalus associated with Chiari malformation Type I-syringomyelia complex via endoscopic third ventriculostomy: an outcome analysis. J Neurosurg. 2008;108(6):1211–4.
25. Metellus P, Dufour H, Levrier O, Grisoli F. Endoscopic third ventriculostomy for treatment of noncommunicating syringomyelia associated with a Chiari I malformation and hydrocephalus: case report and pathophysiological considerations. Neurosurgery. 2002;51(2):500–3; discussion 3-4.
26. Mohanty A, Suman R, Shankar SR, Satish S, Praharaj SS. Endoscopic third ventriculostomy in the management of Chiari I malformation and syringomyelia associated with hydrocephalus. Clin Neurol Neurosurg. 2005;108(1):87–92.
27. Atkinson JL, Weinshenker BG, Miller GM, Piepgras DG, Mokri B. Acquired Chiari I malformation secondary to spontaneous spinal cerebrospinal fluid leakage and chronic intracranial hypotension syndrome in seven cases. J Neurosurg. 1998;88(2):237–42.
28. Kasner SE, Rosenfeld J, Farber RE. Spontaneous intracranial hypotension: headache with a reversible Arnold-Chiari malformation. Headache. 1995;35(9):557–9.
29. Mea E, Chiapparini L, Leone M, Franzini A, Messina G, Bussone G. Chronic daily headache in the adults: differential diagnosis between symptomatic Chiari I malformation and spontaneous intracranial hypotension. Neurol Sci. 2011;32(Suppl 3):291–4.
30. Puget S, Kondageski C, Wray A, Boddaert N, Roujeau T, Di Rocco F, et al. Chiari-like tonsillar herniation associated with intracranial hypotension in Marfan syndrome. Case report. J Neurosurg. 2007;106(1 Suppl):48–52.
31. Udayakumaran S. Post CSF shunting Chiari I malformation--sequel or complication? Hypertension or hypotension? Childs Nerv Syst. 2009;25(11):1391–2; author reply 3.
32. Agostinis C, Caverni L, Montini M, Pagani G, Bonaldi G. "Spontaneous" reduction of tonsillar herniation in acromegaly: a case report. Surg Neurol. 2000;53(4):396–9.
33. Ammerman JM, Goel R, Polin RS. Resolution of Chiari malformation after treatment of acromegaly. Case illustration. J Neurosurg. 2006;104(6):980.
34. Hara M, Ichikawa K, Minemura K, Kobayashi H, Suzuki N, Sakurai A, et al. Acromegaly associated with Chiari-I malformation and polycystic ovary syndrome. Intern Med. 1996;35(10):803–7.
35. Lemar HJ Jr, Perloff JJ, Merenich JA. Symptomatic Chiari-I malformation in a patient with acromegaly. South Med J. 1994;87(2):284–5.
36. Aronson DD, Kahn RH, Canady A, Bollinger RO, Towbin R. Instability of the cervical spine after decompression in patients who have Arnold-Chiari malformation. J Bone Joint Surg Am. 1991;73(6):898–906.
37. Fenoy AJ, Menezes AH, Fenoy KA. Craniocervical junction fusions in patients with hindbrain herniation and syringohydromyelia. J Neurosurg Spine. 2008;9(1):1–9.
38. Grabb PA, Mapstone TB, Oakes WJ. Ventral brain stem compression in pediatric and young adult patients with Chiari I malformations. Neurosurgery. 1999;44(3):520–7; discussion 7-8.
39. Vernooij MW, Ikram MA, Tanghe HL, Vincent AJ, Hofman A, Krestin GP, et al. Incidental findings on brain MRI in the general population. N Engl J Med. 2007;357(18):1821–8.
40. Heiss JD, Patronas N, DeVroom HL, Shawker T, Ennis R, Kammerer W, et al. Elucidating the pathophysiology of syringomyelia. J Neurosurg. 1999;91(4):553–62.
41. McGirt MJ, Atiba A, Attenello FJ, Wasserman BA, Datoo G, Gathinji M, et al. Correlation of hindbrain CSF flow and outcome after surgical decompression for Chiari I malformation. Childs Nerv Syst. 2008;24(7):833–40.
42. Oldfield EH, Muraszko K, Shawker TH, Patronas NJ. Pathophysiology of syringomyelia associated with Chiari I malformation of the cerebellar tonsils. Implications for diagnosis and treatment. J Neurosurg. 1994;80(1):3–15.
43. Elster AD, Chen MY. Chiari I malformations: clinical and radiologic reappraisal. Radiology. 1992;183(2):347–53.
44. Pillay PK, Awad IA, Little JR, Hahn JF. Surgical management of syringomyelia: a five year experience in the era of magnetic resonance imaging. Neurol Res. 1991;13(1):3–9.
45. Wetjen NM, Heiss JD, Oldfield EH. Time course of syringomyelia resolution following decompression of Chiari malformation Type I. J Neurosurg Pediatr. 2008;1(2):118–23.

46. Shetty J, Kandasamy J, Sokol D, Gallo P. Clinical deterioration despite syringomyelia resolution after successful foramen magnum decompression for Chiari malformation - case series. Eur J Paediatr Neurol. 2019;23(2):333–7.
47. Sansur CA, Heiss JD, DeVroom HL, Eskioglu E, Ennis R, Oldfield EH. Pathophysiology of headache associated with cough in patients with Chiari I malformation. J Neurosurg. 2003;98(3):453–8.
48. Vakharia VN, Guilfoyle MR, Laing RJ. Prospective study of outcome of foramen magnum decompressions in patients with syrinx and non-syrinx associated Chiari malformations. Br J Neurosurg. 2011;26:7.
49. Massimi L, Frassanito P, Chieffo D, Tamburrini G, Caldarelli M. Bony decompression for Chiari malformation Type I: long-term follow-up. Acta Neurochir Suppl. 2019;125:119–24.
50. Rocque BG, George TM, Kestle J, Iskandar BJ. Treatment practices for Chiari malformation type I with syringomyelia: results of a survey of the American Society of Pediatric Neurosurgeons. J Neurosurg Pediatr. 2011;8(5):430–7.
51. Waldau B, Domeshek LF, Leigh FA, Lum KC, Fuchs HE, Marcus JR, et al. Spontaneous resolution of a 13-mm Chiari malformation Type I in relation to differential growth of the posterior fossa volume. J Neurosurg Pediatr. 2009;3(2):110–4.
52. Mutchnick IS, Janjua RM, Moeller K, Moriarty TM. Decompression of Chiari malformation with and without duraplasty: morbidity versus recurrence. J Neurosurg Pediatr. 2010;5(5):474–8.
53. Honeyman SI, Warr W. Posterior fossa decompression with or without duraplasty in the treatment of paediatric Chiari malformation Type I: a literature review and meta-analysis. Neurosurgery. 2019;84:E270.
54. Yeh DD, Koch B, Crone KR. Intraoperative ultrasonography used to determine the extent of surgery necessary during posterior fossa decompression in children with Chiari malformation type I. J Neurosurg. 2006;105(1 Suppl):26–32.
55. Batzdorf U, McArthur DL, Bentson JR. Surgical treatment of Chiari malformation with and without syringomyelia: experience with 177 adult patients. J Neurosurg. 2013;118(2):232–42.
56. Kempe LG. Operative neurosurgery. New York: Springer-Verlag; 1970.
57. Heiss JD, Suffredini G, Smith R, DeVroom HL, Patronas NJ, Butman JA, et al. Pathophysiology of persistent syringomyelia after decompressive craniocervical surgery. Clinical article. J Neurosurg Spine. 2010;13(6):729–42.
58. Hultman CS, Riski JE, Cohen SR, Burstein FD, Boydston WR, Hudgins RJ, et al. Chiari malformation, cervical spine anomalies, and neurologic deficits in velocardiofacial syndrome. Plast Reconstr Surg. 2000;106(1):16–24.
59. Mazzola CA, Fried AH. Revision surgery for Chiari malformation decompression. Neurosurg Focus. 2003;15(3):E3.
60. Sacco D, Scott RM. Reoperation for Chiari malformations. Pediatr Neurosurg. 2003;39(4):171–8.
61. Tubbs RS, Webb DB, Oakes WJ. Persistent syringomyelia following pediatric Chiari I decompression: radiological and surgical findings. J Neurosurg. 2004;100(5 Suppl Pediatrics):460–4.
62. Batzdorf U, Klekamp J, Johnson JP. A critical appraisal of syrinx cavity shunting procedures. J Neurosurg. 1998;89(3):382–8.
63. Sgouros S, Williams B. A critical appraisal of drainage in syringomyelia. J Neurosurg. 1995;82(1):1–10.
64. Takayasu M, Shibuya M, Kouketsu N, Suzuki Y. Rapid enlargement of a syringomyelia cavity following syringo-subarachnoid shunt: case report. Surg Neurol. 1996;45(4):366–9.
65. Wester K, Pedersen PH, Krakenes J. Spinal cord damage caused by rotation of a T-drain in a patient with syringoperitoneal shunt. Surg Neurol. 1989;31(3):224–7.
66. Munshi I, Frim D, Stine-Reyes R, Weir BK, Hekmatpanah J, Brown F. Effects of posterior fossa decompression with and without duraplasty on Chiari malformation-associated hydromyelia. Neurosurgery. 2000;46(6):1384–9; discussion 9-90.
67. Jia C, Li H, Wu J, Gao K, Zhao CB, Li M, et al. Comparison decompression by duraplasty or cerebellar tonsillectomy for Chiari malformation-I complicated with syringomyelia. Clin Neurol Neurosurg. 2019;176:1–7.
68. Matsumoto T, Symon L. Surgical management of syringomyelia--current results. Surg Neurol. 1989;32(4):258–65.
69. Van Calenbergh F, Hoorens G, Van den Bergh R. Syringomyelia: a retrospective study part II: diagnostic and therapeutic approach. Acta Neurol Belg. 1990;90(2):100–10.
70. Pare LS, Batzdorf U. Syringomyelia persistence after Chiari decompression as a result of pseudomeningocele formation: implications for syrinx pathogenesis: report of three cases. Neurosurgery. 1998;43(4):945–8.
71. Krayenbuhl H. Evaluation of the different surgical approaches in the treatment of syringomyelia. Clin Neurol Neurosurg. 1975;77(2):111–28.
72. Lee TC, Gau YL, Lui CC. Treatment of symptomatic syringomyelia with ventriculoperitoneal shunt: report of a case. J Formos Med Assoc. 1992;91(5):548–51.
73. Welch K, Shillito J, Strand R, Fischer EG, Winston KR. Chiari I "malformations"--an acquired disorder? J Neurosurg. 1981;55(4):604–9.
74. Batzdorf U. Chiari I malformation with syringomyelia. Evaluation of surgical therapy by magnetic resonance imaging. J Neurosurg. 1988;68(5):726–30.

75. Fischbein NJ, Dillon WP, Cobbs C, Weinstein PR. The "presyrinx" state: a reversible myelopathic condition that may precede syringomyelia. AJNR Am J Neuroradiol. 1999;20(1):7–20.
76. Jinkins JR, Reddy S, Leite CC, Bazan C 3rd, Xiong L. MR of parenchymal spinal cord signal change as a sign of active advancement in clinically progressive posttraumatic syringomyelia. AJNR Am J Neuroradiol. 1998;19(1):177–82.
77. Nishikawa M, Sakamoto H, Hakuba A, Nakanishi N, Inoue Y. Pathogenesis of Chiari malformation: a morphometric study of the posterior cranial fossa. J Neurosurg. 1997;86(1):40–7.
78. Noudel R, Jovenin N, Eap C, Scherpereel B, Pierot L, Rousseaux P. Incidence of basioccipital hypoplasia in Chiari malformation type I: comparative morphometric study of the posterior cranial fossa. Clinical article. J Neurosurg. 2009;111(5):1046–52.

Treatment of the Chiari II Malformation

39

W. Jerry Oakes

In discussing the therapeutic intervention for the Chiari II malformation (CM II), it would be important to emphasize from the beginning our clear understanding that these lesions rarely become symptomatic beyond infancy, and when medullary symptoms or a syrinx does occur, the primary culprit is the lack of adequate shunt function.

In this day of trying to avoid shunt placement in this population, the development of sleep apnea, aspiration pneumonia, or other medullary symptoms in the absence of a shunt should first be addressed by placing a valve-regulated ventriculoperitoneal shunt or endoscopic third ventriculostomy with or without choroid plexus cauterization (ETV-CPC). If ETV-CPC has been performed and medullary dysfunction persists or develops, a valve-regulated shunt should be placed.

If a shunt exists, then its function should be surgically explored. Many of us have learned this lesson at the expense of prior patients. In the setting of a small ventricle on the side of the ventricular catheter and an "unchanged" enlargement on the opposite side (Fig. 39.1) or in the setting of a "totally unchanged ventricular system" and the development of new or progressive medullary or cranio-cervical junction symptoms, one should suspect the shunt. Manipulating the posterior fossa contents without this first and essential step has been the ruin of many a patient. To paraphrase a common neurosurgical saying, "It's the

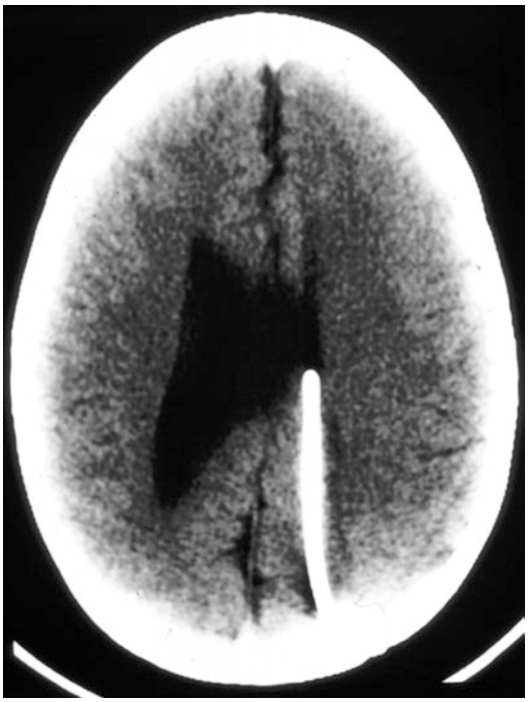

Fig. 39.1 Patient with Chiari malformation II presenting with lower cranial nerve dysfunction. This computed tomography (CT) image demonstrates minimal contralateral dilatation of the ventricular system. The official reading for this image was "unchanged"

W. J. Oakes (✉)
Departments of Neurosurgery and Pediatrics, University of Alabama, Birmingham, AL, USA
e-mail: Jerry.Oakes@childrensal.org

R. S. Tubbs et al. (eds.), *The Chiari Malformations*, https://doi.org/10.1007/978-3-030-44862-2_39

shunt until proven otherwise." This proof demands surgical inspection with good flow from the ventricular catheter and no adherence within the brain. If the catheter fails on either count or if the data are confusing, it should be replaced without going on to Chiari II decompression.

Both symptoms of Chiari II malformations and evaluation preoperatively have been covered in other chapters. Only the highlights will be mentioned here. If you are convinced the symptoms relate to the cranio-cervical junction and the shunt has been explored, then the decision to consider Chiari II decompression is reasonable. Many of the symptom complexes are life-threatening, and the risk of surgical intervention is easily justified.

There is no medical treatment for this condition, and confusion with other explanations for a myelomeningocele infant with a loud inspiratory stridor is generally the inexperience of a poorly informed clinician. Preoperative evaluation of respiration both while awake and during sleep is prudent. Excess snoring is a frequent symptom of medullary compromise, and evaluation will add objective data to assess and allow comparison postoperatively. Swallow studies to determine if aspiration is present and the extent of aspiration are less objective but still useful data.

Radiologic evaluation of the cranio-cervical junction is mandatory. It is helpful if the magnetic resonance imaging (MRI) is done both with and without contrast. The purpose of the contrasted study is to evaluate the position of the choroid plexus as it marks the outlet of the fourth ventricle. The choroid plexus tissue begins embryologically as an extraventricular structure and with normal development rotates into the roof of the ventricle. This migration is frequently arrested in the myelomeningocele patient, and the choroid plexus marks the foramen of Magendie. It is a useful intraoperative marker for the surgeon to avoid dissection through delicate marginally functioning tissue of the lower medulla, trying to find access into the fourth ventricle. Intraoperative ultrasound may also be helpful, but because of the tissue distortion, these may be quite difficult to interpret.

Preoperative studies are also critical to determine the position of the torcular. With the small posterior fossa characteristically seen in myelomeningocele patients, the torcular may be caudally displace and lie at or just above the foramen magnum (Fig. 39.2a). Opening into this venous channel can be avoided simply by knowing its position and extent. Not knowing its position or recognizing its potential for being low-lying is not easily excused. Additionally, flexion-extension evaluation of the cervical spine has occasionally revealed bony instability that had not previously been detected. Not knowing about

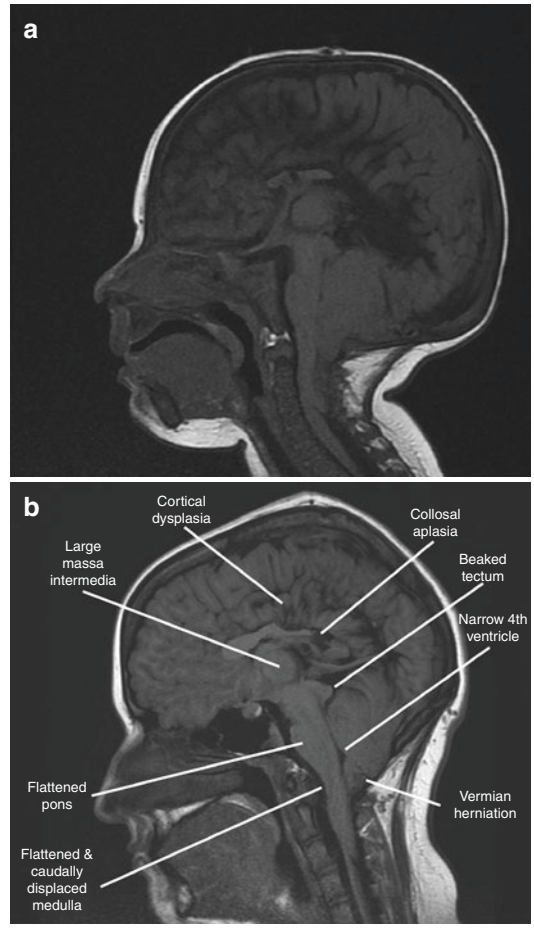

Fig. 39.2 (**a**) Typical magnetic resonance imaging (MRI) of CM II. Note the near vertical straight sinus and torcular near the foramen magnum. (**b**) Sagittal MRI noting typical features of the CM II

this finding can result in a serious neurological deficit during positioning.

Chiari II decompression, particularly in the infant, can be as difficult a technical challenge as is faced in pediatric neurosurgery [1]. Contamination of the subarachnoid space with blood must be avoided to prevent further obliteration of the fourth ventricular outlet; the dural opening itself can be associated with significant loss of blood in a fragile infant. Finding a safe surgical corridor into the floor of the fourth ventricle can be the most challenging of all, but not to pursue this step makes surgical intervention unlikely to be helpful. As with CM I patients, free and unimpeded egress of cerebrospinal fluid (CSF) from the fourth ventricular outlet is the goal of operation.

The procedure is planned to expose the lower brain stem to the outlet of the fourth ventricle (Fig. 39.2b). Again, this is frequently marked by the maintenance of the embryological position of the choroid plexus (Fig. 39.3). It is not necessary to expose the medullary kink, and excess bony removal in the presence of a large cervical syrinx can be associated with the development of a significant kyphotic deformity postoperatively. The bony opening should be limited to the necessary dorsal bony elements only (Fig. 39.4). Bone removal to expand the foramen magnum is rarely necessary, and if the torcular is caudally displaced, it can be life-threatening.

The patient is positioned prone with the neck flexed and the head of the bed elevated. Despite the thin nature of the infant skull, pin fixation can be used with minimal pressure to maintain a constant position. Soft tissue exposure of the appropriate dorsal bony elements is accomplished in the usual manner as well as in a standard laminectomy. This is a midline procedure, and far lateral exposure is unnecessary. Replacement of the bony elements has not proven necessary or easily accomplished in my hands. After bony decompression, if the dura protrudes dorsally and is tense, the intracranial pressure and shunt function should again be assessed. We believe this to occur only in the presence of uncontrolled intracranial hypertension. Again it is the shunt or lack of CSF diversion causing the problem, and if this intraoperative finding occurs, reevaluation of shunt function is necessary immediately.

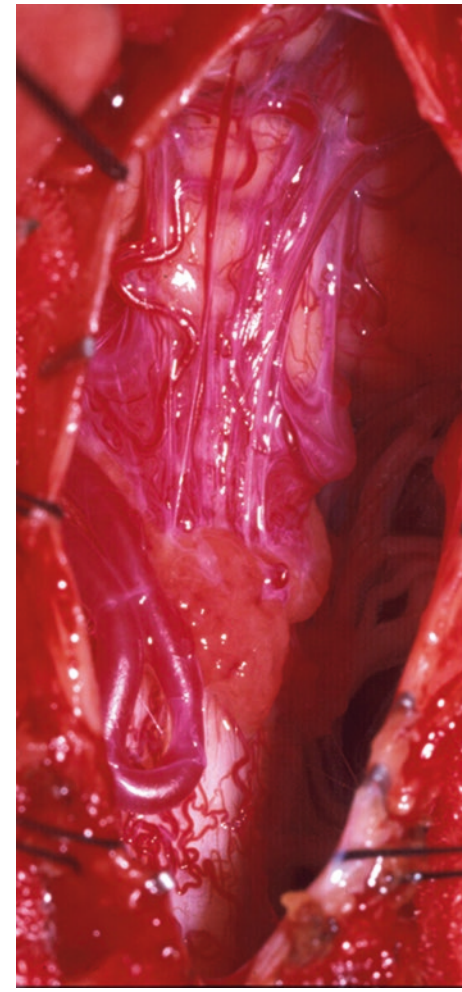

Fig. 39.3 Intradural CM II illustrating the ectopically positioned choroid plexus and a caudal loop of the posterior inferior cerebellar artery

A band of tissue appearing to constrict the dura under C-1 represents the periosteum of the dorsal arch of C-1 and may be present. It should be sectioned and burned back with bipolar coagulation. With the dura exposed, it is opened, usually from caudal to cranial. Above C-1 the dura may contain a large venous sinus. Bipolar coagulation of the outer leaf simply enlarges the opening in the sinus and therefore worsens the bleeding. The solution is to have control of both leaves of the dura and keep them approximated. This may be accomplished with suture or clips. I prefer to maintain sutures opposing both leaves and, if a significant sinus is encountered, simply sew the edges together as you open the dura. This

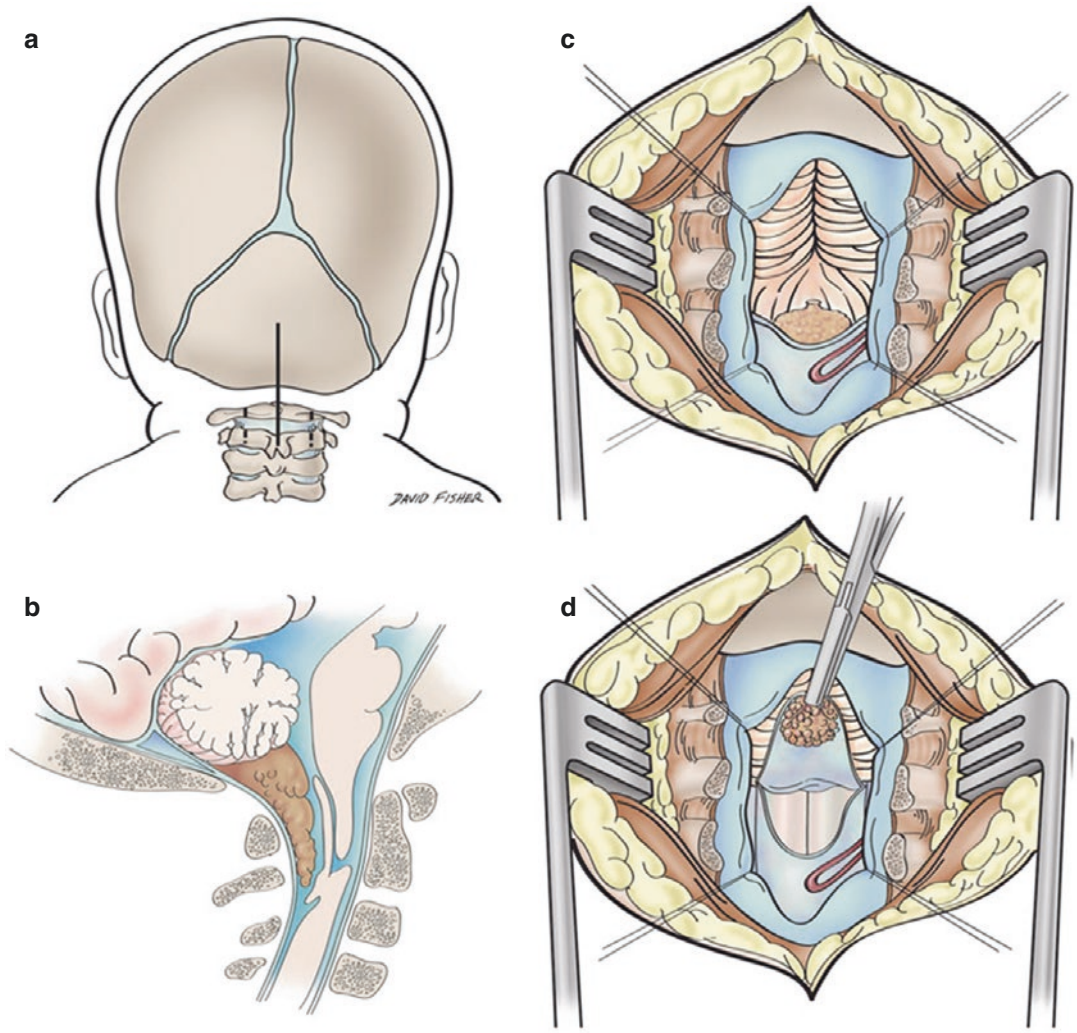

Fig. 39.4 Schematic representation of operative intervention for the CM II. (**a**) Intraoperative view of CM II. The position of the choroid plexus and entry into the fourth ventricle are problematic. The hypervascularity of this region is impressive. (**b**) Intraoperative view of CM II. The hypervascularity of the region with elongation of the dorsal vessels is striking. The site of entrance into the fourth ventricle is not obvious. (**c**) With dissection laterally of Fig. 39.5b, access to the fourth ventricle is eventually obtained. (**d**) Similar patient to the patient seen in Fig. 39.5b, c, but in this patient, a cleft is present in the floor of the fourth ventricle

necessitates that the original opening of the dura be in an area where bleeding is minimal to allow clear visualization of both leaves. Under the arch of C-1 usually accomplishes this purpose. Once the dura is open, the arachnoid is opened as a separate layer and clipped with small titanium clips to the opened dura. The characteristic globular orange-yellow appearance of the choroid plexus is then sought (Figs. 39.4 and 39.5). The dorsal surface of the neural elements may be seen to be covered with a fine excessive network of vessels. This is thought to be due to the chronic ischemia of the caudally displaced neural tissue. Working through and on each side of the choroid plexus will eventually allow visualization of the avascular floor of the fourth ventricle. The opening is enlarged until, at rest, it is maintained (Fig. 39.6). This is the goal of surgery and not to

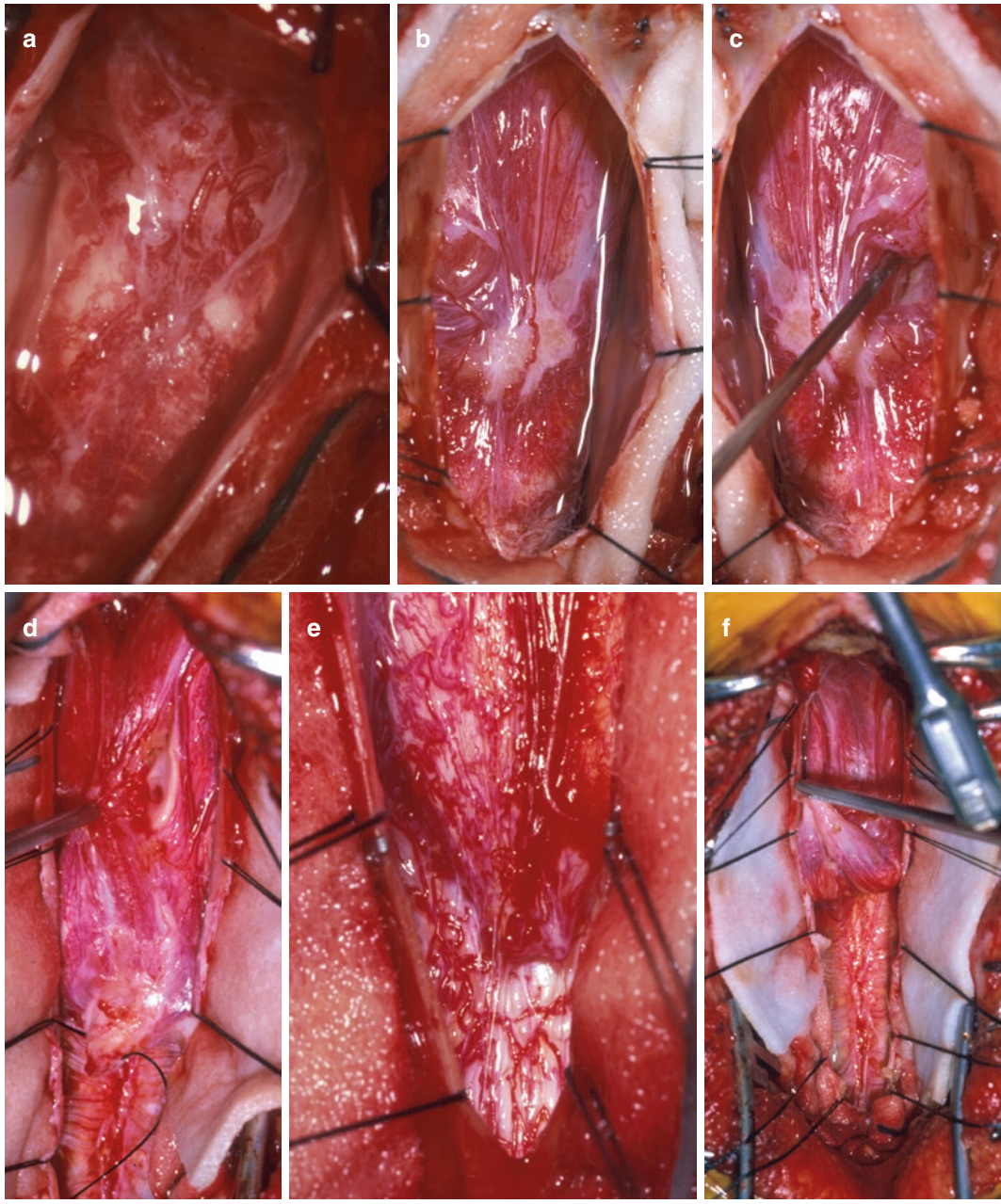

Fig. 39.5 (**a**) Intraoperative view of CM II. The position of the choroid plexus and entry into the fourth ventricle are problematic. The hypervascularity of this region is impressive. (**b**) Intraoperative view of CM II. The hypervascularity of the region with elongation of the dorsal vessels is striking. The site of entrance into the fourth ventricle is not obvious. (**c**) With dissection laterally of (**b**), access to the fourth ventricle is eventually obtained. (**d**) Similar patient to patient seen in (**b**, **c**), but in this patient, a cleft is present in the floor of the fourth ventricle
(**e**) Another intraoperative view of the CM II. Here, the demarcation between the spinal cord and cerebellar tissue is more apparent. (**f**) With dissection of (**e**), the more dorsal tissue is shown to be the medullary kink and *not* a corridor into the fourth ventricle

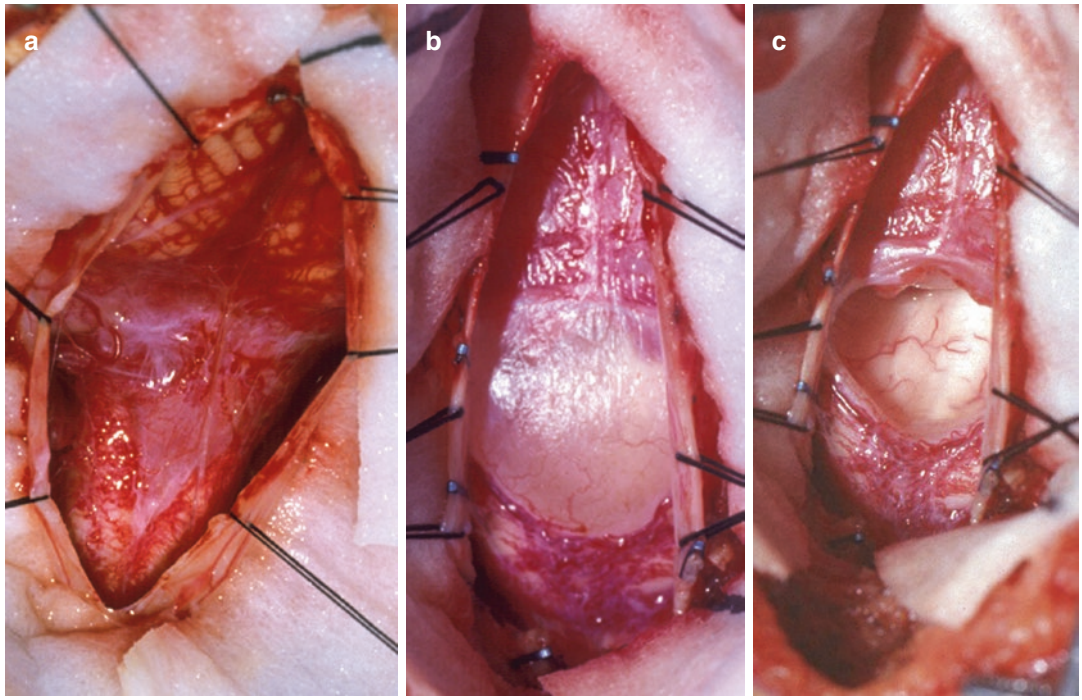

Fig. 39.6 (**a**) A veil over the fourth ventricle is seen as a thin membrane and is easily opened to re-establish outflow. (**b**) Cranio-cervical exposure with dura retracted laterally. A membrane over the fourth ventricular outlet is seen as a thin almost transparent sheet. (**c**) Following opening the membrane seen in (**b**), the relatively avascular floor of the fourth ventricle is obvious

complete this step is likely not to benefit the patient. This is not to minimize the surgical challenge or the risk to the patient of traumatizing marginally functioning portions of the medulla.

Manipulation of the pial surface and blood contamination of the subarachnoid space should be minimized. What can make the procedure difficult is when the opening into the fourth ventricle is not obvious or is blocked by a dominant vessel. Here the decision may be aided by intraoperative ultrasound, although these may be difficult to interpret. Not opening into the fourth ventricle carries much less chance of help for the patient.

With the floor visualized, a small pericranial graft is harvested to sew into place as a dural substitute. Many other tissues and substances have been used for grafting; none is more likely to be sterile or to minimize a foreign body reaction than the patient's own tissue.

The patient is maintained intubated until spontaneous respiration is assured and airway protection is judged to be adequate.

The essential points of the procedure are first and foremost to ensure adequate CSF diversion prior to the procedure. Outside the neonatal age range, this first step will eliminate the need for consideration of further surgery in the vast majority of patients. Once the procedure is deemed justified, maintain dural control with stay sutures, minimize blood contamination of the subarachnoid space, and open into the fourth ventricle.

Reference

1. Oakes WJ. Ch 28. Treatment of the Chiari II Malformation. In: Tubbs RS, Oakes WJ, editors. The Chiari Malformations: New York, NY, Springer Science + Business Media; 2013. p. 315–24.

40 Chiari Type II Malformation: Reversibility Following Myelomeningocele Closure

Pierre-Aurélien Beuriat, Alexandru Szathmari, Federico Di Rocco, and Carmine Mottolese

Introduction

More than half a century before Hans Chiari and Julius Arnold described and explained the peg of the cerebellar tonsil through the foramen magnum now called the Chiari malformation, Jean Cruveilhier, a French surgeon, anatomist, and pathologist, made the first description of the now called "Chiari type II malformation" (CM II). His description came from the observation of a myelomeningocele (MMC) patient: "…the upper part of the cervical region, considerably enlarged, contained both the medulla oblongata and the corresponding parts of the cerebellum which was elongated and covered the fourth ventricle which itself became longer and wider" [1]. Since then, MMCs were thought to be always associated with a CM II [2]. However, since the use of systematic cerebral and spinal radiological exam, first with computed tomography (CT) and then with magnetic resonance imaging (MRI), it was reported that the association was more to a level of 80% [3, 4]. Because of its supposed physiopathology, the cerebellar peg was thought to be irreversible [5]. However, improvement of the hindbrain herniation was proved to be a fact [6–9].

In this chapter, we will review the exciting data on the reversibility of the CM II to allow the reader to better understand this phenomenon.

Generality

The presence of a CM II at birth is a consequence of the neural tube defect and is related to the hydrodynamic consequences of the meningocele sac. Indeed, in McLone's unified theory of the physiopathology of CM II in MMC, CM II is the consequence of cerebrospinal fluid (CSF) leakage causing the decrease of hydrostatic pressure gradient, thus leading to cerebellar peg (CP) descent [3, 4]. The reversibility of this condition can be explained, thanks again to McLone's theory: The MMC closure would restore the normal hydrodynamic forces inside the posterior fossa and the spine, which should lead to the ascent of the CP. It could also be explained by modern management of MMC with early surgical repair and decrease of infectious complications reducing the incidence of an evolutive hydrocephalus, thus reducing the risk of tonsillar herniation because the differential pressure between the infratentorial and spinal CSF space is reestablished.

P.-A. Beuriat · C. Mottolese (✉)
Department of Pediatric Neurosurgery, Hôpital Femme Mère Enfant, Lyon, France
e-mail: Carmine.mottolese@chu-lyon.fr

A. Szathmari
Department of Pediatric Neurosurgery, Hôpital Femme Mère Enfant, Hospices Civils de Lyon, Claude Bernard Lyon 1 University, Lyon, France

F. Di Rocco
Department of Pediatric Neurosurgery, Hôpital Femme Mère Enfant, Université de Lyon, Lyon, France

R. S. Tubbs et al. (eds.), *The Chiari Malformations*, https://doi.org/10.1007/978-3-030-44862-2_40

This knowledge of a possible reversibility of CM II after surgical repair is of tremendous importance because CM II may lead to later symptoms that could require surgery [3, 7, 10, 11]. Historically, CM II was associated with a high rate of surgical decompression of the craniovertebral junction at a very young age and a poor outcome with a high mortality rate and severe morbidity among survivors [12, 13]. The report of the French Society of Neurosurgery edited in 1988 by Lapras et al. was the first to report a low morbidity rate when surgery was postponed after the age of 2 years [11]. The rate of surgery for CM II in MMC is low nowadays but can reach 30% in some series [8]. In our reference center, the rate is 11.5% in a series of 46 patients with no mortality and no need for gastrostomy or tracheostomy [14].

From a clinical point of view, the development of surgical techniques to close the MMC with the use of microscope and the important reduction in infectious complications have undeniably improved the surgical results. Indeed, the overall clinical prognoses of the patients have thus greatly progressed over the years when compared to historical data. The other fact that helped to improve the prognosis of the CM II is the possibility for the malformation to be reversed after MMC closure. This reversibility is now proved to be possible after the prenatal closure of the MMC but also, in some cases, after post-natal closure. The latter was thought not to be possible less than 20 years ago [5].

Reversibility After Prenatal Management of Myelomeningocele

Soon after the first proof of feasibility of the prenatal closure of a MMC, the Vanderbilt University team noticed and published the effect of this closure on the prevalence of CM II. Indeed, in their first prenatal series, 65% of the patients did not have a cerebellar or brainstem herniation [15, 16]. At that time, they were not able to precisely identify the underlying mechanism—that is to say, they did not know if the closure prevented the apparition of the CM II or if the closure helped to reverse the peg. For that purpose, they conducted a study in which they evaluated the presence of a CM II during the prenatal surgical closure with an intraoperative sonography and again after the delivery with a post-natal sonography and an MRI. They graded the cerebellar herniation from 0 (no herniation, normal posterior fossa, and cisterna magma visible) to 6 (severe herniation, fourth ventricle, and vermis entirely below the foramen magnum). On the intraoperative sonography (during the prenatal closure), all the patients had at least a grade 2 herniation with a mean of 4.3. On the control (postdelivery evaluation), the mean herniation grade for the sonographic exam was 0.9 with three grade 0, and the mean herniation grade for the MRI exam was 1.3 with only one grade 0. The first conclusion drawn from this study, yet limited, was that most fetuses with a MMC have a CM II present by at least the 25th week of gestation. The second was the confirmation of the reversibility of the CM II after the closure of the neural tube defect [5]. At that time, they believed that this reversibility was not possible after post-natal closure [5].

This reversibility became one important factor analyzed in prenatal series to assess its effectiveness. In the Management of Myelomeningocele Study (MOMS trial), the absence of tonsil ptosis was not a primary outcome but still was one of the most discussed and put-forward results. Indeed there was a significant difference in the rate of tonsil ptosis in favor of the prenatal group with 64% of the patients in the antenatal group, versus 96% in the post-natal group ($p = 0.001$) having a CM II [6]. Two authors reviewed all the published data on this subject [17, 18]. Reversibility was effective in 15–71% for the open technique [6, 19–21]. For the endoscopic technique, only one study analyzed this factor with a reversal in 85% [22], but the number of patients was very limited ($n = 7$), and therefore no conclusions can be drawn from this experience. Recently, some authors described a mixed technique using an open approach to the uterus with an endoscopic repair of the defect. They published a 57% rate of reversibility of the CM II [23].

Reversibility After Post-natal Management of Myelomeningocele

The reversibility of the CM II after the post-natal management of MMC is in fact possible, but published experience is sparse with only three articles in the literature [7–9]. Less than 10 years after the Vanderbilt team stated that the post-natal closure could not allow the reversal of the CM II [5], Morota et al. published the first evidence that this quote was not correct and that post-natal closure of MMC in born babies after 35 weeks' gestation (WG) could also help to reverse the CM II [7]. Surprisingly, the second evidence of that was published only 8 years after in 2016 [8]. Recently, our team shared the largest series of complete reversibility of CM II [9].

Morota and Ihara [7] studied a population of 20 patients divided into a group 1 (born between 35 and 39 WG) and a group 2 (born between 39 and 41 WG). The surgical management consisted in the closure of the MMC for all patients within 48 hours after birth (after the realization of a MRI) and the placement of a CSF reservoir for those with ventricular dilatation to aspirate CSF to try to manage the hydrocephalus. On the preoperative MRI, 93% and 83% in groups 1 and 2, respectively, of their patients had a caudal end of the CT at least at the level of C2. On the control MRI, 85% and 80% in groups 1 and 2, respectively, of their patients had a caudal end of the CT ascension. In addition to the ascent of CP, they noted an enlargement of the subarachnoid space in the posterior fossa around the brainstem and cerebellum. Surprisingly, in group 1, 61% of their patients developed clinical signs of CM II, but only three required surgery. Concerning the hydrocephalus management, 84.5% of the patients benefited from a ventriculoperitoneal (VP) shunt. They noted that CT ascent began before VP shunt procedure. Therefore, they concluded that the principal factor for CT was not the insertion of a VP shunt. They supported that "the main factor responsible for CM-II ascent after postnatal myelomeningocele repair is the restored hydrodynamic forces following direct closure of the myelomeningocele" as they noted an enlargement of the subarachnoid space in the posterior fossa around the brainstem and cerebellum suggesting better CFS flow inside the posterior fossa in accordance with the expected consequence of MMC closure according to McLone. The last point mentioned by the authors is that there was no relationship between degree of ascent and timing of MMC closure.

Another recent study examined the morphological changes of CM II after post-natal repair [8]. Interestingly, the authors divided their cohort into two groups according to the need of VP shunt. They reported that there was significantly less cerebellar tonsil peg in the group of non-shunted patients, with bigger posterior fossa volume, wider foramen magnum and C1 diameter, and visible CSF fluid at the cranio-vertebral junction. They also studied the timing of the ascent of the cerebellar tonsil. They noted that within the first 6 months after the MMC repair, there was a rapid cerebellar tonsil ascension, which continues up to 3 years but more slowly. They also noted that cerebellar tonsil ascension was possible even in non-shunted patients but that a shunt can help the process. Moreover, they reported some expansion of the posterior fossa and some enlargement of the foramen magnum and C1 diameter after the MMC closure even in patients without VP shunt. These morphological changes seemed to be directly linked to the closure of the MMC, allowing a better circulation of the CSF within the posterior fossa, contributing to the CP ascent [8].

Limitations, such as a small number of patients and limited time of follow-up, led our team to conduct a similar study on this subject. We focused on the complete reversibility, and not just the ascent of the cerebellar tonsil, of the CM II. After blinded reviewed of pre- and post-closure MRI, we evaluated the rate of complete reversibility of CM II in 61 MMC patients with a mean follow-up of 8.1 years (minimum 6 months, maximum 18 years, SD 4.6 years). We also analyzed the reversibility regarding the anatomical level of the MMC, the need for a CSF diversion procedure in case of an evolutive hydrocephalus, and the presence of a syringomyelia. Details of the material and methods with inclusions and exclusions criteria are published elsewhere [9].

In brief, 77% had a CM II at birth (confirmed before the MMC repair) with an average level of the caudal end of the cerebellar tonsil at C3 (ranged C1 to C6). There was a significant correlation between the level of the malformation and the presence of a CM II at birth ($p = 0.003$) with the presence of the CM II at birth in every patient with a malformation strictly above L4. After MMC closure, 45.9% patients had a remaining CM II. The reversibility was better in malformations with an anatomical level of L4 and below ($p = 0.004$). Globally, 11.5% of the children in this cohort needed surgery (craniocervical decompression) for a symptomatic CM II. The overall rate of syringomyelia was 37.7%, with a large predominance of patients without syringomyelia in the group of patients without CM II ($p < 0.001$). Concerning the management of hydrocephalus, 54.1% needed a surgical procedure within an average of 41 days (minimum 3 days, maximum 433 days) after the MMC closure. Three types of CSF diversion procedure were used: endoscopic third ventriculostomy (ETV) alone (3%), a VP shunt alone (30.3%), or a concomitant VP shunt and ETV (66.7%). There were significantly more patients treated in the group with a remaining CM II ($p = 0.004$) and a significant difference in the proportion of patients who had a reversible CM II depending on the type of CSF diversion procedure ($p = 0.004$). Reversibility also occurred in non-hydrocephalic patients, with 52.9% of reversion in these patients. This result proves that the microsurgical repair of the MMC with the aim of recreating the different anatomical layers (neurulation of the medulla, a large dural sac) by restoring the CSF dynamics at the level of the spinal malformation but also along the craniospinal axis might participate to the ascent of the CT.

This series also highlighted several other points. The first one was the relationship between the presence and the reversibility of the CM II with the anatomical level of the malformation. The second was the influence of the hydrocephalus treatment with the possibility of reversibility. Furthermore, it highlights also one new important factor that contributes to the CM II reversibility: the type of surgical procedure. Indeed, the rate of reversibility varies according to the type of CSF diversion with a better rate with the association of an ETV and a VP shunt. One explanation could be that ETV, in addition to help with the control of hydrocephalus, favors the restoration of a good CSF dynamic within the posterior fossa, which helps the cerebellar tonsil to ascend. One parameter that was never studied before this series was the syringomyelia. However, it is an important one to assess the good CSF dynamic within the craniospinal axis. Our team showed that when the CM II reversibility was effective, there was less syringomyelia.

Finally, the reversibility rate of the CM II after post-natal closure of a MMC was 40.4% in this series, which is within the range of the reversibility published in prenatal series [17, 18].

Conclusion

CM II is an important factor to analyze in MMC children as it can be associated with severe complications.

Thanks to the realization of systematic MRI before the closure of the malformation, either prenatally or post-natally, and with the follow-up of these patients in specific multidisciplinary reference centers with systematic brain imaging, it has been proven that ascent of the cerebellar tonsil and even complete reversibility of a CM II after the MMC repair are possible. It was proved in both prenatal and post-natal surgery of MMC.

Our series confirms also that the reduced rate of infectious complications and the better surgical innovations, associated with a high reversibility rate, do not push to the surgical treatment of asymptomatic Chiari II malformation.

References

1. Cruveilhier J. Anatomie Pathologie Du Corps Humain. Paris: JB Baillière; 1829.
2. Goodrich JT. Ch. 1 Historical review of the surgical treatment of spina bifida. In: Özek MM, Cinalli G, Maixner WJ, editors. Spina bifida: management and outcome. Italia: Springer-Verlag; 2008.

3. McLone DG, Dias MS. The Chiari II malformation: cause and impact. Childs Nerv Syst. 2003;19(7–8):540–50.
4. McLone DG, Knepper PA. The cause of Chiari II malformation: a unified theory. Pediatr Neurosci. 1989;15(1):1–12.
5. Tulipan N, Hernanz-Schulman M, Lowe LH, Bruner JP. Intrauterine myelomeningocele repair reverses preexisting hindbrain herniation. Pediatr Neurosurg. 1999;31(3):137–42.
6. Adzick NS, Thom EA, Spong CY, Brock JW 3rd, Burrows PK, Johnson MP, et al; MOMS Investigators. A randomized trial of prenatal versus postnatal repair of myelomeningocele. N Engl J Med. 2011;364(11):993–1004.
7. Morota N, Ihara S. Postnatal ascent of the cerebellar tonsils in Chiari malformation Type II following surgical repair of myelomeningocele. J Neurosurg Pediatr. 2008;2(3):188–93.
8. Hashiguchi K, Morioka T, Murakami N, Togao O, Hiwatashi A, Ochiai M, et al. Sequential morphological change of Chiari malformation type II following surgical repair of myelomeningocele. Childs Nerv Syst. 2016;32(6):1069–78.
9. Beuriat PA, Szathmari A, Rousselle C, Sabatier I, di Rocco F, Mottolese C. Complete reversibility of the Chiari type II malformation following post natal repair of myelomeningocele. World Neurosurg. 2017;108:62–8.
10. Talamonti G, D'Aliberti G, Collice M. Myelomeningocele: long-term neurosurgical treatment and follow-up in 202 patients. J Neurosurg. 2007;107(5 Suppl):368–86.
11. Lapras C, Guilburd JN, Patet JD. [Spina bifida aperta--myelomeningocele. Chiari's malformation type II]. Neurochirurgie. 1988;34 Suppl 1:53–58.
12. Park TS, Hoffman HJ, Hendrick EB, Humphreys RP. Experience with surgical decompression of the Arnold-Chiari malformation in young infants with myelomeningocele. Neurosurgery. 1983;13(2):147–52.
13. Bowman RM, McLone DG, Grant JA, Tomita T, Ito JA. Spina bifida outcome: a 25-year prospective. Pediatr Neurosurg. 2001;34(3):114–20.
14. Beuriat P-A, Poirot I, Hameury F, Szathmari A, Rousselle C, Sabatier I, et al. Postnatal management of myelomeningocele: outcome with a multidisciplinary team experience. World Neurosurg. 2018;110:e24–31.
15. Tulipan N, Hernanz-Schulman M, Bruner JP. Reduced hindbrain herniation after intrauterine myelomeningocele repair: a report of four cases. Pediatr Neurosurg. 1998;29(5):274–8.
16. Bruner JP, Tulipan N, Paschall RL, Boehm FH, Walsh WF, Silva SR, et al. Fetal surgery for myelomeningocele and the incidence of shunt-dependent hydrocephalus. JAMA. 1999;282(19):1819–25.
17. Kabagambe SK, Jensen GW, Chen YJ, Vanover MA, Farmer DL. Fetal surgery for myelomeningocele: a systematic review and meta-analysis of outcomes in fetoscopic versus open repair. Fetal Diagn Ther. 2018;43(3):161–74.
18. Araujo E, Tonni G, Martins WP. Outcomes of infants followed-up at least 12 months after fetal open and endoscopic surgery for meningomyelocele: a systematic review and meta-analysis. J Evid Based Med. 2016;9(3):125–35.
19. Zamłyński J, Olejek A, Koszutski T, Ziomek G, Horzelska E, Gajewska-Kucharek A, et al. Comparison of prenatal and postnatal treatments of spina bifida in Poland–a non-randomized, single-center study. J Matern Fetal Neonatal Med. 2014;27(14):1409–17.
20. Danzer E, Finkel RS, Rintoul NE, Bebbington MW, Schwartz ES, Zarnow DM, et al. Reversal of hindbrain herniation after maternal-fetal surgery for myelomeningocele subsequently impacts on brain stem function. Neuropediatrics. 2008;39(6):359–62.
21. Moldenhauer JS, Soni S, Rintoul NE, Spinner SS, Khalek N, Martinez-Poyer J, et al. Fetal myelomeningocele repair: the post-MOMS experience at the Children's Hospital of Philadelphia. Fetal Diagn Ther. 2015;37(3):235–40.
22. DAL P, Zanon N, Nishikuni K, Moreira de Sá RA, Acacio GL, Chmait RH, et al. Endoscopic surgery for the antenatal treatment of myelomeningocele: the CECAM trial. Am J Obstet Gynecol. 2016;214(1):111.e1–111.e11.
23. Belfort MA, Whitehead WE, Shamshirsaz AA, Bateni ZH, Olutoye OO, Olutoye OA, et al. Fetoscopic open neural tube defect repair: development and refinement of a two-port, carbon dioxide insufflation technique. Obstet Gynecol. 2017;129(4):734–43.

41 Duraplasty Versus Non-dural Opening for the Treatment of Pediatric Chiari Malformation Type I

Susan J. Staulcup, Olufemi Ajani, and Todd C. Hankinson

Introduction

Chiari malformation type I (CM I) is characterized by the herniation of the cerebellar tonsils through the foramen magnum and into the upper cervical spinal canal. Children with CM I may present symptomatically or this entity may be found incidentally. When intervention is required, surgery, generally through posterior fossa decompression, represents first-line treatment for children with CM I. In the pediatric population, there is variability with regard to whether or not the dura is opened as a component of this procedure and if additional intradural maneuvers are performed. This chapter discusses the current literature relevant to this aspect of surgical treatment for children with CM I.

Of note, if hydrocephalus is present, appropriate cerebrospinal fluid (CSF) diversion should be undertaken prior to any other surgical intervention. This may be accomplished through the insertion of a ventricular shunt or performance of an endoscopic third ventriculostomy [1, 2]. This chapter does not discuss the role of intradural maneuvers (i.e., tonsillar reduction/resection) that may be performed along with dural opening procedures. Surgical management for patients with the more recently described Chiari 0 (syringohydromyelia in the absence of cerebellar tonsillar herniation) and Chiari 1.5 (tonsillar herniation with associated brainstem herniation) is based on the principles that will be discussed here in the context of CM I.

General Concepts in Surgical Intervention for Chiari I

First-line surgical therapy for patients with CM I in the absence of hydrocephalus is posterior fossa decompression (PFD) via midline suboccipital craniectomy and (generally) removal of the posterior arch of the atlas. This procedure may be completed with or without subsequent dural opening. PFD attempts to reestablish bidirectional CSF flow across the craniocervical junction. This is accomplished through the expansion of the posterior fossa subarachnoid space, which provides decompression of the cerebellar tonsils and brainstem. PFD may also eliminate the craniospinal CSF pressure differential that is postulated to contribute to syrinx formation [3]. For the remainder of this discussion, the term

S. J. Staulcup (✉)
Department of Neurosurgery, Children's Hospital Colorado/University of Colorado, Aurora, CO, USA
e-mail: susan.staulcup@ucdenver.edu

O. Ajani
Department of Surgery, McMaster Children's Hospital, Hamilton, ON, Canada

T. C. Hankinson
Departments of Neurosurgery and Pediatrics, Children's Hospital Colorado/University of Colorado School of Medicine, Aurora, CO, USA

R. S. Tubbs et al. (eds.), *The Chiari Malformations*, https://doi.org/10.1007/978-3-030-44862-2_41

posterior fossa decompression, when used alone, will refer to bony suboccipital decompression with dural scoring or splitting but without the opening of both layers of the dura mater or the underlying arachnoid mater. Most commonly, PFD is undertaken with duraplasty (PFDD) with or without cerebellar tonsil coagulation or resection. Other intradural interventions, such as fourth ventricular stenting and syrinx shunting, have been largely abandoned or are reserved for second- or third-line therapies [4–7].

Decision-Making Regarding Surgical Technique

Once the decision to operate has been made, the surgeon must determine the most appropriate extent of decompression. The goals of surgery in the CM I population include improvement/resolution of symptoms, stabilization/improvement of scoliosis (when present), and diminution of radiographic syringomyelia (when present). With regard to the postoperative assessment of syringomyelia, there is some debate regarding the extent and timing of diminution that is necessary to demonstrate effective treatment [8, 9].

Studies Directly Comparing Surgical Techniques

Despite significant literature describing the treatment of pediatric CM I, only one randomized control trial comparing PFD against PFDD has been completed [10]. The Park-Reeves Syringomyelia Research Consortium recently completed enrollment of a multicenter prospective randomized trial that compares posterior fossa decompression with or without duraplasty for children with Chiari malformation and syringomyelia. Outcomes to be assessed will include procedure-related complications, syrinx resolution, and quality of life assessments, and results are expected in 1–2 years. Additional published research includes two meta-analyses, one large dataset study, three surveys, and multiple retrospective single-institutional series [5, 7, 10–30].

Durham and Fjeld-Olenec [11] published a meta-analysis of studies that directly compared cohorts of pediatric patients who underwent PFD with cohorts that were treated with PFDD. (Table 41.1) [12–19]. A total of seven studies met their inclusion criteria [12–15, 17–19]. The authors concluded that patients who undergo duraplasty are less likely to require reoperation (2.1% vs. 12.6%) for persistent or recurrent symptoms but are more likely to experience CSF-related complications (18.5% vs. 1.8%). There was no statistical difference in clinical outcomes between the two groups, specifically regarding symptom improvement and syringomyelia. Rates of clinical improvement were 65% in the PFD patients and 79% in the PFDD patients. Rates of radiological syrinx improvement were influenced by small numbers in some studies but were 56% in the PFD patients and 87% in those undergoing PFDD. The authors appropriately acknowledged that their conclusions were limited by the patient selection methods of the studies they examined. Among the seven papers, five used intraoperative ultrasound to help determine whether or not to perform a dural opening [14–16, 18, 19]. The inherent subjectivity of this technique limits the extent to which the resultant findings may be generalized. Additionally, no study included randomization or blinding.

Lu and colleagues [21] conducted a more recent meta-analysis of 12 studies in pediatric CM I. This included data from ten articles and two abstracts. A total of 3455 children were included, of which 57% underwent PFD and 43% underwent PFDD. The authors found PFDD to be associated with greater clinical improvement but longer length of stay (LOS) and higher number of perioperative complications, specifically with regard to CSF and infection. No statistically significant difference was found in reoperations, blood loss, and syrinx or scoliosis improvement between the two surgical techniques.

Jiang and colleagues [10] conducted a randomized controlled trial in which 82 adolescents (ages 10–18 years old) with CM I and syringomyelia were randomized to PFD or PFDD. The authors found that PFDD was associated with significantly longer operative time, longer length

Table 41.1 Meta-analysis by Durham and Fjeld-Olenec: rates of symptom/syrinx improvement and reoperation in studies including both techniques [11]

Author (year)	Pts	Dural opening	Clinical improvement (%)	Syrinx improvement (%)	Scoliosis stable/ improvement (%)
Mutchnick et al. (2010) [12]	56	N	49 (87.5)[a]	NR	NR
	64	Y	62 (96.9)[a]	NR	NR
Galarza et al. (2007) [17]	20	N	4 (33.3, *n* = 12)	2 (40, *n* = 5)	NR
	21	Y	11 (73.3, *n* = 15)	0 (0, *n* = 2)	NR
	19	Y[b]	8 (88.9, *n* = 9)	7 (100, *n* = 7)	NR
Yeh et al. (2006) [14]	40	N	36 (90.0)	4 (66.7)	1 (100)
	85	Y	83 (97.6)	17 (85)	9 (100)
Limonadi, Selden (2004) [18]	12	N	1.67[c]	NR	NR
	12	Y	1.53[c]	7 (70, *n* = 10)	NR
Navarro et al. (2004) [19]	56[d]	N	40[d] (72.2)	NR	NR
	24[d]	Y	16[d] (68.4)	NR	NR
	29[d]	Y[b]	17[d] (60.8)	NR	NR
Ventureyra et al. (2003) [15]	6	N	4 (66.7)	0 (0, *n* = 2)	NR
	10	Y	10 (100)	5 (100, *n* = 5)	NR
Munshi et al. (2000) [13]	11	N	8 (72.7)	3 (50.0, *n* = 6)	NR
	21[e]	Y	18 (85.7)	7 (63.6, *n* = 11)	NR

NR not reported
[a]Extrapolated from reoperation rates
[b]With intradural maneuvers
[c]Aggregate scoring system with range from −1 to 2, with 2 = all preoperative symptoms resolved (p = NS)
[d]Extrapolated from percentages
[e]Dural opening as initial procedure

of stay, and higher incidence of CSF leaks. There was no significant difference in clinical outcome, syrinx resolution, or rates of tonsillar reduction between the two groups. The authors reported a high incidence of CSF leak with dural opening (2.5% PFD versus 38.1% PFDD, $p < 0.001$), likely due to their use of drainage with low vacuum suction postoperatively. They concluded that PFD represents a viable surgical option, as it has comparable outcomes and a lower risk of complications than PFDD.

Shweikeh and colleagues [22] used the Kids' Inpatient Database (KID) to conduct a retrospective analysis of children who underwent PFD or PFDD. The authors concluded that PFD was a more favorable first-line option because it was associated with fewer reoperations (0.7% vs. 2.1%), fewer complications (0.8% vs. 2.3%), a shorter LOS (3.8 days vs. 4.4 days), and lower hospital charges than PFDD. The authors point out that the reoperation rate reported was mainly due to immediate postoperative complications rather than reoperations due to failed resolution of symptoms. In addition, outcome analysis was limited with regard to both symptom resolution and long-term follow-up, during which time PFD-treated patients may have required further surgery due to persistent symptoms.

Single-center retrospective studies [10, 12, 21–30] have demonstrated fluctuating rates of symptom resolution between 50% and 90% for PFD and 64% and 100% for PFDD. Complications rates were lower in the PFD groups with rates between 0% and 11% for PFD and 11% and 19% for PFDD. Reoperation rates were found to be lower in the PFDD groups (2–8%) but varied widely in the PFD groups with rates between 0% and 54%. On balance, PFD is associated with

lower complication rates, operative time, and length of stay and therefore lower hospital cost but with higher rates of reoperation for persistent symptoms [12, 23–30]. Symptom improvement varied among retrospective studies, with some studies finding PFDD to have significantly higher rates of symptom improvement [26, 27] and other studies finding no statistically significant difference with regard to symptom improvement among the two procedures [24, 25, 28–30]. Many studies also reported that there was no significant difference in complication and reoperation rates among the groups [12, 23–30].

Some studies based procedure choice on syrinx presentation with PFD being performed in children without syrinx and dural opening performed in children who presented with syringomyelia [12, 28, 30]. Authors further noted that those undergoing PFDD had a higher prevalence of syrinx as well as a higher degree of tonsillar herniation, which may have affected outcomes and complication rates due to advanced disease [28].

Grahovac and colleagues [31] conducted a retrospective review of 16 children up to the age of 3 years to determine the experience of CM I in infants and toddlers. Ten children (62.5%) underwent PFD and six (37.5%) underwent PFDD. The authors found that symptoms in this age group may differ from older children due to the lack of verbal communication in younger patients. Patients presented mainly with behavioral changes indicating headaches/irritability (75%) and oropharyngeal/respiratory symptoms (62.5%). The incidence of syrinx and scoliosis was rare with only one syrinx and no scoliosis cases. Recurrence rates were found to be higher among patients who underwent PFD versus PFDD (5 vs. 2), although the difference was not statistically significant. They found that PFDD had better decompression and outcomes but had higher risk for CSF complications (36%), especially after reoperation, in this young age group.

The need for further randomized control trials and large multicenter cooperation are necessary to solve the ongoing debate between surgical techniques. The Posterior Fossa Decompression Study, which is a large multi-site randomized, controlled trial led by the Park Reeves Syringomyelia Research Consortium, completed enrollment at the end of 2018. The results of this collaboration are expected to shed light on the ongoing debate between techniques and provide improved patient-selection guidelines moving forward.

Studies of Posterior Fossa Decompression Without Dural Opening

Intraoperative electrophysiological assessments have provided evidence of functional decompression during PFD. Groups from the Children's Hospital of New York/Columbia University and Ohio State University reported that improved conduction of nerve impulses through the brain stem occurs after bony decompression rather than after dural opening [32–34]. Additionally, several groups report the utility of intraoperative ultrasound findings to aid their decision-making with regard to dural opening in children with CM I [14, 19, 35–37]. Yeh and colleagues [14] assessed preoperative characteristics that were associated with successful surgical treatment. The authors reported that age less than 1 year was associated with a high rate of success following PFD. Spinal symptoms (motor, sensory, or scoliosis) and a greater magnitude of tonsillar descent were more likely to require PFDD.

Clinical Outcome

Kennedy and colleagues [38] retrospectively reviewed 156 children who underwent PFD over a 10-year period at their institution. One hundred thirty-eight patients (91%) had symptom improvement or resolution. No major complications were reported. Fourteen patients (9%) required reoperation, with partial C2 laminectomy being a risk factor for reoperation ($p = 0.037$). Of note, no patient with <8 mm tonsillar herniation required reoperation. The authors recommend PFD for the majority of symptomatic patients with CM I. Exceptions include patients with rapidly progressive neurological deficits,

rapidly progressive scoliosis with syrinx, and craniovertebral instability requiring fusion. They also recommend PFDD if the surgeon feels that partial C-2 laminectomy will be necessary to achieve adequate decompression.

Excellent results have been reported in children who underwent PFD alone [8, 31, 39, 40]. Rates have been reported between 91% and 100% of patients who experienced clinical improvement after PFD alone [8, 31, 39]. Genitori and colleagues found that 81.3% of patients without syringomyelia had complete symptom resolution, while 18.8% had partial resolution [39]. Among the patients with syringomyelia, symptoms improved or resolved in all cases with the exception of one of three cases of scoliosis and one of five cases of sensory loss. Rates of complete symptom resolution, however, ranged from 25% (sensory loss) to 100% (vertigo). The authors acknowledged that it is difficult to draw definitive conclusions from their study due to the small numbers in each group [39].

Syrinx Resolution

At this time, there are no clear guidelines regarding the extent or timing of syrinx resolution that should be expected following surgical treatment for CM I (Fig. 41.1). Wetjen et al. [9] have stated that the absence of syrinx distention is more important than complete collapse. Caldarelli and

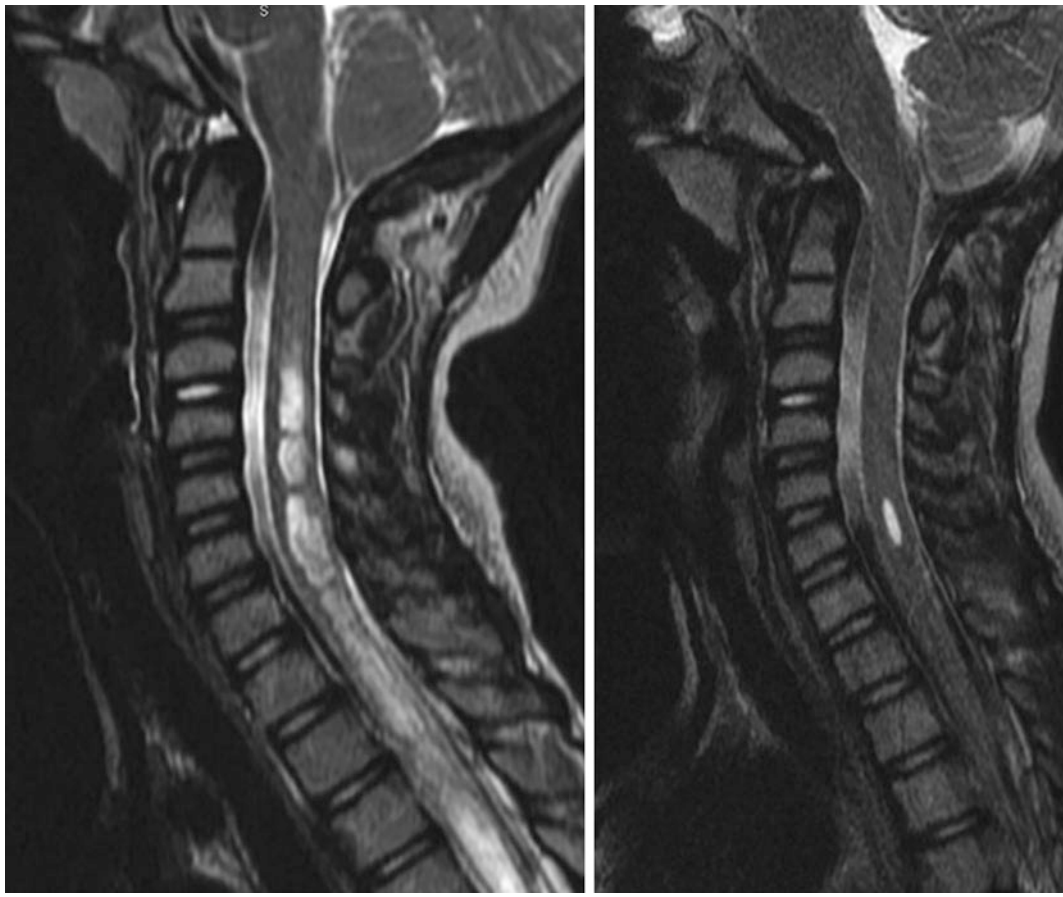

Fig. 41.1 Pre- and postoperative sagittal T2-weighted magnetic resonance imaging (MRI) demonstrating significant improvement of holocord syringomyelia in a child with CM I who was treated with PFD without duraplasty. The postoperative image was acquired 13 months after surgery. (Courtesy of N. Feldstein)

colleagues [8] state that, in the context of clinical improvement, radiological change (either in syrinx size or posterior fossa subarachnoid volume) may not be mandatory for a successful result. In their series, syringomyelia was present preoperatively in 12 of 30 (40%) patients. Postoperatively, half of these patients had a decrease in the size of the syrinx. Two patients (6.7%) demonstrated recurrent symptoms and postoperative syrinx growth (one de novo and another who had a syrinx preoperatively) and required reoperation.

Kennedy and colleagues [40] also found that radiographic syrinx improvement often lags behind clinical improvement following PFD. Two studies by Kennedy et al. [38, 40] showed syrinx improvement/resolution in 70% of patients at a mean of 31.5 months after surgery. In one of the studies, all patients (100%) experienced symptom improvement within the first year after surgery, but only 26% experienced radiographic syrinx improvement during this same time frame. The authors also noted that they typically perform PFD at their institution regardless of syrinx presence. The remaining PFD retrospective studies were influenced by small numbers of patients presenting with syrinx and demonstrated rates of syrinx improvement or resolution ranging between 56% and 100% [11, 39, 41].

Scoliosis Improvement

In the larger study by Kennedy and colleagues [38], 12% of patients (18/156) had scoliosis with a median Cobb angle of 25 degrees. Seventeen of these had an associated syrinx. Five of 17 (29%) patients with syrinx-related scoliosis eventually underwent spinal fusion surgery. Four of 17 (23%) showed scoliosis improvement. Each of these patients had a presenting Cobb angle of 23 degrees or less. Nine patients had stable Cobb angles, with an initial mean Cobb angle of 27 degrees in this group. Four patients had progression of their scoliosis, and this group presented originally with a mean angle of 29 degrees. Of these four patients, two underwent spinal fusion and two underwent reoperation with PFDD followed by spinal fusion.

Three studies with very small numbers of patients with scoliosis treated with PFD showed improvement in four out of six patients (67%), with one patient experiencing scoliosis progression and subsequently undergoing reoperation with PFDD [8, 39, 42].

Studies of Posterior Fossa Decompression with Dural Opening

Clinical Outcome

In a series of 500 pediatric patients with CM I who underwent surgical treatment with PFDD, Tubbs and colleagues reported a 3% rate of reoperation for continued symptoms or persistent large syringomyelia, a 2.4% complication rate, and an 83% rate of relief of preoperative signs or symptoms [43]. Of note, the authors reported no cases of aseptic meningitis [43]. Clinical improvement rates between 92% and 100% and complication rates between 0% and 21.1% have been reported in other series [32, 33, 44–52].

Attenello and colleagues [50] examined outcomes and complication rates comparing different materials for duraplasty (autograft vs. synthetic allograft). The authors reported mild to moderate symptom recurrence at 16 months follow-up in 14/67 patients (20.9%), with 4 of these (6%) requiring revision decompression. Seventeen percent of patients (n = 10) demonstrated a radiographic pseudomeningocele with only one of these becoming symptomatic. A total of five patients (7%) suffered CSF-related complications: two (3%) with CSF leak and two (3%) with aseptic meningitis. Parker and colleagues [52] reported a doubling of their CSF-related complication rate (to as high as 56% in one subgroup) when specific combinations of dural graft and tissue sealant were employed.

In four retrospective single-series reviews, rates of primary symptom resolution were high and ranged from 81% to 93%. Complication and reoperations were found to be low in these studies with complication rates ranging from 4% to 38% and reoperations rates ranging from 4% to 11%. Authors concluded that PFDD was an

effective and safe treatment option with low complication and reoperation rates [53–56].

Kawasaki and colleagues [57] reported a single case study of a 7-year-old who had preoperative neurological symptoms undergoing PFDD. The authors found that intraoperative neurophysiologic monitoring (INM) improvement—specifically motor-evoked potentials (MEPs) and somatosensory-evoked potentials (SSEPs)—observed during surgery may be a positive predictor of good clinical outcome after surgery. This is the first known report showing immediate improvement in INM and corresponding positive clinical outcome and neurological function after PFDD.

Guan and colleagues [58] examined risk factors associated with developing postoperative hydrocephalus after PFDD and the subsequent need for permanent CSF diversion. Their institutional series included a retrospective review of 297 patients who underwent PFDD. Twenty-two patients (7%) subsequently required long-term CSF diversion. The authors identified young age (< 6 years), high intraoperative blood loss, and presence of a fourth ventricular web as risk factors for developing postoperative hydrocephalus.

Syrinx Resolution

Radiographic syrinx improvement following PFDD in pediatric series is reported to range from 55% to 100% [32, 33, 36, 43, 45, 47–51]. As previously mentioned, Durham and Fjeld-Olenec [11] found an overall rate of 87% syrinx reduction in the PFDD arms of studies that compared PFD with PFDD. The variability of syrinx outcomes may be due to the lack of a standard definition of syrinx improvement and from the small sample size of many studies. Additionally, the clinical relevance of specific changes in syrinx characteristics is not well understood (Fig. 41.2).

Following initial PFDD in 500 patients, Tubbs and colleagues [43] reported that 13 of 285 (4.6%) required reoperation for persistent syringomyelia. Eleven of these (84.6%) resolved with reoperative decompression including unilateral tonsillar coagulation (Fig. 41.1).

Xie and colleagues [59] defined significant syrinx resolution as a > 20% decrease in the maximal syrinx/cord ratio on follow-up MRI. In their single-center retrospective study, they noted that an upward shifting of the cerebellar tonsil postoperatively was associated with a 95% likelihood of syrinx improvement, while 76% of patients without this finding had syrinx improvement ($p = 0.008$). The bulbopontine sulcus, the fourth ventricle vertex, and the tip of the cerebellar tonsil were the reference points used to determine the postoperative shifting on imaging.

In the previously mentioned retrospective PFDD studies, rates of syrinx improvement or resolution reported ranged from 7% to 78%, while rates in which the syrinx stabilized ranged from 22% to 42% after surgery. Improvement of symptoms ranged from 54% to 66% [36, 53–56]. Rates of recurring or worsening syrinx remained below 11% in all retrospective studies following PFDD. In their experience, Hildago and colleagues [54] found that children with an associated genetic syndrome or previous surgery had a statistically significant delay in syrinx resolution. Hildago et al. also claimed that favorable outcomes were due to their narrow indications for surgery based on strict definitions of syringomyelia (involvement of at least three spinal levels and expansion of the spinal cord by >4 mm).

Menezes and colleagues [60] analyzed 326 patients who underwent PFDD in which 13 had syringobulbia (4%). Headache and neck pain were noted in all 13 cases. Cranial nerve abnormalities and sleep apnea were also common at presentation. Syringobulbia improved in all cases (100%), while syringomyelia resolved in 12 of the 13 patients. An intradural procedure is recommended by the authors for treatment of syringobulbia.

As previously stated, there is currently no standard definition for the rate or magnitude of syrinx regression that reflects satisfactory treatment. A subjectively significant decrease in the syrinx size on the first postoperative imaging examination is reassuring to the surgeon; however, syrinx obliteration is likely unnecessary [8, 9]. Additionally, delayed syrinx dissipation has been reported [61].

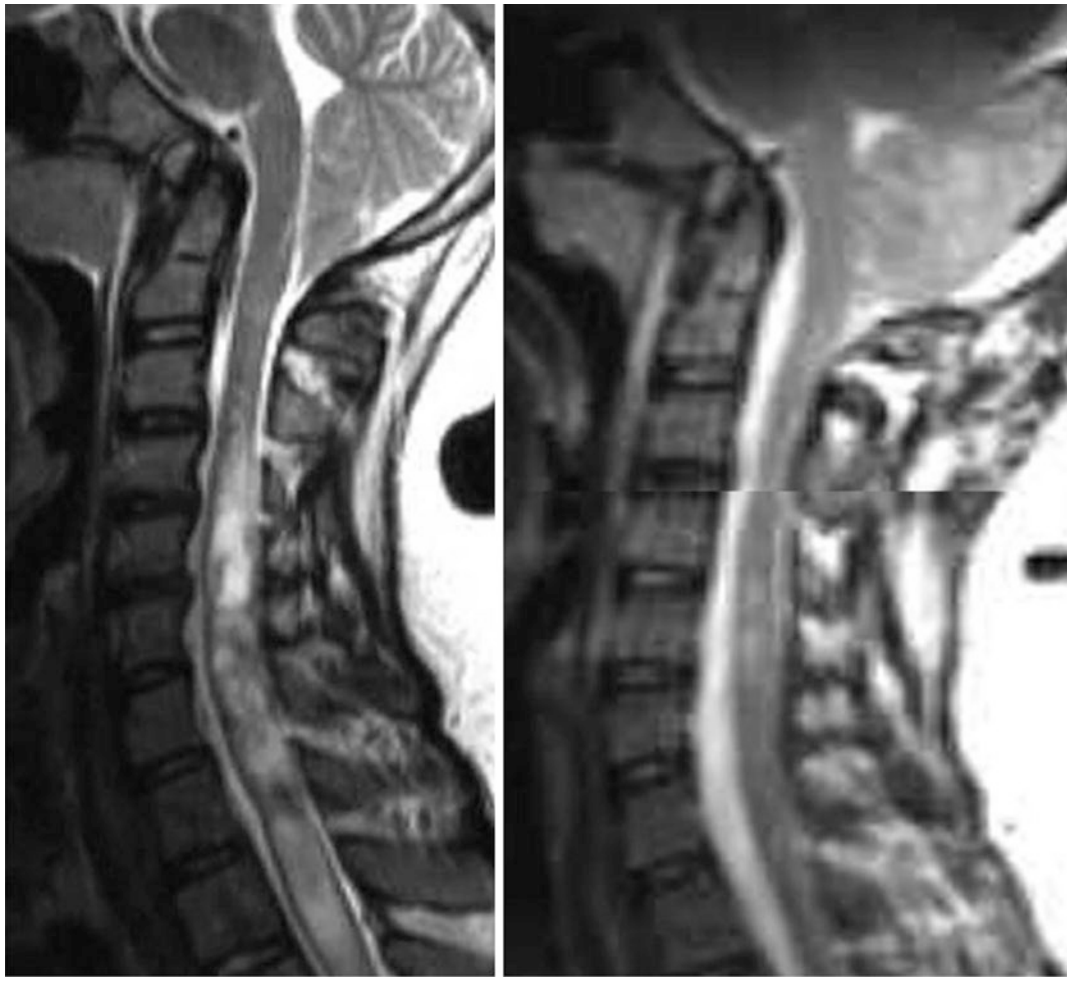

Fig. 41.2 Pre- and postoperative sagittal T2-weighted magnetic resonance imaging (MRI) demonstrating significant improvement of holocord syringomyelia in a child with CM I who was treated with PFD with duraplasty. The postoperative image was acquired 3 months after surgery. (Courtesy of M. Handler)

Scoliosis Progression

In the vast majority of cases, scoliosis in the context of CM I is associated with syringomyelia [62]. Details regarding the neurological impairments that connect these two entities are yet to be fully elucidated. It is believed, however, that scoliosis may result from imbalanced innervation of axial musculature due to syrinx-generated lower motor neuron injury [63–65]. Consistent with this theory, multiple authors have reported scoliosis improvement following PFDD in children with CM I, although Brockmeyer and colleagues found that a decrease in syrinx size did not necessarily correlate with scoliosis improvement [66]. Reported rates of scoliosis improvement and progression vary widely. Rates of improvement are reported at 0–73%, and rates of progression are 18–72% [6, 66–74]. In some series, younger children (less than 8–10 years) have been less likely to suffer from scoliosis progression [6, 31, 66, 68, 73, 74]. Female gender and a smaller presenting Cobb angle have also been associated with improved outcomes. In 20 pediatric patients with CM I-associated scoliosis treated by PFDD, Attenello and colleagues [42] reported that 8

(40%) demonstrated a postoperative improvement of their scoliosis and 9 (45%) progressed. The authors reported that an increased magnitude of scoliosis curve at presentation was predictive of scoliosis progression, as were thoracolumbar junction scoliosis and a lack of postoperative radiological syrinx response.

Two single series retrospective [75, 76] reviews found that PFDD had an effect on the regression of scoliosis in 41% and 65% of the CM I patients, and corrective surgery was needed in 59% and 20%, respectively. Zhu et al. found that age (≥ 10.5 years), curve type (presence of double curve), magnitude (Cobb angle ≥44.5 degrees), and no bracing treatment were independent predictors for curve progression after PFDD, with age and magnitude of Cobb angle being the strongest predictors [75]. Chotai et al. concluded that corrective surgery might not be required in patients with a preoperative scoliosis curve <35 degrees and those with early onset scoliosis [76].

Hwang and colleagues [77] conducted a meta-analysis of 12 published studies evaluating outcomes of children with CM I-associated scoliosis who underwent surgical decompression. The authors found that curve magnitude will improve after surgical treatment of CM I in one-third of patients, and curve progression will stabilize or improve in one-half of patients. They noted the following study limitations: small sample size in most of the studies, retrospective nature of studies, limited details of surgical technique, inconsistent reporting of variables between studies, and differing definitions of curve progression and improvement among studies.

Summary

The Case for Posterior Fossa Decompression

Electrophysiologic data support the assertion that effective PFD occurs with bony decompression and dural scoring, not necessarily requiring dural opening [32–34, 57]. Although rates of reoperation for persistent or recurrent symptoms are higher with PFD, the technique is attractive because it minimizes potential surgical complications. Theoretical complications that are avoided with PFD include pseudomeningocele, chemical meningitis, bacterial meningitis, arterial injury, venous sinus bleeding, stroke, and hydrocephalus. Several studies have demonstrated that CSF-related complication rates are lower with PFD than PFDD [12–14, 18, 19, 25, 29, 30]. Additionally, non-dural opening PFD is likely to require less operative time [12, 18, 28, 29], results in less postoperative pain, and may be of lesser financial burden to the healthcare system [12, 28]. The case for PFD is additionally strengthened by the inability of studies that directly compare PFD to PFDD to demonstrate a statistically significant difference in clinical outcomes. Furthermore, while many studies have demonstrated a trend toward a greater pace and magnitude of syrinx collapse following PFDD, the relevant details of this outcome measure are yet to be determined, making syrinx resolution a suboptimal method for the assessment of efficacy regarding hindbrain decompression for CM I. Lastly, the use of PFD does not in any way preclude patients from undergoing further decompression should this become necessary (Table 41.2).

Table 41.2 Relative advantages of posterior fossa decompression (PFD) and posterior fossa decompression with duraplasty (PFDD)

PFD	PFDD
Lower CSF-related complication rate	Lower reoperation rate
Shorter operative time	Better radiological outcomes
Optional shorter incision	Allows inspection of arachnoid veils/scarring
± Adequate syrinx decompression	± Better clinical outcomes
Shorter hospital stay	
Less postoperative pain	
± Lower cost	

CSF cerebrospinal fluid

The Case for Posterior Fossa Decompression with Duraplasty

Although direct comparisons have not demonstrated a statistically significant difference in clinical outcomes, many consider PFDD to be the treatment that offers the greatest likelihood of improving the presenting signs and symptoms in any given child. Most reports that discuss the clinical efficacy of PFDD demonstrate rates of improvement superior to those of PFD [13–16]. Durham and Fjeld-Olenec [11] demonstrated a significantly lower rate of reoperation following PFDD than PFD (2.1% vs. 12.6%), as did Mutchnick and colleagues [12]. Although the meta-analysis also demonstrated a higher complication rate with PFDD, it must be acknowledged that multiple groups have reported very low complication rates with PFDD [43, 46, 47]. Additionally, up to 12% of patients with CM I and syringomyelia may harbor a radiographically occult arachnoid veil, which cannot be treated without dural opening [43, 78]. Lastly, there are circumstances, such as rapidly progressive neurological decline or scoliosis, where there is very little debate that PFDD is necessary.

Conclusion

At this time, pediatric neurosurgeons lack Class I evidence to guide decision-making with regard to the most appropriate surgical technique for the management of CM I. Most authors concur that, in the absence of hydrocephalus, hindbrain decompression represents the best first-line treatment for CM I. The single published randomized trial (Jiang [10]) was limited to adolescent patients and concluded that PFD was a favorable initial option in most cases. However, current data leave the surgeon and family to choose between a procedure that is more likely to require reoperation (PFD) and one that is more likely to result in perioperative CSF-related complications (PFDD). The frequency of these suboptimal outcomes (12.6% and 18.5%, respectively, in Durham and Fjeld-Olenec's meta-analysis [11]) does little to clarify which approach is most appropriate for a given patient. Furthermore, wide ranges of clinical efficacy and complications have been reported, and additional complicating factors (such as length of hospital stay, perioperative pain, and hospital cost) cloud decision-making. Lastly, the spectrum of presentation in children with CM I extends from asymptomatic to potentially life-threatening symptomatology. It is therefore not surprising that no single surgical approach is universally recommended.

One objective for the future of surgical treatment in CM I should be to improve patient selection in order to identify patients who are likely to be successfully treated with a less-invasive surgical technique, as well as finding more standardized methods of outcome measurements and syrinx/scoliosis treatment guidelines. Efforts to standardize outcome reporting [79] and perform clinical trials for this patient population [20] will hopefully inform future decision-making, as will the results of the forthcoming trial from the Park-Reeves Syringomyelia Research Consortium. Nevertheless, the treating neurosurgeon must always consider the individual characteristics of her/his patient and practice when choosing an operative strategy.

References

1. Massimi L, Pravatà E, Tamburrini G, Gaudino S, Pettorini B, Novegno F, et al. Endoscopic third ventriculostomy for the management of Chiari I and related hydrocephalus: outcome and pathogenetic implications. Neurosurgery. 2011;68(4):950.
2. Hayhurst C, Osman-Farah J, Das K, Mallucci C. Initial management of hydrocephalus associated with Chiari malformation Type I-syringomyelia complex via endoscopic third ventriculostomy: an outcome analysis. J Neurosurg. 2008;108(6):1211–4.
3. Oldfield EH, Muraszko K, Shawker TH, Patronas NJ. Pathophysiology of syringomyelia associated with Chiari I malformation of the cerebellar tonsils. Implications for diagnosis and treatment. J Neurosurg. 1994;80(1):3–15.
4. Alden TD, Ojemann JG, Park TS. Surgical treatment of Chiari I malformation: indications and approaches. Neurosurg Focus. 2001;11(1):E2.
5. Haroun RI, Guarnieri M, Meadow JJ, Kraut M, Carson BS. Current opinions for the treatment of syringomyelia and Chiari malformations: survey of the Pediatric Section of the American Association of Neurological Surgeons. Pediatr Neurosurg. 2000;33(6):311–7.

6. Ozerdemoglu RA, Transfeldt EE, Denis F. Value of treating primary causes of syrinx in scoliosis associated with syringomyelia. Spine. 2003;28(8):806–14.
7. Schijman E, Steinbok P. International survey on the management of Chiari I malformation and syringomyelia. Childs Nerv Syst. 2004;20(5):341–8.
8. Caldarelli M, Novegno F, Vassimi L, Romani R, Tamburrini G, Di Rocco C. The role of limited posterior fossa craniectomy in the surgical treatment of Chiari malformation type I: experience with a pediatric series. J Neurosurg. 2007;106(3 Suppl):187–95.
9. Wetjen NM, Heiss JD, OldÞeld EH. Time course of syringomyelia resolution following decompression of Chiari malformation Type I. J Neurosurg Pediatr. 2008;1(2):118–23.
10. Jiang E, Sha S, Yuan X, Zhu W, Jiang J, Ni H, Liu Z, Qiu Y, Zhu Z. Comparison of clinical and radiographic outcomes for posterior Fossa decompression with and without duraplasty for treatment of pediatric Chiari I malformation: a prospective study. World Neurosurg. 2018;110:e465–72.
11. Durham SR, Fjeld-Olenec K. Comparison of posterior fossa decompression with and without duraplasty for the surgical treatment of Chiari malformation Type I in pediatric patients: a meta-analysis. J Neurosurg Pediatr. 2008;2(1):42–9.
12. Mutchnick IS, Janjua RM, Moeller K, Moriarty TM. Decompression of Chiari malformation with and without duraplasty: morbidity versus recurrence. J Neurosurg Pediatr. 2010;5(5):474–8.
13. Munshi I, Frim D, Stine-Reyes R, Weir BK, Hekmatpanah J, Brown F. Effects of posterior fossa decompression with and without duraplasty on Chiari malformation-associated hydromyelia. Neurosurgery. 2000;46(6):1384–9; discussion 1389–90
14. Yeh DD, Koch B, Crone KR. Intraoperative ultrasonography used to determine the extent of surgery necessary during posterior fossa decompression in children with Chiari malformation type I. J Neurosurg. 2006;105(1 Suppl):26–32.
15. Ventureyra ECG, Aziz HA, Vassilyadi M. The role of cine ßow MRI in children with Chiari I malformation. Childs Nerv Syst. 2003;19(2):109–13.
16. McGirt MJ, Attenello FJ, Datoo G, Gathinji M, Atiba A, Weingart JD, et al. Intraoperative ultrasonography as a guide to patient selection for duraplasty after suboccipital decompression in children with Chiari malformation Type I. J Neurosurg Pediatr. 2008;2(1):52–7.
17. Galarza M, Sood S, Ham S. Relevance of surgical strategies for the management of pediatric Chiari type I malformation. Childs Nerv Syst. 2007;23(6):691–6.
18. Limonadi FM, Selden NR. Dura-splitting decompression of the craniocervical junction: reduced operative time, hospital stay, and cost with equivalent early outcome. J Neurosurg. 2004;101(2 Suppl):184–8.
19. Navarro R, Olavarria G, Seshadri R, Gonzales-Portillo G, McLone DG, Tomita T. Surgical results of posterior fossa decompression for patients with Chiari I malformation. Childs Nerv Syst. 2004;20(5):349–56.
20. Rocque BG, George TM, Kestle J, Iskandar BJ. Treatment practices for Chiari malformation type I with syringomyelia: results of a survey of the American Society of Pediatric Neurosurgeons. J Neurosurg Pediatr. 2011;8(5):430–7.
21. Lu VM, Phan K, Crowley SP, Daniels DJ. The addition of duraplasty to posterior fossa decompression in the surgical treatment of pediatric Chiari malformation Type I: a systematic review and meta-analysis of surgical and performance outcomes. J Neurosurg Pediatr. 2017;20(5):439–49. Review. Erratum in: J Neurosurg Pediatr. 2018;21(2):197.
22. Shweikeh F, Sunjaya D, Nuno M, Drazin D, Adamo MA. National trends, complications, and hospital charges in pediatric patients with Chiari malformation type I treated with posterior fossa decompression with and without duraplasty. Pediatr Neurosurg. 2015;50(1):31–7.
23. Khalsa SSS, Siu A, DeFreitas TA, Cappuzzo JM, Myseros JS, Magge SN, Oluigbo CO, Keating RF. Comparison of posterior fossa volumes and clinical outcomes after decompression of Chiari malformation Type I. J Neurosurg Pediatr. 2017;19(5):511–7.
24. Pomeraniec IJ, Ksendzovsky A, Yu PL, Jane JA Jr. Surgical history of sleep apnea in pediatric patients with Chiari Type 1 malformation. Neurosurg Clin N Am. 2015;26(4):543–53.
25. Pisapia JM, Merkow MB, Brewington D, Henn RE, Sutton LN, Storm PB, Heuer GG. External validity of the chiari severity index and outcomes among pediatric chiari I patients treated with intra- or extra-Dural decompression. Childs Nerv Syst. 2017;33(2):313–20.
26. Pomeraniec IJ, Ksendzovsky A, Awad AJ, Fezeu F, Jane JA Jr. Natural and surgical history of Chiari malformation Type I in the pediatric population. J Neurosurg Pediatr. 2016;17(3):343–52.
27. Raza-Knight S, Mankad K, Prabhakar P, Thompson D. Headache outcomes in children undergoing foramen magnum decompression for Chiari I malformation. Arch Dis Child. 2017;102(3):238–43.
28. Litvack ZN, Lindsay RA, Selden NR. Dura splitting decompression for Chiari I malformation in pediatric patients: clinical outcomes, healthcare costs, and resource utilization. Neurosurgery. 2013;72(6):922–8; discussion 928–9
29. Lee A, Yarbrough CK, Greenberg JK, Barber J, Limbrick D, Smyth MD. Comparison of posterior fossa decompression with or without duraplasty in children with Type I Chiari malformation. Childs Nerv Syst. 2014;30(8):1419–24.
30. Gallo P, Sokol D, Kaliaperumal C, Kandasamy J. Comparison of three different cranio-cervical decompression procedures in children with Chiari malformation type I: does the surgical technique matter? Pediatr Neurosurg. 2017;52(5):289–97.
31. Grahovac G, Pundy T, Tomita T. Chiari type I malformation of infants and toddlers. Childs Nerv Syst. 2018;34(6):1169–76.
32. Anderson RCE, Dowling KC, Feldstein NA, Emerson RG. Chiari I malformation: potential role for intra-

operative electrophysiologic monitoring. J Clin Neurophysiol. 2003;20(1):65–72.
33. Anderson RCE, Emerson RG, Dowling KC, Feldstein NA. Improvement in brainstem auditory evoked potentials after suboccipital decompression in patients with Chiari I malformations. J Neurosurg. 2003;98(3):459–64.
34. Zamel K, Galloway G, Kosnik E, Raslan M, Adeli A. Intraoperative neurophysiologic monitoring in 80 patients with Chiari I malformation: role of duraplasty. J Clin Neurophysiol. 2009;26(2):70–5.
35. Menezes AH. Current opinions for treatment of symptomatic hindbrain herniation or Chiari type I malformation. World Neurosurg. 2011;75(2):226–8.
36. Attenello FJ, McGirt MJ, Gathinji M, Datoo G, Atiba A, Weingart J, et al. Outcome of Chiari-associated syringomyelia after hindbrain decompression in children: analysis of 49 consecutive cases. Neurosurgery. 2008;62(6):1307–13; discussion 1313.
37. McGirt M, Attenello F, Atiba A, Garces-Ambrossi G, Datoo G, Weingart JD, et al. Symptom recurrence after suboccipital decompression for pediatric Chiari I malformation: analysis of 256 consecutive cases. Childs Nerv Syst. 2008;24(11):1333–9.
38. Kennedy BC, Kelly KM, Phan MQ, Bruce SS, McDowell MM, Anderson RC, Feldstein NA. Outcomes after suboccipital decompression without dural opening in children with Chiari malformation Type I. J Neurosurg Pediatr. 2015;16(2):150–8.
39. Genitori L, Peretta P, Nurisso C, Macinante L, Mussa F. Chiari type I anomalies in children and adolescents: minimally invasive management in a series of 53 cases. Childs Nerv Syst. 2000;16(10–11):707–18.
40. Kennedy BC, Nelp TB, Kelly KM, Phan MQ, Bruce SS, McDowell MM, Feldstein NA, Anderson RCE. Delayed resolution of syrinx after posterior fossa decompression without dural opening in children with Chiari malformation Type I. J Neurosurg Pediatr. 2015;16(5):599–606.
41. Lei ZW, Wu SQ, Zhang Z, Han Y, Wang JW, Li F, Shu K. Clinical characteristics, imaging findings and surgical outcomes of Chiari Malformation Type I in pediatric and adult patients. Curr Med Sci. 2018;38(2):289–95.
42. Attenello FJ, McGirt MJ, Atiba A, Gathinji M, Datoo G, Weingart J, et al. Suboccipital decompression for Chiari malformation-associated scoliosis: risk factors and time course of deformity progression. J Neurosurg Pediatr. 2008;1(6):456–60.
43. Tubbs RS, Beckman J, Naftel RP, Chern JJ, Wellons JC 3rd, Rozzelle CJ, et al. Institutional experience with 500 cases of surgically treated pediatric Chiari malformation type I. J Neurosurg Pediatr. 2011;7(3):248–56.
44. Danish SF, Samdani A, Hanna A, Storm P, Sutton L. Experience with acellular human dura and bovine collagen matrix for duraplasty after posterior fossa decompression for Chiari malformations. J Neurosurg. 2006;104(1 Suppl):16–20.
45. Ellenbogen RG, Armonda RA, Shaw DW, Winn HR. Toward a rational treatment of Chiari I malformation and syringomyelia. Neurosurg Focus. 2000;8(3):E6.
46. Feldstein NA, Choudhri TF. Management of Chiari I malformations with holocord syringohydromyelia. Pediatr Neurosurg. 1999;31(3):143–9.
47. Hoffman CE, Souweidane MM. Cerebrospinal fluid-related complications with autologous duraplasty and arachnoid sparing in type I Chiari malformation. Neurosurgery. 2008;62(3 Suppl 1):156–60; discussion 160–1.
48. Alzate JC, Kothbauer KF, Jallo GI, Epstein FJ. Treatment of Chiari I malformation in patients with and without syringomyelia: a consecutive series of 66 cases. Neurosurg Focus. 2001;11(1):E3.
49. Krieger MD, McComb JG, Levy ML. Toward a simpler surgical management of Chiari I malformation in a pediatric population. Pediatr Neurosurg. 1999;30(3):113–21.
50. Attenello FJ, McGirt MJ, Garcés-Ambrossi GL, Chaichana KL, Carson B, Jallo GI. Suboccipital decompression for Chiari I malformation: outcome comparison of duraplasty with expanded polytetrafluoroethylene dural substitute versus pericranial autograft. Childs Nerv Syst. 2009;25(2):183–90.
51. Mottolese C, Szathmari A, Simon E, Rousselle C, Ricci-Franchi AC, Hermier M. Treatment of Chiari type I malformation in children: the experience of Lyon. Neurol Sci. 2011;32 Suppl 3:S325–30.
52. Parker SR, Harris P, Cummings TJ, George T, Fuchs H, Grant G. Complications following decompression of Chiari malformation Type I in children: dural graft or sealant? J Neurosurg Pediatr. 2011;8(2):177–83.
53. Foreman P, Safavi-Abbasi S, Talley MC, Boeckman L, Mapstone TB. Perioperative outcomes and complications associated with allogeneic duraplasty for the management of Chiari malformations Type I in 48 pediatric patients. J Neurosurg Pediatr. 2012;10(2):142–9.
54. Hidalgo ET, Dastagirzada Y, Orillac C, Kvint S, North E, Bledea R, McQuinn MW, Redel-Traub G, Rodriguez C, Wisoff JH. Time to resolution of symptoms after suboccipital decompression with duraplasty in children with Chiari malformation type I. World Neurosurg. 2018;117:e544–51.
55. Liu H, Yang C, Yang J, Xu Y. Pediatric Chiari malformation type I: long-term outcomes following small-bone-window posterior fossa decompression with autologous-fascia duraplasty. Exp Ther Med. 2017;14(6):5652–8.
56. Cools MJ, Quinsey CS, Elton SW. Chiari decompression outcomes using ligamentum nuchae harvest and duraplasty in pediatric patients with Chiari malformation type I. J Neurosurg Pediatr. 2018;22(1):47–51.
57. Kawasaki Y, Uchida S, Onishi K, Toyokuni M, Okanari K, Fujiki M. Intraoperative neurophysiologic monitoring for prediction of postoperative neurological improvement in a child with Chiari type I malformation. J Craniofac Surg. 2017;28(7):1837–41.

58. Guan J, Riva-Cambrin J, Brockmeyer DL. Chiari-related hydrocephalus: assessment of clinical risk factors in a cohort of 297 consecutive patients. Neurosurg Focus. 2016;41(5):E2.
59. Xie D, Qiu Y, Sha S, Liu Z, Jiang L, Yan H, Chen L, Shi B, Zhu Z. Syrinx resolution is correlated with the upward shifting of cerebellar tonsil following posterior fossa decompression in pediatric patients with Chiari malformation type I. Eur Spine J. 2015;24(1):155–61.
60. Menezes AH, Greenlee JDW, Dlouhy BJ. Syringobulbia in pediatric patients with Chiari malformation type I. J Neurosurg Pediatr. 2018;22(1):52–60.
61. Doughty KE, Tubbs RS, Webb D, Oakes WJ. Delayed resolution of Chiari I-associated hydromyelia after posterior fossa decompression: case report and review of the literature. Neurosurgery. 2004;55(3):711.
62. Tubbs RS, Doyle S, Conklin M, Oakes WJ. Scoliosis in a child with Chiari I malformation and the absence of syringomyelia: case report and a review of the literature. Childs Nerv Syst. 2006;22(10):1351–4.
63. Huebert HT, MacKinnon WB. Syringomyelia and scoliosis. J Bone Joint Surg Br. 1969;51(2):338–43.
64. Isu T, Chono Y, Iwasaki Y, Koyanagi I, Akino M, Abe H, et al. Scoliosis associated with syringomyelia presenting in children. Childs Nerv Syst. 1992;8(2):97–100.
65. Williams B. Orthopaedic features in the presentation of syringomyelia. J Bone Joint Surg Br. 1979;61-B(3):314–23.
66. Brockmeyer D, Gollogly S, Smith JT. Scoliosis associated with Chiari 1 malformations: the effect of suboccipital decompression on scoliosis curve progression: a preliminary study. Spine. 2003;28(22):2505–9.
67. Tubbs RS, McGirt MJ, Oakes WJ. Surgical experience in 130 pediatric patients with Chiari I malformations. J Neurosurg. 2003;99(2):291–6.
68. Eule JM, Erickson MA, O'Brien MF, Handler M. Chiari I malformation associated with syringomyelia and scoliosis: a twenty-year review of surgical and nonsurgical treatment in a pediatric population. Spine. 2002;27(13):1451–5.
69. Farley FA, Puryear A, Hall JM, Muraszko K. Curve progression in scoliosis associated with Chiari I malformation following suboccipital decompression. J Spinal Disord Tech. 2002;15(5):410–4.
70. Flynn JM, Sodha S, Lou JE, Adams SB Jr, Whitfield B, Ecker ML, et al. Predictors of progression of scoliosis after decompression of an Arnold Chiari I malformation. Spine. 2004;29(3):286–92.
71. Ghanem IB, Londono C, Delalande O, Dubousset JF. Chiari I malformation associated with syringomyelia and scoliosis. Spine. 1997;22(12):1313.
72. Hida K, Iwasaki Y, Koyanagi I, Abe H. Pediatric syringomyelia with Chiari malformation: its clinical characteristics and surgical outcomes. Surg Neurol. 1999;51(4):383–90; discussion 390–1.
73. Muhonen MG, Menezes AH, Sawin PD, Weinstein SL. Scoliosis in pediatric Chiari malformations without myelodysplasia. J Neurosurg. 1992;77(1):69–77.
74. Sengupta DK, Dorgan J, Findlay GF. Can hindbrain decompression for syringomyelia lead to regression of scoliosis? Eur Spine J. 2000;9(3):198–201.
75. Zhu Z, Wu T, Zhou S, Sun X, Yan H, Sha S, Qiu Y. Prediction of curve progression after posterior fossa decompression in pediatric patients with scoliosis secondary to Chiari malformation. Spine Deform. 2013;1(1):25–32.
76. Chotai S, Basem J, Gannon S, Dewan M, Shannon CN, Wellons JC, Bonfield CM. Effect of posterior fossa decompression for Chiari malformation-I on scoliosis. Pediatr Neurosurg. 2018;53(2):108–15.
77. Hwang SW, Samdani AF, Jea A, Raval A, Gaughan JP, Betz RR, Cahill PJ. Outcomes of Chiari I-associated scoliosis after intervention: a meta-analysis of the pediatric literature. Childs Nerv Syst. 2012;28(8):1213–9.
78. Tubbs RS, Webb DB, Oakes WJ. Persistent syringomyelia following pediatric Chiari I decompression: radiological and surgical Þndings. J Neurosurg. 2004;100(5 Suppl Pediatrics):460–4.
79. Aliaga L, Hekman KE, Yassari R, Straus D, Luther G, Chen J, et al. A novel scoring system for assessing Chiari malformation type I treatment outcomes. Neurosurgery. 2012;70(3):656–64; discussion 664–5.

42 Chiari Decompression Outcomes Using Ligamentum Nuchae Harvest and Duraplasty in Pediatric Patients with Chiari I Malformation

Michael J. Cools, Carolyn S. Quinsey, and Scott W. Elton

Introduction

The surgical treatment of Chiari I malformation in pediatric patients involves suboccipital craniectomy, C1 posterior arch removal, and, depending on surgeon preference and patient's anatomy, a duraplasty. Duraplasty can be complicated by cerebrospinal fluid (CSF) leakage, pseudomeningocele formation, wound infection, meningitis, and reoperation for scarring or restenosis. These complications occur in approximately 3–10% of patients [1, 2]. The complication rate varies based on the use of synthetic or autologous duraplasty graft material [3]. Ideally, graft material used in Chiari malformation treatment would be easy to obtain, non-immunogenic, inexpensive, and robust enough to have low risk of CSF leakage or pseudomeningocele formation.

The ligamentum nuchae is a robust posterior cervical ligament in the midline, spanning from the occiput to the upper cervical spinous processes, and can be used as an autologous graft material. If not harvested for a dural graft, it is divided as part of the standard suboccipital approach in the avascular midline plane. The use of this material in Chiari surgery was described by EJ Kosnik in 1998 [4]. However, a small minority of surgeons utilize ligamentum nuchae as a graft for duraplasty in Chiari decompression [5].

This chapter will demonstrate this technique, as well as report on a single-center experience with outcomes and complications.

Harvest and Implantation of Ligamentum Nuchae Operative Technique

A standard suboccipital incision is made and carried deep until the superficial cervical fascia is identified. A longitudinal incision is made in the fascia slightly off midline until the paraspinal muscle is identified (Fig. 42.1). Using needle tip electric cautery, the muscle is dissected from the ligamentum nuchae on one side until the surface of the rectus capitis posterior minor is identified (Fig. 42.2). This is repeated on the opposite side. The graft is then elevated at its attachment to the

M. J. Cools
Department of Neurosurgery, University of North Carolina, Chapel Hill, NC, USA

C. S. Quinsey
Department of Neurosurgery, University of North Carolina School of Medicine, Chapel Hill, NC, USA

S. W. Elton (✉)
Department of Neurosurgery, University of North Carolina, University of North Carolina School of Medicine, Chapel Hill, NC, USA
e-mail: scott_elton@med.unc.edu

R. S. Tubbs et al. (eds.), *The Chiari Malformations*, https://doi.org/10.1007/978-3-030-44862-2_42

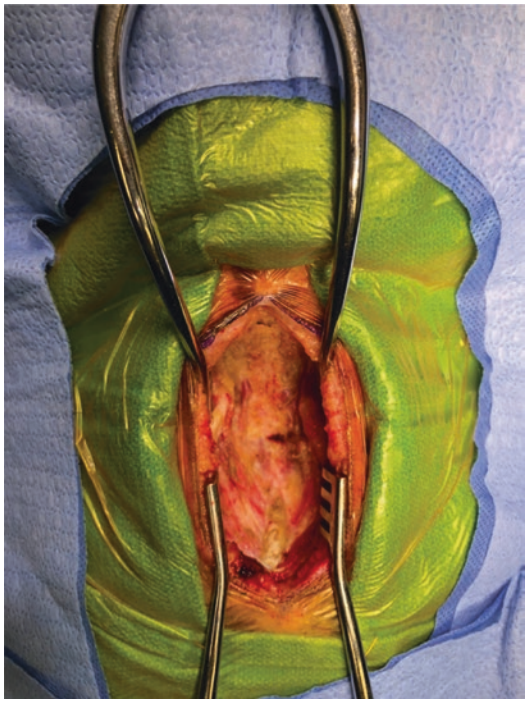

Fig. 42.1 Standard incision opened over posterior cervical spine between inion to C2 spinous process and dissection carried deep to the cervical fascia. Once the cervical fascia is identified, a paramedian incision is made in the fascia until the paraspinous muscle is identified

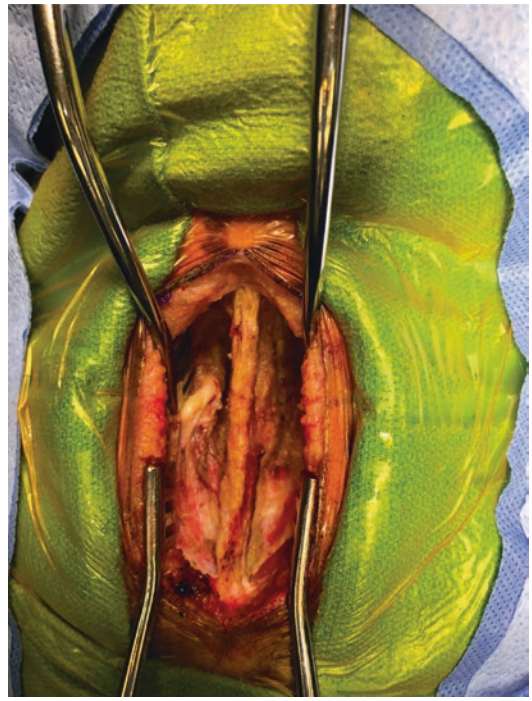

Fig. 42.2 Using needle tip electric cautery, the muscle is dissected from the ligamentum nuchae on one side until the surface of the rectus capitis posterior minor is identified. The rectus capitis posterior minor muscle serves as the base of dissection while dissecting inferiorly, until the surface of C1 and the superior edge of the C2 lamina and spinous process is encountered

occipital bone and amputated along its base while lifting inferiorly. The rectus capitis posterior minor muscle serves as the base of dissection while dissecting inferiorly, until the surface of C1 and the superior edge of the C2 lamina and spinous process is encountered. It is then amputated vertically at C2, removed, and stored in a bacitracin-soaked gauze sponge (Fig. 42.3). The remainder of paraspinal cervical muscle dissection is then completed. The craniectomy and intradural Chiari decompression is completed. The graft is trimmed to the needed size and sewn to native dura with running non-dissolvable braided suture (Fig. 42.4a, b). Representative preoperative and postoperative magnetic resonance imaging (MRI) demonstrates significant decompression of the foramen magnum (Fig. 42.5).

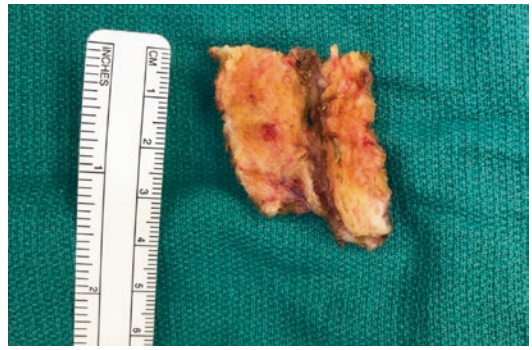

Fig. 42.3 It is then amputated vertically at C2, removed, and stored in a bacitracin-soaked gauze sponge. This graft is both robust and flexible, making an ideal graft material

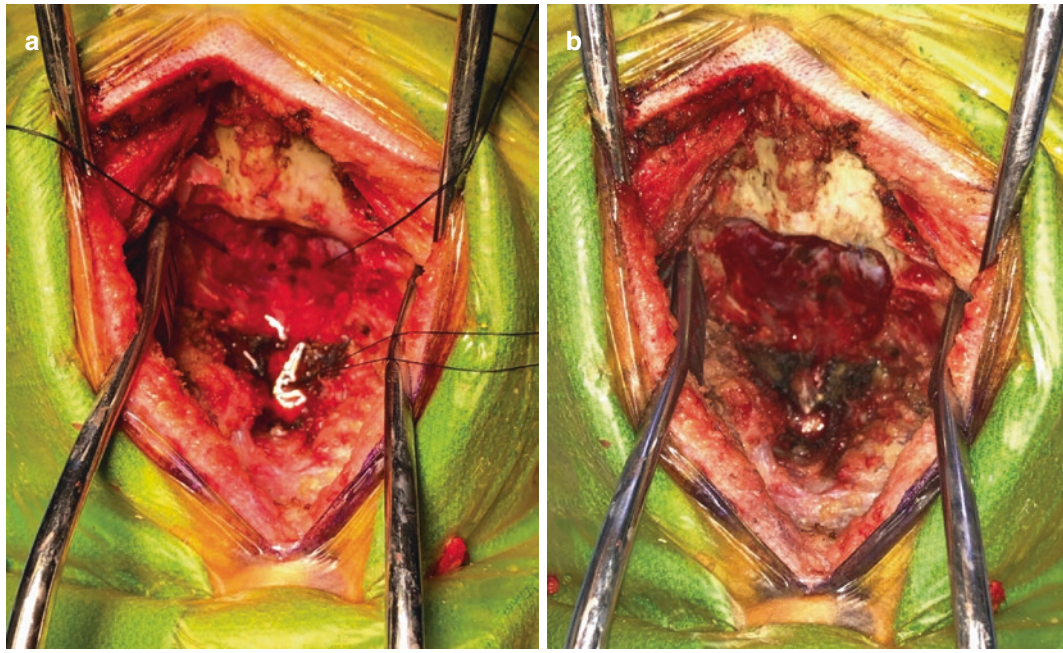

Fig. 42.4 (**a**) The graft is sutured at the corners to secure it to native dura. (**b**) A running 4–0 neurolon is then used to secure the graft to the native dura in a watertight fashion

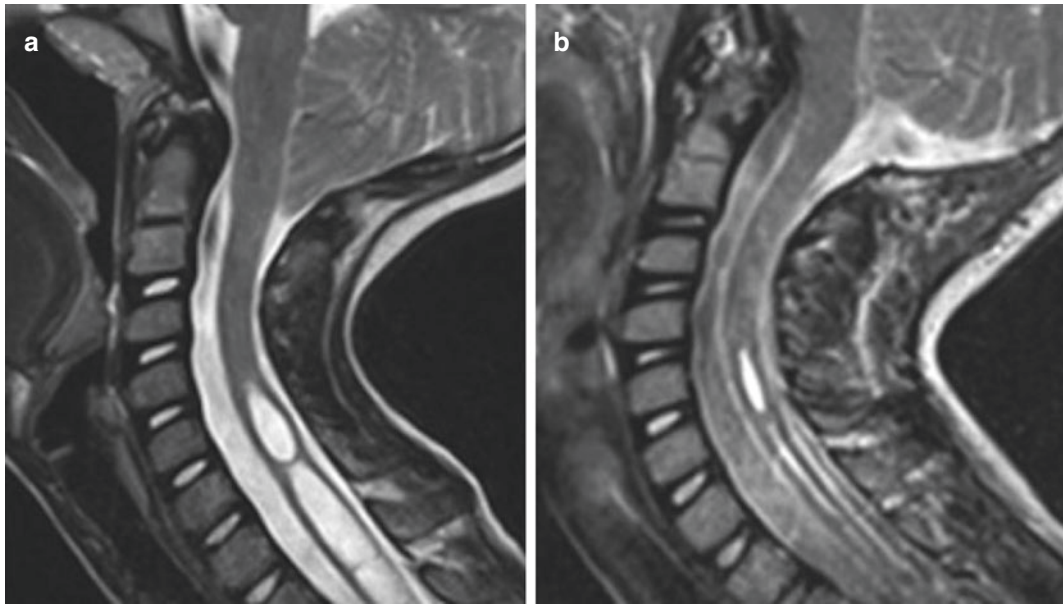

Fig. 42.5 (**a**) Preoperative sagittal T2 MRI with Chiari malformation and associated syrinx. (**b**) Postoperative sagittal T2 MRI following suboccipital decompression, C1 posterior arch removal, and ligamentum nuchae duraplasty. Decompression of the cerebellar tonsils has been achieved, and syrinx has significantly improved

Operative Measurements

All patients were evaluated by clinical exam and MRI of the brain and total spine. Presence, size, and extent of change of spinal cord syrinx were determined by neuroradiology as well as neurosurgical attending evaluation of the T2-weighted hyperintensity within the spinal cord on sagittal and axial MRI sequences. Cerebellar tonsil descent was measured on sagittal MRI using McRae's line. Follow-up includes repeat MRI if the patient had recurrent or non-resolving symptoms or a preoperative syrinx.

Surgical operative time was defined as incision to closure completed as recorded in the anesthesia record, measured in minutes. Graft harvest time is defined as time from incision of cervical fascia until the time the graft is removed from incision.

Literature Search

An English language literature (PubMed.gov) search was undertaken for any previous report of pediatric Chiari decompression using ligamentum nuchae duraplasty (search terms: Chiari decompression, ligamentum nuchae, nuchal ligament, autologous graft).

Table 42.1 Preoperative patient characteristics

Characteristic	**Total *n***	**Percentage**
Male	15	60%
Female	10	40%
Syrinx present	19	76%
Measurement	**Mean**	**Range**
Age at time of surgery	8.6 years	13 months–18 years
Mean tonsillar descent	11.9 mm	SD 7.3 mm
Symptoms	**Total *n***	**Percentage**
Headaches	7	28%
Weakness	3	12%
Vocal cord dysfunction	2	8%
Gait instability	1	4%
Horner's syndrome	1	4%
None	9	36%

Table 42.2 Perioperative factors

Factor	**Mean measurement**	**Range**
Median operative time	163 minutes	IQR 152–187 minutes
Mean EBL	22.4 mL	5–75 mL
Length of hospital stay	3 days	2–6 days
Complications	**Total *n***	**Percentage**
Total	2	8%
CSF leakage	1	4%
Pseudomeningocele	1	4%
Infection	0	0%

CSF Cerebrospinal fluid, *EBL* estimated blood loss, *IQR* Interquartile range

Results

Between 2013 and 2016, 25 suboccipital decompressions for Chiari I malformation were performed by a single pediatric neurosurgeon at our institution using ligamentum nuchae graft for duraplasty. Ten of these patients were female. The average age at time of surgery for all patients was 8.6 years (13 months–18 years). Average tonsillar descent was 11.9 mm (standard deviation 7.3 mm). Nineteen patients presented with a cervical syrinx (Table 42.1).

Median operating time was 163 minutes (interquartile range [IQR] 152–187). Time of ligamentum graft harvest was 10 minutes when completed by a resident surgeon. No grafts became unusable from damage during harvest. Mean estimated blood loss (EBL) was 22.4 mL (5–75 mL), and no patients required blood transfusion. Average length of hospital stay was 3 nights, with a range of 2–6 nights (Table 42.2).

One of the 25 patients (4%) developed a postoperative CSF leak on postoperative day 5, and was taken back to the operating room for a revision. A defect was visualized between the edge of the graft and the dura, and the defect was oversewn. Following revision, the patient did not experience further leakage or pseudomeningocele (Table 42.2).

In our series, no patient developed pseudomeningocele or deep infection. Average follow-up for these patients was 12.8 months (range 0.5–43.5 months). Of the 19 patients who presented with syrinx, ten (53%) had improvement

Table 42.3 Patient outcomes

Outcome and classification	Fraction	Percentage
Syrinx present		
Improved	10/19	53%
Stable	8/19	42%
Worsened	1/19	4%
Symptoms		
Improved	14/16	88%
Stable	1/16	6%
Worsened	1/16	6%

in the syrinx, and eight (42%) had stable imaging. One patient had growth of syrinx and worsening symptoms, which required re-exploration. Of the 16 patients presenting with symptoms, 14 experienced improvement, while 1 remained stable. As previously described, one patient experienced worsening symptoms and syrinx growth (Table 42.3).

The initial description of this technique was published in 1998 by EJ Kosnik [4]. To our knowledge, no other operative descriptions or surgical outcomes of this technique have been reported by any other authors.

Discussion

Despite the large body of research on types of grafts used to treat Chiari I malformation, no consensus exists on the ideal graft material [5, 6]. An ideal graft material must consider several factors, including price, operative time, risk for additional blood loss, robustness of graft, postoperative complication rate, and outcomes of successful decompression of Chiari malformation. Many support the use of pericranial grafts, as the autologous tissue is easily manipulated and has relatively low complication rates [7–11]. However, harvest of pericranial grafts involves extension of incision or extension of dissection outside the standard approach. In addition to the extended incision, the thin pericranium often develops small holes, making it prone to leakage. A recent literature review of pericranial grafts for Chiari decompressions noted up to a 4% CSF leak rate and 10% reoperation rate due to CSF-related complications [7].

The propensity for CSF leak in pericranial grafts led to the evaluation of various types of synthetic graft material, such as AlloDerm, Durepair, DuraGen, and Dura-Guard. Studies of these grafts cite lower complication rates, including CSF leak and pseudomeningocele formation, than pericranial grafts [12–15]. The lower CSF leak rate is used to justify the high cost of the synthetic graft. However, synthetic grafts have higher rates of pseudomeningocele formation, aseptic meningitis, and wound infections when compared to pericranial grafts [7]. Neither the pericranial nor synthetic grafts meet the demands of an ideal graft material. Here, we present the ligamentum nuchae graft as a simple, low complication rate, cost-efficient, autologous graft to treat Chiari I malformation.

In this technique, the ligament is dissected directly from the muscle, but the harvest does not add any blood loss to the case, as the surgical plane remains avascular. Since this ligament is located in the avascular plane routinely dissected in a Chiari decompression, there is no increased loss of stability, need to extend the incision, or increased operative time, which leads to a less complicated graft harvest when compared to other approaches. Additionally, since the ligamentum nuchae harvest does not extend incision and surgery time or require synthetic material, the cost of this approach remains low.

The low complication and reoperation rates also contribute to the cost-efficiency of this graft approach. Overall, we observed low rates of CSF leakage and pseudomeningocele formation and did not note development of holes in the ligamentum nuchae graft. The singular leak was a failure at the suture line. This suggests the ligamentum nuchae provides a more robust autologous graft than the commonly used pericranial graft. In addition to low complication rates, the autologous nature of these grafts does not induce inflammatory reactions observed with synthetic or allogenic grafts. Symptom and radiographic decompression outcomes were similar with this graft compared to reported outcomes of other graft materials [16].

Theoretically, removal of the ligamentum nuchae may impede identification of the midline

for a surgeon on a subsequent surgery, but in our experience, this has not added significant difficulty. Furthermore, it is possible to utilize the midline collagenous scar on repeat operation as further graft material. Our study suggests ligamentum nuchae graft harvest provides a robust, cost-efficient, autologous tissue, which does not require additional dissection, to treat Chiari malformation.

Limitations

While our results suggest ligamentum nuchae graft harvest could be an excellent technique for the treatment of Chiari I malformation, a larger sample size and comparison of this technique to other common autologous and non-autologous grafts would create a more meaningful dataset than presented here. Additionally, because a comparison group does not exist at our institution, a meaningful cost analysis could not be performed. The retrospective nature of this data collection, as well as the potential variation in other parts of the surgical procedure, limits our ability to compare grafts directly. The small sample size and short follow-up limits our ability to make conclusions regarding the long-term results of this technique and avoidance of re-scarring and repeat decompression.

Conclusion

Ligamentum nuchae duraplasty is a simple, fast, low-cost, and durable option in the surgical treatment of Chiari I malformation in children.

Acknowledgments We would like to thank Kathryn Pietrosimone, PhD for editing this manuscript.

References

1. Vedantam A, Mayer RR, Staggers KA, Harris DA, Pan I-W, Lam SK. Thirty-day outcomes for posterior fossa decompression in children with Chiari type 1 malformation from the US NSQIP-pediatric database. Childs Nerv Syst. 2016;32(11):2165–71.
2. Arnautovic A, Splavski B, Boop FA, Arnautovic KI. Pediatric and adult Chiari malformation Type I surgical series 1965–2013: a review of demographics, operative treatment, and outcomes. J Neurosurg Pediatr. 2015;15(2):161–77.
3. Sonntag VH, Abla A, Link T, Fusco D, Wilson D. Comparison of dural grafts in Chiari decompression surgery: review of the literature. J Craniovert Jun Spine. 2010;1(1):29–10.
4. Kosnik EJ. Use of ligamentum nuchae graft for dural closure in posterior fossa surgery. Technical note. J Neurosurg. 1998;89(1):155–6.
5. Haroun RI, Guarnieri M, Meadow JJ, Kraut M, Carson BS. Current opinions for the treatment of syringomyelia and chiari malformations: survey of the Pediatric Section of the American Association of Neurological Surgeons. Pediatr Neurosurg. 2000;33(6):311–7.
6. Schijman E, Steinbok P. International survey on the management of Chiari I malformation and syringomyelia. Childs Nerv Syst. 2004;20(5):341–8.
7. Abla AA, Link T, Fusco D, Wilson DA, Sonntag VKH. Comparison of dural grafts in Chiari decompression surgery: review of the literature. J Craniovert Jun Spine. 2010;1(1):29–37.
8. Lam F, Penumaka A, Chen C, Fischer E, Kasper E. Fibrin sealant augmentation with autologous pericranium for duraplasty after suboccipital decompression in Chiari 1 patients: a case series. Surg Neurol Int. 2013;4(1):6–7.
9. Perrini P. Technical nuances of autologous pericranium harvesting for dural closure in Chiari malformation surgery. J Neurol Surg B Skull Base. 2015;76(2):90–3.
10. Stevens EA, Powers AK, Sweasey TA, Tatter SB, Ojemann RG. Simplified harvest of autologous pericranium for duraplasty in Chiari malformation Type I. Technical note. J Neurosurg Spine. 2009;11(1):80–3.
11. Vanaclocha V, Saiz-Sapena N. Duraplasty with freeze-dried cadaveric dura versus occipital pericranium for Chiari type I malformation: comparative study. Acta Neurochir. 1997;139(2):112–9.
12. Bowers CA, Brimley C, Cole C, Gluf W, Schmidt RH. AlloDerm for duraplasty in Chiari malformation: superior outcomes. Acta Neurochir. 2015;157(3):507–11.
13. Foreman P, Safavi-Abbasi S, Talley MC, Boeckman L, Mapstone TB. Perioperative outcomes and complications associated with allogeneic duraplasty for the management of Chiari malformations Type I in 48 pediatric patients. J Neurosurg Pediatr. 2012;10(2):142–9.
14. Danish SF, Samdani A, Hanna A, Storm P, Sutton L. Experience with acellular human dura and bovine collagen matrix for duraplasty after posterior fossa decompression for Chiari malformations. J Neurosurg. 2006;104(1 Suppl):16–20.
15. Attenello FJ, McGirt MJ, Garcés-Ambrossi GL, Chaichana KL, Carson B, Jallo GI. Suboccipital decompression for Chiari I malformation: outcome comparison of duraplasty with expanded polytetraflu-

oroethylene dural substitute versus pericranial autograft. Childs Nerv Syst. 2008;25(2):183–90.
16. Lu VM, Phan K, Crowley SP, Daniels DJ. The addition of duraplasty to posterior fossa decompression in the surgical treatment of pediatric Chiari malformation Type I: a systematic review and meta-analysis of surgical and performance outcomes. J Neurosurg Pediatr. 2017;20(5):439–49.

Complications of Chiari Surgery

43

Vincent N. Nguyen, Kenneth A. Moore,
David S. Hersh, and Frederick A. Boop

Suboccipital decompression for the treatment of Chiari-related symptoms has been one of the most satisfying surgeries the neurosurgeon can perform due to the fact that most patients derive appreciable and durable benefit from the operation. However, reported complication rates are not as low as many of us would like our patients to believe. Published series report complication rates ranging from 3% to 40% for this procedure [1]. This chapter will review the current literature on these complications in hopes of helping the reader reduce the likelihood of errors. We will detail the complications in an individual format starting with the most common complications and ending with those occurring only rarely. The chapter will not discuss the management of basic wound infections, wound breakdown, and other complications with which all neurosurgeons should be familiar. The authors divide the complications into those related to misdiagnosis and those related to surgical technique.

V. N. Nguyen (✉) · K. A. Moore
Department of Neurosurgery, University of Tennessee Health Science Center, Memphis, TN, USA

D. S. Hersh
Department of Neurosurgery, Connecticut Children's/UConn School of Medicine, Hartford, CT, USA

F. A. Boop
Department of Neurosurgery, University of Tennessee Health Science Center, Le Bonheur Children's Hospital, Memphis, TN, USA

Complications of Misdiagnosis

Incidental Chiari Malformations

When first seeing a patient referred to the neurosurgery clinic with a magnetic resonance imaging (MRI) diagnosis of Chiari malformation, it is important for the neurosurgeon to differentiate the clinical diagnosis from the radiologic picture. The vast majority of patients referred to the neurosurgery clinic with the diagnosis of Chiari I will have mild tonsillar ectopia on a scan unrelated to the clinical condition. The family or the patient has been on the Internet reading about their diagnosis and comes to the clinic certain that many of the symptoms they have read about belong to them as well. Most of the time, the reassurance that this finding has been present since birth and assuring the family that the patient's examination is normal are all that is necessary. Likewise, the small persistent dilatation of the thoracic central canal is often something that can be followed either clinically or radiologically and should not be considered an indication for surgery. One learns quickly that incising the neck muscles in a patient who has muscle tension headaches or fibromyalgia will lead to poor results and a patient who is dissatisfied. Thus, it is of paramount importance that the patient's clinical symptoms suggest Chiari syndrome (e.g., tussive headaches).

R. S. Tubbs et al. (eds.), *The Chiari Malformations*, https://doi.org/10.1007/978-3-030-44862-2_43

Spontaneous Resolution

Prior to any neurosurgical procedure, an up-to-date clinical and radiographic assessment is of the utmost importance. We recently had a patient at our institution who initially presented with headaches that his parents were unable to characterize as being consistently post-tussive or otherwise related to Valsalva. He was also noted to have significant behavioral issues and was scheduled to be seen by a psychiatrist. His initial MRI (Fig. 43.1a) showed a 9-mm descent of the cerebellar tonsils and crowding of the foramen magnum without any evidence of syrinx formation. An interval MRI obtained 1 year later showed complete resolution of his Chiari I malformation (Fig. 43.1b).

Similar cases of spontaneous resolution of Chiari malformation with or without associated syrinx, and without any other underlying pathology, after nonsurgical management have been reported in the literature [2–5]. This further emphasizes the need for a thorough interval history, physical examination, and up-to-date imaging prior to proceeding with Chiari decompression.

Acquired Chiari Malformations

It is not uncommon for the neurosurgeon to see a patient who has radiologic evidence of tonsillar ectopia but whose presenting symptoms are those of raised intracranial pressure (ICP). These patients fall into two subsets. First are patients who present with progressive generalized headaches, visual symptoms, nausea, and perhaps vomiting and who have on imaging either small- or normal-sized ventricles. They may or may not

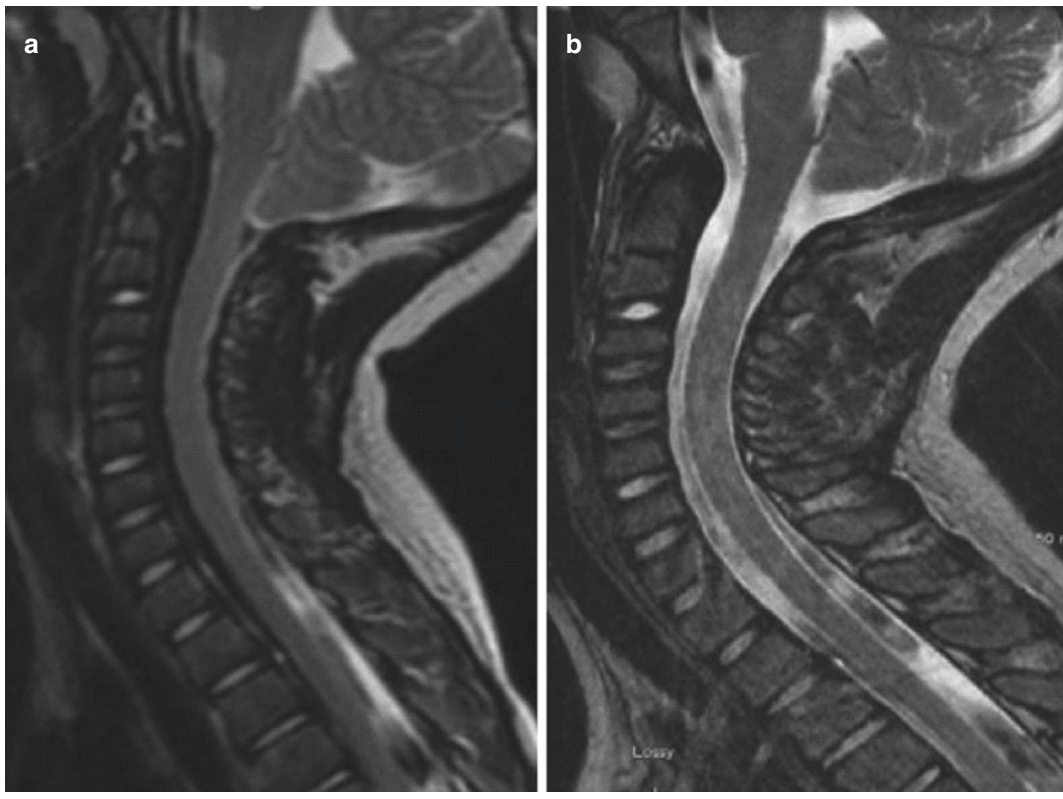

Fig. 43.1 (**a**) This patient's initial magnetic resonance imaging (MRI) showed tonsillar descent of 9 mm with a crowded foramen magnum. (**b**) Subsequent MRI 1 year later showed complete spontaneous resolution of the Chiari malformation

have papilledema, but their symptoms are those of increased intracranial pressure rather than the classic tussive headaches or Chiari symptoms. These patients may have tonsillar ectopia secondary to raised intracranial pressure from pseudotumor cerebri, occult sinus thrombosis, or other causes. In the teenage male, this is often a child who has been started on minocycline for acne, causing a drug-induced pseudotumor. The clinician must recognize that their presenting symptoms are not those of a Chiari patient but instead are those of a patient with raised intracranial pressure. If the clinical suspicion is raised but cannot be confirmed by eye exam, then intracranial pressure monitoring may be necessary. To perform a posterior fossa decompression on such a patient without first addressing the cause of the increased intracranial pressure may lead to further tonsillar descent, brainstem herniation, or neurological deterioration. In papers published looking at patients who present with radiologic evidence of Chiari and have a decompression but continue to be symptomatic, 41% who failed decompression had pseudotumor. This was diagnosed by cine MRI establishing flow and then confirmed by high-flow lumbar puncture with resolution of symptoms [6]. One study, examining the prevalence of Chiari I malformation in patients with pseudotumor cerebri, showed that out of 68 patients with pseudotumor, 7 had MRI evidence of Chiari I; of note, all patients with cerebellar descent in their study were overweight females [7].

The second group of patients is those who again have clinical symptoms of raised intracranial pressure but who have on imaging tonsillar ectopia associated with increased ventricular size. Until proven otherwise, these patients have hydrocephalus causing their cerebellar tonsils to be pushed through the foramen magnum by chronically raised ICP.

Hydrocephalus associated with Chiari malformation has been debated for a long time with regard to pathogenesis. Some authors suggest that hydrocephalus may be associated with 7–10% of patients with Chiari I malformation [8]. In such cases it has been theorized that supratentorial hypertension causes downward pressure on the cerebellum creating a radiologic "Chiari picture" [9]. Though rare, performing a suboccipital craniectomy and duraplasty on such patients may lead to both tonsillar and brainstem descent and has been associated with acute neurological decompensation. Thus, if one feels compelled to perform a suboccipital decompression in patients with ventriculomegaly, consideration should be given to first controlling the intracranial pressure through placement of a ventriculostomy.

Similarly, clinicians will also be asked to treat Chiari II patients shunted early in life and who present with suboccipital headaches, brainstem symptoms, or a progressive syrinx absent of any change in ventricular size. These patients are likely to have a subtle shunt malfunction. Shunt malfunction should be the primary diagnosis in any spina bifida child who presents with neck pain, new onset of bulbar symptoms, or a new cervicothoracic syrinx [10]. In such cases, shunt exploration is warranted before considering suboccipital decompression.

Ventral Compression, Atlas Assimilation, and Atlantoaxial Instability

Another complication that can be avoided with careful preoperative inspection is the patient presenting with a Chiari malformation associated with ventral compressive pathology. Patients with basilar invagination, os odontoideum, a rheumatoid pannus at C1, or atlantoaxial assimilation are at risk to decompensate with dorsal decompression alone. In such patients, careful consideration should be given to addressing their ventral pathology first. Patients with symptomatic anterior compression causing brainstem dysfunction, myelopathy, lower cranial nerve palsies, or quadriparesis often experience no relief with a posterior decompression even with radiologic evidence of Chiari malformation. It is important that these pathologies be recognized preoperatively. In some instances, these patients may improve with traction to reduce the ventral pathology. If not, one must consider ventral

decompression before undertaking a suboccipital decompression. These patients will virtually all require occipitocervical stabilization and fusion for long-term stability.

The final preoperative pathology which we will discuss that can be associated with hindbrain herniation is assimilation of the atlas. Atlas assimilation is caused by failed segmentation of the fourth occipital sclerotome and the first spinal sclerotome, usually occurring in conjunction with other abnormalities, specifically Klippel-Feil syndrome. This pathology leads to basilar invagination secondarily. In one large series of 5300 patients evaluated for cranio-vertebral junction abnormalities, 550 patients (over 10%) had atlas assimilation. Of these, hindbrain herniation occurred in 38% due to diminished posterior fossa volume [11]. This pathology can be compounded with segmentation failures of the second and third cervical vertebrae [12]. If this occurs along with atlas assimilation, it leads to atlantoaxial instability due to abnormal load on this motion segment [13]. This motion segment then leads to a pannus or basilar invagination, which may be reducible with traction up to about 14 or 15 years of age. In older patients, the lesion becomes an irreducible basilar invagination [14]. Hence, an operation just focusing on posterior decompression without addressing the potential for instability can lead to unfortunate results.

Goel recently reported a series of 65 patients with Chiari malformation, 97% of whom improved following posterior atlantoaxial fusion without decompression of the foramen magnum [15]. He postulates atlantoaxial instability as the primary driver of the development of Chiari malformation with or without basilar invagination and syringomyelia, all of which are theorized to be on the same pathologic continuum. According to his theory, tonsillar herniation is a protective mechanism that serves as "nature's airbag" by cushioning neural structures in the setting of atlantoaxial instability; additionally, syringomyelia is a protective response that neutralizes cranial and spinal pressure [16, 17]. However, this theory remains quite controversial, and his patient's demographic likely represents a selected, complex population that is not typical of the standard Chiari patient [18]. Standard-of-care treatment for the majority of patients with a Chiari malformation remains foramen magnum decompression.

Complications of Surgery

Pseudomeningocele

This section addresses the common complications associated with suboccipital decompression, the most common of which is pseudomeningocele. Pseudomeningocele is defined as an abnormal collection of cerebrospinal fluid (CSF) that communicates with the CSF space around the brain or spinal cord (Fig. 43.2). It is the most common complication of Chiari surgery with some papers reporting an incidence as high as 30%. These complications have been attributed to different types of dural patch grafts—both allograft and autograft. Absent the patient with raised intracranial pressure, pseudomeningocele most commonly occurs when a patient vomits, cries, strains, or lifts a heavy object in the postoperative period, thus tearing a suture loose in their dural repair. It is not uncommon, at re-exploration, to find a sin-

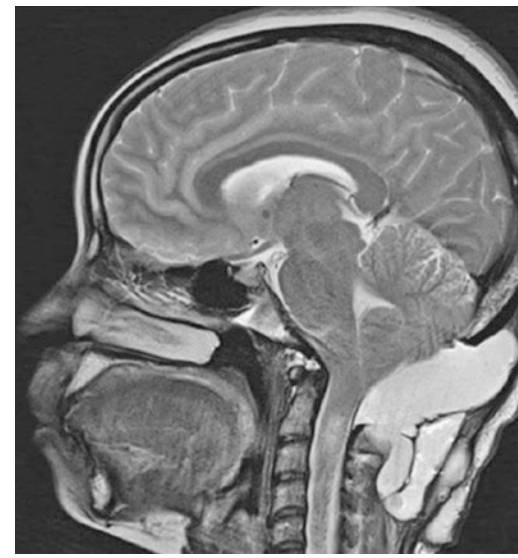

Fig. 43.2 T2-weighted sagittal magnetic resonance image (MRI) showing a postoperative pseudomeningocele

gle small hole in the closure that is responsible for the whole pseudomeningocele [1]. In discussing pseudomeningocele, it is important to recognize that at some centers with large series and good results, the advocated surgical technique is to perform a bony decompression, leave the dura open, and close the paracervical muscles and skin with the intent of creating a pseudomeningocele [19]. Thus, the presence of a small asymptomatic pseudomeningocele should be little cause for concern. Concern arises when a small defect in a dural closure allows CSF to progressively accumulate in the epidural space or to leak through the wound. A progressively expanding mass, which threatens the skin or causes the patient pain, will require additional treatment. Having said that, whenever a large pseudomeningocele occurs in the early postoperative period, it should raise the suspicion of a CSF absorption problem such as pseudotumor cerebri or occult hydrocephalus. In patients with a preexisting ventriculoperitoneal shunt, a pseudomeningocele should suggest the need to rule out a shunt malfunction.

As mentioned, the most common finding at re-exploration is that of a small dural defect where a dural suture has pulled loose either from head movement or from Valsalva, such as crying or vomiting in the acute postoperative period. Although meticulous closure of the dura and muscular layers is essential, requesting that anesthesia extubates the patient a bit deeply and then bags them with a facemask to prevent bucking on the endotracheal tube may reduce the incidence of this complication. In the early postoperative period, scheduled antiemetics can also reduce the risk of retching and disruption of the dural suture line.

As mentioned previously, the presence of a small asymptomatic pseudomeningocele should not be cause for alarm. Parents benefit from knowing this prior to surgery so that they are not surprised by it in the event that they see it postoperatively. Once a pseudomeningocele is deemed concerning, there are several treatment options to be considered.

Re-exploration of the wound for an early acute pseudomeningocele allows the surgeon the most immediate repair of a dural defect. In younger children, this may be the most expeditious means of curing the problem and getting the child home. Since the surgical risks are small, these authors prefer wound re-exploration as the most direct way of dealing with a symptomatic pseudomeningocele in the early postoperative course. Another method of dealing with a pseudomeningocele is by the placement of a lumbar drain. To do so, one must be confident that a good decompression was accomplished at surgery and that CSF flow is restored. Only then is it safe to place a lumbar drain. This allows diversion of CSF flow, which, in return, will hopefully allow the dural closure time to heal. Once the lumbar drain is placed, it is typically left in place from 3 to 7 days. By doing so, the surgeon hopes to avoid another operation. Lumbar drains may not be tolerated well in young infants and children and may be technically difficult to place in patients with concomitant tethered spinal cords or other lumbar pathologies. This treatment requires prolonged hospitalization but is an option for patients with comorbidities that may make return to surgery less appealing.

Some surgeons may elect to percutaneously tap a fluid collection at the bedside. This may differentiate a CSF collection from a wound infection or seroma but is not a treatment for pseudomeningocele. Since this treatment does nothing for the dural defect, it may promote further CSF flow into the epidural space, which may then leak through the needle tract placing the patient at risk for meningitis. Given this, therapeutic tapping of pseudomeningoceles is mentioned only to be condemned. Similarly, there have been case reports of using a blood patch in the epidural space. This is performed by draining the pseudomeningocele and injecting blood mixed with fibrin glue in multiple settings [20].

Meningitis

The second most common complication encountered in Chiari surgery is meningitis. A study by Dubey et al. of 500 patients undergoing posterior fossa surgery reported this complication rate at 9% [19]. Having said this, the incidence of bacterial meningitis following Chiari decompres-

sion is normally quite low. The most common cause of meningeal inflammation is aseptic meningitis or inflammatory meningitis either due to the spillage of blood products into the subarachnoid space or related to an idiosyncratic reaction to a dural allograft. Surgical technique can help decrease this complication. If lysis of arachnoidal adhesions is not planned during the operation, carefully opening the dura and leaving the arachnoid intact decrease the chance of blood spillage into the subarachnoid space. Another surgical technique is placing a temporary Gelfoam patty at the inferior aspect of the opening, stopping any blood products from contaminating the spinal subarachnoid space.

Aseptic meningitis is usually diagnosed subacutely, within 3 weeks of surgery. The diagnosis is made by lumbar puncture with the expected findings of mononuclear pleocytosis, elevated protein, and a negative Gram stain and culture. This complication may either be treated with corticosteroids or by serial lumbar punctures until the symptoms improve.

Bacterial meningitis, though less common, is a more serious complication. Although *Staphylococcus* species are most common, one must rely upon cultures to direct appropriate therapy. In some instances, early return to surgery for removal of an infected dural patch graft may be prudent.

Cerebellar Slump, Sag, or Ptosis

Cerebellar ptosis is a rare iatrogenic complication caused by an excessively large suboccipital craniectomy. Over time, CSF pulsations and gravity may pull the cerebellum through the defect created during the craniectomy, causing cerebellar herniation. Once decompressed the posterior fossa now has a new interface between the brainstem and cerebellar tonsils. As adhesions form between the cerebellum and dura, the CSF outflow, which was once reestablished after surgery, may gradually become obstructed leading to recurrence of a syrinx or preoperative symptoms [21]. Avoidance of an overaggressive craniectomy can help to reduce this complication. A craniectomy of 3 × 3 cm is generally adequate for most straightforward Chiari I patients.

Although the timing of cerebellar sag has been seen within the same calendar year as surgery, it may present much later. This complication most commonly manifests as the insidious return of Chiari symptoms, headache being the most common. Although different in nature than the classic tussive headaches, these have been described as intractable with radiation to the jaw and orbit. Because of the acquired CSF outflow obstruction, patients may develop syringomyelia. Once symptomatic ptosis occurs, surgical correction is generally required. If a patient returns with symptoms related to syringomyelia, one treatment option is a syrinx shunt. A more physiological correction is a suboccipital cranioplasty with dural exploration, allowing visualization and decompression of the cerebellum and dura [22] (see Fig. 43.3).

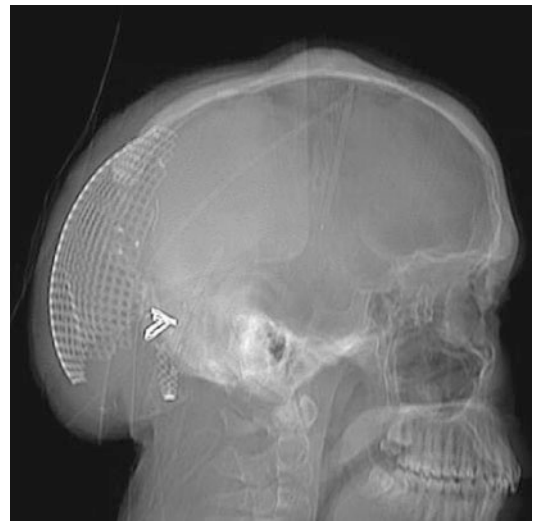

Fig. 43.3 This lateral skull X-ray was taken in a patient who presented after a large occipital decompression at another institution. His presentation was unilateral vocal cord paralysis secondary to syringobulbia secondary to cerebellar sag. Although his vocal cord paralysis was permanent, his syrinx improved with occipital cranioplasty using titanium mesh

Craniocervical Instability/Kyphosis

Another complication is radiologic evidence of craniocervical instability following occipitocervical decompression. In a recently published retrospective review of this complication, the authors reported that five of nine patients (56%) showed evidence of radiologic instability of their cervical spines following surgery for Chiari II malformations. Of the five patients, none developed clinical instability requiring fusion [23]. It should be pointed out that, absent congenitally abnormal anatomy, this complication is generally only seen following laminectomy of C2 and below. It is very uncommon to see instability with just removal of the posterior arch of C1. Thus, in Chiari I children, even though the cerebellar tonsils may extend down to the level of C2, effort should be made to preserve the spinous process and lamina of C2, even if a partial laminectomy of the superior half of C2 is necessary to disimpact the tonsils. Disrupting the facet joints intraoperatively may also lead to a higher probability of instability. Once post-laminectomy deformity develops, it will usually progress until surgical stabilization and fusion corrects the problem.

Bollo et al. defined a subset of "complex Chiari malformation" patients who are at increased risk of developing craniocervical instability following a foramen magnum decompression [24]. Brockmeyer et al. highlighted two radiological features that are highly predictive of progressive craniocervical kyphosis: (1) odontoid retroflexion, defined by a pBC2 distance (the maximum perpendicular distance from the posterior-superior aspect of the odontoid process to the line joining the basion to the posterior-inferior aspect of the C2 vertebral body) >9 mm, and (2) a clival-cervical angle less than 125° [25]. In patients with a pBC2 distance greater than or equal to 9 mm and a clival-axial angle (CXA) less than 125° who have bulbar or myelopathic symptoms, posterior fossa decompression, odontoid reduction, and occipitocervical fusion are recommended as the initial procedures. Those patients who continue to have bulbar or myelopathic symptoms undergo a ventral decompression via an endoscopic endonasal odontoidectomy.

Brainstem Hemorrhage

Although rare, one report detailed two cases of brainstem hemorrhage after suboccipital craniectomy and expansion duraplasty for Chiari decompression. Excessively rapid drainage of cerebrospinal fluid causing intracranial hypotension and stretching of bridging cerebellar veins is an explanation provided by the authors. Care should be taken to have controlled drainage of cerebrospinal fluid when opening the arachnoid to avoid this serious complication. Fortunately, the patients in this series did not suffer any permanent neurologic deficits related to their medullary hemorrhages [26].

Recurrent Syringomyelia

Though not always thought of as a complication, the persistence or recurrence of a syrinx following decompression has been reported in 10–40% of cases [27]. This complication is typically seen months to years following surgery but underscores the need for long-term follow-up of this patient population. One of the arguments favoring intradural exploration for Chiari patients is to confirm that CSF flow has been reestablished and that no arachnoidal webs overlie the fourth ventricular outlet. A delayed postoperative MRI of the cervical spine in patients with syringomyelia will serve as both proof that the syrinx has deflated and to offer a comparison study should future symptoms develop. In most cases, if the syrinx has regressed and symptoms have improved, it is uncommon for the syrinx to return. If the syrinx has not changed in size but the clinical symptoms have improved, it is at this time that assessment of the syrinx and CSF velocity and flow using cine phase-contrast MR imaging may be of benefit. If, by this imaging test, good

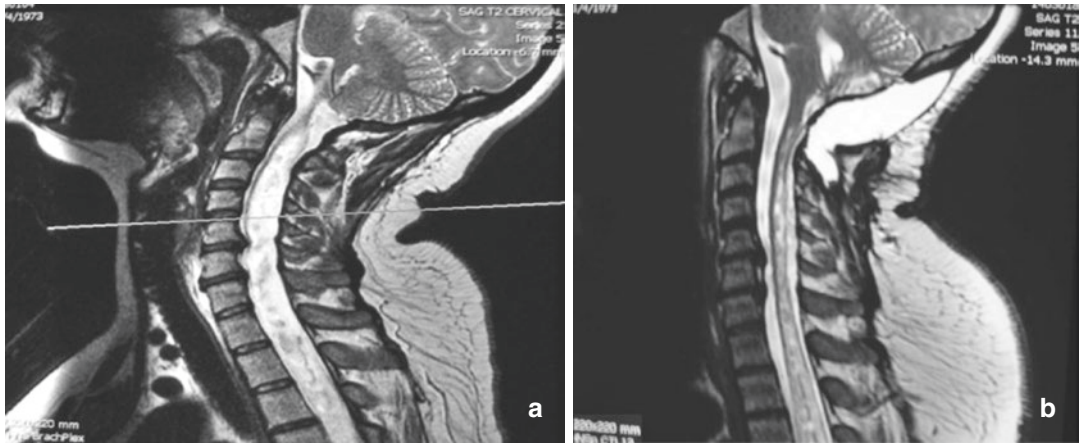

Fig. 43.4 (**a**) This adult female presented with quadriparesis related to a large recurrent syrinx, as noted on her T2-weighted magnetic resonance imaging (MRI). Note her small posterior fossa. Her syrinx had failed prior suboccipital decompression and had been shunted twice before, each time with recurrence. At re-exploration she was found to have a congenital veil of arachnoid over her obex, which had been missed at the initial operation a decade before. (**b**) Postoperative T2-weighted sagittal MRI in this same patient shows resolution of her syrinx and enlargement of her posterior fossa following reoperation. Her quadriparesis significantly improved

CSF flow is observed, then one may follow the patient clinically and radiologically. If the patient's symptoms recur, suboccipital re-exploration should be entertained. The authors treated one patient in whom recurrence of syringomyelia 10 years postoperatively was associated with quadriparesis. At re-exploration, a missed congenital web of arachnoid over the obex was identified. Once resected, the syrinx collapsed and the patient's weakness improved (Fig. 43.4a, b).

The authors also have observed progressive syringomyelia after a bone-only decompression was performed (Fig. 43.5a, b). Although the patient had clinical improvement in his headaches and swallowing function, MRI showed enlargement of his syrinx (Fig. 43.5c). Following intradural exploration, lysis of arachnoid adhesions, and coagulation of the cerebellar tonsils, his syrinx resolved (Fig. 43.5d). Though various reports have demonstrated excellent results with bone-only decompressions, this case demonstrates that techniques without duraplasty may not be universally sufficient, particularly in the presence of syringomyelia [28]. Ongoing randomized clinical trials may help to delineate which patients require duraplasty for durable outcomes [29].

Conclusion

In the current era, the radiologic finding of Chiari I malformation has become very common. Most of these patients and their primary care physicians will not be satisfied until they have had formal neurosurgical evaluation. The majority of these patients either are asymptomatic or have clinical symptoms unrelated to the radiologic picture and will require no intervention. Although neurosurgeons consider suboccipital decompression to be a benign procedure, a careful review of the literature or of one's own series will demonstrate that serious complications can and do occur. It is of paramount importance that the operating surgeon is sure the patient's clinical picture is appropriate before undertaking surgery. Once the operation has been performed, meticulous attention to detail and to postoperative recovery will allow for a healthy patient who is pleased with their surgeon and the results of their surgery.

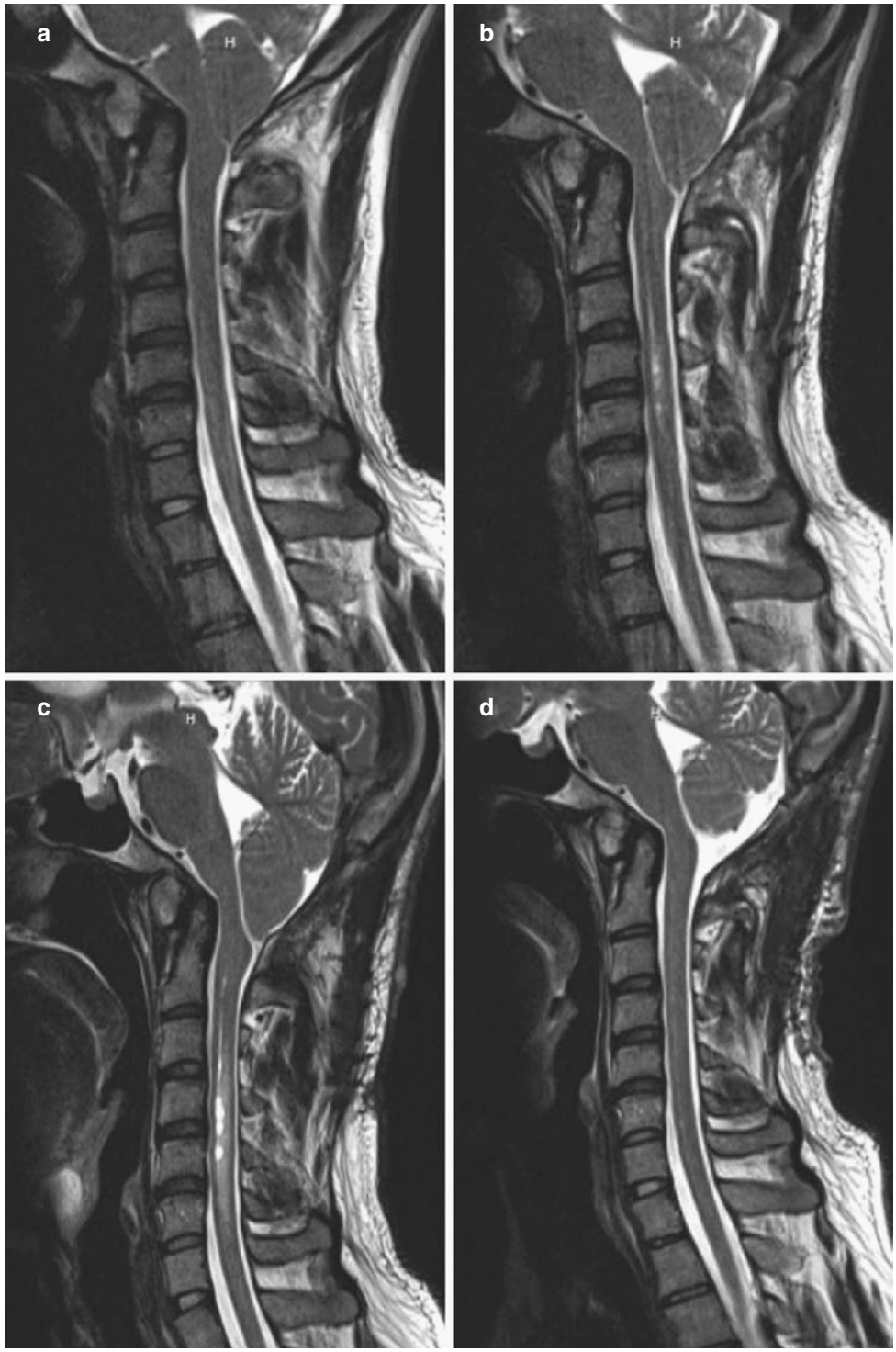

Fig. 43.5 This patient presented with tussive headaches, swallowing dysfunction, and near syncope. His preoperative magnetic resonance imaging (MRI) (**a**) shows a Chiari 1.5 malformation. He was taken for a bone-only decompression with good expansion of the dura at surgery. Though he improved symptomatically, his postoperative MRI showed an early syrinx (**b**). Repeat imaging (**c**) showed progression of his syringomyelia, and he was referred for repeat decompression with intradural exploration, leading to complete resolution of his syrinx (**d**)

References

1. Parker SR, Harris P, Cummings TJ, George T, Fuchs H, Grant G. Complications following decompression of Chiari malformation type I in children: dural graft or sealant? J Neurosurg Pediatr. 2011;8(2):177–83.
2. Ramnarayan R. Spontaneous resolution of Chiari-1-associated syringomyelia: a report of two cases. Pediatr Neurosurg. 2018;53(4):238–42.
3. Briganti F. Spontaneous resolution of Chiari Type 1 malformation, a case report and literature review. Neuroradiol J. 2013;26:304–9.
4. Gaunt T. Spontaneous regression of a Chiari malformation Type 1 in a 58-year-old female. BJR Case Rep. 2016;2:20160016.
5. Williams A. Radiological demonstration of spontaneous resolution of type 1 Chiari malformation in a 17-year-old patient. Br J Neurosurg. 2011;25(6):764–5.
6. Fagan LH, Ferguson S, Yassari R, Frim DM. The Chiari pseudotumor cerebri syndrome: symptom recurrence after decompressive surgery for Chiari malformation type I. Pediatr Neurosurg. 2006;42(1):14–9.
7. Banik R, Lin D, Miller NR. Prevalence of Chiari I malformation and cerebellar ectopia in patients with pseudotumor cerebri. J Neurol Sci. 2006;247(1):71–5.
8. Massimi L, Pravata E, Tamburrini G, Gaudino S, Pettorini B, Novegno F, et al. Endoscopic third ventriculostomy for the management of Chiari I and related hydrocephalus: outcome and pathogenetic implications. Neurosurgery. 2011;68(4):950–6.
9. Di Rocco C, Frassanito P, Massimi L, Peraio S. Hydrocephalus and Chiari type I malformation. Childs Nerv Syst. 2011;27(10):1653–64.
10. Marlin AE. Management of hydrocephalus in the patient with myelomeningocele: an argument against third ventriculostomy. Neurosurg Focus. 2004;16(2):1–3.
11. Menezes AH. Craniocervical developmental anatomy and its implications. Childs Nerv Syst. 2008;24(10):1109–22.
12. Komatsu Y, Shibata T, Yasuda S, Ono Y, Nose T. Atlas hypoplasia as a cause of high cervical myelopathy. Case report. J Neurosurg. 1993;79(6):917–9.
13. Gholve PA, Hosalkar HS, Ricchetti ET, Pollock AN, Dormans JP, Drummond DS. Occipitalization of the atlas in children. Morphologic classification, associations, and clinical relevance. J Bone Joint Surg Am. 2007;89(3):571–8.
14. Menezes AH. Primary craniovertebral anomalies and the hindbrain herniation syndrome (Chiari I): data base analysis. Pediatr Neurosurg. 1995;23(5):260–9.
15. Goel A. Is atlantoaxial instability the cause of Chiari malformation? Outcome analysis of 65 patients treated by atlantoaxial fixation. J Neurosurg Spine. 2015;22:116–27.
16. Goel A. Is Chiari malformation nature's protective "air-bag"? Is its presence diagnostic of atlantoaxial instability? J Craniovertebr Junction Spine. 2014;5:107–9.
17. Goel A. Is syringomyelia pathology or a natural protective phenomenon? J Postgrad Med. 2001;47:87–8.
18. Brockmeyer DL, Oakes WJ, Rozzelle C, Johnston J, Rocque BG, Anderson RC, et al. Chiari malformation Type 1 and atlantoaxial instability: a letter from the Pediatric Craniocervical Society. J Neurosurg Spine. 2015;23(6):820–1.
19. Dubey A, Sung WS, Shaya M, Patwardhan R, Willis B, Smith D, et al. Complications of posterior cranial fossa surgery – an institutional experience of 500 patients. Surg Neurol. 2009;72(4):369–75.
20. Paternoster G, Massimi L, Capone G, Tamburrini G, Caldarelli M, Di Rocco C. Subcutaneous blood patch for iatrogenic suboccipital pseudomeningocele following decompressive suboccipital craniectomy and enlarging duroplasty for the treatment of Chiari I malformation. Technical note. Childs Nerv Syst. 2012;28(2):287–90.
21. Di X, Luciano MG, Benzel EC. Acute respiratory arrest following partial suboccipital cranioplasty for cerebellar ptosis from Chiari malformation decompression. Neurosurg Focus. 2008;25(6):E12.
22. Holly LT, Batzdorf U. Management of cerebellar ptosis following craniovertebral decompression for Chiari I malformation. J Neurosurg. 2001;94(1):21–6.
23. Lam FC, Irwin BJ, Poskitt KJ, Steinbok P. Cervical spine instability following cervical laminectomies for Chiari II malformation: a retrospective cohort study. Childs Nerv Syst. 2009;25(1):71–6.
24. Bollo RJ, Riva-Cambrin J, Brockmeyer MM, Brockmeyer DL. Complex Chiari malformations in children: an analysis of preoperative risk factors for occipitocervical fusion. J Neurosurg Pediatr. 2012;10:134–41.
25. Brockmeyer DL, Spader HS. Complex Chiari malformations in children: diagnosis and management. Neurosurg Clin N Am. 2015;26:555–60.
26. Polster SP. A report of 2 cases of brainstem hemorrhage after suboccipital craniectomy for Chiari decompression. Oper Neurosurg. 2018;14(5):E58–62.
27. Heiss JD, Suffredini G, Smith R, DeVroom HL, Patronas NJ, Butman JA, et al. Pathophysiology of persistent syringomyelia after decompressive craniocervical surgery. Clinical article. J Neurosurg Spine. 2010;13(6):729–42.
28. Kennedy BC. Outcomes after suboccipital decompression without dural opening in children with Chiari malformation Type I. J Neurosurg Pediatr. 2015;16:150–8.
29. ClinicalTrials.gov. Posterior fossa decompression with or without duraplasty for Chiari Type I malformation with syringomyelia. Trial ID NCT02669836. https://clinicaltrials.gov/ct2/show/NCT02669836

Secondary Interventions for Chiari I Malformation

44

Jörg Klekamp

Introduction

Foramen magnum decompression is widely recognized as the procedure of choice for treatment of patients with Chiari I malformation (CM I), with short-term success rates well above 80% reported in numerous reports in the literature. On the other hand, few publications deal specifically with treatment concepts for patients who develop new neurological problems early after such a decompression or in the long term. Furthermore, there still exists considerable disagreement as to how a foramen magnum decompression should be performed: Is it necessary to open both layers of the dura? Should the arachnoid be opened and dissected? How should we deal with the cerebellar tonsils? Should a duraplasty be performed and if yes, what kind of material should be used for grafting? An analysis of patients with failed decompressions may provide some answers to these questions. On the other hand, a neurological deterioration may not always be related to an insufficient decompression or an unrecognized craniospinal instability but caused by another pathology such as a degenerative problem of the cervical spine [1].

J. Klekamp (✉)
Department of Neurosurgery, Christliches Krankenhaus Quakenbrück, Quakenbrück, Lower Saxony, Germany
e-mail: j.klekamp@ckq-gmbh.de

Diagnosis and Decision-Making

Among a series of 856 patients presenting with CM I, 158 patients had already undergone a foramen magnum decompression. Of these, 36 had an additional syrinx shunt implanted. Ninety-two of these 158 patients were not operated: In 64 patients a revision was not recommended because the neurological status was stable or considered unlikely to be stabilized by another intervention, while 28 refused another operation. The majority of patients, in whom a revision was not recommended, presented because they were disappointed by the result of their decompression. Burning-type dysesthesias were the commonest complaint of these patients. Despite postoperative improvements of other symptoms and a reduction of syrinx size, this type of neuropathic pain may persist and turn out to be notoriously difficult to treat. It is important to inform a patient before surgery that burning-type dysesthesias may not respond to an otherwise successful decompression. Bernard Williams even observed postoperative aggravations in a few patients despite regression of a syrinx (personal communication). However, this was not observed in this series. No surgery at the foramen magnum was recommended for most patients with a history of bacterial meningitis or after multiple procedures at the foramen magnum, considering the increased risks of another intervention and the

R. S. Tubbs et al. (eds.), *The Chiari Malformations*, https://doi.org/10.1007/978-3-030-44862-2_44

reduced chances for success under such circumstances.

Sixty-six patients underwent a total of 73 surgical procedures. The decision was based on a detailed clinical and neuroradiological analysis. Once hydrocephalus was ruled out, the evaluation started with the clinical history before the previous decompression and how preoperative symptoms responded to it. Was the neurology unchanged or improved, or did symptoms progress further without a free interval of stable neurology? If symptoms progressed immediately, such a course suggested an insufficient decompression. In most instances, this was related to persistent cerebrospinal fluid (CSF) flow obstruction at the foramen magnum or untreated features such as an associated basilar invagination with craniocervical instability.

In the majority of patients, however, the clinical history revealed a free interval of an improved or unchanged neurological condition before new symptoms of medullary compression developed. The only clinical symptoms, which clearly pointed to a new foramen magnum problem, were occipital headaches and swallowing dysfunctions. If these did not progress or reappeared, the clinical history often provided no clue whether a foramen magnum-related cause or another pathology was responsible for the clinical deterioration. As a general rule, the longer the free interval, the less likely this cause was related to the foramen magnum.

Next, a careful neuroradiological assessment was essential for these patients. The area of the previous operation was evaluated comparing preoperative and postoperative magnetic resonance imaging (MRI) scans. Was there any evidence for an insufficient decompression or recurrent compression? It has been reported that new bone formation may cause recurrent compression, particularly in children [2–4]. However, this was not observed in this series. No example of cerebellar ptosis [5] due to an oversized craniectomy [6] resulting in medullary compression was found either.

Was there a basilar invagination with persistent anterior compression of the odontoid? Was there an indication of craniocervical instability such as an assimilated atlas to the occiput, a Klippel-Feil syndrome of the upper cervical spine, or pannus formation around the odontoid (Fig. 44.1) [7]? Was there a cisterna magna of sufficient size (Figs. 44.1, 44.2, and 44.3)? Was there a pseudomeningocele pushing the dura anteriorly (Figs. 44.1, 44.2, and 44.3) [8]?

Another important aspect was the postoperative course of a syrinx. If the syrinx decreased after surgery and remained so, it was unlikely that new symptoms were related to the foramen magnum with one exception: Craniocervical instability still had to be ruled out.

If all these points were excluded by conventional MRI scans, a cardiac-gated cine MRI was performed to evaluate the CSF passage at the foramen magnum. This modality is the most sensitive method to detect or exclude arachnoid scarring and adhesions that may have reformed or may not have been addressed sufficiently during the previous decompression [9–12]. If such a study demonstrated CSF flow at the foramen magnum and the neuroradiological evaluation had excluded all the other possibilities mentioned above, then the clinical deterioration had to be caused by a process unrelated to the previous decompression.

Fig. 44.1 (**a**) This sagittal T2-weighted magnetic resonance image (MRI) was performed 8 years after decompression of the foramen magnum in another institution in a 46-year-old patient with Chiari I malformation, basilar invagination, and syringomyelia. The syrinx appears of small caliber; a small pseudomeningocele is apparent. C1 is assimilated to the occiput and C2/C3 is fused, i.e., Klippel-Feil syndrome. The patient complained about severe neck pain, dysesthesias, and a slight gait ataxia. (**b**, **c**) The cine MRI shows no flow signals in the foramen magnum region. (**d**, **e**) Functional X-rays of the cervical spine demonstrate the laminectomy of C2 and C3 and instability at C3/C4. Revision surgery incorporated a revision at the foramen magnum with arachnoid dissection and a new duraplasty followed by occipitocervical fusion C0–C5 with lateral mass screws. (**f**) The postoperative MRI demonstrates a large cisterna magna. (**g**) The control X-ray 7 years later shows the correct positions of all implants with a good sagittal profile. Postoperatively, the patient has remained neurologically stable for 7 years with some improvement of her neck pain

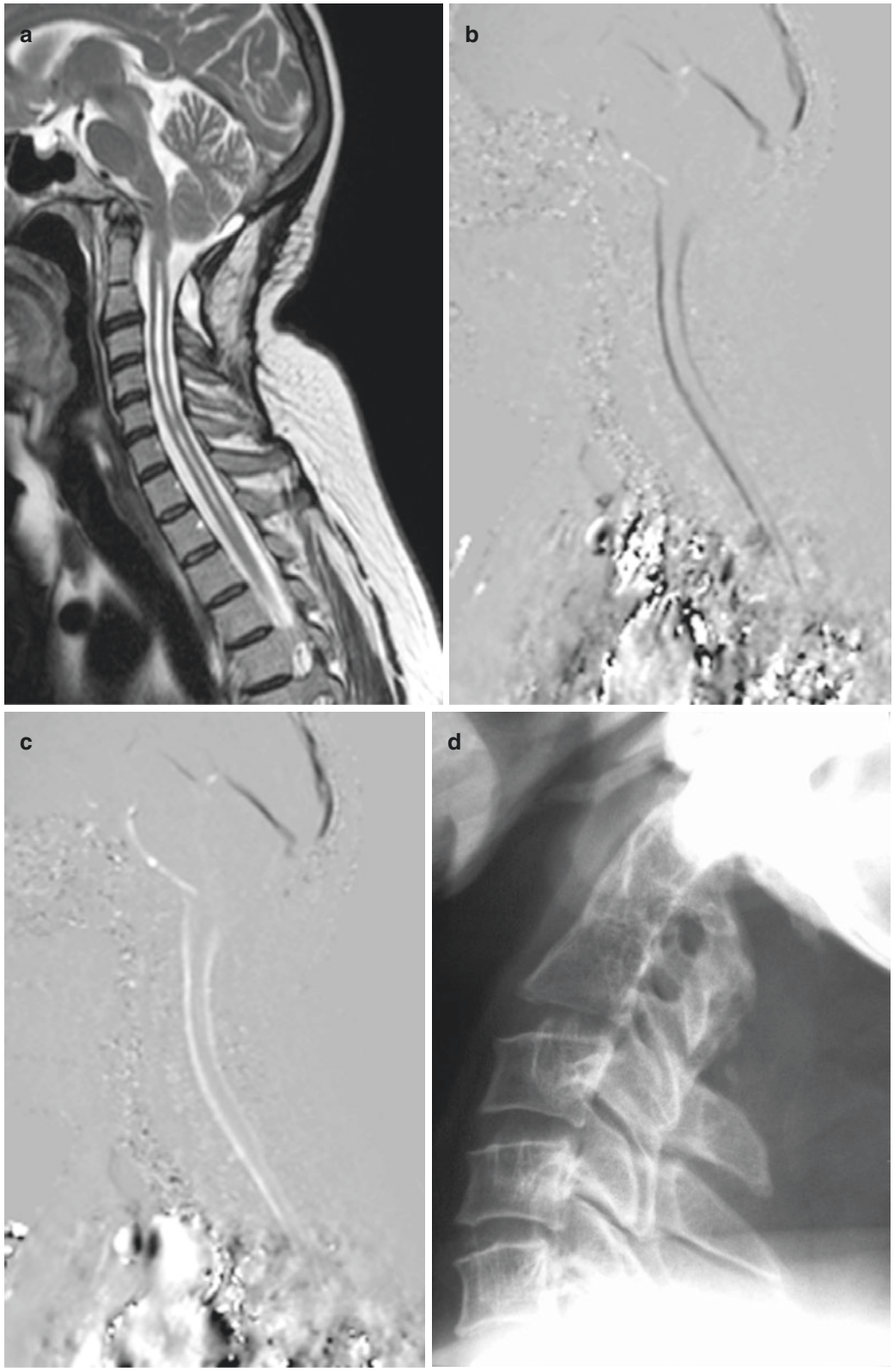
a
b
c
d

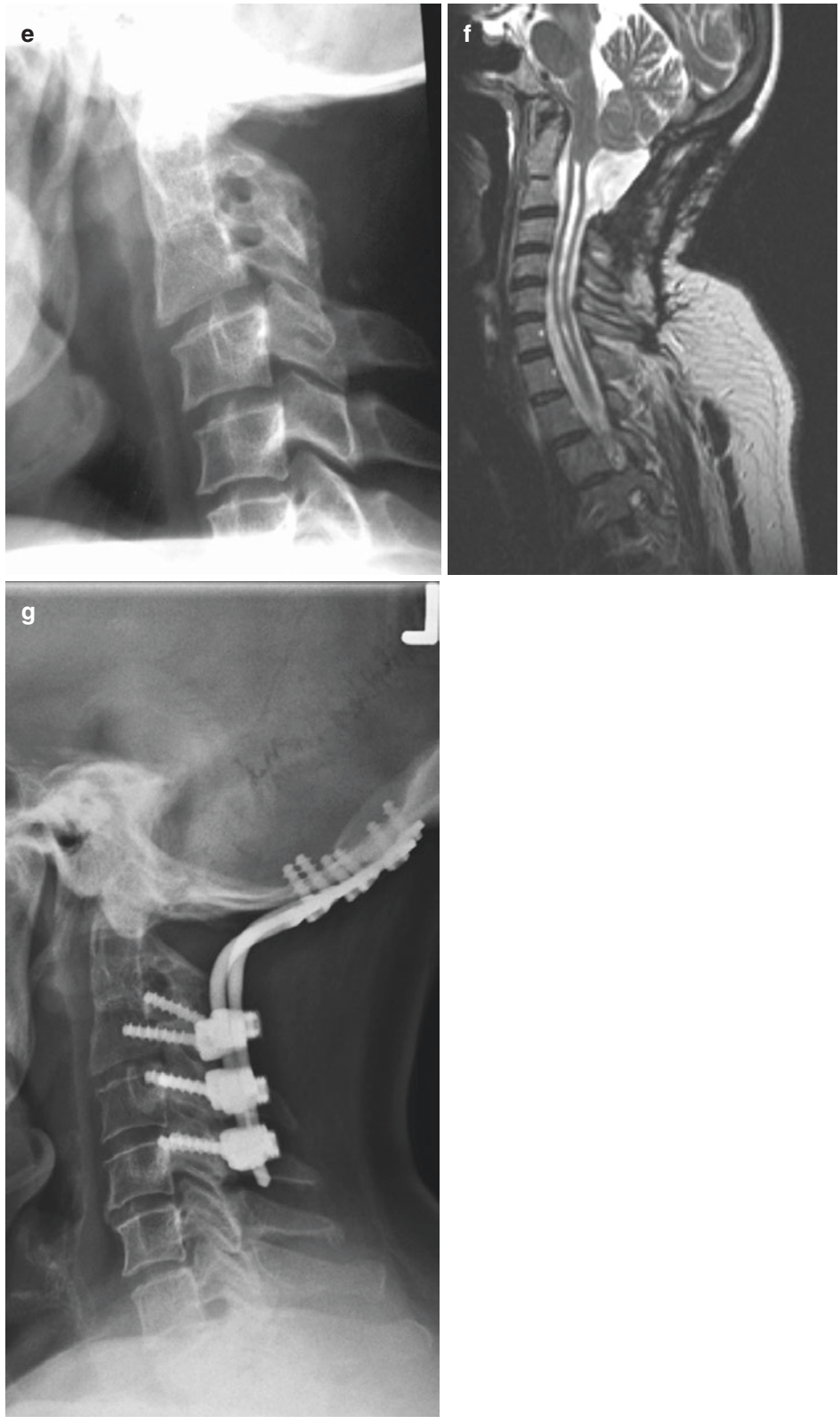

Fig. 44.1 (continued)

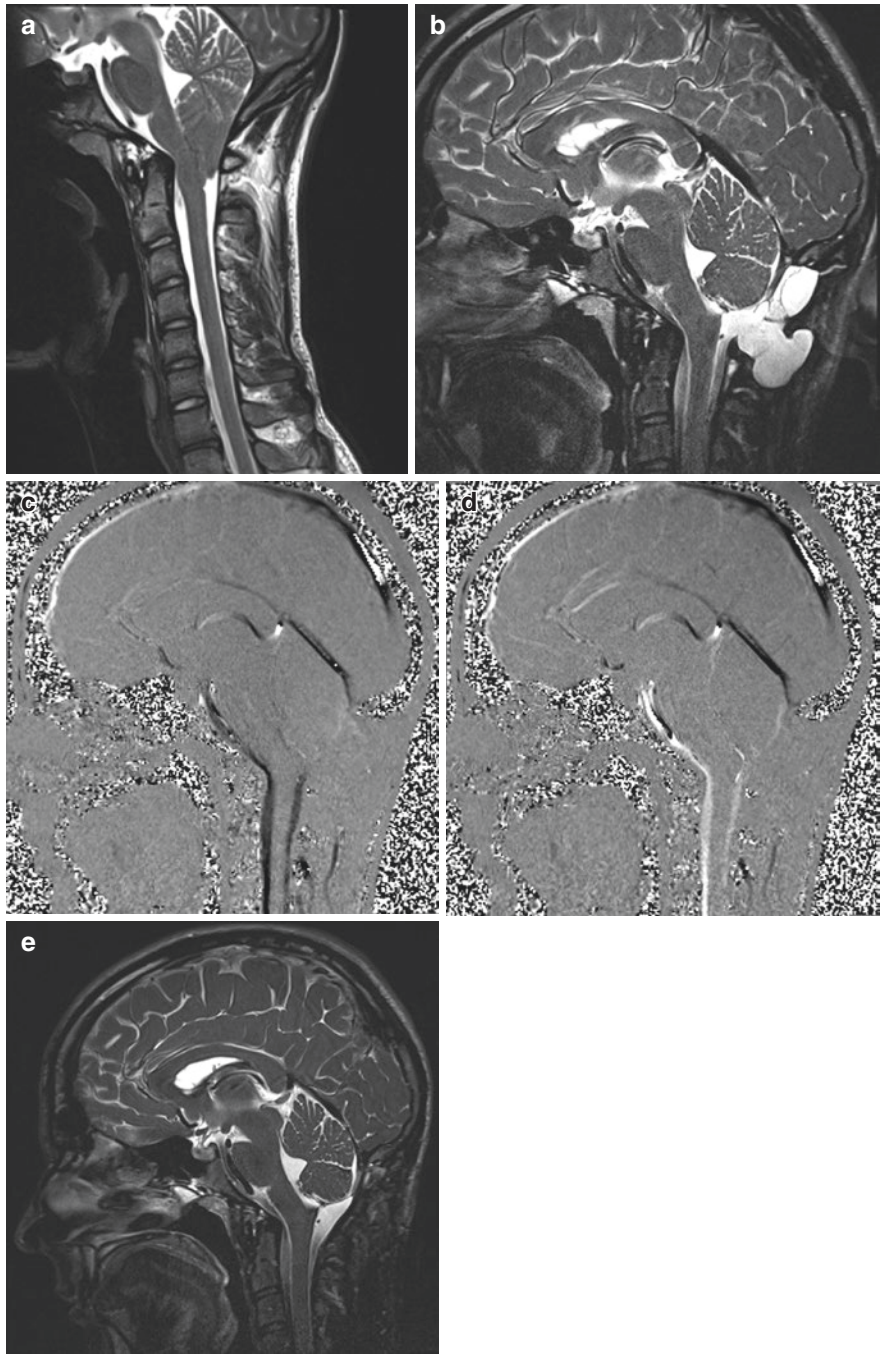

Fig. 44.2 (**a**) This sagittal T2-weighted magnetic resonance image (MRI) shows a classical Chiari I malformation without syringomyelia in a 15-year-old boy with occipital headaches. (**b**) After decompression of the foramen magnum with resection of both tonsils in another institution, the postoperative scan demonstrates a large pseudomeningocele. There appears to be a membrane obstructing the foramen of Magendie. (**c**, **d**) The cine MRI shows no flow signals in the area of the foramen magnum. The patient no longer complained about occipital headaches but reported quite severe local discomfort. At reoperation 2 years later, a large defect in the suture line for the duraplasty was evident. After removal of the duraplasty, profound scarring at both tonsillar stumps was detected. Both posterior inferior cerebellar arteries were embedded in this scar tissue, which also obstructed the foramen of Magendie. The foramen was not opened to avoid any vascular injuries, and a new duraplasty was inserted. (**e**) The postoperative scan shows a free cerebrospinal fluid (CSF) passage across the foramen magnum with normal soft tissue healing. The patient made a full recovery

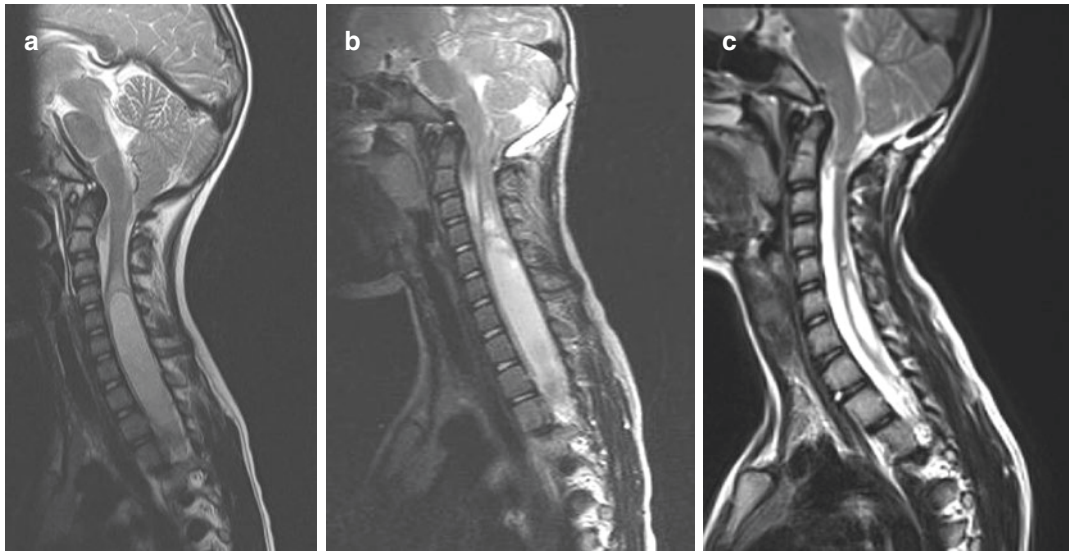

Fig. 44.3 (**a**) This sagittal T2-weighted magnetic resonance image (MRI) shows a Chiari I malformation with a substantial syrinx and scoliosis in a 5-year-old girl. (**b**) After decompression, a pseudomeningocele had formed pushing the duraplasty anteriorly obstructing cerebrospinal fluid (CSF) flow. Consequently, the syrinx did not resolve. Seven years after the first operation, the scoliosis deteriorated, and the decision was made to revise the foramen magnum. (**c**) After this revision, which included arachnoid dissection and insertion of a new duraplasty, the CSF pathway is free and the syrinx has started to decrease. There has been no further progress of her scoliosis

In patients with syrinx shunts, the shunt catheter could lead to a tethering of the nerve roots or spinal cord [13] leading to radicular or myelopathic symptoms, which were often provoked by neck or arm movements. The MRIs in these patients showed adherence of the cord to the dura at the level of the shunt.

If that had been excluded as well, degenerative changes of the cervical spine were evaluated next (Fig. 44.4). Many patients with a well-treated Chiari malformation and a collapsed syrinx demonstrated a considerable amount of spinal cord atrophy as the result of the long-standing syringomyelia. Therefore, MRI scans often gave the impression that a slight or moderate degree of cervical stenosis may not be clinically relevant. However, this is a very dangerous assumption. Such patients have very little functional reserve in their spinal cord as a consequence of their former syringomyelia. Any additional affection—even a minor one—may be enough to cause significant new deficits. It has even been suggested that Chiari patients may be particularly prone to degenerative problems of the cervical spine [14]. Signs of hypermobility of cervical segments should be looked for in particular by X-rays in ante- and retroflexion [1, 15].

Management

Table 44.1 gives an overview on symptoms at presentation for unoperated patients and patients operated again at the foramen magnum or elsewhere in the spinal canal. The percentage of patients suffering from neuropathic or occipital pain was similar in all three groups. For the remaining symptoms, unoperated patients were less severely affected compared to the surgical groups. Patients undergoing a foramen magnum revision presented occipital pain and swallowing problems more commonly, whereas sensory disturbances were more common in patients undergoing surgery for cervical disc diseases. Otherwise, the neurological courses of patients with either a new foramen magnum

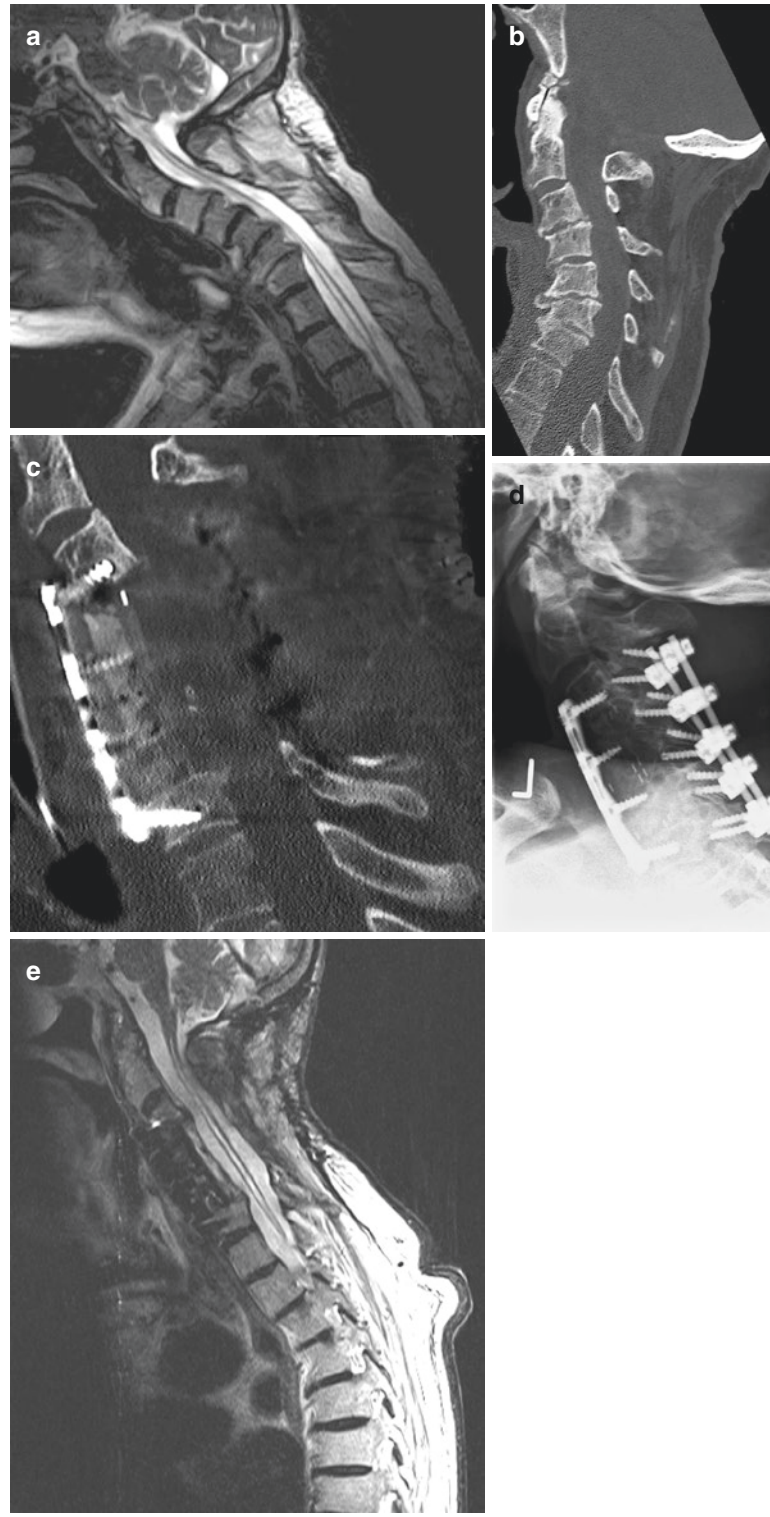

Fig. 44.4 (**a**) This sagittal T2-weighted, upright magnetic resonance image (MRI) was taken 9 years after decompression of the foramen magnum in inclined position and demonstrates profound spinal cord atrophy, a collapsed syrinx, a free cerebrospinal fluid (CSF) passage at the foramen magnum, and multilevel osteochondrosis in his cervical spine with a kyphotic deformity in a patient now 74 years of age. He suffered a progressive tetraparesis confining him to a wheelchair with increasing weakness of his respiratory muscles and loss of upper extremity functions. (**b**) The sagittal computed tomography (CT) reconstruction shows the multiple osteochondroses and the swan neck deformity. The patient underwent a combined decompression with corpectomies C4–C6, reconstruction and ventral fusion C3–C7, followed by posterior decompression C3–C6, and fixation with lateral mass screws C3–C7. The postoperative CT reconstruction (**c**), lateral X-ray (**d**), and the MRI 4 years later (**e**) demonstrate an improved sagittal profile with decompression of the cervical cord. Postoperatively he made a slow recovery. Four months after surgery, he was able to walk for about 20 m with improved respiratory functions, power, and coordination skills in his hands

Table 44.1 Clinical symptoms for patients presenting after foramen magnum decompression

Group	Occ. pain	Neurop. pain	Hypesthesia	Gait	Motor power	Sphincter function	Swallowing function
No surgery	79%	36%	57%	60%	43%	14%	14%
FM group	87%	42%	74%	83%	64%	21%	34%
Spinal group	73%	33%	87%	80%	67%	27%	7%
Total	81%	38%	67%	70%	53%	18%	20%

Abbreviations: *Occ*. occipital, *Neurop*. neuropathic, *FM* foramen magnum

problem or a cervical myelopathy were indistinguishable.

Patients undergoing a foramen magnum revision rather than surgery for cervical disc disease were significantly younger (40 ± 16 years vs. 51 ± 15 years; t-test, $p = 0.03$), with trends for a shorter interval between previous decompression and onset of new symptoms (31 ± 39 months vs. 100 ± 161 months; t-test, $p = 0.12$) and a longer history before the secondary operation (48 ± 89 months vs. 32 ± 65 months; t-test, $p = 0.5$). Eight patients underwent multiple operations: Two patients each underwent foramen magnum revisions followed by removal of syrinx catheters or foramen magnum revisions followed by decompressions for cervical disc diseases or two surgeries on the cervical spine or two foramen magnum revisions in separate operations, respectively.

Secondary Surgeries in the Cervical Spine

In 18 patients, a mechanism independent from the foramen magnum region had caused new neurological symptoms (Table 44.2 and Fig. 44.4). In all these patients, the Chiari malformation had been adequately treated with collapse of the syrinx and a free CSF passage at the foramen magnum. They underwent a total of 20 operations. One patient required a ventriculoperitoneal shunt for hydrocephalus. Four syrinx shunt catheters were removed to release a postoperative tethering of either the nerve roots or spinal cord. In each of these patients, pain and dysesthesias were provoked with certain body movements. The tethering had not caused reappearance of the syrinx in any of them.

For removal of a syrinx catheter, the sharp microsurgical dissection concentrated on untethering the nerve roots and spinal cord first. Once this was achieved, the catheter could be removed in most instances. If it was stuck in the cord, it was transected right at the entry point into the spinal cord. Three of these four patients reported improvement after syrinx catheter removal.

For patients with degenerative disc disease, it was the general policy to restrict one- or two-level ventral fusions to patients with radicular symptoms, whereas multilevel posterior decompressions and fusions were preferred for patients with a progressive myelopathy. This strategy was based on observations that patients with a progressive cervical myelopathy almost always displayed a profound spinal cord atrophy due to the former syringomyelia and often demonstrated multilevel hypermobilities of the cervical spine. The intention was to prevent future deteriorations from adjacent levels in patients with a significantly reduced functional reserve (Fig. 44.4).

Nine patients underwent ten ventral fusions for single- or two-level disc disease of the cervical spine. One of these underwent an additional posterior cervical decompression and fusion 10 years later when she developed a progressive myelopathy. One patient underwent a combined anterior and posterior decompression and fusion for a swan neck deformity (Fig. 44.4). Finally, three patients received a posterior decompression and fusion only. Posterior decompressions consisted of laminectomies C3 to C6 with lateral mass fixation (Table 44.2).

Apart from one patient with a postoperative pneumonia, no complications were observed in this group. One patient undergoing a posterior decompression and lateral mass fixation experienced a permanent worsening of his severe preoperative myelopathy.

Looking at individual symptoms, a trend for improvements of pain, sensory disturbances, and

Table 44.2 Operations for patients after foramen magnum decompressions. One patient required a ventriculoperitoneal shunt

Group	Ventral fusion	Posterior dec. + fusion	Catheter removal	FM revision	FM revision + fusion
FM group				40	13
Spinal group	10	5	4		

Abbreviations: *Dec*. decompression, *FM* foramen magnum

dysesthesias was observed at 3 months after surgery. Other neurological signs such as motor weakness or gait problems tended to remain unchanged. All but one ventral fusion of the cervical spine resulted in some clinical improvement at that time [15].

In the long term, a progression-free survival for at least 5 years was observed for 77% of patients undergoing surgery for degenerative diseases of the cervical spine [15]. Two patients developed adjacent-level disease after ventral fusions and underwent another ventral or posterior operation, respectively, which stabilized the clinical status.

After catheter removal, one patient experienced another deterioration due to postoperative scar formation 4 months after surgery. Her past history had been complicated by meningitis after the initial foramen magnum procedure, and no further operation was undertaken.

Secondary Surgeries at the Foramen Magnum

The 51 patients in this subgroup demonstrated either an untreated or new instability of the craniocervical junction, an insufficient decompression or an obstruction of CSF flow at this level (Figs. 44.1, 44.2, and 44.3). CSF flow obstructions were related to arachnoid scarring or compression of the cisterna magna by a pseudomeningocele. Combinations of these different mechanisms were common (Table 44.3).

In a previous publication, the lack of effect of syrinx shunts in patients with a Chiari I malformation and syringomyelia was demonstrated [16]. Therefore, such shunts were never considered for patients after a failed decompression. If a syrinx had not regressed or reappeared, the reason had to be looked for and treated at the foramen magnum. This required a revision with opening of the dura

Table 44.3 Pathological findings in 53 foramen magnum revisions. As multiple features were often found in a single operation, the total sum is higher than the number of revisions

Feature	Number of observations
Pseudomeningocele	14 (26%)
Slight arachnoid scarring	11 (22%)
Severe arachnoid scarring	36 (73%)
History of meningitis	3 (6%)
Obstruction of foramen of Magendie	33 (67%)
Ventricular dilatation	8 (15%)
Basilar invagination	12 (23%)

exchanging the duraplasty, arachnoid dissection with establishment of a free outflow from the foramen of Magendie, and insertion of a new duraplasty using alloplastic rather than autologeous material [1]. Several authors have mentioned the importance of opening this foramen during foramen magnum decompressions [2, 17, 18] and especially in revisions [18, 19].

Fifty-three revisions at the foramen magnum were performed in 51 patients (Figs. 44.2 and 44.3), of which 13 were combined with posterior craniocervical fusion (Fig. 44.1), where one revision included transoral resection of the odontoid and posterior decompression and fusion in a second operation. In four instances, the revision was restricted to craniocervical fusion only, as no CSF flow obstruction was detectable on preoperative imaging and intraoperatively using ultrasound (Table 44.2). The occiput was fused to C2 or subxial levels in patients with assimilation of the atlas only.

Severe arachnoid scarring was the commonest feature in patients demonstrating a CSF flow obstruction [20–24] and detected in 36 instances (73%) in the form of adhesions either between the dura graft and cerebellum or spinal cord, with obstruction of the foramen of Magendie in 33 of

these (Table 44.3). Whereas the adherence of the dura graft to the underlying nervous tissue was due to either pseudomeningocele formation pushing the dura graft anteriorly, [8] the suture material, autologeous graft material, or insufficient arachnoid dissection at the first operation, the most severe arachnoid scarring at the foramen of Magendie was encountered after obex plugging, resection of tonsils (Fig. 44.2), or in patients with a history of meningitis [16, 20, 25].

The major problem of preoperative evaluation was to determine the severity of arachnoiditis. The more extensive and dense the arachnoid pathology is, the less the probability that a revision may produce a lasting benefit and the higher the risk of surgery. Unless there was a history of meningitis or a clear description of severe arachnoid changes in the operation notes, it was almost impossible to foresee exactly what would be discovered after opening of the dura. Thus, it is difficult to judge the prognosis for a patient before revision surgery. This needs to be discussed with the patient. Reexploration of the foramen magnum is to some degree a diagnostic procedure in order to find out why the first operation did not provide the desired result. Depending on the intraoperative findings, a surgical strategy has to be adopted to improve CSF flow but to minimize the risk of postoperative arachnoid scarring, which may again lead to CSF flow obstruction and prevent a long-term benefit. Limiting the arachnoid dissection to the midline with sharp transection of arachnoid adhesions obstructing the foramen of Magendie and the posterior spinal subarachnoid space is all that is required. Blunt dissection or preparation of arachnoid adhesions laterally carries the risk of damage to small perforating arteries and caudal cranial nerves and should be avoided. Finally, a spacious dura graft using alloplastic material provides reasonable protection against postoperative arachnoid scarring, which may lead to neurological deterioration once again.

Complications were encountered in 26% of foramen magnum revisions with CSF fistulas, hemorrhages, and hydrocephalus occurring after two revisions each. Surgical morbidity was observed after four revisions (7.5%) and encountered exclusively among patients who had undergone their first decompression at other institutions. Compared to patients undergoing the first foramen magnum decompression, the overall complication rate for foramen magnum revisions was slightly higher [26, 27], while permanent surgical morbidity was significantly lower (0.9%) after first decompressions [26].

A postoperative improvement after 3 months was reported after 62% of operations, while 26% resulted in no postoperative change, and neurological worsening was evident after 11% of revisions. Looking at individual symptoms in the first postoperative year, improvements for pain, sensory disturbances, and gait had been revealed. The remainder of symptoms tended to be left unchanged. Improvements tended to be marginal and of little functional significance. Similar experiences have been made for patients with severe foramen magnum arachnoiditis of other causes [28]. The realistic outlook for patients undergoing a foramen magnum revision was clinical stabilization of the previously progressive course [1].

Long-term results determined by Kaplan-Meier statistics revealed rates for progression-free survival of 71% for 5 years and 63% for 10 years, respectively.

Conclusion

Patients presenting with progressive neurological symptoms after a foramen magnum decompression for Chiari I malformation require a detailed clinical and radiological workup to identify the responsible mechanism. Not only the foramen magnum area needs a careful analysis, but degenerative diseases of the cervical spine should also be taken into account. Particularly important are signs of instabilities, as the often atrophic spinal cords of these patients may be extremely vulnerable to hypermobile segments. Multilevel decompressions and fusions may stabilize the course for 77% of such patients for at least 5 years. Foramen magnum revisions are indicated in patients with evidence of CSF flow obstruction, cord compression, or instabilities at this level. They carry a

higher surgical morbidity and are less likely to produce significant neurological improvements compared to a primary decompression. However, still about 63% can be stabilized with such a revision for at least 10 years.

References

1. Klekamp J. Neurological deterioration after foramen magnum decompression for Chiari malformation type I: old or new pathology? J Neurosurg Pediatr. 2012;10(6):538–47.
2. Zerah M. [Syringomyelia in children]. Neurochirurgie. 1999;45(Suppl 1):37–57.
3. Aoki N, Oikawa A, Sakai T. Spontaneous regeneration of the foramen magnum after decompressive suboccipital craniectomy in Chiari malformation: case report. Neurosurgery. 1995;37(2):340–2.
4. Hudgins RJ, Boydston WR. Bone regrowth and recurrence of symptoms following decompression in the infant with Chiari II malformation. Pediatr Neurosurg. 1995;23(6):323–7.
5. Holly LT, Batzdorf U. Management of cerebellar ptosis following craniovertebral decompression for Chiari I malformation. J Neurosurg. 2001;94(1):21–6.
6. Williams B. Surgery for hindbrain related syringomyelia. Adv Tech Stand Neurosurg. 1993;20:107–64.
7. Smith JS, Shaffrey CI, Abel MF, Menezes AH. Basilar invagination. Neurosurgery. 2010;66(3 Suppl):39–47.
8. Pare LS, Batzdorf U. Syringomyelia persistence after Chiari decompression as a result of pseudomeningocele formation: implications for syrinx pathogenesis: report of three cases. Neurosurgery. 1998;43(4):945–8.
9. Armonda RA, Citrin CM, Foley KT, Ellenbogen RG. Quantitative cine-mode magnetic resonance imaging of Chiari I malformations: an analysis of cerebrospinal fluid dynamics. Neurosurgery. 1994;35(2):214–2; discussion 23-43.
10. Bhadelia RA, Bogdan AR, Wolpert SM, Lev S, Appignani BA, Heilman CB. Cerebrospinal fluid flow waveforms: analysis in patients with Chiari I malformation by means of gated phase-contrast MR imaging velocity measurements. Radiology. 1995;196(1):195–202.
11. Hofkes SK, Iskandar BJ, Turski PA, Gentry LR, McCue JB, Haughton VM. Differentiation between symptomatic Chiari I malformation and asymptomatic tonsillar ectopia by using cerebrospinal fluid flow imaging: initial estimate of imaging accuracy. Radiology. 2007;245(2):532–40.
12. McGirt MJ, Atiba A, Attenello FJ, Wasserman BA, Datoo G, Gathinji M, et al. Correlation of hindbrain CSF flow and outcome after surgical decompression for Chiari I malformation. Childs Nerv Syst. 2008;24(7):833–40.
13. Batzdorf U, Klekamp J, Johnson JP. A critical appraisal of syrinx cavity shunting procedures. J Neurosurg. 1998;89(3):382–8.
14. Takeuchi K, Yokoyama T, Ito J, Wada K, Itabashi T, Toh S. Tonsillar herniation and the cervical spine: a morphometric study of 172 patients. J Orthop Sci. 2007;12(1):55–60.
15. Klekamp J. Surgical treatment of multilevel cervical spondylosis in patients with or without a history of syringomyelia. Eur Spine J. 2017;26(4):948–57.
16. Klekamp J, Batzdorf U, Samii M, Bothe HW. The surgical treatment of Chiari I malformation. Acta Neurochir. 1996;138(7):788–801.
17. Menezes AH, Greenlee JD, Donovan KA. Honored guest presentation: lifetime experiences and where we are going: Chiari I with syringohydromyelia--controversies and development of decision trees. Clin Neurosurg. 2005;52:297–305.
18. Tubbs RS, Beckman J, Naftel RP, Chern JJ, Wellons JC 3rd, Rozzelle CJ, et al. Institutional experience with 500 cases of surgically treated pediatric Chiari malformation Type I. J Neurosurg Pediatr. 2011;7(3):248–56.
19. Sacco D, Scott RM. Reoperation for Chiari malformations. Pediatr Neurosurg. 2003;39(4):171–8.
20. Sakamoto H, Nishikawa M, Hakuba A, Yasui T, Kitano S, Nakanishi N, et al. Expansive suboccipital cranioplasty for the treatment of syringomyelia associated with Chiari malformation. Acta Neurochir. 1999;141(9):949–60; discussion 60-1.
21. Ellenbogen RG, Armonda RA, Shaw DW, Winn HR. Toward a rational treatment of Chiari I malformation and syringomyelia. Neurosurg Focus. 2000;8(3):E6.
22. Mazzola CA, Fried AH. Revision surgery for Chiari malformation decompression. Neurosurg Focus. 2003;15(3):E3.
23. Rosen DS, Wollman R, Frim DM. Recurrence of symptoms after Chiari decompression and duraplasty with nonautologous graft material. Pediatr Neurosurg. 2003;38(4):186–90.
24. Yanni DS, Mammis A, Ebersole K, Roonprapunt C, Sen C, Perin NI. Revision of Chiari decompression for patients with recurrent syrinx. J Clin Neurosci. 2010;17(8):1076–9.
25. Vanaclocha V, Saiz-Sapena N, Garcia-Casasola MC. Surgical technique for cranio-cervical decompression in syringomyelia associated with Chiari type I malformation. Acta Neurochir. 1997;139(6):529–39; discussion 39-40.
26. Klekamp J. Surgical treatment of Chiari I malformation--analysis of intraoperative findings, complications, and outcome for 371 foramen magnum decompressions. Neurosurgery. 2012;71(2):365–80; discussion 80.
27. Klekamp J, Samii M. Syringomyelia - diagnosis and treatment. Heidelberg: Springer Verlag; 2001. 195 p.
28. Klekamp J, Iaconetta G, Batzdorf U, Samii M. Syringomyelia associated with foramen magnum arachnoiditis. J Neurosurg Spine. 2002;97(3):317–22.

45 Outcomes for the Surgical Management of Chiari I and Chiari II Malformations

Nathan J. Ranalli, David D. Limbrick Jr., and Tae Sung Park

The details regarding classification, embryology, epidemiology, pathology, presentation, evaluation, and management of Chiari I and II malformations (CM I and CM II) are discussed elsewhere in this text. The objective of this chapter is to provide a literature-based description of the clinical outcomes observed and reported following the surgical treatment of CM I and CM II. The major measurable parameters include the improvement of clinical signs and symptoms, resolution of syringomyelia, and progression of scoliosis. Endpoints such as duration of surgery, findings on intraoperative ultrasonography, and length of hospital stay, each of which has been evaluated in more recent investigations, will be discussed as well. Complications and rates of reoperation will be noted but have been addressed in another chapter. The differences in results documented in patients with CM I or CM II who have undergone either bony decompression alone or in conjunction with duraplasty will also be outlined. In light of the fact that Chiari I and II malformations are congenital disorders truly distinct from one another, they will be addressed separately here.

Chiari I Malformation

First described in 1891 by Hans Chiari, Chiari malformation type I refers to a caudal descent of the cerebellar tonsils through the foramen magnum—sometimes as low as the mid-cervical spine—that results in a variety of clinical signs and symptoms [1]. Multiple theories exist regarding the proposed pathogenesis of CM I, the most routinely cited being that of an anomalous differential craniospinal pressure gradient across the foramen magnum; the lack of pressure equilibration between the intracranial and spinal subarachnoid spaces in this location permits the development of a caudal vector of force that results in worsening downward displacement of posterior fossa tissues [2–10].

The diagnosis of CM I, typically made by magnetic resonance imaging (MRI) criteria, is being delivered with increasing frequency in both children and adults as the threshold for obtaining radiologic studies in the setting of minor clinical

N. J. Ranalli
Department of Neurosurgery, Division of Pediatric Neurosurgery, University of Florida Health Science Center – Jacksonville, Lucy Gooding Pediatric Neurosurgery Center, Wolfson Children's Hospital, Jacksonville, FL, USA

D. D. Limbrick Jr.
Departments of Neurological Surgery and Pediatrics, St. Louis Children's Hospital, Washington University School of Medicine, St. Louis, MO, USA

T. S. Park (✉)
Division of Pediatric Neurosurgery, Department of Neurosurgery, Washington University School of Medicine, St. Louis Children's Hospital, St. Louis, MO, USA
e-mail: tspark@wustl.edu

R. S. Tubbs et al. (eds.), *The Chiari Malformations*, https://doi.org/10.1007/978-3-030-44862-2_45

complaints has continued to decline. Unlike CM I patients of a half-century ago that presented with severe ataxia, quadriplegia, and signs of elevated intracranial pressure, patients today are frequently diagnosed earlier with minor deficits, permitting more elective surgical management [11–13]. An excellent retrospective review of the 20-year institutional experience with pediatric CM I at a major children's hospital conducted by Tubbs et al. revealed the two most common presentations to be headache/neck pain (40% of patients) and scoliosis (18%); they also found that only 20% of patients referred with radiological CM I actually had symptoms likely to be improved by surgical intervention [14]. Numerous authors have similarly determined headache (exertional, Valsalva-induced) and pain to be the dominant presenting complaints in adults [15–19]. In the large pediatric study population evaluated by Tubbs and colleagues, less than 10% of patients presented with cranial neuropathies, and fewer than 5% had central sleep apnea. Other common findings included irritability, opisthotonus, upper extremity pain, paresthesias and weakness, ataxia, and lower extremity hyperreflexia. Among associated diagnoses, shunted hydrocephalus, retroversion of the dens, and scoliosis were observed most often [14].

Syringomyelia (SM), a condition caused by the abnormal accumulation of fluid within the spinal cord, is seen in up to 20% of asymptomatic patients with CM I and 75% of those with symptoms [20–27]. Although difficult to separate from the clinical findings in CM I itself, these patients typically complain of suboccipital headaches and neck pain that may occur in conjunction with uni- or bilateral numbness, weakness, or atrophy, and spasticity depending on the size and location of the syrinx. It is well-recognized from the Boman and Iivanainen study from the 1960s describing the natural history of untreated cervical SM that the condition will gradually progress and ultimately lead to both early disability and death if a timely intervention is not made [28].

Although no causal relationship has been definitively proven, the association between CM I, SM, and scoliosis is well established and has been extensively studied [29–31]. It is believed by many that impairment of the lower motor neurons in the setting of syringomyelia results in aberrant innervation of the trunk musculature and creates an imbalance that directly contributes to the development of scoliotic deformity [32–34]. Several reviews have determined that not only is scoliosis often the earliest presenting sign of SM in children and teens but that it may be present to varying degrees in up to 85% of young patients with SM [35, 36]. The likelihood of an individual case of idiopathic scoliosis (coronal spinal curve with Cobb angle >11 degrees) being associated with CM I and SM is increased in the setting of left-sided thoracic or otherwise atypical curves, hyperkyphosis, loss of thoracic apical segment lordosis, rapidly progressive curves, male gender, pain, and neurological deficits; the evaluation of scoliotic patients with such findings must therefore include spinal MRI [29, 31, 33, 37–47].

Operative Management of Chiari I

With the exception of medical pain management, surgery is the only proven treatment available for CM I. Although traditional approaches have included operations to address the syringomyelia itself via syrinx fenestration and shunting, the mainstay of therapy involves procedures directed at the presumed mechanism of syrinx development. Since some of the first descriptions in the literature of successful surgical management of CM by McConnell and D'Errico in 1938, studies by Fischer, Galarza et al., Krieger et al., and Navarro et al. have demonstrated the safety and efficacy of multiple techniques for decompression of the posterior fossa (PFD) [48–53]. More recently, as the debate regarding the advantages and disadvantages of performing a "bone-only" extradural decompression via removal of the suboccipital bone with or without cervical laminectomy and lysis of fibrous epidural bands (PFD) versus the more invasive intradural maneuvers (PFD with duraplasty [PFDD]) has grown stronger, Durham et al. and Hankinson et al. published meta-analyses of the current literature comparing the results of both approaches [54, 55]. Mutchnick and colleagues added to this growing body of

class IIb and III data in 2010 with a single-institution retrospective review comparing 121 CM I patients who underwent either PFD or PFDD [56]. As has been mentioned previously, however, there is no level I or IIa evidence comparing PFD to PFDD.

Clinical Outcome

In their meta-analysis composed of five retrospective cohort studies and two prospective cohort studies in which both surgical techniques were directly compared, Durham and Fjeld-Olenec found that 65% of patients undergoing PFD experienced clinical improvement as compared to 79% of the PFDD patients [54]. Hankinson and colleagues also reviewed the relatively limited database of studies retrospectively assessing the efficacy of PFD and PFDD separately. Some of these included the use of intraoperative ultrasonography to determine whether or not to perform intradural maneuvers, while others used electrophysiological evidence or preoperative factors to support the selection of PFD versus PFDD [53, 57–62]. Two retrospective studies from Italy reviewed by Hankinson et al. in which patients underwent PFD only demonstrated complete symptom resolution in 81.3% of patients [24] and a significant improvement in clinical condition at nearly 5 years of follow-up in 93.3% of patients [63].

A wealth of class III evidence exists in the form of retrospective, single-institution studies analyzing the outcomes in patients with CM I managed primarily with PFDD. Reports from the 1980s and 1990s by Paul, Nagib, and Nohria, respectively, showed that the majority of patients treated with PFDD experienced either improvement or stabilization of symptoms related to CM I following surgery [25, 64, 65]. Outcomes were better when the onset of symptoms occurred less than 2 years prior to operative intervention [17]. Numerous small studies have shown a range of clinical improvement from 92% to 100% with fairly low complication rates [52, 57, 58, 66–71]. In their extensive analysis of 500 pediatric patients treated for CM I, Tubbs et al. demonstrated relief of preoperative symptoms or signs in 83% of patients; headache (particularly Valsalva-induced and occipital in location), sleep apnea, and syringomyelia were affected more reliably than were preoperative motor or sensory abnormalities [14].

Syrinx Resolution

In the Durham and Fjeld-Olenec meta-analysis reviewing studies in which PFD and PFDD patients were directly compared, radiological syrinx improvement rates were 56% in the PFD patients and 87% in those undergoing PFDD, although this finding did not reach statistical significance [54]. In the study by Genitori et al., eight of ten patients who presented with syringomyelia achieved complete syrinx resolution following PFD alone; Caldarelli and colleagues showed that 50% had a decrease in syrinx size following bony decompression and 16.7% experienced postoperative syrinx growth and persistent or worsening symptoms [24, 63].

Among studies looking at PFDD alone, investigators have reported rates of syringomyelia reduction ranging between 55% and 100%, though no universal criteria defining improvement in syrinx exist [52, 57–59, 66, 68, 70–72]. Tubbs et al. found that of 285 patients with syringomyelia who underwent decompression with duraplasty, only 4 patients were found to have syrinx progression at follow-up 6 months to 1 year postoperatively; 80% of patients had resolution of syringomyelia symptoms following the first operation, and 95% of patients achieved relief following a second operation [14]. Zhang and colleagues reviewed 200 cases and demonstrated collapse or diminished size of syrinx in 60% of CM I patients following PFDD [73]. Although case reports exist in the literature, the likelihood of delayed syrinx resolution is low, and reoperation is recommended for persistent symptomatic syringomyelia at the 3- to 6-month postoperative time point [74].

Scoliosis Improvement

There is a paucity of literature regarding the management of scoliotic CM I patients with PFD alone. Genitori et al. documented radiologic improvement in two of three patients, and Caldarelli's paper reported mild improvement in

two of two patients [24, 63]. Attenello et al. detailed a single patient who had progression of scoliosis requiring reoperation with duraplasty following an initial PFD [75]. The likelihood of improvement in CM I patients with syringomyelia and scoliosis is better defined for the PFDD approach. A detailed search of the literature reveals at least 15 published clinical studies retrospectively evaluating scoliosis outcomes in patients treated primarily with PFDD. Though confounded by a lack of uniformity in surgical criteria and approaches across these series, rates of scoliosis improvement and progression range between 0–73% and 18–72%, respectively [76–87]. An association has been made between better outcomes and both a younger age at intervention and a smaller presenting Cobb angle [76, 77, 83–85]. Isu and colleagues demonstrated that two-thirds of patients with CM I-related syringomyelia and scoliosis might have both a postoperative reduction in the Cobb angle as well as lower rate of scoliosis progression when preoperative Cobb angles were less than 40 degrees [33]. Nagib found that six of ten patients with Cobb angles less than 30 degrees improved, and four patients with preoperative angles greater than 30 degrees stabilized after PFDD [64]. Tubbs et al. observed that 18% of patients in their large series had scoliosis, 82% of whom had syringomyelia; 40 patients (8% of all subjects) ultimately required spinal fusion for deformity correction. The authors observed that a preoperative Cobb angle of more than 40 degrees was associated with higher rates of scoliosis progression even in the setting of decreased syrinx size following surgery [14]. Attenello et al. found that in addition to a larger preoperative Cobb angle, scoliosis located at the thoracolumbar junction and a lack of radiographic improvement in syrinx size following surgery were predictive of scoliosis progression [75]. Most recently, Krieger and colleagues published a 10-year retrospective review of 79 pediatric patients found to have CM I and syringomyelia greater than 6 mm in diameter during an evaluation for scoliosis [87]. Each patient underwent PFDD, and none of the 49 patients with curves less than 20 degrees had progression of their curves postoperatively; 70% of the patients with curves between 25 and 80 degrees required either bracing or spinal instrumentation and fusion for scoliosis after the Chiari decompression. In total, 87% of the 79 patients had a significant size reduction of the syrinx following PFDD, but this, along with the magnitude of the preoperative curvature (in patients with Cobb angle >20 degrees), did not predict the need for subsequent deformity correction. Krieger and colleagues concluded appropriately that timely intervention was the key to improving neurological signs and symptoms and to preventing the need for later spinal fusion surgery [87].

Reoperation Requirement and Complications

In the Durham and Fjeld-Olenec meta-analysis, patients who underwent duraplasty were less likely to require reoperation for persistent or recurrent symptoms (2.1% vs. 12.6%) but were more likely to sustain cerebrospinal fluid (CSF)-related complications (18.5% vs. 1.8%) [54]. McGirt et al. published a 3% incidence of CSF leak in a 2009 retrospective review of 393 adult patients undergoing PFDD [88]. Mutchnick et al. found that 12.5% of PFD patients needed a subsequent PFDD for symptomatic recurrence, though none suffered a complication; only two (3.1%) patients receiving an upfront PFDD in their series underwent a repeated PFDD for lack of symptom improvement, and three patients suffered minor complications [56]. Tubbs and colleagues reported a complication rate of 2.4% in 500 patients; these included posterior fossa extra-axial fluid collections causing acute hydrocephalus (managed with external ventricular drainage); severe brain stem compression within 48 hours of surgery requiring transoral odontoidectomy and occipitocervical fusion, 2 aborted operations due to excessive occipital sinus bleeding, 1 case each of chemical and bacterial meningitis; and 1 patient with CSF leak secondary to untreated hydrocephalus that resolved with shunt placement [14]. Fifteen of 500 patients required reoperation (3.2%). It is estimated that the annual expected mortality rate following CM I decompression is between 2.5% and 4.5% [89].

Operative Time and Length of Stay

In the retrospective review of their own institutional experience published in 2011, Tubbs et al. reported the mean operative duration to be 95 minutes for PFDD [14]. The average hospital stay for their patients (all but one of whom underwent PFDD) was 2–7 days with a mean of 3 days; the length of time away before returning to school ranged between 7 and 16 days, with a mean of 12 days. Mutchnick and colleagues found that those patients in their series undergoing PFDD spent a longer time in the operating room (201 +/− 34 minutes vs. 127 +/− 25 minutes) and in the hospital (4.0 vs. 2.7 days) than the patients who underwent PFD [56]. The 2005–2008 national normative data showed mean lengths of stay between 4.5 and 6 days [89].

Chiari II Malformation

Chiari malformation type II is a disorder of hindbrain development observed in the setting of myelomeningocele that was initially described by Hans Chiari in 1891 and is now known to include a variety of supra- and infratentorial anomalies [90]. In addition to caudal displacement of the cerebellar vermis, brain stem, and fourth ventricle, CM II may include cerebellar inversion, a small posterior fossa, low-lying torcular Herophili, enlargement of the massa intermedia, shallow to absent cerebellar folia, a medullary "kink," and heterotopias [91–95]. The hypothesis currently favored by most neurosurgeons that best explains the myriad of findings in CM II is the unified theory championed by McLone and Knepper: The combination of cranial constriction and settling, spinal cord tethering or traction, intracranial hypertension, and intraspinal hypotension present in this malformation leads to the aforementioned spectrum of anatomical abnormalities [96].

Clinical signs of CM II include apnea and respiratory stridor, neurogenic dysphagia, aspiration, hypotonia or spasticity, and para- or quadriparesis. Symptoms of the disease, which occur in one-third of patients with CM II, range from very subtle to life-threatening. Symptomatic CM II is the leading cause of death in children less than 2 years old with myelomeningocele, and surgical decompression is required in up to one-third of symptomatic patients with CM II [97–101]. Although the malformation is present to variable degrees in every child born with a myelomeningocele and the diagnosis is straightforward, some patients become symptomatic only later in adolescence with deficits or pain related to the more chronic effects of syringomyelia or scoliosis. These older children will manifest classic effects of cervical myelopathy with upper extremity weakness, spasticity, loss of dexterity, and ataxia and occipital headaches and are treated operatively in a more elective fashion [84, 102].

Operative Management of Chiari II

The evaluation of symptomatic CM II in a young child begins with a determination of the presence or absence of hydrocephalus, as many of these children require shunting at birth or shortly thereafter. In those patients with a shunt, the possibility of a malfunction must be addressed first. Because of the potentially fatal nature of the symptoms with which these young children present, whether secondary to cranial nerve traction, lower brain stem compression, or congenitally malformed cranial nerve nuclei, the workup and, if necessary, surgical decompression must be completed in an urgent manner [103–109].

Once hydrocephalus and/or shunt malfunction has been eliminated as the etiology of the CM II patient's symptoms, the options for surgical intervention include suboccipital craniectomy, cervical laminectomy, and durotomy with or without dural augmentation [110–112]. As in CM I operative management, controversy exists regarding the decision to perform a bony decompression only versus the more invasive durotomy and even fourth ventricular fenestration. Each technique has been shown in separate investigations to be safe and effective for the treatment of CM II, but the data remains class IIb or III [113–115]. The advantages of staying outside the intradural space include reduced risk of bleeding and decreased exposure to general anesthesia, while

avoidance of a suboccipital craniectomy eliminates the chance of violating the low-lying torcular in these patients [116, 117].

Clinical Outcome

Overall, the prognosis for patients with symptomatic CM II remains guarded, as up to 15% of these patients die by 3 years old and an additional one-third suffer a permanent neurological disability [99]. Prior to the recognition of hindbrain compression as the cause of apnea, bradycardia, and cranial neuropathies and the establishment of an effective and aggressive surgical treatment, mortality rates for patients presenting with brain stem dysfunction that underwent "less urgent" surgical decompression ranged between 50% and 70%; more recent studies in which surgery was undertaken early in an attempt to reverse the signs of brain stem compression reported postoperative mortality rates between 15% and 23% [106, 109, 118, 119]. Conversely, outcomes in children and adolescents presenting with symptoms related to myelopathy or syringomyelia may mirror those of CM I patients, with mortality rates near 0% and clinical improvement in 79–100% after surgery [106, 120].

As stated earlier, controversy exists regarding the optimal approach for craniovertebral decompression in these patients, in particular whether to include a suboccipital craniectomy and the utility of durotomy with dural augmentation. Tubbs and Oakes found in a 2004 evidence-based review of the literature regarding CM II evaluation and management that all data were class III in nature and no reliable conclusions or recommendations could be made at that time [112].

With regard to the more invasive techniques, Pollack et al. published in 1992 on the use of a suboccipital craniectomy, cervical laminectomy, dural decompression, and, in patients with syringomyelia, a fourth ventricular shunt, in 25 CM II patients with symptoms of increasing brain stem compression and deterioration [106]. The authors found that this approach resulted in near-complete or total reversal of clinical symptoms in 17 patients, while 3 others had mild-moderate residual deficits and 5 experienced no change. They established an association between worse preoperative neurological status, particularly bilateral vocal cord paralysis, and poorer outcomes, with an emphasis on the importance of expeditious treatment. Pollack and colleagues subsequently published a prospective report in 1996 in which children underwent the aforementioned decompression in a protocolized manner at the earliest signs of CM II-related brain stem dysfunction [105]. Ten of 13 patients returned to normal or near-normal brain stem function shortly after surgery, and only 1 required a temporary gastrostomy with no tracheostomies in the group. The remaining three patients presented with bilateral vocal cord paralysis and severe central apnea prior to operative intervention and achieved no meaningful recovery of function following surgery.

In 1992, Vandertop et al. retrospectively reviewed the management of 17 CM II neonates over a decade with cervical laminectomy and duraplasty alone, finding that 88% of patients achieved complete recovery with a mean follow-up of 65 months; 1 patient expired from respiratory arrest 8 months after surgery, and the other died from a remote shunt infection 7 years later [109]. The authors argued that the relatively spacious size of the foramen magnum in CM II patients eliminated the need for routine suboccipital craniectomy as part of the decompression.

With regard to the least-invasive end of the surgical spectrum, a 1996 investigation by Yundt and colleagues found that two children presenting with CM II and stridor experienced clinical improvement following osseous decompression alone [117]. A later retrospective review by James et al. of 22 patients with CM, including 18 children with CM II who underwent a bony decompression only, reported no surgical morbidities or mortality and partial or total symptomatic improvement in 86% [116].

Most recently, Akbari, Limbrick, and colleagues conducted a retrospective analysis of 33 patients who underwent bony decompression with or without dural augmentation for the treatment of symptomatic CM II and compared out-

comes in patients managed with each approach [121]. Twenty-six patients had an osseous decompression alone, including 21 with cervical laminectomy and 5 others with both laminectomy and suboccipital craniectomy; 7 patients underwent cervical laminectomy with or without suboccipital craniectomy and upfront duraplasty. At a median follow-up of 5 years, nearly 70% of patients had symptomatic improvement, 62% of those undergoing bone-only decompression compared to 57% of the patients with dural augmentation (though this did not reach statistical significance). Signs including apnea, opisthotonus, stridor, and dysphagia were most responsive to surgical intervention, and the intraoperative blood loss, time under general anesthesia, and length of hospital stay were less in the bony decompression group, though statistical significance was not achieved. Rates of repeat surgery for lack of improvement or symptomatic recurrence were higher but not statistically significant in the bone-only cohort (19.2% vs. 14.3%); outcomes were not different between the patients who underwent cervical laminectomy alone compared to those who also had a suboccipital craniectomy. Overall, 6 of 33 patients required tracheostomies after surgery, and 1 patient died secondary to fungal sepsis unrelated to the Chiari decompression. The authors concluded that the less-invasive approach of cervical laminectomy and sectioning of the dural band alone avoided the inherent risks of performing a suboccipital craniectomy and durotomy, including injury to the torcular Herophili, CSF leak, pseudomeningocele, and meningitis, and should be considered a first-line option in the operative management of children with CM II. Emphasis must also be placed on the critical need to evaluate each CM II patient for active hydrocephalus or shunt malfunction, whether through radiographic imaging, shunt tap, or exploration, prior to undertaking a decompressive surgery. Undoubtedly, the need exists for a larger retrospective series or randomized controlled trial comparing the aforementioned approaches in order to make an outcome-based decision regarding the optimal technique for CM II treatment.

Fetal Myelomeningocele Repair and Improvement in Hindbrain Herniation

Finally, no discussion of CM II outcomes would be complete without mention of the recently published prospective, randomized controlled trial of prenatal versus postnatal repair of myelomeningocele [122]. Though the primary findings of this study included reduced need for shunting and improved motor outcomes at 30 months, the multiinstitutional investigation also revealed that the proportion of infants without evidence of hindbrain herniation was higher (36%) in the prenatal surgery cohort than in the postnatal surgery group (4%) at 12 months of age. Similarly, the rate of moderate or severe herniation was lower (25%), as were brainstem kinking, abnormal fourth ventricle location, and syringomyelia, in the prenatal surgery group than in the postnatal surgery patients (67%). These data suggest that interruption of CSF flow through the myelomeningocele neural placode in utero, if performed early enough, may halt or even reverse abnormal hindbrain development. Although more work remains to be done, the impact of these findings on the future neurosurgical management of CM II may be enormous.

Conclusion

An up-to-date, evidence-based review of the neurosurgical literature reveals that clinical outcomes following the operative management of Chiari I and II malformations have improved dramatically since these congenital disorders were first recognized as surgical diseases a century ago. A detailed assessment of major measurable postoperative parameters including the improvement of clinical signs and symptoms, resolution of syringomyelia, and progression of scoliosis proves these decompressive procedures to be safe and effective when performed in a timely manner by an experienced neurosurgeon.

Patients with CM I now routinely report a significant reduction in headache, neck pain, apnea, and syrinx-related symptoms and encounter low

rates of complication or reoperation whether a bone-only or intradural posterior fossa decompression is performed.

Neonates and infants with CM II, though facing more significant deficits and frequently presenting in an emergent fashion, have higher rates of symptomatic improvement and reversal of impairment when an operative intervention is made at the first sign of brain stem dysfunction.

The current trend of less-invasive and faster bone-only surgical approaches, if shown in larger prospective trials to be truly superior to traditional intradural decompressions, will only add to the modern-day neurosurgeon's ability to achieve excellent clinical outcomes with minimal risk in the treatment of patients with Chiari I and II malformations.

References

1. Loukas M, Noordeh N, Shoja MM, Pugh J, Oakes WJ, Tubbs RS. Hans Chiari (1851–1916). Childs Nerv Syst. 2008;24:1333–9.
2. Ball MJ, Dayan AD. Pathogenesis of syringomyelia. Lancet. 1972;2:799–801.
3. Oakes WJ, Tubbs RS. Chiari malformations. In: Winn HR, editor. Youmans neurological surgery: a comprehensive guide to the diagnosis and management of neurological problems. 5th ed. Philadelphia, PA: WB Saunders; 2003. p. 3347–61.
4. Oldfield EH, Muraszko K, Shawker TH, Patronas NJ. Pathophysiology of hydrosyringomyelia associated with Chiari I malformation of the cerebellar tonsils. Implications for diagnosis and treatment. J Neurosurg. 1994;80:3–15.
5. Pillay PK, Awad IA, Little JR, Hahn JF. Symptomatic Chiari malformation in adults: a new classification based on magnetic resonance imaging with clinical and prognostic significance. Neurosurgery. 1991;28:639–45.
6. Tubbs RS, Shoja MM, Ardalan MR, Shokouhi G, Loukas M. Hindbrain herniation: a review of embryological theories. Ital J Anat Embryol. 2008;113:37–46.
7. Vega A, Quintana F, Berciano J. Basichondrocranium anomalies in adult Chiari type I malformation: a morphometric study. J Neurol Sci. 1990;99:137–45.
8. Williams B. Pathogenesis of syringomyelia. In: Batzdorf U, editor. Syringomyelia: current concepts in diagnosis and treatment. Current neurosurgical practice series, vol. 4. Baltimore, MD: Williams and Wilkins; 1991. p. 59–90.
9. Williams B. Simultaneous cerebral and spinal fluid pressure recordings. 2. Cerebrospinal dissociation with lesions at the foramen magnum. Acta Neurochir. 1981;59:123–42.
10. Williams B. Syringomyelia. Neurosurg Clin N Am. 1990;1:653–85.
11. Appleby A, Foster JB, Hankinson J, Hudgson P. The diagnosis and management of the Chiari anomalies in adult life. Brain. 1968;91:131–40.
12. Gardner WJ, Goodall RJ. The surgical treatment of Arnold-Chiari malformation in adults; an explanation of its mechanism and importance of encephalography in diagnosis. J Neurosurg. 1950;7:199–206.
13. Malis LI, Cohen I, Gross SW. Arnold-Chiari malformation. Arch Surg. 1951;63:783–98.
14. Tubbs RS, Beckman J, Naftel RP, Chern JJ, Wellons JC III, Rozzelle CJ, Blount JP, Oakes WJ. Institutional experience with 500 cases of surgically treated pediatric Chiari malformation Type I. J Neurosurg Pediatrics. 2011;7:248–56.
15. Dure LS, Percy AK, Cheek WR, Laurent JP. Chiari type I malformation in children. J Pediatr. 1989;115:573–6.
16. Dyste GN, Menezes AH. Presentation and management of pediatric Chiari malformations without myelodysplasia. Neurosurgery. 1988;23:589–97.
17. Dyste GH, Menezes AH, VanGilder JC. Symptomatic Chiari malformations. An analysis of presentation, management, and long-term outcome. J Neurosurg. 1989;71:159–68.
18. Stovner LJ. Headache associated with the Chiari type I malformation. Headache. 1993;33:175–81.
19. Tubbs RS, Oakes WJ. Chiari malformation. J Neurosurg. 2007;106(4 Suppl):329–30.
20. Gardner WJ, Angel J. The mechanism of syringomyelia and its surgical correction. Clin Neurosurg. 1958;6:131–40.
21. Moriwaka F, Tashiro K, Tachibana S, Yada K. Epidemiology of syringomyelia in Japan – the nationwide survey. Rinsho Shinkeigaku. 1995;35(12):1395–7.
22. Williams B. Management schemes for syringomyelia. In: Anson JA, Benzel EC, Awad IA, editors. Syringomyelia and the Chiari malformations. Park Ridge, IL: AANS; 1997. p. 12–144.
23. Schijman E. History, anatomic forms, and pathogenesis of Chiari I malformations. Childs Nerv Syst. 2004;20(5):323–8.
24. Genitori L, Peretta P, Nurisso C, Macinante L, Mussa F. Chiari type I anomalies in children and adolescents: minimally invasive management in a series of 53 cases. Childs Nerv Syst. 2000;16(10–11):707–18.
25. Nohria V, Oakes WJ. Chiari I malformation: a review of 43 patients. Pediatr Neurosurg. 1990;16(4–5):222–7.
26. Elster AD, Chen MY. Chiari I malformations: clinical and radiologic reappraisal. Radiology. 1992;183(2):347–53.
27. Pillay PK, Awad IA, Little JR, Hahn JF. Symptomatic Chiari malformation in adults: a new classification based on magnetic resonance imaging with clinical and prognostic significance. Neurosurgery. 1991;28(5):639–45.

28. Boman K, Iivanainen M. Prognosis of syringomyelia. Acta Neurol Scand. 1967;43(1):61–8.
29. Hankinson TC, Klimo P Jr, Feldstein NA, Anderson RC, Brockmeyer D. Chiari malformations, syringohydromyelia and scoliosis. Neurosurg Clin N Am. 2007;18(3):549–68.
30. Cardoso M, Keating RF. Neurosurgical management of spinal dysraphism and neurogenic scoliosis. Spine. 2009;34(17):1775–82.
31. Akhtar OH, Rowe DE. Syringomyelia-associated scoliosis with and without the Chiari I malformation. J Am Acad Orthop Surg. 2008;16(7):407–17.
32. Huebert HT, MacKinnon WB. Syringomyelia and scoliosis. J Bone Joint Surg Br. 1969;51:338–43.
33. Isu T, Chono Y, Iwasaki Y, Koyanagi I, Akino M, Abe H. Scoliosis associated with syringomyelia presenting in children. Childs Nerv Syst. 1992;8:97–100.
34. Williams B. Orthopaedic features in the presentation of syringomyelia. J Bone Joint Surg Br. 1979;61:314–23.
35. Samuelsson L, Lindell D. Scoliosis as the first sign of a cystic spinal cord lesion. Eur Spine J. 1995;4(5):284–90.
36. Kontio K, Davidson D, Letts M. Management of scoliosis and syringomyelia in children. J Pediatr Orthop. 2002;22(6):771–9.
37. Inoue M, Minami S, Nakata Y. Preoperative MRI analysis of patients with idiopathic scoliosis: a prospective study. Spine. 2005;30(1):108–14.
38. Wu L, Qiu Y, Wang B, Zhu ZZ, Ma WW. The left thoracic curve pattern: a strong predictor for neural axis abnormalities in patients with "idiopathic" scoliosis. Spine. 2010;35(2):182–5.
39. Arai S, Ohtsuka Y, Moriya H, Kitahara H, Minami S. Scoliosis associated with syringomyelia. Spine. 1993;18(12):1591–2.
40. Spiegel DA, Flynn JM, Stasikelis PJ. Scoliotic curve patterns in patients with Chiari I malformation and/or syringomyelia. Spine. 2003;28(18):2139–46.
41. Barnes PD, Brody JD, Jaramillo D, Akbar JU, Emans JB. Atypical idiopathic scoliosis: MR imaging evaluation. Radiology. 1993;186(1):247–53.
42. Whitaker C, Schoenecker PL, Lenke LG. Hyperkyphosis as an indicator of syringomyelia in idiopathic scoliosis: a case report. Spine. 2003;28(1):E16–20.
43. Loder RT, Stasikelis P, Farley FA. Sagittal profiles of the spine in scoliosis associated with an Arnold-Chiari malformation with or without syringomyelia. J Pediatr Orthop. 2002;22(4):483–91.
44. Davids JR, Chamberlin E, Blackhurst DW. Indications for magnetic resonance imaging in presumed adolescent idiopathic scoliosis. J Bone Joint Surg Am. 2004;86A(10):2187–95.
45. Ouellet JA, LaPlaza J, Erickson MA, Birch JG, Burke S, Browne R. Sagittal plane deformity in the thoracic spine: a clue to the presence of syringomyelia as a cause of scoliosis. Spine. 2003;28(18):2147–51.
46. Schwend RM, Hennrikus W, Hall JE, Emans JB. Childhood scoliosis: clinical indications for magnetic resonance imaging. J Bone Joint Surg Am. 1995;77(1):46–53.
47. Zadeh HG, Sakka SA, Powell MP, Mehta MH. Absent superficial abdominal reflexes in children with scoliosis: an early indicator of syringomyelia. J Bone Joint Surg Br. 1995;77(5):762–7.
48. McConnell AA, Parker HL. A deformity of the hindbrain associated with internal hydrocephalus: its relation to the Arnold-Chiari malformation. Brain. 1938;61:415–29.
49. D'Errico A. Surgical procedure for hydrocephalus associated with spina bifida. Surgery. 1938;4:856–66.
50. Fischer EG. Posterior fossa decompression for Chiari I deformity, including resection of the cerebellar tonsils. Childs Nerv Syst. 11:625–9, 195.
51. Galarza M, Sood S, Ham S. Relevance of surgical strategies for the management of pediatric Chiari type I malformation. Childs Nerv Syst. 2007;23:691–6.
52. Krieger MD, McComb JG, Levy ML. Toward a simpler surgical management of Chiari I malformation in a pediatric population. Pediatr Neurosurg. 1999;30:113–21.
53. Navarro R, Olavarria G, Seshadri R, Gonzales-Portillo G, McLone DG, Tomita T. Surgical results of posterior fossa decompression for patients with Chiari I malformation. Childs Nerv Syst. 2004;20:349–56.
54. Durham SR, Fjeld-Olenec K. Comparison of posterior fossa decompression with and without duraplasty for the surgical treatment of Chiari malformation Type I in pediatric patients: a meta-analysis. J Neurosurg Pediatrics. 2008;2:42–9.
55. Hankinson T, Tubbs RS, Wellons JC III. Duraplasty or not? An evidence-based review of the pediatric Chiari I malformation. Childs Nerv Syst. 2011;27:35–40.
56. Mutchnick IS, Janjua RM, Moeller K, Moriarty TM. Decompression of Chiari malformation with and without duraplasty: morbidity versus recurrence. J Neurosurg Pediatrics. 2010;5:474–8.
57. Anderson RC, Dowling KC, Feldstein NA, Emerson RG. Chiari I malformation: potential role for intraoperative electrophysiologic monitoring. J Clin Neurophysiol. 2003;20:65–72.
58. Anderson RC, Emerson RG, Dowling KC, Feldstein NA. Improvement in brain stem auditory evoked potentials after suboccipital decompression in patients with Chiari I malformations. J Neurosurg. 2003;98:459–64.
59. Attenello FJ, McGirt MJ, Gathinji M, Datoo G, Atiba A, Weingart J. Outcome of Chiari-associated syringomyelia after hindbrain decompression in children: analysis of 49 consecutive cases. Neurosurgery. 2008;62:1307–13.
60. McGirt MJ, Attenello FJ, Datoo G, Gathinji M, Atiba A, Weingart JD. Intraoperative ultrasonography as a guide to patient selection for duraplasty after suboccipital decompression in children with Chiari malformation Type I. J Neurosurg Pediatr. 2008;2:52–7.

61. Yeh DD, Koch B, Crone KR. Intraoperative ultrasonography used to determine the extent of surgery necessary during posterior fossa decompression in children with Chiari malformation type I. J Neurosurg. 2006;105:26–32.
62. Zamel K, Galloway G, Kosnik EJ, Raslan M, Adeli A. Intraoperative neurophysiologic monitoring in 80 patients with Chiari I malformation: role of duraplasty. J Clin Neurophysiol. 2009;26:70–5.
63. Caldarelli M, Novegno F, Vassimi L, Romani R, Tamburrini G, DiRocco C. The role of limited posterior fossa craniectomy in the surgical treatment of Chiari malformation Type I: experience with a pediatric series. J Neurosurg. 2007;106:187–95.
64. Nagib MG. An approach to symptomatic children (ages 4-14 years) with Chiari type I malformation. Pediatr Neurosurg. 1994;21:31–5.
65. Paul KS, Lye RH, Strang FA, Dutton J. Arnold-Chiari malformation: review of 71 cases. J Neurosurg. 1983;58:183–7.
66. Alzate JC, Kothbauer KF, Jallo GI, Epstein FJ. Treatment of Chiari I malformation in patients with and without syringomyelia: a consecutive series of 66 cases. Neurosurg Focus. 2001;11:E3.
67. Danish SF, Samdani A, Hanna A, Storm P, Sutton L. Experience with acellular human dura and bovine collagen matrix for duraplasty after posterior fossa decompression for Chiari malformations. J Neurosurg. 2006;104:16–20.
68. Ellenbogen RG, Armonda RA, Shaw DW, Winn HR. Toward a rational treatment of Chiari I malformation and syringomyelia. Neurosurg Focus. 2000;8:E6.
69. Feldstein NA, Choudhri TF. Management of Chiari I malformations with holocord syringohydromyelia. Pediatr Neurosurg. 1999;31:143–9.
70. Hoffman CE, Souweidane MM. Cerebrospinal fluid-related complications with autologous duraplasty and arachnoid sparing in type I Chiari malformation. Neurosurgery. 2008;62:156–60.
71. Park JK, Gleason PL, Madsen JR, Goumnerova LC, Scott RM. Presentation and management of Chiari I malformation in children. Pediatr Neurosurg. 1997;26:190–6.
72. Attenello FJ, McGirt MJ, Garces-Ambrossi GL, Chaichana KL, Carson B, Jallo GI. Suboccipital decompression for Chiari I malformation: outcome comparison of duraplasty with expanded polytetrafluoroethylene dural substitute versus pericranial autograft. Childs Nerv Syst. 2009;25:183–90.
73. Zhang ZQ, Chen YQ, Chen YA, Wu X, Wang YB, Li XG. Chiari I malformation associated with syringomyelia: a retrospective study of 316 surgically treated patients. Spinal Cord. 2008;46:358–63.
74. Doughty KE, Tubbs RS, Webb D, Oakes WJ. Delayed resolution of Chiari I-associated hydromyelia after posterior fossa decompression: case report and review of the literature. Neurosurgery. 2004;55:711.
75. Attenello FJ, McGirt MJ, Atiba A, Gathinji M, Datoo G, Weingart J. Suboccipital decompression for Chiari malformation-associated scoliosis: risk factors and time course of deformity progression. J Neurosurg Pediatrics. 2008;1:456–60.
76. Brockmeyer D, Gollogly S, Smith JT. Scoliosis associated with Chiari I malformations: the effect of suboccipital decompression on scoliosis curve progression: a preliminary study. Spine. 2003;28:2505–9.
77. Eule JM, Erickson MA, O'Brien MF, Handler M. Chiari I malformation associated with syringomyelia and scoliosis: a twenty-year review of surgical and nonsurgical treatment in a pediatric population. Spine. 2002;27:1451–5.
78. Farley FA, Puryear A, Hall JM, Muraszko K. Curve progression in scoliosis associated with Chiari I malformation following suboccipital decompression. J Spinal Disord Tech. 2002;15:410–4.
79. Flynn JM, Sodha S, Lou JE, Adams SB Jr, Whitfield B, Ecker ML. Predictors of progression of scoliosis after decompression of an Arnold Chiari I malformation. Spine. 2004;29:286–92.
80. Ghanem IB, Londono C, Delalande O, Dubousset JF. Chiari I malformation associated with syringomyelia and scoliosis. Spine. 1997;22:1313–7.
81. Hayhurst C, Osman-Farah J, Das K, Mallucci C. Initial management of hydrocephalus associated with Chiari malformation type I-syringomyelia complex via endoscopic third ventriculostomy: an outcome analysis. J Neurosurg. 2008;108:1211–4.
82. Hida K, Iwasaki Y, Koyanagi I, Abe H. Pediatric syringomyelia with chiari malformation: its clinical characteristics and surgical outcomes. Surg Neurol. 1999;51:383–90.
83. Muhonen MG, Menezes AH, Sawin PD, Weinstein SL. Scoliosis in pediatric Chiari malformations without myelodysplasia. J Neurosurg. 1992;77:69–77.
84. Ozerdemoglu RA, Transfeldt EE, Denis F. Value of treating primary causes of syrinx in scoliosis associated with syringomyelia. Spine. 2003;28:806–14.
85. Sengupta DK, Dorgan J, Findlay GF. Can hindbrain decompression for syringomyelia lead to regression of scoliosis? Eur Spine J. 2000;9:198–201.
86. Tubbs RS, McGirt MJ, Oakes WJ. Surgical experience in 130 pediatric patients with Chiari I malformations. J Neurosurg. 2003;99:291–6.
87. Krieger MD, Falkinstein Y, Bowen IE, Tolo VT, McComb JG. Scoliosis and Chiari malformation type I in children. J Neurosurg Pediatrics. 2011;7:25–9.
88. McGirt MJ, Garces-Ambrossi GL, Parker S, Liauw J, Bydon M, Jallo GI. Primary and revision suboccipital decompression for adult Chiari I malformation: analysis of long-term outcomes in 393 patients. Neurosurgery. 2009;65:924.
89. Cleveland Clinic: neurological institute outcomes 2008. Cleveland: The Cleveland Clinic Foundation; 2009, pp 64–66.
90. Chiari H. Uber Veranderungen des Kleinhirns infolge von Hydrocephalie des Grosshirns. Dtsch Med Wschr. 1891;17:1172–5.
91. Callen AL, Filly RA. Supratentorial abnormalities in the Chiari II malformation, I: the ventricular "point". J Ultrasound Med. 2008;27(1):33–8.

92. Callen AL, Stengel JW, Filly RA. Supratentorial abnormalities in the Chiari II malformation, II: tectal morphologic changes. J Ultrasound Med. 2009;28(1):29–35.
93. Filly MR, Filly RA, Barkovich AJ, Goldstein RB. Supratentorial abnormalities in the Chiari II malformation, IV: the too-far-back ventricle. J Ultrasound Med. 2010;29(2):243–8.
94. Miller E, Widjaja E, Blaser S, Dennis M, Raybaud C. The old and the new: supratentorial MR findings in Chiari II malformation. Childs Nerv Syst. 2008;24:563–75.
95. Wong SK, Barkovich AJ, Callen AL, Filly RA. Supratentorial abnormalities in the Chiari II malformation, III: the interhemispheric cyst. J Ultrasound Med. 2009;28(8):999–1006.
96. McLone DG, Knepper PA. The cause of Chiari II malformation: a unified theory. Pediatr Neurosci. 1989;15:1–12.
97. McLone DG, Dias MS. The Chiari II malformation: cause and impact. Childs Nerv Syst. 2003;19:540–50.
98. Rahman M, Perkins LA, Pincus DW. Aggressive surgical management of patients with Chiari II malformation and brain stem dysfunction. Pediatr Neurosurg. 2009;45:337–44.
99. McLone DG. Continuing concepts in the management of spina bifida. Pediatr Neurosurg. 1992;18:254–6.
100. Curnes JT, Oakes WJ, Boyko OB. MR imaging of hindbrain deformity in Chiari II patients with and without symptoms of brain stem compression. Am J Neuroradiol. 1989;10(2):293–302.
101. Talamonti G, Zella S. Surgical treatment of CM2 and syringomyelia in a series of 231 myelomeningocele patients: clinical article. Neurol Sci. 2011;32(3):331–3.
102. Ozerdemoglu RA, Denis F, Transfeldt EE. Scoliosis associated with syringomyelia: clinical and radiologic correlation. Spine. 2003;28(13):1410–7.
103. Gilbert JN, Jones KL, Rorke LB. Central nervous system anomalies associated with meningomyelocele, hydrocephalus, and the Arnold-Chiari malformation: reappraisal of theories regarding the pathogenesis of posterior neural tube closure defects. Neurosurgery. 1986;18:559–64.
104. Holinger PC, Holinger LD, Reichert TJ. Respiratory obstruction and apnea in infants with bilateral abductor vocal cord paralysis, meningomyelocele, hydrocephalus, and Arnold-Chiari malformation. J Pediatr. 1978;92:368–73.
105. Pollack IF, Kinnunen D, Albright AL. The effect of early craniocervical decompression on functional outcome in neonates and young infants with myelodysplasia and symptomatic Chiari II malformations: results from a prospective series. Neurosurgery. 1996;38:703–10.
106. Pollack IF, Pang D, Albright AL. Outcome following hindbrain decompression of symptomatic Chiari malformations in children previously treated with myelomeningocele closure and shunts. J Neurosurg. 1992;77:881–8.
107. Ruge JR, Masciopinto J, Storrs BB. Anatomical progression of the Chiari II malformation. Childs Nerv Syst. 1992;8:86–91.
108. Sieben RL, Hamida MB, Shulman K. Multiple cranial nerve deficits associated with the Arnold-Chiari malformation. Neurology. 1971;21:673–81.
109. Vandertop WP, Asai A, Hoffman HJ. Surgical decompression for symptomatic Chiari II malformation in neonates with myelomeningocele. J Neurosurg. 1992;77:541–4.
110. Guo F, Wang M, Long J, Wang H, Sun H, Yang B, Song L. Surgical management of Chiari malformation: analysis of 128 cases. Pediatr Neurosurg. 2007;43(5):375–81.
111. Haines SJ, Berger M. Current treatment of Chiari malformations types I and II: a survey of the Pediatric Section of the American Association of Neurological Surgeons. Neurosurgery. 1991;28:353–7.
112. Tubbs RS, Oakes WJ. Treatment and management of the Chiari II malformation: an evidence-based review of the literature. Childs Nerv Syst. 2004;20(6):375–81.
113. LaMarca F, Herman M, Grant JA, McLone DG. Presentation and management of hydromyelia in children with Chiari type-II malformation. Pediatr Neurosurg. 1997;26(2):57–67.
114. Stevenson K. Chiari type II malformation: past, present and future. Neurosurg Focus. 2004;16(E5):1–7.
115. Venes JL, Black KL, Latack JT. Preoperative evaluation and surgical management of the Arnold-Chiari II malformation. J Neurosurg. 1986;64(3):363–70.
116. James HE, Brant A. Treatment of the Chiari malformation with bone decompression without durotomy in children and young adults. Childs Nerv Syst. 2002;18(5):202–6.
117. Yundt KD, Park TS, Tantuwaya VS, Kaufman BA. Posterior fossa decompression without duraplasty in infants and young children for treatment of Chiari malformation and achondroplasia. Pediatr Neurosurg. 1996;25(5):221–6.
118. Bell WO, Charney EB, Bruce DA. Symptomatic Arnold-Chiari malformation: a review of experience with 22 cases. J Neurosurg. 1987;66:812–6.
119. Park TS, Hoffman HJ, Hendrick EB. Experience with surgical decompression of the Arnold-Chiari malformation in young infants with myelomeningocele. Neurosurgery. 1983;13:147–52.
120. Oakes WJ, Worley G, Spock A. Surgical intervention in twenty-nine patients with symptomatic Type II Chiari malformations: clinical presentation and outcome. Concepts Pediatr Neurosurg. 1988;8:76–85.
121. Akbari SH, Limbrick DD Jr, Kim DH, Narayan P, Leonard JR, Smyth MD, Park TS. Surgical management of symptomatic Chiari II malformation in infants and children. Childs Nerv Syst. 2013 Jul;29(7):1143–54.
122. Adzick NS, Thom EA, Spong CY, Brock JW 3rd, Burrows PK, Johnson MP, et al; MOMS Investigators. A randomized trial of prenatal versus postnatal repair of myelomeningocele. N Engl J Med. 2011;364(11):993–1004.

Part VIII

Miscellaneous

Chiari-Like Malformation in Dogs

46

Dominic J. Marino and Curtis W. Dewey

Chiari-like malformation (CLM), the canine analog of human Chiari type I malformation, has emerged as the cause of major health problems in several toy-breed dogs, most notably the Cavalier King Charles spaniel (CKCS), Griffon Bruxellois, Yorkshire terriers, Maltese, Pomeranians, and Chihuahuas [1–7]. More than 80% of CKCS [7–9] and 65% of Griffon Bruxellois [5, 10] are reported to have CLM. The prevalence of CLM is difficult to determine as many of these dogs are asymptomatic, and for others, the primary clinical sign of pain is often overlooked or misinterpreted by owners and family veterinarians.

The term craniocervical junction abnormality (CJA), as used in human and veterinary medicine, serves as an "umbrella" term for a variety of malformations that occur in the craniocervical region. The craniocervical junction refers to the occipital bone (primarily the supraoccipital component) that forms the boundaries of the foramen magnum, the atlas (C1), and the axis (C2). With the increased accessibility of advanced imaging techniques and medical awareness, craniocervical junction abnormalities in small-breed dogs are being recognized as common and challenging disorders [1, 2, 4, 5, 8, 11–14].

In veterinary medicine, the term "Chiari-like malformation" has been widely used to describe constrictive disorders at the cervicomedullary junction that are apparent on magnetic resonance imaging (MRI).

Numerous abnormalities of the craniocervical junction in dogs (primarily) and cats (rarely) are presumed to be heritable malformations, and all have been associated with the secondary development of syringomyelia (SM) [6, 15]. Syringomyelia refers to the accumulation of fluid within the spinal cord parenchyma [3, 6, 15–23]. The fluid cavity itself is called a syrinx. The term hydromyelia specifically describes fluid accumulation only within the central canal and is considered a possible precursor to SM.

Although the signalment features for some of the more recently reported disorders have not been clearly defined, all of the disorders tend to affect young, small-breed dogs and infrequently cats. The nomenclature used for these disorders is often confusing and generally assumes that these are all distinctly separate disorders. Included in the nomenclature confusion is Chiari malformation, also termed Arnold-Chiari malformation named after the human analog; caudal occipital malformation syndrome (COMS) named based on an initial understanding of CLM [23]; and occipital hypoplasia based on the reduced development of the basi- and supraoccipital bone [23–26].

D. J. Marino (✉)
Department of Surgery, Long Island Veterinary Specialists, Plainview, NY, USA
e-mail: DMarino@LIVS.org

C. W. Dewey
Department of Neurology/Neurosurgery, College of Veterinary Medicine, Cornell University, Ithaca, NY, USA

R. S. Tubbs et al. (eds.), *The Chiari Malformations*, https://doi.org/10.1007/978-3-030-44862-2_46

In 2006, an international veterinary working group agreed to add the suffix "like" to the term Chiari malformation to reduce the number of variations in the veterinary literature, because dogs do not have cerebellar tonsils and the severity of the condition is not dependent on the size of the cerebellar herniation [27].

It has been found that many dogs have abnormalities in the craniocervical junction region that do not comply with traditional veterinary nomenclature [28]. These include atlanto-occipital overlapping (AOO) and dorsal constriction at the C1–C2 vertebral junction [8, 11, 12, 28–31]. Both of these abnormalities may represent the canine analog of human basilar invagination [32–39]. Finally, it has become apparent that some dogs with suspected "classical" atlantoaxial instability have other concurrent abnormalities at the craniocervical junction. Because the occipital region of the skull and the first two cervical vertebrae develop together embryologically, it makes inherent sense that multiple developmental disorders, as well as combinations of these disorders, should occur in this anatomic region in our patients, as they do in humans [35, 38–41]. For these reasons, we refer to all of these disorders under the general heading of craniocervical junction abnormalities. It has been reported, especially for reasons of surgical planning, optimal individualized patient descriptions of a craniocervical junction disorder often depend on a combination of MRI and computed tomography (CT) scans [7, 28, 42–55]. Although this section will focus on CLM and SM, it should be emphasized that the morphologic description of a particular patient's craniocervical junction abnormality is far more important than a name for that malformation.

Chiari-like malformation is believed to be the canine analog of Chiari type I malformation in people. Similar to the human disorder, the cranial cavity is too small to accommodate the contents of the caudal fossa (cerebellum and brainstem), resulting in overcrowding of the cerebellomedullary region of the brain, alterations in cerebrospinal fluid (CSF) flow, and in some dogs subsequent formation of a syrinx (Fig. 46.1) [2, 5, 23, 43, 44, 50, 56–59]. Increasing evidence suggests that CLM in dogs is a condition in which the entire skull is malformed, although the caudal aspect is the most obvious abnormality on MRI [41].

Cavalier King Charles spaniels with CLM and SM were found to have a shallower and smaller caudal/cranial fossa volumes, compared to CKCS with CLM only and other control dog breeds, that result in caudal cranial fossa overcrowding. In the CKCS, increased cerebellar size is not accommodated by increased occipital bone development. The tentorium cerebelli compensates and is found to be bulging in a rostral direction [59–61]. Brachycephalic breeds in general have earlier closure of the spheno-occipital synchondrosis; however, in the CKCS closure is even earlier. Additionally, CKCS have shorter braincases in relation to width, compared to other brachycephalic breeds, contributing to the caudal fossa overcrowding [62, 63].

The variable association of cerebellar herniation and craniocervical abnormalities with the occurrence and severity of SM portends involvement of additional anatomical abnormalities associated with CLM. Since the full pathophysiology has yet to be fully determined, a broader definition of CLM as a malformation of the skull and craniocervical junction that compromises the neural parenchyma causing pain and/or disruption of the CSF circulation, which can result in SM, has been recommended [41].

The diagnostic challenge is in recognizing fully the abnormalities associated with CLM and SM in an effort to devise a successful treatment strategy. On MRI, the abnormality of the supraoccipital bone that causes an indentation of the caudal cerebellum is often visible in dogs with CLM. In addition, an impingement of the dorsal subarachnoid space typically occurs at the level of the cervicomedullary junction.

In a recent review of MRI studies of 359 dogs (unpublished data) with CLM, 86.9% had evidence of cerebellar herniation through the foramen magnum (Fig. 46.2). Most of these dogs also have cervical SM evident on MRI (Fig. 46.3) [18, 20, 64].

Multiple mechanisms have been proposed for the formation of SM, all of which are based on the pressure differential between cranial and spinal compartments created by constriction at

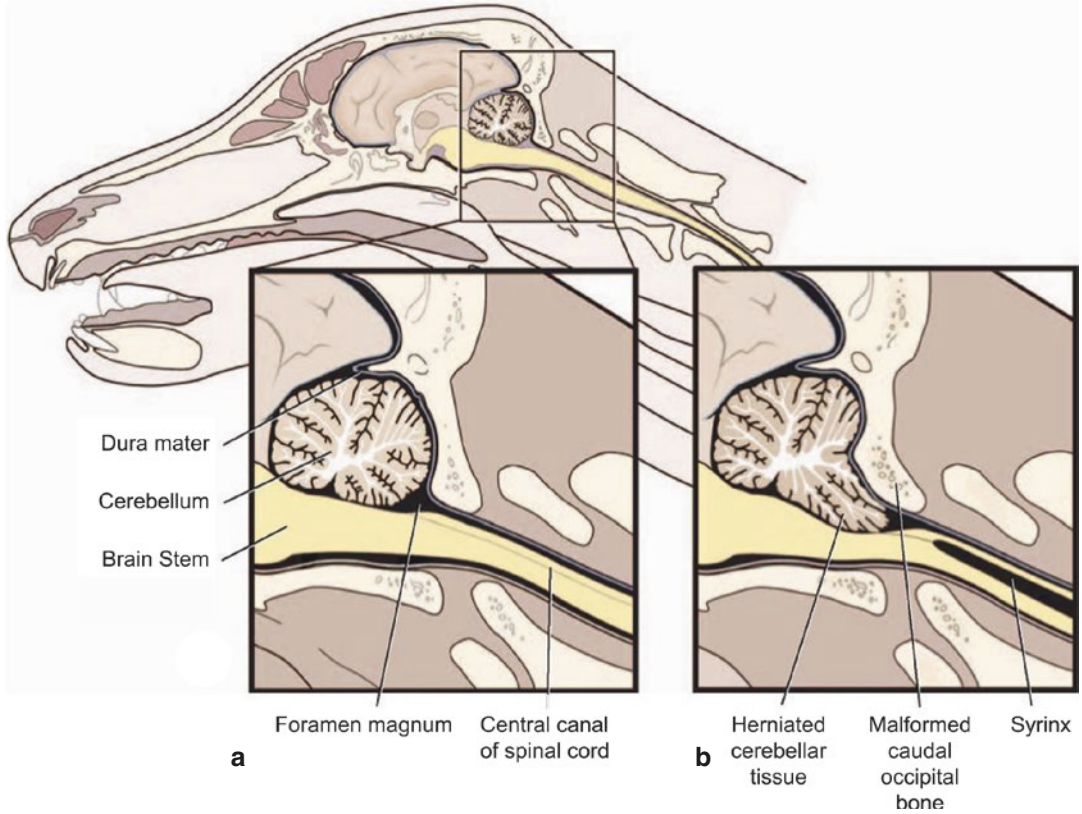

Fig. 46.1 Schematic illustration depicting normal (**a**) versus abnormal (**b**) configurations of the canine occipital/brainstem region. (Modified from Dewey et al. [23])

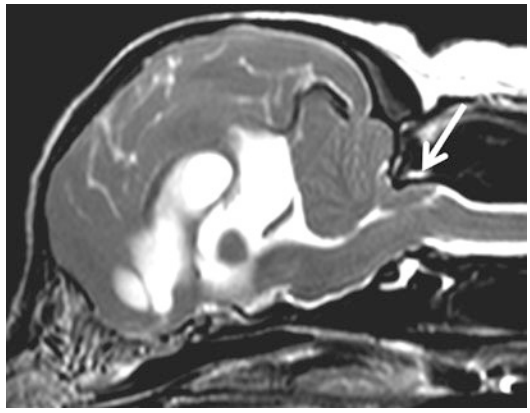

Fig. 46.2 Sagittal T2-weighted magnetic resonance image of a dog with Chiari-like malformation and cerebellar herniation through the foramen magnum (arrow)

the cervicomedullary junction [6, 10, 15–19, 41, 56, 58, 59, 65–70]. Older, probably incorrect theories assume that fluid that accumulates within the spinal cord is cerebrospinal fluid, while newer theories suggest that the syrinx fluid is actually extracellular fluid [18, 26]. The intramedullary pulse pressure hypothesis theorizes that a pressure wave is transmitted across the foramen magnum during systole that is insufficiently dissipated during diastole and that the fluid that is pushed across the craniocervical junction becomes trapped, resulting in SM [18, 71, 72]. Along with the "intramedullary pulse pressure" theory, a phenomenon called the Venturi effect has been proposed to be involved in syrinx formation. The Venturi effect is based on the phenomenon of a jet of CSF flowing from higher to lower velocity. Low pressure outside the spinal cord (cerebrospinal fluid) combines with the high pressure inside the spinal cord, leading to the spinal cord substance being pulled in an outward direction, facilitating the accumulation of fluid in the syrinx cavity. The Venturi

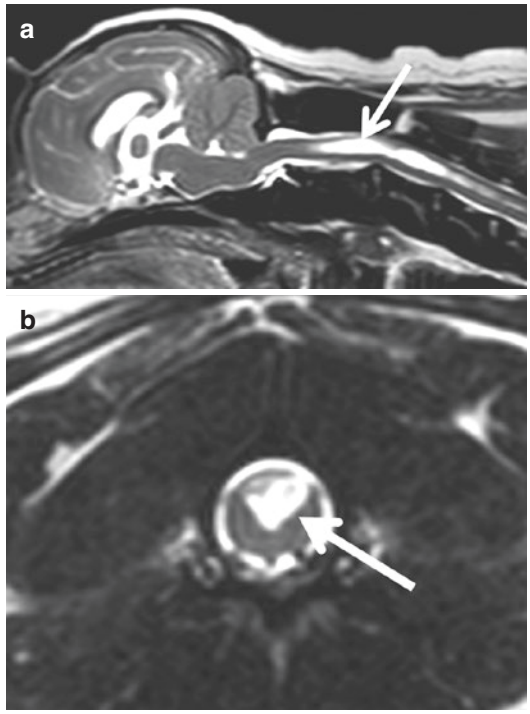

Fig. 46.3 (**a**) Sagittal and (**b**) axial T2-weighted magnetic resonance images of the cervical spine of a Chiari-like malformation depicting syringomyelia

effect has been theorized to be responsible for the formation of syringomyelia in veterinary patients in at least one report [18, 26].

We have found that of dogs that have MRI of their entire spine (i.e., not just the cervical region), most have syrinx cavities in the thoracic and lumbar spinal cord regions, in addition to the cervical region. In a recent review of MRI studies in more than 350 dogs, we found syrinx formation begins in the cervical regions and sequentially progresses to the thoracic region and finally to the lumbar region without skipping over a region (unpublished data). Others have reported similar findings [17, 18, 44, 46, 48, 53–55, 70], supporting the need for brain and full spine MRI study as a requirement for complete patient evaluations rather than financially discounted "abbreviated studies" that are typically limited to the craniocervical regions [53–55].

Chiari-like malformation is typically encountered in small-breed dogs, with the Cavalier King Charles spaniel being the most commonly encountered breed. Other breeds affected by this disorder include Brussels Griffon, miniature poodle, Yorkshire terrier, Maltese, Chihuahua, bichon frise, Staffordshire terrier, pug, Shih Tzu, miniature dachshund, miniature pinscher, French bulldog, Pekingese, and Boston terrier [3, 5, 11, 20, 23, 24, 73–78]. We have observed this disorder in several brachycephalic cats as well, which has been reported by others [79, 80]. The typical age range at presentation appears to have changed over time, with many dogs developing clinical signs within the first year of life. In general, although the age range at clinical presentation is broad, most dogs present by the time they are 4 years old. Dogs that are presented at younger than 2 years of age often have more severe clinical signs than older dogs. In recent years, we have seen an increasing number of younger patients (< 1 year of age); whether this trend reflects increasing severity of the disorder with subsequent generations, increased awareness of the veterinary community and within the general public and hence earlier diagnosis, or a combination of these factors is unknown [78].

Enlarging syrinxes cause progressive damage to the neural parenchyma through a combination of direct pressure and or ischemia. Clinical signs of CLM and SM include neck pain, back pain, vestibular dysfunction, cervical myelopathy, incessant scratching activity, lameness, diminished hearing, and scoliosis. Although clinical signs are variable, the most consistent clinical features are cervical pain and apparent pruritus of the head, neck, and shoulder regions. Cervical myelopathy (with associated neck pain) and cerebellovestibular dysfunction (e.g., strabismus, decreased menace response with normal vision, head tilt, nystagmus) have been reported [15, 18–21, 23, 78, 81–83]. In most cases, cerebellovestibular dysfunction is revealed during a neurologic examination and has not necessarily been observed by the pet owner. Many dogs with CLM will have decreased to absent menace responses with normal vision, as well as varying degrees of positional ventrolateral strabismus. An unusual and distinctive feature of the scratching activity associated with CLM in dogs is that these patients typically do not make contact with

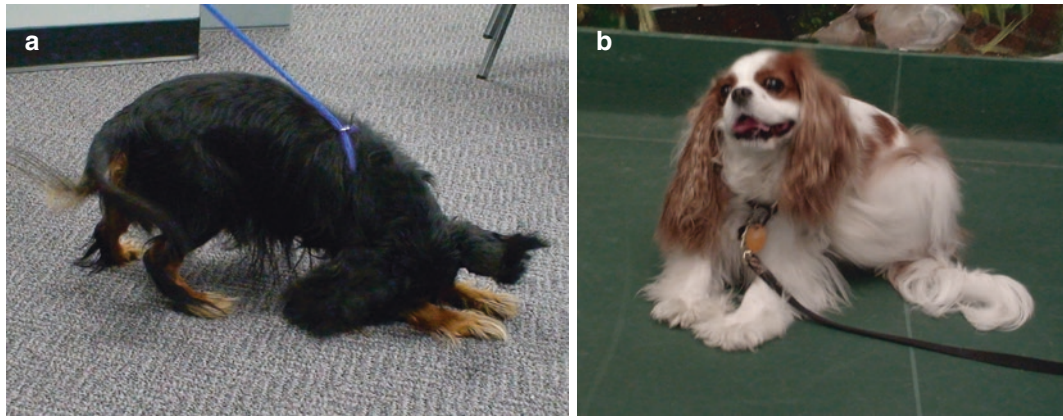

Fig. 46.4 Craniofacial pruritus is the most common clinical sign. (**a**) Rubbing face into the floor or furniture. (**b**) Using the rear limb to scratch at the craniofacial region without making contact known as "air guitar scratching"

the skin while scratching at the head and shoulder regions, so-called phantom scratching or "air guitar." Scratching often occurs on only one side. The pathogenesis of the phantom scratching (Fig. 46.4) is not well understood. It has been presumed it is a response to allodynia and part of the neuropathic pain that these dogs experience. It is possible that damage to inhibitory circuits has permitted overexpression of a hyperactive reflex. It has been established that there are spinal cord central pattern generators for scratching. Hypothetically a syrinx could lead to damage to these networks resulting in a scratch reflex when the appropriate dermatome is stimulated [15, 19, 64, 77]. Facial rubbing (pawing at the face and/or rubbing against objects) is also encountered in some dogs and is considered to be a form of pain and/or paresthesia. Spinal hyperpathia (typically cervical), scratching activity, and scoliosis are all generally believed to be related to interference of the syrinx cavity with ascending sensory pathways in the spinal cord. Pain has been positively correlated with syrinx transverse width and symmetry on the vertical axis [17, 68]. Dogs with a wider asymmetrical syrinx are more likely to experience discomfort, and dogs with a narrow symmetrical syrinx may be asymptomatic [17, 68, 84]. Pain is particularly associated with asymmetrical dorsal horn involvement [17]. Scratching activity and neck discomfort are often exacerbated by abrupt weather changes, stress, or excitement and by physical contact with the neck/shoulder region [11, 19, 23, 78]. The presence of both pain and scoliosis is correlated with syrinx width in CKCS with SM secondary to CLM [64]. Some of the neck pain may be directly related to constriction at the cervicomedullary junction or comorbid CJA [28].

Occasionally, dogs with CLM and cervical SM present with a specific variant of cervical myelopathy called central cord syndrome. In this scenario, the outwardly expanding syrinx in the cervicothoracic intumescence causes damage to the lower motor neurons of the thoracic limbs within the regional gray matter, leading to lower motor neuron paresis of the thoracic limbs, while sparing the more peripherally located white matter tracts (upper motor neurons to pelvic limbs). Damage to the regional white matter would cause general proprioceptive/upper motor neuron paresis to the pelvic limbs. The result is thoracic limb paresis (lower motor neuron in nature) that is notably worse than pelvic limb paresis. In some dogs with this syndrome, the pelvic limbs may appear normal [11, 17, 20, 21]. It is important to realize that, especially in the CKCS, other conditions may account for some or all of the clinical signs identified. It has recently been reported that more than 40% of CKCS with CLM/SM are asymptomatic for the disorder [16, 74, 85]; however, in a recent pilot study, we found that 41% of 227 dogs demonstrated clinical signs that went unrecognized by their owners [53, 54].

Idiopathic epilepsy is also a prevalent disorder in the CKCS. In one report, 32% of the CKCS with CLM had seizures [9]. Additionally, in a long-term study of 48 CKCS with syringomyelia-associated neuropathic pain and where dogs with a history of seizures had been excluded, 12.5% of the study population developed epilepsy in the follow-up period [83]. Seizures have been reported to occur in 10% to 12% of humans with Chiari type I malformation. In the authors' experience, seizure activity is an infrequent concurrent occurrence in dogs with CLM, and it remains impossible to determine whether this is due to CLM or concurrent idiopathic epilepsy.

The severity and rate of progression of CLM in dogs are variable, ranging from asymptomatic (i.e., finding evidence of CLM while imaging for some other reason) to extreme pain and debilitation with rapid worsening over a short time period. In addition, some dogs with CLM have other unrelated, concurrent disorders (e.g., disc extrusion, inflammatory brain disease) that could explain observed clinical signs [8, 11, 12, 78]. In such situations, it may be difficult to discern whether CLM is the main problem, contributory, or an incidental finding.

Finally, other CJAs can occur concurrently with or be mistaken for CLM [28]. In the authors' opinion, a complete and accurate diagnosis including identification of all types of CJA is essential for development of an effective treatment plan.

Diagnosis

The diagnosis of CLM can only be made by MRI, which is also the preferred imaging modality for diagnosing SM. Although there has been some acceptance in the veterinary community of the use of "abbreviated" MRI studies utilizing views of the head and neck region with implementation of limited imaging sequences in an effort to reduce costs, the authors believe these "cost-saving efforts" may lead to incomplete assessments of the patients and result in erroneous conclusions. At the Canine Chiari Institute (CCI) at Long Island Veterinary Specialists, all patients are assessed with a whole body (brain and full spine) 3 Tesla MRI, multi-detector CT scan, medical infrared imaging, as well as skull and cervical radiographs. On MRI, the malformation is best visualized on a midsagittal view (preferably T2-weighted), which includes the caudal fossa and the cranial cervical spinal cord. Consistent findings on MRI indicative of CLM are attenuation/obliteration of the dorsal subarachnoid space at the cervicomedullary junction and rostral displacement of the caudal cerebellum by the occipital bone [11, 20, 23, 78]. Other common MRI findings in CLM include syringomyelia (usually C2 level caudally), herniation of the caudal cerebellum through the foramen magnum, and a "kinked" appearance of the caudal medulla [23, 28]. Phase-contrast MRI (cine MRI) is often used to measure cerebrospinal fluid flow in humans with Chiari type I malformation and has recently been evaluated for use in dogs with CLM. It was found that cerebrospinal fluid flow velocity and flow pattern are useful predictors of CLM/SM in Cavalier King Charles spaniels [86].

Occasionally, dogs with MRI findings consistent with CLM will have evidence of other congenital disorders such as intracranial arachnoid (quadrigeminal) cyst, malformation/malarticulation of the C1 and/or C2 vertebra, and hydrocephalus. In the authors' opinion, most small-breed dogs normally have large lateral ventricles as a breed characteristic (ventriculomegaly) and are not truly hydrocephalic. In the absence of concurrent disease processes, cerebrospinal fluid analysis is usually normal; occasionally, a mild mononuclear pleocytosis will be apparent, however [11, 23, 78].

Although encroachment on the cerebellomedullary region by portions of the occipital bone has been the focus of many studies, evaluation of the entire skull shape and size utilizing multi-slice CT technology with three-dimensional (3D) reconstruction is currently in progress at the CCI at Long Island Veterinary Specialists to identify additional mechanisms of syrinx formation. Some reports describe a volume mismatch between the caudal fossa volume and its neural contents resulting in compression and herniation as the most common finding, while others failed

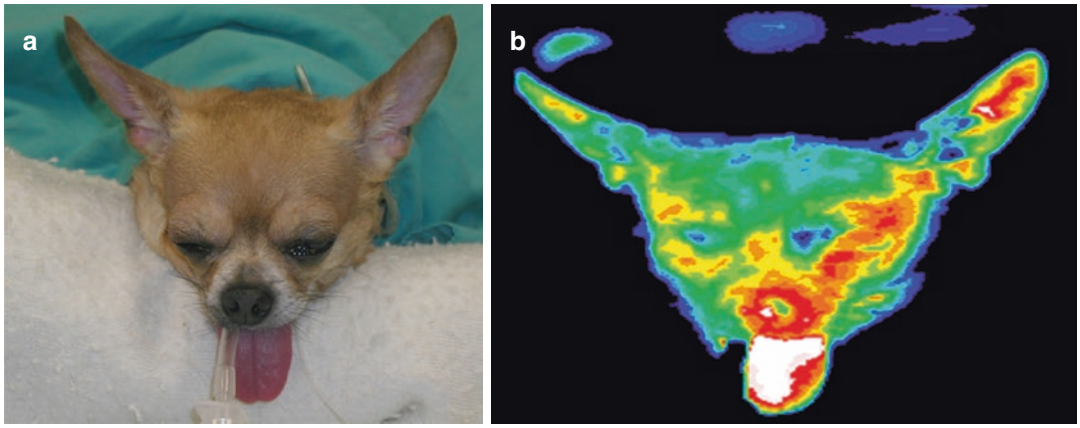

Fig. 46.5 (**a**) A dog with Chiari-like malformation and (**b**) the corresponding medical infrared imaging depicting an asymmetric thermographic pattern

to identify such a mismatch [58, 62, 87, 88]. Patients with "normal" skull volumes may have a loss of the integrity of the brain's collagenous suspensory apparatus allowing for cerebellar "slouching" into the foramen magnum and a state of craniocervical hypermobility as suspected in human patients [89]. An association of CLM and syringomyelia with absent or abnormal frontal sinus formation has been reported [90]. Although CT imaging is able to define volume or conformational abnormalities in affected patients, the clinical focus is now on correcting the flow of CSF as the malformation affects its normal passage around the brain and spinal cord leading to the syrinx formation [18, 30, 59, 66, 69, 70, 79, 86, 91–96].

Medical infrared imaging (MII) is a noninvasive imaging technique involving the recording of cutaneous thermal patterns. This imaging modality provides information about the function of the sympathetic nervous system. Because of recent advances in technology and the ability to image patients without the need for sedation, MII has potential use as a screening test for CLM in dogs. Loughin and others recently concluded a study documenting the reproducibility of image generation in normal canine limbs [97]. A current study by the same authors is attempting to establish a thermographic imaging protocol for dogs suspected of having CLM, to identify thermal imaging patterns for various regions of interest (ROI), to evaluate changes in thermal pattern, and compare the results to those of MRI findings—considered the standard for CLM in dogs [55, 98, 99]. Preliminary results revealed lower temperature thermographic patterns in dogs with abnormal MRI findings compared with a dog with a normal MRI (Fig. 46.5). Severity of compression as determined with MRI was classified as mild, moderate, and severe and was found to correlate with thermographic findings, 100%, 50%, and 0% of the time, respectively. Based on these preliminary findings, MII may be a viable imaging modality to use as a screening tool to detect CLM in dogs [53–55, 98].

Medical Therapy

Medical therapy for dogs with CLM generally falls into three categories: (1) analgesic drugs (implies relief of dysesthesia and paresthesia also), (2) drugs that decrease cerebrospinal fluid production, and (3) corticosteroid therapy. Anecdotally, the most useful drug available for relief of scratching activity associated with syringomyelia has been gabapentin (10 mg/kg body weight PO q8h).

It has been shown that neuropathic pain is accentuated over time because of upregulation of the α(alpha)2δ(delta)1 subunit of voltage-gated calcium channels in dorsal root ganglion neurons

and dorsal horn nociceptive neurons of the spinal cord. Substance P containing primary afferents plays an important part in nociception and neuropathic pain and is found concentrated in the spinal cord dorsal horn. Drugs that affect these neurons are beneficial in the management of neuropathic pain. Gabapentin and the newer gabapentin analog, pregabalin, are believed to exert their antinociceptive effects by selectively binding to the α(alpha)2δ(delta)1 subunit and inhibiting calcium influx in these neurons. Side effects of gabapentin are minimal and are usually restricted to mild sedation, pelvic limb ataxia, and weight gain [11, 19, 23, 78]. Our recent experience with pregabalin (2 to 4 mg/kg q12h) suggests that it is a more effective drug in relieving pain and scratching activity in CLM/SM dogs. Because the half-life of elimination of pregabalin is nearly twice as long as that of gabapentin, twice a day dosing is possible. It is important to start at the low end of the dose range to avoid the side effects of sedation and ataxia. Orally administered opiate drugs are sometimes helpful in alleviating neck and head pain in dogs with CLM/SM. We have had success using oral tramadol (2 to 4 mg/kg q8-12h), especially when used in conjunction with either gabapentin or pregabalin. Nonsteroidal anti-inflammatory drugs (NSAIDs) are inhibitors of cyclooxygenase-1 and/or cyclooxygenase-2. They suppress inflammatory/neuropathic pain by reducing the production of prostanoids, in particular prostaglandin E2. However, the use of NSAIDs alone is unlikely to provide satisfactory relief of neuropathic pain and is not frequently used by the authors.

Several drugs aimed at decreasing cerebrospinal fluid production have been used in dogs with CLM/SM in an effort to diminish CSF pulse pressure. All information regarding efficacy of these drugs is anecdotal. They include omeprazole (a proton pump inhibitor), acetazolamide (a carbonic anhydrase inhibitor), and furosemide (a loop diuretic). Omeprazole, a proton pump inhibitor, has been shown to decrease cerebrospinal fluid production by 26% in experimental studies when administered via the CSF in dogs [100, 101]. The oral dose for dogs is 10 mg (for dogs weighing less than 20 kg) q24h and 20 mg (for dogs weighing more than 20 kg) q24h. Acetazolamide is a carbonic anhydrase inhibitor that is used to treat glaucoma, epileptic seizures, idiopathic intracranial hypertension, altitude sickness, and cystinuria and is also classified as a diuretic. Medically it may be used to treat conditions of moderate to severe metabolic or respiratory alkalosis. It does this by interfering with bicarbonate (HCO3-) resorption in the kidneys, thereby re-acidifying the blood (and thus alkalinizing the urine). Acetazolamide is also used to decrease the production of cerebrospinal fluid in idiopathic intracranial hypertension. Long-term use of acetazolamide is often limited by adverse effects including lethargy, abdominal pain, and bone marrow suppression. Furosemide is a loop diuretic that acts on the distal tubules by abolishing the corticomedullary osmotic gradient and blocking negative as well as positive free water clearance. Its action is independent of any inhibitory effect on carbonic anhydrase or aldosterone. Due to the large NaCl absorptive capacity of the loop of Henle, diuresis is not limited by development of acidosis, as it is with the carbonic anhydrase inhibitors. When treatment decisions are made, the potential side effects of long-term corticosteroid and/or diuretic therapy should be considered, along with the questionable efficacy of this therapy. Electrolyte depletion (especially potassium) and dehydration are concerns when diuretics are used for prolonged periods, particularly when combined with corticosteroids. Corticosteroids are often used in the medical management of CLM/SM in dogs. Potential benefits include anti-inflammatory effects, decreased cerebrospinal fluid production, and decreased substance P (a nociceptive neurotransmitter) expression in spinal cord dorsal horn neurons. An initial anti-inflammatory dosage of 0.5 mg/kg PO q12h is often effective in controlling clinical signs. This dose should be tapered, if at all possible, to an every other day schedule within the first month of therapy. In most cases of CLM/SM, medical therapy will diminish the severity of clinical signs, but resolution is unlikely [11, 20, 22, 78]. It is the authors' opinion that medical therapy should be viewed as a temporary

treatment "bridge" until more definitive therapy, such as surgical decompression with cranioplasty, to restore normal CSF flow can be performed.

Surgical Treatment

We consider CLM/SM to be a surgical disorder. In our opinion, based on more than 400 operated cases, the preferred surgical procedure for treatment of CLM in dogs is foramen magnum decompression (FMD) with cranioplasty utilizing titanium mesh and polymethyl methacrylate (PMMA). This procedure involves a suboccipital craniotomy, dorsal laminectomy of C1, and removal of the cranial 20% of the dorsal spinous process of C2, with subsequent placement of a titanium mesh/PMMA plate on titanium screw anchor posts inserted around the circumference of the occipital bone defect.

For the foramen magnum decompression procedure, the dog is placed in sternal recumbency with the neck flexed (Fig. 46.6). The dorsal aspect of the head and neck is shaved from the level of the bregma to the level of the third or fourth cervical vertebra, with a width approximately equal to the width of the atlas. A dorsal midline incision is made extending from approximately 1 cm rostral to the external occipital protuberance to the middle of the second cervical vertebra. The superficial dorsal cervical musculature is separated at the median raphe, exposing the underlying biventer cervicis muscles (Fig. 46.7). The paired biventer cervicis muscles are then separated on midline, exposing the rectus capitis dorsalis muscles. The caudal aspects of the rectus capitis dorsalis muscles are removed from the cranial half of C2, using sharp dissection and periosteal elevation; these muscles are then split on midline. The cranial aspects of the rectus capitis dorsalis muscles are sharply incised from the nuchal crest, exposing the caudal portion of the occiput and the arch of the atlas. Hemorrhage is controlled with bipolar electrocautery. A high-speed air drill with a 3- to 4-mm-diameter round drill bit and Lempert rongeurs are used to remove a portion of the occiput and the dorsal aspect of the first cervical vertebra (Fig. 46.8). The dorsal arch of C1 and the cranial 20% of the dorsal spinous process of C2 are routinely removed.

The meninges (dura/arachnoid) are incised on midline, and the meningeal tissue in the region of the foramen magnum decompression is resected. Care is taken to identify and resect the fibrous constriction frequently found at the time of the

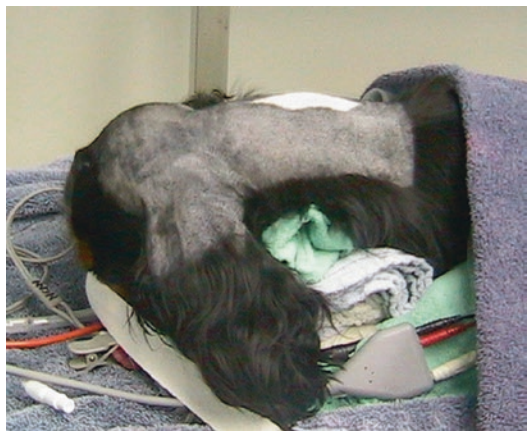

Fig. 46.6 Proper positioning of the head and neck for foramen magnum decompression in a dog with Chiari-like malformation. (Reprinted with permission from Dewey et al. [20])

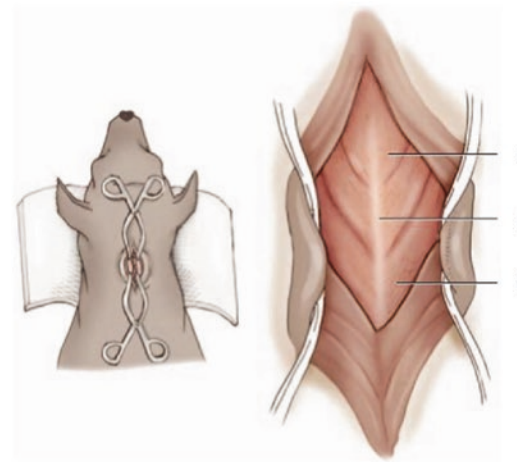

Fig. 46.7 Illustration of the initial surgical approach for foramen magnum decompression in dogs with Chiari-like malformation. (A) Occipitalis muscle; (B) median raphe; (C) cervicoscutularis and cervicoauricularis superficialis muscles

dural resection (Fig. 46.9). Five guide holes are drilled in the occipital bone around the periphery of the skull defect, using a 1.1 mm drill bit. Self-tapping 6-mm-length (1.5-mm-width) screws are inserted into the guide holes for an approximate depth of 2 to 3 mm (Fig. 46.10).

The dog's head is then released from the flexed position and is repositioned at a normal resting angle. The skull plate is fashioned using titanium mesh and PMMA and is fixed to the back of the skull, using the titanium screw heads as anchor posts for the PMMA (Fig. 46.11). The titanium mesh and PMMA "plate" is shaped

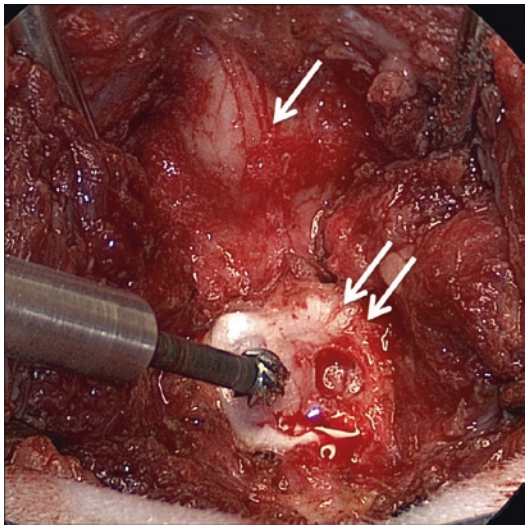

Fig. 46.8 A high-speed air drill with a 3- to 4-mm-diameter round drill bit and Lempert rongeurs are used to remove a portion of the occiput (single arrow) and the dorsal aspect of the first cervical vertebra (double arrow)

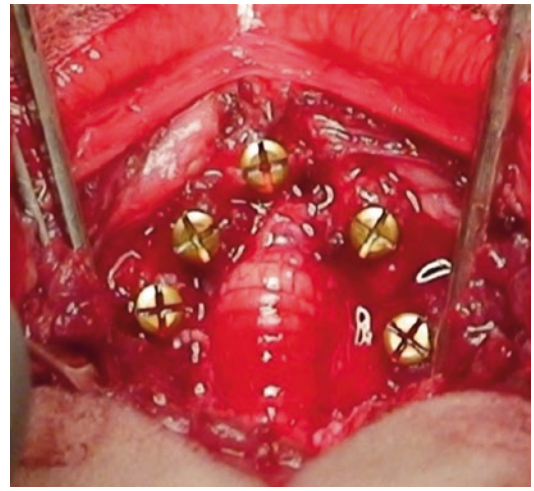

Fig. 46.10 Self-tapping 6-mm-length (1.5-mm-width) titanium screws are inserted into the guide holes for an approximate depth of 2 to 3 mm surrounding the decompression site

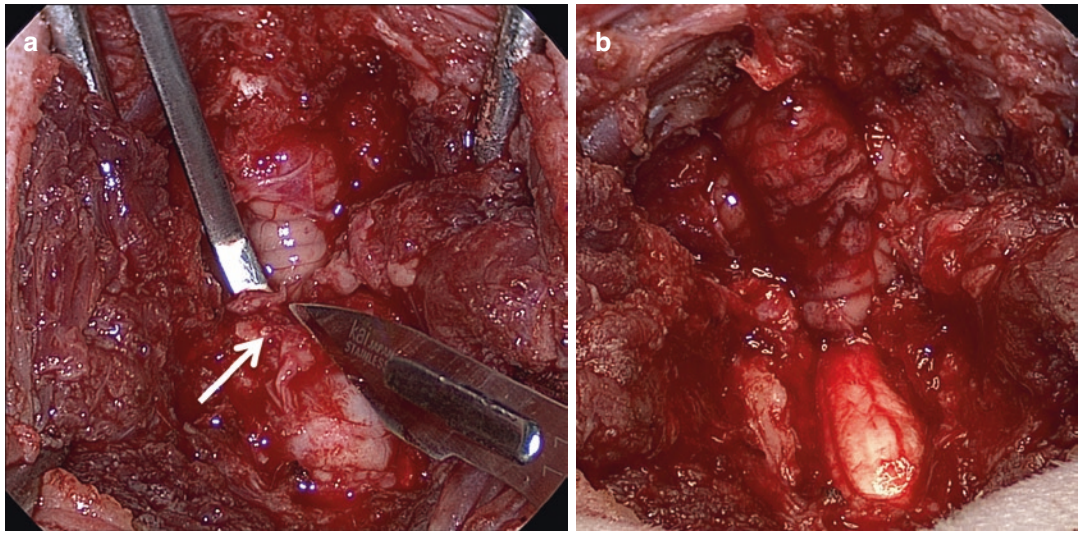

Fig. 46.9 Care is taken to (**a**) identify and (**b**) resect the fibrous constriction (arrow) frequently found at the time of the dural resection

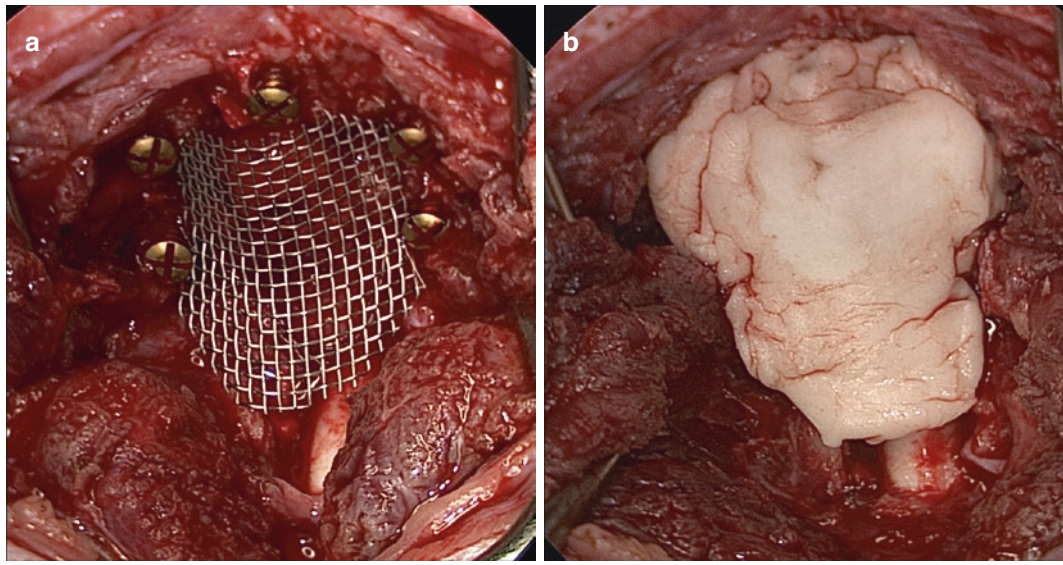

Fig. 46.11 (**a**) The skull plate is fashioned using titanium mesh and polymethyl methacrylate (PMMA) and is fixed to the back of the skull, (**b**) using the titanium screw heads as anchor posts for the PMMA

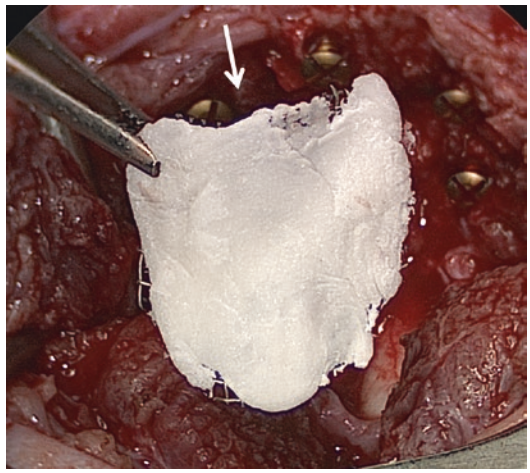

Fig. 46.12 The titanium mesh and polymethyl methacrylate "plate" are shaped somewhat like a guitar pick, with the wide end of the pick toward the occiput (arrow)

somewhat like a guitar pick, with the wide end of the pick toward the occiput (Fig. 46.12). Only a thin layer of PMMA is applied to the outer surface of the titanium mesh to form the plate, with some PMMA extending beyond the edges of the titanium mesh to adhere to the titanium screw heads. The caudal aspect of the plate is made to extend slightly over the dorsal defect of C1; the tail aspect of the plate is curved dorsally to avoid impinging on the medulla or the cranial cervical spinal cord. Prior to routine closure, a locally harvested fat graft is placed between the distal edge of the cranioplasty mesh and the C2 dorsal lamina. Proper plate application is confirmed via radiography or (preferably) CT scan (Fig. 46.13) [20, 21].

The short-term surgical success (sustained improvement in neurologic status and/or pain/scratching relief) rate with foramen magnum decompression in dogs with CLM is found to be approximately 80%, whether or not adjunctive cranioplasty is performed [3, 20, 21]. One report found an inverse relationship between the length of time clinical signs were present before surgical intervention and the extent of postoperative improvement [20]. Unfortunately, a disease relapse rate ranging from 25% to 47% has been reported among cases treated with foramen magnum decompression alone; most of these relapses are suspected to be due to excessive postoperative scar tissue formation at the foramen magnum decompression site [3, 21].

The authors and colleagues developed the cranioplasty procedure (based on a similar procedure used in human foramen magnum decompression surgery) to discourage excessive postoperative scar tissue from recompressing the

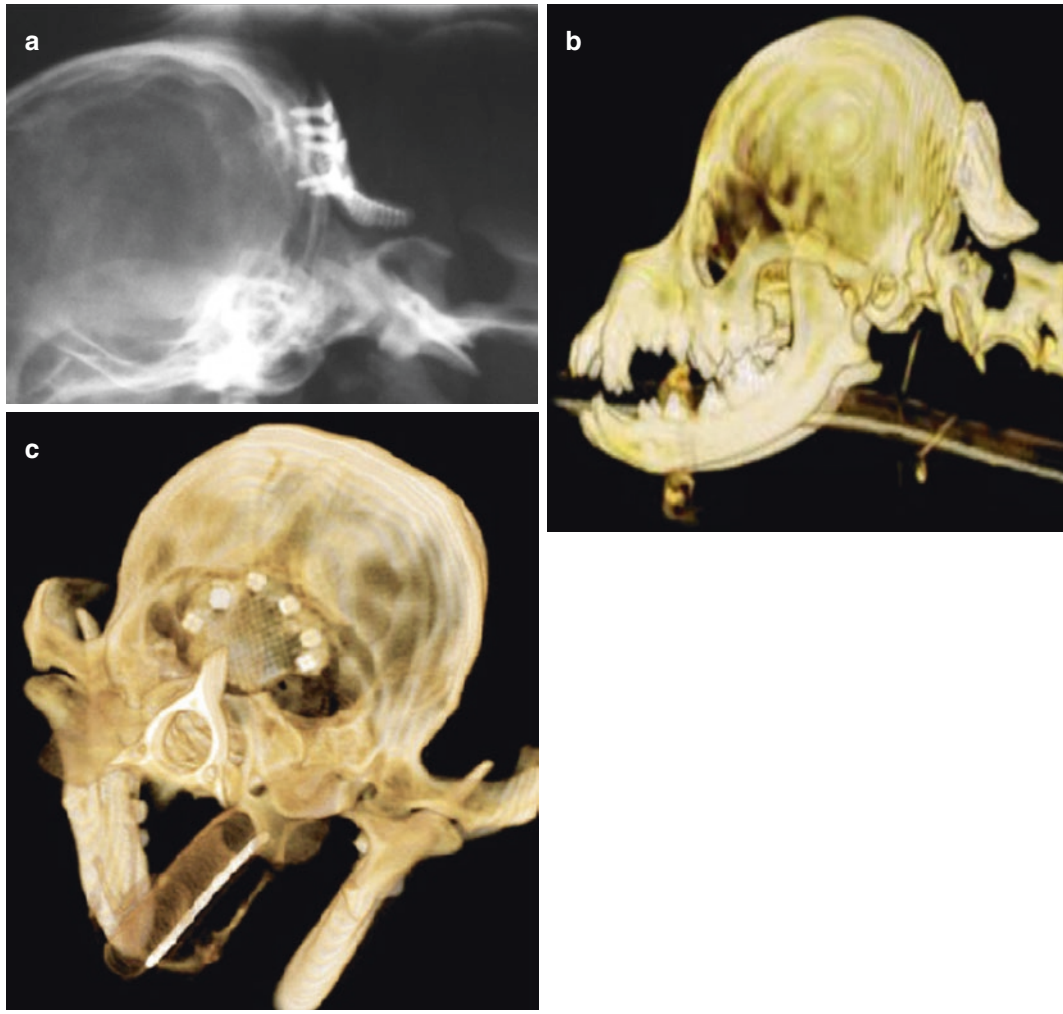

Fig. 46.13 Proper plate application is confirmed via (**a**) radiography or preferably (**b**, **c**) computed tomography scan

operative site. Our initial report suggested a dramatic reduction in the reoperative rate due to scar tissue formation after the cranioplasty procedure was instituted, but this was based on only 21 cases, with about a 1-year follow-up period [21]. In our most recent analysis of more than 400 cases of foramen magnum decompression with cranioplasty, the reoperative rate was less than 1% (unpublished data). In our recent long-term follow-up study of CKCS having FMD and cranioplasty, 103/115 dogs (89.5%) had an improved or static quality of life (QOL) score. The median time to maximum improvement after surgery was 4 months (range 3–12 months) (unpublished data). Historically, recommendations by veterinary neurologists and neurosurgeons have been made to avoid surgery because of the poor long-term success of "surgery" and lack of syrinx resolution, which have been based on reports grouping various surgical techniques performed at different institutions, with scant follow-up information in small numbers of patients with short follow-up duration [3, 6, 16, 67, 74, 75, 83, 102, 103]. In previous reports, 35–81% of dogs were still on medication after surgery to maintain quality of life [3, 20–23, 73, 78, 102–104]. In our recent long-term follow-up study of CKCS having FMD and cranioplasty, 52.4% of dogs did not require any medications to maintain quality of life, while only 47.6% needed intermittent

medications to maintain quality of life according to their owners (unpublished data). These findings are similar to results in human patients with CM after surgical decompression [105–107] and improved from previous report [3, 6, 16, 67, 74, 75, 83, 102, 103]. We found that with the median time between surgery and the last MRI performed being 23.5 months (12–102 months), at the last MRI, the syrinx diameter and length was decreased in 48.6%, static in 33.6%, and increased in 7.5% of the dogs after FMD and cranioplasty. Of the dogs with a decrease in syrinx size, 15.4% had complete resolution of the syrinx (unpublished data). The results of our recent long-term follow-up study are significantly improved from previous reports but are derived from a specific technique: FMD with titanium mesh cranioplasty, performed regularly by a consistent neurosurgical team, in a larger cohort of dogs, with longer follow-up intervals.

Most dogs with CLM/SM will respond favorably to medical therapy, although in many cases this response is temporary. In one group of ten CLM/SM dogs treated medically, five dogs were euthanized within 2 years because of disease progression and diminished responsiveness to therapy [23]. In another study, 36% of CLM/SM dogs treated medically were euthanized at a mean of 1.7 years from the time of diagnosis because of clinical signs of their disease [78]. Although the surgical success rate is favorable for CLM/SM in dogs, the recurrence rate due to excessive postoperative scar tissue formation has been unacceptably high with foramen magnum decompression without cranioplasty. It appears that cranioplasty has improved the success rate of foramen magnum decompression and is currently the recommended procedure by the authors for dogs with CLM/SM exhibiting clinical signs.

Primary Secretory Otitis Media

Most dogs with CLM/SM having foramen magnum decompression and cranioplasty are routinely relieved of clinical signs; however, with some, scratching activity tends to persist. Primary secretory otitis media (PSOM), a common cause of scratching, is the canine analog of otitis media with effusion (OME) in human patients. In a recent study of 120 dogs with CLM, 38.7% of dogs had PSOM [108]. There was a significant difference between the prevalence of PSOM in CKCS (46%) and non CKCS (13%); $p < 0.0001$. Pharyngeal "slouching" associated with brain stem dysfunction in patients with CLM may result in closure or narrowing of the Eustachian tube. The resultant pressure gradient between the middle ear and pharynx is theorized to cause the accumulation of mucus in the middle ear. Affected dogs have a mucus plug in the tympanic cavity that causes the tympanic membrane to bulge. The mucus plug is most evident on MRI (Fig. 46.14). Treatment recommendations for dogs with PSOM include myringotomy and flush/aspiration. A 25–30% recurrence of PSOM has been found within 6 months with the myringotomy and flush/aspiration techniques [108, 109]. Efforts should be made to ascertain whether PSOM is present concurrent with CLM/SM given the prevalence of comorbid disease and appropriate treatment measures instituted. Dogs with recurrent clinical signs after surgery for CLM/SM should be evaluated for PSOM before concluding surgery is deemed a failure.

Atlanto-Occipital Overlapping

An abnormality at the craniocervical junction in small- and toy-breed dogs has recently been described, called atlanto-occipital overlapping (AOO) [11–13]. In this malformation, the atlas (C1) is cranially displaced into the foramen magnum, and overlap of the occipital bone and the atlas occurs. This displacement tends to compress the caudal aspect of the cerebellum and to elevate and compress the caudal medulla (medullary kinking). Atlanto-occipital overlapping is likely a form of basilar invagination. Basilar invagination is a human craniocervical junction disorder in which the atlas and/or the axis (C2) telescopes toward the foramen magnum [38, 110]. We have seen this disorder as a sole entity and in combination with CLM and/or

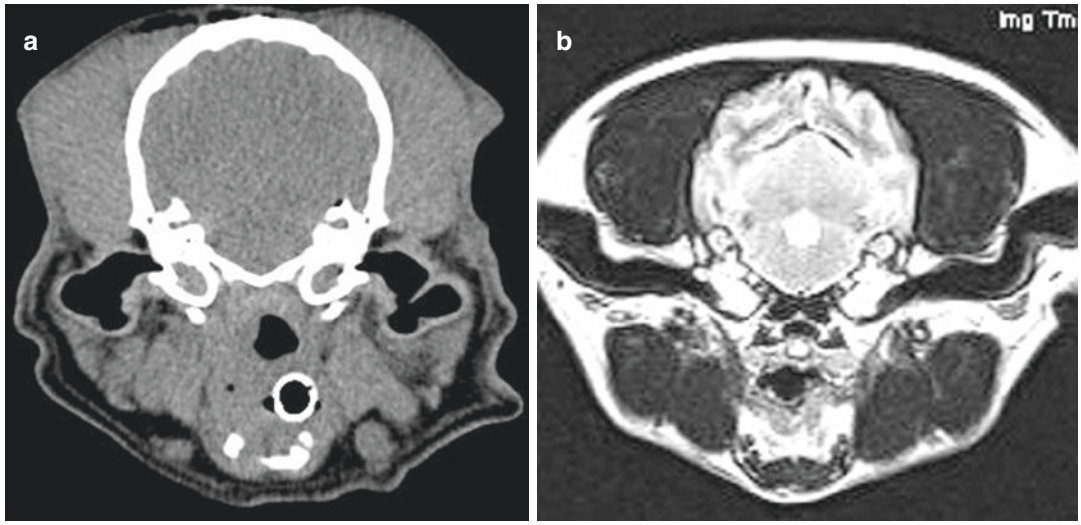

Fig. 46.14 Primary secretory otitis media (PSOM) can be identified on (**a**) computed tomography scan or (**b**) magnetic resonance imaging within the tympanic bullae

atlantoaxial instability. Syringomyelia has been associated with atlanto-occipital overlapping, whether as a sole malformation or as part of several craniocervical malformations in the same patient [7, 8, 12, 29, 111, 112]. Because bony detail is difficult to distinguish on MRI, it is likely that AOO has been underdiagnosed in dogs, with most of these patients incorrectly ascribed a diagnosis of CLM. The precise nature of this and other craniocervical malformations is typically apparent on CT imaging (Fig. 46.15). We routinely follow MRI of craniocervical junction abnormalities with CT imaging to fully evaluate the malformation or malformations in the region.

Clinical signs in dogs with atlanto-occipital overlapping typically include neck pain and varying degrees of ataxia of all four limbs [11–13]. An insufficient number of cases of atlanto-occipital overlapping have been reported in the literature to allow general recommendations concerning therapy. We have found that most dogs with this malformation, similar to dogs with CLM/SM, will respond temporarily to medical management. In a recent review of medical records of 70 dogs with AOO, all dogs have responded to decompression as described in the treatment of CLM (unpublished data). In a recent report, surgical stabilization for relief of clinical signs was reported [13]. At surgery, the compressive mass appears to be soft tissue, possibly due to compensatory ligamentous hypertrophy secondary to chronic instability. We believe that this disorder is also a manifestation of instability at the C1–C2 junction, possibly a form of basilar invagination similar to the atlanto-occipital overlapping problem. This can occur as a sole entity or in combination with CLM and/or atlantoaxial instability. In cases of combined CLM/atlantoaxial instability and C1–C2 dorsal constriction, the authors have pursued combined ventral and dorsal approaches to surgically address both issues (Fig. 46.16). As with atlanto-occipital overlapping in dogs, the optimal treatment strategy for dorsal constriction at C1–C2 has not yet been established. However, because of its compressive nature, we believe that this is most likely a surgical disease.

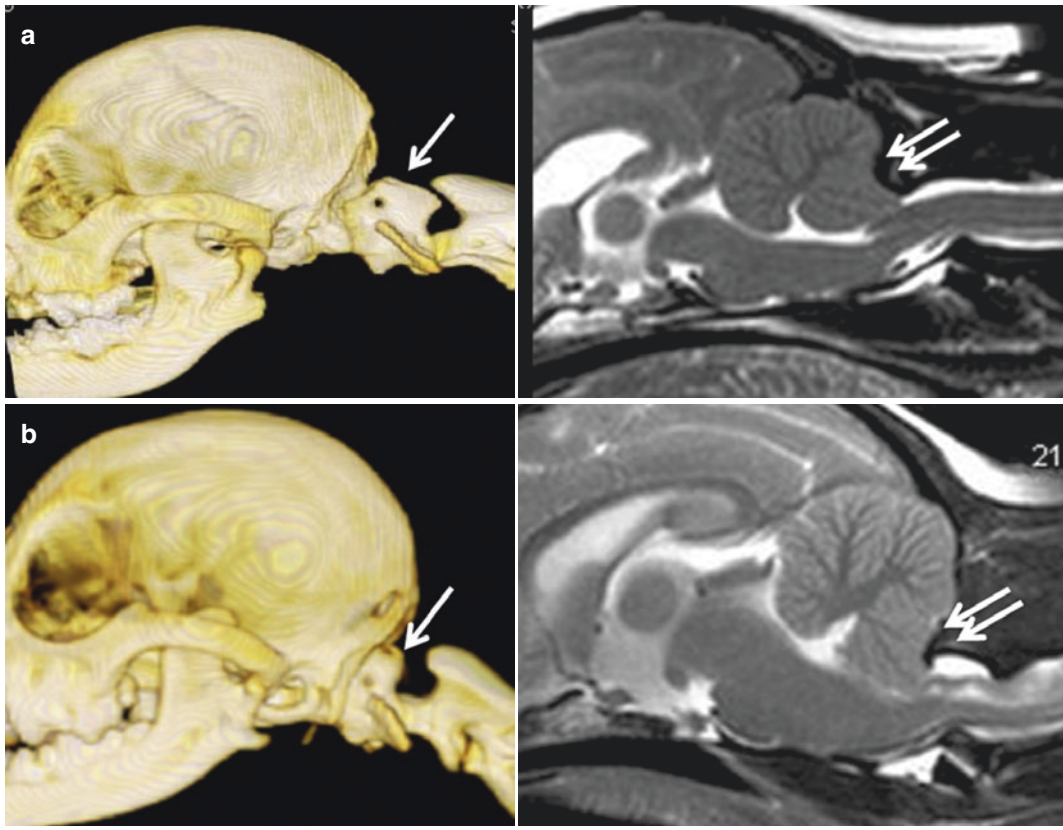

Fig. 46.15 (**a**) A dog with Chiari-like malformation with computed tomography imaging in conjunction with magnetic resonance imaging demonstrating a normal position of the C1 vertebra (single arrow) and broad cerebellar compression (double arrow). (**b**) Compared with a dog with atlanto-occipital overlap revealing the position of the C1 vertebra within the caudal fossa (single arrow) and a linear type compression of the cerebellum (double arrow)

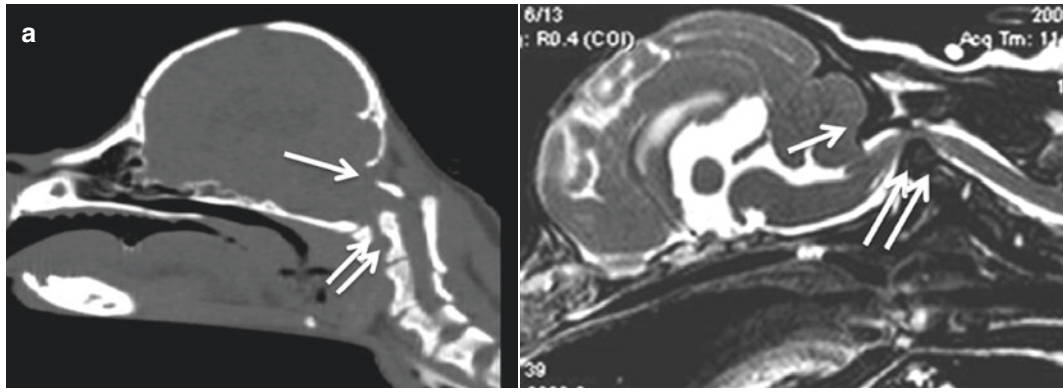

Fig. 46.16 (**a**) A 1 kg dog with Chiari-like malformation and atlanto-occipital overlap with preoperative computed tomography (CT) (top) and magnetic resonance imaging (MRI) (bottom) depicting cerebellar compression (single arrow) and craniocervical instability (double arrow). (**b**) Postoperative CT (top) and radiographic (bottom) imaging depicting cerebellar decompression with cranioplasty (single arrow) and craniocervical stabilization (double arrow)

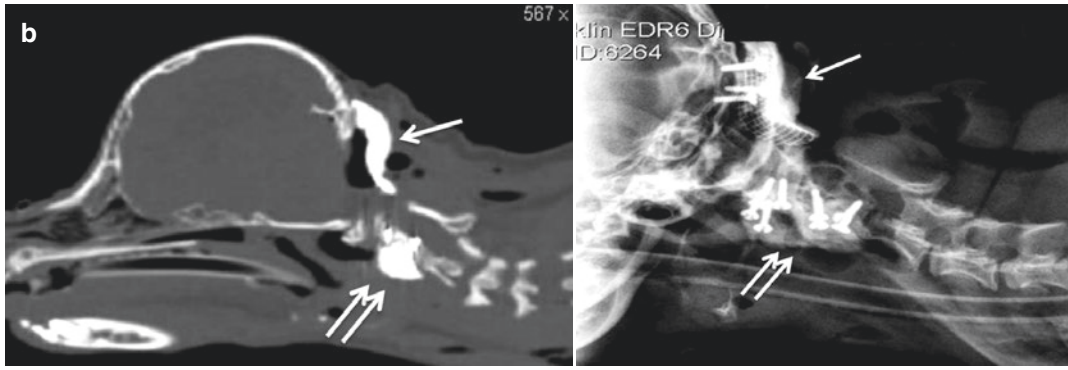

Fig. 46.16 (continued)

References

1. Bynevelt M, Rusbridge C, Britton J. Dorsal dens angulation and a Chiari type malformation in a cavalier king Charles spaniel. Vet Radiol Ultrasound. 2000;41(6):521–4.
2. Rusbridge C. Neurological diseases of the cavalier king Charles spaniel. J Small Anim Pract. 2005;46(6):265–72.
3. Rusbridge C. Chiari-like malformation with syringomyelia in the cavalier king Charles spaniel: long-term outcome after surgical management. Vet Surg. 2007;36(5):396–405.
4. Rusbridge C, Knowler P, Rouleau GA, Minassian BA, Rothuizen J. Inherited occipital hypoplasia/syringomyelia in the cavalier king Charles spaniel: experiences in setting up a worldwide DNA collection. J Hered. 2005;96(7):745–9.
5. Rusbridge C, Knowler SP, Pieterse L, McFadyen AK. Chiari-like malformation in the griffon Bruxellois. J Small Anim Pract. 2009;50(8):386–93.
6. Rusbridge C, MacSweeny JE, Davies JV, Chandler K, Fitzmaurice SN, Dennis R, et al. Syringohydromyelia in cavalier king Charles spaniels. J Am Anim Hosp Assoc. 2000;36(1):34–41.
7. Marino DJ, Loughin CA, Dewey CW, Marino LJ, Sackman JJ, Lesser ML, et al. Morphometric features of the craniocervical junction region in dogs with suspected Chiari-like malformation determined by combined use of magnetic resonance imaging and computed tomography. Am J Vet Res. 2012;73(1):105–11.
8. Cerda-Gonzalez S, Olby NJ, McCullough S, Pease AP, Broadstone R, Osborne JA. Morphology of the caudal fossa in cavalier king Charles spaniels. Vet Radiol Ultrasound. 2009;50(1):37–46.
9. Lu D, Lamb CR, Pfeiffer DU, Targett MP. Neurological signs and results of magnetic resonance imaging in 40 cavalier king Charles spaniels with Chiari type 1-like malformations. Vet Rec. 2003;153(9):260–3.
10. Freeman AC, Platt SR, Kent M, Huguet E, Rusbridge C, Holmes S. Chiari-like malformation and syringomyelia in American Brussels griffon dogs. J Vet Intern Med. 2014;28(5):1551–9.
11. Cerda-Gonzalez S, Dewey CW. Congenital diseases of the craniocervical junction in the dog. Vet Clin North Am Small Anim Pract. 2010;40(1):121–41.
12. Cerda-Gonzalez S, Dewey CW, Scrivani PV, Kline KL. Imaging features of atlanto-occipital overlapping in dogs. Vet Radiol Ultrasound. 2009;50(3):264–8.
13. Dewey CW C-GS, Scrivani PV, et al. Surgical stabilization of a craniocervical junction abnormality with atlanto-occipital overlapping in a dog. Comp Cont Educ Pract Vet. in press.
14. Rusbridge C, Knowler SP. Coexistence of occipital dysplasia and occipital hypoplasia/syringomyelia in the cavalier king Charles spaniel. J Small Anim Pract. 2006;47(10):603–6.
15. Rusbridge C. Canine syringomyelia: a painful problem in man's best friend. Br J Neurosurg. 2007;21(5):468–9.
16. Parker JE, Knowler SP, Rusbridge C, Noorman E, Jeffery ND. Prevalence of asymptomatic syringomyelia in cavalier king Charles spaniels. Vet Rec. 2011;168(25):667.
17. Rusbridge C, Carruthers H, Dube M, Holmes M, Jeffrey N. Syringomyelia in cavalier king Charles spaniels: the relationship between syrinx dimensions and pain. J Small Anim Pract. 2007;48:432–6.
18. Rusbridge C, Greitz D, Iskandar BJ. Syringomyelia: current concepts in pathogenesis, diagnosis, and treatment. J Vet Intern Med. 2006;20(3):469–79.
19. Rusbridge C, Jeffery ND. Pathophysiology and treatment of neuropathic pain associated with syringomyelia. Vet J. 2008;175(2):164–72.
20. Dewey CW, Berg JM, Barone G, Marino DJ, Stefanacci JD. Foramen magnum decompression for treatment of caudal occipital malformation syndrome in dogs. J Am Vet Med Assoc. 2005;227(8):1270–5, 50-1.
21. Dewey CW, Marino DJ, Bailey KS, Loughin CA, Barone G, Bolognese P, et al. Foramen magnum

decompression with cranioplasty for treatment of caudal occipital malformation syndrome in dogs. Vet Surg. 2007;36(5):406–15.
22. Dewey CWBJ, Barone G, et al. Treatment of caudal occipital malformation syndrome in dogs by foramen decompression. J Vet Intern Med. 2005;19(3):418.
23. Dewey CWBJ, Stefanacci JD, Barone G, Marino DJ. Caudal occipital malformation syndrome in dogs. Compend Contin Educ Pract Vet. 2004;26(11):886–95.
24. Rusbridge C, Knowler SP. Hereditary aspects of occipital bone hypoplasia and syringomyelia (Chiari type I malformation) in cavalier king Charles spaniels. Vet Rec. 2003;153(4):107–12.
25. Rusbridge C, Knowler SP. Inheritance of occipital bone hypoplasia (Chiari type I malformation) in cavalier king Charles spaniels. J Vet Intern Med. 2004;18(5):673–8.
26. Rusbridge C, Flint G. Nomenclature. Syringomyelia: Springer; 2014. p. 301–9.
27. Cappello R, Rusbridge C. Report from the Chiari-like malformation and Syringomyelia working group round table. Vet Surg. 2007;36(5):509–12.
28. Marino DJLC, Dewey CW, Marino LJ, Sackman J. Morphometric features of the cranioceervical junction region in dogs with suspected Chiari-Like Malformation Based on Combined MR and CT imaging: 274 cases (2007-2010). AJVR. 2011.
29. Cerda-Gonzalez S, Olby NJ, Griffith EH. Longitudinal study of the relationship among Craniocervical morphology, clinical progression, and Syringomyelia in a cohort of cavalier king Charles spaniels. J Vet Intern Med. 2016;30(4):1090–8.
30. Cerda-Gonzalez S, Olby NJ, Griffith EH. Dorsal compressive atlantoaxial bands and the craniocervical junction syndrome: association with clinical signs and syringomyelia in mature cavalier king Charles spaniels. J Vet Intern Med. 2015;29(3):887–92.
31. Cerda-Gonzalez S, Olby NJ, Griffith EH. Medullary position at the craniocervical junction in mature cavalier king charles spaniels: relationship with neurologic signs and syringomyelia. J Vet Intern Med. 2015;29(3):882–6.
32. Botelho RV, Bittencourt LR, Rotta JM, Tufik S. Polysomnographic respiratory findings in patients with Arnold-Chiari type I malformation and basilar invagination, with or without syringomyelia: preliminary report of a series of cases. Neurosurg Rev. 2000;23(3):151–5.
33. Botelho RV, Neto EB, Patriota GC, Daniel JW, Dumont PA, Rotta JM. Basilar invagination: craniocervical instability treated with cervical traction and occipitocervical fixation. Case Rep J Neurosurg. 2007;7(4):444–9.
34. Goel A. Treatment of basilar invagination by atlantoaxial joint distraction and direct lateral mass fixation. J Neurosurg. 2004;1(3):281–6.
35. Goel A. Craniovertebral anomalies: role for craniovertebral realignment. Neurol India. 2004;52(4):427–9.
36. Goel A. Progressive basilar invagination after transoral odontoidectomy: treatment by atlantoaxial facet distraction and craniovertebral realignment. Spine. 2005;30(18):E551–5.
37. Goel A, Achawal S. The surgical treatment of Chiari malformation association with atlantoaxial dislocation. Br J Neurosurg. 1995;9(1):67–72.
38. Goel A, Bhatjiwale M, Desai K. Basilar invagination: a study based on 190 surgically treated patients. J Neurosurg. 1998;88(6):962–8.
39. Goel A, Sharma P. Craniovertebral junction realignment for the treatment of basilar invagination with syringomyelia: preliminary report of 12 cases. Neurol Med Chir. 2005;45(10):512–7. discussion 8
40. Goel A, Desai KI, Muzumdar DP. Atlantoaxial fixation using plate and screw method: a report of 160 treated patients. Neurosurgery. 2002;51(6):1351–6; discussion 6-7.
41. Knowler SP, Galea GL, Rusbridge C. Morphogenesis of canine Chiari malformation and secondary Syringomyelia: disorders of cerebrospinal fluid circulation. Front Vet Sci. 2018;5:171.
42. Rusbridge C, Stringer F, Knowler S. Clinical application of diagnostic imaging of Chiari-like malformation and syringomyelia. Front Vet Sci. 2018;5(280).
43. Marino D. Foramen magnum decompression with Cranioplasty for the treatment of Chiari-like malformations in dogs. Int Symp Syringomyelia Pro. 2007.
44. Marino D. Chiari like malformation and Syringomyelia in dogs. Am Coll Vet Surg Symp Pro. 2008.
45. Marino D. Chiari like malformation in dogs. Am Coll Vet Surg Symp Pro. 2009.
46. Marino D. Syringomyelia in Dogs. Am Coll Vet Surg Symp Pro. 2009.
47. Marino D. Advances in assessing Chiari-like malformation. Am Coll Vet Surg Symp Pro. 2010.
48. Marino D. Chiari-like malformation and Syringomyelia in dogs. Current Concepts, North American Veterinary Conference proceedings. 2011.
49. Marino D. Chiari-like malformation: the scratching dog only a neurosurgeon can help. North Am Vet Dermatol Forum Pro. 2011.
50. Marino D. Morphometric Features of the Craniocervical Junction Region in Dogs with Suspected Chiari-like Malformation 274 Cases (2007-2010). Am Coll Vet Int Med Forum Pro. 2011.
51. Marino D. Medical infrared imaging (thermography) as a screening modality in dogs with Chiari-like malformation. Am Coll Vet Inter Med Forum Pro. 2011.
52. Marino D. Intractable Pruritus; The Chiari-like Malformation. 7th World Congress of Veterinary Dermatology Forum. 2012.
53. Marino DJ, Editor Chiari-like malformation and syringomyelia in dogs. American College of Veterinary Surgeons Symposium. San Diego, CA; 2008.
54. Marino DJ, editor Chiari-like malformation in dogs. American College of Veterinary Surgeons Symposium. Washington, D.C.; 2009.

55. Marino DJ, editor Advances in assessing Chiari-like malformation. American College of Veterinary Surgeons Symposium. Seattle, WA; 2010.
56. Shaw TA, McGonnell IM, Driver CJ, Rusbridge C, Volk HA. Increase in cerebellar volume in cavalier king Charles spaniels with Chiari-like malformation and its role in the development of syringomyelia. PLoS One. 2012;7(4):e33660.
57. Cross HR, Cappello R, Rusbridge C. Comparison of cerebral cranium volumes between cavalier king Charles spaniels with Chiari-like malformation, small breed dogs and Labradors. J Small Anim Pract. 2009;50(8):399–405.
58. Driver CJ, Rusbridge C, McGonnell IM, Volk HA. Morphometric assessment of cranial volumes in age-matched cavalier king Charles spaniels with and without syringomyelia. Vet Rec. 2010;167(25):978–9.
59. Driver CJ, Rusbridge C, Cross HR, McGonnell I, Volk HA. Relationship of brain parenchyma within the caudal cranial fossa and ventricle size to syringomyelia in cavalier king Charles spaniels. J Small Anim Pract. 2010;51(7):382–6.
60. Carrera I, Dennis R, Mellor DJ, Penderis J, Sullivan M. Use of magnetic resonance imaging for morphometric analysis of the caudal cranial fossa in cavalier king Charles spaniels. Am J Vet Res. 2009;70(3):340–5.
61. Shaw TA, McGonnell IM, Driver CJ, Rusbridge C, Volk HA. Caudal cranial fossa partitioning in cavalier king Charles spaniels. Vet Rec. 2013;172(13):341.
62. Schmidt MJ, Neumann AC, Amort KH, Failing K, Kramer M. Cephalometric measurements and determination of general skull type of cavalier king Charles spaniels. Vet Radiol Ultrasound. 2011;52(4):436–40.
63. Schmidt MJ, Volk H, Klingler M, Failing K, Kramer M, Ondreka N. Comparison of closure times for cranial base synchondroses in mesaticephalic, brachycephalic, and cavalier king Charles spaniel dogs. Vet Radiol Ultrasound. 2013;54(5):497–503.
64. Rusbridge C, Carruthers H, Dube MP, Holmes M, Jeffery ND. Syringomyelia in cavalier king Charles spaniels: the relationship between syrinx dimensions and pain. J Small Anim Pract. 2007;48(8):432–6.
65. Greitz DFO. Modern concepts of syringomyelia. Riv Neuroradiol. 2004;17:360–1.
66. Carruthers H, Rusbridge C, Dube MP, Holmes M, Jeffery N. Association between cervical and intracranial dimensions and syringomyelia in the cavalier king Charles spaniel. J Small Anim Pract. 2009;50(8):394–8.
67. Driver CJ, Volk HA, Rusbridge C, Van Ham LM. An update on the pathogenesis of syringomyelia secondary to Chiari-like malformations in dogs. Vet J. 2013;198(3):551–9.
68. Hu HZ, Rusbridge C, Constantino-Casas F, Jeffery N. Histopathological investigation of syringomyelia in the cavalier king Charles spaniel. J Comp Pathol. 2012;146(2–3):192–201.
69. Lewis T, Rusbridge C, Knowler P, Blott S, Woolliams JA. Heritability of syringomyelia in cavalier king Charles spaniels. Vet J. 2010;183(3):345–7.
70. Loderstedt S, Benigni L, Chandler K, Cardwell JM, Rusbridge C, Lamb CR, et al. Distribution of syringomyelia along the entire spinal cord in clinically affected Cavalier King Charles Spaniels. Vet J. 2011.
71. Greitz D. Unraveling the riddle of syringomyelia. Neurosurg Rev. 2006;29(4):251–63; discussion 64.
72. Milhorat TH, Capocelli AL Jr, Kotzen RM, Bolognese P, Heger IM, Cottrell JE. Intramedullary pressure in syringomyelia: clinical and pathophysiological correlates of syrinx distension. Neurosurgery. 1997;41(5):1102–10.
73. Dewey CRC. Treatment of canine Chiari-like malformation and syringomyelia. In: Bongura J, editor. Kirk's current veterinary therapy. XIV: Saunders Elsevier; 2008. p. 1102–7.
74. Harcourt-Brown TR, Campbell J, Warren-Smith C, Jeffery ND, Granger NP. Prevalence of Chiari-like malformations in clinically unaffected dogs. J Vet Intern Med. 2015;29(1):231–7.
75. Hechler AC, Moore SA. Understanding and treating Chiari-like malformation and Syringomyelia in dogs. Top Companion Anim Med. 2018;33(1):1–11.
76. Knowler SP, McFadyen AK, Freeman C, Kent M, Platt SR, Kibar Z, et al. Quantitative analysis of Chiari-like malformation and syringomyelia in the griffon Bruxellois dog. PLoS One. 2014;9(2):e88120.
77. Rusbridge C. Chiari-like malformation and syringomyelia. Eur J Comp Anim Pract. 2013;23:70–89.
78. Rusbridge C, Dewey C. Treatment of canine Chiari-like malformation and syringomyelia. In: Bonagura J, Twedt D, editors. Kirk's current veterinary therapy. XIV. Philadelphia: Saunders; 2009. p. 1102.
79. Bagley R, Gavin P, Silver G, et al. Syringomyelia and hydromyelia in dogs and cats. Compend Contin Educ Pract Vet. 2000;22(5):471–9.
80. Minato S, Baroni M. Chiari-like malformation in two cats. J Small Anim Pract. 2017.
81. Aghakhani N, Parker F, David P, Morar S, Lacroix C, Benoudiba F, et al. Long-term follow-up of Chiari-related syringomyelia in adults: analysis of 157 surgically treated cases. Neurosurgery. 2009;64(2):308–15. discussion 15
82. Dones J, De Jesus O, Colen CB, Toledo MM, Delgado M. Clinical outcomes in patients with Chiari I malformation: a review of 27 cases. Surg Neurol. 2003;60(2):142–7; discussion 7-8.
83. Plessas IN, Rusbridge C, Driver CJ, Chandler KE, Craig A, McGonnell IM, et al. Long-term outcome of cavalier king Charles spaniel dogs with clinical signs associated with Chiari-like malformation and syringomyelia. Vet Rec. 2012;171(20):501.
84. Hu HZ, Rusbridge C, Constantino-Casas F, Jeffery N. Distribution of substance P and calcitonin gene-related peptide in the spinal cord of cavalier king Charles spaniels affected by symptomatic syringomyelia. Res Vet Sci. 2012;93(1):318–20.

85. Couturier J, Rault D, Cauzinille L. Chiari-like malformation and syringomyelia in normal cavalier king Charles spaniels: a multiple diagnostic imaging approach. J Small Anim Pract. 2008;49(9):438–43.
86. Cerda-Gonzalez S, Olby NJ, Broadstone R, McCullough S, Osborne JA. Characteristics of cerebrospinal fluid flow in cavalier king Charles spaniels analyzed using phase velocity cine magnetic resonance imaging. Vet Radiol Ultrasound. 2009;50(5):467–76.
87. Cross H, Cappello R, Rusbridge C. Comparison of cerebral cranium volumes between cavalier king Charles spaniels with Chiari-like malformation, small breed dogs and Labradors. J Small Anim Pract. 2009;50:399–405.
88. Schmidt MJ, Biel M, Klumpp S, Schneider M, Kramer M. Evaluation of the volumes of cranial cavities in cavalier king Charles spaniels with Chiari-like malformation and other brachycephalic dogs as measured via computed tomography. Am J Vet Res. 2009;70(4):508–12.
89. Milhorat TH, Bolognese PA, Nishikawa M, McDonnell NB, Francomano CA. Syndrome of occipitoatlantoaxial hypermobility, cranial settling, and chiari malformation type I in patients with hereditary disorders of connective tissue. J Neurosurg. 2007;7(6):601–9.
90. Scrivani PV, Thompson MS, Winegardner KR, Dewey CW, Scarlett JM. Association between frontal-sinus size and syringohydromyelia in small-breed dogs. Am J Vet Res. 2007;68(6):610–3.
91. Bhadelia RA, Bogdan AR, Wolpert SM, Lev S, Appignani BA, Heilman CB. Cerebrospinal fluid flow waveforms: analysis in patients with Chiari I malformation by means of gated phase-contrast MR imaging velocity measurements. Radiology. 1995;196(1):195–202.
92. Lee JHLH, Kim JK, et al. CSF flow quantification of the cerebral aqueduct in normal volunteers using phase contrast cine MR imaging. Korean J Radiol. 2004;5(2):81–6.
93. Panigrahi M, Reddy BP, Reddy AK, Reddy JJ. CSF flow study in Chiari I malformation. Childs Nerv Syst. 2004;20(5):336–40.
94. C R. Canine syringomyelia: a painful problem in man's best friend. Br J Neurosurg. 2007;21(5):468–9.
95. Churcher RK, Child G. Chiari 1/syringomyelia complex in a king Charles spaniel. Aust Vet J. 2000;78(2):92–5.
96. Driver CJ, Watts V, Bunck AC, Van Ham LM, Volk HA. Assessment of cerebellar pulsation in dogs with and without Chiari-like malformation and syringomyelia using cardiac-gated cine magnetic resonance imaging. Vet J. 2013;198(1):88–91.
97. Loughin CA, Marino DJ. Evaluation of thermographic imaging of the limbs of healthy dogs. Am J Vet Res. 2007;68(10):1064–9.
98. Marino DJ. Medical infrared imaging (thermography) as a screening modality in dogs with Chiari-like malformation. Denver, CO: American College of Veterinary Internal Medicine Forum; 2011.
99. Marino DJ. Medical infrared imaging (thermography) in veterinary neurology. Chicago, IL: American College of Veterinary Surgeons; 2011.
100. Javaheri S, Corbett WS, Simbartl LA, Mehta S, Khosla A. Different effects of omeprazole and Sch 28080 on canine cerebrospinal fluid production. Brain Res. 1997;754(1–2):321–4.
101. Lindvall-Axelsson M, Nilsson C, Owman C, Winbladh B. Inhibition of cerebrospinal fluid formation by omeprazole. Exp Neurol. 1992;115(3):394–9.
102. Ortinau N, Vitale S, Akin EY, Beasley M, Shores A. Foramen magnum decompression surgery in 23 Chiari-like malformation patients 2007-2010: outcomes and owner survey results. Can Vet J. 2015;56(3):288–91.
103. Vermeersch K, Van Ham L, Caemaert J, Tshamala M, Taeymans O, Bhatti S, et al. Suboccipital craniectomy, dorsal laminectomy of C1, durotomy and dural graft placement as a treatment for syringohydromyelia with cerebellar tonsil herniation in cavalier king Charles spaniels. Vet Surg. 2004;33(4):355–60.
104. Motta L. Does medical therapy influence the size of the syrinx in dogs with Chiari-like malformation/syringohydromyelia complex? J Small Anim Pract. 2016;57(5):278.
105. Tubbs RS, Beckman J, Naftel RP, Chern JJ, Wellons JC 3rd, Rozzelle CJ, et al. Institutional experience with 500 cases of surgically treated pediatric Chiari malformation type I. J Neurosurg Pediatr. 2011;7(3):248–56.
106. Tisell M, Wallskog J, Linde M. Long-term outcome after surgery for Chiari I malformation. Acta Neurol Scand. 2009;120(5):295–9.
107. Valentini L, Visintini S, Saletti V, Chiapparini L, Estienne M, Solero CL. Treatment for Chiari 1 malformation (CIM): analysis of a pediatric surgical series. Neurol Sci. 2011.
108. Marino DJ, Loughin CA. Treatment of primary secretory otitis media (PSOM) with myringotomy in dogs with Chiari-like malformation: 21 dogs (28 bullae) with 24 month follow up. Galviston, TX: North American Dermatology Forum; 2011.
109. Stern-Berthholtz W, Sjostrom L, Wallin HN. Primary secretory otitis media in the cavalier king Charles spaniel: a review of 61 cases. J Small Anim Pract. 2003;44:253–6.
110. Pearce JM. Platybasia and basilar invagination. Eur Neurol. 2007;58(1):62–4.
111. Crockard HA, Stevens JM. Craniovertebral junction anomalies in inherited disorders: part of the syndrome or caused by the disorder? Eur J Pediatr. 1995;154(7):504–12.
112. Dewey CW, Marino DJ, Loughin CA. Craniocervical junction abnormalities in dogs. N Z Vet J. 2013;61(4):202–11.

Experimental Models of Chiari Malformations

47

Kyung Hyun Kim, Ji Yeoun Lee, Ki-Bum Sim, Seung-Ki Kim, and Kyu-Chang Wang

Introduction

Chiari malformation (CM) is defined as the downward displacement of the cerebellar tonsil through the foramen magnum greater than 5 mm. It is not a fixed condition but a dynamic condition. Therefore, the term "malformation" is not adequate for this entity.

Traditionally CM is classified as type I (CM I) or type II (CM II) according to the presence of associated spinal open neural tube defect (ONTD) and the downward displacement of the brain stem and fourth ventricle.

Morphological characteristics of CM are basically a discrepancy between the size or shape of the bony posterior fossa and its contents. In CM II, the degree of discrepancy is more profound and leads to a downward displacement of the brain stem and fourth ventricle in addition to the cerebellar tonsillar herniation and hydrocephalus, which is caused by overcrowding at the area of the fourth ventricular outlet [1].

Experimental models of CM are valuable for understanding its etiology and pathophysiology as well as evaluating the effects of treatment.

In this chapter, the theoretical directions to developing experimental models for CM according to the etiologic background are described. In addition, animal spinal ONTD models and computational models, which are currently most commonly used, are discussed in detail.

Etiology of Chiari Malformation

As mentioned previously, the basic common feature of CM is smaller size of the bony posterior fossa compared to its contents or focal upward deformation of foramen magnum.

For understanding the majority of causative lesions, the following aspects should be noted:

- Among the skull vault bones, the occipital bone is formed earlier than others. The growth of the cerebellum occurs later than other parts of the brain. Therefore, if a small occipital bone is formed in the late fetal period and early infancy, the cerebellum, which grows later, may overgrow the capacity of the bony posterior fossa, making tight subarachnoid

K. H. Kim · J. Y. Lee · K.-C. Wang (✉)
Division of Pediatric Neurosurgery, Seoul National University Children's Hospital and Neural Development and Anomaly Laboratory (NDAL), Department of Anatomy and Cell Biology, Seoul National University College of Medicine, Seoul, South Korea
e-mail: kcwang@snu.ac.kr

K.-B. Sim
Department of Neurosurgery, Jeju National University College of Medicine, Jeju, South Korea

S.-K. Kim
Division of Pediatric Neurosurgery, Seoul National University Children's Hospital, Seoul, South Korea

R. S. Tubbs et al. (eds.), *The Chiari Malformations*, https://doi.org/10.1007/978-3-030-44862-2_47

space and herniation of the contents through the openings of posterior fossa.

- The normal skull bone grows according to the size of its contents if the bone is not involved in intrinsic bone disease such as metabolic disorders. Therefore, if the volume of the posterior fossa content is decreased for reasons such as a cerebrospinal fluid (CSF) leak in the late fetal period and early infancy, the occipital bone is formed small.

A series of events shown below may lead to CM and hydrocephalus in CM II [2].

1. CSF leak.
2. Decreased volume of posterior fossa contents.
3. Small bony posterior fossa.
4. Late growth spurt of cerebellum in the already formed small bony posterior fossa.
5. Overcrowding of posterior fossa.
6. Effacement of CSF pathway in the posterior fossa leading to hydrocephalus or displacement of the posterior fossa contents, mainly cerebellum, through the opening of posterior fossa.

If the bony posterior fossa is formed or is small due to reasons other than CSF leak, then the same sequence of steps occur.

If the degree of posterior fossa crowding is less, then hydrocephalus does not follow.

In other words, the causative lesions of downward displacement (compared to the level of foramen magnum) of the cerebellar tonsils can be classified as follows:

1. Small posterior fossa made in young age.
   A. Abnormal bone growth as the primary bone pathology.
      - Focal upward deviation of bones surrounding foramen magnum such as platybasia or basilar invagination.
      - Bilateral lambdoid suture craniosynostosis.
      - Other bone diseases with abnormal growth.
   B. Abnormal bone growth as the result of other reasons.
      - CSF leak (myelomeningocele or CSF shunting state).
2. Increased posterior fossa content.
   - Posterior fossa space-occupying lesion (usually called a "tonsillar herniation" rather than "CM" and excluded in this chapter).

Experimental Models for Chiari Malformation

Models for CM may be developed according to different pathogenesis. Currently, animal models that have causative elements of CM are used for this purpose. Among the pathogenic mechanisms of CM, only CSF leak is a common feasible target of experimental animal modeling; most spinal ONTDs with CM II are used whether they are genetic, chemical/nutritional, or surgical. CSF diversion early in animal life may be another option, but it has not been widely pursued experimentally.

Although pathogenic mechanisms are not involved, computational models for investigation of fluid dynamic analysis are used for understanding of pathophysiology of CM, mostly CM I, and for expecting outcome of the treatments. The advantage of computational modeling is the isolated control of specific elements. The influence of one factor can be investigated though a theoretical rather than real-life condition. The disadvantage is that it may not accurately simulate a real-life event in spite of laborious computerized simulation. Frequently in the live condition, each factor is interrelated to other factors, and currently investigators cannot simulate all of these aspects in computer modeling. In the future, however, artificial intelligence (AI) technology may develop a computational model much closer to the live condition.

Experimental Animal Models: Spinal Open Neural Tube Defect Models

Spinal ONTD is associated with CM in animals as well as in humans, although it only represents

CM II. Any type of animal spinal ONTD model—whether genetic, chemical/nutritional, or surgical—models CM II. The advantages and disadvantages of each model are described in Table 47.1 [3].

Genetic Models

Genetic models have long been used for research on CM II [4–7], and recent advances in gene analysis and gene manipulation techniques suggest further development in this field. The advantages of genetic models are that the CM is rather natural and not artificial, and it is relatively constant in incidence and morphology in contrast to the chemical/nutritional and surgical models. However, the causal relationship between the spinal ONTD and CM is not as clear as it is unclear in the chemical/nutritional model. One basic error may cause both spinal ONTD and CM. On the other hand, the causal relationship is clear in the surgical model. In addition, the effects of genetic mutation may be not limited to the neural tissue.

Among mutant mouse models, the curly tail mouse and splotch mouse models are most widely used. Representative rodent genetic spinal ONTD models are listed in Table 47.2 [3], and the associated CM is shown in Fig. 47.1 [1].

Chemical/Nutritional Models

There are many teratogens and nutrient deprivations used to induce spinal ONTD in experimental animals (Table 47.3). However, the incidence and phenotypes in spinal ONTD are variable according to the teratogen used and the dose and timing of the administration compared to the genetic and surgical models. As in genetic models, the causal relationship between the spinal ONTD and CM is not clear, and the teratogenic effects are not limited to the neural tissue. Sometimes it is not easy to differentiate spinal

Table 47.1 Advantages and disadvantages of different models for spinal open neural tube defects (ONTDs)

Model category	Advantages	Disadvantages
Genetic models	Spontaneous origin Characteristic features resembling human ONTD Gene manipulation Investigation of environmental factors Constant location of lesion	Multifactorial inheritance Incomplete penetrance High prenatal loss Cannibalism after birth Limited availability Sophisticated maintenance Various lesions
Chemical/nutrient models	Study of molecular mechanism of various chemical/nutrients on ONTD Failure of primary neurulation Short-acting teratogen Possible to pinpoint developmental stage and cell population	High and early prenatal loss Diverse phenotypes according to animal strains Diverse different anomalies in the same animal Systemic cytotoxic effects Long period of dietary treatment
Surgical models	No systemic and cytotoxic effect Establishment of stereotyped surgical procedure Feasibility of in utero or in ovo creation and repair of ONTD Control of lesioning: Timing, location, and size of initial defect Control of time of therapeutic procedure after lesioning Analysis of the causal relationship between the ONTD and associated anomalies Evaluation of secondary effect of mechanical or chemical trauma on lesion Study on fetal therapy Practice of surgical techniques	Not a replication of human ONTD Not a primary defect in neurulation High mortality Long pregnancy duration Technical difficulties such as preterm labor, needs of special facilities and team High cost in large animals

Reprinted by permission from Sim et al. [3]

Table 47.2 Representative genetic models classified according to the response to folate, methionine, and inositol

Characteristics of models	Rodent genetic mutants
Folate-responsive models	Splotch, cart1, cited2, crooked tail
Folate-resistant models	Curly tail, axial defects, ephrin-A5 knockout
Models not classified by response to folate	Loop tail, circle tail, trisomy for chromosomes 12 and 14, homozygous celsr1, shrm, pax3sp
Methionine-responsive model	Axial defects
Methionine-exacerbated model	Splotch
Inositol-responsive model	Grhl3ct

Reprinted by permission from Sim et al. [3]

Table 47.3 Representative chemical/nutritional agents for spinal open neural tube defect (ONTD) models according to animals

Animals	Chemical/nutritional agents
Mouse	Acetaldehyde, copper, cadmium, arsenic, neurotropic drugs, valproic acid, methotrexate, fumonisin B1, cytochalasins D and E, insulin, papaverine, tunicamycin, xylocaine, 5-bromodeoxyuridine, phospholipase C, high glucose and ketone bodies, phenytoin
Rat	Vitamin A, N-methyl N-nitrosourea, trypan blue, thiadiazole, maternal hyperglycemia
Hamster	Aliphatic nitriles, vitamin A, clofibrate, sodium arsenate, dimethyl sulfoxide
Chick	Alpha-methyltyrosine, insulin, phleomycin, papaverine, diazepam, cytochalasin B, caffeine, local anesthetics, colchicine, beta mercaptoethanol, concanavalin A, streptomyces hyaluronidase, aminopterin, retinoic acid, trypan blue, cyclopamine, jervine, spermine, 1,5-hexanedion, high glucose, tetanus toxin

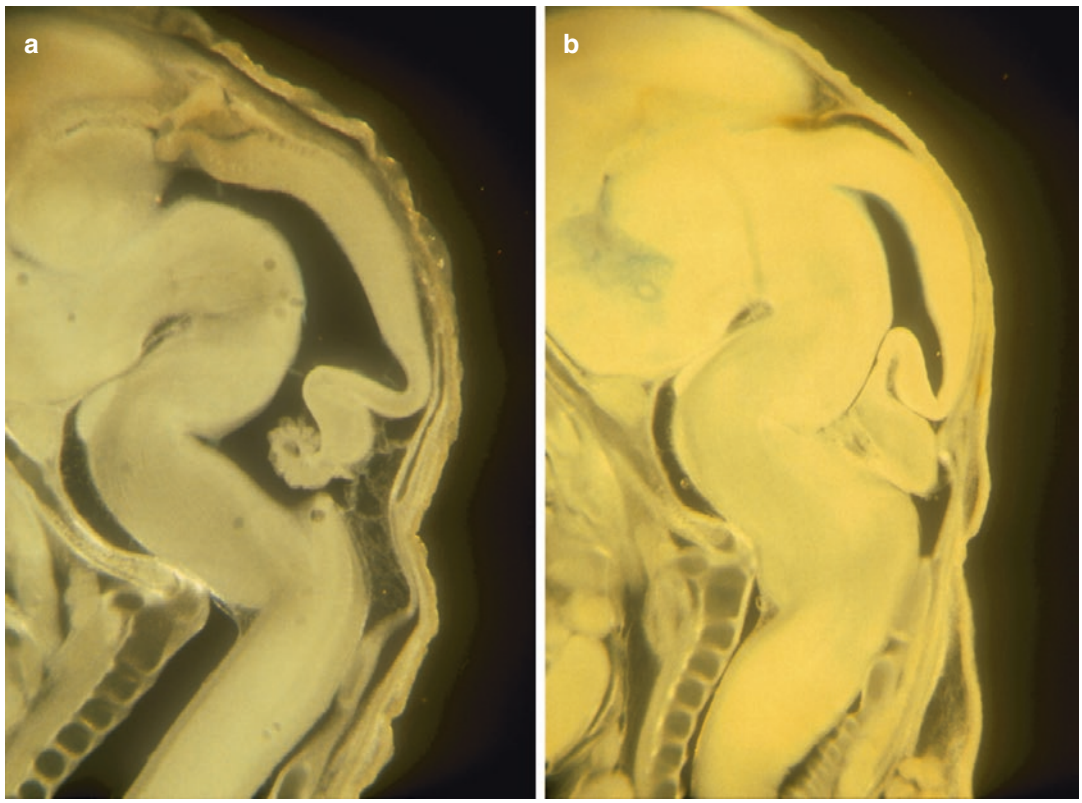

Fig. 47.1 C57BL/6J normal mouse brains on embryonic day 16 (**a**) and a delayed splotch mouse with a spinal open neural tube defect (ONTD) (**b**). Compared to the control, the embryo with spinal ONTD shows a smaller posterior cranial fossa and narrowing of the fourth ventricle and subarachnoid space (**a**, **b**: x 32). (Reprinted with permission from Wang et al. [1])

ONTD from toxin-induced delayed development of the spinal cord. Moreover, the effects of teratogens are different according to the species and genetic background of each individual animal, even if the species is the same. Nevertheless, CM is associated with spinal ONTD once the spinal ONTD is formed, no matter what the teratogen is and how the chemicals or nutrients are manipulated.

Excessive retinoic acid and folate deficiency are the representative chemical/nutritional models.

Chemical models are used for evaluation of therapies just as surgical models are used. Recently, Al-Shanafey et al. [8] used a mouse retinoic acid model to show that both the CM and injury to the exposed spinal cord are progressive during gestation, suggesting protective roles of preterm delivery. Dionigi et al. [9] administered mesenchymal stem cells via trans-amniotic route in a rat retinoic acid model and reported minimized CM II formation.

Surgical Models

Spinal ONTD can be induced by in utero laminectomy and dural opening with or without myelotomy in large animals, and by in utero or in ovo incision of the dorsal part of the neural tube. In spite of the fact that the surgical induction of spinal ONTD is absolutely artificial, it has the advantage that researchers can make lesions at the location, the time, and of the extent as they want. The time at the occurrence of ONTD is clear.

However, they have to consider spontaneous recovery of spinal ONTD during the fetal period, as well as surgical mortality and morbidity depending on the animal species, location, timing, and extent of the lesions made. Moreover, not all of the spinal ONTD animals are associated with CM. Guilbaud et al. [10] made a fetal spinal ONTD in lambs and found that only half of those with spinal ONTD showed CM after birth. They emphasized that the presence of CM should be evaluated by sonography at the time of prenatal repair to evaluate the efficacy of prenatal repair of spinal ONTD on outcome regarding prevention of CM. The degree of CM is also dependent on the time of evaluation. For example, Fontecha et al. [11] used a rabbit fetal surgical model and reported that early birth revealed decreased severity of the CM II.

When the surgery is performed in an early embryonic period, the surgery itself may induce other malformations. In contrast to the genetic and chemical/nutritional models, however, the initial teratogenic insults tend to be limited to the surgical area, and the causal relationship between the spinal ONTD and CM is evident when CM is present, especially if the surgery is performed in the late prenatal period. An example of CM induced by the surgical opening of neural tubes in chick embryos is shown in Fig. 47.2 [12].

In surgical models, because the presence and location of the spinal ONTD is expected to be correct even long after surgery (more so than in genetic or chemical/nutritional models), prenatal surgical management can be performed more adequately, and the detailed evaluation of its therapeutic effects is more feasible. Actually, the surgical model has provided the preclinical background of current practice of fetal surgery for human myelomeningocele, which showed beneficial results in preventing or ameliorating the formation of CM.

The animals and techniques used for the surgical models are listed in Table 47.4 [3, 10, 13–29].

Other Animal Models

Models for spinal and cranial ONTDs using other methods such as hyperthermia or radiation have been tried [30–32]. However, they were used for investigation of teratogenic effects of insults rather than research on the pathophysiology or management outcome of spinal ONTD, including effects on CM.

Computational Experimental Models for Chiari Malformation

In spite of the limited value as a tool for research, CM is a representative disease in which CSF flow dynamics are rigorously investigated with computational methods. Peak flow velocities, pres-

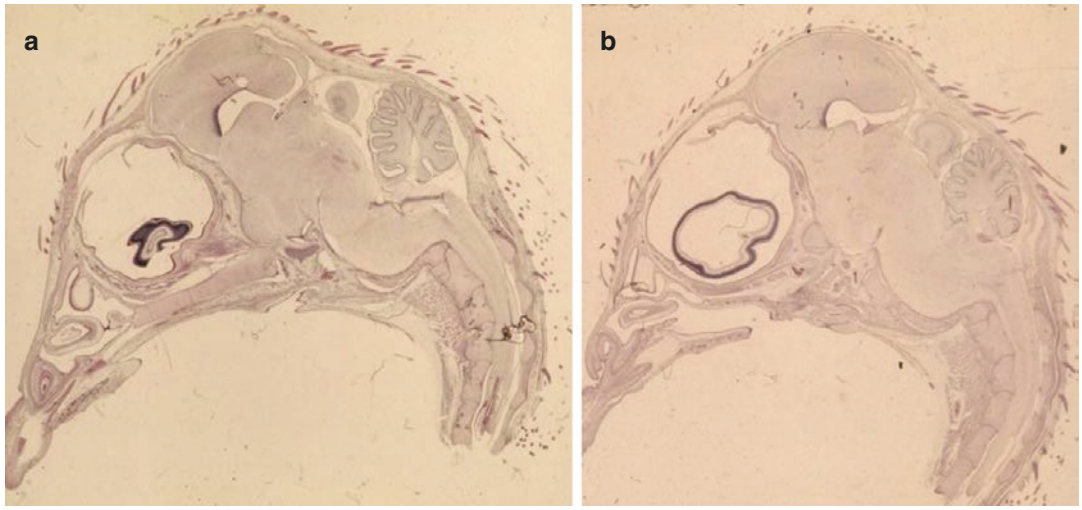

Fig. 47.2 Midsagittal brain sections of chick embryos on total incubation day 14. (**a**) A midsagittal brain section of a control embryo. (**b**) Compared with the control, an embryo of postoperative day 11 (total incubation day 14) with a spinal open neural tube defect shows narrowing of the fourth ventricle and subarachnoid space in the smaller posterior cranial fossa. (Reprinted by permission of the Korean Academy of Medical Sciences from Sim et al. [12])

sure gradients, and flow patterns are studied in models simulating healthy controls and CM cases with or without decompressive operations.

Computational models have an advantage in that each parameter can be controlled separately with ease and the outcome parameters are numerically shown. Nonetheless, there are limitations in their usefulness. In 2011, Shaffer et al. [33] reviewed the literature previously published on the subjects of computational fluid dynamics or experimental flow modeling on CM I and summarized the limitations of computational models:

1. Inconsistent data among different individuals due to factors such as age, gender, or weight, thus recommending simulation or change of parameters in a "subject-specific model" rather than comparison to other individuals.
2. Oversimplification by technical difficulties or lack of in vivo data.
3. Limited resolution of magnetic resonance imaging (MRI) and lack of information on the best boundary condition.
4. Difficulty in interpretation due to limited understanding of influence on "global" CSF dynamics and "subjective nature" of symptoms.

However, continuous efforts have been made to refine computational models for the research of CSF flow dynamics. In 2010, Hentschel et al. [34] reviewed the literature on phase-contrast MRI and computational flow dynamics studies of CSF and performed their own flow simulations. Their review of published data demonstrated greater peak CSF velocities and more complex flow patterns in patients with CM I, and synchronous bidirectional flow was one of the pathologic flow markers. They also showed that the pressure and flow patterns vary according to the spinal level and presence of CM I. In addition to the previous data obtained from the resting state, Linge et al. [35] investigated CSF dynamics during increased heart rates in control and CM I samples with computer simulations. They showed that increasing heart rate from 80 to 120 beats per minute increased superior-inferior pressure gradients and the range of synchronous bidirectional flow velocities in the normal controls, and they are more increased in CM I models.

The studies on CSF flow dynamics are closely related to understanding pathogenesis of syringomyelia in CM; the CSF flow velocity and pressure gradient between the segments or compartments are the main interest. Clarke et al. [36] used computational fluid dynamics models simulating: (1)

Table 47.4 Various techniques for fetal surgery applied to surgical spinal open neural tube defect (ONTD) models

Reference	Animal	ONTD creation (gestation day)	Fetal surgery (gestation day)	Repaired methods
Michejda [13]	Macaca monkey	Late gestation	Immediate	Allogenic bone paste
Heffez [14]	Rat	18	19	Skin suture
	Rat	18	Immediate	Peritoneal patch
	Pig	80–85	Immediate	Human cadaver dura
Copeland [15]	Sheep	90	Immediate	Endoscopic coverage with skin graft, fibrin glue and/or Surgicel®
Meuli [16]	Sheep	75	100	Reversed latissimus dorsi flap
Paek [17]	Sheep	75	100	Dura & skin suture with Alloderm® coverage
Chung [18]	Chick	3	Immediate	Skin graft
Bouchard [19]	Sheep	75	102	Surgical repair
Pedreira [20]	Rabbit	23	Immediate	Cellulose graft coverage with/without skin closure
Kohl [21]	Sheep	90–100	Immediate	Percutaneous fetoscopic patch and fetal skin coverage
von Koch [22]	Sheep	75	100	Two-layer closure or biological glue
Fontecha [23]	Rabbit	23	Immediate	Corticosteroid
Eggink [24]	Sheep	72 or 79	86 or 93	Collagen biomatrix coverage
Fauza [25]	Sheep	75	89–100	Coverage with Alloderm® only or plus NSC delivery
Abou-Jamra [26]	Sheep	75	102	Cellulose graft coverage and skin suture
Hosper [27]	Sheep	79	Immediate	Biodegradable collagen scaffold with growth factors
Fontecha [28]	Sheep	75	95	Fetoscopic inert Silastic® patch with bioadhesive gel or Marlex® mesh without suturing
Saadai [29]	Sheep	75	100	Nanofibrous scaffolds seeded with iPSC-NCSC
Guilbaud [10]	Sheep	75	90	Surgical repair

NSC neural stem cell, *iPSC* induced pluripotent stem cell, NCSC - neural crest stem cell
Reprinted and modified by permission from Sim et al. [3]

normal human subjects, (2) CM subjects without syringomyelia, and (3) CM subjects with syringomyelia to compare CSF velocities. They found a higher peak pressure in CM models. They changed upper spinal geometry and input flow waveform in each separate model, and they confirmed the effects of the two changed parameters on flow velocity, suggesting that they are potential causative factors for syrinx formation.

Flow pattern is another topic. Helgeland et al. [37] measured peak velocity during the cardiac cycle in numerous simulation models of patients with CM I, and the local Reynolds numbers were calculated by a combination of pulsating flow and the geometric complexity of the spinal canal to show the characteristics of turbulent flow.

Computational models are useful as a tool for studying the outcome of surgical treatment. Linge et al. [38] used computational fluid dynamics to calculate the effect of decompression surgery on CSF flow dynamics in the posterior fossa and upper cervical spinal canal during the cardiac cycle comparing data among the states of (1) normal control, (2) preoperative CM I, and (3) three different sizes of surgical defects. They reported normalizing systolic velocities and a decreased pressure gradient along the vertical axis as the surgical defect increased.

More sophisticated models were developed that considered the movement of the brain and the advance of phase-contrast MRI technology. Pahlavian et al. [39] made a computational fluid dynamic model of the cervicomedullary junction, which simulated tonsillar movement during cardiac cycles in a patient with CM I, and it measured the CSF pressure dissociation across the cervicomedullary junction. The same group measured CSF velocity at the cervical subarachnoid space in a healthy control and a patient with CM I using time-resolved three-directional velocity-encoded phase-contrast MRI (4D PCMRI). They compared the data with those obtained from MRI-based computational flow dynamic simulations and described the higher velocity in 4D PCMRI. However, they did not explain the reason for the difference [40]. The application of rapidly advancing artificial intelligence may dramatically change the level of computerized simulation in the field of CM research.

Conclusions

For research on CM, animal spinal ONTD models and computational models are widely used. Each model has its own advantages and limitations, and researchers have to choose one that is the most adequate and efficient for their purpose.

The application of animal models is expanding, and technical advancement is inventing more sophisticated genetic and computational models.

Acknowledgments Parts of this chapter are reprinted by permission from Springer Nature: Sim KB, Lee JY, Phi JH, Kim SK, Wang KC. Experimental models of spinal open neural tube defect and Chiari type II malformation. Childs Nerv Syst. 2013;29(9):1435-49.

This study was supported by grant no.04-2017-0240 from the Seoul National University Hospital Research Fund.

This work was supported by Creative-Pioneering Researchers Program through Seoul National University (SNU No. 800-20160282).

References

1. Wang KC, Higbee R, Knepper PA, McLone DG. Functional opening of the fourth ventricular outlet in C57BL/6J and delayed splotch mouse embryos. Pediatr Neurosurg. 1997;27(4):176–81.
2. McLone DG, Knepper PA. The cause of Chiari II malformation: a unified theory. Pediatr Neurosci. 1989;15(1):1–12.
3. Sim KB, Lee JY, Phi JH, Kim SK, Wang KC. Experimental models of spinal open neural tube defect and Chiari type II malformation. Childs Nerv Syst. 2013;29(9):1435–49.
4. Sulik KK, Sadler TW. Postulated mechanisms underlying the development of neural tube defects. Insights from in vitro and in vivo studies. Ann N Y Acad Sci. 1993;678:8–21.
5. Kibar Z, Capra V, Gros P. Toward understanding the genetic basis of neural tube defects. Clin Genet. 2007;71(4):295–310.
6. Copp AJ, Greene ND. Genetics and development of neural tube defects. J Pathol. 2010;220(2):217–30.
7. Harris MJ, Juriloff DM. An update to the list of mouse mutants with neural tube closure defects and advances toward a complete genetic perspective of neural tube closure. Birth Defects Res A Clin Mol Teratol. 2010;88(8):653–69.
8. Al-Shanafey SN, Fontecha CG, Canyadell MA, Soldado FC, Rojo AA, Conesa XJ, et al. Reduction in neural injury with earlier delivery in a mouse model of congenital myelomeningocele: laboratory investigation. J Neurosurg Pediatr. 2013;12(4):390–4.
9. Dionigi B, Brazzo JA 3rd, Ahmed A, Feng C, Wu Y, Zurakowski D, et al. Trans-amniotic stem cell therapy (TRASCET) minimizes Chiari-II malformation in experimental spina bifida. J Pediatr Surg. 2015;50(6):1037–41.
10. Guilbaud L, Garabedian C, Di Rocco F, Fallet-Bianco C, Friszer S, Zerah M, et al. Limits of the surgically induced model of myelomeningocele in the fetal sheep. Childs Nerv Syst. 2014;30(8):1425–9.
11. Fontecha CG, Aguire M, Soldado F, Peiro JL, Toran N, Vidal N, et al. Effects of birth advancement in Chiari malformation in a surgical myelomeningocele model in rabbits. J Pediatr Surg. 2010;45(3):594–9.
12. Sim KB, Hong SK, Cho BK, Choi DY, Wang KC. Experimentally induced Chiari-like malformation with myeloschisis in chick embryos. J Korean Med Sci. 1996;11(6):509–16.
13. Michejda M. Intrauterine treatment of spina bifida: primate model. Z Kinderchir. 1984;39(4):259–61.
14. Heffez DS, Aryanpur J, Rotellini NA, Hutchins GM, Freeman JM. Intrauterine repair of experimental surgically created dysraphism. Neurosurgery. 1993;32(6):1005–10.

15. Copeland ML, Bruner JP, Richards WO, Sundell HW, Tulipan NB. A model for in utero endoscopic treatment of myelomeningocele. Neurosurgery. 1993;33(3):542–4; discussion 5.
16. Meuli M, Meuli-Simmen C, Hutchins GM, Yingling CD, Hoffman KM, Harrison MR, et al. In utero surgery rescues neurological function at birth in sheep with spina bifida. Nature Med. 1995;1(4):342–7.
17. Paek BW, Farmer DL, Wilkinson CC, Albanese CT, Peacock W, Harrison MR, et al. Hindbrain herniation develops in surgically created myelomeningocele but is absent after repair in fetal lambs. Am J Obstet Gynecol. 2000;183(5):1119–23.
18. Chung YN, Li YC, Kim SK, Cho BK, Wang KC. Skin graft on the surgically induced spinal open neural tube defects does not induce lipomatous malformation but enhances re-closure to the normal state in chick embryos. Neurosci Lett. 2002;329(1):5–8.
19. Bouchard S, Davey MG, Rintoul NE, Walsh DS, Rorke LB, Adzick NS. Correction of hindbrain herniation and anatomy of the vermis after in utero repair of myelomeningocele in sheep. J Pediatr Surg. 2003;38(3):451–8; discussion - 8.
20. Pedreira DA, Valente PR, Abou-Jamra RC, Pelarigo CL, Silva LM, Goldenberg S. Successful fetal surgery for the repair of a 'myelomeningocele-like' defect created in the fetal rabbit. Fetal Diagn Ther. 2003;18(3):201–6.
21. Kohl T, Hartlage MG, Kiehitz D, Westphal M, Buller T, Achenbach S, et al. Percutaneous fetoscopic patch coverage of experimental lumbosacral full-thickness skin lesions in sheep. Surg Endosc. 2003;17(8):1218–23.
22. von Koch CS, Compagnone N, Hirose S, Yoder S, Harrison MR, Farmer DL. Myelomeningocele: characterization of a surgically induced sheep model and its central nervous system similarities and differences to the human disease. Am J Obstet Gynecol. 2005;193(4):1456–62.
23. Fontecha CG, Peiro JL, Aguirre M, Soldado F, Paz P, Oria M, et al. The effect of prenatal treatment with steroids and preterm delivery in a model of myelomeningocele on the rabbit foetus. Pediatr Surg Int. 2007;23(5):425–9.
24. Eggink AJ, Roelofs LA, Feitz WF, Wijnen RM, Lammens MM, Mullaart RA, et al. Delayed intrauterine repair of an experimental spina bifida with a collagen biomatrix. Pediatr Neurosurg. 2008;44(1):29–35.
25. Fauza DO, Jennings RW, Teng YD, Snyder EY. Neural stem cell delivery to the spinal cord in an ovine model of fetal surgery for spina bifida. Surgery. 2008;144(3):367–73.
26. Abou-Jamra RC, Valente PR, Araujo A, Sanchez e Oliveira Rde C, Saldiva PH, Pedreira DA. Simplified correction of a meningomyelocele-like defect in the ovine fetus. Acta Cir Bras. 2009;24(3):239–44.
27. Hosper NA, Eggink AJ, Roelofs LA, Wijnen RM, van Luyn MJ, Bank RA, et al. Intra-uterine tissue engineering of full-thickness skin defects in a fetal sheep model. Biomaterials. 2010;31(14):3910–9.
28. Fontecha CG, Peiro JL, Sevilla JJ, Aguirre M, Soldado F, Fresno L, et al. Fetoscopic coverage of experimental myelomeningocele in sheep using a patch with surgical sealant. Eur J Obstet Gynecol Reprod Biol. 2011;156(2):171–6.
29. Saadai P, Wang A, Nout YS, Downing TL, Lofberg K, Beattie MS, et al. Human induced pluripotent stem cell-derived neural crest stem cells integrate into the injured spinal cord in the fetal lamb model of myelomeningocele. J Pediatr Surg. 2013;48(1):158–63.
30. Cockroft DL, New DA. Effects of hyperthermia on rat embryos in culture. Nature. 1975;258(5536):604–6.
31. Edwards MJ. Hyperthermia as a teratogen: a review of experimental studies and their clinical significance. Teratog Carcinog Mutagen. 1986;6(6):563–82.
32. Craenen K, Verslegers M, Buset J, Baatout S, Moons L, Benotmane MA. A detailed characterization of congenital defects and mortality following moderate X-ray doses during neurulation. Birth Defects Res. 2018;110(6):467–82.
33. Shaffer N, Martin B, Loth F. Cerebrospinal fluid hydrodynamics in type I Chiari malformation. Neurol Res. 2011;33(3):247–60.
34. Hentschel S, Mardal KA, Lovgren AE, Linge S, Haughton V. Characterization of cyclic CSF flow in the foramen magnum and upper cervical spinal canal with MR flow imaging and computational fluid dynamics. AJNR Am J Neuroradiol. 2010;31(6):997–1002.
35. Linge SO, Mardal KA, Haughton V, Helgeland A. Simulating CSF flow dynamics in the normal and the Chiari I subarachnoid space during rest and exertion. AJNR Am J Neuroradiol. 2013;34(1):41–5.
36. Clarke EC, Fletcher DF, Stoodley MA, Bilston LE. Computational fluid dynamics modelling of cerebrospinal fluid pressure in Chiari malformation and syringomyelia. J Biomech. 2013;46(11):1801–9.
37. Helgeland A, Mardal KA, Haughton V, Reif BA. Numerical simulations of the pulsating flow of cerebrospinal fluid flow in the cervical spinal canal of a Chiari patient. J Biomech. 2014;47(5):1082–90.
38. Linge SO, Mardal KA, Helgeland A, Heiss JD, Haughton V. Effect of craniovertebral decompression on CSF dynamics in Chiari malformation type I studied with computational fluid dynamics: Laboratory investigation. J Neurosurg Spine. 2014;21(4):559–64.
39. Pahlavian SH, Loth F, Luciano M, Oshinski J, Martin BA. Neural tissue motion impacts cerebrospinal fluid dynamics at the cervical medullary junction: a patient-specific moving-boundary computational model. Ann Biomed Eng. 2015;43(12):2911–23.
40. Heidari Pahlavian S, Bunck AC, Loth F, Shane Tubbs R, Yiallourou T, Kroeger JR, et al. Characterization of the discrepancies between four-dimensional phase-contrast magnetic resonance imaging and in-silico simulations of cerebrospinal fluid dynamics. J Biomech Eng. 2015;137(5):051002.

Predictive Analysis in Chiari Malformation Type I

48

Sumit Thakar, Saritha Aryan, Subramaniyan Mani, and R. Raghunatha Sarma

Predictive analysis (PA) aims to foretell outcomes based on patterns derived from a set of variables. It uses methods to search through a huge amount of information, analyzing it to predict outcomes for individual patients. The information for PA comes not just from previous treatment outcomes but also from ongoing research. In healthcare, PA can have wide-ranging implications including determining the likelihood of disease, making an accurate diagnosis, optimizing treatment, and predicting outcomes. This is of increasing relevance in patent-centric or value-based care as an accurate predictive model can help in informed decision-making, evidence-based care, and constant quality improvement.

Traditional statistical techniques broadly rely on smaller samples and heavy assumptions about data and its distributions. They pursue generalizations using tests only on the training data set and promote data reduction. These techniques assume linear relationships in data. Real-life data, however, often presents as a nonlinear complex problem. PA applies techniques *without* preconceived theoretical constructs to predict future outcomes and can reveal surprising associations in data that would otherwise never have been suspected. In PA, predictions are made for individuals and not for groups, and their applicability to clinical practice does not come at the cost of their predictive performance.

Utility of Predictive Analysis

Although PA in medicine has traditionally used a Bayesian approach using techniques such as regression models, data mining techniques such as machine learning (ML) are being increasingly used in outcome research. By studying large data sets, ML evaluates clinically meaningful relationships between input and output parameters. It then creates a prediction model from past data that allows a new individual to obtain an instant prediction. The model progressively "learns" and becomes more precise as it gets deployed to new cases over time. Examples of ML include neural networks, support vector machines, and decision trees [1].

PA increases the accuracy of diagnoses and identifies at-risk patients in various conditions. This facilitates early intervention that can significantly ameliorate the clinical course of preventable diseases. The applicability of PA

S. Thakar (✉) · S. Aryan
Department of Neurological Sciences, Sri Sathya Sai Institute of Higher Medical Sciences, Bangalore, Karnataka, India
e-mail: sumit.t@sssihms.org.in

S. Mani
Hospital Management Information System and Telemedicine, Sri Sathya Sai Institute of Higher Medical Sciences, Bangalore, Karnataka, India

R. R. Sarma
Department of Mathematics and Computer Science, Sri Sathya Sai Institute of Higher Learning, Puttaparthi, Andhra Pradesh, India

R. S. Tubbs et al. (eds.), *The Chiari Malformations*, https://doi.org/10.1007/978-3-030-44862-2_48

does not rely upon a "Gaussian bell curve" distribution, allowing for the selection of an optimal treatment modality for *any* given patient. What works best for the middle of a normal distribution of patients may not work best for an individual on either side of the curve. PA helps in selecting the exact treatment for *all* individuals without having the physicians resort to superfluous or even potentially dangerous treatment modalities.

The saying "The decision is more important than the incision" [2] highlights another utility of PA from a surgical perspective: prediction of the risks or benefits of any surgical procedure for a given patient. This information enhances the role of the patient from that of being a mere recipient of care to becoming an informed consumer working along with the physician to achieve better outcomes. This is of added relevance in neurosurgical interventions, where benefits in one dimension may come at the cost of another, and the expectation of a positive outcome is closely associated with the risk of an unfavorable consequence.

Neurosurgery provides a fitting framework for the creation of ML-based PA models, given its complex clinical presentations and varied diagnostic and therapeutic modalities that provide a vast array of multidimensional data. ML models have been explored as tools for outcome prediction across wide-ranging fields encompassing neurovascular conditions, epilepsy, oncology, hydrocephalus, Parkinson disease, spine, and head injury [3]. Examples of these prediction studies include evaluation of seizure freedom after epilepsy surgery [4, 5], survival after varying rates of resection or stereotactic radiosurgery for malignant lesions [6, 7], outcomes after spine surgery [8, 9], and the Glasgow Outcome score prediction after subarachnoid hemorrhage [10]. Some ML models have been demonstrated to outperform prognostic indices [9, 10] and classical statistical models [3], performing similar to or better than clinical experts [4]. Given the complexity of clinical outcomes and the numerous variables that have been postulated to influence outcome in Chiari malformation type I (CM I), it is surprising that the utility of PA remains largely underexplored in CM I.

The Need for Predictive Analysis in Chiari Malformation Type I

Chiari malformations (CMs) are a spectrum of disorders, the pathophysiology of which is still incompletely understood. Traditionally, CMs have been defined as disorders in which there is either herniation of the posterior cranial fossa (PCF) contents below the foramen magnum (FM) or there is hypoplasia of the cerebellum within a small PCF [11, 12]. CM I refers to herniation of the cerebellar tonsils alone; type II refers to herniation of both the cerebellum and lower brainstem; type III is a rare type of brainstem herniation in association with a cervical or occipital encephalocele; and type IV involves extreme cerebellar hypoplasia and caudal displacement of the PCF contents. Two additional types of CM were described later. Chiari type 0 is defined as syringohydromyelia with distortion of contents in posterior fossa but without cerebellar tonsillar herniation (TH) [13]. Chiari type 1.5 has been characterized as caudal migration of the brainstem and cerebellar tonsils often associated with syringomyelia but without spina bifida [14]. However, the exact relevance and distinctiveness of each of these entities remain controversial among clinicians.

Of all the aforementioned types of Chiari malformation, predictive analysis is particularly relevant in CM I—the most common type of the disorder characterized by heterogeneous clinicoradiological presentations, management options, and postsurgical outcomes. Despite being a subject of research for more than a century, CM I is still riddled with controversies related to its diagnosis, optimal management strategy, prediction of clinical improvement, and resolution of syringomyelia. A large number of studies have analyzed different preoperative variables—either individually or in small sets—in relation to clinical and radiological outcomes after CM I surgery. Results from such studies have been diverse and sometimes even conflicting. The sheer numbers of variables that have been postulated to influence postsurgical outcome underscore the need for PA in CM I.

From a diagnostic perspective, a tonsillar herniation more than 5 mm below the foramen magnum is the widely accepted criterion for CM I. The most common cause of TH is a crowded posterior fossa ("classic CM I"). While patients presenting with TH more than 5 mm are readily labeled as having CM I, those presenting with a crowded posterior fossa and lesser degrees of TH are at risk of being underdiagnosed. PA in this regard aids in identifying morphometric measures other than TH to diagnose CM I with higher accuracy [15].

A large majority of CM I patients, including ones with greater degrees of TH, remain asymptomatic [16, 17]. The few patients who do become symptomatic demonstrate a great degree of heterogeneity in their clinical presentations. The range of symptoms includes cough, headache, neck and non-radicular limb pain, weakness, paresthesias, audio-vestibular dysfunction, oculomotor disturbances, syncope, slurred speech, stridor, dysphagia, chronic emesis [18], urinary incontinence, sleep disturbances [19], rage attacks [18], cognitive dysfunction [20], and even sudden death [21]. While this clinical heterogeneity in CM I is morphologically representative of wide anatomical variations in the posterior fossa and cerebrospinal fluid (CSF) dynamics at the craniovertebral junction (CVJ), it also translates to the possibility of these diverse clinical variables having nonlinear and complex relationships with each another. Such relationships can be best explored and uncovered by ML-based predictive model analysis.

An area of considerable research in CM I is related to the commonly observed discordance between clinical and radiological improvement after decompressive surgery. More than half the patients in one study reported unfavorable clinical outcomes despite having achieved adequate radiological decompression [22]. In the light of such findings, a host of clinical, morphological, and hydrodynamic parameters have been evaluated as potential predictors of outcome. Since most of these parameters have been analyzed in isolation or in small groups, the conclusions drawn from these studies have been quite diverse. As an example, while some studies identified age, sex, duration of follow-up, tonsillar and syrinx characteristics [23–26], and pB-C2 distance [27] to correlate with syrinx resolution, another study [28] found none of the analyzed variables to be associated with radiological outcome. A similar inconsistency exists with regard to clinical outcomes as well, with variables such as age [29], duration of symptoms [30, 31], nystagmus [31], trigeminal hypesthesia [31], sensory deficits [29, 31], cough headache [22, 32, 33], myelopathy [33], syrinx diameter [33], pB-C2 distance [27], CSF flow [34, 35], posterior fossa volume (PFV) [35], spinal cord diameter [36], cord displacement, and measures of intracranial compliance [37] being identified to correlate with outcome.

PA-based algorithms for postoperative improvement after CM I surgery would allow for objective and evidence-based preoperative counseling and possibly enhance patient-perceived satisfaction from surgery [38]. This would be of added relevance in a condition that has been identified to have psychological and cognitive connotations [20]. The accuracy of ML-based predictive models improves with changes in the population over time—a phenomenon that would well suit the pathological continuum of CM I.

Review of Various Predictors Identified in Chiari I

Diagnosis of Chiari I

CM I is conventionally described as TH 5 mm or more below the FM. Even though TH is assumed to be caused by a "small" posterior cranial fossa, it is known that it can be caused by multiple mechanisms [39]. It is also accepted that the extent of herniation does not always correlate with disease severity or response to surgery [40–42]. Since the primary pathology is that of the PCF and a uniform surgical technique of posterior fossa decompression is applied to all the different CM types, it has been suggested that radiological TH may not be the best parameter to characterize the diagnosis. Multiple studies have attempted to diagnose CM using additional features [16, 43, 44] so that accuracy is increased and fewer

patients are wrongly diagnosed. Urbizu et al. [45] used logistic regression analysis on seven PCF measures and developed a probability predictor model that had a sensitivity of 93% and a specificity of 92% in differentiating patients with classic CM I from those with a normal PCF. In a recent paper [15], the same group used the technique of machine learning for radiological diagnosis of adult CM. After analyzing TH along with multiple PCF morphometric parameters, they suggested that in addition to TH, alterations in the basion position should be incorporated into making a diagnosis of adult CM. Their final mathematical model based on just three parameters—the distance from the pons to the FM, distance from the fastigium to the FM, and the basal angle—could accurately predict 90% of patients with different CM entities.

Syrinx Formation

The clinical presentation of the various CM entities forms a spectrum. Other than the TH itself, the notable cause for the varying manifestations is the syringomyelia that is seen in a number of patients with CM. Even though multiple theories regarding syrinx formation have been put forward, the risk factors for the same remain unclear. Since asymptomatic Chiari I malformations can be managed conservatively, it would help in counseling patients and determining the frequency of follow-up imaging if the formation of a syrinx could be predicted.

In a magnetic resonance imaging (MRI) study of pediatric CM I, Strahle et al. [46] found that syringes are more common in older children, in girls, and in patients with a greater degree of tonsillar descent and CSF flow impairment. On studying PCF volumes in pediatric CM I patients with and without syrinx, Sgouros et al. [47] found that those with syrinx have significantly smaller-than-normal PCF volumes compared to the patients with isolated CM I. Halvorson et al. [48] searched for morphometric indicators of syrinx formation in CM I. They concluded that the degree of the TH correlated with chances of syrinx formation. The volume of the PCF was not found to be a predictor of syrinx formation even though patients with a syrinx had, on an average, a higher cerebellar to posterior fossa volume ratio.

In a retrospective MRI analysis of 69 patients with CM I, Gad and Jordem [49] found that 36% of symptomatic patients developed syringohydromyelia. On univariate analysis, craniocervical junction osseous anomalies—retroverted odontoid, platybasia, short clivus, and basilar invagination—and a skull base angle of >135° were the features most suggestive of syrinx formation. On multivariate analysis, only the latter had a significant predictive value.

Requirement of Fusion

The basic surgical procedure for the spectrum of CM I is broadly agreed to be posterior fossa decompression, with or without duraplasty. In the presence of syringomyelia, however, the optimal surgical treatment is unclear; a few of the described techniques include suboccipital craniectomy, obex plugging, syringostomy, and syrinx shunting procedures. In addition to these, a subset of patients with what is described as "complex Chiari" may require occipitocervical fusion [50–52]. Brockmeyer [53] defined the complex Chiari malformation as "cerebellar tonsil herniation combined with one or more of the following radiographic findings: brain stem herniation through the foramen magnum (Chiari 1.5 malformation), medullary kink, retroflexed odontoid, abnormal clival-cervical angle, occipitalization of the atlas, basilar invagination, syringohydromyelia or scoliosis." Fenoy et al. [50] suggested that CM I patients with reducible compression or those who previously underwent anterior decompression at the FM would need occipitocervical fusion. Bollo et al. [54] sought to identify which patients undergoing PCF decompression for CM I would ultimately require a stabilization procedure. Of the multiple radiological parameters they studied, they found that CM 1.5, basilar invagination, and a clivoaxial angle <125° correlated with an increasing risk of requiring fusion either along with the primary PCF decompression or at a later stage.

Predicting Postsurgical Clinical Outcomes

In lieu of the complex symptomatology and volatile behavior, it is probably not surprising that predictive analysis in the context of CM I has been maximally used for prognosticating disease outcomes. Dyste et al. [31] attempted to predict disease outcomes in 50 symptomatic patients of CM, both adult and pediatric. In a retrospective analysis, clinical and radiological parameters were correlated with disease outcomes. They found that preoperative signs that are predictive of a less favorable outcome include muscle atrophy, symptoms lasting longer than 24 months, ataxia, nystagmus, trigeminal hypesthesia, and dorsal column dysfunction. Linear regression (LR) analysis and forward and reverse stepwise analysis built up a predictive model that, according to them, could predict outcomes based on the presence or absence of just three clinical features: ataxia, atrophy, and scoliosis.

In a study of 48 patients who underwent surgery for CM I, Arora et al. [55] studied the clinicoradiological determinants of outcome. At 6 months of follow-up, they found that 62.5% of patients had a good outcome. Multivariate analysis showed that the duration of symptoms, absence of respiratory distress, and absence of basilar invagination correlated with good outcomes. However, they did not study the possibly confounding role of concomitant syringomyelia on the treatment results. Attal et al. [30] studied operative efficacy on the sensory symptoms of syringomyelia and stated that only the duration of deficits correlated with improvement; specifically, patients operated on within 2 years of occurrence of symptoms have better outcomes. Of note, they included patients with post-traumatic syringomyelia in addition to CM-associated syrinx.

Kumar et al. [56] analyzed morphometric parameters to identify predictors of surgical outcome. They found that the measured posterior fossa volume was the only factor correlating with clinical improvement, with a cutoff preoperative value of 198.58 cm^3 having 77.8% sensitivity and 100% specificity for prognosticating benefit after surgery.

Aghakhani et al. [57] studied the long-term postoperative outcomes in syrinx associated with CM I. In 157 patients, they had a median follow-up of 88 months. Sixty-three percent of their patients improved, 30% had stable symptoms, and 6% worsened. They found that young age at the time of surgery and clinical signs of paroxysmal intracranial hypertension predicted improvement or stabilization of symptoms. Older age, long-tract involvement, intraoperative finding of adhesive arachnoiditis, and extent of the syrinx on postoperative MRI were predictors of poor clinical outcome in their series.

Liu et al. [58] studied surgical outcomes in a series of 92 children who were diagnosed with CM I and underwent a standard surgical technique of small-bone-window PCF decompression and autologous-fascia duraplasty; 81% of patients had postoperative improvement. They found that a higher grade of TH, basilar invagination, and platybasia were predictors of poor clinical outcome.

Headache Resolution

Headache is the most common symptom of CM I and occurs in 30–90% of patients [16, 59, 60]. The classical CM headache is suboccipital, which worsens with coughing, straining, or neck movements. However, CM I patients can also have poorly localized headaches. In a cohort of 49 patients with CM I, Grangeon et al. [61] reported improvement of headache in 57% and its persistence in the remaining patients. Multivariate regression analysis confirmed occipital location, increasing intensity of the headache, higher number of headache days per month, and classical triggering by Valsalva maneuvers as predictors of headache resolution after surgery in these patients.

Syrinx Resolution

The prognosis of CM I-associated syrinx after a standard surgical procedure of PCF decompression combined with C1 laminectomy and

excision of the outer layer of the dura mater was studied by Nagoshi et al. [23]. Based on the syrinx size on the postoperative MRI, 20 patients were grouped as "decreased" or "unchanged." The clinical symptoms were found to have improved in all patients in the former but only in one patient in the latter. All central syringes decreased after surgery, whereas none of the deviated type did. The authors concluded that in patients with CM-associated syrinx, longer duration of symptoms, a longer length of syrinx and its deviation from the center of the cord, and postoperative residual narrowing of the subarachnoid space—a marker for adhesive arachnoiditis—were associated with poor prognosis after surgery. All their patients with complicated syrinx morphology improved after additional syrinx shunting, and hence they suggested that such patients may be better off undergoing such a shunt as the primary procedure itself.

Cerebrospinal Fluid Studies and Prediction of Outcome

CSF flow abnormalities at the FM in CM I have been demonstrated in multiple studies [62–67]. It has been opined that this pathology may contribute to the symptoms independent of the tonsillar herniation. Arora et al. [68] employed radionuclide cisternography to study CSF dynamics at the FM and to predict the clinical outcome following surgery. They found that PCF decompression provides maximum clinical relief in patients with a demonstrable FM block on cisternography, while those with a normal flow have less relief.

Cine phase-contrast MRI is the most common method of assessing CSF flow dynamics at the FM. McGirt et al. [34] reviewed clinical and radiologic data in 130 patients who underwent PCF decompression for CM I. Patients with no evidence of hindbrain CSF flow abnormality were classified as "normal CSF flow," and those with reduced flow at the FM, either anterior or posterior, were classified as "abnormal CSF flow." Patient outcomes and improvement in CSF flow after surgery were recorded. Cine CSF flow improved in 91% patients with abnormal CSF flow preoperatively. Patients with normal preoperative hindbrain CSF flow were more likely to experience treatment failure after PCF decompression. In addition to normal CSF flow, the other significant predictors of symptom recurrence were the presence of frontal headaches and scoliosis. Syringomyelia, surprisingly, did not correlate with treatment failure.

The same group published their findings of correlation of CSF flow with outcomes in a set of pediatric CMs [69]; 30% of patients had symptom recurrence in the follow-up period. Regression analysis showed that patients with obstructed hindbrain CSF flow responded better to decompression compared to those without CSF flow obstruction. The patients with combined dorsal and ventral CSF flow abnormality had a better response to PCF decompression than patients in whom the CSF flow at the FM was impaired only posteriorly. In fact, the combined CSF flow abnormality was associated with a 2.6-fold reduction in the risk of postoperative symptom recurrence, suggesting that the CSF flow pathology in only the dorsal hindbrain compartment may not in itself predict improved surgical outcome.

Wang et al. [70] in a recent study of CSF dynamics and phase-contrast MRI (PC-MRI) found that patients with pre-surgery posterior cervical CSF peak velocity (PV) > 2.63 cm/s and aqueduct cranial PV > 2.13 cm/s experienced primary symptom improvement after surgery. They concluded that PC-MRI may thus be a useful tool for predicting patient prognosis.

A study by Sakas et al. [71] used another MRI technique called spatial modulation of magnetization (SPAMM) to measure CSF flow velocities in normal people and CM I patients before and after surgery. They found that in CM I, the posterior cervical CSF flow velocity was low, increased minimally after PCF surgery, and by itself had limited predictive value. However, after surgery, an increase of the sum of anterior and posterior cervical CSF flow velocities by more than 20% consistently preceded or coincided with marked headache improvement. Also, postoperatively, the finding that the intrasyringeal CSF pulsatile motion had become absent

was an earlier and more sensitive predictor of motor or sensory improvement than a reduction in syrinx size.

SPAMM was applied to the hydrodynamic analysis of intrasyrinx fluid motion and CSF in a set of patients with syringomyelia of multiple etiology including CM I [72]. Good preoperative intrasyrinx fluid motion and CSF motion, especially the former, as measured on SPAMM-MRI, was predictive of better surgical outcomes.

In a pilot study on 15 patients of CM I, Alperin et al. [37] measured MRI-based morphological and physiological parameters to identify patients who would improve after surgery. These included linear and volumetric morphological measures of the PCF, CSF flow and tissue motion, and intracranial hydrodynamics measures derived from measurements of the blood and CSF flow to and from the cranium [43, 73, 74]. In terms of the chief-complaint response, the preoperative parameters that were the strongest predictors of outcome included maximal cord displacement, the percent venous drainage through the jugular veins, and normalized cerebral blood flow. The parameters that predicted better scores were maximal cord displacement and intracranial volume (ICV) change during the cardiac cycle, which taken together had 93.3% accuracy, 85.7% sensitivity, and 100% specificity. None of the morphometric measures were found to correlate with outcome.

Scoliosis Progression

Chiari-related scoliosis and its progression after PCF decompression have been addressed in multiple studies. CM I surgery was found to aid scoliosis regression in 65% of patients [75]. However, age more than 10 years at scoliosis diagnosis and a Cobb angle more than 35° were seen to be predictive of curve progression and the need for subsequent fusion [75–77]. In a recent study, Ravindra et al. [78] found that along with a higher Cobb angle, an initial pB-C2 (the perpendicular distance between the ventral dura to the line that joins the basion to the posterior portion of the axis body inferior endplate) more than 9 mm and a lower clival-axial angle (CXA) predicted scoliotic curve progression. Lower CXA was also an independent predictor of delayed thoracolumbar fusion.

Chiari I-Related Hydrocephalus

Chiari-related hydrocephalus occurs in about 7–10% of patients with CM I [79, 80]. The need for long-term CSF diversion after CM I surgery was analyzed in a set of 297 pediatric CM patients who underwent PCF decompression [79]. The authors reported that after multivariate regression analysis, age less than 6 years, patients with extensive intraoperative blood loss, and those found during surgery to have the fourth ventricular web were at higher risk for the development of hydrocephalus.

Postoperative Complications

In a recent paper, Farber et al. [81] compared the rates of meningitis and subsequent need for CSF diversion between PCF decompression with duraplasty done with bovine pericardial xenograft and allograft and found that both were higher in the former. Pseudomeningocele formation is another not-uncommon complication of CM I surgery. This is known to occur in 2–6% of patients who undergo PCF decompression [82, 83] and can cause significant morbidity. Menger et al. [81] reported that increasing age of the patient and the use of sealants for duraplasty correlated with increasing risks of pseudomeningocele formation, whereas neither the method nor the material used for duraplasty mattered.

Predictive Scoring Instruments

A good example of a predictive scoring system used to prognosticate outcome in CM I is the Chiari Severity Index (CSI) (Fig. 48.1) put forward by Greenberg et al. [33] in 2015. They integrated clinical and neuroimaging characteristics to propose a preoperative stratification that would

Clinical Grade	Signs/Symptoms
1	Classic Chiari Headache
	Poorly Localized Headache
2	Frontotemporal Headache
	No Headache
3	Myelopathic Symptoms

Neuroimaging Grade	Imaging Finding
A	Syrinx < 6 mm No syrinx
B	Syrinx ≥ 6 mm

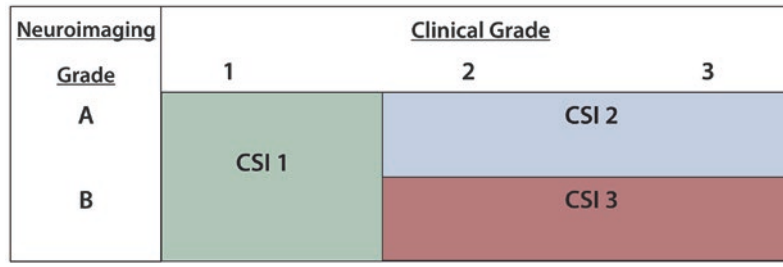

Fig. 48.1 The Chiari Severity Index based on clinical and neuroimaging grades. (Adapted from Greenberg et al. [33], by permission of Oxford University Press)

predict patient-defined improvement following CM I surgery. In a set of 158 pediatric patients who underwent surgery for CM I, the features of headaches and myelopathic symptoms were used to classify patients into three clinical grades; there were two neuroimaging grades on the basis of the presence or absence of syrinx ≥6 mm in size. By combining the two indices, all patients could be preoperatively grouped into three grades with predicted patient-perceived improvement rates ranging from 83% (grade 1) to 45% (grade 3). The authors claimed that the CSI can be used for counseling of patients before surgery and as a means to stratify patients in surgical effectiveness trials.

The Chicago Chiari Outcome Scale (CCOS) (Fig. 48.2) described by Aliaga et al. [84] is the most widely used validated measure in CM I outcome research. This outcome scale designed specifically to measure the success of CM I surgery is composed of four categories: pain, non-pain symptoms, functionality, and complications. A patient is given a score of 1–4 in each category, for a total score of 4–16. A final score of 4 means the person is incapacitated; a score of 8 means an impaired outcome; a score of 12 equates to a functional outcome; and a score of 16 is an excellent outcome. The authors claimed that the CCOS allows for standardized and quantifiable outcome assessment after surgery.

In a retrospective study carried out by the same group [29], 167 patients who underwent surgery for CM were analyzed with respect to preoperative clinical and radiological features, and they were classified into the four categories of the CCOS at follow-up. Patients with higher scores (11–16) were deemed to have experienced a good outcome from surgery (82%); those with lower scores (4–10) were deemed to have experienced a poor outcome from surgery (18%). Odds ratios were generated to identify factors that correlated with poor and good outcomes. Peripheral nerve symptoms such as neuropathy or loss of sensitivity to pinprick were predictors of poor outcome. They found three factors to predict good surgical results: age less than 18 years, male sex, and surprisingly the presence of a syrinx. The degree of TH did not correlate with surgical outcome.

Regression Model for Prognostic Clinical Outcome in Chiari I

Using a total of 40 variables, constituting one of the largest variable arrays used so far in CM I outcome research, we had previously generated a point-based algorithm for predicting postoperative improvement on the CCOS [85]. While a previous study analyzed preoperative clinical variables with respect to outcomes on the CCOS [54], our study utilized both clinical and radiological variables to generate a point-based model to predict outcome. For our study, 120 symptomatic patients with CM I with syringomyelia treated with foramen magnum decompression (FMD), C1 laminectomy, and duraplasty over an 8-year period were screened. From this data set, 82 consecutive adult patients with altered hind-

Chicago Chiari Outcome Scale				
Pain	Non-pain	Functionality	Complications	Total Score
1 - Worse	1 - Worse	1 - Unable to attend	1 - Persistent complication, poorly controlled	4 - Incapacitated outcome
2 - Unchanged and refractory to medication	2 - Unchanged or improved but impaired	2 - Moderate impairment (<50% attendance)	2 - Persistent complication, well controlled	8 - Impaired outcome
3 - Improved or controlled with medication	3 - Improved and unimpaired	3 - Mild impairment (>50% attendance)	3 - Transient complication	12 - Functional outcome
4 - Resolved	4 - Resolved	4 - Fully functional	4 - Uncomplicated course	16 - Excellent outcome

Fig. 48.2 The Chicago Chiari Outcome Scale. (Reproduced from Aliaga et al. [84], by permission of Oxford University Press)

brain CSF flow documented on cine MRI were included in the analysis.

Clinical and Radiological Variables Used

Various preoperative clinical variables used in the analysis included age, sex, body mass index, duration of symptoms, presence of cough headache or non-cough headache, brainstem and cranial nerve symptoms, paresthesias, dysesthesias, bladder incontinence, dysphagia, motor deficits, sensory deficits, abnormal reflexes, gait instability, and cerebellar signs.

The radiological variables recorded on MRI included:

- Degree of tonsillar descent below the FM, syrinx characteristics (diameter, levels, location, and type, i.e., central, enlarged, or deviated) [23, 86].
- Presence or absence of scoliosis.
- Maximum axial width of the fourth ventricle [28].
- Odontoid retroversion (angle between the base of C2 and its intersection with a line from the odontoid tip) and retroflexion (angle formed between a line drawn through the odontoid synchondrosis and its intersection with a line drawn from the odontoid tip) [87, 88].
- Clivus-canal angle (angle between Wackenheim's clivus line and the posterior wall of the C2 vertebral body) [89].
- pB-C2 distance [27].
- Obex position (the distance between the obex and basion-opisthion line, Fig. 48.3a) [33].
- Cervicomedullary angle.
- C2–C7 sagittal alignment (Cobb angle between the lines along the lower endplates of C2 and C7) [90].
- The cervical taper ratio (tapering of the anteroposterior cervical canal dimension from cranial to caudal, Fig. 48.3b) [91].

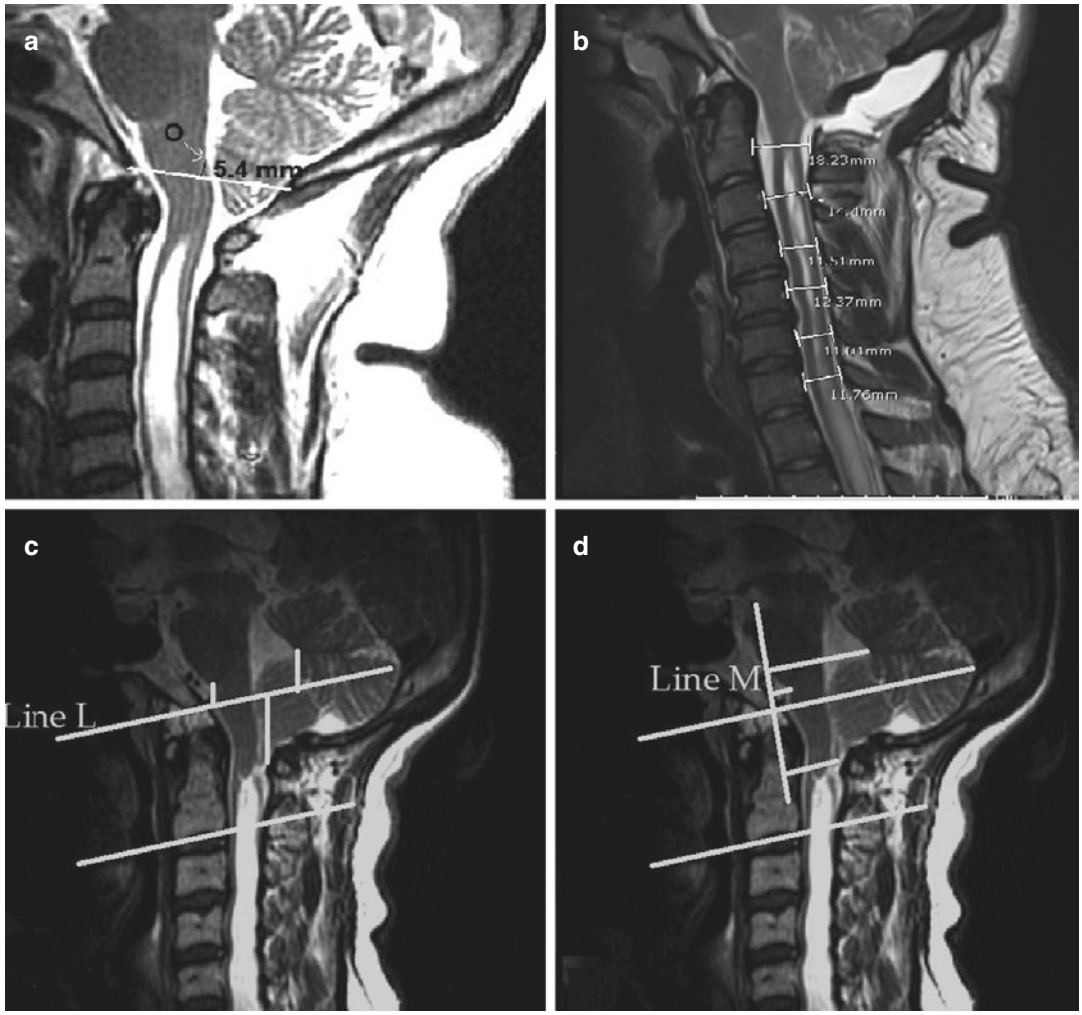

Fig. 48.3 T2-weighted sagittal magnetic resonance imaging (MRI) demonstrating (**a**) the distance of the obex (O) from the cervicomedullary junction; (**b**) the cervical "taper" of the anteroposterior spinal canal dimension from C2 to C7; (**c**) L-line, a line drawn across the clivus vertex and parallel to the C2 endplate; and (**d**) M-line, a line drawn perpendicular to the L-line. Distances from each of these lines were measured to the pontobulbar sulcus, fourth ventricle vertex, and tonsil tip. (Adapted from Thakar et al. [85], by permission from the Journal of Neurosurgery Publishing Group, AANS)

- Posterior fossa morphometry—dimensions of the foramen magnum, posterior fossa/intracranial volume ratio wherein posterior fossa volume was calculated as $4/3 \times \Pi(Pi) \times (x/2 \times y/2 \times z/2)$ with x, y, and z being the posterior fossa dimensions and intracranial volume was calculated as being equal to $948 + (0.478 \times FM\ mm^2)$ [92].
- Hindbrain morphometry in relation to the "L-line" (drawn across the clivus vertex and parallel to the C2 endplate, Fig. 48.3c) and the "M-line" (drawn perpendicular to the L-line, Fig. 48.3d). Distances from each of these lines were measured to the pontobulbar sulcus, fourth ventricle vertex, and tonsil tip (Fig. 48.3c–d), as has been described earlier [93].

Procedure and Outcome Assessment

All patients underwent a 3 x 3 cm suboccipital craniectomy that included the foramen

magnum rim, C1 laminectomy, and intradural exploration for arachnoid adhesions in the fourth ventricular outlet when CSF movement in the cisterna magna or CSF outflow from the fourth ventricle appeared to be insufficient. Tonsillar shrinkage was done when CSF flow was felt to be insufficient even after removing the arachnoidal adhesions. Duraplasty was performed in all cases with the pericranium or an artificial dural substitute. Clinical outcome at the last follow-up was measured by the CCOS on a scale of 4–16. Radiological outcome was measured as the percentage of regression of syringomyelia on MRI.

Results

Of the 82 patients included in the study, the study or test cohort was constituted by 57 consecutive patients, while the remaining 25 patients constituted the validation cohort. Among the various clinical and radiological variables tested, motor deficits, gait instability, and the M-line-fourth ventricular vertex (FVV) distance correlated with the CCOS scores ($p \leq 0.05$), while motor deficits, abnormal reflexes, and the PFV/ICV ratio correlated with regression of syrinx ($p < 0.05$). A multiple linear regression analysis demonstrated gait instability, obex position, and M-line-FVV distance to be associated with CCOS scores (Tables 48.1, 48.2, 48.3), while the presence of motor deficits alone correlated with poor syrinx regression (Table 48.4).

Table 48.1 Multiple linear regression analysis for assessing independent correlations with CCOS

	B	SE	p-Value
Constant	16.25		
Motor deficit	−0.47	0.44	0.31
Gait instability	−0.96	0.43	**0.04**
Obex position	−0.13	0.06	**0.04**
M-line-fourth ventricular vertex distance	−0.08	0.04	**0.05**

Reproduced from Thakar et al. [85], by permission from the Journal of Neurosurgery Publishing Group, AANS
B unstandardized coefficient, *SE* standard error

Table 48.2 Analysis of variance with respect to CCOS

	Sum of squares	df	Mean square	F	p-Value
Regression	34.79	4	8.70	3.86	0.008
Residual	117.14	52	2.25		
Total	151.93	53			

Reproduced from Thakar et al. [85], by permission from the Journal of Neurosurgery Publishing Group, AANS
df degrees of freedom

Table 48.3 Goodness of fit analysis of the linear regression model

R	R square	Adjusted R square	SE
0.68	0.46	0.40	1.50

Reproduced from Thakar et al. [85], by permission from the Journal of Neurosurgery Publishing Group, AANS
SE standard error of estimate

Table 48.4 Multiple linear regression analysis for assessing independent correlations with syrinx regression

	B	SE	p-Value
Constant	85.88		
Cough headache	13.68	10.98	0.23
Abnormal reflexes	−14.27	8.72	0.10
Motor deficits	−34.41	9.57	**0.002**
PFV/ICV ratio	−0.26	0.17	0.12
Cervical taper ratio	−12.72	8.77	0.15

Reproduced from Thakar et al. [85], by permission from the Journal of Neurosurgery Publishing Group, AANS
B unstandardized coefficient, *SE* standard error, *PFV* posterior fossa volume, *ICV* intracranial volume

Point-Based Model

For obtaining the predictive model, we multiplied the regression coefficients from our linear regression model by 10 and rounded them to the nearest integer to use them as weights. We obtained the following weights for the variables that were significant in our regression model: gait instability = −10, obex position = −1, M-line-FVV distance = −1, and intercept = 162. Points were calculated for each individual by multiplying the weights against their values for each of these variables and summed up to obtain a total score. We tested different models for their ability to predict the CCOS scores. The model with the best prediction was

$$\text{Total points} = 162 - \left[(10) * a + (1) * b + (1) * c\right]$$

where a = absence or presence of gait instability (0 or 1), b = obex position in mm, and c = M-line-FVV distance in mm. Thus, patients with no gait instability, a caudally located cervicomedullary junction (obex closer to the FM), and a shorter M-line-FVV distance would score higher on this model.

Performance Metrics of the Model

We performed a receiver operating characteristic (ROC) analysis with the total score using the model and compared it against clinical improvement (Fig. 48.4). A CCOS score of 11 and above was taken as the cutoff for clinical improvement. An optimal threshold score of 128 was identified from the ROC curve of this algorithm. The out-of-sample performance of the model was validated on a cohort of 25 patients. The model demonstrated a fair performance in this validation set in predicting better clinical outcomes, with an area under the curve (AUC) of 0.75, and achieved a sensitivity of 80% (i.e., 80% of the patients with scores <128 would be correctly identified as having a CCOS score of less than 11) and specificity of 70% (i.e., 70% of the patients with scores >128 on the model would demonstrate a CCOS score of 11 or more). The other performance metrics of the algorithm are listed in Table 48.5. Inter-rater reliability analysis of the model demonstrated a κ (kappa) value of 0.85, indicating excellent agreement.

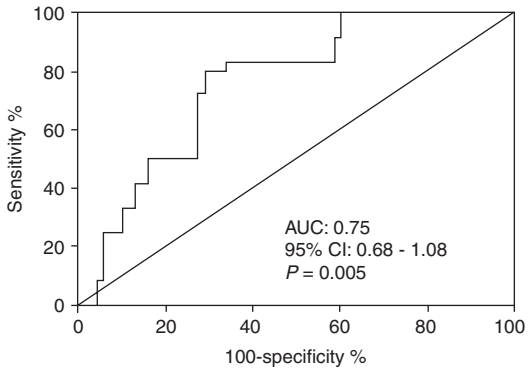

Fig. 48.4 Receiver operating characteristic (ROC) curve of the linear regression model used for predicting outcome as measured by the Chicago Chiari Outcome Scale (CCOS)

The aforementioned scoring system is unique in its simplicity and ease of use and has a good predictive power. It may, however, be cautioned that the predictive value for this model holds good for a relatively short follow-up period of around 3 years. Furthermore, our results need external validation in larger sample sizes and in different patient populations.

Machine Learning-Based Algorithm in Chiari I

The typically used predictive models, like the one detailed previously, utilize statistical regression to identify outcome predictors or risk factors for a particular condition. However, it has been established that regression models are not an optimal approach for complex conditions with possible nonlinearity [94]. Such models often generate misleading conclusions due to factors such as sensitivity to data noise and multicollinearity [95]. An alternative and more robust method of predicting postoperative outcome involves the usage of ML in creating predictive algorithms. For the first time ever, we used ML in predicting outcomes in CM I. With the same data set as used in the previous section, we applied various ML tools using Python 3.6 and generated a "feature importance ranking"

Table 48.5 Comparison of the performance metrics of the different predictive models

	Accuracy	Precision	Recall	AUC	F score
Linear regression	0.68	0.57	0.80	0.75	0.66
SVM	0.82	0.84	0.91	0.75	0.87
Random forest	0.70	0.70	1.00	0.50	0.82
XGBoost	0.84	0.80	1.00	0.80	0.88

AUC area under the curve, *SVM* support vector machine, *XGBoost* Extreme Gradient Boosting

of the predictors. AUC and accuracy were the main measures used to compare the performance between the various models.

At the preprocessing stage of our ML analysis, we first inspected our data for missing values. If information for any particular variable was not available in the hospital records, the group mean for that particular variable was substituted for the missing value. As the next step, data visualization was attempted using principal component analysis (PCA) and the t-distributed stochastic neighbor embedding (t-SNE) technique. PCA is a mathematical technique designed to extract the minimum number of variables that can explain the maximum variation in the original data set. t-SNE, on the other hand, utilizes a probabilistic approach to the problem. It attempts to *minimize the divergence between two distributions: a distribution that measures pair-wise similarities of the input and a distribution that measures similarities of the corresponding low-dimensional points* [96]. t-SNE enabled better visualization of our data set without having to use any output function (Fig. 48.5). Its results also implied that our data set was complex and that the usage of tree-based models (such as random forest and gradient boosting) would probably yield more robust results than those obtained from linear models (like regression and support vector machine [SVM]).

Our data set was found to be imbalanced, with the minority class forming around 12% of the data. In order to obtain a good overall class performance in such a setting, we used an oversampling technique called the Synthetic Minority Over-sampling technique (SMOTE). SMOTE creates synthetic instances of the minority class rather than creating copies. This helps ensemble learning models broaden their decision regions for the minority class [97]. Our data was then normalized and then split into a t*raining and testing set (in an 85:15 ratio). The model was then iteratively trained and validated using K-fold cross validation, a technique that avoids overfitting by generating multiple splits of the training and validation sets.*

We then applied support vector machine and two tree-based ensemble models—random forest (RF) classifier and a "boosting" method and the Extreme Gradient Boosting (XGBoost)—on our data set. A linear SVM is a linear classifier that attempts to find a hyperplane with the largest margin that segregates the input space into regions of interest pertaining to our classes in the data set [98]. Tree-based ensemble models are generally considered superior to other ML algorithms because of their effectiveness in dealing with nonlinearity [98]. The random forest classifier is an ensemble of decision trees trained with the "bagging" method [98, 99]. A "bagging"

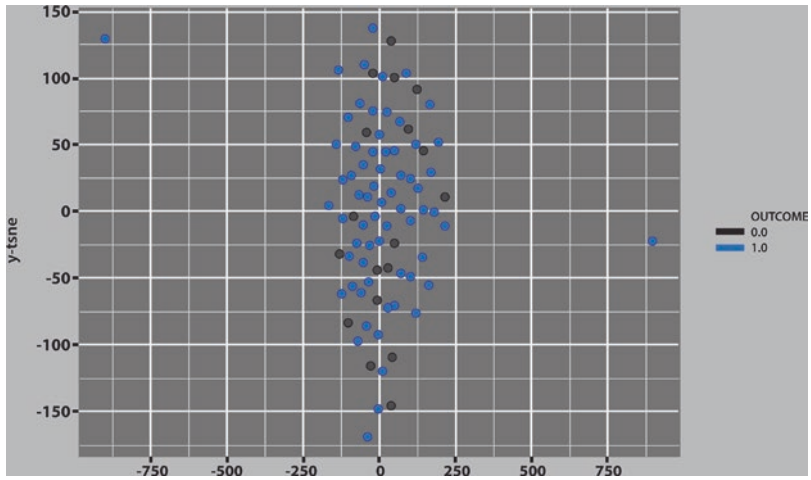

Fig. 48.5 Data visualization by the t-distributed stochastic neighbor embedding (t-SNE) technique

method creates different models by resampling the data to make the model robust. "Boosting" is a method for improving the model predictions of any given learning algorithm by converting a set of "weak learners" to "strong learners." It does so by repetitively learning a set of weak models on the data subsets. Gradient boosting (GB) works by sequentially adding predictors to an ensemble, each one correcting its predecessor. It tries to fit the new predictor to the residual errors made by the previous predictor. XGBoost is an improved version of the GB technique that is designed for speed and performance [98, 100]. It has been one of the most successful ML techniques, because it is computationally efficient and scalable and prevents over-fitting.

Our analysis showed that the XGBoost classifier yielded significantly better results compared to RF and SVM (Fig. 48.6) using a CCOS score of 12 and above as the cutoff for clinical improvement. The parameters that yielded the best results for the XGBoost were as follows: Estimators = 1000, Max_depth = 8, Scale_pos_weight = 1, Objective = Binary-logistic. The most predictive attributes were obtained as a feature ranking list using the inbuilt F estimator. Attributes with weightage <0.1 were excluded from this list, and the algorithm was then rerun. Subsequently, the metrics of the algorithm improved significantly, with an AUC of 0.80 and accuracy of 0.84 (Fig. 48.7). The final feature ranking list is displayed in Fig. 48.8.

Comparison of the Linear Regression and Various Machine Learning Models

As mentioned previously, data visualization techniques in the preliminary ML analysis proved that our data set was nonlinear and multidimensional. This underscores the need to migrate from the traditional linear statistics to ML to be able to perform a more robust outcome analysis in CM I. Our ML model based on XGBoost outperformed the LR model on all metrics (Table 48.5). Besides having higher recall (sensitivity), precision (ratio of correctly predicted positive observations to the total predicted positive observations), F1 score, and accuracy (ratio of correctly predicted observation to the total observations), it had a better overall predictive performance as measured by the AUC. A test with high accuracy and AUC, like our ML model, indicates that the

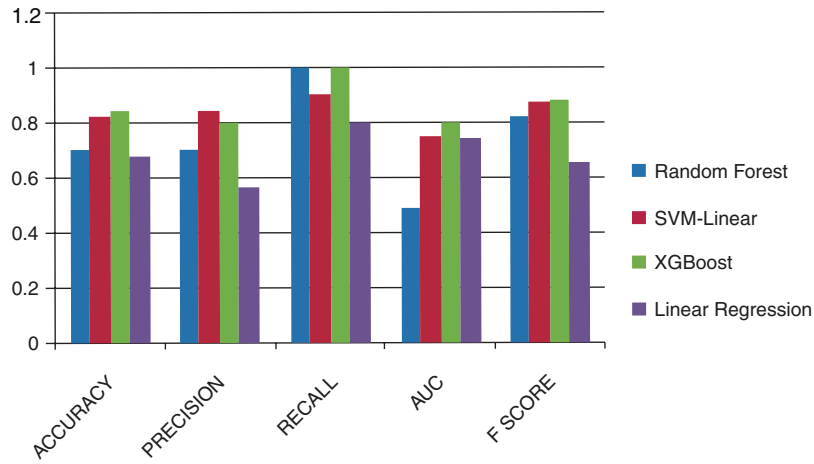

Fig. 48.6 Comparison of the performance metrics of the different machine learning models and the linear regression model (SVM = support vector machine, XGBoost = Extreme Gradient Boosting)

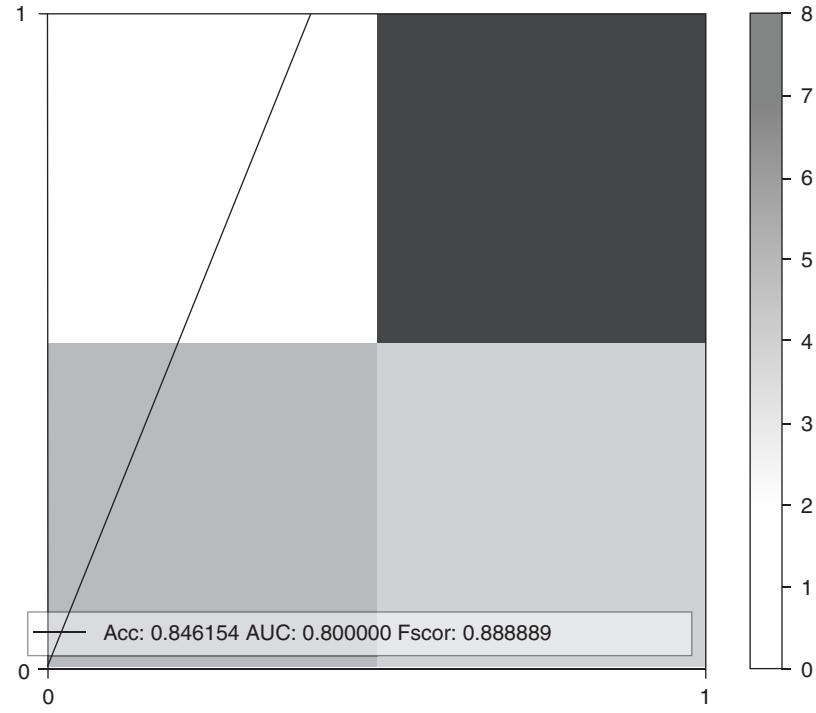

Fig. 48.7 Receiver operating characteristic (ROC) curve of the machine learning (XGBoost)-based predictive model used for predicting outcome as measured by the Chicago Chiari Outcome Scale (CCOS)

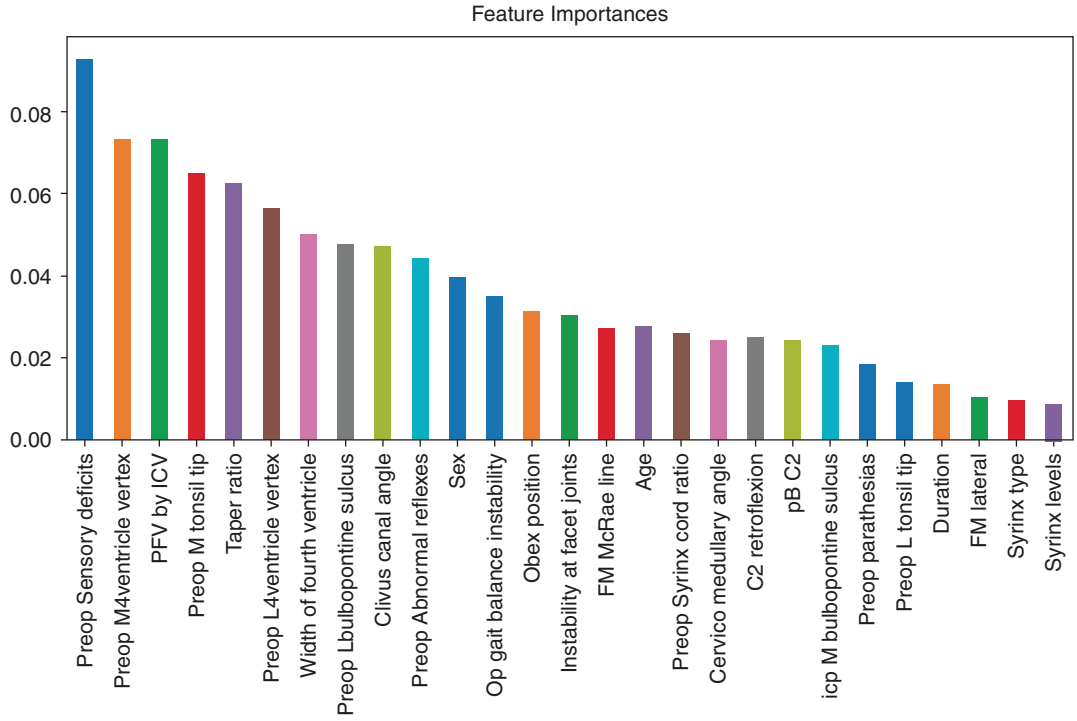

Fig. 48.8 Feature ranking list of variables obtained from the machine learning model

classifier works well at all thresholds. The superiority of the performance of ML over LR has been demonstrated in other neurosurgical conditions [1], but ours is the first one to document this in CM I.

Inferences from our Regression Model

The results of our predictive analysis using the regression model identified the presence of motor deficits, abnormal reflexes, and gait instability to correlate with outcome after CM I surgery [85]. This has been recognized in previous studies as well [31, 32]. It can be construed that by the time patients with CM I develop these specific deficits, severe neurological dysfunction in the alpha-motor neurons and corticospinal or dorsal column tracts occurred to a degree that surgical intervention is unlikely to achieve a good radiological or clinical outcome. At variance with previous reports [29, 33], we found that cough headache or any sensory symptoms or deficits did not correlate with outcome. There was no correlation between clinical improvement and syrinx regression in our study. This finding has been previously described [36] wherein it was noted that while the cord diameter per se correlated with clinical improvement, the syrinx-cord ratio did not. This was hypothesized to be due to differential rates of reduction of the cord and syrinx diameters following surgery.

The hindbrain and posterior fossa morphometric variables that correlated with outcome in our study included the PFV/ICV ratio for its correlation with syrinx regression and the obex position and M-line-FVV distance for their correlations with the CCOS. Posterior fossa morphometry has been demonstrated to be altered in CM I [92], with evidence that patients with smaller posterior fossae respond better to decompressive surgery than their normal-sized counterparts [35]. Our finding of a smaller PFV/ICV ratio correlating with better syrinx regression is consistent with this observation. The position of the obex or the cervicomedullary junction in relation to the FM in CM I has been studied previously [33], with caudal displacement of the same being construed as a marker of CM I severity [101]. Our study suggests that along with the classical tonsillar descent in CM I, the cervicomedullary junction also tends to get caudally displaced toward the FM. A previous study [93] had noted various shifts of hindbrain morphometric lines after surgery indicative of the deformed cerebellum reverting to its normal morphology, with the M-line-FVV being a marker of the deformed cerebellum in the crowded posterior fossa [93]. We noted an inverse relation between this M-line-FVV distance and the CCOS.

Our results underscore the existence of a "worse is better" paradigm in relation to CM I outcomes. This has been previously noted in studies that have documented markers of worse hindbrain pathology such as poor CSF flow [34], smaller posterior fossa volume [35], and a pB-C2 distance >3 mm [27] being associated with *better* outcomes after surgery. The consensus in these studies is that the more severe the hindbrain CSF flow, either due to a smaller posterior fossa or due to ventral encroachment by an angulated odontoid, the more direct is its patho-etiological role in symptomatology, and the better is the response to decompressive surgery. After adjusting for multiple variables, our predictive algorithm identified two novel preoperative markers, the obex position and the M-line-FVV distance, that corroborate the "worse is better" radiological paradigm in CM I. Caudal displacement of the obex (i.e., a shorter distance from the FM) can be considered a marker of disease severity in CM I, as alluded to earlier. Given the fact that posterior fossa overcrowding is considered a hallmark of CM I, it can be inferred that a smaller M-line-FVV distance correlating with smaller PFV/ICV ratios is indicative of it being a marker of worse anomalous hindbrain morphology. Smaller values obtained on both these novel preoperative markers translated to better CCOS scores at follow-up.

Implications of the Machine Learning Algorithm

Our ML algorithm, with an overall predictive performance of 80% and a classification accuracy of 84%, fared better than the LR model in all performance metrics (Table 48.5). As alluded to earlier,

the accuracy of such ML algorithms improves as it "learns" the problem better with the inclusion of new data points over time. Usage of such an algorithm would thus help clinicians prognosticate postsurgical clinical outcome in CM I with increasing accuracy. It should be noted here that while the significant variables identified in the LR model individually reflect positive or negative correlations with the outcome measure, the feature ranking list obtained from the ML algorithm (Fig. 48.8) has a different connotation. The ranking information provided by this list judges the *degree* of class discriminatory information that each variable contains and does not signify the direction of impact (positive or negative) on the class label.

Among the various clinical features used as input variables in our ML analysis, sensory deficits, abnormal reflexes, and gait instability demonstrated the highest degrees of importance in the ML ranking list. Of these, gait instability featured as a significant predictor in our LR model as well. Patients with these clinical features probably represent a relatively advanced stage of the disease and are unlikely to experience clinical improvement. This observation is in line with previous literature [29, 31, 33] and advocates earlier surgical intervention for the symptomatic CM I patients.

Interestingly, almost all the other variables that figured in the final ML ranking list were radiological ones. Many of the highly weighted radiological variables in the predictive algorithm pertain to altered hindbrain morphology. The M-line-FVV distance described earlier (and found to be significant in the LR model as well), the L-line-FVV distance (Fig. 48.3c), and the axial width of the fourth ventricle are representative of the degree of cerebellar deformation in a crowded posterior fossa. The L-line-bulbopontine sulcus distance (Fig. 48.3c) and the M-line-tonsillar tip distance (Fig. 48.3d) are indicative of brainstem deformation and the degree of crowding at the CVJ, respectively. Whether the physical compression or deformation of the neural elements indicated by these variables influences clinical outcomes directly or through altered CSF dynamics needs further elucidation. What stands clear from our ML analysis is that these variables, representative of varying degrees of hindbrain compromise, have a relatively high discriminatory power in predicting clinical improvement.

The other higher-ranked radiological variables that are featured in the ML algorithm included PFV/ICV, cervical taper ratio, and the clivus-canal angle. Posterior fossa morphometry has been demonstrated to be altered in CM I [92, 102], and postoperative increase in PFV has been found to correlate with improvement in headache and overall surgical outcome [103]. While our LR model demonstrated a correlation between PFV/ICV and syrinx regression, the ML algorithm established PFV/ICV to be a predictor of clinical outcome. The cervical taper ratio, a measure of the progressive narrowing of the cervical spinal canal from C1 to C7 (Fig. 48.3b), is being increasingly recognized to be greater in CM I patients than in the normal population [91, 104–106]. The steeper tapering in CM I has been postulated to result in higher CSF pressure gradients between the cranial and caudal ends of the spinal canal, resulting in altered CSF flow that favors syrinx formation [91, 104]. Our algorithm proves for the first time that this also has implications on clinical improvement after surgery. Of the various possible skull base osseous variations seen in CM I, the clivus-canal angle was found to be predictive of clinical improvement. This finding is in concordance with previous studies that reported altered clivus angle gradients to relate to unsatisfactory clinical outcomes [107, 108].

Conclusion

The sheer heterogeneity of clinico-radiological presentations, management options, and outcomes of CM I makes the understanding of the disease a perpetual challenge for both patients and their caregivers. Predictive analytics is a developing field that may hold the key to many of the answers that are being sought. We present a summary of all the work done so far in predictive analysis in CM I. Our ML-based model has thrown up various novel morphological predictors of clinical outcome in CM I. Going forward, external validation of models such as ours in larger and varying populations may help in demystifying this complicated and potentially disabling disease.

Acknowledgments
Source of Support: The authors have not received any support, in the form of grant, from any source for preparation of this chapter. Neither do the authors nor do their institutes have any personal or institutional financial interest in the contents of this submission.

Disclosure: There is no conflict of interest arising from this article.

Parts of this chapter have been published before in Thakar et al. [85]. Permission for reproducing material has been obtained from the Journal of Neurosurgery Publishing Group, AANS.

References

1. Senders JT, Staples PC, Karhade AV, Zaki MM, Gormley WB, Broekman MLD, et al. Machine learning and neurosurgical outcome prediction: a systematic review. World Neurosurg. 2018;109:476–86.
2. Moisi MD, Page J, Gahramanov S, Oskouian RJ. Bullet fragment of the lumbar spine: the decision is more important than the incision. Global Spine J. 2015;5(6):523–6.
3. Arle JE, Perrine K, Devinsky O, Doyle WK. Neural network analysis of preoperative variables and outcome in epilepsy surgery. J Neurosurg. 1999;90(6):998–1004.
4. Emblem KE, Pinho MC, Zöllner FG, Due-Tonnessen P, Hald JK, Schad LR, et al. A generic support vector machine model for preoperative glioma survival associations. Radiology. 2015;275(1):228–34.
5. Knoll MA, Oermann EK, Yang AI, Paydar I, Steinberger J, Collins B, et al. Survival of patients with multiple intracranial metastases treated with stereotactic radiosurgery: does the number of tumors matter? Am J Clin Oncol. 2018;41(5):425–31.
6. Hoffman H, Lee SI, Garst JH, Lu DS, Li CH, Nagasawa DT, et al. Use of multivariate linear regression and support vector regression to predict functional outcome after surgery for cervical spondylotic myelopathy. J Clin Neurosci. 2015;22(9):1444–9.
7. Azimi P, Mohammadi HR, Benzel EC, Shahzadi S, Azhari S. Use of artificial neural networks to predict recurrent lumbar disk herniation. J Spinal Disord Tech. 2015;28(3):E161–5.
8. Lo BW, Macdonald RL, Baker A, Levine MA. Clinical outcome prediction in aneurysmal subarachnoid hemorrhage using Bayesian neural networks with fuzzy logic inferences. Comput Math Methods Med. 2013;2013:904860.
9. Azimi P, Mohammadi HR. Predicting endoscopic third ventriculostomy success in childhood hydrocephalus: an artificial neural network analysis. J Neurosurg Pediatr. 2014;13(4):426–32.
10. Oermann EK, Rubinsteyn A, Ding D, Mascitelli J, Starke RM, Bederson JB, et al. Using a machine learning approach to predict outcomes after radiosurgery for cerebral arteriovenous malformations. Sci Rep. 2016;6:21161.
11. Chiari H. Über Veränderungen des Kleinhirns, des Pons und der Medulla Oblangata in Folge von kongenitaler Hydrocephalie des Grosshirns. Denkschriften Akad Wiss Wien. 1896;63:71–116. Germanica.
12. Chiari H. Über veränderungen des kleinhirns in folge von hydrocephales des grosshirns. Dtsch Med Wochenschr. 1891;17:1172–5. Germanica.
13. Iskandar BJ, Hedlund GL, Grabb PA, Oakes WJ. The resolution of syringohydromyelia without hindbrain herniation after posterior fossa decompression. J Neurosurg. 1998;89:212–6.
14. Tubbs RS, Iskandar BJ, Bartolucci AA, Oakes WJ. A critical analysis of the Chiari 1.5 malformation. J Neurosurg. 2004;101(2 Suppl):179–83.
15. Urbizu A, Martin BA, Moncho D, Rovira A, Poca MA, Sahuquillo J, et al. Machine learning applied to neuroimaging for diagnosis of adult classic Chiari malformation: role of the basion as a key morphometric indicator. J Neurosurg. 2018;129(3):779–91.
16. Milhorat TH, Chou MW, Trinidad EM, Kula RW, Mandell M, Wolpert C, et al. Chiari I malformation redefined: clinical and radiographic findings for 364 symptomatic patients. Neurosurgery. 1999;44(5):1005–17.
17. Meadows J, Kraut M, Guarnieri M, Haroun RI, Carson BS. Asymptomatic Chiari Type I malformations identified on magnetic resonance imaging. J Neurosurg. 2000;92:920–6.
18. Tubbs RS, Beckman J, Naftel RP, Chern JJ, Wellons JC 3rd, Rozzelle CJ, et al. Institutional experience with 500 cases of surgically treated pediatric Chiari malformation Type I. J Neurosurg Pediatr. 2011;7(3):248–56.
19. McVige JW, Leonardo J. Imaging of Chiari type I malformation and syringohydromyelia. Neurol Clin. 2014;32(1):95–126.
20. Rogers JM, Savage G, Stoodley MA. A systematic review of cognition in Chiari I malformation. Neuropsychol Rev. 2018;28(2):176–87.
21. Roohi F, Gropen T, Kula RW. Sudden unexpected nocturnal death in Chiari type 1 malformation and potential role of opioid analgesics. Surg Neurol Int. 2014;5:17.
22. McGirt MJ, Attenello FJ, Atiba A, Garces-Ambrossi G, Datoo G, Weingart JD, et al. Symptom recurrence after suboccipital decompression for pediatric Chiari I malformation: analysis of 256 consecutive cases. Childs Nerv Syst. 2008;24:1333–9.
23. Nagoshi N, Iwanami A, Toyama Y, Nakamura M. Factors contributing to improvement of syringomyelia after foramen magnum decompression for Chiari type I malformation. J Orthop Sci. 2014;19:418–23.
24. Navarro R, Olavarria G, Seshadri R, Gonzales-Portillo G, McLone DG, Tomita T. Surgical results of posterior fossa decompression for patients

with Chiari I malformation. Childs Nerv Syst. 2004;20:349–56.
25. Park YS, Kim DS, Shim KW, Kim JH, Choi JU. Factors contributing improvement of syringomyelia and surgical outcome in type I Chiari malformation. Childs Nerv Syst. 2009;25:453–9.
26. Wu T, Zhu Z, Jiang J, Zheng X, Sun X, Qian B, et al. Syrinx resolution after posterior fossa decompression in patients with scoliosis secondary to Chiari malformation type I. Eur Spine J. 2012;21:1143–50.
27. Ladner TR, Dewan MC, Day MA, Shannon CN, Tomycz L, Tulipan N, et al. Evaluating the relationship of the pB-C2 line to clinical outcomes in a 15-year single-center cohort of pediatric Chiari I malformation. J Neurosurg Pediatr. 2015;15:178–88.
28. Tubbs RS, Webb DB, Oakes WJ. Persistent syringomyelia following pediatric Chiari I decompression: radiological and surgical findings. J Neurosurg. 2004;100(5 Suppl Pediatrics):460–4.
29. Hekman KE, Aliaga L, Straus D, Luther A, Chen J, Sampat A, et al. Positive and negative predictors for good outcome after decompressive surgery for Chiari malformation type 1 as scored on the Chicago Chiari Outcome Scale. Neurol Res. 2012;34:694–700.
30. Attal N, Parker F, Tadié M, Aghakani N, Bouhassira D. Effects of surgery on the sensory deficits of syringomyelia and predictors of outcome: a long term prospective study. J Neurol Neurosurg Psychiatry. 2004;75:1025–30.
31. Dyste GN, Menezes AH, VanGilder JC. Symptomatic Chiari malformations. An analysis of presentation, management, and long-term outcome. J Neurosurg. 1989;71:159–68.
32. Chavez A, Roguski M, Killeen A, Heilman C, Hwang S. Comparison of operative and nonoperative outcomes based on surgical selection criteria for patients with Chiari I malformations. J Clin Neurosci. 2014;21:2201–6.
33. Greenberg JK, Yarbrough CK, Radmanesh A, Godzik J, Yu M, Jeffe DB, et al. The Chiari severity index: a preoperative grading system for Chiari malformation type 1. Neurosurgery. 2015;76:279–85.
34. McGirt MJ, Nimjee SM, Fuchs HE, George TM. Relationship of cine phase-contrast magnetic resonance imaging with outcome after decompression for Chiari I malformations. Neurosurgery. 2006;59:140–6.
35. Badie B, Mendoza D, Batzdorf U. Posterior fossa volume and response to suboccipital decompression in patients with Chiari I malformation. Neurosurgery. 1995;37:214–8.
36. Furtado SV, Thakar S, Hegde AS. Correlation of functional outcome and natural history with clinicoradiological factors in surgically managed pediatric Chiari I malformation. Neurosurgery. 2011;68:319–28.
37. Alperin N, Loftus JR, Bagci AM, Lee SH, Oliu CJ, Shah AH, et al. Magnetic resonance imaging-based measures predictive of short-term surgical outcome in patients with Chiari malformation Type I: a pilot study. J Neurosurg Spine. 2017;26(1):28–38.
38. Soroceanu A, Ching A, Abdu W, McGuire K. Relationship between preoperative expectations, satisfaction, and functional outcomes in patients undergoing lumbar and cervical spine surgery: a multicenter study. Spine (Phila Pa 1976). 2012;37:E103–8.
39. Milhorat TH, Nishikawa M, Kula RW, Dlugacz YD. Mechanisms of cerebellar tonsil herniation in patients with Chiari malformations as guide to clinical management. Acta Neurochir. 2010;152:1117–27.
40. Khan AA, Bhatti SN, Khan G, Ahmed E, Aurangzeb A, Ali A, et al. Clinical and radiological findings in Arnold Chiari malformation. J Ayub Med Coll Abbottabad. 2010;22:75–8.
41. Mueller DM, Oro' JJ. Prospective analysis of presenting symptoms among 265 patients with radiographic evidence of Chiari malformation type I with or without syringomyelia. J Am Acad Nurse Pract. 2004;16:134–8.
42. Noudel R, Gomis P, Sotoares G, Bazin A, Pierot L, Pruvo JP, et al. Posterior fossa volume increase after surgery for Chiari malformation Type I: a quantitative assessment using magnetic resonance imaging and correlations with the treatment response. J Neurosurg. 2011;115:647–58.
43. Alperin N, Loftus JR, Oliu CJ, Bagci A, Lee SH, Ertl-Wagner B, et al. Magnetic resonance imaging measures of posterior cranial fossa morphology and cerebrospinal fluid physiology in Chiari malformation type I. Neurosurgery. 2014;75:515–22.
44. Sekula RF Jr, Jannetta PJ, Casey KF, Marchan EM, Sekula LK, McCrady CS. Dimensions of the posterior fossa in patients symptomatic for Chiari I malformation but without cerebellar tonsillar descent. Cerebrospinal Fluid Res. 2005;2:11.
45. Urbizu A, Poca MA, Vidal X, Rovira A, Sahuquillo J, Macaya A. MRI-based morphometric analysis of posterior cranial fossa in the diagnosis of Chiari malformation type I. J Neuroimaging. 2014;24:250–6.
46. Strahle J, Muraszko KM, Kapurch J, Bapuraj JR, Garton HJ, Maher CO. Chiari malformation type I and syrinx in children undergoing magnetic resonance imaging. J Neurosurg Pediatr. 2011;8:205–13.
47. Sgouros S, Kountouri M, Natarajan K. Posterior fossa volume in children with Chiari malformation type I. J Neurosurg. 2006;105:101–6.
48. Halvorson KG, Kellogg RT, Keachie KN, Grant GA, Muh CR, Waldau B. Morphometric analysis of predictors of cervical Syrinx formation in the setting of Chiari I malformation. Pediatr Neurosurg. 2016;51(3):137–41.
49. Gad KA, Yousem DM. Syringohydromyelia in patients with Chiari I malformation: a retrospective analysis. AJNR Am J Neuroradiol. 2017;38(9):1833–8.

50. Fenoy AJ, Menezes AH, Fenoy KA. Craniocervical junction fusions in patients with hindbrain herniation and syringohydromyelia. J Neurosurg Spine. 2008;9:1–9.
51. Grabb PA, Mapstone TB, Oakes WJ. Ventral brain stem compression in pediatric and young adult patients with Chiari I malformations. Neurosurgery. 1999;44:520–8.
52. Milhorat TH, Bolognese PA, Nishikawa M, McDonnell NB, Francomano CA. Syndrome of occipitoatlantoaxial hypermobility, cranial settling, and Chiari malformation Type I in patients with hereditary disorders of connective tissue. J Neurosurg Spine. 2007;7:601–9.
53. Brockmeyer DL. The complex Chiari: issues and management strategies. Neurol Sci. 2011;32(Suppl 3):S345–7.
54. Bollo RJ, Riva-Cambrin J, Brockmeyer MM, Brockmeyer DL. Complex Chiari malformations in children: an analysis of preoperative risk factors for occipitocervical fusion. J Neurosurg Pediatr. 2012;10(2):134–41.
55. Arora P, Behari S, Banerji D, Chhabra DK, Jain VK. Factors influencing the outcome in symptomatic Chiari I malformation. Neurol India. 2004;52(4):470–4.
56. Kumar A, Pruthi N, Devi BI, Gupta AK. Morphometric factors affecting functional outcome in symptomatic Chiari I malformation and Syrinx. J Spinal Surg. 2017;4(4):145–9.
57. Aghakhani N, Parker F, David P, Morar S, Lacroix C, Benoudiba F, et al. Long-term follow-up of Chiari-related syringomyelia in adults: analysis of 157 surgically treated cases. Neurosurgery. 2009;64:308–15.
58. Liu H, Yang C, Yang J, Xu Y. Pediatric Chiari malformation type I: long-term outcomes following small-bone-window posterior fossa decompression with autologous-fascia duraplasty. Exp Ther Med. 2017;14(6):5652–8.
59. Elster AD, Chen MY. Chiari I malformations: clinical and radiologic reappraisal. Radiology. 1992;183:347–53.
60. Nohria V, Oakes WJ. Chiari headaches. Neurology. 1993;43:1272.
61. Grangeon L, Puy L, Gilard V, Hebant B, Langlois O, Derrey S, et al. Predictive factors of headache resolution after Chiari type 1 malformation surgery. World Neurosurg. 2018;110:e60–6.
62. Armonda RA, Citrin CM, Foley KT, Ellenbogen RG. Quantitative cine-mode magnetic resonance imaging of Chiari I malformations: an analysis of cerebrospinal fluid dynamics. Neurosurgery. 1994;35:214–23.
63. Bhadelia RA, Bogdan AR, Wolpert SM, Lev S, Appignani BA, Heilman CB. Cerebrospinal fluid flow waveforms: analysis in patients with Chiari I malformation by means of gated phase-contrast MR imaging velocity measurements. Radiology. 1995;196:195–202.
64. Curless RG, Quencer RM, Katz DA, Campanioni M. Magnetic resonance demonstration of intracranial CSF flow in children. Neurology. 1992;42:377–81.
65. Oldfield EH, Muraszko K, Shawker TH, Patronas NJ. Pathophysiology of syringomyelia associated with Chiari I malformation of the cerebellar tonsils. Implications for diagnosis and treatment. J Neurosurg. 1994;80:3–15.
66. Pujol J, Roig C, Capdevila A, Pou A, Marti-Vilalta JL, Kulisevsky J, et al. Motion of the cerebellar tonsils in Chiari type I malformation studied by cine phase-contrast MRI. Neurology. 1995;45:1746–53.
67. Wolpert SM, Bhadelia RA, Bogdan AR, Cohen AR. Chiari I malformations: assessment with phase-contrast velocity MR. AJNR Am J Neuroradiol. 1994;15:1299–308.
68. Arora P, Pradhan PK, Behari S, Banerji D, Das BK, Chhabra DK, et al. Chiari I malformation related syringomyelia: radionuclide cisternography as a predictor of outcome. Acta Neurochir. 2004;146(2):119–30.
69. McGirt MJ, Atiba A, Attenello FJ, Wasserman BA, Datoo G, Gathinji M, et al. Correlation of hindbrain CSF flow and outcome after surgical decompression for Chiari I malformation. Childs Nerv Syst. 2008;24(7):833–40.
70. Wang CS, Wang X, Fu CH, Wei LQ, Zhou DQ, Lin JK. Analysis of cerebrospinal fluid flow dynamics and morphology in Chiari I malformation with cine phase-contrast magnetic resonance imaging. Acta Neurochir. 2014;156(4):707–13.
71. Sakas DE, Korfias SI, Wayte SC, Beale DJ, Papapetrou KP, Stranjalis GS, et al. Chiari malformation: CSF flow dynamics in the craniocervical junction and syrinx. Acta Neurochir. 2005;147(12):1223–33.
72. Park CH, Chung TS, Kim DJ, Suh SH, Chung WS, Cho YE. Evaluation of intrasyrinx fluid motion by spatial modulation of magnetization-magnetic resonance imaging in syringomyelia with long-term follow-up: a predictor of postoperative prognosis? J Comput Assist Tomogr. 2008;32(1):135–40.
73. Alperin N, Sivaramakrishnan A, Lichtor T. Magnetic resonance imaging-based measurements of cerebrospinal fluid and blood flow as indicators of intracranial compliance in patients with Chiari malformation. J Neurosurg. 2005;103:46–52.
74. Alperin NJ, Lee SH, Loth F, Raksin PB, Lichtor T. MR-intracranial pressure (ICP): a method to measure intracranial elastance and pressure noninvasively by means of MR imaging: baboon and human study. Radiology. 2000;217:877–85.
75. Zhu Z, Wu T, Zhou S, Sun X, Yan H, Sha S, Qiu Y. Prediction of curve progression after posterior Fossa decompression in pediatric patients with scoliosis secondary to Chiari malformation. Spine Deform. 2013;1(1):25–32.
76. Mackel CE, Cahill PJ, Roguski M, Samdani AF, Sugrue PA, Kawakami N, et al. Factors associated with spinal fusion after posterior fossa decom-

pression in pediatric patients with Chiari I malformation and scoliosis. J Neurosurg Pediatr. 2016;25(6):737–43.
77. Monk SH, Zhao S, Strahle J, Averill C, Couture DE, Johnston JM, et al. Predictors of spinal fusion within 2 years of posterior Fossa decompression in patients with Chiari malformation type 1 and scoliosis: a multi-institutional experience with the Park-Reeves Syringomyelia research consortium. Neurosurgery. 2018;65(Suppl 1):116–7.
78. Ravindra VM, Onwuzulike K, Heller RS, Quigley R, Smith J, Dailey AT, et al. Chiari-related scoliosis: a single-center experience with long-term radiographic follow-up and relationship to deformity correction. J Neurosurg Pediatr. 2018;21(2):185–9.
79. Guan J, Riva-Cambrin J, Brockmeyer DL. Chiari-related hydrocephalus: assessment of clinical risk factors in a cohort of 297 consecutive patients. Neurosurg Focus. 2016;41(5):E2.
80. Zakaria R, Kandasamy J, Khan Y, Jenkinson MD, Hall SR, Brodbelt A, et al. Raised intracranial pressure and hydrocephalus following hindbrain decompression for Chiari I malformation: a case series and review of the literature. Br J Neurosurg. 2012;26:476–81.
81. Menger R, Connor DE Jr, Hefner M, Caldito G, Nanda A. Pseudomeningocele formation following Chiari decompression: 19-year retrospective review of predisposing and prognostic factors. Surg Neurol Int. 2015;6:70.
82. Rieder E, Steinacher-Nigisch A, Weigel G. Human immune-cell response towards diverse xenogeneic and allogeneic decellularized biomaterials. Int J Surg. 2016;36:347–51.
83. Xu H, Wan H, Sandor M, Qi S, Ervin F, Harper JR, et al. Host response to human acellular dermal matrix transplantation in a primate model of abdominal wall repair. Tissue Eng Part A. 2008;14:2009–19.
84. Aliaga L, Hekman KE, Yassari R, Straus D, Luther G, Chen J, et al. A novel scoring system for assessing Chiari malformation type I treatment outcomes. Neurosurgery. 2012;70(3):656–64.
85. Thakar S, Sivaraju L, Jacob KS, Arun AA, Aryan S, Mohan D, et al. A points-based algorithm for prognosticating clinical outcome of Chiari malformation Type I with syringomyelia: results from a predictive model analysis of 82 surgically managed adult patients. J Neurosurg Spine. 2018;28(1):23–32.
86. Milhorat TH, Johnson RW, Milhorat RH, Capocelli AL Jr, Pevsner PH. Clinicopathological correlations in syringomyelia using axial magnetic resonance imaging. Neurosurgery. 1995;37:206–13.
87. Besachio DA, Khaleel Z, Shah LM. Odontoid process inclination in normal adults and in an adult population with Chiari malformation Type I. J Neurosurg Spine. 2015;23:701–6.
88. Tubbs RS, Wellons JC III, Blount JP, Grabb PA, Oakes WJ. Inclination of the odontoid process in the pediatric Chiari I malformation. J Neurosurg. 2003;98(1 Suppl):43–9.
89. Smoker WR, Khanna G. Imaging the craniocervical junction. Childs Nerv Syst. 2008;24:1123–45.
90. Hyun SJ, Moon KY, Kwon JW, Lee CH, Kim J, Kim KJ, et al. Chiari I malformation associated with syringomyelia: can foramen magnum decompression lead to restore cervical alignment? Eur Spine J. 2013;22:2520–5.
91. Hirano M, Haughton V, Munoz del Rio A. Tapering of the cervical spinal canal in patients with Chiari I malformations. AJNR Am J Neuroradiol. 2012;33:1326–30.
92. Furtado SV, Reddy K, Hegde AS. Posterior fossa morphometry in symptomatic pediatric and adult Chiari I malformation. J Clin Neurosci. 2009;16:1449–54.
93. Xie D, Qiu Y, Sha S, Liu Z, Jiang L, Yan H, et al. Syrinx resolution is correlated with the upward shifting of cerebellar tonsil following posterior fossa decompression in pediatric patients with Chiari malformation type I. Eur Spine J. 2015;24:155–61.
94. Jin J, Zhou S, Xu Q, An J. Identification of risk factors in epidemiologic study based on ROC curve and network. Sci Rep. 2017;7:46655.
95. Hui L, Xiaoyi L, Murali R, Aidong Z. Prediction and informative risk factor selection of bone diseases. IEEE/ACM Trans Comput Biol Bioinform. 2015;12(1):79–91.
96. Maaten LV, Hinton G. Visualizing data using t-SNE. J Mach Learn Res. 2008;9:2579–605.
97. Chawla NV, Bowyer KW, Hall LO, Kegelmeyer WP. SMOTE: synthetic minority over-sampling technique. J Artif Intell Res. 2002;16:321–57.
98. Tan PN, Kumar V. Introduction to data mining. India: Doring Kindersely Pvt Ltd, Pearson Education; 2013.
99. Svetnik V, Liaw A, Tong C, Culberson JC, Sheridan RP, Feuston BP. Random forest: a classification and regression tool for compound classification and QSAR modeling. J Chem Inf Comput Sci. 2003;43(6):1947–58.
100. Chen T, Guestrin C. Xgboost. A scalable tree boosting system. In Proceedings of the 22nd ACM Sigkdd international conference on knowledge discovery and data mining. 2016. p. 785–94. ACM.
101. Kim IK, Wang KC, Kim IO, Cho BK. Chiari 1.5 malformation: an advanced form of Chiari I malformation. J Korean Neurosurg Soc. 2010;48:375–9.
102. Nishikawa M, Sakamoto H, Hakuba A, Nakanishi N, Inoue Y. Pathogenesis of Chiari malformation: a morphometric study of the posterior cranial fossa. J Neurosurg. 1997;86(1):40–7.
103. Khalsa SSS, Siu A, DeFreitas TA, Cappuzzo JM, Myseros JS, Magge SN, et al. Comparison of posterior fossa volumes and clinical outcomes after decompression of Chiari malformation Type I. J Neurosurg Pediatr. 2017;19(5):511–7.
104. Hammersley J, Haughton V, Wang Y, del Rio AM. Tapering of the cervical spinal canal in patients with scoliosis with and without the Chiari I malformation. AJNR Am J Neuroradiol. 2012;33:1752–5.

105. Zhu Z, Sha S, Sun X, Liu Z, Yan H, Zhu W, et al. Tapering of the cervical spinal canal in patients with distended or nondistended syringes secondary to Chiari type I malformation. AJNR Am J Neuroradiol. 2014;35:2021–6.
106. Thakar S, Kurudi Siddappa A, Aryan S, Mohan D, Sai Kiran NA, Hegde AS. Does the mesodermal derangement in Chiari Type I malformation extend to the cervical spine? Evidence from an analytical morphometric study on cervical paraspinal muscles. J Neurosurg Spine. 2017;27(4):421–7.
107. Wang X, Gao J, Wang T, Li Z, Li Y. Clinical significance of variable clivus gradients in patients with Chiari malformation Type I after surgical decompression: a retrospective analysis. World Neurosurg. 2018;S1878–8750(18):32365–9.
108. Henderson FC Sr, Henderson FC Jr, Wilson WA 4th, Mark AS, Koby M. Utility of the clivo-axial angle in assessing brainstem deformity: pilot study and literature review. Neurosurg Rev. 2018;41(1):149–63.

Treatment Costs of Chiari Malformation Type 1

49

I-Wen E. Pan and Sandi Lam

Introduction

Health Spending and Quality of Care in the United States

The health spending per capita in 2017 is US$10,209, which was 17% of gross domestic product in the United States. US healthcare has been the most expensive healthcare system among the Organisation for Economic Co-operation and Development (OECD) countries over the past three decades [1]. This health spending did not translate to better quality of healthcare in the United States [2]. Americans are less healthy than their counterparts in other developed nations: Americans are on average overweight, and they have less coverage for a core set of healthcare services. More than one in five people, 22.3% of the US population, have reported skipping a healthcare consultation due to cost [3]. Along with the high spending, healthcare resources in the United States are limited, and the allocation of health resources are unequal geographically. The number of physicians per 1000 population is much higher in capital cities and urban areas than those in rural regions [3]. Ensuring sufficient funding and resources is a continuing challenge in healthcare services.

In the past, all payers adopted cost-based reimbursement systems. Medical providers were paid by fee-for-service (FFS) models. In the 1980s, with contributions from new medical technology, the health insurance premiums were rapidly increasing. The annual premium increase rate is much faster than the annual inflation rate [4]. As a result, public and private payers developed new payment systems to control the growth of medical care expenditures.

The resource-based relative value scale (RBRVS) design for physician payment theoretically reflects the amount of physician work required to perform the service along with the associated costs. The RBRVS and Medicare prospective payment system (PPS) for hospitals were introduced in the 1980s and 1990s [5, 6]. These Medicare payment systems aimed to rationalize FFS under Medicare, reduce the rapid growth of healthcare expenditures, protect access to care, and uphold quality of care.

Meanwhile, managed care health plans including health maintenance organizations (HMOs), preferred provider organizations (PPOs) with out-of-pocket payments, and point-of-service (POS) models in the private payer system were developed. In 1988, 71% of workers had

I.-W. E. Pan (✉)
Department of Health Services Research, Division of OVP, Cancer Prevention and Population Sciences, The University of Texas MD Anderson Cancer Center, Houston, TX, USA

S. Lam
Division of Neurosurgery, Ann & Robert H. Lurie Children's Hospital of Chicago, Chicago, IL, USA

R. S. Tubbs et al. (eds.), *The Chiari Malformations*, https://doi.org/10.1007/978-3-030-44862-2_49

conventional insurance plans, and 29% had managed care plans. In 2008, 90% workers had managed care plans, and 8% had consumer-driven high-deductible plans. The conventional cost-based reimbursement plans shrank to 2% of the private insurance market in 2008 and less than 1% in 2012 [4]. However, these strategies were primarily focused on cost containment rather than the quality of care. Managed care plans focused on controlling and reducing utilization. Healthcare providers merged and consolidated to reduce costs. More hospital systems appeared; small hospitals closed or joined bigger hospital systems. As a result, patients had limited access to healthcare, and the utilization did not decrease overall. In the mid-2000s, the consumer-direct high-deductible (CDHD) health plan was introduced to the market. Because of high-deductible costs, the CDHD health plan gave the consumer more incentive to shop carefully and thus was expected to reduce unnecessary healthcare utilization. This is difficult to apply in reality given the lack of transparency in healthcare services pricing.

From a health services research standpoint, it is important to evaluate the quality of a healthcare system including three dimensions: efficacy (effectiveness), efficiency, and equity [7]. That is, to examine the improvements in health, the efficient resource allocation for health delivery, and fairness of health delivery. The Affordable Care Act (ACA) was enacted in 2010. The goals of the ACA are "making affordable health insurance available to more people by subsidies (premium tax credits) for lowering healthcare costs, expanding the Medicaid program to cover all adults with income below 138% of the federal poverty level, and supporting innovative medical care delivery methods designed to lower the costs of health care" [8]. Subsequently, the uninsured rate declined from 16.0% in 2010 to 9.1% in 2015 [9]. The insurance-covered population was increased; the total healthcare expenditures were also increased from $2.6 trillion in 2010 to $3.2 trillion in 2015 [10].

The healthcare resources are limited; cost containment is always the top priority for health policymakers. To balance between cost and quality of care is the ultimate goal. It is necessary to use the resources wisely and avoid waste.

Bundled Payment

While accessibility to healthcare has increased, quality of care remains a concern. In recent years, the concept of the "bundled payment," which transitions away from the fee-for-service model, has gained significant attraction. Medicare and private insurance plans have begun utilizing this model for reimbursement, as seen in the Centers for Medicare & Medicaid Services (CMS) Medicare Severity-Diagnosis-Related Groups (MS-DRGs) and All Patients Refined Diagnosis-Related Groups (APR-DRGs) [11–13]. Further, CMS employs risk-adjusted models and hierarchical coexisting condition models to adjust Medicare reimbursement [14]. A newly developed scheme of bundled payments named CMS Bundled Payments for Care Improvement (BPCI) was proposed in 2009 and initiated in 2010 [15]. The BPCI links payments for multiple services during an episode of care. The stated purpose is to drive toward a higher quality of care while containing costs. Particularly for surgical hospitalizations, several models proposed by BPCI motivate providers to contain costs with their own risk; initial rollouts started in select adult populations in 2018 [16]. While this payment format has not affected pediatric care or neurosurgical care, it is a trend that is important to recognize and anticipate. The bundled payment concept applies directly for surgical hospitalizations, especially for elective surgeries such as those for a majority of Chiari malformation type 1 (CM 1); it is essential for surgeons, healthcare providers, hospital systems, and payers to understand costs and risks.

Healthcare Costs

The particular stakeholder's viewpoint of healthcare costs defines the scope of healthcare costs and its cost estimation. From the patient's viewpoint, in addition to direct treatment costs, the

indirect travel and other employment opportunity costs need to be added to the total healthcare costs for seeking a healthcare service. Diagnostic tests, medications, imaging services, laboratory services, surgical facilities, medical devices, medical staff, and professional fees consist of total healthcare costs from the payer's perspective, such as when the payer is a private insurance or government entity. To understand why healthcare spending is continuously rising, we must identify what are the drivers of healthcare costs.

In this chapter, our discussion will focus on healthcare costs from a payer's perspective. Chiari malformation type 1 is a common entity treated on a typically elective basis in pediatric neurosurgery, and surgical treatment of this disease presents a significant outlay of healthcare expenditures [17]. Unadjusted cost estimates are between $7000 and $30,000 for a single hospitalization [18, 19]. As payers continue to develop reimbursement models for the bundling of payments, it is becoming increasingly important to define the costs of elective surgical procedures such as that for CM 1. The next section will use an illustrative study to describe how to identify the drivers of hospitalization costs and develop a hospitalization cost model for the surgical treatment of pediatric CM 1 [20].

Illustrative Study: Hospitalization Costs of Chiari Malformation Type 1 in the Pediatric Population

Data Sources

Ideally, itemized cost data collected from the hospital will be the best source of cost estimation; however, it is unlikely the hospital will share data for research purposes with the third party. Thus a common source of data in healthcare cost studies is administrative claims data from public (Medicare and Medicaid) or private insurers. This study [20] used the data extracted from the Kids' Inpatient Database (KID). The KID, one of a families of administrative databases, was developed by the Healthcare Cost and Utilization Project (HCUP) sponsored by the Agency for Healthcare Research and Quality (AHRQ, Rockville, Maryland, USA). Patient discharge data included patient demographics; admission type and source; diagnostic and procedural International Classification of Disease, Ninth Edition (ICD-9) codes; length of stay (LOS); disposition; and payer data. The number of participating states was 44 in 2009, with data from 4100 hospitals. The KID contains information from 2 to three million pediatric discharges, weighted to represent 6.5–7.5 million national discharges. The basic unit of analysis is a patient discharge rather than an individual patient. The KID records were post-stratified by US region, urban or rural location, teaching status, ownership, and bed size, with the addition of a stratum for freestanding children's hospitals [21]. Analysis of this de-identified data typically constitutes nonhuman subjects research by institutional review boards.

Chiari Malformation Type 1 Case Identification from Claims Data

Healthcare providers have claims data to show the reimbursement from their treatment costs from payers. A database containing claims is the best source to identify healthcare costs. However, the codes used to identified clinical cases are not exactly the way medical records are written, and thus it is important to verify how coding reflects clinical care. Ladner and colleagues validated and published an algorithm [22] that helps to identify Chari malformation type 1 cases. Patients with a primary ICD-9-CM diagnosis code of 348.4 and procedure codes consistent with CM 1 decompression, 01.24 for cranial decompression, or 03.09 spinal decompression or laminectomy [22] and excluding patient records associated with Chiari malformation type 2 (741.0) have been described as Chiari malformation type 1 cases.

Treatment Costs and Cost Estimation

Claims data can extract treatment charges but not treatment costs. A consumer price index

(CPI) should be applied if the cost data is taken across multiple years. In this case, patient charges associated with Chiari malformation type 1 hospital admission were extracted. The KID provides two types of cost-to-charge ratios (CCRs). The charges were converted to costs by either hospital-specific cost-to-charge ratio (AP CCR) if available or the group-weighted average CCR in the minority of reporting hospitals who were missing API CCR values [23]. Moreover, hospitalization costs were adjusted by the area wage index to control price factors in a geographic area compared to the national average hospital wage level [23]. In this example, we did not apply a consumer price index because all data was extracted from 1 year: the 2009 KID database.

Cost Model: Factors Associated with the Costs

Several state Medicaid programs including Texas, Arizona, and Florida have adopted prospective payment and pricing systems (PPS) for reimbursement based on All Patient Refined Diagnosis-Related Groups (APR-DRGs) [24, 25]. APR-DRGs include non-Medicare populations such as pediatric patients with adjusted severity of illness [12, 26]. This study included data elements used by APR-DRGs, principal diagnosis, secondary diagnosis, procedures, age, and gender to construct the cost models. Also, consideration of geographical variation, hospital types, registered nurse (RN) full-time equivalents (FTEs), and nonclinical socioeconomic covariates, such as race, insurance status, and income level, were examined for their impact on hospital costs (HC) [27, 28]. Three known disease-specific comorbidities for CM 1 (hydrocephalus, syringomyelia, and scoliosis), pediatric complex chronic conditions (P-CCCs), and perioperative complications were also included in the cost model [29, 30]. Length of stay was not included in the model as it was highly associated with perioperative complications and P-CCCs.

Patient Demographics and Clinical Characteristics

The following patient demographics and clinical characteristics associated with cost were examined: age (0–4 year, 5–9 year, 10–14 year, or 15–20 year), gender (male or female), insurance status (private, public, and other), race (white, black, Hispanic, Asian, others, and unspecified), pediatric complex chronic conditions, and complications. Prior studies on pediatric populations have shown that P-CCC groupings better characterized disease severity and healthcare utilization for the pediatric population than Elixhauser's comorbidity index, which was developed for adults [29, 31]. This study used updated pediatric complex chronic conditions version 2 (CCC v2) as the risk adjustment for Chiari surgery costs [30]. All complications were identified by ICD-9-CM diagnosis and procedure codes [32]. Surgical complications associated with surgery for Chiari malformation type 1 included shunt insertion, revision or exploration, meningitis, wound infection, dural graft complication, wound disruption, iatrogenic cerebrovascular infarction or hemorrhage, other neurosurgery-specific complications (such as cerebrospinal fluid leak and pseudomeningocele), and bleeding requiring transfusion. Medical complications included pulmonary complication/pneumonia, urinary-renal complication, septicemia, cardiac complication, thrombotic complication, gastrostomy, tracheostomy, pressure ulcer, and catheter-associated infection. In addition to P-CCCs and complications, the impact of three disease-specific comorbidities was separately examined: hydrocephalus (331.3, 331.4, and 742.3), syringomyelia (336.0), and scoliosis (737.3X) [29]. Table 49.1 [30], Table 49.2 [33], and Table 49.3 [29] list the codes used in this cohort identification. Fewer than 10 of 1075 observations in this group had an in-hospital death. Sensitivity analysis was conducted for hospital transfers. The hospital costs of the 22 transfer patients (2.2% of total cohort) did not differ significantly from the patients who were not transferred ($p = 0.934$).

Table 49.1 Modified categories of P-CCC v2 [30] and the corresponding ICD-9-CM codes

Categories	Subcategories	ICD-9	Authors' notes
Neurologic and neuromuscular	Brain and spinal cord malformations	740.0–742.9	Remove 741.0X from the original CCC v2. Cases have been removed due to possibly misclassifying to Chiari malformation type 2
	Mental retardation	318.0–318.2	
	CNS degeneration and diseases	330.0–330.9, 334, 335.0–335.9, 331.1, 331.11, 331.19, 331.8, 331.89, 331.9, 333.2, 336.1, 336.8, 337.9, 759.5	Remove 331.4 from the original CCC v2 for solely examining hydrocephalus
	Infantile cerebral palsy	343.0–343.9	
	Epilepsy	345.01, 345.11, 345.3, 345.41, 345.61, 345.71, 345.81, 345.91	
	Other disorders of CNS	341.8, 342.90, 344.0, 344.81, 344.9, 348.1, 780.03, 01.52, 01.53	Remove 348.4 from the original codes for identifying study population
	Occlusion of cerebral arteries	434.01, 434.91	
	Muscular dystrophies and myopathies	359.0–359.3	
	Movement diseases	332.0, 332.1, 333.0, 333.2, 333.4, 333.5, 333.7, 333.9	
	Devices	V45.2, V53.01, V53.02, 02.35, 02.93, 03.93, 03.97, 04.92	Remove 996.2, 996.63, 02.2, 02.21, 02.22, 02.3, 02.31, 02.32, 02.33, 02.34, 02.39, 02.4, 02.41, 02.42, 03.7, 03.71, 03.72, and 03.79 from the original CCC v2 for identifying complications
	Transplantation	N/A	
Cardiovascular	Heart and great vessel malformations	745.0–745.3, 745.60–745.69, 746, 747.1–747.49, 747.81, 747.89, 35.8, 35.81, 35.82, 35.83, 35.84	
	Endocardium diseases	424.0, 424.2, 424.3	
	Cardiomyopathies	425.0–425.4, 425.8, 429.1	
	Conduction disorder	426.0–427.4	
	Dysrhythmias	427.6–427.9	
	Others	416.1, 416.8, 416.9, 428.0, 429.3, 428.83, 433.11, V45.81	
	Devices	996.0, 996.1, 996.61, 996.62, V43.3, V45.0, V53.31, V53.32, V53.39, 00.50, 00.51, 00.53, 00.54, 00.55, 00.57, 17.51, 17.52, 37.41, 37.52, 37.53, 37.54, 37.55, 37.6, 37.60, 37.61, 37.63, 37.65, 37.66, 37.67, 37.68, 37.7, 37.71, 37.72, 37.74, 37.76, 37.79, 37.8, 37.80, 37.81, 37.82, 37.83, 37.85, 37.86, 37.87, 37.89, 37.94, 37.95, 37.96, 37.97, 37.98, 39.81, 39.82, 39.83, 39.84, 39.85, 89.46, 89.47, 89.48, 89.49	
	Transplantation	996.83,V42.1, V42.2, V43.2, 37.5, 37.51	

(continued)

Table 49.1 (continued)

Categories	Subcategories	ICD-9	Authors' notes
Respiratory	Respiratory malformations	748.0–748.9	
	Chronic respiratory diseases	327.25, 416.2, 516.3, 516.31, 518.84, 770.4, V45.76	
	Cystic fibrosis	277.0	
	Others	30.3, 30.4, 32.4, 32.41, 32.49, 32.5, 32.50, 32.59	
	Devices	519.0, V44.0, V55.0, V46.0, V46.1, 31.41, 31.74, 33.21, 34.85, 96.55, 97.23	Remove 31.2, 31.21, and 31.29 from the original list and group into tracheostomy complications
	Transplantation	996.84,V42.6, 33.5, 33.50, 33.51, 33.52, 33.6	
Renal and urologic	Congenital anomalies	753.0–753.9	
	Chronic renal failure	585	
	Others	V45.73, V45.74, 55.5, 55.51, 55.52, 55.53, 55.54, 56.4, 56.41, 56.42, 56.7, 56.71, 56.79, 57.7, 57.71, 57.79	
	Chronic bladder diseases	344.61, 596.4, 596.53, 596.54	
	Devices	996.68, V44.5, V44.6, V45.1, V53.6, V55.5, V55.6, 38.95, 39.27, 39.42, 39.93, 39.94, 39.95, 54.98, 55.02, 55.03, 55.04, 55.12, 55.93, 55.94, 55.97, 56.5, 56.51, 56.52, 56.6, 56.61, 56.62, 56.72, 56.73, 56.74, 56.75, 57.2, 57.21, 57.22, 59.93, 59.94, 86.07, 96.45, 96.46, 96.47	
	Transplantation	996.81,V42.0, 55.6, 55.61, 55.69	
Gastrointestinal	Congenital anomalies	750.3, 751.1–751.9	
	Chronic liver disease and cirrhosis	571.4–571.9	
	Inflammatory bowel diseases	555.0–556.9	
	Others	453.0, 557.1, 560.2, 564.7, V45.3, V45.72, V45.75, 25.3, 25.4, 42.42, 43.9, 43.91, 43.99, 45.63, 45.8, 45.81, 45.82, 45.83, 50.4, 52.6, 52.7, 54.71	
	Devices	536.4, V44.1–V44.4, V53.50, V53.51, V53.59, V55.1–V55.4, 42.1, 42.10, 42.11, 42.81, 44.12, 44.3, 44.32, 44.38, 44.39, 46.1, 46.13, 46.2, 46.22, 46.23, 46.3, 46.32, 46.4, 46.40, 46.41, 46.43, 96.24, 96.36, 97.02	Remove 43.1, 43.11, and 43.19 from the original list and to group into gastrostomy complications
	Transplantation	996.82,996.86,996.87,V42.7, V42.83, V42.84, 46.97, 50.5, 50.51, 50.59, 52.8, 52.80, 52.82, 52.83, 52.84, 52.85, 52.86	

Table 49.1 (continued)

Categories	Subcategories	ICD-9	Authors' notes
Hematologic or immunologic	Hereditary anemias	282.0–282.6	
	Aplastic anemias	284	
	Hereditary immunodeficiency	279.0–279.9, 288.1, 288.2, 446.1	
	Coagulation/ hemorrhagic	286.0, 286.3, 287.32, 287.33, 287.39	
	Leukopenia	288.01, 288.02	
	Hemophagocytic syndromes	288.4	
	Sarcoidosis	135	
	Acquired immunodeficiency	042–044	
	Polyarteritis nodosa and related conditions	446.0, 446.21, 446.4–446.7	
	Diffuse diseases of connective tissue	710.0, 710.1, 710.3	
	Others	41.5	
	Devices	N/A	
	Transplantation	41.00, 41.01, 41.02, 41.03, 41.04, 41.05, 41.06, 41.07, 41.08, 41.09, 41.94	
Metabolic	Amino acid metabolism	270.0–270.9	
	Carbohydrate metabolism	271.0–271.9	
	Lipid metabolism	272.0–272.9	
	Storage disorder	277.3, 277.5	
	Other metabolic disorders	275.0–275.3, 277.2, 277.6, 277.8–277.9	
	Endocrine disorders	243, 253.2, 253.5, 253.6, 235.9, 255.0, 255.13, 255.2, 06.4, 06.52, 06.81, 07.3, 07.64, 07.65, 07.68, 07.69, 62.4, 62.41, 64.5, 65.5, 65.51, 65.53, 65.6, 65.61, 65.63, 68.4, 68.41, 68.49, 68.5, 68.51, 68.59, 68.6, 68.61, 68.69, 68.7, 68.71, 68.79	
	Devices	V45.85, V53.91, 86.06	
	Transplantation	N/A	
Other congenital or genetic defect	Chromosomal anomalies	758.0–758.9	
	Bone and joint anomalies	259.4, 756.0–756.5	Remove 737.3 from the original codes for solely examining scoliosis
	Diaphragm and abdominal wall	553.3, 756.6, 756.7	
	Other congenital anomalies	757.39, 759.7–759.9	
Malignancy	Neoplasms	140–209, 230–239, 00.10, 99.25	
	Devices	N/A	
	Transplantation	996.85,V42.81, V42.82	

(continued)

Table 49.1 (continued)

Categories	Subcategories	ICD-9	Authors' notes
Premature and neonatal	Fetal malnutrition	764.01, 764.02, 764.11, 764.12, 764.21, 764.22, 764.91, 764.92	
	Extreme immaturity	765.01, 765.02, 765.11, 765.12, 765.21–765.23	
	Cerebral hemorrhage at birth	767.0	
	Spinal cord injury at birth	767.4	
	Birth asphyxia	768.5, 768.9	
	Respiratory diseases	770.2, 770.7	
	Hypoxic-ischemic encephalopathy	768.7	
	Others	771.0, 771.1, 772.13, 772.14, 773.3, 773.4, 774.7, 776.5, 777.53, 778.0, 779.7	
Miscellaneous, not elsewhere classified	Devices	996.4, 996.66, 996.67, 996.9, V46.2 81.00, 81.01, 81.02, 81.03, 81.04, 81.05, 81.06, 81.07, 81.08, 81.09, 81.30, 81.31, 81.32, 81.33, 81.34, 81.35, 81.36, 81.37, 81.38, 81.39, 84.51	
	Transplantation	996.80, 996.89, 00.91, 00.92, 00.93	

Abbreviations: *P-CCC* pediatric complex chronic condition, *ICD-9* International Classification of Disease, Ninth Edition, *CM* Chiari malformation; CNS – central nervous system

Table 49.2 Surgical and medical complication and corresponding ICD-9-CM codes [33]

Complication	ICD-9 code(s)
Shunt insertion, revision, or exploration (Pr)	02.2, 02.32–02.34, 02.39, 03.7, 03.71, 03.72, 03.79, 02.41–02.43
Meningitis	003.21, 036.0, 100.81, 320.0–320.7, 047.9, 322.0–322.2, 322.9
Wound infection	324.1, 478.24, 682.1, 730.00, 730.08, 730.20, 996.67, 998.5, 998.51, 998.59
Dural graft complication	996.2, 996.63, 996.75
Wound disruption	998.31–998.32
Iatrogenic cerebrovascular infarction or hemorrhage	997.02
Bleeding complication	998.11–998.12
Other neurosurgical-specific complications (e.g., CSF leak, pseudomeningocele)	349.31 or 349.39, 349.2, 997.00997.01, 997.09
Pulmonary complication/pneumonia	003.22, 020.3–020.5, 021.2, 022.1, 039.1, 073.0–073.9, 083.0, 480.0–480.9, 481, 482.0–482.9, 483, 483.0–483.8, 484, 484.1–484.8, 485, 486, 510.0–510.9, 513.0, 518.81–518.85, 997.31–997.39
Urinary-renal complication	584.5–584.9, 997.5
Septicemia	003.1, 020.2, 022.3, 036.2, 036.42, 038.0–038.9040.82, 449, 421.0–421.9, 422.92, 790.7
Cardiac complication	997.1, 410.00–410.92
Thrombotic complication	415.11, 415.13, 415.19, 453.40–453.42
Gastrostomy (Pr)	43.11–43.19
Tracheostomy (Pr)	31.1–31.29
Pressure ulcer	707.23–707.24
Catheter-associated infection	996.64, 999.31–999.32

ICD-9 International Classification of Disease, Ninth Edition, *CM* Chiari malformation
"Pr" indicates a procedure code. All other ICD-9-CM codes are diagnosis codes

Table 49.3 Hydrocephalus, syringomyelia, and scoliosis and the corresponding ICD-9-CM codes [29]

Comorbidities	ICD-9 code(s)[a]
Hydrocephalus	331.3, 331.4, 742.3
Syringomyelia	336.0
Scoliosis	737.3X

[a]The codes were modified. We excluded 331.5, 258.01–259.03, and 789.51 from the algorithm of Greenberg et al. [29]; there were no such cases in this pediatric cohort

Hospital Characteristics

Hospital characteristics—including bed size, teaching/research status, profit status, and geographic location—associated with overhead costs of the hospital and could impact on total hospitalization costs [34, 35]. Hospital characteristics examined in the study included targeted variables available in KID, census region, number of RN FTEs per 1000 adjusted inpatient days, and hospital type, which was categorized into government-owned, nonprofit (NP) non-children's hospitals, NP freestanding children's hospitals, NP children's units within adult hospitals, investor-owned private hospitals, and unspecified. Teaching status, hospital size, and hospital volume were not included in the analysis due to high collinearity with either hospital type or RN FTEs.

Statistical Analysis

Descriptive statistics with weighted national estimates were conducted. Standard errors were adjusted for the stratification and clustering of the KID sampling design as described in the 2009 KID documentation published by the Agency for Healthcare Research and Quality [36]. We used simple and multivariable generalized linear models (GLM) to build the cost model. Logarithm transform cost used in an ordinary least squares regression model is a method for cost estimation, but it has disadvantages in retransformation cost data that may lead to bias [37, 38]. Alternatively, the GLM method addresses the heavy-tailed and skewness issues in health cost data and avoids retransformation bias. GLM is able to specify a conditional distribution that reflects mean and variance relationship and a link function. A generalized linear model with the Gamma family and the log link function was used to construct the cost model [37–40]. Covariates with p-value >0.2 in the simple GLM were excluded from the multivariable GLM. Due to each inpatient visit being nested within a hospital, a multilevel analysis with a random effect for each hospital was used to account for interclass correlation (individual inpatient visit/hospital) in the final cost model. The rationale for building the final model is described above. Covariates in the final multivariable generalized linear model with test results of p-value <0.05 were considered statistically significantly associated with increased/decreased hospitalization costs.

Results

One thousand seventy-five (1075) patients were included in this study. Mean and median ages were 10.4 and 11 years (interquartile range [IQR], 5–16 years) of age, respectively. Payers included public (32.9%) and private (61.5%) insurers. Patients were most commonly treated in children's units within adult hospitals (39.6%), followed by nonprofit private children's hospitals (31.4%) [20] (Table 49.4). The average number of RN FTEs per 1000 adjusted inpatient days was 5.9 (range 0.3–10.8, median 5.8, IQR 5.1–6.6). Median wage-adjusted cost for Chiari surgery was $13,484.7 (IQR $10,474.6–18,266.0). Average length of stay was 3.8 days (median 3, range 1–48, IQR 3–4).

On univariate analysis (simple GLM) at a significance level p = 0.05, age, gender, race, insurance, the level of median household income in a patient's home ZIP code, and census region did not significantly impact total hospital costs (HC). Hospital type and RN FTEs per 1000 adjusted inpatient days were significantly associated with total HC [20] (Table 49.4). The most common surgical and medical complications were other neurosurgery-specific, including cerebrospinal fluid leak, pseudomeningocele (38 cases, 3.55%) and pulmonary-related (11 cases, 1.05%) [20] (Table 49.5). Hydrocephalus (comorbidities) and

Table 49.4 Patients and hospital characteristics

Characteristics	Categories	National counts	Percentage (%)	No. of obs.[a]	Total costs (median, IQR[a])	P[b]-Value
Total wage-adjusted costs		1615		1075	13484.7 (10474.6, 18266.0)	
Age	0–4	326	20.2	215	13458.7 (10276.1–18598.8)	0.844
	5–9	412	25.5	271	13350.3 (10541.7, 16900.8)	
	10–14	354	21.9	235	13279.7 (10088.6, 18840.2)	
	15–20	525	32.5	354	13884.2 (10712.5, 18149.3)	
Gender	Male	746	46.4	495	13539.3 (10390.3, 18840.2)	0.243
	Female	861	53.6	574	13458.7 (10479.7, 17655.2)	
Insurance	Private	993	61.5	664	13501.7 (10526.0, 18592.6)	0.811
	Public	531	32.9	350	13231.0 (10070.4, 17682.3)	
	Others	91	5.7	61	11166.8 (14577.2, 16977.6)	
Race	White	958	59.3	641	13558.6 (10681.0, 17235.1)	0.146
	Black	92	5.7	62	13899.4 (10681.0, 18385.4)	
	Hispanic	135	8.4	89	14719.8 (10478.4, 21737.3)	
	Asian and others	97	6.0	65	13458.7 (9736.7, 16624.6)	
	Unspecified	334	20.7	218	12960.2 (9769.5, 20328.7)	
ZIP code Median household Income[c]	Quartile 1 (1–39,999)	331	20.5	219	13260.7 (10125.4, 17279.7)	0.400
	Quartile 2 (40,000–49,999)	419	26.0	279	13914.7 (10663.5, 18385.4)	
	Quartile 3 (50,000–65,999)	442	27.4	293	13224.7 (10088.6, 18351.8)	
	Quartile 4 (66,000 +)	395	24.5	265	13864.7 (10546.2, 19193.0)	
	Unspecified	28	1.8	19	11986.3 (11096.3, 15980.8)	
Hospital region	Northeast	211	13.0	152	12701.5 (9736.7, 16331.3)	0.152
	Midwest	516	31.9	341	14855.3 (11900.7, 19243.4)	
	South	575	35.6	369	12372.8 (9771.0, 17655.2)	
	West	314	19.4	213	14022.8 (10478.4, 19282.9)	
Hospital type	Gov. owned	142	8.8	99	11951.9 (9427.3, 15794.4)	0.005
	Nonprofit private, non-children's	148	9.1	104	12960.23 (9591.2, 16935.1)	
	Nonprofit private, children's	507	31.4	314	15544.9 (11986.3, 22278.4)	
	Nonprofit private, children's unit in a hospital	639	39.6	443	12513.4 (9816.3, 15500.5)	
	Private, invest owned	22	1.4	15	8551.6 (6865.8, 16473.4)	
	Unspecified	157	9.7	100	17682.3 (11102.3, 27902.8)	

[a]Abbreviations: No. of obs. = number of observations, IQR = interquartile range
[b]Covariates with p-value <0.2 included in the final model
[c]ZIP Code Median Household Income denotes the median household income of the patient's home ZIP code

surgical and medical complications were significantly associated with total HC. Neurologic and neuromuscular, respiratory gastrointestinal, metabolic, other congenital genetic defect, and device-dependent P-CCCs were also associated with total HC [20] (Table 49.5).

The post estimation of multivariable generalized linear model confirmed that the Gamma function with least Akaike information criterion (AIC) and Bayesian information criterion (BIC) among all other functions (Gaussian, Poisson, and inverse Gaussian) was the preferred family

Table 49.5 Comorbidities, pediatric complex chronic conditions, and complications

Types		National counts	Percentage (%)	No. of obs.	P∗-Value
Comorbidities	Hydrocephalus	72.5	4.49	47	0.002
	Syringomyelia	410.8	25.43	274	0.404
	Scoliosis	190.7	11.81	127	0.856
Pediatric complex chronic conditions (P-CCCs)	Neurologic and neuromuscular	189.2	11.72	123	0.010
	Cardiovascular	65.9	4.08	44	0.075
	Respiratory	21.7	1.34	14	0.004
	Renal and urologic	20.7	1.28	14	0.769
	Gastrointestinal	35.5	2.20	23	<0.001
	Hematologic or immunologic	+	+	+	–
	Metabolic	21.3	1.32	14	<0.001
	Other congenital genetic defects	96.2	5.98	64	0.009
	Malignancy	+	+	+	–
	Premature and neonatal	+	+	+	–
	Device-dependent, miscellaneous, not elsewhere classified	22.1	1.37	15	<0.001
Surgical complication	Yes (total)	90.4	5.60	61	<0.001
	Shunt insertion, revision, or exploration	18.2	1.13	12	–
	Gastrostomy	+	+	+	–
	Meningitis	+	+	+	–
	Wound infection	+	+	+	–
	Dual graft complication	+	+	+	–
	Bleeding complication	+	+	+	–
	Other neurosurgery-specific complications (e.g., cerebrospinal fluid leak, pseudomeningocele)	58.1	3.55	39	–
Medical complication	Yes (total)	35.9	2.22	24	<0.001
	Pulmonary complication/ pneumonia	16.9	1.05	11	–
	Urinary-renal complication	+	+	+	–
	Cardiac complication	+	+	+	–
	Tracheostomy	+	+	+	–
	Thrombotic complication	+	+	+	–
	Catheter-associated infection	+	+	+	–

"+" indicates the number of cases <10

Abbreviation: No. of obs., number of observations; "∗", p-value was the significance test result for the variation of costs among groups. Covariates with p-value <0.2 included in the final model

function fitted into the cost model. Modified Hosmer and Lemeshow's test confirmed that the log link function was fitted ($p = 0.077$). Predicted mean hospitalization cost was $16,069. Analysis of the multivariable generalized linear model demonstrated that none of the patient demographic characteristics were associated with higher costs. Hospital-level factors such as RN FTEs per 1000 adjusted inpatient days and census regions were also not associated with increased hospitalization costs. Hospital type was found to be a risk factor for increased hospitalization costs. Nonprofit private children's hospitals were associated with mean increased costs ($p = 0.001$) compared with nonprofit private children's units within a hospital. Higher total hospitalization costs of CM 1 surgery were significantly associated with medical ($p < 0.001$) and surgical complications ($p < 0.001$) (Table 49.6) [20]. Five P-CCCs categories—neurologic and neuromuscular ($p = 0.021$), gastrointestinal ($p = 0.010$), metabolic ($p = 0.022$), other congenital genetic

Table 49.6 Multilevel multivariable generalized linear model analysis for CM 1 cost estimation

Total wage-adjusted cost			95% confidence interval of Exp(B)		
Covariates	Categories	Exp(B)[a]	Lower	Upper	p-Value
Race	Non-Hispanic white	Ref			
	Non-Hispanic black	0.991	0.926	1.061	0.797
	Hispanic	1.034	0.965	1.107	0.345
	Asian and others	0.945	0.889	1.005	0.072
	Unspecified	0.986	0.899	1.081	0.763
Region	Northeast	Ref			
	Midwest	1.154	0.979	1.359	0.088
	South	1.058	0.898	1.247	0.499
	West	1.137	0.937	1.381	0.193
Hospital type	Nonprofit private, children's units in a hospital	Ref			
	Government owned	1.177	0.991	1.398	0.063
	Nonprofit private, non-children's	1.058	0.937	1.194	0.362
	Nonprofit private, children's	1.320	1.129	1.544	**0.001**
	Private, invest owned	0.836	0.622	1.125	0.237
	Unspecified	1.243	1.018	1.519	0.033
RN FTEs per 1000 adjusted patient days		0.992	0.955	1.030	0.676
Hydrocephalus	Yes	1.082	0.946	1.238	0.248
Pediatric complex chronic conditions					
	Neurologic and neuromuscular	1.004	1.012	1.156	**0.021**
	Cardiovascular	1.128	0.891	1.131	0.950
	Respiratory	1.125	0.929	1.368	0.223
	Gastrointestinal	1.125	1.028	1.232	**0.010**
	Metabolic	1.301	1.039	1.630	**0.022**
	Other congenital genetic defects	1.193	1.077	1.322	**0.001**
	Device-dependent, miscellaneous, not elsewhere classified	2.281	1.854	2.806	**<0.001**
Surgical complication	Yes	1.390	1.226	1.576	**<0.001**
Medical complication	Yes	1.847	1.446	2.359	**<0.001**

RN FTEs registered nurse full-time equivalents

[a]Exp(B): exponential of coefficient, which is the ratio of arithmetic mean costs. For example, if all other covariates are the same, patients who had medical complications would have additional 84.7% of mean costs than patients who without medical complications

defects ($p = 0.001$), and device-dependent conditions ($p < 0.001$)—were also significantly associated with higher total HC (Table 49.6) [20].

The largest cost driver was device-dependent P-CCCs. The average incremental increase in cost per surgical hospitalization was $20,617 (95% confidence interval [CI], $13,721–$29,026) for CM 1 surgery patients with device-dependent P-CCCs compared to those without device-dependent P-CCCs. The second largest cost driver was medical complications. Patients with medical complications had an average incremental increased cost of $13,632 (95% CI, $7163–$21,845) compared with patients without medical complications in a CM 1 surgery hospitalization (Fig. 49.1).

Discussion

Using KID, the largest all-payer national database for pediatric discharge data, we identified multiple factors associated with hospitalization costs of CM 1 surgery. This large-scale cost analysis for pediatric CM 1 surgery provides the initial background to building cost models for reimbursement based on the primary drivers of HC.

Prior studies have demonstrated race and socioeconomic status as variables that may influence the cost of care in pediatric surgery and pediatric hydrocephalus surgery [41, 42]. However, we did not find any patient demographics or socioeconomic status as a cost effect for CM 1 surgery. The proportion of private to public payers in this study cohort is similar to that reported in other studies of pediatric surgical care [29, 41]. In addition, the proportion of private payers did not interact with the geographic distribution of costs reported, as the interaction term did not show a significant difference on the reported costs.

Children's hospitals have been reported to have higher costs [27, 43]. Indeed, this study found a cost difference between nonprofit private children's hospitals and children's units within a hospital with an average cost difference per

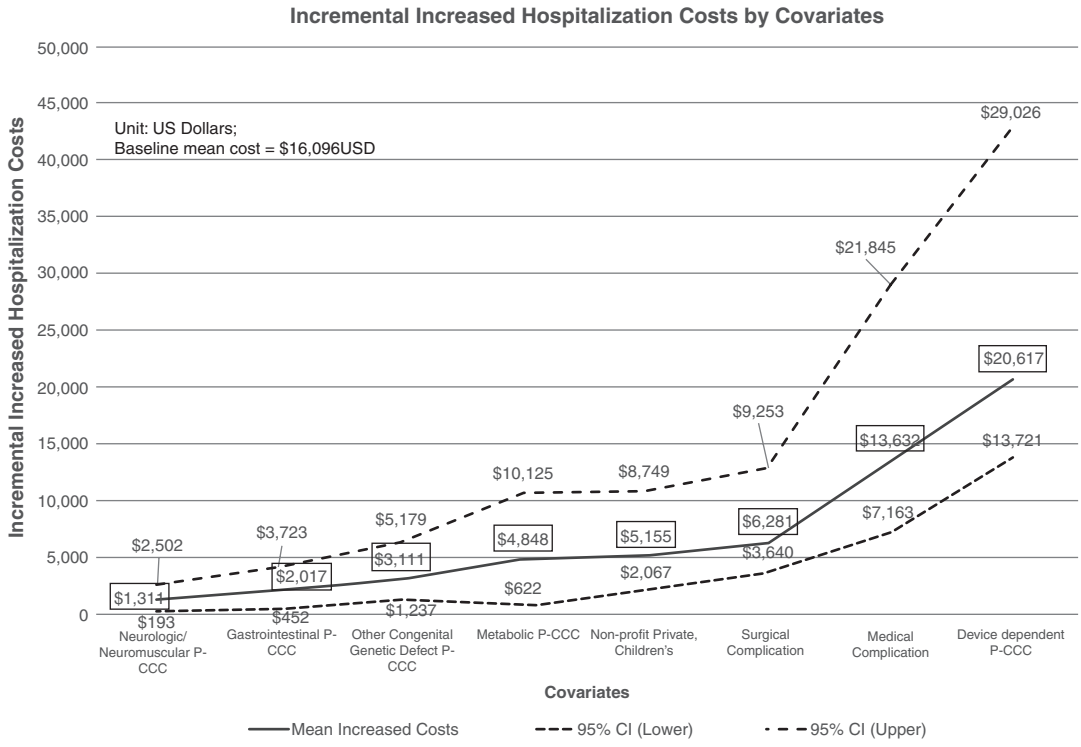

Fig. 49.1 Incremental increased hospitalization costs by covariates. P-CCC, pediatric complex chronic conditions. (Reprinted with permission from Lam et al. [20])

hospitalization of $5155 (95% CI, $2067–$8749). These metrics extend across different domains of care, from radiology to nursing and other ancillary services [27, 44]. The implications of these higher costs are beyond the scope of exploration here but would include considerations on centralization and specialization, along with accreditation efforts of pediatric centers meeting standards for optimal surgical care [45, 46].

Consistent with resource-intensive demands, we found higher nurse-to-patient ratios in NP private children's hospitals—0.25 the number of licensed practical nurse full-time equivalents (LPN FTEs) per 1000 adjusted inpatient days (95% CI, 0.21–0.29) and 7.19 RN FTEs per 1000 adjusted inpatient days (95% CI, 7.02–7.36)—compared to the ratios of average LPN FTE 0.14 (95% CI, 0.12–0.15) and RN FTE 5.41 (95% CI, 5.32–5.50) in children's units within a hospital. This hospital operational component may reflect the higher complexity of provided care and the staffing requirements at dedicated children's hospitals that serve as large referral centers [47]. Children's hospitals also serve as the tertiary referral centers for higher acuity and more complex cases, as well as transfer cases requiring a higher level of care [47]. For instance, 0.68% of patients in nonprofit private children's units within a hospital were transferred in versus 5.73% of patients in children's hospitals. In addition, 6.69% patients in children's hospitals had two or more complex chronic conditions versus only 5.72% patients in NP private children's units within a hospital. However, the proportion of patients with P-CCCs were no different between children's hospitals and NP private children's units within a hospital: 22.93% (95% CI, 18.37–28.23) and 26.13% (95% CI, 22.11–30.59), respectively.

Pediatric complex chronic conditions and complications were major drivers of increased costs. Assuming other covariates were the same, neurologic and neuromuscular P-CCCs, gastrointestinal P-CCCs, metabolic P-CCCs, other congenital genetic defect P-CCCs, and children with device-dependent P-CCCs accounted for increased HC (0.4%, 12.5%, 30.1%, 19.3%, and 128.1%, respectively) compared to children without these P-CCCs. It is not surprising that children with P-CCCs utilized more inpatient resources, as children with P-CCCs are known to be a high-resource-utilization group; this is an area of ongoing study [48]. Meanwhile, children with medical (84.7% higher costs) and surgical (39.0% higher costs) complications incurred higher total HC compared to those without complications (Table 49.6) [20].

These findings may help toward developing a risk-adjusted basis for a bundled or episode-based payment model for CM 1 surgery. Knowledge of each disease and surgery is important, as a single risk-adjusted approach for all surgeries and specialties may not elucidate such nuances. Future studies may build upon this model as much more data is required to more accurately predict surgery or episode-of-care cost.

This case illustration serves to provide an example of building a cost model and the patient-level, hospital-level, and larger socioeconomic factors to take into account for a particular disease, surgery, and patient population.

Study Limitations

Limitations of this study included the inherent nature of KID data. Clinical granularity is limited in this national discharge database, and, like any national administrative claims study, it is not possible to independently verify diagnoses or procedures by chart review. Fortunately, Ladner et al. had already conducted and published an excellent validation study for identification of CM 1 surgery in large administrative databases, and we adopted this standard for the present study [22]. Not all disease processes and surgeries will have undergone this type of validation. Furthermore, clinically relevant details are not able to be examined in this type of study design. For instance, clinical indications for surgery and surgical technique were not known based on administrative claims data. Specific clinical and functional outcomes cannot be included or measured in this study. Further work is needed to examine clinical outcomes, readmission, reoperation, and other

quality metrics. Especially in surgery for Chiari malformation type 1, details of surgical technique and clinical management are topics of debate. Outcomes from practice variation are not yet understood. Thus, it is important to look to multicenter clinical studies such as the Park-Reeves Syringomyelia Research Consortium to provide further clinical study over time (https://park-reeves.wustl.edu/). It remains to be investigated whether surgical technique (such as decompression with or without duraplasty) may impact outcome, LOS, and its cost correlates [19].

While hospital bed assignment is important to consider in costs, we are unable to identify or separate the total LOS in each location (intensive care unit versus ward) due to limitations in KID data. Cost-to-charge ratios provided the opportunity for converting charges to cost; however, this is a surrogate for cost, but not reflective of actual cost data. The impact of differing CCR used in the cost estimates from KID in this study did not have a significant impact on results. Only a small portion of the study cohort did not have API CCRs and used group-weighted CCRs (45 cases, 4% of total cohort); these were calculated from a peer group within the state by HCUP methodology. In this manner, the group-weighted CCRs may not account for aspects of geographic variation in cost. With our analysis of cost estimation by adjusted wage index, census regions were not found to be a driver of increased hospital costs.

The idea of the cost model for pediatric subspecialty surgeries is in its nascent stages. The KID database does not have the level of detail in variables required to build a predictive equation. Further work with more databases is needed. In the future, predictive costing models will likely be more available. Covering risk in such cost models may depend on volume, efficiency, and quality.

There is potential application for more delineation in bundled pricing as we further understand risk adjustment in subspecialty surgery populations. As such, there may be even greater potential, with the advent of ICD-10 and its new level of detail. In the future, the increased specificity with ICD-10 code G93.5 (Chiari type I) may increase the accuracy of database queries and further evaluation of episodes of care related to Chiari treatment (http://www.cdc.gov/nchs/icd/icd10.htm).

There are, of course, many other ways to estimate costs, including from a hospital perspective or from a patient perspective. This illustrative example is one way to use administrative claims data to build a disease-specific, surgery-specific, and patient population-specific rationale to estimate costs from a payer perspective. As it stands, aiming to examine modifiable risks and nonmodifiable risks in drivers of costs in terms of provisioning of care is already quite an undertaking, and much more work needs to be done in the near future. In addition, these studies only complement, and cannot replace, ongoing clinical research to define evolving best practices in surgical care and placing paramount importance on high quality of care for our pediatric patients.

Conclusion

This chapter highlights the background and the importance of studying cost in surgeries, such as for Chiari malformation type 1. We use an illustrative study to show study design with administrative claims data for cost modeling. In this study, we identified drivers of increased hospitalization cost of surgery for CM 1, which included treatment at a nonprofit freestanding children's hospital, presence of complex chronic conditions, and perioperative complications.

This illustrative study initiates informing the development of financial risk models such as bundled payments or prospective payment systems for these procedures, should these efforts be needed in the future of pediatric health payment policy. The study found specific risk factors associated with increased hospital costs. Some of these risk factors are modifiable, but some are not; surgeons, healthcare providers, institutions, and policymakers would need to take notice of these facts. Further development of cost models for CM 1 surgery is warranted to guide reimbursement structures, such as 90-day bundled payments (such as in certain BPCI models proposed by the Centers for Medicare & Medicaid

Services). Targeting areas for cost containment and quality improvement may focus on the balance of costs and delivery of value in healthcare.

References

1. OECD. Health Spending (indicator). 2018 [cited 2018. Available from: https://data.oecd.org/healthres/health-spending.htm.
2. Papanicolas I, Woskie LR, Jha AK. Health care spending in the United States and other high-income countries. JAMA. 2018;319(10):1024–39.
3. OECD. Health at a Glance 2017: OEcD indicators. Paris, France: OECD Publishing; 2017. Available from: http://dx.doi.org/10.1787/health_glance-2017-en.
4. Morrisey MA. History of Health Insurance in the United States. Health Insurance. 2nd ed. Chicago: Health Administration Press; 2013. p. 1–25.
5. Begley CE, Lairson DR, Morgan, RO, Rowan, PJ, Balkrishnan R. Introduction to health services research and policy analysis. evaluating the healthcare system: effectiveness, efficiency, and equity. 4th ed. Chicago, IL: Health Administration Press; 2013. p. 1–26.
6. Epstein AM, Blumenthal D. Physician payment reform: past and future. Milbank Q. 1993;71(2):193–215.
7. Lu Ann Aday CEB, Lairson DR, Balkrishnan R. Evaluating the healthcare system. Chicago, IL: Health Administration Press; 2004. 354 p.
8. Services USDoHaH. Affordable Care Act (ACA) Baltimore, MD: the U.S. Centers for Medicare & Medicaid Services; 2010 [The comprehensive health care reform law enacted in March 2010]. Available from: https://www.healthcare.gov/glossary/affordable-care-act/.
9. Obama B. United States health care reform: progress to date and next steps. JAMA. 2016;316(5):525–32.
10. CMS. National Health Expenditures by types of services and source of funds Baltimore, MD: Centers for Medicare & Medicaid Services; 2018 [updated 12/11/2018. Historical National Health Expenditure Data]. Available from: https://www.cms.gov/Research-Statistics-Data-and-Systems/Statistics-Trends-and-Reports/NationalHealthExpendData/NationalHealthAccountsHistorical.html.
11. de Brantes F, Rosenthal MB, Painter M. Building a bridge from fragmentation to accountability–the Prometheus payment model. N Engl J Med. 2009;361(11):1033–6.
12. Averill RF, Goldfield N, Hughes JS, Bonazelli J, Muldoon J, Turner L. 3M™ APR DRG Classification System Wallingford, CT: 3M Health Information Systems; 2013 [updated 10/2013. 31.0.
13. White C, Reschovsky JD, Bond AM. Inpatient hospital prices drive spending variation for episodes of care for privately insured patients National Institute for Health Care Reform 2014.
14. Pope GC, Kautter J, Ellis RP, Ash AS, Ayanian JZ, Lezzoni LI, et al. Risk adjustment of Medicare capitation payments using the CMS-HCC model. Health Care Financ Rev. 2004;25(4):119–41.
15. CMS. Centers for Medicare & Medicaid Services: Bundled Payments for Care Improvement (BPCI) Initiative: General Information Baltimore, MD: Centers for Medicare & Medicaid Services; 2016 [updated 3/9/2016; cited 2016 3/20/2016]. Available from: https://innovation.cms.gov/initiatives/bundled-payments/.
16. CMS. BPCI Advanced Baltimore, MD: the U.S. Centers for Medicare & Medicaid Services.; 2018 [updated 12/04/2018. Available from: https://innovation.cms.gov/initiatives/bpci-advanced/.
17. Tubbs RS, Beckman J, Naftel RP, Chern JJ, Wellons JC 3rd, Rozzelle CJ, et al. Institutional experience with 500 cases of surgically treated pediatric Chiari malformation type I. J Neurosurg Pediatr. 2011;7(3):248–56.
18. Limonadi FM, Selden NR. Dura-splitting decompression of the craniocervical junction: reduced operative time, hospital stay, and cost with equivalent early outcome. J Neurosurg. 2004;101(2 Suppl):184–8.
19. Litvack ZN, Lindsay RA, Selden NR. Dura splitting decompression for Chiari I malformation in pediatric patients: clinical outcomes, healthcare costs, and resource utilization. Neurosurgery. 2013;72(6):922–8. discussion 8–9
20. Lam SK, Mayer RR, Luerssen TG, Pan IW. Hospitalization cost model of pediatric surgical treatment of Chiari type 1 malformation. J Pediatr. 2016;179:204–10. e3
21. AHRQ. HCUP Sample Design: National Databases: the Agency for Healthcare Research and Quality (AHRQ); 2015 [Available from: http://www.hcup-us.ahrq.gov/tech_assist/sampledesign/508_compliance/508course.htm#{D630D90E-CBB9-4885-A855-6370B80C8E98}.
22. Ladner TR, Greenberg JK, Guerrero N, Olsen MA, Shannon CN, Yarbrough CK, et al. Chiari malformation type I surgery in pediatric patients. Part 1: validation of an ICD-9-CM code search algorithm. Journal of neurosurgery. Pediatrics. 2016:1–6.
23. AHRQ. Agency for Healthcare Research and Quality: Cost to charge ratio files: 2009 Kids' Inpatient Database User Guide Rockville, MD: AHRQ; 2011 [Kids' Inpatient Database (KID) is part of famil of databases and software tools developed for the Healthcare cost and utilization project (HCUP)]. Available from: http://www.hcup-us.ahrq.gov/db/state/CCR2009KIDUserGuide.pdf.
24. AHCCCS. Arizona Health Care Cost Containment System: AHCCCS Transition to DRG-Based payment Arizona: Arizona Health Care Cost Containment System; 2016 [updated 10/30/2015; cited 2016 1/2/2016]. Available from: https://www.azahcccs.gov/PlansProviders/RatesAndBilling/ManagedCare/DRGbasedpayments.html.

25. TMHP. Texas Medicaid & Healthcare Partnership (TMHP): Reimbursement Methodology to Change for some Children's and Rural Hospitals Effective September 1, 2013 Texas: Texas Medicaid & Healthcare Partnership – A State Medicaid Contractor 2013 [updated 8/13/2013; cited 2015 12/1/2015]. Available from: http://www.tmhp.com/Pages/Medicaid/Hospital_APR-DRG.aspx.
26. Quinn K. New directions in Medicaid payment for hospital care. Health Aff. 2008;27(1):269–80.
27. Merenstein D, Egleston B, Diener-West M. Lengths of stay and costs associated with children's hospitals. Pediatrics. 2005;115(4):839–44.
28. Gever M. Improving the quality of care: the continuing debate over nurse-patient ratios. 2009 March 16, 2009.
29. Greenberg JK, Olsen MA, Yarbrough CK, Ladner TR, Shannon CN, Piccirillo JF, et al. Chiari malformation type I surgery in pediatric patients. Part 2: complications and the influence of comorbid disease in California, Florida, and New York. J Neurosurg Pediatr. 2016:1–8.
30. Feudtner C, Feinstein JA, Zhong W, Hall M, Dai D. Pediatric complex chronic conditions classification system version 2: updated for ICD-10 and complex medical technology dependence and transplantation. BMC Pediatr. 2014;14:199.
31. Simon TD, Riva-Cambrin J, Srivastava R, Bratton SL, Dean JM, Kestle JR, et al. Hospital care for children with hydrocephalus in the United States: utilization, charges, comorbidities, and deaths. J Neurosurg Pediatr. 2008;1(2):131–7.
32. Greenberg JK, Ladner TR, Olsen MA, Shannon CN, Liu J, Yarbrough CK, et al. Validation of an international classification of diseases, ninth revision code algorithm for identifying Chiari malformation type 1 surgery in adults. Neurosurgery. 2015;77(2):269–73.
33. Greenberg JK, Ladner TR, Olsen MA, Shannon CN, Liu J, Yarbrough CK, et al. Complications and resource use associated with surgery for Chiari malformation type 1 in adults: a population perspective. Neurosurgery. 2015;77(2):261–8.
34. Kalman NS, Schulman K, Shah B. Hospital overhead costs: the neglected driver of health care spending? J Health Care Finance. 2015;41(4).
35. Jha AK, Orav EJ, Dobson A, Book RA, Epstein AM. Measuring efficiency: the association of hospital costs and quality of care. Health Aff. 2009;28(3):897–906.
36. AHRQ. Introduction to the HCUP KIDS' Inpatient Database (KID), 20092015 12/1/2015 6/7/2016]. Available from: http://www.hcup-us.ahrq.gov/db/nation/kid/KID_2009_Introduction.pdf.
37. Mihaylova B, Briggs A, O'Hagan A, Thompson SG. Review of statistical methods for analysing healthcare resources and costs. Health Econ. 2011;20(8):897–916.
38. Glick HA, Doshi JA, Sonnad SS, Polsky D. Economic Evaluation in Clinical Trials (Handbooks in Health Economic Evaluation). 2nd ed. Oxford: Oxford University Press; 2014. 272 p.
39. Barber J, Thompson S. Multiple regression of cost data: use of generalised linear models. J Health Serv Res Policy. 2004;9(4):197–204.
40. Manning WG, Mullahy J. Estimating log models: to transform or not to transform? J Health Econ. 2001;20(4):461–94.
41. Stone ML, LaPar DJ, Mulloy DP, Rasmussen SK, Kane BJ, McGahren ED, et al. Primary payer status is significantly associated with postoperative mortality, morbidity, and hospital resource utilization in pediatric surgical patients within the United States. J Pediatr Surg. 2013;48(1):81–7.
42. Chern JJ, Bookland M, Tejedor-Sojo J, Riley J, Shoja MM, Tubbs RS, et al. Return to system within 30 days of discharge following pediatric shunt surgery. J Neurosurg Pediatr. 2014;13(5):525–31.
43. Raval MV, Cohen ME, Barsness KA, Bentrem DJ, Phillips JD, Reynolds M. Does hospital type affect pyloromyotomy outcomes? Analysis of the Kids' inpatient database. Surgery. 2010;148(2):411–9.
44. Nguyen C, Hernandez-Boussard T, Davies SM, Bhattacharya J, Khosla RK, Curtin CM. Cleft palate surgery: an evaluation of length of stay, complications, and costs by hospital type. Cleft Palate-Craniofacial J. 2014;51(4):412–9.
45. Surgeons ACo. Optimal Resources for Children's Surgical Care v.1 Chicago, IL: American College of Surgeons; 2015 [updated 2015. Available from: https://www.facs.org/~/media/files/quality%20programs/csv/acs%20csv_standardsmanual.ashx.
46. Surgeons ACo. Children's Surgery Verification Chicago, IL: American College of Surgeons; 2015 [Available from: https://www.facs.org/quality-programs/childrens-surgery/childrens-surgery-verification.
47. Lam SK, Srinivasan VM, Luerssen TG, Pan IW. Cerebrospinal fluid shunt placement in the pediatric population: a model of hospitalization cost. Neurosurg Focus. 2014;37(5):E5.
48. Simon TD, Berry J, Feudtner C, Stone BL, Sheng X, Bratton SL, et al. Children with complex chronic conditions in inpatient hospital settings in the United States. Pediatrics. 2010;126(4):647–55.

A Multidisciplinary Clinic for the Management of Chiari I Malformations

50

Leon S. Dure, W. Jerry Oakes, Curtis J. Rozzelle, Anastasia Arynchyna, and Katherine Barnes

Introduction

A distinction of the Chiari malformation is that it is often a radiographic diagnosis, with no definitive clinical correlates [1, 2]. While certain objective findings, such as ataxia or cranial nerve deficits, may be localizable and consistent with a Chiari I malformation (CM I), these features in no way distinguish it from other posterior fossa pathologies [3]. Therefore, the diagnostician is often confronted with the task of reconciling symptoms with radiographic findings. There is ample literature describing both typical and atypical symptomatic CM I to aid the clinician in this respect. However, the increasing availability of computerized axial tomography (CT) and magnetic resonance imaging (MRI), coupled with the reported incidence of CM I, virtually ensures that referrals to specialty clinics will include patients whose signs and symptoms have no relationship to the radiographic diagnosis.

Given that management of a symptomatic CM I typically involves surgery, most patients are referred to a neurosurgeon for consultation. These referrals may come from neurologists, pediatricians, internists, family practitioners, or any healthcare provider who has obtained a diagnostic MRI and been provided with a report indicating the presence of a CM I. Anecdotally in our institution, the frequency of symptomatic CM I is well under half of referred patients. This illustrates the problem of how to provide efficient and appropriate care for these individuals in a manner that addresses not only the question of whether or not a CM I is symptomatic but also deals with contemporaneous symptoms. Such a situation has been clearly operant at our institution the University of Alabama at Birmingham (UAB), with outstanding neurosurgical expertise in the surgical management of CM I in childhood [4]. Because of the need to address symptoms that are likely distinct from the CM I, a member of the pediatric neurology faculty at UAB (chapter coauthor LSD) was enlisted in 2010 to begin development of a multidisciplinary approach to CM I referrals. In addition, this clinic served as a resource for data collection to examine the characteristics of referrals, the nature of attendant complaints, and outcomes. This chapter will serve as a summary of the experience of the clinic.

L. S. Dure (✉)
Department of Pediatrics/Pediatric Neurology, University of Alabama at Birmingham, Birmingham, AL, USA
e-mail: ldure@peds.uab.edu

W. J. Oakes
Departments of Neurosurgery and Pediatrics, University of Alabama, Birmingham, AL, USA

C. J. Rozzelle · K. Barnes
Department of Neurosurgery, University of Alabama at Birmingham, Birmingham, AL, USA

A. Arynchyna
Department of Neurosurgery, Division of Pediatric Neurosurgery, University of Alabama at Birmingham, Birmingham, AL, USA

R. S. Tubbs et al. (eds.), *The Chiari Malformations*, https://doi.org/10.1007/978-3-030-44862-2_50

Methods

The Children's Hospital of Alabama (COA) is a freestanding tertiary care facility that serves not only the state of Alabama but is a resource for the adjoining states of Georgia, Florida, Mississippi, and Tennessee. Subspecialty pediatric care for children in the region is provided in large measure by physicians at COA, and this is particularly true for neurosurgical services.

Since 1989, COA has offered a neurosurgical clinic specifically focusing on the diagnosis and management of CM I, under the direction of a single neurosurgeon with significant expertise (coauthor JO). Children are typically referred to this clinic after a radiographic diagnosis of CM I is made. Beginning in January 2010, children referred to this clinic were seen and their care incorporated into a multidisciplinary care model, involving a neurosurgeon (coauthors JO, CR) and a neurologist (coauthor LD). Inclusion and evaluation were undertaken only if radiographs (CT or MRI) were available to confirm or exclude a CM I.

In each child, a comprehensive history and physical examination was performed, along with review of radiographic studies. The primary goals of this initial evaluation were to determine (1) if radiographic evidence supported the diagnosis of CM I and (2) if the chief complaint or presenting symptoms could be attributed to a CM I. In situations where these goals were met, the care and management plan remained neurosurgical, typically involving a recommendation for surveillance, or more rarely, the offer of a surgical intervention. However, in patients for whom these criteria were not met, a neurological consultation was obtained, in order to identify other possible etiologies for the presenting complaints. In these latter cases, appropriate recommendations for care and management were made.

Results

Data was collected from January 2010 until December 2016 from 350 patients. Patient demographics are illustrated in Table 50.1. In the group, 53% were male and 47% female. Eighty-five percent were identified as white, with 14% of African-American ethnicity. The average age was 10.1 years, with a range of 9 months to 23 years. In terms of age distribution, 15% (54) were from 0–4 years old, 25% (89) were 5–8 years old, 21% (75) were aged 9–12 years, and 38% (132) were between 13 and 17 years of age.

Table 50.1 Patient demographics (n = 350)

Gender	Male	187 (53%)
	Female	163 (47%)
Ethnicity	White	297 (85%)
	African-American	49 (14%)
	Hispanic	3 (0.8%)
	Unknown	1 (0.2%)
Age	Average	10.1 years (±4.75)
	Range	0–23 years
Age distribution	0–4 years	54 (15.4%)
	5–8 years	89 (25.4%)
	9–12 years	75 (21.4%)
	13+ years	132 (37.7%)

All patients had undergone MRI of the head, and these studies were reviewed and tonsillar descent was measured. Of the total cohort of 350 individuals, 69 had either missing data or had previously undergone a surgical decompression. Of the remaining 281, 71 (25%) failed to demonstrate findings consistent with CM I, with an absence of tonsillar herniation greater than 5 mm. Of the other 210 cases with the presence of a CM I, 131 (62%) were felt to be of mild to moderate severity, as defined as tonsillar herniation measuring between 6 and 10 mm. The remaining 79 (38%) CM I were classified as significant, on the basis of herniation greater than 10 mm. Twenty-five individuals with CM I (12%) were determined to have a coexisting cervical syrinx.

Presenting complaints in the entire population were wide ranging, but headaches predominated, with 183 (51%) being the chief reason for undergoing an MRI. Other reasons for obtaining an MRI in these patients included neck pain, endocrinologic evaluations, assessment of head trauma and concussion, and investigation of musculoskeletal pain of the head and neck, among

Table 50.2 Indications for obtaining magnetic resonance imaging (MRI)

	No radiographic Chiari *N* = 71	Radiographic Chiari *N* = 279
Headache	32 (45%)	151 (54%)
Endocrinologic evaluation	6 (8%)	23 (8%)
Head trauma/concussion	7 (10%)	18 (6%)
Musculoskeletal/neck pain	7 (10%)	14 (5%)
Other	19 (27%)	73 (26%)

other complaints. The incidence of common complaints in children with and without radiographically demonstrated CM I was very similar in both groups. Table 50.2 details the range of reported indications for imaging.

Upon review of MRI findings, clinical history, and the neurologic examination, a determination was made for each child by the neurosurgeon and neurologist of the plan of care. Overall, neurosurgical follow-up was recommended in 171/281 individuals (61%), for longitudinal monitoring, while neurologic follow-up was deemed necessary in only 11 patients (4%). For the 71 patients whose MRI findings did not meet criteria of a CM I, the neurologist and neurosurgeon developed a plan consistent with the clinical history. If there was a neurologic complaint, the neurologist assumed responsibility for any medical management.

Of the 281 patients whose imaging studies were available, correlation of the imaging studies, clinical history, and examination was done to determine if symptoms were related to the CM I. Two hundred forty-seven (88%) patients' symptoms were not felt to be secondary to any imaging findings. This group reported a variety of complaints, summarized in Table 50.3. The most common complaint was that of headache, in some cases diagnosed as tension headache or migraine. Few of these children exhibited characteristic complaints such as headache associated with a Valsalva maneuver, cough, or exercise, and none manifested abnormal findings referable to CM I. None of the children with headaches reported a severity that suggested a significant impact on everyday activities. The next most common instance of detecting a radiographic CM I was as an incidental finding as part of a genetic or endocrinologic evaluation. In terms of ongoing management, these children were referred back to their primary physician for continued observation or to their subspecialist for medical management. Overall, 61% of children seen in the clinic were recommended for neurosurgical follow-up, often with imaging, in order to follow the course of an abnormality.

Table 50.3 Complaints elicited in 247 patients with radiographic Chiari I, but not felt to be symptomatic

Complaint	Number
Headache	134 (54%)
Endocrinologic/genetic	23 (9%)
Musculoskeletal/trauma	23 (9%)
Seizure	16 (6%)
Other (e.g., snoring, tremor, other pain, nystagmus)	51 (22%)

The final group of 34 children included those whose radiographic findings were consistent with CM I and whose clinical history or examination was consistent with a symptomatic process. In most cases, neurologic examination was unremarkable. In this cohort, of the 34 children with symptomatic CM I, 25 had undergone surgical decompression. In other words, of the entire population of patients seen in the clinic over this period with imaging data, 12% were felt to have a surgical indication. Clinical features observed in this surgical group included post-tussive headache in 10 (40%), the presence of a syrinx in 14 (56%), an abnormal sleep study in 6 (24%), and the character of head or neck pain in 4 (16%). The decision to recommend operation was based on the entirety of the clinical phenotype and included an assessment of the severity of symptoms. Of note, one child in this group had undergone an MRI after being struck by lightning, was clinically asymptomatic, but radiographic findings included a large CM I and a cervical syrinx,

and were of such a magnitude that surgery was offered to the family for decompression of the CM I [5].

Discussion

In this report, we summarize our experience with a multidisciplinary model for the management of referrals to a tertiary care facility with expertise in the evaluation and management of CM I. The findings are of interest on a number of levels. Of 281 consecutive patients seen in the clinic with imaging data, 25% were felt to have no radiographic evidence of CM I. It has been the practice in this clinic to evaluate all children referred with a diagnosis of CM I, but it is clear that radiographic diagnoses were made that are inconsistent with guidelines regarding the entity [1]. A limitation of this study is that data were not collected regarding official radiographic interpretations, and therefore no conclusions can be drawn with respect to the possibility that radiographs were either misinterpreted or that guidelines were applied conservatively. However, physicians referring to the clinic did so as a consequence of these radiographic interpretations, suggesting a lack of familiarity with diagnostic criteria for CM I, as well as the clinical features.

Although there is ample literature indicating the frequency of incidental findings on MRI [6, 7], subsequent evaluation and assessment typically falls to subspecialists who must determine if any relationship exists between radiographic abnormalities and clinical phenotypes. In this series, the situation in one-quarter of the cases was one of a diagnosis being applied without radiographic abnormality, thus highlighting a need for either better communication between radiologists and referring physicians or greater education regarding the significance of radiographic findings. A somewhat broader issue is highlighted by our experience, relating to the fact that in our cohort 50% of the referred patients had undergone an MRI for an indication of headache. In the context of management of headache in childhood, it has been demonstrated in a variety of studies that the clinical utility of imaging is low, despite the fact that incidental findings (including CM I) may approach 20% [8, 9]. Thus, it could be argued that overuse of neuroimaging, in combination with misinterpretation of findings, led to the high incidence of inappropriate referrals to our clinic. These findings carry significance in relation to practice patterns and allocation of resources and point toward an important issue for further study.

Another result of our analysis is the fact that upon evaluation of children with a consistent radiographic finding ($n = 210$), more than 80% of these individuals were not felt to have symptoms consistent with a symptomatic CM I. While consistent with other large studies of CM I [2, 10], these findings further underscore a need for better understanding of the clinical features of CM I by referring physicians. Alternatively, the results suggest that a clinic dedicated to CM I evaluation and management should at the very least have access to resources appropriate to care for other diagnoses.

In our clinic, we chose to incorporate neurologic expertise to assist in management of children referred for CM I. With regard to the provision of care, this was successful, as all children were able to access services appropriate to their chief complaints. The model of a multidisciplinary approach to childhood diseases has been successfully implemented for a variety of conditions, including sickle cell disease [11], genetic disorders [12], and diabetes [13, 14], among others, with significant benefits in terms of clinical outcomes. In addition, it has also been shown that multidisciplinary clinics can have a favorable effect on overall healthcare costs [13, 15], while also serving as foundations for innovation and research. On the other hand, as opposed to other medically complex conditions, our experience could be construed as illustrating an overabundance of access, given that 25% of the patients referred to a clinic ostensibly directed at neurosurgical management of CM I had no evidence of the disorder. Therefore, another strategy under consideration would be to develop a screening process, with evaluation of neuroimaging prior to appointing a referral. This could have the effect of more appropriate utiliza-

tion of subspecialty resources, but will demand a higher level of education among primary care providers.

Conclusion

In summary, we have reported our experience with a multidisciplinary approach to the management of CM I in children. Although successful from the standpoint of patient access and care, our findings indicate somewhat problematic issues with respect to utilization and interpretation of radiographic findings in children. We anticipate that our results and conclusions will serve to inform other similar efforts.

References

1. Barkovich AJ, Moore KR, Jones BV, Vézina G, Koch BL, Raybaud C, et al. Diagnostic imaging: pediatric neuroradiology. 1st ed. Salt Lake City: Amirsys, Inc.; 2007.
2. Taylor FR, Larkins MV. Headache and Chiari I malformation: clinical presentation, diagnosis, and controversies in management. Curr Pain Headache Rep. 2002;6(4):331–7.
3. Milhorat TH, Chou MW, Trinidad EM, Kula RW, Mandell M, Wolpert C, et al. Chiari I malformation redefined: clinical and radiographic findings for 364 symptomatic patients. Neurosurgery. 1999;44(5):1005–17.
4. Tubbs RS, Beckman J, Naftel RP, Chern JJ, Wellons JC 3rd, Rozzelle CJ, et al. Institutional experience with 500 cases of surgically treated pediatric Chiari malformation type I. J Neurosurg Pediatr. 2011;7(3):248–56.
5. Tubbs RS, Muhleman M, Loukas M, Oakes WJ. Chiari I malformation and syringomyelia in a child following a lightning strike. Childs Nerv Syst. 2012;28:751–3.
6. Meadows J, Kraut M, Guarnieri M, Haroun RI, Carson BS. Asymptomatic Chiari type I malformations identified on magnetic resonance imaging. J Neurosurg. 2000;92(6):920–6.
7. Morris Z, Whiteley WN, Longstreth WT Jr, Weber F, Lee YC, Tsushima Y, et al. Incidental findings on brain magnetic resonance imaging: systematic review and meta-analysis. BMJ. 2009;339:b3016.
8. Schwedt TJ, Guo Y, Rothner AD. "Benign" imaging abnormalities in children and adolescents with headache. Headache. 2006;46(3):387–98.
9. Lewis DW, Dorbad D. The utility of neuroimaging in the evaluation of children with migraine or chronic daily headache who have normal neurological examinations. Headache. 2000;40(8):629–32.
10. Elster AD, Chen MY. Chiari I malformations: clinical and radiologic reappraisal. Radiology. 1992;183(2):347–53.
11. Brandow AM, Weisman SJ, Panepinto JA. The impact of a multidisciplinary pain management model on sickle cell disease pain hospitalizations. Pediatr Blood Cancer. 2011;56(5):789–93.
12. Heerensperger D. Provision of coordinated care for individuals with Down syndrome: the Calgary perspective. Downs Syndr Res Pract. 2006;10(1):4–9.
13. Kaufman FR, Halvorson M, Carpenter S. Association between diabetes control and visits to a multidisciplinary pediatric diabetes clinic. Pediatrics. 1999;103(5 Pt 1):948–51.
14. Melzer SM, Richards GE, Covington ML. Reimbursement and costs of pediatric ambulatory diabetes care by using the resource-based relative value scale: is multidisciplinary care financially viable? Pediatr Diabetes. 2004;5(3):133–42.
15. Casey PH, Lyle RE, Bird TM, Robbins JM, Kuo DZ, Brown C, et al. Effect of hospital-based comprehensive care clinic on health costs for Medicaid-insured medically complex children. Arch Pediatr Adolesc Med. 2011;165(5):392–8.

Chiari Malformations: A Patient's Guide

51

Nadine Bradley and E. Haley Vance

Introduction

The purpose of this chapter is to provide patients and family members with general medical information concerning the diagnosis and treatment of a Chiari malformation. It is not intended as medical advice. Specific questions or concerns about this diagnosis should be directed toward the treating physician.

Anatomy of the Brain and Spine

To understand you or your family member's diagnosis of a Chiari malformation, it is important to first understand the basic anatomy of the brain and spine. The brain is made up of three main portions: cerebrum, cerebellum, and brain stem (Fig. 51.1). The cerebrum is the largest portion of the brain and is responsible for many higher functions such as hearing, vision, speech, emotion, movement, and sensation. The cerebellum is the second largest portion and is located at the back of the brain. The cerebellum controls things such as balance, coordination, and movement. The brain stem is the portion of the brain that connects to the spinal cord and controls many functions critical for life, such as breathing, swallowing, and heart rate. The spine is made of small vertebrae (bones), which are strong, but flexible. The spinal cord is located inside the spinal canal that is surrounded by the vertebrae of the spine.

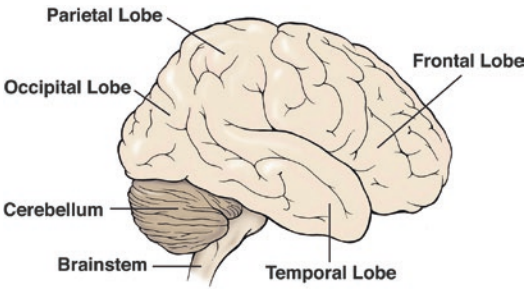

Fig. 51.1 Schematic drawing of the major parts of the brain

What Is a Chiari Malformation?

A Chiari malformation (Fig. 51.2) occurs when a portion of the cerebellum is found outside of the skull and downward into the spinal canal. When the cerebellar tonsils (bottom portion of the cerebellum, i.e., Chiari I malformation) are located in the spinal canal, this disrupts the flow of cere-

N. Bradley (✉)
Department of Pediatric Neurosurgery, Children's of Alabama, Birmingham, AL, USA
e-mail: nadine.bradley@childrensal.org

E. H. Vance
Department of Pediatric Neurosurgery, Vanderbilt University Medical Center, Vanderbilt Children's Neurosurgery, Nashville, TN, USA

R. S. Tubbs et al. (eds.), *The Chiari Malformations*, https://doi.org/10.1007/978-3-030-44862-2_51

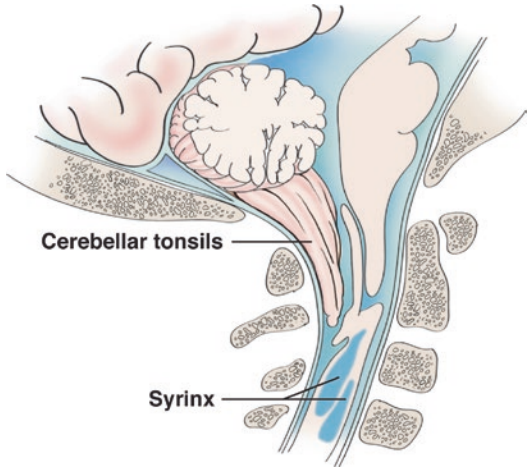

Fig. 51.2 Schematic drawing of the Chiari I malformation with a syrinx

brospinal fluid (CSF) and may cause it to build up in the spinal cord. This buildup of fluid within the spinal cord is called a syrinx (Fig. 51.2).

To be considered a Chiari I malformation, the cerebellar tonsils must extend downward into the spinal canal at least 5 mm. Typically, individuals are thought to be born with this malformation; however, some patients may be found to have cerebellar tonsils that are pathologically descended into the spinal canal due to too much pressure in the head or due to brain tumors. More than one family member may be diagnosed with a Chiari malformation.

Chiari malformations can be classified into several types including:

- *Chiari 0* – The presence of a syrinx without evidence of frank tonsillar herniation (movement of the cerebellar tonsils into the spinal canal). These cases are only diagnosed once surgery results in an improved syrinx.
- *Chiari I* – At least 5 mm of tonsillar herniation into the cervical spine, with or without a syrinx. This is the most common form of these malformations.
- *Chiari II* – Seen only in patients with spina bifida (born with the membranes and/or parts of the spinal cord in a sac on the back). The cerebellum and brain stem herniate into the spinal canal, and there may or may not be a syrinx.
- *Chiari III* – Very rare and the most severe form of cerebellum and brain stem movement into a sac on the back of the head.

Signs and Symptoms

Symptoms of the Chiari malformations vary depending on age and the type of malformation. The most common symptom in these patients is headaches. The headaches are located at the base of the skull/neck area. They are brought on by certain activities such as coughing, sneezing, straining, or exercise and do not last a long time. Headaches have a quick onset and quick relief when the patient stops the activity. Other symptoms may include severe snoring, hoarse voice, difficulty swallowing, choking, abnormal eye movements, weakness, and numbness or tingling in the arms/legs. The list of potential symptoms can be long.

Sometimes a Chiari malformation is diagnosed when a patient is found to have an abnormal curvature of the spine called scoliosis. When present, the scoliosis is due to an underlying syrinx, which is caused by the Chiari malformation. When the Chiari is operated and the syrinx improves, the scoliosis often improves if not severe to begin with.

Diagnosis

A Chiari malformation is best diagnosed with magnetic resonance imaging (MRI) of the brain and neck. To be considered a Chiari I malformation, the cerebellar tonsils must extend downward into the spinal canal at least 5 mm. A computed tomography (CT) scan alone cannot reliably diagnose a Chiari malformation. Occasionally, a Chiari malformation is found when a patient is being evaluated for another condition. Once a Chiari malformation is identified, the individual will be evaluated by a neurosurgeon. The neurosurgeon may request additional tests to be per-

formed to further assist with the diagnosis and treatment. These may include plain X-rays of the neck, MRI of the spine, and swallowing and sleep studies. The MRI of the complete spine will allow the neurosurgeon to evaluate for the presence of a syrinx. The sleep and swallowing studies help evaluate brain stem function.

Treatment Options

Not every individual with a Chiari malformation will require surgery. In fact, most children seen because of an X-ray diagnosis of a Chiari malformation do not have symptoms caused by the malformation. If the individual is not experiencing any symptoms related to the Chiari malformation, the neurosurgeon may recommend routine follow-up to monitor for any future changes. If the individual's symptoms are not related to the Chiari malformation, they may be referred to a neurologist for medical management of their symptoms.

If the neurosurgeon determines that the symptoms are worsening or becoming life altering, surgery may be recommended. If a patient has a large syrinx with a Chiari malformation, then surgery is usually offered.

Surgery

The surgical procedure (called a posterior fossa decompression) carries risks and should not be taken lightly. The goal of this procedure is to make more room at the base of the skull for the herniated cerebellum and allow the spinal fluid to flow in a normal fashion.

The surgical team consists of a neurosurgeon, an anesthesiologist, and the operating room staff. Once the patient is in the operating room, the anesthesiologist will administer medication to put them to sleep. At this time, the neurosurgeon will assist in positioning the individual face down on the operating table holding the head in a surgical frame. The surgical area, extending from the base of the skull to the upper neck, is prepped with a cleaning solution, and the hair will be clipped or shaved. The neurosurgeon will start by making an incision in the skin and pulling back the muscles and other soft tissues to expose the skull and upper neck. A portion of the skull is removed at this time (Fig. 51.3). Depending on the severity of the Chiari malformation, it may be necessary to remove a portion of the upper cervical spine. The neurosurgeon may or may not open the covering of the brain (called the dura mater). If the decision is made to open the dura, then a patch will be sewn over the opening to provide more room. This procedure may take several hours.

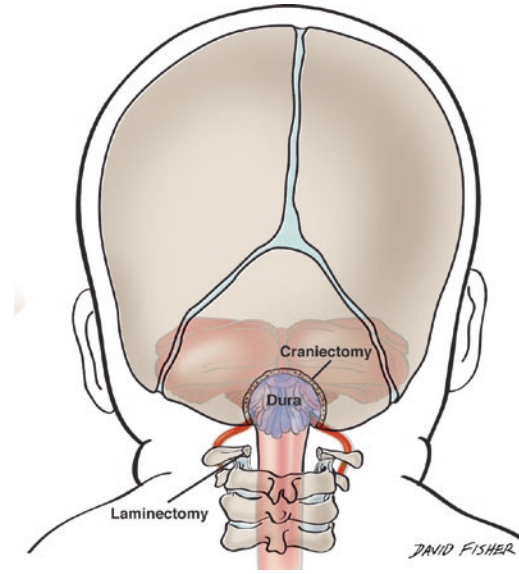

Fig. 51.3 General illustration of the parts of the skull and upper spine that are removed during a posterior fossa decompression

Postoperative Period

After surgery, the patient is observed in the intensive care unit overnight. They will be monitored closely for any complications. If no problems occur overnight, the individual will be transferred to a room, usually on the surgical floor. Neck pain and stiffness are the main complaints after this type of surgery. Nausea and vomiting may also occur, but in general last for the first 2 days. The estimated hospital stay is 2–4 days.

Complications

The risk of complications with this surgical procedure is quite low. The complications that may occur include:

- *Bleeding*.
- *Infection* – this can either be on the outside of the incision (superficial) or deep in the incision. If the infection is superficial, the neurosurgeon may choose to treat the infection with antibiotics that are taken by mouth. If an infection appears to be more severe, then the patient may need to return to the operating room for the incision to be washed out and reclosed. The patient may require intravenous (IV) antibiotics for 10–14 days.
- *Cerebrospinal fluid leak* – this usually occurs only if the surgeon opens the dura (coverings) during the surgical procedure. This increases the risk of an infection called meningitis. Once a leak occurs, the neurosurgeon may place additional sutures (stitches) in the deeper layer of the wound. If the spinal fluid continues to leak, additional surgery may be performed to repair the leak.
- *Fluid collection under the incision* – Fluid can accumulate under the skin without leaking through the incision. This is called a pseudomeningocele. The treatment for this depends on the size and duration of the fluid collection. If the fluid increases in size over several days, the individual may need additional surgery.

Post Hospitalization

Wound Care

The surgeon will typically place a dressing over the incision site. The dressing will be removed by your surgeon. After this, the incision site should be washed daily with plain soap and fresh tap water. The incision should be gently washed and not scrubbed with the fingernails. Do not apply lotions or creams to the site unless instructed to by your surgeon. Do not submerge the incision under water for the first week after surgery.

Activity

After surgery, patients will be tired and have some discomfort near the operative site. Most pain can be treated with over-the-counter pain medicines. The postoperative discomfort will gradually get better over days to weeks. The patient may resume normal activities when they feel they have returned to their baseline. This time varies from patient to patient but is usually in a few weeks. Patients should try to avoid trauma to the area of operation. For pediatric patients, it is recommended that they do not participate in physical education (P.E.) or sports for 3 months.

Reasons to Call Your Surgeon

- *Fever* – 101.5 °F or higher that is persistent or not relieved by medication.
- *Any drainage from the incision site* – red like blood, white like puss, or clear like spinal fluid.
- *Headaches* that increase in frequency or severity and are not relieved with over-the-counter medications; continued *nausea or vomiting; altered sensations* in arms or legs; *worsening pain*; and *fluid collection* at the incision site.

Follow-Up

You will see your neurosurgeon after surgery for a wound check in 1–3 weeks. This visit may consist of removing sutures/staples, evaluation of symptom relief, discussion of returning to school or work, and planning of future testing and appointments. An MRI is not necessary for this appointment. If a preoperative syrinx was present, an MRI will be scheduled 3–6 months after the procedure to allow time for improvements.

Part IX

Conclusions

Conclusions

52

R. Shane Tubbs, Mehmet Turgut, and W. Jerry Oakes

The reader of this text has experienced the breadth of knowledge concerning the Chiari malformations. Every aspect of the conditions we could justify has been included. We are sure other areas will come to us following the publication, but for now this is the limit of our knowledge. As stated in the introduction, we included a section on syringomyelia not caused by cerebrospinal fluid (CSF) equilibrium issues at the craniocervical junction. This was done because the entities are so tightly linked clinically.

Much of the background information concerning the embryology and anatomy is discussed in great detail because it is on this material that our fundamental understanding of the disease process is built. Even a cursory glance at the embryology chapters will impress the reader as to how much we actually understand about the early development of this region. No other reference we are aware of has a section of its equal.

R. S. Tubbs (✉)
Department of Neurosurgery, Tulane University School of Medicine, New Orleans, LA, USA

Department of Neurosurgery and Ochsner Neuroscience Institute, Ochsner Health System, New Orleans, LA, USA

M. Turgut
Department of Neurosurgery, Aydın Adnan Menderes University School of Medicine, Efeler, Aydın, Turkey

W. J. Oakes
Departments of Neurosurgery and Pediatrics, University of Alabama, Birmingham, AL, USA

Dr. Heiss has provided us with insight into the epidemiology of the human occurrence of these conditions. This area is just beginning to be investigated. The genetics have been expertly presented, but as pointed out, this simply goes to emphasize how early we are in our understanding of these problems.

Our two pathology chapters recount the wealth of information concerning the Chiari malformation type II (CM II) but how little pathology plays into our understanding of the Chiari malformation type I (CM I). By investigating the association of CM I with other disease entities, we might gain insight that would help with the genetic analysis as well as the pathophysiology of the conditions. Numerous disease processes may cause a hindbrain hernia as a final common pathway.

One of the most intriguing chapters was contributed by Dr. Marino, our veterinary colleague. Through clinical insight, the discovery of the relatively common occurrence of CM I and syringomyelia in certain dog breeds is of genuine interest. We would wonder if it will be possible to evaluate many of the technical issues associated with the human surgical decompression by randomizing treatment options in the veterinary arena. Few surgical areas are as ripe for exploration as this one.

Dr. Barkovich and colleagues review the explosion of information that occurred in the radiological diagnosis of these conditions. They rightly emphasize that the movement of the cerebellar

R. S. Tubbs et al. (eds.), *The Chiari Malformations*, https://doi.org/10.1007/978-3-030-44862-2_52

tonsils through the foramen magnum is not a true congenital anomaly but simply a reaction to other forces. If there is a pressure differential between the intracranial and intraspinal compartments in utero prior to the full development of the cerebellar tonsils, the vermis and brainstem move caudally. If this same pressure differential occurs later in development, once the tonsils have formed, then they are displaced. The cause for this displacement may be elevated intracranial pressure (ICP) (hydrocephalus, brain tumor, etc.) or inadequate skull growth (growth hormone deficiency, some forms of craniosynostosis, etc.). Alternatively, the cause of the tissue displacement may be abnormally low intraspinal pressure either in utero (myelomeningocele) or following delivery from some type of spinal CSF leak or diversion (e.g., lumbo-peritoneal shunt).

These issues and relationships are further explored by Dr. Iskandar et al. in their discussion of the pathophysiology and CSF flow characteristics of CM I patients. Much more will come from this area in the future. At this point in time, CSF flow studies are interesting but of little concrete assistance in making clinical decisions.

The reader is treated to a brief glimpse into the wealth of experience of a true master of the cranio-cervical junction region in Dr. Menezes' discussion of the bony anomalies found in this region. It is truly difficult to condense the experience of thousands of patients into this succinct chapter, but we believe it was accomplished.

As mentioned previously, the chapter on syringomyelia unassociated with hindbrain hernias was specifically added to help the reader analyze patients who present with similar complaints and findings as those seen with syringes due to CM I. We specifically asked Dr. Klekamp to address the subarachnoid webs causing syrinxes, which are quite difficult to detect radiologically and are only now appreciated as another cause of an "idiopathic" syrinx. His second chapter is devoted to reoperation of adults with continued clinical symptoms. The honest discussion of a difficult group of patients is well worth the reading, and we can all profit from his experience.

Scoliosis and CM I have a separate chapter because of the importance of this clinical problem. In addition to more conventional information, Dr. Brockmeyer et al. mention scoliosis seen in CM I patients without the presence of a syrinx. This subgroup of patients is worth an additional attention in the future.

Of all the chapters, the discussion of the natural history of both CM I and CM II is one of the most important aspects that should be included in any text devoted to a single clinical entity. How can a physician advise a patient on a course of action or inaction without first knowing what will happen without intervention? What becomes obvious from reading this section is that with the advent of readily available magnetic resonance imaging (MRI), a large number of patients are presenting to the neurosurgeon frightened and concerned about their futures. Both this chapter and the discussion of our experience in a multidisciplinary Chiari clinic have gone a long way to reassure asymptomatic patients that surgery is not inevitable and that many individuals remain asymptomatic throughout their length of follow-up.

We then summarize two new entities that do not conveniently fit within Chiari's original classification. It is important to point out that Chiari "0" malformation as described was seen exclusively in the presence of a large syrinx, which was resolved following posterior fossa decompression. The hybrid condition known as Chiari 1.5 has aspects of CM I with caudal movement of the cerebellar tonsils without a neural tube defect and caudal movement of the brainstem typical of CM II. These patients have more significant challenges in regard to their treatment and outcome.

The clinical presentation of both pediatric and adult patients with CM I is summarized and commented on by two experienced clinicians. Their insight into the clinical presentation of this group of patients will be helpful to the reader with limited experience or even a senior consultant.

Additional presentations that are unconventional are divided into two sections: those with objective findings and those without. It appears clear that the weight of evidence dismisses any

association between the patient with fibromyalgia and any form of hindbrain hernia. The chapter devoted to "unconventional" presentations is the most intriguing group of patients. Many are unique in their presentation, which makes pattern recognition by their primary care physician difficult. Many times, the only hint of the problem is localization of the symptoms to the medullary region of the brainstem. Again, the ready availability of MRI has generated many surprised referring physicians and neurosurgeons with a patient and study of singularly unique findings and symptom complex. This aspect of CM I patients is most interesting and a strong stimulus to look for other unusual situations. The balance between explaining unusual patient's symptoms localized to the medulla and trying to cure every patient presenting with headache with an operation is the difficulty.

One of the more difficult areas to discuss is the association of hydrocephalus and pseudotumor to hindbrain hernias. We do not believe the last work that has been written in this area, but the authors summarize the state of our current knowledge.

Dr. Blount discusses the clinical presentation of children with CM II. He emphasizes the need to suspect raised ICP as a common determinant in most patients. Surgical inspection of the shunt is mandatory before any consideration of posterior fossa surgery. The surgical emergency of the situation in infancy is worth reemphasizing.

Treatment of the adult CM I patient is summarized by Dr. Heiss based on his extensive experience at the National Institutes of Health. The reader would be well advised to take many of their surgical tips by heart in approaching their own patients.

The two chapters dealing with the surgical techniques employed in pediatric Chiari decompression do not explore what options are available but rather walk the reader through a single approach and attempts to warn the neurosurgeon of potential pitfalls and how to avoid them. The myriad of surgical options will continue to be explored as long as more than one neurosurgeon is doing these procedures.

Of the various techniques that are available, the controversy over opening or not opening the dura is most poignant. Dr. Hankinson et al. summarize the known information well and outline the advantages and disadvantages of each technique in an even-handed manner.

No text on a surgical subject would be complete without a section on complications and outcomes. Both of these areas are covered in detail by experts with significant experience.

We include a brief lay comment written by two experienced nurses on what to expect as a patient being operated upon for CM I or CM II. We attempt to pitch this section at the average patient/parent level and use language that would be understood by the vast majority of the public. We hope this section could be shared with potential surgical patients and their families.

All in all, one could not but be impressed with the progress we have made in our understanding of these clinical entities in the past 40 years. We have moved from a position of grouping the CM I and syringomyelia patient in the degenerative category to a fundamental understanding of the pathophysiology. This has led to surgical intervention that has generally favorable outcomes. There are many exceptions to this statement, with generalized headaches that do not resolve, to patients whose CSF egress from the fourth ventricle is made worse because of iatrogenic contamination of the subarachnoid space with blood and surgical trauma to the pial surface of the medial cerebellar tonsil. Additional patients with complex issues of ventral compression and micro-movement at the cranio-cervical junction challenge even the experienced neurosurgeon. However, few diseases have progressed so far in such a short time.

The editors of this second edition thank the many experts who have contributed their knowledge on the topic of Chiari malformations. We are sure that the reader will find each of these chapters informative.

Index

R. S. Tubbs et al. (eds.), *The Chiari Malformations*, https://doi.org/10.1007/978-3-030-44862-2